SYNTHESIS OF SUBTYPE SELECTIVE Bz/$GABA_A$ RECEPTOR LIGANDS FOR THE TREATMENT OF ANXIETY, EPILEPSY AND NEUROPATHIC PAIN, AS WELL AS SCHIZOPHRENIA AND ASTHMA

by

Michael M. Poe

A Dissertation Submitted in

Partial Fulfillment of the

Requirements for the Degree of

Doctor of Philosophy

in Chemistry

at

The University of Wisconsin-Milwaukee

August 2016

ABSTRACT

SYNTHESIS OF SUBTYPE SELECTIVE Bz/$GABA_A$ RECEPTOR LIGANDS FOR THE TREATMENT OF ANXIETY, EPILEPSY AND NEUROPATHIC PAIN, AS WELL AS SCHIZOPHRENIA AND ASTHMA

by

Michael M. Poe

The University of Wisconsin-Milwaukee, 2016
Under the Supervision of Professor James M. Cook

The α2/α3 subtype selective Bz/$GABA_A$ receptor positive allosteric modulator HZ-166 (**3**) has been shown to be a nonsedating anxiolytic with anticonvulsant and antihyperalgesic activity. However, instability *in vitro* and *in vivo* has hindered its advancement into clinical trials. A series of ligands based on HZ-166 (**3**) were synthesized. Many of these ligands were designed to increase metabolic stability, while others were synthesized to study the effects that electronics and sterics have on the efficacy exerted when bound to the $GABA_A$ receptor. The α3 subtype selective methyl ester MP-III-024 (**19**) was shown to have increased resistance to metabolism in *in vitro* liver microsomal studies and exhibited significant anxiolytic and antihyperalgesic effects in mice

without showing signs of sedation. However, pharmacokinetic studies indicated that esters as a functional group may not be suitable for extensive preclinical studies.

A series of heterocyclic bioisosteres were synthesized to specifically overcome short half-lives *in vivo*. The oxadiazole MP-III-080 (**34**) and oxazole KRM-II-81 (**36**) underwent pharmacokinetic studies and were both found to exist in plasma and brain samples at high levels. These results indicated these and related heterocycles would be stable *in vivo* to undergo extensive preclinical trials. A dozen ligands were assessed *in vivo* in an anxiolytic marble burying assay as well as a rotarod assay designed to measure ataxic effects. The results from these studies and other *in vitro* protocols led to additional studies using KRM-II-81 (**36**). This oxazole **36** was found to exhibit significant anxiolytic and anticonvulsant properties, including reducing network firing rate frequency in human brain tissue from a patient suffering from resistance epilepsy. In addition, KRM-II-81 (**36**) was found to be more efficacious than gabapentin in reversing the effects of hyperalgesia in a neuropathic pain model at a lower dose than gabapentin in rats, as well as exhibiting antidepressant-like effects.

The α5 $GABA_A$ receptor subtype has been linked to cognitive disorders in such diseases as schizophrenia, bipolar I disorder and major depressive disorder. The enantiomers SH-053-2'F-

S-CH_3 (**51**) and SH-053-2'F-R-CH_3 (**52**) have been shown to be α2/α3/α5- and α5- subtype selective agonists, respectively. Both ligands (*S*)-**51** and (*R*)-**52** have been shown to reduce some positive symptoms of schizophrenia; the *S*-enantiomer **51** was active in the poly(I:C) model of schizophrenia, while the *R*-enantiomer **52** was active in the MAM-model of schizophrenia. Due to the high rate of comorbidity of schizophrenia with anxiety, epilepsy and depression, the *S*-enantiomer (**51**) was shown herein to be useful in these instances because it exhibited both anxiolytic and anticonvulsant properties. In addition, work on analogs of **52** produced MP-III-004 (**63**), an α5 subtype selective ligand with reduced efficacy at the α1, α2 and α3 subtypes as compared to **52**, as well as the very potent α5 positive allosteric modulator MP-III-022 (**65**). This methyl amide **65** was shown to activate α5 subtypes *in vivo* in rats at low concentrations, providing a valuable tool to study the α5 $GABA_A$ receptor subtype. Recent work has shown that *R*-(**52**) and MP-III-022 (**65**) exert antidepressant-like effects in mice, indicating a new use for α5 subtype selective ligands. Moreover, work by Emala *et al*. has discovered a use for α5 subtype selective ligands outside of the central nervous system. Numerous ligands, especially the α5 subtype selective acid **73**, presented herein have been shown to relax precontracted human and guinea pig airway smooth muscle and could provide a novel treatment for those who suffer from asthma.

TABLE OF CONTENTS

LIST OF FIGURES xv

LIST OF TABLES xxv

LIST OF SCHEMES xxvii

LIST OF ABBREVIATIONS xxviii

1 INTRODUCTION 1

1.1 The $GABA_A$ Receptor 1

1.2 Benzodiazepines 4

1.3 Pharmacology of the $GABA_AR$ and Agonistic Effects at Various Subtypes 6

2 MOLECULAR MODELING 11

2.1 Background 11

2.2 Halogen-Acetylene Switch 13

3 DESIGN OF α2/α3 SUBTYPE SELECTIVE LIGANDS AND THEIR USE IN EPILEPSY, ANXIETY AND NEUROPATHIC AND INFLAMMATORY PAIN 16

3.1 Introduction 16

3.2 Background 19

3.3 Chemistry and Results 23

3.3.1 The Synthesis of HZ-166 (3) 23

3.3.2 The Synthesis of Esters to Characterize the L_{Di} Pocket 25

3.3.3 Further Alterations of the C(3) Ester Position of Antinociceptive/ Anxiolytic Agent HZ-166 (3) 45

3.3.4 The Synthesis of Heterocyclic Bioisosteres 59

3.3.5 The *In Vitro* Analysis of HZ-166 (3) and its Analogs 69

3.3.6 Determination of Ataxic and Anxiolytic Effects in Preclinical Models 73

3.3.7 *In Vivo* Characterization of New Lead Compound, KRM-II-81 (36) (CRO) 81

3.4 Discussion 103

3.5 Methods 106

3.5.1 Liver microsomal assay (Revathi Kodali at UWM) 106

3.5.2 Liver microsomal assay (CRO) 107

3.5.3 Time-plasma concentration pharmacokinetic studies (CRO) 107

3.5.4 Efficacy data determined by electrophysiology using *Xenopus laevis* oocytes (Dr. Margot Ernst at the Medical University of Vienna) [172-175] 108

3.5.5 The activity of MP-III-024 (19) in the anxiolytic Vogel conflict assay (Dr. Bradford Fischer at Rowan University) 110

3.5.6 The activity of MP-III-024 (19) in the zymosan A model of inflammatory pain using von Frey filaments (Dr. Bradford Fischer at Rowan University) 110

3.5.7 The activity of MP-III-024 (19) tested for effects in locomotor activity (Dr. Bradford Fischer at Rowan University) 111

3.5.8 The activity of MP-III-024 (19) assessment for operant behavior (Dr. Bradford Fischer at Rowan University) 111

3.5.9 Efficacy data for MP-II-064 (27) using the IonFlux automated patch-clamp (Nina Yuan at UWM) 111

3.5.10 FLIPR functional assay (CRO)[180, 181] 113

3.5.11 Assessment of anxiolytic effects in the marble burying assay (CRO) 116

3.5.12 Assessment for ataxic effects in the rotarod paradigm (CRO) [152] 117

3.5.13 Assessment for muscle relaxation in the inverted screen test (CRO) 117

3.5.14 Assessment for anxiolytic-like effects in the Vogel conflict assay (CRO) [182] 118

3.5.15 Anticonvulsant activity in the MES protocol (CRO) 119

3.5.16 Anticonvulsant activity in the scMET protocol (CRO) 120

3.5.17 Human epileptic cerebral cortex electrophysiology (CRO) 121

3.5.18 Antihyperalgesic activity in the SNL model of neuropathic pain (CRO) 122

3.5.19 Antihyperalgesic activity in the CFA-model of inflammatory pain (Dr. Jun-Xu Li at the University at Buffalo) 123

3.5.20 Depression activity in the forced swim test (CRO) 124

3.6 Experimental Details 125

3.6.1 (2-Amino-5-bromophenyl)(pyridin-2-yl)methanone (6)[91] 125

3.6.2 7-Bromo-5-(pyridin-2-yl)-1*H*-benzo[*e*][1,4]diazepin-2(3*H*)-one (7)[91] 125

3.6.3 Ethyl-8-bromo-6-(pyridin-2-yl)-4*H*-benzo[*f*]imidazo[1,5-*a*][1,4]diazepine-3-carboxylate (8)[91] 127

3.6.4 Ethyl-6-(pyridin-2-yl)-8-((trimethylsilyl)ethynyl)-4*H*-benzo[*f*]imidazo [1,5*a*]-[1,4]diazepine-3-carboxylate (9)[91] 128

3.6.5 Ethyl-8-ethynyl-6-(pyridin-2-yl)-4H-benzo[f]imidazo[1,5-a][1,4] diazepine-3-carboxylate (HZ-166, 3)[91] 128

3.6.6 *tert*-Butyl 8-ethynyl-6-(pyridin-2-yl)-4*H*-benzo[*f*]imidazo[1,5-*a*][1,4]diazepine-3-carboxylate (MP-II-067, 10) 129

3.6.7 Isopropyl 8-ethynyl-6-(pyridin-2-yl)-4*H*-benzo[*f*]imidazo[1,5-*a*][1,4]diazepine-3-carboxylate (MP-II-068, 11) 130

3.6.8 Cyclopropylmethyl 8-ethynyl-6-(pyridin-2-yl)-4H-benzo[f]imidazo[1,5-a][1,4]diazepine-3-carboxylate (MP-II-069, 12) 131

3.6.9 Propyl 8-ethynyl-6-(pyridin-2-yl)-4*H*-benzo[*f*]imidazo[1,5-*a*][1,4]diazepine-3-carboxylate (MP-II-070, 13) 132

3.6.10 *sec*-Butyl 8-ethynyl-6-(pyridin-2-yl)-4*H*-benzo[*f*]imidazo[1,5-*a*][1,4]diazepine-3-carboxylate (MP-II-071, 14) 133

3.6.11 Isobutyl 8-ethynyl-6-(pyridin-2-yl)-4*H*-benzo[*f*]imidazo[1,5-*a*][1,4]diazepine-3-carboxylate (MP-II-072, 15) 134

3.6.12 2-Methoxyethyl 8-ethynyl-6-(pyridin-2-yl)-4*H*-benzo[*f*]imidazo[1,5-*a*][1,4]diazepine-3-carboxylate (MP-II-073, 16) 134

3.6.13 Benzyl 8-ethynyl-6-(pyridin-2-yl)-4*H*-benzo[*f*]imidazo[1,5-*a*][1,4]diazepine-3-carboxylate (MP-II-075, 17) 135

3.6.14 1-Phenyl, ethyl 8-ethynyl-6-(pyridin-2-yl)-4*H*-benzo[*f*]imidazo[1,5-*a*][1,4]diazepine-3-carboxylate (MP-II-076, 18) 136

3.6.15 Methyl 8-ethynyl-6-(pyridin-2-yl)-4*H*-benzo[*f*]imidazo[1,5-a][1,4]diazepine-3-carboxylate (MP-III-024, 19) 137

3.6.16 8-Ethynyl-6-(pyridin-2-yl)-4*H*-benzo[*f*]imidazo[1,5-*a*][1,4]diazepine-3-carboxylic acid (SR-II-54, 20) 138

3.6.17 ^{2}*d*-Ethyl-8-ethynyl-6-(pyridin-2-yl)-4H-benzo[f]imidazo[1,5-a][1,4] diazepine-3-carboxylate (MP-III-068, 21) 139

3.6.18 (8-Ethynyl-6-(pyridin-2-yl)-4*H*-benzo[*f*]imidazo[1,5-*a*][1,4]diazepin-3-yl)methanol (MP-II-023, 22) 139

3.6.19 8-Ethynyl-6-(pyridin-2-yl)-4*H*-benzo[*f*]imidazo[1,5-*a*][1,4]diazepine-3-carbaldehyde (MP-II-050, 23) 140

3.6.20 *N*-Ethyl-8-ethynyl-6-(pyridin-2-yl)-4*H*-benzo[*f*]imidazo[1,5-*a*][1,4]diazepine-3-carboxamide (MP-II-037, 25) 141

3.6.21 *N*-Cyclopropyl-8-ethynyl-6-(pyridin-2-yl)-4*H*-benzo[*f*]imidazo[1,5-*a*][1,4]diazepine-3-carboxamide (MP-II-046, 26) 141

3.6.22 8-Ethynyl-6-(pyridin-2-yl)-4*H*-benzo[*f*]imidazo[1,5-a][1,4]diazepine-3-carbonitrile (MP-II-064, 27) 142

3.6.23 8-Ethynyl-6-(pyridin-2-yl)-4*H*-benzo[*f*]imidazo[1,5-a][1,4]diazepine-3-carboxamide (MP-II-065, 28) 143

3.6.24 5-(8-Ethynyl-6-(pyridin-2-yl)-4*H*-benzo[*f*]imidazo[1,5-*a*][1,4]diazepin-3-yl)-3-methyl-1,2,4-oxadiazole (MP-III-085, 33) 144

3.6.25 3-Ethyl-5-(8-ethynyl-6-(pyridin-2-yl)-4*H*-benzo[*f*]imidazo[1,5-*a*][1,4]diazepin-3-yl)-1,2,4-oxadiazole (MP-III-080, 34) 145

3.6.26 5-(8-Ethynyl-6-(pyridin-2-yl)-4*H*-benzo[*f*]imidazo[1,5-*a*][1,4]diazepin-3-yl)oxazole (KRM-II-81, 36). 147

4 CHIRAL α5 LIGANDS AND THEIR USES IN COGNITIVE DISORDERS AND ASTHMA 148

4.1 Introduction 148

4.2 Background 151

4.3 Chemistry and Results 157

4.3.1 Synthesis of SH-053-2'F-S-CH_3 (51) and SH-053-2'F-R-CH_3 (52) 157

4.3.2 Properties and Pharmacokinetics of SH-053-2'F-S-CH_3 (51) and SH-053-2'F-R-CH_3 (52) 160

4.3.3 Pharmacological Differences between the Enantiomers, SH-053-2'F-S-CH_3 (51) and SH-053-2'F-R-CH_3 (52) and their Potential to Treat Schizophrenia. 167

4.3.4 Synthesis of Analogs 175

4.3.5 MP-III-004, a Superior α5 Bz/$GABA_A$ergic Subtype Selective Ligand 182

4.3.6 MP-III-022 192

4.3.7 The Antidepressant Effects of α5 Subtype Selective Ligands 200

4.3.8 The Use of α5 Subtype Selective Ligands as Bronchodilators for Asthma 203

4.4 Discussion 213

CONCLUSION / FINAL REMARKS 216

4.5 Methods 218

4.5.1 Liver microsomal study (CRO) 218

4.5.2 Cytotoxicity (Kelly Teske at the University of Wisconsin-Milwaukee) 218

4.5.3 Time-concentration (plasma and brain) pharmacokinetic studies (Dr. Miroslav Savić at University of Belgrade)[275] 219

4.5.4 Rat brain metabolism assay 220

4.5.5 Seizure protection in the 6 Hz electroshock assay (ASP at NINDS) 220

4.5.6 Ataxic assessment in the rotorod assay (ASP at NINDS) 221

4.5.7 Prepulse inhibition and the assessment for the development of catalepsy (Dr. David Baker and Nick Raddatz at Marquette University) 221

4.5.8 FLIPR functional assay (CRO)[180, 181] 223

4.5.9 Efficacy data determined by electrophysiology using *Xenopus laevis* oocytes (Dr. Margot Ernst at the Medical University of Vienna)[172-175] 224

4.5.10 Seizure protection against the maximal electroshock (MES) assay (ASP at NINDS)[280-282] 224

4.5.11 Seizure protection against the scMET-induced assay (ASP at NINDS) 224

4.5.12 Determination of plasma and brain concentrations 225

4.5.13 Ataxic assessment in the rotarod assay (Dr. Miroslav Savić at the University of Belgrade) 225

4.5.14 Seizure protection against the scMET-induced assay (Dr. Miroslav Savić at the University of Belgrade) 225

4.5.15 Effects in memory and learning in the Morris water maze (Dr. Miroslav Savić at the University of Belgrade) 226

4.5.16 Effects in the social novelty discrimination (SND) procedure (Dr. Miroslav Savić at the University of Belgrade) 227

4.5.17 Antidepressant effects in the unpredictable chronic mild stress (UCMS) assay (Dr. Etienne Sibille and Sean Piantadosi at the University of Pittsburgh and University of Toronto) 227

4.5.18 Immunohistochemistry of human ASM for α5-containing $GABA_AR$ subunit protein expression[217] 229

4.5.19 Force measurements in human airway smooth muscle strips 230

4.5.20 Force measurements in guinea pig tracheal rings 231

4.6 Experimental 233

4.6.1 *Tert*-butyl (*S*)-(1-((4-bromo-2-(2-fluorobenzoyl)phenyl)amino)-1-oxopropan-2-yl)carbamate (54) 233

4.6.2 (*S*)-7-Bromo-5-(2-fluorophenyl)-3-methyl-1,3-dihydro-2*H*-benzo[*e*][1,4]diazepin-2-one (55) 233

4.6.3 Ethyl (*S*)-8-bromo-6-(2-fluorophenyl)-4-methyl-4*H*-benzo[*f*]imidazo[1,5-*a*][1,4]diazepine-3-carboxylate (56) 234

4.6.4 Ethyl (*S*)-6-(2-fluorophenyl)-4-methyl-8-((trimethylsilyl)ethynyl)-4*H*-benzo[*f*]imidazo[1,5-*a*][1,4]diazepine-3-carboxylate (57) 235

4.6.5 Ethyl (*S*)-8-ethynyl-6-(2-fluorophenyl)-4-methyl-4*H*-benzo[*f*]imidazo[1,5-*a*][1,4]diazepine-3-carboxylate (SH-053-2'F-S-CH_3, 51) 236

4.6.6 *Tert*-butyl (*R*)-(1-((4-bromo-2-(2-fluorobenzoyl)phenyl)amino)-1-oxopropan-2-yl)carbamate (58) 236

4.6.7 (*R*)-7-Bromo-5-(2-fluorophenyl)-3-methyl-1,3-dihydro-2*H*-benzo[*e*][1,4]diazepin-2-one (59) 237

4.6.8 Ethyl (*R*)-8-bromo-6-(2-fluorophenyl)-4-methyl-4*H*-benzo[*f*]imidazo[1,5-*a*][1,4]diazepine-3-carboxylate (60) 237

4.6.9 Ethyl (*R*)-6-(2-fluorophenyl)-4-methyl-8-((trimethylsilyl)ethynyl)-4*H*-benzo[*f*]imidazo[1,5-*a*][1,4]diazepine-3-carboxylate (61) 238

4.6.10 Ethyl (*R*)-8-ethynyl-6-(2-fluorophenyl)-4-methyl-4*H*-benzo[*f*]imidazo[1,5-*a*][1,4]diazepine-3-carboxylate (SH-053-2'F-R-CH$_3$, 52) 238

4.6.11 (*S*)-Methyl 8-ethynyl-6-(2-fluorophenyl)-4-methyl-4*H*-benzo[f]imidazo[1,5-*a*][1,4]diazepine-3-carboxylate (MP-III-021, 62) 239

4.6.12 (*R*)-Methyl 8-ethynyl-6-(2-fluorophenyl)-4-methyl-4*H*-benzo[f]imidazo[1,5-*a*][1,4]diazepine-3-carboxylate (MP-III-004, 63) 239

4.6.13 (*S*)-8-Ethynyl-6-(2-fluorophenyl)-*N*,4-dimethyl-4*H*-benzo[*f*]imidazo[1,5-*a*][1,4]diazepine-3-carboxamide (MP-III-023, 64) 240

4.6.14 (*R*)-8-Ethynyl-6-(2-fluorophenyl)-*N*,4-dimethyl-4*H*-benzo[*f*]imidazo[1,5-*a*][1,4]diazepine-3-carboxamide (MP-III-022, 65) 241

4.6.15 (*S*)-8-Ethynyl-6-(2-fluorophenyl)-4-methyl-4*H*-benzo[*f*]imidazo[1,5-*a*][1,4]diazepine-3-carbonitrile (MP-III-018.A, 66) 241

4.6.16 (*S*)-8-Ethynyl-6-(2-fluorophenyl)-4-methyl-4*H*-benzo[*f*]imidazo[1,5-*a*][1,4]diazepine-3-carboxamide (MP-III-018.B, 67) 243

4.6.17 (*R*)-8-Ethynyl-6-(2-fluorophenyl)-4-methyl-4*H*-benzo[*f*]imidazo[1,5-*a*][1,4]diazepine-3-carbonitrile (MP-III-019.A, 68) 243

4.6.18 (*R*)-8-Ethynyl-6-(2-fluorophenyl)-4-methyl-4*H*-benzo[*f*]imidazo[1,5-*a*][1,4]diazepine-3-carboxamide (MP-III-019.B, 69)..... 244

4.6.19 (*R*)-Isopropyl 8-ethynyl-6-(2-fluorophenyl)-4-methyl-4*H*-benzo[f]imidazo[1,5-*a*][1,4]diazepine-3-carboxylate (MP-III-050, 70) 244

4.6.20 (*R*)-*Tert*-butyl 8-ethynyl-6-(2-fluorophenyl)-4-methyl-4*H*-benzo[*f*]imidazo[1,5-*a*][1,4]diazepine-3-carboxylate (MP-III-051, 71) 245

4.6.21 (*R*)-Cyclopropylmethyl 8-ethynyl-6-(2-fluorophenyl)-4-methyl-4*H*-benzo[*f*]imidazo[1,5-*a*][1,4]diazepine-3-carboxylate (MP-III-052, 72) 246

4.6.22 (*R*)-8-ethynyl-6-(2-fluorophenyl)-4-methyl-4*H*-benzo[*f*]imidazo[1,5-*a*][1,4]diazepine-3-carboxylic acid (SH-053-2'F-R-CH$_3$-Acid, 73) 247

4.6.23 (*R*)-5-(8-ethynyl-6-(2-fluorophenyl)-4-methyl-4*H*-benzo[*f*]imidazo[1,5-*a*][1,4]diazepin-3-yl)-3-methyl-1,2,4-oxadiazole (MP-IV-004, 74)..... 247

4.6.24 (*R*)-3-Ethyl-5-(8-ethynyl-6-(2-fluorophenyl)-4-methyl-4*H*-benzo[*f*]imidazo[1,5-*a*][1,4]diazepin-3-yl)-1,2,4-oxadiazole (MP-IV-005, 75) 248

4.6.25 (*R*)-5-(8-Ethynyl-6-(2-fluorophenyl)-4-methyl-4*H*-benzo[*f*]imidazo[1,5-*a*][1,4]diazepin-3-yl)-3-isopropyl-1,2,4-oxadiazole (MP-IV-010, 76)..... 249

4.6.26 (*R*)-Methyl 8-bromo-6-(2-fluorophenyl)-4-methyl-4*H*-benzo[*f*]imidazo[1,5-*a*][1,4]diazepine-3-carboxylate (MP-III-058, 78) 250

REFERENCES..... 252

APPENDIX A. Characterization of HZ-166 and YT-III-31 (CRO)……...289

APPENDIX B. Oocyte Efficacy and Binding Data of BZDs and β-Carbolines…….309

APPENDIX C. Ester Breakdown of Compounds in Biological Matrices…….…312

APPENDIX D. ADME Evaluation of Test Agents……...…329

APPENDIX E. A Review of the Updated Pharmacophore for the Alpha 5 GABA(A) Benzodiazepine Receptor Model.....338

APPENDIX F. Manuscript Prepared by Miroslav M. Savic, *et al*. on the behavioral characterization of MP-III-022……...394

APPENDIX G. Manuscript Prepared by Etienne Sibille, *et al*. on the Anti-Depressant Effects of SH-053-2'F-R-CH$_3$……...445

APPENDIX H. Manuscript Prepared by Margot Ernst, *et al*. on the Effects of α5-GABA$_A$R Positive Allosteric Modulators in Bronchodilation……....479

APPENDIX I. Provisional Patent on α5 GABA$_A$ Selective Agonists for the Treatment of Depression and Related Disorders…….…513

APPENDIX J. PCT Patent on α2/α3 GABA$_A$ Selective Ligands for the Treatment of Anxiety, Epilepsy, Neuropathic Pain and Depression……..548

APPENDIX K. Crystal Structures……689

APPENDIX L. Results from the Psychoactive Drug Screening Program…….711

LIST OF FIGURES

Figure 1. γ-Aminobutyric acid, the major inhibitory neurotransmitter in the central nervous system. 1

Figure 2. Proposed topology of a GABAA receptor subunit. The extracellular domain begins with the N-terminus and M1-M4 represent the four transmembrane domains (modified from the figures in Burt, *et al*.[16] and Clayton, *et al*.).[17] 2

Figure 3. Longitudinal (A) and cross-sectional (B) schematic representations of the ligand-gated ion channel. The number 1-4 refer to the M1-M4 segments. The M2 segment contributes to the majority of the pore lining within the membrane lipid bilayer (modified from the figures in Keramidas, *et al*[18]. and Clayton *et al.*).[17] 3

Figure 4. Absolute subunit arrangement of the α1β2γ2 GABAA receptor when viewed from the synaptic cleft. The GABA binding sites are located at the β+α- subunit interfaces and the Bz modulatory binding site is located at the α+γ- subunit interface. The part of the schematically drawn subunits marked by the + indicates loop C of the respective subunits (modified from the figures in Clayton, *et al*.[17] and Ernst, *et al*.).[29] 4

Figure 5. Structures of common BZDs diazepam, chlordiazepoxide, triazolobenzodiazepine alprazolam and imidazobenzodiazepine (IBZD) midazolam. The atoms are labeled for both BZDs and IBZDs. 5

Figure 6. Structures of diazepam, which binds only to the DS sites, and flumazenil, which can bind to both the DS and DI sites. 8

Figure 7. Membrane potential over time during the transmission of a nerve signal. A hyperpolarized state represents a potential further away from the threshold potential (modified from the figure in Clayton Ph.D thesis).[73] 10

Figure 8. Relative locations of the descriptors and regions of the unified pharmacophore/ receptor model. The pyrazolo[3,4-c]quinolin-3-one CGS-9896 (dotted line), a diazadiindole (thin line), and diazepam (thick line) aligned within the unified pharmacophore/receptor model for the Bz BS. H_1 and H_2 represent hydrogen bond donor sites within the Bz BS while A_2 represents a hydrogen bond acceptor site necessary for potent inverse agonist activity in vivo. L_1, L_2, L_3 and L_{Di} are four lipophilic regions and S_1, S_2, and S_3 are regions of negative steric repulsion. LP = lone pair of electrons on the ligands (modified from the figure in Clayton, *et al.*). [17] 13

Figure 9. *In vitro* Bz/$GABA_A$ receptor binding data of diazepam and QH-II-066.[75, 94] 14

Figure 10. Comparison of BZD receptor binding data at α1 and α5 GABAA receptors which illustrates increased selectivity at α5 subtypes, as compared to α1 subtypes; where change in selectivity = (Acetyleneα1/α5) / (Halogenα1/α5). 15

Figure 11. Anticonvulsants pregabalin and gabapentin, opioids morphine and methadone, and the COX-2 inhibitor celecoxib, which are used for treatment of neuropathic pain. 17

Figure 12. Structure, binding affinity, and oocyte efficacy of XHe-II-053 (**1**). 20

Figure 13. Structures, binding affinities, and oocyte efficacies of JY-XHe-053 (**2**) and HZ-166 (SH-053-2'N, **3**). 21

Figure 14. Plasma concentration-time profile of SR-II-54 (**20**) when given IV (1 mg/kg) and P.O. (10 mg/kg); n = 3 per time point. 32

Figure 15. Preliminary oocyte efficacy concentration curve of SR-II-54 (**20**) on $GABA_A$ receptors using an EC_3 GABA concentration (n = 2). 34

Figure 16. Preliminary oocyte efficacy concentration curve of MP-III-024 (**19**) on $GABA_A$ receptors using an EC_3 GABA concentration (n = 3). 35

Figure 17. Comparison of a dose-response (DR) curve at EC_3 and EC_{20}. 37

Figure 18. Effects of diazepam and MP-III-024 (**19**) in the Vogel conflict procedure. Male C57BL/6 mice (n = 6) were pretreated i.p. with vehicle (0.5% methyl cellulose, 0.9% sodium chloride), diazepam or MP-III-024 (**19**) 30 minutes prior to testing. Mice were then placed in a chamber and the amount of licks of water was recorded over a 6 minute time period. 39

Figure 19. Effects of MP-III-024 (**19**) on inflammatory pain the in von Frey filament test. Zymosan A (0.06 mg in 20 µL 0.9% sodium chloride) was injected subcutaneously into the plantar surface of the right hindpaw 24 hours prior to testing. Male C57BL/6 mice (n = 6) were then dosed with MP-III-024 (**19**) and mechanical sensitivity was assessed using von Frey filaments. The paw withdrawal threshold was recorded. Open symbols represent the left (non-injured) hindpaw and the closed symbols represent the right (injured) hindpaw. "BL" represents predrug baseline. 41

Figure 20. Effects of diazepam and MP-III-024 (**19**) on locomotor activity. Male C57BL/6 mice (n = 6) were dosed i.p. with vehicle (0.5% methyl cellulose, 0.9% sodium chloride), diazepam or MP-III-024 (**19**). Mice were then assessed for locomotor activity and the total distance traveled was recorded. "V" represents distance traveled after vehicle administration. 43

Figure 21. Effects of MP-III-024 (**19**) on operant behavior. Male C57BL/6 mice (n = 6) were dosed i.p. with MP-III-024 (**19**) and were placed on a fixed ratio of liquid food. Training and test sessions consisted of multiple cycle components, and each culminated in a 5 minute response period. 44

Figure 22. Previously synthesized amides, HJ-I-040 (**24**), ZJW-II-61 and ZJW-II-60 and the oocyte efficacy data of *N*-methyl amide HJ-I-040 (**24**). Concentration curve of 24 on $GABA_A$

receptors suing an EC_3 GABA concentration (n = 4, modified from the figure in Namjoshi, *et al*.).[117] 48

Figure 23. Efficacy testing of MP-II-064 (**27**) in the IonFlux high-throughput patch-clamp instrument. Nitrile MP-II-064 was run against HZ-166 (**3**) to determine how the efficacy profiles compared in parallel experiments. 52

Figure 24. Preliminary oocyte efficacy results of MP-II-064 (**27**) by two-electrode voltage clamp technique (Margot Ernst). Concentration curve of 27 on $GABA_A$ receptors suing an EC_3 GABA concentration (n = 2-3). 53

Figure 25. Proposed structure of a nitrile with an increased degree of freedom at C(3) to interact at H_1 than MP-II-064 (**27**). 54

Figure 26. Structure of imidazenil. 55

Figure 27. Structure and efficacy of ZJW-II-65 (**29**). Concentration curve of **29** on $GABA_A$ receptors using an EC_3 GABA concentration (n = 3). 57

Figure 28. Efficacy comparisons of **19**, **24** and **29** at 1 μM. Efficacy determined on $GABA_A$ receptors using an EC_3 GABA concentration (n = 2 – 4). 58

Figure 29. Structures of a thionoester **30** and thioamide **31**. 59

Figure 30. Common heterocyclic ester bioisosteres. 60

Figure 31. Structure and oocyte efficacy data of ZJW-II-40. Concentration curve of 32 on $GABA_A$ receptors using an EC_3 GABA concentration (n = 3), as reported in Namjoshi, *et al*.[117] 62

Figure 32. Structure and oocyte efficacy of SH-I-85 (**35**), displaying very low efficacy at the α1 subtype. Concentration curve of 35 on $GABA_A$ receptors using an EC_3 GABA concentration (n = 3). 66

Figure 33. Structures of oxazoles (**37** – **40**) and methyl oxazoles (**41** – **46**). These were synthesized based on the pharmacophore/receptor model of Clayton, Poe, *et al*.[74] in collaboration with Dr. Methuku. The synthesis of these can be found in Appendix J..... 68

Figure 34. Analysis of the anxiolytic effects exerted by HZ-166 (**3**) and other ligands. 80

Figure 36. Structure and oocyte efficacy of KRM-II-81 (**36**) and HZ-166 (**3**)..... 83

Figure 37. Plasma concentration-time plot of KRM-II-81 (**36**). Male Sprague-Dawley rats (n = 3 per time point) were dosed i.p. (10 mg/kg) or I.V. (1 mg/kg) and the plasma concentration was analyzed at varying time points for up to 12 hours..... 84

Figure 38. Inverted screen assessment of diazepam, HZ-166 (**3**) and KRM-II-81 (**36**)..... 86

Figure 39. HZ-166 (**3**) and KRM-II-81 (**36**) in the Vogel conflict procedure. 88

Figure 40. Diazepam, HZ-166 (**3**) and KRM-II-81 (**36**) in the MES anticonvulsant activity assay 91

Figure 41. Diazepam, HZ-166 (**3**) and KRM-II-81 (**36**) in the blockage (A) and threshold (B) measurement against scMET-induced seizures. 92

Figure 42. Network Firing Rate. Dampening effects of KRM-II-81 (**36**) on firing rate frequency (Hz) in tissue resected from a human with epilepsy. 94

Figure 43. Antihyperalgesic effects of HZ-166 (**3**) in wild-type (left) and α2 knock-in (right) mice[50] 96

Figure 44. KRM-II-81 (**36**) and gabapentin in the SNL model of neuropathic pain.. 97

Figure 45. Assessment of antihyperalgesic effects of midazolam, **3**, **36** and **38** in CFA-induced inflammatory pain..... 99

Figure 46. Antagonism of BZD effects using flumazenil. The benzodiazepine site antagonist flumazenil shifted the dose-effect curves of PAMs rightward, indicating the effect is modulated by the benzodiazepine receptor. 100

Figure 47. The antidepressant effects of KRM-II-81 (**36**). 102

Figure 48. Typical (haloperidol, chlorpromazine) and atypical (clozapine, olanzapine) antipsychotics. 149

Figure 49. Fast-acting (salbutamol) and long-term control (salmeterol, beclomethasone dipropionate) medications for asthma. 150

Figure 50. Structures of α5 negative allosteric modulators, RY-23, RY-24, RY-79 and RY-80. 151

Figure 51. Structure and binding affinity of α5 antagonist XLi-093 (**47**). 152

Figure 52. Structure and oocyte efficacy of PWZ-029 (**48**)[74] 153

Figure 53. PWZ-029 docked within α5γ2 BzR binding site (BS). Modified from the figure in Clayton, *et al.*[74] 153

Figure 54. PWZ-029 docked with amino acid residues. Modified from the figure in Clayton, *et al.*[74] 154

Figure 55. PWZ-029 docked with A.A. residue interactions. Modified from the figure in Clayton, *et al.*[74] 154

Figure 56. PWZ-029 docked with interactions[74] 154

Figure 57. Structures and oocyte efficacy data of SH-053-S-CH_3 (**49**) and SH-053-R-CH_3 (**50**) 155

Figure 58. Structures and oocyte efficacy data of SH-053-2'F-S-CH_3 (**51**) and SH-053-2'F-R-CH_3 (**52**) 157

Figure 59. Plasma and brain concentration-time profile of SH-053-2'F-S-CH_3 (**51**) after 10 mg/kg i.p. administration in male Wistar rats (n = 3) for up 6 hours..... 163

Figure 60. Plasma and brain concentration-time profile of SH-053-2'F-R-CH_3 (**52**) after 10 mg/kg i.p. administration in male Wistar rats (n = 3) for up to 6 hours 164

Figure 61. Results of **51** and **52** in a rat brain metabolism assay (n = 12)..... 166

Figure 62. Assessment of SH-053-2'F-S-CH_3 (**51**) and SH-053-2'F-R-CH_3 (**52**) to protect mice from electroshock-induced convulsions. 171

Figure 64. Assessment of SH-053-2'F-S-CH_3 (**51**) and SH-053-2'F-R-CH_3 (**52**) to reverse the PPI deficits induced by PCP 172

Figure 65. Assessment of the development of catalepsy of SH-053-2'F-S-CH_3 (**51**) and SH-053-2'F-R-CH_3 (**52**)..... 174

Figure 66. Structure, binding affinity and oocyte efficacy profile of SH-I-75 (**77**). Binding affinity at αxβ3γ2 $GABA_A$/benzodiazepine site subtypes using [^{3}H]-flumazenil displacement studies from two separate experiments..... 183

Figure 67. Structures and oocyte efficacy profiles of SH-053-2'F-R-CH_3 (**52**) and MP-III-004 (**63**). Concentration curves on $GABA_A$ receptors using an EC_3 GABA concentration (n = 3 – 5)..... 184

Figure 68. Assessment of MP-III-004 (**63**) in reversing the PPI deficits induced by MK-801..186

Figure 69. Assessment of the development of catalepsy of MP-III-004 (**63**)..... 187

Figure 70. Assessment of MP-III-004 for protection against 6 Hz electroshock-induced seizures alongside enantiomers **51** and **52**..... 189

Figure 71. Assessment of MP-III-004 (**63**) against seizures when given i.p. or p.o..... 190

Figure 72. Structure, binding affinity and oocyte efficacy profile for MP-III-022 (**65**)..... 192

Figure 73. Plasma and brain concentration-time profile of MP-III-022 (**65**) after 2.5 mg/kg i.p. administration in male Wistar rats (n = 3) for up to 3 hours..... 194

Figure 74. The effects on MP-III-022 (**65**) in basic behavioral tests..... 195

Figure 75. The effects of 2 mg/kg diazepam and 1, 2 and 10 mg/kg MP-III-022 on (a) distance in the target zone (m) and (b) distance in the peripheral ring (%) during probe trial in the water maze. 197

Figure 76. The effects of 1.5 mg/kg diazepam (DZP 1.5) and 1, 2.5 and 10 mg/kg MP-III-022 on discrimination index (a) and the time exploring the familiar and the novel juvenile rat in T2 (b) in the social novelty discrimination procedure. 199

Figure 77. Effect of SH-053-2'F-R-CH_3 (52; α5-PAM) on anxiety- and depressive-like behavior induced by UCMS in female and male mice. 201

Figure 78. Structures of the α4 selective ligands, CMD-45 and XHe-III-74..... 204

Figure 79. Protein expression of the GABAA α5 subunit in intact human trachea-bronchial airway smooth muscle.[217] 205

Figure 80. SH-053-2'F-R-CH_3 (**52**) mediated activation of α5 subunits containing $GABA_A$ channels induces relaxation of pre-contracted airway smooth muscle[217] 206

Figure 81. Structures of α5 selective ligands assessed in an organ bath for the relaxation of precontracted airway smooth muscle; as well as the route to the methyl ester MP-III-058 (**78**). 207

Figure 82. Oocyte efficacy of the α5 selective ligand, SH-053-2'F-R-CH_3 (52), MP-III-004 (**63**), MP-III-058 (**78**) and SH-053-2'F-R-CH_3-Acid (**73**)..... 208

Figure 83. Oocyte efficacy of the super-agonist SH-I-048A (**55**). Concentration curves on $GABA_A$ receptors using an EC_3 GABA concentration (n = 3 – 5). Modified from the figure in Obradovic, *et al*.[272] 210

Figure 84. Assessment of α5 ligands, HZ-166 and SH-I-048A in airway smooth muscle force relaxation 211

LIST OF TABLES

Table 1. Action of benzodiazepines at CNS GABAA α1-6β1-3γ2 receptor subtypes. Presented at the Mona Symposium (2014), University of the West Indies……7

Table 2. Metabolic stability of esters and the carboxylic acid (**20**)…….……..29

Table 3. Time-plasma concentration of **3**, **21** and **20** in IV and P.O. dosing in rats (n = 3 per time point)……..32

Table 4. Brain concentrations at the 2 hour time point of the parent compound which was dosed and **20** after a 10 mg/kg P.O. of either 3, 21, or 20 in rats (n = 3 per time point)……..33

Table 5. *In vitro* metabolic stability, α3 Bz/$GABA_AR$ EC_{50}'s and clogP's of ligands……71

Table 6. Plasma and brain concentrations of HZ-166 (**3**) and KRM-II-81 (**36**) after a 10 mg/kg P.O. dose in rats……85

Table 7. Quantification of Antiseizure Activity: ED_{50} MES, ED_{50} scMET, TD_{50} TOX, and Therapeutic Index (TI) via i.p. and P.O. Routes.[a] Modified from the table in Rivas, *et al*.[115].....90

Table 8. Liver microsomal stability and cytotoxicity of **51** and **52**…….161

Table 9. Pharmacokinetic data of SH-053-2'F-S-CH_3 (**51**) and SH-053-2'F-R-CH_3 (**52**) after 10 mg/kg i.p. administration in male Wistar rats (n = 3)…….164

Table 10. *In vitro* metabolic stability, α3 Bz/$GABA_AR$ EC_{50} values and clogP's of the SH-053-2'F-S-CH_3 (**51**) and SH-053-2'F-R-CH_3 (**52**) and their analogs……180

Table 11. Plasma and brain concentrations of MP-III-022 (**65**) and SH-053-2'F-R-CH_3 (**52**) taken 20 minutes after an i.p. (10 mg/kg) dose, n = 3……193

Table 12. Plasma and brain concentrations taken 20 minutes after an i.p. (10 mg/kg) injection of α5 selective ligands, n = 3…….....209

LIST OF SCHEMES

Scheme 1. Synthesis of HZ-166 (**3**). *Amounts listed are the greatest scale for each reaction. They do not correspond to the product which resulted from the previous reaction.* 24

Scheme 2. Synthesis of esters from HZ-166 (**3**) using lithium and the corresponding alcohols. 26

Scheme 3. Synthesis of the methyl ester MP-III-024 (**19**). 27

Scheme 4. Synthesis of the deuterated ethyl ester, MP-III-068 (**21**)..... 28

Scheme 5. Synthesis of the alcohol MP-II-023 (**22**) and aldehyde MP-II-050 (**23**). 46

Scheme 6. Synthesis of amides, MP-II-037 (**25**) and MP-II-046 (**26**). 49

Scheme 7. Synthesis of nitrile MP-II-064 (**27**) and the byproduct MP-II-065 (**28**)..... 50

Scheme 8. Improved route to the carboxamide MP-II-065 (**28**). 56

Scheme 9. Synthesis of the oximes and methyl (MP-III-085, **33**) and ethyl (MP-III-080, **34**) oxadiazoles..... 63

Scheme 10. Route to SH-I-85 (**35**) as a byproduct..... 64

Scheme 11. Proposed mechanism for the formation of 5-(isocyanomethyl)oxazole. 65

Scheme 12. The synthesis of oxazole KRM-II-81 (**36**)..... 67

Scheme 13. Synthesis of SH-053-2'F-S-CH3 (**51**). 159

Scheme 14. Synthesis of SH-053-2'F-R-CH_3 (**52**). 160

Scheme 15. Synthesis of methyl esters as well as methyl amides..... 176

Scheme 16. Synthesis of nitriles (MP-III-018.A, **66** and MP-III-019.A, 68**)** and carboxamides (MP-III-018.B, **67** and MP-III-019.B, **69**). 177

Scheme 17. Synthesis of esters (**70** – **72**) and SH-053-2'F-R-CH_3-Acid (**73**). 178

Scheme 18. Synthesis of oxadiazoles (**74** – **76**). 179

LIST OF ABBREVIATIONS

ASM	airway smooth muscle
ASP	Anticonvulsant Screening Program
BBB	blood-brain-barrier
BQL	below quantification limit
BZD	benzodiazepine
BzR	benzodiazepine binding site
CCI	chronic constriction injury
CFA	complete Freund's adjuvant
CMC	carboxymethyl cellulose
CNS	central nervous system
CRO	contracted research organization
DI	diazepam-insensitive
DLM	dog liver microsomes
DS	diazepam-sensitive
FLIPR	fluorescence imaging plate reader
GABA	gamma-aminobutyric acid
$GABA_AR$	gamma-aminobutyric acid type A receptors
HLM	human liver microsomes

IBZD	imidazobenzodiazepine
IP	intraperitoneal
IV	intravenously
LR	Lawesson’s reagent
MAM	methylazoxymethanol acetate
MES	maximal electroshock
MLM	mouse liver microsomes
MPE	maximum possible effect
NAM	negative allosteric modulator
NINDS	National Institute for Neurological Disorders and Stroke
PAM	positive allosteric modulator
PCP	phencyclidine
PPI	prepulse inhibition
PTZ	pentylenetetrazole
PWT	paw withdrawal threshold
PO	oral administration
RLM	rat liver microsomes
SAR	structure-activity relationship
scMET	subcutaneous pentylenetetrazole

SEM	standard error of the mean
SNL	sciatic nerve ligation
SSRI	selective serotonin reuptake inhibitors

ACKNOWLEDGEMENTS

I would like to first thank my advisor Professor James M. Cook for the opportunity and support to complete my doctorate in synthetic medicinal chemistry. In addition, Dr. Cook allowed me to gain experience in grant and patent writing to further my development during my time at UW-Milwaukee. I would also like to thank the Cook research group for their helpful discussions and the members of my doctoral committee, Professor's Arnold, Pacheco, Schwabacher and Silvaggi, for their suggestions and instructive discussions.

It was a pleasure working with our numerous collaborators. I have benefitted greatly and gained significant knowledge in various fields through the insightful discussions with each individual, especially Drs. Miroslav Savić (University of Belgrade) and Margot Ernst (Medical University of Vienna). I would also like to thank Professor Robert Carlson, who allowed me to do undergraduate research at the University of Minnesota-Duluth under his supervision. I credit my interest in organic chemistry to this work and experience.

Thank you to my family. To my parents, to which this is dedicated to for all their support and encouragement through my life. To my sister Sarah and her husband Muris, who have offered suggestions and their knowledge regarding the transition out of graduate school.

Finally, I would like to thank my amazing fiancé Kelly Teske, who has made my time in Milwaukee one of the best times of my life.

1 INTRODUCTION

1.1 The $GABA_A$ Receptor

Gamma (γ)-amino butyric acid (GABA; Figure 1) is the major inhibitory neurotransmitter of the central nervous system (CNS) in the mammalian body. When GABA binds to the GABA type A receptor ($GABA_AR$), a transmembrane heteropentameric ion channel,[1, 2] the result is an induction of chloride ions through the pore, which can affect a wide variety of pharmacological actions including anxiety,[3] epilepsy,[4] insomnia,[5] depression,[6] bipolar disorder,[7, 8] schizophrenia[9] and Alzheimer's disease.[10] The response is dependent on the specific composition of the $GABA_A$ subunits which make up the $GABA_AR$.[11] To date, there are 19 individual $GABA_AR$ subunits which have been positively identified; α1-6, β1-3, γ1-3, δ, ε, θ, π, and ρ1-3[12] with additional unidentified subunits plausible. These subunits can arrange in either a hetero- or homo- pentameric ring. Currently, only a small handful of subunit formations have been positively identified to form a functional receptor, with many others highly likely or plausible.[13, 14] The most common and intensively studied arrangement of the $GABA_AR$ consists of $\alpha_{1\text{-}6}\beta_{1\text{-}3}\gamma2$ in a 2:2:1 stoichiometric ratio.[2]

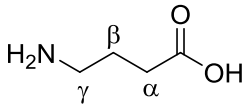


Figure 1. γ-Aminobutyric acid, the major inhibitory neurotransmitter in the central nervous system.

The $GABA_AR$ protein is a polypeptide which possesses an approximate mass of ~50 kD, and each subunit is structurally related. The homology between separate classes (i.e. α versus β) is about 20% sequence identity or 50% sequence similarity, while the homology within a single class is about 70%.[15] A large portion of the *N*-terminal end of each subunit exists in the extracellular

region and contains sites for potential glycosylation and a “Cys-loop” formed by a covalent bond between two conserved cysteines. The protein then proceeds to cross the lipid bilayer four times, with a large intracellular loop located between the M3 and M4 transmembrane regions (Figure 2). Five individual subunits then combine to form the chloride ion pore (Figure 3).

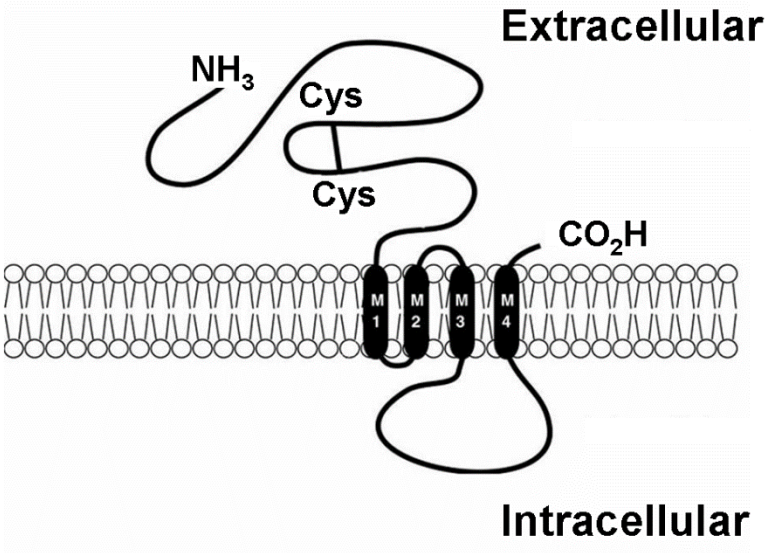


Figure 2. Proposed topology of a GABAA receptor subunit. The extracellular domain begins with the N-terminus and M1-M4 represent the four transmembrane domains (modified from the figures in Burt, *et al.*[16] and Clayton, *et al.*).[17]

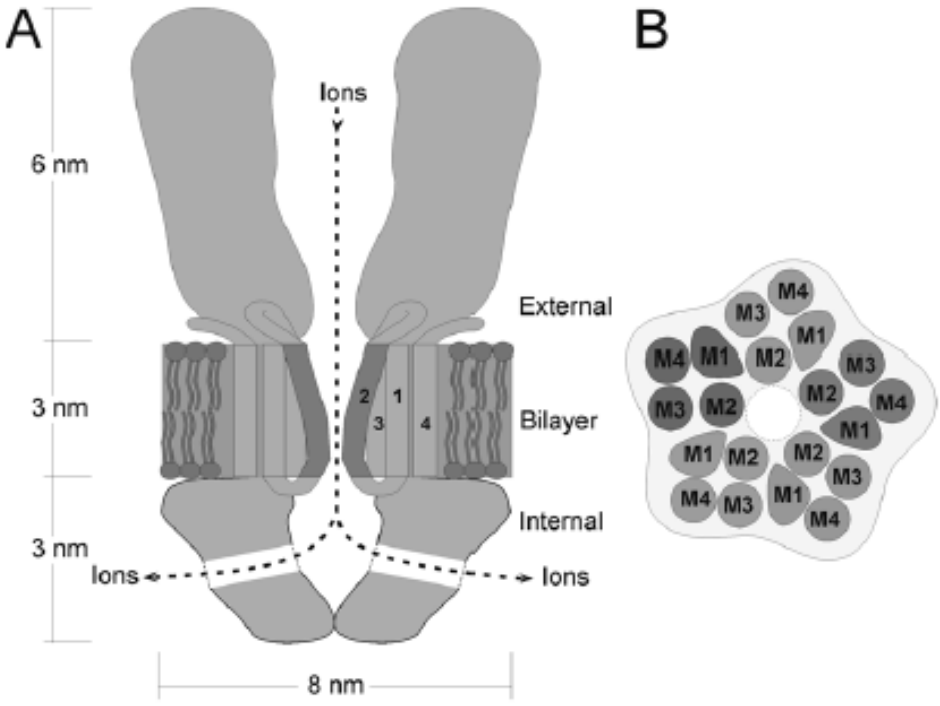


Figure 3. Longitudinal (A) and cross-sectional (B) schematic representations of the ligand-gated ion channel. The number 1-4 refer to the M1-M4 segments. The M2 segment contributes to the majority of the pore lining within the membrane lipid bilayer (modified from the figures in Keramidas, *et al*[18]. and Clayton *et al.*).[17]

The $GABA_AR$ has numerous binding sites located at the synaptic cleft and also within the pore. Activation of the $GABA_AR$ complex can occur due to the binding of a variety of compound classes at these various sites including β-carbolines, barbiturates, ethanol and benzodiazepines, as well as endogenous steroids, among others.[2, 19] Located at the synaptic cleft of the abundant $\alpha_{1\text{-}6}\beta_{1\text{-}3}\gamma2$, which are arranged αβαβγ clockwise when viewed from the extracellular region (Figure 4), are the GABA binding sites at the two $\alpha^-\beta^+$ interfaces, the benzodiazepine binding site (BzR) at the $\gamma^-\alpha^+$ interface,[3, 20] and the more recently discovered CGS 9895 binding site at the $\beta^-\alpha^+$ interface.[21, 22] A number of pyrazoloquinolines have been shown to bind to and activate this $GABA_AR$ site by Ernst, Sieghart, Cook, *et al*. This is based on the seminal work of Sieghart[2] and Sigel.[23] In addition, neurosteroids,[24] ethanol[25, 26] and other compounds may also bind in the interior

of the pore. Research on the interactions of ethanol at the Bz/$GABA_A$ergic subtypes has been reported by Olsen,[27] Platt[28] and others.

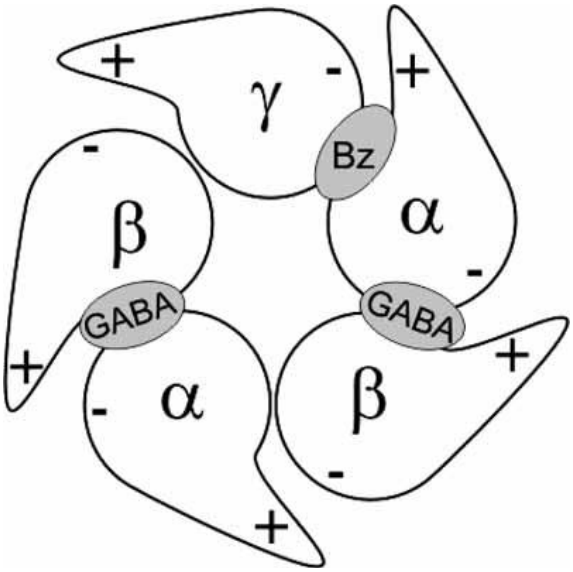


Figure 4. Absolute subunit arrangement of the α1β2γ2 GABAA receptor when viewed from the synaptic cleft. The GABA binding sites are located at the β+α- subunit interfaces and the Bz modulatory binding site is located at the α+γ- subunit interface. The part of the schematically drawn subunits marked by the + indicates loop C of the respective subunits (modified from the figures in Clayton, *et al.*[17] and Ernst, *et al.*).[29]

1.2 Benzodiazepines

Traditional benzodiazepines (BZDs), such as diazepam (Valium) which contain the pendent phenyl C ring (Figure 5), tend to bind non-selectively to the $\alpha_{1\text{-}3,5}\beta_{1\text{-}3}\gamma2$ $GABA_A$ receptors[3, 17, 20] at the BzR site. This class of compounds has been frequently prescribed as a medication for various CNS disorders such as anxiety and convulsions[30, 31] for over half a century. They offer many advantages in drug therapy[32] as they are rapidly absorbed though the gastrointestinal tract when taken orally and generally reach maximum blood concentrations within a couple hours of ingestion. In addition, BZDs are privileged structures, which are able to readily cross the blood-

brain-barrier (BBB) and are rapidly distributed throughout the brain. When used as an emergency anticonvulsant, certain BZDs can reach levels of detection within five minutes when given intravenously (IV),[33-35] but these do develop tolerance in humans after 3 – 5 days which limits their use to status epilepticus in emergency rooms. Other advantages include minimal liver microsomal enzyme inhibition which can cause drug-drug interactions,[36] and a lack of serious toxicity concerns even at high concentrations.[37] Unfortunately, there are also a number of adverse effects that can be produced by BZDs such as drowsiness, sedation, ataxia, muscle-relaxation, amnesia, dependence, withdrawal issues and tolerance to the anticonvulsant and antinociceptive effects limiting their use for the chronic treatment of convulsions and chronic pain syndromes.[19, 38, 39] These adverse effects are a result of the non-selective efficacy of BZDs at multiple $GABA_AR$ subtypes simultaneously.

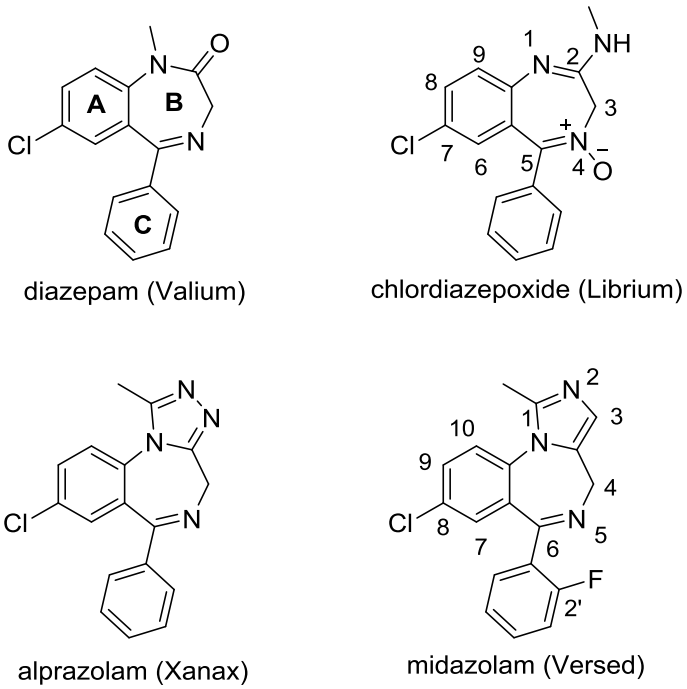


Figure 5. Structures of common BZDs diazepam, chlordiazepoxide, triazolobenzodiazepine alprazolam and imidazobenzodiazepine (IBZD) midazolam. The atoms are labeled for both BZDs and IBZDs.

1.3 Pharmacology of the $GABA_AR$ and Agonistic Effects at Various Subtypes

The pharmacological response to the activation of the $\alpha_{1\text{-}6}\beta_{1\text{-}3}\gamma2$-$GABA_AR$'s is dependent on the composition of the subunits that form the receptor (Table 1), with the presence of different α substituents as the key factor. Over the past couple decades, studies using $GABA_AR$ mutated single-point knock-in mice have been used to identify the actions of different α subunits located within the brain by rendering the BzR insensitive to modulation with BZDs[14] pioneered by Seeburg, Möhler and Rudolph. These studies have been done by replacing a single histidine amino acid of the α subunit with an arginine. In both α1 and α2 subunits, the replacement is an H101R, while the replacements are H126R for α3 and H105R in α5 subunits.[40]

$GABA_A$ receptors containing the α1 subunit have been shown to mediate anterograde amnesia, motor impairment, addiction and sedative effects, as well as part of the anticonvulsant action.[41, 42] Anxiolytic action and some anticonvulsant activity stems from the activation of the α2 subunits,[43, 44] while contribution to the anxiolytic-like effects and possible muscle relaxation at higher receptor occupancy are reported to be mediated by the α3 subunit.[45, 46] Memory and spatial learning, as well as other cognitive effects, are influenced by the α5 subtype.[47] Antihyperalgesic effects also stem from the α2 subunit;[48] however, the site of this action appears to occur from activation of the $GABA_AR$ that are located primarily in the spinal cord[49] as opposed to the brain. A recent triple-point knock-in mutation study was done and shown to confirm which specific α subunit was the source of these pharmacological responses.[50] However, earlier work from this laboratory with the α3 subtype selective ligand YT-III-31 (Poe, Cook, *et al*., unpublished results; see Appendix A) provided evidence that the agonist efficacy at α3 receptors can contribute to the anxiolytic and antinociceptive effects of these ligands. This work, however, may be confounded

by some sedative actions, consequently, unambiguous determination of the processes mediated by the α3β3γ2 subtypes remains to be carried out.

Table 1. Action of benzodiazepines at CNS GABAA α1-6β1-3γ2 receptor subtypes. Presented at the Mona Symposium (2014), University of the West Indies.51

Subtype	Associated Effect
α1	Sedation, anterograde amnesia, some anticonvulsant action, ataxia, some addiction at higher doses and muscle relaxation
α2	Anxiolytic, perhaps hypnotic (EEG) at higher doses, perhaps some muscle relaxation at higher doses, and antihyperalgesic effects
α3	Some anxiolytic action, anticonvulsant action at higher doses, maybe some muscle relaxation at higher doses
α4	Diazepam-insensitive (DI) site, a sedative in the CNS; important in lung disorders in the periphery
α5	Cognition, temporal and spatial memory (Maybe memory component of anxiety)
α6	Diazepam-insensitive (DI) site

The abundance of specific α subtypes in $\alpha_{1\text{-}6}\beta_{2/3}\gamma 2$ $GABA_A$ receptors is not equal throughout the brain. Various studies have been completed by using [^{3}H]-muscimol binding in conjunction with immunoprecipitation using subunit specific antibodies[3, 14] in rat brains, immunohistochemistry,[52, 53] or by monitoring the total decrease in $GABA_A$ receptors after knockout studies in mice.[3] The seminal work by Wisden, *et al*.[54] was key in this regard. The α1 subtype is the most abundant throughout the brain and accounts for 40-50% of the α $GABA_A$ subtypes.[55, 56] The α2 and α3 subtype assemblies account for up to, but not more than, 35% and

14%, respectively[3] and are located mainly in the limbic region. Receptors containing the α5 subtype are the least abundant of the diazepam-sensitive (DS) $GABA_AR$ accounting for about 5% of all α subtypes within the brain, the majority of which are located in the hippocampus.[52, 57] There are some that have been found in the spinal cord.[58]

In addition to the DS $GABA_A$ receptor subtypes ($\alpha_{1\text{-}3,5}\beta_{2/3}\gamma 2$), there are also two diazepam-insensitive (DI) sites in which the binding pocket cannot tolerate the C ring of various benzodiazepines. BZDs, such as flumazenil (Figure 6), which lack the pendent C ring can bind to both the DS and DI $GABA_AR$ binding sites. These two (DI) subtypes are the α4 and α6 subtypes and they account for a smaller percentage of functional $GABA_A$ receptors than the DS subtypes. The α4 makes up 6% of all subtypes[59] and the α6 subtype is found principally in the cerebellum and olfactory bulb.[60] Although these have been studied, the pharmacological effects associated with these two subtypes are still not fully understood. $GABA_A$ receptors are also found in the peripheral nervous system.[61, 62] A major effect of GABA here involves tonic inhibition,[63] but potential uses of BZDs targeting $GABA_AR$ in the peripheral nervous system have been noted within the lungs[64-66] and spleen.[67, 68]

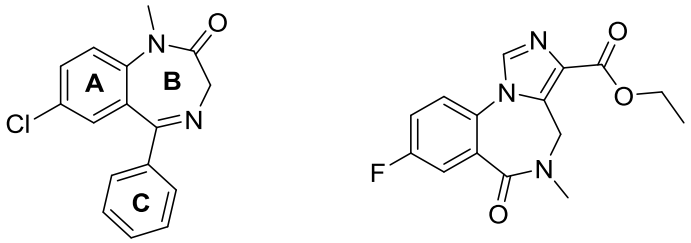


Figure 6. Structures of diazepam, which binds only to the DS sites, and flumazenil, which can bind to both the DS and DI sites.

The pharmacological response due to the modulation of BZDs is dependent not only on which α receptor subtype the BZD binds to, but ultimately the *in vivo* effect it has on the influx of chloride ions through the receptor pore. Under normal physiological conditions, a neuron may become hyperpolarized leading to an action potential and a signal is fired (Figure 7). As GABA binds to the $GABA_A$ receptor and causes a conformational change in the receptor, chloride ions are allowed to travel through the pore. These chloride ions flow into the postsynaptic area and lower the membrane potential, which decreases the likelihood of an action potential being reached and further inhibits neuronal signaling. Benzodiazepines can influence the chloride ion flux in three separate ways; however, GABA must also be present as BZDs alone cannot induce a channel opening.[69-71] A positive allosteric modulator (PAM) alters the conformation of the $GABA_AR$ which results in an increase flux of chloride ions, further inhibiting neuronal firing. PAMs are different from agonists such as muscimol, as agonists bind to the GABA binding site (orthosteric) while all allosteric modulators bind at a separate site by definition. Negative allosteric modulators (NAM) have the opposite effect, termed "inverse agonists", in that the influx of chloride ions is reduced, increasing the chance of an action potential and neuronal firing. The third class of benzodiazepines are null modulators, more commonly referred to as antagonists, which have no discernable effect on the influx of chloride ions. Instead, these antagonists generally have a strong binding affinity for one or more specific BzR sites and limit the ability for other BZDs (such as diazepam, alprazolam, midazolam) to bind and influence the membrane potential.[72] In essence, antagonists occupy the binding site but do not elicit a pharmacological response.[17]

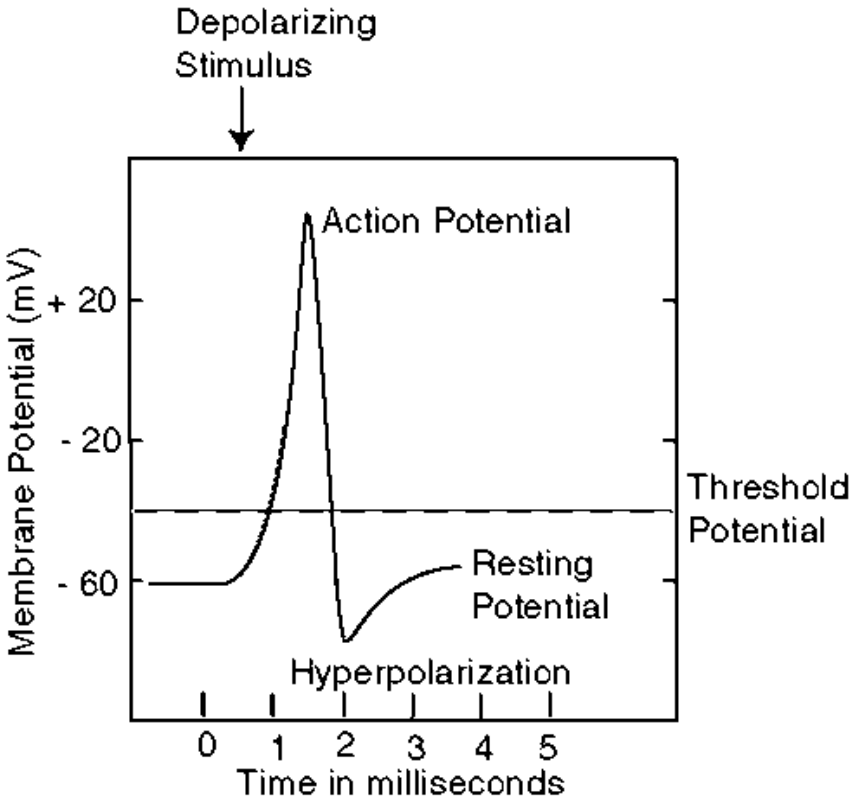


Figure 7. Membrane potential over time during the transmission of a nerve signal. A hyperpolarized state represents a potential further away from the threshold potential (modified from the figure in Clayton Ph.D thesis).[73]

2 MOLECULAR MODELING

2.1 Background

The ability to use BZDs clinically to effectively target various pharmacological diseases is severely hampered by the fact that BZDs generally target multiple α subtypes. This leads to numerous adverse effects including drowsiness, sedation, ataxia, muscle-relaxation, amnesia, dependence, withdrawal issues and tolerance to the anticonvulsant and antinociceptive effects limiting their use for chronic treatment of convulsions.[19, 38, 39] Research in other fields have benefitted from the crystallization of a target receptor protein which allows ligands to be designed based on the binding pocket. Unfortunately for the $GABA_AR$, transmembrane proteins are difficult to crystallize because the removal of the protein from the lipid bilayer destabilizes the protein. Attempts to crystallize a functional $\alpha_{1\text{-}6}\beta_{2/3}\gamma2$ $GABA_AR$ protein have been unsuccessful. Recently, a homopentameric β3 receptor has been crystallized at a 3 Å resolution.[49] Since the BzR is located at the $\gamma^-\alpha^+$ interface, this does not give any insight into the binding pocket for benzodiazepines; however, it does provide hope that a fully functional $\alpha_{1\text{-}6}\beta_{2/3}\gamma2$ may be crystallized in the near future. Certainly, the topology of the β3 receptor can be used to improve homology models reported in the past by Cromer, *et al*.,[1] Sieghart, *et al*.[29] and Clayton, *et al*.[17, 74]

Currently, molecular modeling and structure-activity relationship (SAR) studies are two of the best tools for the study of the activity of benzodiazepines and the design of subtype-selective ligands. Over the past couple decades, extensive work on the BzR pharmacophore has been carried out in Milwaukee[17, 74-76] based on rigid ligands pioneered by Trudell, Diaz, He, Huang and Cook, *et al*.[75-77] This unified Milwaukee-based pharmacophore/receptor model has been built based on the *in vitro* binding affinities of over 150 various ligands which bind to the BzR as PAMs, NAMs or antagonists. These ligands come from over a dozen different classes of compounds including

benzodiazepines,[78, 79] β-carbolines,[80-82] triazolopyrimidines,[83] pyridodiindoles,[84, 85] imidazo-pyridines[86] and pyrazoloquinolines.[87] The predicted binding pocket is created by superimposing ligands from the different compound classes at each individual $\alpha_{1\text{-}3,5}\beta_{2/3}\gamma2$ $GABA_AR$ and aligning them in a way wherein specific elements of the ligands interact with the key descriptors of the pharmacophore model which are used as anchor points. After compounds are docked at these positions, subtle changes in orientation are used around additional lipophilic and steric descriptors. Analysis of these data show that the binding pocket of the DS benzodiazepine binding sites ($\alpha_{1\text{-}3,5}\beta_{2/3}\gamma2$) have very similar topology, and a two-dimensional representation has been produced (Figure 8) with compounds from three separate classes (a quinolinone, a diazadiindole and a benzodiazepine) depicted within. The key descriptors consist of two hydrogen bond donors (H_1 and H_2, corresponding to Y210 and H102, respectively), one hydrogen bond acceptor (A_2, corresponding to T142) and a single, large lipophilic region (L_1) near the center of the binding pocket. Additional descriptors include lipophilic regions (L_2, L_3, and L_{Di}), and regions of negative steric repulsion (S_1, S_2 and S_3). Other lipophilic interactions between the ligand and receptor include van der Waals interactions and $\pi - \pi$ stacking between aromatic regions of the ligand and groups within the receptor protein. Each one of these interactions play an important role in binding affinity, efficacy, potency, and subtype selectivity.[17, 74]

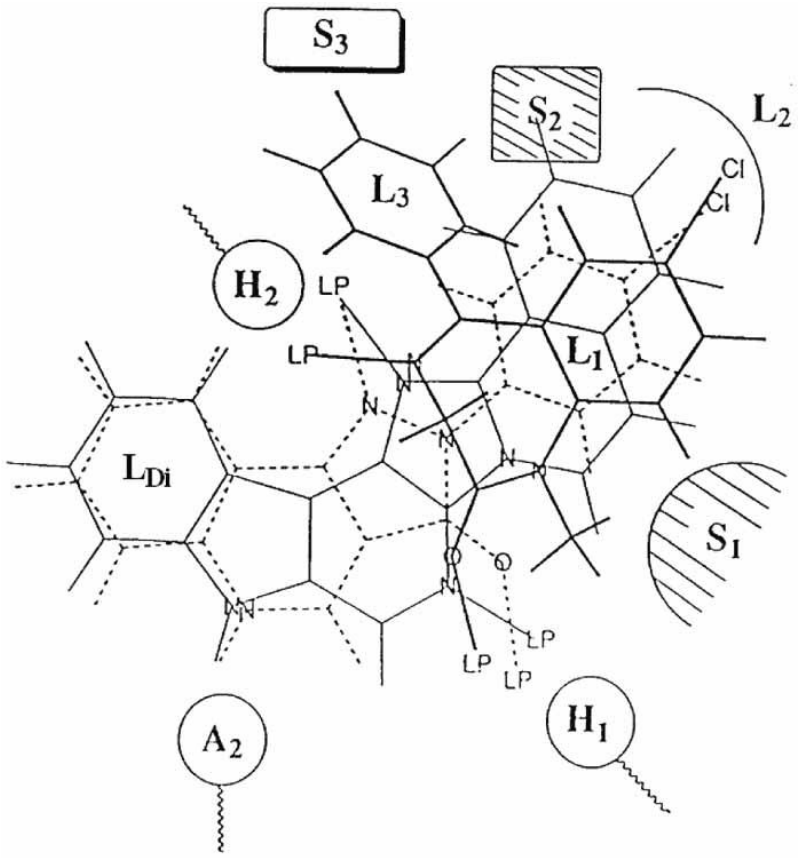
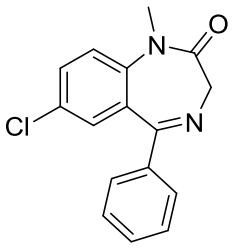


Figure 8. Relative locations of the descriptors and regions of the unified pharmacophore/ receptor model. The pyrazolo[3,4-c]quinolin-3-one CGS-9896 (dotted line), a diazadiindole (thin line), and diazepam (thick line) aligned within the unified pharmacophore/receptor model for the Bz BS. H_1 and H_2 represent hydrogen bond donor sites within the Bz BS while A_2 represents a hydrogen bond acceptor site necessary for potent inverse agonist activity in vivo. L_1, L_2, L_3 and L_{Di} are four lipophilic regions and S_1, S_2, and S_3 are regions of negative steric repulsion. LP = lone pair of electrons on the ligands (modified from the figure in Clayton, *et al.*). [17]

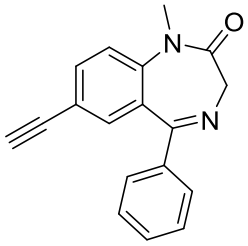
2.2 Halogen-Acetylene Switch

Two lipophilic regions that have been found to be key in the development of ligands for the benzodiazepine binding site of the $GABA_AR$ are the L_2 and L_{Di} regions. A comparison of diazepam and QH-II-066 (Figure 9) shows that switching the chlorine in diazepam to an acetylene in QH-II-066 in the L_2 pocket significantly increased the α5 to α1 selectivity from 1.27 to 11.22, respectively for diazepam and QH-II-066.[75] In terms of selectivity, the switch from a chloride to an acetylene produced an 8.83 selectivity factor for the α5 subtype over the α1 subtype. This was

important for the reduction of the adverse effects commonly exhibited by BZDs.[41, 42] In addition, tolerance has been shown to develop from the coupling of the α1 and α5 subtypes by Möhler, *et al*.[88] Reduction of agonist efficacy at both the α1 and α5 subtypes, disproportionately as compared to other subtypes, has resulted in ligands with little or no development of tolerance.[89-93] This selectivity has been seen in many other cases as well, a few of which are depicted in Figure 10. Two compounds, the data from which *in vitro* and *in vivo* studies, have greatly shaped the development of future ligands, XHe-II-053 (**1**) and JY-XHe-053 (**2**). These two ligands will be discussed in further detail in the next section. The L_{Di} pocket has also been seen as critical in developing new ligands. Based on the molecular modeling,[17, 74] this region appears to be located near the extracellular region of the receptor binding cleft and may be the key to fine tuning ligands.



diazepam



QH-II-066

Bz/$GABA_A$ receptor binding data (K_i = nM)

	α1	α2	α3	α5	α1/α5	**Change in Selectivity**
diazepam	14	20	15	11	1.27	**8.83**
QH-II-066	76.3	42.1	47.4	6.8	11.22	

Figure 9. *In vitro* Bz/$GABA_A$ receptor binding data of diazepam and QH-II-066.[75, 94]

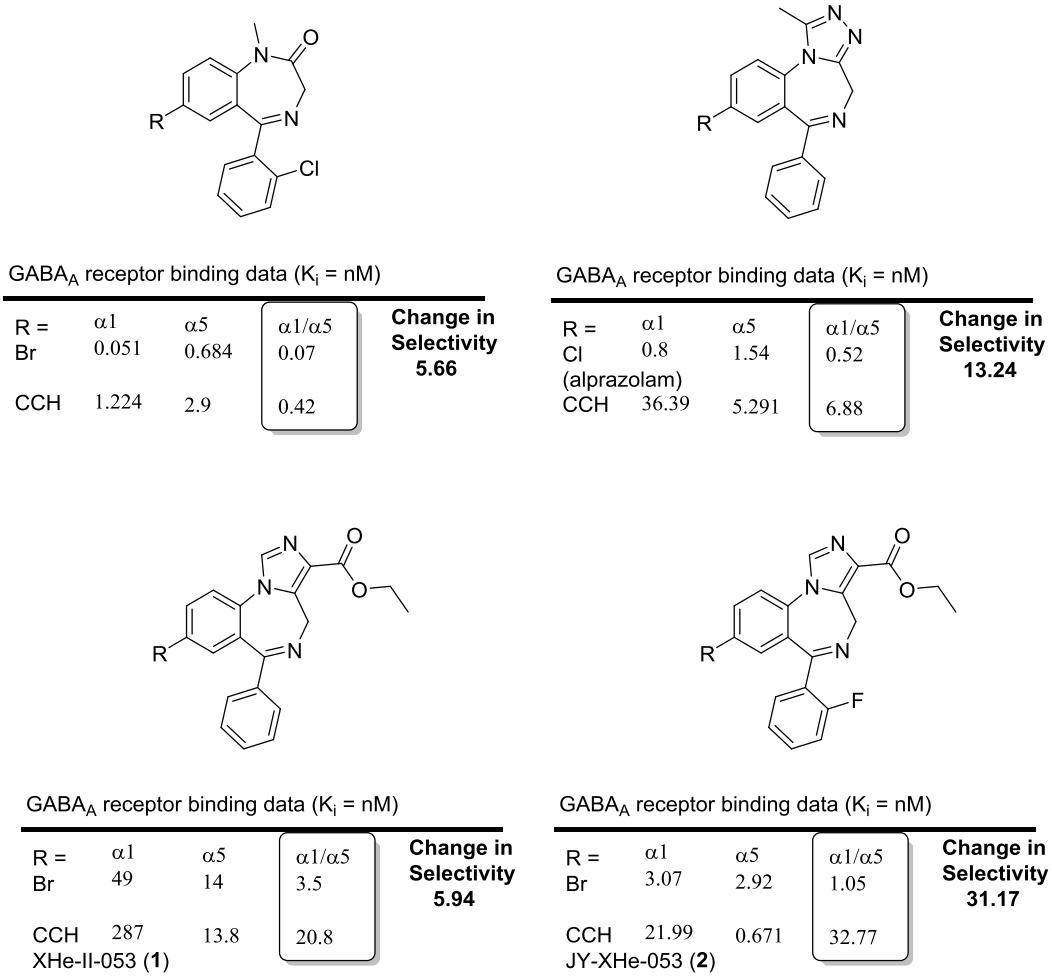


Figure 10. Comparison of BZD receptor binding data at α1 and α5 GABAA receptors which illustrates increased selectivity at α5 subtypes, as compared to α1 subtypes; where change in selectivity = (Acetyleneα1/α5) / (Halogenα1/α5).

In addition to the synthesis of a library of ligands, which bind to the BzR site of the $GABA_AR$, to be used for the study of the basic neuroscience behind the receptor subtype, the goal of this research was to design ligands which can potentially be used in the treatment of epilepsy, anxiety, neuropathic pain and cognition disorders. Because the adverse side effects of BZD ligands are mediated by α1 subtypes and tolerance is effected by the coupling of the α1 subtypes to the α5 subtypes, the goal here is reduced agonist efficacy at α1 subtypes for all ligands, and reduced agonist efficacy at the α1 and α5 subtypes for ligands targeting epilepsy, anxiety, neuropathic and inflammatory pain.

3 DESIGN OF α2/α3 SUBTYPE SELECTIVE LIGANDS AND THEIR USE IN EPILEPSY, ANXIETY AND NEUROPATHIC AND INFLAMMATORY PAIN

3.1 Introduction

Anxiety disorders as a group are among the most common mental disorders afflicting over 18% of the US population.[95] These disorders include generalized anxiety disorder (GAD), obsessive-compulsive disorder (OCD) and panic disorder among others. These disorders can significantly lower a patient's quality of life. Classical BZDs, such as diazepam, and selective serotonin reuptake inhibitors (SSRIs) are two common treatments; however, BZDs are often the drugs of choice since many SSRIs can increase anxiety before becoming effective, and can cause sexual dysfunction and generally take three to four weeks to reach an effect.[96, 97] Diazepam is one classical BZD that has been prescribed for over 50 years for anxiety, but the adverse effects limit its long-term effectiveness and improved treatments are needed that are devoid of sedation, ataxia, amnesia and addiction.

Neuropathic pain is a disease that affects the somatosensory nervous system and is characterized by increased sensitivity to pain (hyperalgesia), or the sensation of pain from stimuli that is, in the absence of neuropathic pain, non-painful (allodynia). Anticonvulsants pregabalin and gabapentin (Figure 11) are two of the first-line treatments for neuropathic pain, but have, in many patients, serious adverse effects including drowsiness, ataxia and an increased risk of suicide in some cases. In addition, they are synergistic with alcohol, which presents a dangerous driving situation. Opioids, such as morphine, fentanyl, dihydrocodiene and methadone, are some of the most effective forms of treatment against neuropathic pain, including in chronic conditions, and

act upon the μ-opioid receptor. These are generally only used in severe cases and never as first-line treatment as the adverse effects include constipation, tolerance, physical dependence and addiction among others.[98] In some cases, they can result in dysphoria. Pain syndromes are also treated with COX-2 inhibitors, such as celecoxib (Celebrex); however, some of these have increased the risk of non-fatal heart attacks and strokes.[99, 100]

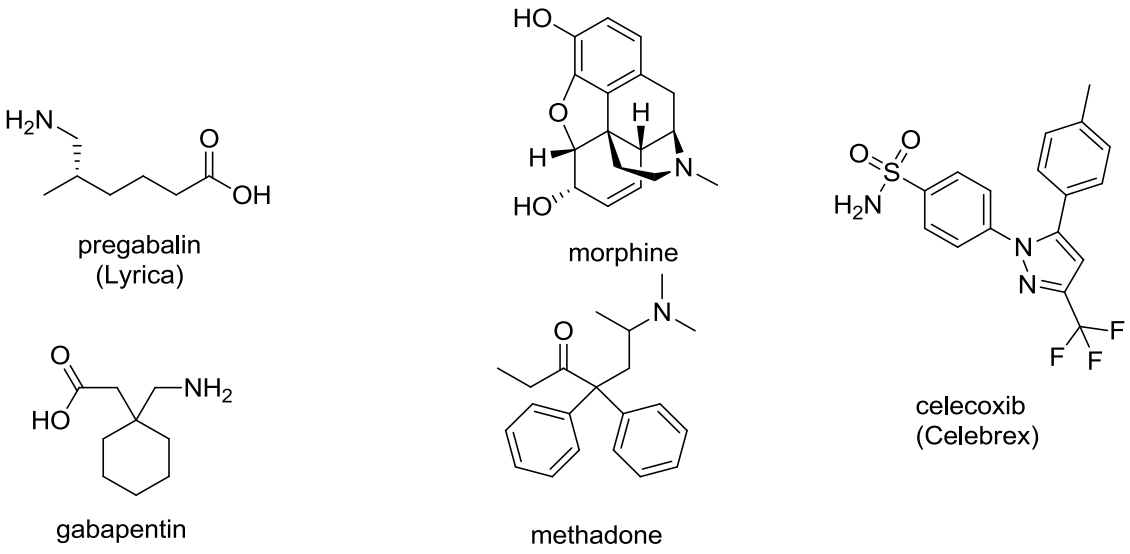


Figure 11. Anticonvulsants pregabalin and gabapentin, opioids morphine and methadone, and the COX-2 inhibitor celecoxib, which are used for treatment of neuropathic pain.

Recently in the pain area, the analogs of salvinorin A by Prisinizano, *et al.*[101] and the enantiomer of (+)-Naloxone by Rice, Hutchinson, Watkins, *et al.*[102] have been found to reduce nociception without tolerance or withdrawal. The enantiomer of Naloxone (marketed, opioid antagonist for overdose) work on toll-like receptor 4 (TLR4)[103] and not opioid receptors. Intense research in these agents are underway and one idea is to mix them with α2/α3 Bz/$GABA_A$ agonists to determine if the effects are synergistic, addictive or neither in the treatment of pain.

Over the years, there have been a number of promising leads for the treatment of anxiety and neuropathic pain that have fallen out of favor for various reasons. A series of

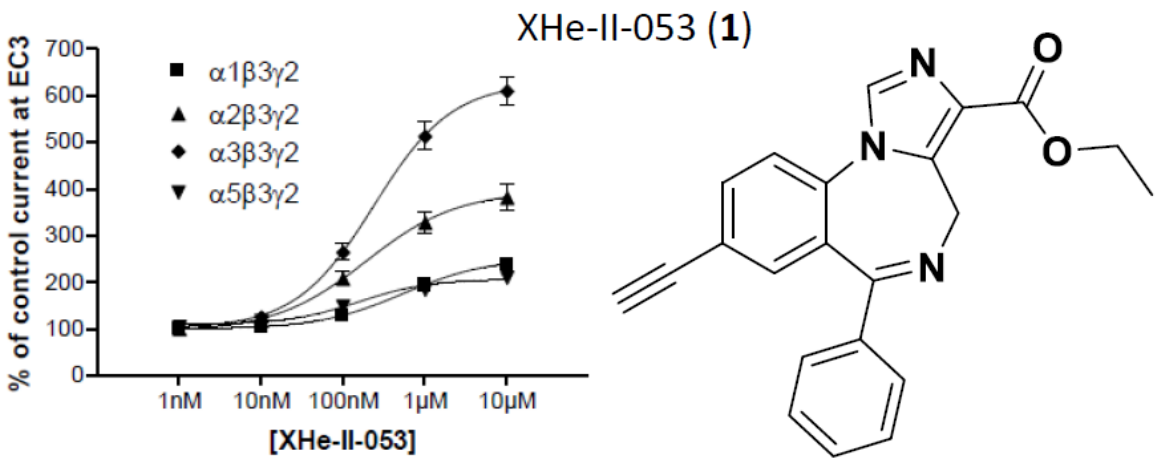
triazolopyridazines, which are partial agonists at the benzodiazepine binding site, were withdrawn from the clinic for various reasons. The L-838417, a partial α2-, α3-, and α5-PAM with antagonistic effects at the α1 subtype promoted anxiolytic properties in rodents[42] and was effective against inflammatory and neuropathic pain;[48] however, the pharmacokinetic profile halted the development.[104] The agent TPA-023, a non-sedating, anticonvulsant, anxiolytic in humans,[105] made it into Phase II clinical trials where long term dosing studies found the formation of cataracts.[106] The ligand MRK-409 (MRK-0343) produced anxiolytic effects in both rodents and primates void of sedation but when given to humans, pronounced sedation was observed at 2 mg/kg.[107] TP023B showed a similar profile to MRK-409 in both rodents and primates, but also displayed sedation and significant ataxia at 2 mg/kg in humans.[108] A benzimidazole, NS11394, exhibited antinociceptive effects in rodents;[109, 110] however, learning and memory impairment has been observed, likely resulting from the high efficacy at the α5 subtype.[111]

Over the past decade there has been growing evidence that an α2 $GABA_AR$ subtype selective ligand can be used in the treatment of neuropathic pain. Molecular modeling[17, 74] has shown that the α2 and α3 binding pockets are nearly identical, which results in ligands that can target both anxiety and neuropathic pain with reduced adverse effects, that exhibit agonist efficacy at α2/α3 Bz/$GABA_A$ subtypes. One of the problems of the Merck compounds was the extremely potent affinity at the DS subtypes (α1, α2, α3 and α5), even though they were reported as antagonists at the α1 and α5 subtypes. This high potency at all four DS subtypes may have led to potent off target effects at other receptor populations and may have resulted in the adverse effects.

3.2 Background

The ligand XHe-II-053 (**1**) was one of the first new generation of ligands which contained the C(8) acetylene in place of a halogen atom in ring A. This halogen-acetylene switch provided a series of BzR/$GABA_A$ ligands with either reduced potency or efficacy at the undesired α1 subtype. In addition, an imidazo-fragment was added to these ligands to further separate them from diazepam and other classical benzodiazepines. Ligands of this type were found to be selective for the α2 and α3 $GABA_A$Rs in both binding affinity and the oocyte efficacy (Figure 12).[112, 113] Anxiolytic XHe-II-053 was in Phase I clinical trials (Bristol-Myers Squibb) and was active as an anticonvulsant and anxiolytic, but the metabolism of the ethyl ester function in the liver kept **1** from progressing to Phase II.

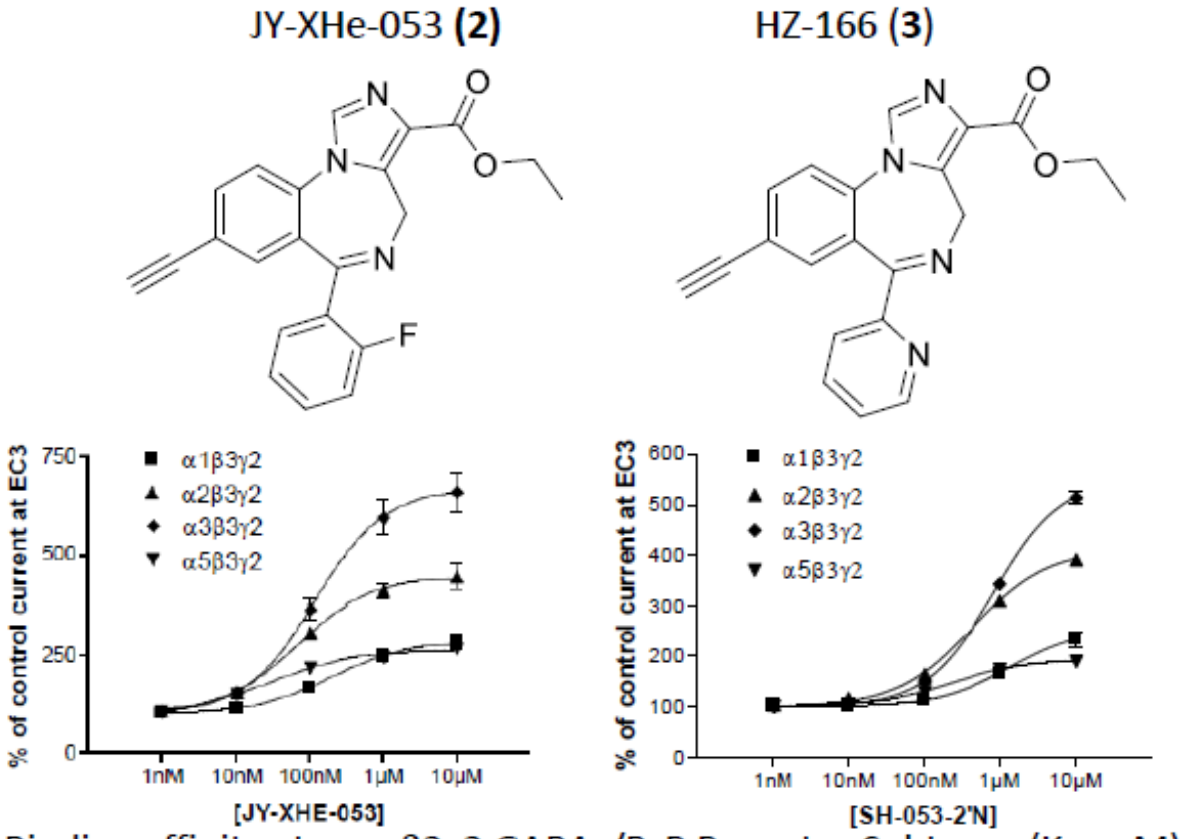
Two related ligands were made replacing the 2'-H atom with a fluorine and nitrogen to obtain JY-XHe-053 (**2**) and HZ-166 (**3**), as depicted in Figure 13. Increased electron density is known to increase the potency in classical 1,4-BZDs,[114] and the reason for this may be due to the ability of the fluorine or nitrogen at the 2'-position to form a three-centered hydrogen bond with the hydrogen bond donor H_2 and the *N*(5) imine lone pair of electrons (see Clayton, Clayton and He for details)[17, 74, 75] While 2'-F ligand **2** was found to be more potent in binding affinity and a more potent anticonvulsant,[89, 90, 115] this trend was seen at all subtypes including an increase at the α1 subtype. This led to minimal sedation at 10 mg/kg in primates[112] which was likely due to the efficacy of the 2'-F compound **2** at the α1 subtype. However, 2'-N ligand HZ-166 (**3**) was found to have a weaker binding affinity at all subtypes, including the greatest decrease at the α1 subtype. However, examining the efficacy profiles of **2** and **3** show that HZ-166 retains the α2/α3 selectivity with reduced efficacy at both the α1 and α5 subtypes, as compared to lead ligand **1**.[112, 113]



Binding affinity at $\alpha_{1\text{-}3,5}\beta3\gamma2$ $GABA_A$/BzR Receptor Subtypes (K_i = nM)

α1	α2	α3	α5
247	40	90	13

Figure 12. Structure, binding affinity, and oocyte efficacy of XHe-II-053 (1).



Binding affinity at $\alpha_{1\text{-}3,5}\beta3\gamma2$ $GABA_A$/BzR Receptor Subtypes (K_i = nM)

	α1	α2	α3	α5
JY-XHe-053 (**2**)	22	12.3	34.9	0.7
HZ-166 (**3**)	300	160	527	82

Figure 13. Structures, binding affinities, and oocyte efficacies of JY-XHe-053 (2) and HZ-166 (SH-053-2'N, 3).

The ligand HZ-166, as well as JY-XHe-053 and others, were sent to the Anticonvulsant Screening Program (ASP) at the National Institutes for Neurological Disorders and Stroke (NINDS) and were evaluated to determine their anticonvulsant activity. In both rat and mouse *in vivo* experiments, **3** was able to protect the test subjects from subcutaneous pentylenetetrazole (scMET)-induced seizures with ED_{50}'s of 16.3 in rats and 98.5 mg/kg in mice when given an i.p. administration.[115] Chronic dosing of **3** for five days at NINDS did not lead to the development of

tolerance in the scMET assay.[116] In addition, HZ-166 was shown to be a non-sedating anxiolytic in the Vogel conflict procedure in rhesus monkeys at 1 mg/kg. Ligand JY-XHe-053 (**2**), on the other hand, was able to protect rodents from seizures and had significant anxiolytic activity at 0.3 mg/kg in monkeys, but the increased efficacy at the α1 subtype likely led to partial sedation in the monkeys at 3 mg/kg; whereas HZ-166 did not exhibit sedation at 10 mg/kg, the highest dose tested.[112]

The 2'-N analog HZ-166 has also been shown to be active in mouse[93] and rat[89, 90] models of inflammatory and neuropathic pain, which exhibited an antihyperalgesic effect without producing general analgesia.[93] A dose-dependent comparison revealed a lower ED_{50} for ligand **3** (5.3 mg/kg) than for gabapentin (6.2 mg/kg), without signs of sedation (ED_{50} = 97 mg/kg) or ataxia (no significant rotarod performance reduction at 160 mg/kg) at the therapeutically relevant dose.[93] A 17-day study of tolerance (chronic versus acute) employing the von Frey filament test in the chronic constriction injury (CCI) paradigm indicated HZ-166 (**3**) performed equally well in the chronic study as it did when naïve mice were treated after 17 days.[93] This lack of tolerance to the antihyperalgesic effects is in agreement with the findings that targeting the α2 subunit will not result in the development of tolerance,[50] as well as the lack of tolerance to the anticonvulsant effects of HZ-166.

In addition to behavioral studies, lead ligands were tested by SRI International *in vitro* for stability on human liver microsomes (HLMs).[117] As expected, based on Phase I clinical trials of the initial lead ligand **1**, XHe-II-053 (**1**) was rapidly metabolized with only 1.5% of the parent compound remaining after a one hour incubation with HLMs while JY-XHe-053 (**3**) exhibited a similar metabolic profile with 0.3% of the parent compound remaining after incubation for one

hour. The more polar 2'-N analog, HZ-166, on the other hand, proved to have an increased resistance to metabolism in HLMs with 80.2% of the parent compound remaining after one hour.[117]

Despite these positive results for HZ-166 (**3**), it was found that rodent metabolism still degraded the compound too rapidly due to the high level of esterases in rodents based on the time-of-effect of HZ-166 in anticonvulsant[115] and antihyperalgesia[93] studies. This was a major problem as many preclinical trials are performed in rodents and evaluation of ligands might be halted due to the metabolic instability. The chemistry and biology that follows focuses on new ligands that are structurally based to HZ-166 and its privileged scaffold. The goal of the development of these ligands was to retain the α2/α3 subtype selectivity, while increasing the metabolic stability in rodents while stability in HLMs remained high.

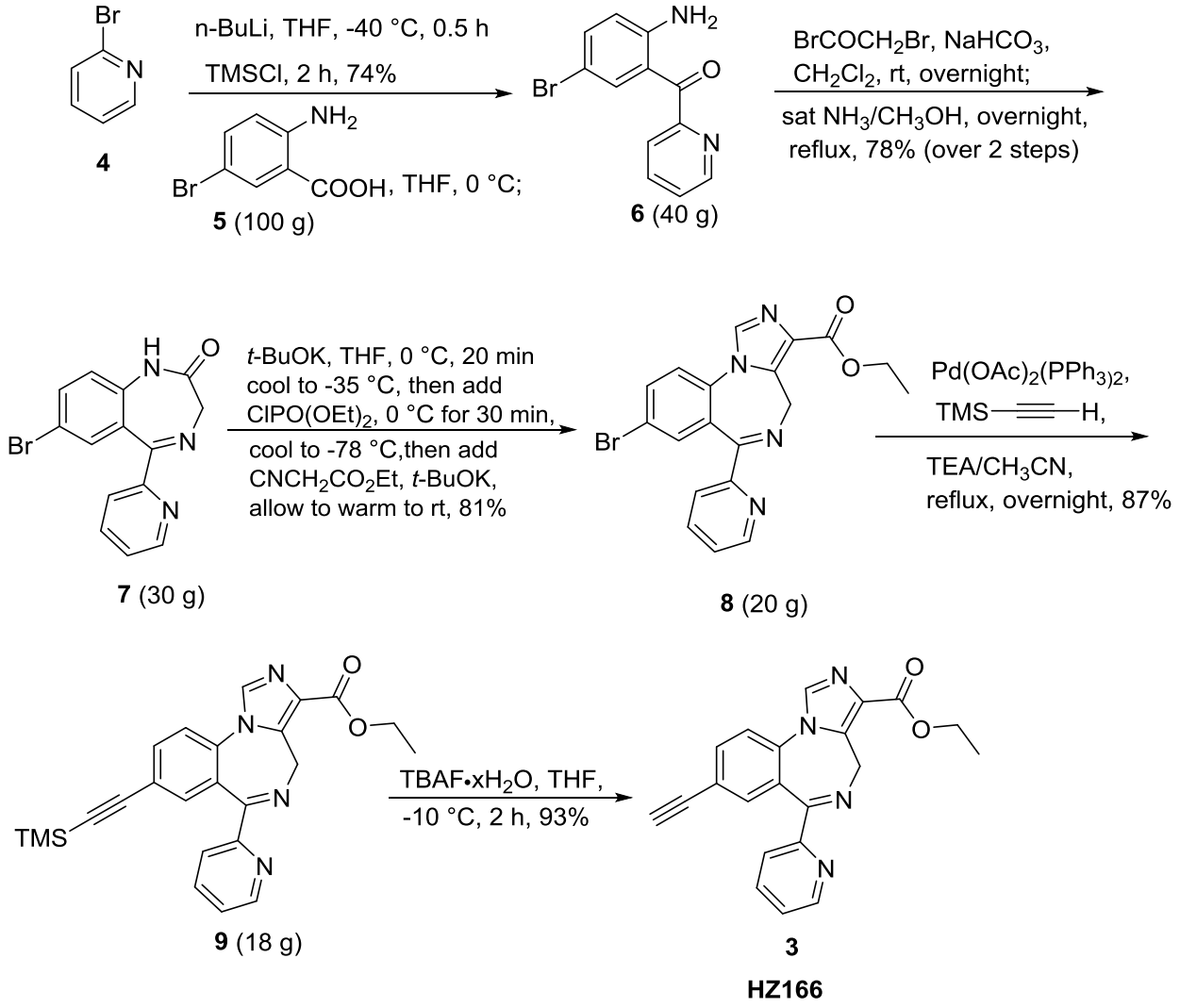
3.3 Chemistry and Results

3.3.1 The Synthesis of HZ-166 (3)

The synthesis of HZ-166 (**3**) was undertaken on a large scale, as illustrated in Scheme 1. The commercially available 2-amino-5-bromobenzoic acid **5** was condensed with the anion of 2-bromopyridine **4** to give the 2'-N ketone **6** in 74% yield on a 100 gram scale. The amine **6** was acetylated with bromoacetyl bromide in the presence of sodium bicarbonate, followed by the cyclization by treatment of a saturated solution of ammonia (gas) in methanol at reflux to form the 1,4-benzodiazepine **7** in 78% overall yield for the two steps. The imidazole ring was prepared using an improved method[118] by treating amide **7** with potassium *tert*-butoxide and diethylchlorophosphate at -35 ^{o}C before the addition of ethyl isocyanate at -78 ^{o}C with potassium *tert*-butoxide to provide imidazobenzodiazepine **8** in 81% yield. The previous method employed sodium hydride as a base at higher temperatures, and yields were consistently below 40%. A Heck-

type coupling reaction with the bromide **8** and trimethylsilylacetylene provided **9**, which was deprotected using tetrabutylammonium fluoride to provide the HZ-166 **3** in 81% overall yield over two steps on a 20 gram scale.

Scheme 1. Synthesis of HZ-166 (3). *Amounts listed are the greatest scale for each reaction. They do not correspond to the product which resulted from the previous reaction.*

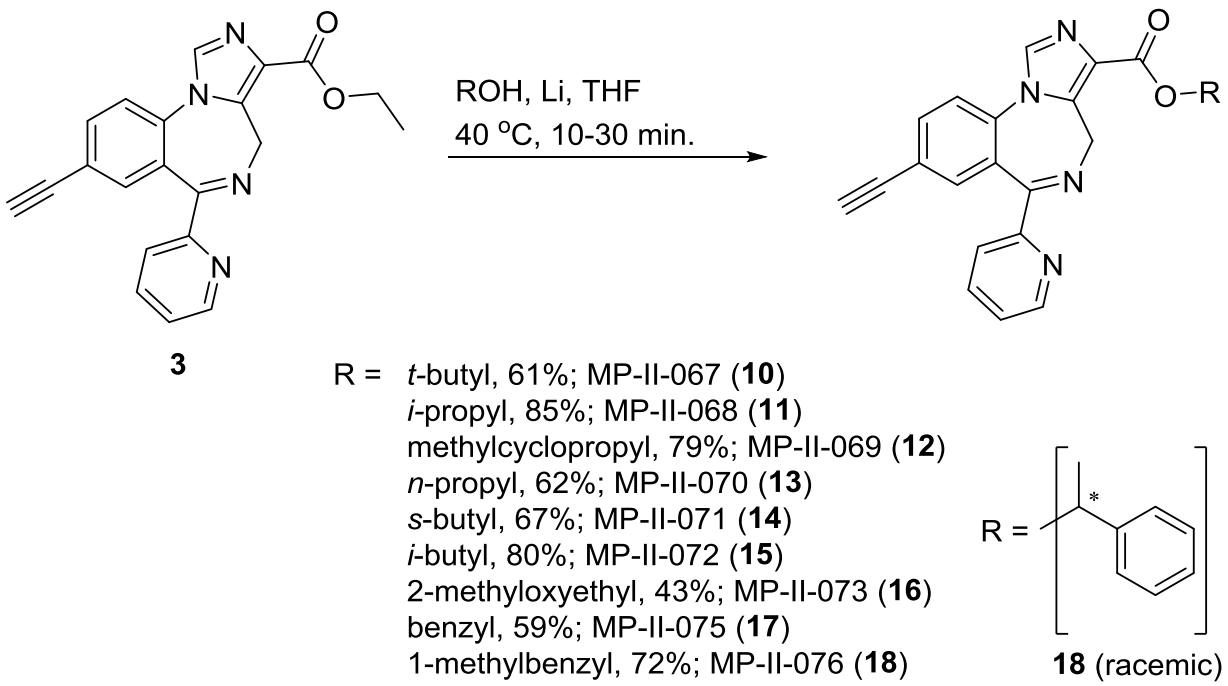


The synthesis of HZ-166 (**3**) on large scale was developed to prepare related analogs for SAR/efficacy at Bz/$GABA_A$ receptors, as well as to send to collaborators for their *in vivo* studies of efficacy, anxiolytic activity, antinociceptive activity and metabolism. Some of these ligands have been found *in vivo* to have clinical potential.[93, 112, 115]

3.3.2 The Synthesis of Esters to Characterize the L_{Di} Pocket

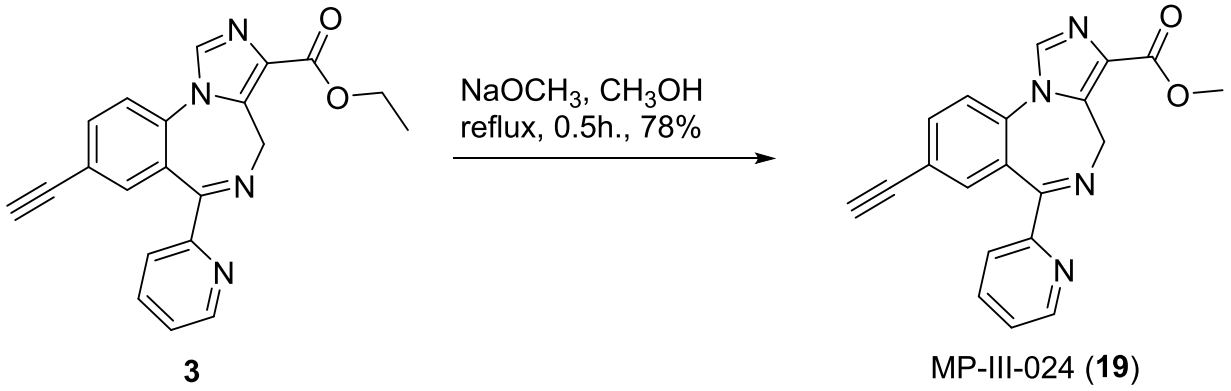
A series of esters were synthesized which were designed to explore the effects of size within the L_{Di} pocket, as well as effects on metabolism. The majority of these reactions were carried out by stirring small freshly cut pieces of lithium rod in an alcohol at 40 ^oC, before adding HZ-166 (**3**) which had been dissolved in THF (Scheme 2). The reaction was monitored by TLC (silica gel), and must be closely monitored. This is because the small changes in polarity and size between the parent ethyl ester **3** with the new esters, especially the isopropyl **11** and *n*-propyl **13** esters, resulted in such similar structures, it was important to make sure all the starting material was consumed so the use of a small wash column could be employed for purification. Additionally, when the reaction was allowed to proceed for longer periods of time after the starting material was consumed, additional byproducts that began to develop would complicate purification. It was also discovered that this reaction was best performed in a dryer atmosphere as moisture and CO_2/O_2 in the air quickly oxidized the freshly cut lithium. To balance this in times of high humidity, the lithium rod was cut while submerged in oil and then transferred to the reaction flask; this, however, resulted in a longer reaction time and also led to longer chromatography (column, silica gel, pressure) during purification to remove all the oil.

Scheme 2. Synthesis of esters from HZ-166 (3) using lithium and the corresponding alcohols.



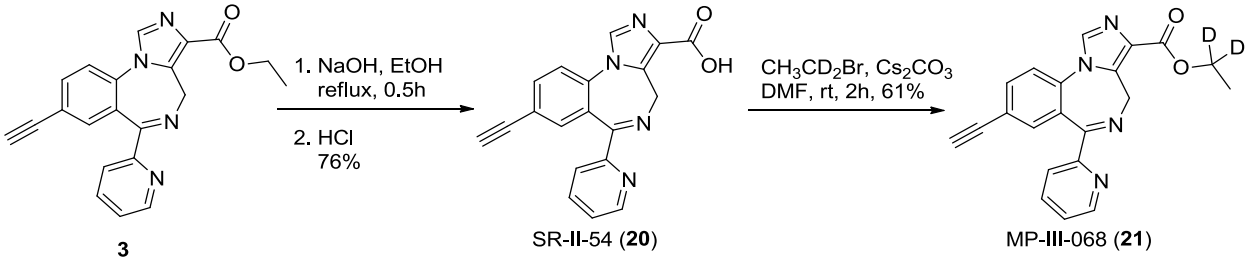
The methyl ester was also desired for this series of esters because of the possibility of beta-oxidation in the liver during the metabolism of ester **3** (HZ-166) to the carboxylic acid SR-II-54 (**20**). This was completed by dissolving **3** in methanol, adding sodium methoxide and refluxing for 30 minutes, as depicted in Scheme 3. It was known (Rowlett, *et al.*, unpublished results) that while the ester **3** was an anxiolytic in the Vogel conflict procedure in monkeys, the acid was not active. This was presumably because the acid does not readily cross the BBB. This was proven earlier for the acid metabolite of **1** which did not cross the BBB (Lelas, *et al.*, BMS, unpublished results).

Scheme 3. Synthesis of the methyl ester MP-III-024 (19).



It has been previously shown that the additional mass from the deuterium isotope can extend the half-life of a compound.[119] The strength of a C-D bond is about 9 times that of a C-H bond.[120] The deuterated ethyl ester **21** was designed and synthesized in an attempt to utilize this technique to increase the half-life of HZ-166. Unlike the synthesis of other esters (**10** – **19**) which were synthesized in one reaction, MP-III-068 (**21**) required preparation in the absence of ethanol, including the ethyl ester function, which could result in a mixture of **3** and **21**. To avoid this mixture of products, HZ-166 was first converted into the acid (SR-II-54, **20**) by saponification with sodium hydroxide at reflux and a subsequent acidification with hydrochloric acid.[121] The d^2-ethyl ester **21** was then synthesized by stirring **20** with 1,1-dideuterated ethyl bromide in the presence of cesium carbonate, as shown in Scheme 4.

Scheme 4. Synthesis of the deuterated ethyl ester, MP-III-068 (21).



3.3.2.1 Analysis of the In vitro Metabolic Stability of the Esters

To analyze the effect of the ester on stability, liver microsomal studies were completed (Table 2); some of which were tested by a contract research organization (CRO) and others by Revathi Kodali at the University of Wisconsin-Milwaukee (UWM). The two assays were both run using liver microsomes from either human (HLM) or mouse (MLM) liver microsomes, while the CRO also ran the compounds in dog (DLM) and rat (RLM) microsomes. Although both assays used microsomes along with NADPH as an energy source at 37 ^{o}C, they were run under different conditions, with the CRO incubating the compound at a 4 μM final concentration for 30 minutes. The assays from UWM were run at a 10 μM final concentration for 60 minutes. In the comparison between the two assays, compounds **3** and **19** were the only ones run in both assays and gave similar results. The results for HZ-166 (**3**) also agree well with previously published data[117] in both assays.

Table 2. Metabolic stability of esters and the carboxylic acid (20).

CRO Results	Metabolic stability in liver microsomes (reported in %-remaining) *Conditions*: 4 µM compound, 37 °C, 30 minutes				clogP[a]
Species	Human (HLM)[b]	Dog (DLM)[b]	Mouse (MLM)[b]	Rat (RLM)[b]	(Diazepam = 2.96)
XHe-II-053 (**1**)	40	83.7	9.9	8.7	3.11
JY-XHe-053 (**2**)	8.9	83.8	5.1	0.7	2.91
HZ-166 (**3**)	80.4	97.2	54.1	50.2	1.71
MP-III-068 (**21**)	95.1	100	63.1	76.6	1.71
MP-III-024 (**19**)	92.2	72.6	73.3	92.7	1.18
SR-II-54 (**20**)	95.9	100	92.7	99.3	1.82
UWM Results	*Conditions*: 10 µM compound, 37 °C, 60 minutes				
Species	HLM		MLM		
HZ-166 (**3**)	69		45		1.71
MP-III-024 (**19**)	80		75		1.18
MP-II-067 (**10**)	66		46		2.42

[a] This was calculated used clogP on the ChemDraw 13.0 software; as compared to diazepam

[b] Human liver microsomes (HLM), dog liver microsomes (DLM), mouse liver microsome (MLM) and rat liver microsomes (RLM).

Analysis of the data on the ethyl esters **1** – **3** from the CRO indicated that, as previously shown, HZ-166 (**3**) was more stable than either **1** or **2** in all species. Rodent microsomes degraded all compounds more rapidly than either human or dog, and this is likely due to a higher concentration of esterases in rodents that in humans or dogs. The short time-of-effect for HZ-166 (**3**) in studies of anticonvulsant[115] and antihyperalgesia[93] may also be explained by this rapid metabolism by esterases in rodents. This low rodent stability of **3** was also seen in MLM's in the results from UWM at 45% remaining after one hour.

Currently, only two additional (non-deuterated) esters have been tested, the methyl ester **19** and the *tert*-butyl ester **10**. The methyl ester (MP-III-024, **19**) was tested in both assays and shows a consistent increase in stability in comparison **3** in all species except DLM, which decreased from 97% to 73%. In rodents, the stability of methyl ester **19** compared to the ethyl ester **3** increased from 45% to 75% and 54% to 73% in the UWM and CRO results, respectively. In addition, **19** exhibited little degradation against RLMs at 93% remaining after 30 minutes. This supports the hypothesis that some of the metabolism of **3** was effected by oxidation in the liver of the ethyl group to acetaldehyde. Compound **10** displays almost no change from **3**. The increased metabolic stability of the methyl ester **19** in rodents led to the decision to test MP-III-024 (**19**) in anxiolytic and antihyperalgesic assays, the positive results of which are presented in Section 3.3.2.3.

The incorporation of deuterium into the ethyl ester functionality, as seen in MP-III-068 (**21**), was successful in decreasing metabolism of the ethyl ester in all species. Slight increases in stability of **21** compared to **3** were exhibited in DLMs, which was already highly stable, and MLMs rose from 54% to 63% remaining. The greatest increase in stability of MP-III-068 (**21**) was seen in RLMs which increased from 50% to 77%. At this juncture it appeared beta oxidation was, in some part, responsible for the metabolism of the ethyl ester in HZ-166 (**3**). This is the reason an *in vivo* pharmacokinetic study on MP-III-068 (**21**) and HZ-166 (**3**) was carried out, and is discussed in Section 3.3.2.2.

One trend that can be seen to occur is that the more polar compounds have an increased resistance to liver microsomes. This of course agrees entirely with the function of liver microsomes since they are there to convert nonpolar ligands into polar metabolites which can be conjugated and excreted more readily via the kidneys. Of the ethyl esters, **3** was the most polar and the most

stable. The varying ester functionalities of **3**, **19**, and **10** also display this trend; it should be noted, however, that the size of the ester could play a role, at least in the case of the methyl ester MP-III-024 (**19**).

3.3.2.2 The In vivo Pharmacokinetics of HZ-166 (3), MP-III-068 (21) and SR-II-54 (20)

The replacement of the ethyl (-CH_2CH_3) group in HZ-166 (**3**) to a deuterated ethyl (-CD_2CH_3) group in **21** was able to increase the amount of parent compound remaining after an incubation in RLMs for 30 minutes from 50% to 77%. In addition, the carboxylic acid **20** was shown to have very little degradation across all species and was a predicted metabolite of the result of the degradation of the ethyl esters **3** and **21**. This was shown earlier by a CRO clearly, that the acid **20** was the principle metabolite of HZ-166 (**3**), see Appendix A. A pharmacokinetic study was completed using the three compounds in rats. The compounds were given intravenously (IV) at a 1 mg/kg dose and oral administration (*per os*; P.O.) at a 10 mg/kg dose. Plasma samples (n = 3/time point) were taken at time points ranging from 0 hours to 16 hours.

Examination of the results found that neither HZ-166 (**3**) nor the deuterated analog (**21**) was stable in the assay *in vivo* as each was below the quantification limit (BQL) at every time point (Table 3). The acid **20**, which showed only a 0.7% degradation in the RLMs, was able to be quantified and the time-plasma concentration curve is depicted in Figure 14. Because neither **3** nor **21** was stable enough in the *in vivo* assay to be quantified, this still does not rule out beta oxidation in part, as a mechanism for conversion of **3** or **21** into the acid **20** and in fact the more stable d^2-analogs **21** is consistent with this pathway, in part.

Table 3. Time-plasma concentration of 3, 21 and 20 in IV and P.O. dosing in rats (n = 3 per time point).

	Total Time Concentrations (time in h.; concentration in nM)			
IV (1 mg/kg)[a]	**0.25**	**0.5**	**1.0**	**2.0**
3	BQL	BQL	BQL	BQL
21	BQL	BQL	BQL	BQL
20	450	148	33.5	3.5
P.O. (10 mg/kg)[b]	**0.25**	**0.5**	**1.0**	**2.0**
3	BQL	BQL	BQL	BQL
21	BQL	BQL	BQL	BQL
20	248	293	161	37.5

BQL – below quantification limit
[a] Quantifiable limit < 2.81 nM in IV samples.
[b] Quantifiable limit < 12.2 nM in PO samples.

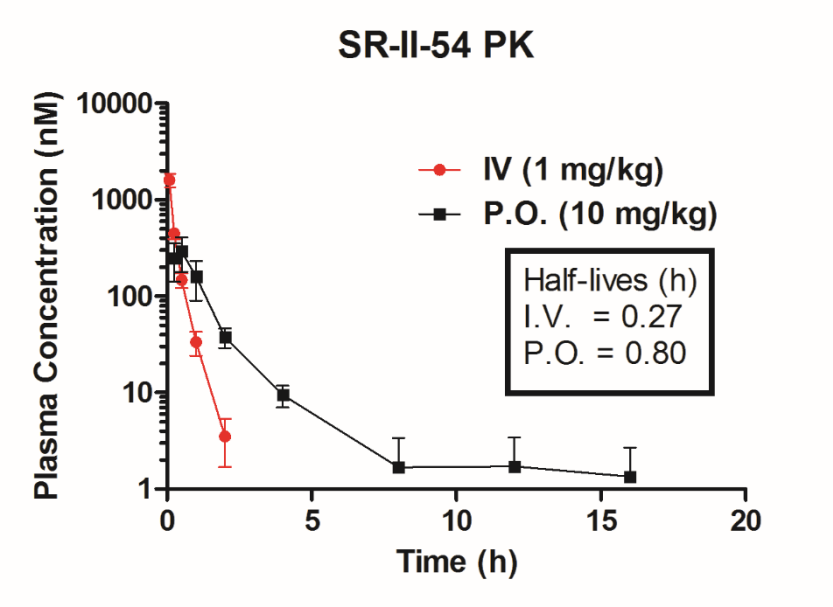


Figure 14. Plasma concentration-time profile of SR-II-54 (20) when given IV (1 mg/kg) and P.O. (10 mg/kg); n = 3 per time point.

Despite the fact that the acid **20** was metabolically stable *in vivo* in this system, it is very far from a useful compound. In a separate experiment, examination of Table 4 shows that **20** was unable to be detected in the brain at the two hour time point when given at a 10 mg/kg P.O. dose. When taken with the plasma concentration-time profile, it can be concluded that **20** was unable to readily penetration the BBB. When the ethyl ester **3** was given, which was not detected in plasma in the initial pharmacokinetic study, analysis of the brain samples found the metabolite **20**, albeit in concentrations just about the quantifiable limit (12.2 nM). This suggests that **3** may be able to rapidly penetrate the brain upon dosing, and it was slowly metabolized to the carboxylic acid **20**. This is consistent with the anxiolytic, anticonvulsant and antinociceptive activity *in vivo* of **3**.

Table 4. Brain concentrations at the 2 hour time point of the parent compound which was dosed and 20 after a 10 mg/kg P.O. of either 3, 21, or 20 in rats (n = 3 per time point).

	3	**21**	**20**
Concentration of Parent compound	BQL[a]	BQL	BQL
Concentration of **20**	10[b]	BQL	BQL

[a] BQL = below quantification limit; Quantification limit < 12.2 nM
[b] The three samples averaged 10 nM; individual samples were BQL, 12.5, and 17.5 nM.

Since the parent ethyl ester **3** was BQL in brain samples after two hours but the acid **20** was detected, it is plausible that **20** may be the compound that is, either in part or in full, producing the pharmacological effects seen when **3** is given; or for that matter, any ester or other compound that may be metabolized to the acid **20**. The oocyte efficacy of **20** is depicted in Figure 15. SR-II-54 (**20**), compared to **3** (Figure 13), is much more potent and less selective. Examination of this oocyte efficacy profile of the acid **20** exhibited potent efficacy at the α1, α3 and α5 subtypes at 500 nM, although α1 was very weak at 100 nM. This does not look like the efficacy profile of a

non-sedating anxiolytic nor anticonvulsant nor antinociceptive agent. It appears HZ-166 (**3**) gets into the brain rapidly and is metabolized into the acid **20**, as mentioned previously.

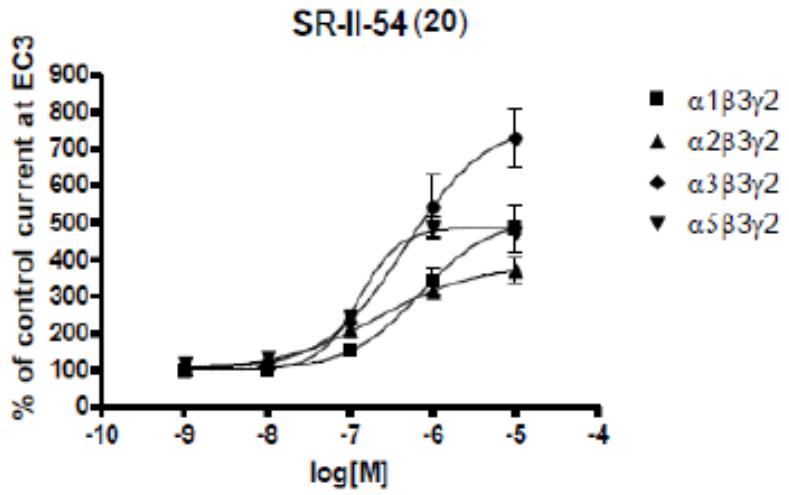


Figure 15. Preliminary oocyte efficacy concentration curve of SR-II-54 (20) on $GABA_A$ receptors using an EC_3 GABA concentration (n = 2).

3.3.2.3 The Efficacy and Behavioral Studies on MP-III-024 (19)

The methyl ester MP-III-024 (**19**), related to HZ-166 (**3**), was found to have significant increased resistance to metabolism by rodent microsomes, as previously mentioned, and has been evaluated further for efficacy to determine the subtype selectivity (Dr. Margot Ernst, Medical University of Vienna) and in behavioral tests to measure the pharmacological effects (Dr. Bradford Fischer, Cooper Medical School of Rowan University).

The methyl ester MP-III-024 (**19**) was tested in *Xenopus laevis* oocytes individually expressing a $GABA_A$ receptor subunit ($\alpha_{1\text{-}3,5}\beta3\gamma2$) for efficacy by Margot Ernst, *et al*. The test consisted of the measurement of chloride currents using a two-electrode voltage clamp at GABA

3% effective concentration (EC_3). Analysis of the results in Figure 16 show that the methyl ester **19** was an α3 subtype selective ligand that is nearly silent at the α1, α2 and α5 subtypes. Within the generally accepted therapeutic range (100 – 300 nM), **19** positively modulated the α3 subtype with low potency. Some researchers have made the case that low potency modulators, sometimes called partial agonists, which stimulate the receptor in the 150 – 200% range are preferred over full agonists which modulate the receptor over 400%. The reasoning is that full agonists which strongly activate receptors can cause desensitization of the receptor. This can lead to the development of tolerance to drug effects (private communication with Dr. Werner Sieghart). It should be noted that the ligands presented here which have been pursued for therapeutic potential are partial agonists in the therapeutic range. In addition, methyl ester **19** should exhibit low risk of the common adverse effects associated with activation of the α1 subtype, especially sedation, tolerance, ataxia and addiction

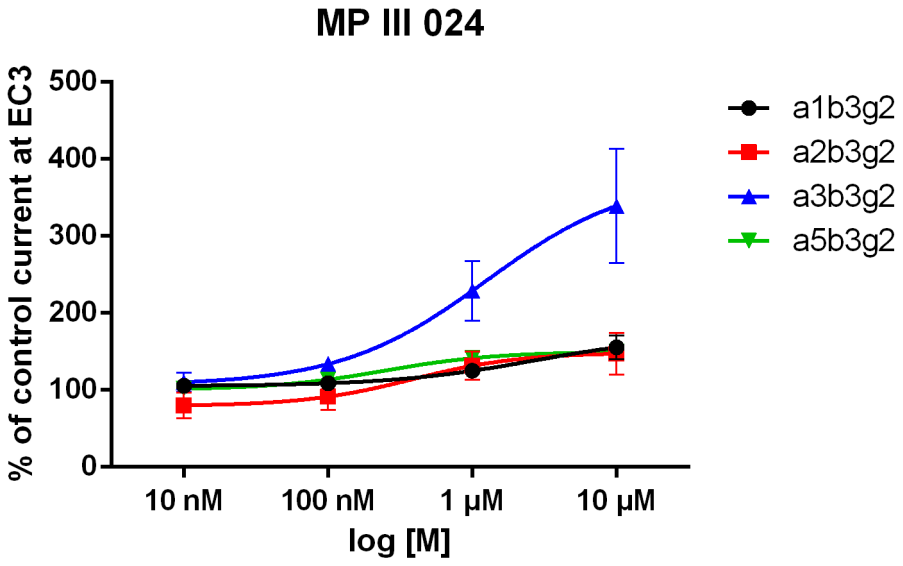


Figure 16. Preliminary oocyte efficacy concentration curve of MP-III-024 (19) on $GABA_A$ receptors using an EC_3 GABA concentration (n = 3).

There have been opposing views on which effective concentration to use when performing these electrophysiology experiments. Dr. Werner Sieghart (Medical University of Vienna), in a private communication, has outlined the complex matter of using EC_3 or EC_{20}. One of the arguments in favor of employing EC_3 in these experiments is that at this concentration the assay is generally stable and exhibits low variability if the concentration is slightly off, since it is not in the steep linear portion of the dose response curve such as the EC_{20} would be, as depicted in Figure 17. In addition, because of a low GABA concentration, the effect seen by a modulator is more clearly visible and generally produces a stronger response by percentage. The EC_{20} was initially chosen because the researchers were in favor of using a dose in the linear range of the dose response curve; however, this high concentration is rarely encountered in physiological situations. For this reason, most of the oocyte efficacy for Bz modulation of $GABA_A$ receptors is run at an EC_3 of GABA in this research.

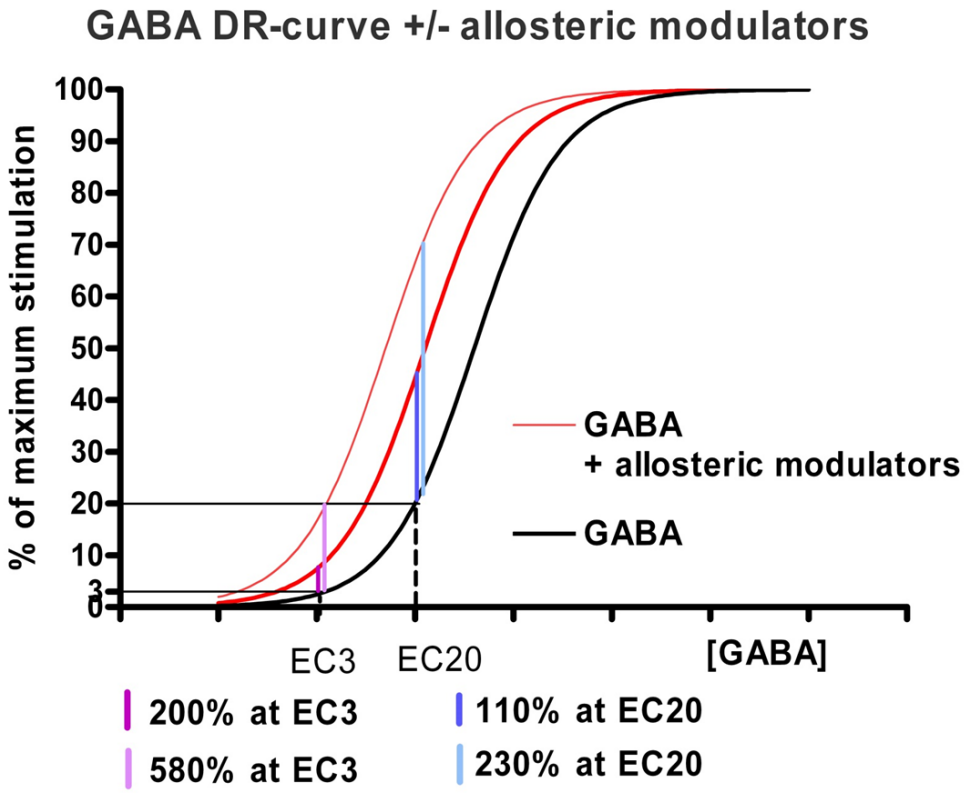


Figure 17. Comparison of a dose-response (DR) curve at EC_3 and EC_{20}.

The α3 subtype selectivity of MP-III-024 (**19**), with little or no activation of the α1 or α5 subtypes, indicated that this ligand **19** could be a valuable therapeutic agent. The partial agonism at the α3 subtype indicated that **19** is an important ligand to study the α3 subtype; as other previous α3 subtype selective ligands were more similar to full agonists. In addition, since the adverse effects generally stem from activation of the α1 subunit and tolerance is due to the coupling of the α1 and α5 subunits,[88] methyl ester **19** should be devoid of these adverse effects.

An assessment of MP-III-024 (**19**) for anxiolytic activity was completed in the operant-based Vogel conflict procedure in mice by Dr. Bradford Fischer at Rowan University (B. Fischer, M. Poe, unpublished results). This procedure first positively reinforces behavior with a food

reinforcement before suppressing this response with a noxious stimulus, such as a mild shock.[122-124] Anxiolytic drugs are able to increase the rate of suppressed responding in spite of the noxious stimulus. BZDs have been shown to reduce the anxiety of test subjects, including HZ-166 (**3**) in rhesus monkeys.[112, 124] One other aspect of the Vogel conflict procedure is that it is also able to test for possible signs of sedation. This is observed when the subjects stop responding in the non-suppressed assay, or when an anxiolytic response is observed in the suppressed portion but decreases at higher doses, as seen previously with 2'-F analog JY-XHe-053 (**2**).[112]

The anxiolytic effects of MP-III-024 (**19**) in the Vogel conflict procedure are illustrated in Figure 18. The C57BL/6 mice (n = 6) were first deprived of water for 24 hours before being placed in a chamber with water access for 6 minutes, which created the vehicle data point. Mice were then deprived of water a second time before being given access to water for another 6 minutes for the suppressed testing session. On the second day of testing, mice were given either vehicle, diazepam (1, 3, or 10 mg/kg) or **19** (10, 32, or 100 mg/kg) 30 minutes prior to testing by intraperitoneal (i.p.) injection. During the 6 minutes of measured response time, a 0.14-mA shock (0.5 sec) was administered for the completion of every 20 consecutive licks from the water spout. Compared to vehicle, diazepam was able to increase the suppressed responding rate at all three doses given, with a further increase seen between the 3 mg/kg and 10 mg/kg doses. Methyl ester **19** produced similar increases, albeit at higher concentrations of 10 and 33 mg/kg.; however, **19** was not tested at lower doses and may still be active in the 1 – 3 mg/kg range. At 100 mg/kg of ester **19**, the response rate of the mice significantly decreased to below vehicle. This indicated that ester **19** may appear to exhibit sedation at high doses. Alternatively, since **19** has a low activation of α1, it is also possible this decrease in responding is due to muscle relaxation, which may occur at higher

receptor occupancy of the α3 subtype. This was observed with α3 subtype selective agonist YT-III-31 at a CRO in mice (M. Poe, *et al*., unpublished results. See Appendix A).

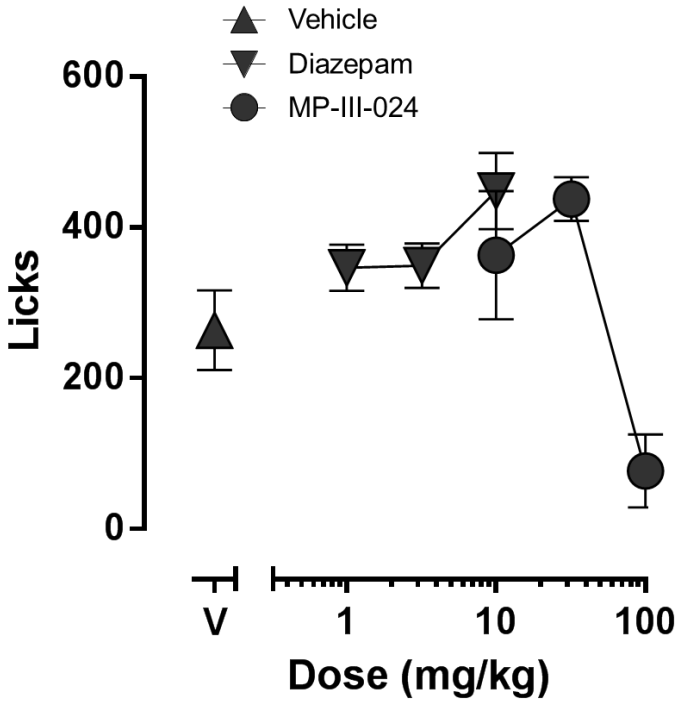


Figure 18. Effects of diazepam and MP-III-024 (19) in the Vogel conflict procedure. Male C57BL/6 mice (n = 6) were pretreated i.p. with vehicle (0.5% methyl cellulose, 0.9% sodium chloride), diazepam or MP-III-024 (19) 30 minutes prior to testing. Mice were then placed in a chamber and the amount of licks of water was recorded over a 6 minute time period.

The selectivity of MP-III-024 (**19**) for the α2 and α3 subtypes and similar efficacy profile to HZ-166 (**3**) resulted in the evaluation of **19** in the mouse model (zymosan A assay) for inflammatory pain (Dr. Bradford Fischer). Zymosan A, a yeast extract, was subcutaneously injected into a test subject's right hindpaw which induced inflammation, consequently, the test subject becomes more sensitive to mechanical force. Von Frey filaments are then used in increasing force to determine the paw withdrawal threshold (PWT). This standard assay has been

used to determine the ability of drugs to reduce this hypersensitivity, and HZ-166 (**3**) has previously been shown to reverse these effects in mice by Zeilhofer, *et al*.[93]

The reversal of hyperalgesia of MP-III-024 (**19**) was evaluated and the results are depicted in Figure 19. The C57BL/6 mice (n = 6) were given a 0.06 mg dose of zymosan A subcutaneously into the plantar surface of the right hindpaw 24 hours prior to testing. On the day of testing, mice were given a 3.2, 10 or 32 mg/kg dose of **19** i.p. and evaluated for the protection against inflammatory pain using a mechanical sensitivity assay. Von Frey filaments were used and increasing force was applied at a rate of 1 gram per second until the paw was withdrawn and the PWT was recorded. Time points consisted of 10, 20, 40, 80, 160 and 320 minutes after injection of methyl ester **19**. The left paw, which was not injected with zymosan A, acted as the control paw and was also assessed for the PWTs. Mice given a dose of 3.2 mg/kg of **19** show a very slight increase in PWT compared to vehicle, while the 10 and 32 mg/kg doses displayed the inflammation-sensitive right paw able to withstand more force beginning at the 20 minute time point. The inflamed paw which was treated with methyl ester **19** was able to withstand nearly as much force as the non-inflamed left paw (control) at time points 40, 80 and 160 in both the 10 and 32 mg/kg doses. Both higher doses given underwent a significant decrease in antinociceptive effect at the 320 minute time point. This was a significant antinociceptive effect.

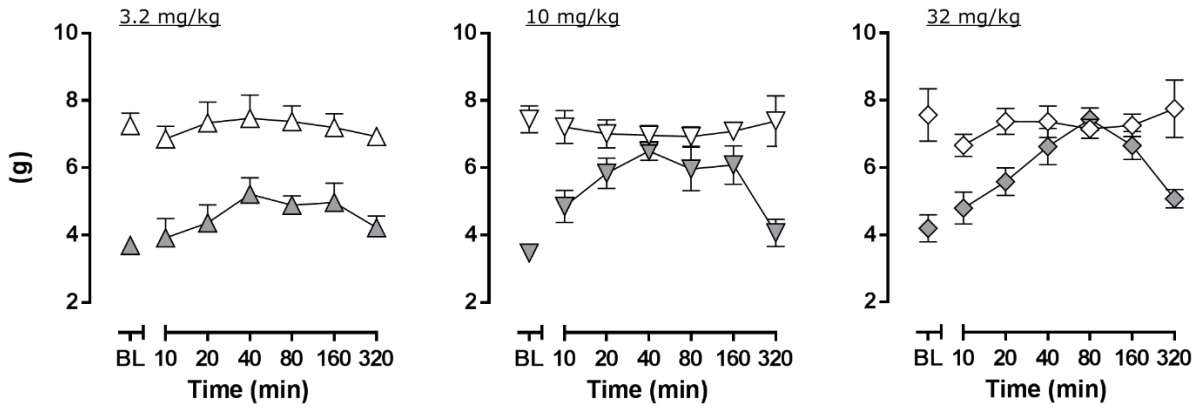


Figure 19. Effects of MP-III-024 (19) on inflammatory pain the in von Frey filament test. Zymosan A (0.06 mg in 20 µL 0.9% sodium chloride) was injected subcutaneously into the plantar surface of the right hindpaw 24 hours prior to testing. Male C57BL/6 mice (n = 6) were then dosed with MP-III-024 (19) and mechanical sensitivity was assessed using von Frey filaments. The paw withdrawal threshold was recorded. Open symbols represent the left (non-injured) hindpaw and the closed symbols represent the right (injured) hindpaw. "BL" represents predrug baseline.

The ethyl ester HZ-166 (**3**) was previously tested in the zymosan A model of inflammatory pain in C57BL/6 mice using von Frey filaments under different, albeit, similar conditions.[93] The major differences were that **3** was used at a 16 mg/kg dose, zymosan A was injected 48 hours prior to the assessment of **3**, but the inflamed paw was still the right paw. Examination of this test indicated that **3** began to exhibit a decreased antinociceptive effect at the 150 minute time point. The study on HZ-166 (**3**) also indicated an increase in PWT; however, the maximum possible effect (MPE) was slightly over 50%, which occurred at the 1 hour time point. It can be speculated that the longer time-of-effect of MP-III-024 (**19**) over **3** could be due to the decreased degradation of **3** seen in the *in vitro* liver metabolism studies presented above (Table 2), and the improved efficacy profile of **19** over **3** lead to an MPE of nearly 100% at 10 mg/kg for methyl ester **19**. However, because these ligands were tested under slightly different conditions, the conclusions need to be verified with further experiments with the methyl ester **19** under the same conditions that HZ-166 (**3**) was evaluated before an accurate direct comparison can be made. Nevertheless, it

is clear that MP-III-024 (**19**) is a more potent antinociceptive agent with a longer duration of action in the mice employed here.

As previously mentioned, traditional BZDs come with a host of adverse effects including sedation, muscle relaxation, ataxia, addiction and amnesia, which primarily originate from interaction at the α1 subtype. Methyl ester **19** and diazepam were assessed in the locomotor activity assay which does evaluate the occurrence of some of these adverse effects (Figure 20). In the locomotor activity test, C57BL/6 mice were dosed with either vehicle, diazepam (0.32, 1, 3.2 or 10 mg/kg), or ester **19** (3.2, 10 or 32 mg/kg) and monitored for 60 minutes; the total amount of distance traveled was tracked. Diazepam, which is known to cause sedation and muscle relaxation, began showing an immediate decrease in distance traveled at the lower dose (0.32 mg/kg) as compared to vehicle. The 1 and 3.2 mg/kg doses of diazepam exhibited similar results to that of 0.32 mg/kg, while the mice dosed with 10 mg/kg were nearly inactive in comparison to the vehicle. Ester MP-III-024 (**19**) showed no significant decrease at any dose test (3.2 – 32 mg/kg). All three doses with **19** performed on par with vehicle, indicating that methyl ester **19** does not affect mice in this assay up to 32 mg/kg, a highly effective dose in both the Vogel conflict and zymosan A models from above. This is a dose of 32 mg/kg at which the therapeutic index of methyl ester **19** is at least 10-fold or more.

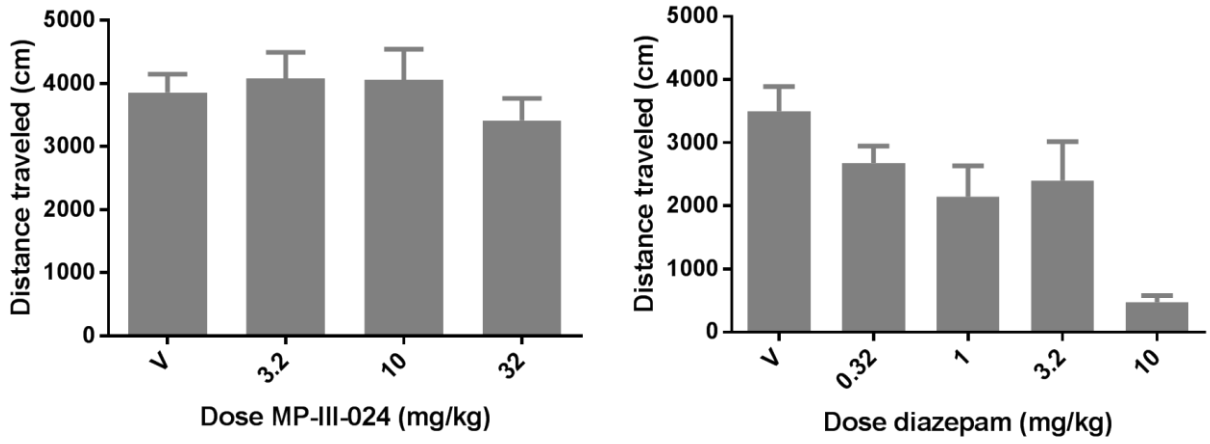


Figure 20. Effects of diazepam and MP-III-024 (19) on locomotor activity. Male C57BL/6 mice (n = 6) were dosed i.p. with vehicle (0.5% methyl cellulose, 0.9% sodium chloride), diazepam or MP-III-024 (19). Mice were then assessed for locomotor activity and the total distance traveled was recorded. "V" represents distance traveled after vehicle administration.

The response rate on operant behavior is another model designed to measure a compounds adverse effects. In many cases, if a subject is given a large enough dose, it should suppress general behavior and is used as an important benchmark to reveal behavioral specificity. If the general behavior is changed at a specific dose, it is possible that other assays may be effected by this suppression of normal behavior at said dose. In this case, MP-III-024 (**19**) was assessed for the change in operant behavior to determine whether the results in the Vogel conflict procedure and antihyperalgesia were true results, or were affected by this suppression.

In the operant behavioral model, C57BL/6 mice (n = 6) were dosed i.p. with vehicle or methyl ester **19** (10, 32 or 100 mg/kg) and examined for a response rate. At all doses, ester **19** performed comparably to vehicle with times ranging from 10 minutes after injection to 160 minutes. These results indicate that MP-III-024 (**19**) has no effect on operant behavior.

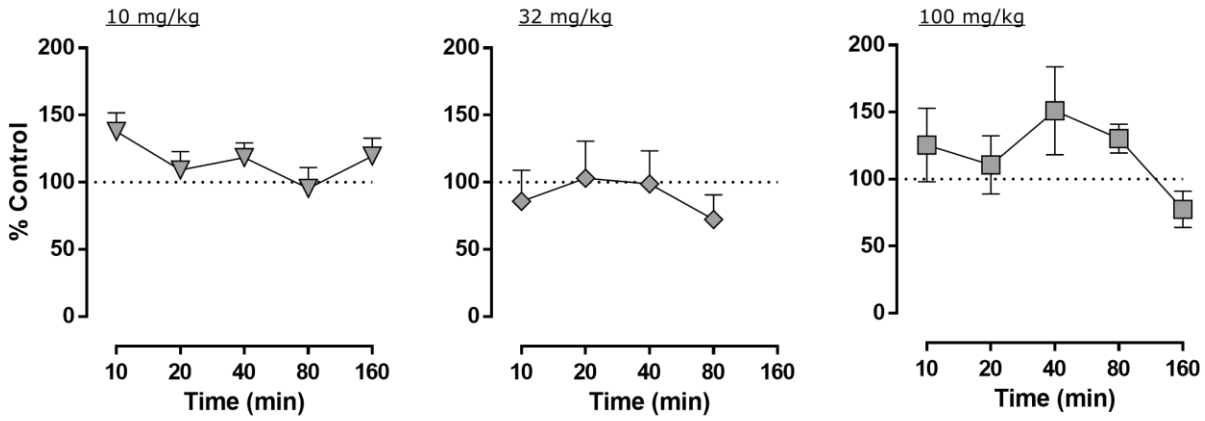


Figure 21. Effects of MP-III-024 (19) on operant behavior. Male C57BL/6 mice (n = 6) were dosed i.p. with MP-III-024 (19) and were placed on a fixed ratio of liquid food. Training and test sessions consisted of multiple cycle components, and each culminated in a 5 minute response period.

Taken together, the efficacy and behavioral results of ester MP-III-024 (**19**) presented here indicate **19** could be a useful tool to study anxiety and pain and has clinical potential for the treatment of anxiety and neuropathic pain. The oocyte efficacy profile indicated that ester **19** would have very few concerns in regard to adverse effects given the low activation at α1 subtypes, as well as little chance for the development of tolerance which stems from the coupling of the α1 and α5 subtypes as reported by Möhler, *et al*.[88] In the anxiolytic Vogel conflict procedure, MP-III-024 (**19**) displayed an increased response rate during the suppressed session at 10 and 32 mg/kg, but a decreased response rate at 100 mg/kg. This is likely not a concern as the 100 mg/kg dose would be well above the pharmacologically relevant dose. Examination of the efficacy indicated that MP-III-024 (**19**) would not be active in neuropathic pain due to the very little positive modulation of the α2 subtype; however, the results in the *in vivo* zymosan A assay have shown the opposite. The antinociceptive inflammation assay indicated **19** was effective in reversing the zymosan A-induced hyperalgesia at the effective doses of 10 and 32 mg/kg. Low activation of the α1 subtype at these effective doses was indicated by the results of the locomotor activity test. Finally, the results of

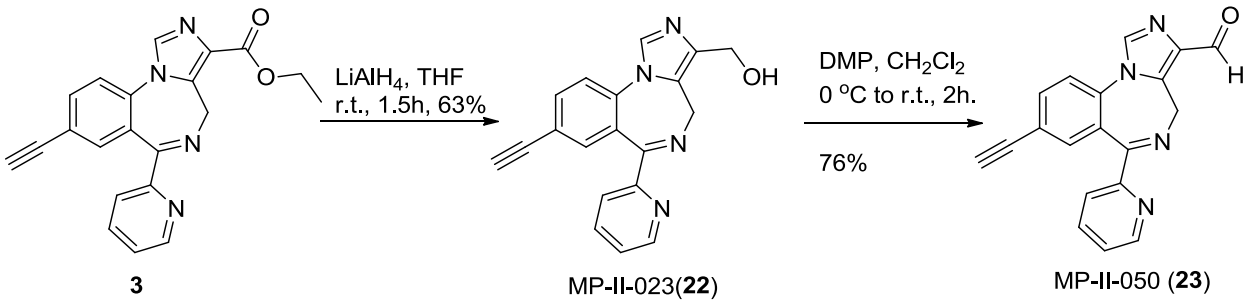
the Vogel conflict procedure and the zymosan A assay for inflammatory pain can confidently be attributed to anxiolysis and antihyperalgesic actions exerted by the imidazobenzodiazepine (IBZD) **19** because ester **19** did not reduce the responding rate in the operant behavior test even at 100 mg/kg. The high resistance to rodent liver metabolism is also encouraging; however, the ester functionality may still be too readily metabolized as the time-of-effect is shown to be between 160 and 320 minutes (> 5 hours) based on the zymosan A model of inflammatory pain. It should be noted however, that an effect which lasts 2 hours in mice/rats will be about 4 hours in dogs, 8 hours in primates and 12 hours in humans. Because MP-III-024 (**19**) exerted an antihyperalgesic effect as an α3 selective ligand, this agent bears further preclinical trials.

3.3.3 Further Alterations of the C(3) Ester Position of Antinociceptive/ Anxiolytic Agent HZ-166 (3)

3.3.3.1 The Synthesis of Oxygen-Containing Analogs

In addition to the esters, which were designed to explore the effect the alkyl chain would have on affinity at the binding pocket and efficacy, the alcohol MP-II-023 (**22**) and aldehyde MP-II-050 (**23**) were synthesized to determine the effects of electronics on receptor binding. The alcohol, **22**, was synthesized by dissolving **3** in dry THF at room temperature and adding lithium aluminum hydride, as depicted in Scheme 5. The alcohol **22** which resulted was then oxidized using Dess-Martin periodinane in methylene chloride to afford the aldehyde, MP-II-050 (**23**) in good yield.

Scheme 5. Synthesis of the alcohol MP-II-023 (22) and aldehyde MP-II-050 (23).



The synthesis of the alcohol went through several stages of development before the determination of the best reaction conditions, illustrated here. Initially, milder reducing agents, such as lithium and sodium borohydride, were used but these were unable to reduce the ester at room temperature or higher temperatures. When lithium aluminum hydride was employed, the *N*(5)-C(6) imine bond was reduced in some molecules, even when one equivalent was used at low temperatures. This also complicated the purification process as the two alcohols were difficult to separate by column chromatography (streaking occurred). Diisobutylaluminium hydride (DIBAL) was also used in attempts to directly convert ethyl ester **3** to the aldehyde **23**. These attempts were either unsuccessful, or successful in low yields, again with the reduced imine bond at the *N*(5)-C(6) position. It should also be noted that during oxidation of the alcohol **22** to the aldehyde **23**, a mixture of the imine at *N*(5)-C(6) with the C(3) alcohol along with the reduced imine with the C(3) alcohol were used, the imine would also be oxidized to recover product. However, the imine bond also isomerized to the C(4)-*N*(5) position.

Based on the pharmacophore/receptor model,[17, 74] it is unlikely that the alcohol, MP-II-023 (**22**), would result in a compound active for anxiety or neuropathic pain. The reason for this is that the loss of the ester function creates a molecule **22** with fewer hydrogen-bond acceptors in the L_{Di}

region limiting interaction with the H_1 (Y210) descriptor. This descriptor has been shown to be an important interaction for positive allosteric modulation.[17, 74]

3.3.3.2 The Synthesis of Nitrogen-Containing Analogs at C(3)

Previously the synthesis of nitrogen-containing analogs of HZ-166 (**3**) at C(3) included the methyl (**24**), dimethyl, and diethyl amides, illustrated in Figure 22. Ligand HJ-I-040 (**24**) has been tested in oocytes for efficacy and was found to be a potent α3 subtype selective PAM.[117] In relation to the methyl ester MP-III-024 (**19**), ligand **24** was much more selective for the α3 subtype; however, the potency at the α1 and α5 subtypes are greater for **24** as well as exhibiting a weaker potency at the α2 subtype. Based solely on the efficacy profile, methyl ester **19** appeared more likely to be useful for the treatment of anxiety and neuropathic pain, although *N*-methyl amide **24** remains a great research tool for the study of the physiological effects of selective efficacy at the α3 subtype.

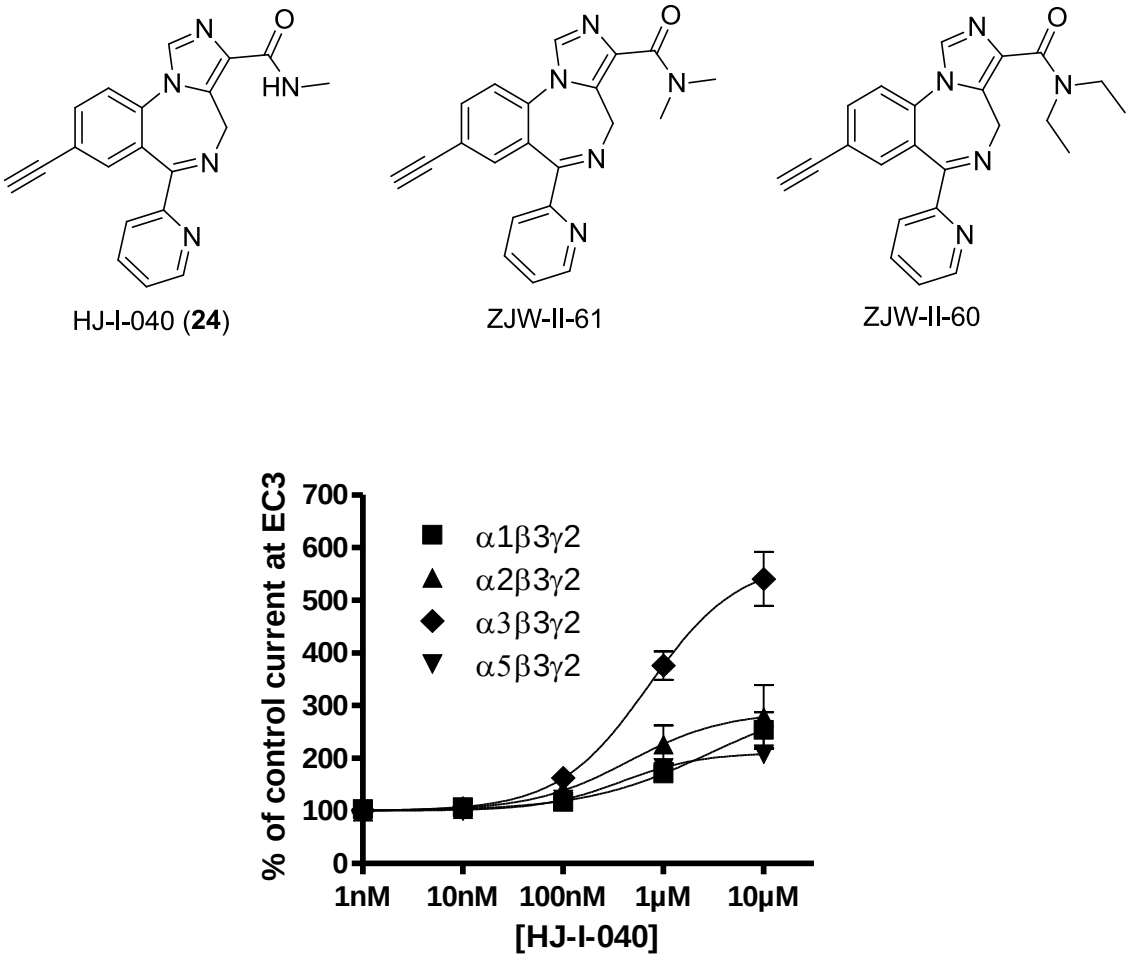
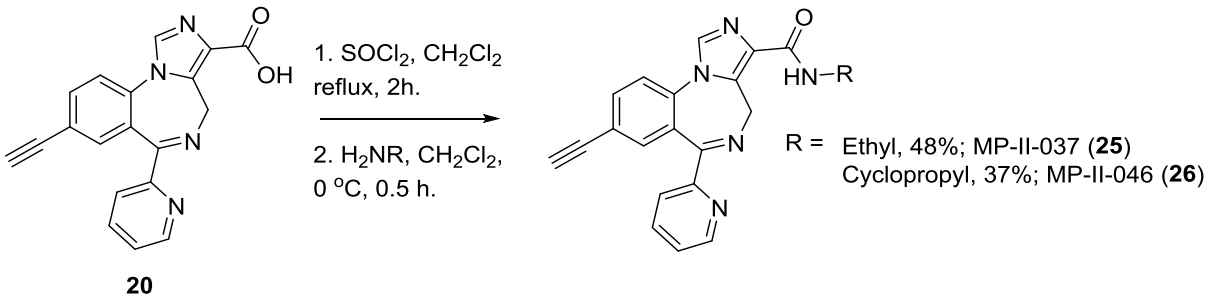


Figure 22. Previously synthesized amides, HJ-I-040 (24), ZJW-II-61 and ZJW-II-60 and the oocyte efficacy data of *N*-methyl amide HJ-I-040 (24). Concentration curve of 24 on $GABA_A$ receptors suing an EC_3 GABA concentration (n = 4, modified from the figure in Namjoshi, *et al.*).[117]

To expand the scope of the amides, the ethyl amide, MP-II-037 (**25**) and cyclopropyl amide, MP-II-046 (**26**), were synthesized, as depicted in Scheme 6. The acid SR-II-54 (**20**) was stirred in methylene chloride with thionyl chloride and then heated to reflux. The conversion to the acid chloride was complete when the solution became homogeneous, since acid **20** is insoluble in CH_2Cl_2 and was initially suspended in the mixture. The reaction was cooled to room temperature and the solvent was removed under reduced pressure. Methylene chloride was added and flash evaporated three times to eliminate any excess hydrochloric acid and thionyl chloride. The residue

was redissolved in CH_2Cl_2, cooled to 0 ^oC and the required amine was added. This solution was slowly allowed to warm to room temperature and monitored for the appearance of the amide on TLC (silica gel). The reactions were worked up in the usual manner (see Experimental for details) and purified by column chromatography. The structures were determined by ^1H and ^{13}C NMR and compared to the spectrum of HZ-166 (**3**). The high resolution mass spectroscopy was in complete agreement with the structure determination.

Scheme 6. Synthesis of amides, MP-II-037 (25) and MP-II-046 (26).

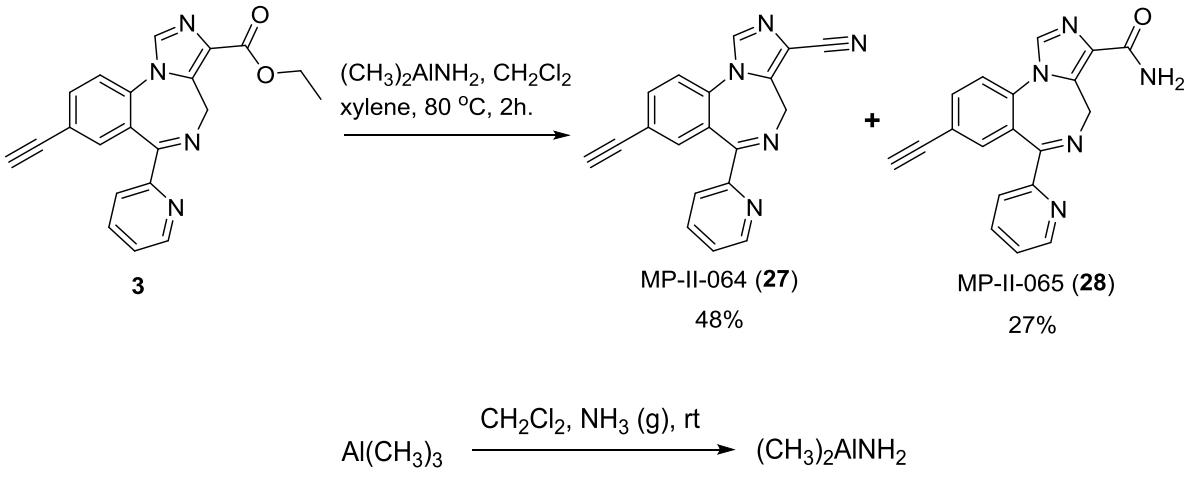


20

The ethyl amide **25** was chosen as a direct comparison to **3** to further evaluate an SAR between esters and amides because of the structural similarity at C(3) to **3**. The cyclopropyl amide **26** was chosen to substitute an amide with an alkyl group which was similar in size to the ethyl ester function, but less prone to hydrolysis by peptidases or hydrolases *in vivo*. The synthesis of a larger number of amides was initially reduced until the ester series had been screened in regard to binding or efficacy data. This data would then be analyzed to determine the effects of the size of the alkyl chain and the corresponding amides would subsequently be synthesized. Currently, the esters are awaiting oocyte efficacy evaluation and binding affinity.

The nitrile, MP-II-064 (**27**), was designed to help determine how the degrees of freedom of the hydrogen-bond acceptor H_1 in the binding site play a role in binding and efficacy because of the linearity of the nitrile function. This synthesis is illustrated in Scheme 7 where HZ-166 (**3**) was stirred in xylene and heated to 80 ^oC, followed by the addition of dimethylaluminum amine.[125] The dimethylaluminum amine was made fresh[126] immediately prior to its use by saturating CH_2Cl_2 with ammonia gas and adding trimethylaluminum. The nitrile reaction was stirred at 80 ^oC for two hours before cooling the solution to room temperature and working up. The reaction mixture contained two products, the desired nitrile **27** and the carboxamide MP-II-065 (**28**). Additional dimethylaluminum amine was added in attempts to produce only the nitrile **27**, since the carboxamide **28** was an intermediate, but these were unsuccessful. Repeated reaction attempts resulted in no consistent trend when the temperature or equivalents of dimethylaluminum amine were varied in the production of the nitrile **27** over the carboxamide **28**. The side-by-side reactions of two enantiomers, seen and discussed further in Section 4.3, resulted in different yields of each product.

Scheme 7. Synthesis of nitrile MP-II-064 (27) and the byproduct MP-II-065 (28); as well as the preparation of dimethylaluminum amine.



Preliminary efficacy using human embryonic kidney (HEK) 293T cells was evaluated on nitrile MP-II-064 (**27**) using the high-throughput patch-clamp IonFlux instrument (Nina Yuan, Alexander "Leggy" Arnold, *et al.*, unpublished results) and the results are depicted in Figure 23. The two-electrode voltage clamp technique has been the standard method for collecting efficacy data, but has its drawbacks. The primary hindrance is the time-consuming nature of the assay. Assays are performed one oocyte at a time for each individual subunit, creating a large number of experiments to reach *n*-values great enough to verify a compounds' effects confidently. In comparison, the automated patch-clamp averages the general response of 20 parallel cell currents to form into a single data point. Transiently transfected cells were produced and **27** was tested in the preliminary stages of development. It is noteworthy that the % of control current exerted by a compound in the IonFlux cannot be directly compared to the results reported in the oocyte two-electrode voltage clamp technique. For the preliminary results of the IonFlux technique, the assay was designed to run a test compound along with a control compound to determine whether or not the test compound exerted a greater or lesser potency at each subtype.

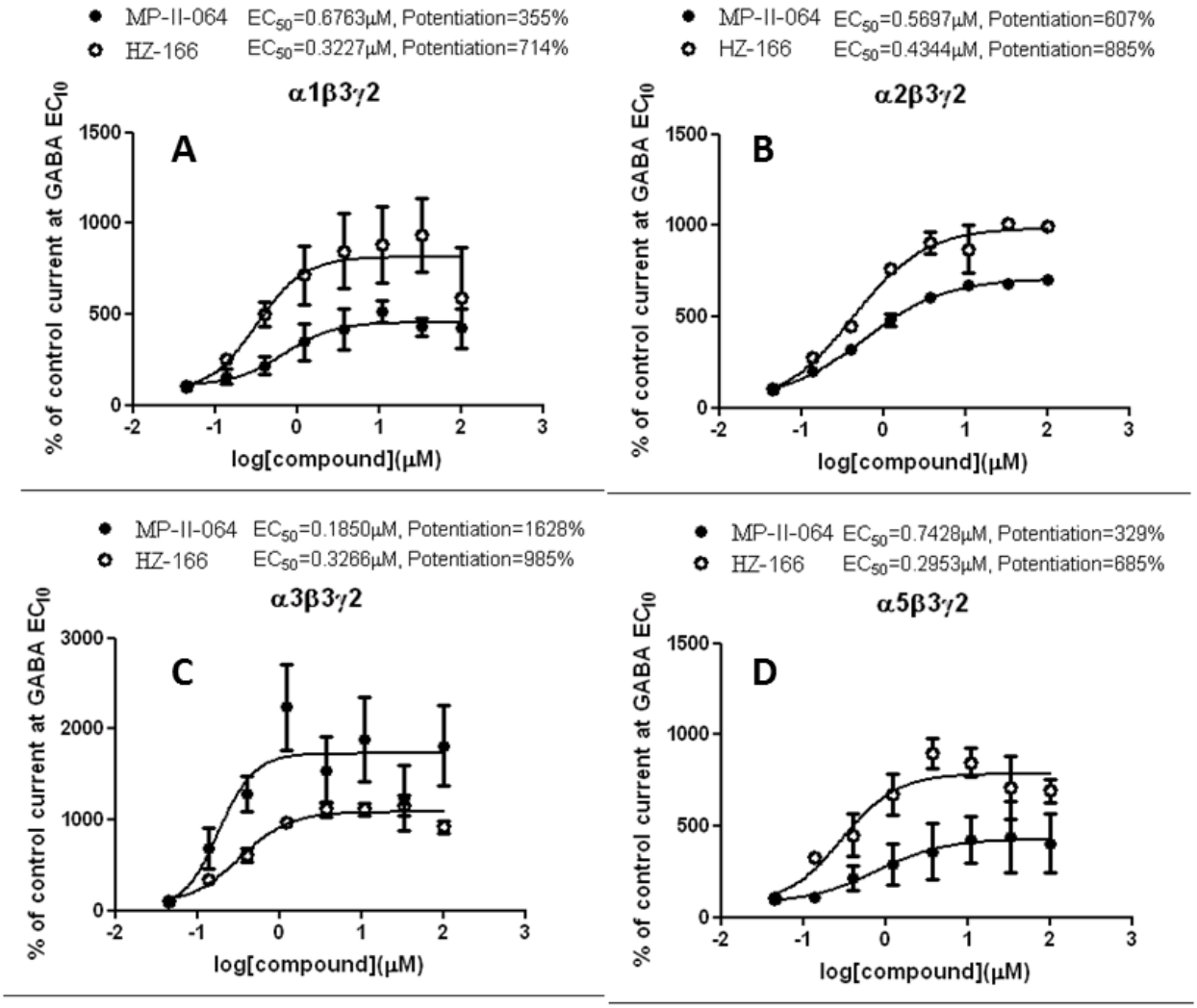


Figure 23. Efficacy testing of MP-II-064 (27) in the IonFlux high-throughput patch-clamp instrument. Nitrile 27 was run against HZ-166 (3) to determine how the efficacy profiles compared in parallel experiments.

The results of the IonFlux assay indicated that MP-II-064 (**27**) was an α3 preferring subtype selective ligand with weak efficacy at α1 and α5 subtypes compared to control HZ-166 (**3**). Examination of the data in Figure 23A illustrates **27** has a lower potency at the α1 subtype than **3**, which was used as a control compound. Similar results at the α2 subtype are shown in Figure 23B. At the α3 subtype in Figure 23C, **27** was shown to have a greater potency than HZ-166 (**3**). Examination of the data from the α5 subtype indicates that **27** was less potent than **3** at that subtype.

To test the accuracy of the IonFlux patch-clamp technique, the Ernst group in Austria agreed to assess the efficacy of nitrile **27** in the two-electrode voltage clamp technique, and the results are depicted in Figure 24.

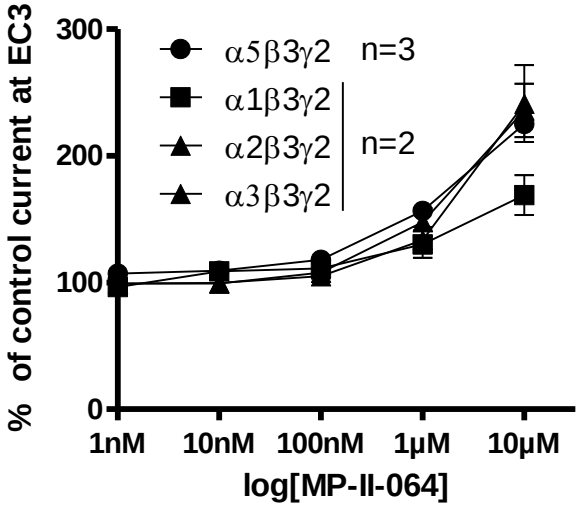


Figure 24. Preliminary oocyte efficacy results of MP-II-064 (27) by two-electrode voltage clamp technique (Margot Ernst). Concentration curve of 27 on $GABA_A$ receptors suing an EC_3 GABA concentration (n = 2-3).

Examination of the data from the oocyte assay in the two-electrode voltage clamp technique indicated of MP-II-064 (**27**) has no selectivity at all in oocytes, as well as very little potency. When compared to the predicted IonFlux results, nitrile **27** showed no selectivity for the α3 subtype in oocytes; however, nitirle **27** does show lower potency at the α1, α2 and α5 subtypes, as predicted. It is also worth mentioning that the two-electrode voltage clamp technique commonly assesses a ligands' efficacy in the 1 nM – 10 µM range, while the IonFlux patch-clamp technique assessed **27** in the high nanomolar range to 100 µM, and these concentration differences could reveal different results. Since the two-electrode voltage clamp technique is currently the 'gold-standard' for efficacy evaluation, it was concluded that the methodology for generating the different subtypes for the IonFlux patch-clamp technique needed more investigation and have

targeted stable cell lines now in place of transiently transfected cell lines. However, it must be emphasized the oocyte efficacy experiments are now within statistical significance at n = 2. More oocytes are required for accurate analysis of the efficacy in Figure 24.

In regard to the results of the two-electrode voltage clamp technique, it can be hypothesized that the lack of significant potency at any subtype below a high concentration (10 μM) by MP-II-064 (**27**) likely results from the lack of interaction of the C(3) substituent with the H_1 (Y210) descriptor, or possibly the lack of lipophilic-lipophilic interactions in the L_{Di} pocket. This L_{Di} pocket is a lipophilic pocket and the polar nitrile may have been incompatible. Because the nitrile (Ar-C≡N:) is a linear molecule with much of the electron density projecting straight out, this may have hindered the ability of the N: lone pair to interact with the hydrogen bond donor H_1. One way that may be able to overcome this lack of interaction at H_1 would be to add a methylene function between the C(3) aromatic ring and the nitrile, as shown in Figure 25. This would provide more flexibility for the lone pair of electrons on the -C≡N: bond to interact with H_1. Further work in the series is ongoing.

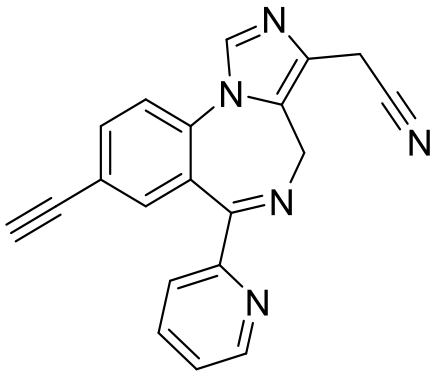


Figure 25. Proposed structure of a nitrile with an increased degree of freedom at C(3) to interact at H_1 than MP-II-064 (27).

The byproduct of the nitrile reaction, MP-II-065 (**28**), is also of interest. The C(3) carboxamide functional group is the same as imidazenil, shown in Figure 26. Imidazenil has been thoroughly studied and has been shown to be a non-sedating anticonvulsant and anxiolytic, without developing tolerance to the anticonvulsant effects.[127] It has been suggested that imidazobenzodiazepine carboxamides, such as **28**, possess these properties as a class of compounds.[128] Imidazenil has also shown the ability to alleviate withdrawal symptoms that has been associated with long-term BZD usage.[129]

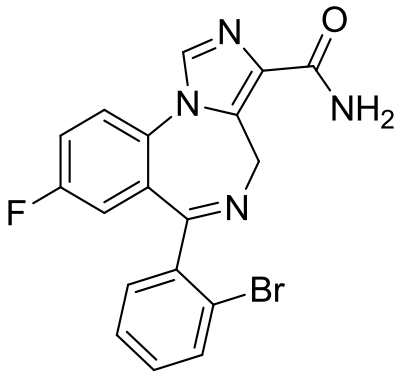
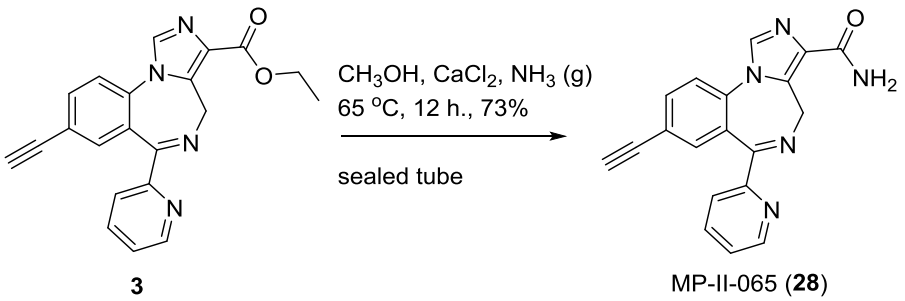


Figure 26. Structure of imidazenil.

An improved route was needed to synthesize the carboxamide because the route depicted in Scheme 7, which provided MP-II-065 (**28**) as a byproduct, was unacceptable. An improved route to **28** employed stirring HZ-166 (**3**) in a saturated ammonia (gas)/methanol solution with calcium chloride in a sealed tube and then heated at 65 ^{o}C for 18 hours,[130] as illustrated in Scheme 8. The calcium chloride was necessary and served as a Lewis acid[130] for the transformation from an ester to the carboxamide. In the absence of calcium chloride, the product which resulted was the methyl ester MP-III-024 (**19**). Heating **3** in the presence or absence of ammonia (g) under these conditions did not result in a higher yield of **19** than previously described (Scheme 3). With its

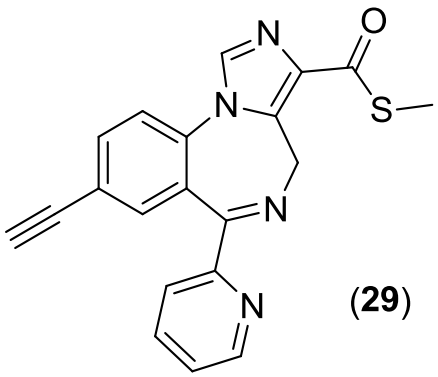
similarities to imidazenil and therapeutic potential, MP-II-065 (**28**) has been assessed for anxiolytic activity and the data is described in Section 3.3.6.

Scheme 8. Improved route to the carboxamide MP-II-065 (28).



3.3.3.3 Attempts to Synthesize the Thionoester (30) and Thioamide (31)

Previously, the methyl thioester, ZJW-II-65 (**29**), had been synthesized by Wang, *et al.* and is shown with the efficacy data in Figure 27. This thioester ligand **29** exhibited low potency with almost no efficacy at α1 subtypes, even at 10 μM (log[-5]), but did exhibit a slight agonist preference at the α3 subtype. A comparison of the efficacy data at 1 μM of the methyl ester (**19**), methyl amide (**24**) and methyl thioester (**29**) is illustrated in Figure 28. Here, the influence of the heteroatom next to the carbonyl can be examined. The 1 μM concentration was chosen to be evaluated because this concentration has the greatest degree of selectivity.



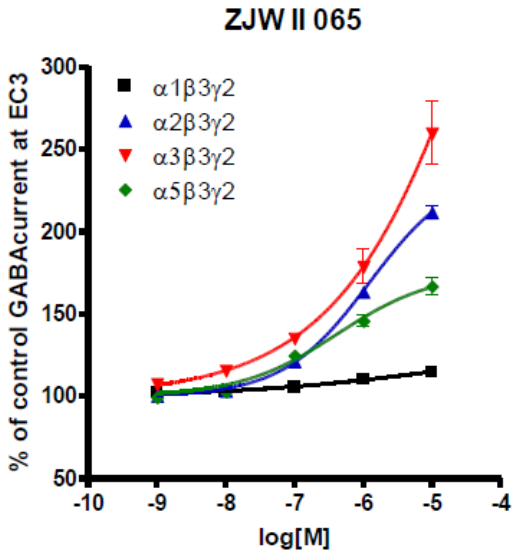


Figure 27. Structure and efficacy of ZJW-II-65 (29). Concentration curve of 29 on $GABA_A$ receptors using an EC_3 GABA concentration (n = 3).

Analysis of the data in Figure 28 show that methyl ester **19** and methyl amide **24** are both more potent in oocytes than the corresponding methyl thioester **29**, espeically at the α2 and α3 subtypes. One hypothesis for this is that both the oxygen and nitrogen are more electronegative than the sulfur, and may have stronger interactions with the pharmacophore descriptor at H_1. The amide **24** is the only compound of the three which contains a hydrogen-bond donor group, which could interact with A_2, as well as the H-bond donor H_1. This may result in higher potency at the α1 and α3 subtypes. Overall, one trend that can be seen by comparison of the efficacy of these

three compounds was the necessity for strong hydrogen-bond interactions in the binding site; however, this hypothesis is based on a the three examples presented in Figure 28 at C(3) and must be explored more thoroughly to see if the pattern continues.

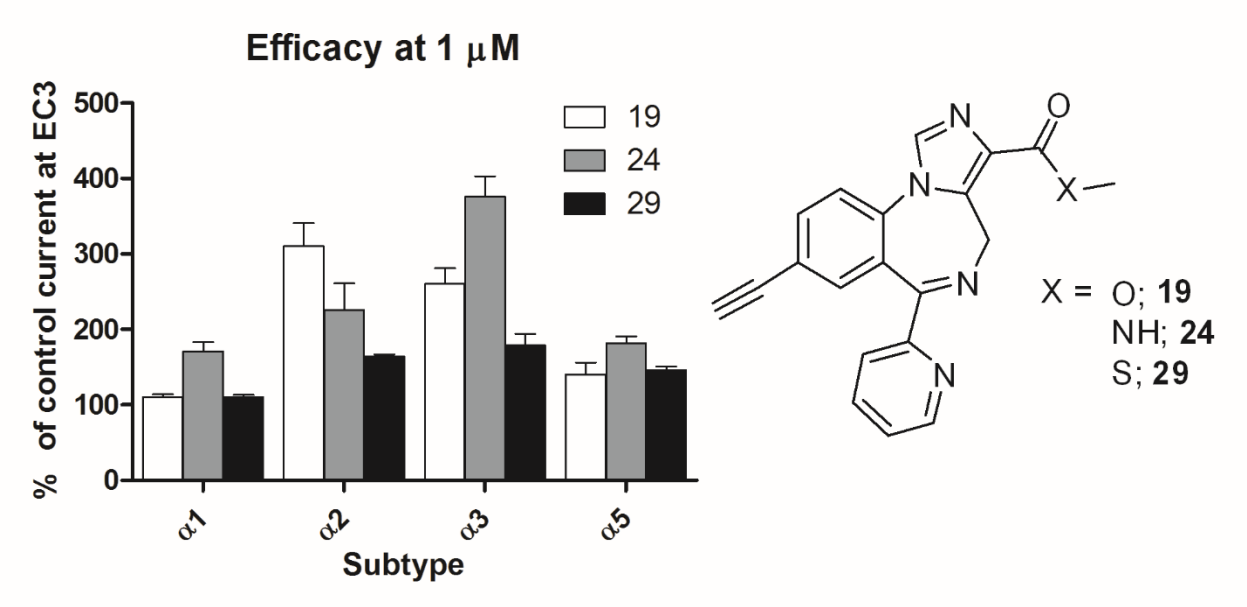


Figure 28. Efficacy comparisons of 19, 24 and 29 at 1 μM. Efficacy determined on $GABA_A$ receptors using an EC_3 GABA concentration (n = 2 – 4).

Attempts were made to synthesize the thionoester **30**, as well as the thioamide **31** (structures shown in Figure 29), to examine whether replacing the carbonyl oxygen with sulfur would affect the same decrease in potency as replacing the carboxylic oxygen did, as seen in **29** compared **19**. Initial attempts to complete this conversion employed Lawesson's reagent (LR),[131] which is a reagent that is commonly used to replace a carbonyl oxygen with a sulfur atom. Ligand HZ-166 (**3**) was first stirred in benzene at room temperature with LR with no conversion observed, as indicated by mass spectrometry. The reaction was repeatedly attempted heating incrementally up to reflux for up to 48 hours with no success. Similar reaction conditions were carried out using toluene, xylene, dimethylformamide and dimethylsulfoxide with no conversion, which was

monitored by mass spectrometry. Other conditions were attempted to no avail.[132, 133] Although the carbonyl oxygen in esters has been replaced with sulfur in many cases, it is reportedly one of the more difficult carbonyl oxygens to replace[133] and generally requires harsher conditions than other molecules. Conversion of MP-II-065 (**28**) to a thioamide **31** was also attempted to determine the compatibility of the BZD scaffold to undergo thionation. Initial attempts used reaction conditions as described above. Another route reported quantitative yields using LR in hexamethylphosphoramide,[134] but these conditions failed to work with amide **28**.

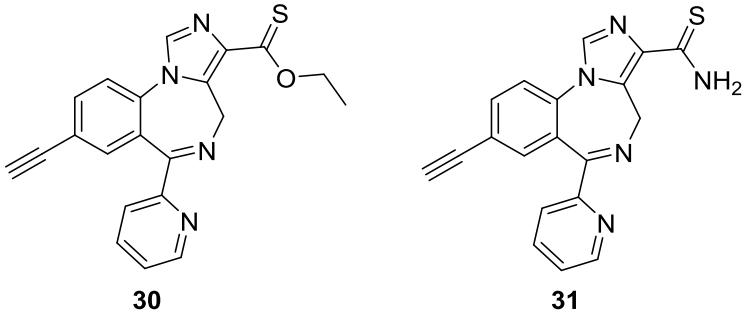


Figure 29. Structures of a thionoester 30 and thioamide 31.

Attempts to thionate the carbonyl oxygen of esters and amides were unsuccessful. There have been reports of the synthesis of newer generation fluorous LRs[135] and conditions using a microwave;[136, 137] however, these were not attempted due to lack of material.

3.3.4 The Synthesis of Heterocyclic Bioisosteres

The isostere concept has been around since the early 1900's. It initially referred to the octet theory of valence electrons and if two compounds existed, which had the same number of atoms and electrons, the electrons would arrange themselves in the same fashion.[138] The initial Group 2 of isosteres identified by Langmuir consisted of O^{2-}, F^{-}, Ne, Na^{+}, Mg^{2+} and $Al.^{3+}$ Through the years,

the terms and meaning expanded and eventually evolved into a new concept of bioisosteres which was defined by compounds exerting a similar biological effect. More recently, bioisosteres have been defined by Burger as, "Compounds or groups that possess near-equal molecular shapes and volumes, approximately the same distribution of electrons, and which exhibit similar physical properties".[139]

Classical bioisosteres consisted of simple replacements such as switching a hydrogen for fluorine or deuterium, or a phenyl ring for a thiophene ring.[140] Nonclassical bioisosteres are generally structurally distinct and contain a different number of atoms. Changes also include different electronic and steric properties. One subclass of nonclassical bioisosteres includes cyclic versus noncyclic compounds.

Ligand HZ-166 (**3**) has previously been shown to be an important non-sedating anxiolytic, with anticonvulsant and antihyperalgesic properties; however, the metabolism of the ester function in rodents *in vivo* hinders the ability to study the ADME toxicity for a clinical candidate due to the short half-life in rodents. The use of a bioisostere to replace the ester function could increase the *in vivo* stability of the ligand, while retaining its pharmacological properties. Esters have a number of bioisosteres, and some of the heterocyclic bioisosteres are depicted in Figure 30.

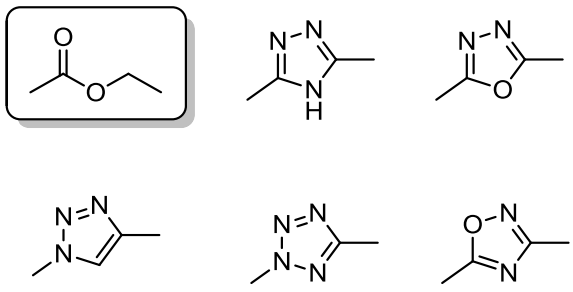


Figure 30. Common heterocyclic ester bioisosteres.

3.3.4.1 The Synthesis of Oxadiazoles

An oxadiazole is a common ester bioisostere.[141] It has been previously utilized with HZ-166 (**3**) to provide the isopropyl oxadiazole ZJW-II-40 (**32**; Namjoshi, *et al.*),[117] depicted in Figure 31. The replacement of the ester function was able to significantly increase the stability in a one-hour human liver microsomal assay over HZ-166 (**3**) by SRI, and it increased the stability of bioisostere **32** over the parent compound HZ-166 (**3**) *in vitro* from 76% to 95%, respectively.[117] Analysis of the efficacy data of **3** and **32** indicated that the isopropyl oxadiazole lost efficacy at the α2 subtype, while retaining potency at the α5 subtype. The activation of the α1 and α3 subtypes remained about the same as in **3**. The results indicated that the bioisostere replacement of the ethyl ester with an isopropyl oxadiazole has a negative effect of the efficacy profile. However, it should be noted that the isopropyl function of the oxadiazole would more similarly correspond to an isobutyl ester group in reference to sterics. Instead, a methyl oxadiazole would be a better replacement of the ethyl ester in this respect and was synthesized, along with the ethyl oxadiazole.

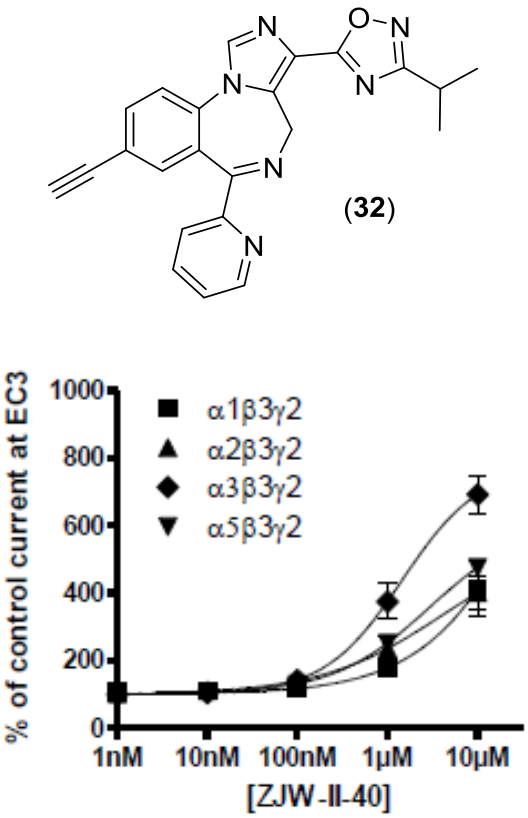
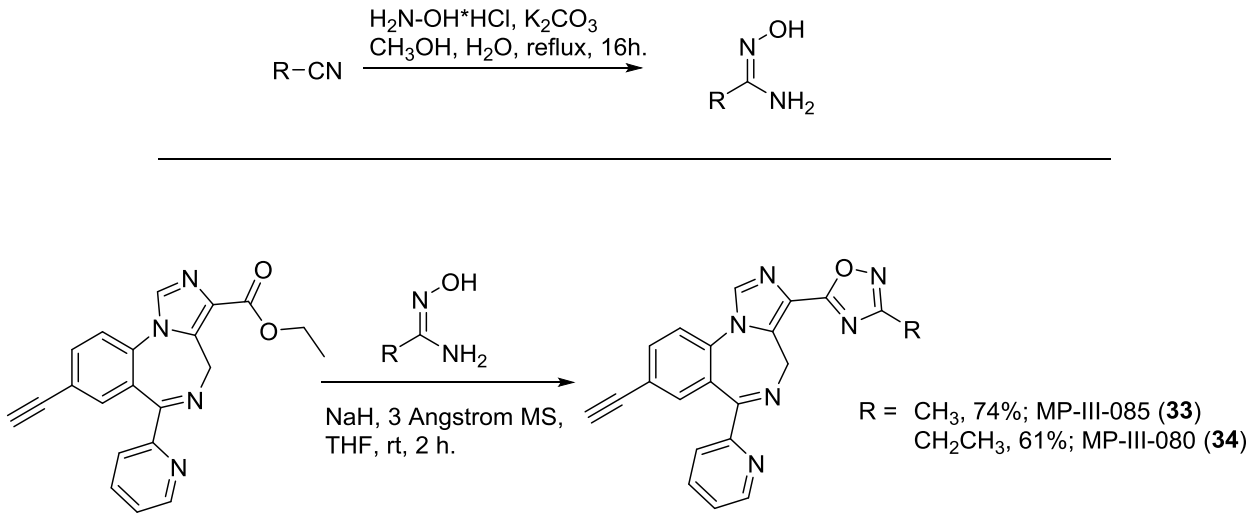


Figure 31. Structure and oocyte efficacy data of ZJW-II-40. Concentration curve of 32 on $GABA_A$ receptors using an EC_3 GABA concentration (n = 3), as reported in Namjoshi, *et al.*[117]

The methyl oxadiazole, MP-III-085 (**33**), and the ethyl oxadiazole, MP-III-080 (**34**), were synthesized to expand the scope of the bioisosteres and this work is illustrated in Scheme 9. The oxime was first synthesized by refluxing an alkyl nitrile and hydroxylamine hydrochloride with potassium carbonate in water and methanol.[142] This oxime was then stirred with sodium hydride in the presence of 3 Å molecular sieves before adding HZ-166 (**3**) and permitting the solution, which resulted, to stir at room temperature for two hours to produce the corresponding oxadiazoles. We thank Dr. Merle Johnson and Dr. Ranjit Verma for earlier work on the synthesis of oxadiazoles.

Scheme 9. Synthesis of the oximes and methyl (MP-III-085, 33) and ethyl (MP-III-080, 34) oxadiazoles.



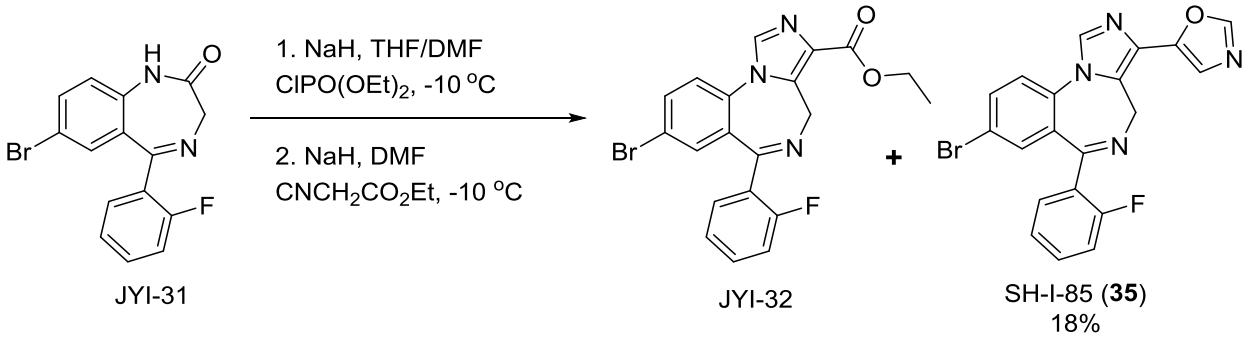
The methyl oxadiazole MP-III-085 (**33**) is a good bioisostere for the ethyl ester **3** and should display a similar efficacy profile. This, along with the ethyl oxadiazole **34** are awaiting evaluation of their efficacy in oocytes or via HTPS on a stable human cell lines. However, they have been characterized through *in vitro* metabolic stability studies and *in vivo* on the rotarod assay. In addition, they have been evaluated in the marble burying assay for anxiolytic activity. These studies are discussed in Sections 3.3.5 and 3.3.6, respectively.

3.3.4.2 Ligand SH-I-85 and the Synthesis of Oxazoles

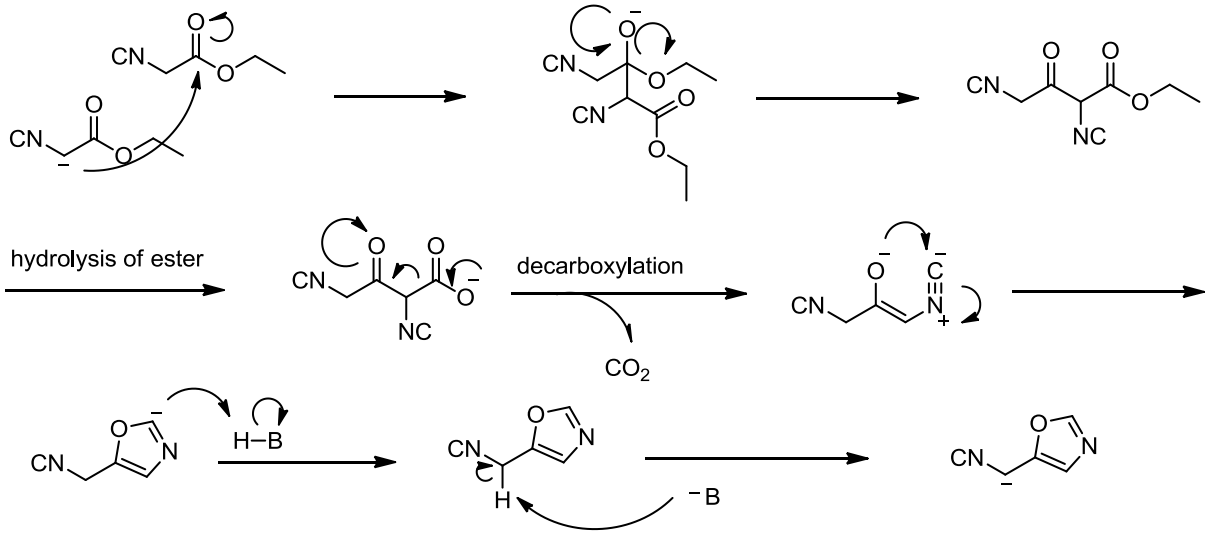
During the synthesis of JY-XHe-053 (**2**), Shengming Huang isolated SH-I-85 (**35**) as am 18% byproduct[143] while building on the imidazole ring in going from benzodiazepine JYI-31 to imidazobenzodiazepine JYI-32, as shown in Scheme 10. The use of sodium hydride was utilized

in an earlier route to prepare ethyl ester JYI-32, prior to the development of the improved route to imidazobenzodiazepines using potassium *tert*-butoxide at low temperature.[118] This earlier route was carried out by stirring the ethyl isocyanate in dimethylformamide with sodium hydride for one hour. This resulted in the formation of a byproduct which ultimately led to 1,3-oxazole **35** when the benzodiazepine JYI-31 was added to the mixture. Attempts to increase the yield by stirring the ethyl isocyanate with sodium hydride for three hours resulted in the isocyanate attacking another isocyanate molecule and eventually forming the 5-(isocyanomethyl)oxazole, illustrated in Scheme 11.[143] The methyl (CH_2) group was then deprotonated and reacted with the BZD JYI-32 to form the imidazobenzodiazepine SH-I-85 (**35**) with a 1,3-oxazole at the C(3) position.

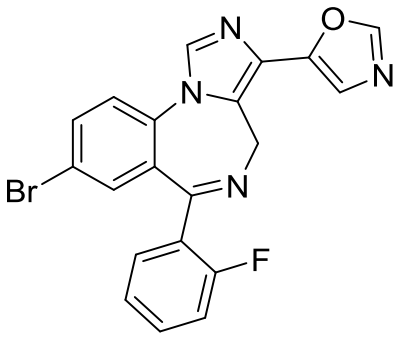
Scheme 10. Route to SH-I-85 (35) as a byproduct.



Scheme 11. Proposed mechanism for the formation of 5-(isocyanomethyl)oxazole.



The 1,3-oxazole found in byproduct **35** was not a common bioisosteric replacement for an ester, but has been used before.[144] The five-membered ring relates to a methyl ester in size, but the electronics are less similar to an ester than those of the oxadiazole. The two-electrode voltage-clamp technique was performed to attain the oocyte efficacy profile, shown in Figure 32. Agonist (PAM) SH-I-85 (**35**) was found to be a potent α2/α3/α5 subtype selective agonist with very low α1 agonist efficacy. The concentration at which the ligand **35** begins to increase the chloride flux began around 10 nM which means byproduct **35** was able to affect the chloride current at lower concentrations than most compounds, although this is similar to **2**, another 2'-fluoro compound. Although there is no direct comparison to the bromo, ethyl ester ligand JYI-32, a discussion resulted in the exploration of the oxazole as a C(3) ester replacement in HZ-166 (**3**) and other compounds in order to increase the half-life *in vivo* and *in vitro* in rodents and humans.



SH-I-85 (**35**)

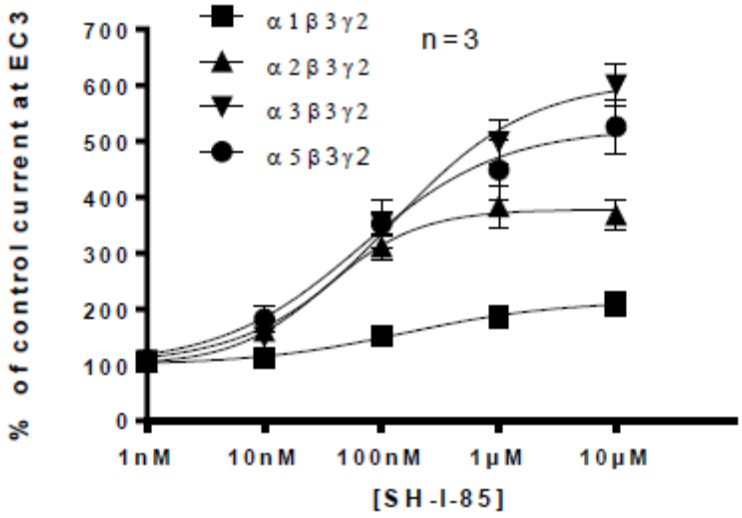
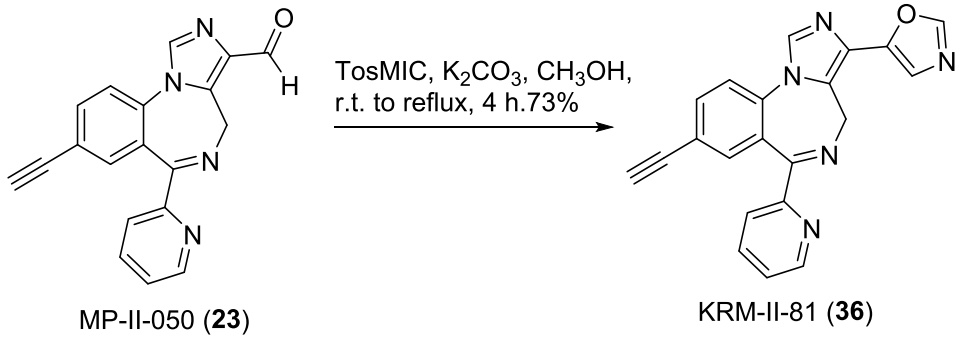


Figure 32. Structure and oocyte efficacy of SH-I-85 (35), displaying very low efficacy at the α1 subtype. Concentration curve of 35 on $GABA_A$ receptors using an EC_3 GABA concentration (n = 3).

In collaboration with a coworker, Dr. Kashi Reddy Methuku was tasked to find an improved route to the synthesis of ligands with the 1,3-oxazole ester replacement at C(3) based on the pharmacophore/receptor model.[74] Initial reactions attempted to improve the yield of the byproduct in a similar reaction sequence, as depicted in Scheme 10 by stirring the ethyl isocyanate with a base (potassium *tert*-butoxide) before combining this solution with JYI-31. Replacement of sodium hydride with potassium *tert*-butoxide did increase the yield slightly, but this route was still unacceptable. Attempts to synthesize 5-(isocyanomethyl)oxazole were unsuccessful. Eventually,

a route through the aldehyde using toluenesulfonylmethyl isocyanide (TosMIC) and potassium carbonate[145, 146] was developed by Methuku, Cook, *et al.*[147] The synthesis using this new route was employed to produce the oxazole (KRM-II-81, **36**) of HZ-166 (**3**) and is depicted in Scheme 12. A number of other related 1,3-oxazoles, based on modeling,[74] were also synthesized by Dr. Methuku in the 2'-H and 2'-F series to obtain KRM-II-82 (**37**) and KRM-II-18B (**38**), respectively, and are shown in Figure 33. After preliminary testing of oxazoles **36** – **38** indicated they exhibited anxiolytic activity in a marble burying assay (see Section 3.3.6), Dr. Methuku, myself and others worked together to synthesize these three (**36** – **38**) compounds on large scale, with a heavy focus on the 2'-N analog of HZ-166, KRM-II-81 (**36**). In addition, the 2'-N 8-bromo analogs (**39**) and 2'-H (**40**) versions of **35** were synthesized as well as six methyl oxazole compounds, **41** – **46**, by Dr. Methuku. All of these were designed based on the fit into the L_{Di} pocket of the pharmacophore/receptor model by Clayton, Poe, *et al*.[74] These methyl oxazoles were synthesized by replacing TosMIC with 1-((1-isocyanoethyl)sulfonyl-4-methylbenzene.[147] The synthesis and characterization of these oxazoles and methyl oxazoles **37** – **46** can be found in Appendix J.

Scheme 12. The synthesis of oxazole KRM-II-81 (36).



MP-II-050 (**23**) KRM-II-81 (**36**)

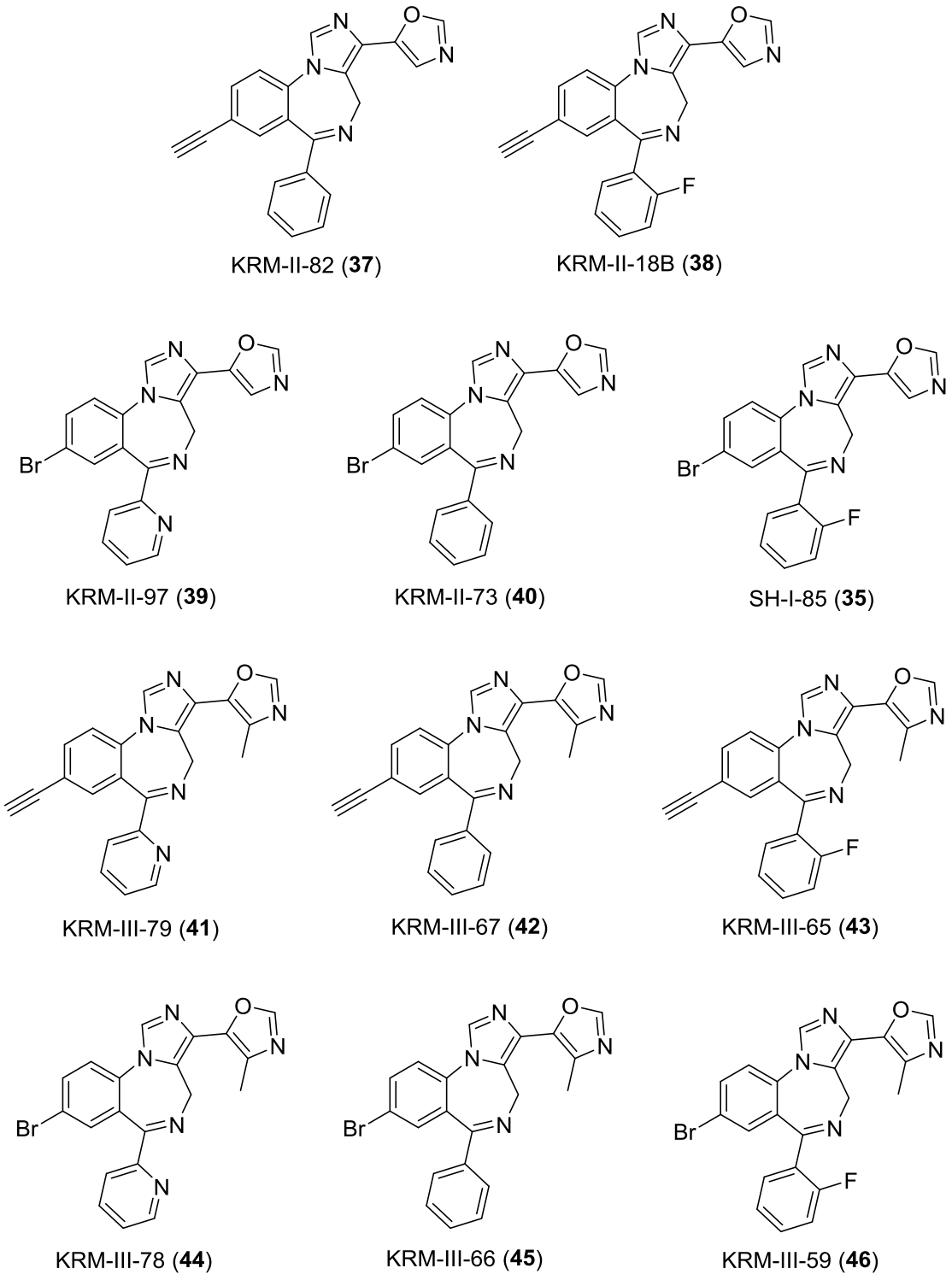


Figure 33. Structures of oxazoles (37 – 40) and methyl oxazoles (41 – 46). These were synthesized based on the pharmacophore/receptor model of Clayton, Poe, *et al.*[74] in collaboration with Dr. Methuku. The synthesis of these can be found in Appendix J.

3.3.5 The *In Vitro* Analysis of HZ-166 (3) and its Analogs

Many of the compounds were tested by a big pharma CRO (under a Confidential Disclosure Agreement) for affinity at α1 and α3 $GABA_AR$ subtypes on the fluorescence imaging plate reader (FLIPR) functional assay, as shown in Table 5. Examination of the data at the α1 subtype in the FLIPR assay indicated that all ligands tested had an EC_{50} greater than 20 μM, which was the highest concentration tested. This illustrated they have little to no affinity at the sedating, ataxic, amnesic, addictive α1 subtype. In contrast, they exhibited good affinity at the α3 subtypes, indicating they have significant selectivity for the α3 subtype over the α1 subtype. Because α2 and α3 subtypes are very similar in binding topology[74] this indicated they should exhibit efficacy at the key α2 subtypes as well. Based on data by Möhler, Zeilhofer, Cook and others on ligand HZ-166 (**3**); agonist efficacy at the α2 subtypes is the most important in treating anxiety and pain. This indicated that all compounds should have a high likelihood of being active against anxiety and possibly hyperalgesia with a low risk of adverse effects. This was a key breakthrough in Bz/$GABA_A$ receptor studies with worldwide importance.

Analysis of ethyl esters **1** – **3** and oxazoles **36** – **38** indicated that the 2'-F compounds **2** and **38** showed a greater affinity for the α3 subtype (0.0346 and 0.0112 μM, respectively) than their 2'-H (**1** and **37**; 0.146 and 0.0321 μM, respectively) or 2'-N (**3** and **36**; 0.844 and 0.937 μM, respectively) counterparts, with the more polar 2'-N compounds **3** and **36** were the least potent of the three in each series. Examination of the metabolic stability of these compounds indicated that the 2'-N containing ligands are much more stable than either of the other two series *in vitro* on MLMs and RLMs. Analysis of each species shows that, other than DLMs, replacing the ethyl ester

with the atypical bioisosteric oxazole significantly increased the resistance to metabolism by liver microsomes.

The metabolism and clogP of the esters **3**, **21** and **19** were previously discussed in Section 3.3.2.1. Examination of the data from the FLIPR assay indicated that a smaller alkyl side chain exhibited a more potent EC_{50} value at the α3 subtype. This general trend in sterics can be seen throughout the series of compounds analyzed. The two compounds with the largest C(3) substituents, oxadiazoles **33** and **34**, displayed two of the poorest EC_{50} values at 5.15 and 3.02 μM, respectively at the α3 subtype. Although it may be that lipophilic-lipophilic interactions of the larger alkyl substituent prevented the rotation of the bioisostere to interact at H_1. On the other hand, the low potency could be just the result of repulsive lipophilic-lipophilic interactions with the receptor protein. The only other compound with an EC_{50} greater than 2 μM was the nitrile **27** which we classify as inactive at Bz/$GABA_A$ receptors. This may be due to the lack of degree of freedom to interact with hydrogen-bond donor H_1, as discussed previously in Section 3.3.3.2. Although the C(3)-nitrile was not active, the four 2'-N compound (methyl ester **19**, methyl amide **24**, carboxylic acid **20** and carboxamide **28**), displayed the most potent EC_{50}'s at the α3 subtype: 0.461, 0.757, 0.47 and 0.166 μM, respectively. Of all the 2'-N compounds, carboxamide **28** displayed the strongest affinity towards the α3 subtype. This may be due to the fact that it contained two hydrogen-bond acceptors, as well as two hydrogen-bond donor groups in the $–NH_2$ group.

Table 5. *In vitro* metabolic stability, α3 Bz/GABA$_A$R EC$_{50}$'s and clogP's of ligands.

CRO Results		Metabolic stability in liver microsomes (reported in %-remaining) *Conditions*: 4 μM compound, 37 °C, 30 minutes				α3 FLIPR assay[a]	clogP[b]
Compound and C(3) substituent		HLM [c]	DLM [c]	MLM [c]	RLM [c]	EC$_{50}$ (μM)	(Diazepam = 2.96)
1	Ethyl ester (2'H) XHe-II-053	40	83.7	9.9	8.7	0.146	3.11
2	Ethyl ester (2'F) JY-XHe-053	8.9	83.8	5.1	0.7	0.0346	2.91
3	Ethyl ester (2'N) HZ-166	80.4	97.2	54.1	50.2	0.844	1.71
21	^{2}*d*-Ethyl ester (2'N)	95.1	100	63.1	76.6	1.17	1.71
19	Methyl ester	92.2	72.6	73.3	92.7	0.461	1.18
20	Acid	95.9	100	92.7	99.3	0.47	1.82
23	Aldehyde[d]	70		56			1.41
24	Me. amide	95.3	70.6	82.7	87.6	0.757	1.32
27	Nitrile	87.8	65.6	77.2	76.6	5	1.29
28	Carboxamide	94.1	89.4	90.6	71.4	0.166	0.99
33	Methyl Oxadiazole	80.8	92.5	85.4	92.9	5.15	1.50
34	Ethyl Oxadiazole	90.6	96.9	91.6	94.2	3.02	2.03
36	1,3-Oxazole (2'N)	91.4	94.1	89.9	90.4	0.937	1.58
37	1,3-Oxazole (2'H)	73.5	85.5	73.1	72.2	0.0321	2.98
38	1,3-Oxazole (2'F)	77.6	86.5	78.5	67.9	0.0112	2.78

[a] The α1 subtype was also examined for all compounds (except 23), and the EC$_{50}$ > 20 μM was very poor for all compounds.

[b] This was calculated used clogP on the ChemDraw 13.0 software; as compared to diazepam

[c] Human liver microsomes (HLM), dog liver microsomes (DLM), mouse liver microsome (MLM) and rat liver microsomes (RLM).

[c] Aldehyde 23 was tested by Revathi Kodali at UWM under separate conditions (10 μM, 37 °C, 60 minutes). Analysis of all compounds that were assayed by both places exhibited similar results.

There does not seem to be a general trend when replacing an oxygen atom with an –NH group, as seen from methyl ester **19** to methyl amide **24** and carboxylic acid **20** to carboxamide **28**. The results in the HLMs are nearly identical, while the DLMs and MLMs show up to 10% changes, but with no particular trend. The largest discrepancy is seen from the acid **20** to carboxamide **28** in RLMs, with %-parent compound decreasing from 99.3% to 71.4%, respectively. The carboxamide **28** also has decreased stability in DLMs, decreasing from 100% remaining in the acid **20** to 89.4% remaining in **28**; however, this may not be statistically significant. In addition, the methyl amide **24** increased in stability from 73.3% in the methyl ester **19** to 82.7% in MLMs, which indicated the methyl amide is worthy of preclinical assays on sedation, anxiety as well as neuropathic and inflammatory pain.

The heterocyclic 2'-N oxadiazoles **33** and **34**, as well as 1,3-oxazole **36** (KRM-II-81), were designed to combat rodent degradation and all show significant increases in metabolic stability in MLMs and RLMs. This is very important. Lead ligand HZ-166 (**3**) was degraded to about 50% of the parent HZ-166 remaining in both rodent species after a 30 minute incubation, whereas the methyl oxadiazole **33**, which exhibited the greatest degradation of the heterocycles, was still much more stable as compared to lead ester HZ-166 (**3**) with 85.4% of **33** remaining in mouse microsomes after 30 minutes. This clearly shows that the replacement of an ethyl ester function at C(3) was effective in reducing metabolism in rodent liver microsomes, as anticipated. Increased stability in HLMs was also seen in **36** (91.4% remaining) and **34** (90.6%) as compared to **3** (80.4%). These are extremely important findings since most preclinical studies in drug design are carried out in rodents.

Although tested under different conditions, the aldehyde **23** exhibited the least resistance to degradation in human and mouse liver microsomes at 70% and 56% of the parent **23** remaining,

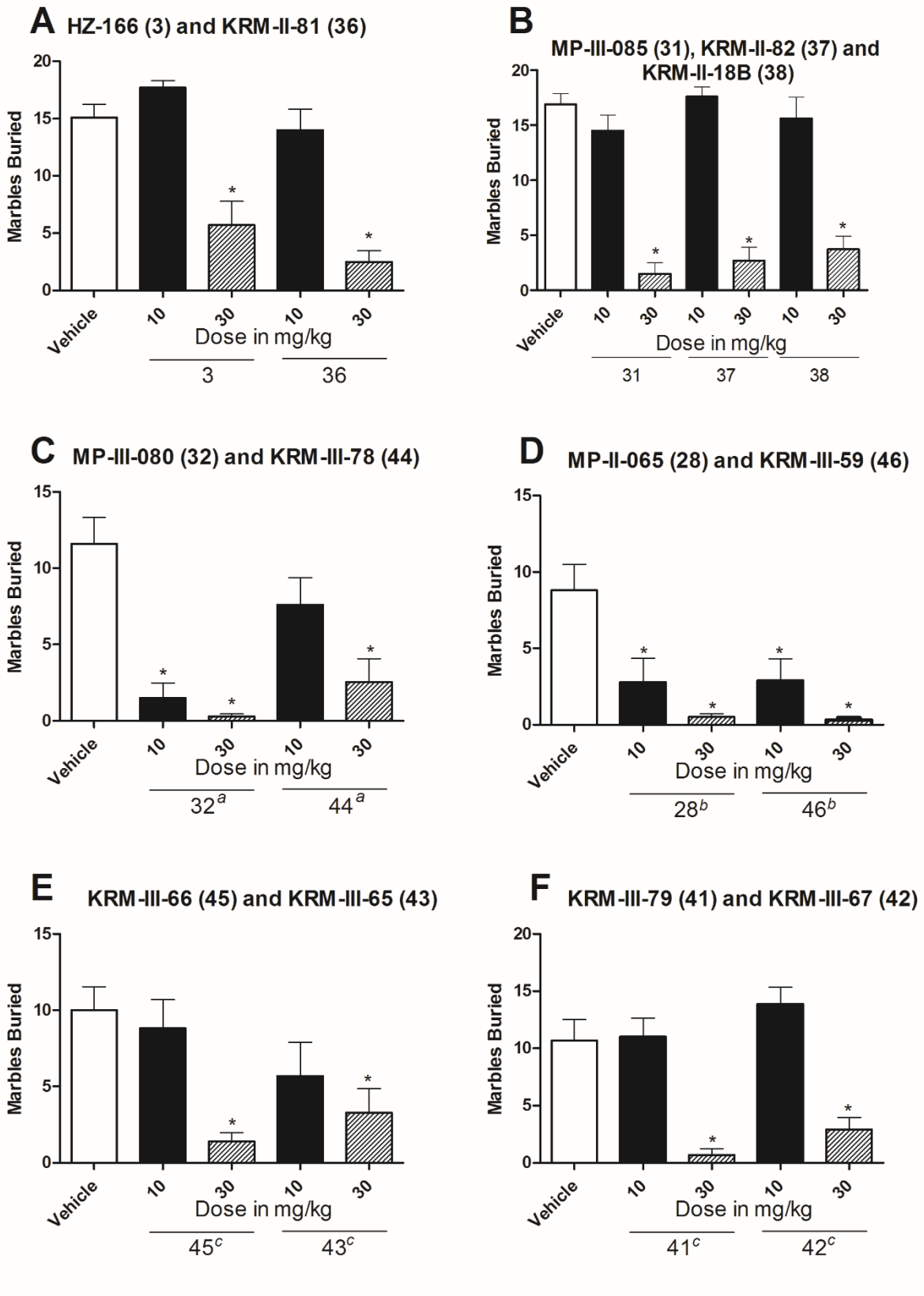
respectively, of the compounds containing the 2'-nitrogen. Analysis of the results shown in Table 2 illustrated that the same compounds **3** and **19** assayed, which had similar profiles, indicated that the results on the aldehyde **23** shown in Table 4 can be roughly compared to all other results. It is reasonable to assume the aldehyde **23** would be metabolically more stable in HLM than in MLM because of the increase in metabolic activity in mice as compared to humans.

3.3.6 Determination of Ataxic and Anxiolytic Effects in Preclinical Models

The increased stability of the heterocyclic oxadiazoles **33** and **34** as well as the 1,3-oxazoles **36** – **38** in rodent liver microsomes resulted in *in vivo* testing in search of a clinical candidate for the treatment of anxiety disorders, epilepsy and pain syndromes in collaboration with the same CRO that did the *in vitro* testing on the ligands. The initial round of testing included HZ-166 (**3**) as a standard because it is a non-sedating anxiolytic and antinociceptive agent that does not develop tolerance to the anticonvulsant and antinociceptive effects. These initial *in vivo* experiments consisted of a marble burying assay to test the ligands' anxiolytic effects[148] and a rotarod assay to determine whether or not the compounds induced ataxia.[149] After the positive initial results, a second round of testing assessed the methyl 1,3-oxazoles **41** – **46**, due to their heterocyclic replacement of the ester function at C(3), and the carboxamide **28**, due to its potent affinity at the α3 subtype in the FLIPR assay while still not interacting at the sedating α1 subtype (EC_{50} > 20 μM). Despite the potent affinity and metabolic affinity of the acid **20** in HLMs, DLMs, MLMs and RLMs, it was not tested due to the poor brain penetration, as described in Section 3.3.2.1. The methyl ester, or any other ester, were also excluded from testing due to the high concentration of esterases found in rodents, which would likely hinder the esters from future development.

3.3.6.1 The Results from the Marble Burying Assay for Anxiolytic-like Effects

The marble burying assay was designed to measure the anxiolytic effect a ligand exerts on a test subject.[148, 150] This assay has been an effective way to assess traditional BZDs, such as diazepam,[151] and analysis of the imidazobenzodiazepines (1,3-oxazoles, oxadiazoles, etc.) is illustrated in Figure 34. The male Swiss mice (n = 10) were dosed i.p. with either vehicle (1% carboxymethyl cellulose (CMC; a surfactant) or a test compound (10 or 30 mg/kg) 30 minutes prior to testing. During testing, mice were set inside a box with 20 marbles placed throughout the container in a bed of shredded paper. When dosed with vehicle, mice begin to 'nest', or bury the marbles for fear of them being taken.[152] A ligand which exhibited anxiolytic effects will reduce this urge, resulting in a fewer number of marbles buried over a 30 minute time period.


A HZ-166 (3) and KRM-II-81 (36)
Marbles Buried
Vehicle
10
30
10
30
Dose in mg/kg
3
36
B
MP-III-085 (31), KRM-II-82 (37) and KRM-II-18B (38)
Marbles Buried
Vehicle
10
30
10
30
10
30
Dose in mg/kg
31
37
38
C MP-III-080 (32) and KRM-III-78 (44)
Marbles Buried
Vehicle
10
30
10
30
Dose in mg/kg
32a
44a
D MP-II-065 (28) and KRM-III-59 (46)
Marbles Buried
Vehicle
10
30
10
30
Dose in mg/kg
28b
46b
E KRM-III-66 (45) and KRM-III-65 (43)
Marbles Buried
Vehicle
10
30
10
30
Dose in mg/kg
45c
43c
F KRM-III-79 (41) and KRM-III-67 (42)
Marbles Buried
Vehicle
10
30
10
30
Dose in mg/kg
41c
42c

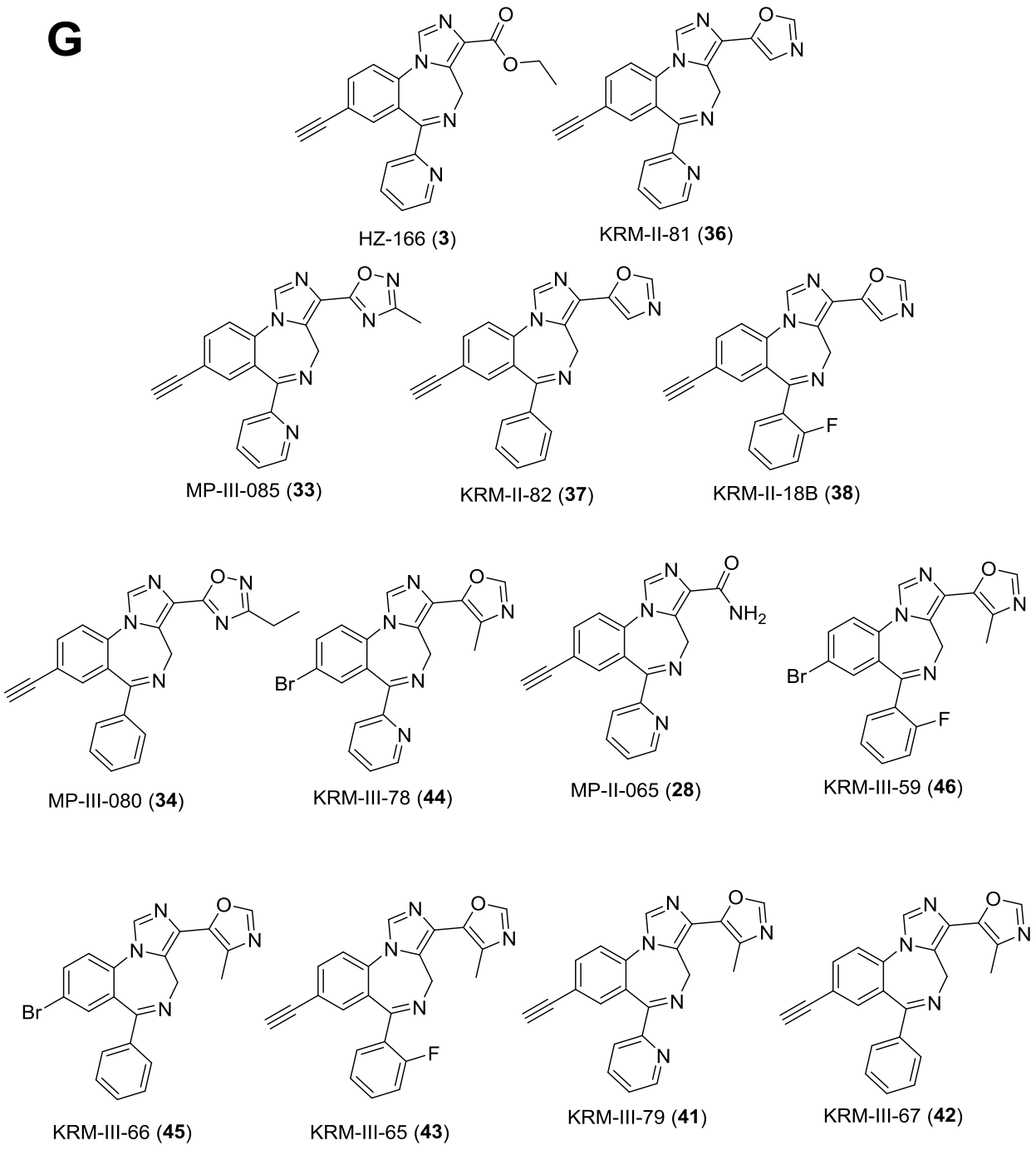


Figure 34. Analysis of the anxiolytic effects exerted by HZ-166 (3) and other ligands. Male Swiss mice (n = 10) were given an i.p. 30 minute pretreatment of vehicle (1% CMC) or a test ligand (10 or 30 mg/kg) and were then placed in a chamber with 20 marbles, and were observed for 30 minutes and the number of marbles buried was recorded. Analyzed using ANOVA (Dunnet's test: * $P < 0.05$). [a] Sedation-like effects observed at 30 mg/kg. [b] Sedation-like effects observed at 10 and 30 mg/kg. [c] Modest sedation-like effects observed at 30 mg/kg. Structures depicted in (G).

Analysis of the results in Figures 34A-F indicated each ligands (Figure 34G) ability to reduce the anxiety-driven behavior of marble burying. All compounds exhibited a significant anxiolytic-like effect when compared to vehicle after a 30 mg/kg dose. Only the ethyl oxadiazole (**34**), carboxamide (**28**), and one of the methyl oxazoles (**46**) exhibited a significant decrease in marble burying at 10 mg/kg. It has been noted in the past that the reduction in buried marbles is sometimes a results of sedation,[151] and observers reported sedation-like effects in both **28** and **46** at the both the 10 and 30 mg/kg doses. Sedation-like effects were also observed in **34**, but only at 30 mg/kg which indicated the results seen at 10 mg/kg may be a true anxiolytic-like effect exerted by the ligand. Other compounds that were noted for signs of sedation at 30 mg/kg were methyl oxadiazoles **41** – **45**.

A closer look at the methyl oxazoles show that compounds with the C(8)-bromide (**44** – **46**) display greater signs of sedation then the corresponding methyl oxazoles with an acetyleno-functionality (**41** – **43**) in keeping with the Milwaukee hypothesis.[17, 74-76] Although these ligands display sedative effects, the 2'-N bromide **44** was noted to display sedative-like effects at 30 mg/kg (Figure 34C), while the 2'-N acetylene **41** was noted to elicit only modest sedation at 30 mg/kg (Figure 34F). The similar result is seen in the 2'-fluoro compounds, with the bromide **46** displaying sedation at 10 and 30 mg/kg (Figure 34D) and the acetylene **43** only having modest sedation at 30 mg/kg (Figure 34E). On the other hand, the 2'-H compounds **43** and **42** were reported to exhibit the same degree of sedation (Figures 34E and 34F, respectively). This is not unexpected and follows the trend that replacing the C(8) halogen with an acetylene can reduce the binding affinity and/or efficacy at the α1 subtype by interaction in the L_2 pocket, as previously discussed in Section 2.2. This is based on the pharmacophore/receptor model[17, 75, 76] which was designed employing rigid ligands as a template and the use of 12 other families overlaid in this model.

It was also interesting to note that in comparison between corresponding oxazoles (**36** – **38**) and methyl oxazoles (**41** – **43**), all the methyl oxazoles were reported to have sedative-like effects. It is possible that the methyl functions increase the potency at the α1 subtype. However, because testing of the oxazoles and methyl oxazoles occurred at different times, it may also be possible that the observers were different, as observation of sedation-like effects can be considered subjective. That said, the oxazoles **36** – **38** and methyl oxadiazole **33** were the only compounds that were reported to have significant reduction in marble burying at 30 mg/kg without the observation of sedative-like effects.

3.3.6.2 Assessment for the Presence of Ataxia by the Rotarod Protocol

The ligands which were tested in the marble burying assay were also assessed for ataxic effects in the rotarod paradigm and the results are depicted in Figure 35A-F. Ataxia, or the partial or full loss of control of body movements, has been observed in many patients when given traditional BZDs[41, 153, 154] such as diazepam, alprazolam and midazolam, and is an adverse effect that stems from the activation of the α1 subtype. The male Swiss mice (n = 10) were dosed i.p. with either vehicle (1% CMC) or one of the test compounds (10 or 30 mg/kg) 30 minutes prior to testing. The testing consisted of placing the mice on a rotating rod at 4 r.p.m. Any mouse that was able to stay on for the two minute testing period were called a 'Success', while mice that fell once were given a 'Partial' designation. Mice that fell off twice during the two minute time period failed the test.

The ethyl ester HZ-166 (**3**) has previously been shown to complete a rotarod trial comparably to vehicle at 48 mg/kg,[93] therefore there was no sedation nor ataxia. Ligand HZ-166 (**3**) is shown here in Figure 35A to have no change at 10 mg/kg in relation to vehicle, but one failure occurred as well as a few additional 'Partial' trials at 30 mg/kg. However, in mice and rats

by Stables *et al*., showed **3** elicited no sedation up to 500 mg/kg.[115] The oxazole KRM-II-81 (**36**) performed the best of the oxazoles **36** – **38**, as both the 2'-H (**37**) and 2'-F (**38**) oxazoles had no 'Success' trials as 30 mg/kg. Both the oxadiazoles **33** and **34** and carboxamide **37** performed similarly to **3**, with the ethyl oxadiazole **34** undergoing a few more successful trials than its methyl counterpart **33**. All methyl oxazoles **41** – **46** performed comparable to its corresponding vehicle with the exception of the 2'-F, C(8)-bromo methyl oxazole **46**. These results indicated that 1,3-oxazoles **37** and **38** have the greatest risk of exerting ataxic-like effects. However, it is important to note that these ataxic-like symptoms were observed in some mice dosed with vehicle as some mice trained on a rotating rod were unable to successfully complete the task.

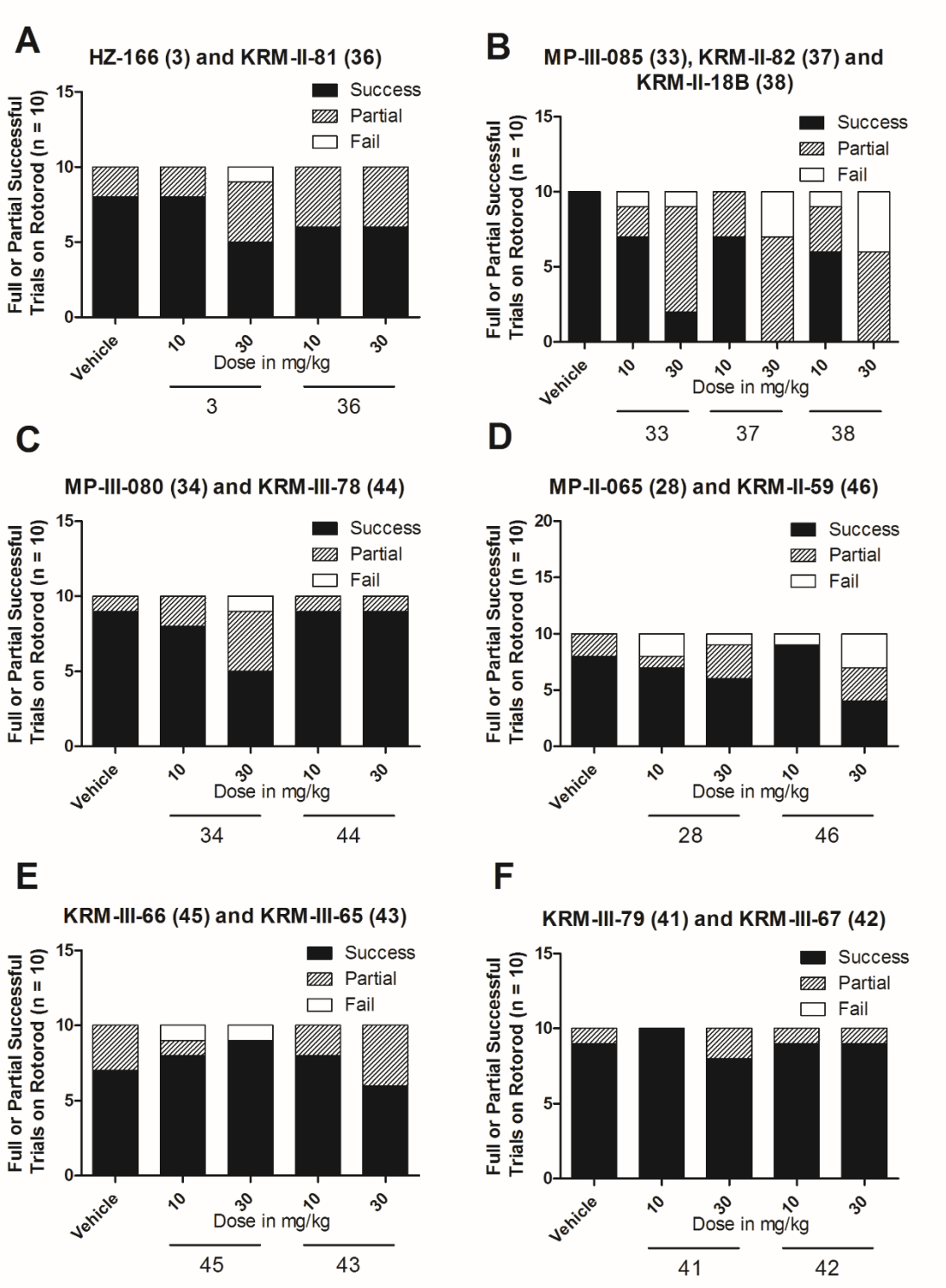


Figure 35. Results of BzR ligands in the rotarod assay. Male Swiss mice (n = 10) were given a 30 minute i.p. pretreatment of either vehicle (1% CMC) or a test ligand (10 or 30 mg/kg) and were then run for two minutes on a rotarod at 4 revolutions per minute. Mice that did not fall were designated a "Success", while mice that fell once during the timing were given a "Partial" designation. Mice that fell twice "Fail" the testing.

It is interesting to note that with the exception of KRM-III-59 (**46**), all compounds which were observed to induce sedation-like effects in Figures 34C-F did not perform significantly worse than vehicle on the rotarod assay, shown in Figures 35C-F. This was initially an odd finding as both adverse effects stem from the activation of the α1 subtype. Arguably, 1,3-oxazoles **37** and **38** performed the worst in the rotarod paradigm, and neither were reported to induce sedation. However, this could be attributed to the subjectiveness of observing sedation-like effects described above in Section 3.3.6.1. Alternatively, it is possible that the sedation-like effects could be attributed to muscle relaxation, which can occur from activation of the α3 subtype at higher receptor occupancy. Although sedation and muscle relaxation may appear to result in the same observation in some assays, others protocols have been able to distinguish between the two; however, these are not explored here.

3.3.7 *In Vivo* Characterization of New Lead Compound, KRM-II-81 (36) (CRO)

A new lead ligand was chosen to further characterize in anticonvulsant, anxiolytic and neuropathic pain assays as a potential clinical candidate. The oxazole KRM-II-81 (**36**) was chosen for a number of reasons. In the *in vitro* metabolic analysis, KRM-II-81 (**36**) was highly stable in all species tested, with the greatest degradation occurring in mice, however, only 10.1% of the parent compound was metabolized over a 30 minute time period. Ligand **36** also exhibited potent affinity at the α3 subtype, with a sub-micromolar EC_{50} at 0.937 nM. Of all the compounds analyzed in Table 4, the only other ligand to display these characteristics was the acid **20**, which had already been shown to have poor BBB penetration. The two oxadiazoles **33** and **34** displayed a high resistance to degradation as well, but the micromolar EC_{50}'s of 5.15 and 3.02 μM, respectively, were slighter higher than desired, but this did not immediately exclude them from consideration.

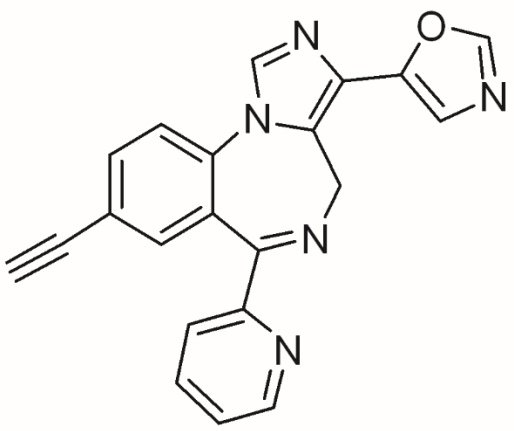
On the other hand, the carboxamide **27**, the 2'-H (**37**) and 2'-F (**38**) oxazoles displayed good affinity for the α3 subtype (0.166, 0.0321 and 0.0112 μM, respectively), but also had lower stability against rodent microsomes, particularly in RLMs at 71.4%, 72.2% and 67.9% of the parent compound remaining, respectively, over 30 minutes.

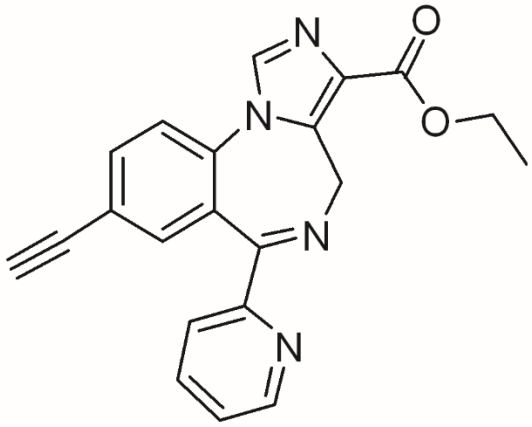
Analysis of the *in vitro* data alone promoted moving forward with KRM-II-81 (**36**). In the marble burying assay, all mice dosed with a methyl oxazole, **41** – **46**, showed some degree of sedative-like effects, as reported in the marble burying assay by the observer; however, this was subjective and requires further characterization on the matter. This, along with the lack of *in vitro* data excluded the methyl oxazoles from being considered further as the lead compound. Oxazole **36** and the two oxadiazoles **33** and **34** performed well in the marble burying assay at 30 mg/kg. Ethyl oxazole **34** also exerted anxiolytic-like effects in mice at 10 mg/kg; however, sedative-like effects were observed at 30 mg/kg. In the rotarod assay, **36** performed comparable to **3** and vehicle at both 10 and 30 mg/kg, whereas mice dosed with methyl oxadiazole **33** only had two successful trials at 30 mg/kg. Because of the higher likelihood of α1 activation by the oxadiazoles, it was decided that oxazole KRM-II-81 (**36**) would be investigated in greater detail, as mentioned above.

3.3.7.1 Oocyte Efficacy Data

The efficacy for KRM-II-81 (**36**) was investigated by Dr. Margot Ernst in a direct comparison against HZ-166 (**3**). Examination of the results have shown that the two compounds have similar efficacies at all subtypes $\alpha_{1\text{-}3,5}\beta3\gamma2$ subtypes at 100 nM and 1 μM when tested, as depicted in Figure 36. At a 10 μM concentration, KRM-II-81 was shown to have increased efficacy at the α1 and α5 subtypes in comparison to HZ-166; however, it is highly unlikely to reach this high of a concentration within the brain. Gratifyingly, analysis of all these results indicate that

KRM-II-81 (**36**) should perform as well or better than HZ-166 (**3**). This circumstance is due to the fact that KRM-II-81 (**36**) is less rapidly metabolized in mouse and rat liver microsomes than HZ-166 (**3**). The low activation at the α1 and α5 subtypes also indicated that 1,3-oxazole **36** should be devoid of adverse effects such as sedation, muscle relaxation, dependence and tolerance issues.





Change of GABA EC $_{3\text{-}6}$ current (100%), n=3 -4

	KRM-II-81 (36)			**HZ-166 (3)**		
	100 nM	1 μM	10 μM	100 nM	1 μM	10 μM
α1	n.d.	155.2 ± 9.9	231.7 ± 13.75	n.d.	147.4 ± 11.43	178.4 ± 19.55
α2	100 ± 11.85	200.6 ± 15.67	258.3 ± 18.07	111 ± 6.48	207.4 ± 19.72	244 ± 18
α3	109.3 ± 6.33	187.5 ± 25.25	332 ± 48.14	119.1 ± 8.62	195.2 ± 32.82	305 ± 31
α5	n.d.	157.5 ± 11	246.4 ± 6.15	n.d.	134 ± 9.4	158.5 ± 2.6

Figure 36. Structures and oocyte efficacy comparison of KRM-II-81 (36) and HZ-166 (3). Dose-dependent modulation of GABA ($EC_{3\text{-}6}$ concentration) by ligands 9 and 2 on *Xenopus laevis* oocytes expressing $GABA_AR$ subtypes $\alpha_{1\text{-}3,5}\beta3\gamma2S$ was determined by two-electrode voltage clamp current recordings. Data represents mean ± SEM.

3.3.7.2 Pharmacokinetic Data

The plasma concentration-time profile was next examined to evaluate the pharmacokinetic properties of PAM **36**, and is depicted in Figure 37. Male rats (n = 3 for each data point) were dosed with oxazole **36** (1 mg/kg I.V., or 10 mg/kg i.p.) and the concentration in the rat plasma was determined at various time points up to 24 hours. Analysis of the data from the IV injection indicated a half-life of 1.36 hours with a plasma C_{max} of 2480 nM at the first measured time point of 5 minutes. The i.p. dosing resulted in a half-life of 3.1 hours and a plasma C_{max} of 3090 nM at the two-hour time point. This is important for it indicated that oxazole **36** is stable *in vivo* whereas HZ-166 (**3**) was metabolized immediately upon administration. Comparison of the results of the I.V. injections of **36** and **3** (Table 3) show that the oxazole **36** is incredibly more stable in rats since the analysis of HZ-166 (**3**) was found to be below the quantifiable limit.

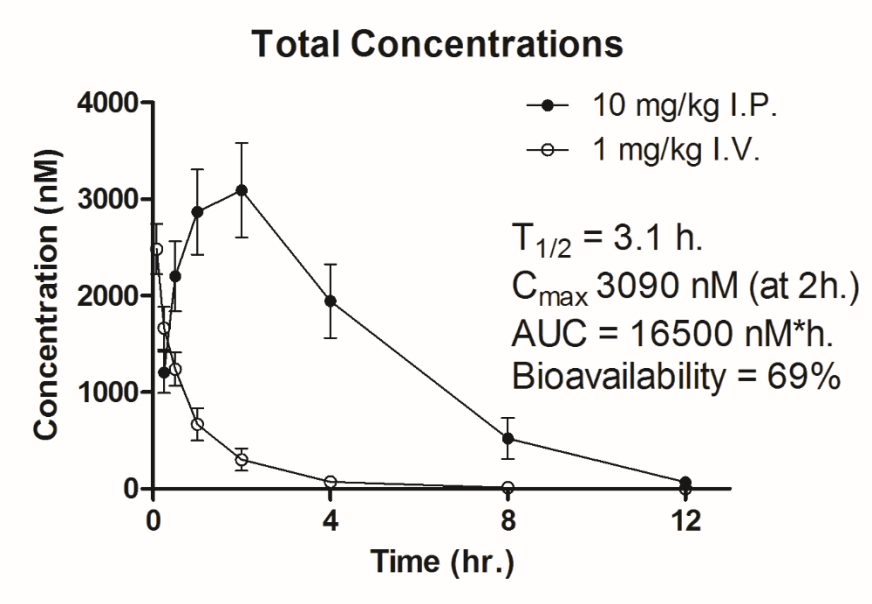


Figure 37. Plasma concentration-time plot of KRM-II-81 (36). Male Sprague-Dawley rats (n = 3 per time point) were dosed i.p. (10 mg/kg) or I.V. (1 mg/kg) and the plasma concentration was analyzed at varying time points for up to 12 hours.

The analysis of the results from oral dosing in rats also provided similar results, as shown in Table 6. The ethyl ester **3** went similarly undetected in the oral dosing as it did in the I.V. dosing because of hydrolysis to the acid which prevented penetration through the BBB, with the parent compound HZ-166 undetected in plasma at 1 hour, and brain samples at 2 hours. The 1,3-oxazole **36** had a 3910 nM concentration found in the plasma at one hour and 3640 nM in brain samples. This is a terrific level for KRM-II-81 (**36**). Although HZ-166 (**3**) went undetected, it was still able to produce pharmacological effects in anxiolytic, convulsant, and hyperalgesic assays. As mentioned previously, this may be due to the ester immediately entering the brain and being converted to the acid **20** very rapidly. The acid **20** may then exert some anxiolytic and anticonvulsant effects on its own.

Table 6. Plasma and brain concentrations of HZ-166 (3) and KRM-II-81 (36) after a 10 mg/kg P.O. dose in rats.

	3	**36**
Plasma concentration at 1 h. (nM)	BQL[a]	3910 ± 1870
Brain concentration (nM)	BQL[a,b]	3640 ± 1680

BQL = below quantification limit
[a] Quantifiable limit < 12.2 nM
[b] Brain concentration for 3 taken at 2 hour time point

3.3.7.3 Assessment for Motor Impairment in the Inverted Screen Paradigm

In addition to the rotarod paradigm, the inverted screen assay was carried out to further assess the levels of motor impairment exerted by KRM-II-81 (**36**). The inverted screen test has been used for years to measure whether a compound induced muscle relaxation,[155] which can stem from the α1 subtype, and possibly the α3 subtype at higher receptor occupancy. Muscle relaxation can be observed in the inverted screen test where the rats were placed on a wire screen which was subsequently inverted and suspended a few centimeters above a soft bedding. The reaction of the test subject was to climb to the opposite side of the screen so that they are no longer hanging upside

down. If a compound induced muscle relaxation, the test subject will either be unable to hold onto the screen while upside down and fall, or hang onto the screen without successfully climbing to the other side. The male Sprague-Dawley rats (n = 5) were dosed i.p. with vehicle (1% CMC), diazepam (3, 10 or 30 mg/kg), **3** (30 mg/kg) or **36** (10, 30 or 60 mg/kg) 25 minutes prior to testing. The rats were then placed on the screen which was then inverted and observed for one minute and scored (0 = climbed over; 1 = hanging upside down; 2 = fell off).

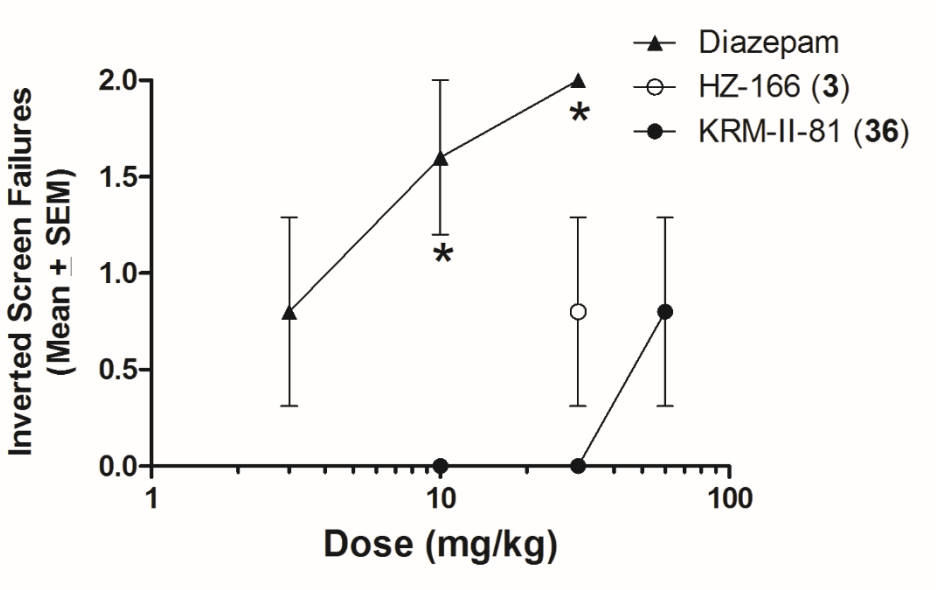


Figure 38. Inverted screen assessment of diazepam, HZ-166 (3) and KRM-II-81 (36). Vehicle scored 0.1. Male Sprague-Dawley rats (n = 5) were dosed i.p. with vehicle (1% carboxymethyl cellulose), diazepam (3, 10 or 30 mg/kg), KRM-II-81 (10, 30 or 60 mg/kg) or HZ-166 (30 mg/kg) 30 minutes prior to testing. Analyzed using ANOVA (Dunnett's test: * $P < 0.05$).

Diazepam was shown to induce signs of muscle relaxation at 3 mg/kg, with significant results at 10 and 30 mg/kg. This was not unexpected since diazepam notably has many of the common adverse effects that are associated with traditional BZDs and binds non-selectively to α1, α2, α3 and α5 subtypes.[17] Rats dosed with **3** exhibited some signs of muscle relaxation at 30 mg/kg. Oxazole KRM-II-81 (**36**) was shown to induce no signs of muscle relaxation at the 10 and 30

mg/kg doses, while it begins to show some mild signs at 60 mg/kg. If the pharmacological effects seen after dosing of **3** are in fact from the ethyl ester, and not the acid **20**, it might be possible that the muscle relaxation was due to activation of the α3 subtype, which would indicate that KRM-II-81 (**36**) may have a lower efficacy activation of the α3 subtype, which resulted in **36** interacting more at the α2 subtype selective ligand rather than a α2/α3. Because there are no α2 subtype selective ligands known, to date, this could be an extremely valuable compound. Alternatively, if the pharmacological effects are due to the acid **20**, than the oxazole top of **36** is very effective in combating the degradation that was seen in ethyl ester **3**. Nevertheless, the lack of muscle relaxant effects of KRM-II-81 (**36**) as compared to the lead anxiolytic/antinociceptive agent HZ-166 (**3**) are exciting and provide the impetus for further evaluation of 1,3-oxazole **36** below.

3.3.7.4 Assessment of Anxiolytic Activity in the Vogel Conflict Procedure

The marble burying assay was a good general anxiolytic test, but did not do a great job in distinguishing which ligands in the oxazole or oxadiazole series are the best clinical candidates. The Vogel conflict protocol (previously described in Section 3.3.2.3) is the gold standard for anxiolytic activity and was employed as a second assay with KRM-II-81 (**36**) for anxiolytic activity,[112, 124] illustrated in Figure 39. In this, male Sprague-Dawley rats (n = 6 – 8) were dosed with vehicle (1% CMC), **3** (30 mg/kg), **36** (3, 10, 30 or 60 mg/kg) or the positive control chlordiazepoxide (CDAP; 20 mg/kg). CDAP is a traditional BZD which is commonly prescribed as a short-term anxiolytic, but tolerance is a concern limiting its long-term use,[156] especially as an anticonvulsant or antinociceptive agent.

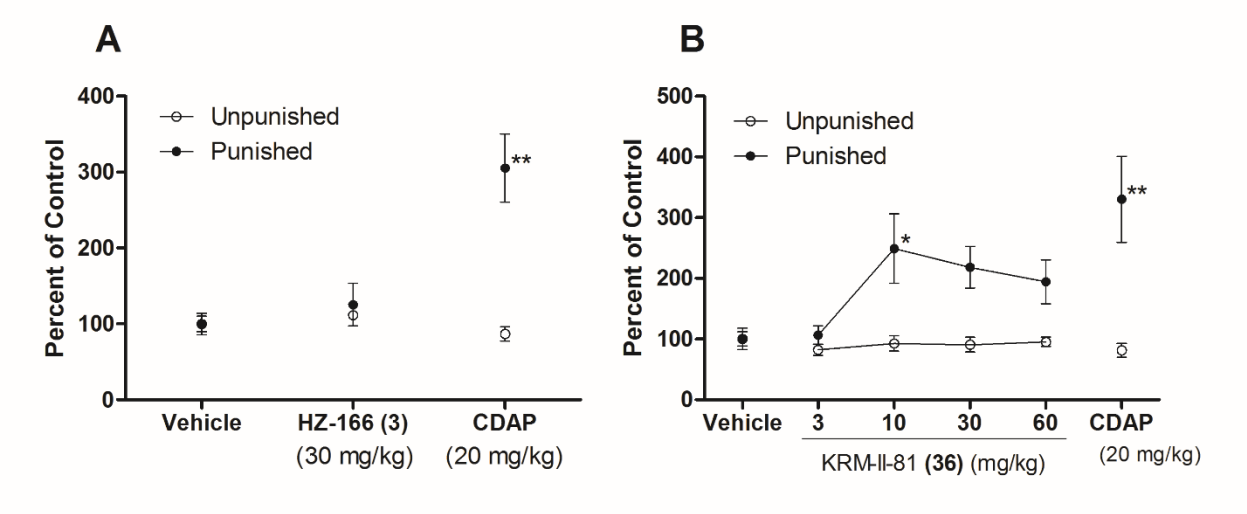


Figure 39. HZ-166 (3) and KRM-II-81 (36) in the Vogel conflict procedure. After a baseline is established using a vehicle (1% 2-hydroxyethyl cellulose), male Sprague-Dawley rats (n = 6-8) were dosed i.p. with either KRM-II-81 (3, 10, 30, or 60 mg/kg) or chlordiazepoxide (20 mg/kg) 30 minutes prior to testing. Analyzed using ANOVA (Dunnett's test: * $P < 0.05$; Student t-test: ** $P < 0.05$).

HZ-166 (**3**) was shown to be ineffective in increasing the response in the punished session at 30 mg/kg (Figure 39A), whereas KRM-II-81 (**36**) showed a significant increase in responses at 10 mg/kg (Figure 39B). Oxazole **36** also produced increased response rates at 30 and 60 mg/kg, but these did not reach significance. In examination of the inverted screen test, the 60 mg/kg dose did produce slight muscle relaxation; however, muscle relaxation should not play a major role in the Vogel conflict procedure and the test subjects could remain at the water source with little movement required. Muscle relaxation should not influence the Vogel conflict at 30 mg/kg dose either since there was none observed in the inverted screen with oxazole **36** at the same dose.

Ethyl ester **3** had previously been shown to perform well in the Vogel conflict procedure in rhesus monkeys at 1 mg/kg[112] where esterase levels are much lower than in rodents; but the 30 mg/kg dose of **3** in this test had no effect. It is highly possible that the high concentration of esterases in rats may degrade **3** too rapidly to have an effect as mentioned above. Alternatively,

these results cannot be directly compared because rats and monkeys are significantly different species. Regardless, because KRM-II-81 (**36**) performed well in rats at 10 mg/kg, it can be assumed that the 1,3-oxazole **36** would also exhibit non-sedating anxiolytic properties in monkeys. This work is currently underway.

3.3.7.5 Evaluation of Anticonvulsant Activity in the MES and scMET Procedures

Epilepsy is a common neurological disease that is often treated with BZDs[157] in status epilepticus in emergency rooms. The seizures that are associated can range from nearly undetectable, to mild or severe uncontrollable shaking for an extended period of time. BZDs elicit anticonvulsant activity from both the α1 and α2 subtypes. Ligands which target the α1 subtype also come with the adverse effects of sedation, ataxia, amnesia, addiction, tolerance, etc. The development of tolerance is the greatest drawback of the use of BZDs to treat convulsions as the prescribed ligands become ineffective with continued use[158] due to the development of tolerance. BZDs which target only the α2 subtype can avoid these concerns while also being effective in the management of seizures, especially since these ligands would avoid the coupling of the α1 and α5 subtypes which have been shown to be the source of the development of tolerance by Möhler, *et al*.[88] and demonstrated by Cook *et al*.[89, 90, 93]

Ligand HZ-166 (**3**) was previously characterized by ASP at NINDS. It was found to be inactive when mice were given a 100 mg/kg i.p. dose in the maximal electroshock (MES) assay, which was designed to evaluate a compounds ability to prevent seizures in a generalized tonic-clonic response, when all neuronal circuits in the brain are firing. Tonic seizures generally set in first, and are characterized by the stiffening of muscles. These are commonly followed by the clonic phase, which is the uncontrollable spasming of muscles. Alternatively, **3** was active in the

scMET assay for antiseizure activity[115]. In mice, **3** had an ED_{50} of 16.28 mg/kg when given i.p., and an ED_{50} of 98.5 mg/kg when dosed P.O. in rats, as depicted in Table 7. Both of these ED_{50}'s are better than has been reported for carbamazepine and phenytoin, both of which are commonly prescribed for epileptic seizures, in similar assays.

Table 7. Quantification of Antiseizure Activity: ED_{50} MES, ED_{50} scMET, TD_{50} TOX, and Therapeutic Index (TI) via i.p. and P.O. Routes.[a] Modified from the table in Rivas, *et al*.[115]

	Mouse i.p.			Rat P.O.			TI Mouse i.p.	TI Rat P.O.
entry	ED_{50} MES[d]	ED_{50} scMET[d]	TD_{50} TOX[d]	ED_{50} MES[d]	ED_{50} scMET[d]	TD_{50} TOX[d]	TD_{50}/ED_{50} (scMET)	TD_{50}/ED_{50} (scMET)
3	>300	**16.28**	**>500**	>250	**98.5**	**>500**	**>30.2**	**>>5**[c]
Cbz[b]	7.81	>50	45.4	5.35	>250	364	<0.9	1.5
Cl[b]	25.6	0.02	0.26	7.86	0.61	2.38	13	3.9
Pn[b]	5.64	>50	41.0	28.1	>500	>1000	<0.82	2.0

[a] MES, maximal electroshock induced seizures; scMET, subcutaneous pentylenetetrazole induced seizures; TOX, observed minimal muscular or neurological impairment as indicated by rotarod paradigm (mice) or abnormal, uncoordinated gait (rats); TI, therapeutic index = TD_{50}/ED_{50}; ED_{50}, median effective dose; TD_{50}, median toxic dose; i.p., intraperitoneal; P.O., oral.
[b] Refer to reference.[159]
[c] A higher dose was not tested, since 500 mg/kg was clearly not sedating. [d]All values are in mg/kg; Cbz, carbamazepine; Cl, clonazepam; Pn, Phenytoin

The maximal electroshock (MES) assay is a common choice in search of new antiepileptic drugs[160] and KRM-II-81 (**36**) was evaluated, along with diazepam and HZ-166 (**3**) for comparison. Male CD-1 mice (n = 10) were dosed i.p. with vehicle (1% CMC), diazepam (1, 3 or 6 mg/kg), **3** (3, 10 or 30 mg/kg) or **36** (3, 10 or 30 mg/kg) 30 minutes prior to testing. During the testing, mice were given a 7mA electroshock for 0.2 seconds and observed for tonic and/or clonic seizures and the results are illustrated in Figure 40.

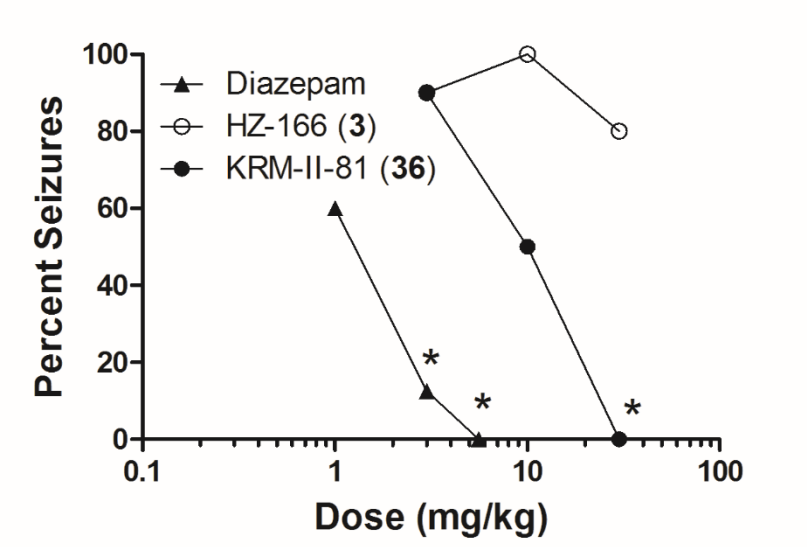


Figure 40. Diazepam, HZ-166 (3) and KRM-II-81 (36) in the MES anticonvulsant activity assay. Male CD-1 mice (n = 10) were dosed i.p. 30 minutes prior to being tested with either vehicle (1% CMC), diazepam (1, 3 or 6 mg/kg), KRM-II-81 (3, 10 or 30 mg/kg) or HZ-166 (3, 10 or 30 mg/kg). Analyzed using ANOVA (Dunnett's test versus vehicle: * $P < 0.05$).

Examination of the results indicated that HZ-166 (**3**) produced little to no protection against MES-induced seizures at 3, 10 or 30 mg/kg. This was consistent with the findings at ASP (NINDS, Stables, *et al.*), which had seen no protection at 100 mg/kg, albeit under somewhat different conditions [115]. Diazepam, which is a potent anticonvulsant, was able to significantly reduce the percent of seizure outcomes to about 10% at 3 mg/kg and provided full protection at 6 mg/kg. The 1 mg/kg dose did reduce the number of seizures to 60% of the total number of outcomes, but this was not a significant effect. Oxazole **36** performed comparably to **3** at 3 mg/kg and exerting little effect, but began to show activity in reducing convulsions at 10 mg/kg and protected all test subjects at 30 mg/kg. This was exciting and long-lived *in vivo*.

KRM-II-81 (**36**) was also evaluated for its anticonvulsant activity against scMET-induced clonic seizures. Male Sprague-Dawley rats (n = 5) were dosed i.p. with either vehicle (1% CMC), diazepam (3 or 10 mg/kg), **3** (30 mg/kg) or **36** (10, 30 or 60 mg/kg). Thirty minutes post

administration of a test compound, the convulsant pentylenetetrazole (in saline), was then given i.p. at a 35 mg/kg dose and the rats were observed for convulsions, as depicted in Figure 41A. Another assessment of the protection from scMET-induced seizures is shown in Figure 41B. This assay consisted of first dosing rats i.p. with either vehicle (1% CMC), diazepam (0.1, 0.3 or 1 mg/kg), **3** (3, 10, 30 or 60 mg/kg), **36** (3, 10, 30 or 60 mg/kg), or valproic acid (300 mg/kg) before determining the concentration of metrazole that was needed to induce a seizure. Thirty minutes after administration of a test compound, pentylenetetrazole (PTZ) was infused I.V. at a rate of 0.5 mL/minute (10 mg/mL) until the appearance of a clonic seizure.

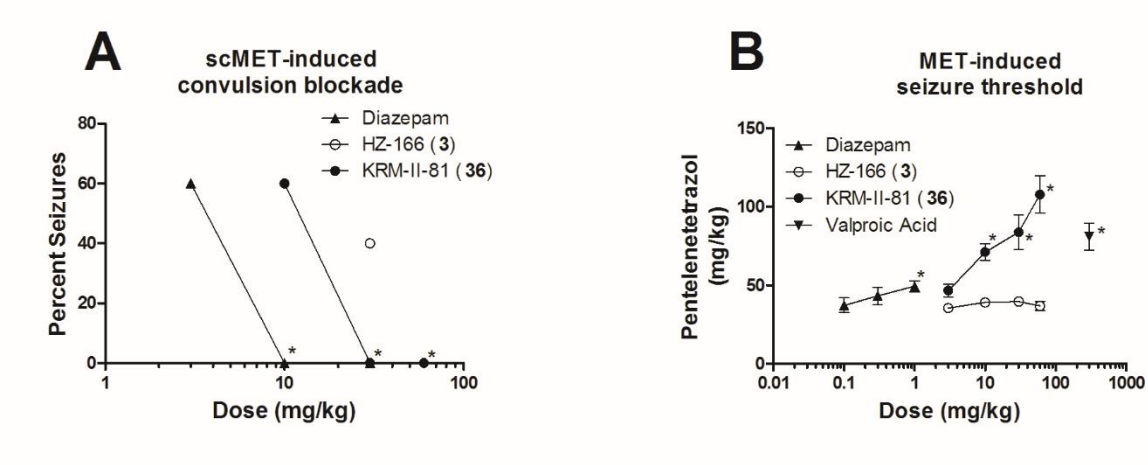


Figure 41. Diazepam, HZ-166 (3) and KRM-II-81 (36) in the blockage (A) and threshold (B) measurement against scMET-induced seizures. In the blockage procedure (A), mice were dosed i.p. with either diazepam (3 or 10 mg/kg), KRM-II-81 (10, 30 or 60 mg/kg) or HZ-166 (30 mg/kg) 30 minutes prior to testing. The threshold procedure (B) dosed diazepam, KRM-II-81, HZ-166 or valproic acid 30 minutes prior to an I.V. infusion of the convulsant pentylenetetrazole until convulsions were observed. Analyzed using ANOVA (Dunnett's test: * $P < 0.05$).

The ability of diazepam, **3** and **36** to prevent convulsions is shown in Figure 41A. Diazepam was able to produce some reduction of scMET-induced seizures at 3 mg/kg, and offered

full protection at 10 mg/kg. At a 30 mg/kg, ethyl ester **3** was able to protect rats from some seizures, but not significantly different than vehicle. Oxazole **36** showed some reduction at 10 mg/kg, and full protection at 30 and 60 mg/kg. These results are in alignment with the results from the MES-induced seizure assay.

The follow-up study to determine the threshold limit of protection of the test compounds is shown in Figure 41B. At 1 mg/kg, diazepam was able to increase the required dose of PTZ to 49 mg/kg, which was significantly different than vehicle (PTZ threshold = 37.1 ± 1.9 mg/kg). Ligand HZ-166 (**3**) was unable to increase the amount of PTZ required to induce seizures up to 60 mg/kg, whereas KRM-II-81 (**36**) began to require a significant increase of PTZ at 10 mg/kg, requiring a 71 mg/kg dose of PTZ to induce seizures. When rats were given a 60 mg/kg dose of KRM-II-81 (**36**), the amount of PTZ required to induce a convulsion rose to 108 mg/kg. This was greater than the 81 mg/kg of PTZ required when given a 300 mg/kg of the antiepileptic drug valproic acid at a fifth of the dose.

Analysis of the anticonvulsant data indicated that **36** was better at protecting rodents from seizures than the known anticonvulsant **3**. In the threshold test (Figure 41B), oxazole **36** was able to significantly increase the amount of PTZ required to induce a seizure at 10 mg/kg, which was a sixth of the dose that **3** was unable to produce a significant effect. It is interesting that HZ-166 (**3**) was unable to produce significant effects at 60 mg/kg here in rats when given i.p. Earlier in a scMET mouse study by ASP, an ED_{50} of 16.28 mg/kg resulted when dosed i.p. The rat P.O. study by ASP also showed HZ-166 (**3**) performed well with an ED_{50} of 98.5 mg/kg.[115] However, these test conditions are not identical, along with the species of animals and cannot be directly compared. The most important finding is that KRM-II-81 (**36**) was effective against convulsions at a fifth of the dose to achieve the same effect with the known anticonvulsant valproic acid.

3.3.7.5.1 Assessment of Seizure Protection in Resistant Epileptic Human Brain Tissue

Recently, human brain tissue from a patient suffering from intractable, or resistance, epilepsy was obtained and KRM-II-81 (**36**) was assessed to determine if it would reduce the firing rate in epileptic brain tissue after surgical treatment, as illustrated in Figure 42. The slice was first monitored while in a picrotoxin solution which determined that the tissue was active while recording over a one-hour time period (open circles) and resulted in an average firing rate of 0.05 Hz ± 0.01. The oxazole **36** was then added (30 μM) which inhibited the firing rate activity (closed circles) and resulted in a firing rate of 0.01 Hz ± 0.005. Data was collected for 1 hour under each condition.

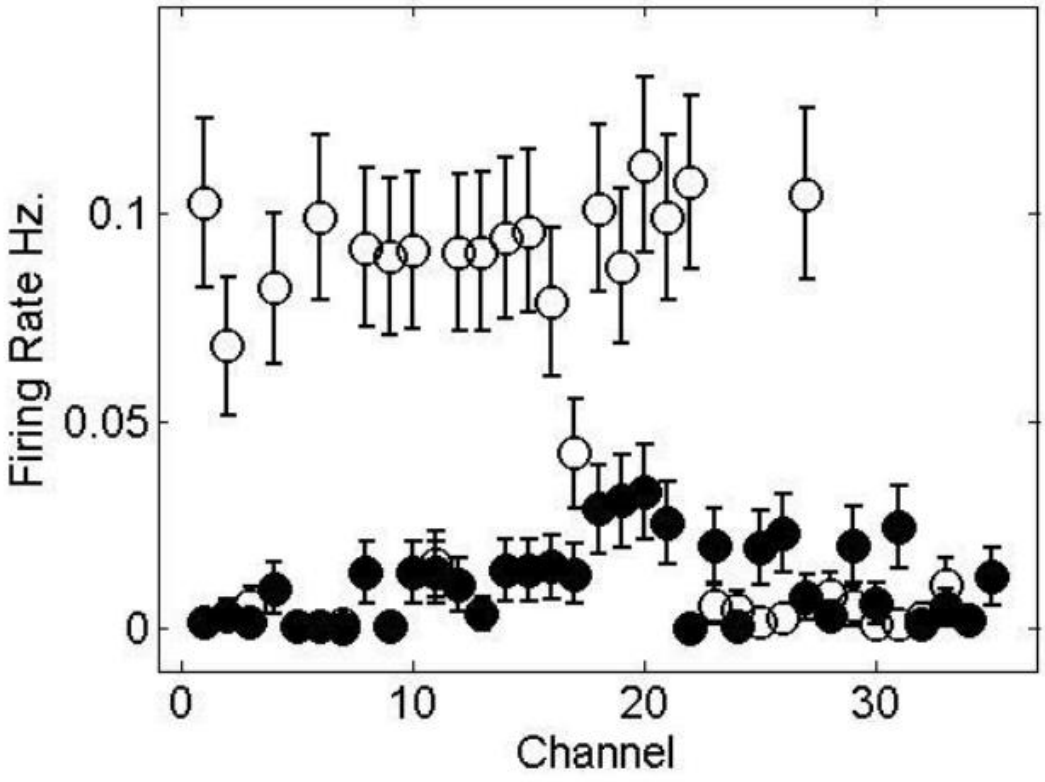


Figure 42. Network Firing Rate. Dampening effects of KRM-II-81 (36) on firing rate frequency (Hz) in tissue resected from a human with epilepsy. Data was collected for 1 hour under each condition (circle/baseline EACSF) (filled circle EACSF + 30uM 36). KRM-II-81 (36) significantly reduced the firing rate frequency (paired t-test: $P < 0.05$).

These results indicated that KRM-II-81 (**36**) was able to significantly reduce the firing rate of epileptic seizures that were resistant to other forms of treatment. This data is a very important step forward for **36** and the treatment of epileptic seizures!

3.3.7.6 Reversal of Hyperalgesia in Neuropathic and Inflammatory Pain Models

The use of BZDs for the treatment of neuropathic pain is one study that has become a topic of growing interest over the past few years. It has been shown by Zeilhofer, *et al*. with HZ-166 and a triple knock-in mouse that the positive activation of the α2 subtype is responsible for most of the antihyperalgesic effects[161] exerted by BZDs. More recently, instead of being effected in the brain, it appears that the action stems from the α2 Bz/$GABA_AR$ subunits that are located supraspinal region of the CNS (Paul, Cook, Zeilhofer, *et al*.).[162] As previously discussed, HZ-166 (**3**) has been shown to be active in inflammatory pain models and the CCI model of neuropathic pain[93] by Zeilhofer, Cook, *et al*. More recently, **3** was used in a knock-in CCI model of mechanical sensitization in which the α2 subtype was rendered insensitive with a H101R replacement.[50] Here, ethyl ester **3** exerted an antihyperalgesic effect in wild-type mice using von Frey filaments, but the α2 knock-in mice showed little difference from vehicle, as illustrated in Figure 43. This indicated that most of the antihyperalgesic effects do stem from the α2 subtype. In a different study, the α3 subtype selective agent YT-III-31[117] did show some antinociceptive activity but sedation confounded the results of this study; a sedative effect would slow down paw withdrawal (M. Poe, J. Cook, unpublished results; see Appendix A). Oxazole **3** was investigated for its antihyperalgesic effects to further assess its pharmacological profile.

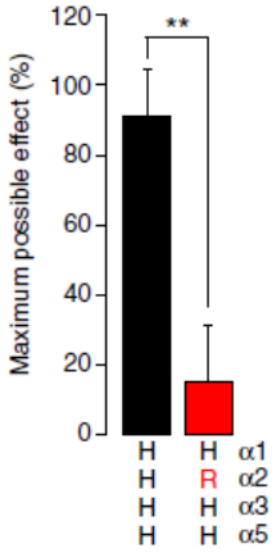


Figure 43. Antihyperalgesic effects of HZ-166 (3) in wild-type (left) and α2 knock-in (right) mice. Mice (n = 7-8) were dosed with 3 (16 mg/kg) and assessed in the CCI antihyperalgesic procedure using von Frey filaments. Analyzed using the unpaired *t*-test: ** $P < 0.01$. Modified from the figure in Ravlenius, *et al*.[50]

3.3.7.6.1 The Potential Treatment of Neuropathic Pain

The oxazole KRM-II-81 (**36**) was assessed in a neuropathic pain model in which the sciatic nerve ligation (SNL) model was used. The SNL model induces hypersensitivity to pain by tying spinal nerves[163] and is similar to the CCI model. It can be measured by mechanical sensitization or thermal methods. This model employed male Sprague-Dawley rats (n = 5) that went through SNL 90 days prior to testing. After determining a baseline for the study, rats were injected i.p. with either vehicle (1% CMC), gabapentin (50 mg/kg) or **36** (30 mg/kg). Every hour for 4 hours, rats were subjected to mechanical sensitization using von Frey filaments to determine the paw withdrawal threshold (PWT) and the results are shown in Figure 44. Gabapentin was chosen as a positive control as it is commonly used for neuropathic pain, as discussed in Section 3.1.

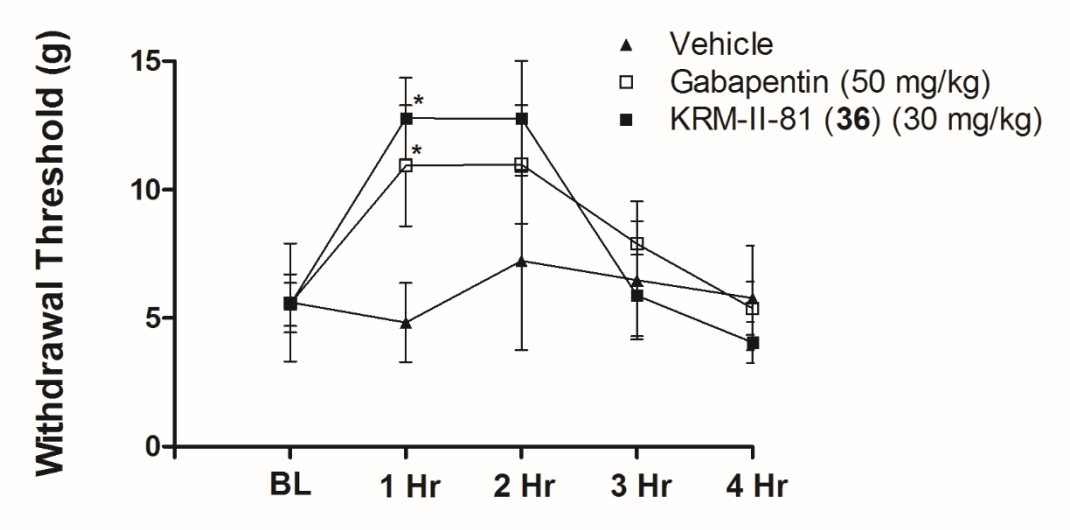


Figure 44. KRM-II-81 (36) and gabapentin in the SNL model of neuropathic pain. Male Sprague-Dawley rats (n = 5) were dosed i.p. either vehicle, KRM-II-81 (30 mg/kg), or gabapentin (50 mg/kg) and tested in the von Frey filament assay after undergoing SNL 90 days prior. Analyzed using ANOVA (Dunnett's test: * $P < 0.05$). It is clear that KRM-II-81 is more potent than gabapentin in this model of neuropathic pain. KRM-II-81 in von Frey filament assay for antihyperalgesia.

The results of the SNL model of neuropathic pain show that oxazole **36** and gabapentin were able to significantly reverse the effects of hyperalgesia at the one-hour time point after dosing. The PWT of rats dosed with KRM-II-81 (**36**) produced the same medium value at the one- and two-hour time points, but the results at two hours were not significant due to a slightly higher vehicle PWT and a greater SEM. It should be noted that in addition to the mediation of a greater antihyperalgesic effect at a lower dose than gabapentin, although not significantly so, the more than double molecular weight of KRM-II-81 (**36**) also indicates that it is acting at a lower respective concentration than gabapentin. This corresponds to **36** exerting a greater reversal of hyperalgesia than gabapentin at about a third of the concentration which would further help reduce the concerns of adverse effects which could result in doses of higher concentrations that would result in the activation of off-target $GABA_AR$ subtypes or other receptors. These interactions were assessed by the National Institute for Mental Health (Psychoactive Drug Screening Program, Dr.

Bryan Roth, UNC) and screened against a panel of cloned human and rodent CNS receptors determine any off-target effects. The oxazole **36** was found to have little to no binding affinity for a wide-array of receptors, including dopamine, histamine, opioid, adrenergic, and serotonin receptors among other. In addition, KRM-II-81 had no hERG activity,[164] which is involved in coordinating the electrical activity associated with the heart's beating, decreasing the risk of inducing heart arrhythmias.[165]

3.3.7.6.2 The Activity of KRM-II-81 (36) and KRM-II-18B (38) in a Model of Inflammatory Pain

The antihyperalgesic effects of KRM-II-81 (**36**) and KRM-II-18B (**38**) were assessed in an assay which uses the complete Freund's adjuvant (CFA) model of inflammatory pain by Dr. Jun-Xu Li (University at Buffalo). CFA contains *Mycobacterium butyricum* which induces inflammation.[166] Male Sprague-Dawley rats (n = 6) were injected with 0.1 mL of CFA into the right hind paw. Three days post injection, rats were injected with either midazolam, **3**, **36** or **38** and tested for antihyperalgesic activity using von Frey filaments. The results are illustrated in Figure 45. Von Frey filaments were used slowly increasing the pressure on the left hind paw (control). Once the left paw was withdrawn, the amount of force applied was recorded as 100% maximum possible effect (MPE), with a maximum of 26 g.

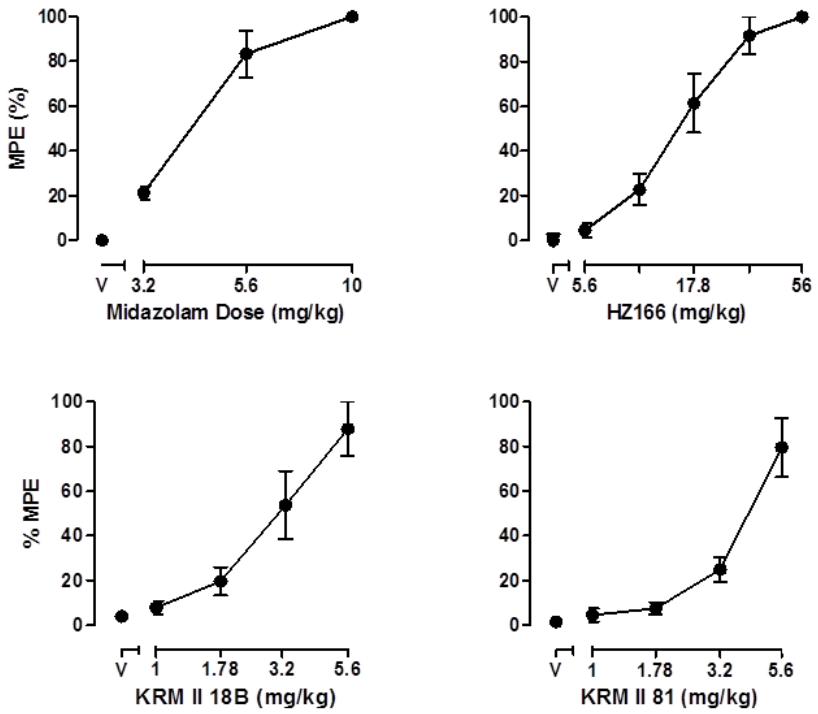


Figure 45. Assessment of antihyperalgesic effects of midazolam, 3, 36 and 38 in CFA-induced inflammatory pain. $GABA_A$ receptor PAMs, Midazolam (nonselective PAM), HZ166, KRM-II-18B, and KRM-II-81 dose-dependently attenuated mechanical hyperalgesia in a CFA-induced inflammatory pain rat model. Raw data (paw withdrawal threshold, expressed in g of von Frey filament) was converted to a maximal possible effect value according the following equation:

% MPE = [(test threshold (g)- control threshold (g) / (pre-CFA threshold – control threshold)] x 100

HZ-166 (**3**) had been previously shown to reverse the antihyperalgesia in the zymosan A model of inflammatory pain.[93] Here in the CFA model, **3** was able to reduce hypersensitivity; however, it only reached 50% MPE at 17.8 mg/kg, and did not offer full protection until rats were given a 56 mg/kg dose. This was much higher than midazolam, which was used as a positive control, which was shown to offer 80% MPE at 5.6 mg/kg, and full protection at 10 mg/kg. However, it must be remembered that sedation caused by midazolam may seriously confound these

results. KRM-II-81 (**36**) on the other hand elicited very similar results to midazolam, with an MPE near 80% at the 5.6 mg/kg dose but there was no sedation to confound the results. Ligand KRM-II-18B appeared to be much more potent at lower concentrations, for it showed a 57% MPE at 3.2 mg/kg, but at the 5.6 mg/kg dose it offered the same protection as **36**.

The antihyperalgesic effects of ligands **3**, **36** and **38** were examined to verify the source of the pharmacological effect. This was done by using flumazenil, which is a $GABA_AR$ antagonist which tightly binds to all $GABA_AR$ subtypes and blocks the effect of DS BzR ligands. Rats were dosed with **3**, **36** and **38** at the same doses as was completed previously, but an additional pretreatment of flumazenil (1, 3.2 or 10 mg/kg) 10 minutes prior to the test compound was given. These results are shown in Figure 46.

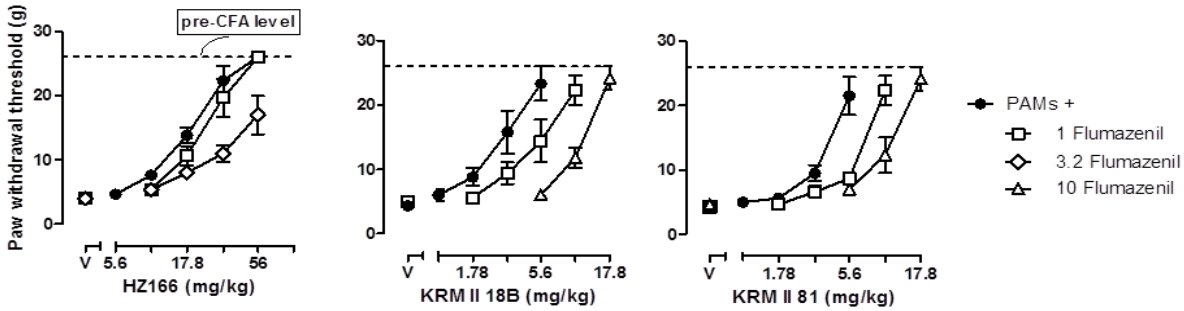


Figure 46. Antagonism of BZD effects using flumazenil. The benzodiazepine site antagonist flumazenil shifted the dose-effect curves of PAMs rightward, indicating the effect is modulated by the benzodiazepine receptor.

The $GABA_AR$ antagonist, flumazenil, was able to dose-dependently right-shift the antihyperalgesic effects, which resulted in a lower MPE at each concentration of a given test compound. With increasing flumazenil doses, the greater the concentration was needed to reach the pre-CFA level, or 100% MPE. This key result indicated clearly that HZ-166 (**3**), KRM-II-81

(**36**) and the 2'-F analog (**38**) exerted their effects through benzodiazepine receptors and not some other receptor system.

3.3.7.7 The Treatment of Depression in the Forced Swim Test

A hypothesis that predicts depression can be treated through a GABAergic pathway has been proposed,[6] and some clinical studies have seen BZDs alprazolam and adinazolam exert some antidepressant nature similar to marketed antidepressants;[167, 168] however the Bz/$GABA_AR$ subtype is unknown. The forced swim test is used as a primary screen for the antidepressant nature of a test compound. One knockout study has suggested that the α2 subunit may be the source of the activity[169] and KRM-II-81 (**36**) was assessed for antidepressant activity. Mice NIH Swiss mice were dosed i.p. with vehicle (1% CMC), **36** (3, 10 or 30 mg/kg) or positive control imipramine (15 mg/kg) 30 minutes prior to being placed in a cylinder filled with a small amount of water, and the results are illustrated in Figure 47. Mice that were more mobile during the test were determined to be less depressed as they continued to search for an escape, opposed to treading water.

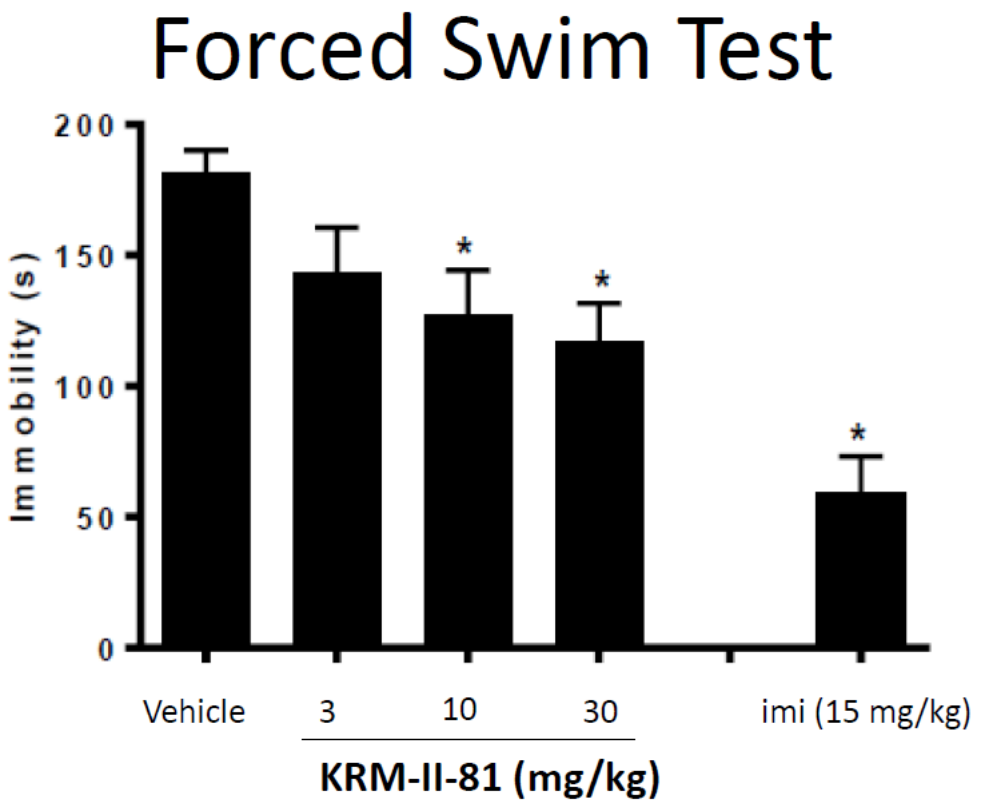


Figure 47. The antidepressant effects of KRM-II-81. Male NIH Swiss mice (n = 7 – 8) were dosing i.p. with vehicle (1% HEC, 0.25% Tween 80, 0.05% antifoam), KRM-II-81 (3, 10 or 30 mg/kg) or imipramine (15 mg/kg) and assessed in the forced swim test. Analyzed using ANOVA (Dunnett's test * $P < 0.05$).

The results indicated that KRM-II-81 (**36**) was able induce an antidepressant effect at 10 and 30 mg/kg, characterized by the decreased immobility time as compared to vehicle. Because the majority of antidepressants, which have their drawbacks, act upon the serotonergic and/or noradrenergic systems,[170] there is a need for agents that target different pathways.[171] The data presented here is exciting and encouraging that nonsedating nor addicting BZDs could be used in the treatment of depression by targeting $GABA_A$ receptors.

3.4 Discussion

Prior to this work, lead compound ethyl ester HZ-166 (**3**) had been shown to be a very good non-sedating anxiolytic,[112] anticonvulsant,[115] and it was also active against inflammatory and neuropathic pain.[50, 93, 162] It was shown by Stables (NINDS) and Zeilhofer that **3** did not develop tolerance to the anticonvulsant and antinociceptive effects. This lack of tolerance by low efficacy at α1 and α5 subtypes indicated HZ-166 (**3**) was in a very special class of ligands which target the benzodiazepine binding site of $GABA_A$ receptors. It was shown to be stable when incubated with human liver microsomes;[117] however, the short time-of-effect seen in the *in vivo* assays in rodents[93, 115] led to the realization that **3** was not stable enough in rodents required for extensive preclinical trials. The research in this thesis was designed to address the stability issues, in regard to preclinical testing, as well as to design better subtype selective ligands to understand the physiological effects of α2 and/or α3 subtype Bz/$GABA_A$R ligands. This work has led to a number of important findings.

Pharmacokinetic studies of **3** (Table 3) show that the ethyl ester was not detected in plasma or brain of rodents when dosed I.V. or orally; however, the acid **20** was found in the brain in very small amounts. This indicated that **3** was possibly a prodrug of the pharmacologically active acid **20** or the ester **3** enters the brain very rapidly and is hydrolyzed to **20** in the brain. The acid **20** itself, however, was also dosed in PK studies and it was shown that **20** has very poor BBB penetration, indicated by the absence of **20** in brain samples. The deuterated ethyl ester **21** of **3** was designed and synthesized, which was successful in combating degradation when incubated *in vitro* with liver microsomes, but was still metabolized *in vivo* in rodents.

The methyl ester **19** was also found to have an increased resistance to metabolism by liver microsomes *in vitro*. We believe that the metabolism of **3** is effected by esterases and β-oxidation

of the ethyl group in MLMs, whereas the methyl ester would not undergo β-oxidation in the liver. This is speculation at the moment but is in agreement with the longer half-life of the methyl ester **19** when compared to the ethyl ester **3**. This compound was tested *in vivo* for anxiolytic and antihyperalgesic activity by Dr. Bradford Fischer. It was found to be active in both assays and appeared to have a longer time-of-effect than **3** when tested in similar experiments. Because of poor metabolic results with other esters described above, it was concluded that esters as a group, although active, were too metabolically unstable *in vivo* to be regarded as promising preclinical candidates.

A series of heterocyclic bioisosteres were designed using the pharmacophore/receptor model[74] and synthesized, including various oxazoles and oxadiazoles, to resist rodent metabolic degradation. The 2'-N compounds which are more polar were found to have increased stability in *in vitro* rodent and human liver microsomes. KRM-II-81 (**36**) was found to be the most promising of the heterocyclic compounds based on an α3 FLIPR assay, liver microsomal stability, anxiolytic marble burying assay and a rotarod assay which indicated no ataxia at the therapeutic dose. Further studies on KRM-II-81 were carried out with HZ-166 employed as a comparison ligand. Oxazole **36** was found to be a better anticonvulsant, anxiolytic and more active against neuropathic and inflammatory pain than published lead non-sedating anxiolytic **3**. This includes two critical pieces of data which indicate that **36** was able to reduce network firing in resistant human epileptic brain tissue and was able to decrease depression. Moreover, KRM-II-81 had much greater BBB penetration, as indicated by the high concentration of compound found within brain samples two hours after oral administration whereas **3** was below the quantifiable limit (< 12 nM). Additional studies on **36**, as well as other heterocycles and amides, are currently being completed to further characterize these compounds. The results of these studies indicate that KRM-II-81 or its analogs

have great potential to advance to clinical trials as non-sedating anxiolytic, anticonvulsant and antinociceptive agents which do not develop tolerance to the anticonvulsant or antinociceptive effects.

3.5 Methods

3.5.1 Liver microsomal assay (Revathi Kodali at UWM)

Chemicals and Reagents

Test compound (1 mM in DMSO), Verapamil HCl (1 µM in Acetonitrile), phosphate buffer (0.5 M) pH 7.4, 18 mΩ water, NADPH Regenerating System Solution A (BD Bioscience Cat. No. 451220), NADPH Regenerating System Solution B (BD Bioscience Cat. No. 451200), Human pooled liver microsome (BD Gentest, Cat. No. 452156), Mouse liver microsomes (Life Technologies, Cat. No. MSMC-PL).

Microsomal stability assay

Test compounds (10 µM) were incubated with human and mouse liver microsomes at a protein concentration of 0.5 mg/mL in a total volume of 400 µL containing 282 µL of water, 80 µL of phosphate buffer (0.5 M) pH 7.4, 20 µL of NADPH Solution A, 4 µL of NADPH Solution B, 4 µL of test compound (1 mM in DMSO) and 8.8 µL of liver microsomes. After preincubation at 37 °C for 5 minutes, the reaction was initiated by addition of microsomes and vials were stirred using a digital heat-shaking dry bath (Fischer Scientific, Cat. No. S08040). Aliquots of 50 µL were taken at time intervals of 0 (without microsomes), 10, 20, 30, 40, 50 and 60 min. Each aliquot was added to 100 µL of cold acetonitrile solution containing 1 µM of the internal standard verapamil, followed by sonication for 10 seconds and centrifugation at 10,000 rpm for 5 minutes. The 100 µL of the supernatant was transferred into Spin-X HPLC filter tubes and centrifuged at 13,000 rpm for 5 min. The filtrate was diluted and subsequently analyzed by LC-MS/MS (Shimadzu LCMS 8040). The ratio of the peak areas of the internal standard and test compound was calculated for every time point and the natural log of this ratio was plotted against the time to determine the linear slope (k). The metabolic rate ($k*C_0/C$), half-life (0.693/k), and internal clearance (V*k) were

calculated, where k is the slope, C_0 is the initial concentration of test compound (μM), C is the concentration of microsomes (mg/mL), and V is the volume of incubation (μL)/protein in the incubation (mg). All incubations throughout the study were performed in three experiments carried out in duplicate and the data was presented as the average value with the standard deviation.

3.5.2 Liver microsomal assay (CRO)

The compounds were incubated in hepatic microsomes (human, dog, mouse and rat) over a 30-minute incubation period at 37ºC. Incubations both with and without NADPH (2 mM) were performed in a 96-well plate format. The reaction was initiated with the addition of substrate and was terminated by protein precipitation with acetonitrile. All incubations are performed using a final substrate concentration of 4 μM in 50 mM sodium phosphate buffer, pH 7.4. The final organic solvent content was 0.5 % acetonitrile and 0.02% DMSO. The amount of enzyme present was fixed at 1.11mg/mL protein irrespective of the species of microsomes used. Samples were analyzed by LC/MS-MS to determine the percent loss in the NAPDH incubations relative to the NADPH free incubations.

3.5.3 Time-plasma concentration pharmacokinetic studies (CRO)

The single-dose pharmacokinetics were determined in femoral artery/vein cannulated Sprague-Dawley rats. The rats received a 1mg/kg intravenous and 10 mg/kg oral gavage dose of compound in individual experiments, respectively. Blood samples were collected at 0.08 (I.V. only), 0.25, 0.5, 1, 2, 4, 8, 12 and 24 hrs after initiation of compound administration. Plasma was obtained via centrifugation. Plasma samples were then analyzed by LC-MS, and pharmacokinetic parameters calculated using Watson (version 7.4; Thermo Fisher Scientific). Calculated parameters included clearance (C_L), volume of distribution (V_{dss}), area-under-the-curve (AUC), half-life ($T_{1/2}$),

maximum plasma concentration (C_{max}), time of maximum concentration (T_{max}), and bioavailability (%F).

3.5.4 Efficacy data determined by electrophysiology using *Xenopus laevis* oocytes (Dr. Margot Ernst at the Medical University of Vienna) [172-175]

Ligand effects on $GABA_A$ receptors were tested by two-electrode voltage clamp experiments in cRNA injected Xenopus oocytes that functionally expressed several subtype combinations of $GABA_A$ receptors.

Preparation of cloned mRNA

Cloning of $GABA_A$ receptor subunits α1, β3 and γ2 into pCDM8 expression vectors (Invitrogen, CA) has been described elsewhere.[176] The cDNAs for subunits α2, α3 and α5 were gifts from P. Malherbe and were subcloned into a pCI-vector. After linearizing the cDNA vectors with appropriate restriction endonucleases, capped transcripts were produced using the mMessage mMachine T7 transcription kit (Ambion, TX). The capped transcripts were polyadenylated using yeast poly(A) polymerase (USB, OH) and were diluted and stored in diethylpyrocarbonate-treated water at –70 °C.

Functional expression of $GABA_A$ receptors

The methods used for isolating, culturing, injecting and defolliculating of the oocytes were identical as described previously.[173, 177, 178] Briefly, mature female *Xenopus* laevis (Nasco, WI) were anaesthetized in a bath of ice-cold 0.17 % Tricain (Ethyl-m-aminobenzoate, Sigma, MO) before decapitation and removal of the frog ovary. Stage 5 to 6 oocytes with the follicle cell layer around them were singled out of the ovary using a platinum wire loop. Oocytes were stored and incubated at 18 °C in modified Barths medium [MB, containing 88 mM NaCl, 10 mM HEPES-

NaOH (pH 7.4), 2.4 mM $NaHCO_3$, 1 mM KCl, 0.82 mM MgSO4, 0.41 mM $CaCl_2$, 0.34 mM $Ca(NO_3)_2$] that was supplemented with 100 units/mL penicillin and 100 µg/mL streptomycin. Oocytes with follicle cell layers still around them were injected with a total of 2.25 ng of cRNA. This solution contained the transcripts for the different α subunits and the β 3 subunit at a concentration of 0.0065 ng/nL as well as the transcript for the γ2 subunit at 0.032 ng/nL. After injection of the cRNA, oocytes were incubated for at least 36 h before the enveloping follicle cell layers were removed. To this end, oocytes were incubated for 20 min at 37 °C in MB that contained 1 mg/mL collagenase type IA and 0.1 mg/mL trypsin inhibitor I-S (both Sigma). This was followed by osmotic shrinkage of the oocytes in doubly concentrated MB medium supplied with 4 mM Na-EGTA. Finally, the oocytes were transferred to a culture dish containing MB and were gently pushed away from the follicle cell layer which stuck to the surface of the dish. After removal of the follicle cell layer, oocytes were allowed to recover for at least 4 h before being used in electrophysiological experiments.

Electrophysiological experiments[112, 115, 175]

For electrophysiological recordings, oocytes were placed on a nylon-grid in a bath of *Xenopus* Ringer solution (XR, containing 90 mM NaCl, 5 mM HEPES NaOH (pH 7.4), 1 mM $MgCl_2$, 1 mM KCl and 1 mM $CaCl_2$). The oocytes were constantly washed by a flow of 6 mL/min XR which could be switched to XR containing GABA and/or drugs. Drugs were diluted into XR from DMSO solutions resulting in a final concentration of 0.1 % DMSO perfusing the oocytes. Drugs were preapplied for 30 sec before the addition of GABA, which was coapplied with the drugs until a peak response was observed. Between the two applications, oocytes were washed in XR for up to 15 min to ensure full recovery from desensitization. For current measurements the oocytes were impaled with two microelectrodes (2–3 mΩ) which were filled with 2 mM KCl. All recordings

were performed at rt at a holding potential of –60 mV using a Warner OC-725C two-electrode voltage clamp (Warner Instruments, Hamden, CT). Data were digitized, recorded and measured using a Digidata 1322A data acquisition system (Axon Instruments, Union City, CA). Results of concentration response experiments were fitted using GraphPad Prism 3.00 (GraphPad Software, San Diego, CA). The equation used for fitting the concentration response curves was Y=Bottom + (Top-Bottom)/(1+10^((LogEC_{50}-X)*HillSlope)); X represents the logarithm of the concentration, Y represents the response; Y starts at the Bottom and goes to the Top with a sigmoid shape.

3.5.5 The activity of MP-III-024 (19) in the anxiolytic Vogel conflict assay (Dr. Bradford Fischer at Rowan University)

Experimentally naive adult male C57BL/6 mice (n = 6) were used as subjects. Water was withheld for 24 h prior to the first training session (habituation period). After 30 min, mice were placed in an experimental chamber for 6 min with water access. The mice went through a second 24 h water deprivation period before an i.p. pretreatment of either vehicle (0.5% methyl cellulose, 0.9% NaCl), diazepam or MP-III-024. The mice were then placed in the chamber after 30 min for another 6 min test period (suppressed session). During the suppressed session, every completion of 20 consecutive licks from the water spout was suppressed by a 0.14-mA shock (0.5 sec) to the tongue. The number of licks was recorded.

3.5.6 The activity of MP-III-024 (19) in the zymosan A model of inflammatory pain using von Frey filaments (Dr. Bradford Fischer at Rowan University)

Experimentally naive adult male C57BL/6 mice (n = 6) were used as subjects. Zymosan A (0.06 mg) was suspended in 20 µL of 0.9% NaCl solution and injected subcutaneously into the plantar surface of the right hindpaw. Mechanical sensitivity was assessed 24 h after the zymosan A

injection with a Dynamic Plantar Aesthesiometer (Ugo Basile, Varese, Italy). A pretreatment of MP-III-024 was given 30 minutes prior to testing. Von Frey filaments were used in increasing force (1 gram per second) until the paw withdrawal threshold had been reached. The left hindpaw served as the non-injured paw for a baseline (control).

3.5.7 The activity of MP-III-024 (19) tested for effects in locomotor activity (Dr. Bradford Fischer at Rowan University)

Experimentally naive adult male C57BL/6 mice (n = 6) were used as subjects. Mice were dosed i.p. with either vehicle, diazepam or MP-III-024 and the ambulatory behavior was assessed in a locomotor activity chamber (Med Associates, St Albans, VT). The total distance was recorded over a 60 min span, and expressed in 5-min bins.

3.5.8 The activity of MP-III-024 (19) assessment for operant behavior (Dr. Bradford Fischer at Rowan University)

Experimentally naive adult male C57BL/6 mice (n = 6) were used as subjects. Mice were on a fixed ratio 3 (FR3) schedule of liquid food (Ensure) and observed in an experimental operant chamber (Med Associates, St Albans, VT). Training and test sessions consisted of multiple cycle components, each culminating with a 5 minute response period. Predrug response rate was recorded over 160 minutes and used as a 100% baseline. Mice were injected i.p. with MP-III-024 and observed for 160 minutes and the response rates were expressed as a percent control relative to the pre-drug baseline value.

3.5.9 Efficacy data for MP-II-064 (27) using the IonFlux automated patch-clamp (Nina Yuan at UWM)

Patch Clamp Solutions

The intracellular solution (ICS) contained (mM): 60 KCl, 15 NaCl, 70 KF, 5 EGTA, 5 HEPES, pH 7.25 with KOH. The extracellular solution (ECS) contained (mM): 138 NaCl, 4 KCl, 1 MgCl, 1.8 $CaCl_2$, 5.6 D-glucose monohydrate, and 10 HEPES, pH 7.4 with NaOH. EC_{10} was approximated to be 0.25uM GABA.

Automated patch-clamp electrophysiology

Measurements were performed with the IonFlux instrument (Molecular Devices, Sunnyvale, CA), which utilizes microfluidic compound delivery on timescales below 100 ms, facilitating the recording of fast activating ligand gated ion channels. Using this platform, a large number of cells (20 per ensemble) can be held under voltage clamp and exposed to a series of concentrations of compound within a short time period in parallel across a plate. Continuous recording coupled with fast solution exchange enables high-throughput. The IonFlux 16 plate layout consists of units of twelve wells; two wells contain intracellular solution (cytosolic), one contains cells diluted in extracellular solution, eight contain the compounds of interest diluted in extracellular solution, and one well is for waste collection. Cells are captured from suspension by applying suction to microscopic channels in ensemble recording arrays. Once the array is fully occupied, the applied suction breaks the cell membranes of captured cells, establishing whole cell voltage clamp. For compound applications, pressure is applied to the appropriate compound wells, introducing the compound into the extracellular solution rapidly flowing over the cells. For recording $GABA_A$ currents, cell arrays were voltage clamped at a holding potential of -80 mV. IonFlux software (IonFlux App) was used for data acquisition and exported to an Excel file (Microsoft) for organization. The data was uploaded to GraphPad Prism 5 (GraphPad Software) for automated analysis of the concentration dose-response curves.

Plasmid Propagation Reagents

Plasmids containing the genes for α1-6, β3, and γ2 were generously donated by Dr. Werner Sieghart's Lab in Vienna, Austria.

Cell Culture Reagents and Instrumentation

A commercially available, stably transfected, human embryonic kidney (HEK 293T) cell containing the simian vacuolating (SV) virus 40 T-antigen origin of replication [179] was used in all the stable cell lines. The HEK 293T cells were purchased (ATCC) and cultured in 75 cm^2 flasks (CellStar) coated in Matrigel (BD Bioscience, #354234), a gelatinous protein secreted by mouse sarcoma that facilitates cell adhesion to the flask. Cells are grown in DMEM/High Glucose (Hyclone, SH3024301) media to which non-essential amino acids (Hyclone, SH30238.01), 10 mM HEPES (Hyclone, SH302237.01), 5 x 10^6 units of penicillin and streptomycin (Hyclone, SV30010), and 10% of heat-inactivated premium US-sourced fetal bovine serum (FBS) (Biowest, SO1520HI) were added. Cells were rinsed with phosphate buffered saline (Hyclone SH30256.01) without calcium or magnesium. Cells are harvested using 0.05% Trypsin (Hyclone, SH3023601) or Detachin (Genlantis T100100) which both disrupts the cell monolayer and proteolytically cleaves the bonds between the cells and flask; the latter more gently for patch-clamp study. The media utilized in transient transfections contains the same components only the FBS was heat-inactivated and dialyzed FBS (Atlanta Bio, S12650H), then cells were rinsed and shaken in Serum Free Media (Hyclone, SH30521.01).Cell transfection was conducted by lipid-based methods using Lipofectamine with PLUS reagent (Life Technologies, #15338020).

3.5.10 FLIPR functional assay (CRO)[180, 181]

Compounds

Compounds tested were synthesized internally and solubilized in DMSO at a 10 mM concentration. GABA was purchase from Sigma (#A2129) and prepared at 100 mM in water.

Cells expressing the $GABA_A$ receptor

HEK-293 cells stably transfected with the α1, β3, γ2 GABA A receptor subunits (GenBank accession numbers NM_000806.3, NM_000814.5, and NM_198904.1, respectively) or α3, β3, γ2 (NM_000808 for α3) where obtained from ChanTest Co. (Catalog # CT6216 and CT6218, respectively).

Cells were cultivated in Dulbeco's Modified Eagle's Medium (DMEM, Sigma D5796) supplemented with 10 % Fetal Bovine Serum (FBS, Gibco 16000), 0.5 mg/ml Geneticin (Gibco), 0.04 mg/ml Hygromycin B (Gibco), 0.1 mg/ml Zeocin (Gibco) and 20 mM HEPES (Sigma). Cells were grown at 37 ºC in a humidified atmosphere of 5% CO_2. In the experiments described here frozen cells were used. For this purpose, cells were gown and maintained under confluency during 2-3 weeks and then frozen down at different cell densities using Recovery™ Cell Culture Freezing Medium (Gibco).

FLIPR assays in 384 format

18 hours prior to the experiment, cells were quickly thawed at 37 ºC and seeded on Poly-D-Lys 384 plates (Corning 356663) at a density of 25,000 cells/well and in 25 uL of complete cell medium as described above.

Membrane potential changes induced by the flux of ions through the receptor were measured as relative fluorescence units (RFU) using the Fluorometric Imaging Plate Reader (FLIPR Tetra®, Molecular Devices) and the FLIPR Membrane Potential Blue Assay kit (Molecular Devices). Prior to the addition of the compounds, the medium was removed and cells were loaded with 20 µL of dye prepared in assay buffer composed of Hank's Balanced Salt Solution (HBSS with Ca^{+2} and Mg^{+2}; Gibco 14025) with 20 mM Hepes. After 1 hour of incubation at room temperature (RT), the

plate was placed into the FLIPR instrument and experiments were run adding first 10 uL from the 1st addition plate (compound plate) and after a 3 min incubation adding 20 uL of the 2nd addition or agonist plate. The response to this last GABA addition was monitored for another 3 min.

1st Addition plates or compound plates.

First addition plates containing the compounds to be tested were prepared as follows: compounds in 10 mM dimethyl sulfoxide (DMSO) stock were serially diluted from column 3 to 12 and 13 to 22 in 100 % DMSO using Corning 3657 plates and a Tecan Freedom Evo ® platform. Then, compounds were further diluted 1:100 in assay buffer. A GABA EC_0 (assay buffer alone) and EC_{100} (150 or 100 uM final GABA concentration after 1st addition for α1 or α3-containing receptor cell lines, respectively) were also included in these plates and used as minimum and maximum response controls, respectively, to analyze any possible compound agonist response.

2nd Addition plate or agonist plate.

Second addition plates were generated using a GABA EC_{20} to test the potentiation profile of the compounds. EC_{20} and EC_{100} GABA (final assay concentrations) were used as minimum and maximum response controls, respectively. EC_{20} was 2 or 1.2 uM final GABA concentration for α1 or α3-containing receptor cell lines, respectively.

Data analysis.

The difference between the maximum and the minimum (Max-Min) fluorescence reached during the first addition or read interval and the second read interval were used for data analysis (agonist and potentiation, respectively). Data was normalized according to the following formula:

$$\% \text{ activation} = 100 \times \left(\frac{\text{Test well} - \text{Median EC0 or EC20 Control}}{\text{Median EC100 Control} - \text{Median EC0 or EC20 Control}}\right)$$

Where Test well refers to those that contain test compounds.

EC_{50} and maximum stimulation values were determined from concentration-response curves at 10 distinct concentrations. The four-parameter logistic model was used to fit each data set.

3.5.11 Assessment of anxiolytic effects in the marble burying assay (CRO) [152]

Animals

Experimentally naïve, male NIH Swiss mice (Harlan Sprague–Dawley, Indianapolis, IN) were allowed to acclimate to a vivarium for at least 3 days prior to testing. They weighed between 28 and 32 g and were housed in groups of 10 to 12 in plastic cages (24 x 45 x 15 cm high) with sawdust bedding in a temperature-controlled vivarium with a 12-h light dark cycle (lights on: 0600–1800 hours). Experiments were conducted during the light phase of this cycle. The facilities in which the animals were maintained are fully accredited by the American Association for the Accreditation of Laboratory Animal Care (AAALAC) and the studies described herein were conducted in accordance with the Guide for Care and Use of Laboratory Animals under protocols approved by a local animal care and use committee.

Protocol

Mice were dosed i.p. with either vehicle (1% CMC) or a test compound 30 min prior to testing. Mice were placed in a 17 x 28 x 12 cm high plastic tub with 5 mm sawdust shavings (Harlan Sani-Chips, Harlan-Teklad, Indianapolis, IN) on the floor that were covered with 20 blue marbles (1.5

cm diameter) placed in the center. Mice were left in the tub for 30 min. The number of marbles buried (2/3 covered with sawdust) were counted and recorded.

3.5.12 Assessment for ataxic effects in the rotarod paradigm (CRO) [152]

Animals

See 3.5.11 for description

Protocol

Mice were dosed i.p. with either vehicle (1% CMC) or a test compound 30 min prior to testing. Mice were then placed on a rotarod (Ugo Basile 7650) operating at a speed of 4 revolutions/minute and observed for falling. Mice that did not fall during the 2 minutes of testing were given a "Success" designation. Mice that fell once were given a "Partial" score, while the mice that fell twice failed the test.

3.5.13 Assessment for muscle relaxation in the inverted screen test (CRO)

Animals

Male Sprague Dawley rats, (from Harlan Sprague Dawley. Indianapolis, IN), weighing 90-110 grams at time of test were employed. The animals were housed 5 per cage with *ad lib*itum food and water in a large colony room with a standard light cycle (lights on 6am, lights off 6pm). Animals were maintained in the colony room for at least 3 days before testing. Animals were moved to the quiet room 1 h prior to the start of the test.

Equipment

The apparatus for the inverted screen is made of six 13 cm x 16 cm squares or round holes, perforated stainless steel mesh (18 holes/square inch; 3/16 inch diameter, ¼ inch staggered centers, 50% open area) which are mounted 15 cm apart on a metal rod, 42 cm above the table top.

Procedure

Male Sprague-Dawley rats (n = 5) were dosed i.p. (vehicle = 1% carboxymethyl cellulose) with diazepam (3, 10 or 30 mg/kg), KRM-II-81 (10, 30 or 60 mg/kg) or HZ-166 (30 mg/kg) 30 min prior to testing. Rats were then placed onto the top of a wire screen, which was then inverted 180^{o} over a 2 – 3 second time span, so that the rats were hanging upside down. Rats were observed for 60 seconds, at which point they were scored (0 = climbed over; 1 = hanging onto screen; 2 = fell off).

3.5.14 Assessment for anxiolytic-like effects in the Vogel conflict assay (CRO) [182]

Animals

Experimentally naive adult male Sprague-Dawley rats (Harlan Industries, Indianapolis, IN), weighing between 200 and 300 g, were used as subjects. The rats were housed in Plexiglas cages (4 per cage), and given free access to Lab Diet #5001 for rodents (PMI Nutrition International Inc., St. Louis, MO). Water was withheld for 20 – 24 h prior to the first training session. A 12-h light/dark cycle was maintained, and all experimental sessions were conducted during the light phase of the cycle at about the same time each day. All experiments were conducted in accordance with the NIH regulations of animal care covered in "Principles of Laboratory Animal Care", NIH Publication 85-23, and were approved by the Institutional Animal Care and Use Committee.

Apparatus

The experiments were conducted using operant behavior test chambers ENV-007 (Med Associates Inc., Georgia, Vermont, USA), 30.5 x 24.1 x 29.2 cm. The test chambers were contained within light and sound attenuating shells. On the front wall of the chamber, a food trough was mounted 2 cm off the grid floor on the centerline. Two response levers were centered 8 cm off the centerline

and 7 cm off the grid floor. Three lights were located above each response lever at 15 cm off the grid floor. Responding on the levers was without consequences for all sessions. On the rear of the chamber, a sipping tube was mounted 3 cm off the grid floor and 3 cm from the door. The sipping tube was wrapped with electrical tape to prevent the circuit from being completed if the animals were holding/touching the tube. All events were controlled and licking data were recorded by a Compaq computer running MED-PC Version IV (Med Associates Inc., Georgia, Vermont, USA).

Sipper tube training

Rats were put into the chamber on day 1 and 2 with white noise and the houselight illuminated, and allowed to drink for a total of 6 min after the first lick was made. The 6 min was broken into two components, the first 3 min was recorded as the unpunished component and the second 3 min was recorded as the punished component. During the 2 training days no shock was delivered in the punished component. After training, animals were returned to the home cage and given access to water for 30 min. For the second and third tests for each group, water was withheld for 24 h before the training session. Animals were re-trained for 1 day. After training, animals were returned to the home cage and given access to water for 30 min.

Sipper tube testing, conflict session

On day 3, animals were weighed and injected with either vehicle or compound and returned to the home cage. Thirty minutes after injection, animals were placed into the test chamber. The session was identical to the training session except that during the punishment component the sipper tube delivered a brief electric shock (100 ms, 0.5 mA) after every 20th lick (FR20).

3.5.15 Anticonvulsant activity in the MES protocol (CRO)

Animals

Experimentally naive adult male CD mice (Harlan Industries, Indianapolis, IN), weighing between 20 and 30 g, were used as subjects. The mice were housed in Plexiglas cages (4 per cage), and given free access to Lab Diet #5001 for rodents (PMI Nutrition International Inc., St. Louis, MO).

Protocol

Male CD mice (n = 10) were pretreated i.p. with vehicle (1% CMC), KRM-II-81 (3, 10, 30 mg/kg) or HZ-166 (3, 10, 30 mg/kg) and examined for anticonvulsant effects at 30 minutes after treatment. Mice were then given a 7mA electroshock (using a Wahlquist Model H) for 0.2 seconds, and observed for the presence or absence of seizure activity. Each mouse was tested only once, and euthanized immediately following the test.

3.5.16 Anticonvulsant activity in the scMET protocol (CRO)

Animals

Male Sprague Dawley rats, (from Harlan Sprague Dawley. Indianapolis, IN), weighing 90-110 grams at time of test were employed. Animals were housed 5 per cage with *ad lib*itum food and water in a large colony room with a standard light/dark cycle (lights on 6am, lights off 6pm). Animals were maintained in the colony room for at least 3 days before testing. Animals were moved to a quiet room 1 h prior to the start of the test.

Protocol (scMET blockade)

Male Sprague-Dawley rats (n = 5) were dosed i.p. (vehicle = 1% CMC) with either diazepam (3 or 10 mg/kg), KRM-II-81 (10, 30 or 60 mg/kg), or HZ-166 (30 mg/kg) 30 min prior to testing and placed in an observation cage covered with ¼ inch of woodchips. After 30 min pentylenetetrazole (in saline) in a volume of 1 mL/kg was then injected i.p. at 35 mg/kg, and rats were observed for 30 min for signs of seizures, demonstrated by loss of righting reflex.

Protocol (scMET threshold)

Male Sprague-Dawley rats (n = 8) were dosed i.p. (vehicle = 1% CMC) with diazepam (0.1, 0.3 or 1 mg/kg) or a test compound (3, 10, 30 or 60 mg/kg) 30 min prior to testing. After the 30 min, pentylenetetrazole was administered IV to each group (10 mg/mL at 0.5 mL/min) until each animal exhibited a clonic convulsion, or for four min. Each animal was used only once, and was euthanized post testing.

3.5.17 Human epileptic cerebral cortex electrophysiology (CRO)

Tissue preparation and recording:

The block of tissue from the patient described above was then sliced into coronal sections with a thickness of 250 μm using a vibratome tissue slicer. Coronal sections were cut using white matter as landmark. After cutting, slices were bathed for ~1hr at room temperature in Artificial cerebrospinal fluid (ACSF), with 125 mM NaCl to restore Na^+ and allow cells to fire action potentials again.

In preparation for recording, slices were adhered to microelectrode arrays (MEA; Multichannel Systems, Reutlingen, Germany) with a solution of 0.1% polyethelinamine that had been previously applied and let dry for 2 hrs.[183] We attempted to place the tissue so that neocortical layers I-V covered the array. Slices were maintained thermostatically at 37° C and were perfused at 1.0 ml/min first with normal ACSF (NACSF) for one hour to see if the tissue was spontaneously active. If spontaneous activity did not develop after one hour the tissue was bathed in excitable ACSF (EACSF) solution containing 5 mM KCl and 0 mM Mg^{+2}. These external ionic concentrations are known to produce robust local field potential (LFP) activity in cortical brain slices.[184-186] Tissue was then recorded in EACSF with a concentration of 10 μM of picrotoxin for more than 1 hour. Subsequently, tissue was recorded in EACSF with a concentration of 10μM of

picrotoxin with perampanel and recorded for 1 hour. Following the perampanel addition, tissue was recorded in a washout solution of EACSF and 10 μM picrotoxin for 1 hour.

Electrode arrays.

Recordings were performed on microelectrode arrays purchased from Multichannel Systems (Reutlingen, Germany). Each array had 60 electrodes, and each electrode was 30 μm in diameter, and 30 μm high. Electrodes were arranged in a square grid with 200 μm spacing between electrodes.

Local field potential (LFP) detection.

Extracellular activity from slices was recorded in the same manner as previously reported.[187] Activity was sampled from all 60 electrodes (Fig. 3B) at 1 kHz and amplified before being stored to disk for offline analysis. Local field potentials (LFPs) that showed sharp negative peaks below a threshold set at 3 standard deviations of the signal were marked, and the time of the maximum excursion was recorded as the time of that LFP. Time points were binned at 4 ms resolution, as this was previously shown to match the average time between successive LFP events across electrodes.[188]

In characterizing network activity, we closely followed the methods as previously described.[188, 189] An avalanche is a sequence of consecutively active frames that is preceded by a blank frame and terminated by a blank frame. The length of an avalanche is given by the total number of active frames and the size of an avalanche is given by the total number of electrodes activated during the avalanche.

3.5.18 Antihyperalgesic activity in the SNL model of neuropathic pain (CRO)

Animals

Experimentally naive adult male Sprague-Dawley rats (Harlan Industries, Indianapolis, IN), weighing between 200 and 300 g, were used as subjects. The rats were housed in Plexiglas cages (4 per cage), and given free access to Lab Diet #5001 for rodents (PMI Nutrition International Inc., St. Louis, MO). Rats underwent SNL at least 90 days prior to testing.

Protocol

Rats were first tested without given an injection to determine a baseline. Following baseline establishment, rats (n = 5 for all groups) were dosed i.p. with either vehicle (1% CMC), KRM-II-81 (30 mg/kg), or gabapentin (50 mg/kg). Subjects were then tested every hour for four hours to determine the antihyperalgesic effect of the test compounds; for testing, pressure using von Frey filaments was applied to the forelimb of the rat, increasing in pressure until the limb was withdrawn and the amount of pressure recorded versus the control (opposite unaffected forelimb).

3.5.19 Antihyperalgesic activity in the CFA-model of inflammatory pain (Dr. Jun-Xu Li at the University at Buffalo)

Model of Pain

Complete Freund's adjuvant (CFA) contains *Mycobacterium butyricum,* inducing inflammation and an increase in paw thickness. The 0.1 mL of CFA was injected in the right hind paw of Sprague Dawley male rats under isoflurane anaesthesia.

Drugs

The following drugs were used: HZ-166 (**3**), KRM-II-81 (**36**), and KRM-II-18B (**38**), and were dissolved in a mixture containing 20% dimethyl sulfoxide (DMSO), 10% Emulphor-620 (Rhodia Inc.), and 70% of 0.9% saline. Flumazenil (purchased from Cayman Chemical Company, MI) was dissolved in a mixture containing 10% ethanol, 40% propylene glycol, and 50% sterile water.

Midazolam (Akorn, Inc.) was dissolved in 0.9% saline. Doses were expressed as the weight of the drug in milligrams per kilogram of body weight and drugs were administered intraperitoneally.

Mechanical hyperalgesia

Mechanical hyperalgesia was measured 3 days after CFA treatment. Rats (n=6) were placed in elevated boxes with a mesh floor. Von Frey filaments (expressed in g) were applied perpendicularly to the hindpaws, starting with the lowest filament (1.4 g) then increased until hindpaw withdrawal was observed. After each measurement, rats received the next dose of drug (every 20 min) until the maximum threshold (26 g) was observed. For the antagonist study, rats were pretreated with the benzodiazepine site antagonist flumazenil (10 min), then received the next dose of drug (every 20 min) until the pre-CFA threshold was observed.

3.5.20 Depression activity in the forced swim test (CRO)

Full experimental details are described by Porsolt *et al.*[190] Mice were placed individually in clear plastic cylinders (10 cm in diameter x 25 cm in height) filled to 6 cm with 22 – 25 ºC water for 6 minutes. The duration of immobility was recorded during the last 4 minutes of a 6-min trial. A mouse was regarded as immobile when floating motionless or making only those movements necessary to keep its head above the water.

3.6 Experimental Details

3.6.1 (2-Amino-5-bromophenyl)(pyridin-2-yl)methanone (6)[91]

To a stirred solution of 2-bromopyridine **4** (295.5 g, 1.9 mol) in dry diethyl ether under an argon atmosphere at -40 °C was added dropwise a solution of 2.5 M *n*-butyl lithium in hexanes (815 mL, 2.04 mol). The temperature was maintained at -40 °C during the addition. The resultant dark orange solution which resulted was stirred further for 1 h at -40 °C. In a separate flask, a solution of 2-amino-5-bromobenzoic acid **2** (100 g, 0.5 mol) in dry THF under a nitrogen atmosphere at 0 °C (ice bath) was transferred by cannula in one portion into the former bromopyridine solution. The mixture was stirred for 4 h at 0 °C and then treated with Me_3SiCl (75.5 g, 0.7 mol) while the stirring was continued. The reaction mixture was allowed to warm to rt and hydrolyzed with a solution of 1N aq HCl (2.3 L). The two-phase system which resulted was separated. The aq phase was neutralized with an aq solution of 3N NaOH under ice cold conditions and extracted with Et_2O (3 x 150 mL). The combined organic extracts were dried (Na_2SO_4) and the solvent was removed under reduced pressure. The yellow oil, which resulted, was purified by flash chromatography using ethyl acetate/hexanes (2 : 3) as eluent to give the title compound **3** as yellow needles (101 g, 79%): **^{1}H NMR** (300 MHz, $CDCl_3$) δ 8.73 (ddd, *J* = 4.8, 1.6, 1.0 Hz, 1H), 7.93 – 7.87 (m, 2H), 7.81 (dt, *J* = 7.8, 1.0 Hz, 1H), 7.48 (ddd, *J* = 7.5, 4.8, 1.3 Hz, 1H) 7.37 (dd, *J* = 8.8, 2.4 Hz, 1H), 6.65 (d, *J* = 8.8 Hz, 1H), 6.31 (br s, 1H). This material was used in the next step without any further characterization.

3.6.2 7-Bromo-5-(pyridin-2-yl)-1*H*-benzo[*e*][1,4]diazepin-2(3*H*)-one (7)[91]

Benzophenone **6** (40 g, 144 mmol) was dissolved in dry CH_2Cl_2 (300 mL) in a 3-neck flask and stirred using an overhead mechanical stir until a homogenous solution was obtained. Then solid $NaHCO_3$ (24.3 g, 289 mmol) was slowly added to the solution and the mixture was cooled to 0^{o}C

(ice bath). Using an addition funnel, the bromoacetyl bromide (35.0 g, 173 mmol; dissolved in 100 mL dry CH_2Cl_2) was added dropwise at 0^oC . The reaction mixture was allowed to stir overnight at ambient temperature or until the the starting material was consumed as indicated by TLC (EtOAc/hexanes, 2:1). Ice-water (400 mL) was then added to the reaction mixture to quench the reaction. The organic layer was separated, and the water layer was extracted with CH_2Cl_2 (3 x 120 mL). The organic layers were combined, and washed (200 mL each) sequentially with a sat'd aq $NaHCO_3$ solution, water, 10% HCl, brine and then dried (Na_2SO_4). The organic solution was then concentrated to 1/3 of its original volume under reduced pressure and employed in the following step without further purification.

Methanol (800 mL) was cooled to -10^oC using an ice-brine mixture in the cooling bath and saturated with anhydrous ammonia gas. The former organic solution from above was added to the solution of saturated methanolic-ammonia at 0^oC. The mixture was allowed to warm to rt and slowly heated to reflux overnight or until the starting material was consumed, as indicated by analysis by TLC (silica gel). The reaction mixture was then cooled to rt and the solvent was removed under reduced pressure. The solid which remained was washed with water as well as EtOAc and filtered to give the amide **7** as an off-white colored solid (32.4 g, 71% yield over the two steps): **^{1}H NMR** (300 MHz, $CDCl_3$) δ 8.65 (ddd, *J* = 4.8, 1.7, 09 Hz, 1H), 8.02 (dt, *J* = 7.9, 0.9 Hz, 1H), 7.85 (td, *J* = 7.7, 1.8 Hz, 1H), 7.59 (dd, *J* = 8.6, 2.3 Hz, 1H), 7.50 (d, *J* = 2.2 Hz, 1H), 7.41 (ddd, *J* = 7.5, 4.8, 1.2 Hz, 1H), 7.02 (d, *J* = 8.6 Hz, 1H), 4.39 (s, 2H); **HPLC-MS** (ESI) *m/z* (M+H) 316.00. This material was used in the next step without any further characterization.

3.6.3 Ethyl-8-bromo-6-(pyridin-2-yl)-4*H*-benzo[*f*]imidazo[1,5-*a*][1,4]diazepine-3-carboxylate (8)[91]

Amide **7** (30 g, 94.9 mmol) was dissolved in dry THF (1500 mL), and cooled to -20^{o}C, after which potassium *tert*-butoxide (13.8 g, 123.3 mmol) was added in one portion. The reaction mixture was stirred until it reached 0^{o}C and then stirred for 0.5h at 0^{o}C. The mixture was then cooled to -50^{o}C after which diethyl chlorophosphate (22.9 g, 132.8 mmol) was added and the stirring continued. Upon reaching 0^{o}C, after which it was allowed to stir for 0.5h, the solution was then cooled to -78^{o}C and ethyl isocyanoacetate (14.0 g, 123.3 mmol) was added, immediately followed by a second portion of potassium *tert*-butoxide (13.8 g, 123.3 mmol). This solution was allowed to stir overnight, during which it was allowed to warm to rt. The reaction was quenched by addition of a cold sat'd aq solution of $NaHCO_3$ (2 L) and extracted with EtOAc. The organic layers were combined and washed with brine (2 x 200 mL), dried (Na_2SO_4) and the solvent was removed under reduced pressure to afford a dark brown solid. The solid was washed with Et_2O/EtOAc (9:1) to remove some of the impurities and the remaining solid was purified by column chromatography (silica gel, EtOAc/hexanes 2:1) to afford the pure imidazobenzodiazepine **8** as an off-white solid (30.4 g, 78% yield): **^{1}H NMR** (300 MHz, $CDCl_3$) δ 8.57 (d, *J* = 4.11 Hz, 1H), 8.09 (d, *J* = 7.9 Hz, 1H), 7.90 (s, 1H), 7.83 (td, *J* = 7.7, 1.8 Hz, 2H), 7.60 (d, *J* = 2.2 Hz, 1H), 7.55 (d, *J* = 31 Hz, 1H), 7.28 (t, *J* = 7.7, 2.1 Hz. 1H), 6.11 (d, *J* = 10.4 Hz, 1H), 4.45 (m, 2H), 4.13 (d, *J* = 10.0 Hz, 1H), 1.44 (t, *J* = 7.1 Hz, 3H); **^{13}C NMR** (75 MHz, $CDCl_3$) δ 167.0, 162.8, 156.1, 148.6, 138.3, 136.8, 135.2, 134.9, 134.5, 134.3, 128.4, 124.8, 124.2, 123.9, 120.5, 60.7, 44.9, 14.3; **HPLC-MS** (ESI) *m/z* (M+H) 411.04.

3.6.4 Ethyl-6-(pyridin-2-yl)-8-((trimethylsilyl)ethynyl)-4*H*-benzo[*f*]imidazo [1,5*a*]-[1,4]diazepine-3-carboxylate (9)[91]

Imidazobenzodiazepine **8** (20 g, 48.6 mmol) from the above step was dissolved in triethylamine (650 mL) and acetonitrile (800 mL). Trimethylsilylacetylene (7.2 g, 72.9 mmol) and bis(triphenylphosphine)-palladium (II) acetate (2.0 g, 2.7 mmol) were added. A reflux column was attached and the mixture was degassed under vacuum and argon; the process was repeated four times. The solution was then heated to reflux under argon and stirred overnight. The reaction mixture was cooled to rt, filtered through celite and the celite washed with EtOAc. The filtrate was concentrated under reduced pressure. The black residue which resulted was purified by a wash column (silica gel, EtOAc/hexanes 2:1 with 1% each E_3N and CH_3OH) to afford **9** as an off-white solid (18.1 g, 87% yield): **^{1}H NMR** (300 MHz, $CDCl_3$) δ 8.56 (d, *J* = 4.11 Hz, 1H), 8.06 (d, *J* = 7.9 Hz, 1H), 7.92 (s, 1H), 7.83 (td, *J* = 7.7, 1.8 Hz, 2H), 7.55 (dd, *J* = 8.6, 1.8 Hz, 2H), 7.38 (ddd, *J* = 7.5, 4.8, 1.1 Hz, 1H), 6.13 (d, *J* = 10.4 Hz, 1H), 4.45 (m, 2H), 4.17 (d, *J* = 10.0 Hz, 1H), 1.45 (t, *J* = 7.1 Hz, 3H), 0.25 (s, 9H); **^{13}C NMR** (75 MHz, $CDCl_3$) δ 167.7, 162.8, 156.4 148.7, 138.4, 136.8, 135.6, 135.1, 135.0, 134.4, 126.9, 124.7, 123.9, 122.6, 122.2, 102.7, 97.0, 60.7, 44.9, 14.3, -0.3, (one quaternary carbon atom is embedded in one of the above peaks); **HPLC-MS** (ESI) *m/z* (M+H) 429.17.

3.6.5 Ethyl-8-ethynyl-6-(pyridin-2-yl)-4H-benzo[f]imidazo[1,5-a][1,4] diazepine-3-carboxylate (HZ-166, 3)[91]

Intermediate **9** (18 g, 42 mmol) was dissolved in THF (1 L) and cooled to -78^{o}C. This was treated with tetrabutylammonium fluoride hydrate (1 M solution in THF, 50 mmol), followed by water (18 mL). The reaction mixture was stirred at -78 ^{o}C until the starting material was consumed as indicated by TLC (silica gel), in about 0.5h. The reaction mixture was allowed to warm to -20 ^{o}C

and quenched by a slow addition of water (500 mL), followed by extraction with EtOAc (5 x 500 mL). The combined organic extracts were washed with brine (2 x 500 mL), dried (Na_2SO_4), and the solvent was removed under reduced pressure. The residue which resulted was purified by a wash column (silica gel, EtOAc/hexanes 4:1 with 1% each Et_3N and CH_3OH) to afford pure **3** as a white powder (13.6 g, 91% yield): **^{1}H NMR** (300 MHz, $CDCl_3$) δ 8.56 (d, *J* = 4.11 Hz, 1H), 8.06 (d, *J* = 7.9 Hz, 1H), 7.92 (s, 1H), 7.83 (td, *J* = 7.7, 1.8 Hz, 2H), 7.55 (dd, *J* = 8.6, 1.8 Hz. 2H), 7.38 (ddd, *J* = 7.5, 4.8, 1.1 Hz, 1H), 6.13 (d, *J* = 10.4 Hz, 1H), 4.45 (m, 2H), 6.13 (d, *J* = 10.4 Hz, 1H), 4.17 (d, *J* = 10.0 Hz, 1H), 3.17 (s, 1H), 1.45 (t, *J* = 7.1 Hz, 2H); **^{13}C NMR** (75 MHz, $CDCl_3$) δ 167.68, 162.94, 156.43, 148.75, 138.47, 136.91, 136.22, 135.45, 135.28, 134.52, 129.34, 127.08, 124.82, 124.03, 122.86, 121.2, 81.68, 79.52, 60.81, 45.04, 14.44; **HRMS** (LCMS-IT-TOF) Calc. for $C_{21}H_{17}N_4O_2$ $(M + H)^+$ 357.1307, found 357.1321.

HRMS (LCMS-IT-TOF) Calc. for $C_{22}H_{17}FN_4O$ $(M + H)^+$ 373.1459, found: 373.1462.

3.6.6 *tert*-Butyl 8-ethynyl-6-(pyridin-2-yl)-4*H*-benzo[*f*]imidazo[1,5-*a*][1,4]diazepine-3-carboxylate (MP-II-067, 10)

Ethyl ester HZ-166 **3** (200 mg, 0.56 mmol) was stirred in dry THF (10mL) in an oven-dried flask under argon at 40 ^oC; while anhydrous *tert*-butanol (3mL) was stirred in a separate oven-dried flask under an argon atmosphere at 40 ^oC. Small pieces of freshly cut Li rod (~50mg) were quickly added to *tert*-butanol and the suspension was stirred for 10 min under argon. The ethyl ester solution was then added to *tert*-butanol and it was monitored by TLC (silica gel) until most of the starting material was consumed, about 30 min. The reaction mixture was then quenched with sodium bicarbonate (sat'd aq solution, 5 mL) and the product was extracted with EtOAc. The organic layers were combined, washed with brine, dried (Na_2SO_4) and the solvent was removed under reduced pressure. The solid which resulted was purified by flash chromatography (3:2

EtOAc:hexanes with 1% each of Et_3N and CH_3OH added to the eluent) to afford pure *t*-butyl ester **10** as a white solid (132 mg, 61%): **^{1}H NMR** (300 MHz. $CDCl_3$) δ 8.58 (d, *J* = 4.6 Hz, 1H), 8.07 (d, *J* = 7.9 Hz, 1H), 7.91 (s, 1H), 7.88 – 7.78 (m, 1H), 7.75 (dd, *J* = 8.3, 1.6 Hz, 1H), 7.54 (d, *J* = 8.6 Hz, 2H), 7.37 (dd, *J* = 7.0, 5.2 Hz, 1H), 6.10 (d, *J* = 11.7 Hz, 1H), 4.14 (d, *J* = 7.9 Hz, 1H), 3.17 (s, 1H), 1.65 (s, 9H); **^{13}C NMR** (75 MHz. $CDCl_3$) δ 167.64, 162.18, 156.50, 148.78, 138.02, 136.90, 136.16, 135.61, 135.26, 134.27, 130.50, 127.07, 124.78, 124.07, 122.87, 121.09, 81.72, 81.54, 79.43, 45.16, 28.38; **HRMS** (LCMS-IT-TOF) Calc. for $C_{23}H_{21}N_4O_2$ $(M + H)^+$ 385.1620, found 385.1614.

3.6.7 Isopropyl 8-ethynyl-6-(pyridin-2-yl)-4*H*-benzo[*f*]imidazo[1,5-*a*][1,4]diazepine-3-carboxylate (MP-II-068, 11)

Ethyl ester HZ-166 **3** (500 mg, 1.403 mmol) was stirred in dry THF (10mL) in an oven-dried flask under an argon atmosphere at 40 ^oC; while anhydrous isopropanol (3mL) was stirred in a separate oven-dried flask under argon at 40 ^oC. Small pieces of freshly cut Li rod (~50mg) were quickly added to isopropanol at 40 ^oC and the suspension was stirred for 10 min under argon. The ethyl ester solution was then added to isopropanol and the mixture monitored by analysis of TLC (silica gel) until most of the starting material had been consumed (TLC, silica gel), about 30 min. The reaction solution was then quenched with sodium bicarbonate (sat'd aq solution, 5 mL) and the product was extracted with EtOAc. The organic layers were combined, washed with brine, dried (Na_2SO_4), and the solvent was removed under reduced pressure. The solid which resulted was purified by flash chromatography (3:2 EtOAc:hexanes with 1% each of Et_3N and CH_3OH added to the eluent) to afford pure *iso*-propyl ester **11** as a white solid (439.4 mg, 84.6%): **^{1}H NMR** (300 MHz. $CDCl_3$) δ 8.59 (d, *J* = 4.5 Hz, 1H), 8.08 (d, *J* = 8.0 Hz, 1H), 7.93 (s, 1H), 7.83 (t, *J* = 7.7 Hz, 1H), 7.76 (dd, *J* = 8.3, 1.5 Hz, 1H), 7.55 (d, *J* = 8.5 Hz, 2H), 7.38 (dd, *J* = 7.3, 5.0 Hz, 1H), 6.12

(s, 1H), 5.43 – 5.24 (m, 1H), 4.18 (s, 1H), 3.17 (s, 1H), 1.43 (d, *J* = 5.6 Hz, 6H); **^{13}C NMR** (75 MHz. $CDCl_3$) δ 167.64, 162.55, 156.45, 148.76, 138.44, 136.90, 136.20, 135.51, 135.26, 134.44, 129.64, 127.09, 124.80, 124.04, 122.85, 121.17, 81.70, 79.47, 68.32, 45.07, 22.01; **HRMS** (LCMS-IT-TOF) Calc. for $C_{22}H_{19}N_4O_2$ $(M + H)^+$ 371.1463, found 371.1476.

3.6.8 Cyclopropylmethyl 8-ethynyl-6-(pyridin-2-yl)-4H-benzo[f]imidazo[1,5-a][1,4]diazepine-3-carboxylate (MP-II-069, 12)

Ethyl ester HZ-166 **3** (600 mg, 1.683 mmol) was stirred in dry THF (10mL) in an oven-dried flask under argon at 40 ^oC; while anhydrous cyclopropylmethyl alcohol (3mL) was stirred in a separate oven-dried flask under an argon atmosphere at 40 ^oC. Small pieces of freshly cut Li rod (~50mg) were quickly added to cyclopropylmethyl alcohol and the suspension was stirred for 10 min under argon. The ethyl ester solution was then added to cyclopropylmethyl alcohol at 40 ^oC and monitored by analysis by TLC (silica gel) until most of the starting material had been consumed (TLC, silica gel), about 30 min. The reaction was then quenched with sodium bicarbonate (sat'd aq solution, 5 mL) and the product was extracted with EtOAc. The organic layers were combined, washed with brine, dried (Na_2SO_4), and the solvent was removed under reduced pressure. The solid which resulted was purified by flash chromatography (3:2 EtOAc:hexanes with 1% each of Et_3N and CH_3OH added to the eluent) to afford pure cyclopropyl methyl ester **12** as a white solid (508.6 mg, 79.0%): **^{1}H NMR** (300 MHz. $CDCl_3$) δ 8.60 (d, *J* = 4.8 Hz, 1H), 8.09 (d, *J* = 7.9 Hz, 1H), 7.95 (s, 1H), 7.84 (t, *J* = 7.7 Hz, 1H), 7.77 (dd, *J* = 8.4, 1.3 Hz, 1H), 7.57 (dd, *J* = 4.9, 3.3 Hz, 2H), 7.39 (dd, *J* = 7.3, 4.9 Hz, 1H), 6.13 (s, 1H), 4.15 (dd, *J* = 19.0, 11.8 Hz, 3H), 3.18 (s, 1H), 1.41 – 1.24 (m, 1H), 0.63 (q, *J* = 5.2 Hz, 2H), 0.40 (q, *J* = 5.0 Hz, 2H); **^{13}C NMR** (75 MHz. $CDCl_3$) δ 167.69, 163.06, 156.43, 148.76, 138.50, 136.93, 136.20, 135.48, 135.29, 134.56, 129.38, 127.09,

124.82, 124.03, 122.86, 121.21, 81.69, 79.50, 69.69, 45.07, 10.03, 3.55; **HRMS** (LCMS-IT-TOF) Calc. for $C_{23}H_{19}N_4O_2$ $(M + H)^+$ 383.1463, found 383.1451.

3.6.9 Propyl 8-ethynyl-6-(pyridin-2-yl)-4*H*-benzo[*f*]imidazo[1,5-*a*][1,4]diazepine-3-carboxylate (MP-II-070, 13)

Ethyl ester HZ-166 **3** (200 mg, 0.56 mmol) was stirred in dry THF (10mL) in an oven-dried flask under an argon atmosphere at 40 ^oC; while anhydrous propanol (3mL) was stirred in a separate oven-dried flask under Argon at 40 ^oC. Small pieces of freshly cut Li rod (~50mg) were quickly added to the propanol and the suspension was stirred for 10 min under argon. The ethyl ester solution was then added to propanol at 40 ^oC and monitored by analysis of the TLC (silica gel) until most of the starting material had been consumed, about 30 min. The reaction mixture was then quenched with sodium bicarbonate (sat'd aq solution, 5 mL) and the product was extracted with EtOAc. The organic layers were combined, washed with brine, dried (Na_2SO_4), and the solvent was removed under reduced pressure. The solid which resulted was purified by flash chromatography (3:2 EtOAc:hexanes with 1% each of Et_3N and CH_3OH added to the eluent) to afford pure propyl ester **13** as a white solid (128 mg, 61.5%): **^{1}H NMR** (300 MHz. $CDCl_3$) δ 8.59 (d, *J* = 4.6 Hz, 1H), 8.08 (d, *J* = 7.9 Hz, 1H), 7.93 (s, 1H), 7.89 – 7.73 (m, 2H), 7.57 (t, *J* = 4.2 Hz, 2H), 7.38 (dd, *J* = 6.8, 5.5 Hz, 1H), 6.12 (d, *J* = 9.4 Hz, 1H), 4.34 (d, *J* = 6.0 Hz, 2H), 4.23 – 4.10 (m, 1H), 3.17 (d, *J* = 1.2 Hz, 1H), 1.94 – 1.78 (m, 2H), 1.05 (dd, *J* = 8.0, 6.8 Hz, 3H); **^{13}C NMR** (75 MHz. $CDCl_3$) δ 167.66, 163.03, 156.42, 148.76, 138.44, 136.91, 136.22, 135.47, 135.28, 134.55, 129.37, 127.09, 124.81, 124.02, 122.86, 121.20, 81.69, 79.49, 66.40, 45.08, 22.12, 10.52; **HRMS** (LCMS-IT-TOF) Calc. for $C_{22}H_{19}N_4O_2$ $(M + H)^+$ 371.1463, found 371.1455.

3.6.10 *sec*-Butyl 8-ethynyl-6-(pyridin-2-yl)-4*H*-benzo[*f*]imidazo[1,5-*a*][1,4]diazepine-3-carboxylate (MP-II-071, 14)

Ethyl ester HZ-166 **3** (200 mg, 0.561 mmol) was stirred in dry THF (10mL) in an oven-dried flask under an argon atmosphere at 40 ^{o}C; while anhydrous *sec*-butanol (3mL) was stirred in a separate oven-dried flask under argon at 40 ^{o}C. Small pieces of freshly cut Li rod (~50mg) were quickly added to *sec*-butanol and the suspension was stirred for 10 min under argon. The ethyl ester solution was then added to *sec*-butanol at 40 ^{o}C and monitored by analysis by TLC (silica gel) until most of the starting material had been consumed (TLC, silica gel), about 30 min. The reaction solution was then quenched with sodium bicarbonate (sat'd aq solution, 5 mL) and the product was extracted with EtOAc. The organic layers were combined, washed with brine, dried (Na_2SO_4), and the solvent was removed under reduced pressure. The solid which resulted was purified by flash chromatography (3:2 EtOAc:hexanes with 1% each of Et_3N and CH_3OH added to the eluent) to afford pure racemic *sec*-butyl ester **14** as a white solid (145 mg, 67.1%): **^{1}H NMR** (300 MHz. $CDCl_3$) δ 8.59 (d, *J* = 4.8 Hz, 1H), 8.09 (d, *J* = 7.9 Hz, 1H), 7.93 (s, 1H), 7.83 (t, *J* = 7.7 Hz, 1H), 7.76 (dd, *J* = 8.3, 1.0 Hz, 1H), 7.56 (d, *J* = 8.6 Hz, 2H), 7.38 (dd, *J* = 7.4, 4.9 Hz, 1H), 6.12 (s, 1H), 5.25 – 5.08 (m, 1H), 4.16 (d, *J* = 9.0 Hz, 1H), 3.17 (s, 1H), 1.84 (dd, *J* = 13.9, 6.8 Hz, 1H), 1.76 – 1.64 (m, 1H), 1.39 (d, *J* = 5.7 Hz, 3H), 1.07 – 0.91 (m, 3H); **^{13}C NMR** (75 MHz. $CDCl_3$) δ 167.55, 162.63, 156.29, 148.66, 138.40, 137.03, 136.18, 135.50, 135.32, 134.48, 129.56, 127.04, 124.85, 124.11, 122.89, 121.22, 81.69, 79.50, 72.94, 45.07, 28.92, 19.68, 10.01; **HRMS** (LCMS-IT-TOF) Calc. for $C_{23}H_{21}N_4O_2$ $(M + H)^+$ 385.1620, found 385.1613.

3.6.11 Isobutyl 8-ethynyl-6-(pyridin-2-yl)-4*H*-benzo[*f*]imidazo[1,5-*a*][1,4]diazepine-3-carboxylate (MP-II-072, 15)

Ethyl ester HZ-166 **3** (200 mg, 0.56 mmol) was stirred in dry THF (10mL) in an oven-dried flask under an argon atmosphere at 40 ^{o}C; while anhydrous *iso*-butanol (3mL) was stirred in a separate oven-dried flask under argon at 40 ^{o}C. Small pieces of freshly cut Li rod (~50mg) were quickly added to *iso*-butanol and the suspension was stirred for 10 min under argon. The ethyl ester solution was then added to *iso*-butanol at 40 ^{o}C and the mixture was monitored by analysis by TLC (silica gel) until most of the starting material had been consumed (TLC, silica gel), about 30 min. The reaction was then quenched with sodium bicarbonate (sat'd aq solution, 5 mL) and the product was extracted with EtOAc. The organic layers were combined, washed with brine, dried (Na_2SO_4), and the solvent was removed under reduced pressure. The solid which resulted was purified by flash chromatography (3:2 EtOAc:hexanes with 1% each of Et_3N and CH_3OH added to the eluent) to afford pure *iso*-butyl ester **15** as a white solid (173 mg, 80.1%): **^{1}H NMR** (300 MHz. $CDCl_3$) δ 8.58 (d, *J* = 4.3 Hz, 1H), 8.08 (d, *J* = 7.9 Hz, 1H), 7.93 (s, 1H), 7.82 (td, *J* = 7.8, 1.5 Hz, 1H), 7.76 (dd, *J* = 8.3, 1.7 Hz, 1H), 7.56 (d, *J* = 8.6 Hz, 2H), 7.37 (dd, *J* = 6.5, 5.0 Hz, 1H), 6.11 (d, *J* = 10.5 Hz, 1H), 4.17 (s, 3H), 3.17 (s, 1H), 2.17 (dp, *J* = 13.4, 6.7 Hz, 1H), 1.05 (d, *J* = 6.7 Hz, 6H); **^{13}C NMR** (75 MHz. $CDCl_3$) δ 167.64, 163.01, 156.41, 148.75, 138.40, 136.91, 136.21, 135.48, 135.27, 134.62, 129.38, 127.09, 124.81, 124.01, 122.86, 121.20, 81.70, 79.49, 70.89, 45.13, 27.84, 19.32; **HRMS** (LCMS-IT-TOF) Calc. for $C_{23}H_{21}N_4O_2$ $(M + H)^+$ 385.1620, found 385.1611.

3.6.12 2-Methoxyethyl 8-ethynyl-6-(pyridin-2-yl)-4*H*-benzo[*f*]imidazo[1,5-*a*][1,4]diazepine-3-carboxylate (MP-II-073, 16)

Ethyl ester HZ-166 **3** (200 mg, 0.56 mmol) was stirred in dry THF (10mL) in an oven-dried flask under an argon atmosphere at 40 ^{o}C; while 2-methoxyethanol (3mL) was stirred in a separate oven-

dried flask under argon at 40 °C. Small pieces of freshly cut Li rod (~50mg) were quickly added to the 2-methoxyethanol and the suspension was stirred for 10 min under argon. The ethyl ester solution was then added to 2-methoxyethanol at 40 °C under argon and monitored by analysis by TLC (silica gel) until most of the starting material had been consumed, about 30 min. The reaction was then quenched with sodium bicarbonate (sat'd aq solution, 5 mL) and the product was extracted with EtOAc. The organic layers were combined, washed with brine, dried (Na_2SO_4), and the solvent was removed under reduced pressure. The solid which resulted was purified by flash chromatography (3:2 EtOAc:hexanes with 1% each of Et_3N and CH_3OH added to the eluent) to afford pure 2-methoxyethyl ester **16** as a white solid (94 mg, 43.4%): **^{1}H NMR** (300 MHz. $CDCl_3$) δ 8.57 (d, *J* = 4.3 Hz, 1H), 8.06 (d, *J* = 7.9 Hz, 1H), 7.93 (s, 1H), 7.81 (td, *J* = 7.8, 1.5 Hz, 1H), 7.75 (dd, *J* = 8.4, 1.5 Hz, 1H), 7.55 (dd, *J* = 4.8, 3.3 Hz, 2H), 7.36 (dd, *J* = 6.9, 5.3 Hz, 1H), 6.10 (d, *J* = 11.1 Hz, 1H), 4.51 (s, 2H), 4.15 (d, *J* = 10.9 Hz, 1H), 3.76 (t, *J* = 4.9 Hz, 2H), 3.42 (s, 3H), 3.17 (s, 1H); **^{13}C NMR** (75 MHz. $CDCl_3$) δ 167.56, 162.73, 156.16, 148.63, 138.63, 137.11, 136.19, 135.43, 135.38, 134.68, 129.03, 127.01, 124.92, 124.13, 122.90, 121.30, 81.65, 79.57, 70.37, 63.53, 59.00, 45.05; **HRMS** (LCMS-IT-TOF) Calc. for $C_{22}H_{19}N_4O_3$ $(M + H)^+$ 387.1412, found 387.1426.

3.6.13 Benzyl 8-ethynyl-6-(pyridin-2-yl)-4*H*-benzo[*f*]imidazo[1,5-*a*][1,4]diazepine-3-carboxylate (MP-II-075, 17)

Ethyl ester HZ-166 **3** (200 mg, 0.56 mmol) was stirred in dry THF (10mL) in an oven-dried flask under an argon atmosphere at 40 °C; while anhydrous benzyl alcohol (3mL) was stirred in a separate oven-dried flask under argon at 40 °C. Small pieces of freshly cut Li rod (~50mg) were quickly added to the benzyl alcohol and the suspension was stirred for 10 min under argon. The ethyl ester solution was then added to benzyl alcohol at 40 °C under argon and monitored by

analysis by TLC (silica gel) until most of the starting material had been consumed (TLC, silica gel), about 30 min. The reaction was then quenched with sodium bicarbonate (sat'd aq solution, 5 mL) and the product was extracted with EtOAc. The organic layers were combined, washed with brine, dried (Na_2SO_4), and the solvent was removed under reduced pressure. The solid which resulted was purified by flash chromatography (3:2 EtOAc:hexanes with 1% each of Et_3N and CH_3OH added to the eluent) to afford pure benzyl ester **17** as a white solid (138 mg, 58.8%): **^{1}H NMR** (300 MHz. $CDCl_3$) δ 8.61 – 8.56 (m, 1H), 8.08 (d, *J* = 7.9 Hz, 1H), 7.94 (s, 1H), 7.82 (td, *J* = 7.8, 1.7 Hz, 1H), 7.76 (dd, *J* = 8.3, 1.8 Hz, 1H), 7.57 (s, 2H), 7.55 – 7.47 (m, 2H), 7.42 – 7.31 (m, 4H), 6.11 (d, *J* = 11.7 Hz, 1H), 5.43 (d, *J* = 20.8 Hz, 2H), 4.15 (d, *J* = 11.4 Hz, 1H), 3.17 (s, 1H); **^{13}C NMR** (75 MHz. $CDCl_3$) δ 167.66, 162.71, 156.34, 148.73, 138.76, 136.94, 136.19, 136.05, 135.38, 135.30, 134.69, 129.02, 128.54, 128.48, 128.16, 127.07, 124.84, 124.02, 122.88, 121.25, 81.67, 79.60, 66.42, 45.05; **HRMS** (LCMS-IT-TOF) Calc. for $C_{26}H_{19}N_4O_2$ $(M + H)^+$ 419.1463, found 419.1466.

3.6.14 1-Phenyl, ethyl 8-ethynyl-6-(pyridin-2-yl)-4*H*-benzo[*f*]imidazo[1,5-*a*][1,4]diazepine-3-carboxylate (MP-II-076, 18)

Ethyl ester HZ-166 **3** (205 mg, 0.57 mmol) was stirred in dry THF (10mL) in an oven-dried flask under an argon atmosphere at 40 ^oC; while anhydrous 1-phenylethanol (5 mL) was stirred in a separate oven-dried flask under argon at 40 ^oC. Small pieces of freshly cut Li rod (~50mg) were quickly added to 1-phenylethanol and the suspension was stirred for 10 min under argon. The ethyl ester solution was then added to 1-phenylethanol at 40 ^oC under argon and the reaction mixture was stirred and monitored by analysis by TLC (silica gel) until most of the starting material had been consumed, about 30 min (TLC, silica gel). The reaction solution was then quenched with sodium bicarbonate (sat'd aq solution, 5 mL) and the product was extracted with EtOAc. The

organic layers were combined, washed with brine, dried (Na_2SO_4), and the solvent was removed under reduced pressure. The solid which resulted was purified by flash chromatography (3:2 EtOAc:hexanes with 1% each of Et_3N and CH_3OH added to the eluent) to afford pure 1-phenyl, ethyl ester **18** as a white solid (173 mg, 71.6%): **^{1}H NMR** (300 MHz. $CDCl_3$) δ 8.58 (d, *J* = 4.5 Hz, 1H), 8.08 (d, *J* = 7.7 Hz, 1H), 8.01 (s, 1H), 7.84 (dd, *J* = 11.0, 4.5 Hz, 1H), 7.76 (dd, *J* = 8.4, 1.6 Hz, 1H), 7.56 (t, *J* = 7.7 Hz, 2H), 7.50 (d, *J* = 7.2 Hz, 2H), 7.37 (dd, *J* = 14.2, 7.5 Hz, 3H), 7.28 (dd, *J* = 8.1, 6.3 Hz, 1H), 6.17 (dd, *J* = 13.2, 6.6 Hz, 2H), 4.15 (s, 1H), 3.17 (s, 1H), 1.72 (d, *J* = 5.8 Hz, 3H); **^{13}C NMR** (75 MHz. $CDCl_3$) δ 167.44, 161.98, 155.93, 148.49, 141.69, 138.60, 137.29, 136.11, 135.45, 135.35, 134.74, 128.95, 128.52, 127.83, 126.95, 126.27, 125.00, 124.22, 123.00, 121.39, 81.62, 79.66, 72.96, 44.97, 22.43; **HRMS** (LCMS-IT-TOF) Calc. for $C_{27}H_{21}N_4O_2$ $(M + H)^+$ 433.1586, found 433.1592.

3.6.15 Methyl 8-ethynyl-6-(pyridin-2-yl)-4*H*-benzo[*f*]imidazo[1,5-a][1,4]diazepine-3-carboxylate (MP-III-024, 19)

Ethyl ester HZ-166 **3** (500 mg, 1.40 mmol) was dissolved in methanol (40 mL). Sodium methoxide (303 mg, 5.61 mmol) was added in one portion and the solution was heated to reflux. The reaction mixture was monitored by analysis by TLC (silica gel, 4:1 EtOAc:hexanes) until the starting material had been consumed; approximately 30 min. The reaction solution was then cooled to rt and then quenched with a saturated aq solution of sodium bicarbonate (10 mL). Water (30 mL) was then added to the solution and the methanol was removed under reduced pressure. The product was then extracted with EtOAc (3 x 100 mL) and the organic layers were combined, washed with brine, and as well as dried (Na_2SO_4). The solution was concentrated under reduced pressure. The solid which resulted was purified via a wash column (silica gel, 4:1 EtOAc:hexanes with 1% each of Et_3N and CH_3OH added to the eluent) which provided pure methyl ester **19** as an off-white solid

(374 mg, 78.0% yield): **^{1}H NMR** (300 MHz, $CDCl_3$) δ 8.60 (d, *J* = 4.7 Hz, 1H), 8.09 (d, *J* = 7.9 Hz, 1H), 7.99 (s, 1H), 7.90 – 7.81 (m, 1H), 7.78 (dd, *J* = 8.4, 1.6 Hz, 1H), 7.59 – 7.54 (m, 1H), 7.41 (dd, *J* = 6.9, 5.4 Hz, 1H), 7.28 (s, 1H), 6.10 (s, 1H), 4.20 (s, 1H), 3.96 (s, 3H), 3.18 (s, 1H); **^{13}C NMR** (75 MHz, $CDCl_3$) δ 167.51, 163.15, 155.92, 148.49, 138.36, 137.36, 136.16, 135.49, 135.37, 134.69, 128.94, 126.94, 125.04, 124.25, 122.97, 121.41, 81.59, 79.67, 51.94, 44.94; **HRMS** (LCMS-IT-TOF) Calc. for $C_{20}H_{15}N_4O_2$ $(M + H)^+$ 343.1150, found 343.1146.

3.6.16 8-Ethynyl-6-(pyridin-2-yl)-4*H*-benzo[*f*]imidazo[1,5-*a*][1,4]diazepine-3-carboxylic acid (SR-II-54, 20)

Ethyl ester HZ-166 **3** (4 g, 11.22 mmol) was stirred in ethanol (100 mL) and sodium hydroxide (3 M, 44 mL) was added and the solution was heated at reflux for one h. The reaction solution was then cooled to rt and diluted with water (100 mL). The solution was evaporated under reduced pressure until half the solvent remained. The remaining reaction mixture was stirred at rt and aqueous hydrochloric acid (1 M) was added dropwise until the product precipitated out. The product was filtered, rinsed with water and dried to afford pure acid **20** as a white solid (2.63 g, 71.3%): **^{1}H NMR** (300 MHz, DMSO-*d*^{6}) δ 8.51 (d, *J* = 4.3 Hz, 1H), 8.41 (s, 1H), 8.06 (d, *J* = 7.8 Hz, 1H), 7.94 (t, *J* = 7.7 Hz, 1H), 7.86 (q, *J* = 8.5 Hz, 2H), 7.48 (dd, *J* = 7.1, 5.8 Hz, 2H), 5.84 (d, *J* = 9.8 Hz, 1H), 4.34 (s, 1H), 4.20 (d, *J* = 9.7 Hz, 1H).; **^{13}C NMR** (75 MHz, DMSO-*d*^{6}) δ 167.68, 164.42, 156.64, 148.77, 138.43, 137.60, 136.23, 135.92, 135.57, 135.15, 129.12, 127.19, 125.47, 124.20, 123.86, 120.35, 82.98, 82.42, 45.10; **HRMS** (LCMS-IT-TOF) Calc. for $C_{19}H_{13}N_4O_2$ $(M + H)^+$ 329.1033, found 329.1032.

3.6.17 ^{2}d-Ethyl-8-ethynyl-6-(pyridin-2-yl)-4H-benzo[f]imidazo[1,5-a][1,4] diazepine-3-carboxylate (MP-III-068, 21)

Carboxylic acid SR-II-54 **20** (2.3 g, 7.01 mmol) and cesium carbonate (4.5 g, 14 mmol) were dissolved in dry DMF (dry, 25 mL) at rt. The 1,1-dideuterated bromoethane was added and the reaction was stirred for two hr at rt. The reaction mixture was then filtered, and the solid CsBr rinsed with EtOAc. The organic layers were combined and the solvent was removed under reduced pressure. The residue that resulted was purified by flash chromatography (4:1 EtOAc:hexanes with 1% each of Et_3N and CH_3OH added to the eluent) which provided pure C(3) subtituted d^2-ethyl ester **21** as a white solid (1.34 g, 61.2%): **^{1}H NMR** (300 MHz, $CDCl_3$) δ 8.57 (d, *J* = 4.2 Hz, 1H), 8.06 (d, *J* = 7.9 Hz, 1H), 7.95 (s, 1H), 7.82 (dd, *J* = 10.7, 4.8 Hz, 1H), 7.75 (d, *J* = 8.3 Hz, 1H), 7.61 – 7.52 (m, 1H), 7.41 – 7.33 (m, 1H), 7.28 (d, *J* = 1.9 Hz, 1H), 6.09 (s, 1H), 4.16 (s, 1H), 3.16 (d, *J* = 1.7 Hz, 1H), 1.40 (s, 3H); **^{13}C NMR** (75 MHz, $CDCl_3$) δ 167.59, 162.79, 156.16, 148.62, 138.36, 137.11, 136.15, 135.40, 135.37, 134.61, 129.16, 126.98, 124.91, 124.12, 122.94, 121.28, 81.62, 79.61, 60.25, 44.98, 14.20 (-CD_2 carbon does barely appears at 60.25); **HRMS** (LCMS-IT-TOF) Calc. for $C_{21}H_{15}D_2N_4O_2$ $(M + H)^+$ 359.1462, found 359.1468.

3.6.18 (8-Ethynyl-6-(pyridin-2-yl)-4*H*-benzo[*f*]imidazo[1,5-*a*][1,4]diazepin-3-yl)methanol (MP-II-023, 22)

Ethyl ester HZ-166 **3** (1.0 g, 2.81 mmol) was dissolved in dry THF (100 mL). The $LiAlH_4$ (181 mg, 4.77 mmol) was added in one portion and the mixture was stirred at rt for 90 min. Once the starting the material was consumed, as indicated by analysis by TLC (silica gel), ice-cold water (50 mL) was slowly added to quench the excess $LiAlH_4$, and the product was extracted with EtOAc (3 x 100 mL). The organic layers were combined, washed with brine, dried (Na_2SO_4), and the solvent was removed under reduced pressure. The solid, which resulted, was purified by flash

chromatography (basic alumina, EtOAc with 3% each Et_3N and CH_3OH added to the eluent) to afford the alcohol **22** as an off-white powder (0.56 g, 63%): **^{1}H NMR** (300 MHz, DMSO) δ 8.50 (d, *J* = 4.6 Hz, 1H), 8.24 (s, 1H), 8.03 (d, *J* = 7.9 Hz, 1H), 7.94 (td, *J* = 7.7, 1.7 Hz, 1H), 7.79 (s, 2H), 7.51 – 7.44 (m, 1H), 7.38 (s, 1H), 5.31 (d, *J* = 9.7 Hz, 1H), 4.47 (d, *J* = 5.5 Hz, 2H), 4.31 (s, 1H), 4.16 (s, 1H); **^{13}C NMR** (75 MHz, DMSO) δ 167.13, 159.96, 157.12, 148.73, 138.22, 137.52, 136.49, 134.89, 129.96, 126.82, 125.28, 123.75, 119.49, 100.07, 82.58, 72.54, 56.56, 50.42, 44.71; **HRMS** (ESI) *m/z* calc'd for $C_{19}H_{15}N_4O$ $(M+H)^+$ 315.1246, found 315.1216.

3.6.19 8-Ethynyl-6-(pyridin-2-yl)-4*H*-benzo[*f*]imidazo[1,5-*a*][1,4]diazepine-3-carbaldehyde (MP-II-050, 23)

Alcohol MP-II-023 **22** (200 mg, 0.636 mmol) was dissolved in dry DCM (50 mL) under argon and cooled to 0^{o}C with an ice bath. Dess-Martin periodinane (405 mg, 0.954 mmol) was added and the reaction was stirred for 30 min at 0^{o}C. The ice bath was then removed and the reaction was allowed to stir for an additional 1.5 hours. The reaction was quenched by adding $Na_2S_2O_3$ (sat'd aq solution, 10 mL) and $NaHCO_3$ (sat'd aq solution, 10 mL), and the product was extracted with EtOAc (3 x 50 mL). The organic layers were combined, washed with brine, dried (Na_2SO_4), and the solvent was removed under reduced pressure. The solid which resulted was purified by flash chromatography (silica gel, EtOAc with 1% each Et_3N and CH_3OH added to the eluent) to afford the aldehyde **23** as a white powder (151 mg, 76%): **^{1}H NMR** (300 MHz. $CDCl_3$) δ 10.08 (s, 1H), 8.60 (d, *J* = 4.2 Hz, 1H), 8.11 (d, *J* = 7.9 Hz, 1H), 7.99 (s, 1H), 7.86 (t, *J* = 7.1 Hz, 1H), 7.79 (d, *J* = 8.4 Hz, 1H), 7.59 (d, *J* = 7.9 Hz, 2H), 7.44 – 7.38 (m, 1H), 6.04 (s, 1H), 4.21 (s, 1H), 3.19 (s, 1H); **^{13}C NMR** (75 MHz, $CDCl_3$) δ 186.92, 167.50, 155.91, 148.38, 137.66, 137.47, 136.71, 136.19, 135.51, 127.09, 125.09, 125.06, 124.22, 122.92, 122.89, 121.59, 81.54, 79.78, 44.44; **HRMS** (ESI) *m/z* calc'd for $C_{19}H_{13}N_4O$ $(M+H)^+$ 313.1089, found 313.1060.

3.6.20 *N*-Ethyl-8-ethynyl-6-(pyridin-2-yl)-4*H*-benzo[*f*]imidazo[1,5-*a*][1,4]diazepine-3-carboxamide (MP-II-037, 25)

The carboxylic acid SR-II-54 **20** (200 mg, 0.609 mmol) was suspended and stirred in CH_2Cl_2 (dry, 15 mL), after which thionyl chloride (2 mL) was added and the reaction mixture was heated to reflux. After the conversion of the acid to the acid chloride was complete, as observed by the conversion into a homogeneous solution (about 2 h.), the reaction was cooled to rt and the solvent was removed under reduced pressure. The residue which resulted was redissolved in CH_2Cl_2 (dry, 15 mL) and the solution was cooled to 0 ^oC. Ethyl amine was added and the reaction mixture was allowed to stir until the amide product formed, as indicated by analysis by TLC (silica gel). The solvent was removed under reduced pressure and the mixture was purified by flash column chromatography (3:1 EtOAc/hex with 1% each of methanol and trimethylamine added to the eluent) to afford pure cyclopropyl amide **25** (103.9 mg, 48%): **^{1}H NMR** (300 MHz. $CDCl_3$) δ 8.61 – 8.53 (m, 1H), 8.16 (d, *J* = 7.9 Hz, 1H), 7.90 – 7.79 (m, 2H), 7.76 (dd, *J* = 8.3, 1.8 Hz, 1H), 7.58 (d, *J* = 1.7 Hz, 1H), 7.53 (d, *J* = 8.4 Hz, 1H), 7.41 – 7.30 (m, 2H), 6.34 (s, 1H), 4.14 (dd, *J* = 14.3, 7.1 Hz, 1H), 3.17 (s, 1H), 2.94 – 2.82 (m, 2H), 0.88 – 0.78 (m, 3H); **^{13}C NMR** (75 MHz. $CDCl_3$) δ 167.48, 161.34, 155.72, 148.39, 138.27, 136.84, 136.05, 135.36, 135.18, 134.49, 129.98, 126.82, 124.76, 123.94, 122.75, 121.06, 81.51, 79.40, 44.86, 34.12, 14.76**; HRMS** (LCMS-IT-TOF) Calc. for $C_{21}H_{18}N_5O$ $(M + H)^+$ 356.1467, found 356.1476.

3.6.21 *N*-Cyclopropyl-8-ethynyl-6-(pyridin-2-yl)-4*H*-benzo[*f*]imidazo[1,5-*a*][1,4]diazepine-3-carboxamide (MP-II-046, 26)

The carboxylic acid SR-II-54 **20** (200 mg, 0.609 mmol) was suspended and stirred in CH_2Cl_2 (dry, 15 mL) and thionyl chloride (2 mL) was added, after which the reaction mixture was heated to reflux. After the conversion of the acid to the acid chloride was complete, observed by the

conversion to a homogeneous solution (about 2 h.), the reaction mixture was cooled to rt and the solvent was removed under reduced pressure. The residue which resulted was redissolved in CH_2Cl_2 (dry, 15 mL) and the solution was cooled to 0 ^oC. The cyclopropyl amine was added and the reaction mixture was allowed to stir until the amide product formed, as indicated by analysis by TLC (silica gel). The solvent was removed under reduced pressure and the residue was purified by flash column chromatography (3:1 EtOAc:hexanes with 1% each of methanol and trimethylamine added to the eluent) to afford pure cyclopropyl amide **26** (82.8 mg, 37%): **^{1}H NMR** (300 MHz. $CDCl_3$) δ 8.56 (d, *J* = 4.7 Hz, 1H), 8.14 (d, *J* = 7.9 Hz, 1H), 7.83 (dd, *J* = 7.7, 1.6 Hz, 1H), 7.78 (s, 1H), 7.74 (dd, *J* = 8.4, 1.7 Hz, 1H), 7.57 (d, *J* = 1.6 Hz, 1H), 7.51 (d, *J* = 8.3 Hz, 1H), 7.35 (dd, *J* = 6.8, 5.0 Hz, 1H), 7.19 (s, 1H), 6.30 (s, 1H), 4.14 (s, 1H), 3.16 (s, 1H), 2.88 (dt, *J* = 10.7, 3.6 Hz, 1H), 1.43 (t, *J* = 7.3 Hz, 2H), 0.84 (dd, *J* = 12.2, 6.9 Hz, 2H); **^{13}C NMR** (75 MHz. $CDCl_3$) δ 167.39, 161.48, 155.83, 148.45, 138.21, 136.77, 136.01, 135.42, 135.17, 134.56, 130.10, 126.71, 124.65, 124.06, 122.81, 120.98, 81.54, 79.32, 44.78, 26.14, 7.81; **HRMS** (LCMS-IT-TOF) Calc. for $C_{22}H_{18}N_5O$ $(M + H)^+$ 369.1433, found 369.1441.

3.6.22 8-Ethynyl-6-(pyridin-2-yl)-4*H*-benzo[*f*]imidazo[1,5-a][1,4]diazepine-3-carbonitrile (MP-II-064, 27)

Ethyl ester HZ-166 **3** (500 mg, 1.40 mmol) was stirred in dry xylene (35 mL) at rt; while an oil bath was heated to 80 ^oC. Using a glass syringe and metal needle, dimethylaluminum amine (0.67 M, 12.5 mL, 8.42 mmol) was carefully added to the starting material. ***Caution*: Do not breathe this amine or get it on you!** The reaction was then heated to 80^{o}C in the oil bath and the solution was monitored by analysis by TLC (silica gel) until the starting material had been consumed, about 2h. Once the reaction was complete, the mixture was cooled to rt, and quenched with cold water (15 mL). The product was extracted with EtOAc (5 x 50 mL) and the organic layers were

combined, washed with brine, dried (Na_2SO_4), and the solvent was removed under reduced pressure. The solid which resulted was purified by flash chromatography (Gradient elution; Step 1: remove excess xylene with 1:4 EtOAc:hexanes eluent; Step 2: collect the nitrile product with 1:1 EtOAc:hexanes; Step 3: collect the amide product, 4:1 EtOAc:hexanes with 1% each Et_3N and CH_3OH added to the eluent) which afforded the nitrile **27** as a white solid (208 mg, 48%) and the amide **28** (124 mg, 27%). The spectral data for nitrile **27**: **^{1}H NMR** (300 MHz, $CDCl_3$) δ 8.59 (d, *J* = 4.7 Hz, 1H), 8.09 (d, *J* = 7.9 Hz, 1H), 7.94 (s, 1H), 7.86 (td, *J* = 7.8, 1.7 Hz, 1H), 7.79 (dd, *J* = 8.3, 1.8 Hz, 1H), 7.57 (dd, *J* = 7.1, 5.1 Hz, 2H), 7.45 – 7.38 (m, 1H), 5.45 (s, 1H), 4.26 (d, *J* = 12.0 Hz, 1H), 3.20 (s, 1H); **^{13}C NMR** (75 MHz, $CDCl_3$) δ 167.64, 155.98, 148.64, 140.92, 137.23, 136.49, 135.80, 135.57, 134.77, 126.93, 125.13, 124.00, 122.70, 121.79, 113.72, 112.22, 81.41, 79.96, 44.56; **HRMS** (LCMS-IT-TOF) Calc. for $C_{19}H_{12}N_5$ $(M + H)^+$ 310.1048, found 310.1053.

Preparation of 0.67 M dimethylaluminum amine solution, CAUTION

You begin by stirring 20 mL of methylene chloride (dry) at 0 ^oC. You then bubble NH_3 (g) through the CH_2Cl_2 until the solution is saturated, about 10-15 min. The 10 mL trimethylaluminum (2.0 M in toluene) was then added while avoiding contact with air (use glass/metal syringe and needle). The solution was stirred at rt for 5 min and transferred directly for use in the reaction above using a glass syringe and metal needle. ***DO NOT BREATHE OR GET ON YOU!***

3.6.23 8-Ethynyl-6-(pyridin-2-yl)-4*H*-benzo[*f*]imidazo[1,5-a][1,4]diazepine-3-carboxamide (MP-II-065, 28)

Ethyl ester HZ-166 **3** (1 g, 2.81 mmol) and calcium chloride (311 mg, 2.81 mmol) were placed inside a sealable vessel with a stir bar. Methanol (dry, 20 mL) was added and a septum was placed on the top to seal the vessel. In a separate flask, ammonia (g) was bubbled into methanol (dry, 20 mL) until saturated; this took about 10 min. The ammonia-methanol solution was then added to

the vessel containing HZ-166 **3** and the vessel was sealed with a screw cap. The reaction mixture was heated and stirred at 85 ^{o}C for 18 hours. The reaction solution was allowed to cool to rt and the methanol was removed under reduced pressure. The solid which remained was dissolved in EtOAc and filtered to remove the calcium chloride. The filtrate was washed with brine, dried (Na_2SO_4), and the solvent removed under reduced pressure. The residue which remained was purified using flash column chromatography (EtOAc with 1% methanol and 1% trimethylamine added to the eluent) to afford the pure carboxamide **28** as a white solid (661 mg, 72%): **^{1}H NMR** (300 MHz, $CDCl_3$) δ 8.57 (d, *J* = 4.6 Hz, 1H), 8.14 (d, *J* = 8.0 Hz, 1H), 7.84 (s, 2H), 7.81 – 7.73 (m, 1H), 7.61 – 7.51 (m, 2H), 7.42 – 7.32 (m, 1H), 7.01 (s, 1H), 6.26 (s, 1H), 5.38 (s, 1H), 4.13 (s, 1H), 3.17 (s, 1H); **^{13}C NMR** (75 MHz, $CDCl_3$) δ 167.38, 164.71, 156.59, 148.59, 136.87, 136.52, 136.32, 135.53, 135.14, 133.29, 131.01, 127.14, 124.72, 124.04, 122.76, 121.07, 81.77, 79.35, 44.80; **HRMS** (LCMS-IT-TOF) Calc. for $C_{19}H_{14}N_5O$ $(M + H)^+$ 328.1154, found 328.1161.

3.6.24 5-(8-Ethynyl-6-(pyridin-2-yl)-4*H*-benzo[*f*]imidazo[1,5-*a*][1,4]diazepin-3-yl)-3-methyl-1,2,4-oxadiazole (MP-III-085, 33)

The ethyl ester HZ-166 **3** (1 g, 2.8 mmol) was dissolved in dry THF (100 mL) at rt under argon. In a separate flask which contained 3Å molecular sieves, *N*-hydroxyacetimidamide (831 mg, 11.2 mmol) was dissolved in dry THF (100 mL) under argon and treated with sodium hydride (60% dispersion in mineral oil, 281 mg, 7.0 mmol). The mixture which resulted was stirred for 15 min at which point the solution of 2'-pyridine **3** was added. The reaction mixture which resulted was stirred at rt for 3h or until the starting material was consumed as indicated by TLC (silica gel). The reaction mixture was quenched with a saturated aq $NaHCO_3$ solution (10 mL). Water (200 mL) was then added and the product was extracted with EtOAc (3 x 200 mL). The organic layers were combined, washed with brine, dried (Na_2SO_4) and the solvent was removed under reduced

pressure. The solid which resulted was purified by flash chromatography (silica gel, EtOAc/hexanes 4:1 with 1% each of Et_3N and CH_3OH added to the eluent) to afford pure methyl oxadiazole **33** as a white powder (0.76 g, 74% yield): **^{1}H NMR** (300 MHz, $CDCl_3$) δ 8.62 (d, *J* = 4.2 Hz, 1H), 8.11 (d, *J* = 7.9 Hz, 1H), 8.07 (s, 1H), 7.89 (t, *J* = 7.7 Hz, 1H), 7.81 (dd, *J* = 8.3, 1.6 Hz, 1H), 7.62 (d, *J* = 8.4 Hz, 1H), 7.57 (d, *J* = 1.5 Hz, 1H), 7.49 – 7.40 (m, 1H), 6.17 (s, 1H), 4.31 (s, 1H), 3.19 (s, 1H), 2.49 (s, 3H); **^{13}C NMR** (75 MHz, $CDCl_3$) δ 170.77, 167.76, 167.48, 156.16, 148.62, 137.15, 136.32, 136.15, 135.92, 135.48, 135.24, 127.08, 124.99, 124.70, 124.12, 122.85, 121.48, 81.59, 79.70, 44.90, 11.68; **HRMS** (LCMS-IT-TOF) Calc. for $C_{21}H_{15}N_6O$ $(M + H)^+$ 367.1263, found 367.1254.

Synthesis of the methyl oxime (N-hydroxyacetimidamide*)*

The hydroxylamine hydrochloride salt (9.73 g, 0.14 mol), potassium carbonate (41.5 g, 0.3 mol), methanol (400 mL) and water (80 mL) were mixed and stirred as well as heated to reflux. Acetonitirle (5.2 mL, 0.1 mol) was added dropwise and the reaction was stirred at reflux overnight. The next day, the reaction was cooled to 0 ^oC and a precipitate formed. The reaction mixture was filtered and the solvent of the filtrate was removed under reduced pressure. The solid which resulted was dissolved in EtOAc and washed with water, brine, and dried (Na_2SO_4). The solvent was then removed under reduced pressure to afford the methyl oxime (4.35 g, 59%) which was used in the synthesis of **33**: **HPLC-MS** (ESI) *m/z* (M+H) 75.05. This was used in the previous step without further characterization.

3.6.25 3-Ethyl-5-(8-ethynyl-6-(pyridin-2-yl)-4*H*-benzo[*f*]imidazo[1,5-*a*][1,4]diazepin-3-yl)-1,2,4-oxadiazole (MP-III-080, 34)

Ethyl ester HZ-166 **3** (200 mg, 0.561 mmol) was dissolved in dry THF (20 mL) at rt under argon. In a separate flask which contained 3Å molecular sieves, *N'*-hydroxypropionimidamide (198 mg,

2.25 mmol) was dissolved in dry THF (20 mL) under argon and treated with sodium hydride (60% dispersion in mineral oil, 56 mg, 1.40 mmol). The mixture was stirred for 15 min at which point the solution of ethyl ester **3** was added. The reaction mixture which resulted was stirred at rt for 2h or until the starting material was consumed as indicated by TLC (silica gel). The reaction mixture was quenched with a saturated aq $NaHCO_3$ solution (5 mL). Water (50 mL) was then added and the product was extracted with EtOAc (3 x 100 mL). The organic layers were combined, washed with brine, dried (Na_2SO_4) and the solvent was removed under reduced pressure. The solid which resulted was purified by flash chromatography (silica gel, EtOAc/hexanes 4:1 with 1% each Et_3N and CH_3OH added to the eluent) to afford pure ethyl oxadiazole **34** as a white powder (130 mg, 61.0%): **^{1}H NMR** (300 MHz, $CDCl_3$) δ 8.63 (d, *J* = 3.6 Hz, 1H), 8.16 – 8.05 (m, 2H), 7.91 (t, *J* = 7.4 Hz, 1H), 7.81 (d, *J* = 8.0 Hz, 1H), 7.63 (d, *J* = 8.3 Hz, 1H), 7.57 (s, 1H), 7.47 (d, *J* = 5.3 Hz, 1H), 6.20 (s, 1H), 4.32 (s, 1H), 3.19 (s, 1H), 2.86 (dd, *J* = 15.0, 7.5 Hz, 2H), 1.41 (t, *J* = 7.5 Hz, 3H); **^{13}C NMR** (75 MHz, $CDCl_3$) δ 171.93, 170.64, 167.12, 155.34, 148.00, 138.11, 136.05, 136.00, 135.89, 135.76, 135.35, 126.77, 125.33, 124.91, 124.53, 122.98, 121.64, 81.48, 79.87, 44.96, 19.78, 11.53; **HRMS** (LCMS-IT-TOF) Calc. for $C_{22}H_{17}N_6O$ $(M + H)^+$ 381.1419, found 381.1423.

Synthesis of the ethyl oxime (N'-hydroxypropionimidamide*)*

The hydroxylamine hydrochloride (9.73 g, 0.14 mol), potassium carbonate (41.5 g, 0.3 mol), methanol (400 mL) and water (80 mL) were mixed and stirred, after which the mixture was heated to reflux. The propionitrile (7.1 mL, 0.1 mol) was added dropwise and the reaction was stirred at reflux overnight. The next day, the reaction mixture was cooled to 0 ^oC and a precipitate formed. The reaction mixture was filtered and the solvent from the filtrate was removed under reduced pressure. The solid which resulted was dissolved in EtOAc and washed with water, brine, and

dried (Na_2SO_4), after which the solvent was removed under reduced pressure to afford the ethyl oxime (6.03 g, 69%) which was used in the synthesis of **34**: **HPLC-MS** (ESI) *m/z* (M+H) 89.06. This was used in the previous step without further characterization.

3.6.26 5-(8-Ethynyl-6-(pyridin-2-yl)-4*H*-benzo[*f*]imidazo[1,5-*a*][1,4]diazepin-3-yl)oxazole (KRM-II-81, 36).

The toluenesulfonylmethyl isocyanide (TosMIC, 750 mg, 3.84 mmol) was placed in a dry two neck round bottom flask and dry MeOH (100 mL) was added under an argon atmosphere. At rt, solid K_2CO_3 (1.33 g, 9.6 mmol) and the aldehyde MP-II-050 **23** (1.0 g, 3.2 mmol) were added to the reaction solution and the mixture was heated to reflux for 3 to 4 h. After the completion of the reaction on analysis by TLC (silica gel, 1:10 MeOH and EtOAc), which was indicated by the absence of aldehyde starting material [and complete conversion to the 1,3-oxazole (lower R_f,)] the reaction mixture was quenched with cold water. The solution was now reduced by one-third of the solvent volume under reduced pressure and the product was extracted with EtOAc (3 x 30 mL). The combined organic layers were washed with water, brine and dried (Na_2SO_4). The solvent was then removed under reduced pressure and the residue was purified by flash chromatography (silica gel) to give the pure 1,3-oxazole **36** as white solid (821 mg, 73%): **^{1}H NMR** (300 MHz, $CDCl_3$) δ 8.62 (d, *J* = 4.2 Hz, 1H), 8.12 (s, 1H), 8.06 (d, *J* = 7.8 Hz, 1H), 7.96 (s, 1H), 7.85 (ddd, *J* = 1.8, 6.0 Hz, 1H), 7.79 (dd, *J* = 1.8, 6.6 Hz, 1H), 7.62 (d, *J* = 8.4 Hz, 1H), 7.55 (d, *J* = 1.5 Hz, 1H), 7.53 (s, 1H), 7.41 (ddd, *J* = 1.5, 4.8 Hz, 1H), 5.78 (d, *J* = 12.9 Hz, 1H), 4.31 (d, *J* = 12.9 Hz, 1H). **^{13}C NMR** (75 MHz, $CDCl_3$) δ 167.9, 156.7, 149.9, 149.0, 146.6, 137.0, 136.4, 135.8, 135.5, 135.3, 129.8, 127.5, 127.0, 124.9, 124.0, 122.8, 122.7, 121.0, 81.8.7, 79.5, 45.3; **HRMS** (LCMS-IT-TOF) Calc. for $C_{21}H_{14}N_5O$ $(M + H)^+$ 352.1188, found 352.1193.

The synthesis of characterization of ligands 37 – 46 can be found in Appendix J.

4 CHIRAL α5 LIGANDS AND THEIR USES IN COGNITIVE DISORDERS AND ASTHMA

4.1 Introduction

The α5 $GABA_AR$ subtypes account for about 5% of all BzR-modulated α subtypes within the brain and are located primarily in the hippocampus.[53, 57] They have been implicated in cognitive effects, including memory and spatial learning.[47] Among these cognitive disorders include Alzheimer's disease,[191] Huntington's disease,[192] Down syndrome,[193] schizophrenia[194-198] and possibly depression.[199]

Schizophrenia is a mental disorder that affects nearly 1% of people worldwide[200, 201] and is characterized by positive (disorganized thought, hallucinations, delusions, psychosis) and negative symptoms (little emotion, social withdrawal), as well as cognitive deficits (working memory deficits, reversal in learning, failure in executive function).[202, 203] The most common form of management for schizophrenia is antipsychotics. Haloperidol, chlorpromazine (Figure 48) and other first-generation typical antipsychotics are thought to influence schizophrenia by targeting the dopamine D_2 receptor (D2).[204] They are effective at reducing the positive symptoms of schizophrenia; however, associated adverse effects include the development of catalepsy[205] and a range of extrapyramidal symptoms such as dystonia and parkinsonism.[205] Second-generation atypical antipsychotics, such as clozapine and olanzapine, affect the serotonin receptor 5HT-2A in addition to D2.[206] These have been shown to mildly reduce some of the negative symptoms of schizophrenia[207] and cause fewer extrapyramidal symptoms,[208] in addition to reducing the positive symptoms. However, second-generation antipsychotics are thought to be only a mild improvement over first-generation antipsychotics,[204, 207] and as many patients discontinue these forms of

treatment due to ineffectiveness and adverse effects,[203, 209] there is a need for improved forms of medication.

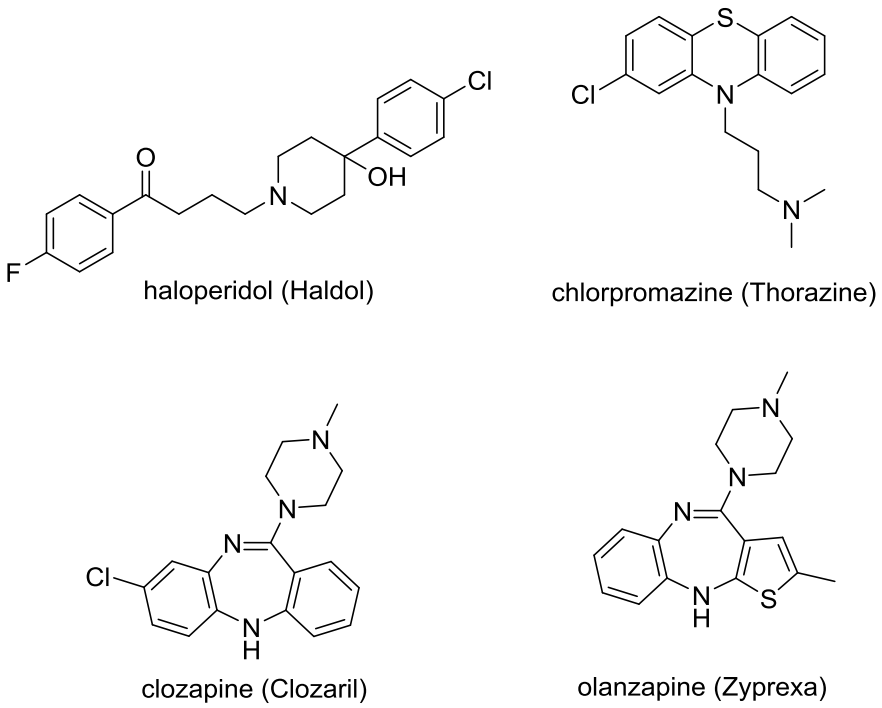


Figure 48. Typical (haloperidol, chlorpromazine) and atypical (clozapine, olanzapine) antipsychotics.

In addition to these, schizophrenia has a high rate of comorbidity,[210] in which depression, anxiety and substance abuse are common,[211, 212] along with epilepsy to a lesser extent.[213, 214] The result of these symptoms can lead to an extremely low quality of life in which patients with schizophrenia have a 10% lifetime risk of attempting suicide.[215, 216]

Outside of the CNS, the α5 and α4 subtypes have been found in the peripheral nervous system in the lungs.[66] Here, positive Bz/$GABA_A$ allosteric modulators have been shown to exhibit therapeutic potential as bronchodilators for the treatment of asthma.[64, 217] Asthma is a chronic inflammatory disease of the airways characterized by airway hyper-responsiveness, increased inflammation and increased mucous production.[218] Current treatments include beta-2 adrenoceptor

agonists, such as salbutamol or salmeterol (Figure 49), which act as bronchodilators, or corticosteroids such as beclometasonse dipropionate which acts as an anti-inflammatory agent. However, down sides to these forms of treatment include route-of-administration (mainly by inhalation), and adverse effects including cataracts and regression in stature,[219] which creates a need for an improved form of treatment. In addition, treating patients with steroids over a long period of time can lead to severe side effects.

Targeting the $GABA_A$Rs in the airway may provide an alternative approach. It is possible that a long-lived *in vivo* α4- or α5-subtype selective ligand that targets the Bz/$GABA_A$R in the lungs that does not exert CNS effects may be used as an pill to dilate the airway smooth muscle for the treatment of asthma or may be used in an inhaler. With fewer adverse effects, compliance with an oral dose or an inhaler would be much improved.

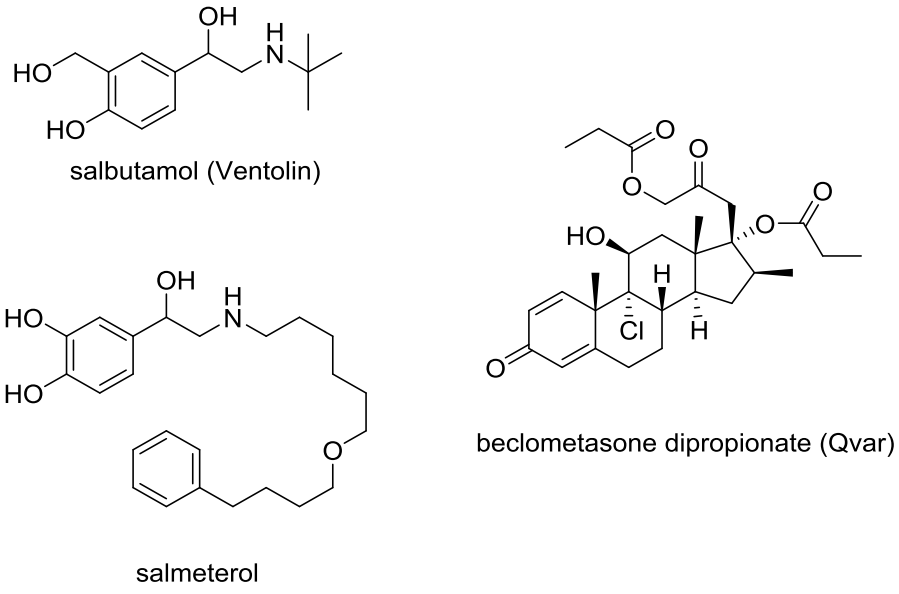


Figure 49. Fast-acting (salbutamol) and long-term control (salmeterol, beclomethasone dipropionate) medications for asthma.

4.2 Background

The α5 $GABA_AR$ subtype has been of significant interest following reports by Möhler, *et al*. using knock-in mice. In relation to this, a series of α5 negative allosteric modulators (RY-023, RY-024, RY-079 and RY-080, Figure 50) were synthesized in Milwaukee and were found to enhance memory and learning.[74, 220, 221] These were based on the structure of Ro15-4513[221] and other ligands by Roche,[222] such as flumazenil, and have been shown to be important by Helmstetter, Cook, *et al*. in the involvement of hippocampal learning and anxiety.[17, 74, 220]

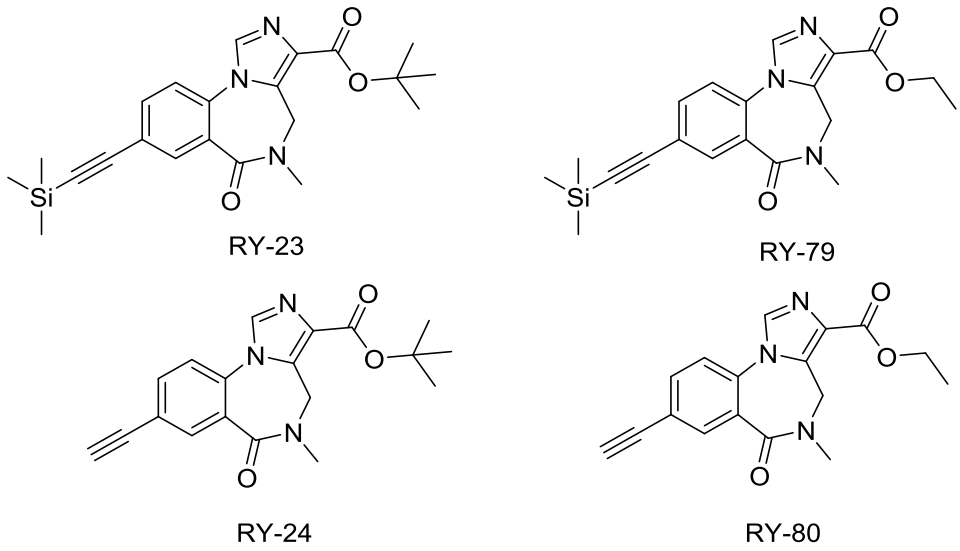
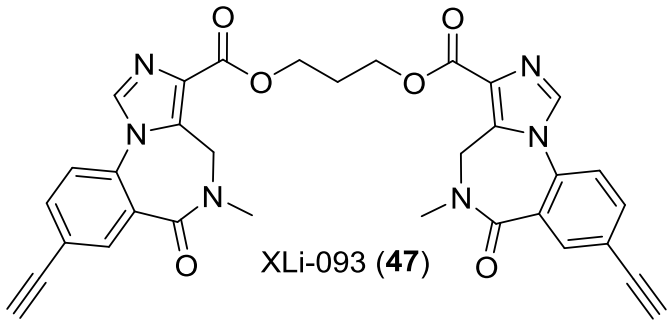


Figure 50. Structures of α5 negative allosteric modulators, RY-23, RY-24, RY-79 and RY-80.

In attempts to increase the subtype selectivity, a dimer of RY-80 was prepared to provide XLi-093 (**47**). The *in vitro* binding affinity was completed on $\alpha_{1\text{-}6}\beta3\gamma2$-$GABA_ARs$ and revealed that the bivalent ligand **47** binds selectively to the α5 subtype with a K_i of 15 nM, as depicted in Figure 51.[223] The *Xenopus laevis* oocyte efficacy was conducted by Sieghart, *et al*.[223, 224] and the analysis indicated that at concentrations up to 1 μM, XLi-093 does not trigger chloride flux though the α1, α2 or α3 $GABA_AR$ subtype, but slightly inhibited the flux through the α5 subtype. This

resulted in the development of XLi-093 (**47**) as a potent α5 antagonist. This useful tool has been shown to shift the dose-response curve of other BZDs, including diazepam, to the right and has been used extensively to study the effects of agonists (PAMs) and inverse agonists (NAMs) at the α5 subtype.[76, 220, 225, 226]



$GABA_A$ receptor binding data (K_i = nM)

α1	α2	α3	α4	α5	α6
>1000	>1000	858	>1000	15	>1000

Figure 51. Structure and binding affinity of α5 antagonist XLi-093 (47).

Additional work in this area provided the nontoxic NAM PWZ-029 (**48**), whose structure is depicted in Figure 52. Electrophysiology efficacy experiments completed by Sieghart, *et al.* demonstrated that **48** was an α5 NAM with little or no effect at the α1, α2 or α3 subtypes.[227] At physiologically relevant concentrations about 100 to 180 nM, the negative modulation can be seen at the α5 subtype with no effect at other subtypes. This ligand **48** has been shown to improve cognitive performance in the object recognition test in both rats[228] and rhesus monkeys,[74, 229] which discriminates between exploration time between familiar and novel objects. For a review of these ligands, and the forthcoming PAMs, refer to Clayton, *et al.*,[74] (see Appendix E). Because of the importance of PWZ-029 (**48**), modeling studies have been carried out to provide a rendering of **48** docked within the α5γ2 BzR subunit homology model, as depicted in Figures 53 – 56 (legend in

Figure 56 caption). These models illustrate the molecule interacting with specific amino acids, as well as π-stacking and hydrogen bonding interactions.

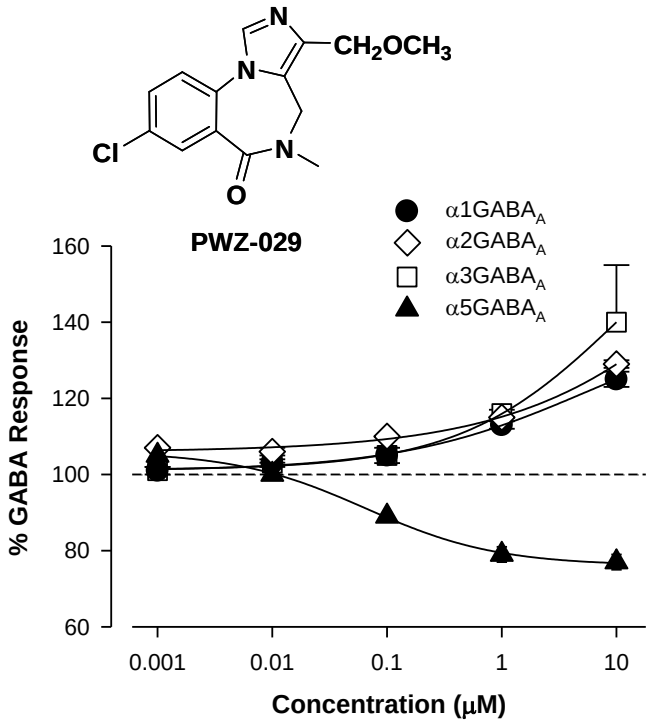


Figure 52. Structure and oocyte efficacy of PWZ-029 (48). Concentration curve of 48 on $GABA_A$ receptors using an EC_3 GABA concentration (n = 4, modified from the figure in Clayton, *et al.*).[74]

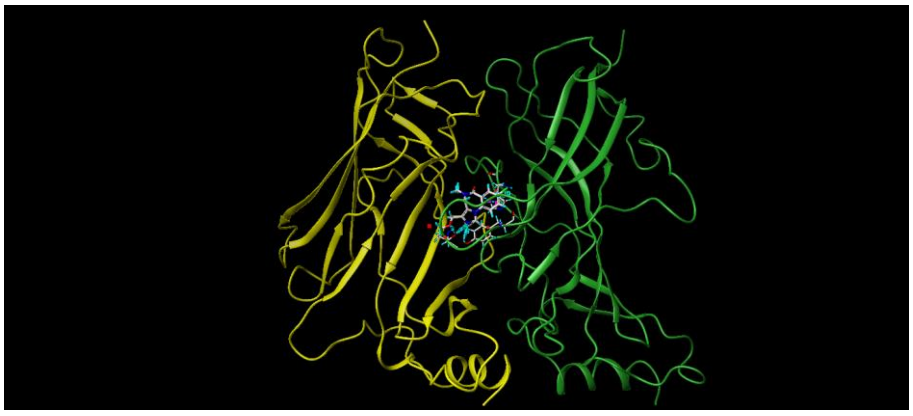


Figure 53. PWZ-029 docked within α5γ2 BzR binding site (BS). Modified from the figure in Clayton, *et al.*[74]

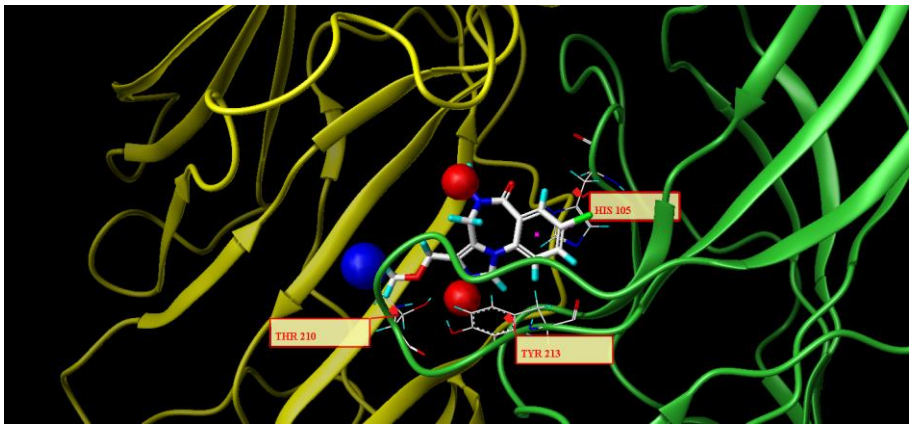


Figure 54. PWZ-029 docked with amino acid residues. Modified from the figure in Clayton, *et al*.[74]

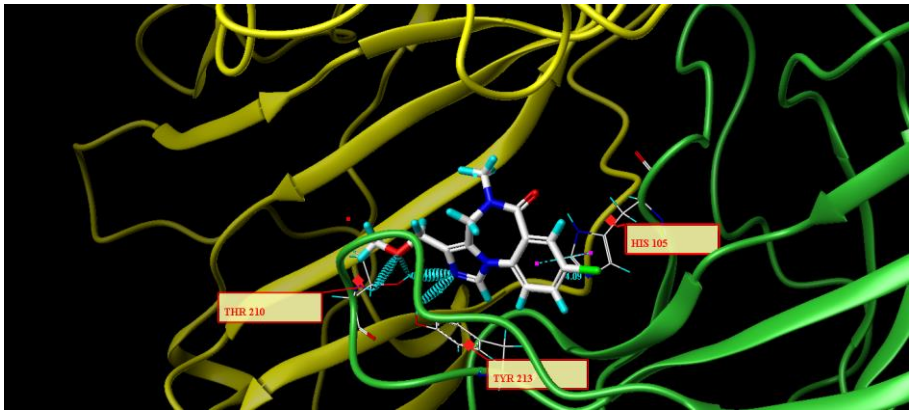


Figure 55. PWZ-029 docked with A.A. residue interactions. Modified from the figure in Clayton, *et al*.[74]

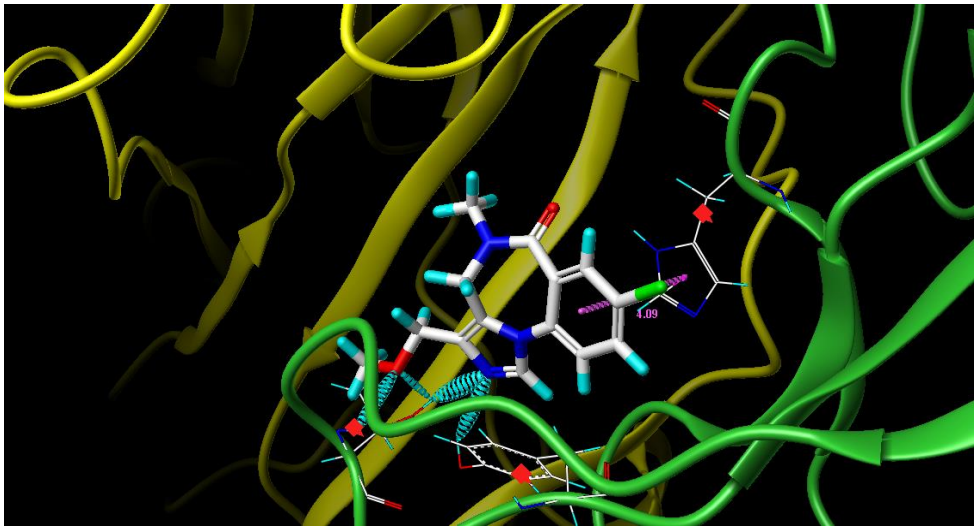
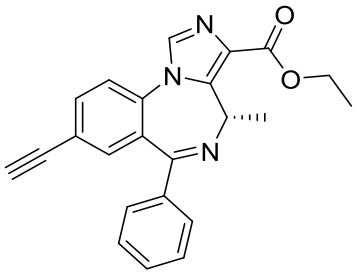
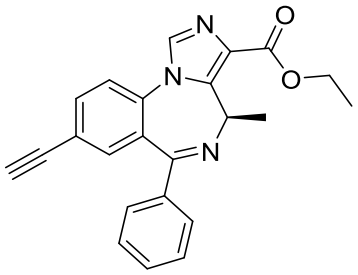


Figure 56. PWZ-029 docked with interactions. (1) HIS 105 π-stacking interaction with centroid of PWZ-029; (2) TYR 213 phenol OH hydrogen bonding to imidazole nitrogen lone pair; (3)THR 210 OH and lone pair on methoxy group of PWZ029; (4) α5 ribbon is green; (5) γ2 ribbon is yellow; (6) hydrogen bonding is aqua blue; (7) π-stacking is magenta. Modified from the figure in Clayton, *et al*.[74]

While α5 negative allosteric modulators (NAMs) decrease the flux of chloride ions through the pore which results in an excitatory effect and enhances cognition, positive allosteric modulators (PAMs) increase the concentration of chloride ions and has been shown to decrease the firing rate of synapses controlling cognition. A series of chiral enantiomeric α5 PAMs have also been used to study the α5 subtype. The first of these, SH-053-S-CH_3 (**49**) and SH-053-R-CH_3 (**50**), were found to be α2-, α3-, α5-subtype selective and α5-subtype selective ligands, respectively, as illustrated in Figure 57.



SH-053-S-CH_3 (**49**)



SH-053-R-CH_3 (**50**)

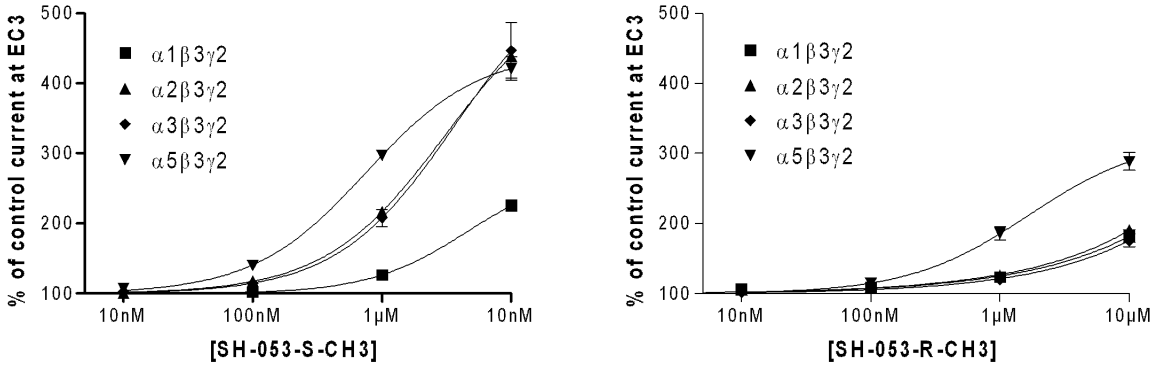
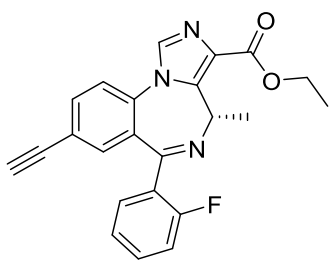


Figure 57. Structures and oocyte efficacy data of SH-053-S-CH_3 (49) and SH-053-R-CH_3 (50). Concentration curves of 49 and 50 on $GABA_A$ receptors using an EC_3 GABA concentration (n = 3-4, modified from the figures in Clayton, *et al.*).[17] These ligands were not very potent as compared to diazepam.

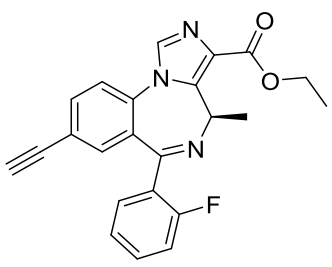
These ligands both target the α5 subtype, and as a result they have been tested in a number of behavioral assays. These included the elevated plus maze, spontaneous locomotor activity and

the rotarod for anxiolytic, sedative and ataxic properties, respectively.[230] These studies revealed that while the *S*-enantiomer **49** exerted anxiolytic-like properties, likely due to the activation of the α2 and α3 subtypes, both ligands decreased locomotor activity at 30 mg/kg in rats. Because both these ligands are α1-sparing, this indicated that sedation may be partially dependent on the activation mediated by the α5 subtype. It is possible that the sedative-like effect observed is due to the activation of the α5 subunits located in the spinal cord.[47, 57] It should be noted, however, that a decrease in locomotor activity can be attributed to a variety of causes other than sedation.[231] These ligands were not potent enough to observe robust pharmacological effects and work was discontinued.

A second series of ligands replaced the 2'-H in the pendant phenyl ring with a fluorine to produce SH-053-2'F-S-CH_3 (**51**) and SH-053-2'F-R-CH_3 (**52**), as shown in Figure 58. It was shown by Haefley many years ago that replacement of a hydrogen with an electronegative substituent at the 2'-position enhanced the potency of a ligand. This can be rationalized by a 3-centered hydrogen-bond this ligand undergoes with the receptor protein.[17, 74] These, like their predecessors, resulted in a α2-, α3-, α5-subtype selective ligand for the *S*-enantiomer **51** and an α5-subtype selective ligand for the *R*-enantiomer **52**. While the *S*-enantiomer **51** displayed an efficacy profile similar to **49** with increased potency, SH-053-2'F-R-CH_3 (**52**) remained an α5 selective ligand, but was much more potent than its 2'-H predecessor **50**.



SH-053-2'F-S-CH_3 (**51**)



SH-053-2'F-R-CH_3 (**52**)

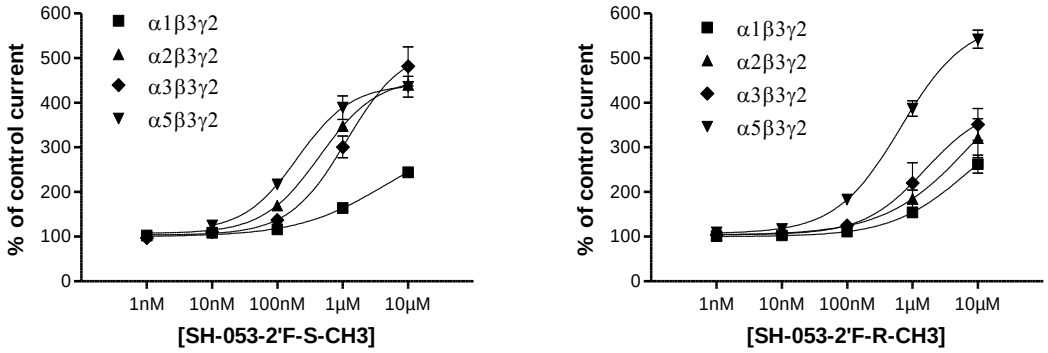


Figure 58. Structures and oocyte efficacy data of SH-053-2'F-S-CH_3 (49) and SH-053-2'F-R-CH_3 (50). Concentration curves of 49 and 50 on $GABA_A$ receptors using an EC_3 GABA concentration (n = 3-5).

These ligands have undergone behavioral studies and have indicated that the *S*-enantiomer **51** exerts anxiolytic activity in both rats[113] and rhesus monkeys[112] while **52** does not unless administered at a very high dose. This, again, was due to efficacy activation at the α2 and α3 subtypes by the *S*-enantiomer **51**. These ligands provided a framework of how chiral enantiomers can be applied for different therapeutic uses similar to many other drugs including (+)-naloxone versus (-)-naloxone.

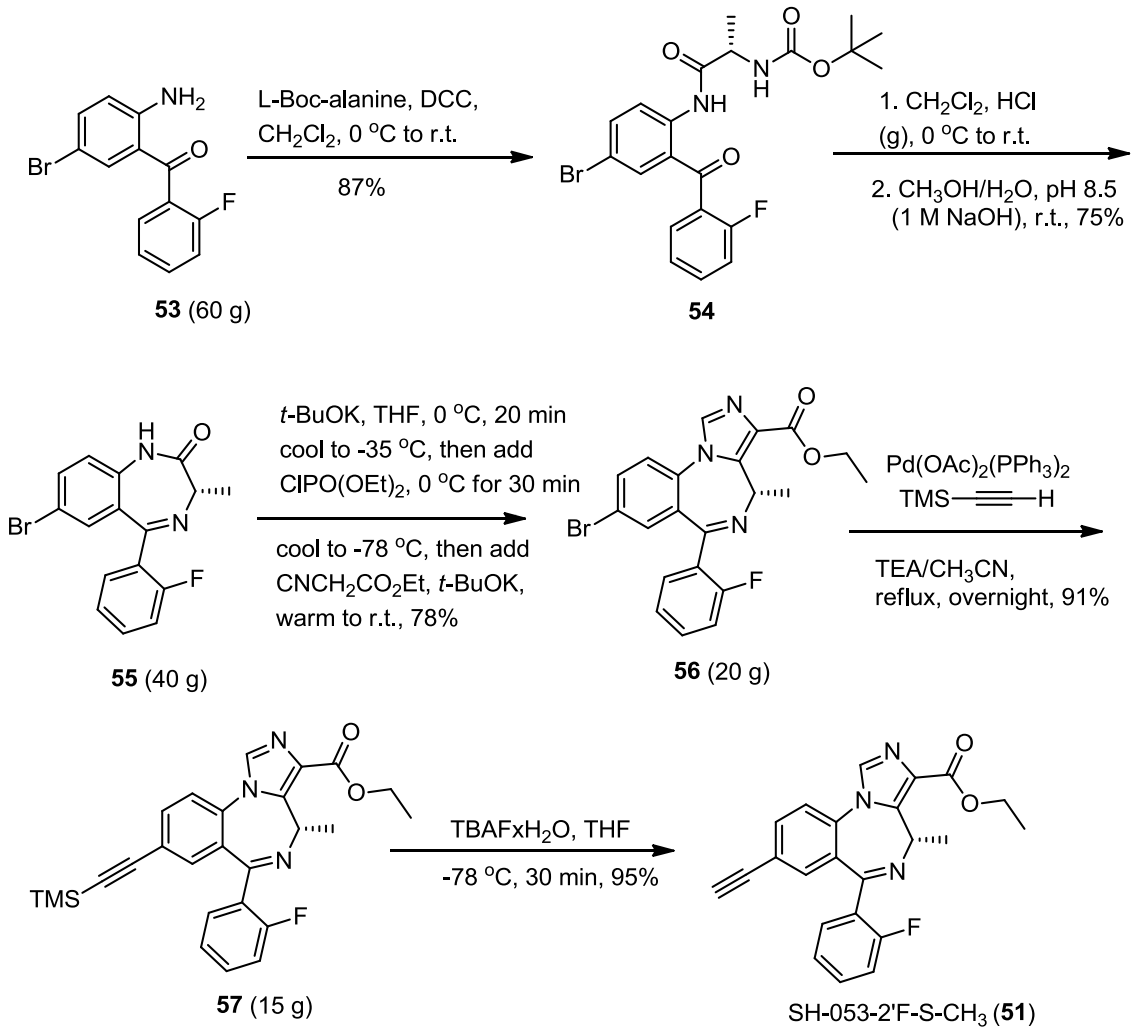
4.3 Chemistry and Results

4.3.1 Synthesis of SH-053-2'F-S-CH_3 (51) and SH-053-2'F-R-CH_3 (52)

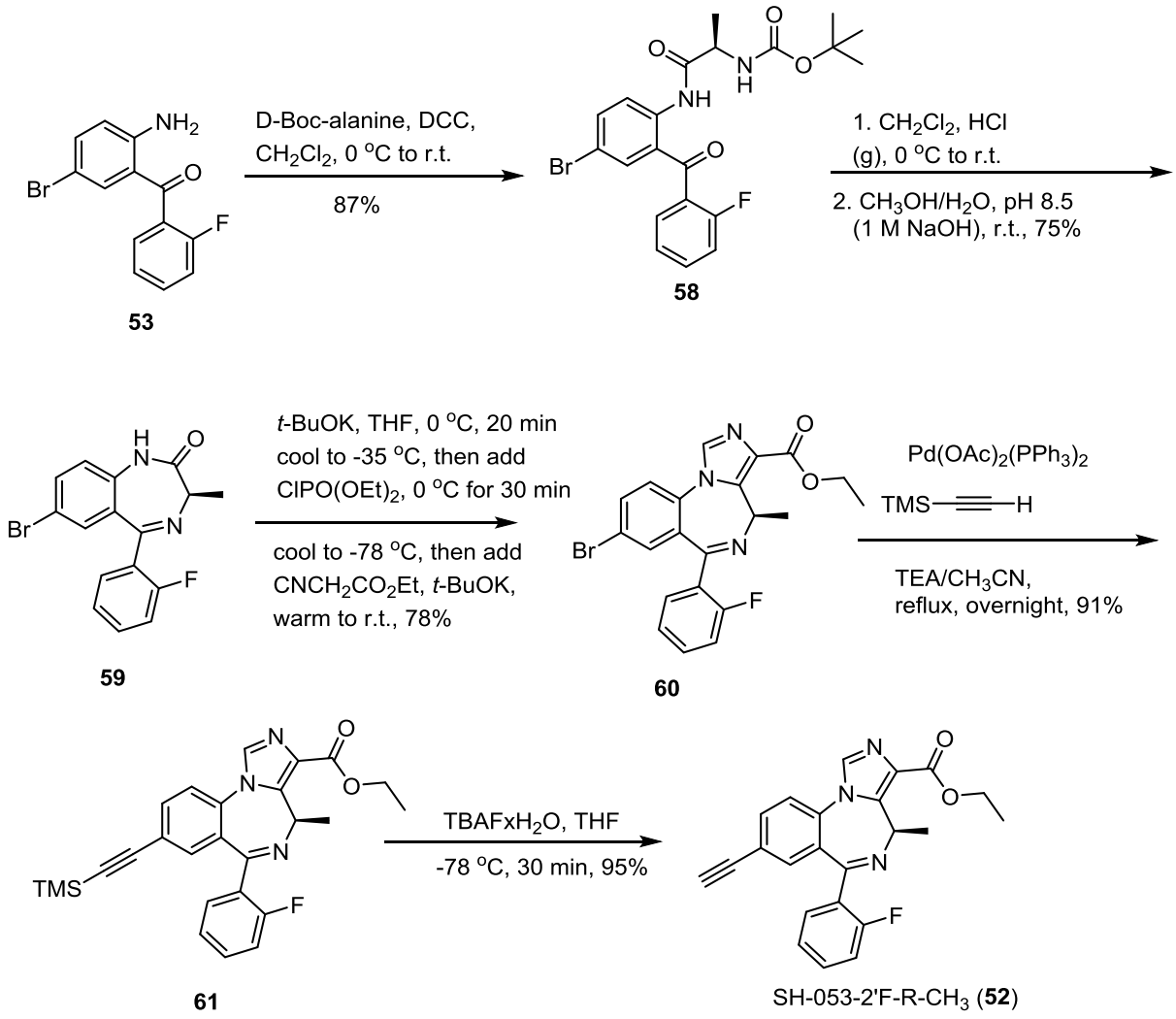
The synthesis of SH-053-2'F-S-CH_3 (**51**) was undertaken on large scale, as illustrated in Scheme 13. An amidation reaction coupling commercially available (2-amino-5-bromophenyl)(2-fluorophenyl)methanone **53** and L-Boc-alanine was performed to provide the amide **54** using *N*,*N*'-dicyclohexylcarbodiimde at room temperature in 87% yield. The amide was then subjected to a Boc-deprotection in a saturated methylene chloride-ammonia (g) solution, followed by cyclization

to form the basic 1,4-benzodiazepine structure **55** in 75% yield. The imidazole ring was prepared using the improved method[118] by treating amide **55** with potassium *tert*-butoxide and diethylchlorophosphate at -35 ^{o}C and this was followed by the addition of potassium *tert*-butoxide and ethyl isocyanate at -78 ^{o}C to provide **56** in 78% yield. The previous method used sodium hydride as a base, and yields were consistently below 40%. A Heck-type coupling reaction with the bromide **56** and trimethylsilylacetylene provided the TMS ligand **57**, which was deprotected using tetrabutylammonium fluoride at -78 ^{o}C to provide SH-053-2'F-R-CH_3 **51** in 86% overall yield over the final two steps. The enantiomer, SH-053-2'F-R-CH_3 **52**, was prepared in similar yields via the same route by replacing L-Boc-alanine with D-Boc alanine in the first step, and is shown in Scheme 14.

Scheme 13. Synthesis of SH-053-2'F-S-CH3 (51). *Amounts listed are the largest scale for each reaction in the synthesis of either (S)- **51** or (R)- **52**. They do not correspond to the product which resulted from the previous reaction.*



Scheme 14. Synthesis of SH-053-2'F-R-CH_3 (52).



4.3.2 Properties and Pharmacokinetics of SH-053-2'F-S-CH_3 (51) and SH-053-2'F-R-CH_3 (52)

An advantage to this synthetic route was that it provided each compound enantiomerically pure, as shown by analysis by chiral HPLC by Huang.[143] This also confirmed these ligands do not undergo racemization during the synthesis. This is important because enantiomers can exert different pharmacological responses, as mentioned previously, and is a common occurrence with enantiomeric drugs. In some cases, one enantiomer has been shown to have a therapeutic use,

while the other causes harmful adverse effects or is toxic, as seen with thalidomide and others.[232-236] These instances require chiral resolution and is an expensive, yet necessary, added step.[237] In other cases, a chiral pharmaceutical drug is given as a racemic mixture, when one enantiomer is active and the other is inactive.[232] This can lead to waste that can be as high as 50%. Although these enantiomers **51** and **52** were made enantiomerically pure, it was still possible that they could undergo chiral inversion *in vitro* or *in vivo*, which can lead to the development of the unwanted enantiomer, as was the case with thalidomide.[237] Examination of the liver microsomal studies in Table 8 illustrates that this does not happen.

Table 8. Liver microsomal stability and cytotoxicity of 51 and 52.

Ligand	Liver Microsomes Stability (%-Remaining) *Conditions*: 4 µM compound, 37 °C, 30 minutes				Cytotoxicity[b] (18 h.)
	HLM[a]	DLM[a]	MLM[a]	RLM[a]	LD_{50} (µM)
SH-053-2'F-S-CH_3 (**51**)	2.3	90.7	66.5	6	142
SH-053-2'F-R-CH_3 (**52**)	100	90.3	59.1	5.4	271

[a] Human liver microsomes (HLM), dog liver microsomes (DLM), mouse liver microsome (MLM) and rat liver microsomes (RLM).
[b] Ligands were incubated in HEK293T cells for 18 hours and the cell death was assessed by luminescence.

Analysis of the data on HLMs indicated that it was very unlikely that either enantiomer **51** nor **52** underwent chiral inversion. This was clear because the *S*-enantiomer **51** was at nearly 0% of the parent ligand **51** remaining after a 30 minute incubation time and the *R*-enantiomer **52** was not degraded at all; 100% of the parent ligand **52** remained after the 30 minute incubation. If one of these ligands were to undergo chiral inversion, the results would not be as dramatically different for the *S*-enantiomer **51** as compared to the *R*-enantiomer **52**. The metabolic stability would be similar rather than completely opposite. The results of this study have been repeated, albeit under slightly different conditions, and also confirmed that SH-053-2'F-S-CH_3 (**51**) was completely

degraded during the HLM incubation while SH-053-2'F-R-CH_3 (**52**) remained at 100% of the parent ligand **52** at the end of the study (Rahul Edwankar, Ph.D. Thesis, see reference in his Appendix).[116] The same conclusion cannot be made in DLMs, MLMs or RLMs, as the metabolism of each enantiomer was nearly the same at around 90%, 63% and 6%, respectively. This may also not translate into the same results *in vivo*. However, even chemically both the *S*- and *R*-enantiomers were stable for the conversion of the benzodiazepine to the imidazobenzodiazepine, which required stirring the ligand in the presence of potassium tertbutoxide at room temperature took place with no racemization (Shengming Huang, Ph.D. Thesis).[143]

Benzodiazepines are widely considered to have low toxicity concerns.[154] To confirm this, the cytotoxicity of **51** and **52** were investigated in HEK293T cells (Kelly Teske, University of Wisconsin-Milwaukee). As expected, the LD_{50} of neither SH-053-2'F-S-CH_3 (**51**) nor SH-053-2'F-R-CH_3 (**52**) are a concern, at 142 µM and 271 µM, respectively, after 18 hours of incubation time. Moreover, they are different as expected. The assays were also run for a 48-hour time span and similar results were observed. These concentrations are 150- and 10,000-fold higher than the respective binding constants for **51** and **52**.[112] This was also consistent with data for **51** and **52** from the PDSP program (B. Roth, UNC) where these two analogs did not bind to other receptors nor had hERG activity.

In regard to metabolism, the concentration-time profiles of the enantiomers **51** and **52** in rat plasma and brain were taken following a 10 mg/kg i.p. dose, and the results are displayed in Figures 59 and 60, and Table 9. These studies by Dr. Miroslav Savić, *et al*. yielded interesting results. Because the *in vitro* rat liver microsomal studies resulted in about 6% remaining for both enantiomers, it was expected that the *in vivo* pharmacokinetic studies would also lead to similar results between the *S*-enantiomer **51** and the *R*-enantiomer **52**. Instead, SH-053-2'F-R-CH_3 (**52**)

was found to be much more stable *in vivo* than SH-053-2'F-S-CH_3 (**51**), with half-lives of 5.39 and 2.84 hours in plasma, respectively. In addition, importantly the *R*-enantiomer **52** had a C_{max} of nearly 10-fold greater than the *S*-enantiomer **51**, with 154.85 and 18.13 ng/mL, respectively. Interestingly, there were some similarities in brain concentrations more than what would be expected based on the plasma concentrations. The *S*-enantiomer **51** exhibited a brain C_{max} greater than what was reached when dosed with the *R*-enantiomer **52**, at 304.65 and 123.16 ng/mL, respectively. It must be remembered that the *R*-CH_3 enantiomer **52** was synthesized by the employment of the unnatural D-alanine and would be expected to be metabolized *in vivo* at a slower rate than the *S*-CH_3 enantiomer **51** which was synthesized using the natural L-alanine.

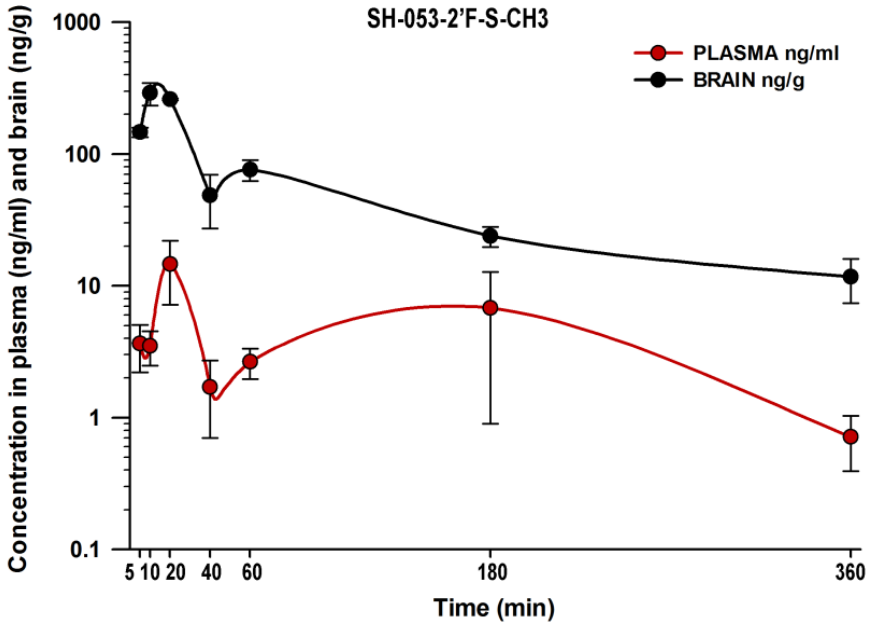


Figure 59. Plasma and brain concentration-time profile of SH-053-2'F-S-CH_3 (51) after 10 mg/kg i.p. administration in male Wistar rats (n = 3) for up 6 hours.

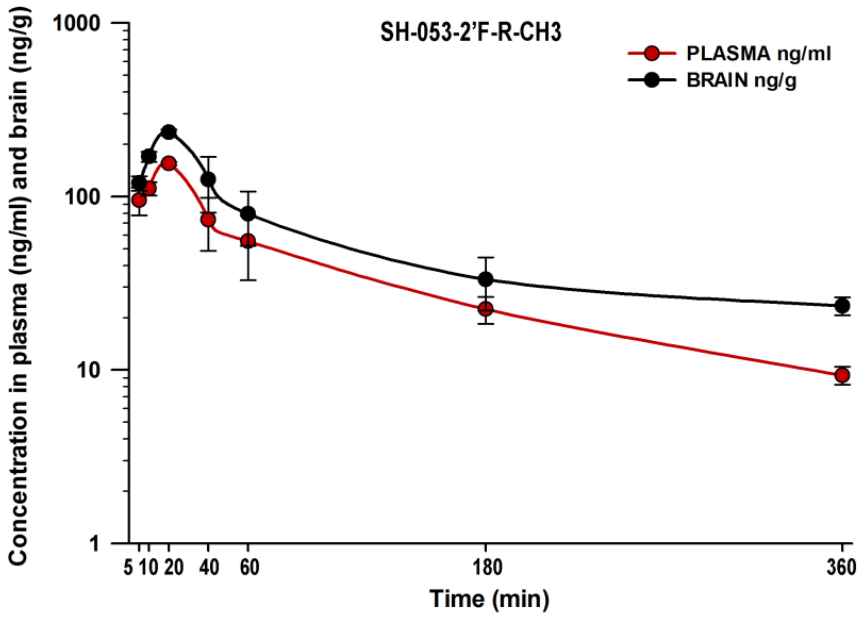


Figure 60. Plasma and brain concentration-time profile of SH-053-2'F-R-CH_3 (52) after 10 mg/kg i.p. administration in male Wistar rats (n = 3) for up to 6 hours

Table 9. Pharmacokinetic data of SH-053-2'F-S-CH_3 (51) and SH-053-2'F-R-CH_3 (52) after 10 mg/kg i.p. administration in male Wistar rats (n = 3)

SH-053-2'F-S-CH_3 (**51**)					
Plasma	Mean	SEM	**Brain**	Mean	SEM
C_{max} (ng/ml)	18.13	6.58	C_{max} (ng/g)	304.65	49.27
T_{max} (h)	1.14	0.93	T_{max} (h)	0.28	0.06
AUC_{0-6} (ng*h/ml)	26.04	13.95	AUC_{0-6} (ng*h/g)	289.61	8.14
$AUC_{0-\infty}$ (ng*h/ml)	29.96	16.61	$AUC_{0-\infty}$ (ng*h/g)	336.35	26.05
β	0.33	0.11	β	0.39	0.12
$t_{1/2}$ (h)	2.84	1.14	$t_{1/2}$ (h)	2.22	0.76
SH-053-2'F-R-CH_3 (**52**)					
Plasma	Mean	SEM	**Brain**	Mean	SEM
C_{max} (ng/ml)	154.85	3.56	C_{max} (ng/ml)	234.16	9.49
T_{max} (h)	0.33	0.00	T_{max} (h)	0.33	0.00
AUC_{0-6} (ng*h/ml)	215.61	28.75	AUC_{0-6} (ng*h/g)	337.62	60.46
$AUC_{0-\infty}$ (ng*h/ml)	289.24	25.66	$AUC_{0-\infty}$ (ng*h/g)	511.45	21.29
β	0.30	0.12	β	0.20	0.07
$t_{1/2}$ (h)	5.39	3.73	$t_{1/2}$ (h)	5.94	3.36

4.3.2.1 Potential Metabolism of SH-053-2'F-S-CH_3 (51) and SH-053-2'F-S-CH_3 (52) in the CNS

Analysis of the concentration-time pharmacokinetic profiles resulted in a few theories as to why the brain concentration levels are similar, yet there is a significant discrepancy between the plasma concentrations of SH-053-2'F-S-CH_3 (**51**) and SH-053-2'F-R-CH_3 (**52**). One hypothesis is that the *S*-enantiomer **51** which was synthesized from the natural Boc-L-alanine underwent active transport into the brain at a much fast rate than the *R*-enantiomer **52** which was prepared from the unnatural Boc-D-alanine. A second hypothesis assumed that both ligands are actively transported into the brain; however, the *R*-enantiomer **52** was readily metabolized within the brain as compared to the *S*-enantiomer **51**. Cytochrome P450 isozymes primarily metabolize exogenous compounds in the liver, but are also found in the brain,[238] albeit at about 1% concentration compared to the liver.[239] This second hypothesis has a low probability based on; 1) RLMs degrade the isomers at a comparable rate, and; 2) HLMs quickly degrade the *S*-enantiomer **51** while the *R*-enantiomer **52** is completely stable over a 30 minute time span. These two factors indicated a low likelihood that the second hypothesis, wherein the *R*-enantiomer **52** was metabolized faster, was the case. Irregardless, a 24 hour *in vitro* rat brain metabolism assay was conducted and the results are presented in Figure 61. The brain of a male Wistar rat was extracted and homogenized with phosphate buffer solution. The ligands **51** and **52** were then incubated at 37 ^{o}C for 24 hours, and the % of the parent compound remaining was analyzed by mass spectrometry. The results show that the *S*-isomer (50% remaining after 24 hours) was degraded at a faster rate than the *R*-isomer (84%).

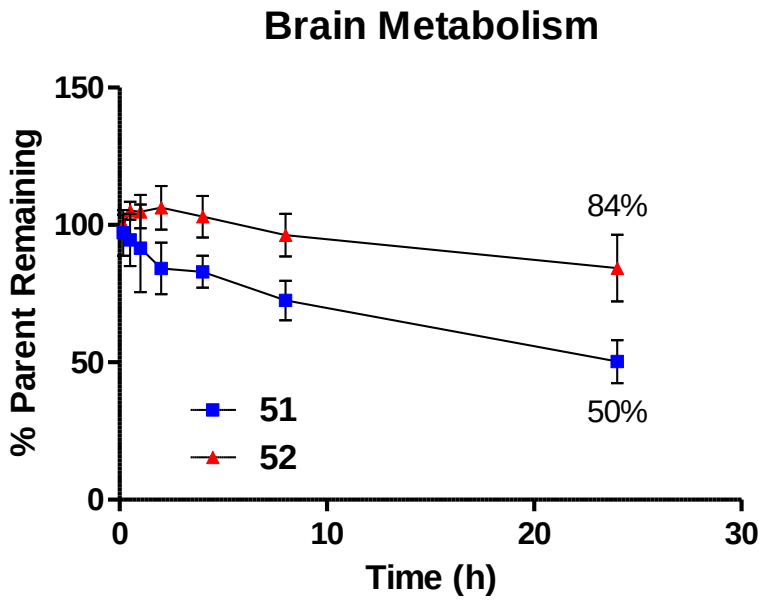


Figure 61. Results of 51 and 52 in a rat brain metabolism assay (n = 12). Brains were extracted from male Wistar rats, homogenized and incubated individually with each compound (10 µM compound concentration) for 24 hours. Results presented as average ± SEM.

These ligands have also been sent to PDSP for screening at the multidrug-resistance transport (MDR-1) transporter, which is a P-glycoprotein that transports xenobiotic compounds out of the brain.[240] It is possible that the *R*-enantiomer **52** is a substrate for MDR-1 which rapidly transports the ligand out of the brain and lowers the brain concentration while the *S*-enantiomer **51** is not. These studies are currently underway. Until the MDR-1 study has been completed, the reason for the contrast in brain concentrations is unknown, but appears that the *S*-enantiomer **51** was actively transported into the brain at a faster rate than the *R*-enantiomer **52**.

4.3.3 Pharmacological Differences between the Enantiomers, SH-053-2'F-S-CH_3 (51) and SH-053-2'F-R-CH_3 (52) and their Potential to Treat Schizophrenia.

Recently, these ligands, **51** and **52**, have been studied due to their ability to activate the α5 $GABA_AR$ subtype while remaining near-silent at α1 reducing the risks of adverse effects. Avoiding activation of the α1 subtype when targeting schizophrenia is important. First, cognitive disorders in schizophrenia have been proposed to involve the α5 subtype and the coupling of the α1 subtypes to the α5 subtypes would certainly confound this study including observations in the PCP- or MK-801-mediated prepulse inhibition of acoustic startle paradigm and also studies of catalepsy; an adverse effect of some antipsychotic drugs. Also, it has been predicted that increased firing of dopaminergic neurons can be triggered by activation of the α1 subtype and should be avoided as this could further exacerbate the symptoms of schizophrenia.[52, 170] Hyperdopaminergic levels have long been correlated with the etiology of schizophrenia.

Studies which have focused on schizophrenia have determined that SH-053-2'F-S-CH_3 (**51**)[241] and SH-053-2'F-R-CH_3 (**52**)[196, 197] are able to mitigate some of the positive symptoms of schizophrenia. The *S*-enantiomer **51** was studied in an immune-mediated neurodevelopmental disruption model in mice which resulted in abnormalities implicated in schizophrenia. This was done by a prenatal administration of the viral mimetic polyriboinosinic-polyribocytidilic acid [poly(I:C)].[242, 243] This resulted in schizophrenia-like behavioral and cognitive dysfunctions, such as reduced social approach behavior, impaired working memory and increased amphetamine sensitivity.[244] Administration of SH-053-2'F-S-CH_3 (**51**) failed to correct the deficits in working memory and social interaction, as was also seen with both **51** and **52** by Soto *et al*.,[245] but was highly effective in alleviating the poly(I:C)-induced amphetamine hypersensitivity, a positive symptom of schizophrenia, without causing adverse effects.[241]

Similar studies using SH-053-2'F-R-CH_3 (**52**) in the methylazoxymethanol acetate (MAM) developmental disruption model of schizophrenia in rats indicated agonist activity of the selective *R*-enantiomer **52** at the α5 receptor subtype reduced the hyperactivity of amphetamine-induced locomotor hyperactivity.[196, 197] The MAM-model of schizophrenia was derived by administering the DNA-methylating agent MAM to pregnant dams and the offspring exhibit schizophrenia-like symptoms,[246-248] similar to those seen in the poly(I:C) model of schizophrenia. The results of these studies using **51** and **52**[196, 197, 241] indicated that these α5 PAMs can be used in the treatment of schizophrenia.

While the α5 subtype selective SH-053-2'F-R-CH_3 (**52**) exhibited the potential to be used in the treatment of schizophrenia with a low risk of exerting non-α5 subtype effects, the comorbidity[210] of schizophrenia with other disorders created a very useful situation for the α2/α3/α5 agonist SH-053-2'F-S-CH_3 (**51**). It is not uncommon for a patient to be suffering from both schizophrenia and anxiety.[211, 212] The *S*-isomer **51** has previously been shown to be a non-sedating anxiolytic in the elevated plus maze paradigm in rats[230] and the Vogel conflict procedure in rhesus monkeys,[112] which indicated that **51** could be useful in treating both these disorders in regard to comorbidity. Epilepsy is also known to coexist with schizophrenia in some patients,[213, 214] and with the efficacy at the α2 subtype, it is likely that SH-053-2'F-S-CH_3 (**51**) would be useful in treating patients displaying symptoms from both schizophrenia and epilepsy. The prepulse inhibition model of schizophrenia and the assessment of the development of catalepsy were also investigated to determine the practicality in the treatment of schizophrenia.

4.3.3.1 Evaluation of SH-053-2'F-S-CH_3 (51) and SH-053-2'F-R-CH_3 (52) at the Anticonvulsant Screening Program for Seizure Protection and Signs of Ataxia

The enantiomers SH-053-2'F-S-CH_3 (**51**) and SH-053-2'F-R-CH_3 (**52**) were assessed for their ability to protect from epileptic seizures by the Anticonvulsant Screening Program (ASP) at the National Institute for Neurological Disorders and Stroke (NINDS). The treatment of epilepsy by BZDs has previously been discussed in Section 3.3.7.5. As pointed out, tolerance develops to the anticonvulsant effect of typical BZDs in 3 – 5 days. The initial screen for **51** and **52** was a low-frequency (6 Hz), long-duration (3 sec.) electroshock test (Figure 62A). Mice (n = 4) were dosed i.p. with either 100 mg/kg of the *S*-enantiomer **51** or 150 mg/kg of the *R*-enantiomer **52** and subjected to the electroshock test to determine the ability of each compound to protect mice from electroshock-induced seizures. The *S*-enantiomer **51** offered protection at all time points, ranging from 15 minutes to 4 hours, as expected due to the positive modulation of the α2 subtype. The *R*-enantiomer **52** had no effect at a higher dose at any time point. The ED_{50} of the *S*-enantiomer **51** was then calculated at the time-of-peak effect, 1 hour. Doses of 5, 15, 30 and 60 mg/kg led to an ED_{50} of 14.2 mg/kg against electroshock-induced seizures (Figure 62B). These results are promising for the use of SH-053-2'F-S-CH_3 (**51**) in the treatment of patients who exhibit the symptoms of schizophrenia comorbid with epilepsy.

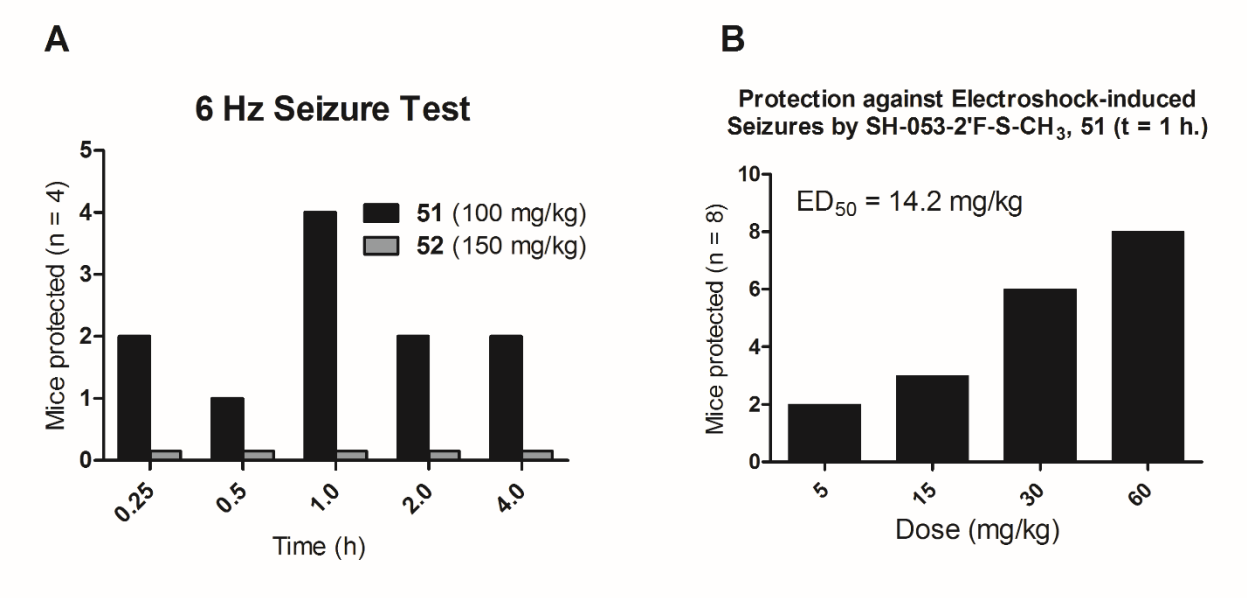


Figure 62. Assessment of SH-053-2'F-S-CH_3 (51) and SH-053-2'F-R-CH_3 (52) to protect mice from electroshock-induced convulsions. A) Mice were dosed i.p. with either 51 (100 mg/kg) or 52 (150 mg/kg) and a 6 Hz shock by a corneal electrode was administered at various time points and observed for convulsions and 51 was able to protect some subjects while 52 was not; B) The dose-response of 51 in protection in the 6 Hz electroshock test at 1 hour post i.p. administration.

Mice were also assessed for ataxic properties in the rotorod paradigm by ASP at NINDS. Both compounds were dosed i.p. at 100 mg/kg in mice (n = 8) and neither had significant ataxic properties since only one mouse failed to complete the assay when dosed with **51**, as depicted in Figure 63. Rudolph *et al.*[170] predicted that activation of the α1 subtype can increase dopamine firing,[52, 170] further increasing the schizophrenia-like symptoms. The lack of ataxia, which also stems from the α1 subtype,[41, 42] at high doses is encouraging and important for the treatment of schizophrenia with *S*-enantiomer **51** or the *N*-methyl analogs as well as other *N*-alkyl ligands of **51** also including C(3)-oxadiazoles.

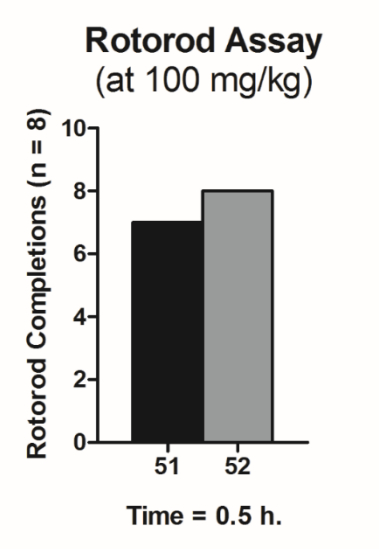


Figure 63. Assessment of SH-053-2'F-S-CH_3 (51) and SH-053-2'F-R-CH_3 (52) in the rotarod assay. Mice were dosed i.p. with 51 or 52 (100 mg/kg) 30 minutes prior to being tested on a rotating rod (6 rpm). Mice that fell 3 times during a 1-minute trial were deemed toxic (ataxic).

4.3.3.2 Prepulse Inhibition of SH-053-2'F-S-CH_3 (51) and SH-053-2'F-R-CH_3 (52)

The deficits in prepulse inhibition (PPI) to acoustic startle reflex are observed in patients which exhibit schizophrenic-like symptoms.[249] The trait that is characterized by PPI is when a weak prestimulus (prepulse) is able to inhibit the reaction (startle response) of a subject to a subsequent strong stimulus (pulse).[250, 251] This can be induced by *N*-methyl-D-aspartate (NMDA) antagonists such as phencyclidine (PCP) and dizocilpine (MK-801).[250] A traditional antipsychotic haloperidol was unable to reverse the PPI deficits induced by PCP and MK-801; however, the atypical antipsychotic clonzapine was able to correct the deficits.

The enantiomers SH-053-2'F-S-CH_3 (**51**) and SH-053-2'F-R-CH_3 (**52**) were assessed for PPI (Dr. David Baker and Nick Raddatz) to further characterize the ability of these IBZDs to be used in the management of schizophrenia beyond the correction of amphetamine-induced hyperactivity previously observed.[196, 197, 241] Male Sprague-Dawley rats (n = 6 – 8) were trained in

a sound-attenuating chamber which rested on a motion sensing plate to determine the magnitude of the startle response. The sessions consisted of a 50 dB pulse above a 60 dB background noise which determined the baseline. Rats where then given a 60 minute pretreatment of vehicle (DMSO), **51** or **52** (30 mg/kg), followed by a subcutaneous injection of either PCP-hydrochloride (1.5 mg/kg) or saline 10 minutes prior to testing. Subjects were then tested for PPI with the 50 dB pulse immediately preceded (100 ms) by a 5, 10 or 15 dB prepulse to determine the ability of **51** and **52** to reverse the effects of PCP, as depicted in Figure 64.

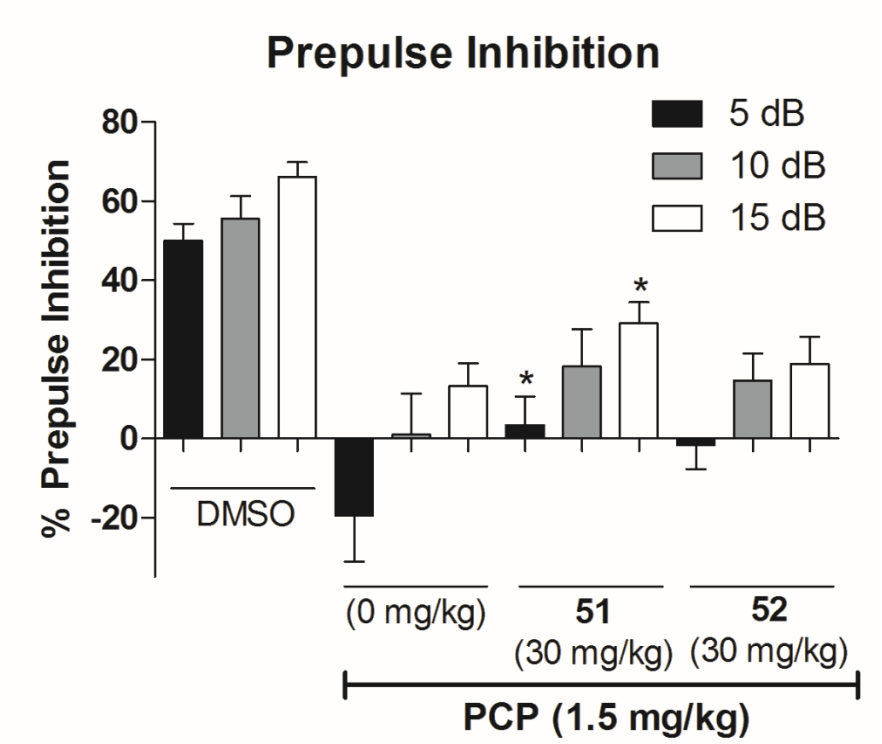


Figure 64. Assessment of SH-053-2'F-S-CH$_3$ (51) and SH-053-2'F-R-CH$_3$ (52) to reverse the PPI deficits induced by PCP. SH-053-2'F-S-CH$_3$, but not SH-053-2'F-R-CH$_3$, (30 mg/kg, dosed i.p.) antagonized deficits in prepulse inhibition produced by phencyclidine when given one hour before testing. The data are expressed as the mean (+SEM) percent prepulse inhibition of the startle response to an auditory stimulus (50 dB above a 60 dB background) when preceded by a nonstartle-eliciting auditory cue at 5, 10, and 15 decibels above a 60 dB background. Disruption of prepulse inhibition was obtained in rats by an acute injection of phencyclidine (PCP.HCl, 1.5 mg/kg, subcutaneous) ten minutes prior to testing. *p<0.05, difference from controls receiving phencyclidine with 0 mg/kg drug pretreatment. The *R*-enantiomer 52 was trending towards significance in this protocol but would have required many more animals to reach significance and logistics prevented the completion of this study with 52.

Analysis of the results indicated that the *S*-isomer **51**, which activated the α2, α3 and α5 subtypes, significantly reversed the schizophrenic-like symptoms induced by PCP when using a 5 and 15 dB prepulse (over 60 dB background) prior to a pulse (50 dB over 60 dB background). The *R*-enantiomer **52**, which activated only the α5 subtype, was unable to reach a significant effect, but did show improvement over the vehicle that was treated with PCP. The use of more animals would have reached significance with **52** but was not executed due to cost. Although the α5 subtype has been implicated as a target for the treatment of schizophrenia, it is possible that the anxiolytic effect exerted by the α2 subtype may have aided in the ability of **51** to reduce the startle response. However, there are protocols which separate out these two processes. The results may be more accurate by a shorter pretreatment time as the concentration-time profile in Section 4.3.2 displayed that the maximum brain concentration was reached around 20 minutes after injection rather than the 60 minutes employed here. It is reasonable to assume much of **51** and some of **52** were already metabolized when the PPI test was carried out.

4.3.3.3 Catalepsy of SH-053-2'F-S-CH₃ (51) and SH-053-2'F-R-CH₃ (52)

Catalepsy, which is defined as a failure to correct an externally imposed posture,[252] is associated with drugs that treat schizophrenia because of the effects on dopamine levels.[253] Unfortunately, some antipsychotics, such as haloperidol, have been found to cause catalepsy,[254] limiting their use in the treatment of schizophrenia. While BZDs are currently a first-line treatment for catalepsy,[255] SH-053-2'F-S-CH_3 (**51**) and SH-053-2'F-R-CH_3 (**52**) were assessed against haloperidol to measure the development of catalepsy.

Male Sprague-Dawley rats were dosed i.p. with vehicle (DMSO), haloperidol (0.1 mg/kg), **51** or **52** (30 mg/kg) and their front paws were placed on a bar that was positioned 12.5 cm above the floor. The time from the placement of the paws until one paw was moved or slipped from the

bar was measured at 30, 60 and 90 minutes post treatment, as illustrated in Figure 65. As expected, haloperidol significantly increased the amount of time in between the placement of the paws and the first movement as compared to vehicle, which indicated the development of catalepsy. Neither **51** nor **52** displayed signs of catalepsy as both ligands performed comparable to vehicle. Moreover, the observer noted that neither animal appeared sedated, as mentioned by Nick Raddatz (private communication).

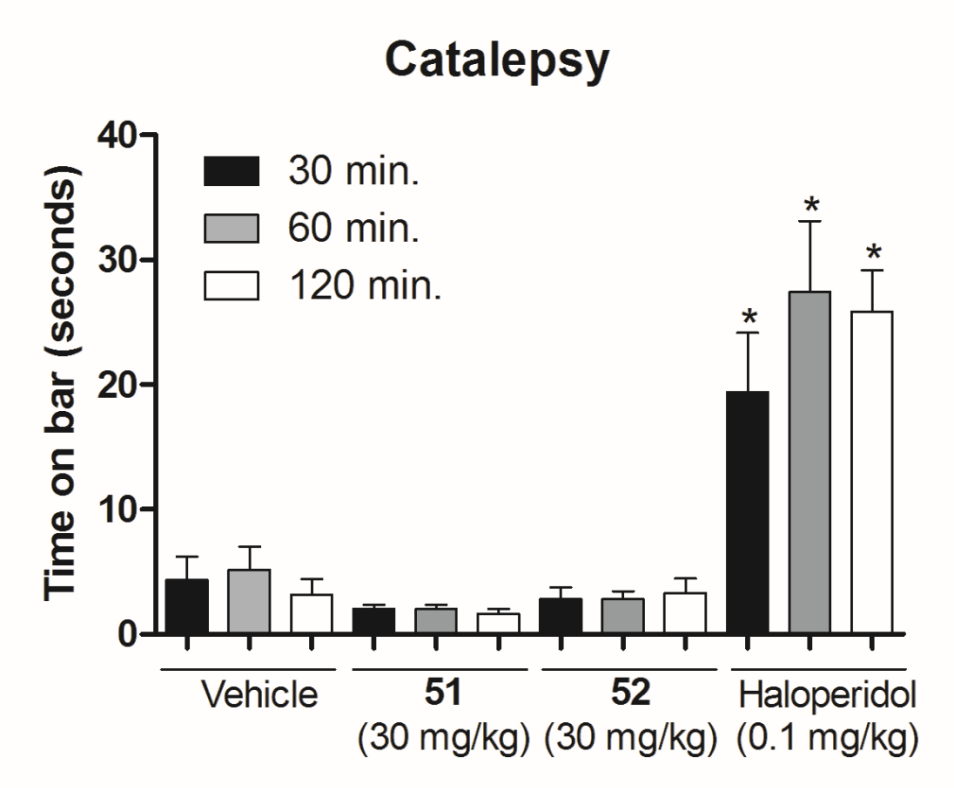


Figure 65. Assessment of the development of catalepsy of SH-053-2'F-S-CH$_3$ (51) and SH-053-2'F-R-CH$_3$ (52). Haloperidol, but not 51 nor 52 (30 mg/kg, i.p.) produced a significant cataleptic response at 30, 60, and 120 minutes post-injection. The data are expressed as the mean (+SEM) time (sec) subjects spent with both front paws on an elevated bar. *p<0.001, difference from controls receiving vehicle alone.

The results of these studies indicated that SH-053-2'F-S-CH_3 (**51**), which has been shown to be an anxiolytic,[112, 230] active against electroshock-induced seizures and reversed the PCP-induced deficits of acoustic startle in the PPI paradigm, as well as reducing amphetamine-induced hyperactivity,[241] would be useful in the management of the positive symptoms of schizophrenia which are comorbid with either anxiety, epilepsy or both. In addition, SH-053-2'F-R-CH_3 (**52**) has been shown to reduce amphetamine-induced hyperactivity[196, 197] and was nearly able to reverse the effects of PCP in the PPI test, which make it a strong candidate for further evaluation as well.

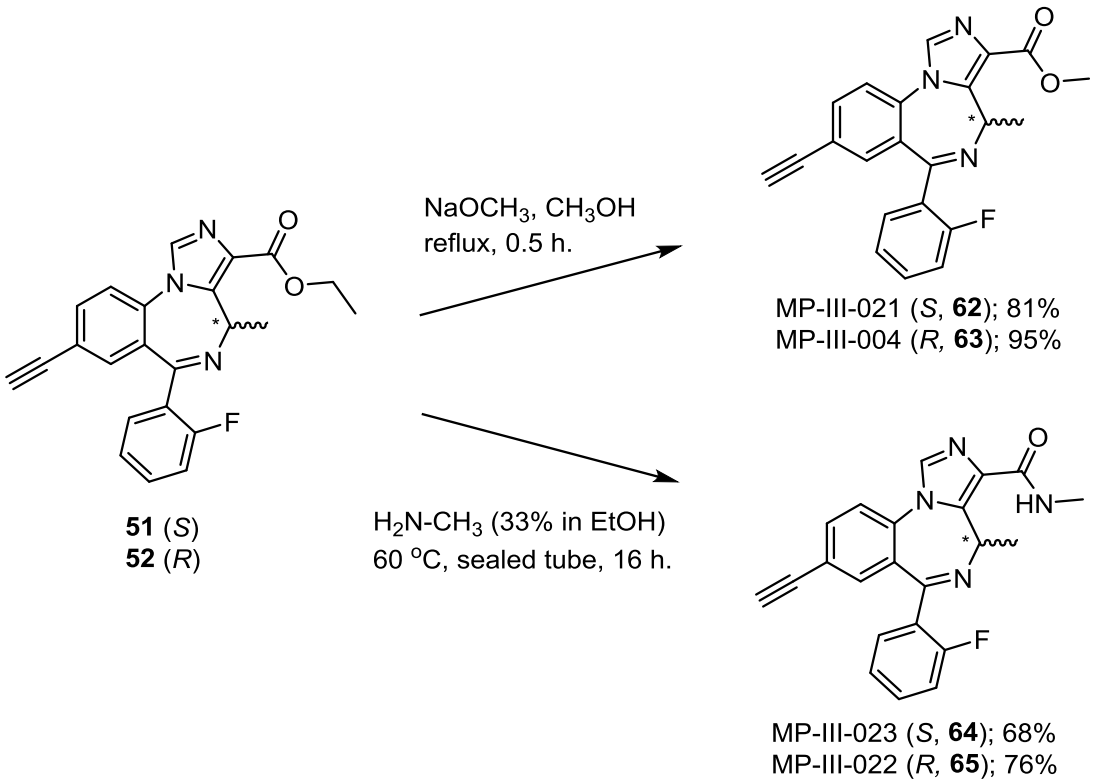
Along with the positive results for targeting schizophrenia with the *S*-enatiomer **51** and the *R*-enantiomer **52**, these ligands provided a framework from which new analogs were made to improve the current pharmacokinetic and pharmacodynamic characteristics. The results of this research are presented in the following sections.

4.3.4 Synthesis of Analogs

It was well known by examination of the pharmacophore/receptors model[17, 74] and SAR[73] that drastic changes in a subtype selective ligand in the Bz/$GABA_A$ system will alter the subtype selectivity. Consequently, a few selected analogs of SH-053-2'F-S-CH_3 (**51**) and SH-053-2'F-R-CH_3 (**52**) were synthesized to minimize changes in the sterics and electronics of the ligands as compared to those in **51** and **52**. The methyl esters MP-III-021 (**62**) and MP-III-004 (**63**) and methyl amides MP-III-023 (**64**) and MP-III-022 (**65**) were synthesized (Scheme 15) since the corresponding ligands in the 2'-N series, MP-III-024 (**19**) and HJ-I-040 (**24**), respectively, retained similar efficacy profiles as the parent. On analysis of preliminary data on the efficacy of **19**, it appears to be an α2/α3 subtype selective ligand, while **24** became more selective towards the α3 subtype. It was thought that the related ligands in the enantiomic series would exhibit a similar

profile to their parents **51** or **52**. The oocyte efficacy of MP-III-004 (**63**) and MP-III-022 (**65**) were investigated and the data are presented in Sections 4.3.5 and 4.3.6, respectively.

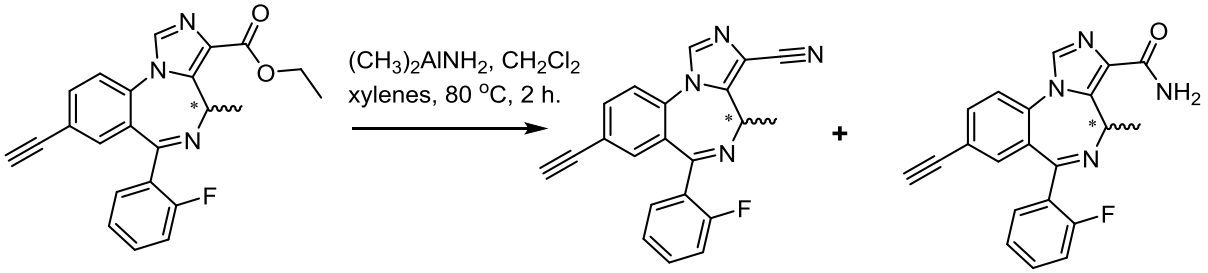
Scheme 15. Synthesis of methyl esters (MP-III-021, 62 and MP-III-004, 63) as well as methyl amides (MP-III-023, 64 and MP-III-022, 65).



Dimethylaluminum amine was prepared, as described in Section 3.3.3.2, and utilized to convert the ethyl esters **51** and **52** into the nitriles MP-III-018.A (**66**) and MP-III-019.A (**68**) as well as the carboxamides MP-III-018.B (**67**) and MP-III-019.B (**69**), as illustrated in Scheme 16. ***Caution*: *Do not breathe or get trimethylaluminum or dimethylaluminum amide on you!*** These nitriles were prepared before the nitrile in the 2'-N series (**27**) was found to lose all potency, likely due to the linearity of the nitrile which in turn, presumably, loses the ability to interact with H_1. These two reactions on the enantiomers were run side-by-side under identical conditions and

resulted in different yields. The overall conversion of the starting material to the combined products were high, at 92% and 89% overall for the *S*- and *R*-enantiomers, respectively; however, the ratio of the resulting nitriles and carboxamides were not similar, for the *S*-enantiomer **51** series produced a 4:1 nitrile to carboxamide ratio while the *R*-enantiomer **52** series produced a 1:1 ratio. It is possible the sterics of the chiral C(4) methyl group impacted the reactions because the preferred conformation of the seven membered BZD ring is different depending on whether you have the *S*-CH_3 enantiomer **51** or the *R*-CH_3 enantiomer **52**. This has been clearly shown in at least two cases, wherein two rotomers were observed in the NMR spectrum which collapsed to a single set of signals when the NMR spectrum was run at higher temperature. This was observed often in chiral BZDs.

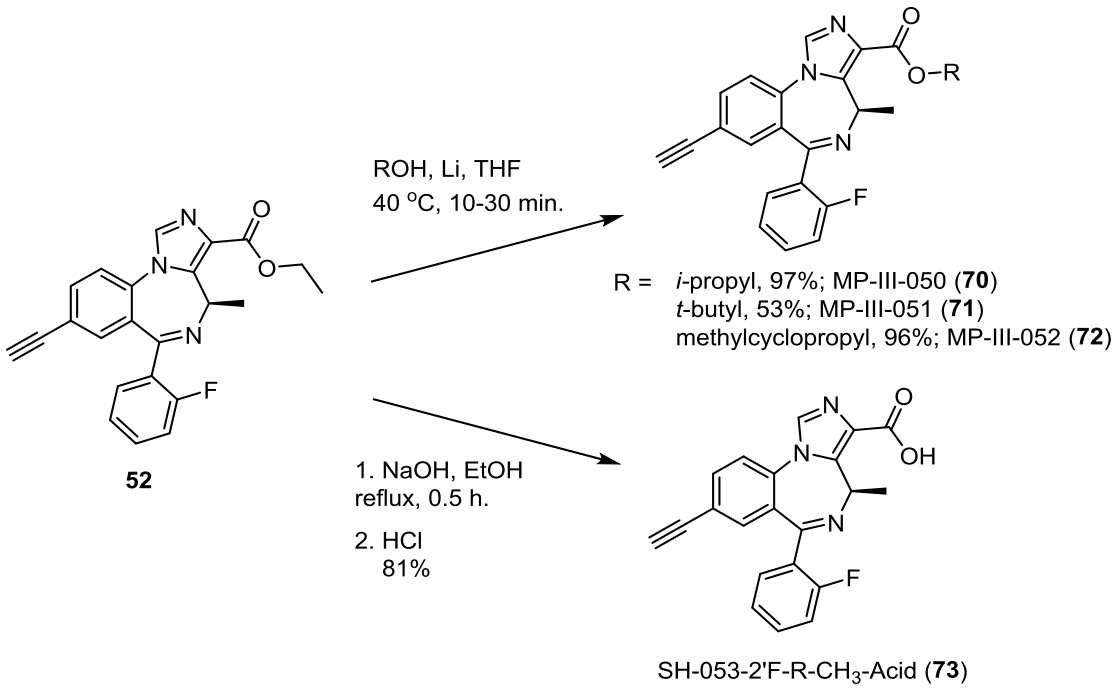
Scheme 16. Synthesis of nitriles (MP-III-018.A, 66 and MP-III-019.A, 68) and carboxamides (MP-III-018.B, 67 and MP-III-019.B, 69).



The α5 selectivity seen in MP-III-004 (**63**), discussed in Section 4.3.5, prompted the synthesis of additional esters and the predicted carboxylic acid metabolite, SH-053-2'F-R-CH_3-Acid (**73**), as shown in Scheme 17. The esters which were afforded by a transesterification process with lithium metal and the corresponding alcohol, were restricted to *i*-propyl (MP-III-050, **70**), *t*-

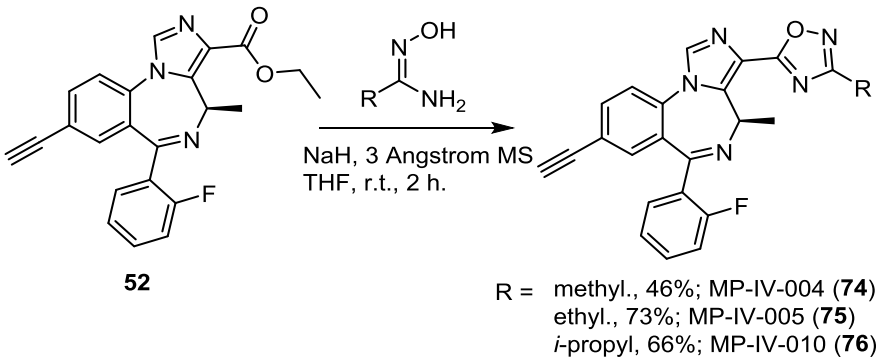
butyl (MP-III-051, **71**) and methylcyclopropyl (MP-III-052, **72**) until more analysis could be completed.

Scheme 17. Synthesis of esters (70 – 72) and SH-053-2'F-R-CH$_3$-Acid (73).



Additionally, the methyl (MP-IV-004, **74**), ethyl (MP-IV-005, **75**) and *i*-propyl (MP-IV-010, **76**) oxadiazoles were synthesized with the corresponding oximes, as illustrated in Scheme 18. These were synthesized in attempts to increase the metabolic stability in rodent microsomes, which had clearly been seen with the heterocycles in the 2'-N (HZ-166, **3**) series (see Section 3.3.5).

Scheme 18. Synthesis of oxadiazoles (74 – 76).



Additional analogs of both SH-053-2'F-S-CH_3 (**51**) and SH-053-2'F-R-CH_3 (**52**) have been synthesized by Guanguan Li.

4.3.4.1 In Vitro Analysis of the Analogs of SH-053-2'F-S-CH_3 (51) and SH-053-2'F-R-CH_3 (52)

The analogs of SH-053-2'F-S-CH_3 (**51**) and SH-053-2'F-R-CH_3 (**52**) were investigated *in vitro* by a CRO to assess the metabolic stability and efficacy at the α3 subtype in the FLIPR functional assay, the results of which are reported in Table 10. As previously discussed in Section 4.3.2, the *R*-enantiomer **52** was not degraded in HLMs, while the *S*-enantiomer **51** was completely metabolized at the end of a 30 minute incubation time. The α3 FLIPR EC_{50} values which are reported indicated that the *S*-enantiomer analogs all have greater efficacy at this subtype. This was expected as it had been the case in previously investigated compounds such as **49** and **50**,[230] as well as **51** and **52**.[112, 113] Based on molecular modeling, the *S*-enantiomer analogs would also have a greater efficacy at the α2 subtype.[17, 74] For a review on the subject, see Clayton, *et al*. (Appendix E).[74]

CRO Results		Metabolic stability in liver microsomes (reported in %-remaining) Conditions: 4 μM compound, 37 °C, 30 minutes				α3 FLIPR assay[a]	clogP[b]
Compound		HLM[c]	DLM[c]	MLM[c]	RLM[c]	EC_{50} (μM)	(Diazepam = 2.96)
51	Ethyl ester (*S*)	2.3	90.7	66.4	6	0.427	3.42
52	Ethyl ester (*R*)	100	90.3	59.1	5.4	0.973	
63	Methyl ester (*R*)[d]	64.5		68.0			
64	Methyl amide (*S*)					0.048	3.04
65	Methyl amide (*R*)	89.6	53.7	47.7	2.7	2.54	
67	Carboxamide (*S*)					0.0505	2.71
69	Carboxamide (*R*)	86.9	65.1	71.2	30.3	0.316	
66	Nitrile (*S*)					0.353	3.00
68	Nitrile (*R*)	86.9	6.3	49.6	38.3	20	
74	Me. oxadiazole (*R*)	86.4	65.3	74.3	46.4	2.37	3.21
75	Et. oxadiazole (*R*)	89.3	57.5	50.3	49	20	3.74
76	*i*-Pr. Oxadiazole (*R*)	74.3	51.9	26.6	30.9	14.6	4.14

Table 10. *In vitro* metabolic stability, α3 Bz/$GABA_AR$ EC_{50} values and clogP's of the SH-053-2'F-S-CH_3 (51) and SH-053-2'F-R-CH_3 (52) and their analogs

[a] The α1 subtype was also examined for all compounds, and the EC_{50} > 20 μM for all compounds.
[b] This was calculated used clogP on the ChemDraw 13.0 software; as compared to diazepam
[c] Human liver microsomes (HLM), dog liver microsomes (DLM), mouse liver microsome (MLM) and rat liver microsomes (RLM)
[d] Methyl ester 63 was tested by Revathi Kodali at UWM under similar conditions (10 μM, 37 °C, 60 minutes)

Similar to the 2'-N series presented in Section 3.3.5, the *S*-enantiomer amides **64** and **67** displayed greater affinity for the α3 subtype as compared to ethyl ester **52**, perhaps due to containing a hydrogen bond donator which can interact with A_2. Unlike the 2'-N nitrile **28**, nitrile

(*S*) **66** displayed greater affinity than the parent ethyl ester **51** at 0.353 and 0.427 μM, respectively. In the 2'-N series, it was believed that the lack of degree of freedom of the linear nitrile hindered its ability to interact with H_1. It is plausible to suggest that the chiral methyl group of **66** altered the conformation of the C(3) functional group to interact with H_1. In the *R*-enantiomer series, it was interesting to note that the methyl amide **65** has decreased efficacy at the α3 subtype, whereas increased efficacy has occurred in other cases. Similar to the 2'-N series, the oxadiazoles **74** – **76** have decreased efficacy at the α3 subtype, likely due to the increased size of the C(3) functional group. It is possible that the larger size hinders rotation as compared to the parent and does not permit as effective of an interaction of the heteroatoms with H_1.

The *R*-enantiomers were analyzed for their resistance to metabolism in liver microsomes. The *R*-enantiomer ethyl ester **52** was not degraded over the 30 minute incubation time in HLMs, and all analogs exhibited good resistance, ranging from 74 – 90% of the parent remaining. All analogs significantly were metabolized more rapidly in DLMs, with the majority of analogs exhibiting 50 – 65% remaining; the exception being the nitrile **68** which was severely degraded to 6% remaining. It was interesting to note that the metabolic behavior of the *S*-enantiomer ethyl ester **51**. It was nearly completely metabolized in HLM but was very stable in DLMs (90%). Moreover, it was much more stable in MLMs (66%) as compared to RLMs (6% remaining). Most of the analogs exhibited similar resistance to MLMs compared to **52**, while the low initial stability in RLMs of **52** (5% remaining) was the same as *S*-**51** and *R*-**65** but the other analogs **68** and **74** – **76** were moderately more stable. The methyl and ethyl oxadiazoles **74** and **75** performed similarly to **52** in HLMs, DLMs and MLMs but exhibited moderately increased stability when incubated in RLMs. In contrast, the isopropyl oxadiazole **76** was less stable than the other oxadiazoles in all species with the most significant drop in rodent liver microsomes.

The methyl ester **63**, which was tested under slightly different conditions, exhibited lower resistance to HLMs as compared to the ethyl ester **52**, at 64.5% and 100%, respectively. In MLMs, methyl ester **63** displayed a similar resistance to liver microsomes as the ethyl ester **52**, at 68% of the parent **63** remaining after a one-hour incubation time. It should be noted that although the comparison made between **52** and **63** were tested under different conditions, ligands which were assessed in both experiments had similar results, as mentioned in Section 3.3.5.

4.3.5 MP-III-004, a Superior α5 Bz/GABA$_A$ergic Subtype Selective Ligand

One of the goals of this research was to discover superior α5 subtype selective ligands as compared to SH-053-2'F-R-CH_3 (**52**). Analysis of previous data found SH-I-75 (**77**),[143] a low potency, α5 selective ligand in regards to efficacy, as well as an α5 selective binding ligand, as depicted in Figure 66. The binding data was tested twice. Although the α5 affinities are more than 1000-fold different, both sets indicate that **77** was more potent at α5 subtypes as compared to non-α5 subtypes.

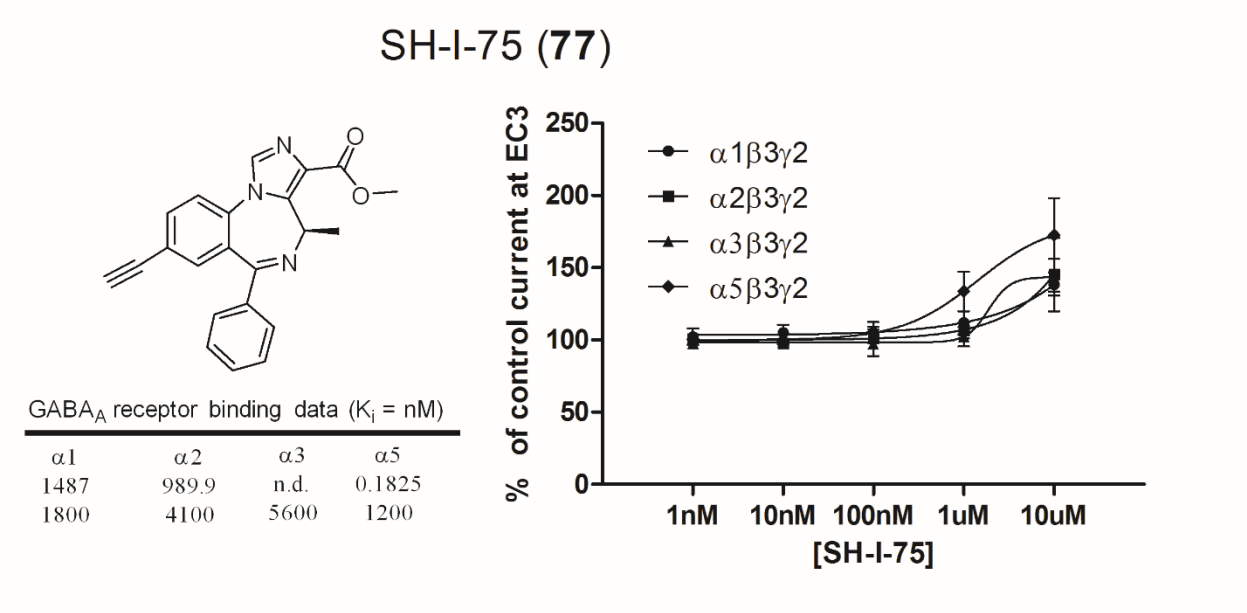


Figure 66. Structure, binding affinity and oocyte efficacy profile of SH-I-75 (77). Binding affinity at αxβ3γ2 GABA$_A$/benzodiazepine site subtypes using [^{3}H]-flumazenil displacement studies from two separate experiments. Efficacy concentration curve on GABA$_A$ receptors using an EC$_3$ GABA concentration (n = 3).

There were two subtle differences between **52** and **77**. Ligand **52** contained a 2'-F and a C(3) ethyl ester while **77** had a 2'-H and methyl ester as the C(3) functional group. The combination of these resulted in a 2'-F and C(3) methyl ester ligand, MP-III-004 (**63**), which was predicted to be an α5 subtype selective GABA$_A$R ligand. These data were relayed to Dr. Margot Ernst who agreed to examine the oocyte efficacy on **63**, and the results are presented in a side-by-side comparison to SH-053-2'F-R-CH$_3$ (**52**) in Figure 67.

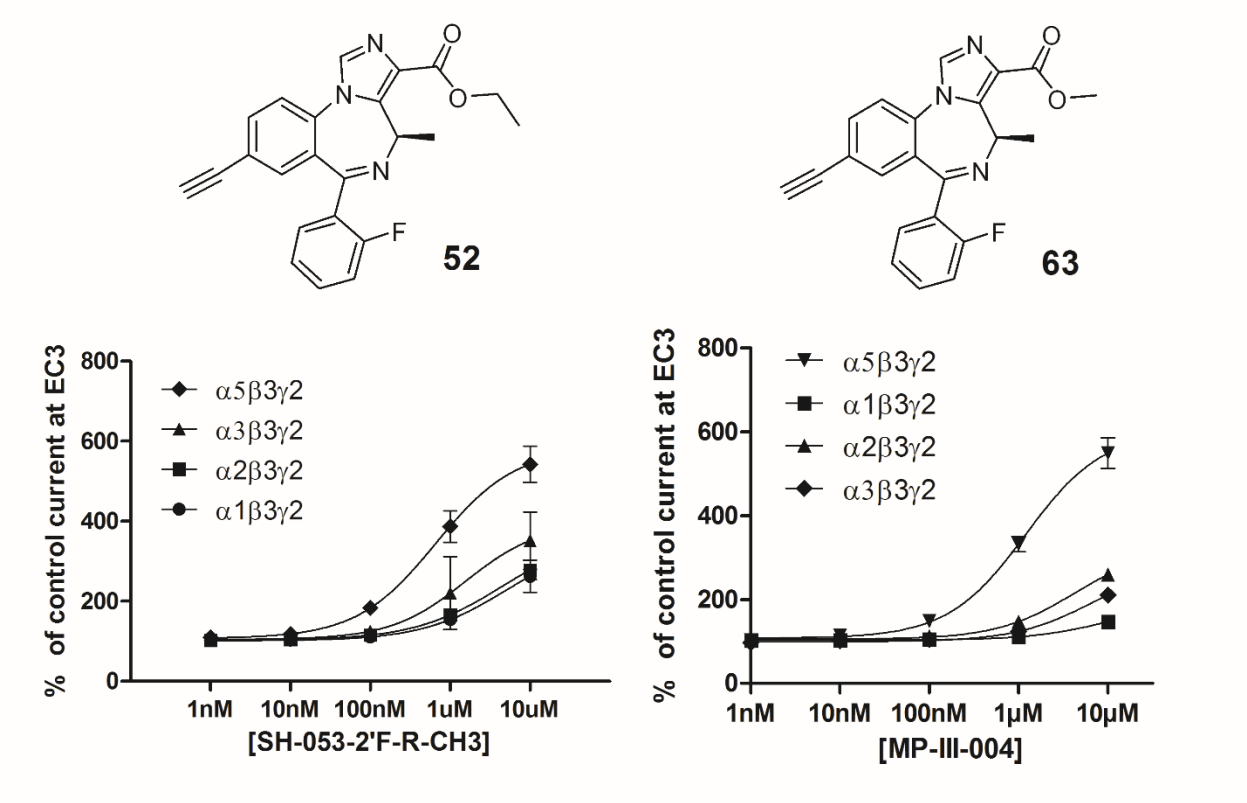


Figure 67. Structures and oocyte efficacy profiles of SH-053-2'F-R-CH$_3$ (52) and MP-III-004 (63). Concentration curves on GABA$_A$ receptors using an EC$_3$ GABA concentration (n = 3 – 5).

As predicted based on the α5 selectivity of **52** and **77**, the combined structural changes in MP-III-004 (**63**) resulted in an α5 subtype selective ligand. Comparison of the efficacy data in oocytes of the methyl ester **63** and ethyl ester **52** indicated that while both compounds exerted similar efficacy at the α5 subtype, MP-III-004 (**63**) had significantly reduced efficacy at the α1, α2 and α3 subtypes as compared to **52**. At 1 μM, ethyl ester **52** modulated GABA currents to 150 – 200% at non-α5 subtypes; while the methyl ester modulated currents at less than 150% for the same subtypes. This resulted in an excellent tool for studying GABA$_A$Rs containing the α5 subtype since it has reduced efficacy at non-α5 receptors which decreased the chances of adverse effects. This finding prompted the work on additional esters, as described in Section 4.3.4, as well as the investigation of the oocyte efficacy of MP-III-022 (**65**), which is presented in Section 4.3.6.

4.3.5.1 Prepulse Inhibition and Catalespy of MP-III-004

Because of the α5 subtype selectivity of MP-III-004 (**63**), it was tested for the effect in prepulse inhibition and catalepsy by Dr. David Baker and Nick Raddatz at Marquette University. The assays were performed as described in Sections 4.3.3.2 and 4.3.3.3. However, complications with consistency using phencyclidine (PCP) led to the use of MK-801 to induce PPI deficits.[256] The ethyl ester SH-053-2'F-S-CH_3 (**51**) was assessed using MK-801 (*unpublished results*) to first validate the switch from PCP to MK-801 and was found to significantly reverse the deficits of PPI, as was seen earlier using PCP. Similar to the protocol with **51** and **52**, rats (n = 11 – 12) were dosed i.p. with MP-III-004 (**63**) sixty minutes prior to testing, with a subcutaneous injection of MK-801 (0.1 mg/kg) and the results are depicted in Figure 68. Additionally, MP-III-004 (**63**) was assessed for the development of catalepsy, as illustrated in Figure 69.

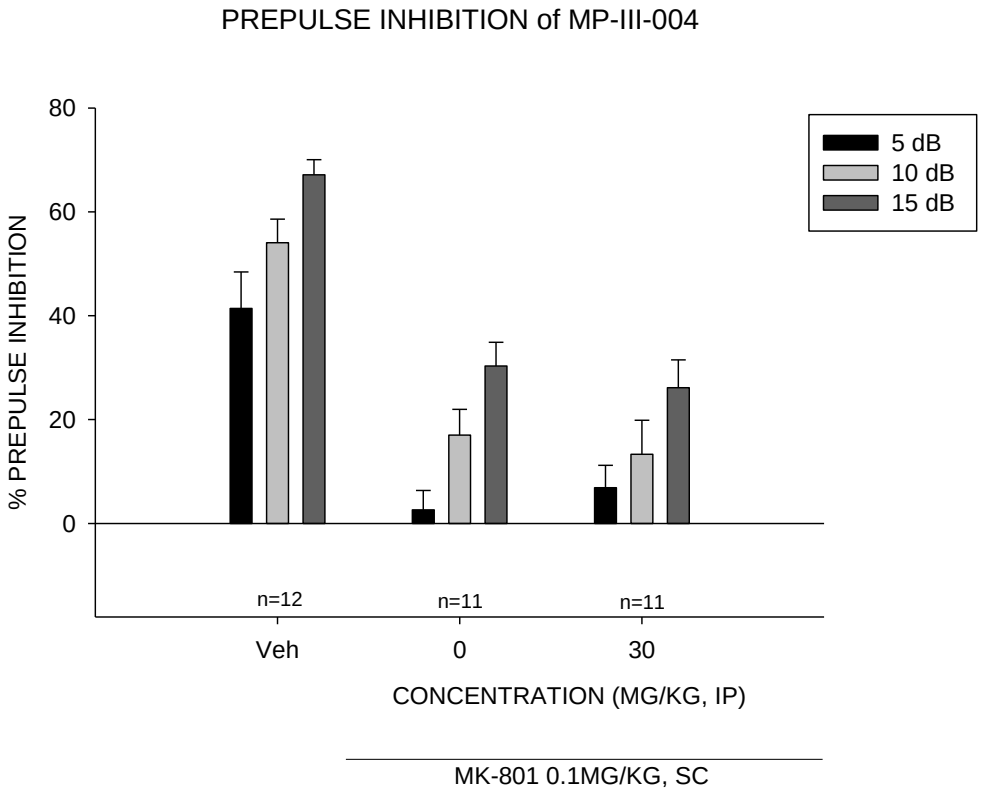


Figure 68. Assessment of MP-III-004 (63) in reversing the PPI deficits induced by MK-801. MP-III-004 (30 mg/kg, dosed i.p.) was unable to antagonize deficits in prepulse inhibition produced by MK-801 when given one hour before testing. The data are expressed as the mean (+SEM) percent prepulse inhibition of the startle response to an auditory stimulus when preceded by a nonstartle-eliciting auditory cue at 5, 10, and 15 decibels. Disruption of prepulse inhibition was obtained in rats by an acute injection of MK-801 (0.1 mg/kg, sc) ten minutes prior to testing. *p<0.05, difference from controls receiving MK-801 with 0 mg/kg drug pretreatment.

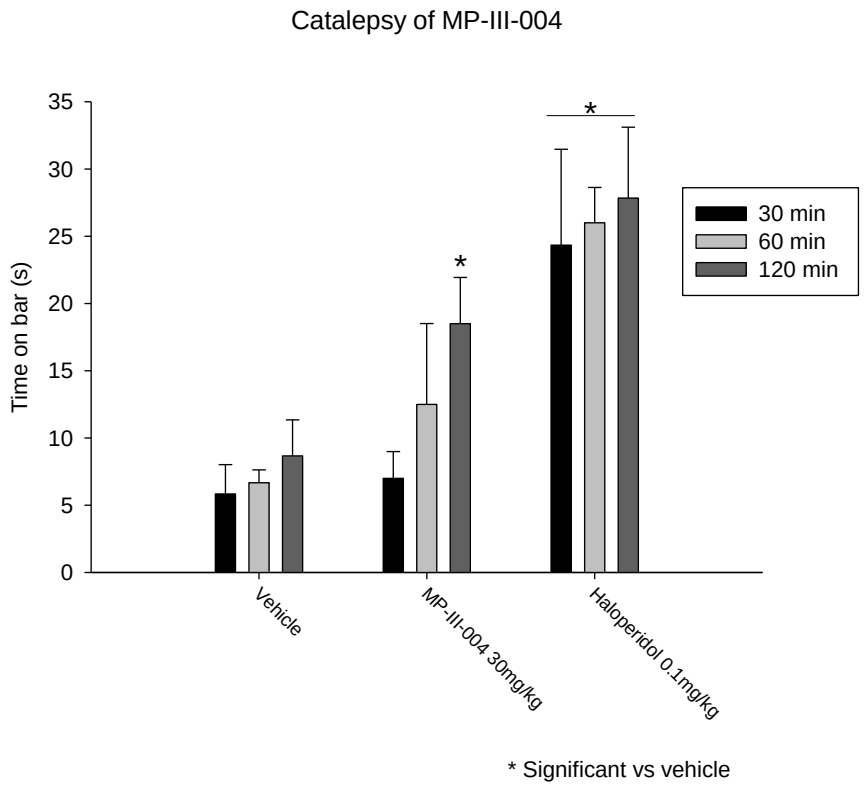


Figure 69. Assessment of the development of catalepsy of MP-III-004 (63). Haloperidol and MP-III-004 at 2 hours (30 mg/kg, i.p.) post administration produced a significant cataleptic response. The data are expressed as the mean (+SEM) time (sec) subjects spent with both front paws on an elevated bar. *p<0.001, difference from controls receiving vehicle alone.

The results indicated that methyl ester MP-III-004 (**63**) did not exert a noticeable effect in the reversal of the MK-801-induced deficits of PPI as compared to vehicle. This was similar to the results seen with the related α5 selective ethyl ester SH-053-2'F-R-CH_3 (**52**); however, a shorter pretreatment time is clearly necessary to produce superior results. This is based on numerous concentration-time profiles which indicate the C_{max} of related ligands was at 20 minutes. In the assessment for the development of catalepsy, MP-III-004 (**63**) was found to induce catalepsy at two-hours after administration as compared to vehicle, but not at 30 or 60 minutes.

Although catalepsy did not reach significance at 60 minutes post administration, a slight catalepsy was observed during testing. This is the time point at which the PPI was tested and it is possible that it had an effect on the PPI results; however, the *n*-value was high at 11 rats. It was also discouraging to find that MP-III-004 (**63**) induced catalepsy, but the dose may be too high. Many prescribed antipsychotics elicit their effects acting upon D2 (dopamine receptor 2) receptors, which has been shown to be involved in catalepsy using knock-out mice.[257] Because the $GABA_A$ and dopamine pathways are linked,[258] it is possible that the potent activation of α5-containing $GABA_A$Rs by MP-III-004 may cause a down-stream effect that activates the dopamine pathway at too high a level which caused catalepsy. Although unfortunate in terms of the elucidation of catalepsy, it is possible that the strong modulation of α5 $GABA_A$Rs could engender MP-III-004 (**63**) as a very good therapeutic agent for cognitive disorders since it may play a role in multiple pathways which could ultimately lead to a better pharmaceutical drug. Further studies on PPI employing MP-III-004 are to be carried out with a shorter pretreatment time.

4.3.5.2 The Unexpected Anticonvulsant Data of MP-III-004

It was known that the α1 and perhaps α2 $GABA_A$R subtypes play a role in the anticonvulsant nature of BZDs.[41, 42] Because the *R*-enantiomer MP-III-004 (**63**) exerted a similar modulation of chloride currents upon activation of the $GABA_A$R as SH-053-2'F-R-CH_3 (**52**), preferring the α5 subtype, it was not expected that **63** would have any anticonvulsant effects. Nevertheless, **63** was sent to ASP and assessed in the 6 Hz seizure test, as described in Section 4.3.3.1. The results were expected to be similar to *R*-enantiomer ethyl ester **52** and are depicted alongside **52** as well as the *S*-enantiomer SH-053-2'F-S-CH_3 (**51**) in Figure 70.

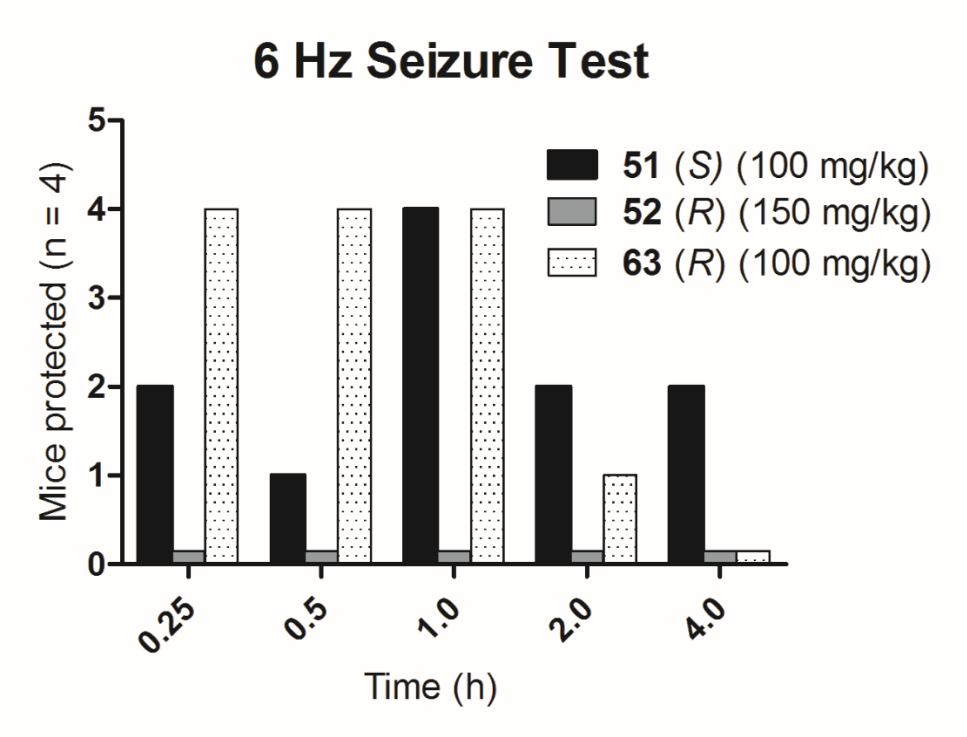


Figure 70. Assessment of MP-III-004 for protection against 6 Hz electroshock-induced seizures alongside enantiomers 51 and 52. Mice were dosed i.p. with a test compound (100 or 150 mg/kg) and a 6 Hz shock by a corneal electrode was administered at various time points and observed for convulsions. MP-III-004 offered the greatest protection against convulsions.

Examination of the results were quite exciting and indicated that MP-III-004 (**63**) did protect mice from the development of seizures in the 6 Hz test. At 15, 30 and 60 minutes post administration, all four mice tested were protected. Only one mouse was protected at 2 hours and all mice exhibited convulsions at 4 hours. This was unexpected since no mice were protected with the *R*-enantiomer ethyl ester **52** at any time point. Moreover, **63** was able to protect more mice than the α2/α3/α5 selective SH-053-2'F-S-CH_3 (**51**) at 15 and 30 minutes; however, the time of effect of *R*-**63** appeared shorter than *S*-**51** since the *S*-enantiomer ethyl ester **51** protected two of the four mice at both 2 and 4 hours post administration. These unexpected results led to further characterization of the anticonvulsant effects of MP-III-004 (**63**) by ASP at NINDS in the maximal

electroshock (MES) assay and scMET (subcutaneous pentylenetetrazole) both by i.p. and oral administration of **63**.

The MES assay is a more powerful electroshock assay than the 6 Hz electroshock, where 60 Hz of alternating current at 50 mA are delivered by corneal electrodes for 2 seconds. Mice (n = 4) were dosed i.p. with *R*-**63** (30, 100 or 300 mg/kg) and subjected to the electroshock to determine each compounds ability to protect mice from these seizures and the results are presented in Figure 71A. The scMET procedure dosed mice (n = 8) i.p. with **63** (13, 25, 45 or 75) prior to a subcutaneous 85 mg/kg IV infusion of pentylenetetrazole (PTZ or MET) was administered and the number of mice protected from seizures was counted (Figure 71B). Oral dosing was conducted in each test and the ED_{50} values were reported.

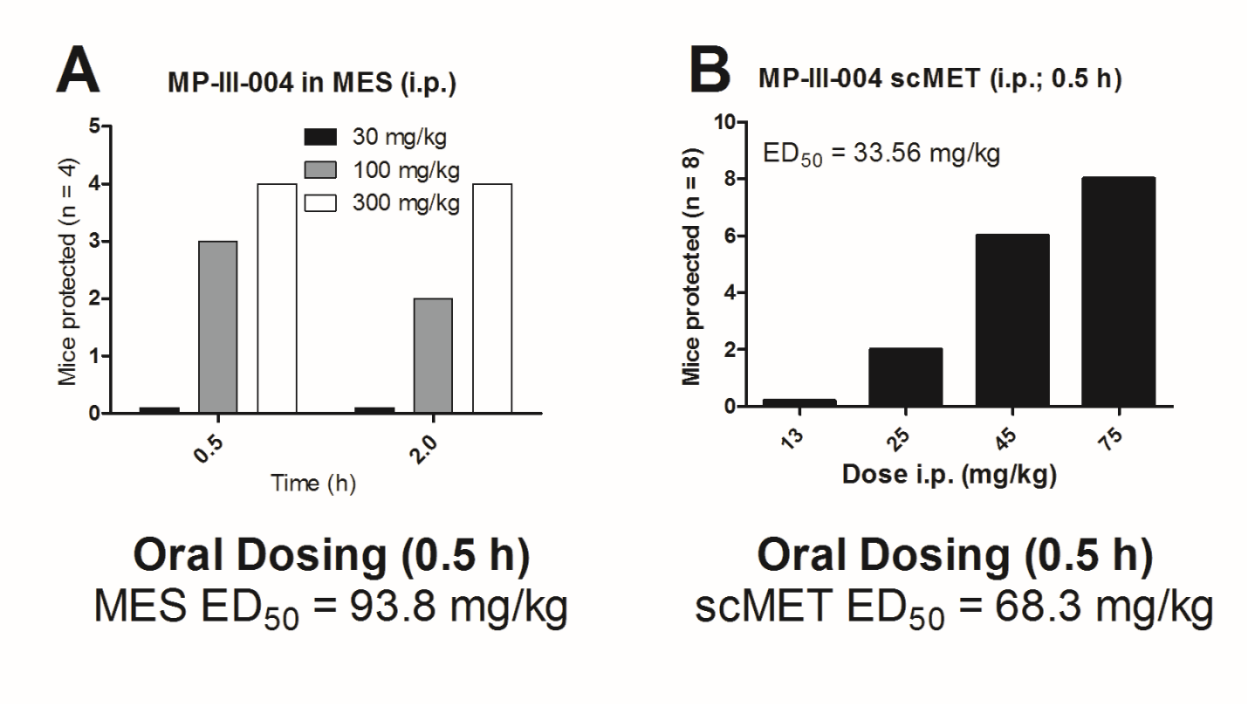


Figure 71. Assessment of MP-III-004 (63) against seizures when given i.p. or p.o. A) Mice were dosed i.p. with 63 (30, 100 or 300 mg/kg) and observed for convulsions in the MES assay; the oral dosing provided an ED_{50} of 93.8 mg/kg. B) Mice were dose with 63 (13, 25, 45 or 75) in the scMET seizure assay to determine both the i.p. and p.o. ED_{50} values, which were found to be 33.56 and 68.3 mg/kg, respectively.

The MES results indicated that MP-III-004 (**63**) was able to provide protection against these seizures at 100 and 300 mg/kg, but not at 30 mg/kg. The MES oral dosing produced an ED_{50} of 93.8 mg/kg at 30 minutes post administration. In the scMET assay, methyl ester **63** produced an ED_{50} of 33.56 and 68.3 mg/kg when dosed i.p. or orally, respectively. This lower ED_{50} which resulted when dosed i.p. was expected since it is not subjected to first-pass metabolism while oral dosing is. These results indicated that, unexpectedly, MP-III-004 (**63**) has robust anticonvulsant effects and further studies are underway at ASP, including testing in rats.

It is unknown as to why MP-III-004 (**63**) was able to protect mice from electroshock- and pentylenetetrazole-induced seizures. Further studies on anticonvulsant effects are necessary including the use of XLi-093 (**47**) to antagonize the α5 Bz/$GABA_A$ effects. Additionally, the low modulation of the non-α5 $GABA_A$Rs tested for efficacy are unlikely to play a role in the behavioral effects seen in these studies. Examination of the Tables 11 (Section 4.3.6) and 12 (Section 4.3.8.2) show that MP-III-004 (**63**) had very good brain penetration and was somewhat better than MP-III-022 (**65**) at 1696 and 1031 nmol/kg, respectively. The methyl amide **65** was tested in a separate PTZ-infusion test (Section 4.3.6.1) and did not protect from seizures; taken together with the fact that **65** has a higher potency at all $GABA_A$Rs (discussed below), this data suggests that a different receptor site not described is responsible for the effects. However, the anticonvulsant studies on the methyl amide **65** were not done in the same animals; moreover, the full metabolic stability of the methyl ester **63** must be completed and compared to the results of the methyl amide **65**. The methyl amide **65** is currently being tested at ASP (NINDS) to obtain a better comparison of the anticonvulsant activities. The fact that Uwe Rudolph, *et al*. in a triple knock in mouse just reported that α5 subtypes exhibit anxiolytic activity[259] indicated that the anticonvulsant effects of MP-III-004 (**63**) are possibly via an α5 Bz/$GABA_A$ergic pathway. Through private discussions with Drs.

Werner Sieghart, Margot Ernst and Miroslav Savic, it is also possible that the anticonvulsant effects are due to a yet untested, functional $GABA_AR$.

4.3.6 MP-III-022

The findings from MP-III-004 (**63**) led directly to the investigation of MP-III-022 (**65**) in *Xenopus laevis* oocytes for efficacy (Dr. Margot Ernst) and binding affinity (Dr. Petra Scholze) and is illustrated in Figure 72.

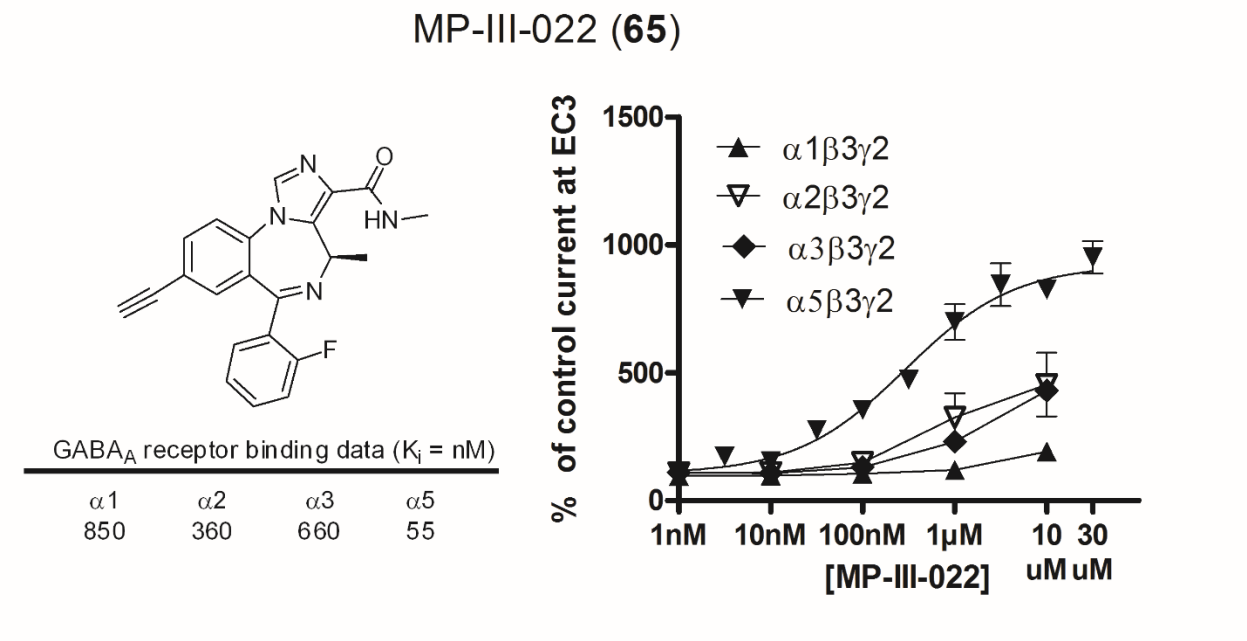


Figure 72. Structure, binding affinity and oocyte efficacy profile for MP-III-022 (65). Binding affinity at αxβ3γ2 $GABA_A$/benzodiazepine site subtypes using [^{3}H]-flumazenil displacement studies. Efficacy concentration curve on $GABA_A$ receptors using an EC_3 GABA concentration (n = 3 – 4).

Examination of the results from Ernst and Scholze indicated that MP-III-022 (**65**) was a very potent α5-$GABA_AR$ subtype selective agonist. At concentrations as low as 10 nM, *R*-**65** exerted a 154% control current at the α5 subtype, while the α2 subtype displayed the next greatest

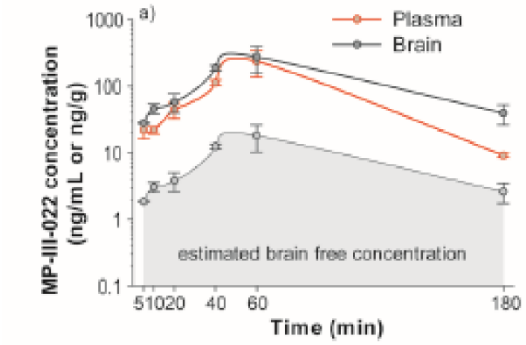
efficacy at 109%. In addition, the binding data indicated a strong affinity for *R*-**65** for the α5 subtype at 55 nM. The ligand **65** selectively bound to the α5 subtype at a 5:1 ratio over the α2 subtype and greater than a 10:1 ratio over both the α1 and α3 subtypes. Analysis of both the binding and efficacy data indicated the methyl amide **65** should have a low potential for the development of tolerance since **65** only very slightly modulated the α1 subtype at high concentrations.

The brain and plasma concentrations of both total and free MP-III-022 (**65**) and SH-053-2'F-R-CH_3 (**52**) were measured 20 minutes after a 10 mg/kg i.p. injection in male Wistar rats (Dr. Miroslav Savić), and are depicted in Table 11. With the exception of the free plasma concentrations, dosing of the two compounds resulted in similar concentrations, all within 2.5-fold. The major discrepancy in dosing between the ligands was seen in conjunction with the efficacy data. The 10 mg/kg dose of the parent *R*-**52** resulted in a 29 nM free brain concentration which correlated to a 135% modulation of the α5 subtype; while the more potent methyl amide **65** when dosed resulted in a 68 nM free brain concentration which correlated to a 314% modulation of the α5 subtype.

Table 11. Plasma and brain concentrations of MP-III-022 (65) and SH-053-2'F-R-CH_3 (52) taken 20 minutes after an i.p. (10 mg/kg) dose, n = 3.

Ligand	Plasma (nmol/L)		Brain (nmol/kg)	
	Total	Free	Total	Free
MP-III-022 (65)	645 ± 166	87 ± 23	1031 ± 278	68 ± 18
SH-053-2'F-R-CH3 (52)	406 ± 76	279 ± 52	752 ± 132	29 ± 5

These results, along with the subsequent full pharmacokinetic study at 2.5 mg/kg (Figure 73), indicated that MP-III-022 (**65**) should have exceptional characteristics required to study the functions mediated by the α5 Bz/$GABA_A$ergic subtype at a very low dose.



	Brain	Plasma
C_{max} (ng/g)	314 ± 87	257 ± 86
T_{max} (min)	53 ± 7	53 ± 7
AUC_{0-3} (ng*h/g)	446 ± 145	340 ± 121
$t_{1/2}$ (min)	71 ± 28	35 ± 4

Figure 73. Plasma and brain concentration-time profile of MP-III-022 (65) after 2.5 mg/kg i.p. administration in male Wistar rats (n = 3) for up to 3 hours. Statistics calculated analogous to the methods described in Section 4.5.

4.3.6.1 Basic Behavioral Studies with MP-III-022 (Dr. Miroslav Savić)

To assess the capabilities of the potent α5 subtype selective MP-III-022 (**65**), a variety of behavioral tests were completed by Dr. Miroslav Savić (for an in-depth review, see Appendix F). A rotarod assay and determination of the protection from pentylenetetrazole (PTZ)-induced seizures were completed to evaluate the general characteristics of *R*-**65**. Because amide **65** has great brain penetration, it was important to determine if non-α5 subtypes were activated at a given dose. The rotarod assay was employed to assess whether methyl amide **65** would induce ataxia which would indicate activation of the α1 subtype. Male Wistar rats (n = 3 – 9) were dosed i.p. 20 minutes prior to testing, at which point they were placed on a rotating rod at 15 r.p.m. and the number of falls observed over a three minute time period, as illustrated in Figure 74A. The dosing consisted of amide **65** (10, 15 or 20 mg/kg), or **65** (15 mg/kg) in combination with α5 antagonist XLi-093 (20 mg/kg) or Bz/$GABA_AR$ antagonist flumazenil (15 mg/kg).

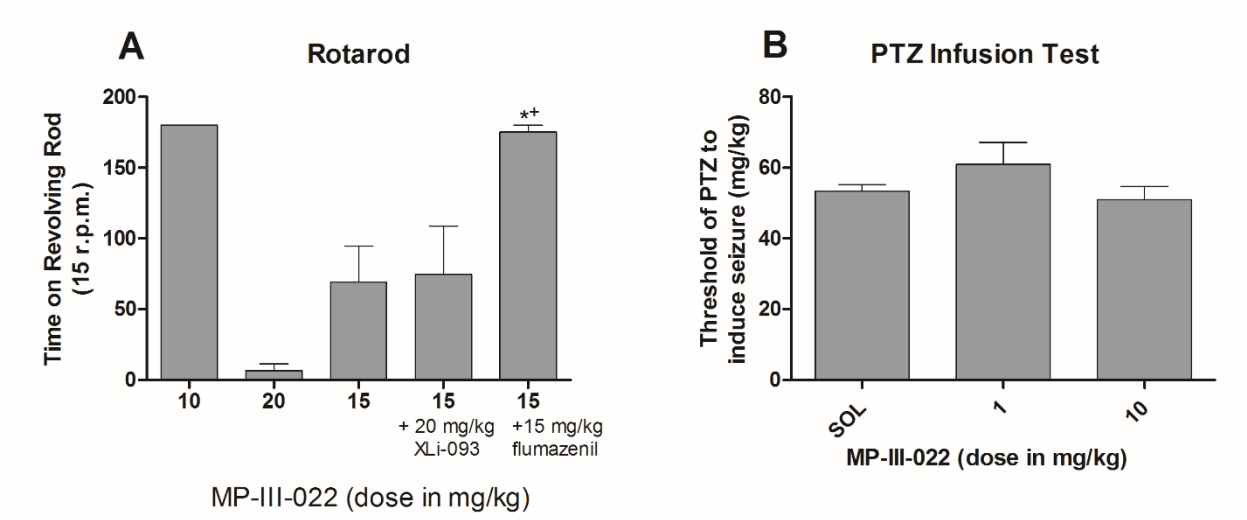


Figure 74. The effects on MP-III-022 (65) in basic behavioral tests. A) Male Wistar rats (n = 3 – 9) were dosed i.p. with MP-III-022 (10, 15 or 20 mg/kg) 20 minutes prior to assessment on the rotarod for ataxic effects. Additionally, MP-III-022 (15 mg/kg) was coadministered with the α5 anatagonist XLi-093 (20 mg/kg) or the Bz/GABA$_A$R antagonist flumazenil; B) Male Wistar rats (n = 11) were dosed with vehicle or MP-III-022 (1 or 10 mg/kg) for the assessment of seizure protection in the PTZ infusion (scMET) test. *p < 0.05 compared to 15 mg/kg MP-III-022, +p < 0.05 compared to combination of 15 mg/kg MP-III-022 and 20 mg/kg XLi-093.

Examination of the results indicated that a 10 mg/kg i.p. dose of amide MP-III-022 (**65**) does not lead to ataxia, while doses of 15 and 20 mg/kg led to failures in the rotarod assay. Co-administration of 15 mg/kg of **65** with α5 antagonist XLi-093 (20 mg/kg) did not result in any change from dosing with solely 15 mg/kg of **65**. This indicated that the ataxic effects which were observed do not stem from the α5 GABA$_A$R subtype. The combination of **65** (15 mg/kg) with the non-selective Bz/GABA$_A$R antagonist flumazenil (15 mg/kg) was able to reverse the ataxic effects induced by *R*-**65**. This indicated that the ataxic effects which were observed at a 15 or 20 mg/kg dose of **65** were a result of the activation of one or more of the α1, α2 and/or α3 GABA$_A$R subtypes, most likely α1. This may have occurred because of the rapid penetration of methyl amide **65** into the brain.

The PTZ-infusion test was to determine if MP-III-022 (**65**) exerted any anticonvulsant effects, which would be expected to originate from the α1 and α2 subtypes.[41, 42] Male Wistar rats (n = 11) were pretreated i.p. with vehicle solvent (85% water, 14% propylene glycol, 1% Tween 80) or **65** (1 or 10 mg/kg) 20 minutes prior to IV administration of PTZ, which was infused until seizures were observed, as depicted in Figure 74B). Analysis of the results indicated that **65** at doses up to 10 mg/kg did not offer protection from PTZ-induced seizures as compared to vehicle, which demonstrated that **65** at 10 mg/kg did not modulate the α1 or α2 subtypes. Taken together with the results from the rotarod study, it can be concluded that the effects observed in male Wistar rats following a 10 mg/kg dose of MP-III-022 (**65**) can be attributed solely to positive modulation of the α5 subtype; at higher doses other receptors became involved. This was taken into account for the following studies.

4.3.6.2 In Vivo Cognition Performance of MP-III-022

4.3.6.2.1 Morris Water Maze

The Morris water maze is a commonly used behavioral test to study spatial learning and memory[260] associated with the α5 subtype. The test consists of placing a rodent into a circular pool of water which has a platform placed just beneath the water level. The platform is left in one constant spot with visual cues for orientation to aide in locating the platform.[261, 262] After a rodent is trained to quickly locate the platform, a cognition-altering drug can be administrated to determine the effect it has on locating the platform.[260] Because activation of the α5 Bz/$GABA_AR$ subtype is inhibitory in learning, it was expected that MP-III-022 (**65**) would decrease performance in the Morris water maze.[245]

The Morris water maze was conducted using male Wistar rats (n = 6 – 7). After successful training, rats were given a 20 minute pretreatment i.p. injection of vehicle, diazepam (2 mg/kg) or *R*-**65** (1, 2.5 or 10 mg/kg) and placed into the pool of water at varying locations to negate swimming patterns with a platform oriented 2 cm below the surface of the water. Rats were tracked to determine the distance in the target zone that was traveled, as well as the distance (in %) traveled outside of the target area, as illustrated in Figure 75.

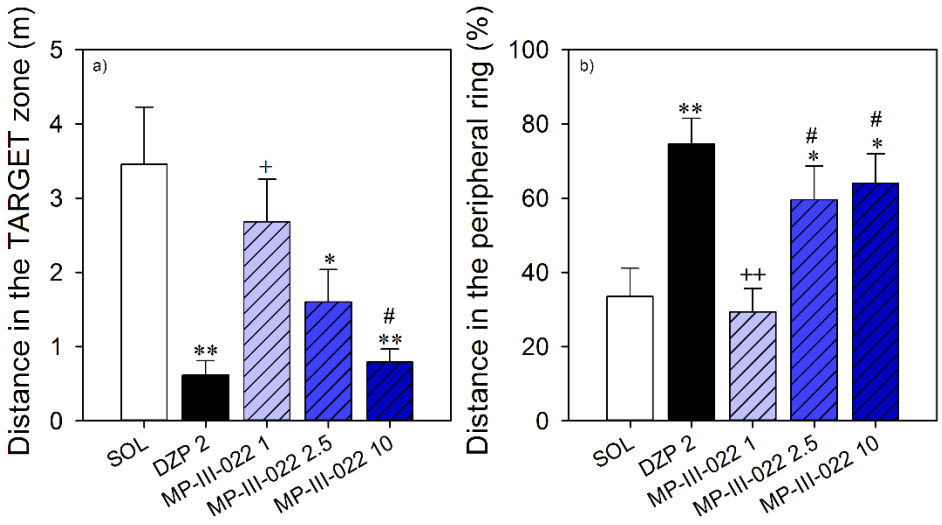


Figure 75. The effects of 2 mg/kg diazepam and 1, 2 and 10 mg/kg MP-III-022 on (a) distance in the target zone (m) and (b) distance in the peripheral ring (%) during probe trial in the water maze. *p < 0.05, **p < 0.01 compared to solvent (SOL) group; +p < 0.05, ++p < 0.01 compared to 2 mg/kg diazepam (DZP 2) group; #p<0.05 compared to 1 mg/kg MP-III-022 (MP-III-022 1) group. Animals per treatment group were 6-7. SOL = solvent, DZP 2 = 2 mg/kg diazepam, MP-III-022 1 = 1 mg/kg MP-III-022, MP-III-022 2.5 = 2.5 mg/kg MP-III-022, MP-III-022 10 = 10 mg/kg MP-III-022

Examination of the results indicated that a 10 mg/kg dose of **65** had similar results to a 2 mg/kg dose of diazepam at decreasing the distance traveled in the target zone which is likely due to the positive activation of the α5 subtype altering spatial learning. A 1 mg/kg dose of **65** had no change as compared to vehicle, indicating that the α5 subtype was not significantly modulated at that dose to decrease cognition. However, this dose might be useful in reversing the effects which

occur in schizophrenia to reset the correct oscillation effect or simply decrease the number of signals over-stimulating the hippocampus via α5 subtypes in long-term potentiation or perhaps even short-term potentiation. The 2.5 mg/kg dose of **65** resulted in a decrease in the target zone, which implied that a 2.5 mg/kg dose of **65** was potent enough to have an effect on spatial learning and memory. Consequently, diazepam and the 2.5 and 10 mg/kg doses of **65** increased the % of distance traveled in the peripheral ring, while the 1 mg/kg dose of **65** displayed no change from vehicle. These results were expected as they are generally inversely correlated with the distance traveled in the target zone.

4.3.6.2.2 Social Novelty Discrimination Procedure

The social novelty discrimination procedure is used to compare the social investigation time of an adult rat with a familiar and a novel juvenile rat.[263] The first phase (T1) introduced a juvenile rat to an adult rat for five minutes. After a 30 minute break, the second phase (T2) consisted of the adult rat being placed in the cage with the same juvenile rat along with a second, novel juvenile rat. The time spent with each of the two rats in T2 is measured. Typically, the adult rat will spend more time with the familiar rat opposed to the novel rat. This procedure was conducted on adult male Wistar rats (n = 8) which were dosed i.p. with vehicle, diazepam (1.5 mg/kg) or **65** (1, 2.5 or 10 mg/kg) 20 minutes prior to testing and the results are presented in Figure 76.

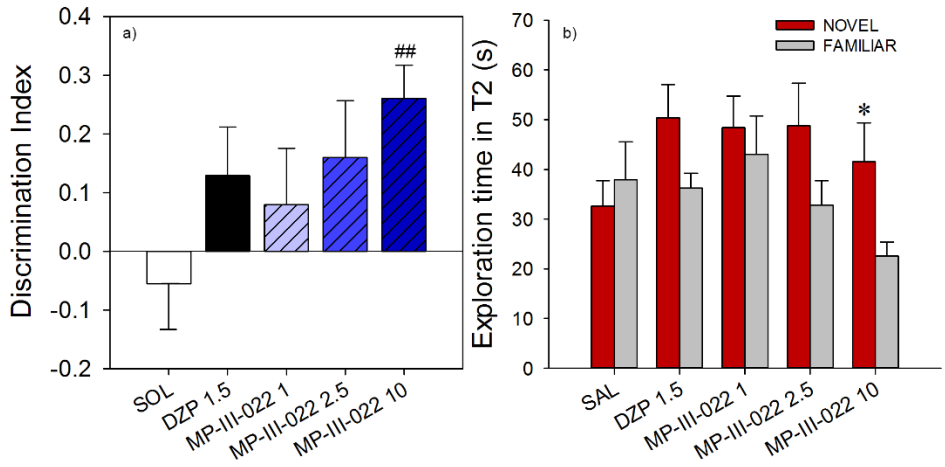


Figure 76. The effects of 1.5 mg/kg diazepam (DZP 1.5) and 1, 2.5 and 10 mg/kg MP-III-022 on discrimination index (a) and the time exploring the familiar and the novel juvenile rat in T2 (b) in the social novelty discrimination procedure. A significant difference from zero for discrimination index is indicated with: (one simple t-test, ##p < 0.01). *p < 0.05 for the familiar vs. novel exploration times (paired-samples t-test). Data are represented as mean + SEM. Number of animals per treatment group was 8. SOL = solvent, DZP 1.5 = 1.5 mg/kg diazepam, MP-III-022 1 = 1 mg/kg MP-III-022, MP-III-022 2.5 = 2.5 mg/kg MP-III-022, MP-III-022 10 = 10 mg/kg MP-III-022

Analysis of the results indicated that a 10 mg/kg dose of MP-III-022 (**65**) facilitated the adult rat to spend a significantly greater amount of time with the novel rat than the familiar rat. This was consistent with the observation that a 10 mg/kg dose strongly modulated the α5 subtype in the Morris water maze.

Expanded statistics can be found in the prepared manuscript by Timic, *et al*. in Appendix F. Taken together, the results of these studies present a ligand that can be given at very low doses (1 – 5 mg/kg) to evaluate the therapeutic significance of positively modulating the α5 $GABA_AR$ subtype. The importance of MP-III-022 (**65**) as a potential use in the treatment of schizophrenia has yet to be evaluated.

4.3.7 The Antidepressant Effects of α5 Subtype Selective Ligands

The α5 subtype selective SH-053-2'F-R-CH_3 (**52**) was sent to Sean Piantadosi and Dr. Etienne Sibille (University of Pittsburgh) with the intention of further characterizing the ligand for the use in cognition disorders. Unexpectedly, **52** was found to produce antidepressant effects in female, but not male, C57BL/6J mice. Although there is some rationale for the role of the α2 subtype playing a part in treating depression[170] and previously supported by the results of KRM-II-81 (**36**) as discussed in Section 3.3.7.7, other evidence suggests that positively modulating the α5 subtype which inhibits GABA could also be useful.[6, 199] There is a wealth of reports in the scientific literature correlating decreased expression of α5 Bz/$GABA_A$ subunits in both schizophrenia and bipolar depression.[264-266]

The effect of α5 $GABA_A$Rs on schizophrenia and bipolar I disorder are genetically and etiology linked.[264-266] The unpredictable chronic mild stress (UCMS) procedure was known to precipitate anxiety- and depressive-like behavior.[267] The procedure exposed test subjects (male and female C57BL/6J mice) to multiple mild stressors each day over a 6 weeks span; these stressors include wet bedding, brief restraint, forced bath, no bedding and predator odor present, along with single-cage isolation towards the end of the 6-week period. The study evaluated both chronic (28 days) and acute dosing of SH-053-2'F-R-CH_3 (**52**) given at 30 mg/kg by i.p. administration. The behavioral testing consisted of the elevated plus maze (EPM), open field test (OFT), novelty suppressed feeding test (NSF) and a cookie test. The EPM and OFT tests are designed to measure the movement and location of the mice, where the greater the movement indicated a decrease in anxiety and/or depression; while the novelty suppressed feeding test and cookie test measured the latency to bite food placed in an unfamiliar area, where an increased latency time indicated a greater level of anxiety and/or depression (for expanded descriptions, refer

to Section 4.5.17 in the Methods section). The results of these behavioral tests are presented in Figure 77 (EPM and OFT are depicted in panels A and B; NSF in panel C; cookie test in panel D).

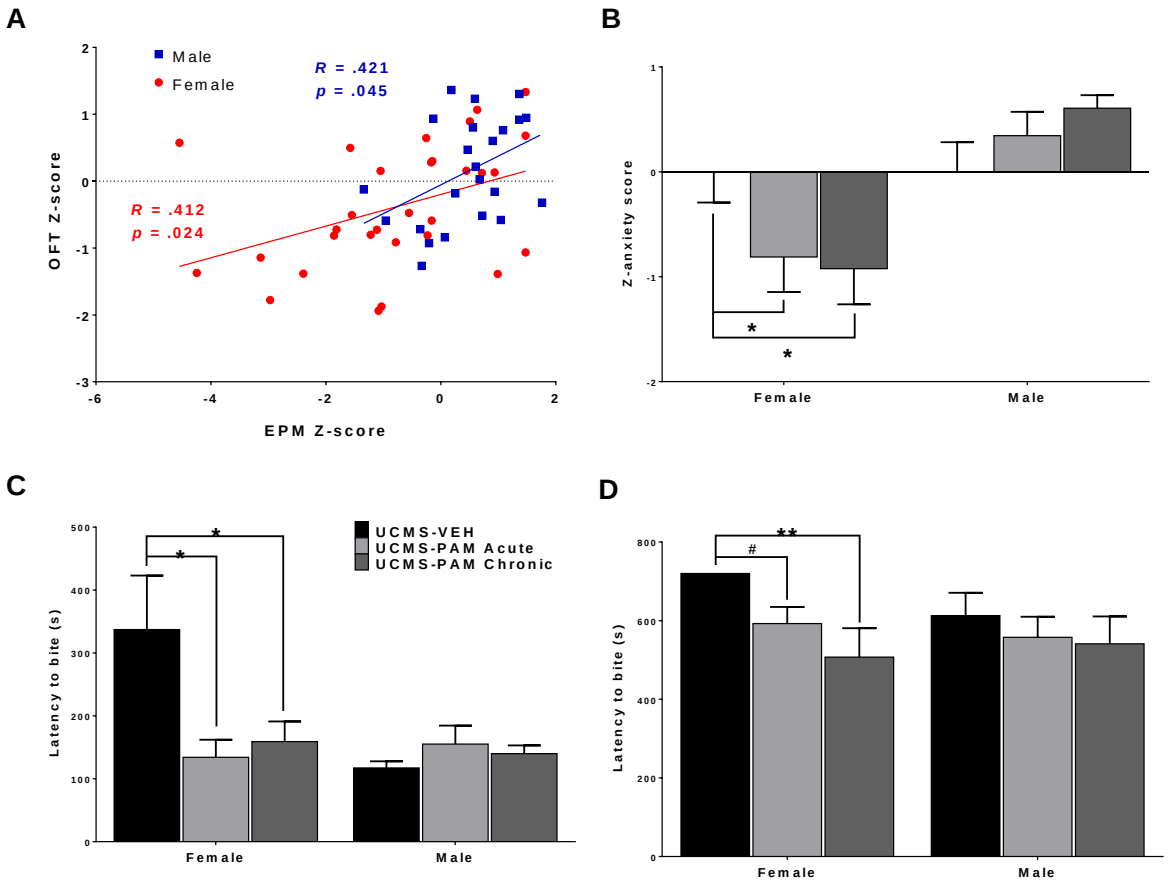


Figure 77. Effect of SH-053-2'F-R-CH$_3$ (52; α5-PAM) on anxiety- and depressive-like behavior induced by UCMS in female and male mice. A) Shown are significant positive correlations of Z-anxiety scores from the EPM and OFT. B) Female mice treated acutely and chronically with α5-PAM had reduced anxiety-like behavior across both tests while no effect of treatment was observed in male mice. C) Treatment with acute and chronic α5-PAM reduced latency to bite a food pellet in the NSF in female but not male mice. D) Chronic α5-PAM treatment reduced latency to bite a piece of cookie in the cookie test in female mice, while a trend in the same direction was observed following acute treatment. No significant effect of α5-PAM was detected in males. *p<.05, **p<.01, ***p<.001.

Analysis of the results presented in Figure 77 indicated that female, but not male, mice when given SH-053-2'F-R-CH_3 (**52**) exhibited reduced anxiety- and/or depression-like symptoms in both chronic and acutely dosed assays as compared to vehicle. The results from the EPM and OFT observed that female mice exhibited an anxiolytic-like response indicated by the increased time in the open arms of the EPM and the greater locomotor activity count in the OFT. A significant difference between sexes was observed in the NSF and cookie test as the latency to bite was significantly lower for females than for males as compared to an individual vehicle for each sex. The increased time to react in both the NSF and cookie test indicated a higher rate of depression. Taken together, this data indicated that treatment with SH-053-2'F-R-CH_3 (**52**) reduced stress-induced emotionality in female mice; whereas administration of **52** in male mice had no effect as compared to the male vehicle.

One observation that can be seen is the increased latency to bite in the NSF (Figure 77C) for female vehicle as compared to male vehicle. It is known that the prevalence of major depressive disorders in humans is higher in females than in males; although the causes are still being investigated.[268] This may play a role in rodents as well as humans; regardless, a significant effect was seen when females were dosed with **52**. The results of the EPM in which males exhibited no difference from vehicle is in agreement with a previous study which assessed male rats in the EPM; females were not tested.[113] Additionally, a Vogel conflict procedure using male rhesus monkeys (n = 4) were dosed with SH-053-2'F-R-CH_3 (**52**) which was found to be inactrive as an anxiolytic unless at a very high dose.[112] This data supports the possibility that targeting the α5 subtype may have antidepressant-like effects in females but not males, although more studies are necessary for this to be concluded.

Expanded statistics on SH-053-2'F-R-CH_3 (**52**) in a prepared manuscript by Piantadosi *et al*. on this topic are located in Appendix G. Additionally, this work has led to the assessment of the antidepressant effects of MP-III-022 (**65**). Preliminary data indicated that **65** is able to reduce the depressant effects induced by UCMS (preliminary results by Catherine Belzung, Etienne Sibille, M. Poe, J. Cook, *et al*. can be found in Appendix I).

4.3.8 The Use of α5 Subtype Selective Ligands as Bronchodilators for Asthma

Over the past decade, research by Dr. Charles Emala, *et al*. have identified functional $GABA_AR$ ion channels containing either the α4 or α5 subunit by reverse transcription polymerase chain reaction (RT-PCR) studies and Western blot as well as immunohistochemistry analysis in airway smooth muscle (ASM).[66] Initial studies found that the $GABA_AR$ agonist muscimol was able to induce relaxation of precontracted guinea pig tracheal rings or human bronchial ASM using an organ bath.[269] The ability to selectively modulate $GABA_ARs$ for bronchodilation would offer a novel new treatment for asthma beyond the current clinical bronchodilators such as methylxanthines, anticholinergics and β-adrenoceptor agonists.[270] Because activation of all $GABA_ARs$ can lead to numerous adverse effects, including mucus production in the lungs[271] which can exacerbate the symptoms of asthma, the employment of an α4- or α5-subtype selective ligand is needed to reduce these liabilities. Two α4 subtype selective ligands CMD-45[64] and XHe-III-74[272] (Figure 78) have been shown to successfully relax precontracted guinea pig tracheal rings. This ability to target $GABA_ARs$ for bronchorelaxation was also attempted using the α5 subtype selective agonist (PAM) SH-053-2'F-R-CH_3 (**52**).[217]

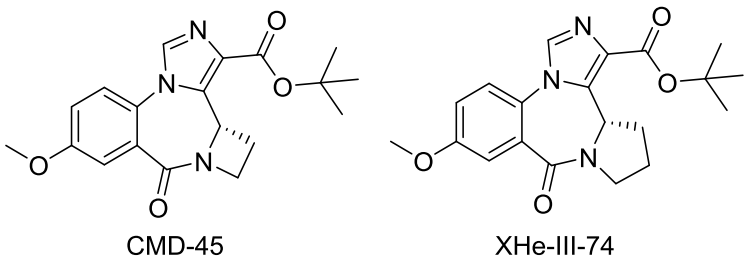


Figure 78. Structures of the α4 selective ligands, CMD-45 and XHe-III-74.

4.3.8.1 Assessment of the α5 Subtype Selective Ligand SH-053-2'F-R-CH₃ (52) as a Bronchodilator (Gallos, et. al.)[217]

The contraction of airway smooth muscle (ASM) is due, in part, to the actin-myosin interactions[273] which results in bronchoconstriction.[274] Because α5 $GABA_A$Rs are known to be present in ASM,[66] the co-localization of smooth muscle α actin and α5 $GABA_A$Rs was assessed by immunohistochemistry in human trachea (Figure 79). The first (1st) panel shows the α5-$GABA_A$R subunit in an ASM section nuclear stained with DAPI (4',6-diamidino-2-phenylindole) and appears in fluorescent green and blue. The second (2nd) panel is the same muscle section stained with an anti-α-smooth muscle actin antibody, appearing in red. The third (3rd) panel is the overlay of the first two panels confirming the co-localization of the α5 subunit and smooth muscle actin in human trachea. The final (4th) panel was used as a control with DAPI staining but omitting primary antibodies.[217]

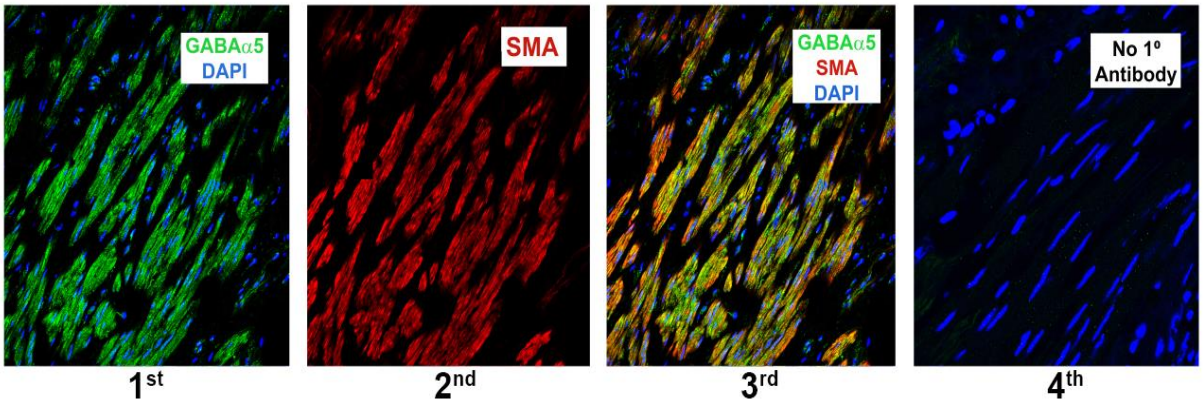


Figure 79. Protein expression of the GABAA α 5 subunit in intact human trachea-bronchial airway smooth muscle. Representative images of human tracheal airway smooth muscle sections using confocal microscopy are depicted following single, double, and triple immunofluorescence labeling. The antibodies employed were directed against the GABAA α5 subunit (green), α-smooth muscle actin (SMA; red) and/or the nucleus via DAPI counterstain (blue). Panels illustrate the following staining parameters from left to right: (1st) co-staining of DAPI and GABAA α5 subunit (2nd) α-SMA staining alone (3rd) triple-staining of GABAA α5, α-SMA, and DAPI (4th) DAPI nucleus counterstain, with primary antibodies omitted as negative control. Modified from the figure in Gallos, *et al.*[217]

Following the demonstration of protein expression of $GABA_AR$ containing the α5 $GABA_A$ subunit, the ability of SH-053-2'F-R-CH_3 (**52**) to relax precontracted ASM in human and guinea pig ASM was executed. The smooth muscle was suspended in an organ bath and monitored using a force transducer. The ASM was first pre-contracted using acetylcholine at the predetermined EC_{50} concentration. The induced contraction was then relaxed with a β-agonist (isoproterenol) in the absence or presence of *R*-**52**. Examination of the results indicated that the amount of relaxation induced by isoproterenol (10 nM) was significantly increased when **52** was co-administered at 50 μM, as depicted in Figure 80A. Additional studies using substance P, a contractile agent, in guinea pig tracheal rings measured the ability of the α5 selective **52** to relax ASM 30 minutes after substance P-induced contraction, as illustrated in Figure 80B. The α5 subtype selective ligand SH-053-2'F-R-CH_3 (**52**) was also shown to significantly decrease the amount of muscle force, which indicated that **52** successfully promoted relaxation of the tracheal ring.[217]

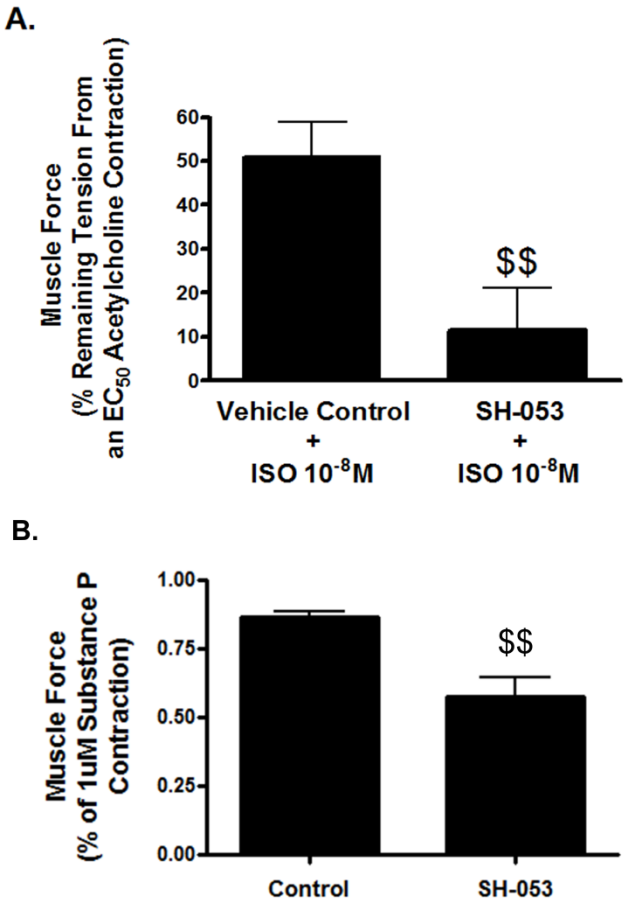


Figure 80. SH-053-2'F-R-CH$_3$ (52) mediated activation of α5 subunits containing GABA$_A$ channels induces relaxation of pre-contracted airway smooth muscle. A) SH-053-2'F-R-CH$_3$ (labeled as SH-053) potentiated β-agonist-mediated relaxation of human airway smooth muscle. Co-treatment of human airway smooth muscle strips with SH-053-2'F-R-CH$_3$ (50 μM) significantly enhanced isoproterenol (10 nM) mediated relaxation of an acetylcholine EC$_{50}$ contraction compared to isoproterenol alone. (N=8/group, $$=p <0.01). B) SH-053-2'F-R-CH$_3$ activation of α5 containing GABA$_A$ receptors induces direct relaxation of substance P-induced airway smooth muscle contraction. Compiled results demonstrating enhanced spontaneous relaxation (expressed as % remaining force at 30 minutes following a 1 μM substance P mediated contraction) following treatment with SH-053-2'F-R-CH$_3$ compared to treatment with vehicle control (n=4-5/group, $$ = p< 0.01). Modified from the figure in Gallos *et al.*[217]

4.3.8.2 Additional Studies using α5 Ligands as Bronchodilators

The results from SH-053-2'F-R-CH$_3$ (**52**) prompted additional studies using α5 subtype selective ligands as potential bronchodilators. The structurally related methyl ester MP-III-004 (**63**), methyl ester, C(8)-bromide MP-III-058 (**78**), as well as the SH-053-2'F-R-CH$_3$-Acid (**73**), the predicted metabolite of **52** and **63**, were investigated (structures shown in Figure 81).

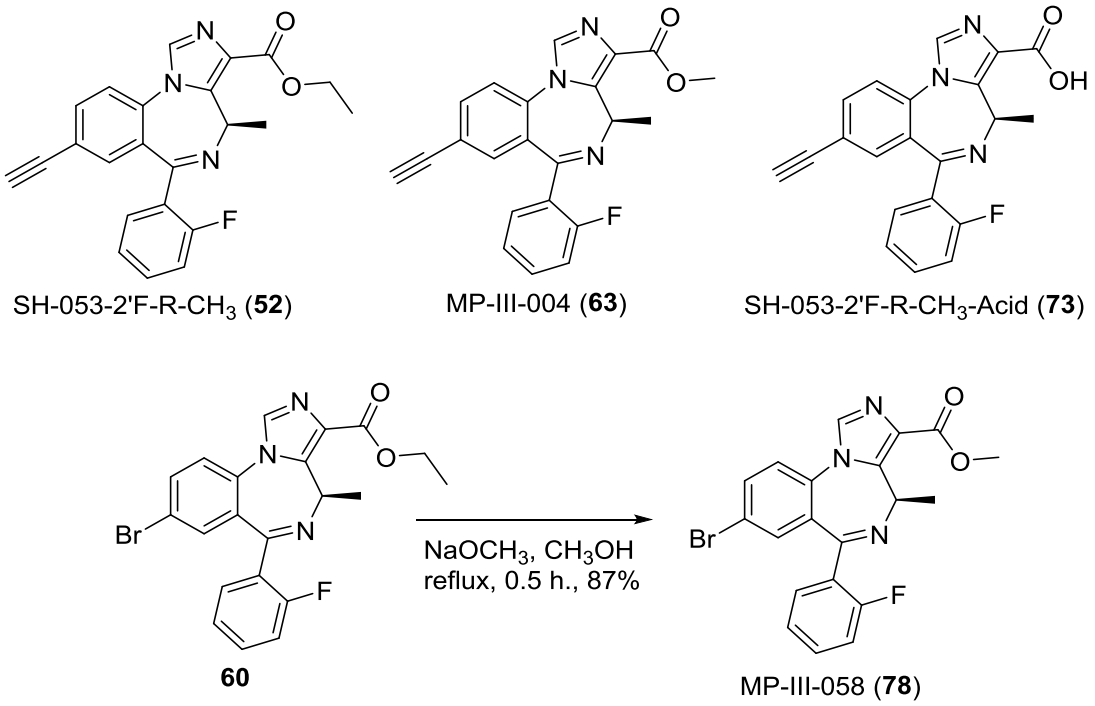


Figure 81. Structures of α5 selective ligands assessed in an organ bath for the relaxation of precontracted airway smooth muscle; as well as the route to the methyl ester MP-III-058 (78).

As previously discussed, the methyl ester MP-III-004 (**63**) has an improved oocyte efficacy profile as compared to the ethyl ester **52** in regards to α5 selectivity. The carboxylic acid **73** and bromide MP-III-058 (**78**) were first assessed for their modulation of chloride currents in *Xenopus laevis* oocytes, as depicted in Figure 82 (note the Y-axis scale for **73** is different than the remaining compounds). The bromide **78** was found to have similar receptor preference as the C(8)-acetlyene counterpart **63**, albeit higher efficacy towards non-α5 containing receptors at higher concentrations; although bromide **78** does appear to be more potent towards the α5 subtype modulating currents greater at 100 nM than MP-III-004 (**63**). The carboxylic acid **73** was found to be extremely efficacious at the α5 subtype with a modulation of ~600% above baseline at 100 nM

with little to no activation of non-α5 subtypes. This potentially permits strong modulation of the α5 subtype without off-target effects with the correct dosing.

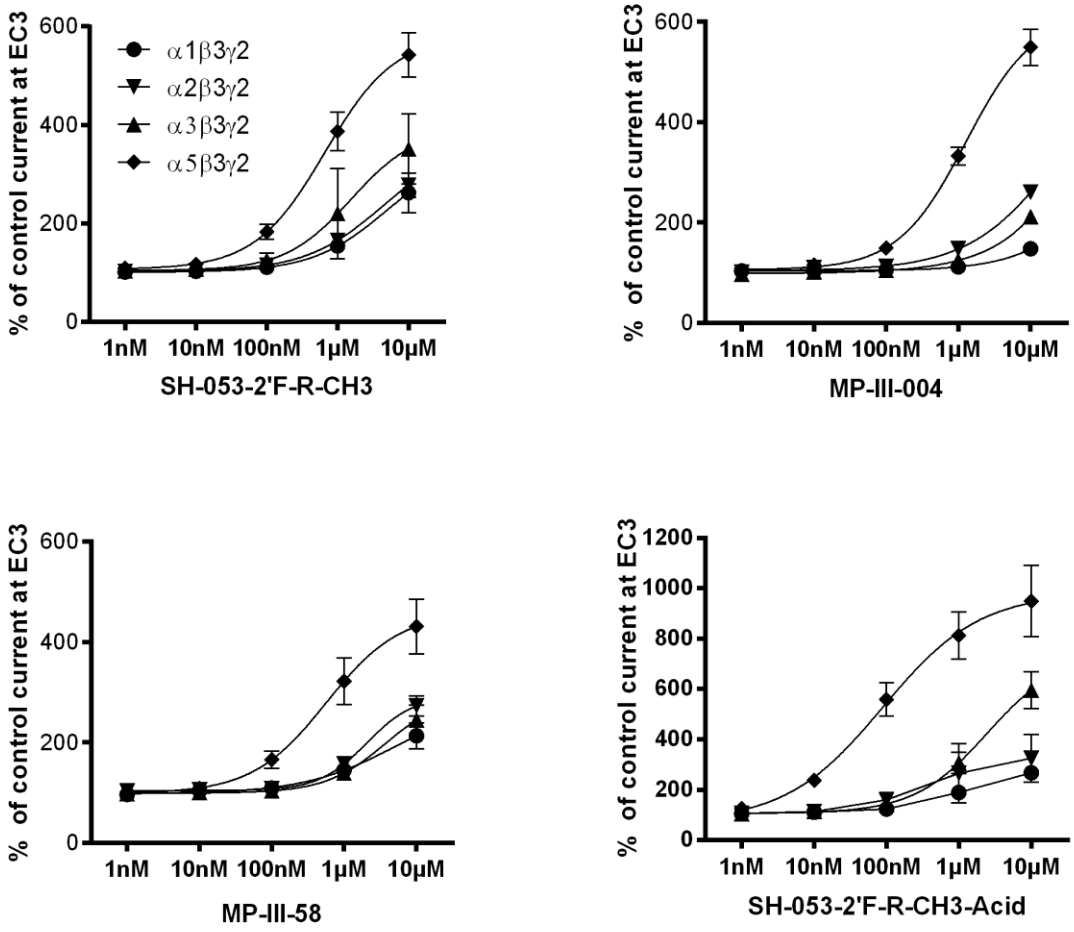


Figure 82. Oocyte efficacy of the α5 selective ligand, SH-053-2'F-R-CH$_3$ (52), MP-III-004 (63), MP-III-058 (78) and SH-053-2'F-R-CH$_3$-Acid (73). Concentration curves on GABA$_A$ receptors using an EC$_3$ GABA concentration (n = 3 – 5).

One necessary consideration when using ligands as bronchodilators in the lungs which target GABA$_A$Rs, either selectively or non-selectively, is the possibility of CNS adverse effects. Many current treatments of asthma use an aerosol for the method of delivery. If this is the case for

acid **73**, there would be a low chance for BBB penetration which would lead to a reduced risk of CNS effects. If CNS adverse effects were to occur, it would likely result in learning and memory complications in the case of α5 subtype selective ligands.[192] One goal of using BZDs in the treatment of asthma is that they could be taken orally, eliminating the drawbacks of aerosols. For this to be feasible with an α5 selective ligand, there needs to be low BBB permeability. This was investigated by dosing male Wistar rats (n = 3) i.p. with 10 mg/kg of the test compounds and the plasma and brain concentrations were analyzed (Table 12) 20 minutes after treatment.

Table 12. Plasma and brain concentrations taken 20 minutes after an i.p. (10 mg/kg) injection of α5 selective ligands, n = 3.

Compound	**Plasma (nmol/L)**		**Brain (nmol/kg)**	
	Total	**Free**	**Total**	**Free**
52 (ethyl ester)	337 ± 145	231 ± 99	553 ± 242	21 ± 9
63 (methyl ester)	1182 ± 546	418 ± 193	1696 ± 270	106 ± 17
78 (methyl ester)	95 ±64	61 ±41	903 ± 395	11 ± 4
73 (acid)	1511 ± 815	272 ± 146	**BQL**[a]	**BQL**

[a] BQL = below quantification limit

Analysis of the results *in vivo* indicated that the carboxylic acid **73** had very little or no brain penetration, with amounts undetectable in brain samples. This is in agreement with the expectation that the carboxylic acids of these molecules are too hydrophilic to cross the BBB, as seen previously with SR-II-54 (**20**). The acid **73** also appeared to be the most stable to degradation, as indicated by the greatest plasma concentration at 1511 nmol/L. It is interesting that methyl ester MP-III-004 (**63**) exhibited significantly higher brain and plasma concentrations than the similarly related ethyl ester **52** and methyl ester **78**. However, this is completely compatible with the rapid hydrolysis of esters as compared to the longer half-life of some amides. Despite the low plasma

concentrations of bromide **78**, the 10-fold increase in brain concentration indicated that **78** was able to readily cross the BBB, although at a low free concentration in the CNS.

These ligands, along with HZ-166 (**3**) and SH-I-048A (**55**) were assessed to determine their ability to relax precontracted guinea pig tracheal rings. HZ-166 (**3**) was used as a negative control since the α2/α3 subtype selective agonist with very low efficacy at the α1 and α5 subtypes was not expected to induce relaxation since only functional receptors containing α4 and α5 subtypes have been identified in ASM. The ligand SH-I-048A (**55**) has been previously reported as a super-agonist at all DS sites ($\alpha_{1\text{-}3,5}\beta_{2/3}\gamma 2$),[275] becoming extremely potent at concentrations as low as 10 nM, as illustrated in Figure 83. Based on the *in vitro* electrophysiology of the ligands, it was expected that the acid **73** and super-agonist **55** would induce the greatest relaxation, while the methyl esters **63** and **78** would have similar results to ethyl ester **52**. These ligands were assessed in the organ bath using precontracted guinea pig tracheal rings as described previously (Figure 84).

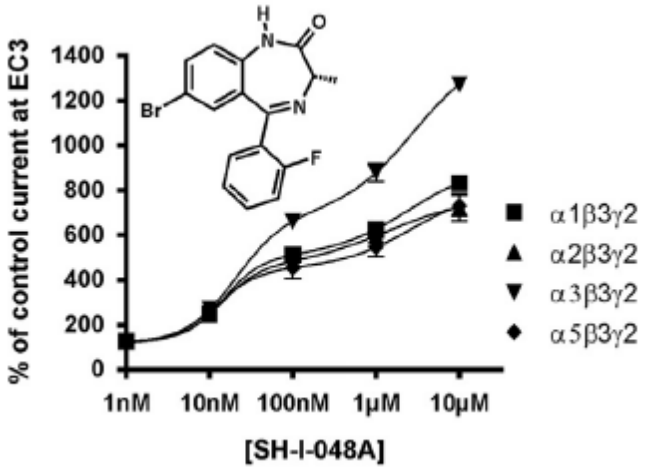


Figure 83. Oocyte efficacy of the super-agonist SH-I-048A (55). Concentration curves on $GABA_A$ receptors using an EC_3 GABA concentration (n = 3 – 5). Modified from the figure in Obradovic, *et al*.[275]

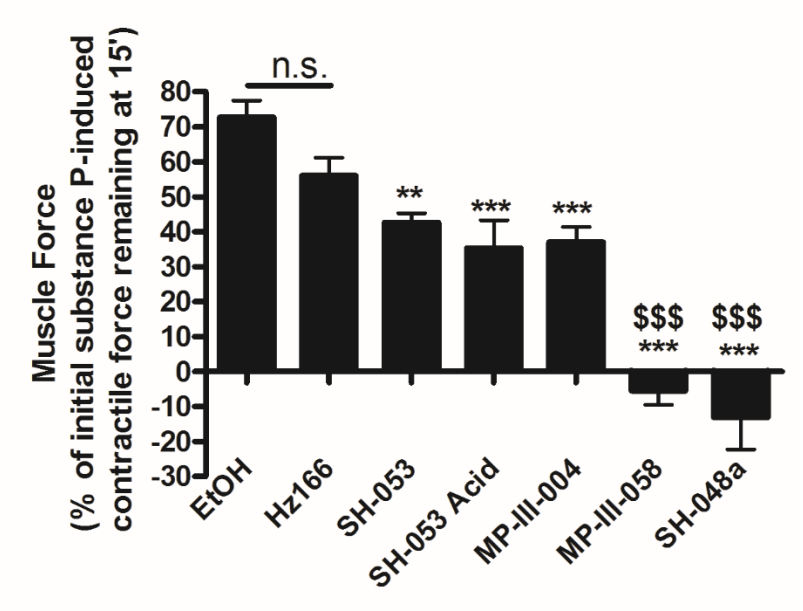


Figure 84. Assessment of α5 ligands, HZ-166 and SH-I-048A in airway smooth muscle force relaxation. Guinea pig tracheal rings were suspended in an organ bath and precontracted with substance P (1 μM), followed by vehicle (0.1% EtOH) or a test ligand (50 μM) and the force was measured. ** and *** p< 0.01 and 0.001 compared to vehicle control, respectively; $$$ p< 0.001 compared to SH-053, n = 6-17. (SH-053 = SH-053-2'F-R-CH_3; SH-053 Acid = SH-053-2'F-R-CH_3-Acid).

The results indicated that the α2/α3 selective HZ-166 (**3**) did not induce a significant relaxation as compared to vehicle (EtOH). The C(8)-acetylene methyl ester MP-III-004 (**63**) improved performance over ethyl ester **52** as compared to vehicle; however, the two ligands did not perform statistically different when compared to each other. The super-agonist **55** induced the greatest relaxation, causing the ASM to produce less force than what was initially measured. Unexpectedly, the acid **73**, which had a similar α5 efficacy profile as **55**, performed on par with ethyl (**52**) and methyl (**63**) esters. Additionally, the C(8)-bromide **78** was found to relax the ASM as well as the super-agonist **55**. This activity of **73** which is similar to ethyl ester **52** and methyl ester **63** may indicate one can use them to treat asthma depending on the vehicle and route of administration (aerosol or oral) because these esters are metabolized to the acid **73** rapidly and even on first pass metabolism.

These results indicated that positive modulation of the α5-containing functional $GABA_AR$s induce relaxation of precontracted ASM. Part of this is evidenced by the α2/α3 PAM HZ-166 (**3**) which was unable to relax the guinea pig tracheal rings as indicated before. An additional study to further support this conclusion would be to antagonize the α5 subtype. Unfortunately, the non-selective diazepam-sensitive (DS) $GABA_AR$ antagonist flumazenil,[276] as well as the selective α5 antagonist XLi-093 (**47**),[220] both cause positive modulation of the α4 subtype. This could result in the relaxation of ASM through modulation of the α4 $GABA_AR$ rather than the α5 subtype. It was interesting to observe that the relaxation induced by **78** is as nearly as potent as the super-agonist **55**, while the carboxylic acid **73** induced relaxation similar to ethyl ester **52**, despite its potency *in vitro* at the α5 subtype. It is worth mentioning that *in vitro* experiments do not always correlate to *in vivo*, or *ex vivo* in these examples since results on neuronal firing are not always consistent from one type of experiment to another and is not surprising.

Because invoking CNS effects is a concern when using IBZDs as a treatment for asthma, the route of administration and potential brain penetration must be taken into account. With an inhaler or nebulizer, although the ligand would be delivered directly into the lungs, there is still the risk of the compound reaching the brain. For a compound such as the super-agonist **55** which targets all DS sites, it could exert a number of adverse effects upon dosing; although it was not tested for brain concentrations, it is structurally related to diazepam and would be expected to have good penetration. Some of these adverse effects of **55** including ataxia and sedation have been reported by Savic, *et al.*[275] The pharmacokinetic studies indicated that, regardless of route of administration, the acid **73** would be the preferred α5 ligand as it was not detected in brain levels. This would also allow **73** to potentially be given orally if lung exposure levels are deemed

acceptable (not yet tested). Similar to CNS adverse effects, there is also a risk of off-target effects within the lungs.

4.4 Discussion

The importance of the α5-$GABA_AR$ has been of significant interest following findings by Möhler, *et al*., since it related to cognition disorders such as schizophrenia, bipolar disorder and Alzheimer's disease. The enantiomers SH-053-2'F-S-CH_3 (**51**) and SH-053-2'F-R-CH_3 (**52**) both positively modulated the α5 subtype, while the *S*-enantiomer **51** also activated the α2 and α3 Bz/$GABA_A$ subtypes.[112] These ligands have both been reported to mitigate the hyperactivity induced by amphetamine, one of the positive symptoms of schizophrenia, when studied in the MAM- or the poly(I:C)- model of schizophrenia.[196, 197, 241] The *S*-enantiomer **51** was found here to reverse the deficits in prepulse inhibition (PPI) while the *R*-enantiomer **52** failed to do so; however, a shorter pretreatment time may provide superior results. Moreover, SH-053-2'F-R-CH_3 (**52**) in PPI was trending toward significance although the pharmacologist ran into logistic problems. Additionally, **51** was able to protect mice from electroshock-induced seizures. These results indicated that while the *R*-enantiomer **52** may be useful in treating some positive symptoms of schizophrenia, the *S*-enantiomer **51** may be used in the comorbidity in schizophrenia which occurs with anxiety[211, 212] and/or epilepsy.[213, 214]

The oocyte efficacy of the methyl ester MP-III-004 (**63**, Figure 67) and the methyl amide MP-III-022 (**65**, Figure 72) present two improved α5 ligands over SH-053-2'F-R-CH_3 (**52**); since **63** has reduced efficacy at α1, α2 and α3 subtypes while α5 is increased, and the amide **65** is much more potent at α5 receptors at low concentrations than the parent ethyl ester (*R*)-**52**. These two new ligands provide superior tools to study the neuroscience and behavioral aspects associated

with the α5 $GABA_AR$ subtype. The importance of the potent MP-III-022 (**65**) has been presented in a number of behavioral assays, which highlight the ability to modulate the α5 subtype in the absence of other α subtype effects at low concentrations in rats. Unexpectedly, MP-III-004 (**63**) protected mice from both electroshock- and pentylenetetrazole-induced seizures when dosed i.p. and orally. To date, there is no data to confirm that positive modulation of the $\alpha5\beta_{2/3}\gamma2$ can offer protection from seizures. Rudolph, *et al*. in a triple knock in mouse recently reported α5 $BzR/GABA_A$ subtypes can mediate anxiety. This, if confirmed, would provide some evidence for an α5-mediated anticonvulsant effect, but much research must be done to shed light on this result.

The ethyl ester SH-053-2'F-R-CH_3 (**52**) was assessed in mice that were subjected to unpredictable chronic mild stress (UCMS) and **52** was found to exhibit anxiolytic- and especially antidepressant-like effects in female, but not male mice. Although the underlying mechanisms for the role α5 $GABA_AR$ subtypes exhibit unequivocally in treating depression are not known, there have been many reports that the α5 subtype is involved[6, 199] and these data here, along with preliminary data on **65** (see Appendix I), offer additional support. As mentioned before, the α5 subtype is associated with schizophrenia and bipolar I depression. These two CNS disorders are genetically linked and the etiology is so similar that doctors misdiagnose one for the other. In addition, the anxiolytic-like effects of (*R*)-**52** in the elevated plus maze and open field test may be due to activation of the α5 subtypes, which has just recently been reported in a model of anxiety.[259, 277] This antianxiety effect will have to be confirmed in numerous studies because a triple knock-in mouse model may indeed have compensatory effects.

In addition to targeting CNS disorders, the α5 $GABA_AR$ subtype had been identified in airway smooth muscle.[66] The ethyl ester SH-053-2'F-R-CH_3 (**52**) was found to relax precontracted airway smooth muscle,[217] which led to the investigation of additional α5 subtype selective ligands

which were tested in organ baths studies. The primary concern of using α5 Bz/$GABA_AR$ subtype selective ligands as bronchodilators in the treatment of asthma is the possibility of CNS effects. Low brain penetration is necessary to avoid these adverse effects. This indicates that SH-053-2'F-R-CH_3-Acid (**73**) or a prodrug may be the best ligand to treat asthma. It does not go through the BBB, yet relaxes airway smooth muscle. Additionally, a tetrazole, which is a bioisostere of a carboxylic acid, may also provide desired results in organ bath studies while having low brain penetration.

CONCLUSION / FINAL REMARKS

The $GABA_A$ receptor has long been a topic of interest and has been targeted for a wide range of therapeutic uses, some of which include the treatment of anxiety, seizures, neuropathic pain, schizophrenia, bipolar disorder and Alzheimer's disease. Despite recent advances by Miller, *et al.*, the lack of a crystallized functional receptor has left researchers without definitive knowledge of the specific target site within the $GABA_AR$. Through molecular modeling, the Milwaukee-based pharmacophore/receptor model based on binding affinities of known ligands has certainly aided in the design of ligands for the Bz/$GABA_AR$ site containing $\alpha_{1\text{-}6}\beta_{2/3}\gamma2$ subtypes, the efficacy of a bound ligand can only be predicted with a certain level of error.

Seminal studies by Möhler, Rudolph, McKernan and others have greatly advanced the knowledge in the field of $GABA_AR$ with the use of knock-in mice to determine effects of specific subtypes. The exploitation of the pharmacological response evoked by the modulation of a specific $GABA_AR$ can be done ideally through a subtype selective ligand which activates a single subtype. The α2 containing $GABA_AR$ is of particular interest for anxiety and neuropathic pain; however, there are no α2 subtype selective ligands known to date. The similar homology of the α2 and α3 subtypes has led to many α2/α3 subtype selective ligands, such as HZ-166 (**3**), to be characterized for their ability to treat these disorders. The work here illustrated the discovery of the oxazole KRM-II-81 (**36**), which has improved pharmacokinetic and pharmacodynamics properties over HZ-166. Continued assessment of KRM-II-81 is underway, as well as work on many other similarly related ligands in the search for a therapeutic drug with improved properties for anxiety, epilepsy and neuropathic pain.

The work presented here on α5 selective ligands has produced significant improvements. The methyl ester MP-III-004 (**63**) has been shown to have reduced efficacy towards non-α5 subtypes over SH-053-2'F-R-CH_3, which has resulted in a more subtype selective ligand with a decreased risk of off-target effects. Additionally, the anticonvulsant activity of MP-III-004 discovered at ASP (NINDS) was an unexpected result that may lead to some interesting and important findings as it continues to be studied. The methyl amide MP-III-022 (**65**) is a very potent α5 subtype selective PAM and was found to modulate the α5 subtype at very low concentrations, permitting the behavioral effects to be studied with minimal dosing necessary.

The goal of this research was to develop ligands for the Bz/$GABA_A$ receptor to aid in the understanding of the $GABA_AR$. It is hoped that the framework of this research may continue to shed light directly on these subjects, or provide advancements for the next generation of ligands, which can be used for the treatment of anxiety disorders, epilepsy, neuropathic pain, schizophrenia and depression, as well as asthma; to create a better quality of life to those who suffer from these disorders.

4.5 Methods

4.5.1 Liver microsomal study (CRO)

Refer to Section 3.5.2 for details.

4.5.2 Cytotoxicity (Kelly Teske at the University of Wisconsin-Milwaukee)

Human embryonic kidney (HEK) 293T cells were purchased (ATCC) and cultured in 75 cm^2 flasks (CellStar) coated in Matrigel (BD Bioscience, #354234). Cells were grown in DMEM/High Glucose (Hyclone, #SH3024301) media to which non-essential amino acids (Hyclone, #SH30238.01), 10 mM HEPES (Hyclone, #SH302237.01), 5 x 10^6 units of penicillin and streptomycin (Hyclone, #SV30010), and 10% of heat inactivated fetal bovine serum (Gibco, #10082147) were added. HEK293T cells at 70-80% confluency were harvested with 0.05% Trypsin (Hyclone, #SH3023601), added to 10 mL of the assay buffer, DMEM/High Modified buffer without phenol red (Hyclone, #SH30284.01) containing all the above mentioned additives plus 10 mM sodium pyruvate and 2% percent charcoal treated FBS (Invitrogen, #12676-011) instead of HI FBS, and spun down for 2 min at 1000 rpm. The media was removed and cells were resuspended in the assay buffer. Prior to adding cells to a sterile white, optical bottom 384-well plates, plates were treated with 20 µL per well of a 0.25% Matrigel solution. To each well, 20 µL of cells were added to yield a final concentration of 15,000 cells per well for the 18 h timed assay. Cells were further diluted for the 48 h timed assay to yield 7,000 cells per well which allowed cells to grow without causing their own programmed cell death due to insufficient space and resources in each well. Plates were incubated for 4 h at 37 ºC with 5% CO_2 before 100 nL of serially diluted (1:3 in DMSO) small molecules (final maximum concentration at 150 µM) were transferred using a Tecan Freedom EVO liquid handling system with a 50H hydrophobic coated pin tool. The controls for the cytotoxicity assay used were 3-dibutylamino-1-(4-hexyl-phenyl)-propan-1-one

(150 μM in DMSO, positive) and DMSO (negative). After 18 h, assay plates were evaluated by adding 20 μL of Cell Titer-Glo™ Luminescence Assay Kit (Promega, Madison, WI) to each well and reading luminescence on a Tecan Infinite M1000 plate reader. Controls were measured within each plate to determine the z' factor and to enable data normalization. Three independent experiments were performed in quadruplicate and data was analyzed using nonlinear regression with variable slope (GraphPrism).

4.5.3 Time-concentration (plasma and brain) pharmacokinetic studies (Dr. Miroslav Savić at University of Belgrade)[275]

Male Wistar rats were divided into two cohorts of six groups each, which corresponded to predetermined time intervals (5, 10, 20, 40, 60, 180 and 360 min), each containing three animals. Ligands, dosed at 10 mg/kg, were administered by i.p. injection in a volume of 2 mL/kg (85% distilled water, 14% propylene glycol, 1% Tween 80). The blood samples were collected in heparinized syringes via cardiac puncture of rats anesthetized with ketamine solution (10% Ketamidor, Richter Pharma Ag, Wels, Austria, dosed i.p. at 100 mg/kg), and centrifuged at 2500 rpm for 10 min to obtain plasma. Thereafter, rats were decapitated and brains were weighed, homogenized in 5 mL of methanol and centrifuged at 6000 rpm for 20 min. To determine the concentrations of the ligands in plasma and supernatants of brain tissue homogenates, compounds were extracted from these samples by solid phase extraction, using Oasis HLB cartridges (Waters Corporation, Milford, Massachusetts). Concentrations of ligands in plasma and brain tissue were determined by ultra-performance liquid chromatography-tandem mass spectrometry (UPLC/MS/MS). The sample pretreatment procedure was carried out using solid-phase extraction (SPE) on Oasiss HLB cartridges (Waters, Milford, MA, USA). The procedure was adapted from the method reported by Mercolini *et al.*[278] Briefly, cartridges preconditioned with methanol and

water were loaded with samples (plasma or supernatant of brain tissue homogenate) and the internal standard solution. Endogenous impurities were removed by washing the cartridges with water and methanol. Finally, analyte elution was carried out with 1 mL of methanol for 1 minute.

4.5.4 Rat brain metabolism assay

Male Wistar rats (250-350 g.) were housed in pairs and kept on a 12h dark/light cycle (lights on at 7:00 am) with food and water provided *ad libitum*. For testing, a single rat was euthanized (asphyxiated) in accordance with IACUC, and decapitated with a small animal guillotine. The top of the skull was removed using bone rongeurs and the brain was extracted and placed in a pre-weighed 15 mL centrifuge tube. The tube was weighed to determine the weight of the brain, an equal amount of PBS was added and the mixture was homogenized. Individual centrifuge vials (1.5 mL) were prepared (100 μL PBS, 20 μL of a 100 μM stock solution of test compound, 80 μL brain homogenate) for eight (0, 10, 30, 60, 120, 240, 480, 1440 min) time points (n = 4 per time point) and placed in an oscillating heat-block (37 ^{o}C, 300 r.p.m.). At each time point, the reaction vial was quenched with cold acetonitrile (400 μL) containing a 10 μM internal standard and placed on ice. The vials were centrifuged (10,000 r.p.m.) for three minutes and the supernatant was pipetted into a spin filter centrifuge tube (0.22 micron nylon) and recentrifuged. Samples were diluted 20x (25 μL into 475 μL into LC-MS grade methanol) and analyzed using a Shimadzu LCMS-8040. Three independent experiments were performed (n = 4 for each independent experiment).

4.5.5 Seizure protection in the 6 Hz electroshock assay (ASP at NINDS)

Adult male CF1 mice (18-25 g) were pretreated intraperitoneally (i.p.) with the test compound at either 100 or 150 mg/kg. Each treatment group (n = 4 mice / group) was examined for anticonvulsive effects at one of five time points (1/4, 1/2, 1, 2, and 4 hr) after treatment with the

test compound. Following pretreatment, each mouse receiveed a drop of 0.5% tetracaine hydrochloride applied to each eye. The mouse was then challenged with the low-frequency (6 Hz) stimulation for 3 sec delivered through corneal electrodes. The low-frequency (6 Hz), long-duration (3 sec) stimuli are initially delivered at 32 mA intensity. Animals are manually restrained and released immediately following the stimulation and observed for the presence or absence of seizure activity. If the test compound is effective in the 6 Hz screen, mice were assessed in a dose-response using 5, 15, 30 and 60 mg/kg i.p. doses to determine the ED_{50} value

4.5.6 Ataxic assessment in the rotorod assay (ASP at NINDS)

Adult mice were dosed (i.p.) 30 minutes prior to being placed on a rotating rod at a speed of 6 rpm, as described in Dunham and Miya, 1957.[279] The ligand was considered toxic (sedating) if the animal fell off this rotating rod three times during a 1-min period. In addition to minimal motor impairment, animals may exhibit a circular or zigzag gait, abnormal body posture and spread of the legs, tremors, hyperactivity, lack of exploratory behavior, somnolence, stupor, catalepsy, loss of placing response and changes in muscle tone, and are noted accordingly by the observer. Toxicity at NINDS equates to sedation or ataxia.

4.5.7 Prepulse inhibition and the assessment for the development of catalepsy (Dr. David Baker and Nick Raddatz at Marquette University)

Animals

Male Sprague Dawley rats (350-450g) were singly housed and kept on a reverse 12hr dark/light cycle (lights on 7:00 pm) with food and water provided ad libitum. Behavioral testing occurred between the hours of 9:00 am and 4:00 pm with all animals individually handled a minimum of five minutes each for two days prior to the testing days.

Drugs

SH-053-2'F-R-CH_3 (**52**), SH-053-2'F-S-CH_3 (**51**), and haloperidol (Sigma-Aldrich, St. Louis, MO) were dissolved in dimethyl sulfoxide to a final concentration of 30 and 0.1 mg/mL, respectively. Dimethyl sulfoxide, while not an ideal vehicle for animal behavioral work, is an acceptable formulation for rats (Gad et al., 2006). Phencyclidine hydrochloride or MK-801 (NIDA Drug Supply Program, Research Triangle, NC) was dissolved in saline at a concentration of 1.5 or 0.1 mg/mL, respectively.

Prepulse Inhibition

Prepulse inhibition testing was run according to Bakshi and Geyer (1995).[249] Subjects were placed on a platform in a sound-attenuating chamber (10.75"x14"x19.5"; Hamilton Kinder, CA) that rested on a motion sensing plate. A matching session was conducted to determine the magnitude of the startle response for each subject. This session consisted of a five minute habituation period followed by 20 trials; 17 trials involved the presentation of a single auditory stimulus (pulse stimulus; 50 dB above a 60 dB background noise) and three trials in which a prepulse stimulus (10 dB above background) was presented 100 milliseconds before the pulse auditory stimulus. Subjects were then assigned to the various treatment groups based on the magnitude of their startle response. At least one day later, an experimental session was conducted to assess sensorimotor gating. Subjects were given an intraperitoneal injection of SH-053-2'F-R-CH_3 (30 mg/kg), SH-053-2'F-S-CH_3 (30 mg/kg), or vehicle 60 minutes before testing, followed by a subcutaneous injection of either phencyclidine hydrochloride (1.5 mg/kg), MK-801 (0.1 mg/kg) or saline ten minutes prior to testing. In the experimental session, after a five or ten minute habituation period, subjects received 58 discrete trials; 26 trials during which the pulse stimulus (50 dB above background) was presented alone, 8 trials each in which the pulse stimulus was preceded by a prepulse stimulus (5, 10, or 15 dB above background) and 8 background trials with no pulse and

only background noise. The first 6 pulse alone trials were not included in the average startle stimulus to achieve a relatively stable level of startle reactivity. The percent of prepulse inhibition was determined as 100-(average prepulse startle response/average startle stimulus alone) x 100.

Catalepsy

Catalepsy was tested as per the methods reviewed by Sanberg et al (1988).[252] In short, the subjects were placed in a test box that has an open top and a stainless steel floor and grey plastic walls (34.50 cm x 19.60 cm x 23.00 cm). The box contains a stainless steel bar 1.25 cm in diameter laterally mounted 12.50 cm above the floor and 8.50 cm from one end of the box. Haloperidol (0.1 mg/kg), SH-053-2'F-S-CH_3, SH-053-2'F-R-CH_3 (30 mg/kg), or vehicle was administered intraperitoneally and subjects were tested at 30, 60, and 120 min post injection with a maximum of five trials per session. Time (seconds) was measured from placement of the subject's front paws on the bar until one paw moves or slips from the bar. A maximum of five consecutive trials were attempted. Criteria time for a completed trial was between ten seconds and five minutes. After five trials, if the subject had not remained on the bar for a minimum of five seconds, the longest time of the five trials was recorded.

Statistics

Comparisons in each experiment were analyzed using a repeated measures analysis of variance (ANOVA) with drug treatment as between-subject variables and time or prepulse intensity as within-subjects variables for catalepsy and prepulse inhibition, respectively. Significant interactions and main effects were further analyzed using a Fisher LSD post hoc test ($p<0.05$).

4.5.8 FLIPR functional assay (CRO)[180, 181]

Refer to Section 3.5.10 for details.

4.5.9 Efficacy data determined by electrophysiology using *Xenopus laevis* oocytes (Dr. Margot Ernst at the Medical University of Vienna)[172-175]

Refer to Section 3.5.4 for details.

4.5.10 Seizure protection against the maximal electroshock (MES) assay (ASP at NINDS)[280-282]

The MES is a model for generalized tonic-clonic seizures and provides an indication of a compound's ability to prevent seizure spread when all neuronal circuits in the brain are maximally active.These seizures are highly reproducible and are electrophysiologically consistent with human seizures.For all tests based on MES convulsions, 60Hz of alternating current (50 mA in mice and 150 mA in rats) is delivered for 2s by corneal electrodes which have been primed with an electrolyte solution containing an anesthetic agent (0.5% tetracaine HCL).In our initial screens, mice or rats are tested at various intervals following doses of 30, 100 and 300 mg/kg of test compound given by i.p. injection or through oral dosing (p.o.). An animal is considered "protected" from MES-induced seizures upon abolition of the hindlimb tonic extensor component of the seizure.

4.5.11 Seizure protection against the scMET-induced assay (ASP at NINDS)

Subcutaneous injection of the $GABA_AR$ antagonist convulsant Metrazol (MET, pentylenetetrazole, PTZ) produces clonic seizures in laboratory animals. The scMET test detects the ability of a test compound to raise the seizure threshold of an animal and thus protect it from exhibiting a clonic seizure in response to a normally convulsant dose of Metrazol. Animals are pretreated with various doses of the test compound given by i.p. injection or through oral dosing. At various times after dosing with the test compound, the dose of Metrazol which will induce convulsions in 97% of animals (CD97: 85 mg/kg mice or 56.4 mg/kg rats) is injected into a loose

fold of skin in the midline of the neck. The animals are placed in isolation cages to minimize stress[283] and observed for the next 30 minutes for the presence or absence of a seizure. An episode of clonic spasms, approximately 3-5 seconds, of the fore and/or hindlimbs, jaws, or vibrissae is taken as the endpoint. Animals which do not meet this criterion are considered protected.

4.5.12 Determination of plasma and brain concentrations

Male Wistar rats (n = 3) were dosed i.p. with a test ligand at 10 mg/kg. Refer to Section 4.5.3 for experimental details.

4.5.13 Ataxic assessment in the rotarod assay (Dr. Miroslav Savić at the University of Belgrade)

Motor performance was assessed using an automated rotarod (Ugo Basile, Italy). Before testing, male Wistar rats (n = 3 – 9) were trained for three days until they could remain for 180 s on the rod revolving at 15 rpm. On the fourth day, selection was made and rats fulfilling the given criteria were included in the experiment. Seven groups received one of the following treatments 20 minutes before testing: solvent, MP-III-022 (10, 15 and 20 mg/kg), and 15 mg/kg MP-III-022 in combination with XLi-093 (20 mg/kg) or flumazenil (15 mg/kg). Latency to fall from the rotarod was recorded automatically.

4.5.14 Seizure protection against the scMET-induced assay (Dr. Miroslav Savić at the University of Belgrade)

A butterfly cannula (needle size 25 G, ¾ in.) attached to a 20 ml syringe prefilled with pentylenetetrazole (PTZ) solution was used. The syringe was held in an adjustable motor driven infusion pump (Stoelting Co., Wood Dale Illinois, USA). Before infusing PTZ, the rat's tail vein was dilated with warm water. A single male Wistar rat was then placed in the restrainer. A butterfly needle was inserted into the lateral tail vein and PTZ was infused at a constant rate of 0.5 ml/min.

The animal was observed throughout the infusion by two trained and blind observers. The threshold doses of PTZ (mg/kg) required to elicit clonic and tonic seizures were calculated using the following formula: volume of PTZ (ml) x concentration of PTZ (mg/ml)/body weight (kg).

4.5.15 Effects in memory and learning in the Morris water maze (Dr. Miroslav Savić at the University of Belgrade)

Experiments were performed in a 2 m diameter circular pool filled to a height of 30 cm with water at 22 ± 1 °C. The escape platform (15 cm × 10 cm) was submerged 2 cm below the water surface. An indirect illumination in the experimental room was provided by white neon tubes and many distal cues were present. On each of the five consecutive days, rats were given one swimming block, consisting of four trials. For each trial the rat was placed in the water at one of four pseudo–randomly determined starting positions. Once the rat has found and mounted the escape platform it was permitted to remain on the platform for 15 s. The rat was guided to the platform by the experimenter if it failed to locate it within 120 s. During the acquisition phase, treatments were applied once daily before the swimming block. On the sixth day, rats were given a treatment–free probe test (60 s) without the platform. In order to ensure that any spatial bias is a consequence of the spatial memory of escape location, rather than of a specific swim strategy, the probe test was started from the novel, most distant location.[284] The pool was virtually divided into four quadrants, three concentric annuli and a target region consisting of the intersection of the platform quadrant and the platform (middle) annulus, as represented in Savić *et al*.[285] The selected parameters in the probe test were the distance swam in the target zone (s) and % of the distance swam in the peripheral annulus. We tested the effects of 1, 2.5 and 10 mg/kg MP-III-022 and 2 mg/kg diazepam.

4.5.16 Effects in the social novelty discrimination (SND) procedure (Dr. Miroslav Savić at the University of Belgrade)

SND experiments compared the social investigation times of an adult rat with a familiar and a novel juvenile rat. The procedure is replicated from previous studies.[263, 286] Testing consisted of two consecutive juvenile presentation periods to an adult subject: test period 1 (T1) and test period 2 (T2). At the beginning of T1, one juvenile was placed into the adult home cage and the time spent by the adult investigating the juvenile (anogenital sniffing, licking, close pursuing and pawing) was recorded manually for 5 min. During T2, the same juvenile and a second, novel juvenile were placed in the cage together with the adult, and the times spent by the adult investigating each juvenile were measured independently for 3 min. A different pair of juvenile rats was presented to each adult tested. Manual scoring was conducted in a blinded manner. SND was impaired by the parametric manipulation applied, as there was 30 min delay between T1 and T2, and SND was expected to be low in control rats. The influence of MP-III-022 (1, 2.5 or 10 mg/kg) on such induced impairment in SND was examined. There were five groups of rats which received one of the following treatments 20 min before T1: solvent, 1.5 mg/kg diazepam and 1, 2.5 and 10 mg/kg MP-III-022. The amount of time investigating familiar (Tf) and novel (Tn) juvenile during T2 was manually scored, and discrimination indexes (Tn-Tf/Tn+Tf) was calculated. Total exploration time during T1 and T2 was also manually recorded.

4.5.17 Antidepressant effects in the unpredictable chronic mild stress (UCMS) assay (Dr. Etienne Sibille and Sean Piantadosi at the University of Pittsburgh and University of Toronto)

Animals

C57BL/6J mice (Jackson Laboratories, Bar Harbor, Maine USA) were housed under normal conditions with a 12/12 light/dark cycle and ad libitum access to food and water in accordance with the University of Pittsburgh Institutional Animal Care and Use Committee.

Unpredictable chronic mild stress (UCMS)

Mice underwent 6 weeks of UCMS. Briefly, animals were exposed to multiple mild stressors a day, including wet bedding, brief restraint, forced bath, no bedding, and predator odor over a period of several weeks (for a comprehensive review of the procedure, see Lin, *et al*.[267] and Edgar, *et al*.).[287] In one experiment, UCMS was augmented with single-cage isolation starting at the fourth week until sacrifice.

Drug treatment

Beginning on the third week of UCMS and continuing for 28 days until sacrifice, mice received daily i.p injections of vehicle (85% ddH2O, 14% propylene glycol, 1% Tween 80) or 30 mg/kg SH-053-2'F-R-CH3 (α5-PAM) in a volume of 10 mg/mL.Thirty minutes prior to behavioral testing all animals received a second injection of either vehicle (for chronic α5-PAM treated animals and UCMS-vehicle treated animals) or an α5-PAM acutely.

Behavioral testing

After five weeks of UCMS animals were assessed in a battery of behavioral tests including (each test separated by 24 hours, UCMS continued throughout behavioral testing): Elevated plus maze: under red light, animals were placed on a plus maze with two open and two closed arms (30x5 cm). Number of entries into all arms as well as the time spent in the open arms was recorded manually for 10 minutes. Open field test: The open field test was conducted in a 43x43 cm arena under full (800 lux) light. Using AnyMaze software (Stoelting), the center 50% of the arena was

identified and animals were tracked for 10 minutes. Novelty suppressed feeding test: Mice were food deprived for 24 hours the day before testing. Testing occurred in brightly lit (~1000 lux) open field arenas covered in bedding. A normal food pellet was placed into the brightly lit center and the latency for an animal to approach and bite the cookie was manually recorded over a 12 minute session. Immediately following the 12 minute session, animals were placed into their home cage and allowed to eat a weighed food pellet to assess hunger drive. Cookie test: The cookie test apparatus contains three identically sized chambers (40x20x20) separated by two offset doors. The walls of each chamber were clear and the only difference between each was the color of the divider with one divider shaded white and the other black. One week prior to experimentation, mice were habituated in their home cage to a piece of (2 ± 1g) Keebler Fudge Stripe Cookie (Kellogg's Company, Battle Creek, MI USA). On the first and second day of testing, a piece of cookie (2 ± 1g) was placed into the chamber separated by the black wall. Mice were then placed into the white chamber and monitored for 10 minutes. The time it took for each mouse to bite the cookie was recorded.

4.5.18 Immunohistochemistry of human ASM for α5-containing $GABA_AR$ subunit protein expression[217]

All human airway tissue protocols were reviewed by Columbia University Institutional Board and were deemed not human subjects research under 45 CFR 46. Human tracheal tissue was obtained from discarded airway from healthy lung donors during transplantation surgery at Columbia University, N.Y. The trachea and first generation bronchi of the airway were processed for immediate fixation in 4% paraformaldehyde (4^{o}C overnight), then incubated in 30% sucrose in PBS at 4^{o}C for an additional 24 hrs prior to processing for cryostat sectioning (6 μm). The sections were washed in PBS, incubated with 0.1% Triton X-100 for 10 min, blocked with 15 % goat serum

then incubated overnight at 4 ^{o}C in primary antisera. The primary antibodies used were (1) anti-GABA α5 (rabbit, polyclonal: Chemicon # AB9678, 1:300 dilution in PBS) (2) anti-α smooth muscle actin (mouse, monoclonal; Sigma-Aldrich, #A2547, 1:10,000 dilution in PBS). The secondary antibodies consisted of FITC-conjugated goat anti-rabbit IgG (1:400 dilution), and Alexa Fluor 594 goat anti-mouse IgG (1:400 dilution; Invitrogen) incubated for 1 hr. Nuclear staining was performed using mounting medium pre-mixed with DAPI stain (Vector laboratories, #H-1500). Negative controls omitted all primary antibodies, but included secondary staining and nuclear staining steps. All the immunofluorescence experiments were repeated on at least 3 independent samples. Samples were viewed under confocal microscopy (Nikon A1 Eclipse, Japan) and images were acquired with NIS software version 4.10.

4.5.19 Force measurements in human airway smooth muscle strips

Human airway smooth muscle strips were dissected from trachea and mainstem bronchi and epithelium was removed under a dissecting microscope. Strips were suspended at 1.5 grams resting tension in Krebs-Henseleit (KH) buffer as previously described in Gallos *et al*.[64] Trachea and bronchi were obtained from surgical discards from healthy donor lungs incidental to lung transplant surgery and studies were deemed not human subjects research after review by Columbia University's Institutional Review Board. The KH buffer contained in mM: 118 NaCl, 5.6 KCl, 0.5 $CaCl_2$, 0.24 $MgSO_4$, 1.3 NaH_2PO_4, 25 $NaHCO_3$, and 5.6 glucose, pH 7.4). 10μM indomethacin was added to the buffer to block endogenous release of prostanoids. Strips were allowed to equilibrate for 1 hour with KH buffer exchanges every 15 minutes. Strips underwent contractile challenges with acetylcholine (100nM-100 μM) for three cycles with extensive buffer exchanges and resetting of resting tension to 1.5 grams between cycles. Tetrodotoxin (1 μM), pyrilamine (10 μM), and MK501 (10 μM) were then added to the buffer to eliminate potentially confounding

effects of neural activation, histamine release or leukotriene release from other cell types (neurons, mast cells) present in the ASM strip preparation during muscle force studies. ASM strips were then contracted with an EC_{50} concentration of acetylcholine, and after establishing a stable plateau of muscle force (typically ~30 min), 10 nM of isoproterenol was added with or without 50 μM SH-053-2'F-R-CH_3 or vehicle (0.2% ethanol). The magnitude of remaining muscle force was measured 15 min after the addition of isoproterenol +/- SH-053-2'F-R-CH_3 and expressed as a percentage of the initial acetylcholine-induced force.

4.5.20 Force measurements in guinea pig tracheal rings

All guinea pig protocols were approved by the Columbia University Animal Care and Use Committee. Studies were conducted as previously described in Gallos *et al*.[217] Briefly, male Hartley guinea pigs (~400 g) were anesthetized with intraperitoneal pentobarbital (100 mg/kg) and their tracheas dissected free of epithelium and suspended in physiological buffer with 10uM indomethacin in organ baths at 37°C and continuously aerated with 95% O_2/5% CO_2 (bubbled). Tracheal rings were placed under a resting tension of 1.0 g and allowed to equilibrate for 1h with buffer exchanges every 15 min. Tracheal rings were pretreated with *N*-vanillylnonanamide (10 μM) to activate and then deplete nonadrenergic, noncholinergic nerves contained within the tissue. After buffer exchanges the tracheal rings were subjected to two cycles of increasing cumulative concentrations of acetylcholine (0.1 μM to 0.1 mM). Following extensive buffer exchanges, pyrilamine (10 μM), and tetrodotoxin (1 μM) were added to the buffers to block confounding effects of released histamine or nerve depolarization on endogenous airway smooth muscle contractile force. Tracheal rings were then contracted with 1uM substance P. After contractions achieved a steady-state plateau of increased force (typically 30 min), 50 μM of the indicated $GABA_A$ ligand or the vehicle control (0.1% ethanol) was added to the buffers. The maintenance

of force was measured after 15 min and was expressed as a percent of the initial contractile substance P-induced force for each ring and the resultant relaxation was compared to the vehicle control.

4.6 Experimental

4.6.1 *Tert*-butyl (*S*)-(1-((4-bromo-2-(2-fluorobenzoyl)phenyl)amino)-1-oxopropan-2-yl)carbamate (54)

The (2-amino-5-bromophenyl)(2-fluorophenyl)methanone **53** (60 g., 204 mmol) and Boc-L-alanine (38.6 g., 204 mmol) were dissolved in dry CH_2Cl_2 (500 mL) and stirred at 0 ^oC. Dicyclohexylcarbodiimide (DCC; 50.5 g., 249 mmol) dissolved in dry CH_2Cl_2 was added dropwise over a 30 min period at 0 ^oC. The solution was allowed to stir for 8 h at rt. The dicyclohexyl urea byproduct which was formed was filtered off and washed with CH_2Cl_2. The organic layers were combined and concentrated under reduced pressure to afford the Boc analog **54** (82.6 g., 87%): **^{1}H NMR** (300 MHz, $CDCl_3$) δ 11.68 (s, 1H), 8.71 (d, *J* = 9.0 Hz, 1H), 7.69 (dd, *J* = 9.0, 2.3 Hz, 1H), 7.55-7.62 (m, 2H), 7.46 (td, *J* = 7.6, 1.4 Hz, 1H), 7.30 (t, *J* = 7.5 Hz, 1H), 7.21 (t, *J* = 9.1 Hz, 1H), 5.13 (bs, 1H), 4.37 (bs, 1H), 1.51 (d, *J* = 7.2 Hz, 3H), 1.45 (s, 9H); this was used in the next step without further characterization. The spectral data for **54** was identical to the literature.[143]

4.6.2 (*S*)-7-Bromo-5-(2-fluorophenyl)-3-methyl-1,3-dihydro-2*H*-benzo[*e*][1,4]diazepin-2-one (55)

Benzophenone **54** (40 g., 86 mmol) was dissolved in dry CH_2Cl_2 (400 mL) and cooled to -10 ^oC. Anhydrous HCl (g) was slowly added until the solution was saturated, about 20 min, and the solution was allowed to stir overnight at rt. The reaction mixture was then washed with a sat'd aq solution of $NaHCO_3$ (2 x 100 mL) and water (2 x 100 mL). The organic layer was concentrated under reduced pressure and the oil which resulted was dissolved in methanol-water (1:1, 400 mL) with the pH adjusted to 8.5 using a solution of 1 M aq NaOH. The reaction mixture was allowed stir at rt overnight. The solution was concentrated under reduced pressure and water (100 mL) was added. The solution was extracted with CH_2Cl_2 and the organic layer was washed with brine, dried

(Na_2SO_4), and concentrated under reduced pressure. The solid which resulted was purified by recrystallization from methanol/water to provide benzodiazepine **55** as a white solid (22.4 g., 75%): **^{1}H NMR** (300 MHz, $CDCl_3$) δ 9.50 (bs, 1 H), 7.62 - 7.65 (m, 2 H), 7.50 (q, *J*= 6.5 Hz, 1 H), 7.40 (d, *J*=2.0 Hz, 1 H), 7.29 (t, *J*=7.5 Hz 1 H) 7.15 (d, *J*=8.6 Hz, 1 H), 7.11 (t, *J*=8.9 Hz, 1 H), 3.84 (q, *J*= 6.5 Hz, 1 H), 1.82 (d, *J*=6.5 Hz, 3 H); **^{13}C NMR** (75 MHz, $CDCl_3$) δ 171.87, 162.14, 158.79, 136.68, 135.00, 132.21, 131.72, 129.73, 124.46, 124.41, 123.03, 116.53, 116.45, 116.17, 58.69, 16.66; **HPLC-MS** (ESI) *m/z* (M+H) 347.01; **[α] $^{26}_D$** = +168.8 (c 0.73, EtOAc). The spectral data for **55** were identical to the literature.[143]

4.6.3 Ethyl (*S*)-8-bromo-6-(2-fluorophenyl)-4-methyl-4*H*-benzo[*f*]imidazo[1,5-*a*][1,4]diazepine-3-carboxylate (56)

Amide **55** (20 g., 58 mmol) was dissolved in dry THF (800 mL) and cooled to -35 ^{o}C. K-*t*-BuO (8.4 g., 75 mmol) was then added in one portion and the solution was allowed to warm to rt where the temperature was held for 30 min. The reaction was then cooled to -50 ^{o}C and diethyl chlorophosphate (14.1 g., 81 mmol) was added. The solution was allowed to warm to rt and the temperature was held there for 1 hour. The reaction was then cooled to -78 ^{o}C and ethyl isocyanoacetate (8.5 g., 75 mmol) was added, followed by a second portion of K-*t*-BuO (8.4 g., 75 mmol). The reaction was allowed to warm to rt and stirred overnight. The reaction was quenched by addition of a cold sat'd aq solution of $NaHCO_3$ (1 L) and extracted with EtOAc. The organic layers were combined and washed with brine (2 x 150 mL), dried (Na_2SO_4) and the solvent was removed under reduced pressure to afford a brown solid. The solid was washed with Et_2O/EtOAc (9:1) to remove some of the impurities and the remaining solid was purified by column chromatography (silica gel, EtOAc/hexanes 2:1) to afford pure imidazobenzodiazepine **56** as an off-white solid (19.9 g., 78%): **^{1}H NMR** (300 MHz, $CDCl_3$) δ 7.92 (s, 1 H), 7.72 (dd, *J*= 8.5, 1.5

Hz, 1 H), 7.6 (t, *J*= 6.9 Hz, 1H), 7.48 (d, *J*=8.5 Hz, 1 H), 7.42-7.49 (m, 2 H), 7.23-7.29 (m, 1 H), 7.05 (t, *J*= 9.3 Hz, 1H), 6.71 (q, *J*=7.3Hz, 1 H), 4.41 (m, 2H), 1.42 (t, *J*=7.1 Hz, 3H), 1.29 (d, *J*=7.2, 3H); **^{13}C NMR** (75 MHz, $CDCl_3$) δ 163.38, 162.36, 158.44, 141.18, 135.35, 135.09, 133.52, 133.26, 132.54, 131.32, 130.70, 128.91, 124.63, 124.00, 121.30, 116.45, 116.17, 61.03, 49.80, 14.88, 14.38; **HPLC-MS** (ESI) *m/z* (M+H) 441.05; **[α] $^{26}_{D}$** = +10.6 (c 0.53, EtOAc). The spectral data for **56** were identical to the literature.[143]

4.6.4 Ethyl (*S*)-6-(2-fluorophenyl)-4-methyl-8-((trimethylsilyl)ethynyl)-4*H*-benzo[*f*]imidazo[1,5-*a*][1,4]diazepine-3-carboxylate (57)

Imidazobenzodiazepine **56** (15 g., 34 mmol) was dissolved in triethylamine (500 mL) and acetonitrile (600 mL). Trimethylsilylacetylene (5.0 g., 51 mmol) and bis(triphenylphosphine)-palladium (II) acetate (1.40 g., 1.9 mmol) were added. A reflux condenser was attached and the mixture was degassed under vacuum with argon; this process was repeated four times. The reaction mixture was heated to reflux under argon and stirred for 8 hours. The solution was cooled to rt, filtered through celite, and the celite was washed with EtOAc. The filtrate was concentrated under reduced pressure. The black residue which resulted was purified by a wash column (silica gel, EtOAc/hexanes 2:1) to afford the TMS-analog **57** as an off-white solid (14.2 g., 91%): **^{1}H NMR** (300 MHz, $CDCl_3$) δ 8.00 (s, 1H), 7.74 – 7.60 (m, 2H), 7.57 (d, *J* = 8.3 Hz, 1H), 7.47 (dd, *J* = 12.7, 6.5 Hz, 1H), 7.37 (s, 1H), 7.27 (dd, *J* = 9.2, 5.6 Hz, 1H), 7.06 (t, *J* = 9.2 Hz, 1H), 6.70 (q, *J* = 7.1 Hz, 1H), 4.49 – 4.31 (m, 2H), 1.41 (t, *J* = 7.1 Hz, 3H), 1.27 (d, *J* = 7.3 Hz, 3H), 0.23 (s, 9H); **^{13}C NMR** (75 MHz, $CDCl_3$) δ 164.13, 162.69, 158.49, 141.32, 135.62, 134.96, 134.11, 133.67, 132.42, 131.35, 129.41, 129.08, 124.51, 122.89, 122.29, 116.44, 116.17, 102.30, 97.62, 60.87, 49.82, 14.81, 14.40, -0.48; **HPLC-MS** (ESI) *m/z* (M+H) 459.18; **[α] $^{26}_{D}$** = -27.8 (c 0.46, EtOAc). The spectral data for **57** were identical to the literature.[143]

4.6.5 Ethyl (*S*)-8-ethynyl-6-(2-fluorophenyl)-4-methyl-4*H*-benzo[*f*]imidazo[1,5-*a*][1,4]diazepine-3-carboxylate (SH-053-2'F-S-CH_3, 51)

The intermediate **57** (10 g, 21.8 mmol) was dissolved in THF (400 mL) and cooled to -78 ^oC. This was treated with tetrabutylammonium fluoride hydrate (1 M solution in THF, 25 mmol), followed by water (10 mL). The reaction mixture was stirred until the starting material was consumed as indicated by TLC (silica gel), about 30 min. The reaction mixture was allowed to warm to -20 ^oC, and water (200 mL) was slowly added. The solution was extracted with EtOAc and the organic extracts were combined, washed with brine, dried (Na_2SO_4), and the solvent was removed under reduced pressure. The residue which resulted was purified by a wash column (silica gel, EtOAc/hexanes 4:1) to afford pure **51** as a white powder (8.0 g., 95%): **^{1}H NMR** (300 MHz, $CDCl_3$) δ 8.03 (s, 1H), 7.72 (d, *J* = 8.0 Hz, 1H), 7.62 (t, *J* = 7.9 Hz, 2H), 7.45 (dd, *J* = 15.0, 8.1 Hz, 2H), 7.32 – 7.20 (m, 1H), 7.04 (t, *J* = 9.3 Hz, 1H), 6.70 (q, *J* = 7.1 Hz, 1H), 4.47 – 4.33 (m, 2H), 3.16 (s, 1H), 1.40 (t, *J* = 7.1 Hz, 3H), 1.29 (d, *J* = 7.3 Hz, 3H).); **^{13}C NMR** (75 MHz, $CDCl_3$) δ 163.94, 162.65, 158.43, 141.30, 135.60, 135.02, 134.48, 134.18, 132.34, 131.32, 129.39, 129.15, 124.54, 122.42, 121.84, 116.40, 116.11, 81.27, 79.94, 60.90, 49.84, 14.91, 14.40.; **HRMS** (ESI *m/z*) for $C_{23}H_{19}FN_3O_2$ calc'd 388.1456, found 388.1456 $(M+H)^+$; **[α] $^{26}_D$** = -21.5 (c 0.89, EtOAc). The spectral data for (*S*)-**51** were in excellent agreement with the literature.[143]

4.6.6 *Tert*-butyl (*R*)-(1-((4-bromo-2-(2-fluorobenzoyl)phenyl)amino)-1-oxopropan-2-yl)carbamate (58)

The amide **58** was synthesized as described in 4.6.1, by replacing Boc-L-alanine with Boc-D-alanine to afford **58** in 87% yield: **^{1}H NMR** (300 MHz, $CDCl_3$) δ 11.68 (s, 1H), 8.71 (d, *J* = 9.0 Hz, 1H), 7.69 (dd, *J* = 9.0, 2.3 Hz, 1H), 7.55-7.62 (m, 2H), 7.46 (td, *J* = 7.6, 1.4 Hz, 1H), 7.30 (t, *J* = 7.5 Hz, 1H), 7.21 (t, *J* = 9.1 Hz, 1H), 5.13 (bs, 1H), 4.37 (bs, 1H), 1.51 (d, *J* = 7.2 Hz, 3H),

1.45 (s, 9H); this was used in the next step without further characterization. The spectral data for **55** were identical to the literature.[143]

4.6.7 (*R*)-7-Bromo-5-(2-fluorophenyl)-3-methyl-1,3-dihydro-2*H*-benzo[*e*][1,4]diazepin-2-one (59)

The 1,4-benzodiazepine **59** was synthesized as described in 4.7.2, by using amide **58** as the starting material to afford **59** in 75% yield: **^{1}H NMR** (300 MHz, $CDCl_3$) δ 9.50 (bs, 1 H), 7.62 - 7.65 (m, 2 H), 7.50 (q, *J*= 6.5 Hz, 1 H), 7.40 (d, *J*=2.0 Hz, 1 H), 7.29 (t, *J*=7.5 Hz 1 H) 7.15 (d, *J*=8.6 Hz, 1 H), 7.11 (t, *J*=8.9 Hz, 1 H), 3.84 (q, *J*= 6.5 Hz, 1 H), 1.82 (d, *J*=6.5 Hz, 3 H); **^{13}C NMR** (75 MHz, $CDCl_3$) δ 171.87, 162.14, 158.79, 136.68, 135.00, 132.21, 131.72, 129.73, 124.46, 124.41, 123.03, 116.53, 116.45, 116.17, 58.69, 16.66; **HPLC-MS** (ESI) *m/z* (M+H) 347.01; **[α] $^{26}_{D}$** = -169.1 (c 0.71, EtOAc). The spectral data for **59** were identical to the literature.[143]

4.6.8 Ethyl (*R*)-8-bromo-6-(2-fluorophenyl)-4-methyl-4*H*-benzo[*f*]imidazo[1,5-*a*][1,4]diazepine-3-carboxylate (60)

The imidazobenzodiazepine **60** was synthesized as described in 4.6.3, by using 1,4-benzodiazepine **59** as the starting material to afford **60** in 78% yield: **^{1}H NMR** (300 MHz, $CDCl_3$) δ 7.92 (s, 1 H), 7.72 (dd, *J*= 8.5, 1.5 Hz, 1 H), 7.6 (t, *J*= 6.9 Hz, 1H), 7.48 (d, *J*=8.5 Hz, 1 H), 7.42-7.49 (m, 2 H), 7.23-7.29 (m, 1 H), 7.05 (t, *J*= 9.3 Hz, 1H), 6.71 (q, *J*=7.3Hz, 1 H), 4.41 (m, 2H), 1.42 (t, *J*=7.1 Hz, 3H), 1.29 (d, *J*=7.2, 3H); **^{13}C NMR** (75 MHz, $CDCl_3$) δ 163.38, 162.36, 158.44, 141.18, 135.35, 135.09, 133.52, 133.26, 132.54, 131.32, 130.70, 128.91, 124.63, 124.00, 121.30, 116.45, 116.17, 61.03, 49.80, 14.88, 14.38; **HPLC-MS** (ESI) *m/z* (M+H) 441.05; **[α] $^{26}_{D}$** = -10.9 (c 0.53, EtOAc). The spectral data for **60** were identical to the literature.[143]

4.6.9 Ethyl (*R*)-6-(2-fluorophenyl)-4-methyl-8-((trimethylsilyl)ethynyl)-4*H*-benzo[*f*]imidazo[1,5-*a*][1,4]diazepine-3-carboxylate (61)

The TMS-protected acetylene **61** was synthesized as described in 4.6.4, by using imidazobenzodiazepine **60** as the starting material to afford **61** in 91% yield: **^{1}H NMR** (300 MHz, $CDCl_3$) δ 8.00 (s, 1H), 7.74 – 7.60 (m, 2H), 7.57 (d, *J* = 8.3 Hz, 1H), 7.47 (dd, *J* = 12.7, 6.5 Hz, 1H), 7.37 (s, 1H), 7.27 (dd, *J* = 9.2, 5.6 Hz, 1H), 7.06 (t, *J* = 9.2 Hz, 1H), 6.70 (q, *J* = 7.1 Hz, 1H), 4.49 – 4.31 (m, 2H), 1.41 (t, *J* = 7.1 Hz, 3H), 1.27 (d, *J* = 7.3 Hz, 3H), 0.23 (s, 9H); **^{13}C NMR** (75 MHz, $CDCl_3$) δ 164.13, 162.69, 158.49, 141.32, 135.62, 134.96, 134.11, 133.67, 132.42, 131.35, 129.41, 129.08, 124.51, 122.89, 122.29, 116.44, 116.17, 102.30, 97.62, 60.87, 49.82, 14.81, 14.40, -0.48; **HPLC-MS** (ESI) *m/z* (M+H) 459.18; **[α] $^{26}_D$** = +28.2 (c 0.48, EtOAc). The spectral data for **61** were identical to the literature.[143]

4.6.10 Ethyl (*R*)-8-ethynyl-6-(2-fluorophenyl)-4-methyl-4*H*-benzo[*f*]imidazo[1,5-*a*][1,4]diazepine-3-carboxylate (SH-053-2'F-R-CH_3, 52)

The ethyl ester SH-053-2'F-R-CH_3 **52** was synthesized as described in 4.6.5, by using the benzodiazepine **61** as the starting material to afford **52** in 95% yield: **^{1}H NMR** (300 MHz, $CDCl_3$) δ 8.03 (s, 1H), 7.72 (d, *J* = 8.0 Hz, 1H), 7.62 (t, *J* = 7.9 Hz, 2H), 7.45 (dd, *J* = 15.0, 8.1 Hz, 2H), 7.32 – 7.20 (m, 1H), 7.04 (t, *J* = 9.3 Hz, 1H), 6.70 (q, *J* = 7.1 Hz, 1H), 4.47 – 4.33 (m, 2H), 3.16 (s, 1H), 1.40 (t, *J* = 7.1 Hz, 3H), 1.29 (d, *J* = 7.3 Hz, 3H).); **^{13}C NMR** (75 MHz, $CDCl_3$) δ 163.94, 162.65, 158.43, 141.30, 135.60, 135.02, 134.48, 134.18, 132.34, 131.32, 129.39, 129.15, 124.54, 122.42, 121.84, 116.40, 116.11, 81.27, 79.94, 60.90, 49.84, 14.91, 14.40.; **HRMS** (ESI *m/z*) for $C_{23}H_{19}FN_3O_2$ calc'd 388.1456, found 388.1456 $(M+H)^+$; **[α] $^{26}_D$** = +20.9 (c 0.89, EtOAc). The spectral data for (*R*)-**52** were in excellent agreement with the literature.[143]

4.6.11 (*S*)-Methyl 8-ethynyl-6-(2-fluorophenyl)-4-methyl-4*H*-benzo[f]imidazo[1,5-*a*][1,4]diazepine-3-carboxylate (MP-III-021, 62)

Ethyl ester SH-053-2'F-S-CH_3 **51** (150 mg, 0.387 mmol) was dissolved in methanol (20 mL). Sodium methoxide (84 mg, 1.55 mmol) was added in one portion and the solution was heated to reflux. The reaction mixture was monitored by analysis by TLC (silica gel, 4:1 EtOAc:hexanes) until the starting material had been consumed; approximately 30 min. The reaction solution was cooled to rt and then quenched with a saturated aq solution of sodium bicarbonate (4 mL). Water (10 mL) was then added to the solution and the methanol was removed under reduced pressure. The product was then extracted with EtOAc (3 x 40 mL), and the organic layers were combined, washed with brine, as well as dried (Na_2SO_4). The solution was then concentrated under reduced pressure. The solid which resulted was purified via a wash column (silica gel, 4:1 EtOAc:hexanes) which provided pure methyl ester **62** as an off-white solid (117 mg, 80.8% yield): **^{1}H NMR** (300 MHz, $CDCl_3$) δ 7.96 (s, 1H), 7.71 (d, 1H, *J* = 8.3 Hz), 7.59 (t, 2H, *J* = 9.5 Hz), 7.49-7.40 (m, 2H), 7.29-7.21 (m, 1H), 7.04 (t, 1H, *J* = 9.3 Hz), 6.69 (q, 1H, 7.2 Hz), 3.92 (s, 3H), 3.16 (s, 1H), 1.29 (d, 3H, *J* = 7.1 Hz); **^{13}C NMR** (75 MHz, $CDCl_3$) δ 163.17, 161.77, 158.45, 141.47, 135.49, 135.01, 134.46, 134.13, 132.30, 131.30, 129.21, 124.58, 124.54, 122.33, 121.83, 116.40, 116.11, 81.31, 79.90, 51.93, 49.88, 14.92; **HRMS** (LCMS-IT-TOF) Calc. for $C_{22}H_{17}FN_3O_2$ $(M + H)^+$ 374.1299, found 374.1307.

4.6.12 (*R*)-Methyl 8-ethynyl-6-(2-fluorophenyl)-4-methyl-4*H*-benzo[f]imidazo[1,5-*a*][1,4]diazepine-3-carboxylate (MP-III-004, 63)

Ethyl ester SH-053-2'F-R-CH_3 **52** (4.0 g, 10.32 mmol) was dissolved in methanol (250 mL). Sodium methoxide (2.23 g, 41.3 mmol) was added in one portion and the solution was heated to reflux. The reaction mixture was monitored by analysis by TLC (silica gel, 4:1 EtOAc:hexanes)

until the starting material had been consumed; approximately 30 min. The reaction solution was cooled to rt and then quenched with a saturated aq solution of sodium bicarbonate (40 mL). Water (100 mL) was then added to the solution and the methanol was removed under reduced pressure. The product was then extracted with EtOAc (3 x 100 mL), and the organic layers were combined, washed with brine, as well as dried (Na_2SO_4). The solution was then concentrated under reduced pressure. The solid which resulted was purified via a wash column (silica gel, 4:1 EtOAc:hexanes) which provided pure methyl ester **63** as an off-white solid (3.66 g, 95% yield): **^{1}H NMR** (300 MHz, $CDCl_3$) δ 7.96 (s, 1H), 7.71 (d, 1H, *J* = 8.3 Hz), 7.59 (t, 2H, *J* = 9.5 Hz), 7.49-7.40 (m, 2H), 7.29-7.21 (m, 1H), 7.04 (t, 1H, *J* = 9.3 Hz), 6.69 (q, 1H, 7.2 Hz), 3.92 (s, 3H), 3.16 (s, 1H), 1.29 (d, 3H, *J* = 7.1 Hz); **^{13}C NMR** (75 MHz, $CDCl_3$) δ 163.17, 161.77, 158.45, 141.47, 135.49, 135.01, 134.46, 134.13, 132.30, 131.30, 129.21, 124.58, 124.54, 122.33, 121.83, 116.40, 116.11, 81.31, 79.90, 51.93, 49.88, 14.92; **HRMS** (LCMS-IT-TOF) Calc. for $C_{22}H_{17}FN_3O_2$ $(M + H)^+$ 374.1299, found 374.1307.

4.6.13 (*S*)-8-Ethynyl-6-(2-fluorophenyl)-*N*,4-dimethyl-4*H*-benzo[*f*]imidazo[1,5-*a*][1,4]diazepine-3-carboxamide (MP-III-023, 64)

Ethyl ester SH-053-2'F-S-CH_3 **51** (200 mg, 0.516 mmol) was added to a sealed vessel fitted with a septum at 0 ^{o}C and treated with methyl amine (10 mL; 33% wt solution in EtOH). The vessel was sealed with a screw-cap and stirred at 60 ^{o}C for 18 h. The solution was then cooled to rt and the methyl amine and ethanol were removed under reduced pressure. The residue which resulted was purified by a wash column (silica gel, 4:1 EtOAc:hexanes) to afford pure amide **64** as a white powder (131 mg, 68.2%): **^{1}H NMR** (300 MHz, $CDCl_3$) δ 7.88 (s, 1H), 7.67 (dd, *J* = 16.3, 7.8 Hz, 2H), 7.55 (d, *J* = 8.3 Hz, 1H), 7.50 – 7.41 (m, 2H), 7.29 – 7.18 (m, 2H), 7.04 (t, *J* = 9.3 Hz, 1H), 6.93 (q, *J* = 7.4 Hz, 1H), 3.16 (s, 1H), 2.97 (d, *J* = 5.0 Hz, 3H), 1.29 (d, *J* = 6.4 Hz, 3H); **^{13}C NMR**

(75 MHz, $CDCl_3$) δ 162.24, 161.81, 158.48, 138.25, 137.12, 135.73, 134.41, 133.57, 132.53, 131.57, 129.03, 125.15, 124.92, 124.58, 122.50, 116.33, 116.05, 81.25, 79.99, 49.42, 25.73, 25.27; **HRMS** (LCMS-IT-TOF) Calc. for $C_{22}H_{18}FN_4O$ $(M + H)^+$ 373.1459, found: 373.1462.

4.6.14 (*R*)-8-Ethynyl-6-(2-fluorophenyl)-*N*,4-dimethyl-4*H*-benzo[*f*]imidazo[1,5-*a*][1,4]diazepine-3-carboxamide (MP-III-022, 65)

Ethyl ester SH-053-2'F-R-CH_3 **52** (1.0 g, 2.58 mmol) was added to a sealed vessel fitted with a septum at 0 ^oC and treated with methyl amine (15 mL; 33% wt solution in EtOH). The vessel was sealed with a screw-cap and stirred at 60 ^oC for 18 h. The solution was then cooled to rt and the methyl amine and ethanol were removed under reduced pressure. The residue which resulted was purified by a wash column (silica gel, 4:1 EtOAc:hexanes) to afford pure amide **65** as a white powder (731 mg, 1.96 mmol, 76%): **^{1}H NMR** (300 MHz, $CDCl_3$) δ 7.88 (s, 1H), 7.67 (dd, *J* = 16.3, 7.8 Hz, 2H), 7.55 (d, *J* = 8.3 Hz, 1H), 7.50 – 7.41 (m, 2H), 7.29 – 7.18 (m, 2H), 7.04 (t, *J* = 9.3 Hz, 1H), 6.93 (q, *J* = 7.4 Hz, 1H), 3.16 (s, 1H), 2.97 (d, *J* = 5.0 Hz, 3H), 1.29 (d, *J* = 6.4 Hz, 3H); **^{13}C NMR** (75 MHz, $CDCl_3$) δ 162.24, 161.81, 158.48, 138.25, 137.12, 135.73, 134.41, 133.57, 132.53, 131.57, 129.03, 125.15, 124.92, 124.58, 122.50, 116.33, 116.05, 81.25, 79.99, 49.42, 25.73, 25.27; **HRMS** (LCMS-IT-TOF) Calc. for $C_{22}H_{18}FN_4O$ $(M + H)^+$ 373.1459, found: 373.1462.

4.6.15 (*S*)-8-Ethynyl-6-(2-fluorophenyl)-4-methyl-4*H*-benzo[*f*]imidazo[1,5-*a*][1,4]diazepine-3-carbonitrile (MP-III-018.A, 66)

Ethyl ester SH-053-2'F-S-CH_3 **51** (500 mg, 1.40 mmol) was stirred in dry xylene (35 mL) at rt; while an oil bath was heated to 80 ^oC. Using a glass syringe and metal needle, dimethylaluminum amine (0.67 M, 12.5 mL, 8.42 mmol) was carefully added to the starting material. ***Caution*: Do not breathe this amine or get it on you!** The reaction was then heated to 80 ^oC in the oil bath and

the solution was monitored by analysis by TLC (silica gel) until the starting material had been consumed, about 2 h. Once the reaction was complete, the mixture was cooled to rt, and quenched with cold water (15 mL). The product was extracted with EtOAc (5 x 50 mL) and the organic layers were combined, washed with brine, dried (Na_2SO_4), and the solvent was removed under reduced pressure. The solid which resulted was purified by flash chromatography (Gradient elution; step 1: remove excess xylene with 1:4 EtOAc:hexanes as the eluent; step 2: collect the nitrile product with 1:1 EtOAc:hexanes; step 3: collect the amide product, 4:1 EtAOc:hexanes) which afforded the nitrile **66** as a white solid (331 mg, 75.4%) and the amide **67** (78.5 mg, 17.0%). The spectral data for nitrile **66**: **^{1}H NMR** (300 MHz, $CDCl_3$) δ 7.98 (s, 1H), 7.78 (d, *J* = 7.1 Hz, 1H), 7.67 (s, 1H), 7.62 – 7.53 (m, 1H), 7.49 (s, 2H), 7.28 (s, 1H), 7.04 (t, *J* = 8.7 Hz, 1H), 4.36 (d, *J* = 4.8 Hz, 1H), 3.20 (s, 1H), 2.18 (d, *J* = 4.6 Hz, 3H); **^{13}C NMR** (75 MHz, $CDCl_3$) δ 163.64, 158.60, 143.66, 135.69, 133.97, 133.35, 132.89, 132.78, 131.37, 129.22, 124.73, 122.88, 122.64, 116.50, 116.22, 114.54, 110.74, 81.13, 80.33, 51.68, 18.09; **HRMS** (LCMS-IT-TOF) Calc. for $C_{21}H_{14}FN_4$ $(M + H)^+$ 341.1137, found 341.1142.

Preparation of 0.67 M dimethylaluminum amine solution, ***CAUTION: Do not breathe this or get it on you!***

You begin by stirring 20 mL of methylene chloride (dry) at 0 ^oC. You then bubble NH_3 (g) through the CH_2Cl_2 until the solution is saturated, about 10-15 min. Then, 10 mL trimethylaluminum (2.0 M in toluene) was added while avoiding contact with air (use glass/metal syringe and needle). The solution was stirred at rt for 5 minutes and transferred directly for use in the reaction above using a glass syringe and metal needle. ***DO NOT BREATHE OR GET ON YOU!***

4.6.16 (*S*)-8-Ethynyl-6-(2-fluorophenyl)-4-methyl-4*H*-benzo[*f*]imidazo[1,5-*a*][1,4]diazepine-3-carboxamide (MP-III-018.B, 67)

The carboxamide **67** was synthesized as a product in the experimental in Section 4.6.15 as a white solid in 17% yield. The spectral data for carboxamide **67**: **^{1}H NMR** (300 MHz, DMSO-d^6) δ 8.41 (s, 1H), 7.94 (d, *J* = 8.4 Hz, 1H), 7.81 (d, *J* = 8.2 Hz, 1H), 7.57 (dd, *J* = 15.7, 7.9 Hz, 3H), 7.33 (t, *J* = 7.3 Hz, 2H), 7.22 (t, *J* = 9.4 Hz, 2H), 6.66 (d, *J* = 7.0 Hz, 1H), 4.36 (s, 1H), 1.15 (d, *J* = 6.8 Hz, 3H); **^{13}C NMR** (75 MHz, . DMSO-d^6) δ 164.99, 162.68, 161.44, 158.17, 138.36, 135.45, 134.82, 133.20, 132.58, 131.84, 131.36, 129.31, 125.12, 123.86, 120.97, 116.50, 116.22, 83.35, 82.03, 49.45, 25.24; **HRMS** (LCMS-IT-TOF) Calc. for $C_{21}H_{16}FN_4O$ $(M + H)^+$ 359.1227, found 359.1231.

4.6.17 (*R*)-8-Ethynyl-6-(2-fluorophenyl)-4-methyl-4*H*-benzo[*f*]imidazo[1,5-*a*][1,4]diazepine-3-carbonitrile (MP-III-019.A, 68)

The nitrile **68** was synthesized by the experimental procedure as described in 4.6.15 using SH-053-2'F-R-CH_3 **52** (500 mg, 1.40 mmol) as the starting material. The products which resulted were the nitrile **68** (193 mg, 41.6%) and the carboxamide **69** (204 mg, 46.5%). The spectral data for the nitrile **68**: **^{1}H NMR** (300 MHz, $CDCl_3$) δ 7.98 (s, 1H), 7.78 (d, *J* = 7.1 Hz, 1H), 7.67 (s, 1H), 7.62 – 7.53 (m, 1H), 7.49 (s, 2H), 7.28 (s, 1H), 7.04 (t, *J* = 8.7 Hz, 1H), 4.36 (d, *J* = 4.8 Hz, 1H), 3.20 (s, 1H), 2.18 (d, *J* = 4.6 Hz, 3H); **^{13}C NMR** (75 MHz, $CDCl_3$) δ 163.64, 158.60, 143.66, 135.69, 133.97, 133.35, 132.89, 132.78, 131.37, 129.22, 124.73, 122.88, 122.64, 116.50, 116.22, 114.54, 110.74, 81.13, 80.33, 51.68, 18.09; **HRMS** (LCMS-IT-TOF) Calc. for $C_{21}H_{14}FN_4$ $(M + H)^+$ 341.1137, found 341.1142.

4.6.18 (*R*)-8-Ethynyl-6-(2-fluorophenyl)-4-methyl-4*H*-benzo[*f*]imidazo[1,5-*a*][1,4]diazepine-3-carboxamide (MP-III-019.B, 69)

The carboxamide **69** was synthesized as a product in the experimental in Section 4.6.17 as a white solid in 46.5% yield. The spectral data for carboxamide **69**: **^{1}H NMR** (300 MHz, DMSO-d^6) δ 8.41 (s, 1H), 7.94 (d, *J* = 8.4 Hz, 1H), 7.81 (d, *J* = 8.2 Hz, 1H), 7.57 (dd, *J* = 15.7, 7.9 Hz, 3H), 7.33 (t, *J* = 7.3 Hz, 2H), 7.22 (t, *J* = 9.4 Hz, 2H), 6.66 (d, *J* = 7.0 Hz, 1H), 4.36 (s, 1H), 1.15 (d, *J* = 6.8 Hz, 3H); **^{13}C NMR** (75 MHz, DMSO-d^6) δ 164.99, 162.68, 161.44, 158.17, 138.36, 135.45, 134.82, 133.20, 132.58, 131.84, 131.36, 129.31, 125.12, 123.86, 120.97, 116.50, 116.22, 83.35, 82.03, 49.45, 25.24; **HRMS** (LCMS-IT-TOF) Calc. for $C_{21}H_{16}FN_4O$ $(M + H)^+$ 359.1227, found 359.1231.

4.6.19 (*R*)-Isopropyl 8-ethynyl-6-(2-fluorophenyl)-4-methyl-4*H*-benzo[f]imidazo[1,5-*a*][1,4]diazepine-3-carboxylate (MP-III-050, 70)

Ethyl ester SH-053-2'F-R-CH_3 **52** (196 mg, 0.506 mmol) was stirred in dry THF (20 mL) in an oven-dried flask under an argon atmosphere at 40 ^{o}C; meanwhile, anhydrous isopropanol (4 mL) was stirred in a separate oven-dried flask under argon at 40 ^{o}C. Small pieces of freshly cut Li rod (~50 mg) were quickly added to the dry isopropanol and the suspension was stirred for 10 min under argon. The ethyl ester solution was then added to isopropanol and the mixture monitored by analysis of TLC (silica gel) until most of the starting material had been consumed (TLC, silica gel), about 30 min. The reaction solution was then quenched with sodium bicarbonate (sat'd aq solution, 5 mL) and the product was extracted with EtOAc (3 x 100 mL). The organic layers were combined, washed with brine, dried (Na_2SO_4), and the solvent was removed under reduced pressure. The solid which resulted was purified by flash chromatography (3:2 EtOAc:hexanes) to afford pure *iso*-propyl ester **70** as a white solid (197 mg, 97.0%): **^{1}H NMR** (300 MHz, $CDCl_3$) δ

7.95 (s, 1H), 7.71 (d, *J* = 8.1 Hz, 1H), 7.59 (dd, *J* = 19.4, 7.8 Hz, 2H), 7.46 (dd, *J* = 14.7, 7.3 Hz, 2H), 7.25 (d, *J* = 7.5 Hz, 1H), 7.05 (t, *J* = 9.2 Hz, 1H), 6.71 (q, *J* = 6.9 Hz, 1H), 5.30 (dt, *J* = 12.4, 6.2 Hz, 1H), 3.16 (s, 1H), 1.41 (dd, *J* = 9.8, 6.4 Hz, 6H), 1.29 (d, *J* = 7.0 Hz, 3H); **^{13}C NMR** (75 MHz, $CDCl_3$) δ 163.98, 162.21, 158.44, 141.23, 135.64, 134.98, 134.53, 134.18, 132.38, 131.33, 129.67, 129.12, 124.55, 122.47, 121.85, 116.41, 116.13, 81.28, 79.94, 68.48, 49.87, 21.94, 14.91.; **HRMS** (LCMS-IT-TOF) Calc. for $C_{24}H_{21}FN_3O_2$ $(M + H)^+$ 402.1551, found 402.1545.

4.6.20 (*R*)-*Tert*-butyl 8-ethynyl-6-(2-fluorophenyl)-4-methyl-4*H*-benzo[*f*]imidazo[1,5-*a*][1,4]diazepine-3-carboxylate (MP-III-051, 71)

Ethyl ester SH-053-2'F-R-CH_3 **52** (207 mg, 0.535 mmol) was stirred in dry THF (20 mL) in an oven-dried flask under argon at 40 ºC; meanwhile, anhydrous *tert*-butanol (3 mL) was stirred in a separate oven-dried flask under an argon atmosphere at 40 ºC. Small pieces of freshly cut Li rod (~50 mg) were quickly added to *tert*-butanol and the suspension was stirred for 10 min under argon. The ethyl ester solution was then added to *tert*-butanol and monitored by TLC (silica gel) until most of the starting material was consumed, about 30 min. The reaction mixture was then quenched with sodium bicarbonate (sat'd aq solution, 5 mL) and the product was extracted with EtOAc (3 x 100 mL). The organic layers were combined, washed with brine, dried (Na_2SO_4) and the solvent was removed under reduced pressure. The solid which resulted was purified by flash chromatography (3:2 EtOAc:hexanes) to afford pure *t*-butyl ester **71** as a white solid (118 mg, 53.1%). **^{1}H NMR** (300 MHz, $CDCl_3$) δ 7.96 (s, 1H), 7.71 (d, *J* = 8.4 Hz, 1H), 7.62 (t, *J* = 7.4 Hz, 1H), 7.56 (d, *J* = 8.3 Hz, 1H), 7.46 (dd, *J* = 16.9, 9.5 Hz, 2H), 7.26 (d, *J* = 7.7 Hz, 1H), 7.10 – 7.00 (m, 1H), 6.73 – 6.63 (m, 1H), 3.16 (s, 1H), 1.63 (s, 9H), 1.29 (d, *J* = 7.2 Hz, 3H); **^{13}C NMR** (300 MHz, $CDCl_3$) δ 161.80, 159.91, 158.44, 139.60, 137.25, 135.40, 134.99, 134.10, 131.98, 131.82,

124.92, 124.82, 123.49, 122.93, 116.72, 116.44, 100.15, 83.36, 80.85, 80.12, 48.96, 28.27, 14.95; **HRMS** (LCMS-IT-TOF) Calc. for $C_{25}H_{23}FN_3O_2$ $(M + H)^+$ 416.1705, found 416.1711.

4.6.21 (*R*)-Cyclopropylmethyl 8-ethynyl-6-(2-fluorophenyl)-4-methyl-4*H*-benzo[*f*]imidazo[1,5-*a*][1,4]diazepine-3-carboxylate (MP-III-052, 72)

Ethyl ester SH-053-2'F-R-CH_3 **52** (206 mg, 0.534 mmol) was stirred in dry THF (20 mL) in an oven-dried flask under argon at 40 ^oC; meanwhile, anhydrous cyclopropylmethyl alcohol (4 mL) was stirred in a separate oven-dried flask under an argon atmosphere at 40 ^oC. Small pieces of freshly cut Li rod (~50 mg) were quickly added to cyclopropylmethyl alcohol and the suspension was stirred for 10 min under argon. The ethyl ester solution was then added to cyclopropylmethyl alcohol and monitored by analysis by TLC (silica gel) until most of the starting material had been consumed (TLC, silica gel), about 30 min. The reaction was then quenched with sodium bicarbonate (sat'd aq solution, 5 mL) and the product was extracted with EtOAc (3 x 100 mL). The organic layers were combined, washed with brine, dried (Na_2SO_4), and the solvent was removed under reduced pressure. The solid which resulted was purified by flash chromatography (3:2 EtOAc:hexanes) to afford pure cyclopropyl methyl ester **72** as a white solid (213 mg, 96.2%): **^{1}H NMR** (300 MHz, $CDCl_3$) δ 7.98 (s, 1H), 7.73 (d, *J* = 8.4 Hz, 1H), 7.63 (t, *J* = 7.7 Hz, 1H), 7.58 (d, *J* = 8.3 Hz, 1H), 7.53 – 7.40 (m, 2H), 7.32 – 7.24 (m, 1H), 7.06 (t, *J* = 9.2 Hz, 1H), 6.78 – 6.69 (m, 1H), 4.28 – 4.10 (m, 3H), 3.17 (s, 1H), 1.30 (d, *J* = 7.4 Hz, 3H), 0.62 (q, *J* = 5.2 Hz, 2H), 0.38 (q, *J* = 4.9 Hz, 2H); **^{13}C NMR** (75 MHz, $CDCl_3$) δ 162.81, 161.77, 158.45, 141.40, 135.57, 135.05, 134.50, 134.14, 132.31, 131.31, 129.44, 129.21, 124.53, 122.41, 121.83, 116.40, 116.11, 81.30, 79.92, 69.75, 49.90, 14.91, 10.01.; **HRMS** (LCMS-IT-TOF) Calc. for $C_{25}H_{21}FN_3O_2$ $(M + H)^+$ 414.1534, found 414.1538.

4.6.22 (*R*)-8-ethynyl-6-(2-fluorophenyl)-4-methyl-4*H*-benzo[*f*]imidazo[1,5-*a*][1,4]diazepine-3-carboxylic acid (SH-053-2'F-R-CH$_3$-Acid, 73)

Ethyl ester SH-053-2'F-R-CH$_3$ **52** (2.0 g, 5.16 mmol) was stirred in ethanol (100 mL) and 3 M sodium hydroxide (20 mL, 60 mmol) was added and the solution was heated and refluxed for 1 h. The reaction solution was then cooled to rt and diluted with water (100 mL). The solution was placed under reduced pressure until half of the solvent remained. The remaining reaction mixture was stirred at rt and hydrochloric acid (1 M) was added dropwise at rt until the product precipitated out. The product was filtered, rinsed with water and dried to afford pure acid **73** as a white solid: **^{1}H NMR** (300 MHz, DMSO-d^6) δ 8.42 (s, 1H), 7.94 (d, 1H, *J* = 8.4 Hz), 7.82 (d, 1H, *J* = 8.2 Hz), 7.56 (dt, 2H, *J* = 7.8, 6.5 Hz), 7.33 (t, 1H, *J* = 7.4 Hz), 7.22 (t, 2H, *J* = 9.3 Hz), 6.53 (d, 1H, *J* = 7.1 Hz), 2.51 (s, 1H), 1.16 (d, 3H, *J* = 6.8 Hz); **^{13}C NMR** (75 MHz, DMSO-d^6) δ 164.76, 162.81, 158.19, 140.57, 136.57, 135.54, 134.74, 133.18, 132.65, 131.88, 129.88, 129.35, 125.17, 123.98, 121.09, 116.53, 116.25, 83.42, 82.01, 49.79, 15.08; **HRMS** (LCMS-IT-TOF) Calc. for $C_{21}H_{15}FN_3O_2$ $(M + H)^+$ 360.1143, found 360.1140.

4.6.23 (*R*)-5-(8-ethynyl-6-(2-fluorophenyl)-4-methyl-4*H*-benzo[*f*]imidazo[1,5-*a*][1,4]diazepin-3-yl)-3-methyl-1,2,4-oxadiazole (MP-IV-004, 74)

Ethyl ester SH-053-2'F-R-CH$_3$ **52** (300 mg, 0.774 mmol) was dissolved in dry THF (30 mL) at rt under argon. In a separate flask which contained 3Å molecular sieves, *N*-hydroxyacetimidamide (273 mg, 3.01 mmol) was dissolved in dry THF (30 mL) under argon and treated with sodium hydride (60% dispersion in mineral oil, 77 mg, 1.94 mmol). The mixture which resulted was stirred for 15 min at which point the solution containing **52** was added. The reaction mixture which resulted was stirred at rt for 3 h or until the starting material was consumed as indicated by TLC (silica gel). The reaction mixture was quenched with a saturated aq $NaHCO_3$ solution (5 mL).

Water (50 mL) was then added and the product was extracted with EtOAc (3 x 100 mL). The organic layers were combined, washed with brine, dried (Na_2SO_4) and the solvent was removed under reduced pressure. The solid which resulted was purified by flash chromatography (silica gel, EtOAc:hexanes 4:1) to afford pure methyl oxadiazole **74** as a white powder (141 mg, 45.8%): **^{1}H NMR** (300 MHz, $CDCl_3$) δ 8.13 (s, 1H), 7.79 (dd, *J* = 8.4, 1.4 Hz, 1H), 7.74 – 7.61 (m, 2H), 7.51 (dd, *J* = 13.9, 6.4 Hz, 2H), 7.35 – 7.26 (m, 1H), 7.13 – 7.04 (m, 1H), 6.78 (q, *J* = 7.1 Hz, 1H), 3.20 (s, 1H), 2.46 (s, 3H), 1.40 (d, *J* = 7.3 Hz, 3H); **^{13}C NMR** (75 MHz, $CDCl_3$) δ 170.30, 167.49, 161.80, 158.46, 138.42, 136.46, 135.48, 134.78, 134.30, 133.29, 131.63, 128.32, 125.12, 124.67, 122.53, 122.26, 116.52, 116.24, 80.98, 80.39, 49.58, 15.13, 11.66; **HRMS** (LCMS-IT-TOF) Calc. for $C_{23}H_{17}FN_5O$ $(M + H)^+$ 398.1347, found 398.1350.

Synthesis of the methyl oxime (N-hydroxyacetimidamide)

The synthesis of the methyl oxime can be found in Section 3.6.24

4.6.24 (*R*)-3-Ethyl-5-(8-ethynyl-6-(2-fluorophenyl)-4-methyl-4*H*-benzo[*f*]imidazo[1,5-*a*][1,4]diazepin-3-yl)-1,2,4-oxadiazole (MP-IV-005, 75)

Ethyl ester SH-053-2'F-R-CH_3 **52** (300 mg, 0.774 mmol) was dissolved in dry THF (30 mL) at rt under argon. In a separate flask which contained 3Å molecular sieves, *N'*-hydroxypropionimidamide (273 mg, 3.10 mmol) was dissolved in dry THF (20 mL) under argon and treated with sodium hydride (60% dispersion in mineral oil, 77 mg, 1.94 mmol). The mixture which resulted was stirred for 15 min at which point the solution containing **52** was added. The reaction mixture which resulted was stirred at rt for 2 h or until the starting material was consumed as indicated by TLC (silica gel). The reaction mixture was quenched with a saturated aq $NaHCO_3$ solution (5 mL). Water (50 mL) was then added and the product was extracted with EtOAc (3 x 100 mL). The organic layers were combined, washed with brine, dried (Na_2SO_4) and the solvent

was removed under reduced pressure. The solid which resulted was purified by flash chromatography (silica gel, EtOAc:hexanes 4:1) to afford pure ethyl oxadiazole **75** as a white powder (232 mg, 72.8%): **^{1}H NMR** (300 MHz, $CDCl_3$) δ 8.09 (s, 1H), 7.76 (d, *J* = 7.8 Hz, 1H), 7.63 (d, *J* = 8.2 Hz, 2H), 7.47 (d, *J* = 11.7 Hz, 2H), 7.33 – 7.24 (m, 1H), 7.06 (t, *J* = 9.1 Hz, 1H), 6.76 (dd, *J* = 14.1, 7.0 Hz, 1H), 3.18 (s, 1H), 2.83 (q, *J* = 7.5 Hz, 2H), 1.40 (dd, *J* = 14.7, 7.1 Hz, 6H); **^{13}C NMR** (75 MHz, $CDCl_3$) δ 171.93, 170.51, 161.79, 158.45, 138.81, 136.34, 135.83, 134.44, 134.29, 132.61, 131.37, 125.16, 124.63, 124.58, 122.33, 122.07, 116.46, 116.18, 81.19, 80.11, 49.96, 19.76, 15.07, 11.52; **HRMS** (LCMS-IT-TOF) Calc. for $C_{24}H_{19}FN_5O$ $(M + H)^+$ 412.1501, found 412.1497.

Synthesis of the ethyl oxime (N'-hydroxypropionimidamide)

The synthesis of the ethyl oxime can be found in Section 3.6.25.

4.6.25 (*R*)-5-(8-Ethynyl-6-(2-fluorophenyl)-4-methyl-4*H*-benzo[*f*]imidazo[1,5-*a*][1,4]diazepin-3-yl)-3-isopropyl-1,2,4-oxadiazole (MP-IV-010, 76)

Ethyl ester SH-053-2'F-R-CH_3 **52** (300 mg, 0.774 mmol) was dissolved in dry THF (30 mL) at rt under argon. In a separate flask which contained 3Å molecular sieves, *N'*-hydroxyisobutyrimidamide (316 mg, 3.10 mmol) was dissolved in dry THF (30 mL) under argon and treated with sodium hydride (60% dispersion in mineral oil, 77 mg, 1.94 mmol). The mixture which resulted was stirred for 15 min at which point the solution containing **52** was added. The reaction mixture which resulted was stirred at rt for 2 h or until the starting material was consumed as indicated by TLC (silica gel). The reaction mixture was quenched with a saturated aq $NaHCO_3$ solution (5 mL). Water (50 mL) was then added and the product was extracted with EtOAc (3 x 100 mL). The organic layers were combined, washed with brine, dried (Na_2SO_4) and the solvent was removed under reduced pressure. The solid which resulted was purified by flash

chromatography (silica gel, EtOAc:hexanes 4:1) to afford pure ethyl oxadiazole **34** as a white powder (216 mg, 65.7%): **^{1}H NMR** (300 MHz, $CDCl_3$) δ 8.09 (s, 1H), 7.75 (d, *J* = 7.8 Hz, 1H), 7.63 (d, *J* = 8.3 Hz, 2H), 7.46 (d, *J* = 12.1 Hz, 2H), 7.27 (dd, *J* = 9.4, 5.5 Hz, 1H), 7.06 (t, *J* = 9.2 Hz, 1H), 6.74 (q, *J* = 7.0 Hz, 1H), 3.24 – 3.10 (m, 2H), 1.38 (t, *J* = 8.3 Hz, 9H); **^{13}C NMR** (75 MHz, $CDCl_3$) δ 175.35, 170.27, 161.77, 158.43, 138.51, 136.39, 135.58, 134.70, 134.32, 133.01, 131.47, 128.52, 125.31, 124.67, 122.48, 122.19, 116.52, 116.23, 81.04, 80.31, 49.76, 26.76, 20.59, 20.54, 15.13; **HRMS** (LCMS-IT-TOF) Calc. for $C_{25}H_{21}FN_5O$ $(M + H)^+$ 426.1663, found 426.1659.

Synthesis of the isopropyl oxime (N'-hydroxyisobutyrimidamide)

The hydroxylamine hydrochloride (9.73 g, 0.14 mol), potassium carbonate (41.5 g, 0.3 mol), methanol (400 mL) and water (80 mL) were mixed as well as stirred and the mixture was heated to reflux. The isobutyronitrile (9.0 mL, 0.1 mol) was added dropwise and the reaction was stirred at reflux overnight. The next day the reaction mixture was cooled to 0 ^oC and a precipitate formed. The reaction mixture was filtered and the solvent from the filtrate was removed under reduced pressure. The solid which resulted was dissolved in EtOAc and washed with water, brine, and dried (Na_2SO_4) and the solvent removed under reduced pressure to afford the ethyl oxime (6.03 g, 59%) which was used in the synthesis of **76**: **HPLC-MS** (ESI) *m/z* (M+H) 103.08. This was used in the previous step without further characterization.

4.6.26 (*R*)-Methyl 8-bromo-6-(2-fluorophenyl)-4-methyl-4*H*-benzo[*f*]imidazo[1,5-*a*][1,4]diazepine-3-carboxylate (MP-III-058, 78)

Ethyl ester **55** (2.0 g, 4.52 mmol) was dissolved in methanol (120 mL). Sodium methoxide (0.98 g, 18.1 mmol) was added in one portion and the solution was heated to reflux. The reaction mixture was monitored by analysis by TLC (silica gel, 4:1 EtOAc:hexanes) until the starting material had

been consumed; approximately 30 min. The reaction solution was cooled to rt and then quenched with a saturated aq solution of sodium bicarbonate (20 mL). Water (50 mL) was then added to the solution and the methanol was removed under reduced pressure. The product was then extracted with EtOAc (3 x 100 mL), and the organic layers were combined, washed with brine, as well as dried (Na_2SO_4). The solution was concentrated under reduced pressure. The solid which resulted was purified via a wash column (silica gel, 4:1 EtOAc:hexanes) which provided pure methyl ester **78** as an off-white solid (1.68 g, 87% yield): **^{1}H NMR** (300 MHz, $CDCl_3$) δ 7.93 (s, 1H), 7.74 (d, 1H, *J* = 8.5 Hz), 7.61 (t, 1H, *J* = 7.2 Hz), 7.52-7.42 (m, 3H), 7.30-7.23 (m, 1H), 7.11-7.01 (m, 1H), 6.71 (q, 1H, *J* = 7.1 Hz), 3.94 (s, 3H), 1.30 (d, 3H, *J* = 7.4 Hz); **^{13}C NMR** (75 MHz, $CDCl_3$) δ 163.90, 162.64, 158.45, 141.03, 135.70, 135.20, 133.51, 132.99, 131.46, 130.32, 128.68, 127.09, 124.69, 124.10, 121.46, 116.52, 116.24, 52.08, 49.61, 14.96; **HRMS** (LCMS-IT-TOF) Calc. for $C_{20}H_{16}BrFN_3O_2$ $(M + H)^+$ 428.0404, found 428.0400.

REFERENCES

1. Cromer, B. A.; Morton, C. J.; Parker, M. W. Anxiety over $GABA_A$ receptor structure relieved by AChBP. *Trends Biochem. Sci.* **2002,** 27, 280 - 287.
2. Sieghart, W. Structure and pharmacology of g-aminobutyric $acid_A$ receptor subtypes. *Pharmacol. Rev.* **1995,** 47, 181 - 234.
3. Sieghart, W.; Ernst, M. Heterogeneity of $GABA_A$ receptors: revived interest in the development of subtype-selective drugs. *Curr. Med. Chem. - Central Nervous System Agents* **2005,** 5, 217 - 242.
4. Bowser, D. N.; Wagner, D. A.; Czajkowski, C.; Cromer, B. A.; Parker, M. W.; Wallace, R. H.; Harkin, L. A.; Mulley, J. C.; Marini, C.; Berkovic, S. F.; Williams, D. A.; Jones, M. V.; Petrou, S. Altered kinetics and benzodiazepine sensitivity of a GABA(A) receptor subunit mutation [g2(R43Q)] found in human epilepsy. *Proc. Natl. Acad. Sci.* **2002,** 99, 15170 - 15175.
5. Bateson, A. N. The benzodiazepine site of the GABA(A) receptor: An old target with new potential? *Sleep Medicine* **2004,** 5, S9 - S15.
6. Luscher, B. P.; Shen, Q.; Sahir, N. The GABAergic deficit hypothesis of major depressive disorder. *Mol. Psychiatry* **2011,** 16, 383 - 406.
7. Otani, K.; Ujike, H.; Tanaka, Y.; Morita, Y.; Katsu, T.; Nomura, A.; Uchida, N.; Hamamura, T.; Fujiwara, Y.; Kuroda, S. The GABA type A receptor alpha 5 subunit gene is associated with bipolar I disorder. *Neuroscience Letters* **2005,** 381, 108 - 113.
8. Dean, B.; Scarr, E.; McLeod, M. Changes in hippocampal GABA(A) receptor subunit composition in bipolar I disorder. *Brain Res. Mol. Brain Res.* **2005,** 138, 145 - 155.

9. Guidotti, A.; Auta, J.; Davis, J. M.; Dong, E.; Grayson, D. R.; Veldic, M.; Zhang, X.; Costa, E. GABAergic dysfunction in schizophrenia: new treatment strategies on the horizon. *Psychopharmacol.* **2005,** 180, 191 - 205.

10. Maubach, K. GABA(A) receptor subtype selective cognition enhancers. *Drug Targets-CNS & Neuro. Disorders* **2003,** 2003, 233 - 239.

11. Barnard, E. A.; Skolnick, P.; Olsen, R. W.; Mohler, H.; Sieghart, W.; Biggio, G.; Braestrup, C.; Bateson, A. N.; Langer, Z. International Union of Pharmacology. XV. Subtypes of g-aminobutyric $acid_A$ receptors: Classification on the basis of subunit structure and receptor function. *Pharmacol. Rev.* **1998,** 50, 291 - 313.

12. Simon, J.; Wakimoto, H.; Fujita, N.; Lalande, M.; Barnard, E. A. Analysis of the set of $GABA_A$ receptor genes in the human genome. *J. Biol. Chem.* **2004,** 279, 41422 - 41435.

13. Olsen, R. W.; Sieghart, W. $GABA_A$ receptors: Subtypes provide diversity of function and pharmacology. *Neuropharmacology* **2009,** 56, 141 - 148.

14. Sieghart, W.; Sperk, G. Subunit composition, distribution and function of $GABA_A$ receptor subtypes. *Curr. Topics Med. Chem.* **2002,** 2, 785 - 816.

15. Olsen, R. W.; Tobin, A. J. Molecular biology of $GABA_A$ receptors. *FASEB J.* **1990,** 4, 1469 - 1480.

16. Burt, D. R.; Kamatchi, G. L. $GABA_A$ receptor subtypes: from pharmacology to molecular biology. *FASEB J.* **1991,** 5, 2916 - 2923.

17. Clayton, T.; Chen, J. L.; Ernst, M.; Richter, L.; Cromer, B. A.; Morton, C. J.; Ng, H.; Kaczorowski, C. C.; Helmstetter, F. J.; Furtmuller, R.; Ecker, G.; Parker, M. W.; Sieghart, W.; Cook, J. M. An updated unified pharmacophore model of the benzodiazepine binding site

on g-aminobutyric acid$_a$ receptors: Correlation with comparative models. *Curr. Med. Chem.* **2007,** 14, 2755 - 2775.

18. Keramidas, A.; Moorhouse, A.; Schofield, P. C.; Barry, P. Ligand-gated ion channels: mechanisms underlying ion selectivity. *Prog. Biophys. Mol. Biol.* **2004,** 86, 161 - 204.
19. MacDonald, R. L. Benzodiazepine mechanisms of action. In *Antiepileptic Drugs*, Levy, R. H.; Mattson, R. H.; Meldrum, B. S.; Perucca, E., Eds. Lippincott Williams and Wilkins: Philadelphia, 2002; pp 179 - 186.
20. Sigel, E.; Luscher, B. P. A closer look at the high affinity benzodiazepine binding site on GABA(A) receptors. *Curr. Topics Med. Chem.* **2011,** 11, 241 - 246.
21. Ramerstorfer, J.; Furtmuller, R.; Sarto-Jackson, I.; Varagic, Z.; Sieghart, W.; Ernst, M. The $GABA_A$ receptor a+b- interface: A novel target for subtype selective drugs. *J. Neurosci.* **2011,** 31, 870 - 877.
22. Varagic, Z.; Ramerstorfer, J.; Huang, S.; Rallapalli, S.; Sarto-Jackson, I.; Cook, J.; Sieghart, W.; Ernst, M. Subtype selectivity of a+b- site ligands of $GABA_A$ receptors: identification of the first highly specific positive modulators at a6b2/3g2 receptors *Br. J. Pharmacol.* **2013,** 169, 384 - 399.
23. Sigel, E. Mapping of the benzodiazepine recognition site of $GABA_A$ receptors. *Curr. Topics Med. Chem.* **2002,** 2, 833-839.
24. Belelli, D.; Lambert, J. J. Neurosteriods: endogenous regulators of the GABA(A) receptor. *Nat. Rev. Neurosci.* **2005,** 6, 565 - 575.
25. Harris, R. A. Ethanol actions on multiple ion channels: which are important? *Alcohol Clin. Exp. Res.* **1999,** 23, 1563 - 1570.

26. Lobo, I. A.; Harris, R. A. $GABA_A$ receptors and alcohol. *Pharmacol. Biochem. Behav.* **2008,** 90, 90 - 94.

27. Olsen, R. W.; Hanchar, H. J.; Meera, P.; Wallner, M. GABAA receptor subtypes: the "one glass of wine" receptors. *Alcohol* **2007,** 41, 201 - 209.

28. Sawyer, E.; Moran, C.; Sirbu, M. H.; Szafir, M.; Van Linn, M.; Namjoshi, O.; Tiruveedhula, V. V. N. P. B.; Cook, J. M.; Platt, D. M. Little evidence of a role for the a1 $GABA_A$ subunit-containing receptor in rhesus monkey model of alcohol drinking. *Alcohol Clin. Exp. Res.* **2014,** 38, 1108 - 1117.

29. Ernst, M.; Brauchart, D.; Boresch, S.; Sieghart, W. Comparative modeling of $GABA_A$ receptors: Limits, insights, future developments. *Neurosci.* **2003,** 119, 933 - 943.

30. Haefely, W. The biological basis of benzodiazepine actions. *J. Psychoactive Drugs* **1983,** 15, 19 - 39.

31. Haefely, W.; Facklam, M.; Schoch, P.; Martin, J. R.; Bonetti, E. P.; Moreau, J. L.; Jenck, F.; Richards, J. G. Partial agonists of benzodiazepine receptors for the treatment of epilepsy, sleep, and anxiety disorders. *Adv. Biochem. Psychopharmacol.* **1992,** 47, 379 - 394.

32. Gorman, J. M. Benzodiazepines: Taking the good with the bad and the ugly. *CNS Spectrums* **2005,** 10, 14 - 15.

33. Garattini, S.; Mussini, E.; Marucci, F.; Guaitani, A. Metabolic studies on benzodiazepines in various animal species. In *The Benzodiazepines*, Garattini, S.; Mussini, E.; Randall, L. O., Eds. Raven Press: New York, 1973; pp 75 - 97.

34. Rutherford, D. M.; Okoko, A.; Tyrer, P. J. Plasma concentrations of diazepam and desmethyldiazepam during chronic diazepam therapy. *Br. J. Clin. Pharmacol.* **1978,** 1978.

35. Bond, A. J.; Hailey, D. M.; Lader, M. H. Plasma concentrations of benzodiazepines. *Br. J. Clin. Pharmacol.* **1977,** 4, 51 - 56.

36. Stevenson, I. H.; Browning, M.; Crooks, J.; O'Malley, K. Changes in human drug metabolism after long-term exposure to hypnotics. *Br. Med. Journal* **1972,** 4, 322 - 324.

37. Hillestad, L.; Hansen, T.; Melsom, H.; Drivenes, A. Diazepam metabolism in normal man I. Serum concentrations and clinical effects after intravenous, intramuscular, and oral administrations. *Clin. Pharmacol. Therapeutics* **1974,** 16, 479 - 484.

38. Killam, E. K.; Suria, A. Benzodiazepines. In *Antiepileptic Drugs: Mechanisms of Action*, Glaser, G. H.; Penry, J. K.; Woodbury, D. M., Eds. Raven Press: New York, 1980; pp 597 - 615.

39. Rogawski, M. A. Principles of antiepileptic drug action. In *Antiepileptic Drugs*, 5th ed.; Levy, R. H.; Mattson, R. H.; Meldrum, B. S.; Perucca, E., Eds. Lippincott Williams and Wilkins: Philadelphia, 2002; pp 3 - 22.

40. Rudolph, U.; Mohler, H. Analysis of $GABA_A$ receptor function and dissection of the pharmacology of benzodiazepines and general anesthetics through mouse genetics. *Ann. Rev. Pharmacol. Toxicol.* **2004,** 44, 475 - 498.

41. Rudolph, U.; Crestani, F.; Benke, D.; Brunig, I.; Benson, J. A.; Fritschy, J.-M.; Martin, J. R.; Bluethmann, H.; Mohler, H. Benzodiazepine actions mediated by specific g-aminobutyric $acid_A$ receptor subtypes. *Nature* **1999,** 401, 796 - 800.

42. McKernan, R. M.; Rosahl, T. W.; Reynolds, D. S.; Sur, C.; Wafford, K. A.; Atack, J. R.; Farrar, S.; Myers, J.; Cook, G.; Ferris, P.; Garrett, L.; Bristow, L.; Marshall, G.; Macaulay, A.; Brown, N.; Howell, O.; Moore, K. W.; Carling, R. W.; Street, L. J.; Castro, J. L.; Ragan,

C. I.; Dawson, G. R.; Whiting, P. J. Sedative but not anxiolytic properties of benzodiazepines are mediated by the $GABA_A$ receptor a_1 subtype. *Nat. Neurosci.* **2000,** 3, 587 - 592.

43. Low, K.; Crestani, F.; Keist, R.; Benke, D.; Brunig, I.; Benson, J. A.; Fritschy, J.-M.; Rulicke, T.; Bluethmann, H.; Mohler, H.; Rudolph, U. Molecular and neuronal substrate for the selective attenuation of anxiety. *Science* **2000,** 290, 131 - 134.
44. Morris, H. V.; Dawson, G. R.; Reynolds, D. S.; Atack, J. R.; Stephens, D. N. Both a2 and a3 $GABA_A$ receptor subtypes mediate the anxiolytic properties of benzodiazepine site ligands in the conditioned emotional response paradigm. *Eur. J. Neurosci.* **2006,** 23, 2498 - 2504.
45. Dias, R.; Sheppard, W. F. A.; Fradley, R. L.; Garrett, E. M.; Stanley, J. L.; Tye, S. J.; Goodacre, S.; Lincoln, R. J.; Cook, S. M.; Conley, R.; Hallett, D.; Humphries, A. C.; Thompson, S. A.; Wafford, K. A.; Street, L. J.; Castro, J. L.; Whiting, P. J.; Rosahl, T. W.; Atack, J. R.; McKernan, R. M.; Dawson, G. R.; Reynolds, D. S. Evidence for a significant role of a3-containing $GABA_A$ receptors in mediating the anxiolytic effects of benzodiazepines. *J. Neurosci.* **2005,** 25, 10682 - 10688.
46. Yee, B. K.; Keist, R.; von Boehmer, L.; Studer, R.; Benke, D.; Hagenbuch, N.; Dong, Y.; Malenka, R. C.; Fritschy, J.-M.; Bluethmann, H.; Feldon, J.; Mohler, H.; Rudolph, U. A schizophrenia-related sensorimotor deficit links a3-containing $GABA_A$ receptors to a dopamine hyperfunction. *Proc. Natl. Acad. Sci. U.S.A.* **2005,** 102, 17154 - 17159.
47. Crestani, F.; Keist, R.; Fritschy, J.-M.; Benke, D.; Vogt, K.; Prut, L.; Bluthmann, H.; Mohler, H.; Rudolph, U. Trace fear conditioning involving hippocampal a5 $GABA_A$ receptors. *Proc. Natl. Acad. Sci. U.S.A.* **2002,** 99, 8980 - 8985.
48. Knabl, J.; Witschi, R.; Hosl, K.; Reinold, H.; Zeilhofer, U. B.; Ahmadi, S.; Brockhaus, J.; Sergejeva, M.; Hess, A.; Brune, K.; Fritschy, J.-M.; Rudolph, U.; Mohler, H.; Zeilhofer, H.

U. Reversal of pathological pain through specific spinal $GABA_A$ receptor subtypes. *Nature* **2008,** 451, 330 - 335.

49. Miller, P. S.; Aricescu, A. R. Crystal structure of a human $GABA_A$ receptor. *Nature* **2014,** 512, 270 - 275.
50. Ralvenius, W. T.; Benke, D.; Acuna, M. A.; Rudolph, U.; Zeilhofer, H. U. Analgesia and unwanted benzodiazepine effects in point-mutated mice expressing only one benzodiazepine-sensitive $GABA_A$ receptor subtype. *Nat. Commun.* **2015,** 6.
51. Cook, J. M.; Edwankar, R.; Poe, M. M.; Tiruveedhula, V. V. N. P. B.; Witzigmann, C. Synthesis of natural products and related heterocyclic compounds. Search for agents to treat neuropathic pain, epilepsy and anxiety disorders as well as simple molecules to treat TB and MRSA infections. In *Mona Symposium on Natural Products and Medicinal Chemistry*, Kingston, Jamaica, 2014.
52. Fritschy, J. M.; Mohler, H. $GABA_A$-receptor heterogeneity in the adult rat brain: differential regional and cellular distribution of seven major subunits. *J. Comp. Neurol.* **1995,** 359, 154 - 194.
53. Fritschy, J. M.; Benke, D.; Mertens, S.; Oertel, W. H.; Bachi, T.; Mohler, H. Five subtypes of type A gamma-aminobutyric acid receptors identified in neurons by double and triple immunofluorescence staining with subunit-specific antibodies. *Proc. Natl. Acad. Sci.* **1992,** 89, 6726 - 6730.
54. Korpi, E. R.; Mattila, M. J.; Wisden, W.; Luddens, H. GABAA-receptor subtypes: clinical efficacy and selectivity of benzodiazepine site ligands. *Ann. Med.* **1997,** 29, 275 - 282.

55. Vicini, S.; Ferguson, C.; Prybylowski, K.; Kralic, J.; Morrow, A. L.; Homanics, G. E. $GABA_A$ receptor a1 subunit deletion prevents developmental changes of inhibitory synaptic currents in cerebellar neurons. *J. Neurosci.* **2001,** 21, 3009 - 3016.

56. Sur, C.; Wafford, K. A.; Reynolds, D. S.; Hadingham, K. L.; Bromidge, F.; Macaulay, A.; Collinson, N.; O'Meara, G.; Howell, O.; Newman, R.; Myers, J.; Atack, J. R.; Dawson, G. R.; McKernan, R. M.; Whiting, P. J.; Rosahl, T. W. Loss of the major $GABA_A$ receptor subtype in the brain is not lethal in mice. *J. Neurosci.* **2001,** 21, 3409 - 3418.

57. Collinson, N.; Kuenzi, F. M.; Jarolimek, W.; Maubach, K. A.; Cothliff, R.; Sur, C.; Smith, A.; Otu, F. M.; Howell, O.; Atack, J. R.; McKernan, R. M.; Seabrook, G. R.; Dawson, G. R.; Whiting, P. J.; Rosahl, T. W. Enhanced learning and memory and altered GABAergic synaptic transmission in mice lacking the a5 subunit of the $GABA_A$ receptor. *J. Neurosci.* **2002,** 22, 5572 - 5580.

58. Bohlhalter, S.; Weinmann, O.; Mohler, H.; Fritschy, J. M. Laminar compartmentalization of GABAA-receptor subtypes in the spinal cord: an immunohistochemical study. *J. Neurosci.* **1996,** 16, 283 - 297.

59. Bencsits, E.; Ebert, V.; Tretter, V.; Sieghart, W. A significant part of native g-aminobutyric $acid_A$ receptors containing a4 subunits do not contain g or d subunits. *J. Biol. Chem.* **1999,** 274, 19613 - 19616.

60. Quirk, K.; Gillard, N. P.; Ragan, I.; Whiting, P. J.; McKernan, R. M. Model of subunit composition of g-aminobutyric acid A receptor subtypes expressed in rat cerebellum with respect to their a and g/d subunits. *J. Biol. Chem.* **1994,** 169, 16020 - 16028.

61. Tanaka, C.; Taniyama, K. The role of GABA in the peripheral nervous system. In *GABA Outside the CNS*, Erdo, S. L., Ed. Springer: 1992; pp 3 - 17.

62. Magnaghi, V.; Ballabio, M.; Consoli, A.; Lambert, J. J.; Roglio, I.; Melcangi, R. C. GABA receptor-mediated effects in the peripheral nervous system: A cross-interaction with neuroactive steroids. *J. Mol. Neuroscience* **2006,** 28, 89 - 102.

63. Farrant, M.; Nusser, Z. Variations on an inhibitory theme: phasic and tonic activation of $GABA_A$ receptors. *Nat. Rev. Neurosci.* **2005,** 6, 215 - 229.

64. Gallos, G.; Yim, P.; Chang, S.; Zhang, Y.; Xu, D.; Cook, J. M.; Gerhoffer, W. T.; Emala Sr., C. W. Targeting the restricted a-subunit repertoire of airway smooth muscle $GABA_A$ receptors augments airway smooth muscle relaxation. *Am. J. Physiol. Lung Cell Mol. Physiol.* **2012,** 302, L248 - L256.

65. Gallos, G.; Yocum, G. T.; Siviski, M. E.; Yim, P. D.; Fu, X. W.; Poe, M. M.; Cook, J. M.; Harrison, N.; Perez-Zoghbi, J.; Emala Sr., C. W. Selective targeting of the a5-subunit of GABAA receptors relaxes airway smooth msucle and inhibits cellular calcium handling. *Am. J. Physiol. Lung Cell Mol. Physiol.* **2015,** 308, L931 - L942.

66. Mizuta, K.; Xu, D.; Pan, Y.; Comas, G.; Sonett, J. R.; Zhang, Y.; Panettieri Jr., R. A.; Yang, J.; Emala Sr., C. W. $GABA_A$ receptors are expressed and facilitate relaxation in airway smooth muscle. *Am. J. Physiol. Lung Cell Mol. Physiol.* **2008,** 294, L1206 - L1216.

67. Bergeret, M.; Khrestchatisky, M.; Tremblay, E.; Bernard, A.; Gregoire, A.; Chany, C. GABA modulates cytotoxicity of immunocompetent cells expressing GABA(A) receptor subunits. *Biomed. Pharmacother.* **1998,** 52, 214 - 219.

68. Labonte, D.; Thies, E.; Kneussel, M. The kinesin KIF21B participates in the cell surface delivery of g2 subunit-containing GABAA receptors. *Eur. J. Cell Biol.* **2014,** 93, 338 - 346.

69. Davies, M.; Bateson, A. N.; Dunn, S. M. J. Structural requirements for ligand interactions at the benzodiazepine recognition site of the GABA(A) receptor. *J. Neurochem.* **1998,** 70, 2188 - 2194.

70. Dunn, S. M. J.; Davies, M.; Muntoni, A. L.; Lambert, J. J. Mutagenesis of the rat a1 subunit of the g-aminobutyric Acid(A) receptor reveals the importance of residue 101 in determining the allosteric effects of benzodiazepine site ligands. *Mol. Pharmacol.* **1999,** 56, 768 - 774.

71. Sigel, E.; Schaerer, M. T.; Buhr, A.; Baur, R. The benzodiazepine binding pocket of recombinant a1b2g2 g-aminobutyric acid(A) receptors: Relative orientation of ligands and amino acid side chains. *Mol. Pharmacol.* **1998,** 54, 1097 - 1105.

72. Divljakovic, J.; Milic, M.; Namjoshi, O. A.; Tiruveedhula, V. V.; Timic, T.; Cook, J. M.; Savic, M. M. bCCT, an antagonist selective for a1 $GABA_A$ receptors, reverses diazepam withdrawal-induced anxiety in rats. *Brain Res. Bulletin* **2013,** 91, 1 - 7.

73. Clayton, T. S. Ph.D. Thesis, Part I. Unified Pharmacophoric Protein Models of the Benzodiazepine Receptor Subtypes. Part II. Subtype Selective Ligands for a5 $GABA_A$/Bz Receptors. University of Wisconsin-Milwaukee, 2011.

74. Clayton, T.; Poe, M. M.; Rallapalli, S.; Biawat, P.; Savic, M. M.; Rowlett, J. K.; Gallos, G.; Emala, C. W.; Kaczorowski, C. C.; Stafford, D. C.; Arnold, L. A.; Cook, J. M. A review of the updated pharmacophore for the alpha 5 GABA(A) benzodiazepine receptor model. *Intl. J. Med. Chem.* **2015**.

75. He, X.; Huang, Q.; Ma, C.; Yu, S.; McKernan, R.; Cook, J. M. Pharmacophore/receptor models for $GABA_A$/BzR a2b3g2, a3b3g2 and a4b3g2 recombinant subtypes. Included volume analysis and comparison to a1b3g2, a5b3g2 and a6b3g2 subtypes. *Drug Des. Discov.* **2000,** 17, 131 - 171.

76. Huang, Q.; He, X.; Ma, C.; Liu, R.; Yu, S.; Dayer, C. A.; Wenger, G. R.; McKernan, R.; Cook, J. M. Pharmacophore/receptor models for $GABA_A$/BzR subtypes (a1b3g2, a5b3g2, and a6b3g2) via a comprehensive ligand-mapping approach. *J. Med. Chem* **2000,** 43, 71 - 95.

77. Martin, M.; Trudell, M. L.; Diaz-Arauzo, H.; Allen, M. S.; LaLoggia, A.; Deng, L.; Schultz, C. A.; Tan, T.-C.; Bi, Y.; Narayanan, K.; Dorn, L.; Koehler, K.; Skolnick, P.; Cook, J. M. Molecular yardsticks. Rigid planar ligands to define the spatial dimensions of the benzodiazepine receptor binding site. *J. Med. Chem* **1992,** 35, 4105 - 4117.

78. Gu, Z. Q.; Wong, G.; Dominguez, C.; de Costa, B. R.; Rice, K. C.; Skolnick, P. Synthesis and evaluation of imidazo[1,5a][1,4]benzodiazepine esters with high affinities and selectivities at diazepam insensitive (DI) benzodiazepine receptors. *J. Med. Chem* **1993,** 36, 1001 - 1006.

79. Wong, G.; Koehler, K. F.; Skolnick, P.; Gu, Z. Q.; Ananthan, S.; Schonholze, P.; Hunkeler, W.; Zhang, W.; Cook, J. M. Synthetic and computer-assisted analysis of the structural requirements for selective, high affinity ligand binding to 'diazepam-insensitive' benzodiazepine receptors. *J. Med. Chem* **1993,** 36, 1820 - 1830.

80. Lippke, K. P.; Schunack, W. G.; Wenning, W.; Muller, W. E. b-Carbolines as benzodiazepine receptor ligands. I. Synthesis and benzodiazepine receptor interactino of esters of b-carboline-3-carboxylic acid. *J. Med. Chem* **1983,** 26, 499 - 503.

81. Haefely, W.; Martin, J. R.; Schoch, P. Novel anxiolytics that act as partial agonists at benzodiazepine receptors. *Trends Pharmacol. Sci.* **1990,** 11, 452 - 456.

82. Hagen, T. J.; Guzman, F.; Schultz, C.; Cook, J. M. Synthesis of 3,6-disubstituted b-carbolines which possess either benzodiazepine antagonist or agonist activity. *Heterocycles* **1986,** 24, 2845 - 855.

83. Gee, K. W.; Brinton, R. E.; Yamamura, H. I. CL-218872 antagonism of diazepam induced loss of righting reflex: Evidence for partial agonistic activity at the benzodiazepine receptor. *Life Sci.* **1983,** 32, 1037 - 1040.

84. Allen, M. S.; Hagen, T. J.; Trudell, M. L.; Codding, P. W.; Skolnick, P.; Cook, J. M. Synthesis of novel 3-substituted b-carbolines as benzodiazepine receptor ligands: probing the benzodiazepine receptor pharmacophore. *J. Med. Chem* **1988,** 31, 1854 - 1861.

85. Trudell, M. L.; Lifer, S. L.; Tan, Y. C.; Martin, M. J.; Deng, T.; Skolnick, P.; Cook, J. M. Synthesis of substituted 7,12-dihydropyrido[3,2-*b*:5,4-*b*'] diindoles: rigid planar benzodiazepine receptor ligands with inverse agonist/antagonist properties. *J. Med. Chem* **1990,** 33, 2412 - 2420.

86. Arbilla, S.; Depoortere, H.; Geroge, P.; Langer, S. Z. Pharmacological profile of the imidazopyridine zolpidem at benzodiazepine receptors and electrocorticogram in rats. *Naunym Schmiederbergs Arch. Pharmacol.* **1985,** 330, 248 - 251.

87. Yokoyama, N.; Ritter, B.; Neubert, A. D. 2-Arylpyrazolo[4,3-*c*]quinolin-3-ones: novel agonist, partial agonist, and antagonist of benzodiazepines. *J. Med. Chem* **1982,** 25, 337 - 339.

88. van Rijnsoever, C.; Tauber, M.; Choulli, M. K.; Keist, R.; Rudolph, U.; Mohler, H.; Fritschy, J.-M.; Crestani, F. Requirement of a5-$GABA_A$ receptors for the development of tolerance to the sedative action of diazepam in mice. *J. Neurosci.* **2004,** 24, 6785 - 6790.

89. Cook, J.; Huang, S.; Edwankar, R.; Namjoshi, O. A.; Wang, Z.-j. Selective agents for pain suppression. US 2010/0317619 A1, 2010.

90. Cook, J.; Huang, S.; Edwankar, R.; Namjoshi, O. A.; Wang, Z.-J. Selective agents for pain suppression. US 8,835,424 B2, Sep. 16, 2014, 2014.

91. Cook, J. M.; Zhou, H.; Huang, S.; Sarma, P. V. V. S.; Zhang, C. Stereospecific anxiolytic and anticonvulsant agents with reduced muscle-relaxant, sedative-hypnotic and ataxic effects. US 2006/0003995 A1, Jan. 5, 2006, 2006.

92. Cook, J. M.; Zhou, H.; Huang, S.; Sarma, P. V. V. S.; Zhang, C. Stereospecific anxiolytic and anticonvulsant agents with reduced muscle-relaxant, sedative-hypnotic and ataxic effects. US 7,618,958 B2, Nov. 17, 2009, 2009.

93. Di Lio, A.; Benke, D.; Besson, M.; Desmeules, J.; Daali, Y.; Wang, Z.-j.; Edwankar, R.; Cook, J. M.; Zeilhofer, H. U. HZ166, a novel $GABA_A$ receptor subtype-selective benzodiazepine site ligand, is antihyperalgesic in mouse models of inflammatory and neuropathic pain. *Neuropharmacology* **2011,** 60, 626 - 632.

94. Huang, Q.; Zhang, W.; Liu, R.; McKernan, R. M.; Cook, J. M. Benzo-fused benzodiazepines employed as topological probes for the study of benzodiazepine receptor subtypes. *Med. Chem. Res.* **1996,** 6, 384 - 391.

95. Kessler, R. C.; Chiu, W. T.; Demler, O.; Walters, E. E. Prevalence, severity, and comorbidity of 12-month *DSM-IV* disorders in the National Comorbidity Survey Replication. *Arch. Gen. Psychiatry* **2005,** 62, 617 - 627.

96. Baldwin, D. S.; Polkinghorn, C. Evidence-based pharmacotherapy of generalized anxiety disorder. *Int. J. Neuropsychopharmacol.* **2005,** 8, 293 - 302.

97. Nutt, D. J. Overview of diagnosis and drug treatments of anxiety disorders. *CNS Spectrums* **2005,** 10, 49 - 56.

98. Benyamin, R.; Trescot, A. M.; Datta, S.; Buenaventura, R.; Adlaka, R.; Sehgal, N.; Glaser, S. E.; Vallejo, R. Opioid complications and side effects. *Pain Physician* **2008,** 11, S105 - S120.

99. Antman, E. M.; Bennett, J. S.; Daugherty, A.; Furberg, C.; Roberts, H.; Taubert, K. A. Use of nonsteroidal antiinflammatory drugs: an update for clinicians: a scientific statement from the American Heart Association. *Circulation* **2007,** 115, 1634 - 1642.

100. Kearney, P. M.; Baigent, C.; Godwin, J.; Halls, H.; Emberson, J. R.; Patrono, C. Do selective cyclo-oxygenase-2 inhibitors and traditional non-steroidal anti-inflammatory drugs increase the risk of atherothrombosis? Meta-analysis of randomised trials. *Brit. Med. J.* **2006,** 332, 1302 - 1308.

101. Cunningham, C. W.; Rothman, R. B.; Prisinzano, T. E. Neuropharmacology of the naturally occuring kappa-opioid hallucinogen salvinorin A. *Pharmacol. Rev.* **2011,** 63, 316 - 347.

102. Watkins, L. R.; Hutchinson, M. R.; Rice, K. C.; Maier, S. F. The "toll" of opioid-induced glial activation:improving the clinical efficacy of opioids by targeting glia. *Trends Pharmacol. Sci.* **2009,** 30, 581 - 591.

103. Hutchinson, M. R.; Zhang, Y.; Shridhar, M.; Evans, J. H.; Buchanan, M. M.; Zhao, T. X.; Slivka, P. F.; Coats, B. D.; Rezvani, N.; Wieseler, J.; Hughes, T. S.; Landgraf, K. E.; Chan, S.; Fong, S.; Phipps, S.; Falke, J. J.; Leinwand, L. A.; Maier, S. F.; Yin, H.; Rice, K. C.; Watkins, L. R. Evidence that opioids may have toll-like receptor 4 and MD-2 effects. *Brain, Behav., and Immunity* **2010,** 24, 83 - 95.

104. Scott-Stevens, P.; Atack, J. R.; Sohal, B.; Worboys, P. Rodent pharmacokinetics and receptor occupancy of the $GABA_A$ receptor subtype selective benzodiazepine site ligand L-838417. *Biopharm. Drug Dispos.* **2005,** 26, 13 - 20.

105. Atack, J. R.; Wafford, K. A.; Tye, T. J.; Cook, S. M.; Sohal, B.; Pike, A.; Sur, C.; Melillo, D.; Bristow, L.; Bromidge, F.; Ragan, I.; Kerby, J.; Street, L.; Carling, R.; Castro, J. L.; Whiting, P.; Dawson, G. R.; McKernan, R. M. TPA023 [7-(1,1Dimethylethyl)-6-(2-ethyl-2*H*-1,2,4-

triazol-3-ylmethoxy)-3-(2-fluorophneyl)-1,2,4-triazolo[4,3-*b*]pyridazine], an agonist selective for a2- and a3-containing $GABA_A$ receptors, is a nonsedating anxiolytic in rodents and primates. *J. Pharmacol. Exp. Ther.* **2006,** 316, 410 - 422.

106. Mohler, H. The rise of a new GABA pharmacology. *Neuropharmacology* **2011,** 60, 1042 - 1049.

107. Atack, J. R.; Wafford, K. A.; Street, L. J.; Dawson, G. R.; Tye, S.; Van Laere, K.; Bormans, G.; Sanabria-Bohorquez, S. M.; De Lepeleire, I.; de Hoon, J. N.; Van Hecken, A.; Burns, H. D.; McKernan, R. M.; Murphy, M. G.; Hargreaves, R. J. MRK-409 (MK-0343), a $GABA_A$ receptor subtype-selective partial agonist, is a non-sedating anxiolytic in preclinical species but causes sedation in humans. *J. Psychopharmacol.* **2010,** 25, 314 - 328.

108. Atack, J. R.; Hallett, D. J.; Tye, S.; Wafford, K. A.; Ryan, C.; Sanabria-Bohorquez, S. M.; Eng, W.-s.; Gibson, R. E.; Burns, H. D.; Dawson, G. R.; Carling, R. W.; Street, L. J.; Pike, A.; De Lepeleire, I.; Van Laere, K.; Bormans, G.; De Hoon, J. N.; Van Hecken, A.; McKernan, R. M.; Murphy, M. G.; Hargreaves, R. J. Preclinical and clinical pharmacology of TPA023B, a $GABA_A$ receptor a2/a3 subtype-selective partial agonist. *J. Psychopharmacol.* **2010,** 25, 329 - 344.

109. Mirza, N. R.; Larsen, J. S.; Mathiasen, C.; Jacobsen, T. A.; Munro, G.; Erichsen, H. K.; Nielsen, A. N.; Troelsen, K. B.; Nielsen, E. O.; Ahring, P. K. NS11394 [3'-[5-(1-Hydroxy-1-methyl-ethyl)-benzoimidazol-1-yl]-biphenyl-2-carbonitrile], a unique subtype-selective $GABA_A$ receptor positive allosteric modulator: In vitro actions, pharmacokinetic properties and in vivo anxiolytic Efficacy. *J. Pharmacol. Exp. Ther.* **2008,** 327, 954-968.

110. Munro, G.; Lopez-Garcia, J. A.; Rivera-Arconada, I.; Erichsen, H. K.; Nielsen, E. O.; Larsen, J. S.; Ahring, P. K.; Mirza, N. R. Comparison of the novel subtype-selective $GABA_A$ receptor-

positive allosteric modulator NS11394 [3'-[5-(1-Hydroxy-1-methyl-ethyl)benzoimidazol-1-yl]-biphenyl-2-carbonitrile] with diazepam, zolpidem, bretazenil, and gaboxadol in rat models of inflammatory and neuropathic pain. *J. Pharmacol. Exp. Ther.* **2008,** 327, 969-981.

111. Hofmann, M.; Kordas, K. S.; Gravius, A.; Bolcskei, K.; Parsons, C. G.; Dekundy, A.; Danysz, W.; Dezsi, L.; Wittko-Schneider, I. M.; Saghy, K.; Gyertyan, I.; Horvath, C. Assessment of the effects of NS11394 and L-838417, a2/3 subunit-selective $GABA_A$ receptor-positive allosteric modulators, in tests of pain, anxiety, memory and motor function. *Behavioural Pharmacology* **2012,** 23, 790-801.

112. Fischer, B. D.; Licata, S. C.; Edwankar, R. V.; Wang, Z.-j.; Huang, S.; He, X.; Yu, J.; Zhou, H.; Jr., E. M. J.; Cook, J. M.; Furtmuller, R.; Ramerstorfer, J.; Sieghart, W.; Roth, B. L.; Majumder, S.; Rowlett, J. K. Anxiolytic-like effects of 8-acetylene imidazobenzodiazepines in a rhesus monkey conflict procedure. *Neuropharmacology* **2010,** 59, 612 - 618.

113. Savic, M. M.; Majumder, S.; Huang, S.; Edwankar, R. V.; Furtmuller, R.; Joksimovic, S.; Clayton Sr., T.; Ramerstorfer, J.; Milinkovic, M. M.; Roth, B. L.; Sieghart, W.; Cook, J. M. Novel positive allosteric modulators of GABAA receptors: do subtle differences in activity at a1 plus a5 versus a2 plus a3 subunits account for dissimilarities in behavioral effects in rats? *Prog. Neuro-Pyschopharmacology and Biol Psychiatry* **2010,** 2010, 376 - 386.

114. Haefely, W.; Kyburz, E.; Gerecke, M.; Mohler, H. Recent advances in the molecular pharmacology of benzodiazepine receptors and in the structure-activity relationships of their agonists and antagonists. In *Advances in Drug Research*, Testa, B., Ed. Academic Press: New York, 1985; pp 165 - 322.

115. Rivas, F.; Stables, J. P.; Murphree, L.; Edwankar, R. V.; Edwankar, C. R.; Huang, S.; Jain, K. D.; Zhou, H.; Majumder, S.; Sankar, S.; Roth, B. L.; Ramerstorfer, J.; Furtmuller, R.; Sieghart,

W.; Cook, J. M. Antiseizure activity of novel g-aminobutyric acid (A) receptor subtype-selective benzodiazepine analogues in mice and rat models. *J. Med. Chem* **2009,** 52, 1795 - 1798.

116. Edwankar, R. Ph.D. Thesis, I. Hz166, A Novel g-Aminobutyric Acid (A) Receptor Subtype Selective Ligand Active Against Neuropathic Pain; II. The First Enantiospecific, Stereospecific Total Synthesis Of The C-19 Methyl Substituted Sarpagine Indole Alkaloids 19(S),20(R)-Dihydroperaksine, 19(S),20-(R)-Dihydroperaksine-17-Al And Peraksine; III. Application Of Metal-Carbenoid Chemistry And Brönsted Acid Mediated Cyclization Of Enaminones For The Rapid And Efficient Access To The Tetracyclic (Abce) Skeleton Of The Strychnos Alkaloids Contained In Bisindole Alkaloids. University of Wisconsin-Milwaukee, 2010.
117. Namjoshi, O. A.; Wang, Z.-j.; Rallapalli, S. K.; Jr., E. M. J.; Johnson, Y.-T.; Ng, H.; Ramerstorfer, J.; Varagic, Z.; Sieghart, W.; Majumder, S.; Roth, B. L.; Rowlett, J. K.; Cook, J. M. Search for a3b$_{2/3}$g2 subtype selective ligands that are stable on human liver microsomes. *Bioorg. Med. Chem.* **2013,** 21, 93 - 101.
118. Yang, J.; Teng, Y.; Ara, S.; Rallapalli, S.; Cook, J. M. An improved process for the synthesis of 4*H*-imidazo[1,5*a*][1,4]benzodiazepines. *Synthesis* **2009,** 40.
119. Sharma, R.; Strelevitz, T. J.; Gao, H.; Clark, A. J.; Schildknegt, K.; Obach, R. S.; Ripp, S. L.; Spracklin, D. K.; Tremaine, L. M.; Vaz, A. D. N. Deuterium isotope effects on drug pharmacokinetics. I. System-dependent effects of specific deuteration with aldehyde oxidase cleared drugs. *Drug Metab. Desposition* **2012,** 40, 625 - 634.
120. Scheiner, S.; Martin, C. Relative stability of hydrogen and deuterium bonds. *J. Am. Chem. Soc.* **1996,** 118, 1511 - 1521.

121. Rallapalli, S. Ph.D. Theis, Part I. The First Enantiospecific, Stereospecific Total Synthesis of the Indole Alkaloid Ervincidine. Part II. The Synthesis of Alpha 5 Subtype Selective Ligands for GABA(A)/Benzodiazepine Receptors. University of Wisconsin-Milwaukee, 2012.

122. Geller, I.; Seifter, J. The effects of meprobamate, barbiturate, damphetamine and promazine on experimentally-induced conflict in the rat. *Psychopharmacologia* **1960,** 1, 482 - 492.

123. Cook, L.; Davidson, A. B. Effects of behaviorally active drugs in a conflict-punishment procedure in rats. In *The Benzodiazepines,* Garattini, S.; Mussini, E.; Randall, L. O., Eds. Raven Press: New York, 1973; pp 327 - 345.

124. Rowlett, J. K.; Lelas, S.; Tornatzky, W.; Licata, S. C. Anti-conflict effects of benzodiazepines in rhesus monkeys: relationship with therapeutic doses in humans and role of GABAA receptors. *Psychopharmacol. (Berl.)* **2006,** 184, 201 - 211.

125. Theodore, L. J.; Nelson, W. L. Stereospecific synthesis of the enantiomers of verapamil and gallopamil. *J. Org. Chem.* **1987,** 52, 1309 - 1315.

126. Ndibwami, A.; Deslongchamps, P. Study on the enolization of alkylation of *cis* and *trans* 2-*tert*-5-X-1,3-dioxanes (X = CO_2CH_3, CHO, COPh, NO_2, and CN). Evidence for stereoelectronic control. *Can. J. Chem.* **1986,** 9, 1788 - 1794.

127. Auta, J.; Impagnatiello, F.; Kadriu, B.; Guidotti, A.; Costa, E. Imidazenil: A low efficacy agonist at a1- but high efficacy at a5-$GABA_A$ receptors fail to show anticonvulsant cross tolerance to diazepam or zolpidem. *Neuropharmacology* **2008,** 55, 148 - 153.

128. Auta, J.; Kadriu, B.; Giusti, P.; Costa, E.; Guidotti, A. Anticonvulsant, anxiolytic, and non-sedating actions of imidazenil and other imidazo-benzodiazepine carboxamide derivatives. *Pharmacol. Biochem. Behav.* **2010,** 95, 383 - 389.

129. Auta, J.; Costa, E.; Davi, s. J. M.; Guidotti, A. Imidazenil: An antagonist of the sedative but not the anticonvulsant action of diazepam. *Neuropharmacology* **2005,** 49, 425 - 429.

130. Bundesmann, M. W.; Coffey, S. B.; Wright, S. W. Amidation of esters assisted by $Mg(OCH_3)_2$ or $CaCl_2$. *Tett. Letters* **2010,** 51, 3879 - 3882.

131. Cava, M. P.; Levinson, M. I. Thionation reactions of Lawesson's reagents. *Tetrahedron* **1985,** 41, 5061 - 5087.

132. Curphey, T. J. Thionation with the reagent combination of phosphorus pentasulfide and hexamethyldisiloxane. *J. Org. Chem.* **2002,** 67, 6461 - 6473.

133. Jesberger, M.; Davis, T. P.; Barner, L. Applications of Lawesson's reagent in organic and organometallic syntheses. *Synthesis* **2003,** 13, 1929 - 1958.

134. Cherkasov, R. A.; Kutyrev, G. A.; Pudovik, A. N. Organothiophosphorus reagents in organic synthesis. *Tetrahedron* **1985,** 41, 2567 - 2624.

135. Kaleta, Z.; Makowski, B. T.; Soos, T.; Dembinski, R. Thionation using fluorous Lawesson's reagent. *Org. Letters* **2006,** 8, 1625 - 1628.

136. Varma, R.; Kumar, D. Microwave-accelerated solvent-free synthesis of thioketones, thiolactones, thioamides, thionoesters, and thioflavonoids. *Org. Letters* **1999,** 1, 697 - 700.

137. Pathak, U.; Pandey, L. K.; Tank, R. Expeditious microwave-assisted thionation with the system $PSCl_3/H_2O/Et_3N$ under solvent-free condition. *J. Org. Chem.* **2008,** 73, 2890 - 2893.

138. Langmuir, I. Isomorphism, isosterism and covalence. *J. Am. Chem. Soc.* **1919,** 41, 1543 - 1559.

139. Burger, A. Isosterism and bioisosterism in drug design. *Prog. Drug Res.* **1991,** 37, 287 - 371.

140. Patani, G. A.; LaVoie, E. J. Bioisosterism: A rational approach in drug design. *Chem. Rev.* **1996,** 96, 3147 - 3176.

141. Bostrom, J.; Hogner, A.; Llinas, A.; Wellner, E.; Plowright, A. T. Oxadiazoles in medicinal chemistry. *J. Med. Chem* **2012,** 55, 1817 - 1830.

142. Yang, X.; Liu, G.; Li, H.; Zhang, Y.; Song, D.; Li, C.; Wang, R.; Liu, B.; Liang, W.; Jing, Y.; Zhao, G. Novel oxadiazole analogues derived from ethacrynic acid: Design, synthesis, and structure-activity relationships in inhibiting the activity of glutathione *S*-transferase P1-1 and cancer cell proliferation. *J. Med. Chem* **2010,** 53, 1015 - 1022.

143. Huang, S. Ph.D. Thesis, Synthesis of Optically Active Subtype Selective Benzodiazepine Receptor Ligands. University of Wisconsin-Milwaukee, 2007.

144. Bach, P.; Bostrom, J.; Brickmann, K.; Burgess, L. E.; Clarke, D.; Groneberg, R. D.; Harvey, D. M.; Laird, E. R.; O'Sullivan, M.; Zetterberg, F. 5-Alkyl-1,3-oxazole derivatives of 6-amino-nicotinic acids as alkyl ester bioisosteres are antagonists of the $P2Y_{12}$ receptor. *Future Med. Chem.* **2013,** 5, 2037 - 2056.

145. Bull, J. A.; Balskus, E. P.; Horan, A. J.; Langner, M.; Ley, S. V. Total synthesis of potent antifungal marine bisoxazole natural products Bengazoles A and B. *Chem. Eur. J.* **2007,** 13, 5515 - 5538.

146. Webb, M. R.; Donald, C.; Taylor, R. J. K. A general route to the *Streptomyces*-derived inthomycin family: the first synthesis of (+)-inthomycin B. *Tett. Letters* **2006,** 47, 549 - 552.

147. Cook, J. M.; Poe, M. M.; Methuku, K. R.; Li, G. GABAergic ligands to treat CNS disorders including anxiety and depression as well as neuropathic pain. March 18, 2016, 2016.

148. Broekkamp, C. L.; Rijk, H. W.; Joly-Gelouin, D.; Lloyd, K. Major tranquillizers can be distinguished from minor tranquillizers on the basis of effects on marble burying and swim-induced grooming in mice. *Eur. J. Pharmacol.* **1986,** 126, 223 - 229.

149. Cendelin, J.; Voller, J.; Vozeh, F. Ataxic gait analysis in a mouse model of the olivocerebellar degeneration. *Behav. Brain Res.* **2010,** 210, 8 - 15.

150. Njung'e, K.; Handley, S. L. Evaluation of marble-burying behavior as a model of anxiety. *Pharmacol. Biochem. Behav.* **1991,** 38, 63 - 67.

151. Kinsey, S. G.; O'Neal, S. T.; Long, J. Z.; Cravatt, B. F.; Lichtman, A. H. Inhibition of endocannabinoid catabolic enzymes elicits anxiolytic-like effects in the marble burying assay. *Pharmacol. Biochem. Behav.* **2011,** 98, 21 - 27.

152. Li, X.; Morrow, D.; Witkin, J. M. Decreases in nestlet shredding of mice by serotonin uptake inhibitors: Comparison with marble burying. *Life Sci.* **2006,** 78, 1933 - 1939.

153. Browne, T. R. Clonazepam. A review of a new anticonvulsant drug. *Arch. Neurol.* **1976,** 33, 326 - 323.

154. Gaudreault, P.; Guay, J.; Thivierge, R. L.; Verdy, I. Benzodiazepine poisoning. Clinical and pharmacological considerations and treatment. *Drug Safety* **1991,** 6, 247 - 265.

155. Kondziela, W. Eine neue method zur messung der muskularen relaxation bei weissen mausen. *Arch. Int. Pharmacodyn.* **1964,** 152, 277 - 284.

156. Liljequist, R.; Palva, E.; Linnoila, M. Effects on learning and memory of 2-week treatments with chlordiazepoxide lactam, N-desmethyldiazepam, oxaezpam and methyloxazepam, alone or in combination with alcohol. *Int. Pharmacopsychiatry* **1979,** 14, 190 - 198.

157. Riss, J.; Cloyd, J.; Gates, J.; Collins, S. Benzodiazepines in epilepsy: pharmacology and pharmacokinetics. *Acta Neurol. Scand.* **2008,** 118, 69 - 86.

158. Rundfeldt, C.; Wlaz, P.; Honack, D.; Loscher, W. Anticonvulsant tolerance and withdrawal characteristics of benzodiazepine receptor ligands in different seizure models in mice.

Comparison of diazepam, bretazenil and abecarnil. *J. Pharmacol. Exp. Ther.* **1995,** 275, 693 - 702.

159. White, S. H.; Woodhead, J. H.; Wilcox, K. S.; Stables, J. P.; Kupferberg, H. J.; Wolf, H. H. Discovery and Preclinical Development of Antiepileptic Drugs. In *Antiepileptic Drugs*, 5th ed.; Levy, R. H.; Mattson, R. H.; Meldrum, B. S.; Perucca, E., Eds. Lippincott Williams and Wilkins: Philadelphia, PA, 2002; pp 36 - 48.
160. Castel-Branco, M. M.; Alves, G. L.; Figueiredo, I. V.; Falcao, A. C.; Caramona, M. M. The maximal electroshock seizure (MES) model in the preclinical assessment of potential new antiepileptic drugs. *Methods Find. Exp. Clin. Pharmacol.* **2009,** 31, 101 - 106.
161. Knabl, J.; Zeilhofer, U. B.; Crestani, F.; Rudolph, U.; Zeilhofer, H. U. Genuine antihyperalgesia by systemic diazepam revealed by experiments in $GABA_A$ receptor point-mutated mice. *Pain* **2009,** 141, 233 - 238.
162. Paul, J.; Yevenes, G. E.; Benke, D.; Lio, A. D.; Ralvenius, W. T.; Witschi, R.; Scheurer, L.; Cook, J. M.; Rudolph, U.; Fritschy, J.-M.; Zeilhofer, H. U. Antihyperalgesia by a2-$GABA_A$ receptors occurs via a genuine spinal action and does not involve supraspinal sites. *Neuropsychopharm.* **2014,** 39, 477 - 487.
163. Chung, J. M.; Kim, H. K.; Chung, K. Segmental spinal nerve ligation model of neuropathic pain. *Methods Mol. Med.* **2004,** 99, 35 - 45.
164. Huang, X. P.; Mangano, T.; Hufeisen, S.; Setola, V.; Roth, B. L. Identification of human Ether-a-go-go related gene modulators by three screening platforms in an academic drug-discovery setting. *Assay Drug Dev. Technol.* **2010,** 8, 727 - 742.
165. Sanguinetti, M. C.; Tristani-Firouzi, M. hERG potassium channels and cardiac arrhythmia. *Nature* **2006,** 440, 463 - 469.

166. Gould, H. J. Complete Freund's adjuvant-induced hyperalgesia: a human perception. *Pain* **2000,** 85, 301 - 303.

167. Amsterdam, J. D.; Hornig-Rohan, M.; Maislin, G. Efficacy of alprazolam in reducing fluoxetine-induced jitteriness in patients with major depression. *J. Clin. Psychiatry* **1994,** 55, 394 - 400.

168. Petty, F.; Trivedi, M. H.; Fulton, M.; Rush, A. J. Benzodiazepines as antidepressants: does GABA play a role in depression? *Biol. Psychiatry* **1995,** 38, 578 - 591.

169. Vollenweider, I.; Smith, K. S.; Keist, R.; Rudolph, U. Antidepressant-like properties of a2-containing $GABA_A$ receptors. *Behav. Brain Res.* **2011,** 217, 77 - 80.

170. Rudolph, U.; Knoflach, F. Beyond classical benzodiazepines: novel therapeutic potential of $GABA_A$ receptor subtypes. *Nature Reviews* **2011,** 10, 685 - 697.

171. Berton, O.; Nestler, E. J. New approaches to antidepressant drug discovery beyond monoamines. *Nat. Rev. Neurosci.* **2006,** 7, 137 - 151.

172. El Hadri, A.; Abouabdellah, A.; Thomet, U.; Baur, R.; Furtmuller, R.; Sigel, E.; Sieghart, W.; Dodd, R. H. N-substituted 4-amino-3,3-dipropyl-2(3*H*)-furanones: New positive allosteric modulators of the $GABA_A$ receptor sharing electrophysiological properties with the anticonvulsant Loreclezole. *J. Med. Chem* **2002,** 45, 2824 - 2831.

173. Li, X.; Cao, H.; Zhang, C.; Furtmuller, R.; Fuchs, K.; Huck, S.; Sieghart, W.; Deschamps, J.; Cook, J. M. 6,7-Dihydro-2-benzothiophen-4(5*H*)-ones: A novel class of GABA-A a5 receptor inverse agonists. *J. Med. Chem* **2003,** 46, 5567 - 5570.

174. Sieghart, W. Pharmacology of benzodiazepine receptors: an update. *J. Psychiatry Neurosci* **1994,** 19, 24 - 29.

175. Schreibmayer, W.; Lester, H. A.; Dascal, N. Voltage clamping of *Xenopus laevis* oocytes utilizing agarose-cushion electrodes. *Pflugers Arch-Eur. J. Physiol.* **1994,** 426, 453 - 458.

176. Fuchs, K.; Zezula, J.; Slany, A.; Sieghart, W. Endogenous [3H]flunitrazepam binding in human embryonic kidney cell line 293. *Eur. J. Pharmacol.* **1995,** 289, 87 - 95.

177. Sigel, E. Properties of single sodium channels translated by *Xenopus* oocytes after injection with messenger ribonucleic acid. *J. Physiol.* **1987,** 386, 73 - 90.

178. Sigel, E.; Baur, R.; Trube, G.; Mohler, H.; Malherbe, P. The effect of subunit composition of rat brain GABAA receptors on channel function. *Neuron* **1990,** 5, 703 - 711.

179. Huang, Z.; Li, G.; Pei, W.; Sosa, L. A.; Niu, L. Enhancing protein expression in single HEK 293 cells. *J. Neurosci. Methods* **2005,** 142, 159 - 166.

180. Liu, J.; Chen, T.; Norris, T.; Knappenberger, K.; Huston, J.; Wood, M.; Bostwick, R. A high-throughput functional assay for characterization of g-aminobutyric acid A channel modulators. *Assay Drug Dev. Technol.* **2008,** 6, 781 - 786.

181. Joesch, C.; Guevarra, E.; Parel, S. P.; Bergner, A.; Zbinden, P.; Konrad, D.; Albrecht, H. Use of FLIPR membrane potential dyes for validation of high-throughput screening with the FLIPR and microARCS technologies: identification of ion channel modulators acting on the GABA(A) receptor. *J. Biomol. Screen.* **2008,** 13, 218 - 228.

182. Alt, A.; Weiss, B.; Ornstein, P. L.; Gleason, S. D.; Bleakman, D.; Stratford Jr., R. E.; Witkin, J. M. Anxiolytic-like effects through a GLU_{K5} kainate receptor mechanism. *Neuropharmacology* **2007,** 52, 1482 - 1487.

183. Wirth, C.; Luscher, H. R. Spatiotemporal evolution of excitation and inhibition in the rat barrel cortex investigated with multielectrode arrays. *J. Neurophysiol.* **2004,** 91, 1635 - 1647.

184. Schiff, S. J.; Jerger, K.; Duong, D. H.; Chang, T.; Spano, M. L.; Ditto, W. L. Controlling chaos in the brain. *Nature* **1994,** 370, 615 - 620.

185. Wu, Y.; Guan, L.; Tsau, Y. Propagating activation during oscillations and evoked responses in neocortical slices. *J. Neurosci.* **1999,** 19, 5005 - 5015.

186. Hobbs, J. P.; Smith, J. L.; Beggs, J. M. Aberrant neuronal avalanches in cortical tissue removed from juvenile epilepsy patients. *J. Clin. Neurophysiol.* **2010,** 27, 380 - 386.

187. Tang, A.; Jackson, D.; Hobbs, J. P.; Chen, W.; Smith, J. L.; Patel, H.; Prieto, A.; Petrusca, D.; Grivich, M. I.; Sher, A.; Hottowy, P.; Dabrowski, W.; Litke, A. M.; Beggs, J. M. A maximum entropy model applied to spatial and temporal correlations from cortical networks *in vitro*. *J. Neurosci.* **2008,** 28, 505 - 518.

188. Beggs, J. M.; Plenz, D. Neuronal avalanches in enocortical circuits. *J. Neurosci.* **2003,** 23, 11167 - 11177.

189. Beggs, J. M.; Plenz, D. Neuronal avalanches are diverse and precise activity patterns that are stable for many hours in cortical slice cultures. *J. Neurosci.* **2004,** 24, 5216 - 5229.

190. Porsolt, R. D.; Bertin, A.; Jalfre, M. Behavioral despair in mice: a primary screening test for antidepressants. *Arch. Int. Pharmacodyn. Ther.* **1977,** 229, 327 - 336.

191. Gill, K. M.; Grace, A. A. The role of a5 $GABA_A$ receptor agonists in the treatment of cognitive deficits in schizophrenia. *Curr. Pharm. Des.* **2014,** 20, 5069 - 5076.

192. Soh, M. S.; Lynch, J. W. Selective modulators of a5-containing $GABA_A$ receptors and their therapeutic significance. *Current Drug Targets* **2015,** 16, 735 - 746.

193. Martinez-Cue, C.; Martinez, P.; Rueda, N.; Vidal, R.; Garcia, S.; Vidal, V.; Corrales, A.; Montero, J. A.; Pazos, A.; Florez, J.; Gasse, R.; Thomas, A. W.; Honer, M.; Knoflach, F.; Trejo, J. L.; Wettstein, J. G.; Hernandez, M. C. Reducing $GABA_A$ a5 receptor-mediated

inhibition rescues functional and neuromorphological deficits in a mouse model of down syndrome. *J. Neurosci.* **2013,** 33, 3953 - 3966.

194. Benes, F. M. A new paradigm for understanding gamma-aminobutyric acid cell pathology in schizophrenia? *Biol. Psychiatry* **2012,** 72, 712 - 713.

195. Benes, F. M.; Lim, B.; Matzilevich, D.; Walsh, J. P.; Subburaju, S.; Minns, M. Regulations of the GABA cell phenotype in hippocampus of schizophrenics and bipolars. *Proc. Natl. Acad. Sci.* **2007,** 104, 10164 - 10169.

196. Gill, K. M.; Cook, J. M.; Poe, M. M.; Grace, A. A. Prior Antipsychotic Drug Treatment Prevents Response to Novel Antipsychotic Agent in the Methylazoxymethanol Acetate Model of Schizophrenia. *Schizophrenia Bulletin* **2014,** 40, 341-350.

197. Gill, K. M.; Lodge, D. J.; Cook, J. M.; Aras, S.; Grace, A. A. A Novel a5$GABA_AR$-Positive Allosteric Modulator Reverses Hyperactivation of the Dopamine System in the MAM Model of Schizophrenia. *Neuropsychopharm.* **2011,** 36, 1903-1911.

198. Lodge, D. J.; Grace, A. A. Hippocampal dysfunction and disruption of dopamine system regulation in an animal model of schizophrenia. *Neurotox Rex.* **2008,** 14, 97 - 104.

199. Papadimitriou, G. N.; Dikeos, D. G.; Karadima, G.; Avramopoulos, D.; Daskalopoulou, E. G.; Vassilopoulos, D.; Stefanis, C. N. Association between the $GABA_A$ receptor a5 subunit gene locus ($GABRA_5$) and bipolar affective disorder. *AM. J. Med. Gen. (Neuropsychiatric Genetics)* **1998,** 81, 73 - 80.

200. McGrath, J.; Saha, S.; Welham, J.; El Saadi, O.; MacCauley, C.; Chant, D. A systematic review of the incidence of schizophrenia: the distribution of rates and the influence of sex, urbanicity, migrant status and methodology. *BMC Medicine* **2004,** 2.

201. Stilo, S. A.; Murray, R. M. The epidemiology of schizophrenia: replacing dogma with knowledge. *Dialogues Clin. Neurosci.* **2010,** 12, 305 - 315.

202. Perez, S. M.; Lodge, D. J. New approaches to the management of schizophrenia: focus on aberrant hippocampal drive of dopamine pathways. *Drug Des. Dev. Therapy* **2014,** 8, 887 - 896.

203. Lieberman, J. A.; Stroup, T. S.; McEvoy, J. P.; Swartz, M. S.; Rosenheck, R. A.; Perkins, D. O.; Keefe, R. S. E.; Davis, S. M.; Davis, C. E.; Lebowitz, B. D.; Severe, J.; Hsiao, J. K. Effectiveness of antipsychotic drugs in patients with chronic schizophrenia. *N. Engl. J. Med.* **2005,** 353, 1209 - 1223.

204. Miyamoto, S.; Duncan, G. E.; Marx, C. E.; Lieberman, J. A. Treatments for schizophrenia: a critical review of pharmacology and mechnisms of action of antipsycotic drugs. *Mol. Psychiatry* **2005,** 10, 79 - 104.

205. Hattori, K.; Uchino, S.; Isosaka, T.; Maekawa, M.; Iyo, M.; Soato, T.; Kohsaka, S.; Yagi, T.; Yuasa, S. Fyn is required for haloperidol-induced catalepsy in mice. *J. Biol. Chem.* **2006,** 281, 7129 - 7135.

206. Abi-Dargham, A.; Laruelle, M. Mechanisms of action of second generation antipsychotic drugs in schizophrenia: insights from brain imaging studies. *Eur. Psychiatry* **2005,** 20, 15 - 27.

207. Leucht, S.; Pitschel-Walz, G.; Abraham, D.; Kissling, W. Efficacy and extrapyramidal side-effects of the new antipsychotics olanzapine, quitiapine, risperidone, and sertindole compared to conventional antipsychotics and placebo. A meta-analysis of randomized controlled trials. *Schizophrenia Res.* **1999,** 35, 51 - 68.

208. Geddes, J.; Freemantle, N.; Harrison, P.; Bebbington, P. Atypical antipsychotics in the treatment of schizophrenia: systematic overview and meta-regression analysis. *Br. Med. Journal* **2000,** 321, 1371 - 1376.

209. Komossa, K.; Rummel-Kluge, C.; Hunger, H.; Schmid, F.; Schwarz, S.; Duggan, L.; Kissling, W.; Leucht, S. Olanzapine versus other atypical antipsychotics for schizophrenia. *Cochrane Database Syst. Rev.* **2010,** 3.

210. Pincus, H. A.; Tew Jr., J. D.; First, M. B. Psychiatric comorbidity: is more less? *World Psychiatry* **2004,** 3, 18 - 23.

211. Green, A. I.; Canuso, C. M.; Brenner, M. J.; Wijcik, J. D. Detection and management of comorbidity in schizophrenia. *Psychiatr. Clin. N. Am.* **2003,** 26, 115 - 139.

212. Buckley, P. F.; Miller, B. J.; Lehrer, D. S.; Castle, D. J. Psychiatric comorbidities and schizophrenia. *Schizophrenia Bulletin* **2009,** 35, 383 - 402.

213. Perez, M. M.; Trimble, M. R. Epileptic psychosis--diagnostic comparison with process schizophrenia. *Br. J. Psychiatry* **1980,** 137, 245 - 249.

214. Cascella, N. G.; Schretlen, D. J.; Sawa, A. Schizophrenia and epilepsy: is there a shared susceptibility. *Neurosci. Res.* **2009,** 63, 227 - 235.

215. Lewis, D. A.; Lieberman, J. A. Catching up on schizophrenia: natural history and neurobiology. *Neuron* **2000,** 28, 325 - 334.

216. De Hert, M.; McKenzie, K.; Peuskens, J. Risk factors for suicide in young people suffering from schizophrenia: a long-term follow-up study. *Schizophrenia Res.* **2001,** 47, 127 - 134.

217. Gallos, G.; Yocum, G. T.; Siviski, M. E.; Yim, P. D.; Fu, X. W.; Poe, M. M.; Cook, J. M.; Harrison, N.; Perez-Zoghbi, J.; Emala, C. W. Selective targeting of the a5-subunit of $GABA_A$

receptors relaxes airway smooth muscle and inhibits cellular calcium handling. *Am J Physiol Lung Cell Mol Physiol* **2015,** 308, L931 - L942.

218. Pascual, R. M.; Peters, S. P. Airway remodeling contributes to the progressive loss of lung function in asthma: an overview. *J. Allergy and Clinical Immunology* **2005,** 116, 477 - 486.

219. Rachelefsky, G. Inhaled corticosteroids and asthma control in children: assessing impairment and risk. *Pediatrics* **2009,** 123, 353 - 366.

220. Li, X.; Cao, H.; Zhang, C.; Furtmuller, R.; Fuchs, K.; Huck, S.; Sieghart, W.; Deschamps, J.; Cook, J. M. Synthesis, in Vitro Affinity, and Efficacy of a Bis 8-Ethynyl-4*H*-imidazo[1,5*a*]-[1,4]benzodiazepine Analogue, the First Bivalent a5 Subtype Selective BzR/$GABA_A$ Antagonist. *J. Med. Chem* **2003,** 46, 5567-5570.

221. Bailey, D. J.; Tetzlaff, J. E.; Cook, J. M.; He, X.; Helmstetter, F. J. Effects of hippocampal injections of novel ligands selective for the a5b2g2 subunits of the GABA/benzodiazepine receptor on Pavlovian conditioning. *Neurobiol. Learn. Mem.* **2002,** 78, 1 - 10.

222. Atack, J. R.; Alder, L.; Cook, S. M.; Smith, A. J.; McKernan, R. M. *In vivo* labelling of a5 subunit-containing $GABA_A$ receptors using the selecetive radioligand [^{3}H]L-655,708. *Neuropharmacology* **2005,** 49, 220 - 229.

223. Li, X. Ph.D. Thesis, Synthesis of Selective Ligands for $GABA_A$/Benzodiazepine Receptors. University of Wisonsin-Milwaukee, Milwaukee, WI, 2004.

224. Abadi, A. H.; Lankow, S.; Hoefgen, B.; Decker, M.; Kassack, M. U.; Lehman, J. Dopamine/serotonin receptor ligands, part III: synthesis and biological activities of 7,7'-alkylene-bis-6,7,8,9,14,15-hexahydro-5H-benz[d]indolo[2,3g]azecines- application of the bivalent ligand approach to a novel type of dopamine receptor antagonist. *Archiv. der Pharmazie* **2002,** 355, 367 - 373.

225. Han, D. M.; Forsterling, F. H.; Li, X.; Deschamps, J. R.; Parrish, D.; Cao, H.; Rallapalli, S.; Clayton, T.; Teng, Y.; Majumder, S.; Sankar, S.; Roth, B. L.; Sieghart, W.; Furtmuller, R.; Rowlett, J. K.; Weed, M. R.; Cook, J. M. A study of the structure-activity relationship of $GABA_A$-benzodiazepine receptor bivalent ligands by conformational analysis with low temperature NMR and X-ray analysis. *Bioorg. Med. Chem.* **2008,** 16, 8853 - 8862.

226. Liu, R. Y.; Hu, R. J.; Zhang, P. W.; Skolnick, P.; Cook, J. M. Synthesis and pharmacological properties of novel 8-substituted imidazobenzodiazepines: high-affinity, selective porbes for a5-containing $GABA_A$ receptors. *J. Med. Chem* **1996,** 39, 1928 - 1934.

227. Savic, M. M.; Clayton, T.; Furtmuller, R.; Gavrilovic, I.; Samardzic, J.; Savic, S.; Huck, S.; Sieghart, W.; Cook, J. M. PWZ-029, a compound with moderate inverse agonist functional selectivity at $GABA_A$ receptors containing a5 subunits, improves passive, but not active, avoidance learning in rats. *Brain Research* **2008,** 1208, 150-159.

228. Milic, M.; Timic, T.; Joksimovic, S.; Biawat, P.; Rallapalli, S.; Divljakovic, J.; Radulovic, T.; Cook, J. M.; Savic, M. M. Pwz-029, an inverse agonist selective for a5 $GABA_A$ receptors, improves object recognition, but not water-maze memory in normal and scopolamine-treated rats. *Behav. Brain Res.* **2012,** 241, 206-213.

229. Rowlett, J. K.; Moran, C. A.; Clayton, T.; Rallapalli, S.; Roth, B. L.; Cook, J. M. In *PWZ-029, an inverse agonist selective for a5 subunit containing GABA(A) receptors, enhances performance on an executive function task in monkeys*, European Behavioral Pharmacology Society, Rome, Italy, 2009; Rome, Italy, 2009.

230. Savic, M. M.; Huang, S.; Furtmuller, R.; Clayton, T.; Huck, S.; Obradovic, D. I.; Ugresic, N. D.; Sieghart, W.; Bokonjic, D. R.; Cook, J. M. Are $GABA_A$ receptors containing a5 subunits

contributing to the sedative properties of benzodiazepine site agonists? *Neuropharmacology* **2008,** 33, 332 - 339.

231. Porsolt, R. D.; McArthur, R. A.; Lenegre, A. Psychotropic Screening Procedures. In *Methods in Behavioral Pharmacol.*, Haaren, V., Ed. Elsevier: Amsterdam, Netherlands, 1993; pp 23 - 51.

232. Nguyen, L. A.; He, H.; Pham-Huy, C. Chiral drugs: an overview. *Int. J. Biomed. Sci.* **2006,** 2, 85 - 100.

233. Mellin, G. W.; Katzenstein, M. The saga of thalidomide: neuropathy to embryopathy, with case reports and congenital abnormalities. *N. Engl. J. Med.* **1962,** 267, 1184 - 1193.

234. Landoni, M. F.; Soraci, A. Pharmacology of chiral compounds: 2-arylpropionic acid derivatives. *Current Drug Metabolism* **2001,** 2, 37 - 51.

235. Drayer, D. E. Pharmacodynamic and pharmacokinetic differences between drug enantiomers in humans: an overview. *Clin. Pharmacol. Therapeutics* **1986,** 40, 125 - 133.

236. Patocka, J.; Dvorak, A. Biomedical aspects of chiral molecules. *J. Applied Medicine* **2004,** 2, 95 - 100.

237. Izake, E. L. Chiral discrimination and enantioselective analysis of drugs: an overview. *J. Pharmaceutical Sci.* **2007,** 96, 1659 - 1676.

238. Ferguson, C. S.; Tyndale, R. F. Cytochrome P450 enzymes in the brain: emerging evidence for biological significance. *Trends Pharmacol. Sci.* **2011,** 32, 708 - 714.

239. Hedlund, E.; Gustafsson, J. A.; Warner, M. Cytochrome P450 in the brain; a review. *Curr. Drug Metab.* **2001,** 2, 245 - 263.

240. Schinkel, A. H. P-glycoprotein, a gatekeeper in the blood-brain barrier. *Adv. Drug Deliv. Rev.* **1999,** 36, 179 - 194.

241. Richetto, J.; Labouesse, M. A.; Poe, M. M.; Cook, J. M.; Grace, A. A.; Riva, M. A.; Meyer, U. Behavioral effects of the benzodiazepine-positive allosteric modulator SH-053-2'F-S-CH_3 in an immune-mediated neurodevolpmental disruption model. *Int. J. Neuropsychopharmacol* **2015,** 18, 1 - 11.

242. Meyer, U. Prenatal poly(I:C) exposure and other devlopmental immune activation models in rodent systems. *Biol. Psychiatry* **2014,** 75, 307 - 315.

243. Meyer, U.; Feldon, J. Epidemiology-driven neurodevelopmental animal models in schizophrenia. *Prog. Neurobiol.* **2010,** 90, 285 - 326.

244. Brown, A. S.; Derkitis, E. J. Prenatal infection and schizophrenia: a review of epidemiologic and translational studies. *Am. J. Psychiatry* **2010,** 167, 261 - 280.

245. Soto, P. L.; Ator, N. A.; Rallapalli, S. K.; Biawat, P.; Clayton, T.; Cook, J. M.; Weed, M. R. Allosteric modulation of $GABA_A$ receptor subtypes: effects on visual recognition and visuospatial working memory in rhesus monkeys. *Neuropsychopharm.* **2013,** 38, 2315 - 2325.

246. Lodge, D. J.; Grace, A. A. Aberrant hippocampal activity underlies the dopamine dysregulation in an animal model of schizophrenia. *J. Neurosci.* **2007,** 27, 11424 - 11430.

247. Moore, H.; Jentsch, J. D.; Ghajarnia, M.; Geyer, M. A.; Grace, A. A. A neurobehavioral systems analysis of adult rats exposed to methylazoxymethanol acetate on E17: implications for the neuropathology of schizophrenia. *Biol. Psychiatry* **2006,** 60, 253 - 264.

248. Cattabeni, F.; Di Luca, M. Developmental models of brain dysfunctions induced by targeted cellular ablations with methylazooxymethanol. *Physiol Rev.* **1997,** 77, 199 - 215.

249. Bakshi, V. P.; Geyer, M. A. Antagonism of phencyclidine-induced deficits in prepulse inhibition by the putative atypical antipsychotic olanzapine. *Psychopharmacol.* **1995,** 122, 198 - 201.

250. Geyer, M. A.; Swerdlow, N. R.; Masbach, R. S.; Braff, D. L. Startle response models of sensorimotor gating and habituation deficits in schizophrenia. *Brain Res. Bulletin* **1990,** 25, 485 - 498.

251. Swerdlow, N. R.; Braff, D. L.; Taaid, N.; Geyer, M. A. Assessing the validity of an animal model of deficient sensorimotor gating in schizophrenic patients. *Arch. Gen. Psychiatry* **1994,** 51, 139 - 154.

252. Sanberg, P. R.; Bunsey, M. D.; Giordano, M.; Norman, A. B. The catalepsy test: its ups and downs. *Behavioural Neuroscience* **1988,** 102, 748 - 759.

253. Garver, D. L. Disease of the Nervous System: Psychiatric Disorders. In *Clinical chemistry: Theory analysis and correlations*, Kaplan, L. A.; Pesce, A. J., Eds. C.V. Mosby: St. Louis, MO, 1984; pp 864 - 881.

254. Sanberg, P. R. Haloperidol-induced catalepsy is mediated by postsynaptic dopamine receptors. *Nature* **1980,** 284, 472 - 473.

255. Daniels, J. Catatonia: clinical aspects and neurobiological correlates. *J. Neuropsychiatry Clin. Neurosci.* **2009,** 21, 371 - 380.

256. Bast, T.; Zhang, W.; Feldon, J.; White, I. M. Effects of MK801 and neuroleptics on prepulse inhibition: re-examination in two strains of rats. *Pharmacol. Biochem. Behav.* **2000,** 67, 647 - 658.

257. Boulay, D.; Depoortere, R.; Oblin, A.; Sanger, D. J.; Schoemaker, H.; Perrault, G. Haloperidol-induced catalepsy is absent in dopamine D_2, but maintained in dopamine D_3 receptor knock-out mice. *Eur. J. Pharmacol.* **2000,** 391, 63 - 73.

258. Garbutt, J. C.; van Kammen, D. P. The interaction between GABA and dopamine: implications for schizophrenia. *Schizophrenia Bulletin* **1983,** 9, 336 - 356.

259. Behlke, L. M.; Foster, R. A.; Liu, J.; Benke, D.; Benham, R. S.; Nathanson, A.; Yee, B. K.; Zeilhofer, H. U.; Engin, E.; Rudolph, U. A pharmaco-genetic 'restriction-of-function' approach reveals evidence for anxiolytic-like actions mediated by a5-containing $GABA_A$ receptors in mice. *Neuropsychopharm.* **2016**.

260. D'Hooge, R.; De Deyn, P. P. Applications of the Morris water maze in the study of learning and memory. *Brain Res. Rev.* **2001,** 36, 60 - 90.

261. Wongwitdecha, N.; Marsden, C. A. Effects of social isolation rearing on learning in the Morris water maze. *Brain Research* **1996,** 715, 119 - 124.

262. Sharma, S.; Rakoczy, S.; Brown-Borg, H. Assessment of sptial memory in mice. *Life Sci.* **2010,** 87, 521 - 536.

263. Terranova, J.-P.; Chabot, C.; Barnouin, M.-C.; Perrault, G.; Depoortere, R.; Griebel, G.; Scatton, B. SSR181507, a dopamine D(2) receptor antagonist and 5-HT(1A) receptor agonist, alleviates disturbances of novelty discrimination in a social context in rats, a putative model of selective attention deficit. *Psychopharmacol.* **2005,** 181, 134 - 144.

264. Craddock, N.; Owen, M. J. The Kraepelinian dichotomy - going, going... but still not gone. *Br. J. Psychiatry* **2010,** 196, 92 - 95.

265. Fung, S. J.; Fillman, S. G.; Webster, M. J.; Weickert, C. S. Schizophrenia and bipolar disorder show both common and distinct changes in cortical interneuron markers. *Schizophrenia Res.* **2014,** 155, 26 - 30.

266. Lin, L. C.; Sibille, E. Reduced brain somatostatin in mood disorders: a common pathophysiological substrate and drug target? *Front. Pharmacology* **2013,** 4, 110.

267. Lin, L. C.; Sibille, E. Somatostatin, neuronal vulnerability and behavioral emotionality. *Mol. Psychiatry* **2015,** 20, 377 - 387.

268. Seney, M. L.; Chang, L. C.; Oh, H.; Wang, X.; Tseng, G. C.; Lewis, D. A.; Sibille, E. The role of genetic sex in affect regulation and expression of GABA-related genes across species. *Front. Psychiatry* **2013,** 4, 104.

269. Gallos, G.; Gleason, N. R.; Zhang, Y.; Pak, S. W.; Sonett, J. R.; Yang, J.; Emala, C. W. Activation of endogenous $GABA_A$ channels on airway smooth muscle potentiates isoproterenol-mediated relaxation. *Am J Physiol Lung Cell Mol Physiol* **2008,** 295, L1040 - L1047.

270. Chu, E. K.; Drazen, J. M. Asthma: one hundred years of treatment and onward. *Am. J. Respir. Crit. Care Med.* **2005,** 171, 1202 - 1208.

271. Xiang, Y. Y.; Wang, S.; Liu, M.; Hirota, J. A.; Li, J.; Ju, W.; Fan, Y.; Kelly, M. M.; Ye, B.; Orser, B.; O'byrne, P. M.; Inman, M. D.; Yang, X.; Lu, W. Y. A GABAergic system in airway epithelium is essential for mucus overproduction in asthma. *Nature Medicine* **2007,** 13, 862 - 867.

272. Yocum, G. T.; Gallos, G.; Zhang, Y.; Jahan, R.; Stephen, M. R.; Varagic, Z.; Puthenkalam, R.; Ernst, M.; Cook, J. M.; Emala, C. W. Targeting the g-aminobutyric acid A receptor a4 subunit in airway smooth muscle to alleviate bronchoconstriction. *Am. J. Respir. Cell Mol. Biol* **2016,** 54, 546 - 553.

273. Fredberg, J. J.; Inouye, D. S.; Mijailovich, S. M.; Butler, J. P. Perturbed equilibrium of myosin binding in airway smooth muscle and its implications in bronchospasm. *Am. J. Respir. Crit. Care Med.* **1999,** 159, 959 - 967.

274. Doeing, D. C.; Solway, J. Airway smooth muscle in the pathophysiology and treatment of asthma. *J. Appl. Physiol.* **2013,** 114, 834 - 843.

275. Obradovic, A. L.; Joksimovic, S.; Batinic, B.; Radulovic, T.; Poe, M. M.; Namjoshi, O. A.; Cook, J. M.; Ramerstorfer, J.; Varagic, Z.; Sieghart, W.; Karovic, B.; Roth, B.; Savic, M. M. SH-I-048A, an *in vitro* nonselective super-agonist at the benzodiazepine site of $GABA_A$ receptors: the approximated activation of receptor subtypes may explain behavioral effects. *Brain Res.* **2014,** 1554, 36 - 48.

276. Ramerstorfer, J.; Furtmuller, R.; Vogel, E.; Huck, S.; Sieghart, W. The point mutation gamma 2F77I changes the potency and efficacy of benzodiazepine site ligands in different $GABA_A$ receptor subtypes. *Eur. J. Pharmacol.* **2010,** 636, 18 - 27.

277. Botta, P.; Demmou, L.; Kasugai, Y.; Markovic, M.; Xu, C.; Fadok, J. P.; Lu, T.; Poe, M. M.; Xu, L.; Cook, J. M.; Rudolph, U.; Sah, P.; Ferraguti, F.; Luthi, A. Regulating anxiety with extrasynaptic inhibition. *Nat. Neurosci.* **2015,** 18, 1493 - 1500.

278. Mercolini, L.; Mandrioli, R.; Iannello, C.; Matrisciano, F.; Nicoletti, F.; Raggi, M. A. Simultaneous analysis of diazepam and its metabolites in rat plasma and brain tissue by HPLC-UV and SPE. *Talanta* **2009,** 80, 279 - 285.

279. Dunham, M. S.; Miya, T. A. A note on a simple apparatus for detecting neurological deficit in rats and mice. *J. Amer. Pharm. Ass. Sci.* **1957,** 46, 208 - 209.

280. Swinyard, E. A.; Woodhead, J. H.; White, H. S.; Franklin, M. R. General Principles: Experimental Selection, Quantification, and Evaluation of Anticonvulsants. In *Antiepileptic Drugs*, 3rd ed.; Levy, R. H.; Mattson, R. H.; Melrum, B.; Penry, J. K.; Dreifuss, F. E., Eds. Raven Press: New York, 1989; pp 85 - 102.

281. White, H. S.; Woodhead, J. H.; Franklin, M. R. General Principles: Experimental Selection, Quantification, and Evaluation of Antiepileptic Drugs. In *Antiepileptic Drugs*, 4th ed.; Levy, R. H.; Mattson, R. H.; Meldrum, B. S., Eds. Raven Press: New York, 1995; pp 99 - 110.

282. White, H. S.; Johnson, M.; Wolf, H. H.; Kupferberg, H. J. The early identification of anticonvulsant activity: role of the maximal electroshock and subcutaneous pentylenetetrazole seizure models. *Italian Journal of Science* **1995,** 16, 73 - 77.

283. Swinyard, E. A.; Clark, L. D.; Miyahara, J. T.; Wolf, H. H. Studies on the mechanism of amphetamine toxicity in aggregated mice. *J. Physiol.* **1961,** 132, 97 - 102.

284. Vorhees, C. V.; Williams, M. T. Value of water mazes for assessing spatial and egocentric learning and memory in rodent basic research and regulatory studies. *Neurotoxicol. Teratol.* **2014,** 45, 75 - 90.

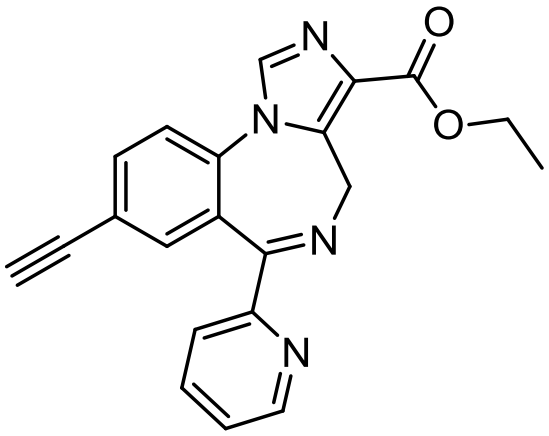
285. Savic, M. M.; Milinkovic, M. M.; Rallapalli, S.; Clayton, T.; Joksimovic, S.; Van Linn, M.; Cook, J. M. The differential role of alpha1- and alpha5-containing GABA(A) receptors in mediating diazepam effects on spontaneous locomotor activity and water-maze learning and memory in rats. *Int. J. Neuropsychopharmacol* **2009,** 12, 1179 - 1193.

286. Engelmann, M.; Wotjak, C. T.; Landgraf, R. Social discrimination procedure: an alternative method to investigate juvenile recognition abilities in rats. *Physiol. Behav.* **1995,** 58, 315 - 321.

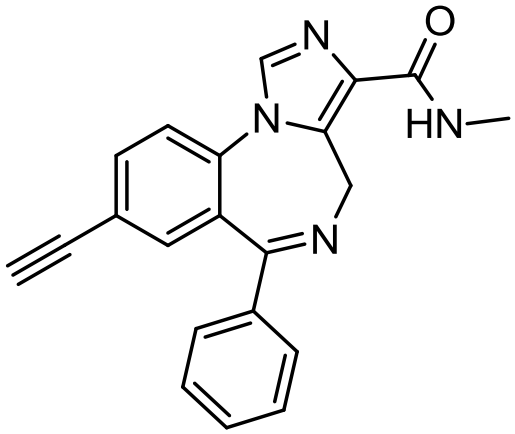
287. Edgar, N. M.; Touma, C.; Palme, R.; Sibille, E. Resilient emotionality and molecular compensation in mice lacking the oligodendrocyte-specific gene Cnp1. *Transl. Psychiatry* **2011,** 20.

APPENDIX A. Characterization of HZ-166 and YT-III-31 (CRO).

Structures:



HZ-166



YT-III-31

HZ166 Characterization

Nov 17, 2011

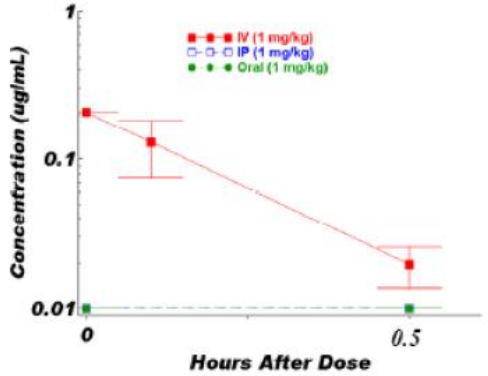
Progress-at-a-Glance

UW MTA Request (HZ166)	Progress
1. Mouse PK study: i.v., i.p, and p.o. pharmacokinetic time course @ 1 mg/kg.	Completed
2. Replicate the recent CCI (Bennett) neuropathic pain data at a couple of time points (~0.5 and 1.5 hr) @ 10,30,100 mg/kg ip, (n=12) and collect plasma and brain to quantify drug concentrations.	Rat CCI, 30 mg/KG, i.p.
3. Evaluate these compounds in the mouse Carrageenan hyperalgesia pain assay @ 10,30,100 mg/kg ip. (n=12).	Completed (new data)
4. Assess the level of CNS sedation using the exploratory locomotor activity assay @ ~30 and 100 mg/kg depending on the results of the above experiments.	Planned
5. Collect in vitro ADME data including: Plasma protein binding; human, rat and mouse liver microsomal stability; metabolism identification studies to identify oxidative and reactive soft spots; and in vitro brain free fraction prediction.	Completed
6. Run HERG interaction/binding for HZ-166 and JY-XHE-053(if possible), also run for YT-III-31 and YT-III-271 (if possible).	Completed
7. Run binding on whole set of other types of receptors for all 4 compounds (if possible) to show they don't interact with other types (if possible).	Completed

HZ166 is highly selective

- hERG IC50: 18 μM
- No activity against 41 tested receptors (IC50/EC50: > 10 μM)
  - Ion channels and GPCRs (e.g., Cav1.2, 5HTs, CB1)

Mouse PK: 1 mg/kg IV, IP and PO



	$t_{1/2}$	V_{ss}	V_β	CL_p	C_{max}	AUC	T_{max}	F	AUC/D	MRT
IV (1 mg/kg)		_·_		21.4	0.21	0.047				0.00
IP (1 mg/kg)										
PO (1 mg/kg)										

* harmonic mean ; $t_{1/2}$ [hr]; C_{max} [ug/mL]; V_{ss} [L/kg]; V_β [L/kg]; T_{max} [hr]; AUC [ug*hr/mL]; CL_p [L/hr/kg]; F [%]; MRT [hr]; AUC/D [ug*hr/mL per mg/kg];

- High clearance in mouse PK 24 hr study (CLp = 21.4 L/hr/kg)
- No measurable drug following 1 mg/kg IP and PO

PPB and Microsomal Stability

❑ Plasma and Brain Protein Binding (free fraction: fu)

Rat Plasma	Mouse Plasma	Human Plasma	Rat Brain
NV	NV	0.0513	0.197

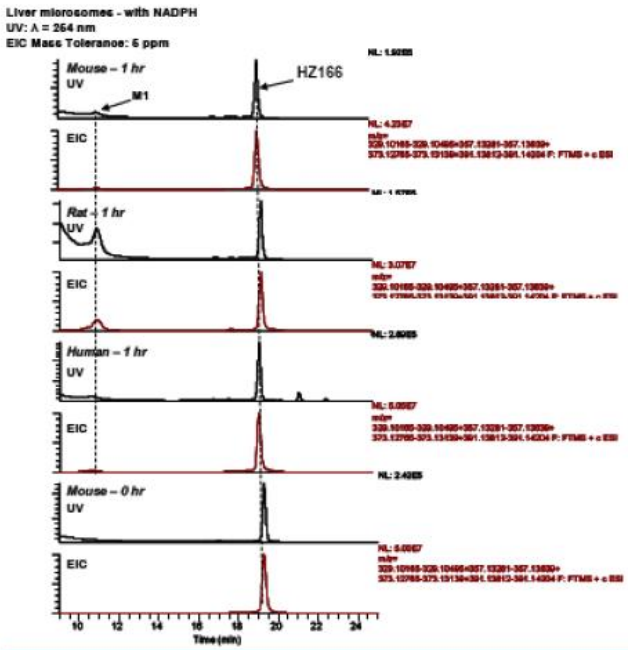
NV: low recovery, due to rodent-specific plasma esterase activity

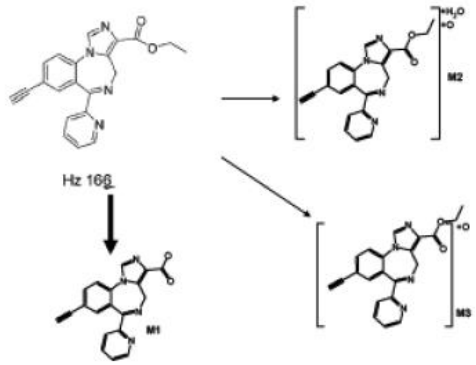
❑ Liver Microsomal Stability ($Cl_{int\text{-}scaled}$: L/hr/kg)

Rat	Mouse	Human
10.7	15.2	< 1.5

- ❑ Moderately bound to human plasma protein; less bound to rat brain
- ❑ Stable in human liver microsome; less stable in mouse and rat

Liver Microsomal MetID

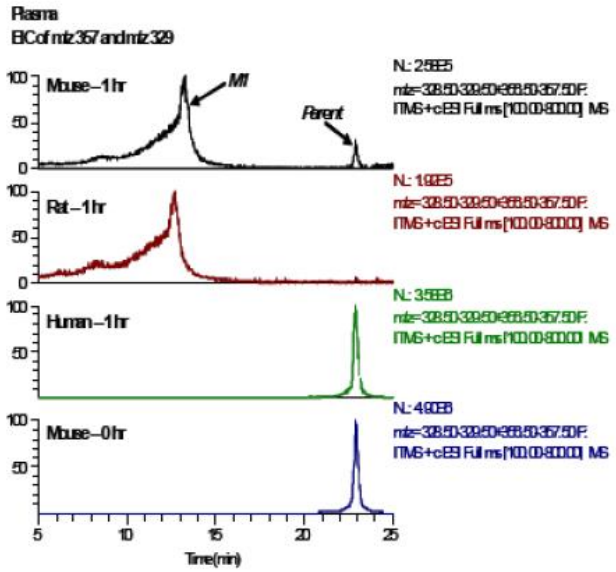


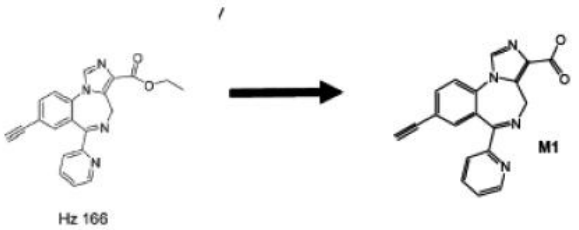


				Mouse	Rat	Human
				MS	*MS*	*MS*
	RT	*m/z*	*Δ m/z*	*% Parent*	*% Parent*	*% Parent*
Parent	19.2	357	0	100.00	100.00	100.00
M1	10.6	329	-28	6.29	47.20	6.10
M2	10.0	391	34	0.60	1.70	0.49
M3	16.0	373	16		0.19	0.03
MS = Detected on MS only; no UV peak						

❑ In LMs, HZ166 was primarily metabolized to form M1 *via* non-NADPH dependent esterase activity.

Plasma MetID





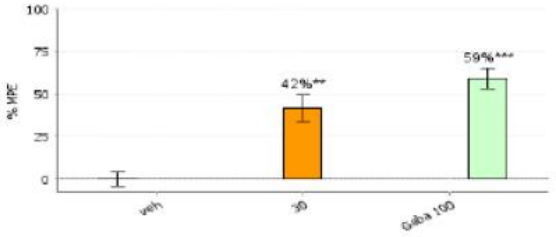
Hz 166

				Mouse	Rat	Human
				MS	*MS*	*MS*
	RT	*m/z*	*Δ m/z*	*% Parent*	*% Parent*	*% Parent*
Parent	19.2	357	0	100.00	100.00	100.00
M1	10.6	329	-28	2334.94	33908.27	0.00

❑ HZ166 was also metabolized by rodent specific plasma esterase activity to form M1.

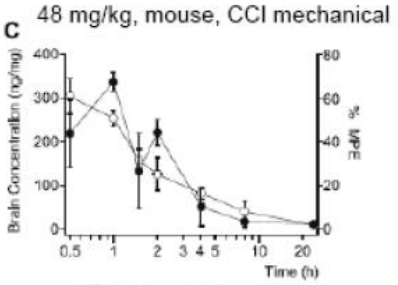
Rat CCI: 30 mg/kg, IP, 0.5 hr

COMPANY



HZ166, mg/kg, ip

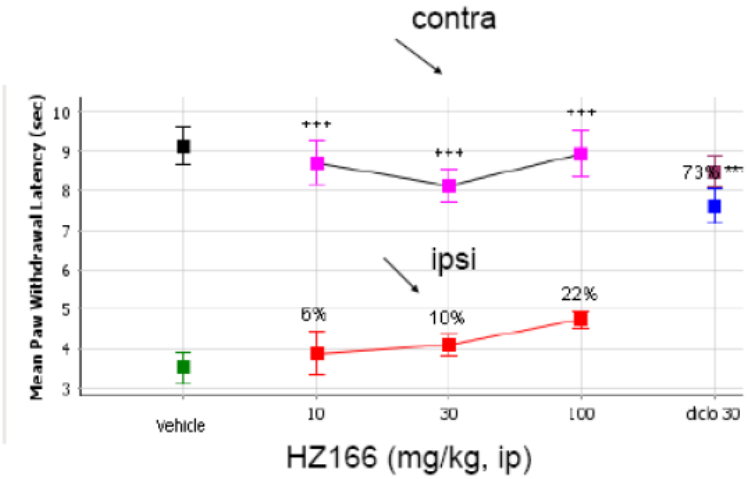
UW



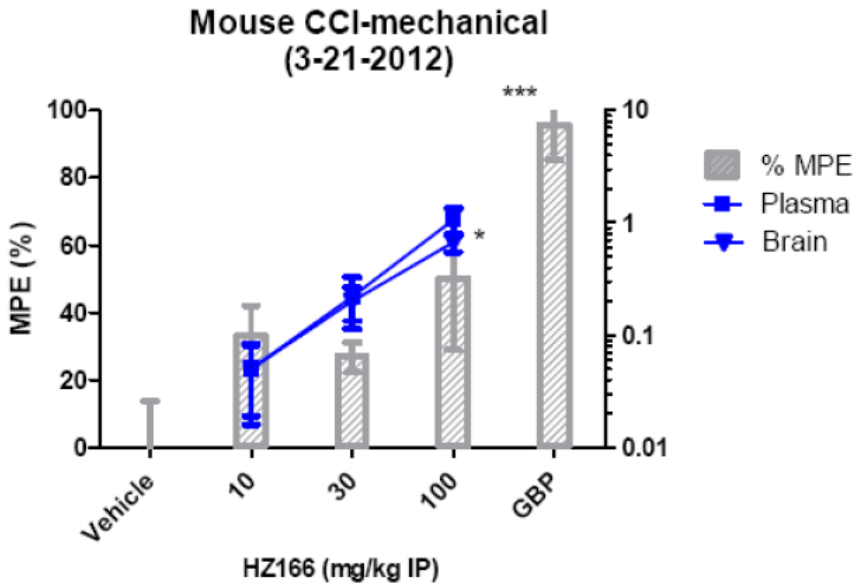
(Di, Lio et al)

- 42% efficacy 0.5 hr after 30 mg/kg, IP
- Plasma con = 0.1 µg/ml, brain con = 0.116 µg/ml
- No obvious deficits from visual observation
- Results consistent with UW 48 mg/kg dosing in mouse CCI

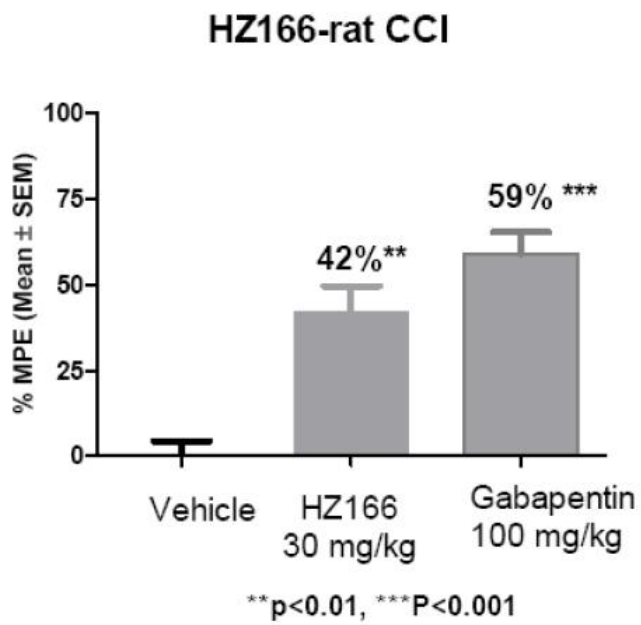
Mouse Carrageenan: no significant effect



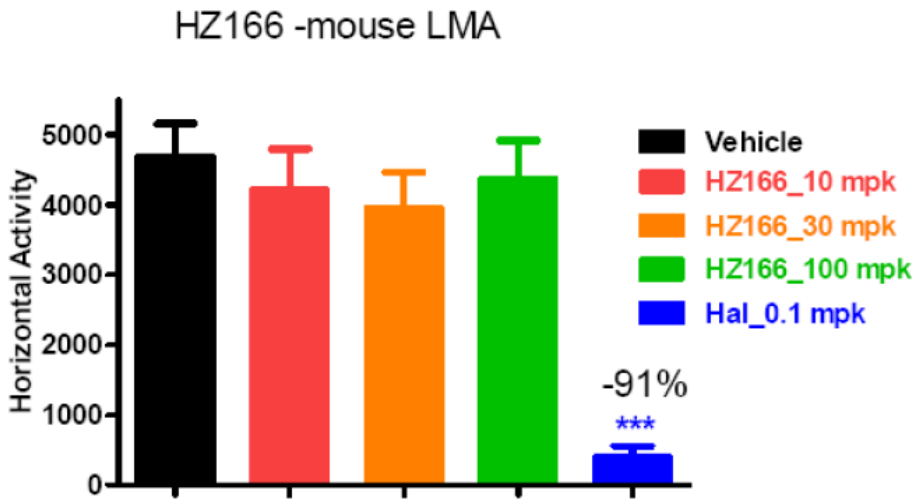
- Lack of efficacy could be due to lack of peripheral exposure (PK ongoing)
- Other experiments pending: mouse CCI and LMA



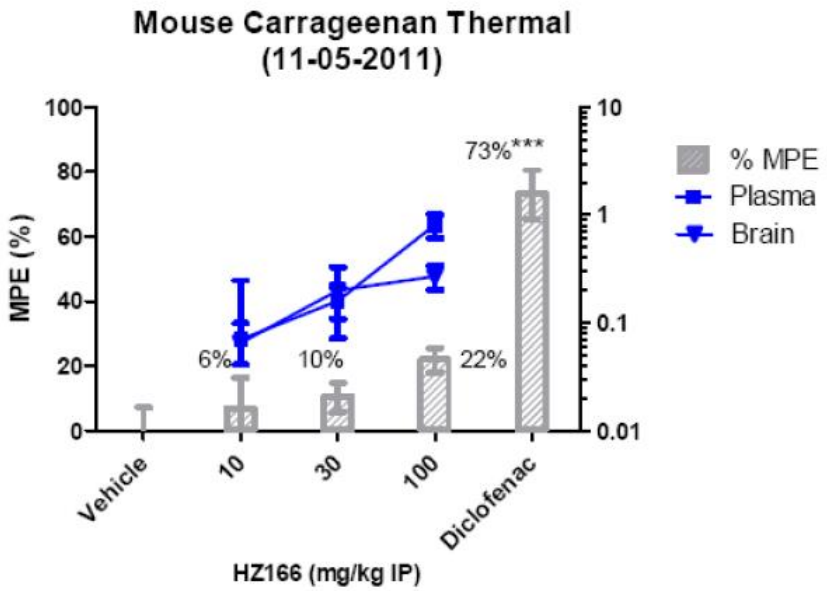
HZ166 at 10.30 and 100 mg/kg, ip 10 ml/kg, Vehicle: 0.5% HPMC
Positive control: Gabapentin 100 mg/kg, 10 mL/Kg in water
Von Frey test after 60 min pretreatment (n=8)
Post-hoc: *p<0.05; ***p<0.001



HZ166 rCCI, 05-16-2011, 30 mg/kg (Vehicle, 10%DMSO/PEG), Gabapentin 100 mg/kg in water, 2.0 mL/kg, 30 min after treatment
[Plasma]= 0.27 uM, [brain]= 0.3 uM (n=6)
** p<0.01; *** p<0.001



HZ166 at 10.30 and 100 mg/kg, ip 10 ml/kg, Vehicle: 0.5% HPMC
Positive control: Haloperidal 0.1 mg/kg, ip (10%DMSO/PEG, 10 mL/kg), 60 min treatment
*** p<0.001, n=8



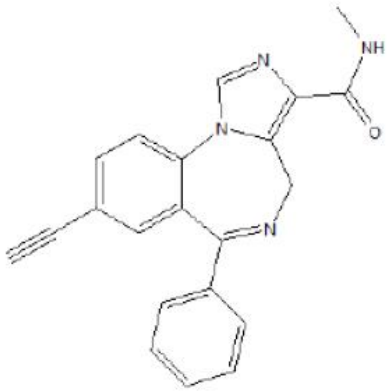
HZ mouse Carrageenan, 11/02/2011, 310/30/100 mg/kg (Vehicle, 0.5% HPMC),
Diclofeanc 30 mg/kg, 60 min treatment, 10 mL/kg
Mouse Carrageenan hotbox test after 60 min pretreatment
Post-hoc: ***p<0.001, n=8

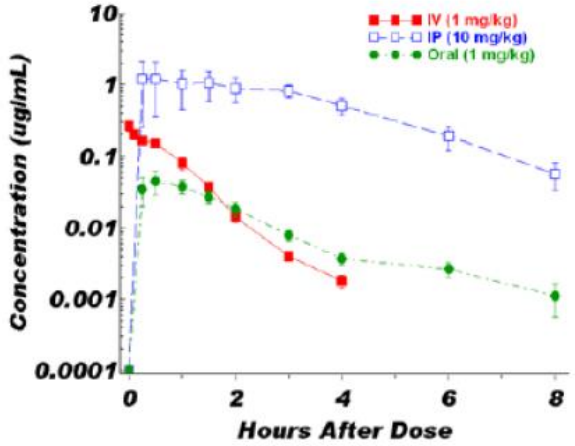
YT-III-31 Characterization

UW MTA Request

UW MTA (Fully Executed on 6-18-2012) (YT-III-31)	Progress
1. Rat PK study: i.v., i.p., and p.o. pharmacokinetic time course.	Completed
2. Test compound(s) in neuropathic pain (e.g., Bennett), or an inflammatory pain (e.g., CFA) models. Collect plasma and/or brain to quantify drug exposure.	CCI completed
3. Evaluate compound(s) in locomotor activity assay or other CNS side effect assays (if necessary).	LMA completed
4. Evaluate compound(s) selectivity by testing against a panel of receptors and ion channels, including hERG.	Completed

YT-III-31 PK in Rats



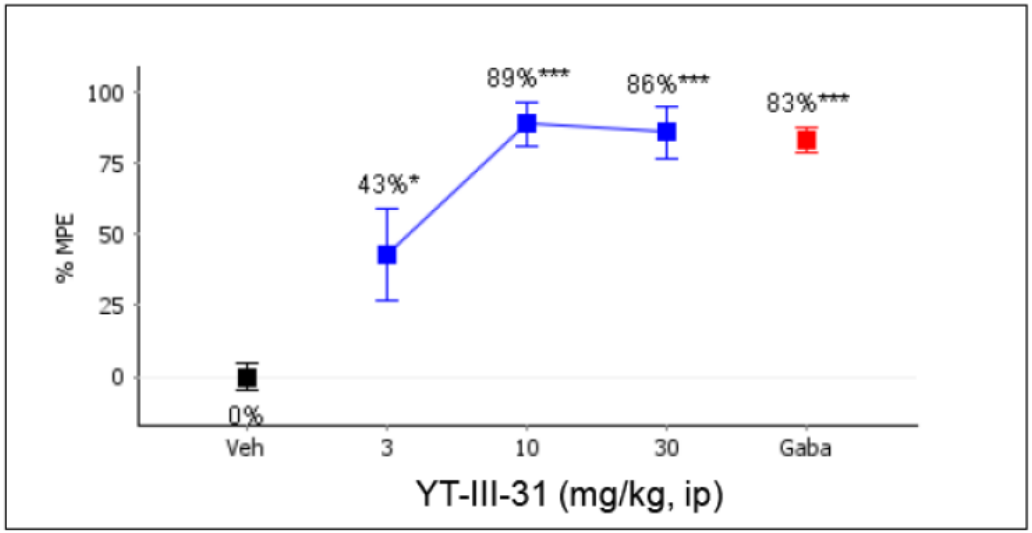


	IV (1 mg/kg)						IP (10 mg/kg)					PO (1 mg/kg)				
Rat #	$t_{1/2}$	C_0	V_{ss}	V_β	AUC	CL_P	$t_{1/2}$	C_{max}	T_{max}	AUC	F	$t_{1/2}$	C_{max}	T_{max}	AUC	F
1,4,7	0.6	0.2	4.9	5.3	0.16	6.31	0.9	0.8	1.5	2.54	124	1.8	0.0	1.00	0.05	26
2,5,8	0.5	0.3	3.5	3.4	0.22	4.50	1.6	0.8	3.0	3.32	161	1.0	0.1	0.50	0.11	56
3,6,9	0.7	0.3	2.9	4.1	0.24	4.22	1.3	3.1	0.3	7.90	384	1.5	0.1	0.25	0.11	56
Mean	0.6°	0.3	3.8	4.2	0.21	5.01	1.2°	1.6	1.6	4.59	223	1.4°	0.0	0.58	0.09	46
SEM		0.0	0.6	0.5	0.02	0.65		0.8	0.8	1.67	81		0.0	0.22	0.02	10

° harmonic mean ; $t_{1/2}$ [hr]; C_0 and C_{max} [ug/mL]; V_{ss} [L/kg]; V_β [L/kg]; T_{max} [hr]; AUC [ug*hr/mL]; CL_P [L/hr/kg]; F [%]; V12-1415

Formulation: 10:90 (v/v) DMSO:PEG-400 dosed at 1 mL/kg; Fasted

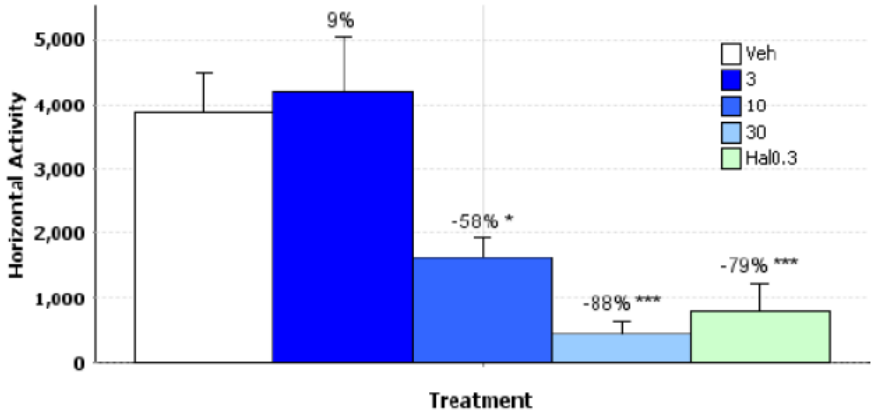
YT-III-31: Rat CCI



YT-III-31	Brain, uM	Fu-brain, uM	Plasma, uM	Fu-PI, uM
3 mpk, ip	1.675±0.694	0.05±0.02	0.872±0.35	0.09±0.037
10 mpk, ip	10.86±1.69	0.33±0.05	6.04±0.68	0.64±0.072
30 mpk, ip	55.75±9.74	1.67±0.29	17.85±6.72	1.89±0.71

- Efficacy tested 30 min post dosing (3/10/30 mpg, ip)
- Hypoactivity observed in 2/6 animals at 3 mpk, and 6/6 animals at 10 and 30 mpk

YT-III-31: Locomotor Activity Assay



YT-III-31	Brain (uM)	Fu Brain (uM)	Plasma (uM)	Fu Plasma (uM)
3 mg/kg, ip	0.457±0.085	0.014±0.003	0.179±0.028	0.019±0.003
10 mg/kg, ip	5.825±1.08	0.175±0.032	2.132±0.282	0.226±0.03
30 mg/kg, ip	39.98±3.14	1.20±0.09	17.54±1.68	1.86±0.18

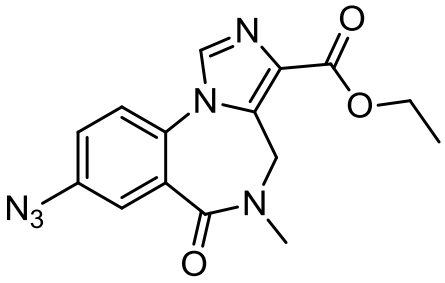
•Significant LMA effects in rats (10/30 mpk, ip, tested 30 min post dosing)

YT-III-31 Bioprofiling

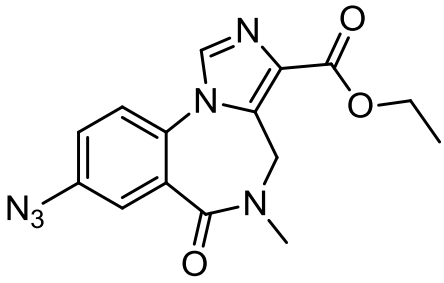
- hERG IC50: 11.8 μM
- IC50: 5.1 μ M on PDE3
- Lack of effect on 40 other GPCR, ion channels at 10 μM
  - e.g., 5HT1a, Cav1.2 and CB1

APPENDIX B. Oocyte efficacy and binding of BZDs (including flumazenil) and β-carbolines (data from Scott Harvey).

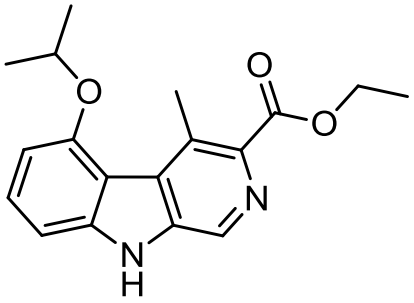
Structures:



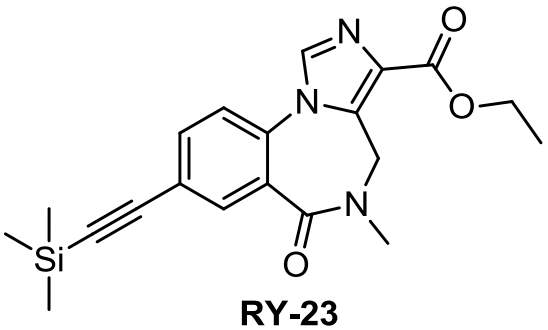
Ro15-4513



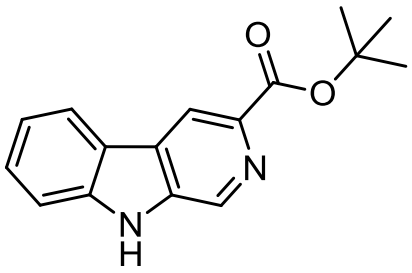
Ro15-1788
Flumazenil



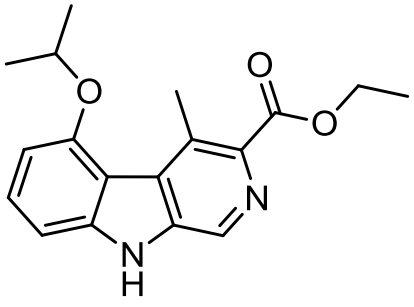
ZK-93426



RY-23

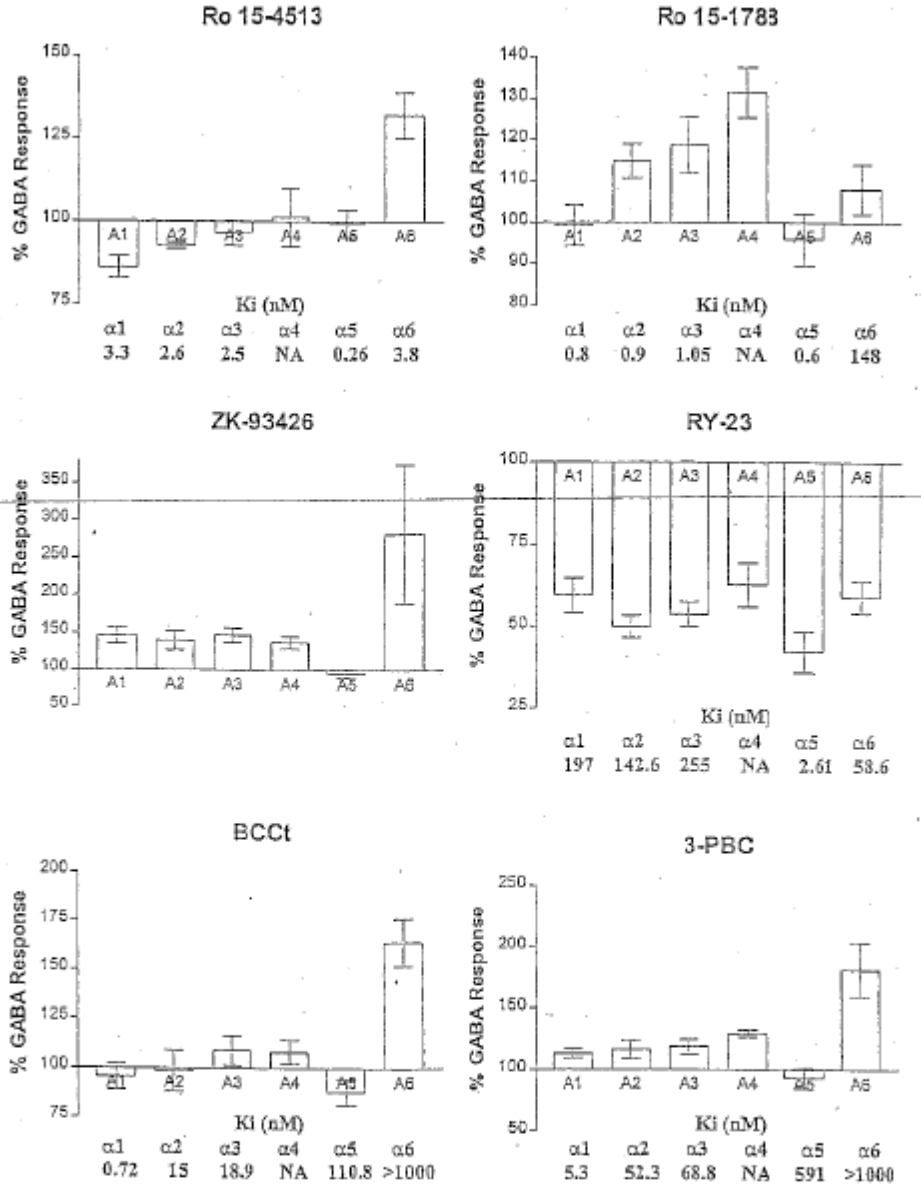


BCCt



3-PBC

Efficacy of $GABA_A$ Receptor Modulators



Percent modulation of GABA-evoked current responses in voltage clamped *Xenopus* oocytes expressing recombinant $GABA_A$ receptors. Each oocyte was injected with cRNA of indicated α subunit together with cRNA of β3 and γ2 subunits. GABA concentration is at the EC_{50} for each receptor subunit combination. Concentration of indicated modulator is saturating (1-10 μM). The peak whole cell current response from application of GABA and modulator is reported as the percentage of the peak response to GABA alone (% GABA Response). Each value is the mean ± standard deviation for 3 or more separate oocytes (Harvey, June, Cook et. al. in press).[19-22, 75]

METHODS

Materials. Xenopus laevis frogs were purchased from Xenopus-1 (Dexter, MI). Collagenase B was from Boehringer Mannheim (Indianapolis, IN). GABA was from RBI, all other compounds were synthesized by James Cook (UW)

cDNA clones. The rat GABA receptor alpha 1-5, beta 3 and gamma 2 clones were gifts from Dr. Luddens (Department of Psychiatry, University of Mainz, Germany).

Injection of in vitro synthesized RNA into Xenopus oocytes. Capped cRNA was synthesized from linearized template cDNA encoding the subunits using mMESSAGE mMACHINE kits (Ambion, Austin, TX). Oocytes were injected with the alpha, beta and gamma subunits in a molar ratio of 1:1:1 as determined by UV absorbance.

Mature *X. laevis* frogs were anesthetized by submersion in 0.1% 3-aminobenzoic acid ethyl ester, and oocytes were surgically removed. Follicle cells were removed by treatment with collagenase B for 2 hr. Each oocyte was injected with 50-100 ng of cRNA in 50 nl of water and incubated at 19° C in modified Barth's saline (88 mM NaCl, 1mM KCl, 2.4 mM $NaHCO_3$, 0.41 mM $CaCl_2$, 0.82 mM $MgSO_4$, 100 µg/ml gentamicin, and 15 mM HEPES, pH 7.6). Oocytes were recorded from after 3 to 10 days post-injection.

Electrophysiological recordings. Oocytes were perfused at room temperature in a Warner Instruments oocyte recording chamber #RC-5/18 (Hamden, CT) with perfusion solution (115 mM NaCl, 1.8 mM $CaCl_2$, 2.5 mM KCl, 10 mM HEPES, pH 7.2). Perfusion solution was gravity fed continuously at a rate of 15 ml/min. Compounds were diluted in perfusion solution, and applied until a peak current was reached.

APPENDIX C. Ester Breakdown of Compounds in Biological Matrices (data report by Mithridion, Inc.).

Summary: Metabolic stability studies of Bz/$GABA_A$ ligands incubated in whole blood, brain, liver and liver microsomes.

CONFIDENTIAL

Technical Report

Ester Breakdown of Compounds in Biological Matrices

Experimentation and Author: Melinda Verdone

Mithridion, Inc.

November 3, 2008

Study Objectives

A. Ester breakdown in biological tissues

The objective is to determine the rate of breakdown of the ester in human blood, brain, liver and kidney.

B. Development of a bioanalytical method for parent ester compound

The proteins will be precipitated using formic acid, followed by centrifugation and ultra-filtration; or using acetonitrile or methanol, followed by SpeedVacing and redissolution in LC mobile phase. Alternatively the compounds will be extracted into organic phase, SpeedVaced and redissolved in LC mobile phase. The initial choice of extraction method and LC method will be made based upon chemical structure, chemical stability and physicochemical properties of the compounds. If the compounds are poorly soluble in aqueous buffers, if they are tightly protein bound, or if reverse-phase LC is unsatisfactory, additional work may be required.

We will consult with the Cook lab on method selection and if initial standard methods are unsatisfactory, meaning that additional work is required.

Initially, for economy, we will measure the parent compounds simply using the peak areas of the parent ester compounds in the MS-MS using characteristic parent and product ions. The quantification may not be exact.

C. Semi-quantitative test of ester breakdown

The compounds will be incubated with the tissue or tissue homogenate for various times, the parent compound and its breakdown products will be extracted from the biological materials, and assayed using LC-MS-MS.

The area of the parent (ester) will be determined at time zero and at various times. The breakdown will be expressed as follows:

Fraction broken down = 1- ((Area at time t) /(Area at time 0))

Providing all samples are treated identically, the time zero sample will serve to normalize for extraction efficiency. The experiment will then be repeated. We will look for characteristic breakdown products, in particular the acid, though this may be further metabolized.

D. Interim report

We will produce an interim report and discuss the initial results with Prof Cook. We can then decide whether further work is required. The semi-quantitative assay should enable the relative susceptibilities of the compounds to breakdown to be determined.

An estimate of breakdown rates will be obtained. We may be able to detect and identify breakdown products other than those formed by simple de-esterification. If desired, we could use inhibitors to part-characterize the enzymes responsible.

Initial Setup and Evaluation

A. Solubility Determination and Solution Formulation

All compounds were initially dissolved in dimethyl sulfoxide (DMSO) at a concentration of 20 mg/mL. Gentle heating was applied to dissolve the compound if necessary. Portions of these DMSO stocks were added to phosphate buffered saline (PBS) in an attempt to form 2 mM solutions. However, six out of the seven compounds precipitated immediately. The six solutions that showed precipitation were centrifuged at 16,000 x *g* for 10 minutes at 4°C, and the saturated solutions were removed from the undissolved material. These saturated solutions were aliquoted and stored at -20°C until needed for the rest of the experiments outlined herein.

Compound	Saturated Stock (uM)
HZ166	144
YT-TC-3	774
JY-XHe-053	480
EMJ-026	146
XLi-210	1,214
DM-II-20	147
XHe053	199

B. Sample Preparation and Compound Recovery

It is necessary to use an extraction method that shows good recovery of the compound from all matrices used in experimentation in order to give accurate results. Based upon the compounds' high logPs, an organic extraction was the most logical choice for compound recovery from biological matrices. The procedure used for sample preparation is outlined below.

Samples were kept on ice throughout the entire preparation procedure. Six hundred microliters of acetonitrile (AcN) was added to 200 uL of sample and vortexed. The precipitated sample was centrifuged at 16,000 x *g* for 10 minutes at 4°C. The supernatant was removed and transferred to a capless tube and dried overnight *in vaccuo* at room temperature by Savant SpeedVac (Model SC110). The dried material was resuspended in 200 uL of 0.1% formic acid and filtered through a 0.2 um spin filter (Pall) at 16,000 x *g* for 3 minutes. The solution was diluted 8-fold in 0.1% formic acid, placed in a 96-well plate with a plate seal, and analyzed by LC/MS/MS as described below. The sample remained at 4°C in the LC autosampler until analyzed.

Compound recovery was tested by performing the above sample preparation procedure on each compound added to 200 uL of whole blood, brain, kidney and liver homogenates. These samples were immediately precipitated with 600 uL of AcN and prepared as above. Control samples were prepared by substituting the matrix with an equal volume of water. These matrix samples were compared to control samples to calculate percent recovery.

C. Liquid Chromatography and Mass Spectrometry Methods

Multiple Reaction Monitoring (MRM) methods were developed for each compound and its corresponding metabolite. Solutions were prepared by adding 1 uL of each DMSO stock to 500 uL of 50% AcN + 0.1% formic acid. Samples were infused at a rate of 10 uL/min by syringe pump. Samples were analyzed on an API3200 (Applied Biosystems) triple quadrupole mass spectrometer. The parent ion, product ion, and mass spec settings for each compound were determined automatically through quantitative optimization by the Analyst 1.4.2 (Applied Biosystems) software. The MS/MS settings for each compound and metabolite are summarized in Table 1 below.

Table 1. Mass Spectrometer Settings

Compound Name	**Q1 Parent ion *m/z***	**Q3 Product ion *m/z***	**Polarity**	**DP**	**EP**	**CE**	**CXP**
HZ166	357.1	311.0	Positive	51	9.5	23	4
YT-TC-3	651.2	274.0	Positive	101	9.5	47	6
JY-XHe-053	374.1	328.0	Positive	46	8	25	4
EMJ-026	394.2	310.1	Positive	56	5	27	4
XLi-210	631.2	264.1	Positive	111	7.5	45	6
DM-II-20	410.1	310.1	Positive	61	7.5	29	4
XHe053	356.1	310.1	Positive	46	10	25	4
HZ166 acid	329.1	232.1	Positive	46	9.5	35	4
YT-TC-3 acid	292.0	274.0	Positive	46	8.5	19	4
JY-XHe-053 acid	346.1	249.1	Positive	41	6.5	31	4
EMJ-026, XHe053, DM-II-20 acid	328.2	231.1	Positive	46	8.5	33	4
XLi-210 acid	282.1	264.1	Positive	46	9.5	19	4

The same LC method was used for all compounds and metabolites. See details in Table 2.

Table 2. LC Settings

Variable	Setting
HPLC	Shimadzu Prominence
Column	Agilent Zorbax 300SB-C8, 2.1x150mm, 3.5um
Solvent A	H_2O + 0.1% formic acid
Solvent B	AcN + 0.1% formic acid
Gradient	0-100% B, 5 min; 100% B, 2 min
Flowrate	0.3 mL/min
Column Oven Temp.	40°C
Injection Volume	5 uL

Table 3 shows the retention times for each compound and metabolite obtained with this LC method.

Table 3. LC Retention Times

Compound Name	t_R (min)
HZ166	5.4
YT-TC-3	5.7
JY-XHe-053	5.8
EMJ-026	6.2
XLi-210	5.5
DM-II-20	6.0
XHe053	5.8
HZ166 acid	4.8
YT-TC-3 acid	5.1
JY-XHe-053 acid	5.5
EMJ-026, XHe053, DM-II-20 acid	5.4
XLi-210 acid	5.0

It is important that the parent compound and its metabolite have different retention times, for if there is some "breakthrough" in signal for MRM methods between the two due to similar product ions, the two signals may be differentiated from one another on the basis of their retention times. In this situation, all parent compound/metabolite pairs are separated by 0.3-0.8 minutes, which is more than adequate to distinguish between the two signals.

Ester Breakdown *In Vitro*

A. Sample Composition

The composition of samples is listed in Table 4. Each sample had a total volume of 200 uL. All samples were incubated at 37°C in a water bath during each experiment.

Table 4. Sample Composition

Assay	Component	Volume (uL)
Brain Esterase	Brain Homogenate	80
	H_2O	30
	100 mM Tris + 600 mM NaCl + 20 mM $CaCl_2$	50
	Compound	40
Kidney or Liver Esterase	Kidney or Liver Homogenate	40
	H_2O	70
	100 mM Tris + 600 mM NaCl + 20 mM $CaCl_2$	50
	Compound	40
Whole Blood Esterase	Whole Blood	160
	Compound	40

B. B. Timecourse Studies

In order to determine the appropriate incubation time for each matrix, an initial timecourse study was conducted. All seven compounds were incubated in whole blood, brain, kidney and liver homogenates at 37°C. Aliquots were removed at selected time points and enzymatic activity halted by the addition of 600 uL of AcN. For brain, kidney and liver homogenates, the time points were 0, 20, 40, 60, and 120 minutes. For whole blood, the time points were 0, 10, 20, 30, and 60 minutes. All samples were kept on ice until all time points were completed. Samples were prepared for analysis by LC/MS/MS as outlined above.

C. Standard Curves

Standard curves for each compound were prepared with a known concentration of compound dissolved in DMSO by serially diluting into PBS. Parent compound standards were made up at the following concentrations: 62.5, 125, 250, 500, 1000, 2000 uM. Standards and stock solutions were diluted 1:8 or 1:80 into 0.1% formic acid. These diluted solutions were analyzed by LC/MS/MS to form standard curves used to calculate the concentrations of each compound and metabolite.

D. Comprehensive *In Vitro* Esterase Experiments

Triplicate samples were set up as outlined in Table 4. Brain homogenate samples were incubated at 37°C for 120 minutes, and kidney and liver homogenates and whole blood samples were incubated at 37°C for 60 minutes. Time 0 samples for each compound and matrix were also prepared in triplicate. Samples were prepared for MS analysis as outlined above. The samples were quantitatively analyzed by LC/MS/MS for each compound and its predicted metabolite. Any statistical outliers were discarded and not used in the final calculations.

E. LC/MS Scans for Novel Metabolites

LC/MS Scans (Q1) were performed on all samples to attempt to identify novel metabolites not predicted previously. The same LC/MS settings were used as outlined in Table 1. The resulting scan for each sample was compared to its corresponding Time 0 scan to look for the introduction of new masses. ChemDraw Ultra 10.0 software was used in an attempt to elucidate the chemical structures for the discovered masses.

Experimental Results

A. Compound Recovery

The recovery of the compounds from the biological matrices used in this set of experiments was 58-163%. The raw data are listed in Appendix A at the end of this report. This sample extraction procedure is adequate for use in further experiments.

B. Timecourse Studies

The optimal incubation time for each matrix is one in which the breakdown of parent compound has reached a steady state for all compounds of interest. At this point, differences in the metabolism of each compound can be delineated. For this set of experiments, the optimal incubation time was determined to be 60 minutes for kidney and liver homogenates, and 120 minutes for brain homogenate.

C. Standard Curves

The raw data for all standard curves can be found in Appendix B at the end of this report. These curves were used to calculate the concentrations of stock solutions used in these experiments.

D. Comprehensive *In Vitro* Esterase Experiments

A summary of these experimental results can be found in Table 5 below. The raw data obtained from these experiments can be found in Appendix C at the end of this report.

Compounds YT-TC-3 and XLi-210 had similar breakdown profiles to each other, but different from the rest of the compounds. YT-TC-3 was 57% broken down in the brain; Xli-210 was 32% broken down under the same conditions. Both compounds were metabolized less in liver, and kidney and were quite stable in 80% whole blood. Both compounds formed their predicted acid metabolites.

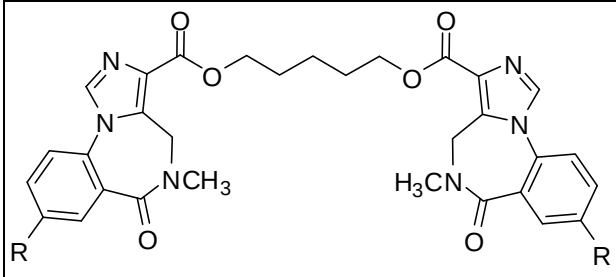
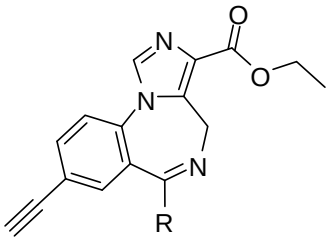
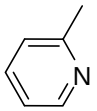
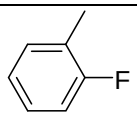
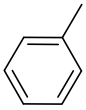
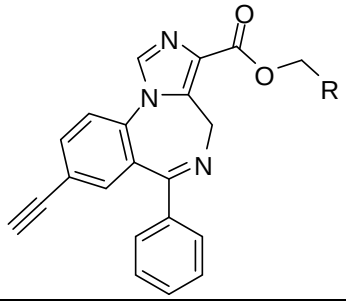
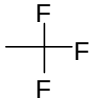
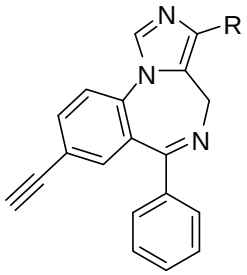
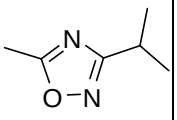
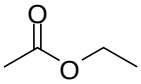
Compounds HZ166, JY-XHe-053, and XHe053 had similar breakdown profiles to each other. These compounds were 43%, 39% and 32% broken down by liver homogenate, respectively. In addition, HZ166 was susceptible to breakdown by

kidney homogenate (51% breakdown), while the other two compounds were not. All compounds were stable in 80% whole blood. These three compounds formed their predicted acid metabolites.

DM-II-20 was the most susceptible to breakdown of all the compounds tested. 59% breakdown was observed in kidney, 99% in liver homogenates, and 25% in brain homogenates, forming its predicted acid metabolite. In contrast, this compound was stable in 80% whole blood. XHe053 was more stable in liver and brain that DM-II-20, and was stable in kidney and 80% whole blood. This outcome might be expected as the trifluoroethyl group of DM-II-20 is a better leaving group than the ethyl group of XHe053.

Compounds EMJ-026 and XHe053 had similar breakdown profiles. However, EMJ-026 was more susceptible to brain and kidney esterase activity, than XHe053. XHe053 was stable in kidney and 80% whole blood. XHe053 formed the predicted acid metabolite, whereas EMJ-026 did not form its predicted acid metabolite.

Table 5. Summary of Esterase Breakdown of Parent Compounds

Structure	R	Compound Name	% Compound Remaining				Predicted Metabolite
			Br	Ki	Li	WB	
		YT-TC-3	42.8	80.9	69.0	78.7	+
		XLi-210	68.0	72.4	59.9	111.7	+
		HZ166	98.1	49.3	58.9	97.0	+
		JY-XHe-053	84.4	108.5	61.3	113.8	+
		XHe053	88.7	103.5	67.5	109.4	+
		DM-II-20	74.7	40.9	1.1	101.7	+
		XHe053	88.7	103.5	67.5	109.4	+
		EMJ-026	57.5	66.7	59.4	97.9	-
		XHe053	88.7	103.5	67.5	109.4	+

E. LC/MS Scans for Novel Metabolites

Homogenates containing compounds incubated for 60 or 120 minutes at 37°C were scanned using LC/MS and compared to control homogenates that had not been incubated, to attempt to identify novel metabolites. Ions with masses other than the predicted metabolites were observed. However, none of the novel masses could be translated into predicted structures derived from the structures of the parent compounds. Clearly EMJ-026 forms a metabolite other than the one predicted, but its structural identity was not elucidated through these methods.

Comments on the Experimental Results

These compounds were difficult to work with, because of their highly hydrophobic natures and relatively low aqueous solubilities. This precluded the use of LC-UV, which might have made it easier to track the major metabolites. Additionally, only minute amounts of each compound were available to use for testing purposes. With the experience gained in the current project, we could design sound quantitative evaluations, though it might be difficult to estimate Vmax or Km, given their low solubilities.

We would recommend that *in vivo* PK and metabolism studies should be undertaken before further *in vitro* studies. It would be important to establish whether the *in vitro* tests model *in vivo* metabolism well. These experiments might be quite challenging, because formulation has proven difficult, again due to hydrophobicity and low solubility. This is not to suggest it is impossible, but typically, a good deal of empirical work is required with such compounds to establish the best formulations and dosing regimens.

It is important to bear in mind that metabolism varies greatly between species. In previous work in this laboratory, we found that human and rat serum (surprisingly) did not hydrolyze alkyl esters in a series of carboxylic acids. However, whole blood did cause hydrolysis, and it was the blood cells that caused the hydrolysis. While it is difficult to identify enzymes in complex tissue homogenates by inhibitor profiling, we had a strong suspicion that the ester hydrolysis was not caused by typical non-specific esterases.

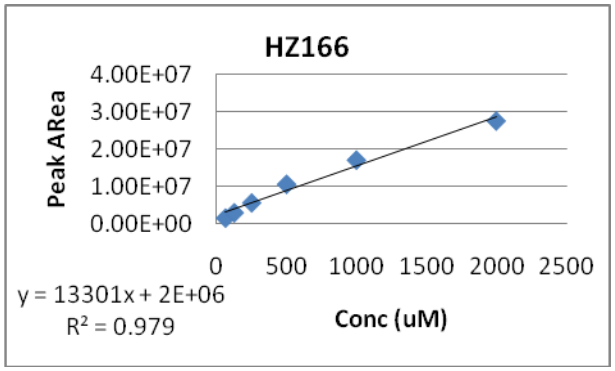
Appendix A. Compound Recovery

Compound	Brain (Peak Area)			Kidney (Peak Area)			Liver (Peak Area)			Whole Blood (Peak Area)		
	Matrix	H_2O	% Recov	Matrix	H_2O	% Recov	Matrix	H_2O	% Recov	Matrix	H_2O	% Recov
HZ166	1.51E+06	1.79E+06	84	2.78E+06	1.79E+06	155	1.63E+06	1.79E+06	91	1.38E+06	1.79E+06	77
YT-TC-3	3.93E+04	3.58E+04	110	5.44E+04	3.58E+04	152	4.71E+04	3.58E+04	132	2.27E+04	3.58E+04	63
JY-XHe-053	5.27E+05	6.06E+05	87	7.08E+05	6.06E+05	117	6.92E+05	6.06E+05	114	4.44E+05	6.06E+05	73
EMJ-026	9.17E+03	9.30E+03	99	1.07E+04	9.30E+03	115	1.06E+04	9.30E+03	114	8.81E+03	9.30E+03	95
XLi-210	5.95E+03	4.52E+03	132	6.40E+03	4.52E+03	142	6.20E+03	4.52E+03	137	7.35E+03	4.52E+03	163
DM-II-20	1.88E+05	2.96E+05	64	2.62E+05	2.96E+05	89	2.33E+05	2.96E+05	79	1.72E+05	2.96E+05	58
XHe053	9.06E+05	1.14E+06	79	1.03E+06	1.14E+06	90	8.89E+05	1.14E+06	78	7.83E+05	1.14E+06	69

Appendix B. Standard Curves

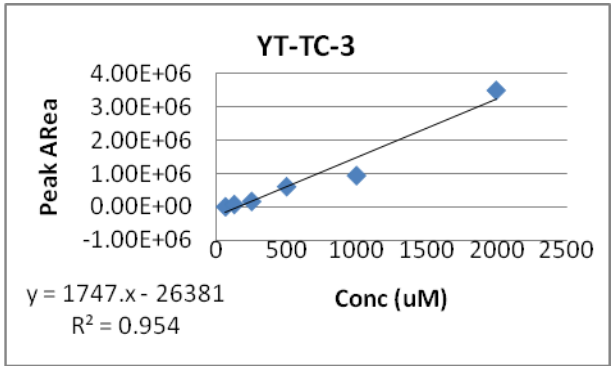
HZ166

Conc (uM)	Peak Area	Slope	Calc Conc (uM)
62.5	1.53E+06	2.45E+04	-
125	2.95E+06	2.36E+04	-
250	5.62E+06	2.25E+04	-
500	1.06E+07	2.12E+04	-
1000	1.71E+07	1.71E+04	-
2000	2.76E+07	1.38E+04	
Stock	3.24E+06	-	144.1



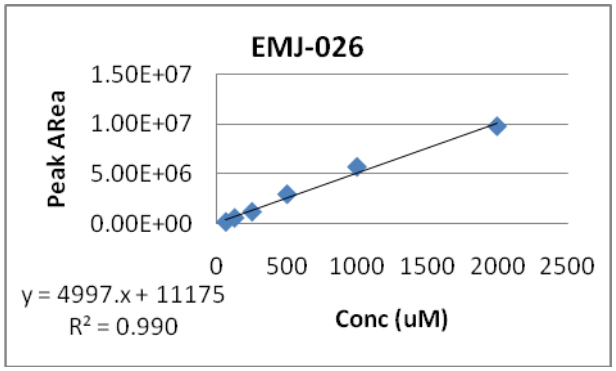
YT-TC-3

Conc (uM)	Peak Area	Slope	Calc Conc (uM)
62.5	9.36E+03	1.50E+02	-
125	7.70E+04	6.16E+02	-
250	1.69E+05	6.76E+02	-
500	6.11E+05	1.22E+03	-
1000	9.43E+05	9.43E+02	-
2000	3.49E+06	1.75E+03	
Stock	9.46E+05	-	774.1



EMJ-026

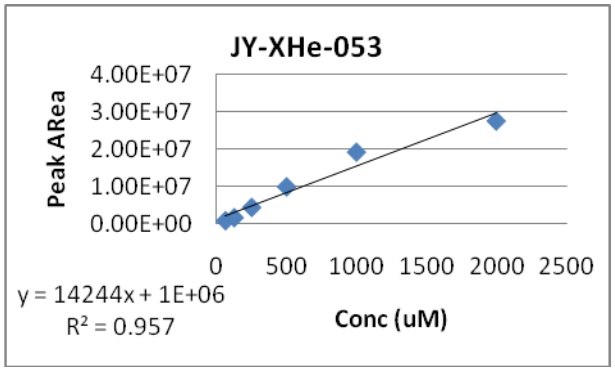
Conc (uM)	Peak Area	Slope	Calc Conc (uM)
62.5	1.70E+05	2.72E+03	-
125	5.77E+05	4.62E+03	-
250	1.19E+06	4.76E+03	-
500	2.95E+06	5.90E+03	-
1000	5.69E+06	5.69E+03	-
2000	9.77E+06	4.89E+03	
Stock	3.97E+05	-	146.0



Appendix B., continued

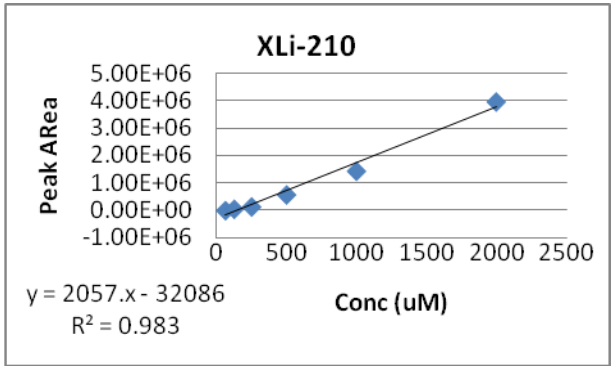
JY-XHe-053

Conc (uM)	Peak Area	Slope	Calc Conc (uM)
62.5	7.30E+05	1.17E+04	-
125	1.54E+06	1.23E+04	-
250	4.32E+06	1.73E+04	-
500	9.85E+06	1.97E+04	-
1000	1.92E+07	1.92E+04	-
2000	2.76E+07	1.38E+04	
Stock	9.45E+06	-	479.7



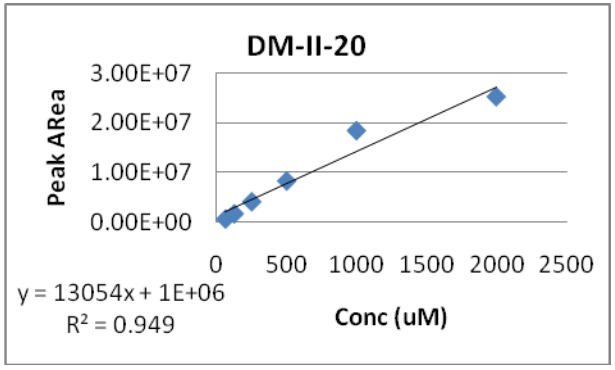
XLi-210

Conc (uM)	Peak Area	Slope	Calc Conc (uM)
62.5	3.01E+03	4.82E+01	-
125	5.23E+04	4.18E+02	-
250	1.36E+05	5.44E+02	-
500	5.76E+05	1.15E+03	-
1000	1.44E+06	1.44E+03	-
2000	3.97E+06	1.99E+03	
Stock	2.41E+06	-	1214.1



DM-II-20

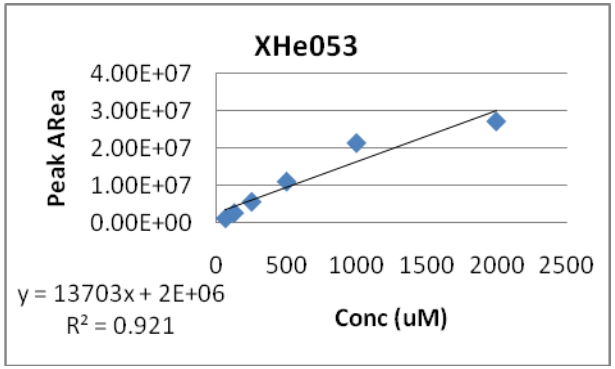
Conc (uM)	Peak Area	Slope	Calc Conc (uM)
62.5	6.92E+05	1.11E+04	-
125	1.73E+06	1.38E+04	-
250	4.15E+06	1.66E+04	-
500	8.31E+06	1.66E+04	-
1000	1.84E+07	1.84E+04	-
2000	2.52E+07	1.26E+04	
Stock	2.03E+06	-	146.7



Appendix B., continued

XHe053

Conc (uM)	Peak Area	Slope	Calc Conc (uM)
62.5	1.18E+06	1.89E+04	-
125	2.61E+06	2.09E+04	-
250	5.60E+06	2.24E+04	-
500	1.10E+07	2.20E+04	-
1000	2.13E+07	2.13E+04	-
2000	2.71E+07	1.36E+04	
Stock	4.15E+06	-	198.8



Appendix C. Esterase Breakdown Raw Data

A. Brain Homogenate

Compound	t_0 (Peak Area)					t_{120} (Peak Area)					Δ	% Breakdown	p
	1	2	3	Avg	% CV	1	2	3	Avg	% CV			
HZ166	2.61E+06	2.15E+06	2.09E+06	2.28E+06	12.46	2.26E+06	2.26E+06	2.20E+06	2.24E+06	1.55	4.33E+04	1.9	0.403
YT-TC-3	5.71E+04	7.58E+04	5.03E+04	6.11E+04	21.62	6.24E+04*	2.35E+04	2.88E+04	2.62E+04	14.33	3.49E+04	57.2	0.020
JY-XHe-053	5.48E+05	5.00E+05	5.01E+05	5.16E+05	5.31	4.84E+05	4.32E+05	3.91E+05	4.36E+05	10.70	8.07E+04	15.6	0.031
EMJ-026	7.53E+03	4.30E+03	5.36E+03	5.73E+03	28.73	3.83E+03	2.96E+03	3.09E+03	3.29E+03	14.25	2.44E+03	42.5	0.035
XLi-210	9.79E+03	8.26E+03	1.02E+04	9.42E+03	10.86	6.94E+03	5.62E+03	6.65E+03	6.40E+03	10.83	3.01E+03	32.0	0.007
DM-II-20	1.84E+05	2.29E+05	1.91E+05	2.01E+05	12.03	1.39E+05	1.60E+05	1.52E+05	1.50E+05	7.05	5.10E+04	25.3	0.014
XHe053	9.93E+05	9.81E+05	1.04E+06	1.00E+06	3.10	9.15E+05	9.03E+05	8.55E+05	8.91E+05	3.56	1.14E+05	11.3	0.006

* Outlier

B. Kidney Homogenate

Compound	t_0 (Peak Area)					t_{60} (Peak Area)					Δ	% Breakdown	p
	1	2	3	Avg	% CV	1	2	3	Avg	% CV			
HZ166	5.17E+06	4.39E+06	2.56E+06*	4.78E+06	11.54	2.62E+06	2.15E+06	2.30E+06	2.36E+06	10.19	2.42E+06	50.7	0.003
YT-TC-3	5.66E+04	4.85E+04	5.50E+04	5.34E+04	8.04	3.75E+04	4.78E+04	4.42E+04	4.32E+04	12.11	1.02E+04	19.1	0.030
JY-XHe-053	5.05E+05	5.55E+05	5.22E+05	5.27E+05	4.82	6.05E+05	5.06E+05	6.06E+05	5.72E+05	10.04	-4.50E+04	-8.5	0.141
EMJ-026	1.17E+04	1.18E+04	1.09E+04	1.15E+04	4.30	8.24E+03	7.89E+03	6.83E+03	7.65E+03	9.59	3.81E+03	33.3	0.001
XLi-210	1.71E+04	1.36E+04	1.10E+04	1.39E+04	22.02	7.64E+03	9.63E+03	1.29E+04	1.01E+04	26.41	3.84E+03	27.6	0.088
DM-II-20	2.27E+05	2.84E+05	2.65E+05	2.59E+05	11.22	9.79E+04	1.36E+05	8.34E+04	1.06E+05	25.69	1.53E+05	59.1	0.001
XHe053	1.26E+06	1.26E+06	1.15E+06	1.22E+06	5.19	1.25E+06	1.28E+06	1.27E+06	1.27E+06	1.21	-4.33E+04	-3.5	0.157

* Outlier

Appendix C., continued

C. Liver Homogenate

Compound	t_0 (Peak Area)					t_{60} (Peak Area)					Δ	% Breakdown	p
	1	2	3	Avg	% CV	1	2	3	Avg	% CV			
HZ166	5.24E+05	4.16E+05	1.27E+05*	4.70E+05	16.25	3.50E+05	2.78E+05	2.03E+05	2.77E+05	26.54	1.93E+05	41.1	0.033
YT-TC-3	1.45E+04	1.62E+04	1.56E+04	1.54E+04	5.59	1.07E+04	1.18E+04	9.45E+03	1.07E+04	11.04	4.78E+03	31.0	0.0024
JY-XHe-053	1.06E+05	1.06E+05	1.09E+05	1.07E+05	1.62	6.91E+04	7.25E+04	5.52E+04	6.56E+04	13.97	4.14E+04	38.7	0.0008
EMJ-026	1.92E+03	1.84E+03	1.85E+03	1.87E+03	2.33	1.09E+03	1.17E+03	1.07E+03	1.11E+03	4.77	7.60E+02	40.6	0.00002
XLi-210	4.37E+04	4.17E+04	4.38E+04	4.31E+04	2.75	2.53E+04	2.79E+04	2.42E+04	2.58E+04	7.36	1.73E+04	40.1	0.00009
DM-II-20	5.15E+04	5.04E+04	5.45E+04	5.21E+04	4.07	4.42E+02	6.10E+02	6.49E+02	5.67E+02	19.40	5.16E+04	98.9	0.000001
XHe053	2.67E+05	2.63E+05	2.57E+05	2.62E+05	1.92	1.89E+05	1.76E+05	1.66E+05	1.77E+05	6.52	8.53E+04	32.5	0.00015

* Outlier

D. Whole Blood

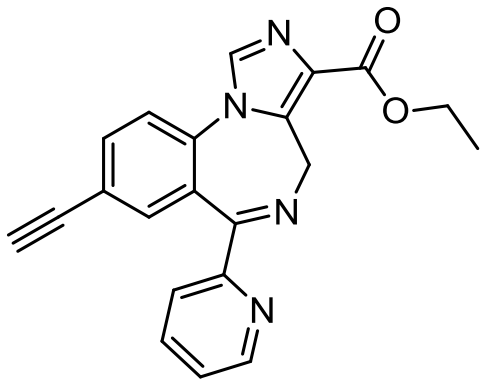
Compound	t_0 (Peak Area)					t_{60} (Peak Area)					Δ	% Breakdown	p
	1	2	3	Avg	% CV	1	2	3	Avg	% CV			
HZ166	2.12E+06	1.84E+06	1.09E+06*	1.98E+06	10.00	2.17E+06	2.01E+06	1.58E+06	1.92E+06	15.89	6.00E+04	3.0	0.41
YT-TC-3	8.85E+04	1.06E+05	9.28E+04	9.58E+04	9.52	8.13E+04	7.41E+04	7.07E+04	7.54E+04	7.18	2.04E+04	21.3	0.015
JY-XHe-053	4.80E+05	4.51E+05	5.40E+05	4.90E+05	9.26	4.53E+05	5.97E+05	6.24E+05	5.58E+05	16.47	-6.77E+04	-13.8	0.16
EMJ-026	1.28E+04	1.09E+04	1.02E+04	1.13E+04	11.91	1.16E+04	1.05E+04	1.11E+04	1.11E+04	4.98	2.33E+02	2.1	0.40
XLi-210	2.28E+04*	1.47E+04	1.18E+04	1.33E+04	15.48	1.85E+04	1.08E+04	1.51E+04	1.48E+04	26.07	-1.55E+03	-11.7	0.32
DM-II-20	1.84E+05	1.55E+05	1.44E+05	1.61E+05	12.83	1.44E+05	1.59E+05	1.88E+05	1.64E+05	13.67	-2.67E+03	-1.7	0.44
XHe053	1.12E+06	9.33E+05	4.98E+05*	9.33E+05	14.17	6.59E+05	8.57E+05	8.32E+05	7.83E+05	13.78	1.50E+05	16.1	0.053

* Outlier

APPENDIX D. ADME Evaluation of Test Agents (data by Apredica).

Summary: Ligand HZ-166 was incubated in rabbit, guinea pig and dog liver microsomes for metabolic stability.

Structure:



HZ-166



Apredica Study Number: CYP0692-R1

ADME Evaluation of Test Agents

Draft Final Report

Sponsor:	Milwaukee Institute for Drug Discovery University of Wisconsin-Milwaukee Chemistry Bldg., Room 272A PO Box 413 Milwaukee, WI 53201-0413
Sponsor's Representative	Douglas C. Stafford, PhD, MS, CLP Professor Email: dcstaff@uwm.edu
Test Facilities:	Apredica 313 Pleasant Street Watertown, MA 02472 Telephone Number: 617.600.4300
Study Director	Mohammed Taimi In Vitro ADMET, Bioanalysis 617.600.4300x116 mtaimi@apredica.com

Approved: Mohammed Taimi

Date: 01/10/13

TABLE OF CONTENTS

1 Objective....3
1.1 Regulatory Guidelines....3
2 Test Articles....3
3 Test Methods....4
3.1 Analytical Methods....4
3.1.1 Method development....4
3.1.2 Analysis....4
3.2 In vitro ADME-Tox Experimental Conditions....4
3.2.1 Liver microsomal stability experimental conditions....4
4 Results....5
4.1 Analytical....5
4.1.1 Method development....5
4.2 In vitro ADME-Tox Summary....6
4.2.1 Liver Microsomal stability screen summary....6
4.3 In vitro ADME-Tox Individual Data....7
4.3.1 Liver microsomal stability screen, Individual Data....7
5 References....8
6 Storage and Retention of Records....8

1 Objective

The objective of this study was to determine ADME profile of test agents.

1.1 *Regulatory Guidelines*

This study was not conducted under US FDA Good Laboratory Practice Regulations (GLPs). Standard operating procedures of Apredica were used throughout the study.

2 Test Articles

Client ID	Parent MW	Stock solution
HZ-166	356.38	10mM DMSO

Stock solutions were stored at -20 °C.

3 Test Methods

Testing was performed at Apredica in Watertown, MA.

3.1 *Analytical Methods*

3.1.1 Method development

The signal was optimized for each compound by ESI positive or negative ionization mode. An MS2 scan or a SIM scan was used to optimize the fragmenter voltage and a product ion analysis was used to identify the best fragment for analysis, and the collision energy was optimized using a product ion or MRM scan. An ionization ranking was assigned indicating the compound's ease of ionization.

3.1.2 Analysis

Samples were analyzed by LC/MS/MS using an Agilent 6410 mass spectrometer coupled with an Agilent 1200 HPLC and a CTC PAL chilled autosampler, all controlled by MassHunter software (Agilent). After separation on a C18 reverse phase HPLC column (Agilent, Waters, or equivalent) using an acetonitrile-water gradient system, peaks were analyzed by mass spectrometry (MS) using ESI ionization in MRM mode.

3.2 In vitro *ADME-Tox Experimental Conditions*

3.2.1 Liver microsomal stability experimental conditions

Client ID	Test conc.	Micro-some source	Protein conc.	Incub-ation	Ref. comp.	Analytical method
HZ-166	1 µM	Rabbit, guinia pig, dog	0.3 mg/mL	0, 60 min 37 °C	verapamil warfarin	LC/MS/MS

Liver microsomal stability screen

The test agent is incubated in duplicate with microsomes at 37 °C. The reaction contains microsomal protein in 100 mM potassium phosphate, 2 mM NADPH, 3 mM $MgCl_2$, pH 7.4. A control is run for each test agent omitting NADPH to detect NADPH-free degradation. The indicated times, an aliquot is removed from each experimental and control reaction and mixed with 3 volumes of ice-cold Stop Solution (methanol containing internal standards). Stopped reactions are incubated at least ten minutes on ice. The samples are centrifuged to remove precipitated protein, and the supernatants are analyzed by LC/MS/MS to quantitate the remaining parent. Data are reported as % remaining of parent compound

4 Results

4.1 *Analytical*

4.1.1 Method development

Client ID	MW	Polari-zation	Precursor m/z	Product m/z	Ionization classification[a]
HZ-166	356.4	Pos.	356.8	283.1	1

[a]Ionization classification:
1 = Highly ionizable
2 = Intermediately ionizable
3 = Poorly ionizable

4.2 In vitro *ADME-Tox Summary*

4.2.1 Liver Microsomal stability screen summary

Client ID	test conc (μM)	test species	mean remaining parent with NADPH (%)	mean remaining parent NADPH-free (%)	comment
Verapamil	1	Rabbit	0.01%	92.2%	high CL control
		Guinea pig	0.2%	92.2%	
		Dog	13.1%	96.5%	
Warfarin	1	Rabbit	97.9%	98.2%	low CL control
		Guinea pig	101%	98.8%	
		Dog	95.8%	98.7%	
HZ-166	1	Rabbit	1.3%	2.5%	
		Guinea pig	15.0%	30.3%	
		Dog	96.9%	103%	

4.3 In vitro *ADME-Tox Individual Data*

4.3.1 Liver microsomal stability screen, Individual Data

Client ID	test species	NADPH	% remaining		
			1st (%)	2nd (%)	Mean (%)
HZ-166	Rabbit	Yes	1.3%	1.3%	1.3%
		No	2.5%	2.5%	2.5%
	Guinea pig	Yes	14.5%	15.5%	15.0%
		No	32.1%	28.6%	30.3%
	Dog	Yes	93.9%	99.9%	96.9%
		No	98.7%	108%	103%

5 References

Houston, JB (1994) "Utility of in vitro drug metabolism data in predicting in vivo metabolic clearance." Biochem. Pharmacol. 47:1469.

6 Storage and Retention of Records

All documents generated in this study (raw data, the study plan, a copy of this report, etc.) will be stored for three years from the date of this document. Only authorized Apredica employees will have access to the archives.

The original final report will be provided to the sponsor and will be kept by the sponsor under its sole responsibility.

APPENDIX E. A Review of the Updated Pharmacophore for the Alpha 5 GABA(A) Benzodiazepine Receptor Model

Authors: Terry Clayton, Michael M. Poe, Sundari Rallapalli, Poonam Biawat, Miroslav M. Savic, James K. Rowlett, George Gallos, Charles W. Emala, Catherine C. Kaczorowski, Douglas C. Stafford, Leggy A. Arnold and James M. Cook

International Journal of Medicinal Chemistry, Volume **2015**, Article ID 430248;

Doi: 10.1155/2015/430248

Hindawi Publishing Corporation
International Journal of Medicinal Chemistry
Volume 2015, Article ID 430248, 54 pages
http://dx.doi.org/10.1155/2015/430248

Review Article

A Review of the Updated Pharmacophore for the Alpha 5 GABA(A) Benzodiazepine Receptor Model

Terry Clayton,[1] Michael M. Poe,[1] Sundari Rallapalli,[1] Poonam Biawat,[1] Miroslav M. Savić,[2] James K. Rowlett,[3] George Gallos,[4] Charles W. Emala,[4] Catherine C. Kaczorowski,[5] Douglas C. Stafford,[6] Leggy A. Arnold,[1,6] and James M. Cook[1,6]

[1]*Department of Chemistry and Biochemistry, University of Wisconsin-Milwaukee, Milwaukee, WI 53201, USA*
[2]*Department of Pharmacology, Faculty of Pharmacy, University of Belgrade, Belgrade, Serbia*
[3]*Department of Psychiatry and Human Behavior, University of Mississippi Medical Center, Jackson, MS 39216, USA*
[4]*Department of Anesthesiology, Columbia University, New York, NY 10032, USA*
[5]*Department of Anatomy and Neurobiology, University of Tennessee Health Science Center, Memphis, TN 38163, USA*
[6]*Milwaukee Institute of Drug Discovery, University of Wisconsin-Milwaukee, Milwaukee, WI 53201, USA*

Correspondence should be addressed to James M. Cook; capncook@uwm.edu

Received 11 February 2015; Revised 16 June 2015; Accepted 2 July 2015

Academic Editor: Hussein El-Subbagh

Copyright © 2015 Terry Clayton et al. This is an open access article distributed under the Creative Commons Attribution License, which permits unrestricted use, distribution, and reproduction in any medium, provided the original work is properly cited.

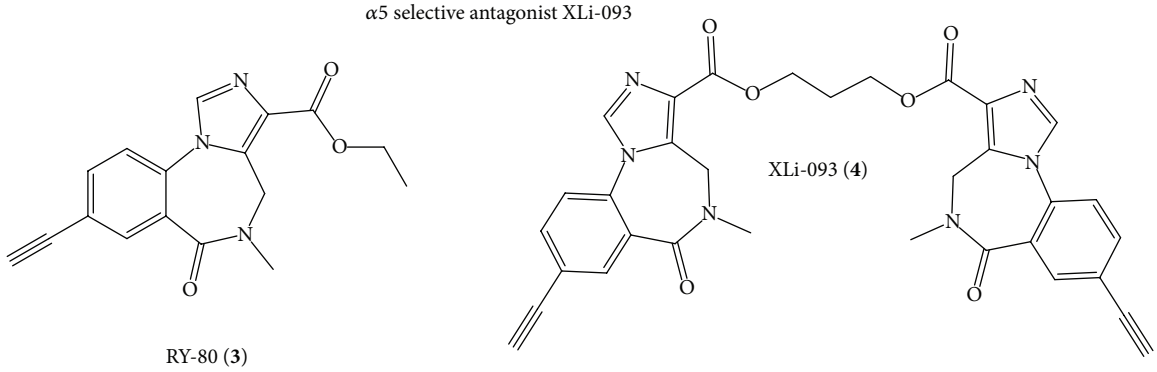
An updated model of the GABA(A) benzodiazepine receptor pharmacophore of the α5-BzR/GABA(A) subtype has been constructed prompted by the synthesis of subtype selective ligands in light of the recent developments in both ligand synthesis, behavioral studies, and molecular modeling studies of the binding site itself. A number of BzR/GABA(A) α5 subtype selective compounds were synthesized, notably α5-subtype selective inverse agonist PWZ-029 (**1**) which is active in enhancing cognition in both rodents and primates. In addition, a chiral positive allosteric modulator (PAM), SH-053-2′F-R-CH_3 (**2**), has been shown to reverse the deleterious effects in the MAM-model of schizophrenia as well as alleviate constriction in airway smooth muscle. Presented here is an updated model of the pharmacophore for $\alpha5\beta2\gamma2$ Bz/GABA(A) receptors, including a rendering of PWZ-029 docked within the α5-binding pocket showing specific interactions of the molecule with the receptor. Differences in the included volume as compared to $\alpha1\beta2\gamma2$, $\alpha2\beta2\gamma2$, and $\alpha3\beta2\gamma2$ will be illustrated for clarity. These new models enhance the ability to understand structural characteristics of ligands which act as agonists, antagonists, or inverse agonists at the Bz BS of GABA(A) receptors.

1. Introduction

The gamma-amino butyric acid A ($GABA_A$) receptor is a heteropentameric chloride ion channel. This channel is generally made up of two α-subunits, two β-subunits, and a single γ-subunit arranged in an $\alpha\beta\alpha\beta\gamma$ fashion. The $GABA_A$ receptors ($GABA_AR$) are responsible for a myriad of brain functions. Positive allosteric modulators (PAMs) and negative allosteric modulators (NAMs) act on the benzodiazepine (BZ) site of the $GABA_AR$ which can change the conformation of the receptor to inhibit or excite the neurons associated with the ion channel. To date, researchers have been unable to get an X-ray crystal structure of a functional Bz/$GABA_AR$ ion channel. Recently, Miller and Aricescu [1] have reported the crystal structure of a homopentameric $GABA_AR$ containing the β3-subunit at 3 Å resolution. Although this work provides great promise that other heteropentameric $GABA_ARs$ will be crystallized in the near future, molecular modeling and structure-activity-relationships (SARs) still remain key tools to find better subtype-selective binding agents.

2. Subtype Selective Ligands for α5 GABA(A)/Bz Receptors

Interest in BzR/GABA(A) α5 subtypes began years ago when it was realized that $\alpha5\beta3\gamma2$ Bz/GABA(A) subtypes are located



Ligand	α1	α2	α3	α4	α5	α6
RY-80 (**3**)	2834	21.4	25.8	5.3	0.49	28.8
XLi-093 (**4**)	>1000	>1000	858	1550	15	>2000

Figure 1: Alpha 5 selective compounds [13]. This figure is modified from that reported in [13].

primarily in the hippocampus. More recently this interest has been confirmed by the report of Möhler et al. [2–5] on $\alpha 5$ "knock-in mice." This group has provided strong evidence that hippocampal extrasynaptic $\alpha 5$ GABA(A) receptors play a critical role in associative learning as mentioned above [6–11].

Earlier we synthesized a series of $\alpha 5$ subtype selective ligands (RY-023, RY-024, RY-079, and RY-080) based on the structure of Ro 15-4513 and reported their binding affinity [6], as well as several ligands by Atack et al. [12]. These ligands are benzodiazepine receptor (BzR) negative modulators *in vivo* and a number of these compounds have been shown to enhance memory and learning [13]. One of these ligands was shown by Bailey et al. [6] to be important in the acquisition of fear conditioning and has provided further evidence for the involvement of hippocampal GABA(A)/BzR in learning and anxiety [13]. This is in agreement with the work of DeLorey et al. [7] in a memory model with a ligand closely related to $\alpha 5$ subtype selective inverse agonists RY-024 and RY-079 including PWZ-029 (**1**).

In order to enhance the $\alpha 5$ subtype selectivity, the bivalent form of RY-80 (**3**) was prepared to provide XLi-093 (**4**) [13]. The binding affinity of XLi-093 *in vitro* was determined on $\alpha_{1-6}\beta 3\gamma 2$ LTK cells and is illustrated in Figure 1. This bivalent ligand exhibited little or no affinity at $\alpha_{1-4,6}\beta 3\gamma 2$ BzR/GABA(A) subtypes, but this $\alpha 5$ ligand had a K_i of 15 nM at the $\alpha 5\beta 3\gamma 2$ subtype [14]. Since this receptor binding study indicated bivalent ligand XLi-093 bound almost exclusively to the $\alpha 5$ subtype, the efficacy of this ligand on GABA(A) receptor subtypes expressed in *Xenopus* oocytes was investigated by Sieghart, Furtmueller, Li, and Cook [14, 15]. Analysis of the data indicated that XLi-093 up to a concentration of 1 μM did not trigger chloride flux in any one of the GABA(A) subtypes tested. At 1 μM XLi-093 did not modulate GABA induced chloride flux in $\alpha 1\beta 3\gamma 2$, $\alpha 2\beta 3\gamma 2$, or $\alpha 3\beta 3\gamma 2$ receptors, but very slightly inhibited chloride flux in $\alpha 5\beta 3\gamma 2$ subtypes. At 1 μM, XLi-093 barely influenced benzodiazepine (Valium) stimulation of GABA-induced current in $\alpha 1\beta 3\gamma 2$, $\alpha 2\beta 3\gamma 2$, and $\alpha 3\beta 3\gamma 2$ BzR but shifted the diazepam dose response curve to the right in $\alpha 5\beta 3\gamma 2$ receptors in a very significant manner [16]. Importantly, bivalent ligand XLi-093 was able to dose dependently and completely inhibit diazepam-stimulated currents in $\alpha 5\beta 3\gamma 2$ receptors. This was the first subtype selective benzodiazepine receptor site antagonist at $\alpha 5$ receptors. This bivalent ligand XLi-093 provided a lead compound for all of the bivalent ligands in this research [16].

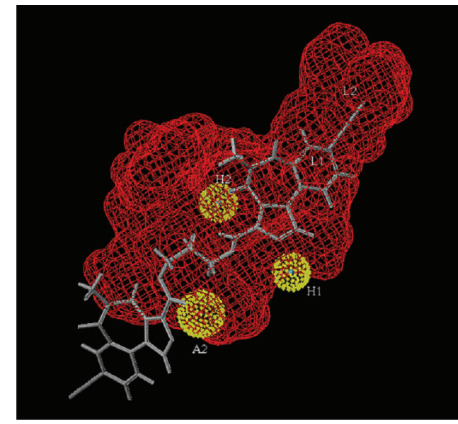


Figure 2: XLi-093 (**4**) aligned in the included volume of the pharmacophore receptor model for the $\alpha 5\beta 3\gamma 2$ subtype [17, 18] (this figure is modified from the figure in Clayton et al., 2007) [23].

Illustrated in Figure 2 is XLi-093 (**4**) aligned excellently within the pharmacophore-receptor model of the $\alpha 5\beta 3\gamma 2$ subtype [14, 16–19]. The fit to the pharmacophore-receptor and the binding data indicate that bivalent ligands will bind to BzR subtypes [14, 19]. It is believed that the dimer enters the binding pocket with one monomeric unit docking while the other monomer tethered by a linker extends out of the protein into the extracellular domain. If this is in fact true that the second imidazole unit is protruding into the extracellular domain of the BzR/GABA(A) $\alpha 5$ binding site,

Table 1: Full PDSP panel receptor binding reported (Roth [138]) for XLi-093 and XLi-356.

Cook code	5ht1a	5ht1b	5ht1d	5ht1e	5ht2a	5ht2b	5ht2c	5ht3	5ht5a	5ht6	5ht7	α1A	β1B	α2A	α2B
XLi093	*	Repeat	*	*	*	*	*	*	*	*	*	*	*	*	*
XLi356	*	*	*	*	*	*	*	*	*	*	*	*	*	*	*
Cook code	α2C	Beta1	Beta2	CB1	CB2	D1	D2	D3	D4	D5	DAT	DOR	H1	H2	H3
XLi093	*	*	*	*	*	*	*	*	*	*	*	*	*	*	*
XLi356	*	*	*	*	*	*	*	*	*	*	*	*	*	*	*
Cook code	H4	Imidaz oline	KOR	M1	M2	M3	M4	M5	MDR	MOR	NET	NMDA	SERT	σ1	σ2
XLi093	*	*	***2,024.00***	*	*	*	*	*	*	*	*	*	*	*	*
XLi356	*	*	**6,118.00**	*	*	*	*	*	*	*	*	*	*	*	*

Data ("secondary binding") are K_i values. K_i values are reported in nanomolar concentration, Case Western Reserve University. "*" indicates "primary missed" (<50% inhibition at 10 μM). See full data of the PDSP screen in the report of Clayton [22].

it could have a profound effect on the ligand design. This means other homodimers or even heterodimers may bind to BzR/GABA(A)ergic sites.

In this vein, Wenger, Li, and Cook et al. [13, 20, 21] earlier described preliminary data that XLi-093, an α5 subtype selective antagonist, enhances performance of C57BL/6J mice under a titrating delayed matching to position schedule of cognition, as illustrated in Figure 3 [14, 16–19]. This indicates, however, that this agent does cross the blood brain barrier.

Bivalent ligands have a preferred linker of 3–5 methylene units, between the two pharmacophores (see XLi-093). This was established by NMR experiments run at low temperatures, X-ray crystallography, and molecular modeling of the ligands in question and will be discussed [14, 17, 18].

Based on this data, additional α5-subtype selective ligands have been prepared (see Figure 4). The basic imidazobenzodiazepine structure has been maintained [7]; however substituents were varied in regions around the scaffold based on molecular modeling [6]. These are now the most α5 subtype selective ligands ever reported [22]. Moreover, the ability to increase the subtype selectivity can be done by selecting specific substituents on these ligands to new agents with 400–1000-fold α5-selectivity over the remaining 5 subtypes. *This is an important step forward to understanding the true, unequivocal physiological responses mediated by α5 subtypes in regard to cognition (amnesia), schizophrenia, anxiety, and convulsions, all of which in some degree are influenced by α5 subtypes*. Based on the ligands in Figures 4 and 5, affinity has occurred principally at α5 subtypes. In addition, since XLi-093 bound very tightly only to α5 BzR subtypes, the bivalent nature and functionality presented here can be incorporated into other dimeric ligands.

As shown previously in Figure 3, α5-antagonist XLi-093 (**4**) was shown to enhance cognition. In another study, a reduction of the two acetylenic groups of XLi-093 resulted in ethyl groups [14], providing a new bivalent ligand (XLi-356, **10**) which shows α5-selective binding with very low affinity for α1 subtypes (Figure 5). Efficacy (oocyte) data shows XLi-356 is an α5 negative allosteric modulator [7, 13]. DeLorey et al. have recently shown in mice that XLi-356 does potently reverse scopolamine induced memory deficits [7]. This bivalent α5 inverse agonist enhanced cognition

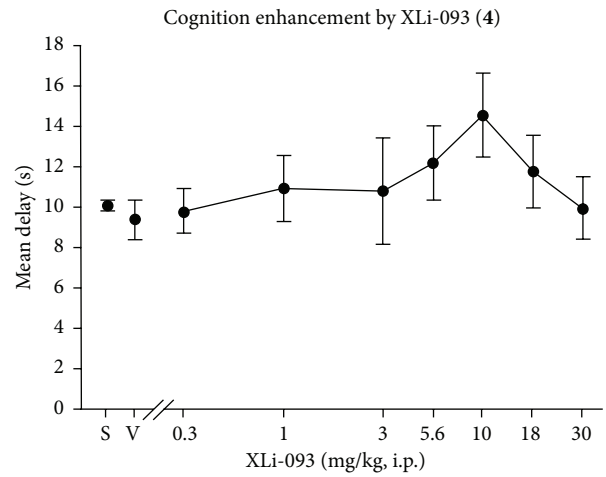


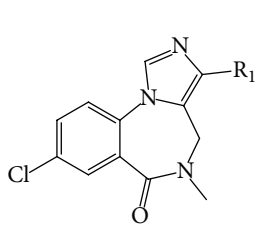
Figure 3: XLi-093 (**4**) effects on cognition enhancement by Wenger et al. (data on statistical significance not shown, unpublished results). Effects of **4** on cognition from the mean delay achieved by C57BL/6J mice titrating delayed matching-to-position schedule.

in agreement with work reported from our laboratory on monovalent inverse agonists RY-10 [6] and RY-23 [7].

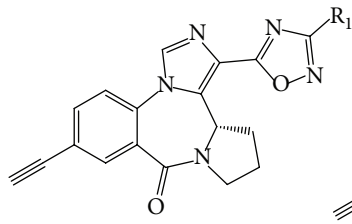
The dimers XLi-093 (**4**) and XLi-356 (**10**) were sent to Case Western Reserve (NIMH supported PDSP program, Roth et al.) for full panel receptor binding and they do not bind to other receptors at levels of concern (Table 1).

Although XLi-093 (**4**) was found to be an antagonist at the α5 subtype, XLi-356 (**10**) was found to be a weak agonist-antagonist. XLi-356 was found to reverse scopolamine induced memory deficits in mice. When XLi-356 was looked at in audio cued fear conditioning, the results show no activity. This suggests that the effect of XLi-356 is selective through α5 receptors which are abundant in the hippocampus which is highly associated with contextual memory. Audio cued memory instead is amygdala-based and should not be affected by an α5 subtype selective compound [39–42].

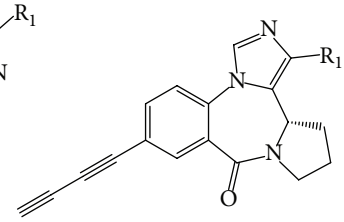
As illustrated in Figure 6, scopolamine (1 mg/kg) reduced freezing (i.e., impairs memory) generally due to coupling the



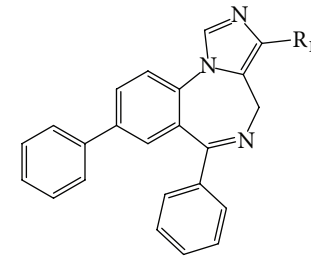
1a–c, **5**, **6**



7



8



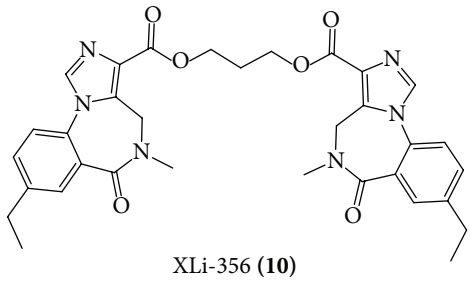
DM-I-81 (**9**)

Ligand	R_1	K_i (nM)[a] $\alpha1$	$\alpha2$	$\alpha3$	$\alpha4$	$\alpha5$	$\alpha6$
1a[b]	CH_2OCH_3	>300	>300	>300	ND	38.8	>300
1b[b]	CH_2OCH_3	920	ND	ND	ND	30	ND
1c[b]	CH_2OCH_3	362.4	180.3	328.2	ND	6.185	ND
5	CH_2Cl	>300	>300	>300	ND	28.5	>300
6	CH_2OEt	>300	>300	>300	ND	82.7	>300
7	CH_3	>89	>70	>91	ND	3.7	>301
8	CO_2Et	>1000	>1000	>1000	>1000	64	>1000
9	CO_2Et	>2000	>2000	>2000	>2000	176	>2000

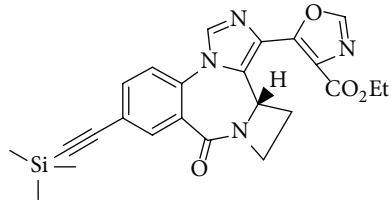
[a]Data shown here are the means of two determinations which differed by less than 10%. ND: not determined (presumably similar to $\alpha6$).

[b]**1a–c** are binding datasets of PWZ-029 (**1**) from three separate laboratories. This figure is modified from that illustrated in reference [22] to indicate the $\alpha5$ subtype selectivity.

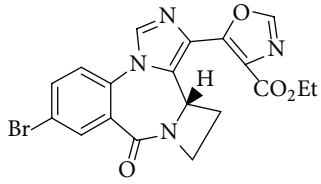
Figure 4: Binding data of selected imidazobenzodiazepines [22].



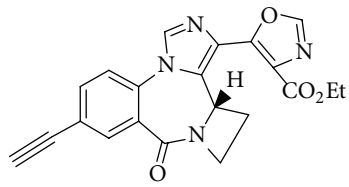
XLi-356 (**10**)



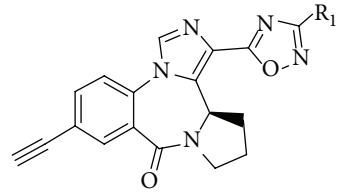
RY-068 (**11**)



RY-062 (**12**)



RY-069 (**13**)



RY-I-29 (**14**)

Ligand	K_i (nM)[a] $\alpha1$	$\alpha2$	$\alpha3$	$\alpha4$	$\alpha5$	$\alpha6$
XLi-356 (**10**)	1852	4203	8545	ND	101	5000
RY-068 (**11**)	>500	877	496	ND	37	>1000
RY-062 (**12**)	>1000	>1000	>500	ND	172	>2000
RY-069 (**13**)	692	622	506	ND	19	>1000
RY-I-29 (**14**)	>1000	>1000	>1000	ND	157	>1000

[a]Data shown here are the means of two determinations which differed by less than 10%. ND: not determined (presumably greater than 1000 nM; similar to $\alpha6$).

Figure 5: Binding data of selected imidazobenzodiazepines substituted with an E-ring as compared to XLi-356 (**10**).

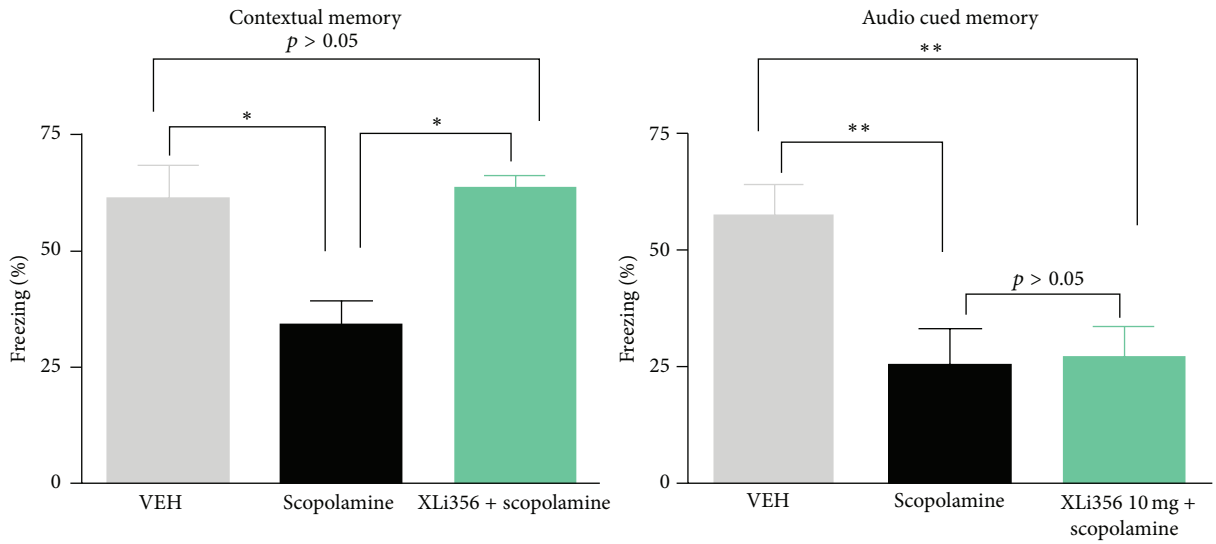


Figure 6: Visual and audio cued data for XLi-356 (**10**). This figure was modified from that in [22].

context (the cage) with a mild shock. XLi-356 (10 mg/kg) attenuated the impairment of memory returning the freezing to the levels on par with subjects dosed with vehicle. In audio cued memory the response was activated by sound, not the context. XLi-356 was not able to reverse this type of memory effect which is amygdala driven. A similar effect was observed for XLi-093 by Harris et al. [43]. XLi-093 is the most selective antagonist for $\alpha 5$ subtypes reported to date [13, 43] and is a very useful $\alpha 5$ antagonist used by many *in vivo* [22, 44, 45].

Molecular modeling combined with this knowledge was used to generate new lead compounds aimed at the development of $\alpha 5$-subtype selective positive and negative allosteric modulators to study cognition as well as amnesia mediated by the hippocampus. All of these compounds have been prepared based on the structure of current $\alpha 5$-subtype selective ligands synthesized in Milwaukee [46] (see Figures 4 and 5), as well as the binding affinity (15 nM)/selectivity of bivalent $\alpha 5$ antagonist XLi-093 (**4**) [13].

In efforts to enhance $\alpha 5$-selectivity in regards to cognition, Cook, Bailey, and Helmstetter et al. have employed RY-024 to study the hippocampal involvement in the benzodiazepine receptor in learning and anxiety [14, 19]. Supporting this Harris, DeLorey et al. show in mice that $\alpha 5$ NAMs (**1**) and RY-10 potently reversed scopolamine-induced memory impairment. These $\alpha 5$ NAMs provide insight as to how $GABA_A$Rs influence contextual memory, an aspect of memory affected in age associated memory impairment and especially in Alzheimer's disease [13, 62–64]. In addition, Savić et al. have used the $\alpha 1$ preferring antagonist, BCCt, in passive avoidance studies, in which midazolam's amnesic effects are shown to be due to interaction of agonist ligands at $\alpha 5$ in addition to $\alpha 1\beta 3\gamma 2$ BzR subtypes [24, 65].

3. PWZ-029: A Negative Allosteric Modulator

PWZ-029 (**1**) has been studied extensively as an $\alpha 5$-$GABA_A$R inverse agonist and in certain experimental models has been shown to enhance cognition. The binding data from three separate laboratories (Table 2) have all shown that it exhibits remarkable selectivity for the $\alpha 5$ subunit-containing receptors, all greater than 60-fold compared to the next subunit.

Table 2: Affinity of PWZ-029 (**1**); K_i (nM)[a].

Code	MW	$\alpha 1$	$\alpha 2$	$\alpha 3$	$\alpha 4$	$\alpha 5$	$\alpha 6$
PWZ-029 (**1**)	291.73	>300	>300	>300	ND	**38.8**	>300
PWZ-029 (**1**)	291.73	920	ND	ND	ND	**30**	ND
PWZ-029 (**1**)	291.73	362	180	328	ND	**6**	ND

[a]Data from three separate laboratories.

Electrophysiological efficacy testing done by Sieghart et al. in oocytes demonstrated that PWZ-029 (**1**) acts as a negative allosteric modulator at the $\alpha 5$-subunit, with a very weak agonist activity at the $\alpha 1$, $\alpha 2$, and $\alpha 3$ subunits (Figure 7). At a pharmacologically relevant concentration of 0.1 μM, PWZ-029 exhibits moderate negative modulation at the $\alpha 5$-subunit, while showing little or no effect at the $\alpha 1$, $\alpha 2$, or $\alpha 3$-subunits.

Milić et al. reported on the effects of PWZ-029 in the widely used novel object recognition test, which differentiates between the exploration time of novel and familiar objects. As shown by significant differences between the exploration times of the novel and familiar object (Figure 8(a)), as well as the respective discrimination indices (Figure 8(b)), all the three tested doses of PWZ-029 (2, 5 and 10 mg/kg) improved object recognition in rats after the 24 h delay period. Additionally, in the procedure with the 1 h delay between training and testing, the lowest of the tested doses of PWZ-029 (2 mg/kg) successfully reversed the deficit in recognition memory induced by 0.3 mg/kg scopolamine (Figure 9) [25].

The results of the described study showed for the first time that inverse agonism at $\alpha 5$-$GABA_A$ receptors may be efficacious in both improving cognitive performance in

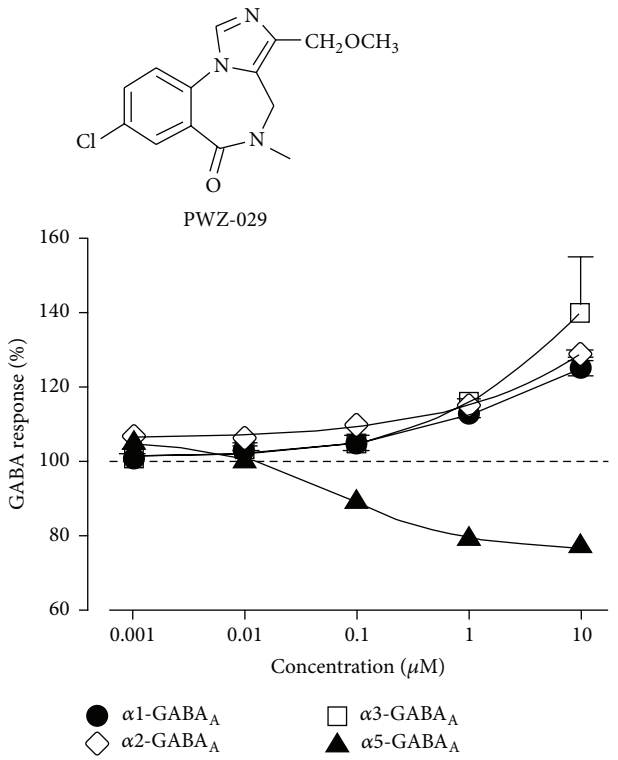


Figure 7: Oocyte electrophysiological data of PWZ-029 (**1**) [24].

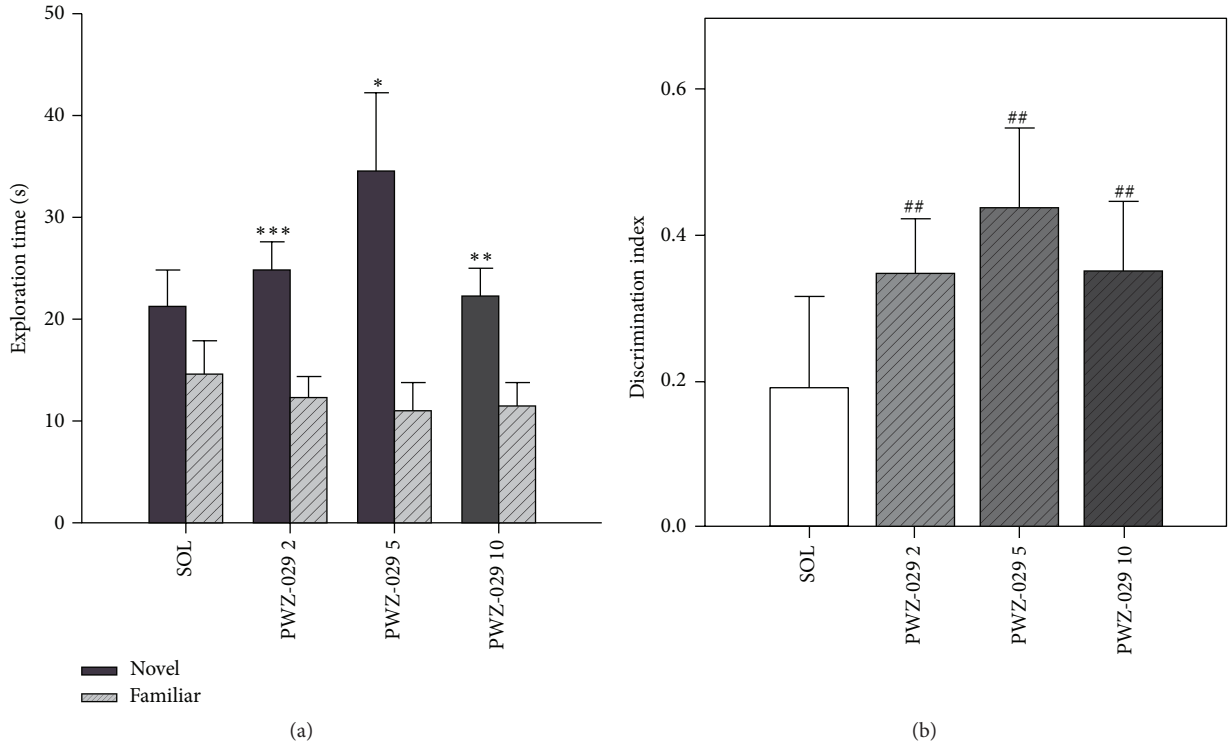


Figure 8: The effects of PWZ-029 (**1**) (2, 5 and 10 mg/kg) on (a) time exploring familiar and novel objects and (b) discrimination indices in the novel object recognition test using a 24 h delay (mean + SEM). Significant differences are indicated with asterisks (paired-samples t-test, novel versus familiar, $^{*}p < 0.05$, $^{**}p < 0.01$, $^{***}p < 0.001$). A significant difference from zero is indicated with hashes (one sample t-test, $^{\#\#}p < 0.01$). The number of animals per each treatment group was 10. SOL = solvent [25].

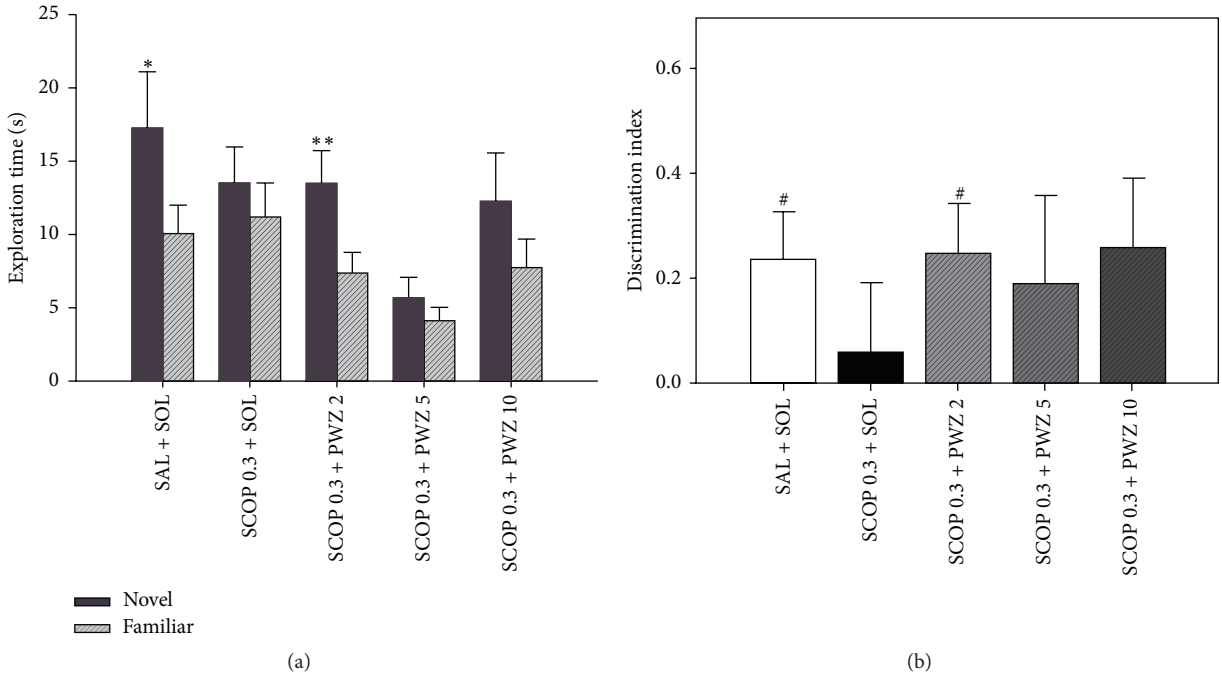


FIGURE 9: The effects of 0.3 mg/kg scopolamine (SCOP 0.3) and combination of 0.3 mg/kg scopolamine and PWZ-029 (**1**) (2, 5, and 10 mg/kg) on the rats' performance in the object recognition task after a 1 h delay: (a) time exploring familiar and novel objects and (b) discrimination index. Data are represented as mean + SEM. Significant differences are indicated with asterisks (paired-samples t-test, novel versus familiar, $^{*}p < 0.05$, $^{**}p < 0.01$). A significant difference from zero is indicated with hashes (one sample t-test, $^{\#}p < 0.05$). The number of animals per each treatment group was 12–15. SAL = saline, SOL = solvent [25].

unimpaired subjects and ameliorating cognitive deficits in pharmacologically impaired subjects, as assessed in two protocols of the same animal model [25].

In a recent by Rowlett et al. [26], negative allosteric modulator PWZ-029 was evaluated in female rhesus monkeys (n = 4) in an Object Retrieval test with Detours (ORD; Figure 10 for details). **1** was administered via i.v. catheters in ORD trained monkeys and evaluated for cognition enhancement. A successful trial was determined by the ability of the subject to obtain a food reward within a transparent box with a single open side, with varying degrees of difficulty ("easy" or "difficult" or "mixed" as a combination of both) based on food placement within the box. In "mixed" trials using PWZ-029, no significant results were observed when compared to vehicle (Figure 11(a)). "Difficult" trials, however, exhibited an increasing dose-dependent curve for successful trials (Figure 11(b)). These results were attenuated by a coadministration α5-antagonist XLi-093 (Figure 11(c)). PWZ-029 was also shown to dose-dependently reverse the cholinergic deficits that were induced by scopolamine (Figure 11(d)) [26].

These findings suggest that PWZ-029 can enhance performance on the ORD task, only under conditions in which baseline performance is attenuated. The effects of PWZ-029 were antagonized in a surmountable fashion by the selective α5-GABA$_A$ ligand, XLi-093, consistent with PWZ-029's effects being mediating via the α5-GABA$_A$ receptor. The results are consistent with the view that α5 GABA$_A$ receptors may represent a viable target for discovery of cognitive enhancing agents.

In addition, we have new data showing that modulation of α5-GABA$_A$Rs by PWZ-029 rescues Hip-dependent memory in an AD rat model [PMID: 23634826] as evidenced by a significant decrease in the latency to reach the hidden platform (memory probe trials) on spatial water maze task (Figure 12). Roche has employed a similar strategy at α5 subtypes and recently has a drug in the clinic to treat symptoms of dementia in Down syndrome patients. It is well known many Down syndrome patients develop Alzheimer's disease or a dementia with a very similar etiology. This is aimed at treating early onset Alzheimer's patients.

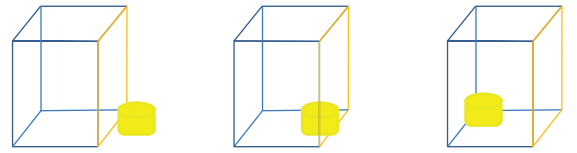
4. PWZ-029 Docking within $\alpha5\gamma2$ GABA$_A$ Receptor Subunit Homology Model

These studies with PWZ-029 led to the molecular model rendering of the compound docked within the $\alpha5\gamma2$ BzR subtype (Figures 13–16). The model figures have the following features:

The docking of PWZ-029 within the GABA$_A$/BzR shows the molecule bound and interacting with specific amino acids. The A and B rings of the benzodiazepine framework undergo a π-stacking interaction with HIS 105, indicated by the magenta coloring. At the other end of the molecule the methoxy lone pair and imidazole nitrogen lone pair act as a hydrogen bond acceptors with THR 210 and TYR 213, respectively. These interactions are shown by the aqua-blue descriptors.

Methods

ORD task examples of different types of trials



Easy-right outside Easy-right inside Difficult-right deep

Note: open side indicated with orange lines

Mixed trials		
Type of trial	Position of opening	Position of food
Easy	Left	Outside
Easy	Right	Outside
Easy	Front	Outside
Easy	Left	Outside
Easy	Front	Outside
Easy	Left	Inside
Difficult	Right	Deep
Easy	Left	Inside
Easy	Right	Inside
Easy	Left	Inside
Difficult	Right	Deep
Difficult	Left	Deep
Difficult	Right	Deep
Easy	Left	Inside
Easy	Right	Inside

Difficult trials		
Type of trial	Position of opening	Position of food
Difficult	Left	Deep
Difficult	Right	Deep
Difficult	Left	Deep
Difficult	Right	Deep
Difficult	Left	Deep
Difficult	Left	Deep
Difficult	Right	Deep
Difficult	Left	Deep
Difficult	Right	Deep
Difficult	Left	Deep
Difficult	Left	Deep
Difficult	Right	Deep
Difficult	Left	Deep
Difficult	Right	Deep
Difficult	Left	Deep

Subjects:

Rhesus monkeys (*Macaca mulatta*)

$N = 5$

Implanted with chronic i.v. catheters

Procedure:

Object retrieval with detours (ORD)

15 trials per session
Easy, difficult, and mixed trials (see diagram)

Tests:

(i) PWZ-029 · mixed trials

(ii) PWZ-029 · difficult trials

(iii) PWZ-029 + XLi-093 · difficult trials

(iv) Scopolamine · mixed trials

(v) PWZ-029 + scopolamine · mixed trials

Measurements: % correct trials—trial in which food is obtained with the first reach

Errors: barrier reaches (hand in contact with closed side of box) and incomplete trials (food grasped but dropped)

Figure 10: ORD methods and procedure [26].

5. Subtype Selective Agonists for $\alpha5$ $GABA_A$/Bz Receptors

Möhler has proposed that $\alpha5$ selective inverse agonists or $\alpha5$ selective agonists might enhance cognition [5, 13, 16–18, 86]. This is because of the extrasynaptic pyramidal nature of $\alpha5\beta3\gamma2$ subtypes, located almost exclusively in the hippocampus. Because of this, a new "potential agonist" which binds solely to $\alpha5\beta3\gamma2$ subtypes was designed by computer modeling (see Figure 17). This ligand (DM-I-81, **9**) has an agonist framework and binds only to $\alpha5\beta3\gamma2$ subtypes [13, 17, 18, 86]. The binding potency at $\alpha5$ subtypes is 176 nM. Although the 8-pendant phenyl of DM-I-81 was lipophilic and bound to the L_2 pocket, additional work on the 8-position of this scaffold has been abandoned and generally left as an acetylene or halide function, with a few exceptions. The steric bulk of the 8-phenyl moiety was felt detrimental to activity and potency which may have led to the weak binding affinity.

6. Alpha 5 Positive Allosteric Modulators in Schizophrenia

In addition to inverse agonists, a number of other $\alpha5$-$GABA_AR$ positive allosteric modulators (PAMs) have been synthesized. These compounds, such as SH-053-2′F-R-CH_3 (**2**), have been shown to decrease the firing rate of synapses controlling cognition and can be used to treat schizophrenia.

The following is reported by Gill, Cook, and Grace et al. [27–38].

There are a number of novel benzodiazepine-positive allosteric modulators (PAMs), selective for the $\alpha5$ subunit of the $GABA_A$ receptor, including SH-053-2′F-R-CH_3 (**2**), which has been tested for its ability to effect the output of the HPC (hippocampal) in methylazoxymethanol-(MAM-) treated animals, which can lead to hyperactivity in the dopamine system [27–38]. In addition, the effect of this compounds (**2**) response to amphetamine in MAM-animals on the hyperactive locomotor activity was examined. Schizophrenic-like symptoms can be induced into rats when treated prenatally with DNA-methylating agent, methylazoxymethanol, on gestational day (GD) 17. These neurochemical outcomes and changes in behavior mimic those found in schizophrenic patients. Systemic treatment with (**2**) resulted in a reduced number of spontaneously active DA (dopamine) neurons in the VTA (ventral tegmental area) of MAM animals (Figure 18) to levels seen in animals treated with vehicle (i.e., saline). To confirm the location of action, **2** was also directly infused into the ventral HPC (Figure 19)

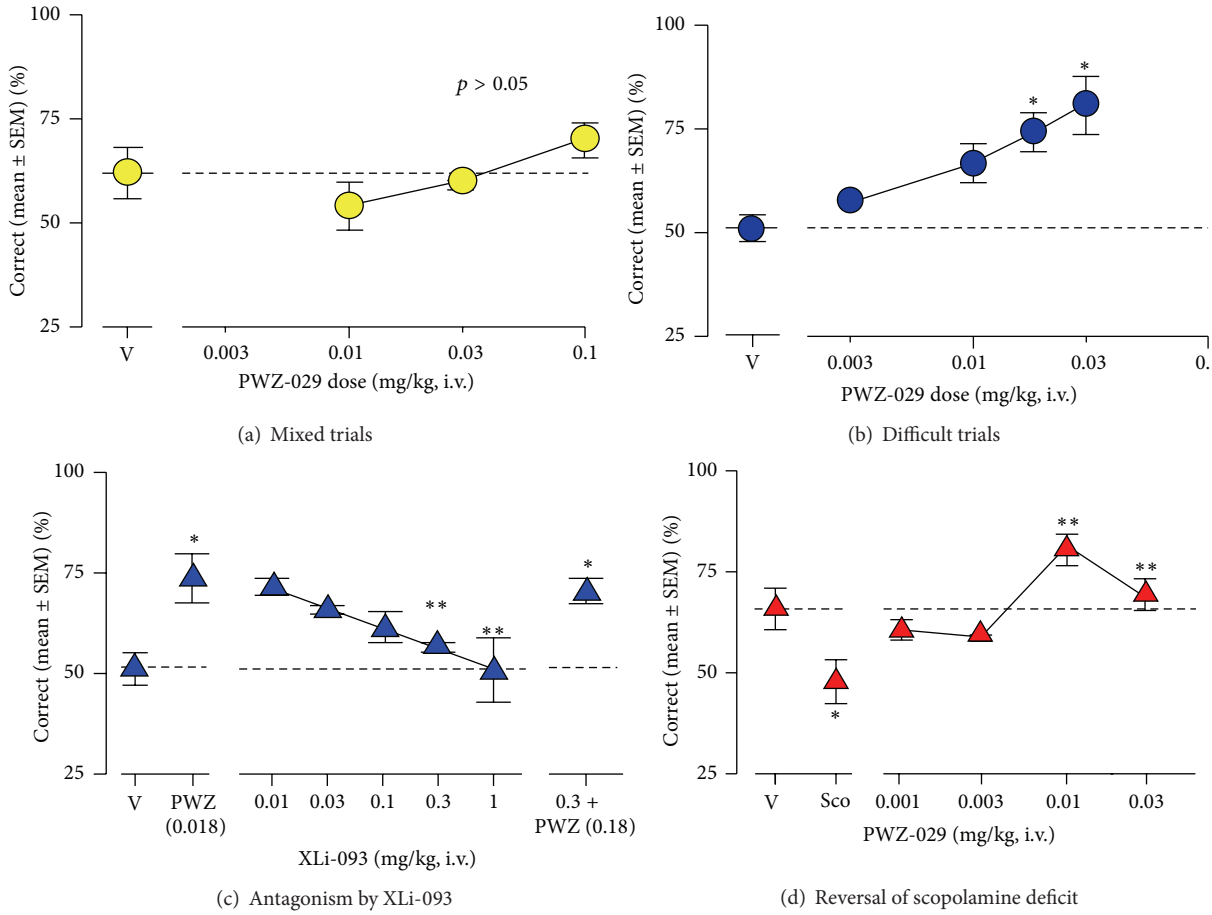


Figure 11: Cognitive-enhancing effects of PWZ-029 in the rhesus monkey Object Retrieval with Detours (ORD) task (n = 5 monkeys). (a) Effects of PWZ-029 on ORD tests consist of both easy and difficult trials: (b) PWZ-029 enhanced performance on the ORD task when tested with difficult trials only; (c) enhancement of ORD performance by 0.018 mg/kg of PWZ-029 was attenuated by the α5 $GABA_A$-preferring antagonist XLi-093 and this antagonism was surmountable by increasing the PWZ-029 dose; (d) PWZ-029 reversed performance impaired by 0.01 mg/kg of scopolamine [26]. $^{*}p < 0.05$ versus vehicle, $^{**}p < 0.05$ versus Scopolamine.

and was shown to have the same effect. Moreover, HPC neurons in both SAL and MAM animals showed diminished cortical-evoked responses following α5-$GABA_A$R PAM treatment. This study is important for it supports a treatment of schizophrenia that targets abnormal HPC output, which in turn normalized dopaminergic neuronal activity [27–38]. This is a novel approach to treat schizophrenia.

The pathophysiology of schizophrenia has identified hippocampal (HPC) dysfunction as a major mediator as reported by many including Anthony Grace [27–38]. This included morphological changes, reduced HPC volume, and GAD67 expression [27, 28] that have been reported after death in the brains of patients with schizophrenia. Both HPC activation and morphology changes have been identified that can precede psychotic symptoms or correlate with severity of cognitive deficits [29–33]. This has been shown in a cognitive test during baseline and activation.

Many animal models of schizophrenia were essential to behavioral pathology and have delivered new knowledge about the network disturbances that contribute to CNS disorder. This study shows that the offspring of MAM-treated animals showed both structural and behavioral abnormalities. These were consistent with those observed in patients with schizophrenia. The animals had reduced limbic cortical and HPC volumes with increased cell packing density and showed increased sensitivity to psychostimulants [34–36]. In addition, the startle response in prepulse inhibition was reduced in MAM-treated animals and deficits in latent inhibition were observed [35]. Furthermore, a pathological rise in spontaneous dopamine (DA) activity by the ventral tegmental area (VTA) was observed that can be attributed to aberrant activation within the ventral HPC [36]. It was suggested that reductions in parvalbumin- (PV-) stained interneurons might be the reason for the hyperactivation of the HPC and disruption of normal oscillatory activity in the HPC and cortex of MAM animals [38, 61]. At least this is the prevailing hypothesis at the moment put forth by many investigators (see references cited in [27–38]).

Selective α5-$GABA_A$R positive allosteric modulator (**2**) was successful in reversing the pathological increase in tonic DA transmission in methylazoxymethanol rats by targeting abnormal hippocampal activity. In addition, the α5-PAM was

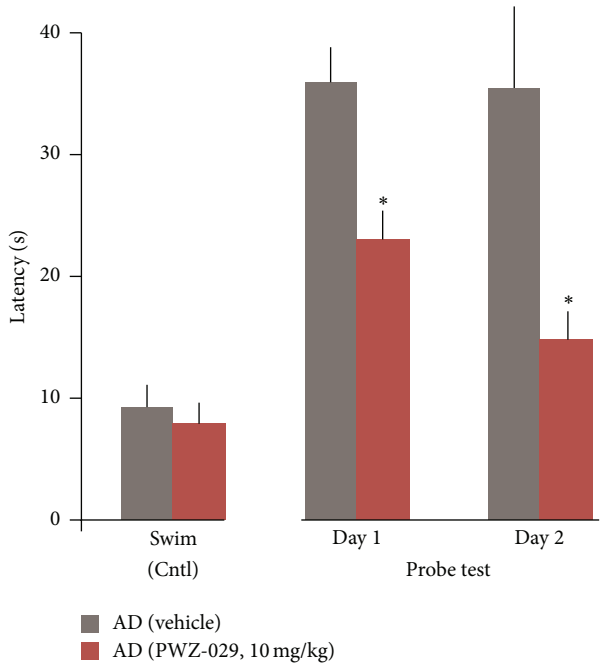


Figure 12: PWZ-029 rescues spatial memory deficits in AD model as evidenced by a decrease in the latency to reach the hidden platform (probe test) in the water maze relative to vehicle (VEH, $^{*}p < 0.05$).

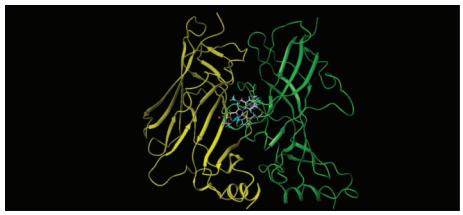


Figure 13: PWZ-029 docked within $\alpha 5\gamma 2$ BzR binding site (BS).

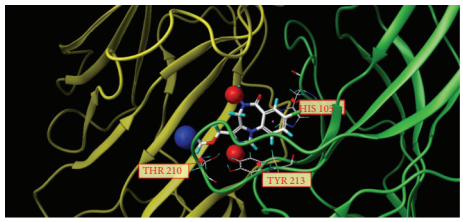


Figure 14: PWZ-029 docked with amino acid residues.

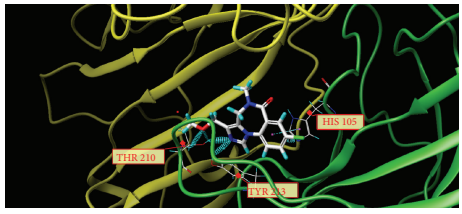


Figure 15: PWZ-029 docked with A.A. residue interactions.

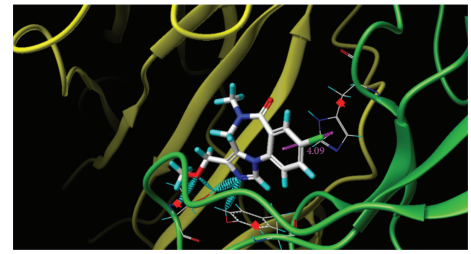


Figure 16: PWZ-029 docked with interactions. (1) HIS 105 π-stacking interaction with centroid of PWZ-029. (2) TYR 213 phenol OH hydrogen bonding to imidazole nitrogen lone pair. (3) THR 210 OH and lone pair on methoxy of PWZ029. (4) $\alpha 5$ ribbon being green. (5) $\gamma 2$ ribbon being yellow. (6) Hydrogen bonding being aqua blue. (7) π-stacking being magenta.

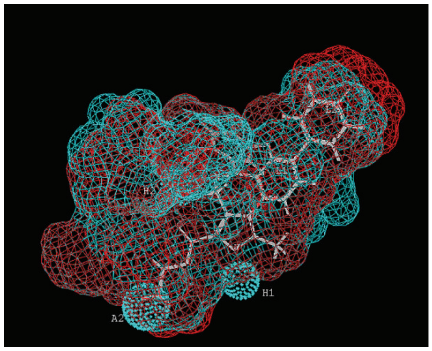
able to reduce the behavioral sensitivity to psychostimulants observed in MAM rats (Figures 20 and 21). This suggests that novel $\alpha 5$-partial allosteric modulators should be effective in alleviating dopamine-mediated psychosis. However, if this drug can also restore rhythmicity within HPC-efferent structure, it may also affect other aspects of this disease state such as cognitive disabilities and negative symptoms. This study, using the MAM-model to induce symptoms of schizophrenia, shows that the use of $\alpha 5$-$GABA_AR$ targeting compounds could be an effective treatment in schizophrenic patients. The selective targeting solely of $\alpha 5\beta 3\gamma 2$ subunits, as opposed to unselective BZDs such as diazepam, could provide relief from the psychotic symptoms without producing adverse effects such as sedation [27–38].

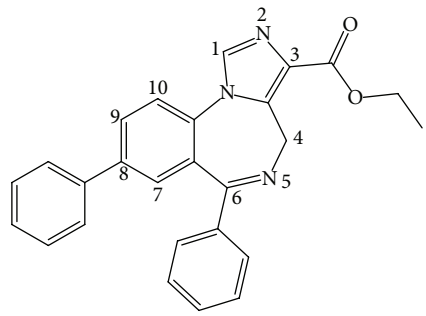
As reported by Gill, Grace et al. [36, 38, 47–61].

Often initial antipsychotic drug treatments (APD) for schizophrenia are ineffective, requiring a brief washout period prior to secondary treatment. The impact of withdrawal from initial APD on the dopamine (DA) system is unknown. Furthermore, an identical response to APD therapy between normal and pathological systems should not be assumed. In another study by Gill, Grace et al., $\alpha 5$ positive allosteric modulator SH-053-2′F-R-CH_3 (**2**) was used in the MAM neurodevelopmental model of schizophrenia which was used to study impact of withdrawal from repeated haloperidol (HAL) on the dopamine system [36, 38, 47–61].

The following studies were designed to provide insight as to why a new drug to treat schizophrenia may be effective in Phase II clinical trials but fail in Phase III because of the large number of patients required for the study. Many of these patients in Phase III studies have altered neuronal pathways in the CNS because of long-term treatment with antipsychotics (sometimes 10–20 years) [36, 38, 47–61].

Importantly, spontaneous dopamine activity reduction was observed in saline rats withdrawn from haloperidol with an enhanced locomotor response to amphetamine, indicating the development of dopamine supersensitivity. In addition, PAM treatment, as well as ventral HPC inactivation, removed the depolarization block of DA neurons in withdrawn HAL treated SAL rats. In contrast, methylazoxymethanol rats withdrawn from HAL displayed a reduction in spontaneous dopamine activity and enhanced locomotor response that





9

DM-I-81 aligned in the included volume of the pharmacophore/receptor model for the $\alpha1\beta3\gamma2$ (blue) and $\alpha5\gamma3\beta2$ (red) subtypes

Binding data	$\alpha1$	$\alpha2$	$\alpha3$	$\alpha4$	$\alpha5$	$\alpha6$
DM-I-81 (**9**)	>2000	>2000	>2000	>2000	176	>2000

FIGURE 17: The $\alpha5$ selective agonist DM-I-81 (**9**), bound within the $\alpha1$ and $\alpha5$ subtypes. Binding data shown as K_i (nM).

was unresponsive to PAM treatment with SH-053-2′F-R-CH_3 or ventral HPC inactivation [36, 38, 47–61].

Prior HAL treatment withdrawal can restrict the efficacy of subsequent pharmacotherapy in the MAM model of schizophrenia. This is an extremely important result indicating that testing a new drug for schizophrenia in humans treated for years with both typical and atypical antipsychotics may result in a false negative with regard to treatment. Studies that support this hypothesis follow here [36, 38, 47–61].

Novel therapeutics for the treatment of schizophrenia that exhibit initial promise in preclinical trials often fail to demonstrate sufficient efficacy in subsequent clinical trials. In addition, relapse or noncompliance from initial treatments is common, necessitating secondary antipsychotic intervention [47, 48]. Studies have shown that between 49 and 74% of schizophrenia patients discontinue the use of antipsychotic drug (APD) treatments within 18 months due to adverse side-effects [48, 49]. Current pharmacotherapies for schizophrenia target the pathological increase in dopamine system activity, as mentioned above. Common clinical practice for secondary antipsychotic application involves a brief withdrawal period from the initial APD. Unfortunately, the success of even secondary treatments is far from being optimal with the rehospitalization of patients being a common occurrence. The impact of repeated antipsychotic treatment and subsequent withdrawal on the dopamine system has not been adequately assessed [36, 38, 47–61].

As indicated above, schizophrenia is a complex chronic psychiatric illness characterized by frequent relapses despite ongoing treatment. The search for more effective pharmacotherapies for the treatment of schizophrenia continues unabated. It is not uncommon for novel pharmaceuticals to demonstrate promise in preclinical trials but fail to show an adequate response in subsequent clinical trials. Indeed, evaluating the benefits of one APD versus another is complicated by clinical trials beset with high attrition rates and poor efficacy in satisfactorily reducing rehospitalization [47, 49–52].

Previous work from the Gill, Grace et al.'s laboratory [36, 38, 47–61] with the MAM model of schizophrenia has identified a potential novel therapeutic, a $\alpha5$GABAAR PAM. The dopamine system pathology in the MAM model is likely the result of excessive output from the ventral HPC [36]. The $\alpha5$GABAAR PAM was identified as a potential therapeutic due to the relatively selective expression of $\alpha5$GABAAR in the ventral HPC and its potential for reducing HPC activity [53–60]. When either administered systemically or directly infused into the ventral HPC, the $\alpha5$GABAAR PAM (SH-053-2′F-R-CH_3) was effective in reducing the dopamine system activation in MAM rats [38]. Anthony Grace, Gill et al. showed $\alpha5$GABAAR PAM treatment was also effective in reducing the enhanced behavioral response to amphetamine in MAM rats, as stated above. Data from the present study sought to delineate whether the $\alpha5$GABAAR PAM (SH-053-2′F-R-CH_3) would remain effective in MAM rats withdrawn from prior neuroleptic treatment, a common occurrence in the patient population. In both SAL and MAM rats, there was a reduction in the spontaneous activity of dopamine neurons in the VTA after 7 days withdrawal from repeated HAL treatment. However, MAM rats continued to exhibit a greater activation of the dopamine system in comparison to SAL rats. Treatment with the $\alpha5$GABAAR PAM was no longer effective in reducing the activity of dopamine neurons in the VTA in withdrawn HAL treated MAM rats. In contrast, $\alpha5$GABAAR PAM treatment in the withdrawn HAL treated SAL rats instead increased the spontaneous activity of dopamine in the VTA (Figures 22–25) [36, 38, 47–61].

Similar to the effects seen following $\alpha5$GABAAR PAM treatment, ventral HPC inactivation in withdrawn HAL treated SAL rats restored normal dopamine system activity by increasing the number of spontaneously active dopamine neurons. The disparate effect of withdrawal from HAL on

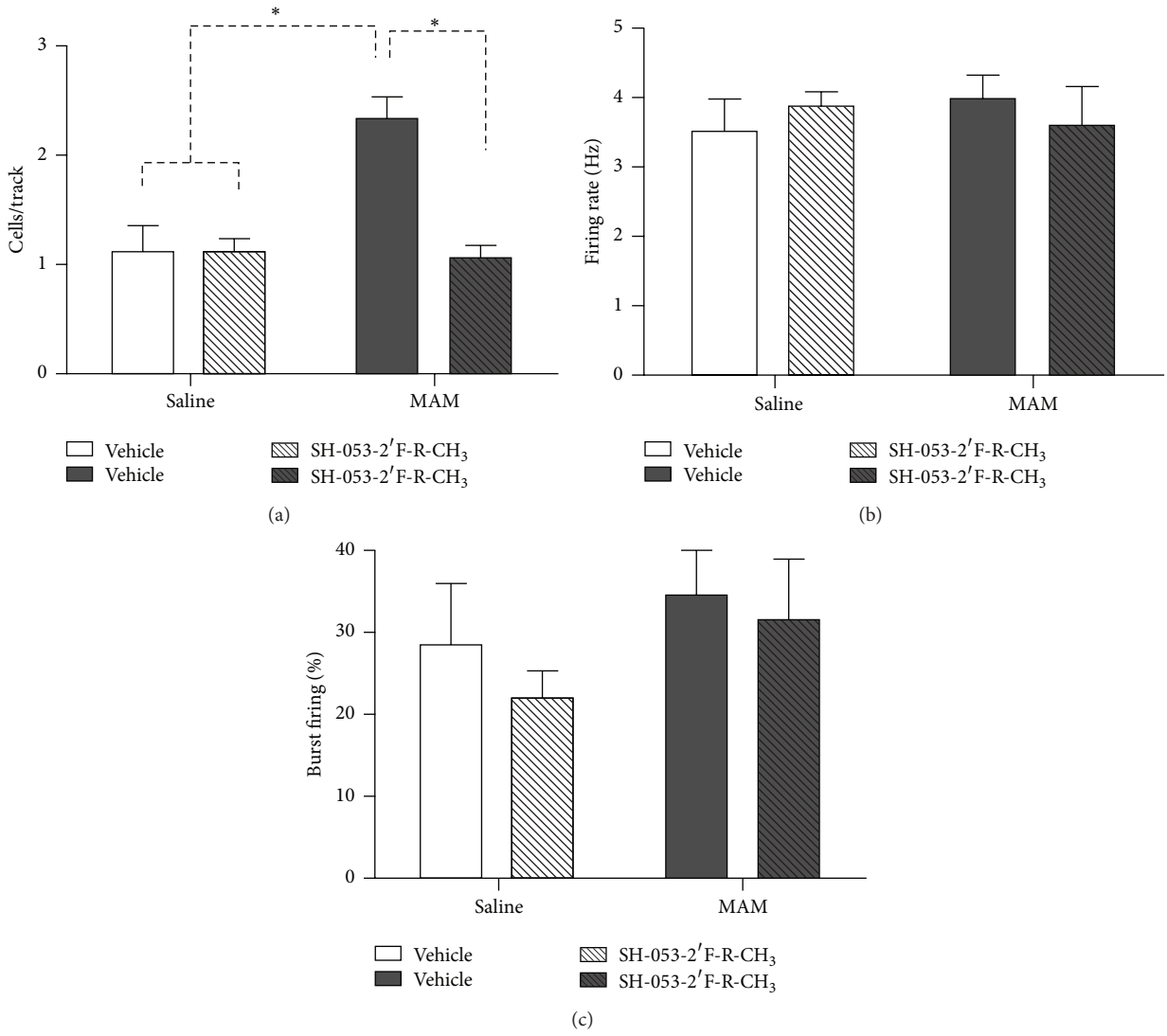


FIGURE 18: Treatment with SH-053-2′F-R-CH_3 (0.1 mg/kg, i.v.; patterned bars) normalizes the aberrant increase in the number of spontaneously firing dopamine neurons (expressed as cells/track) in methylazoxymethanol acetate- (MAM-) treated animals (a). There was no effect of SH-053-2′F-R-CH_3 treatment in control animals (open bars, (a)–(c)) or on firing rate and burst activity in MAM animals (dark bars; (b)-(c)) ($^*p < 0.05$, two-way ANOVA, Holm-Sidak *post hoc*; $N = 5$–7 rats/group) [27–38].

the dopamine system between SAL and MAM rats provides a vital clue for the inconsistencies between preclinical trials for novel therapeutics that utilize normal subjects and subsequent clinical trials in a patient population [36, 38, 47–61].

The data suggests underlying dopamine system pathology alters the impact of withdrawal from prior repeated HAL in the MAM model of schizophrenia. In addition, subsequent novel APD treatment loses efficacy following withdrawal from repeated HAL in MAM animals. This certainly has relevance to Phase III clinical trials of new drugs to treat schizophrenia [36, 38, 47–61].

7. $GABA_A$ α5 Positive Allosteric Modulators Relax Airway Smooth Muscle

Emala, Gallos, et al. [66–75] have found that novel α5-subtype selective $GABA_A$ positive allosteric modulators relax airway smooth muscle from rodents and humans. The clinical need for new classes of bronchodilators for the treatment of bronchoconstrictive diseases such as asthma remains a major medical issue. Few novel therapeutics have been approved for targeting airway smooth muscle (ASM) relaxation or lung inflammation in the last 40 years [66]. In fact, several asthma-related deaths are attributed, in part, to long-acting β-agonists (LABA) [67]. Adherence to inhaled corticosteroids, the first line of treatment for airway inflammation in asthma, is very poor [68, 69]. Therapies that break our dependence on β-agonism for ASM relaxation would be a novel and substantial advancement.

These ASM studies were undertaken due to a pressing clinical need for novel bronchodilators in the treatment of asthma and other bronchoconstrictive diseases such as COPA. There are only three drug classes currently in clinical

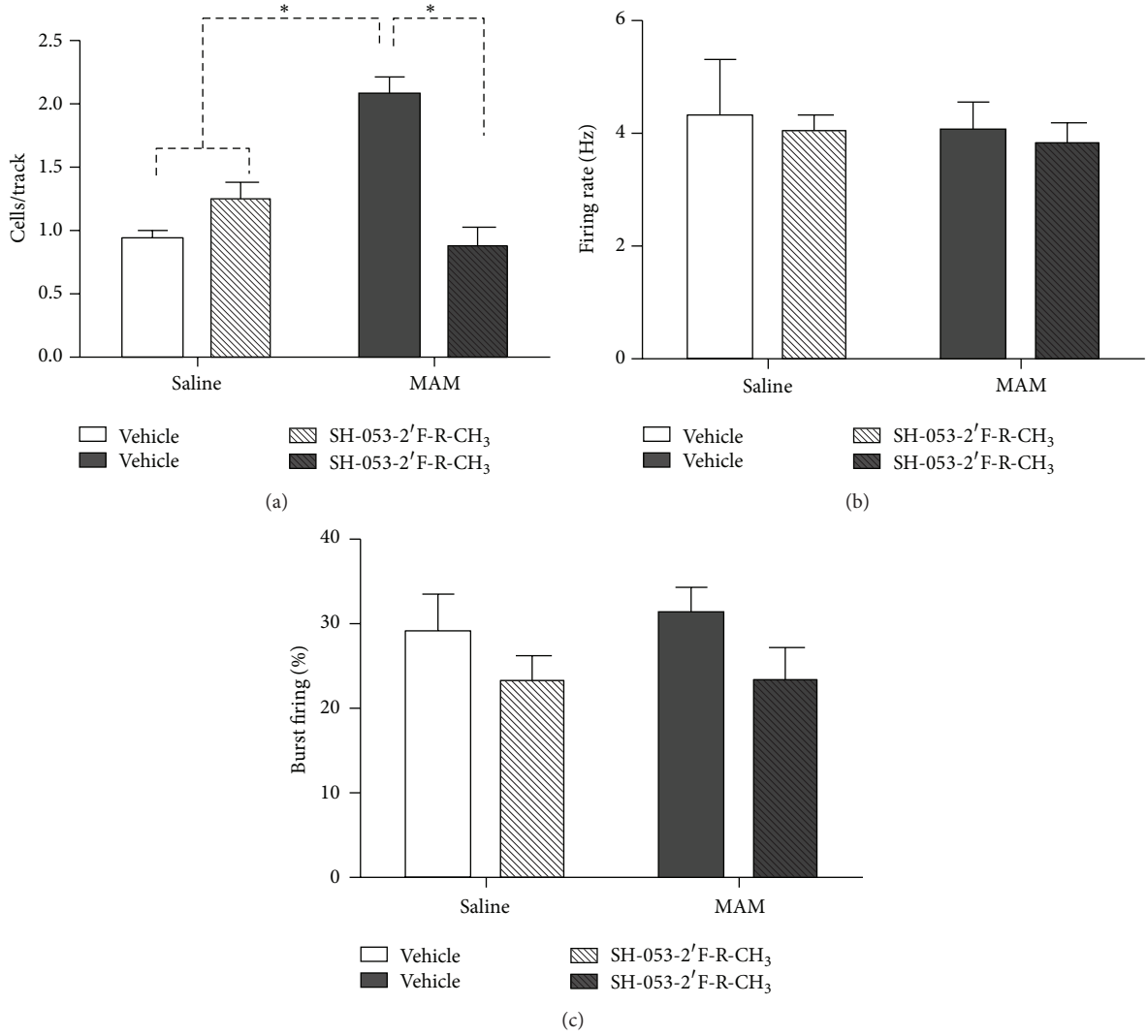


Figure 19: Hippocampal (HPC) infusion of SH-053-2′F-R-CH_3 (1 μM/side; patterned bars) normalizes the aberrant increase in the number of spontaneously firing dopamine neurons (expressed as cells/track) in methylazoxymethanol acetate- (MAM-) treated animals (a). There was no effect of SH-053-2′F-R-CH_3 treatment in control animals (open bars, (a)–(c)) or on firing rate in MAM animals (dark bars; (b)). Hippocampal (HPC) infusion of SH-053-2′F-R-CH_3 significantly reduced the percentage of spikes occurring in bursts of dopamine (DA) neurons in MAM and control animals (c) ($^*p < 0.05$, two-way ANOVA, Holm-Sidak *post hoc*; $N = 7$ rats/group) [27–38].

use as acute bronchodilators in the United States (methylxanthines, anticholinergics, and β-adrenoceptor agonists) [70]. Thus, a novel therapeutic approach that would employ cellular signaling pathways distinct from those used by these existing therapies involves modulating airway smooth muscle (ASM) chloride conductance via $GABA_A$ receptors to achieve relaxation of precontracted ASM [71, 72]. However, widespread activation of all $GABA_A$ receptors may lead to undesirable side effects (sedation, hypnosis, mucus formation, etc.). Thus, a strategy that selectively targets a subset of $GABA_A$ channels, those containing α subunits found to be expressed in airway smooth muscle, may be a first step in limiting side effects. Since human airway smooth muscle contains only α4 or α5 subunits [72], ligands with selectivity for these subunits are an attractive therapeutic option. Concern regarding nonselective $GABA_A$ receptor activation is not limited to the airway or other peripheral tissues. $GABA_A$ receptor ligands are classically known for their central nervous system effects of anxiolysis, sedation, hypnosis, amnesia, anticonvulsion, and muscle relaxant effects. Such indiscriminate activation of $GABA_A$ receptors in the CNS is exemplified by the side effects of classical benzodiazepines (such as diazepam) which were the underpinning for the motivation of a search for benzodiazepine (BZD) ligands that discriminate among the α subunits of $GABA_A$ receptors [73–75].

A novel approach to identify novel benzodiazepine derivatives to selectively target $GABA_A$ channels containing specific α subunits was developed by Cook et al. in the 1980s that employed a pharmacophore receptor model based on the binding affinity of rigid ligands to BDZ/$GABA_A$ receptor sites (as reviewed in 2007 [23]). From this series

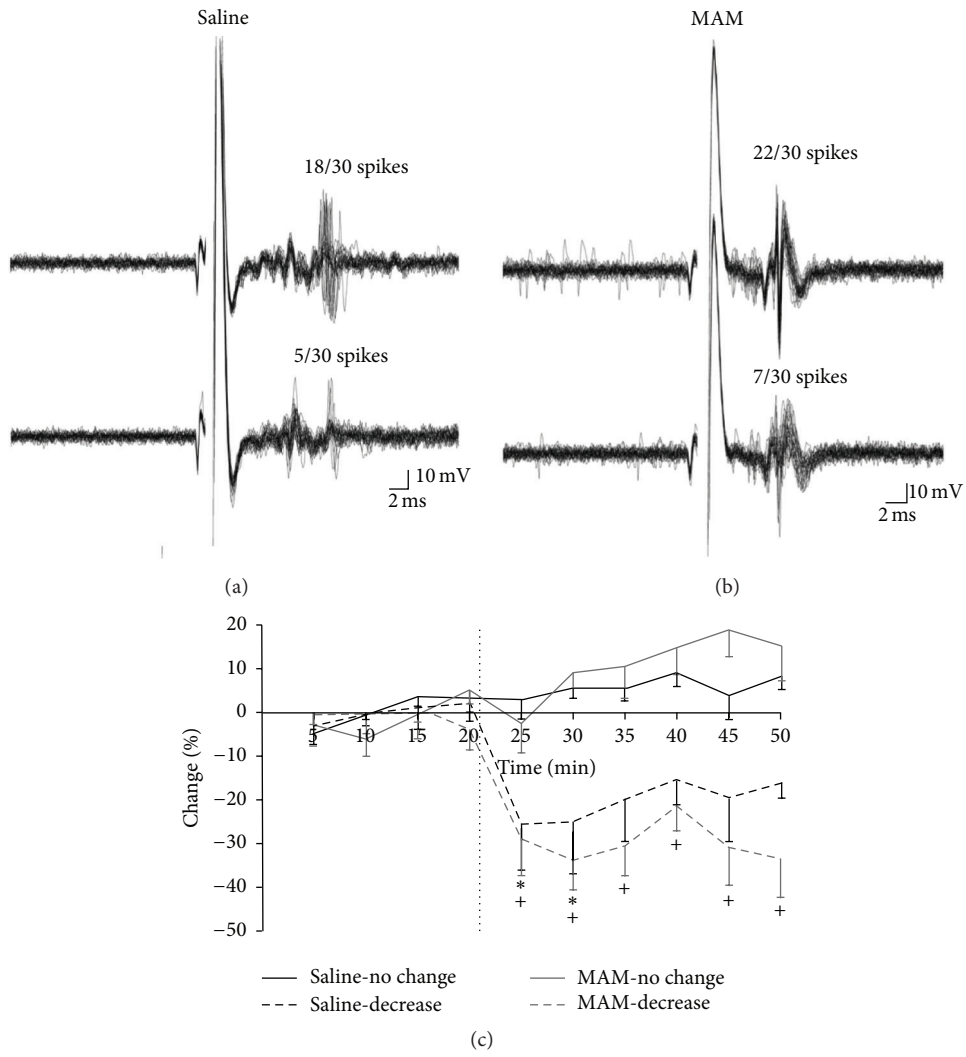


Figure 20: Extracellular recording traces illustrate the reduction in evoked responses in the ventral hippocampal (HPC) to entorhinal cortex stimulation in both MAM- and saline-treated animals (a, b). Treatment with SH-053-2′F-R-CH_3 (0.1 mg/kg, i.v.) decreases the evoked excitatory response (dashed lines) of ventral HPC neurons to entorhinal cortex stimulation in both MAM- and saline-treated animals (c) ($^{*}p < 0.05$ for saline and $^{+}p < 0.05$, two-way repeated measures ANOVA, Holm-Sidak *post hoc*) [27–38].

of receptor models for $\alpha_{1-6}\beta3\gamma2$ subtypes a robust model for $\alpha5$ subtype selective ligands emerged, the result of which included the synthesis of a novel $\alpha5\beta3\gamma2$ partial agonist modulator, SH-053-2′F-R-CH_3 (**2**). The discovery of this and related ligands selective for $\alpha5$ BDZ/$GABA_A$-ergic receptors and the realization that only $\alpha4$ and $\alpha5$ subunits are expressed in $GABA_A$ channels on human airway smooth muscle yielded an ideal opportunity for targeting these $\alpha5$-subunit containing $GABA_A$ channels for bronchorelaxation [66–75].

The $GABA_A\alpha5$ subunit protein was first localized to the ASM layer of human trachea while costaining for the smooth muscle specific protein α actin (Figure 26). The first panel of Figure 26 shows $GABA_A$ $\alpha5$ protein stained with fluorescent green and blue fluorescent nuclear staining (DAPI). The second panel is the same human tracheal smooth muscle section simultaneously stained with a protein specific for smooth muscle, α actin, and the third panel is a merge of the first two panels showing costaining of smooth muscle with $GABA_A$ $\alpha5$ and α actin proteins. The fourth panel is a control omitting primary antibodies but including nuclear DAPI staining [66–75].

After demonstrating the protein expression of $GABA_A$ receptors containing the $\alpha5$ subunit, functional studies of isolated airway smooth muscle were performed in tracheal airway smooth muscle from two species. Human airway smooth muscle suspended in an organ bath was precontracted with a concentration of acetylcholine that was the EC_{50} concentration of acetylcholine for each individual airway smooth muscle preparation. The induced contraction was then relaxed with a β-agonist (isoproterenol) in the absence or presence of the $GABA_A$ $\alpha5$ ligand SH-053-2′F-R-CH_3 (**2**). Figure 27(a) shows that the amount of relaxation

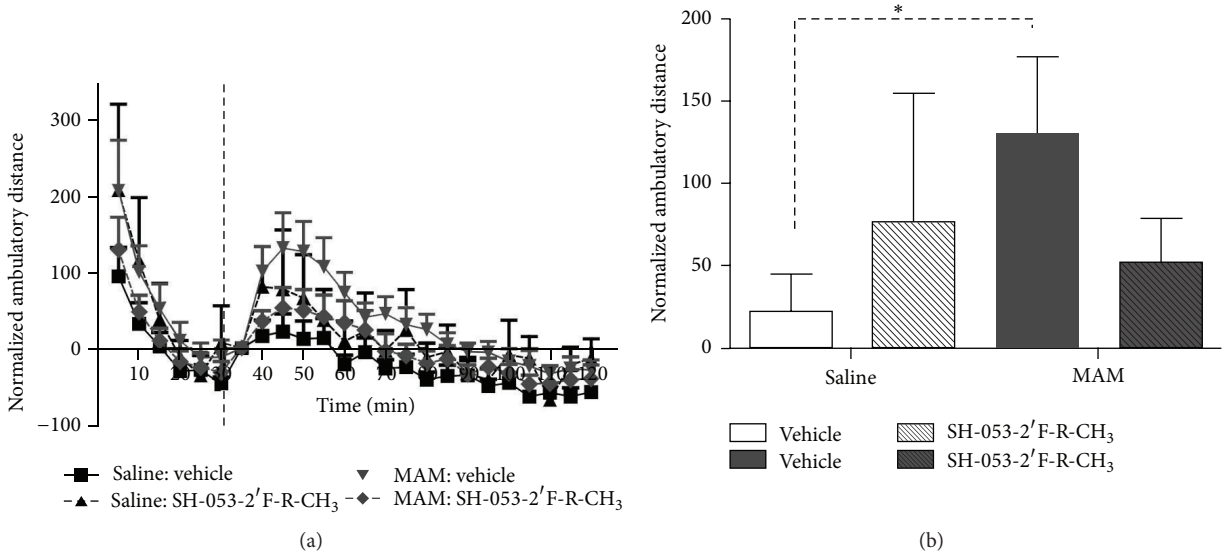


FIGURE 21: Treatment with SH-053-2′F-R-CH_3 (10 mg/kg, i.p.) reduced the aberrant increased locomotor response to D-amphetamine (0.5 mg/kg i.p.) observed in MAM rats (a). MAM animals demonstrated a significantly larger peak locomotor response than both saline-treated animals and MAM animals pretreated with the alpha-5 PAM (b) (there was a significant difference between MAM-vehicle and all other groups, $^{*}P < 0.05$, two-way repeated measures ANOVA, Holm-Sidak *post hoc*) [27–38].

induced by 10 nM isoproterenol was significantly increased if 50 μM SH-053-2′F-R-CH_3 (**2**) was also present in the buffer superfusing the airway smooth muscle strip. Studies were also performed in airway smooth muscle from another species, guinea pig, that measured direct relaxation of a different contractile agonist, substance P. As shown in Figure 27(b), the amount of remaining contractile force 30 minutes after a substance P-induced contraction was significantly reduced in airway smooth muscle tracheal rings treated with SH-053-2′F-R-CH_3 (**2**) [66–75].

Following these studies in intact airway smooth muscle, cell based studies were initiated in cultured human airway smooth muscle cells to directly measure plasma membrane chloride currents and the effects of these currents on intracellular calcium concentrations. SH-053-2′F-R-CH_3 (**2**) induced a Cl^- current *in vitro* using conventional whole cell patch clamp techniques [66–75]. These electrophysiology studies were then followed by studies to determine the effect of these plasma membrane chloride currents on intracellular calcium concentrations following treatment of human airway smooth muscle cells with a ligand whose receptor couples through a Gq protein pathway, a classic signaling pathway that mediates airway smooth muscle contraction.

SH-053-2′F-R-CH_3 (**2**) attenuated an increase in intracellular calcium concentrations induced by a classic Gq-coupled ligand, bradykinin (Figure 28(a)) [66–75]. The attenuation by SH-053-2′F-R-CH_3 (**2**) was significantly blocked by the $GABA_A$ antagonist gabazine (Figure 28(b)) indicating that SH-053-2′F-R-CH_3 (**2**) was modulating $GABA_A$ receptors for these effects on cellular calcium [66–75].

The major findings of these studies are that human airway smooth muscle expresses α5 subunit containing $GABA_A$ receptors that can be pharmacologically targeted by a selective agonist. The $GABA_A$ α5 subunit selective ligand SH-053-2′F-R-CH_3 (**2**) relaxed intact guinea pig airway smooth muscle contracted with substance P and augmented β-agonist-mediated relaxation of intact human airway smooth muscle. The mechanism for these effects was likely mediated by plasma membrane chloride currents that contributed to an attenuation of contractile-mediated increases in intracellular calcium, a critical event in the initiation and maintenance of airway smooth muscle contraction [66–75].

8. Recent Discovery of Alpha 5 Included Volume Differences: L_4 Pocket as Compared to Other Bz/GABAergic Subtypes

The findings in both the MAM-model of schizophrenia and the relaxation of airway smooth muscle have led to the study of SH-053-2′F-R-CH_3 and related compounds bound within the α5-$GABA_A$/BzR (Figure 29). The SH-053-R-CH_3 (**15**) and SH-053-S-CH_3 (**16**) isomers have been previously described [23]. These compounds along with SH-053-2′F-R-CH_3 and SH-053-2′F-S-CH_3 have been tested for binding affinity and show selectivity for the α5-subunit (Table 3).

From examination of Figure 30 and Tables 3 and 4, it is clear the (R)-isomers bound to the α5 subtype while the (S)-isomers were selective for α2/α3/α5 subtypes.

From this data, these compounds were then used in examining the α5-binding pocket, most specifically the fluoroseries. In regard to molecular modeling, depicted in Figure 30 is the included volume and ligand occupation of the SH-053-2′F-S-CH_3 (**17**) and SH-053-2′F-R-CH_3 (**2**) enantiomers in the α5 subtype as well as the α2 subtype. It

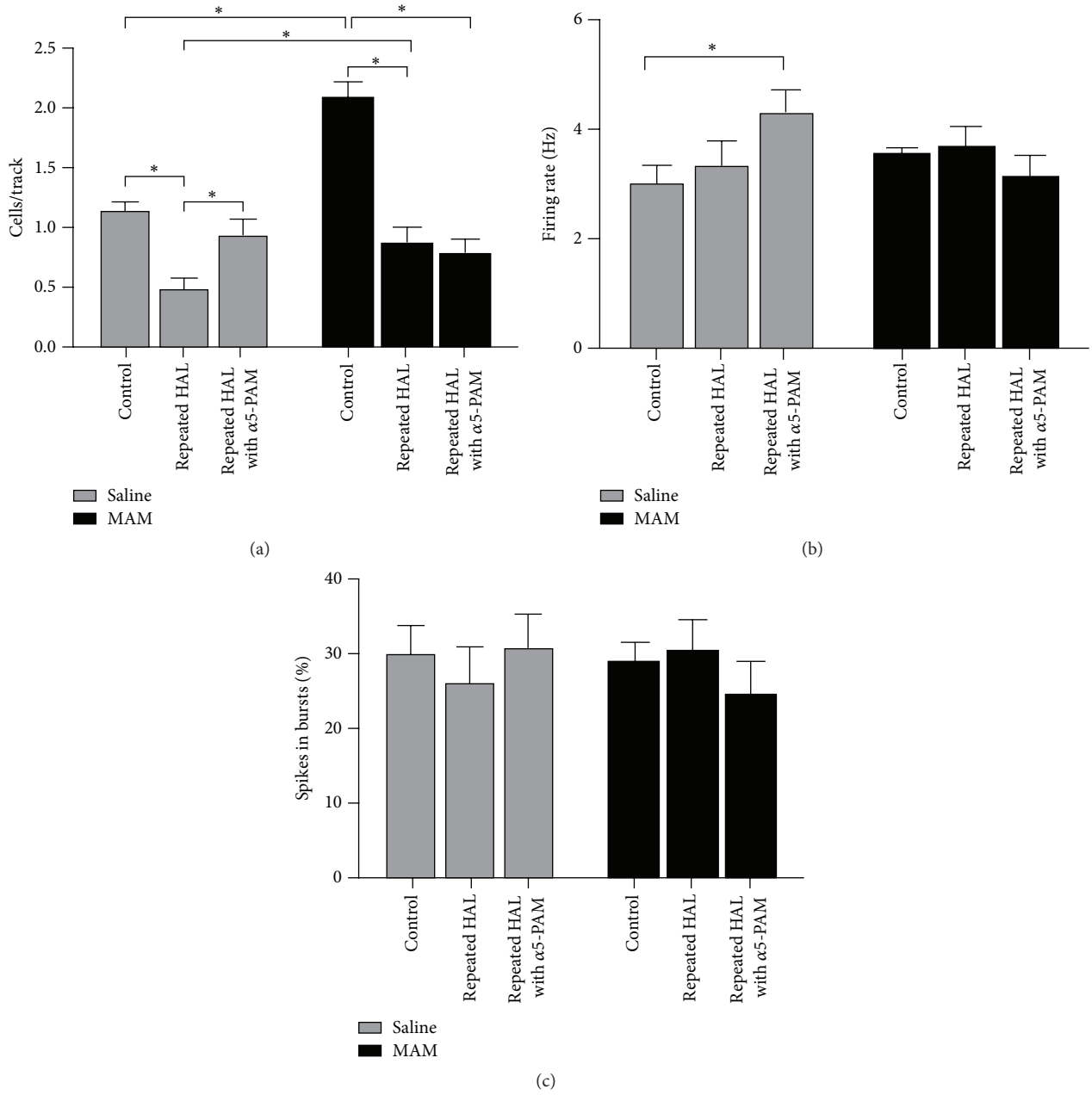


FIGURE 22: Repeated haloperidol treatment caused a reduction in the number of spontaneously active dopamine neurons in both SAL and MAM rats injected with vehicle compared to untreated control animals. Treatment with SH-053-2′F-R-CH_3 (0.1 mg/kg, i.v.) reversed the haloperidol-induced reduction in cells/track in SAL, but not MAM, rats (a). Repeated haloperidol treatment had no effect on the firing rate of dopamine neurons recorded in SAL or MAM rats treated with vehicle. However, SH-053-2′F-R-CH_3 caused an increase in firing rate of dopamine neurons in repeatedly haloperidol-treated SAL rats (b). Repeated haloperidol treatment, as well as SH-053-2′F-R-CH_3 injection, had no impact on the percentage of spikes occurring in bursts for dopamine neurons recorded in SAL and MAM rats (c) [36, 38, 47–61]. $^*p < 0.05$.

is clear a new pocket (L_4) has been located in the α5 subtype permitting **2** as well as **17** to bind to the α5 subtype. Examination of both ligands in the α2 subtype clearly illustrates the analogous region in the α2 subtype is not present and thus does not accommodate **2** for the pendant phenyl which lies outside the included volume in the space allocated for the receptor protein itself [23].

9. BzR GABA(A) Subtypes

In terms of potency, examination of the values in Table 4 [87], it is clear the R-isomer (**2**) shows more selectivity towards the α5-subunit, while the S-isomer (**17**) is potent at the α2/3/5 subunits. It is important, as postulated earlier [23], that the major difference in GABA(A)/Bz receptors subtypes stems

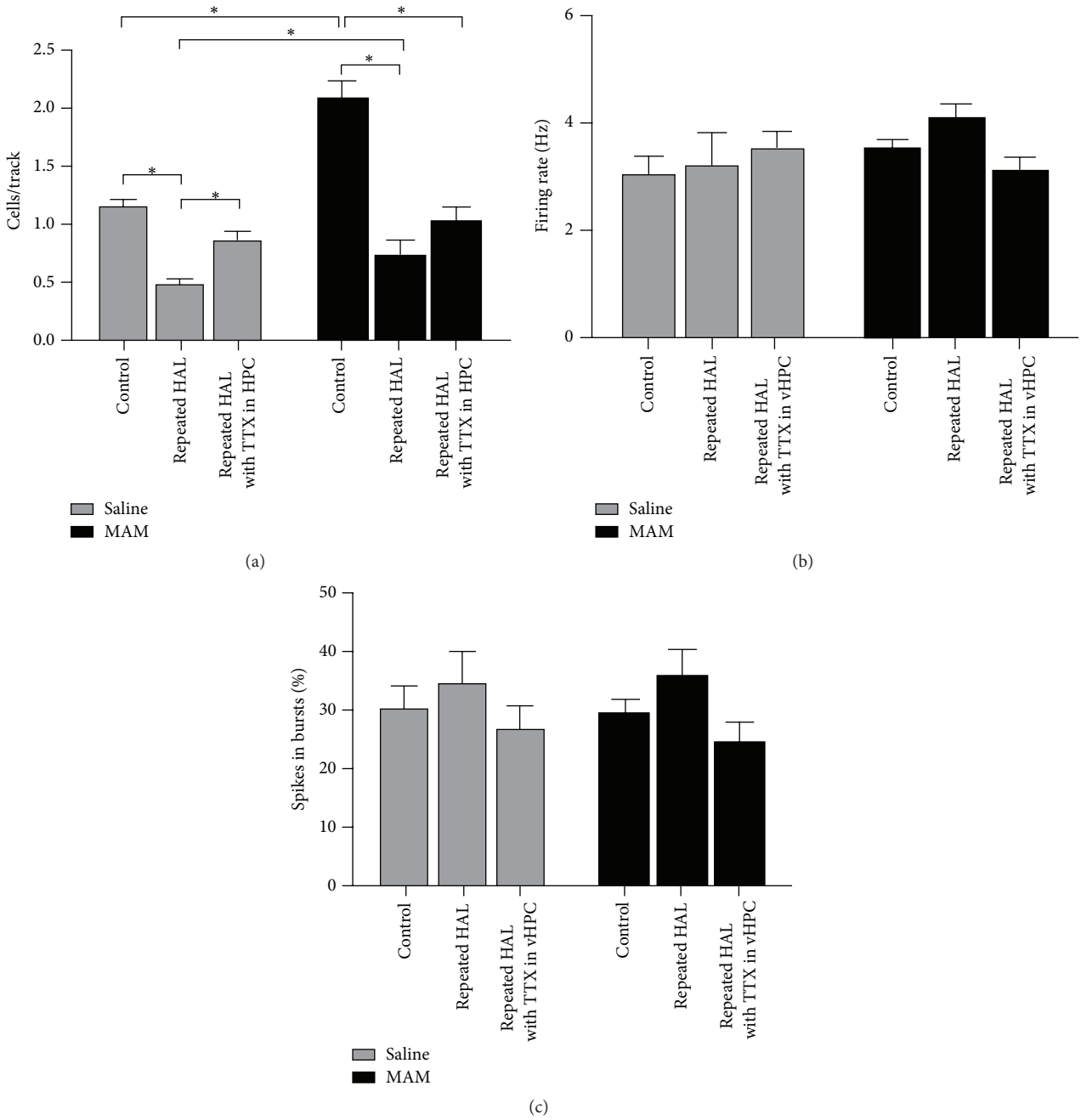


Figure 23: Repeated haloperidol treatment caused a reduction in the number of spontaneously active dopamine neurons in both SAL and MAM rats microinfused with vehicle in the ventral HPC compared to untreated control animals. Infusion of TTX in the ventral HPC reversed the haloperidol-induced reduction in cells/track in SAL, but not MAM, rats (a). Repeated haloperidol treatment had no effect on the firing rate of dopamine neurons recorded in SAL or MAM rats infused with vehicle or TTX in the ventral HPC (b). Repeated haloperidol treatment had no effect on the percentage of spikes occurring in bursts for dopamine neurons recorded in SAL or MAM rats infused with vehicle or TTX in the ventral HPC (c) [36, 38, 47–61]. $^{*}p < 0.05$.

from differences in asymmetry in the lipophilic pockets L_1, L_2, L_3, L_4, and L_{Di} in the pharmacophore/receptor model and indicates even better functional selectivity is possible with asymmetric BzR ligands.

The synthetic switching of chirality at the C-4 position of imidazobenzodiazepines to induce subtype selectivity was successful. Moreover, increase of the potency of imidazobenzodiazepines can be achieved by substitution of the 2′-position hydrogen atom with an electron rich atom (fluorine) on the pendant phenyl ring in agreement with Haefely et al. [88], Fryer [89, 90], and our own work [22, 91]. The biological data on the two enantiomeric pairs of benzodiazepine ligands

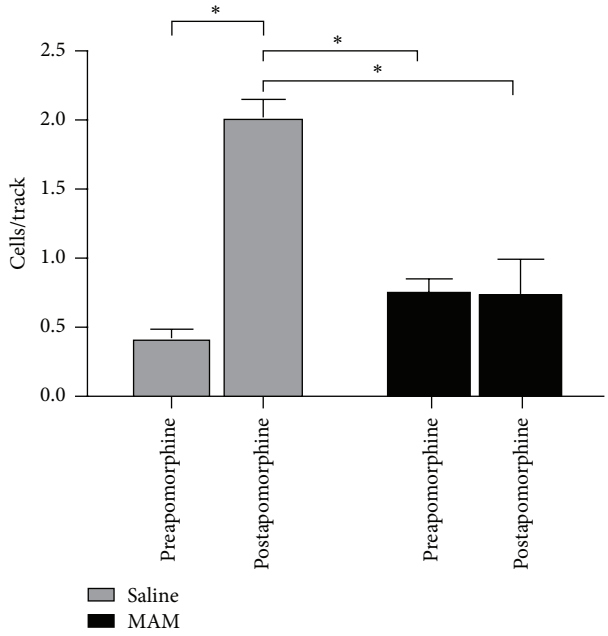


Figure 24: Administration of apomorphine (80 mg/kg i.v.) increased the number of spontaneously active dopamine neurons in SAL rats withdrawn from repeated HAL, while having no effect on the number of active dopamine neurons in MAM rats withdrawn from repeated HAL [36, 38, 47–61]. $^{*}p < 0.05$.

Table 3: Binding affinity at $\alpha x\beta 2\gamma 2$ $GABA_A$ receptor subtypes (values are reported in nM).

Compound[a]	$\alpha 1$	$\alpha 2$	$\alpha 3$	$\alpha 4$	$\alpha 5$	$\alpha 6$
SH-053-R-CH_3, (**15**)	2026	2377	1183	>5000	949.1	>5000
SH-053-S-CH_3, (**16**)	1666	1263	1249	>5000	206.4	>5000
SH-053-2′F-R-CH_3, (**2**)	759.1	948.2	768.8	>5000	95.17	>5000
SH-053-2′F-S-CH_3, (**17**)	350	141	1237	>5000	19.2	>5000

[a]Data shown here are the means of two determinations which differed by less than 10%.

Table 4: Oocyte electrophysiological data of benzodiazepines[a] [87].

Compound	$\alpha 1$	$\alpha 2$	$\alpha 3$	$\alpha 5$
SH-053-2′F-R-CH_3 (**2**)	111/154	124/185	125/220	183/387
SH-053-2′F-S-CH_3 (**17**)	116/164	170/348	138/301	218/389

[a]Efficacy at $\alpha x\beta 3\gamma 2$ $GABA_A$ receptor subtypes as % of control current at 100 nM and 1 μM concentrations. Data presented as percent over baseline (100) at concentrations of 100 nM/1 μM.

confirm the ataxic activity of BZ site agonists is mediated by $\alpha 1\beta 2/3\gamma 2$ subtypes, as reported in [23, 91–93]. The antianxiety activity in primates of the S isomers was preserved with no sedation. In only one study in rodents was any sedation observed; the confounding sedation was observed in both the S isomer (functionally selective for $\alpha 2$, $\alpha 3$, and $\alpha 5$ receptor subtypes) and R isomer (essentially selective for $\alpha 5$ subtype) and may involve at least, in part, agonist activity at $\alpha 5$ BzR subtypes. There are some $\alpha 5$ BzR located in the spinal cord which might be the source of the decrease in locomotion with SH-053-2′F-R-CH_3 and SH-053-2′F-S-CH_3; however, this is possibly some type of stereotypical behavior. Hence in agreement with many laboratories including our own [23, 92, 93] the best potential nonsedative, nonamnesic, antianxiety agents stem from ligands with agonist efficacy at $\alpha 2$ subtypes essentially silent at $\alpha 1$ and $\alpha 5$ subtypes (to avoid sedation) [91]. It must be pointed out again; however, in primates Fischer et al. [87] observed a potent anxiolytic effect with no sedation with the 2′F-S-CH_3 (**17**) isomer, while the 2′F-R-CH_3 (**2**) isomer exhibited only a very weak anxiolytic effect.

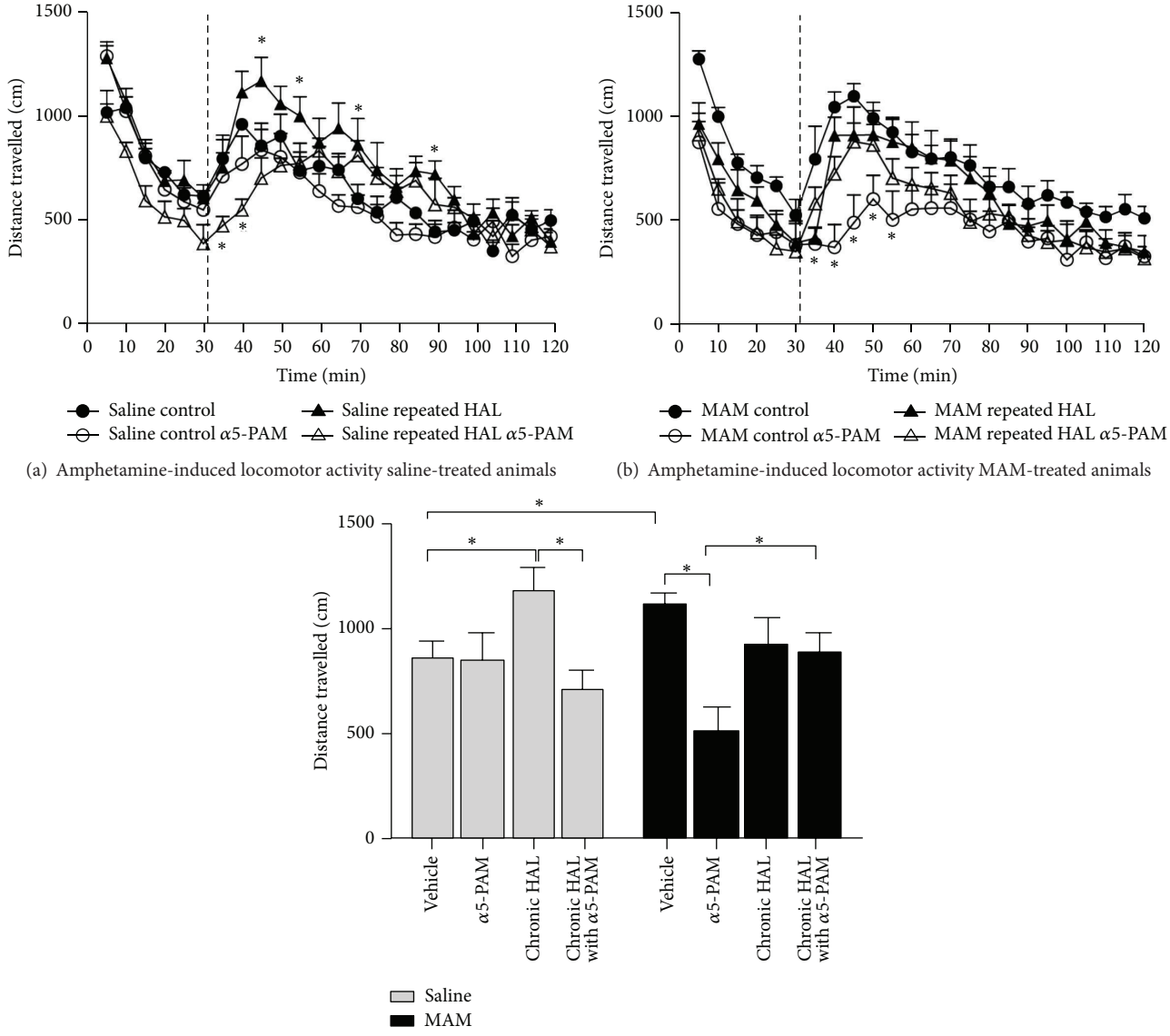
Numerous groups have done modeling and SAR studies on different classes of compounds which have resulted in a few different pharmacophore models based on the benzodiazepine binding site (BS) of the $GABA_A$ receptor [94]. These models are employed to gain insight in the interactions between the BS and the ligand. These have been put forth by Loew [7, 95, 96], Crippen [97, 98], Codding [76, 77, 99–101], Fryer [89, 90, 94], Gilli and Borea [102–105], Tebib et al. [106], and Gardner [107], as well as from Professors Sieghart, Cromer, and our own laboratory [21, 39, 40, 76, 78–82, 108–118].

The Milwaukee-based pharmacophore/receptor model is a comprehensive building of the BzR using radioligand binding data and receptor mapping techniques based on 12 classes of compounds [20, 23, 39, 40, 42, 111, 119–122]. This model (Figure 31) [79] has brought together previous models which have used data from the activity of antagonists, positive allosteric modulators, and negative allosteric modulators and included the new models for the "diazepam-insensitive" (DI) sites [123]. Four basic anchor points, H_1, H_2, A_2, and L_1, were assigned, and 4 additional lipophilic regions were defined as L_2, L_3, L_{Di}, and the new L_4 (see captions in Figure 31 for details); regions S_1, S_2, and S_3 represent negative areas of steric repulsion. As previously reported, the synthesis of both partial agonists and partial inverse agonists has been achieved by using parts of this model [99, 100, 104, 105, 119, 124–127].

The cloning, expression, and anatomical localization of multiple GABA(A) subunits have facilitated both the identification and design of subtype selective ligands. With the availability of binding data from different recombinant receptor subtypes, affinities of ligands from many different structural classes of compounds have been evaluated.

Illustrated in Figure 31 is the [*3,4-c*]quinolin-3-one CGS-9896 (**18**) (dotted line), a diazadiindole (**19**) (thin line), and diazepam (**20**) (thick line) fitted initially to the inclusive pharmacophore model for the BzR. Sites H_1 (Y210) and H_2 (H102) represent hydrogen bond donor sites on the receptor protein complex while A_2 (T142) represents a hydrogen bond acceptor site necessary for potent inverse activity *in vivo*. L_1, L_2, L_3, L_4, and L_{Di} are four lipophilic regions in the binding pharmacophore. Descriptors S_1, S_2, and S_3 are regions of negative steric repulsion.

Based on SAR data obtained for these ligands at 6 recombinant BzR subtypes [128–132], an effort has been undertaken to establish different pharmacophore/receptor models for BzR subtypes. The alignment of the twelve different structural classes of benzodiazepine receptor ligands was earlier based on the least squares fitting of at least three points. The coordinates of the four anchor points (A_2, H_1, H_2, and L_1) employed in the alignment are outlined in Figure 32.



(a) Amphetamine-induced locomotor activity saline-treated animals

(b) Amphetamine-induced locomotor activity MAM-treated animals

(c) Postamphetamine average peak distance travelled

FIGURE 25: Repeated haloperidol treatment causes an enhancement in the locomotor response to D-amphetamine (0.5 mg/kg, i.p.) in SAL animals that is reduced by pretreatment with SH-053-2′F-R-CH$_3$ (10 mg/kg, i.p.) (a). MAM rats treated repeatedly with haloperidol exhibit a locomotor response following D-amphetamine similar to untreated MAM rats. However, repeated haloperidol treatment blocks the effect of SH-053-2′F-R-CH$_3$ pretreatment in decreasing the locomotor response in MAM rats (b). Untreated MAM rats demonstrated a significantly larger peak locomotor response than untreated SAL rats. In addition, SH-053-2′F-R-CH$_3$ pretreatment significantly reduced the peak locomotor response in untreated MAM rats, while having no effect in repeatedly haloperidol-treated MAM rats. In contrast, repeated haloperidol treatment enhanced the peak locomotor response to amphetamine in SAL rats that was reduced by SH-053-2′F-R-CH$_3$ pretreatment (c) [36, 38, 47–61]. $^*P < 0.05$.

Herein are described the results from ligand-mapping experiments at recombinant BzR subtypes of 1,4-benzodiazepines, imidazobenzodiazepines, β-carbolines, diindoles, pyrazoloquinolinones, and others [126]. Some of the differences and similarities among these subtypes can be gleaned from this study and serve as a guide for future drug design.

10. α1 Updates

10.1. Beta-Carbolines. A series of 3,6-disubstituted β-carbolines was prepared and evaluated for their *in vitro* affinity at $\alpha x\beta 3\gamma 2$ GABA(A)/BzRr subtypes by radioligand binding assays in search of $\alpha 1\beta 3\gamma 2$ subtype selective compounds (Figure 33). A potential therapeutic application of such antagonist analogs is to treat alcohol abuse [133, 134]. Analogues of βCCt (**21**) were synthesized *via* a carbonyldiimidazole-mediated method by Yin et al. [85] and the related 6-substituted β-carboline-3-carboxylates including WYS8 (**27**) were synthesized from 6-iodo βCCt (**29**). Bivalent ligands (**42** and **43**) were also synthesized to increase the scope of the structure-activity relationships (SAR) to larger ligands. An

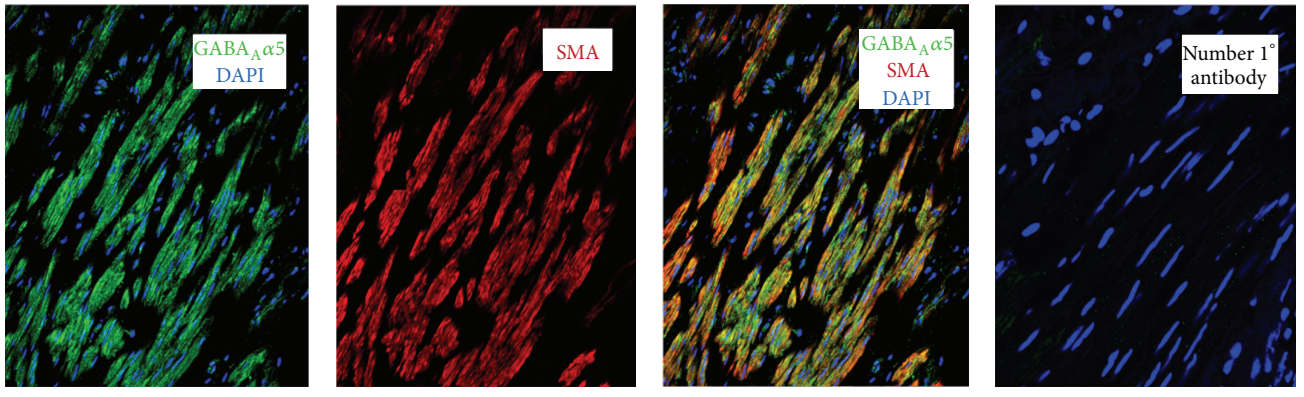


FIGURE 26: Protein expression of the GABA$_A$ α5 subunit in intact human trachea-bronchial airway smooth muscle. Representative images of human tracheal airway smooth muscle sections using confocal microscopy are depicted following single, double, and triple immunofluorescence labeling. The antibodies employed were directed against the GABA$_A$ α5 subunit (green), α-smooth muscle actin (SMA; red), and/or the nucleus via DAPI counterstain (blue). Panels illustrate the following staining parameters from left to right: (1st) costaining of DAPI and GABA$_A$ α5 subunit; (2nd) α-SMA staining alone; (3rd) triple-staining of GABA$_A$ α5, α-SMA, and DAPI; (4th) DAPI nucleus counterstain, with primary antibodies omitted as negative control. Modified from [66–75].

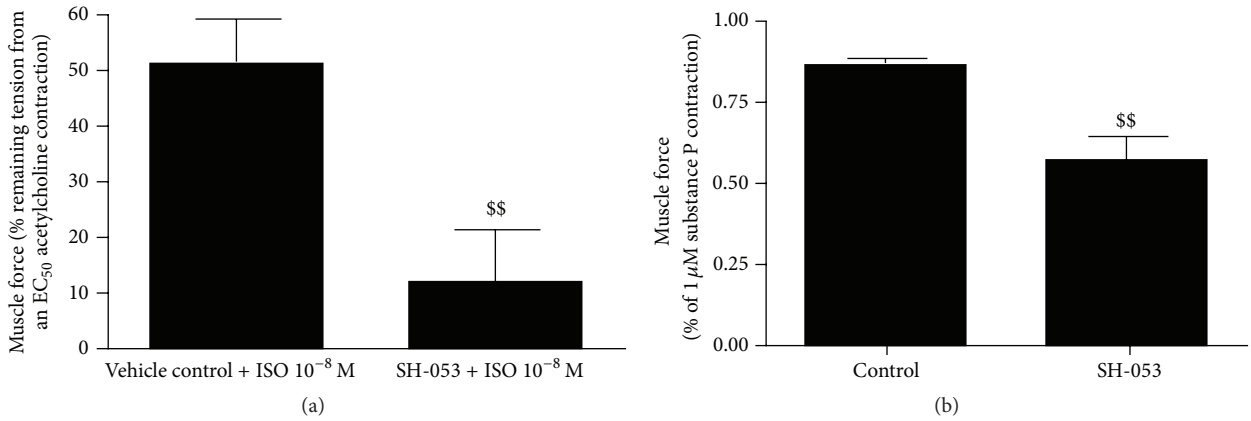


FIGURE 27: SH-053-2′F-R-CH$_3$ (**2**) mediated activation of α5 subunit containing GABA$_A$ channels induces relaxation of precontracted airway smooth muscle. (a) SH-053-2′F-R-CH$_3$ (**2**) (SH-053) potentiates β-agonist-mediated relaxation of human airway smooth muscle. Cotreatment of human airway smooth muscle strips with SH-053-2′F-R-CH$_3$ (**2**) (50 μM) significantly enhances isoproterenol (10 nM) mediated relaxation of an acetylcholine EC$_{50}$ contraction compared to isoproterenol alone (N = 8/group, \$\$ = $p < 0.01$). Modified from [66–75]. (b) SH-053-2′F-R-CH$_3$ (**2**) activation of α5 containing GABA$_A$ receptors induces direct relaxation of substance P-induced airway smooth muscle contraction. Compiled results demonstrating enhanced spontaneous relaxation (expressed as % remaining force at 30 minutes following a 1 μM substance P mediated contraction) following treatment with SH-053-2′F-R-CH$_3$ (**2**) compared to treatment with vehicle control (n = 4-5/group, \$\$ = $p < 0.01$) [66–75].

initial SAR on the first analogs demonstrated that compounds with larger side-groups at C6 were well tolerated as they projected into the L_{Di} domain (see **42** and **43**) [85]. Moreover, substituents located at C3 exhibited a conserved stereo interaction in lipophilic pocket L_1, while N2 likely participated in hydrogen bonding with H_1. Three novel β-carboline ligands (**21**, **23**, and **27**) permitted a comparison of the pharmacological properties with a range of classical benzodiazepine receptor antagonists (flumazenil, ZK93426) from several structural groups and indicated these β-carbolines were "near GABA neutral antagonists." Based on the SAR, the most potent (*in vitro*) α1 selective ligand was the 6-substituted acetylenyl βCCt (WYS8, **27**). In a previous study both **21** and **23** were able to reduce the rate at which rats self-administrated alcohol in alcohol preferring and HAD rats but had little or no effect on sucrose self-administration [85].

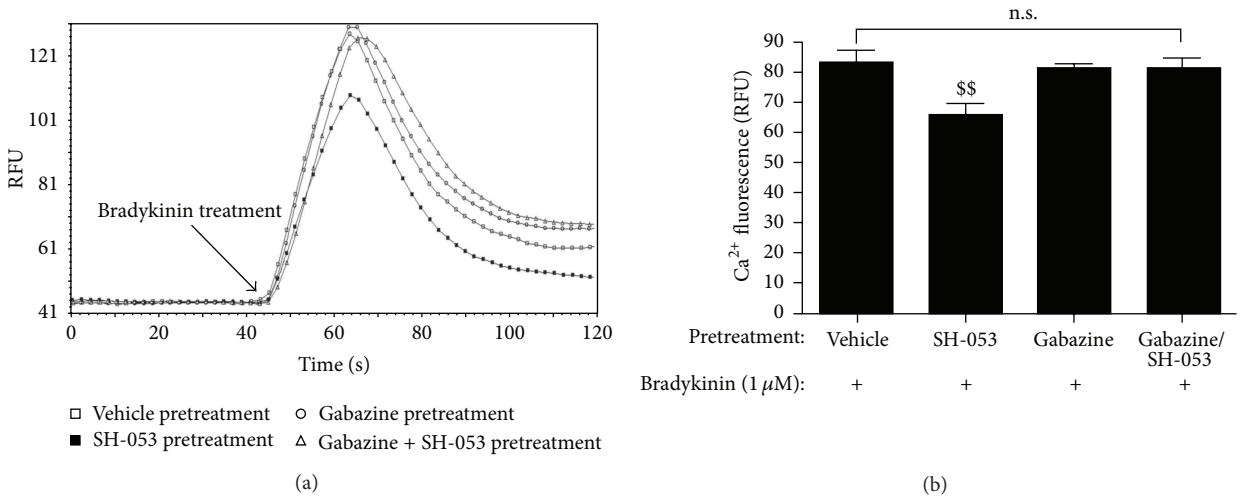
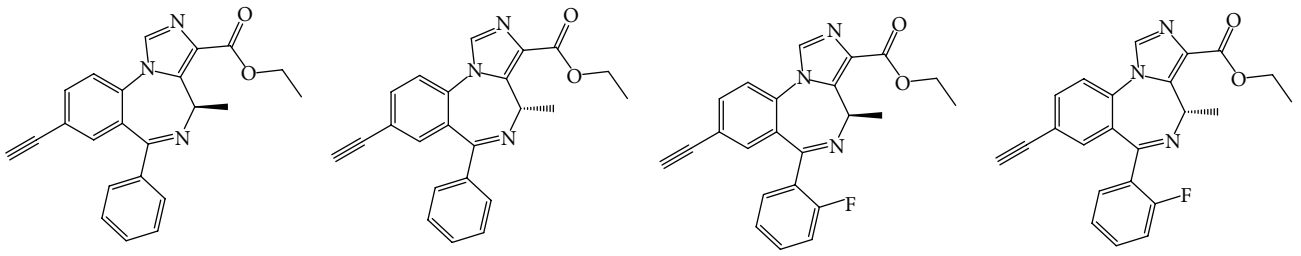


FIGURE 28: SH-053-2′F-R-CH_3 (**2**) mediated activation of α5 containing $GABA_A$ receptors attenuates bradykinin-induced elevations in cytosolic Ca^{2+} in human airway smooth muscle cells. (a) Representative Fluo-4 Ca^{2+} fluorescence (RFU) tracing illustrating pretreatment with SH-053-2′F-R-CH_3 (**2**) (SH-053) (10 μM) reduces cytosolic Ca^{2+} response to bradykinin (1 μM). This effect is reversed in the presence of gabazine (200 μM, $GABA_A$ receptor antagonist). Modified from [66–75]. (b) Compiled results illustrating SH-053-2′F-R-CH_3 (**2**) pretreatment of $GABA_A$ α5 receptors on human airway smooth muscle cells attenuates bradykinin-induced elevations in intracellular Ca^{2+} compared to levels achieved following pretreatment with vehicle control ($$ = $p < 0.01$). While gabazine-mediated blockade of $GABA_A$ channels does not significantly affect bradykinin-induced intracellular calcium increase compared to vehicle control, gabazine treatment did reverse SH-053-2′F-R-CH_3 (**2**) ability to attenuate bradykinin-induced elevations in intracellular calcium thereby illustrating a $GABA_A$ channel specific effect (n.s. = not significant). Modified from [66–75].



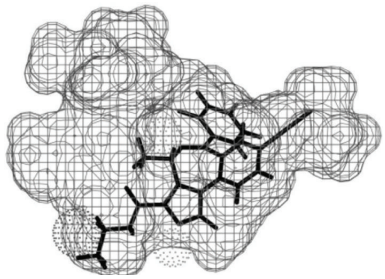
SH-053-R-CH_3, **15** SH-053-S-CH_3, **16** SH-053-2′F-R-CH_3, **2** SH-053-2′F-S-CH_3, **17**

FIGURE 29: Structures of enantiomers with 2′H (**15**, **16**) and 2′F (**2**, **17**).

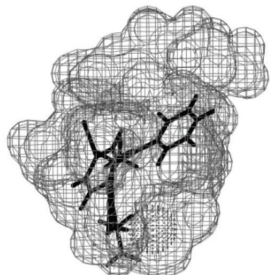
3-PBC (**23**) was also active in baboons [134]. This data has been used in updating the pharmacophore model in the α1-subtype.

11. The Updated Included Volume Models

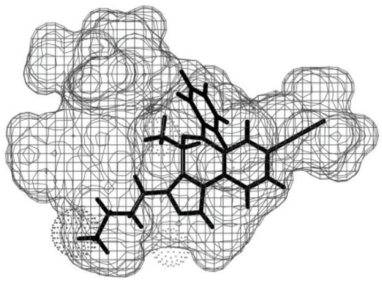
Illustrated in Figure 34 is the included volume of the updated pharmacophore receptor model of the $\alpha1\beta3\gamma2$ subtype of Clayton [22]. The current model for the $\alpha1\beta3\gamma2$ subtype has several new features. The cyclopropyl group of CD-214 extended 2 Å past the A_2 descriptor slightly increasing its volume. The trimethylsilyl group of QH-II-82 and WYS7 illustrates how well bulky groups are tolerated near the entrance of the binding pocket. Despite not being as potent, dimers of beta carbolines, WYS2 and WYS6, bound to α1 subtypes at 30 nM and 120 nM, respectively. Their ability to bind, albeit weakly, supports the location of the binding site entrance from the extracellular domain. The included volume of the $\alpha1\beta3\gamma2$ subtype was previously 1085.7 cubic angstroms. The volume has now been measured as 1219.2 cubic angstroms. Volume measurements should be used carefully as the binding site is not enclosed and the theoretical opening near L_{DI} is not clearly demarcated. Dimers were excluded from the included volume exercise because although they bound to the receptor, they represented compounds which were felt to extend outside the receptor binding pocket when docked to the protein. Where appropriate,



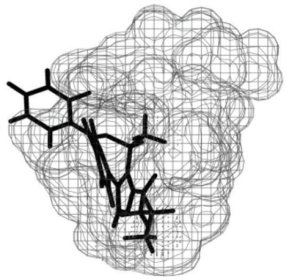
SH-053-2′F-S-CH_3 **17** fits the pharmacophore in the included volume of the alpha 2 subtype



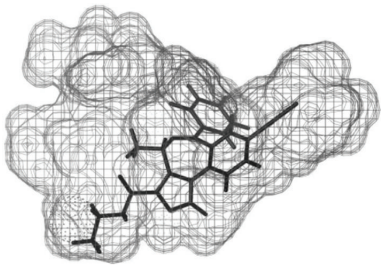
The left image of figure rotated 90°. It can be clearly seen that **17** fits within the included volume



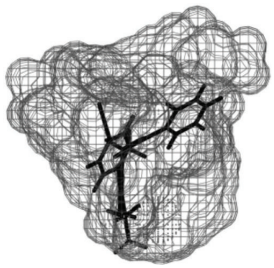
SH-053-2′F-R-CH_3 **2** does not fit the pharmacophore in the included volume of the alpha 2 subtype



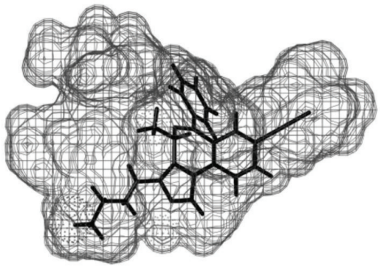
The left image of figure rotated 90°. It can be clearly seen that the conformation of **2** is such that the pendant 6-phenyl sticks outside the included volume



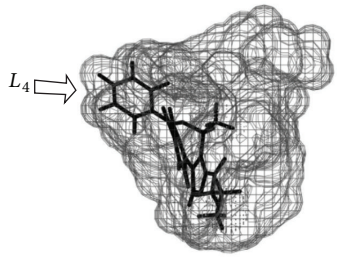
SH-053-2′F-S-CH_3 **17** fits the pharmacophore in the included volume of the alpha 5 subtype



The left image of figure rotated 90°. It can be clearly seen that **17** fits within the included volume



SH-053-2′F-R-CH_3 **2** fits the pharmacophore in the included volume of the alpha 5 subtype



The left image of figure rotated 90°. It can be clearly seen that **2** fits within the included volume

FIGURE 30: Included volume and ligand occupation of the SH-053-2′F-S-CH_3 **17** and SH-053-2′F-R-CH_3 **2** enantiomers in the $\alpha 5$ and $\gamma 2$ pharmacophore/receptor models. This figure was modified and reproduced from that reported by Clayton et al. in [22, 23].

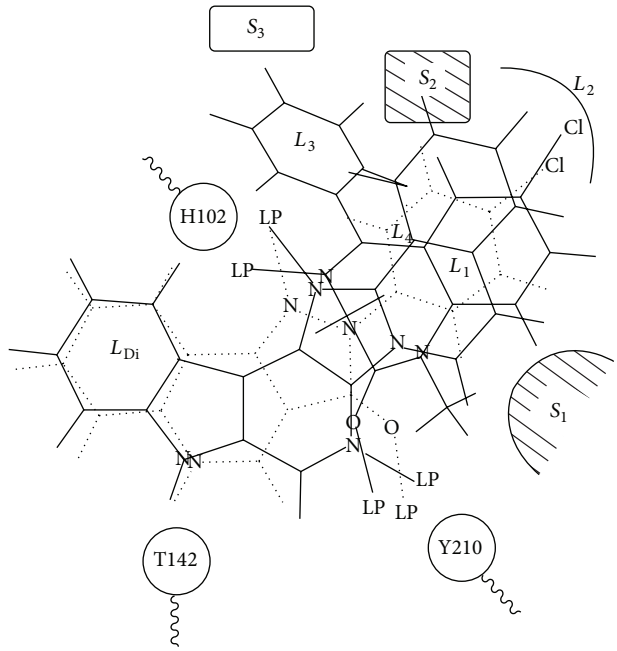


FIGURE 31: The two-dimensional representation of the Milwaukee-based unified pharmacophore with 3 amino acids in the binding site based on the rigid ligand template [23, 39, 42, 76–80]. This figure has been modified from that reported for PAMs, NAMs, and antagonists in [22, 23].

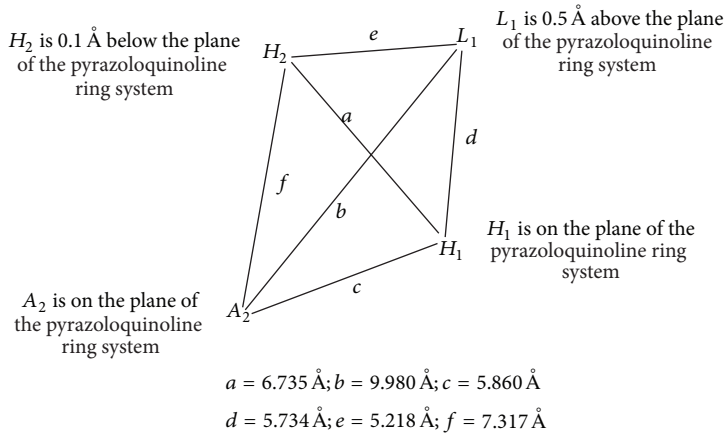
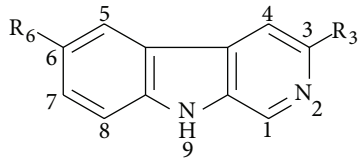


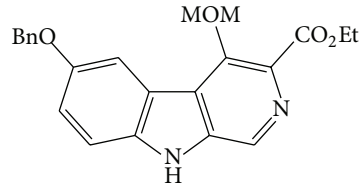
FIGURE 32: The schematic representation of the descriptors for the initial inclusive BzR pharmacophore based on the rigid ligands (diindoles) [79, 81–84]. This figure has been modified from that reported in [79].

their monomers were included in the included volume analysis. Ligands considered for the included volume in Table 5 exhibited potent binding at $\alpha 1$ subtypes ($K_i \leq 20$ nM) but were not necessarily subtype selective. The binding data for ligands at α_{2-6}-subtypes follow (Tables 6–10; structures located in Clayton [22] and Supporting Information, Appendix III in Supplementary Material available online at http://dx.doi.org/10.1155/2015/430248).

12. The $\alpha 1\beta 3\gamma 2$ Receptor Subtype

The focus of this research was aimed at diazepam sensitive receptors; additional features to the $\alpha 4\beta 3\gamma 2$ and $\alpha 6\beta 3\gamma 2$ receptors were not identified (see Table 5, Figures 34 and 35). The major new feature identified for the $\alpha 5\beta 3\gamma 2$ receptor was a new L_4 pocket. This new lipophilic pocket was identified with SH-053-R-CH_3 (**15**) and SH-053-S-CH_3 (**16**) chiral enantionmers as well as the 2′F analogs [74, 135, 136].





ZK-93423

Ligands	R_6	R_3	$\alpha1$	$\alpha2$	$\alpha3$	$\alpha4$	$\alpha5$	$\alpha6$
21(βCCt)	**H**	**CO_2tBu**	**0.72**	**15**	**18.9**	**1000**	**111**	**>5,000**
22(βCCE)	**H**	**CO_2Et**	**1.2**	**4.9**	**5.7**	**ND**	**26.8**	**2,700**
23(3-PBC)	H	OnPr	5.3	52.3	68.8	1000	591	>1,000
24(WYB14)	TMS—≡	CO_2tBu	6.8	30	36	2000	108	1000
25(WY-B-25)	TMS—≡	$CO_2CH_2CF_3$	17	59	88	200	1444	>3000
26(WY-B-99-1)	TMS—≡	CO_2Et	4.4	4.5	5.58	2000	47	2000
27(WYS8)	H—≡	CO_2tBu	**0.972**	**111**	**102**	**2000**	**1473**	**1980**
28(WY-B-26-2)	H—≡	$CO_2CH_2CF_3$	4.5	44.6	42.7	2000	124	2000
29(iodo-βCCt)	I	CO_2tBu	14.4	44.9	123	>4000	65.3	>4000
30(WY-B-20)	I	$CO_2CH_2CF_3$	12	39	47	2000	122	3000
31(iodo-βCCE)	I	CO_2Et	4.8	31	34	1000	286	1000
32(WY-B-08)	I	$CO_2CH_2(CF_3)_2$	78	301	131	3000	681	3000
33(WYS13)		CO_2tBu	2.4	13	27.5	NA	163	5000
34(WYB27-1)		$CO_2CH_2CF_3$	26	143	117	3000	127	2000
35(WYS12)		CO_2tBu	37	166	314	NA	2861	5000
36(WYB27-2)		$CO_2CH_2CF_3$	9.2	13	72	2000	449	2000
37(WYS15)		CO_2tBu	3.63	2.02	44.3	NA	76.5	5000
38(WYB29-2)		$CO_2CH_2CF_3$	25	137	125	2000	299	2000
39(CMA57)	F	COC_3H_7	3.7	27	40	NA	254	>2500
40(CM-A-82a)	$C(CH_3)_3$	CO_2tBu	2.78	8.93	24.5	1000	7.49	1000
41(CM-A-87)	F	CO_2tBu	1.62	4.54	14.7	1000	4.61	1000
42(WY-S-2)	Bcct—≡—Bcct		30	124	100	>300	>300	>4000
43(WY-S-6)	Bcct—≡≡—Bcct		120	1059	3942	5000	5000	5000

[a]Affinity of compounds at GABA(A)/BzR recombinant subtypes was measured by competition for [^{3}H]flunitrazepam or [^{3}H] Ro-15-4513 binding to HEK cell membranes expressing human receptors of composition $\alpha1\beta3\gamma2$, $\alpha2\beta3\gamma2$, $\alpha3\beta3\gamma2$, $\alpha4\beta3\gamma2$, $\alpha5\beta3\gamma2$, and $\alpha6\beta3\gamma2$ [85]. Data represent the average of at least three determinations with a SEM of ±5%.

Figure 33: [a]Affinities (K_i = nM) of 3,6-disubstituted β-carbolines at $\alpha x\beta3\gamma2$ (x = 1–3, 5, 6) receptor subtypes [85]. The structures versus code numbers of all ligands in the tables of this review can be found in the Ph.D. thesis of Terry Clayton (Ph.D. thesis, University of Wisconsin-Milwaukee, Milwaukee, WI, December, 2011) [22] and in the Supporting Information.

Table 5: These ligands bound with potent affinity for $\alpha 1$; ligands bound with K_i values <20 nM at this subtype.

Cook code[a]	$\alpha 1$	$\alpha 2$	$\alpha 3$	$\alpha 4$	$\alpha 5$	$\alpha 6$
WY-TSC-4 (WYS8)	0.007	0.99	1.63		51.04	
SH-TSC-2 (BCCT)	0.03	0.0419	0.035		69.32	
QH-II-090 (CGS-8216)	0.05	0.08	0.12		0.25	17
XLI-286	0.051	0.064	0.118		0.684	
QH-II-077	0.06	0.08	0.05		0.12	4
QH-II-092	0.07	0.03	0.04	ND	0.17	ND
JYI-57	0.076	0.076	0.131	ND	0.036	ND
QH-II-085	0.08	0.06	0.02	ND	0.08	ND
XHE-II-024	0.09	0.18	0.32	14	0.24	11
PWZ-007A	0.11	0.1	0.09	ND	0.2	10
CGS8216	0.13	ND	ND	ND	ND	46
SPH-121	0.14	1.19	1.72	ND	4	479
QH-II-075	0.18	0.21	0.25	ND	1.3	40
PZII-028	0.2	ND	0.2	ND	0.32	1.9
CGS9895	0.21	ND	ND	ND	ND	9.3
PWZ-0071	0.23	0.17	0.12	ND	0.44	17.31
XHE-III-24	0.25	ND	8	222	10	328
JYI-42	0.257	0.146	0.278	ND	0.256	ND
CGS9896	0.28	ND	ND	ND	ND	181
JYI-64 (C17H12N4FBr)	0.305	1.111	0.62	ND	0.87	5000
PZII-029	0.34	ND	0.79	ND	0.52	10
BRETAZENIL	0.35	0.64	0.2	ND	0.5	12.7
FG8205	0.4	2.08	1.16	ND	1.54	227
YT-5	0.421	0.6034	36.06	ND	1.695	ND
6-PBC	0.49	1.21	2.2	ND	2.39	1343
QH-146	0.49	ND	0.76	ND	7.7	10000
DM-II-90 (C17H12N4BrCl)	0.505	1	0.63	ND	0.37	5000
SPH-165	0.63	2.79	4.85	ND	10.4	1150
BCCt	0.72	15	18.9	ND	110.8	5000
SH-I-048A	0.774	0.1723	0.383	ND	0.11	ND
alprazolam	0.8	0.59	1.43	ND	1.54	10000
Ro15-1788	0.8	0.9	1.05	ND	0.6	148
WYS10 C14H9F3N2O2	0.88	36	25.6	ND	548.7	15.3
WY-B-15	0.92	0.83	0.58	2080	4.42	646
WY-A-99-2 (WYS8)	0.972	111	102	2000	208	1980
XHE-III-06a	1	2	1	5	1.8	37
Xli366 C22H21N3O2	1	ND	ND	ND	ND	ND
JYI-59 (C22H13N3O2F4)	1.08	2.6	11.82	ND	11.5	5000
WYSC1 C16H16N2O2	1.094	5.44	12.3	ND	69.8	21.2
MLT-I-70	1.1	1.2	1.1	ND	40.3	1000
SVO-8-30	1.1	5.3	5.3	2.8	0.6	15
BCCE	1.2	4.9	5.7	ND	26.8	2700
XHE-III-04	1.2	2	1.1	219	0.4	500
XLi350 C17H11ClN2O	1.224	1.188	ND	ND	2.9	ND
XHE-III-49	1.3	5.5	4.2	38.7	11.3	85.1
PWZ-009A1	1.34	1.31	1.26	ND	0.84	2.03
DM-239	1.5	ND	0.53	ND	0.14	6.89
XLi351 C21H21ClN2OSi	1.507	0.967	ND	ND	1.985	ND
XLi352 C18H13ClN2O	1.56	0.991	ND	ND	1.957	ND

Table 5: Continued.

Cook code[a]	α1	α2	α3	α4	α5	α6
TG-4-39	1.6	34	24	5.6	1.4	23
TG-II-82	1.6	2.9	2.8	ND	1	1000
CM-A87	1.62	4.54	14.73	1000	4.61	1000
QH-II-082	1.7	1.8	1.6	ND	6.1	100
JYI-49 (C20H12N3O2F4Br)	1.87	2.38	ND	ND	6.7	3390
LJD-III-15E	1.93	14	19	ND	70.8	1000
SPH-38	2	5.4	10.8	ND	18.5	3000
XHE-I-093	2	7.1	8.9	1107	20	1162
MSA-IV-35	2.1	16	21	ND	995	3000
JYI-19 (C23H23N3O3S)	2.176	205	ND	ND	34	12.7
FLUNITRAZEPAM	2.2	2.5	4.5	ND	2.1	2000
YCT-5	2.2	11.46	16.3	ND	200	10000
TJH-IV-51	2.39	17.4	14.5	ND	316	10000
WYS13 C20H18N2O3	2.442	13	27.5	ND	163	5000
YT-III-25	2.531	5.786	5.691	ND	0.095	ND
XHE-III-14	2.6		10	13	2	7
WYS9 C16H15IN2O2	2.72	22.2	23.1	ND	562	122
JYI-47	2.759	2.282	0.511	ND	0.427	ND
CM-A82a	2.78	8.93	24.51	1000	7.49	1000
TG-4-29	2.8	3.9	2.7	2.1	0.18	3.9
XLi268 C17H13BrN4	2.8145	0.6862	ND	ND	0.6243	ND
JYI-54 (C24H15N3O3F4)	2.89	172	6.7	ND	57	1890
MMB-II-74	3	24.5	41.7	500	125.7	1000
MMB-III-016	3	1.97	2	1074	0.26	211
MMB-III-16	3	1.97	2	1074	0.26	211
QH-II-080b	3	3.7	4.7	ND	24	1000
YCT-7A	3	23.8	30.5	ND	240	10000
JYI-32 (C20H15N3O2BrF)	3.07	4.96	ND	ND	2.92	52.24
Ro15-4513	3.3	2.6	2.5	ND	0.26	3.8
XHE-II-017	3.3	10	7	258	17	294
XLi-JY-DMH ANX3	3.3	0.58	1.9	ND	4.4	5000
MLT-II-18	3.4	11.7	11	ND	225	10000
TJH-V-88	3.41		30	ND	140.9	10000
XLI-2TC	3.442	1.673	44.08	ND	1.121	
WYS15 C22H20N2O2	3.63	2.02	44.3	ND	76.5	5000
CM-A57	3.7	27	40	ND	254	1000
XHE-II-006b	3.7	15	12	1897	144	1000
JYI-60	3.73	1.635	4.3	ND	1.7	5000
RY-008	3.75	7.2	4.14	ND	1.11	44.3
MLT-II-18	3.9	12.2	24.4	ND	210	10000
OMB-18	3.9	1.2	3.4	1733	0.8	5
WY-B-09-1	3.99	8	32	1000	461	2000
SHU-1-19	4	12	7	48	14	84
ZK 93423	4.1	4.2	6	ND	4.5	1000
WY-B-23-2 (WYS11)	4.2	37.7	39	2000	176	69.4
WY-B-23-2 (WYS11)	4.2	37.7	73	ND	176	69.4
WY-B-99-1	4.4	4.5	5.58	2000	47	2000
WY-B-26-2	4.45	44.57	42.66	2000	124	2000
XHE-II-006a	4.7	4.4	20	1876	89	3531

Table 5: Continued.

Cook code[a]	α1	α2	α3	α4	α5	α6
CM-B01	4.8	31	34	1000	286	1000
PWZ-085	4.86	13	8.5	ND	0.55	40
MLT-II-16	5.05	10.41	18.4	ND	260	10000
3 PBC	5.3	52.3	68.8	ND	591	1000
MA-3-PROPOXYL	5.3	52.3	68.8	ND	591	1000
TJH-IV-43	5.42	30.19	48.9	ND	475	10000
DMCM	5.69	8.29	4	ND	1.04	134
DM-139	5.8	ND	169	ND	9.25	325
XHE-II-073A (R ENRICHED)	5.9	11	10	15	1.18	140
MSR-I-032	6.2	18.7	4	ND	3.3	74.9
JYI-70 (C19H13N4F)	6.3	2.1	ND	ND	0.56	5000
XLi343 C20H19ClN2OSi	6.375	17.71	ND	ND	150.5	ND
3 EBC	6.43	25.1	28.2	ND	826	1000
DM-146	6.44	ND	148	ND	4.23	247
DM-215	6.74	ND	7.42	ND	0.293	8.28
ZG69A	6.8	16.3	9.2	ND	0.85	54.6
ZG-69a (Ro15-1310)	6.8	16.3	9.2	ND	0.85	54.6
WY-B-14 (WYS7)	6.84	30	36	2000	108	1000
YT-II	6.932	0.8712	3.518	ND	5.119	ND
SVO-8-67	7	41	26	15	2.3	191
MLT-II-34	7.04	15.95	22.3	ND	158	1000
SPH-195	7.2	168.5	283.5	ND	271	10000
XHE-I-065	7.2	17	18	500	57	500
ZG-234	7.25	22.14	9.84	ND	0.3	5.25
SH-I-04	7.3	6.136	5.1	ND	7.664	ND
XHE-I-038	7.3	5	34	ND	132	1000
XHE-III-13	7.3	ND	7.1	880	1.6	311
WY-B-25	7.6	40	66	2000	263	2000
CM-A49 (R)	7.7	32.5	43	ND	69	1000
SVO-8-14	8	25	8	6.9	0.9	14
TG-4-29	8.3	10.2	6.9	ND	0.4	7.61
XHE-II-002	8.3	18	13	3.9	1.5	11
WY-B-14 (WYS7)	8.5	165	245	ND	1786	5000
XHE-II-011	9	60	39	3233	90	1000
WY-B-27-2	9.19	111	72	2000	449	2000
QH-II-063	9.4	9.3	31	ND	7.7	3000
JC184 C13H9BrN2OS	9.606	10.5	ND	ND	6.709	ND
ZG-208	9.7	11.2	10.9	ND	0.38	4.6
RY-I-31	10	45	19	ND	6	1000
WY-B-23-1	10	33	43	1000	189	2000
RY-098	10.1	22.2	16.5	ND	1.68	100
Hz148 C18H15N3	10.98	5000	ND	ND	256	5000
SVO-8-20	11	40	28	19	8.6	138
XHE-II-073B (S-ENRICHED)	11	17	12	33	2.1	269
SH-I-085	11.08	4.866	13.75	ND	0.24	ND
PWZ-096	11.1	36	16.9	ND	1.07	51.5
ZG-168	11.2	10.7	9.2	ND	0.47	9.4
CM-A77	11.51	51.9	105.16	1000	42.62	1000
WY-B-20	12	39	47	2000	122	3000
ABECARNIL	12.4	15.3	7.5	ND	6	1000

Table 5: Continued.

Cook code[a]	α1	α2	α3	α4	α5	α6
SH-I-89S	12.78	8.562	8.145	ND	3.23	ND
ZG-213	12.8	49.8	30.2	ND	3.5	22.5
EDC-I-071	12.9	83.1	ND	ND	314	5000
MMB-III-14	13	13	6.9	333	1.1	333
DM-173	13.1	ND	38.1	ND	0.78	118
XLI-348	13.56	11.17	1.578	ND	82.05	ND
EDC-I-093	13.6	423	ND	ND	2912	5000
diazepam	14	20	15	ND	11	ND
XLi223 C22H20BrN3O2	14	8.7	18	1000	10	2000
WYSC2 C15H11F3N2O2	14.14	113	170	ND	518	61.2
SH-I-030	14.42	11.04	19.09	ND	1.89	ND
CM-A100	14.49	44.91	123.8	1000	65.31	1000
RY-033	14.8	56	25.3	ND	1.72	22.9
HJ-I-037	15.07	8.127	28.29	ND	0.818	ND
YT-6	15.31	87.8	60.49	ND	1.039	ND
EDC-II-044	15.4	ND	293	ND	323	1000
CM-A58	16	120	184	ND	1000	1012
QH-II-067a	16	31	52	ND	199	3000
CD-214	16.4	48.2	42.5	ND	9.8	168
JYI-06 (C23H23N3O4)	16.5	5.48	5000	ND	12.6	5000
CM-A50 (S)	17	59	88	ND	144	1000
RY-061	17	13	6.7	ND	0.3	31
ZG-224	17.1	33.7	50	ND	2.5	30.7
ZG-63A	17.3	21.6	29.1	ND	0.65	4
DM-II-30 (C20H13N3O2BrF3)	17.6	13.4	28.51	ND	7.8	5000
CM-A64	18	60	116	ND	216	1000
RY-071	19	56	91	ND	7.2	266
WZ-113	19.2	13.2	13.4	ND	11.5	300
YT-III-23	19.83	23.65	19.87	ND	1.105	ND
CM-E09b	20	22	19	55	0.45	69
MMB-II-90	20	24	5.7	9	0.25	36

[a]Affinity of compounds at $GABA_A$/BzR recombinant subtypes was measured by competition for [^{3}H]flunitrazepam or [^{3}H] Ro15-4513 binding to HEK cell membranes expressing human receptors of compositions $\alpha1\beta3\gamma2$, $\alpha2\beta3\gamma2$, $\alpha3\beta3\gamma2$, $\alpha4\beta3\gamma2$, $\alpha5\beta3\gamma2$, and $\alpha6\beta3\gamma2$ [139]. Data represent the average of at least three determinations with a SEM of ±5%. The structures of these ligands are in the Ph.D. thesis of Clayton (2011) [22] and Supporting Information.

13. The $\alpha2\beta3\gamma2$ Receptor Subtype

See Table 6 and Figures 36 and 37.

14. The $\alpha3\beta3\gamma2$ Receptor Subtype

See Table 7 and Figures 38 and 39.

15. The $\alpha4\beta3\gamma2$ Receptor Subtype

See Table 8 and Figures 40 and 41.

16. The $\alpha5\beta3\gamma2$ Receptor Subtype

The multiple volume contours displayed in Figures 34–47 were created using the mvolume function (multiple volume contour function) in Sybyl and compounds with binding affinity at the receptor less than or equal to 20 nM. To create the overlays, first, the display (dsp) and contour (cnt) files were created for the $\alpha5\beta3\gamma2$ receptor subtype and the $\alpha1\beta3\gamma2$ receptor subtype by overlaying the compounds for each of these receptors (see Table 9 and Figures 42–45). Using the mvolume function, a logical expression was entered to create the surfaces making up the union as well as the included volume for each receptor subtype itself. It is clear from the

Table 6: Ligands with potent affinity for $\alpha 2$; ligands bound with K_i values <20 nM at this subtype. The structures of these ligands are in the Ph.D. thesis of Clayton (2011) [22].

Cook code[a]	$\alpha 1$	$\alpha 2$	$\alpha 3$	$\alpha 4$	$\alpha 5$	$\alpha 6$
QH-II-092	0.07	0.03	0.04	ND	0.17	ND
SH-TSC-2 (BCCT)	0.03	0.0419	0.035	ND	69.32	ND
QH-II-085	0.08	0.06	0.02	ND	0.08	ND
XLI-286	0.051	0.064	0.118	ND	0.684	ND
JYI-57	0.076	0.076	0.131	ND	0.036	ND
QH-II-090 (CGS-8216)	0.05	0.08	0.12	ND	0.25	17
QH-II-077	0.06	0.08	0.05	ND	0.12	4
PWZ-007A	0.11	0.1	0.09	ND	0.2	10
JYI-42	0.257	0.146	0.278	ND	0.256	ND
PWZ-0071	0.23	0.17	0.12	ND	0.44	17.31
SH-I-048A	0.774	0.1723	0.383	ND	0.11	ND
XHE-II-024	0.09	0.18	0.32	14	0.24	11
QH-II-075	0.18	0.21	0.25	ND	1.3	40
XLi-JY-DMH ANX3	3.3	0.58	1.9	ND	4.4	5000
alprazolam	0.8	0.59	1.43	ND	1.54	10000
YT-5	0.421	0.6034	36.06	ND	1.695	ND
BRETAZENIL	0.35	0.64	0.2	ND	0.5	12.7
XLi268 C17H13BrN4	2.8145	0.6862	ND	ND	0.6243	ND
WY-B-15	0.92	0.83	0.58	2080	4.42	646
YT-II	6.932	0.8712	3.518	ND	5.119	
Ro15-1788	0.8	0.9	1.05	ND	0.6	148
XLi351 C21H21ClN2OSi	1.507	0.967	ND	ND	1.985	ND
WY-TSC-4 (WYS8)	0.007	0.99	1.63	ND	51.04	ND
XLi352 C18H13ClN2O	1.56	0.991	ND	ND	1.957	ND
DM-II-90 (C17H12N4BrCl)	0.505	1	0.63	ND	0.37	5000
JYI-64 (C17H12N4FBr)	0.305	1.111	0.62	ND	0.87	5000
XLi350 C17H11ClN2O	1.224	1.188	ND	ND	2.9	ND
SPH-121	0.14	1.19	1.72	ND	4	479
MLT-I-70	1.1	1.2	1.1	ND	40.3	1000
OMB-18	3.9	1.2	3.4	1733	0.8	5
6-PBC	0.49	1.21	2.2	ND	2.39	1343
YT-III-271	32.54	1.26	2.35	ND	103	ND
PWZ-009A1	1.34	1.31	1.26	ND	0.84	2.03
DM-II-72 (C15H10N20BrCl)	5000	1.37	ND	ND	2.02	5000
JYI-60 (C17H11N2OF)	3.73	1.635	4.3	ND	1.7	5000
XLI-2TC	3.442	1.673	44.08	ND	1.121	ND
QH-II-082	1.7	1.8	1.6	ND	6.1	100
TC-YT-II-76	101.1	1.897	5.816	ND	11.99	ND
MMB-III-016	3	1.97	2	1074	0.26	211
MMB-III-16	3	1.97	2	1074	0.26	211
XHE-III-06a	1	2	1	5	1.8	37
XHE-III-04	1.2	2	1.1	219	0.4	500
WYS15 C22H20N2O2	3.63	2.02	44.3	ND	76.5	5000
FG8205	0.4	2.08	1.16	ND	1.54	227
JYI-70 (C19H13N4F)	6.3	2.1	ND	ND	0.56	5000
JYI-47	2.759	2.282	0.511	ND	0.427	ND
JYI-49 (C20H12N3O2F4Br)	1.87	2.38	ND	ND	6.7	3390
FLUNITRAZEPAM	2.2	2.5	4.5	ND	2.1	2000
JYI-59 (C22H13N3O2F4)	1.08	2.6	11.82	ND	11.5	5000

Table 6: Continued.

Cook code[a]	α1	α2	α3	α4	α5	α6
Ro15-4513	3.3	2.6	2.5	ND	0.26	3.8
SPH-165	0.63	2.79	4.85	ND	10.4	1150
YT-II-76	95.34	2.797	0.056	ND	0.04	ND
TG-II-82	1.6	2.9	2.8	ND	1	1000
QH-II-080b	3	3.7	4.7	ND	24	1000
TG-4-29	2.8	3.9	2.7	2.1	0.18	3.9
PS-1-34B C20H17N4BrO	ND	4.198	3.928	ND	ND	ND
ZK 93423	4.1	4.2	6	ND	4.5	1000
XHE-II-006a	4.7	4.4	20	1876	89	3531
WY-B-99-1	4.4	4.5	5.58	2000	47	2000
CM-A87	1.62	4.54	14.73	1000	4.61	1000
OMB-19	22	4.6	20	3333	3.5	40
SH-I-085	11.08	4.866	13.75	ND	0.24	ND
BCCE	1.2	4.9	5.7	ND	26.8	2700
JYI-32 (C20H15N3O2BrF)	3.07	4.96	ND	ND	2.92	52.24
XHE-I-038	7.3	5	34	ND	132	1000
SVO-8-30	1.1	5.3	5.3	2.8	0.6	15
SPH-38	2	5.4	10.8	ND	18.5	3000
WYSC1 C16H16N2O2	1.094	5.44	12.3	ND	69.8	21.2
JYI-06 (C23H23N3O4)	16.5	5.48	5000	ND	12.6	5000
XHE-III-49	1.3	5.5	4.2	38.7	11.3	85.1
YT-III-25	2.531	5.786	5.691	ND	0.095	ND
SH-I-04	7.3	6.136	5.1	ND	7.664	ND
XHE-I-093	2	7.1	8.9	1107	20	1162
RY-008	3.75	7.2	4.14	ND	1.11	44.3
DMH-D-053 (C43H30N6O4)	236	7.4	272	5000	194.2	5000
WY-B-09-1	3.99	8	32	1000	461	2000
HJ-I-037	15.07	8.127	28.29	ND	0.818	ND
DMCM	5.69	8.29	4	ND	1.04	134
SH-I-89S	12.78	8.562	8.145	ND	3.23	ND
XLi223 C22H20BrN3O2	14	8.7	18	1000	10	2000
CM-A82a	2.78	8.93	24.51	1000	7.49	1000
QH-II-063	9.4	9.3	31	ND	7.7	3000
	9.4	9.3	31	ND	7.7	3000
XHE-II-017	3.3	10	7	258	17	294
TG-4-29	8.3	10.2	6.9	ND	0.4	7.61
MLT-II-16	5.05	10.41	18.4	ND	260	10000
JC184 C13H9BrN2OS	9.606	10.5	ND	ND	6.709	ND
ZG-168	11.2	10.7	9.2	ND	0.47	9.4
XHE-II-073A (R ENRICHED)	5.9	11	10	15	1.18	140
XLI-8TC	21.52	11.01	2.155	ND	4.059	ND
SH-I-030	14.42	11.04	19.09	ND	1.89	ND
XLI-348	13.56	11.17	1.578	ND	82.05	ND
ZG-208	9.7	11.2	10.9	ND	0.38	4.6
YT-TC-3	141.4	11.43	118.1	ND	29.22	ND
YCT-5	2.2	11.46	16.3	ND	200	10000
MLT-II-18	3.4	11.7	11	ND	225	10000
XHE-II-O53-ACID	50.35	11.8	44	ND	5.9	5000
SHU-1-19	4	12	7	48	14	84
RY-067	21	12	10	ND	0.37	42

Table 6: Continued.

Cook code[a]	$\alpha1$	$\alpha2$	$\alpha3$	$\alpha4$	$\alpha5$	$\alpha6$
DM-III-01 (C18H12N3O2Br)	5000	12	ND	ND	4.73	5000
MLT-II-18	3.9	12.2	24.4	ND	210	10000
SH-053-2′F	21.99	12.34	34.9	ND	0.671	ND
WYS13 C20H18N2O3	2.442	13	27.5	ND	163	5000
PWZ-085	4.86	13	8.5	ND	0.55	40
MMB-III-14	13	13	6.9	333	1.1	333
RY-061	17	13	6.7	ND	0.3	31
WZ-113	19.2	13.2	13.4	ND	11.5	300
YT-II-83	32.74	13.22	24.1	ND	3.548	ND
DM-II-30 (C20H13N3O2BrF3)	17.6	13.4	28.51	ND	7.8	5000
LJD-III-15E	1.93	14	19	ND	70.8	1000
YT-III-272	295.9	14.98	10.77	ND	103.3	ND
BCCt	0.72	15	18.9	ND	110.8	5000
XHE-II-006b	3.7	15	12	1897	144	1000
ABECARNIL	12.4	15.3	7.5	ND	6	1000
MLT-II-34	7.04	15.95	22.3	ND	158	1000
MSA-IV-35	2.1	16	21	ND	995	3000
JYI-04 (C21H23N3O3)	28.3	16	ND	ND	0.51	1.57
PS-1-35 C23H22N5OBr	ND	16.03	24.41	ND	ND	ND
ZG69A	6.8	16.3	9.2	ND	0.85	54.6
ZG-69a (Ro15-1310)	6.8	16.3	9.2	ND	0.85	54.6
YT-III-42	382.9	16.83	44.04	ND	9.77	ND
XHE-I-065	7.2	17	18	500	57	500
XHE-II-073B (S-ENRICHED)	11	17	12	33	2.1	269
TJH-IV-51	2.39	17.4	14.5	ND	316	10000
SH-I-047	1710	17.52	1222	ND	1519	ND
XLi343 C20H19ClN2OSi	6.375	17.71	ND	ND	150.5	ND
XHE-II-002	8.3	18	13	3.9	1.5	11
YT-III-38	1461	18.21	14.63	ND	3999	
JYI-72 (C22H21N4SiF)	48.5	18.5	ND	ND	11.5	5000
MSR-I-032	6.2	18.7	4	ND	3.3	74.9
JC208 C15H10N2OS	22.42	18.89	ND	ND	5.039	ND
diazepam	14	20	15	ND	11	ND

[a]Affinity of compounds at $GABA_A$/BzR recombinant subtypes was measured by competition for [^{3}H]flunitrazepam or [^{3}H] Ro15-4513 binding to HEK cell membranes expressing human receptors of compositions $\alpha1\beta3\gamma2$, $\alpha2\beta3\gamma2$, $\alpha3\beta3\gamma2$, $\alpha4\beta3\gamma2$, $\alpha5\beta3\gamma2$, and $\alpha6\beta3\gamma2$ [22, 139]. Data represent the average of at least three determinations with a SEM of ±5%. ND: not determined.

included volume overlay that the L_2 pocket is deeper for the $\alpha5$ subtype, as determined previously [13, 21–23, 110, 119]. The new L_4 pocket can be distinguished as the new yellow region of the $\alpha5\beta3\gamma2$ subtype which is due to recently designed R-isomers by Huang [135], Poe and Li.

17. The $\alpha6\beta3\gamma2$ Receptor Subtype

See Table 10 and Figures 46 and 47.

18. Updates to the Previous Model

In addition to the newly discovered L_4 pocket, the updated library of binding affinity led to two specific updates in the previous model (Figure 48).

19. QSAR

A nontraditional quantitative structure activity relationship (QSAR) approach was executed to observe steric and electrostatic preferences for each receptor subtype. A subset of the compounds used in each subtype pharmacophore/receptor model were chosen with a good cross section of scaffold variety. The compounds used in the COMFA maps are the imidazobenzodiazepines published previously [110, 137] and additionally alternative scaffolds which bound with <20 nM at the respective subtype [22].

The interest here was in creation of steric and electrostatic maps of the comparative molecular field analyses (COMFA) created from molecular spreadsheets. A variety of compounds selective for each subtype were selected and placed into a dataset used to build the CoMFA models. Activities (K_i

Table 7: Ligands with potent affinity for $\alpha 3$; ligands bound with K_i values <20 nM at this subtype. The structures of these ligands are in the Ph.D. thesis of Clayton (2011) [22].

Cook code[a]	$\alpha 1$	$\alpha 2$	$\alpha 3$	$\alpha 4$	$\alpha 5$	$\alpha 6$
QH-II-085	0.08	0.06	0.02	ND	0.08	ND
SH-TSC-2 (BCCT)	0.03	0.0419	0.035	ND	69.32	ND
QH-II-092	0.07	0.03	0.04	ND	0.17	ND
QH-II-077	0.06	0.08	0.05	ND	0.12	4
YT-II-76	95.34	2.797	0.056	ND	0.04	ND
PWZ-007A	0.11	0.1	0.09	ND	0.2	10
XLI-286	0.051	0.064	0.118	ND	0.684	ND
QH-II-090 (CGS-8216)	0.05	0.08	0.12	ND	0.25	17
PWZ-0071	0.23	0.17	0.12	ND	0.44	17.31
JYI-57	0.076	0.076	0.131	ND	0.036	ND
BRETAZENIL	0.35	0.64	0.2	ND	0.5	12.7
PZII-028	0.2	ND	0.2	ND	0.32	1.9
QH-II-075	0.18	0.21	0.25	ND	1.3	40
JYI-42	0.257	0.146	0.278	ND	0.256	ND
XHE-II-024	0.09	0.18	0.32	14	0.24	11
SH-I-048A	0.774	0.1723	0.383	ND	0.11	ND
JYI-55	41.39	ND	0.504	ND	24.75	ND
JYI-47	2.759	2.282	0.511	ND	0.427	ND
DM-239	1.5	ND	0.53	ND	0.14	6.89
WY-B-15	0.92	0.83	0.58	2080	4.42	646
JYI-64 (C17H12N4FBr)	0.305	1.111	0.62	ND	0.87	5000
DM-II-90 (C17H12N4BrCl)	0.505	1	0.63	ND	0.37	5000
QH-146	0.49	ND	0.76	ND	7.7	10000
PZII-029	0.34	ND	0.79	ND	0.52	10
WYS19 C26H32N2O4Si	ND	ND	0.89	ND	ND	ND
XHE-III-06a	1	2	1	5	1.8	37
Ro15-1788	0.8	0.9	1.05	ND	0.6	148
MLT-I-70	1.1	1.2	1.1	ND	40.3	1000
XHE-III-04	1.2	2	1.1	219	0.4	500
FG8205	0.4	2.08	1.16	ND	1.54	227
PWZ-009A1	1.34	1.31	1.26	ND	0.84	2.03
alprazolam	0.8	0.59	1.43	ND	1.54	10000
XLI-348	13.56	11.17	1.578	ND	82.05	ND
QH-II-082	1.7	1.8	1.6	ND	6.1	100
WY-TSC-4 (WYS8)	0.007	0.99	1.63	ND	51.04	ND
SPH-121	0.14	1.19	1.72	ND	4	479
XLi-JY-DMH ANX3	3.3	0.58	1.9	ND	4.4	5000
MMB-III-016	3	1.97	2	1074	0.26	211
MMB-III-16	3	1.97	2	1074	0.26	211
XLI-8TC	21.52	11.01	2.155	ND	4.059	ND
6-PBC	0.49	1.21	2.2	ND	2.39	1343
YT-III-271	32.54	1.26	2.35	ND	103	ND
Ro15-4513	3.3	2.6	2.5	ND	0.26	3.8
TG-4-29	2.8	3.9	2.7	2.1	0.18	3.9
TG-II-82	1.6	2.9	2.8	ND	1	1000
OMB-18	3.9	1.2	3.4	1733	0.8	5
YT-II	6.932	0.8712	3.518	ND	5.119	ND

Table 7: Continued.

Cook code[a]	α1	α2	α3	α4	α5	α6
PS-1-34B C20H17N4BrO	ND	4.198	3.928	ND	ND	ND
DMCM	5.69	8.29	4	ND	1.04	134
MSR-I-032	6.2	18.7	4	ND	3.3	74.9
RY-008	3.75	7.2	4.14	ND	1.11	44.3
XHE-III-49	1.3	5.5	4.2	38.7	11.3	85.1
JYI-60 (C17H11N2OF)	3.73	1.635	4.3	ND	1.7	5000
FLUNITRAZEPAM	2.2	2.5	4.5	ND	2.1	2000
XLI-317	60.24	24.05	4.562	ND	0.295	ND
QH-II-080b	3	3.7	4.7	ND	24	1000
SPH-165	0.63	2.79	4.85	ND	10.4	1150
SH-I-04	7.3	6.136	5.1	ND	7.664	ND
SVO-8-30	1.1	5.3	5.3	2.8	0.6	15
WY-B-99-1	4.4	4.5	5.58	2000	47	2000
YT-III-25	2.531	5.786	5.691	ND	0.095	ND
BCCE	1.2	4.9	5.7	ND	26.8	2700
MMB-II-90	20	24	5.7	9	0.25	36
TC-YT-II-76	101.1	1.897	5.816	ND	11.99	ND
ZK 93423	4.1	4.2	6	ND	4.5	1000
RY-061	17	13	6.7	ND	0.3	31
JYI-54 (C24H15N3O3F4)	2.89	172	6.7	ND	57	1890
TG-4-29	8.3	10.2	6.9	ND	0.4	7.61
MMB-III-14	13	13	6.9	333	1.1	333
XHE-II-017	3.3	10	7	258	17	294
SHU-1-19	4	12	7	48	14	84
XHE-III-13	7.3	ND	7.1	880	1.6	311
DM-215	6.74	ND	7.42	ND	0.293	8.28
ABECARNIL	12.4	15.3	7.5	ND	6	1000
SVO-8-14	8	25	8	6.9	0.9	14
XHE-III-24	0.25	ND	8	222	10	328
SH-I-89S	12.78	8.562	8.145	ND	3.23	ND
PWZ-085	4.86	13	8.5	ND	0.55	40
XHE-I-093	2	7.1	8.9	1107	20	1162
ZG-168	11.2	10.7	9.2	ND	0.47	9.4
ZG69A	6.8	16.3	9.2	ND	0.85	54.6
ZG-69a (Ro15-1310)	6.8	16.3	9.2	ND	0.85	54.6
ZG-234	7.25	22.14	9.84	ND	0.3	5.25
XHE-II-073A (R ENRICHED)	5.9	11	10	15	1.18	140
RY-067	21	12	10	ND	0.37	42
XHE-III-14	2.6	ND	10	13	2	7
YT-III-272	295.9	14.98	10.77	ND	103.3	ND
SPH-38	2	5.4	10.8	ND	18.5	3000
ZG-208	9.7	11.2	10.9	ND	0.38	4.6
MLT-II-18	3.4	11.7	11	ND	225	10000
DM-II-33 (C20H13N3O2BrCl3)	88.6	85	11.6	ND	26.2	5000
JYI-59 (C22H13N3O2F4)	1.08	2.6	11.82	ND	11.5	5000
XHE-II-006b	3.7	15	12	1897	144	1000
XHE-II-073B (S-ENRICHED)	11	17	12	33	2.1	269
CM-B44 (ss)	32	43	12	379	4.3	485

Table 7: Continued.

Cook code[a]	$\alpha1$	$\alpha2$	$\alpha3$	$\alpha4$	$\alpha5$	$\alpha6$
WYSC1 C16H16N2O2	1.094	5.44	12.3	ND	69.8	21.2
JYI-48	75.59	90.68	12.78	ND	31.28	ND
XHE-II-002	8.3	18	13	3.9	1.5	11
RY-076	26	27	13	ND	0.7	22
WZ-113	19.2	13.2	13.4	ND	11.5	300
SH-I-085	11.08	4.866	13.75	ND	0.24	ND
CM-E10	23	26	14	215	0.51	96
TJH-IV-51	2.39	17.4	14.5	ND	316	10000
YT-III-38	1461	18.21	14.63	ND	3999	ND
CM-A87	1.62	4.54	14.73	1000	4.61	1000
diazepam	14	20	15	ND	11	ND
RY-053	49	29	15	ND	1	46
YCT-5	2.2	11.46	16.3	ND	200	10000
RY-098	10.1	22.2	16.5	ND	1.68	100
PWZ-096	11.1	36	16.9	ND	1.07	51.5
XLi223 C22H20BrN3O2	14	8.7	18	1000	10	2000
XHE-I-065	7.2	17	18	500	57	500
SH-I-02B	29.82	1315	18	ND	74.05	ND
MLT-II-16	5.05	10.41	18.4	ND	260	10000
RY-024 C19H19N3O3	26.9	26.3	18.7	ND	0.4	5.1
BCCt	0.72	15	18.9	ND	110.8	5000
LJD-III-15E	1.93	14	19	ND	70.8	1000
CM-E09b	20	22	19	55	0.45	69
RY-I-31	10	45	19	ND	6	1000
SH-I-030	14.42	11.04	19.09	ND	1.89	ND
YT-III-23	19.83	23.65	19.87	ND	1.105	ND
XHE-II-006a	4.7	4.4	20	1876	89	3531
OMB-19	22	4.6	20	3333	3.5	40
XHE-III-06b	32	33	20	299	28.6	740

[a]Affinity of compounds at $GABA_A$/BzR recombinant subtypes was measured by competition for [^{3}H]flunitrazepam or [^{3}H] Ro15-4513 binding to HEK cell membranes expressing human receptors of compositions $\alpha1\beta3\gamma2$, $\alpha2\beta3\gamma2$, $\alpha3\beta3\gamma2$, $\alpha4\beta3\gamma2$, $\alpha5\beta3\gamma2$, and $\alpha6\beta3\gamma2$ [22, 139]. Data represent the average of at least three determinations with a SEM of ±5%. ND: not determined.

values) were converted to logarithmic units for this study. A CoMFA descriptor set was created based on the –log (K_i) of over 70 structures. The goal was to derive an alternative three-dimensional shape of the receptor using biological activity of the most selective compounds. Structures were determined by crystal structure where available or by calculation. Charges were provided based on the Gasteiger-Huckel model. Conformations were kept consistent based on previous studies of low energy conformations [110]. It should be noted that this was not a traditional QSAR study as nonselective compounds were excluded. Therefore, K_i values did not cross 3 log units. This was acceptable since the goal was not to create a predictive QSAR predictive algorithm, rather a map of the receptor based on sterics and electrostatics. Hydrogen acceptor radii were set to 3.0 and the hydrogen donor radii were set to 2.6 based on recommendations from Certara (Tripos). Analyses were executed using PLS (partial least squares). The details of modeling will be further discussed in the SI.

For each of the following QSAR models (Figures 49–64), green areas represent desirable steric bulk and yellow represents undesirable steric bulk. Positive electrostatic contributions are represented by blue and negative electrostatic contributions are represented by red.

20. The $\alpha1\beta3\gamma2$ Receptor Subtype

See Figures 49–52.

21. The $\alpha2\beta3\gamma2$ Receptor Subtype

See Figures 53–56.

Table 8: Ligands with potent affinity for $\alpha 4$; ligands bound with K_i values <20 nM at this subtype. The structures of these ligands are in the Ph.D. thesis of Clayton (2011) [22].

Cook code[a]	$\alpha 1$	$\alpha 2$	$\alpha 3$	$\alpha 4$	$\alpha 5$	$\alpha 6$
CM-D45 C19H21N3O4	90.5	65.5	30.3	0.15	1.65	0.23
CM-D44	34.3	56.3	20.7	0.33	0.57	0.92
XHE-III-74	77	105	38	0.42	2.2	5.8
TG-4-29	2.8	3.9	2.7	2.1	0.18	3.9
SVO-8-30	1.1	5.3	5.3	2.8	0.6	15
XHE-II-002	8.3	18	13	3.9	1.5	11
XHE-III-06a	1	2	1	5	1.8	37
RY-080 C17H15N3O3	28.4	21.4	25.8	5.3	0.49	28.8
TG-4-39	1.6	34	24	5.6	1.4	23
SVO-8-14	8	25	8	6.9	0.9	14
RY-023 C22H27N3O3Si	197	142.6	255	7.8	2.61	58.6
MMB-II-90	20	24	5.7	9	0.25	36
XHE-III-14	2.6		10	13	2	7
XHE-II-024	0.09	0.18	0.32	14	0.24	11
XHE-II-073A (R ENRICHED)	5.9	11	10	15	1.18	140
SVO-8-67	7	41	26	15	2.3	191
CM-B31i (ss)	90	184	78	18	4.9	121
SVO-8-20	11	40	28	19	8.6	138

[a]Affinity of compounds at $GABA_A$/BzR recombinant subtypes was measured by competition for [^{3}H]flunitrazepam or [^{3}H] Ro15-4513 binding to HEK cell membranes expressing human receptors of compositions $\alpha 1\beta 3\gamma 2$, $\alpha 2\beta 3\gamma 2$, $\alpha 3\beta 3\gamma 2$, $\alpha 4\beta 3\gamma 2$, $\alpha 5\beta 3\gamma 2$, and $\alpha 6\beta 3\gamma 2$ [22, 139]. Data represent the average of at least three determinations with a SEM of ±5%. ND: not determined.

22. The $\alpha 3\beta 3\gamma 2$ Receptor Subtype

See Figures 57–60.

23. The $\alpha 5\beta 3\gamma 2$ Receptor Subtype

From the CoMFA maps several observations (Figure 65) can be made. The yellow steric regions near L_3 in the $\alpha 5\beta 3\gamma 2$ map are unique. This illustrated that, in general, benzodiazepines lacking a pendant phenyl are more suited to targeting the $\alpha 5$ subtype. The L_{Di} region of the $\alpha 1$ subtype is most tolerable for compounds with steric interactions in this location while the $\alpha 3$ subtype receptor compounds prefer no steric interaction in this location. Negative electrostatics are most preferred by the L_3 pocket of the $\alpha 2$ and $\alpha 5$ receptors. In general, the $\alpha 1$ subtype receptor prefers molecules without a dipole. It should be noted that none of the analogs are ionic in nature and the charges for this model were provided by the Gasteiger-Huckel model. For this reason more emphasis is placed on the steric relationships which exclude interactions in the pharmacophores. In the future a QSAR study which includes nonbinding benzodiazepines in the data set along with activity data will permit the creation of a predictive algorithm which will be very useful in lead targeting (see Figures 61–65).

24. Conclusion

Benzodiazepines, β-carbolines, and other classes of compounds readily target the $GABA_A$ receptors. The difficulty is finding subtype selective ligands, since there is no crystal structure of the Bz/$GABA_A$-ergic site itself, just one composed of five beta-subunits which has no Bz site to date. The $\alpha 5$-BzR/$GABA_A$ subunit has recently been shown to be important in the search to treat numerous cognition-based illnesses including Alzheimer's, schizophrenia, bipolar, and depression, as well as more recently a bronchodilator, potentially important in the treatment of asthma. As an inverse agonist, PWZ-029 was able to counteract the memory-impairing effects of scopolamine, a muscarinic antagonist, in both object recognition tests and object retrieval tests in rodents, and was active in primates, as well as samaritan Alzheimer's rats. The implications of these tests point to a use as a possible treatment for Alzheimer's disease. The docking of PWZ-029 in the $\alpha 5\gamma 2$ $GABA_A$R-subunit details the interactions between the pharmacophore/receptor model binding site and this important negative allosteric modulator. Furthermore, $\alpha 5$-BzR/$GABA_A$ positive allosteric modulator, SH-053-2′F-R-CH_3, was shown to reverse deleterious effects in the MAM-model of schizophrenia. The recent discovery of $\alpha 5$-$GABA_A$R in airway smooth muscle by Emala et al. has also lead to the testing of SH-053-2′F-R-CH_3 as a bronchodilator. This SH-053-2′F-R-CH_3 was found to be effective in relaxing preconstricted airway smooth muscle, as well as attenuating calcium-ion entry through the plasma membrane. In addition, XLi-093 (an $\alpha 5$ receptor antagonist), a potently binding $\alpha 5$-subtype selective bivalent ligand, has been shown to inhibit the $\alpha 5$-cognition deficits effected by diazepam and is a very good $\alpha 5$ benzodiazepine receptor site antagonist. It has also been shown to reverse the effects of $\alpha 5$ PAMs and NAMs in both rodent and primate models. These findings led to the exploration of the $\alpha 5$-binding pocket in the Milwaukee-based pharmacophore.

New features have been introduced to the unified pharmacophore/receptor model based on many substance classes that act at the diazepam sensitive and diazepam insensitive BzR binding sites of $GABA_A$ receptors. The major new feature identified for the $\alpha 5\beta 3\gamma 2$ receptor was a new L_4 pocket which was found by using pendant 6-phenyl benzodiazepines with a R-CH_3 at the prochiral center at C4. Further enhancement of potency was achieved by addition of 2′-F or 2′-N substituent in the pendant phenyl ring at C-6. While these changes have led to enhanced subtype selective ligands, the overall development guided by this pharmacophore model described here has led to new agents with varying, fascinating pharmacological profiles, ranging from use in cognition-based diseases such as Alzheimer's and schizophrenia, to use as a bronchodilator. This research on updating the Milwaukee-based pharmacophore/receptor model can be used in the rational design for improving the selectivity of $\alpha 5$ ligands. As the library of compounds increases, the data which follows can then be further evaluated and can lead to more insight to the identification of the possible roles each individual residue may have with the binding pocket.

Table 9: Ligands with potent affinity for $\alpha 5$; ligands bound with K_i values <20 nM at this subtype. The structures of these ligands are in the Ph.D. thesis of Clayton (2011) [22].

Cook code[a]	$\alpha 1$	$\alpha 2$	$\alpha 3$	$\alpha 4$	$\alpha 5$	$\alpha 6$
JYI-57	0.076	0.076	0.131	ND	0.036	ND
YT-II-76	95.34	2.797	0.056	ND	0.04	ND
QH-II-085	0.08	0.06	0.02	ND	0.08	ND
YT-III-25	2.531	5.786	5.691	ND	0.095	ND
SH-I-048A	0.774	0.1723	0.383	ND	0.11	ND
QH-II-077	0.06	0.08	0.05	ND	0.12	4
DM-239	1.5	ND	0.53	ND	0.14	6.89
QH-II-092	0.07	0.03	0.04	ND	0.17	ND
TG-4-29	2.8	3.9	2.7	2.1	0.18	3.9
SH-I-75	1487	989.9	773	ND	0.1825	ND
PWZ-007A	0.11	0.1	0.09	ND	0.2	10
XHE-II-024	0.09	0.18	0.32	14	0.24	11
SH-I-085	11.08	4.866	13.75	ND	0.24	ND
MMB-II-90	20	24	5.7	9	0.25	36
QH-II-090 (CGS-8216)	0.05	0.08	0.12	ND	0.25	17
JYI-42	0.257	0.146	0.278	ND	0.256	ND
MMB-III-016	3	1.97	2	1074	0.26	211
MMB-III-16	3	1.97	2	1074	0.26	211
Ro15-4513	3.3	2.6	2.5	ND	0.26	3.8
DM-215	6.74	ND	7.42	ND	0.293	8.28
XLI-317	60.24	24.05	4.562	ND	0.295	ND
RY-061	17	13	6.7	ND	0.3	31
ZG-234	7.25	22.14	9.84	ND	0.3	5.25
PZII-028	0.2	ND	0.2	ND	0.32	1.9
RY-067	21	12	10	ND	0.37	42
DM-II-90 (C17H12N4BrCl)	0.505	1	0.63	ND	0.37	5000
ZG-208	9.7	11.2	10.9	ND	0.38	4.6
XHE-III-04	1.2	2	1.1	219	0.4	500
TG-4-29	8.3	10.2	6.9	ND	0.4	7.61
RY-024 C19H19N3O3	26.9	26.3	18.7	ND	0.4	5.1
JYI-47	2.759	2.282	0.511	ND	0.427	ND
PWZ-0071	0.23	0.17	0.12	ND	0.44	17.31
CM-E09b	20	22	19	55	0.45	69
ZG-168	11.2	10.7	9.2	ND	0.47	9.4
RY-080 C17H15N3O3	28.4	21.4	25.8	5.3	0.49	28.8
BRETAZENIL	0.35	0.64	0.2	ND	0.5	12.7
CM-E10	23	26	14	215	0.51	96
JYI-04 (C21H23N3O3)	28.3	16	ND	ND	0.51	1.57
PZII-029	0.34	ND	0.79	ND	0.52	10
PWZ-085	4.86	13	8.5	ND	0.55	40
JYI-70 (C19H13N4F)	6.3	2.1	ND	ND	0.56	5000
CM-D44	34.3	56.3	20.7	0.33	0.57	0.92
SVO-8-30	1.1	5.3	5.3	2.8	0.6	15
Ro15-1788	0.8	0.9	1.05	ND	0.6	148
XLi268 C17H13BrN4	2.8145	0.6862	ND	ND	0.6243	ND
ZG-63A	17.3	21.6	29.1	ND	0.65	4
SH-053-2′F	21.99	12.34	34.9	ND	0.671	ND
XLI-286	0.051	0.064	0.118	ND	0.684	ND
SH-I-S66	22.93	30.36	55.26	ND	0.69	ND

Table 9: Continued.

Cook code[a]	α1	α2	α3	α4	α5	α6
RY-076	26	27	13	ND	0.7	22
DM-173	13.1	ND	38.1	ND	0.78	118
OMB-18	3.9	1.2	3.4	1733	0.8	5
HJ-I-037	15.07	8.127	28.29	ND	0.818	ND
PWZ-009A1	1.34	1.31	1.26	ND	0.84	2.03
ZG69A	6.8	16.3	9.2	ND	0.85	54.6
ZG-69a (Ro15-1310)	6.8	16.3	9.2	ND	0.85	54.6
JYI-64 (C17H12N4FBr)	0.305	1.111	0.62	ND	0.87	5000
SVO-8-14	8	25	8	6.9	0.9	14
JYI-03 (C21H21N3O3)	185.4	107	ND	ND	0.954	3.34
TG-II-82	1.6	2.9	2.8	ND	1	1000
RY-053	49	29	15	ND	1	46
YT-6	15.31	87.8	60.49	ND	1.039	ND
DMCM	5.69	8.29	4	ND	1.04	134
PWZ-096	11.1	36	16.9	ND	1.07	51.5
MMB-III-14	13	13	6.9	333	1.1	333
YT-III-23	19.83	23.65	19.87	ND	1.105	ND
RY-008	3.75	7.2	4.14	ND	1.11	44.3
XLI-2TC	3.442	1.673	44.08	ND	1.121	ND
XHE-II-073A (R ENRICHED)	5.9	11	10	15	1.18	140
QH-II-075	0.18	0.21	0.25	ND	1.3	40
RY-054	59	44	27	ND	1.3	126
TG-4-39	1.6	34	24	5.6	1.4	23
XHE-II-002	8.3	18	13	3.9	1.5	11
RY-031 (RY-10)	20.4	27	26.1	ND	1.5	176
FG8205	0.4	2.08	1.16	ND	1.54	227
alprazolam	0.8	0.59	1.43	ND	1.54	1000
XHE-III-13	7.3	ND	7.1	880	1.6	311
CM-D45 C19H21N3O4	90.5	65.5	30.3	0.15	1.65	0.23
RY-098	10.1	22.2	16.5	ND	1.68	100
YT-5	0.421	0.6034	36.06	ND	1.695	ND
JYI-60 (C17H11N2OF)	3.73	1.635	4.3	ND	1.7	5000
RY-033	14.8	56	25.3	ND	1.72	22.9
XHE-III-06a	1	2	1	5	1.8	37
SH-I-030	14.42	11.04	19.09	ND	1.89	ND
XLi352 C18H13ClN2O	1.56	0.991	ND	ND	1.957	ND
XLi351 C21H21ClN2OSi	1.507	0.967	ND	ND	1.985	ND
XHE-III-14	2.6	ND	10	13	2	7
DM-II-72 (C15H10N20BrCl)	5000	1.37	ND	ND	2.02	5000
XHE-II-073B (S-ENRICHED)	11	17	12	33	2.1	269
FLUNITRAZEPAM	2.2	2.5	4.5	ND	2.1	2000
XHE-III-74	77	105	38	0.42	2.2	5.8
SVO-8-67	7	41	26	15	2.3	191
6-PBC	0.49	1.21	2.2	ND	2.39	1343
RY-058	86	40	85	ND	2.4	150
ZG-224	17.1	33.7	50	ND	2.5	31.7
RY-066	83	60	48	ND	2.6	180
RY-023 C22H27N3O3Si	197	142.6	255	7.8	2.61	58.6
XLi350 C17H11ClN2O	1.224	1.188	ND	ND	2.9	ND
JYI-32 (C20H15N3O2BrF)	3.07	4.96	ND	ND	2.92	52.24

Table 9: Continued.

Cook code[a]	α1	α2	α3	α4	α5	α6
SH-I-89S	12.78	8.562	8.145	ND	3.23	ND
MSR-I-032	6.2	18.7	4	ND	3.3	74.9
OMB-19	22	4.6	20	3333	3.5	40
ZG-213	12.8	49.8	30.2	ND	3.5	22.5
YT-II-83	32.74	13.22	24.1	ND	3.548	ND
RY-059	89	70	91	ND	3.7	301
SPH-121	0.14	1.19	1.72	ND	4	479
RY-047	200	124	79	ND	4	340
XLI-8TC	21.52	11.01	2.155	ND	4.059	ND
YT-I-38	945.9	326.8	245.9	ND	4.07	ND
DM-146	6.44	ND	148	ND	4.23	247
CM-B44 (ss)	32	43	12	379	4.3	485
CM-B47	32	63	34	2007	4.4	717
XLi-JY-DMH ANX3	3.3	0.58	1.9	ND	4.4	5000
WY-B-15	0.92	0.83	0.58	2080	4.42	646
ZK 93423	4.1	4.2	6	ND	4.5	1000
JYI-12 (C19H16N3O3F3)	91	39	ND	ND	4.5	6.8
CM-A87	1.62	4.54	14.73	1000	4.61	1000
DM-III-01 (C18H12N3O2Br)	5000	12	ND	ND	4.73	5000
RY-057	73	85	97	ND	4.8	333
JYI-15 (C19H14N3O3F3)	205	812	ND	ND	4.8	22
CM-B31i (ss)	90	184	78	18	4.9	121
RY-079	121.1	141.9	198.4	159	5	113.7
JC208 C15H10N2OS	22.42	18.89	ND	ND	5.039	ND
YT-II	6.932	0.8712	3.518	ND	5.119	ND
XLi270 C19H14N4	36.39	25.81	ND	ND	5.291	ND
XHE-I-051	35	39	42	ND	5.3	979
MMB-II-87	200	333	107	109	5.4	333
XLI-210	231	661	2666	ND	5.4	54.22
XHE-II-O53-ACID	50.35	11.8	44	ND	5.9	5000
ABECARNIL	12.4	15.3	7.5	ND	6	1000
RY-I-31	10	45	19	ND	6	1000
QH-II-082	1.7	1.8	1.6	ND	6.1	100
SH-TSC-1 (PWZ-029)	362.4	180.3	328.2	ND	6.185	ND
XHE-II-065	1000	409	216	37	6.4	175
JYI-49 (C20H12N3O2F4Br)	1.87	2.38	ND	ND	6.7	3390
JC184 C13H9BrN2OS	9.606	10.5	ND	ND	6.709	ND
QH-II-066	76.3	42.1	47.4	2000	6.8	3000
XLI-381	619.9	285.6	3639	ND	7.051	ND
RY-071	19	56	91	ND	7.2	266
RY-I-28	283	318	102	ND	7.2	61
CM-A82a	2.78	8.93	24.51	1000	7.49	1000
YT-III-31	36.39	67.85	129.7	ND	7.59	ND
SH-I-04	7.3	6.136	5.1	ND	7.664	ND
QH-146	0.49	ND	0.76	ND	7.7	1000
QH-II-063	9.4	9.3	31	ND	7.7	3000
JC221 ANX1	106.175	49.405	182	ND	7.7495	362
DM-II-30 (C20H13N3O2BrF3)	17.6	13.4	28.51	ND	7.8	5000
SH-TS-CH_3	107.2	50.09	20.95	ND	8.068	ND
RY-073	156	88	122	ND	8.5	267

Table 9: Continued.

Cook code[a]	α1	α2	α3	α4	α5	α6
SVO-8-20	11	40	28	19	8.6	138
SHU-221-1	66	41	43	3000	9	3000
YT-III-231	51.09	61.46	26.34	ND	9.124	ND
CM-E09a	176	192	122	490	9.2	718
DM-139	5.8	ND	169	ND	9.25	325
YT-III-42	382.9	16.83	44.04	ND	9.77	ND
CD-214	16.4	48.2	42.5	ND	9.8	168
XHE-III-24	0.25	ND	8	222	10	328
XLi223 C22H20BrN3O2	14	8.7	18	1000	10	2000
SPH-165	0.63	2.79	4.85	ND	10.4	1150
JYI-01 (C19H20N3O3Br)	59.2	159	96	ND	10.6	2.88
diazepam	14	20	15	ND	11	ND
XHE-III-49	1.3	5.5	4.2	38.7	11.3	85.1
WZ-113	19.2	13.2	13.4	ND	11.5	300
JYI-59 (C22H13N3O2F4)	1.08	2.6	11.82	ND	11.5	5000
JYI-72 (C22H21N4SiF)	48.5	18.5	ND	ND	11.5	5000
TC-YT-II-76	101.1	1.897	5.816	ND	11.99	ND
JYI-10 (C17H13N3O3F3Br)	5000	368	ND	ND	12.3	23
WZ-069	40	30.5	38.5	ND	12.6	1000
JYI-06 (C23H23N3O4)	16.5	5.48	5000	ND	12.6	5000
RY-072	220	150	184	ND	12.7	361
JYI-14 (C17H14N3O3F3)	32	25	ND	ND	13	565
XHE-II-053	287	45	96	1504	13.8	1000
Xli-347 C34H28N6O7	828.05	690.2	ND	ND	13.87	ND
SHU-1-19	4	12	7	48	14	84
CM-C28 (SR)	176	752	244	290	14	141
CM-E11	333	308	161	394	14	750
XHE-II-012	49	24	31	1042	14	2038
MMB-III-018	117	140	78	3500	14	976
MMB-III-18	117	140	78	3500	14	976
CM-B31c (ss)	118	319	173	37	15	137
CM-B45	230	557	336	265	15	230
XLI-093	1000	1000	858	1550	15	2000
DM-II-20 (C22H14N3O2F3)	54.3	27.14	35.68	ND	15.35	5000
XLi269 C22H22N4Si	221.8	154.2	ND	ND	15.51	ND
SH-O53-S-CH_3-2′F	350	141	1237	ND	16	5000
JYI-13 (C21H16N3O4F3)	5000	63.7	ND	ND	16	8.38
CM-B34	472	451	223	114	17	175
XHE-II-017	3.3	10	7	258	17	294
JC222 C16H12N2OS	86.7	45.11	ND	ND	17.63	ND
SPH-38	2	5.4	10.8	ND	18.5	3000
WZ-070	72.7	30.7	53.2	ND	18.6	300
RY-069	692	622	506	ND	19	1000
SH-053-2′F-S-CH_3	468.2	33.27	291.5	ND	19.2	ND
XHE-I-093	2	7.1	8.9	1107	20	1162

[a]Affinity of compounds at $GABA_A$/BzR recombinant subtypes was measured by competition for [^{3}H]flunitrazepam or [^{3}H] Ro15-4513 binding to HEK cell membranes expressing human receptors of compositions $\alpha1\beta3\gamma2$, $\alpha2\beta3\gamma2$, $\alpha3\beta3\gamma2$, $\alpha4\beta3\gamma2$, $\alpha5\beta3\gamma2$, and $\alpha6\beta3\gamma2$ [22, 139]. Data represent the average of at least three determinations with a SEM of ±5%. ND: not determined.

Table 10: Ligands with potent affinity for $\alpha 6$; ligands bound with K_i values <20 nM at this subtype. The structures of these ligands are in the Ph.D. thesis of Clayton (2011) [22].

Cook code[a]	$\alpha 1$	$\alpha 2$	$\alpha 3$	$\alpha 4$	$\alpha 5$	$\alpha 6$
CM-D45 C19H21N3O4	90.5	65.5	30.3	0.15	1.65	0.23
CM-D44	34.3	56.3	20.7	0.33	0.57	0.92
JYI-04 (C21H23N3O3)	28.3	16	ND	ND	0.51	1.57
PZII-028	0.2	ND	0.2	ND	0.32	1.9
PWZ-009A1	1.34	1.31	1.26	ND	0.84	2.03
JYI-01 (C19H20N3O3Br)	59.2	159	96	ND	10.6	2.88
JYI-03 (C21H21N3O3)	185.4	107	ND	ND	0.954	3.34
Ro15-4513	3.3	2.6	2.5	ND	0.26	3.8
TG-4-29	2.8	3.9	2.7	2.1	0.18	3.9
JYI-11 (C22H22N3O3F3Si)	5000	5000	ND	ND	648	3.97
QH-II-077	0.06	0.08	0.05	ND	0.12	4
ZG-63A	17.3	21.6	29.1	ND	0.65	4
ZG-208	9.7	11.2	10.9	ND	0.38	4.6
OMB-18	3.9	1.2	3.4	1733	0.8	5
RY-024 C19H19N3O3	26.9	26.3	18.7	ND	0.4	5.1
ZG-234	7.25	22.14	9.84	ND	0.3	5.25
XHE-III-74	77	105	38	0.42	2.2	5.8
JYI-12 (C19H16N3O3F3)	91	39	ND	ND	4.5	6.8
DM-239	1.5	ND	0.53	ND	0.14	6.89
XHE-III-14	2.6	ND	10	13	2	7
TG-4-29	8.3	10.2	6.9	ND	0.4	7.61
DM-215	6.74	ND	7.42	ND	0.293	8.28
JYI-13 (C21H16N3O4F3)	5000	63.7	ND	ND	16	8.38
CGS9895	0.21	ND	ND	ND	ND	9.3
ZG-168	11.2	10.7	9.2	ND	0.47	9.4
PWZ-007A	0.11	0.1	0.09	ND	0.2	10
PZII-029	0.34	ND	0.79	ND	0.52	10
XHE-II-024	0.09	0.18	0.32	14	0.24	11
XHE-II-002	8.3	18	13	3.9	1.5	11
BRETAZENIL	0.35	0.64	0.2	ND	0.5	12.7
JYI-19 (C23H23N3O3S)	2.176	205	ND	ND	34	12.7
SVO-8-14	8	25	8	6.9	0.9	14
SVO-8-30	1.1	5.3	5.3	2.8	0.6	15
WYS10 C14H9F3N2O2	0.88	36	25.6	ND	548.7	15.3
QH-II-090 (CGS-8216)	0.05	0.08	0.12	ND	0.25	17
PWZ-0071	0.23	0.17	0.12		0.44	17.31

[a]The affinity of compounds at $GABA_A$/BzR recombinant subtypes was measured by competition for [^{3}H]flunitrazepam binding to HEK cell membranes expressing human receptors of compositions $\alpha 1\beta 3\gamma 2$, $\alpha 2\beta 3\gamma 2$, $\alpha 3\beta 3\gamma 2$, $\alpha 4\beta 3\gamma 2$, $\alpha 5\beta 3\gamma 2$, and $\alpha 6\beta 3\gamma 2$ [139]. Data represent the average of at least three determinations with a SEM of ±5%. ND: not determined.

The X-ray structure determination of the $\alpha 5\beta 3\gamma 2$ GABA(A) receptor is eagerly awaited, while that with five $\beta 3$-subunits has been reported recently (Miller and Aricescu, *Nature* 2014). It is hoped that the proposed orientation may be used by others to gain additional insight into the potential mechanisms underlying binding and modulation at the Bz site, all of which will lead to a better understanding of the structure and function of GABA(A) receptors, ultimately targeted toward treatment of diseases.

25. Synthesis of Ligands with $\alpha 5$ BzR Subtype Selectivity

Briefly, bromoacetyl bromide was added to 2-aminobenzophenone **44**, followed by treatment with methanol, which had been saturated with ammonia (g) under the cooling of an ice-water bath. The benzodiazepine, **45**, was brominated to provide **46** and then reacted with ethyl isocyanoacetate to generate the imidazobenzodiazepine, **47**. A much better one-pot process has now been devised using KtBuO at −30°C [140]. The bromide **48** was subjected to a Stille-type coupling to give DM-I-81 (**9**) [126]. This route (Scheme 1) can be executed on several hundred gram scales.

The benzodiazepine monomers were prepared by the method of Fryer and Gu [89, 141]. The isatoic anhydride was heated with sarcosine in dimethyl sulfoxide to provide amide **49**. Bromination of **49** in a mixture of acetic acid, bromine, and sodium acetate afforded the corresponding monosubstituted bromide **50** in good yield. Deprotonation of **50** with lithium diisopropyl amide (LDA) in THF was followed by treatment with diethyl chlorophosphate to provide the intermediate enol phosphate. The enol phosphate was stirred with a solution of ethyl isocyanoacetate and LDA to yield the imidazo congener. Again, a better one-pot procedure has been developed using KtBuO at −30°C in place of LDA at 0°C. A Heck type coupling reaction was employed with the bromide **51** with bis(acetate)bis(triphenylphosphine)palladium(II) to provide the TMS-acetylene **52**. Treatment of **52** with Bu_4NF removed the trimethylsilyl group. Hydrolysis of the ester function of **53** provided the acid **54** in excellent yield and this material was dried scrupulously and subjected to a standard CDI-mediated coupling reaction to furnish bivalent ligand XLi-093 (**4**). The imidazobenzodiazepine diethyl diester XLi-356 (**10**) was obtained from XLi-093 (Scheme 2) in high yield *via* catalytic hydrogenation (Pd/C, H_2).

26. Synthesis of Bivalents

Inverse agonist **53** was synthesized via the reported procedure. Hydrolysis of the ester function of **53** provided the acid **54** in excellent yield. This material was dried scrupulously and was subjected to a standard CDI-mediated coupling reaction to furnish bivalent ligands **4**, **55**, and **56** in 60% yield (Scheme 3) [13].

The acid **57**, obtained from the ester **47**, which was available from the literature [13], was stirred with CDI in DMF, followed by stirring with the required diol and DBU to provide bromide substituted dimers **58** or **59**, respectively. They were converted into the trimethylsilylacetylenyl **60** or **61**, respectively, under standard conditions (Pd-mediated, Heck-type coupling) [142]. The bisacetylene **62** or **63** (individually) was easily obtained by treatment of the trimethylsilyl ligand **60** or **61** with fluoride anion, as shown in Scheme 4.

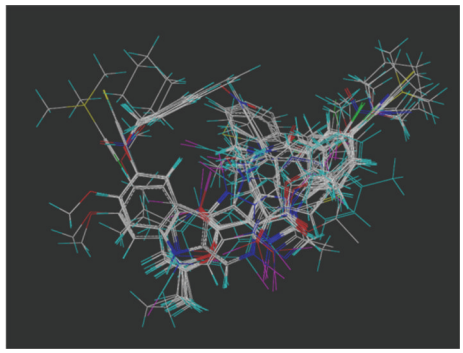


Figure 34: Overlay of selected compounds for $\alpha 1\beta 3\gamma 2$ subtype from Table 5.

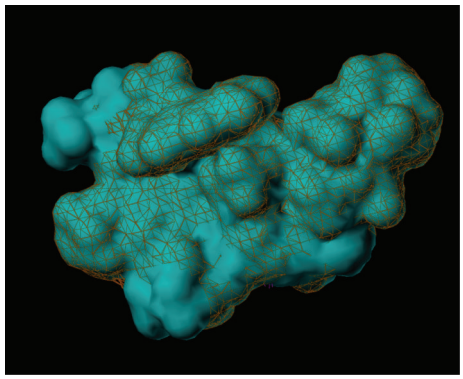


Figure 35: Updated $\alpha 1\beta 3\gamma 2$ subtype (blue solid) overlaid with the previous model (red wire). Overlap identified where wire and solid overlap.

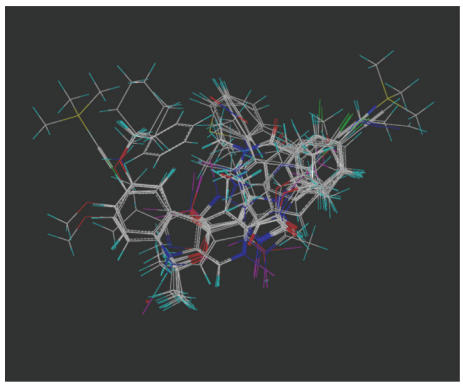


Figure 36: Overlay of compounds selective for $\alpha 2\beta 3\gamma 2$ subtype.

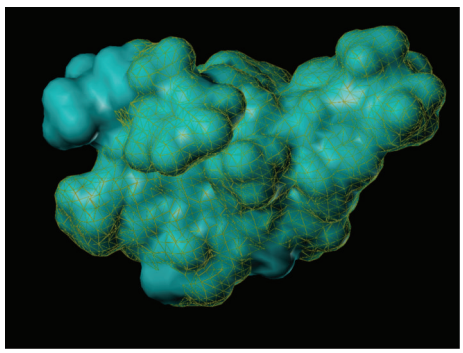


Figure 37: Updated $\alpha 2\beta 3\gamma 2$ subtype (solid) overlaid with the previous model (red wire). Overlap identified where wire and solid overlap.

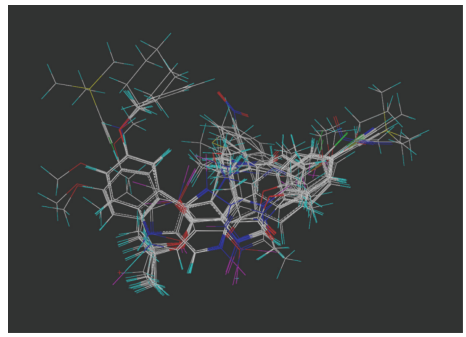


Figure 38: Overlay of compounds selective for $\alpha 3\beta 3\gamma 2$ subtype.

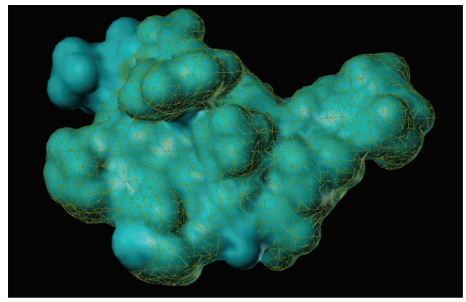


Figure 39: Updated $\alpha 3\beta 3\gamma 2$ subtype (blue solid) overlaid with the previous model (red wire). Overlap identified where wire and solid overlap.

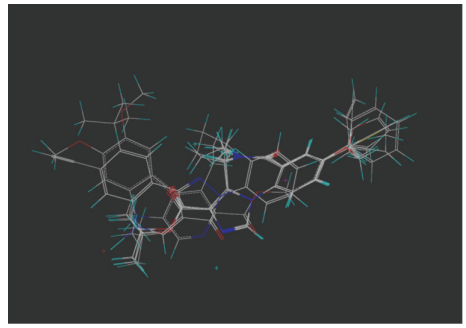


Figure 40: Overlay of selected compounds selective for $\alpha 4\beta 3\gamma 2$ subtype.

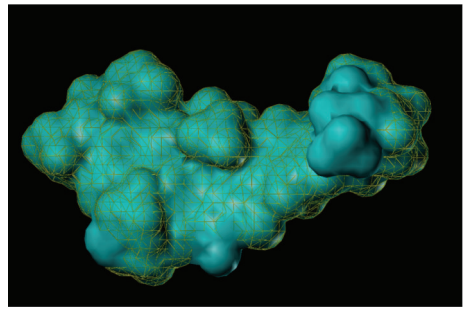


Figure 41: Updated $\alpha 4\beta 3\gamma 2$ subtype (blue solid) overlaid with the previous model (yellow wire). Overlap identified where wire and solid overlap.

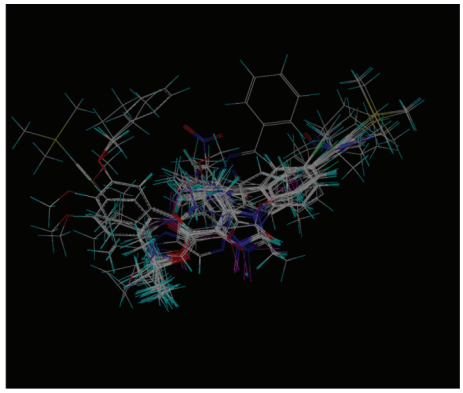


Figure 42: Overlay of selected compounds selective for $\alpha5\beta3\gamma2$ subtype.

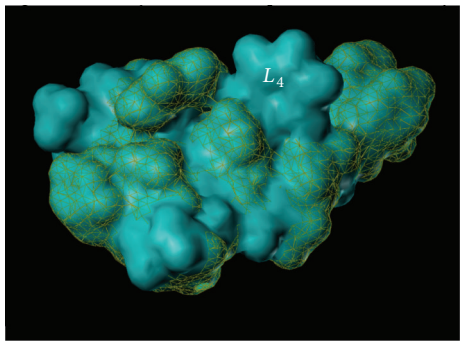


Figure 43: Updated $\alpha5\beta3\gamma2$ subtype (blue solid) overlaid with the previous model (yellow wire). Overlap identified where wire and solid overlap.

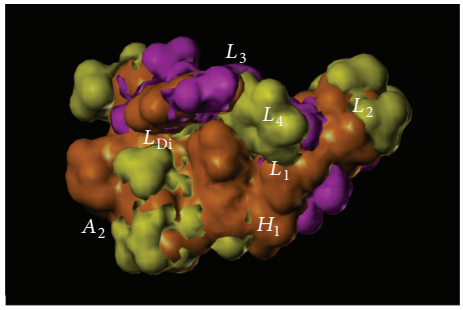


Figure 44: Overlay of the $\alpha5\beta3\gamma2$ receptor (yellow) subtype with the $\alpha1\beta3\gamma2$ receptor (magenta) subtype. Orange surfaces indicate overlapping regions.

27. Materials, Methods, and Experimental

27.1. Materials and General Instrumentation. Chemicals were purchased from Aldrich Chemical Co. or Tokyo Chemical Industries and were used without further purification except where otherwise noted. Anhydrous THF was distilled from sodium/benzophenone ketyl. TLC analyses were carried out on Merck Kieselgel 60 F_{254}, and flash column chromatography was performed on silica gel 60b purchased from E. M. Laboratories. Melting points were taken on a Thomas-Hoover melting point apparatus or an Electrothermal Model IA8100 digital melting point apparatus and are reported uncorrected. NMR spectra were recorded on a Bruker 300 or 500 MHz multiple-probe spectrometer. Infrared spectra were recorded on a Nicolet DX FTIR BX V5.07 spectrometer or a Mattson Polaris IR-10400 instrument. Low-resolution mass spectral data (EI/CI) were obtained on a Hewlett-Packard 5985B GC-mass spectrometer, while high resolution mass spectral data were taken on a VG autospectrometer (Double Focusing High Resolution GC/Mass Spectrometer, UK). Microanalyses were performed on a CE Elantech EA1110 elemental analyzer. Methods of specific experiments can be found in corresponding cited works.

27.2. Competition Binding Assays. Competition binding assays were performed in a total volume of 0.5 mL of a 50 mM Tris-acetate at 4° degree centigrade for 1 hour using [^{3}H]flunitrazepam as the radioligand. For these binding assays, 20–50 mg of membrane protein harvested with hypotonic buffer (50 mM Tris-acetate pH 7.4 at 4 degree) was incubated with the radiolabel as previously described [139, 143]. Nonspecific binding was defined as radioactivity bound in the presence of 100 μM diazepam and represented less than 20% of total binding. Membranes were harvested with a Brandel cell harvester followed by three ice-cold washes onto polyethyleneimine-pretreated (0.3%) Whatman GF/C filters. Filters were dried overnight and then soaked in Ecoscint A liquid scintillation cocktail (National Diagnostics; Atlanta, GA). Bound radioactivity was quantified by liquid scintillation counting. Membrane protein concentrations were determined using an assay kit from Bio-Rad (Hercules, CA) with bovine serum albumin as the standard.

27.3. Radioligand Binding Assays (Drs. McKernan and Atack) [12]. In brief, the affinity of compounds for human recombinant GABA(A) receptors was measured by competition binding using 0.5 nM [^{3}H]flunitrazepam. Transfected HEK cells (beta2 gamma2 and desired alpha subtype) were harvested into phosphate-buffered saline, centrifuged at 3,000 g, and stored at −70°C until required. On the day of the assay, pellets were thawed and resuspended in sufficient volume of 50 mM Tris/acetate (pH 7.4 at 4°C) to give a total binding of approximately 1500–2000 dpm. Nonspecific binding was defined in the presence of 100 mM (final concentration) diazepam. Test compounds were dissolved in DMSO at a concentration of 10 mM and diluted in assay buffer to give an appropriate concentration range in the assay, such that the final DMSO concentration in the assay was always less than 1%. Total assay volume was 0.5 mL and assays were carried out in 96-well plates and incubation time started by the addition of 0.1 mL of resuspended cell membranes. Following incubation for 1 hour at 4°C, assays were terminated by filtration through GF/B filters, washed with 10 mL ice cold buffer, dried, and then counted using a liquid scintillation counter. The percentage of inhibition of [^{3}H]flunitrazepam binding, the IC_{50}, and the K_i values were calculated using the Activity Base Software Package (ID Business Solutions,

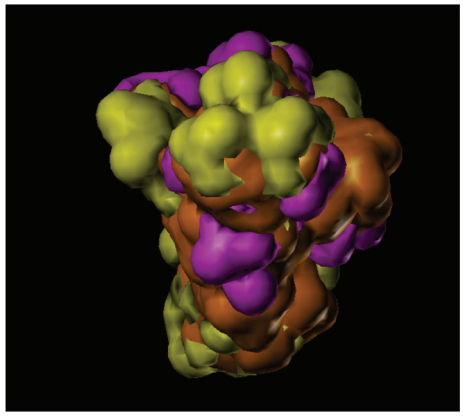


Figure 45: Overlay of the $\alpha5\beta3\gamma2$ receptor (yellow) subtype with the $\alpha1\beta3\gamma2$ receptor (magenta) subtype (Figure 44 rotated 90°). Orange surfaces indicate overlapping regions.

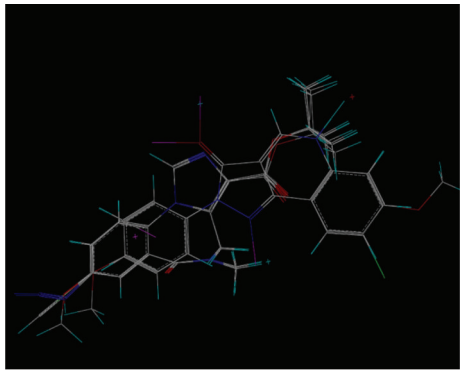


Figure 46: Overlay of selected compounds selective for $\alpha6\beta3\gamma2$ subtype.

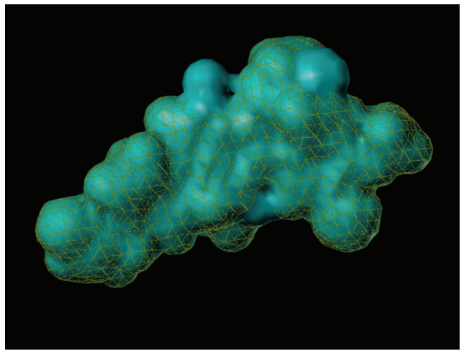
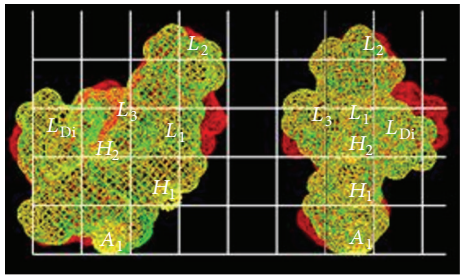


Figure 47: Updated $\alpha6\beta3\gamma2$ subtype (blue solid) overlaid with the previous model (yellow wire). Overlap identified where wire and solid overlap.

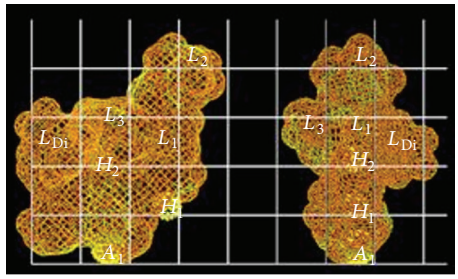
Guildford, UK) according to the Cheng-Prusoff equation [143]. We have previously reported the synthesis of the following.

1,3-Bis(8-acetyleno-5,6-dihydro-5-methyl-6-oxo-4H-imidazo[1,5a][1,4]benzodiazepine-3-carboxy) propyl diester ***4*** (XLi-093) (Procedure A), experimental details previously reported [17].

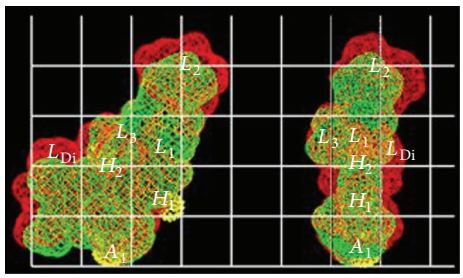
1,5-Bis(8-acetyleno-5,6-dihydro-5-methyl-6-oxo-4H-imidazo[1,5a][1,4]benzodiazepine-3-carboxy) pentyl diester ***56*** (XLi-210), experimental details previously reported [17].



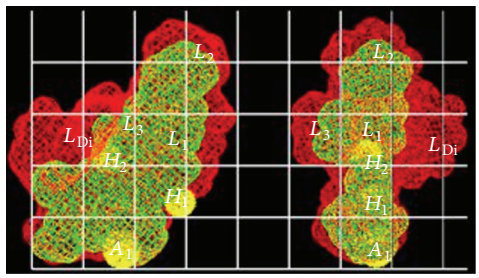
(a) Orthogonal views of the overlap (yellow) volumes of $\alpha1\beta3\gamma2$ (red) and $\alpha2\beta3\gamma2$ (green)



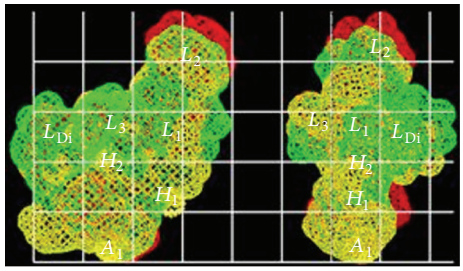
(b) Orthogonal views of the overlap (yellow) volumes of $\alpha2\beta3\gamma2$ (red) and $\alpha3\beta3\gamma2$ (green)



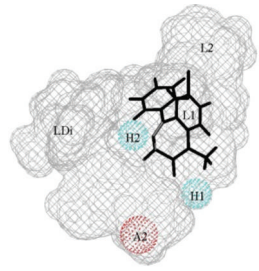
(c) Orthogonal views of the overlap (yellow) volumes of $\alpha4\beta3\gamma2$ (red) and $\alpha6\beta3\gamma2$ (green)



(d) Orthogonal views of the overlap (yellow) volumes of $\alpha1\beta3\gamma2$ (red) and $\alpha6\beta3\gamma2$ (green)



(e) Orthogonal views of the overlap (yellow) volumes of $\alpha5\beta3\gamma2$ (red) and $\alpha1\beta3\gamma2$ (green)



(f) Diazepam and the unified pharmacophore descriptors

FIGURE 48: The previous benzodiazepine subtype selective receptor pharmacophore models [23]. (1) The L_2 region in the $\alpha5$ subtype is larger than the $\alpha1$ subtypes. This is a key result. It is the principle difference between $\alpha5$ subtypes compared to $\alpha2$ and $\alpha3$ subtypes, but especially in regard to $\alpha1$ subtypes (L_2 smaller in $\alpha1$). (2) The L_3 region is larger in the $\alpha5$ subtype as compared to the $\alpha1$, $\alpha2$, $\alpha3$, $\alpha4$, and $\alpha6$ BzR sites. R analogs of benzodiazepines with pendant phenyls had increased affinity to $\alpha5$ supporting the larger L_3 pocket in this receptor subtype, while S isomers bound to $\alpha2$, $\alpha3$, and $\alpha5$ subtypes because of different conformational constraints.

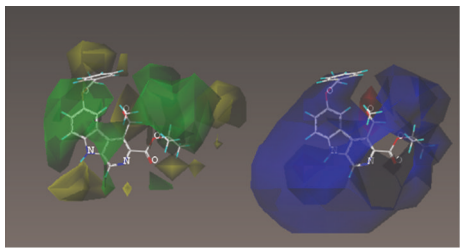


FIGURE 49: Steric (left) and electrostatic maps of the $\alpha1\beta3\gamma2$ receptor subtype shown in the transparent mode as seen from the classic perspective.

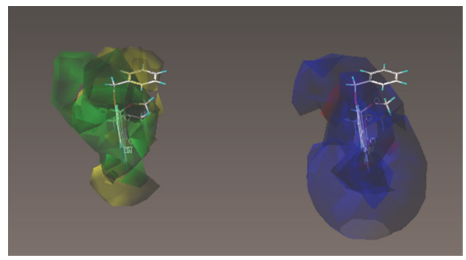


FIGURE 50: Steric (left) and electrostatic maps of the $\alpha1\beta3\gamma2$ receptor subtype shown in the transparent mode as seen from the classic perspective (Figure 45) rotated 90°.

1,3-Bis(8-ethyl-5,6-dihydro-5-methyl-6-oxo-4H-imidazo[1,5a][1,4]benzodiazepine-3-carboxy) propyl diester ***10*** (Xli-356), experimental previously published [144].

Bis(8-acetyleno-5,6-dihydro-5-methyl-6-oxo-4H-imidazo[1,5a][1,4]benzodiazepine-3-carboxy) dimethyl glycol dies-

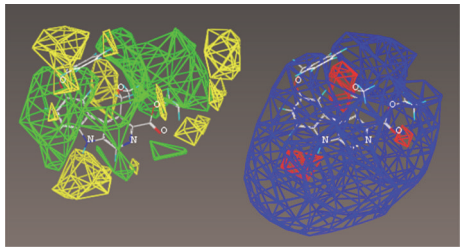


Figure 51: Steric (left) and electrostatic maps of the $\alpha 1\beta 3\gamma 2$ receptor subtype shown in line mode as seen from the classic perspective.

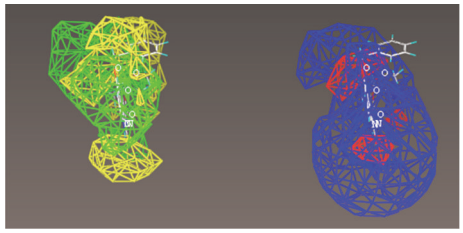


Figure 52: Steric (left) and electrostatic maps of the $\alpha 1\beta 3\gamma 2$ receptor subtype shown in line mode as seen from the classic perspective rotated 90°.

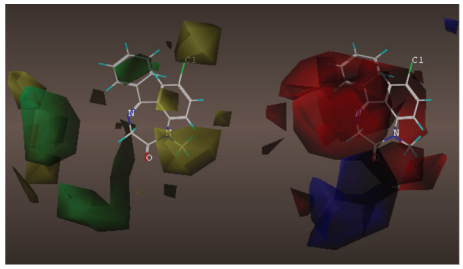


Figure 53: Steric (left) and electrostatic maps of the $\alpha 2\beta 3\gamma 2$ receptor subtype shown in the transparent mode as seen from the classic perspective.

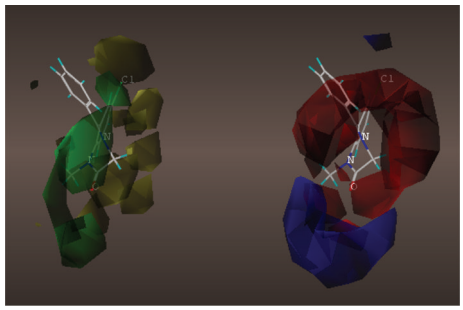


Figure 54: Steric (left) and electrostatic maps of the $\alpha 2\beta 3\gamma 2$ receptor subtype shown in the transparent mode as seen from the classic perspective rotated 90°.

ter **55** (Xli-374), experimental details previously reported [17].

8-Bromo-6-phenyl-4H-benzo[f]imidazo[1,5-a][1,4]diazepine-3-carboxylic acid **57**, experimental details previously reported [17].

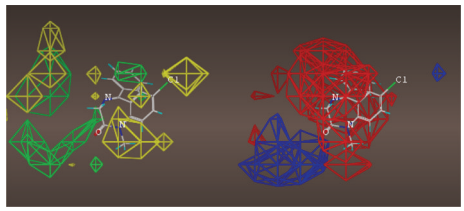


Figure 55: Steric (left) and electrostatic maps of the $\alpha 2\beta 3\gamma 2$ receptor subtype shown in line mode as seen from the classic perspective.

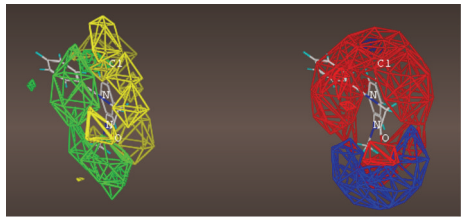


Figure 56: Steric (left) and electrostatic maps of the $\alpha 2\beta 3\gamma 2$ receptor subtype shown in line mode as seen from the classic perspective rotated 90°.

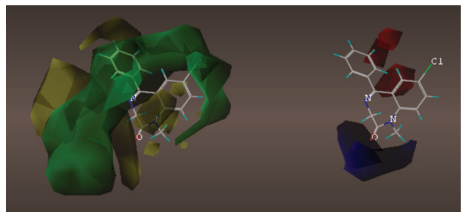


Figure 57: Steric (left) and electrostatic maps of the $\alpha 3\beta 3\gamma 2$ receptor subtype shown in the transparent mode as seen from the classic perspective.

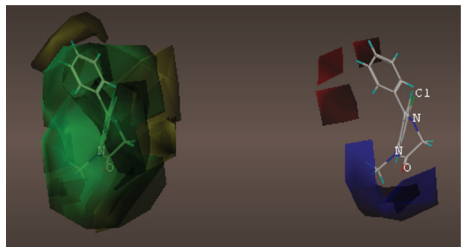


Figure 58: Steric (left) and electrostatic maps of the $\alpha 3\beta 3\gamma 2$ receptor subtype shown in the transparent mode as seen from the classic perspective rotated 90°.

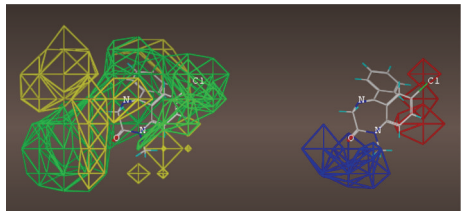


Figure 59: Steric (left) and electrostatic maps of the $\alpha 3\beta 3\gamma 2$ receptor subtype shown in line mode as seen from the classic perspective.

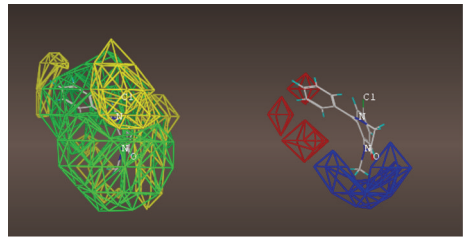


Figure 60: Steric (left) and electrostatic maps of the $\alpha 3\beta 3\gamma 2$ receptor subtype shown in line mode as seen from the classic perspective rotated 90°.

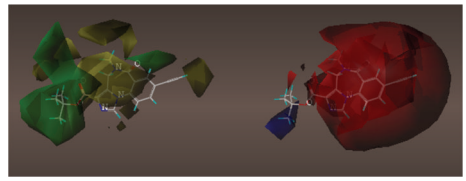


Figure 61: Steric (left) and electrostatic maps of the $\alpha 5\beta 3\gamma 2$ receptor subtype shown in the transparent mode as seen from the classic perspective.

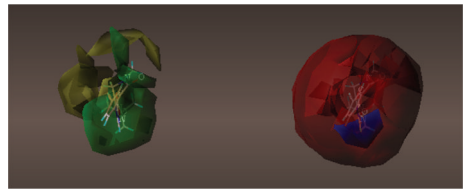


Figure 62: Steric (left) and electrostatic maps of the $\alpha 5\beta 3\gamma 2$ receptor subtype shown in the transparent mode as seen from the classic perspective rotated 90°.

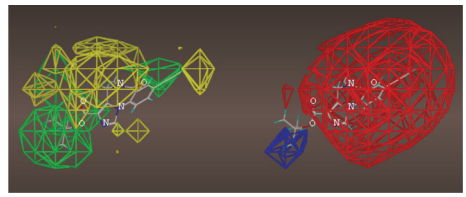


Figure 63: Steric (left) and electrostatic maps of the $\alpha 5\beta 3\gamma 2$ receptor subtype shown in line mode as seen from the classic perspective.

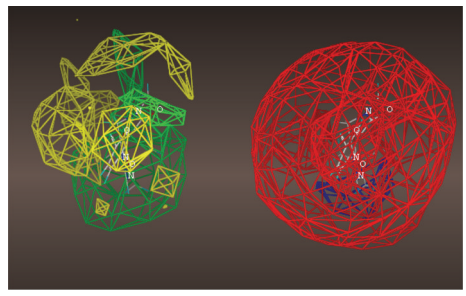


Figure 64: Steric (left) and electrostatic maps of the $\alpha 5\beta 3\gamma 2$ receptor subtype shown in line mode as seen from the classic perspective rotated 90°.

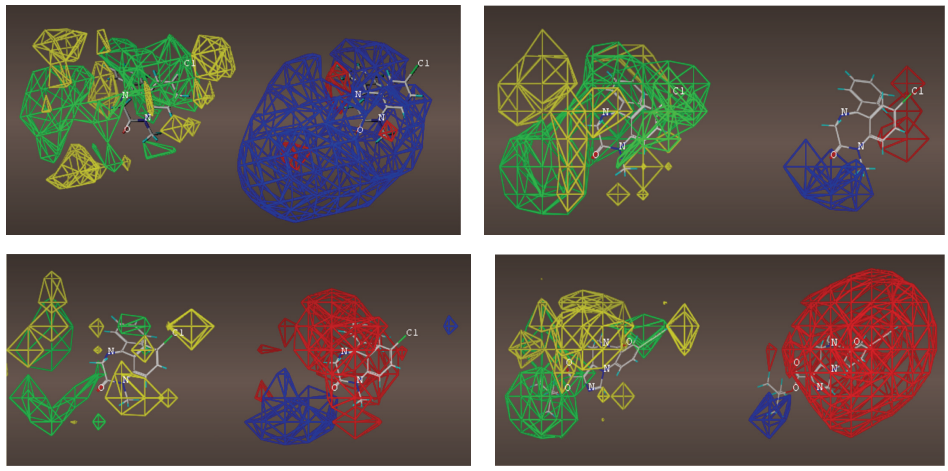
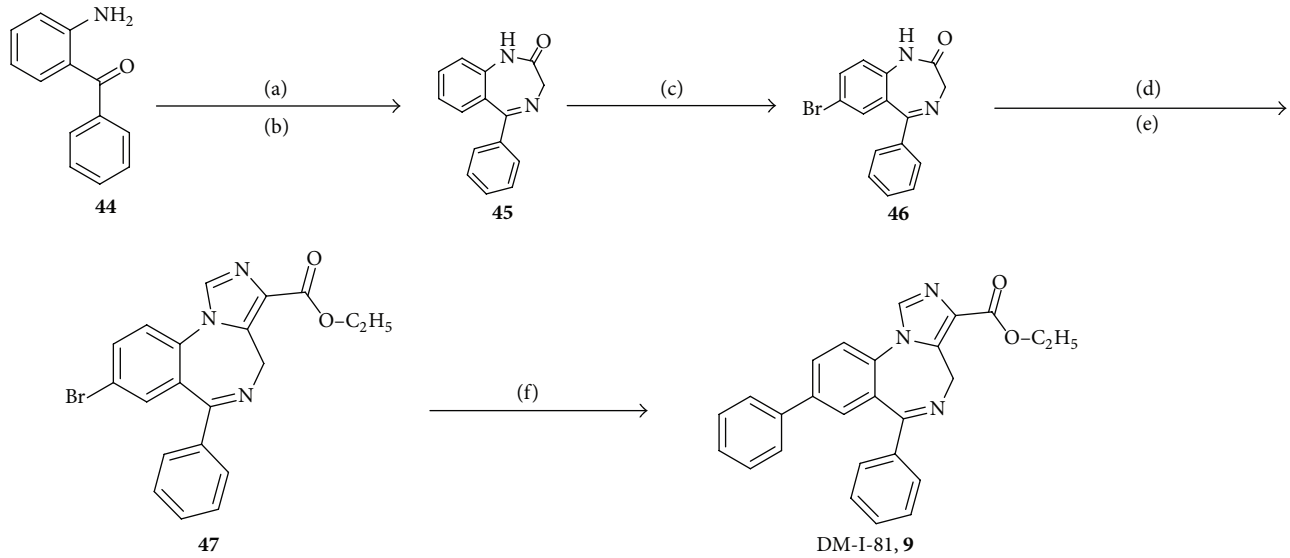


Figure 65: Clockwise from the top left, line maps of the $\alpha 1\beta 3\gamma 2$, $\alpha 2\beta 3\gamma 3$, $\alpha 3\beta 3\gamma 2$, and $\alpha 5\beta 3\gamma 2$ CoMFA.



Scheme 1: Synthesis of 8-substituted imidazobenzodiazepines following chemistry earlier developed by Sternbach, Fryer et al. *Reagents and Conditions*. (a) Bromoacetyl bromide, sodium bicarbonate, and chloroform; (b) ammonia (anhydrous), methanol, and reflux; (c) bromine, sulfuric acid, and acetic acid; (d) sodium hydride, diethyl chlorophosphate, and tetrahydrofuran; (e) sodium hydride, ethyl isocyanoacetate, and tetrahydrofuran, −30°C to r.t.; (f) tributyl(phenyl)stannane, $Pd(PPh_3)_4$.

1,3-Bis(8-bromo-6-phenyl-4H-benzo[f]imidazo[1,5-a][1,4]diazepine-3-carboxy) propyl diester ***59*** (DMH-D-070) (Procedure B), experimental details previously reported [17].

1,3-Bis(8-trimethylsilylacetylenyl-6-phenyl-4H-benzo[f]imidazo[1,5-a][1,4]-diazepine-3-carboxy) propyl diester ***61*** (DMH-D-048) (Procedure C), experimental details previously reported [17].

1,3-Bis(8-acetylenyl-6-phenyl-4H-benzo[f]imidazo[1,5-a][1,4]diazepine-3-carboxy) propyl diester ***63*** (DMH-D-053): experimental details previously reported [17].

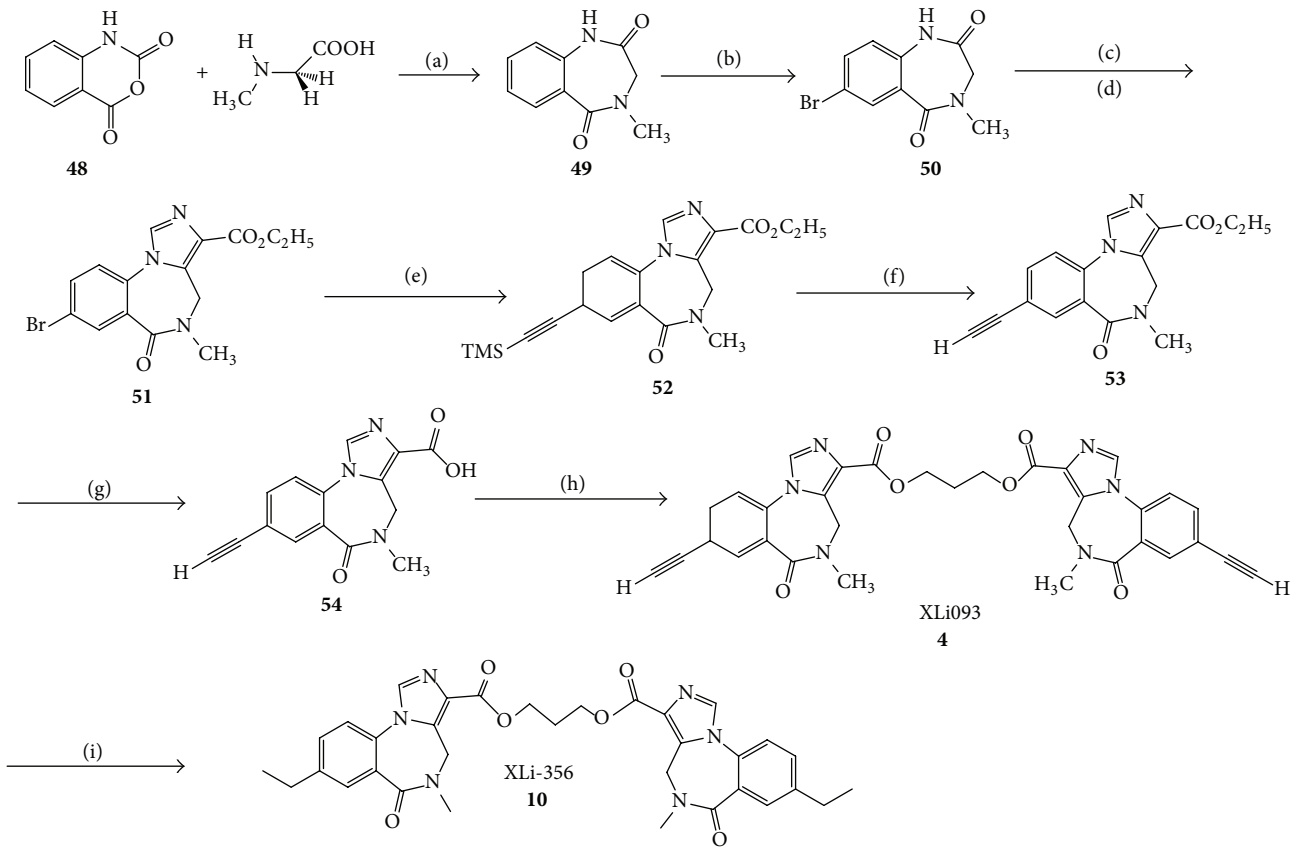
Bis(8-bromo-6-phenyl-4H-benzo[f]imidazo[1,5-a][1,4]diazepine-3-carboxy) diethylene glycol diester ***58*** (DM-III-93), experimental details previously reported [17].

Bis(8-trimethylsilylacetylenyl-6-phenyl-4H-benzo[f]imidazo[1,5-a][1,4]diazepine-3-carboxy) diethylene glycol diester ***60*** (DM-III-94), experimental details previously reported [17].

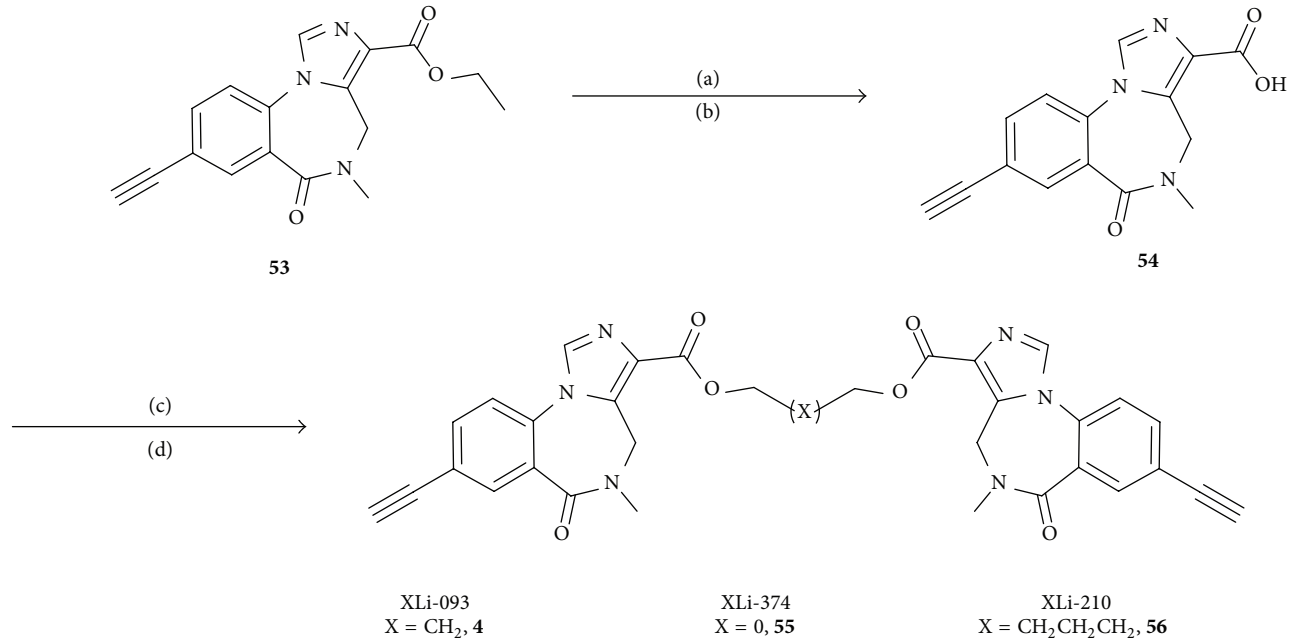
Bis(8-acetylenyl-6-phenyl-4H-benzo[f]imidazo[1,5-a][1,4]diazepine-3-carboxy) diethylene glycol diester ***62*** (DM-III-96), experimental details previously reported [17].

Abbreviations

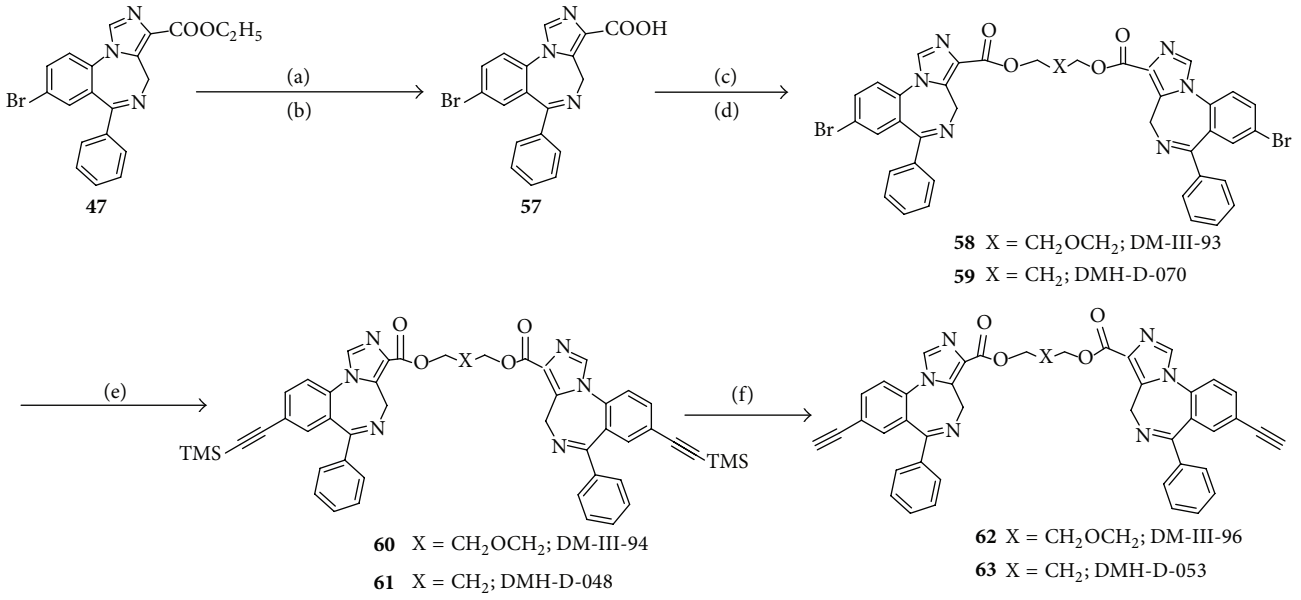
APD: Antipsychotic drug
ASM: Airway smooth muscle
BS: Binding site
BZD, Bz: Benzodiazepine
BzR: Benzodiazepine receptor
DA: Dopamine
DAPI: 4′,6-Diamidino-2-phenylindole



Scheme 2: Synthesis of 8-substituted imidazobenzodiazepine bivalent ligands. *Reagents and Conditions*. (a) DMSO, 180°C, 90%; (b) bromine, sodium acetate, and acetic acid, r.t., 80%; (c) LDA, THF, and diethyl chlorophosphate, 0°C; (d) LDA, THF, and ethyl isocyanoacetate; (e) trimethylsilyl acetylene, $Pd(OAc)_2(PPh_3)_2$, triethylamine, acetonitrile, and reflux, 80%; (f) tetrabutylammonium fluoride, THF, and H_2O, r.t., 88%; (g) 2N NaOH and ethanol, 70°C, 90%; (h) CDI, DMF, $HO(CH_2)_3OH$, and DBU, 60%; (i) Pd/C, H_2, ethanol, and DCM, 90%.



Scheme 3: Synthesis of bivalent analogs of XLi-093 (**4**). *Reagents and Conditions*. (a) 2 M NaOH, EtOH, 70°C; (b) 10% aq HCl; (c) CDI, DMF; (d) diol, DBU.



Scheme 4: Synthesis of bivalent analogues of DMH-D-053 (**63**). *Reagents and Conditions*. (a) 2 N NaOH, EtOH, and reflux; (b) 10% aq. HCl; (c) CDI, DMF; (d) diol, DBU; (e) trimethylsilylacetylene, $Pd(OAc)_2(PPH_3)_2$, Et_3N, CH_3CN, and reflux; (f) TBAF$*0.5H_2O$, THF, −78°C.

GABA:	Gamma amino butyric acid
$GABA_A$:	Gamma amino butyric acid A
$GABA_AR$:	Gamma amino butyric acid A receptor
HAL:	Haloperidol
HEK:	Human embryonic kidney
HPC:	Hippocampal
LTK:	Leukocyte tyrosine kinase
MAM:	Methylazoxymethanol
NAM:	Negative allosteric modulator
QSAR:	Quantitative structure-activity relationship
PAM:	Positive allosteric modulator
PV:	Parvalbumin
SAL:	Saline
SH-053:	SH-053-2′F-R-CH_3
SMA:	Smooth muscle actin
TTX:	Tetrodotoxin
VTA:	Ventral tegmental area.

Conflict of Interests

The authors declare that there is no conflict of interests regarding the publication of this paper.

Authors' Contribution

Terry Clayton and Michael M. Poe contributed equally to this work.

Acknowledgments

The authors gratefully acknowledge the work of Dr. Ruth McKernan and Dr. Bryan Roth for receptor binding. This was supported by NS-076517, MH-096463, NIA AG-039511, and AG-048446. The authors acknowledge support from the Milwaukee Institute for Drug Design.

References

[1] P. S. Miller and A. R. Aricescu, "Crystal structure of a human $GABA_A$ receptor," *Nature*, vol. 512, no. 7514, pp. 270–275, 2014.

[2] K. H. Backus, M. Arigoni, U. Drescher et al., "Stoichiometry of a recombinant $GABA_A$ receptor deduced from mutation-induced rectification," *Neuroreport*, vol. 5, no. 3, pp. 285–288, 1993.

[3] H. Möhler, "Brain disorders and novel therapeutics," *Chimia*, vol. 58, no. 10, pp. 718–720, 2004.

[4] H. Möhler, J.-M. Fritschy, F. Crestani, T. Hensch, and U. Rudolph, "Specific $GABA_A$ circuits in brain development and therapy," *Biochemical Pharmacology*, vol. 68, no. 8, pp. 1685–1690, 2004.

[5] U. Rudolph and H. Möhler, "Analysis of $GABA_A$ receptor function and dissection of the pharmacology of benzodiazepines and general anesthetics through mouse genetics," *Annual Review of Pharmacology and Toxicology*, vol. 44, pp. 475–498, 2004.

[6] D. J. Bailey, J. E. Tetzlaff, J. M. Cook, X. He, and F. J. Helmstetter, "Effects of hippocampal injections of a novel ligand selective for the $\alpha5\beta2\gamma2$ subunits of the GABA/benzodiazepine receptor on Pavlovian conditioning," *Neurobiology of Learning and Memory*, vol. 78, no. 1, pp. 1–10, 2002.

[7] T. M. DeLorey, R. C. Lin, B. McBrady et al., "Influence of benzodiazepine binding site ligands on fear-conditioned contextual memory," *European Journal of Pharmacology*, vol. 426, no. 1-2, pp. 45–54, 2001.

[8] M. S. Chambers, J. R. Atack, F. A. Bromidge et al., "6,7-Dihydro-2-benzothiophen-4(5*H*)-ones: a novel class of GABA-A $\alpha5$ receptor inverse agonists," *Journal of Medicinal Chemistry*, vol. 45, no. 6, pp. 1176–1179, 2002.

[9] M. S. Chambers, J. R. Atack, H. B. Broughton et al., "Identification of a novel, selective GABAa $\alpha5$ receptor inverse agonist

which enhances cognition," *Journal of Medicinal Chemistry*, vol. 46, no. 11, pp. 2227–2240, 2003.

[10] C. Sur, K. Quirk, D. Dewar, J. Atack, and R. Mckernan, "Rat and human hippocampal alpha 5 subunit-containing gamma-aminobutyric acid(A) receptors have alpha 5 beta 3 gamma 2 pharmacological characteristics," *Molecular Pharmacology*, vol. 54, no. 5, pp. 928–933, 1998.

[11] M. Sarter, "Taking stock of cognition enhancers," *Trends in Pharmacological Sciences*, vol. 12, pp. 456–461, 1991.

[12] J. R. Atack, L. Alder, S. M. Cook, A. J. Smith, and R. M. McKernan, "In vivo labelling of α5 subunit-containing $GABA_A$ receptors using the selective radioligand [^{3}H]L-655,708," *Neuropharmacology*, vol. 49, no. 2, pp. 220–229, 2005.

[13] X. Y. Li, H. Cao, C. C. Zhang et al., "Synthesis, in vitro affinity, and efficacy of a bis 8-ethynyl-4*H*-imidazo[1,5α]-[1,4]benzodiazepine analogue, the first bivalent α5 subtype selective BzR/$GABA_A$ antagonist," *Journal of Medicinal Chemistry*, vol. 46, no. 26, pp. 5567–5570, 2003.

[14] X. Li, *Synthesis of selective ligands for GABAA/benzodiazepine receptors [Ph.D. thesis]*, University of Wisconsin-Milwaukee, Milwaukee, Wis, USA, 2004.

[15] A. H. Abadi, S. Lankow, B. Hoefgen, M. Decker, M. U. Kassack, and J. Lehmann, "Dopamine/serotonin receptor ligands, part III: synthesis and biological activities of 7,7′-alkylene-bis-6,7,8,9,14,15-hexahydro-5H-benz[d]indolo[2,3-g]azecines—application of the bivalent ligand approach to a novel type of dopamine receptor antagonist," *Archiv der Pharmazie*, vol. 335, no. 8, pp. 367–373, 2002.

[16] W. Yin, F. Rivas, R. Furtmueller et al., "Synthesis, in-vitro affinity and efficacy of the first bivalent alpha 5 subtype selective BzR/GABA(A) antagonist," in *Proceedings of the 2004 Neuroscience Meeting*, San Diego, Calif, USA, 2004.

[17] D. Han, F. Holger Försterling, X. Li et al., "A study of the structure-activity relationship of GABAA-benzodiazepine receptor bivalent ligands by conformational analysis with low temperature NMR and X-ray analysis," *Bioorganic and Medicinal Chemistry*, vol. 16, no. 19, pp. 8853–8862, 2008.

[18] D. M. Han, F. H. Försterling, X. Y. Li, J. R. Deschamps, H. Cao, and J. M. Cook, "Determination of the stable conformation of $GABA_A$-benzodiazepine receptor bivalent ligands by low temperature NMR and X-ray analysis," *Bioorganic & Medicinal Chemistry Letters*, vol. 14, no. 6, pp. 1465–1469, 2004.

[19] C. C. Zhang, *Structure Activity Relationships and Cytotoxic Activity of Analogs of Tryprostatin A and B. Preparation of Irreversible Inhibitors for Studies of Mechanism and Action. II. Pharmacophore Receptor Models of GABA(A)/BzR*, University of Wisconsin-Milwaukee, Milwaukee, Wis, USA, 2004.

[20] R. Y. Liu, R. J. Hu, P. W. Zhang, P. Skolnick, and J. M. Cook, "Synthesis and pharmacological properties of novel 8-substituted imidazobenzodiazepines: high-affinity, selective probes for α5-containing GABAA receptors," *Journal of Medicinal Chemistry*, vol. 39, no. 9, pp. 1928–1934, 1996.

[21] Q. Huang, X. H. He, C. R. Ma et al., "Pharmacophore/receptor models for $GABA_A$/BzR subtypes ($\alpha1\beta3\gamma2$, $\alpha5\beta3\gamma2$, and $\alpha6\beta3\gamma2$) via a comprehensive ligand-mapping approach," *Journal of Medicinal Chemistry*, vol. 43, no. 1, pp. 71–95, 2000.

[22] T. Clayton, *Part I. Unified pharmacophore protein models of the benzodiazepine receptor subtypes. Part II. Subtype selective ligands for alpha5 Gaba(A) /BZ receptors [Ph.D. thesis]*, University of Wisconsin-Milwaukee, Milwaukee, Wis, USA, 2011.

[23] T. Clayton, J. L. Chen, M. Ernst et al., "An updated unified pharmacophore model of the benzodiazepine binding site on γ-aminobutyric acida receptors: correlation with comparative models," *Current Medicinal Chemistry*, vol. 14, no. 26, pp. 2755–2775, 2007.

[24] M. M. Savić, T. Clayton, R. Furtmüller et al., "PWZ-029, a compound with moderate inverse agonist functional selectivity at GABA-A receptors containing alpha5 subunits, improves passive, but not active, avoidance learning in rats," *Brain Research*, vol. 1208, pp. 150–159, 2008.

[25] M. Milić, T. Timić, S. Joksimović et al., "PWZ-029, an inverse agonist selective for α5 GABAA receptors, improves object recognition, but not water-maze memory in normal and scopolamine-treated rats," *Behavioural Brain Research*, vol. 241, no. 1, pp. 206–213, 2013.

[26] J. K. Rowlett, C. A. Moran, T. Clayton, S. Rallapalli, B. Roth, and J. M. Cook, *PWZ-029, An Inverse Agonist Selective for α5 Subunit Containing GABA(A) Receptors, Enhances Performance on an Executive Function Task in Monkeys*, European Behavioral Pharmacology Society, Rome, Italy, 2009.

[27] F. M. Benes, B. Lim, D. Matzilevich, J. P. Walsh, S. Subburaju, and M. Minns, "Regulation of the GABA cell phenotype in hippocampus of schizophrenics and bipolars," *Proceedings of the National Academy of Sciences of the United States of America*, vol. 104, no. 24, pp. 10164–10169, 2007.

[28] L. M. Rimol, C. B. Hartberg, R. Nesvåg et al., "Cortical thickness and subcortical volumes in schizophrenia and bipolar disorder," *Biological Psychiatry*, vol. 68, no. 1, pp. 41–50, 2010.

[29] C. Pantelis, D. Velakoulis, P. D. McGorry et al., "Neuroanatomical abnormalities before and after onset of psychosis: a cross-sectional and longitudinal MRI comparison," *The Lancet*, vol. 361, no. 9354, pp. 281–288, 2003.

[30] S. A. Schobel, M. A. Kelly, C. M. Corcoran et al., "Anterior hippocampal and orbitofrontal cortical structural brain abnormalities in association with cognitive deficits in schizophrenia," *Schizophrenia Research*, vol. 114, no. 1–3, pp. 110–118, 2009.

[31] S. A. Schobel, N. M. Lewandowski, C. M. Corcoran et al., "Differential targeting of the CA1 subfield of the hippocampal formation by schizophrenia and related psychotic disorders," *Archives of General Psychiatry*, vol. 66, no. 9, pp. 938–946, 2009.

[32] A. P. Weiss, D. Goff, D. L. Schacter et al., "Fronto-hippocampal function during temporal context monitoring in schizophrenia," *Biological Psychiatry*, vol. 60, no. 11, pp. 1268–1277, 2006.

[33] R. C. Wolf, A. Höse, K. Frasch, H. Walter, and N. Vasic, "Volumetric abnormalities associated with cognitive deficits in patients with schizophrenia," *European Psychiatry*, vol. 23, no. 8, pp. 541–548, 2008.

[34] H. Moore, J. D. Jentsch, M. Ghajarnia, M. A. Geyer, and A. A. Grace, "A neurobehavioral systems analysis of adult rats exposed to methylazoxymethanol acetate on E17: implications for the neuropathology of schizophrenia," *Biological Psychiatry*, vol. 60, no. 3, pp. 253–264, 2006.

[35] P. Flagstad, A. Mørk, B. Y. Glenthøj, J. Van Beek, A. T. Michael-Titus, and M. Didriksen, "Disruption of neurogenesis on gestational day 17 in the rat causes behavioral changes relevant to positive and negative schizophrenia symptoms and alters amphetamine-induced dopamine release in nucleus accumbens," *Neuropsychopharmacology*, vol. 29, no. 11, pp. 2052–2064, 2004.

[36] D. J. Lodge and A. A. Grace, "Aberrant hippocampal activity underlies the dopamine dysregulation in an animal model of schizophrenia," *The Journal of Neuroscience*, vol. 27, no. 42, pp. 11424–11430, 2007.

[37] D. J. Lodge, M. M. Behrens, and A. A. Grace, "A loss of parvalbumin-containing interneurons is associated with diminished oscillatory activity in an animal model of schizophrenia," *The Journal of Neuroscience*, vol. 29, no. 8, pp. 2344–2354, 2009.

[38] K. M. Gill, D. J. Lodge, J. M. Cook, S. Aras, and A. A. Grace, "A novel α5GABA$_A$R-positive allosteric modulator reverses hyperactivation of the dopamine system in the MAM model of schizophrenia," *Neuropsychopharmacology*, vol. 36, no. 9, pp. 1903–1911, 2011.

[39] W. Zhang, K. F. Koehler, P. Zhang, and J. M. Cook, "Development of a comprehensive pharmacophore model for the benzodiazepine receptor," *Drug Design and Discovery*, vol. 12, no. 3, pp. 193–248, 1995.

[40] W. Zhang, H. Diaz-Arauzo, M. S. Allen, K. F. Koehler, and J. M. Cook, "Chemical and computer assisted development of the inclusive pharmacophore of benzodiazepine receptors," in *Studies in Medicinal Chemistry*, M. I. Choudhary, Ed., p. 303, Harwood Academic Publishers, 1996.

[41] P. W. Zhang, W. J. Zhang, R. Y. Liu, B. Harris, P. Skolnick, and J. M. Cook, "Synthesis and SAR study of novel imidazobenzodiazepines at 'diazepam-insensitive' benzodiazepine receptors," *Journal of Medicinal Chemistry*, vol. 38, no. 10, pp. 1679–1688, 1995.

[42] Q. Huang, E. D. Cox, T. Gan et al., "Studies of molecular pharmacophore/receptor models for GABA(A)/benzodiazepine receptor subtypes: binding affinities of substituted β-carbolines at recombinant $\alpha1\beta3\gamma2$ subtypes and quantitative structure-activity relationship studies via a comparative molecular field analysis," *Drug Design and Discovery*, vol. 16, no. 1, pp. 55–76, 1999.

[43] D. Harris, T. Clayton, J. Cook et al., "Selective influence on contextual memory: physiochemical properties associated with selectivity of benzodiazepine ligands at GABA$_A$ receptors containing the α5 subunit," *Journal of Medicinal Chemistry*, vol. 51, no. 13, pp. 3788–3803, 2008.

[44] D. Rüedi-Bettschen, J. K. Rowlett, S. Rallapalli, T. Clayton, J. M. Cook, and D. M. Platt, "Modulation of α5 subunit-containing GABAA receptors alters alcohol drinking by rhesus monkeys," *Alcoholism: Clinical and Experimental Research*, vol. 37, no. 4, pp. 624–634, 2013.

[45] M. M. Savić, M. M. Milinković, S. Rallapalli et al., "The differential role of alpha1- and alpha5-containing GABAA receptors in mediating diazepam effects on spontaneous locomotor activity and water-maze learning and memory in rats," *International Journal of Neuropsychopharmacology*, vol. 12, no. 9, pp. 1179–1193, 2009.

[46] X. Y. Li, C. R. Ma, X. H. He et al., "Studies in search of diazepam-insensitive subtype selective agents for GABA$_A$/Bz receptors," *Medicinal Chemistry Research*, vol. 11, no. 9, pp. 504–537, 2003.

[47] L. Duggan, M. Fenton, J. Rathbone, R. Dardennes, A. El-Dosoky, and S. Indran, "Olanzapine for schizophrenia," *Cochrane Database of Systematic Reviews*, no. 2, Article ID CD001359, 2005.

[48] J. A. Lieberman, T. S. Stroup, J. P. McEvoy et al., "Effectiveness of antipsychotic drugs in patients with chronic schizophrenia," *The New England Journal of Medicine*, vol. 353, no. 12, pp. 1209–1223, 2005.

[49] K. Komossa, C. Rummel-Kluge, H. Hunger et al., "Olanzapine versus other atypical antipsychotics for schizophrenia," *Cochrane Database of Systematic Reviews*, no. 3, Article ID CD006654, 2010.

[50] K. Komossa, C. Rummel-Kluge, H. Hunger et al., "Zotepine versus other atypical antipsychotics for schizophrenia," *Cochrane Database of Systematic Reviews*, no. 1, p. CD006628, 2010.

[51] K. Komossa, C. Rummel-Kluge, H. Hunger et al., "Amisulpride versus other atypical antipsychotics for schizophrenia," *Cochrane Database of Systematic Reviews*, no. 1, p. CD006624, 2010.

[52] K. Komossa, C. Rummel-Kluge, F. Schmid et al., "Quetiapine versus other atypical antipsychotics for schizophrenia," *Cochrane Database of Systematic Reviews*, no. 1, Article ID CD006625, 2010.

[53] C. Sur, L. Fresu, O. Howell, R. M. McKernan, and J. R. Atack, "Autoradiographic localization of α5 subunit-containing GABA(A) receptors in rat brain," *Brain Research*, vol. 822, no. 1-2, pp. 265–270, 1999.

[54] H. L. June, S. C. Harvey, K. L. Foster et al., "GABAA receptors containing α5 subunits in the CA1 and CA3 hippocampal fields regulate ethanol-motivated behaviors: an extended ethanol reward circuitry," *The Journal of Neuroscience*, vol. 21, no. 6, pp. 2166–2177, 2001.

[55] A. Lingford-Hughes, S. P. Hume, A. Feeney et al., "Imaging the GABA-benzodiazepine receptor subtype containing the alpha5-subunit in vivo with [11C]Ro15 4513 positron emission tomography," *Journal of Cerebral Blood Flow and Metabolism*, vol. 22, no. 7, pp. 878–889, 2002.

[56] B. Hutcheon, J. M. Fritschy, and M. O. Poulter, "Organization of GABAA receptor alpha-subunit clustering in the developing rat neocortex and hippocampus," *European Journal of Neuroscience*, vol. 19, no. 9, pp. 2475–2487, 2004.

[57] B. Ramos, J. F. Lopez-Tellez, J. Vela et al., "Expression of α5 GABAA receptor subunit in developing rat hippocampus," *Developmental Brain Research*, vol. 151, no. 1-2, pp. 87–98, 2004.

[58] S. K. Towers, T. Gloveli, R. D. Traub et al., "Alpha5 subunit-containing GABAA receptors affect the dynamic range of mouse hippocampal kainate-induced gamma frequency oscillations in vitro," *Journal of Physiology*, vol. 559, no. 3, pp. 721–728, 2004.

[59] S. A. Heldt and K. J. Ressler, "Forebrain and midbrain distribution of major benzodiazepine-sensitive GABAA receptor subunits in the adult C57 mouse as assessed with in situ hybridization," *Neuroscience*, vol. 150, no. 2, pp. 370–385, 2007.

[60] C. Papatheodoropoulos and E. Koniaris, "α5GABAA receptors regulate hippocampal sharp wave-ripple activity in vitro," *Neuropharmacology*, vol. 60, no. 4, pp. 662–673, 2011.

[61] K. M. Gill, J. M. Cook, M. M. Poe, and A. A. Grace, "Prior antipsychotic drug treatment prevents response to novel antipsychotic agent in the methylazoxymethanol acetate model of schizophrenia," *Schizophrenia Bulletin*, vol. 40, no. 2, pp. 341–350, 2014.

[62] C. C. Kaczorowski and J. F. Disterhoft, "Memory deficits are associated with impaired ability to modulate neuronal excitability in middle-aged mice," *Learning and Memory*, vol. 16, no. 6, pp. 362–366, 2009.

[63] C. C. Kaczorowski, E. Sametsky, S. Shah, R. Vassar, and J. F. Disterhoft, "Mechanisms underlying basal and learning-related intrinsic excitability in a mouse model of Alzheimer's disease," *Neurobiology of Aging*, vol. 32, no. 8, pp. 1452–1465, 2011.

[64] C. C. Kaczorowski, S. J. Davis, and J. R. Moyer Jr., "Aging redistributes medial prefrontal neuronal excitability and impedes extinction of trace fear conditioning," *Neurobiology of Aging*, vol. 33, no. 8, pp. 1744–1757, 2012.

[65] S. I. Rallapalli, *Synthesis of Agents to Enhance Cognition. II. Synthesis of Indole Alkaloids*, University of Wisconsin-Milwaukee, 2014.

[66] P. J. Barnes, "Biochemistry of asthma," *Trends in Biochemical Sciences*, vol. 16, pp. 365–369, 1991.

[67] D. W. Cockcroft, "Clinical concerns with inhaled β2-agonists: adult asthma," *Clinical Reviews in Allergy and Immunology*, vol. 31, no. 2-3, pp. 197–208, 2006.

[68] R. W. Morton, M. L. Everard, and H. E. Elphick, "Adherence in childhood asthma: the elephant in the room," *Archives of Disease in Childhood*, vol. 99, no. 10, pp. 949–953, 2014.

[69] N. S. Jentzsch, P. Camargos, E. S. C. Sarinho, and J. Bousquet, "Adherence rate to beclomethasone dipropionate and the level of asthma control," *Respiratory Medicine*, vol. 106, no. 3, pp. 338–343, 2012.

[70] E. K. Chu and J. M. Drazen, "Asthma: one hundred years of treatment and onward," *The American Journal of Respiratory and Critical Care Medicine*, vol. 171, no. 11, pp. 1202–1208, 2005.

[71] G. Gallos, N. R. Gleason, Y. Zhang et al., "Activation of endogenous GABAA channels on airway smooth muscle potentiates isoproterenol-mediated relaxation," *The American Journal of Physiology—Lung Cellular and Molecular Physiology*, vol. 295, no. 6, pp. L1040–L1047, 2008.

[72] K. Mizuta, D. Xu, Y. Pan et al., "GABAA receptors are expressed and facilitate relaxation in airway smooth muscle," *The American Journal of Physiology—Lung Cellular and Molecular Physiology*, vol. 294, no. 6, pp. L1206–L1216, 2008.

[73] M. M. Savić, T. Clayton, R. Furtmüller et al., "PWZ-029, a compound with moderate inverse agonist functional selectivity at $GABA_A$ receptors containing α5 subunits, improves passive, but not active, avoidance learning in rats," *Brain Research*, vol. 1208, pp. 150–159, 2008.

[74] M. M. Savić, S. Huang, R. Furtmüller et al., "Are GABAA receptors containing alpha5 subunits contributing to the sedative properties of benzodiazepine site agonists?," *Neuropsychopharmacology*, vol. 33, no. 2, pp. 332–339, 2008.

[75] G. Gallos, G. T. Yocum, M. E. Siviski et al., "Selective targeting of the α5 subunit of $GABA_A$ receptors relaxes airway smooth muscle and inhibits cellular calcium handling," *American Journal of Physiology—Lung Cellular and Molecular Physiology*, vol. 308, no. 9, pp. L931–L942, 2015.

[76] M. S. Allen, Y.-C. Tan, M. L. Trudell et al., "Synthetic and computer-assisted analyses of the pharmacophore for the benzodiazepine receptor inverse agonist site," *Journal of Medicinal Chemistry*, vol. 33, no. 9, pp. 2343–2357, 1990.

[77] M. S. Allen, T. J. Hagen, M. L. Trudell, P. W. Codding, P. Skolnick, and J. M. Cook, "Synthesis of novel 3-substituted β-carbolines as benzodiazepine receptor ligands: probing the benzodiazepine receptor pharmacophore," *Journal of Medicinal Chemistry*, vol. 31, no. 9, pp. 1854–1861, 1988.

[78] H. Diaz-Arauzo, G. E. Evoniuk, P. Skolnick, and J. M. Cook, "The agonist pharmacophore of the benzodiazepine receptor. Synthesis of a selective anticonvulsant/anxiolytic," *Journal of Medicinal Chemistry*, vol. 34, no. 5, pp. 1754–1756, 1991.

[79] H. Diaz-Arauzo, K. F. Koehler, T. J. Hagen, and J. M. Cook, "Synthetic and computer assisted analysis of the pharmacophore for agonists at benzodiazepine receptors," *Life Sciences*, vol. 49, no. 3, pp. 207–216, 1991.

[80] W. J. Zhang, K. F. Koehler, B. Harris, P. Skolnick, and J. M. Cook, "Synthesis of benzo-fused benzodiazepines employed as probes of the agonist pharmacophore of benzodiazepine receptors," *Journal of Medicinal Chemistry*, vol. 37, no. 6, pp. 745–757, 1994.

[81] M. L. Trudell, S. L. Lifer, Y.-C. Tan et al., "Synthesis of substituted 7,12-dihydropyrido[3,2-b:5,4-b′]diindoles: rigid planar benzodiazepine receptor ligands with inverse agonist/antagonist properties," *Journal of Medicinal Chemistry*, vol. 33, no. 9, pp. 2412–2420, 1990.

[82] M. L. Trudell, A. S. Basile, H. E. Shannon, P. Skolnick, and J. M. Cook, "Synthesis of 7,12-dihydropyrido[3,4-b:5,4-b′]diindoles. A novel class of rigid, planar benzodiazepine receptor ligands," *Journal of Medicinal Chemistry*, vol. 30, no. 3, pp. 456–458, 1987.

[83] M. J. Frisch, G. W. Trucks, M. Head-Gordon et al., *Gaussian 92*, Gaussian, Pittsburgh, Pa, USA, 1992, http://www.lct.jussieu.fr/manuels/Gaussian98/00000119.htm.

[84] M. L. I. Trudell, *The synthesis and study of the pharmacologic activity of 7,12 dihydropyrido[3,2 b:5,4 b′]diindoles. A novel class of rigid, planar benzodiazepine receptor ligands. II. The total synthesis of the indole alkaloid, (±) suaveoline [Ph.D. thesis]*, University of Wisconsin-Milwaukee, Milwaukee, Wis, USA, 1989.

[85] W. Yin, S. Majumder, T. Clayton et al., "Design, synthesis, and subtype selectivity of 3,6-disubstituted β-carbolines at Bz/GABA(A)ergic receptors. SAR and studies directed toward agents for treatment of alcohol abuse," *Bioorganic and Medicinal Chemistry*, vol. 18, no. 21, pp. 7548–7564, 2010.

[86] D. Han, F. H. Forsterling, X. Li, J. Deschamps, H. Cao, and J. M. Cook, "Study of the structure activity relationships of $GABA_A$-benzodiazepine receptor ligands by low termperature NMR spectroscopy and X-ray analysis," in *Proceedings of the 227th ACS National Meeting*, Anaheim, Calif, USA, March-April 2004.

[87] B. D. Fischer, S. C. Licata, H. Zhou et al., "Anxiolytic-like effects of 8-acetylene imidazobenzodiazepines in a rhesus monkey conflict procedure," *Neuropharmacology*, vol. 59, no. 7-8, pp. 612–618, 2010.

[88] W. Haefely, E. Kyburz, M. Gerecke, and H. Mohler, "Recent advances in the molecular pharmacology of benzodiazepine receptors and in the structure—activity relationships of their agonist and antagonists," in *Advances in Drug Research*, vol. 99, pp. 165–322, Academic Press, New York, NY, USA, 1985.

[89] R. I. Fryer, Z.-Q. Gu, and C.-G. Wang, "Synthesis of novel, substituted 4H-imidazo[1,5-a][1,4]benzodiazepines," *Journal of Heterocyclic Chemistry*, vol. 28, no. 7, pp. 1661–1669, 1991.

[90] R. I. Fryer, P. Zhang, R. Rios, Z.-Q. Gu, A. S. Basile, and P. Skolnick, "Structure-activity relationship studies at the benzodiazepine receptor (Bzr)—a comparison of the substituent effects of pyrazoloquinolinone analogs," *Journal of Medicinal Chemistry*, vol. 36, no. 11, pp. 1669–1673, 1993.

[91] F. M. Rivas, C. R. Edwankar, J. M. Cook et al., "Antiseizure activity of novel γ-aminobutyric acid (A) receptor subtype-selective benzodiazepine analogues in mice and rat models," *Journal of Medicinal Chemistry*, vol. 52, no. 7, pp. 1795–1798, 2009.

[92] J. M. Cook, D. Han, X. He et al., "Anxiolytic agents with reduced sedative and ataxic effects," 7119196 B2, 2006.

[93] J. M. Cook, H. Zhao, S. Huang, P. S. Sarma, and C. C. Zhang, "Stereospecific anxiolytic and anticonvulsant agents with reduced muscle-relaxant, sedative-hypnotic and ataxic effects," US Patent 2006004945, 2007.

[94] R. I. Fryer, *Comprehensive Medicinal Chemistry*, vol. 99, Pergamon Press, Oxford, UK, 1989.

[95] H. O. Villar, M. F. Davies, G. H. Loew, and P. A. Maguire, "Molecular models for recognition and activation at the benzodiazepine receptor: a review," *Life Sciences*, vol. 48, no. 7, pp. 593–602, 1991.

[96] H. O. Villar, E. T. Uyeno, L. Toll, W. Polgar, M. F. Davies, and G. H. Loew, "Molecular determinants of benzodiazepine receptor affinities and anticonvulsant activities," *Molecular Pharmacology*, vol. 36, no. 4, pp. 589–600, 1989.

[97] G. M. Crippen, "Distance geometry analysis of the benzodiazepine binding site," *Molecular Pharmacology*, vol. 22, no. 1, pp. 11–19, 1982.

[98] A. K. Ghose and G. M. Crippen, "Modeling the benzodiazepine receptor binding site by the general three-dimensional structure-directed quantitative structure-activity relationship method REMOTEDISC," *Molecular Pharmacology*, vol. 37, no. 5, pp. 725–734, 1990.

[99] P. W. Codding and A. K. S. Muir, "Molecular structure of Ro15-1788 and a model for the binding of benzodiazepine receptor ligands. Structural identification of common features in antagonists," *Molecular Pharmacology*, vol. 28, no. 2, pp. 178–184, 1985.

[100] A. K. S. Muir and P. W. Codding, "Structure-activity studies of β-carbolines. 3. Crystal and molecular structures of methyl β-carboline-3-carboxylate," *Canadian Journal of Chemistry*, vol. 63, no. 10, pp. 2752–2756, 1985.

[101] M. G. Codding, A. W. Roszak, M. B. Szkaradzinska, J. M. Cook, and L. J. Aha, *Modeling of the Benzodiazepine Receptor Using Structural and Theoretical Characterization of Novel Beta-Carbolines*, Elsevier Science, Amsterdam, The Netherlands, 1989.

[102] V. Ferretti, P. Gilli, and P. A. Borea, "Structural features controlling the binding of β-carbolines to the benzodiazepine receptor," *Acta Crystallographica Section B: Structural Science*, vol. 60, no. 4, pp. 481–489, 2004.

[103] P. A. Borea, G. Gilli, V. Bertolasi, and V. Ferretti, "Stereochemical features controlling binding and intrinsic activity properties of benzodiazepine-receptor ligands," *Molecular Pharmacology*, vol. 31, no. 4, pp. 334–344, 1987.

[104] V. Bertolasi, V. Feretti, G. Gilli, and P. A. Borea, "Stereochemistry of benzodiazepine-receptor ligands.1. Structure of methyl beta-carboline-3-carboxylate (beta-CCM), $C_{13}H_{10}N_2O_2$," *Acta Crystallographica Section C: Crystal Structure Communications*, vol. 40, p. 1981, 1984.

[105] V. Ferretti, V. Bertolasi, G. Gilli, and P. A. Borea, "Structures of two 2-arylpyrazolo[4,3-c]quinolin-3-ones: CGS8216, $C_{16}H_{11}N_3O$, and CGS9896, $C_{16}H_{10}ClN_3O$," *Acta Crystallographica Section C: Crystal Structure Communications*, vol. 41, no. 1, pp. 107–110, 1985.

[106] S. Tebib, J.-J. Bourguignon, and C.-G. Wermuth, "The active analog approach applied to the pharmacophore identification of benzodiazepine receptor ligands," *Journal of Computer-Aided Molecular Design*, vol. 1, no. 2, pp. 153–170, 1987.

[107] C. R. Gardner, "A review of recently-developed ligands for neuronal benzodiazepine receptors and their pharmacological activities," *Progress in Neuropsychopharmacology and Biological Psychiatry*, vol. 16, no. 6, pp. 755–781, 1992.

[108] M. S. Allen, A. J. LaLoggia, L. J. Dorn et al., "Predictive binding of β-carboline inverse agonists and antagonists via the CoMFA/GOLPE approach," *Journal of Medicinal Chemistry*, vol. 35, no. 22, pp. 4001–4010, 1992.

[109] Q. Huang, E. Cox, T. Gan et al., "Studies of molecular pharmacophore/receptor models for $GABA_A$/benzodiazepine receptor subtypes: binding affinities of substituted β-carbolines at recombinant alpha x beta 3 gamma 2 subtypes and quantitative structure-activity relationship studies via a comparative molecular field analysis," *Drug Design and Discovery*, vol. 16, no. 1, pp. 55–76, 1999.

[110] X. He, Q. Huang, C. Ma, S. Yu, R. McKernan, and J. M. Cook, "Pharmacophore/receptor models for GABA(A)/BzR $\alpha 2\beta 3\gamma 2$, $\alpha 3\beta 3\gamma 2$ and $\alpha 4\beta 3\gamma 2$ recombinant subtypes. Included volume analysis and comparison to $\alpha 1\beta 3\gamma 2$, $\alpha 5\beta 3\gamma 2$ and $\alpha 6\beta 3\gamma 2$ subtypes," *Drug Design and Discovery*, vol. 17, no. 2, pp. 131–171, 2000.

[111] E. D. Cox, H. Diaz-Arauzo, Q. Huang et al., "Synthesis and evaluation of analogues of the partial agonist 6- (propyloxy)-4-(methoxymethyl)-β-carboline-3-carboxylic acid ethyl ester (6-PBC) and the full agonist 6-(benzyloxy)-4-(methoxymethyl)-β-carboline-3-carboxylic acid ethyl ester (Zk 93423) at wild type and recombinant GABA(A) receptors," *Journal of Medicinal Chemistry*, vol. 41, no. 14, pp. 2537–2552, 1998.

[112] M. J. Martin, M. L. Trudell, H. D. Araúzo et al., "Molecular yardsticks—rigid probes to define the spatial dimensions of the benzodiazepine receptor binding site," *Journal of Medicinal Chemistry*, vol. 35, no. 22, pp. 4105–4117, 1992.

[113] K. Naryanan and J. M. Cook, "Probing the dimensions of the benzodiazepine receptor inverse agonist site," *Heterocycles*, vol. 31, no. 2, pp. 203–209, 1990.

[114] S. P. Hollinshead, M. L. Trudell, P. Skolnick, and J. M. Cook, "Structural requirements for agonist actions at the benzodiazepine receptor: studies with analogues of 6-(benzyloxy)-4-(methoxymethyl)-beta-carboline-3-carboxylic acid ethyl ester," *Journal of Medicinal Chemistry*, vol. 33, no. 3, pp. 1062–1069, 1990.

[115] J. M. Cook, H. Diaz-Arauzo, and M. S. Allen, "Inverse agonists: probes to study the structure, topology and function of the benzodiazepine receptor," in *Proceedings of the 51st Annual Scientific Meeting*, L. S. Harris, Ed., National Institute on Drug Abuse Research Monograph, pp. 133–139, The College on Problems of Drug Dependence, 1991.

[116] R. Trullas, H. Ginter, B. Jackson et al., "3-Ethoxy-beta-carboline: a high affinity benzodiazepine receptor ligand with partial inverse agonist properties," *Life Sciences*, vol. 43, no. 15, pp. 1189–1197, 1988.

[117] M. Cain, R. W. Weber, F. Guzman et al., "β-Carbolines: synthesis and neurochemical and pharmacological actions on brain benzodiazepine receptors," *Journal of Medicinal Chemistry*, vol. 25, no. 9, pp. 1081–1091, 1982.

[118] X. H. He, C. C. Zhang, and J. M. Cook, "Model of the BzR binding site: correlation of data from site-directed mutagenesis and the pharmacophore/receptor model," *Medicinal Chemistry Research*, vol. 10, no. 5, pp. 269–308, 2001.

[119] Q. Huang, R. Y. Liu, P. W. Zhang et al., "Predictive models for $GABA_A$/benzodiazepine receptor subtypes: studies of quantitative structure-activity relationships for imidazobenzodiazepines at five recombinant $GABA_A$/benzodiazepine receptor subtypes [$\alpha x\beta 3\gamma 2$ ($x = 1$–3, 5, and 6)] via comparative molecular field analysis," *Journal of Medicinal Chemistry*, vol. 41, no. 21, pp. 4130–4142, 1998.

[120] R. Y. Liu, P. W. Zhang, T. Gan, R. M. McKernan, and J. M. Cook, "Evidence for the conservation of conformational topography at five major GABA(A)/benzodiazepine receptor subsites. Potent affinities of the (S)-enantiomers of framework-constrained 4,5-substituted pyrroloimidazo-benzodiazepines," *Medicinal Chemistry Research*, vol. 7, no. 1, pp. 25–35, 1997.

[121] Q. Huang, W. Zhang, R. Liu, R. M. McKernan, and J. M. Cook, "Benzo-fused benzodiazepines employed as topological probes

for the study of benzodiazepine receptor subtypes," *Medicinal Chemistry Research*, vol. 6, no. 6, pp. 384–391, 1996.

[122] S. Yu, X. H. He, C. R. Ma, R. McKernan, and J. M. Cook, "Studies in search of α2 selective ligands for GABAA/BzR receptor subtypes. Part I. Evidence for the conservation of pharmacophoric descriptors for DS subtypes," *Medicinal Chemistry Research*, vol. 9, no. 3, pp. 186–202, 1999.

[123] S. Arbilla, H. Depoortere, P. George, and S. Z. Langer, "Pharmacological profile of the imidazopyridine zolpidem at benzodiazepine receptors and electrocorticogram in rats," *Naunyn-Schmiedeberg's Archives of Pharmacology*, vol. 330, no. 3, pp. 248–251, 1985.

[124] G. Wong, K. F. Koehler, P. Skolnick et al., "Synthetic and computer-assisted analysis of the structural requirements for selective, high-affinity ligand binding to diazepam-insensitive benzodiazepine receptors," *Journal of Medicinal Chemistry*, vol. 36, no. 13, pp. 1820–1830, 1993.

[125] A. Camerman and N. Camerman, "Stereochemical basis of anticonvulsant drug action. 2. Molecular structure of diazepam," *Journal of the American Chemical Society*, vol. 94, no. 1, pp. 268–272, 1972.

[126] A. Hempel, N. Camerman, and A. Camerman, "Benzodiazepine stereochemistry: crystal structures of the diazepam antagonist Ro 15-1788 and the anomalous benzodiazepine Ro 5-4864," *Canadian Journal of Chemistry*, vol. 65, no. 7, pp. 1608–1612, 1987.

[127] S. Neidle, G. D. Webster, G. B. Jones, and D. E. Thurston, "Structures of two DNA minor-groove binders, based on pyrrolo[2,1-c][1,4]-benzodiazepines," *Acta Crystallographica Section C: Crystal Structure Communications*, vol. 47, no. 12, pp. 2678–2680, 1991.

[128] T. A. Halgren, "Merck molecular force field. V. Extension of MMFF94 using experimental data, additional computational data, and empirical rules," *Journal of Computational Chemistry*, vol. 17, no. 5-6, pp. 616–641, 1996.

[129] T. A. Halgren, "Merck molecular force field. III. Molecular geometries and vibrational frequencies for MMFF94," *Journal of Computational Chemistry*, vol. 17, no. 5-6, pp. 553–586, 1996.

[130] T. A. Halgren, "Merck molecular force field. II. MMFF94 van der Waals and electrostatic parameters for intermolecular interactions," *Journal of Computational Chemistry*, vol. 17, no. 5-6, pp. 520–552, 1996.

[131] T. A. Halgren, "Merck molecular force field. I. Basis, form, scope, parameterization, and performance of MMFF94," *Journal of Computational Chemistry*, vol. 17, no. 5-6, pp. 490–519, 1996.

[132] T. A. Halgren and R. B. Nachbar, "Merck molecular force field. IV. Conformational energies and geometries for MMFF94," *Journal of Computational Chemistry*, vol. 17, no. 5-6, pp. 587–615, 1996.

[133] H. L. June, S. C. Harvey, K. L. Foster et al., "$GABA_A$ receptors containing α5 subunits in the CA1 and CA3 hippocampal fields regulate ethanol-motivated behaviors: an extended ethanol reward circuitry," *Journal of Neuroscience*, vol. 21, no. 6, pp. 2166–2177, 2001.

[134] B. J. Kaminski, M. L. Van Linn, J. M. Cook, W. Yin, and E. M. Weerts, "Effects of the benzodiazepine GABAA α1-preferring ligand, 3-propoxy-β-carboline hydrochloride (3-PBC), on alcohol seeking and self-administration in baboons," *Psychopharmacology*, vol. 227, no. 1, pp. 127–136, 2013.

[135] S. Huang, *Synthesis of Optically Active Subtype Selective Benzodiazepine Receptor Ligands*, University of Wisconsin, Milwaukee, Wis, USA, 2007.

[136] M. M. Savić, S. Majumder, S. Huang et al., "Novel positive allosteric modulators of $GABA_A$ receptors: do subtle differences in activity at α1 plus α5 versus α2 plus α3 subunits account for dissimilarities in behavioral effects in rats?" *Progress in Neuro-Psychopharmacology and Biological Psychiatry*, vol. 34, no. 2, pp. 376–386, 2010.

[137] M. Ernst, D. Brauchart, S. Boresch, and W. Sieghart, "Comparative modeling of GABAA receptors: limits, insights, future developments," *Neuroscience*, vol. 119, no. 4, pp. 933–943, 2003.

[138] B. L. Roth, "Ki determinations were generously provided by the National Institute of Mental Health's Psychoactive Drug Screening Program," Contract # HHSN-271-2013-00017-C (NIMH PDSP), The NIMH PDSP, 2013, https://pdspdb.unc.edu/pdspWeb/.

[139] M. S. Choudhary, S. Craigo, and B. L. Roth, "Identification of receptor domains that modify ligand binding to 5-hydroxytryptamine2 and 5-hydroxytryptamine1c serotonin receptors," *Molecular Pharmacology*, vol. 42, no. 4, pp. 627–633, 1992.

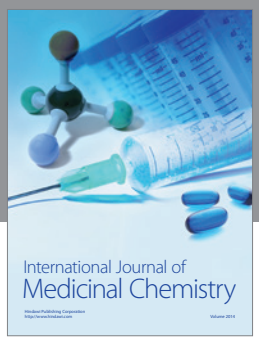
[140] J. Yang, Y. Teng, S. Ara, S. Rallapalli, and J. M. Cook, "An improved process for the synthesis of 4H-imidazo[1,5-a][1,4]benzodiazepines," *Synthesis*, no. 6, pp. 1036–1040, 2009.

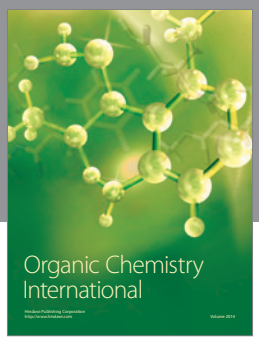
[141] Z.-Q. Gu, G. Wong, C. Dominguez, B. R. De Costa, K. C. Rice, and P. Skolnick, "Synthesis and evaluation of imidazo[1,5-a][1,4]benzodiazepine esters with high affinities and selectivities at 'diazepam-insensitive' benzodiazepine receptors," *Journal of Medicinal Chemistry*, vol. 36, no. 8, pp. 1001–1006, 1993.

[142] J. Buckingham, *Dictionary of Organic Compounds*, vol. 2, Chapman & Hall, New York, NY, USA, 1982.

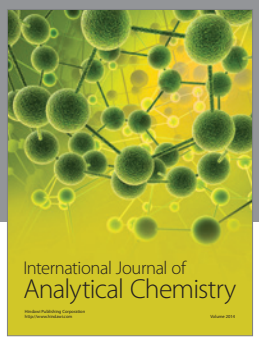
[143] C. Yung-Chi and W. H. Prusoff, "Relationship between the inhibition constant (KI) and the concentration of inhibitor which causes 50 per cent inhibition (I50) of an enzymatic reaction," *Biochemical Pharmacology*, vol. 22, no. 23, pp. 3099–3108, 1973.

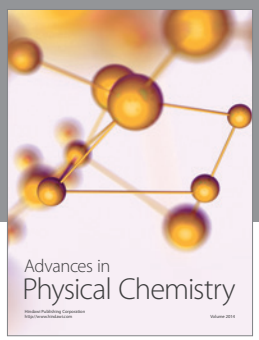
[144] J. M. Cook, T. Clayton, Y. T. Johnson, S. Rallapalli, and D. Han, "GABAergic agents to treat memory deficits," US Patent 2010/0130479 A1, 2010.

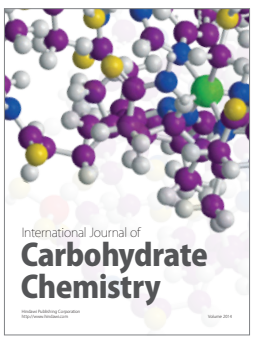


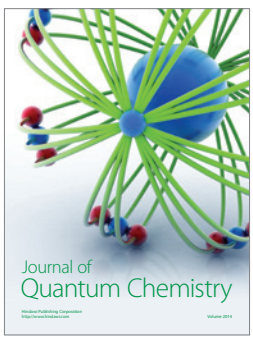












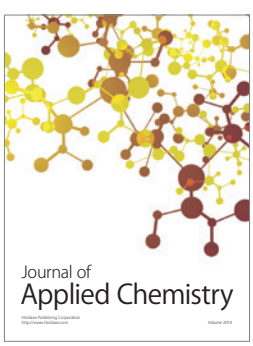


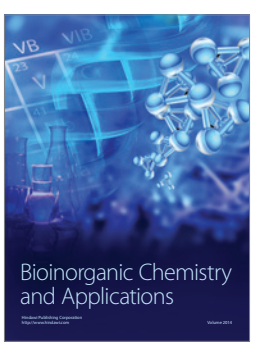




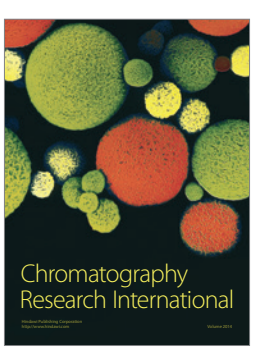




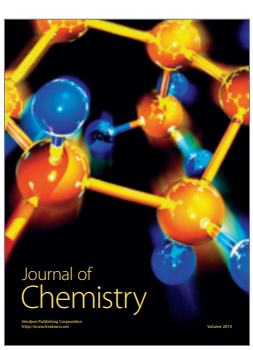














Hindawi
Submit your manuscripts at
http://www.hindawi.com

APPENDIX E. A Review of the Updated Pharmacophore for the Alpha 5 GABA(A) Benzodiazepine Receptor Model – *Supporting Information*

Supporting information can be found at:

http://www.hindawi.com/journals/ijmc/2015/430248/

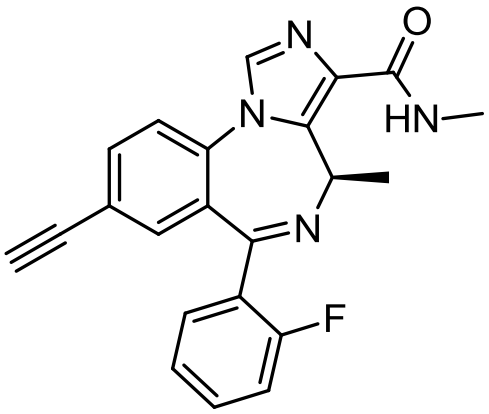
Authors: Terry Clayton, Michael M. Poe, Sundari Rallapalli, Poonam Biawat, Miroslav M. Savic, James K. Rowlett, George Gallos, Charles W. Emala, Catherine C. Kaczorowski, Douglas C. Stafford, Leggy A. Arnold and James M. Cook

International Journal of Medicinal Chemistry, Volume **2015**, Article ID 430248;

Doi: 10.1155/2015/430248

APPENDIX F. Manuscript prepared by Miroslav M. Savic, *et al.* on the behavioral characterization of MP-III-022.

Structure:



MP-III-022

A NOVEL BENZODIAZEPINE MP-III-022 IMPAIRS SPATIAL COGNITION AND IMPROVES SOCIAL RECOGNITION BY STRONG SELECTIVE POSITIVE MODULATION OF $GABA_A$ RECEPTORS CONTAINING THE α5 SUBUNIT

Tamara Timić Stamenić[a], Michael M. Poe[b], Sabah Rehman[c], Anja Santrač[a], Branka Divović[a], Petra Scholze[d], Margot Ernst[c], James M. Cook[b], Miroslav M. Savić[a]*

[a]Department of Pharmacology, Faculty of Pharmacy, University of Belgrade, Vojvode Stepe 450, 11221 Belgrade, Serbia

[b]Department of Chemistry and Biochemistry, University of Wisconsin-Milwaukee, P.O. Box 413, Milwaukee, Wisconsin 53201, USA

[c]Department of Molecular Neurosciences, Center for Brain Research, Medical University of Vienna, Vienna, Austria

[d]Department of Pathobiology of the Nervous System, Center for Brain Research, Medical University of Vienna, Vienna, Austria

*Corresponding author: Dr Miroslav M. Savić, Department of Pharmacology, Faculty of Pharmacy, University of Belgrade, Vojvode Stepe 450, 11221 Belgrade, Serbia

Tel.:+381-11-3951280

Fax: +381-11-3972840

E-mail address: miroslav@pharmacy.bg.ac.rs (M. M. Savić)

ABSTRACT

Selective modulation of $GABA_A$ receptors containing the α5 subunit (α5$GABA_A$Rs) is believed to have considerable therapeutic potential in several psychiatric and neurological conditions characterized by cognitive dysfunction. We have synthesized and characterized MP-III-022 ((*R*)-8-ethynyl-6-(2-fluorophenyl)-*N*,4-dimethyl-4*H*-benzo[*f*]imidazo[1,5-*a*][1,4]diazepine-3-carboxamide) *in vitro* and *in vivo* as an affinity and especially efficacy selective positive allosteric modulator of α5$GABA_A$Rs. By approximation of the electrophysiological responses which the estimated free rat brain concentrations can induce, we demonstrated that convenient systemic administration of MP-III-022 in the dose range 1-10 mg/kg resulted in a selective potentiation, over a wide range from mild to moderate to strong, of α5βγ2 $GABA_A$ receptors. For eliciting a similar range of potentiation, the parent ligand SH-053-2′F-R-CH3 needs to be administered over a much wider dose range (10-200 mg/kg), but at the price of activating non-α5 $GABA_A$Rs as well as the desired α5$GABA_A$Rs at the highest dose. At the dose of 10 mg/kg, which elicits a strong positive modulation of α5$GABA_A$Rs, MP-III-022 caused mild, but significant muscle relaxation, devoid of ataxia or sedation characteristic for non-selective benzodiazepines. Concomitantly, the same dose deteriorated spatial learning and memory of rats in the Morris water maze and the animals' performance in the sociability trial in the three-chamber test, but improved social recognition in the social discrimination test. However, a mild potentiation of α5βγ2 $GABA_A$ receptors, produced by the 1 mg/kg dose, resulted in a faster acquisition of spatial learning in the water maze. These results provide additional insight into graded modulation of α5$GABA_A$Rs as a potential treatment for distinct cognition-related clinical manifestations. Moreover, MP-III-022 may represent an improved tool to study the effects of α5$GABA_A$Rs on the neuronal pathways related to CNS disorders such as schizophrenia, Alzheimer's disease, Down syndrome or autism, aimed at finding the optimal levels of selective modulation needed for their amelioration.

Keywords: receptor efficacy; binding assay; free brain concentration; Morris water maze; social novelty discrimination; three-chamber test

INTRODUCTION

Gamma-aminobutyric acid (GABA) is the main inhibitory neurotransmitter in adult brain. $GABA_A$ receptors mediate the majority of inhibitory neurotransmission and at the same time represent a prominent therapeutic target for many psychiatric and neurological conditions. Most notably, benzodiazepines are GABAergic drugs widely used for decades in treatment of anxiety, insomnia, epilepsy and muscular spasms, and detailed elucidation of their mechanism of action has helped the understanding of the role of various $GABA_A$ receptor populations in normal and pathological conditions. Specifically, $GABA_A$ receptors are pentameric assemblies composed of five subunits recruited from a pool of 19 subunits designated as α1-6, β1-3, γ1-3, δ, ε, π and ρ1-3. Despite the huge number of possible subunit combinations, the vast majority of $GABA_A$ receptors contain an α1, α2, α3 or α5 subunits together with a neighboring γ2 subunit, and benzodiazepines such as diazepam act as positive allosteric modulators at all these receptors. An approach based on knock-in modification of α1, α2, α3 or α5 subunits in mice, aimed at linking the distinct pharmacological effects of benzodiazepines with a particular receptor subtype, and thus developing selective, better-tolerated ligands for known and novel indications, was a substantial breakthrough.[1] A number of studies assessing the behavioral activity of diazepam in mice which harbor such point-mutated receptors have attributed the sedative, ataxic and addictive properties of benzodiazepines to α1-containing $GABA_A$ receptors, the anxiolytic and antihyperalgesic actions to the α2- and α3-containing $GABA_A$ receptors, the muscle relaxant actions to the α2/α3/α5-subtypes, anterograde amnesic effects to the α1- and α5-subtypes, and anticonvulsant activity to all the α1/α2/α3-containing receptors.[2]

Among these diazepam-sensitive target populations, α5$GABA_A$Rs are the least abundant (<5% of total) and with the most restricted distribution,[1] both of which are excellent characteristics for development of subtype selective ligands. Indeed, in a recent overview of patents in the field of benzodiazepines, it was stated that most of the analyzed patents claim the therapeutic usefulness of both, positive and negative selective modulators of α5$GABA_A$Rs.[3] As genetic studies revealed pro-cognitive effects by reduction of GABAergic neurotransmission at α5$GABA_A$Rs,[4,5] development of negative allosteric modulators selective for these receptors has been initiated firstly,[6] and resulted in claims of the effectiveness of such ligands in cognitive symptoms of schizophrenia, Down syndrome or mood disorders.[3,7] On the other hand, development of positive allosteric modulators with selectivity for α5$GABA_A$Rs has been recognized more recently as a potentially fruitful approach in

treatment of aging-related dementia[8] and cognitive impairment in neurodevelopmental disorders such as schizophrenia[9] or autism[10].

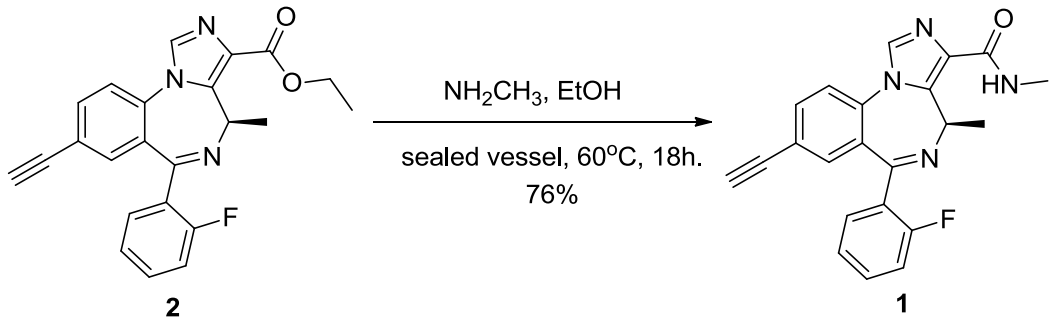
Although synthesis and discovery of ligands selective for distinct $GABA_A$ receptor subtypes have become a research priority,[11] many encouraging preclinical results failed to translate to the clinical setting so far (e.g. Atack et al.[12]). Poor tolerability or toxicity, suboptimal selectivity or kinetics and lack of the needed magnitude of receptor modulation are among possible explanations for such failure.[13-15] In the present work, we have synthesized and pharmacokinetically and pharmacologically characterized MP-III-022 **(1)**, the ligand prepared in a one-step reaction from SH-053-2′F-R-CH3 **(2)**, which has been characterized and widely studied as one of the most selective positive modulators at α5$GABA_A$Rs.[9,18-22] When compared with the published ligands, MP-III-022 demonstrated an improved selectivity for α5βγ2 $GABA_A$ receptors, both in binding and functional assays (cf. the recent reviews by Clayton et al.[23] and Soh and Lynch[7]). Moreover, by approximation of the electrophysiological responses which estimated free rat brain concentrations can induce,[16,17] it was demonstrated that systemic administration of MP-III-022 at doses between 1 and 10 mg/kg should result in a wide range of selective potentiation at α5$GABA_A$Rs, which is not conveniently attainable after dosing with the parent compound SH-053-2′F-R-CH3. This was accompanied by distinct changes in cognitive tests, but not in overt behavioral impairments suggestive of safety issues.

RESULTS AND DISCUSSION

CHEMISTRY

Synthesis of (*R*)-8-Ethynyl-6-(2-fluorophenyl)-*N*,4-dimethyl-4*H*-benzo[*f*]imidazo[1,5-*a*][1,4]diazepine-3-carboxamide (MP-III-022) was performed, as depicted in Scheme 1.

Scheme 1. Synthesis of MP-III-022 (**1**)



IN VITRO CHARACTERIZATION

Binding studies

Membranes from HEK-293 cells transiently expressing different $GABA_A$ receptor subunit combinations were characterized using ^{3}H-Flunitrazepam binding. In order to determine radioligand affinities to the four tested receptor subtypes (which are needed to convert the IC_{50} values of a test compound into K_i values), saturation binding experiments were performed. Cells were incubated with various concentrations of ^{3}H-flunitrazepam and binding data were subjected to Scatchard analysis, as described in the methods section. The equilibrium dissociation constants of the ligand-receptor complex obtained in saturation binding experiments for four $GABA_A$ receptor subtypes are presented in Table S1.

In other experiments the potency of MP-III-022 to inhibit 2 nM ^{3}H-flunitrazepam binding to membranes from HEK-293 cells expressing four different receptor subtypes was studied. Membranes from HEK cells transfected with the four subunit combinations were incubated with 2 nM ^{3}H-flunitrazepam in the absence or presence of either 5 µM diazepam (to determine nonspecific binding) or increasing concentrations of MP-III-022. IC50 values (i.e. drug concentrations resulting in half maximal inhibition of specific ^{3}H-flunitrazepam binding) were converted to Ki values by using the Cheng-Prusoff relationship (for details see methods-section).

The determined K_i values (Table 1) of α5$GABA_A$Rs differ statistically significantly from α1- ($p=0.0011$) and from α3-containing receptors ($p=0.0041$) (one-way ANOVA analysis followed by Tukey's multiple comparison test). The Ki values demonstrate that MP-III-022 possesses a 15, 6 and 12-fold selectivity in binding to α5$GABA_A$Rs when compared to binding to α1, α2 and α3-containing $GABA_A$ receptors, respectively. For comparison, the Ki values for SH-053-2′F-R-CH3 at α1β3γ2, α2β3γ2, α3β3γ2, and α5β3γ2 $GABA_A$ receptors were 759.1, 948.2, 768.8 and 95.2 nM, respectively,[19] which means that relative selectivity of the two ligands is of the same order of magnitude. However, it is clear that selectivity for α5- against α1-containing $GABA_A$ receptors is 15-fold for MP-III-022, and 8-fold for SH-053-2′F-R-CH3; this approximately two-fold greater selectivity ratio may be relevant because α1-containing $GABA_A$ receptors are the subtype predominantly connected with adverse effects of potentiation at $GABA_A$ receptors.[1]

Table 1: Binding affinities of MP-III-022 (K_i) for the different receptor subtypes

α1β3γ2S	α2β3γ2S	α3β3γ2S	α5β3γ2S
850 ± 110 nM	360 ± 56 nM	660 ± 170 nM	55 ± 17 nM

The concentrations resulting in half maximal inhibition of radioligand binding were converted into Ki values by using the Cheng-Prusoff relationship and the respective KD values given in Table S1. Ki values are presented as mean values ± SEM from 3 independent experiments performed in duplicates.

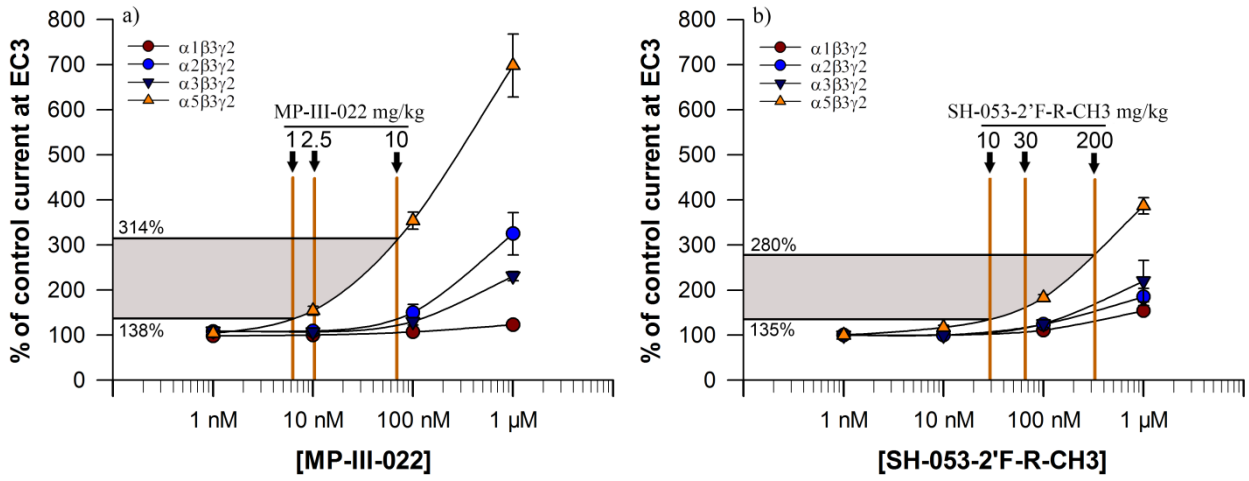
Ligand MP-III-022 exerted negligible activity in 50 other receptor and enzyme assays (B. Roth et al., NIMH Psychoactive Drug Screening Program, UNC, unpublished results). The only exception was the κ opioid receptor (KOR), at which the secondary binding study gave the Ki value of 381 nM. The value is of the same order of magnitude as that of SH-053-2′F-R-CH3 (240 nM; B. Roth et al., NIMH Psychoactive Drug Screening Program, UNC, unpublished results). As these are at least 100-fold weaker affinities than that of the declared KOR selective ligands,[24] the findings have no plausible biological relevance. However, as the KOR Ki for MP-III-022 is on par with that determined for α2GABA$_A$Rs (360 nM), KOR-mediated effects might be seen after the doses (15 mg/kg and above) connected with high free brain concentrations of this ligand, at which selectivity for α5-containing receptors was lost, as discussed below.

Electrophysiological effects

Two electrode voltage clamp experiments were performed as indicated in the methods section. Dose response curves for MP-III-022 are shown in Figure 1a, while the exact data are available in the Supplementary table S2. At the α5β3γ2 GABA$_A$ receptors, MP-III-022 elicited a significant allosteric modulatory efficacy at concentrations starting at 10 nM, and the potentiation values obtained at concentrations approaching 100 nM can be described as strong efficacy (above 300%). On the other hand, its activity tended to be weakly modulatory at α2- and α3-containing receptors only at concentrations of about 100 nM and above. Finally, MP-III-022 lacked modulatory actions at α1-containing GABA$_A$ receptors in the whole range of *in vivo* free brain concentrations which were obtained (*vide infra* and Table S3). For comparison, a concentration of 100 nM of SH-053-2′F-R-CH3 resulted in 111 ± 2%, 124 ± 9%, 125 ± 8%, and 183 ± 7% of control current in α1β3γ2, α2β3γ2, α3β3γ2, and α5β3γ2 GABA$_A$ receptors, respectively.[19] Analogous to the data with MP-III-022, in Figure 1b are presented dose response curves for SH-053-2′F-R-CH3[19] with approximated actions of *in vivo* obtainable free brain concentrations. The exact values of potentiation read from the curves in

Figure 1 (Table S3), suggest that efficacy selectivity of MP-III-022 is obtainable in the range from mild (below 140%) via moderate (about 160%) to strong (above 300%) potentiation at α5GABA$_A$Rs. While SH-053-2′F-R-CH3 displays similar selectivity for mild (below 140%) to moderate potentiation (about 160%), its strong potentiation at α5GABA$_A$Rs (below 300%) has been accompanied by substantial activation of all non-α5 receptors.

Figure 1. The approximated electrophysiological responses elicited by the estimated free brain concentrations of MP-III-022 (given in Table 2) and SH-053-2′F-R-CH3 (given in Table 3), presented on the concentration-response curves of MP-III-022 (a) and SH-053-2′F-R-CH3 (b) at rat recombinant α1-, α2-, α3,- and α5β3γ2 GABA$_A$ receptors



Pharmacokinetic and free fraction studies

The concentration–time profiles of MP-III-022 and SH-053-2′F-R-CH3 in rat plasma and brain after intraperitoneal administration of the 2.5 mg/kg and 10 mg/kg dose, respectively, with the calculated pharmacokinetic parameters, are given in Figure 2. The doses chosen elicit a moderate degree of selective potentiation at α5GABA$_A$Rs; see vertical markers in Figure 1. AUC values for plasma and brain were 2-fold and 1.75-fold, respectively, greater for MP-III-022 than for SH-053-2′F-R-CH3, despite the fact that MP-III-022 was administered at a 4-fold lower dose. In line with *in vivo* data of superior systemic exposure, the amide compound MP-III-022 displayed an excellent *in vitro* metabolic stability during incubation in rat plasma, which is in clear contrast with the values obtained with the less stable ester compound SH-053-2′F-R-CH3 (Table S4). Analysis of these rodent data demonstrated that MP-III-022, as a

highly brain-bioavailable benzodiazepine, possesses a more favorable pharmacokinetic profile for *in vivo* investigation of the role of α5GABA$_A$Rs than SH-053-2′F-R-CH3.

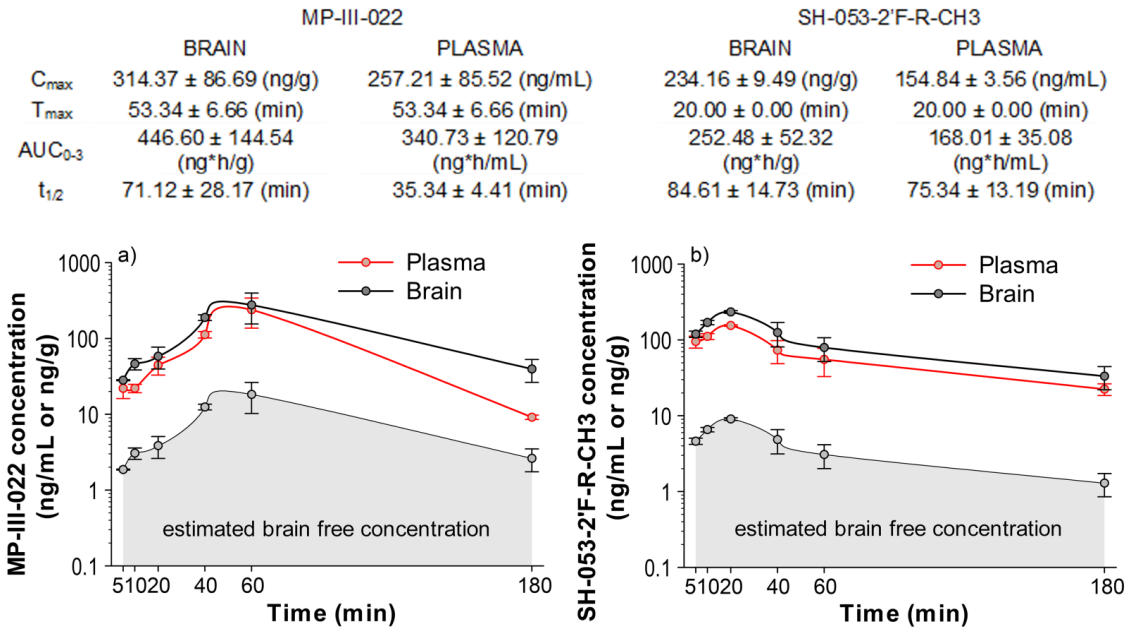


Figure 2. Plasma and brain concentration–time profiles of MP-III-022 (a) and SH-053-2′F-R-CH3 (b) after intraperitoneal administration of the 2.5 mg/kg and 10 mg/kg dose, respectively (n = 3 per time point).

The concentrations of MP-III-022 in rat plasma (nmol/L) and brain tissue (nmol/kg), both total and free (estimated), measured 20 min after i.p. injection of MP-III-022 dosed at 1, 2.5, 10, 15 and 20 mg/kg, are shown in Table 2. Free concentrations of MP-III-022 were calculated by multiplying the obtained total plasma and brain concentrations with the appropriate free fractions (13.51% for plasma and 6.61% for brain tissue) determined by rapid equilibrium dialysis. The analogous results for SH-053-2′F-R-CH3 over the same 20-fold dose schedule, but in the range from 10 mg/kg to 200 mg/kg, are presented in Table 3. Free fractions for this ester compound were 68.55% for plasma and 3.87% for brain.

Table 2. Total and estimated free concentration of MP-III-022 (1, 2.5, 10, 15 and 20 mg/kg) in plasma and brain 20 minutes after treatment in rats. Mean ± SEM, n = 3-6

Dose (mg/kg)		**1**	**2.5**	**10**	**15**	**20**
Plasma (nmol/L)	*Total*	62.43 ± 4.97	120.01 ± 31.74	645.07 ± 166.29	3709.24 ± 2012.04	5378.01 ± 1936.91
	Free	8.47 ± 0.67	16.29 ± 4.31	87.57 ± 22.57	503.51 ± 273.13	730.04 ± 262.93
Brain	*Total*	96.47 ± 12,04	156.46 ± 50.33	1030.52 ± 278.03	4804.44 ± 2821.77	8465.45 ± 886.18

(nmol/kg)	*Free*	**6.38 ± 0.80**	**10.34 ± 3.33**	**68.12 ± 18.38**	**317.57 ± 186.52**	**559.57 ± 58.58**

Table 3. Total and estimated free concentration of SH-053-2′F-R-CH3 (10, 20, 30, 150 and 200 mg/kg) in plasma and brain 20 minutes after treatment in rats. Mean ± SEM, n = 2-4

Dose (mg/kg)		**10**	**20**	**30**	**150**	**200**
Plasma (nmol/L)	*Total*	406.43 ± 76.45	420.63 ± 70.01	555.51 ± 68.18	1604.96 ± 271.88	2737.87 ± 286.86
	Free	278.60 ± 52.39	288.32 ± 47.99	380.78 ± 46.73	1100.14 ± 186.36	1876.71 ± 196.63
Brain (nmol/kg)	*Total*	752.00 ± 132.84	1003.57 ± 87.55	1663.84 ± 378.29	3816.79 ± 965.21	8374.25 ± 2322.03
	Free	**29.10 ± 5.14**	**38.85 ± 3.39**	**64.40 ± 14.64**	**147.74 ± 37.36**	**324.16 ± 89.88**

The combined *in vitro* and pharmacokinetic results suggest that MP-III-022 in the dose range 1-10 mg/kg can selectively and gradually potentiate the α5GABA$_A$Rs in a wide span from 138% to 314%. At higher doses (15 mg/kg and above), the selectivity of receptor activation disappears, and other, mostly α2/α3-containing GABA$_A$ receptors, would begin to substantially contribute to the overall pharmacological activity of MP-III-022. On the other hand, the estimated potentiation of GABA-mediated currents at α5GABA$_A$Rs obtained with SH-053-2′F-R-CH3 reached the value of 280% after a huge, experimentally inconvenient dose of 200 mg/kg, and was accompanied with higher levels of potentiation at the respective non-α5GABA$_A$Rs when compared with the 10 mg/kg dose of MP-III-022. In this vein, SH-053-2′F-R-CH3 is not as applicable as MP-III-022 for *in vivo* studies of the role of strong potentiation of α5GABA$_A$Rs.

BASIC BEHAVIORAL TESTING

Grip strength, rotarod test and intravenous PTZ infusion test

MP-III-022 induced a dose-dependent decrease of muscle tension as measured by grip strength (Table 4). Studies in knock-in mice have suggested that all, the α2-, α3- and α5-containing GABA$_A$ receptors, contribute to the muscle relaxant action of diazepam.[2] We have previously demonstrated that the α5-selective antagonist XLi-093[25] can significantly diminish the myorelaxant actions of diazepam in rats. Consistent with these results, the first muscle relaxant effect of MP-III-022 was observed at a dose (10 mg/kg) postulated to elicit a selective strong potentiation of α5-GABA$_A$ receptors. The involvement of α2/α3-containing GABA$_A$ receptors at higher doses of MP-III-022 is expected to have contributed to the further gradual decrease of muscle tension seen in rats.

In contrast to the grip strength results, the rats treated with 10 mg/kg MP-III-022 displayed normal motor coordination and balance as assessed in the rotarod test, far different from the

animals treated with the 15 mg/kg, and especially 20 mg/kg dose (Table 4). The ataxic effect of 15 mg/kg MP-III-022 was preventable by flumazenil, but not XLi-093. Namely, one-way ANOVA ($F(2,18) = 5.05$, $p = 0.018$) and Student–Newman–Keuls (SNK) *post hoc* revealed significant differences in performance between the rats treated with 15 mg/kg MP-III-022 alone or in combination with 20 mg/kg of XLi-093, and the combination of 15 mg/kg MP-III-022 and 15 mg/kg flumazenil ($p = 0.021$ and $p = 0.019$, respectively, Table 4). The rotarod studies in knock-in mice have suggested that the α1-, but not the α2- or α3-containing $GABA_A$ receptors contribute to the ataxic action of diazepam.[2] In line with this, the administration of L-838,417, a ligand with significant, but comparably small efficacy at α2-, α3- and α5-$GABA_A$Rs, did not cause deficits in rotarod performance in rats[26] or mice.[27] Nonetheless, the experiments using the nonselective, α1- and α5-subunit-selective antagonists flumazenil, βCCt and XLi-093, respectively, have suggested that an effect of diazepam mediated by α2- or α3-, but not α5-containing $GABA_A$ receptors may have contributed to the impairing influence of diazepam on the rotarod performance of rats.[25] Accordingly, the present results imply that a pronounced modulatory action at α2/3$GABA_A$Rs (the estimated respective potentiations at α2- and α3$GABA_A$Rs were 225% and 175% after the 15 mg/kg dose, and 280% and 200% after the 20 mg/kg dose; for comparison, the estimated potentiation at α2$GABA_A$Rs after the dose of 10 mg/kg was 138%) still can induce ataxia. The differences in dose-dependency of behavioral response in two tests demonstrate that the rotarod-ataxic effects of MP-III-022 may encompass, but do not solely rely on muscle relaxation. When testing SH-053-2′F-R-CH3 on the rotarod, the first, mild and insignificant deterioration (154±26 s vs. 180 s with control animals; $n = 4$) was noticed at the dose as high as 200 mg/kg, at which the estimated potentiations at α2- and α3$GABA_A$Rs were 171% and 155%, respectively. Furthermore, even higher doses most probably required for marked incapacitation (for comparison, the S-isomer of this ligand, SH-053-2′F-S-CH3, displayed a median incapacitating dose of 219 mg/kg[28]) were not tested due to ethical constraints and irrelevancy, bearing in mind that they need to be accompanied by a distinct lack of selectivity of receptor subtype action. Keeping in mind the efficacy and kinetic properties of MP-III-022, the whole set of grip strength and rotarod results unambiguously demonstrated that the 15 mg/kg dose of MP-III-022 is behaviorally non-selective and thus in further experiments was used only once more, in the spontaneous locomotor activity test.

One-way ANOVA applied to the PTZ test (Table 4) did not show a statistically significant effect of treatment with either of two tested doses of MP-III-022 selective for α5$GABA_A$Rs

(F(2,30) = 1.50, p = 0.239). This is consistent with the proposed contribution of the non-α5 containing receptors to the anticonvulsant action of GABAergic drugs.[2]

Table 4. Effect of different doses of MP-III-022 in the grip strength, rotarod, and pentylenetetrazole (PTZ) test; mean ± SEM. Grip strength: *p < 0.05, **p < 0.01, ***p < 0.001 compared to SOL, +p < 0.05 compared to combination of 1 mg/kg MP-III-022. Rotarod: *p < 0.05 compared to 15 mg/kg MP-III-022, +p < 0.05 compared to combination of 15 mg/kg MP-III-022 and 20 mg/kg XLi-093; SOL = solvent, FLU = flumazenil

grip strength the peak force of experimenter's pull necessary to overcome the strength of the animal's grip		
Treatment	**Mean ± SEM (kg/kg)**	**n**
SOL	2.87 ± 0.17	10
1 mg/kg MP-III-022	2.57 ± 0.08	10
2.5 mg/kg MP-III-022	2.41 ± 0.28	8
10 mg/kg MP-III-022	1.94 ± 0.22**+	8
15 mg/kg MP-III-022	1.86 ± 0.16*	5
20 mg/kg MP-III-022	1.78 ± 0.16***+	11
rotarod test the time remaining on the rod revolving at 15 rpm		
Treatment	**Mean ± SEM (s)**	**n**
10 mg/kg MP-III-022	180	3
20 mg/kg MP-III-022	6.67 ± 4.81	3
15 mg/kg MP-III-022	69.09 ± 25.58	9
15 mg/kg MP-III-022/20 mg/kg XLi-093	74.61 ± 34.03	6
15 mg/kg MP-III-022/15 mg/kg FLU	175.17 ± 4.83*+	6
PTZ test the threshold doses of PTZ required to elicit seizures		
Treatment	**Mean ± SEM (mg/kg PTZ)**	**n**
SOL	53.38 ± 1.84	11
1 mg/kg MP-III-022	60.99 ± 6.11	11
10 mg/kg MP-III-022	50.99 ± 3.72	11

Spontaneous and amphetamine induced locomotor activity

The spontaneous locomotor activity test was performed with the highest selective (10 mg/kg) and lowest non-selective (15 mg/kg) dose of MP-III-022. One-way ANOVA for total distance traveled revealed a significant effect of treatment (F(2,25) = 3.64, p = 0.041) and analysis of the SNK test showed differences between control and 15 mg/kg MP-III-022 (p = 0.029, Fig 3a). Similarly, when the two-way repeated measures ANOVA was applied on distance traveled in the 5-min bins, a significant effect of treatment and time was revealed (F(2,25) = 3.64, p = 0.041, F(8,200) = 32.90, p < 0.001, respectively), without a significant interaction of factors (F(16,200) = 1.63, p = 0.065, Figure 3b). The *post hoc* SNK test showed the differences between control and 15 mg/kg MP-III-022 (p = 0.032). The slight hyperlocomotion observed after treatment with the 15 mg/kg dose could be ascribed to a kind

of behavioral disinhibition induced by potentiation of α2/3-containing $GABA_A$ receptors unopposed by activity at α1-containing receptors.[29] As an important corollary, the assertion that α5$GABA_A$Rs may contribute to the sedative properties of benzodiazepine site agonists[19,28] could certainly not apply to a substantial level of potentiation, such as that elicited by 10 mg/kg MP-III-022.

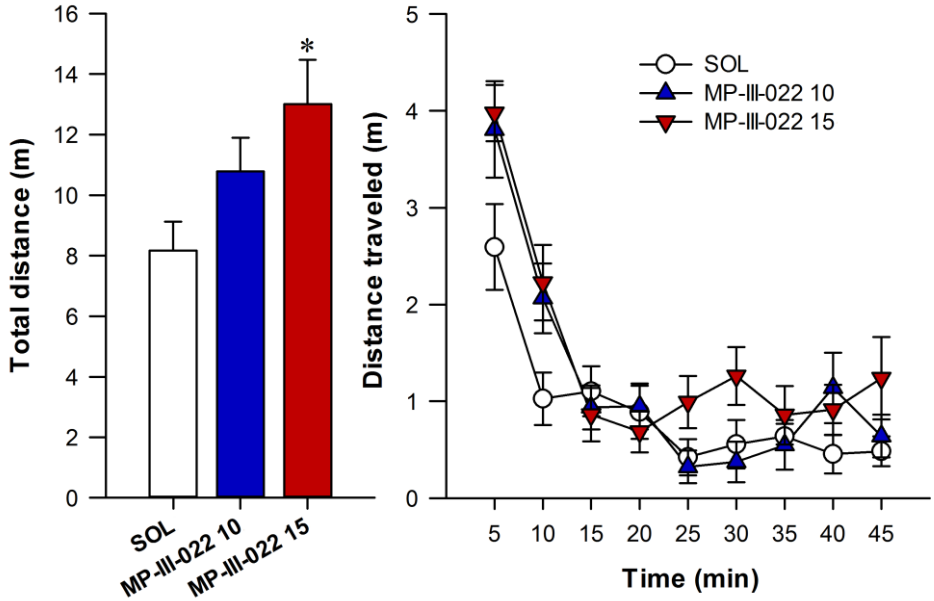


Figure 3. The effects 10 and 15 mg/kg MP-III-022 on the total distance traveled (a) and on distance traveled in 5-min bins (b) during 45 min in SLA. *p < 0.05 compared to control (SOL/SOL) group. All data are presented as the mean +/± SEM. Number of animals per treatment group was 8-10. SOL = solvent, MP-III-022 10 = 10 mg/kg MP-III-022, MP-III-022 15 = 15 mg/kg MP-III-022.

Moreover, the present results lead to an assumption that activation of α5$GABA_A$Rs is not sufficient to either enhance or decrease locomotion, as one-way ANOVA applied on data with three selective doses of MP-III-022 (1, 2.5 and 10 mg/kg) from the first part of the amphetamine-induced locomotor activity test did not show any effect of treatment ($F(3,28) = 0.08$, $p = 0.970$, Figure 4a). The same lack of effect was observed with two-way repeated measures ANOVA on results of 5-min intervals: Treatment: $F(3,28) = 0.08$, $p = 0.970$; Time: $F(3,84) = 78.36$, $p < 0.001$: Interaction: $F(9,84) = 0.49$, $p = 0.879$.

One-way ANOVA applied on the data from 60-min recordings after administration of amphetamine revealed a significant effect on total distance traveled ($F(3,35) = 4.16$, $p = 0.007$); *post hoc* SNK results were given in Figure 4b. When two-way ANOVA with repeated

measures was applied on distance traveled in 5-min bins, the same significant effect was observed (Treatment: $F(4,35) = 4.16$, $p = 0.007$, Time: $F(11,385) = 5.47$, $p < 0.001$, Interaction: $F(44,385) = 2.02$, $p < 0.001$). The SNK test confirmed differences between control and all amphetamine-treated groups. Recent studies with allegedly selective positive as well as negative modulators of $\alpha5GABA_A$ receptors reported a slight, but still significant suppression of the amphetamine-induced locomotor stimulation in the sensitized, behaviorally altered, animals[9,30]; the present data demonstrate the lack of influence of α5 receptor-selective doses of MP-III-022 on amphetamine's effects in normal wild-type animals.

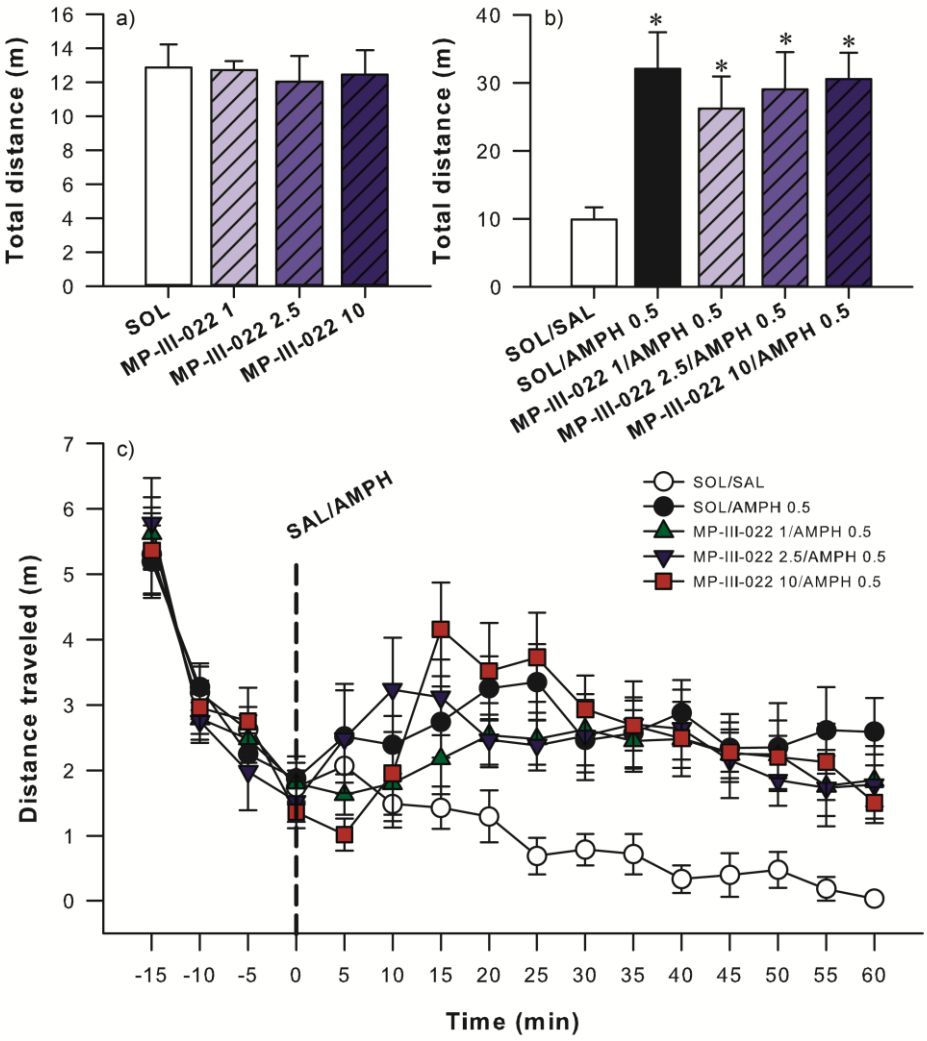


Figure 4. The effect of 1, 2.5, and 10 mg/kg MP-III-022 on locomotor activity during 20 minutes before amphetamine treatment (a), the influence of 1, 2.5, and 10 mg/kg MP-III-022 on amphetamine induced hyperlocomotion during 60 min (b) and effect on distance traveled in 5-min bins during all testing (c) in locomotor activity test. *$p < 0.05$ compared to control (SAL/SAL) group. All data are presented as the mean + or ± SEM. Number of animals per treatment group was 8. SOL = solvent, SAL = vehicle, AMPH 0.5 = 0.5 mg/kg amphetamine,

MP-III-022 1 = 1 mg/kg MP-III-022, MP-III-022 2.5 = 2.5 mg/kg MP-III-022, MP-III-022 10 = 10 mg/kg MP-III-022

IN VIVO TESTS OF COGNITIVE PERFORMANCE

Morris water maze

The results of the five-day acquisition phase of the water maze test are presented in Figure 5, while the accompanying statistical analysis is given in Table 5. For all parameters measured, significant effects of factors Treatment and Days were observed. Our results demonstrated that at the highest dose selective for α5GABA$_A$Rs (10 mg/kg), MP-III-022 elicited spatial learning incapacitation indistinguishable from that induced by diazepam 2 mg/kg used as a positive control. The effect included the percent of distance swam in the peripheral ring, as the parameter of thigmotaxic behavior. This is the first result which directly demonstrates that water maze impairments characteristic for benzodiazepines[31] are achievable through positive modulation of α5GABA$_A$Rs solely. The receptors that mediate the effect are most probably those located in the hippocampus,[32] bearing in mind that the water maze is commonly seen as a hippocampal-dependent cognitive task.[33] As the two-way repeated measures ANOVA for mean speed was not statistically significant for factor Treatment ($F(4,27) = 1.112$, $p = 0.317$), any sensorimotor disturbances during acquisition sessions can be excluded.

Notably, the *post hoc* tests revealed that the group treated with 1 mg/kg MP-III-022 differed overall (for all five days) from both, 2 mg/kg diazepam and 10 mg/kg MP-III-022 group for all parameters: the animals receiving 1 mg/kg MP-III-022 had shorter escape latencies, shorter distances, swam less distance in the peripheral ring and had higher path efficiencies (Figure 5). Moreover, *post hoc* analysis after one-way ANOVA on Day II revealed that rats treated with 1 mg/kg MP-III-022 had higher path efficiencies compared to the control and all other treatment groups (Day II, Figure 5d), suggesting together with the previous finding that a mild level of selective modulation, associated with the lowest dose of MP-III-022, tended to make rats faster to acquire the task. While the observation needs further investigation, we can hypothesize that it involves a certain degree of potentiation of α5GAB$_A$ARs in the neocortex,[32,34] which may accelerate action potential firing during up states.[20] Here, it seems relevant to comment on our published results with 30 mg/kg SH-053-2′F-R-CH3 in the same MWM protocol[19]; a detailed presentation of those results is given in Supplementary material (Figures S3 and S4; Table S5). SH-053-2′F-R-CH3 at 30 mg/kg did not affect rats' water maze behavior, which can be seen as analogous to the results obtained with 2.5 mg/kg MP-III-022; both of these treatments are supposed to elicit a moderate level of positive modulation at

α5GABA$_A$Rs. The single significant effect of SH-053-2′F-R-CH3 on distance in the peripheral ring (Table S5) additionally supports the notion that a much higher, experimentally inconvenient, dose of this ligand would be needed to exert a complete deterioration of spatial performance mediated by α5GAB$_A$A receptors.

Table 5. The effects of 2 mg/kg DZP and 1, 2.5 and 10 mg/kg MP-III-022 administration on the rat's behavior in the MWM. Two-way repeated measures ANOVA and overall *post hoc* results for latency to platform (s), total distance (m), distance swam in the peripheral annulus (%) and path efficiency. SOL = solvent; DZP = diazepam; MP = MP-III-022; ns = not significant.

Factor	**Latency (s)**	**Total distance (m)**	**Distance in the peripheral ring (%)**	**Path efficiency**
Treatment: F(4,27)	3.962	4.946	6.994	6.445
p	0.012	0.004	< 0.001	< 0.001
Days: F(4,108)	43.761	22.438	37.268	19.000
p	< 0.001	< 0.001	< 0.001	< 0.001
Interaction: F(16,108)	1.527	1.135	1.460	2.074
p	0.103	0.333	0.128	0.014
SNK *post hoc* for Treatment				
SOL vs. 2 mg/kg DZP	ns	0.086	**0.018**	0.086
SOL vs. 1 mg/kg MP	ns	ns	ns	0.052
SOL vs. 2.5 mg/kg MP	ns	0.099	ns	ns
SOL vs. 10 mg/kg MP	ns	**0.038**	**0.030**	0.077
2 mg/kg DZP vs. 1 mg/kg MP	**0.017**	**0.019**	**0.001**	**0.001**
2 mg/kg DZP vs. 2.5 mg/kg MP	ns	ns	ns	ns
2 mg/kg DZP vs. 10 mg/kg MP	ns	ns	ns	ns
1 mg/kg MP vs. 2.5 mg/kg MP	ns	**0.036**	**0.018**	**0.022**
1 mg/kg MP vs. 10 mg/kg MP	**0.026**	**0.007**	**0.002**	**0.002**

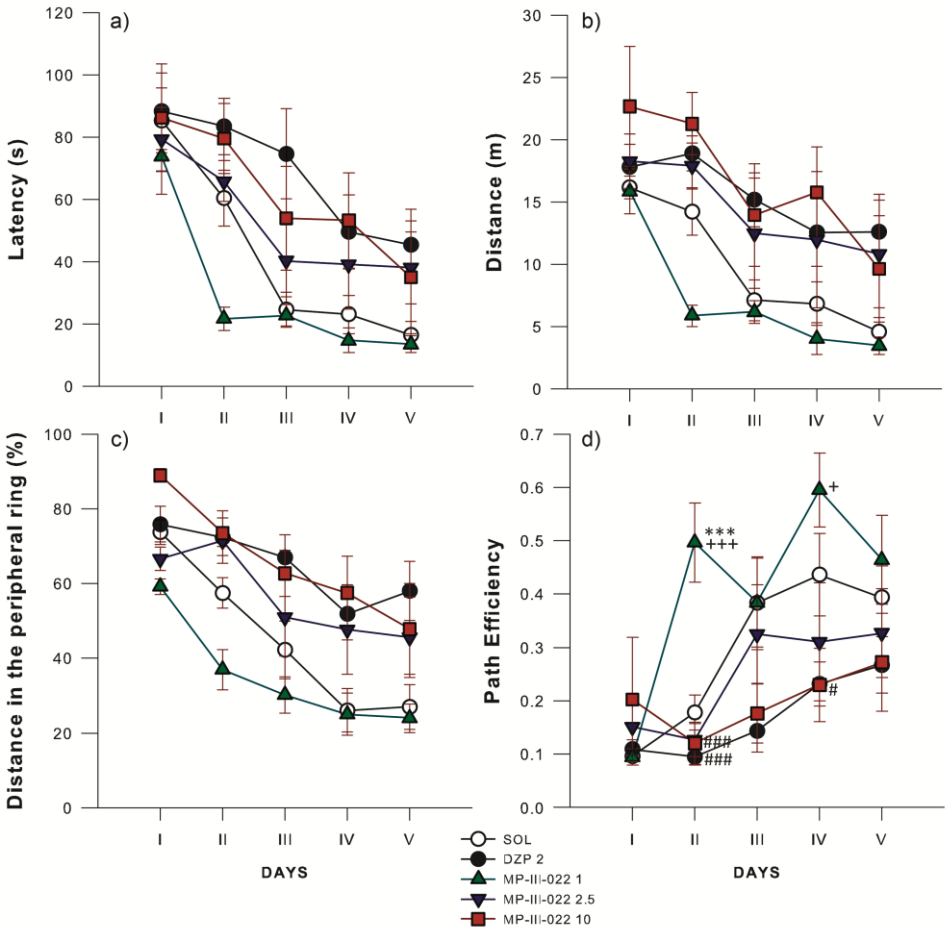


Figure 5. The effects of diazepam 2 mg/kg and MP-III-022 1, 2 and 10 mg/kg on (a) latency to platform, (b) total distance, (c) distance in the peripheral ring (%) and (d) path efficiency during acquisition trials in the water maze. ***p < 0.001 compared to solvent (SOL) group; +p < 0.05, +++p < 0.001 compared to 2 mg/kg diazepam (DZP 2) group; #p < 0.05, ###p < 0.001 compared to 1 mg/kg (MP-III-022 1) group. Animals per treatment group were 6-7. SOL = solvent, DZP 2 = 2 mg/kg diazepam, MP-III-022 1 = 1 mg/kg MP-III-022, MP-III-022 2.5 = 2.5 mg/kg MP-III-022, MP-III-022 10 = 10 mg/kg MP-III-022

One–way ANOVA applied on results from the probe test revealed a significant influence of MP-III-022 on both parameters analyzed: the distance swam in the target region ($F(4,27) = 6.26$, $p = 0.001$; Figure 6a), and the percent of distance swam in the peripheral ring ($F(4,27) = 6.84$, $p < 0.001$; Figure 6b). All groups, with the exception of 1 mg/kg MP-III-022, differed significantly from control animals, confirming cognitive-disruptive effects of diazepam and 10 mg/kg, but also 2.5 mg/kg MP-III-022 on long-lasting spatial memory. The latter finding is at odds with the lack of action of 30 mg/kg SH-053-2′F-R-CH3 (Figure S4), and points to the role of expected differences in pharmacokinetic profiles of two ligands in a repeated-dose

study. With respect to the effects of profound deterioration of both, memory acquisition and retrieval, obtained with the dose of MP-III-022 eliciting a high level of potentiation of α5GABA$_A$Rs (10 mg/kg), they demonstrate that impairments of spatial cognition elicited by benzodiazepines are dependent on this population of receptors.

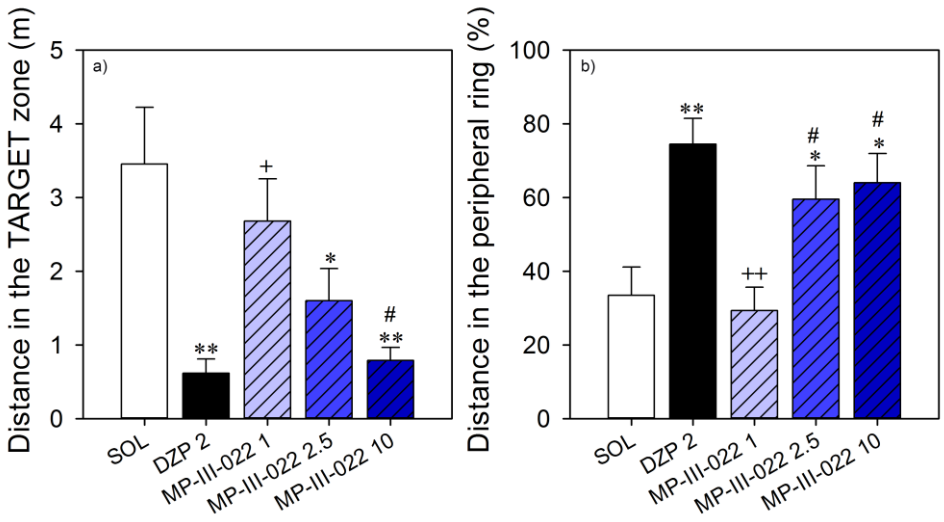


Figure 6. The effects of 2 mg/kg diazepam and 1, 2 and 10 mg/kg MP-III-022 on (a) distance in the target zone (m) and (b) distance in the peripheral ring (%) during probe trial in the water maze. *p < 0.05, **p < 0.01 compared to solvent (SOL) group; +p < 0.05, ++p < 0.01 compared to 2 mg/kg diazepam (DZP 2) group; #p<0.05 compared to 1 mg/kg MP-III-022 (MP-III-022 1) group. Animals per treatment group were 6-7. SOL = solvent, DZP 2 = 2 mg/kg diazepam, MP-III-022 1 = 1 mg/kg MP-III-022, MP-III-022 2.5 = 2.5 mg/kg MP-III-022, MP-III-022 10 = 10 mg/kg MP-III-022

Social novelty discrimination procedure

The effects of 1.5 mg/kg diazepam and 1, 2.5 and 10 mg/kg MP-III-022 on the rats' behavior in the social novelty discrimination procedure are presented in Figure 7. One-sample t-test for discrimination indices revealed significant differences from zero (i.e. chance level) only for the 10 mg/kg MP-III-022 group ($t(7) = 2.446$; $p = 0.023$, Figure 7a). Similarly, paired t-test revealed significance of time spent in exploring the familiar and the novel juvenile rat during P2, showing that only the 10 mg/kg MP-III-022 group spent significantly more time in exploring the new rat ($t(7) = -2.921$, $p = 0.022$, Figure 7b). The same statistical analysis on exploration time revealed a statistical trend in rats treated with 1.5 mg/kg diazepam ($t(7) = -2.076$, $p = 0.077$). The finding of facilitation of social novelty discrimination by a benzodiazepine that selectively potentiates α5GABA$_A$Rs is novel. We can hypothesize that

the significant expression of α5-subunit in the olfactory bulb[32,35] is associated with the observed effect. Namely, the primary cue for social discrimination is olfactory,[36] and there is an intricate network of extensively connected structures involved in forming the 'olfactory signature'.[36,37] It is of interest to note that lesions to one of these structures, the perirhinal cortex, but not to the hippocampus, cause significant deficits for social odor recognition memory.[38]

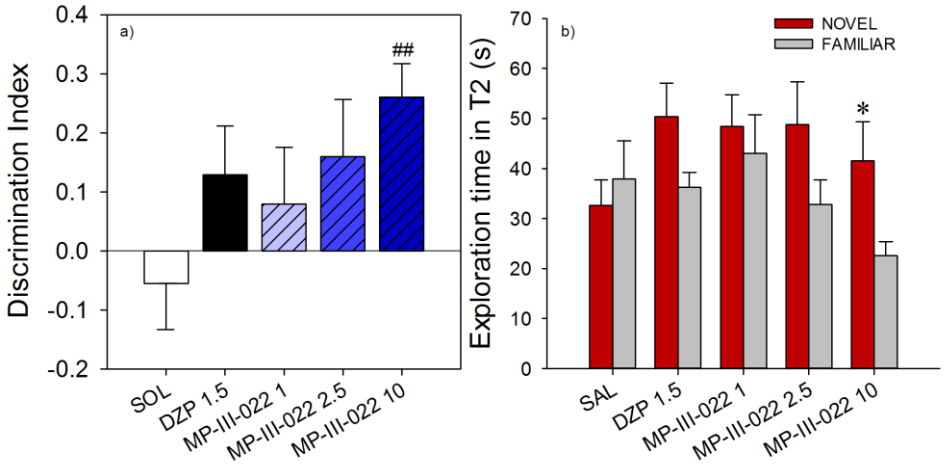


Figure 7. The effects of 1.5 mg/kg diazepam (DZP 1.5) and 1, 2.5 and 10 mg/kg MP-III-022 on discrimination index (a) and the time exploring the familiar and the novel juvenile rat in P2 (b) in social novelty discrimination procedure. A significant difference from zero for discrimination index is indicated with # (one sample t-test, ##$p < 0.01$). *$p < 0.05$ for the familiar vs. novel exploration times (paired-samples t-test). Data are represented as mean + SEM. Number of animals per treatment group was 8. SOL = solvent, DZP 1.5 = 1.5 mg/kg diazepam, MP-III-022 1 = 1 mg/kg MP-III-022, MP-III-022 2.5 = 2.5 mg/kg MP-III-022, MP-III-022 10 = 10 mg/kg MP-III-022

Three-chamber test

The non-competitive antagonist of the NMDA receptors ketamine is widely used at subanesthetic doses to induce cognitive deficits and social withdrawal in rats.[39] The effects of 15 mg/kg ketamine and 10 mg/kg MP-III-022, on their own and in combination, on the rats' behavior in the three chamber test are presented in Figure 8. Examination of the one-sample t-test, for sociability indices (SI) revealed significant differences from zero (i.e. chance level) only for the control group ($t(7) = 4.734$; $p = 0.002$, Figure 8a). In the same way, paired t-test revealed significance on time spent in exploring the animal and object during T2, showing that only control can discriminate between object and rat group ($t(7) = 4.58$, $p = 0.003$, Figure

8b). The same statistical analyses on the social recognition trial (T3) showed no discrimination between the familiar and novel rat during testing in any treatment group (Figure 8c and 8d).

It is remarkable that mice with reduced α5 subunit expression selectively in the granule cells of the dentate gyrus of the hippocampus showed impairments in cognitive tasks characterized by high interference, without any deficiencies in low-interference tasks.[40] Memory interference refers to antagonistic processes whereby either new memories impair retrieval of previously learned information or earlier memories prevent future learning, and is most likely to occur between memories that are similar.[41] Our settings of selective positive modulation of α5$GABA_A$Rs may be seen as opposite to those with reduced expression of α5 $GABA_A$ receptors given by Engin and co-workers[40], and hence they may be expected to favor facilitation in cognitive tasks characterized by high interference, but also impairment in low-interference tasks. The results from the social novelty discrimination, exemplifying the former, and the Morris water maze and the sociability trial of the three-chamber test, exemplifying the latter kind of tasks (cf. Engin et al.[40]), comply with this hypothesis. Moreover, when looking at the results in the social novelty trial of the three-chamber test, which is a task characterized by high interference, it is notable that the discrimination index of animals exposed to 10 mg/kg MP-III-022 was 2.18, while only 1.02 in control rats, without reaching a statistical significance of the difference. The high rate of attrition in the three-chamber test in all groups receiving either MP-III-022, ketamine or their combination (7, 6 and 9 rats, respectively, did not reach the criterion in either the second or the third trial; Supplementary Table 6S) demonstrated that the impairing effects of ketamine,[42, 43] and also 10 mg/kg MP-III-022, on spatial orientation and memory could have substantially influenced the results obtainable in this paradigm. It should be emphasized that such effects are not pertinent for behavioral performance in the social novelty discrimination procedure.

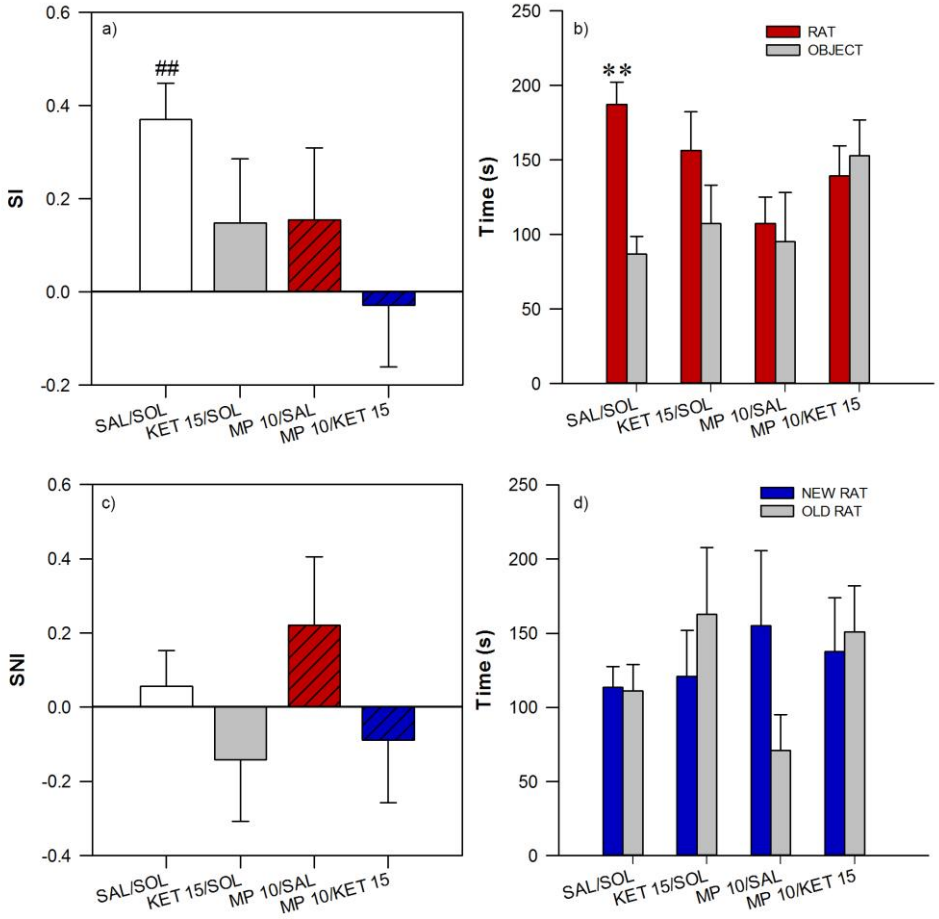


Figure 8. The effects of 15 mg/kg ketamine and 10 mg/kg MP-III-022, alone and in combination, on sociability index (SI) (a), the time exploring the rat and the object in sociability trial (T2) (b), social novelty preference index (SNI) (c) and the time exploring the novel and the familiar rat in social recognition trial (T3) (d) in the three-chamber test. A significant difference from zero is indicated with # (one sample t-test, ##p < 0.01). **p < 0.01 for the rat vs. object exploration times (paired-samples t-test). Data are represented as mean + SEM. Number of animals per treatment group was 8. SOL = solvent, SAL = saline, KET 15 = 15 mg/kg ketamine, MP-III-022 1 = 1 mg/kg MP-III-022, MP-III-022 10 = 10 mg/kg MP-III-022

CONCLUSIONS

Several sets of data unequivocally suggest that $GABA_A$ receptors containing the α5 subunit play a major role in modulating cognition-related behaviors. The novel ligand MP-III-022 was synthesized from SH-053-2′F-R-CH3, a benzodiazepine widely used in research as a positive allosteric modulator selective for α5$GABA_A$Rs. In comparison with the starting ligand, *in vitro* studies demonstrated an improved affinity- and especially efficacy-selectivity of MP-III-

022 for α5GABA$_A$Rs, while it was mainly inactive in a standard screening panel of 50 GPCRs, ion channels, enzymes, and transporters (PDSP, Dr Bryan Roth, UNC). The parent compound SH-053-2'F-R-CH3 has already permitted important insights into the role of α5βγ2 receptors, and its improved derivative MP-III-022 enables researchers to investigate effects of α5βγ2 positive modulation with even lower interference from residual activity at other subtypes. Namely, by combining the results of electrophysiological and pharmacokinetic studies, we predict that the *in vivo* effects of MP-III-022 are solely dependent on positive modulation of α5GABA$_A$Rs (at doses up to 10 mg/kg) and can be differentiated from those involving also some other diazepam-sensitive GABA$_A$ receptor subtypes, most probably the receptors containing α2 and/or α3 subunits (15 mg/kg and above). Moreover, when compared with SH-053-2′F-R-CH3, an improved applicability of MP-III-022 stems from a wide range of selective potentiation of α5GABA$_A$Rs, from mild to moderate to strong, which can be accomplished by its convenient administration in the dose range 1 mg/kg to 10 mg/kg. Indeed, in the rotarod, pentylenetetrazole as well as spontaneous and amphetamine-induced locomotor activity tests, MP-III-022 at doses up to 10 mg/kg proved to be behaviorally silent in rats, and the only motor effect of the highest dose was a mild, though significant muscle relaxation expectedly observed in the grip strength test. Thus, it was possible to assess the behavioral consequences of eliciting a wide range of potentiation of α5GABA$_A$Rs in a set of cognitive tests, free of safety issues such as ataxia or sedation. It was found that strong selective potentiation of α5GABA$_A$Rs (more than three times the current level elicited by low concentrations of GABA) can induce at the same time both a facilitatory action on social recognition, and an impairing effect on spatial learning and memory, as assessed in the social novelty discrimination procedure and Morris water maze test, respectively. On the other hand, in the three-chamber test, there was impairment in the sociability trial, while an apparent tendency of improved social recognition in the social novelty trial for the group receiving 10 mg/kg MP-III-022 was far from significance, possibly due to the expected concomitant deterioration of spatial acuity. The presented behavioral results demonstrate that MP-III-022 may be used as an excellent experimental tool to assess protective or therapeutic potential of selective potentiation of α5GABA$_A$Rs in various medical states putatively connected with pathological changes in this receptor population.

METHODS

Chemistry

(*R*)-8-Ethynyl-6-(2-fluorophenyl)-*N*,4-dimethyl-4*H*-benzo[*f*]imidazo[1,5-*a*][1,4]diazepine-3-carboxamide (MP-III-022) (**1**) was synthesized as follows.

Ester **2** (1.0 g, 2.58 mmol)[44] was added to a sealed vessel fitted with a septum at 0°C and treated with methyl amine (15 mL; 33% wt solution in ethanol). The vessel was sealed with a cap and stirred at 60°C for 18 h. The solution was then cooled to rt and the methyl amine and ethanol were removed under reduced pressure. The residue was purified by a wash column (silica column, 4:1 EtOAc:hexanes) to afford amide **1** as a white powder (731 mg, 1.96 mmol, 76%). Characterization of compound **1**: ^{1}H NMR (300 MHz, $CDCl_3$) δ 7.88 (s, 1H), 7.67 (dd, *J* = 16.3, 7.8 Hz, 2H), 7.55 (d, *J* = 8.3 Hz, 1H), 7.50 – 7.41 (m, 2H), 7.29 – 7.18 (m, 2H), 7.04 (t, *J* = 9.3 Hz, 1H), 6.93 (q, *J* = 7.4 Hz, 1H), 3.16 (s, 1H), 2.97 (d, *J* = 5.0 Hz, 3H), 1.29 (d, *J* = 6.4 Hz, 3H). ^{13}C NMR (300 MHz, $CDCl_3$) δ 162.24, 161.81, 158.48, 138.25, 137.12, 135.73, 134.41, 133.57, 132.53, 131.57, 129.03, 125.15, 124.92, 124.58, 122.50, 116.33, 166.05, 81.25, 79.99, 49.42, 25.73, 25.27. HRMS (LCMS-IT-TOF) Calc. for $C_{22}H_{17}FN_4O$ $(M + H)^+$ 373.1459, found: 373.1462. Detailed spectra are provided in the Supporting Information (Figures S1 – S2).

Competition binding assays

Materials

3H-Flunitrazepam (specific activity 83 Ci/mmol) was purchased from Perkin Elmer NEN (New England Nuclear)(Waltham, Massachusetts, USA). Diazepam (7-chloro-1,3-dihydro-1-methyl-5-phenyl-2H-1,4, benzodiazepine-2-one) from Nycomed (Opfikon, Switzerland). Standard chemicals came from Sigma-Aldrich (St. Louis, Missouri, USA)

Culturing of human embryonic kidney 293 cells

Human embryonic kidney (HEK) 293 cells (American Type Culture Collection ATCC® CRL-1574™) were maintained in Dulbecco's modified Eagle medium (DMEM, high glucose, GlutaMAX™ supplement, Gibco 61965-059, ThermoFisher, Waltham, Massachusetts, USA) supplemented with 10% fetal calf serum (Sigma-Aldrich F7524, St. Louis, Missouria, USA), 100 U/ml Penicillin-Streptomycin (Gibco 15140-122, ThermoFisher, Waltham, Massachusetts, USA) and MEM (Non-Essential Amino Acids Gibco 11140-035,

ThermoFisher, Waltham, Massachusetts, USA) on 10cm Cell culture dishes (Cell$^+$, Sarstedt, Nürnbrecht, Germany) at 37°C and 5% CO_2.

HEK293 cells were transfected with cDNAs encoding rat $GABA_A$-receptor subunits subcloned into pCI expression vectors. The ratio of plasmids used for transfection with the calcium phosphate precipitation method[45] were 3µg α(1,2,3 or 5): 3µg β3 and 15 µg γ2 per 10 cm dish. Medium was changed 4-6 hours after transfection.

Cells were harvested 72 days after transfection by scraping into phosphate buffered saline. After centrifugation (10 min, 12000 g, 4°C) cells were resuspended in TC50 (50 mM Tris-Citrate pH=7.1), homogenized with an ULTRA-TURRAX® (IKA, Staufen, Germany) and centrifuged (20 min, 50 000g). Membranes were washed three times in TC50 as described above and frozen at -20°C until use.

Radioligand binding assay

Frozen membranes were thawed, resuspended in TC50 and incubated for 90 min at 4°C in a total of 500 µl of a solution containing 50 mM Tris/citrate buffer, pH=7.1, 150 mM NaCl and 2 nM [^{3}H]-Flunitrazepam in the absence of presence of either 5 µM diazepam (to determine unspecific binding) or various concentrations of receptor ligands (dissolved in DMSO, final DMSO-concentration 0.5%). Membranes were filtered through Whatman GF/B filters and the filters were rinsed twice with 4 ml of ice-cold 50mM Tris/citrate buffer. Filters were transferred to scintillation vials and subjected to scintillation counting after the addition of 3 ml Rotiszint Eco plus liquid scintillation cocktail. Nonspecific binding determined in the presence of 5 µM Diazepam was subtracted from total [^{3}H]-Flunitrazepam binding to result in specific binding.

In order to determine the equilibrium binding constant K_D of 3H-Flunitrazepam for the various receptor-subtypes, membranes were incubated with various concentrations of 3H-Flunitrazepam in the absence or presence of 5 µM Diazepam.

Data calculation

Saturation binding experiments were analyzed using the equation Y=Bmax*X/(KD+X).

Nonlinear regression analysis of the displacement curves used the equation: log(inhibitor) vs. response - variable slope with Top=100% and Bottom=0% Y=100/(1+10^((logIC50-x)*Hillslope)). Both analyses were performed using GraphPad Prism version 5.0a for Mac OS X, GraphPad Software, La Jolla California USA, www. graphpad.com.

Drug concentrations resulting in half maximal inhibition of specific 3H-Flunitrazepam binding (IC50) were converted to Ki values by using the Cheng-Prusoff relationship[46] Ki=

IC50/(1+(S/KD)) with S being the concentration of the radioligand (2 nM) and the KD values listed in table S1.

Electrophysiological experiments

cDNAs of rat $GABA_A$ receptor subunits were used for generating the respective mRNAs that were then injected into Xenopus laevis oocytes (Nasco, WI) as described previously.[47] For electrophysiological recordings, oocytes were placed on a nylon-grid in a bath of Xenopus Ringer solution (XR, containing 90 mM NaCl, 5 mM HEPES-NaOH (pH 7.4), 1 mM MgCl2, 1 mM KCl and 1 mM CaCl2). The oocytes were constantly washed by a flow of 6 mL/min XR which could be switched to XR containing GABA or MP-III-022 and GABA. Test compounds were diluted into XR from DMSO-solutions resulting in a final concentration of 0.1% DMSO perfusing the oocytes. For current measurements the oocytes were impaled with two microelectrodes (2–3 mΩ) which were filled with 2 mM KCl. To test for modulation of GABA-induced currents by MP-III-022, a concentration of GABA was used that was titrated to trigger 3-5% of the respective maximum GABA-elicited current of the individual oocyte (EC3-5). At this low GABA concentration, within-day and between-day currents are reproducible and effects of drugs (% of modulation) are much higher than that at higher GABA concentrations. GABA at EC3-5 was then coapplied with varying concentrations of MP-III-022 until a peak response was observed. Between two applications, oocytes were washed in XR for up to 15 min to ensure full recovery from desensitization. All recordings were performed at room temperature at a holding potential of –60 mV using Dagan TEV-200 two-electrode voltage clamp amplifiers (Warner Instruments, Hamden, CT). Data were digitized, recorded and measured using Digidata 1322A and 1550 data acquisition systems (Axon Instruments, Union City, CA). Results of concentration response experiments were graphed using GraphPad Prism 4.00 (GraphPad Software, San Diego, CA).

Studies in rats

Animals

Male outbred Wistar rats were supplied by Military Farm, Belgrade, Serbia. Rats were housed in groups of five and were maintained under standard laboratory conditions (21 ± 2°C, relative humidity 40-45%) with free access to pellet food and tap water. They were kept on 12:12 h light/dark cycle with lights on at 07.00 h. All handling and testing took place during the light phase of the diurnal cycle.

Behavioral experiments were carried out on nine weeks old (adults weighing 200–250 g) or 21 days old (juvenile) Wistar male rats. For social discrimination novelty procedure adults were isolated in individual cages two days before testing. The animals received two intraperitoneal (i.p.) injections, one of which was the solvent if not otherwise stated. The behavior was recorded by a ceiling–mounted camera and analyzed by ANY–maze Video Tracking System software (Stoelting Co., USA). Throughout the study, experimentally naïve animals were used.

Ethics Statement

Experiments were approved by the Ethical Commission on Animal Experimentation of the Faculty of Pharmacy in Belgrade and were carried out in accordance with the EEC Directive 86/609.

Drugs

The ligands MP-III-022, SH-053-2′F-R-CH3 and XLi-093 were synthesized at the Department of Chemistry and Biochemistry, University of Wisconsin–Milwaukee, USA. XLi-093 is an α_5GABA$_A$ receptor selective antagonist. D-Amphetamine-sulfate and ketamine were purchased from Sigma–Aldrich, flumazenil from Feicheng BoYuan Fine Chemicals Co., Ltd, China, while diazepam was obtained from Galenika (Belgrade, Serbia). The ligands MP-III-022, SH-053-2′F-R-CH3, XLi-093, flumazenil and diazepam were suspended/dissolved with the aid of sonication in the solvent (85% distilled water, 14% propylene glycol, and 1% Tween 80), while d-amphetamine and ketamine were dissolved in saline. All compounds were administered i.p. in a volume of 2 mL/kg, 20 min before the behavioral testing, with the exception of the experiment with d-amphetamine, in which the animal's behavior was recorded immediately after the respective treatments.

For determination of free fractions in plasma and brain tissue, stock solutions of MP-III-022 and SH-053-2′F-R-CH3 were prepared in dimethyl sulfoxide (DMSO).

Pharmacokinetic study

Rats were divided in two cohorts of six groups which corresponded to predetermined time intervals (5, 10, 20, 40, 60 and 180 min), each containing three animals. MP-III-022 and SH-053-2′F-R-CH3, dosed at 2.5 mg/kg and 10 mg/kg, respectively, were administered by i.p. injection in a volume of 2 mL/kg. Additional experiments were performed in order to determine brain and plasma concentration 20 min after i.p. injection, as well as to calculate free brain and plasma levels of MP-III-022 dosed at 1, 2.5, 10, 15 and 20 mg/kg, and SH-053-2′F-R-CH3 dosed at 10, 20, 30, 150 and 200 mg/kg. The blood samples were collected in heparinized syringes via cardiac puncture of rats anesthetized with ketamine solution (10%

Ketamidor, Richter Pharma Ag, Wels, Austria, dosed i.p. at 100 mg/kg), and centrifuged at 2500 rpm for 10 min to obtain plasma. Thereafter, rats were decapitated and brains were weighed, homogenized in 5 mL of methanol and centrifuged at 6000 rpm for 20 min. To determine the concentration of MP-III-022 and SH-053-2′F-R-CH3 in plasma and supernatants of brain tissue homogenates, MP-III-022 and SH-053-2′F-R-CH3 were extracted from these samples by solid phase extraction, using Oasis HLB cartridges (Waters Corporation, Milford, Massachusetts). The procedure of sample preparation and determination of MP-III-022 and SH-053-2′F-R-CH3 by ultraperformance liquid chromatography–tandem mass spectrometry (UPLC–MS/MS) with Thermo Scientific Accela 600 UPLC system connected to a Thermo Scientific TSQ Quantum Access MAX triple quadrupole mass spectrometer (Thermo Fisher Scientific, San Jose, California), equipped with electrospray ionization (ESI) source, has been already described in detail.[16]

Plasma protein and brain tissue binding studies

The rapid equilibrium dialysis assay used to determine free fraction of MP-III-022 and SH-053-2′F-R-CH3 in rat plasma and brain tissue was the same as in Obradović et al.[16]

Grip strength

Muscle strength was assessed by the grip strength meter (Ugo Basile, Milan, Italy, model 47105). When pulled by the tail, the rat grasps the trapeze connected to a force transducer, and the apparatus measures the peak force of experimenter's pull (in grams) necessary to overcome the strength of the animal's forelimbs grip. Six groups received one of the following treatments 20 minutes before testing: solvent, MP-III-022 (1, 2.5, 10, 15 and 20 mg/kg). Each animal was given three consecutive trials, and the median value of three readings, normalized against body weight, was used for further statistics.

Rotarod test

Motor performance was assessed using an automated rotarod (Ugo Basile, Italy). Before testing, rats were trained for three days until they could remain for 180 s on the rod revolving at 15 rpm. On the fourth day, selection was made and rats fulfilling the given criteria were included in the experiment. Seven groups received one of the following treatments 20 minutes before testing: solvent, MP-III-022 (10, 15 and 20 mg/kg), SH-053-2′F-R-CH3 (200 mg/kg) and 15 mg/kg MP-III-022 in combination with XLi-093 (20 mg/kg) or flumazenil (15 mg/kg). Latency to fall from the rotarod was recorded automatically.

Intravenous pentylenetetrazole infusion test

A butterfly cannula (needle size 25 G, ¾ in.) attached to a 20 ml syringe prefilled with pentylenetetrazole (PTZ) solution was used. The syringe was held in adjustable motor driven infusion pump (Stoelting Co., Wood Dale Illinois, USA). Before infusing PTZ, the rat's tail vein was dilated with warm water. Single rat was then placed in the restrainer. A butterfly needle was inserted into the lateral tail vein and PTZ was infused at a constant rate of 0.5 ml/min. The animal was observed throughout the infusion by two trained and blind observers. The threshold doses of PTZ (mg/kg) required to elicit clonic and tonic seizures were calculated using the following formula: volume of PTZ (ml) x concentration of PTZ (mg/ml)/body weight (kg).

Spontaneous and amphetamine induced locomotor activity

Activity of single rats in a clear Plexiglas chamber (40×25×35 cm) under dim red light (20 lux) was recorded for a total of 45 min, without any habituation period but with 20 min acclimatization time. One of two doses of MP-III-022 (10 and 15 mg/kg) or solvent were applied 20 min before testing. The same apparatus was used for assessing the amphetamine-induced locomotor activity, with an adapted protocol. Here, rats received the appropriate treatment (solvent, 1, 2.5 or 10 mg/kg MP-III-022) and were immediately placed in the tracking chamber. Behavior was recorded for 20 min and then rats were injected with saline or 0.5 mg/kg amphetamine and locomotor activity was recorded for an additional 60 min.

Morris water maze

Experiments were performed in a 2 m diameter circular pool filled to a height of 30 cm with water at 22 ± 1 °C. The escape platform (15 cm × 10 cm) was submerged 2 cm below the water surface. An indirect illumination in the experimental room was provided by white neon tubes and many distal cues were present. On each of the five consecutive days rats were given one swimming block, consisting of four trials. For each trial the rat was placed in the water at one of four pseudo–randomly determined starting positions. Once the rat has found and mounted the escape platform it was permitted to remain on the platform for 15 s. The rat was guided to the platform by the experimenter if it failed to locate it within 120 s. During the acquisition phase, treatments were applied once daily before the swimming block. On the sixth day, rats were given a treatment–free probe test (60 s) without the platform. In order to ensure that any spatial bias is a consequence of the spatial memory of escape location, rather than of a specific swim strategy, the probe test was started from the novel, most distant location.[48] The pool was virtually divided into four quadrants, three concentric annuli and a target region consisting of the intersection of the platform quadrant and the platform (middle) annulus, as represented in Savić et al.[29] Dependent variables chosen for tracking during the

acquisition trials were: escape latency (s), total distance traveled (m), path efficiency (the ratio of the shortest possible path length to actual path length), % of distance swam in the peripheral annulus and mean speed (m/s). The selected parameters in the probe test were the distance swam in the target zone (s) and % of the distance swam in the peripheral annulus. We tested the effects of 1, 2.5 and 10 mg/kg MP-III-022 and 2 mg/kg diazepam.

Social novelty discrimination (SND) procedure

SND experiments compared the social investigation times of an adult rat with a familiar and a novel juvenile rat. The procedure is replicated from previous studies.[49,50] Testing consisted of two consecutive juvenile presentations periods to an adult subject: period 1 (P1) and period 2 (P2). At the beginning of P1, one juvenile was placed into the adult home cage and the time spent by the adult investigating the juvenile (anogenital sniffing, licking, close pursuing and pawing) was recorded manually for 5 min. During P2, the same juvenile and a second, novel juvenile were placed in the cage together with the adult, and the times spent by the adult investigating each juvenile were measured independently for 3 min. A different pair of juvenile rats was presented to each adult tested. Manual scoring was conducted in a blinded manner. SND was impaired by the parametric manipulation applied, as there was 30 min delay between P1 and P2, and SND was expected to be low in control rats. The influence of MP-III-022 (1, 2.5 or 10 mg/kg) on such induced impairment in SND was examined. There were five groups of rats which received one of the following treatments 20 min before P1: solvent, 1.5 mg/kg diazepam and 1, 2.5 and 10 mg/kg MP-III-022. The amount of time investigating familiar (Tf) and novel (Tn) juvenile during P2 was manually scored, and discrimination indexes (Tn-Tf/Tn+Tf) was calculated. Total exploration time during P1 and P2 was also manually recorded.

Three-chamber test

The three-chamber test investigates the ability of the tested animal to discriminate between an object and another animal in the sociability trial, as well as to differentiate two animals in the social novelty trial. The procedure is replicated from a previous study.[51] The test was performed in an apparatus consisting of three compartments, one central and two lateral chambers, with an overall dimension of 95×50×35 cm. The 10-minute habituation was performed in the central chamber immediately before the sociability trial. In the latter trial, an object was positioned in one of the lateral chambers, and an animal was placed in the opposite lateral chamber. The object was an empty cage identical to that used to enclose the rat in the other chamber. The investigation times of the tested rat were recorded. Time spent in each chamber, as well as the time spent exploring the novel rat or the novel object, were analyzed

automatically during 10 minutes. Immediately thereafter, the social novelty test began with introducing an additional, unfamiliar rat. This rat was placed in the empty wire cage. Time spent in each chamber and time spent sniffing each rat/wire cage was recorded during 10 minutes. The rats which did not explore all three chambers during the sociability test were excluded from the statistical analysis. Since the social novelty test aims to evaluate the preference for social novelty and the formation of social memories, rodents that did not interact with both the familiar and the novel rat were also excluded from the analysis. The calculated parameters for the three-chamber test were a Sociability Index (SI) and, in an analogous manner, a Social Novelty Preference Index (SNI).[51,52]

Statistics

All numerical data presented in figures are given as the mean ± SEM. Pharmacokinetic parameters were calculated using PK Functions for Microsoft Excel software (by Joel Usansky, Atul Desai, and Diane Tang-Liuwere). In SND procedure the discrimination indexes were analyzed by one-sample t-test, and exploration times by paired-t test. The data from the acquisition days in the Morris water maze were averaged for each rat (total data/total number of trials per day) and analyzed using two–way ANOVA with repeated measures (factors: Treatment and Days) with Days as the repeated measure. In the case of significant interaction, separate one–way ANOVAs were conducted to assess the influence of treatment within individual levels of factor Days. The data from the probe test were assessed using one–way ANOVA. In SLA test one-way ANOVA (for overall effect) or two-way ANOVA with repeated measures (factors: Treatment and Time) with Time as the repeated measure (for effect during 5-min bins) were applied. For the binding study, as well as in the PTZ and rotarod test, one-way ANOVA were applied. *Post hoc* comparisons, where applicable, were performed using SNK test, with exception of the binding study, where Tukey test was applied. Statistical analysis was performed using SigmaPlot 11 (Systat Software Inc., Richmond, USA) software. Differences were considered significant when $p < 0.05$, while $0.1 > p > 0.05$ was considered as a trend toward significance.

ACKNOWLEDGEMENTS

Financial support was provided by the Ministry of Education, Science and Technological Development, R. Serbia – Grant No. 175076 (MMS) and by FWF grant P 27746 (ME). We also wish to thank the NIH (MH096463, NS076517) for generous financial support (JMC).

The authors acknowledge support from the Milwaukee Institute for Drug Discovery. Analytical instrumentation support was provided by University of Wisconsin - Milwaukee's Shimadzu Laboratory for Advanced and Applied Analytical Chemistry.

We appreciate the skilled work of Dr. Bojan Marković, who performed the mass spectrometry measurements. We also thank Ms Karin Schwarz and Ms Friederike Steudle for excellent technical assistance in radioligand binding experiments and Ms Roshan Puthenkalam for some oocyte measurements.

AUTHOR CONTRIBUTIONS

TTS, ME, PS, JMC and MMS conceived and designed the experiments. MMP synthesized and characterized the compound. TTS, AS, BD, SR, PS and ME performed the biological assays and analyzed the data. MMS, TTS, MP, PS, ME and JMC wrote the manuscript. All authors read and approved the final manuscript.

The authors declare no competing financial interest.

REFERENCES

1. Rudolph, U. and Möhler, H. (2014) GABAA receptor subtypes: Therapeutic potential in Down syndrome, affective disorders, schizophrenia, and autism. Annu. Rev. Pharmacol. Toxicol. 54, 483-507.

2. Rudolph, U. and Knoflach, F. (2011) Beyond classical benzodiazepines: novel therapeutic potential of GABAA receptor subtypes. Nat. Rev. Drug. Discov. 10, 685–697.

3. Guerrini, G. and Ciciani, G. (2006-2012) Benzodiazepine receptor ligands: a patent review. Expert. Opin. Ther. Pat. 23, 843-866.

4. Collinson, N., Kuenzi, F.-M., Jarolimek, W., Maubach, K.-A., Cothliff, R., Sur, C., Smith, A., Otu, F.-M., Howell, O., Atack, J.-R., McKernan, R.-M., Seabrook, G.-R., Dawson, G.-R., Whiting, P.-J. and Rosahl, T.-W. (2002) Enhanced learning and memory and altered GABAergic synaptic transmission in mice lacking the alpha 5 subunit of the GABAA receptor. J. Neurosci. 22, 5572-5580.

5. Crestani, F., Keist, R., Fritschy, J.-M., Benke, D., Vogt, K., Prut, L., Blüthmann, H., Möhler, H. and Rudolph, U. (2002) Trace fear conditioning involves hippocampal alpha5 GABA(A) receptors. Proc. Natl. Acad. Sci. USA. 99, 8980-8985.

6. Maubach, K. (2003) GABA(A) receptor subtype selective cognition enhancers. Curr. Drug. Targets. CNS. Neurol. Disord. 2, 233-239.

7. Soh, M.-S. and Lynch, J.-W. (2015) Selective Modulators of α5-Containing GABAA Receptors and their Therapeutic Significance. Curr. Drug. Targets. 16, 735-746.

8. Koh, M.-T., Rosenzweig-Lipson, S. and Gallagher, M. (2013) Selective GABAA α5 positive allosteric modulators improve cognitive function in aged rats with memory impairment. Neuropharmacology. 64, 145–152.

9. Gill, K.-M., Lodge, D.-J., Cook, J.-M., Aras, S. and Grace, A.-A. (2011) A novel α5GABA(A)R-positive allosteric modulator reverses hyperactivation of the dopamine system in the MAM model of schizophrenia. Neuropsychopharmacology. 36, 1903-1911.

10. Mendez, M.-A., Horder, J., Myers, J., Coghlan, S., Stokes, P., Erritzoe, D., Howes, O., Lingford-Hughes, A., Murphy, D. and Nutt, D. (2013) The brain GABA-benzodiazepine receptor alpha-5 subtype in autism spectrum disorder: a pilot [(11)C]Ro15-4513 positron emission tomography study. Neuropharmacology. 68, 195-201.

11. Skolnick, P. (2012) Anxioselective anxiolytics: on a quest for the Holy Grail. Trends. Pharmacol. Sci. 33, 611-620.

12. Atack, J.-R., Wafford, K.-A., Street, L.-J., Dawson, G.-R., Tye, S., Van Laere, K., Bormans, G., Sanabria-Bohórquez, S.-M., De Lepeleire, I., de Hoon, J.-N., Van Hecken, A., Burns, H.-D., McKernan, R.-M., Murphy, M.-G. and Hargreaves, R.-J. (2011) MRK-409 (MK-0343), a GABAA receptor subtype-selective partial agonist, is a non-sedating anxiolytic in preclinical species but causes sedation in humans. J. Psychopharmacol. 25, 314-328.

13. Atack, J.-R. (2010) GABAA receptor alpha2/alpha3 subtype-selective modulators as potential nonsedating anxiolytics. Curr. Top. Behav. Neurosci. 2, 331-360.

14. Atack, J.-R. (2011a) GABAA receptor subtype-selective modulators. I. α2/α3-selective agonists as non-sedating anxiolytics. Curr. Top. Med. Chem. 11, 1176-1202.

15. Atack, J.-R. (2011b) GABAA receptor subtype-selective modulators. II. α5-selective inverse agonists for cognition enhancement. Curr. Top. Med. Chem. 11, 1203-1214.

16. Obradović, A.-Lj., Joksimović, S., Poe, M.-M., Ramerstorfer, J., Varagic, Z., Namjoshi, O., Batinić, B., Radulović, T., Marković, B., Roth, B.-L., Sieghart, W., Cook, J.-M and, Savić, M.-M. (2014) Sh-I-048A, an in vitro non-selective super-agonist at the benzodiazepine site of GABAA receptors: the approximated activation of receptor subtypes may explain behavioral effects. Brain. Res. 1554, 36-48.

17. Timić Stamenić, T., Joksimović, S., Biawat, P., Stanković, T., Marković, B., Cook, J.-M. and Savić, M.-M. Negative modulation of α5 GABAA receptors in rats may partially prevent memory impairment induced by MK-801, but not amphetamine- or MK-801-elicited hyperlocomotion. J. Psychopharmacol. 29, 1013-1024.

18. Fischer, B.-D., Licata, S.-C., Edwankar, R.-V., Wang, Z.-J., Huang, S., He, X., Yu, J., Zhou, H., Johnson, E.-M. Jr, Cook, J.-M., Furtmüller, R., Ramerstorfer, J., Sieghart, W., Roth, B.-L., Majumder, S. and Rowlett, J.-K. (2010) Anxiolytic-like effects of 8-acetylene imidazobenzodiazepines in a rhesus monkey conflict procedure. Neuropharmacology. 59, 612-618.

19. Savić, M.-M., Majumder, S., Huang, S., Edwankar, R.-V., Furtmüller, R., Joksimović, S., Clayton, T. Sr, Ramerstorfer, J., Milinković, M.-M., Roth, B.-L., Sieghart, W. and Cook, J.-M. (2010) Novel positive allosteric modulators of GABAA receptors: do subtle differences in activity at alpha1 plus alpha5 versus alpha2 plus alpha3 subunits account for dissimilarities in behavioral effects in rats? Prog. Neuropsychopharmacol. Biol. Psychiatry. 34, 376-386.

20. Drexler, B., Zinser, S., Huang, S., Poe, M.-M., Rudolph, U., Cook, J.-M. and Antkowiak, B. (2013) Enhancing the function of alpha5-subunit-containing GABAA receptors promotes action potential firing of neocortical neurons during up-states. Eur. J. Pharmacol. 703, 18-24.

21. Soto, P.-L., Ator, N.-A., Rallapalli, S.-K., Biawat, P., Clayton, T., Cook, J.-M. and Weed, M.-R. (2013) Allosteric modulation of GABA(A) receptor subtypes:effects on visual recognition and visuospatial working memory in rhesus monkeys [corrected]. Neuropsychopharmacology. 38, 2315-2325.
22. Gallos, G., Yocum, G.-T., Siviski, M.-E., Yim, P.-D., Fu, X.-W., Poe, M.-M., Cook, J.-M., Harrison, N., Perez-Zoghbi, J. and Emala, C.-W. Sr. (2015) Selective targeting of the α5-subunit of GABAA receptors relaxes airway smooth muscle and inhibits cellular calcium handling. Am. J. Physiol. Lung. Cell. Mol. Physiol. 308, L931-L942.
23. Clayton, T., Poe, M.-M., Rallapalli, S., Biawat, P., Savić, M.-M., Rowlett, J.-K., Gallos, G., Emala, C.-W., Kaczorowski, C.-C., Stafford, D.-C., Arnold, L.A. and Cook, J.-M. (2015) A review of the updated pharmacophore for the alpha 5 GABA(A) benzodiazepine receptor model. Int J Med Chem. 2015, 430248.
24. Frankowski, K.-J., Hedrick, M.-P., Gosalia, P., Li, K., Shi, S., Whipple, D., Ghosh, P., Prisinzano, T.-E., Schoenen, F.-J., Su, Y., Vasile, S., Sergienko, E., Gray, W., Hariharan, S., Milan, L., Heynen-Genel, S., Mangravita-Novo, A., Vicchiarelli, M., Smith, L.-H., Streicher, J.-M., Caron, M.-G., Barak, L.-S., Bohn, L.-M., Chung, T.-D. and Aubé, J. (2012) Discovery of Small Molecule Kappa Opioid Receptor Agonist and Antagonist Chemotypes through a HTS and Hit Refinement Strategy. ACS Chem. Neurosci. 3, 221-236.
25. Milić, M., Divljaković, J., Rallapalli, S., van Linn, M.-L., Timić, T., Cook, J.-M. and Savić, M.-M. (2012) The role of α1 and α5 subunit-containing GABAA receptors in motor impairment induced by benzodiazepines in rats. Behav. Pharmacol. 23, 191-197.
26. Knabl, J., Witschi, R., Hösl, K., Reinold, H., Zeilhofer, U.-B., Ahmadi, S., Brockhaus, J., Sergejeva, M., Hess, A., Brune, K., Fritschy, J.-M., Rudolph, U., Möhler, H. and Zeilhofer, H.-U. (2008) Reversal of pathological pain through specific spinal GABAA receptor subtypes. Nature 451, 330-334.
27. McKernan, R.-M., Rosahl, T.-W., Reynolds, D.-S., Sur, C., Wafford, K.-A., Atack, J.-R., Farrar, S., Myers, J., Cook, G., Ferris, P., Garrett, L., Bristow, L., Marshall, G., Macaulay, A., Brown, N., Howell, O., Moore, K.-W., Carling, R.-W., Street, L.-J., Castro, J-.L., Ragan, C.-I., Dawson, G.-R. and Whiting, P.-J. (2000). Sedative but not anxiolytic properties of benzodiazepines are mediated by the GABA(A) receptor alpha1 subtype. Nat Neurosci 3, 587-592.
28. Savić MM, Huang S, Furtmüller R, Clayton T, Huck S, Obradović DI, Ugresić ND, Sieghart W, Bokonjić DR, Cook JM. Are GABAA receptors containing alpha5 subunits

contributing to the sedative properties of benzodiazepine site agonists? Neuropsychopharmacology. 2008 Jan;33(2):332-9.

29. Savić, M.-M., Milinković, M.-M., Rallapalli, S., Clayton, T. Sr, Joksimović, S., Van Linn, M. and Cook, J.-M. (2009) The differential role of alpha1- and alpha5-containing GABA(A) receptors in mediating diazepam effects on spontaneous locomotor activity and water-maze learning and memory in rats. Int. J. Neuropsychopharmacol. 12, 1179-1193.

30. Redrobe, J.-P., Elster, L., Frederiksen, K., Bundgaard, C., de Jong, I.-E., Smith, G.-P., Bruun, A.-T., Larsen, P.-H. and Didriksen, M. (2012) Negative modulation of GABAA α5 receptors by RO4938581 attenuates discrete sub-chronic and early postnatal phencyclidine (PCP)-induced cognitive deficits in rats. Psychopharmacology 221, 451-468.

31. McNamara, R.-K. and Skelton, R.-W. (1993) The neuropharmacological and neurochemical basis of place learning in the Morris water maze. Brain. Res. Brain. Res. Rev. 18, 33-49.

32. Pirker, S., Schwarzer, C., Wieselthaler, A., Sieghart, W. and Sperk, G. (2000) GABA(A) receptors : immunocytochemical distribution of 13 subunits in the adult rat brain. Neuroscience. 101, 815–850.

33. Gerlai, R. (2001) Behavioral tests of hippocampal function: simple paradigms complex problems. Behavioural. Brain. Research. 125, 269–277.

34. Yamada, J., Furukawa, T., Ueno, S., Yamamoto, S. and Fukuda, A. (2007) Molecular basis for the GABAA receptor-mediated tonic inhibition in rat somatosensory cortex. Cerebral. Cortex. 17, 1782–1787.

35. Panzanelli, P., Fritschy, J.-M., Yanagawa, Y., Obata, K. and Sassoè-Pognetto, M. (2007) GABAergic phenotype of periglomerular cells in the rodent olfactory bulb. J. Comp. Neurol. 502, 990-1002.

36. Ferguson, J.-N., Young, L.-J. and Insel, T.-R. (2002) The neuroendocrine basis of social recognition. Front. Neuroendocrinol. 23, 200–224.

37. Haberly, L.-B. (2001) Parallel-distributed processing in olfactory cortex: new insights from morphological and physiological analysis of neuronal circuitry. Chem. Senses. 26, 551-576.

38. Feinberg, L.-M., Allen, T.-A., Ly, D. and Fortin, N.-J. (2012) Recognition memory for social and non-social odors: differential effects of neurotoxic lesions to the hippocampus and perirhinal cortex. Neurobiol. Learn. Mem. 97, 7-16.

39. Kocsis, B., Brown, R.-E., McCarley, R.-W. and Hajos, M. (2013) Impact of ketamine on neuronal network dynamics: translational modeling of schizophrenia-relevant deficits. CNS Neurosci. Ther. 19, 437-447.

40. Engin, E., Zarnowska, E.-D., Benke, D., Tsvetkov, E., Sigal, M., Keist, R., Bolshakov, V.-Y., Pearce, R.-A. and, Rudolph, U. (2015) Tonic Inhibitory Control of Dentate Gyrus Granule Cells by α5-Containing GABAA Receptors Reduces Memory Interference. J. Neurosci. 35, 13698-13712.

41. Colgin, L.-L., Moser, E.-I. and Moser, M.-B. (2008) Understanding memory through hippocampal remapping. Trends. Neurosci. 31, 469-477.

42. Moosavi, M., Yadollahi, Khales G., Rastegar, K. and Zarifkar, A. (2012) The effect of sub-anesthetic and anesthetic ketamine on water maze memory acquisition, consolidation and retrieval. Eur. J. Pharmacol. 677, 107-110.

43. Sabbagh, J.-J., Heaney, C.-F., Bolton, M.-M., Murtishaw, A.-S. and Kinney, J.-W. (2012) Examination of ketamine-induced deficits in sensorimotor gating and spatial learning. Physiol. Behav. 107, 355-363.

44. Cook, J.-M., Zhou, H., Huang, S., Sarma, P.-V.-V.-S. and Zhang, C. (2009) Stereospecific anxiolytic and anticonvulsant agents with reduced muscle-relaxant, sedative-hypnotic and ataxic effects, PCT WO2006/004945A1, US Patent 7,618,958.

45. Chen, C. and Okayama, H. (1987) High-efficiency transformation of mammalian cells by plasmid DNA. Mol. Cell. Biol. 7, 2745-2752.

46. Cheng, Y. and Prusoff, W.-H. (1973) Relationship between the inhibition constant (K1) and the concentration of inhibitor which causes 50 per cent inhibition (I50) of an enzymatic reaction. Biochem. Pharmacol. 22, 3099-3108.

47. Ramerstorfer, J., Furtmüller, R., Vogel, E., Huck, S. and Sieghart, W. (2010) The point mutation gamma 2F77I changes the potency and efficacy of benzodiazepine site ligands in different GABAA receptor subtypes. Eur. J. Pharmacol. 636, 18–27.

48. Vorhees, C.-V. and Williams, M.-T. (2014) Value of water mazes for assessing spatial and egocentric learning and memory in rodent basic research and regulatory studies. Neurotoxicol. Teratol. 45, 75–90.

49. Engelmann, M., Wotjak, C.-T. and Landgraf, R. (1995) Social discrimination procedure: an alternative method to investigate juvenile recognition abilities in rats. Physiol. Behav. 58, 315-321.

50. Terranova, J.-P., Chabot, C., Barnouin, M.-C., Perrault, G., Depoortere, R., Griebel, G. and Scatton, B. (2005) SSR181507, a dopamine D(2) receptor antagonist and 5-HT(1A)

receptor agonist, alleviates disturbances of novelty discrimination in a social context in rats, a putative model of selective attention deficit. Psychopharmacology. 181, 134-144.
51. Bambini-Junior, V., Zanatta, G., Della Flora Nunes, G., Mueller de Melo, G., Michels, M., Fontes-Dutra, M., Nogueira Freire, V., Riesgo, R. and Gottfried, C. (2014) Resveratrol prevents social deficits in animal model of autism induced by valproic acid. Neurosci. Lett. 583, 176-181.
52. Kim, K.-C., Kim, P., Go, H.-S., Choi, C.-S., Yang, S.-I., Cheong, J.-H., Shin, C.-Y. and Ko, K.-H. (2011) The critical period of valproate exposure to induce autistic symptoms in Sprague-Dawley rats. Toxicol. Lett. 201, 137-142.

SUPPORTING INFORMATION

Table of contents

Figure S1

Figure S2

Figure S3

Figure S4

Table S1

Table S2

Table S3

Table S4

Table S5

Table S6

HPLC and LCMS Spectra

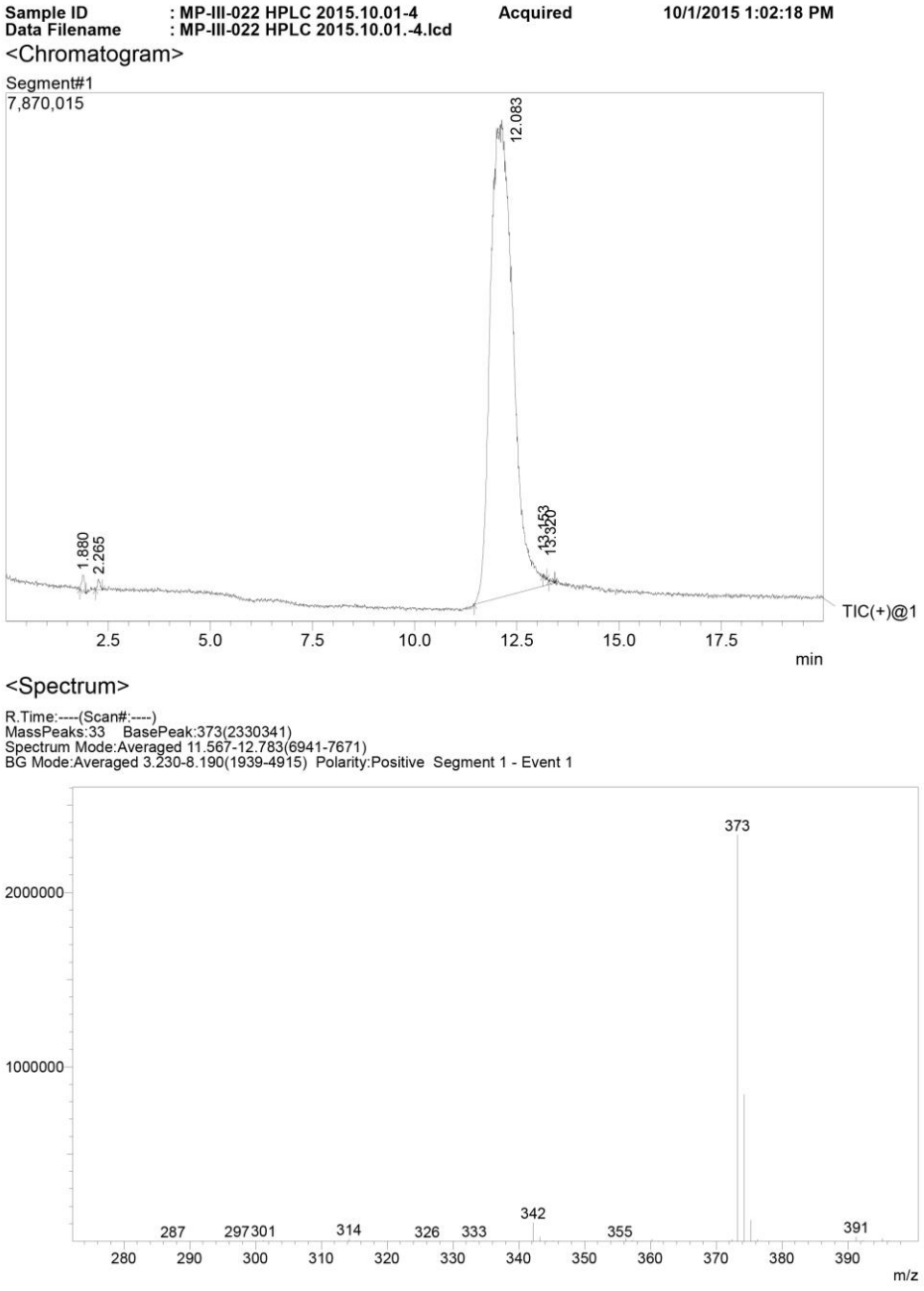


Figure S1. HPLC total ion chromatogram with associated LC-MS spectrum (positive ion mode) of MP-III-022 (Shimadzu Single Quadrupole Mass Spectrometer (2020)).

HRMS Report

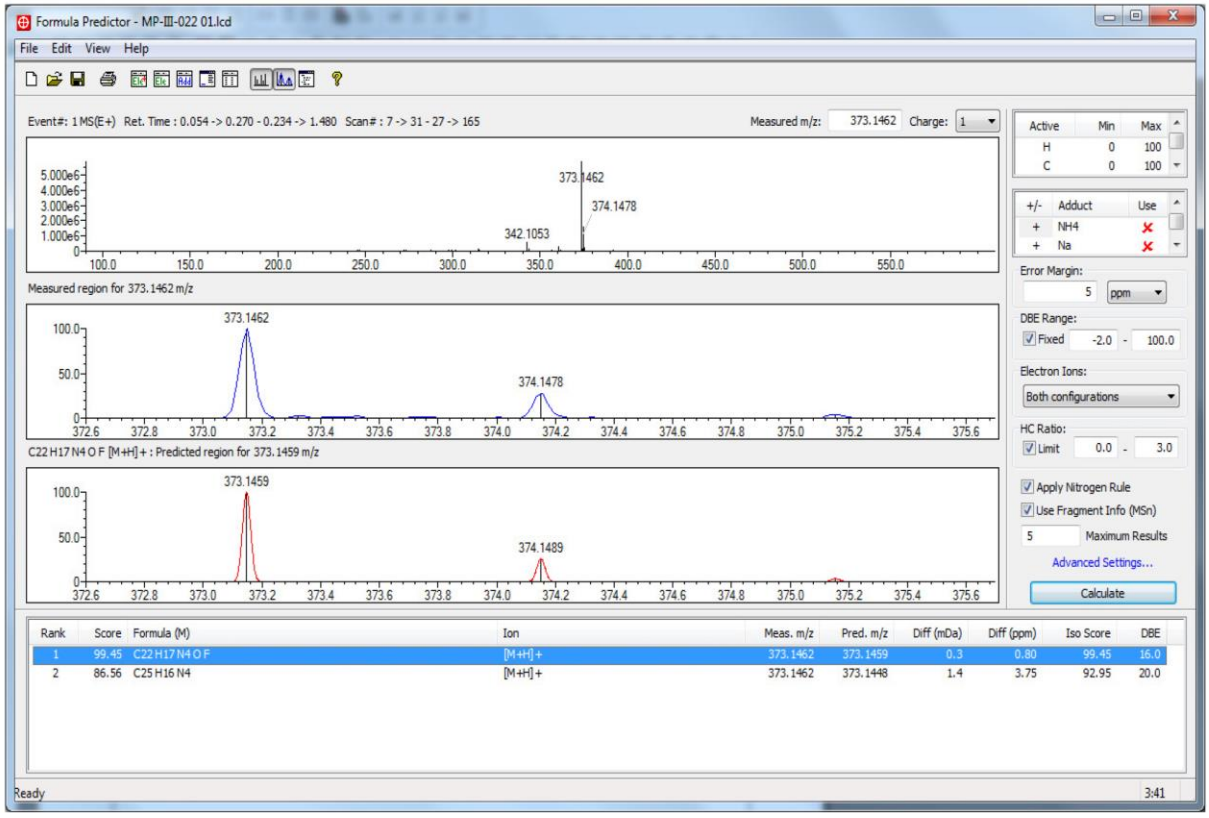


Figure S2. High-resolution-Mass spectrum of MP-III-022 (Shimadzu Ion Trap Time-of-Flight)

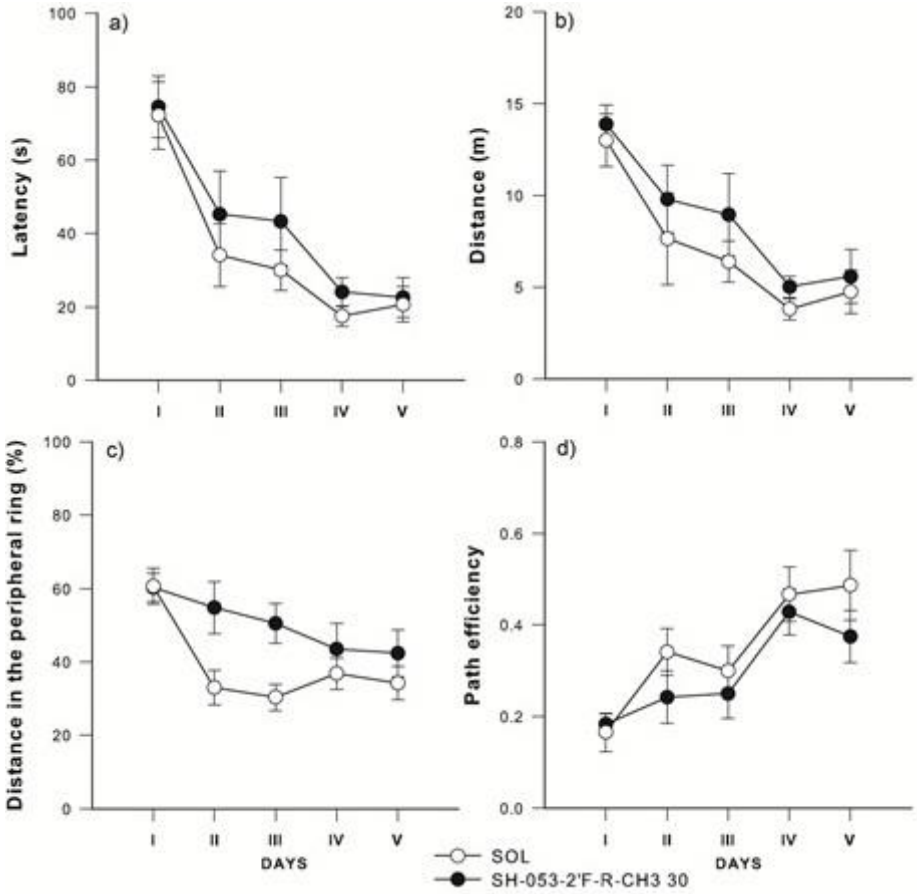


Figure S3. The effects of 30 mg/kg SH-053-2′F-R-CH3 on (a) latency to platform, (b) total distance, (c) distance in the peripheral ring (%) and (d) path efficiency during acquisition trials in the water maze. Animals per treatment group were 8. SOL = solvent, SH-053-2′F-R-CH3 30 = 30 mg/kg SH-053-2′F-R-CH3. The original data used for preparation of the figure were published in reference 19.

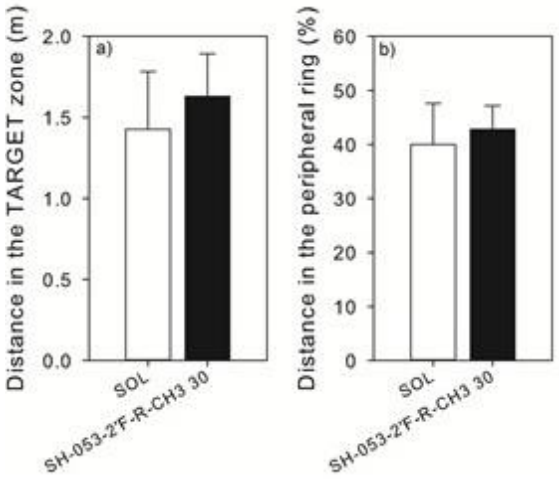


Figure S4. The effects of 30 mg/kg SH-053-2′F-R-CH3 on (a) distance in the target zone (m) and (b) distance in the peripheral ring (%) during probe trial in the water maze. Animals per treatment group were 8. SOL = solvent, SH-053-2′F-R-CH3 30 = 30 mg/kg SH-053-2′F-R-CH3. Distance in the target zone (m): $t(14) = -0.462$, $p = 0.651$; distance in the peripheral ring (%): $t(14) = -0.320$, $p = 0.754$. The original data used for preparation of the figure were published in reference 19.

Table S1: Equilibrium binding constant (KD) for the different receptor subtypes

α1β3γ2S	α2β3γ2S	α3β3γ2S	α5β3γ2S
7.2 ± 0.2 nM	2.9 ± 0.6 nM	4.1 ± 0.2 nM	2.2 ± 0.3 nM

Legend:

Membranes from HEK-293 cells transfected with the subunit combinations as indicated were incubated with various concentrations of 3H-Flunitrazepam in the absence or presence of either 5 µM diazepam (to determine unspecific binding). Results were analyzed using the equation Y=Bmax*X/(KD+X). KD values are presented as mean values ± SEM from 3-4 independent experiments performed in duplicates.

Table S2. Measured positive modulation of GABA EC3-5 currents by MP-III-022 at rat recombinant α1-, α2-, α3,- and α5β3γ2 $GABA_A$ receptors

	1 nM	**10 nM**	**100 nM**	**1 µM**	**10 µM**	
α1	98 ± 3	100 ± 6	107 ± 3	123 ± 6	185 ± 7	n=4
α2	108 ± 2	109 ± 6	150 ± 18	325 ± 47	454 ± 62	n=4
α3	109 ± 9	107 ± 4	130 ± 8	231 ± 10	429 ± 28	n=4
α5	104 ± 4	154 ± 10	354 ± 19	698 ± 70	825 ± 36	n= 5

Table S3. The approximated % of GABA potentiation, read from Figure 1, for the estimated brain free concentrations of SH-053-2′F-R-CH3, in the dose range 10 mg/kg to 200 mg/kg, and MP-III-022, in the dose range 1 mg/kg to 10 mg/kg.

	SH-053-2′F-R-CH3 (dose (mg/kg)			MP-III-022 (dose (mg/kg)		
	10	30	200	1	2.5	10
Estimated brain free concentration (nmol/kg)						
	29.10	64.40	324.16	6.38	10.34	68.12
Approximated % of GABA potentiation from Figure…						
α1β3γ2	102.14	108.27	130.99	102.74	104.99	107.25
α2β3γ2	107.28	122.63	171.10	109.74	114.57	137.96
α3β3γ2	106.29	120.72	154.70	108.30	111.99	123.74
α5β3γ2	**135.14**	**165.96**	**280.16**	**137.96**	**158.57**	**314.31**

Metabolic stability in rat plasma

Table S4. Estimated *in vitro* metabolic stability (total plasma concentration of MP-III-022 or SH-053-2′F-R-CH3 in 30, 60, 120 and 240 minutes). Mean ± SEM, n = 3

MP-III-022	**µM**	**%**	**SH-053-2′F-R-CH3**	**µM**	**%**
0 min	0.5556	**100**	0 min	0.5556	**100**
30 min	0.5402 ± 0.0146	**97.23**	30 min	0.4258 ± 0.0042	**76.64**
60 min	0.5403 ± 0.0193	**97.25**	60 min	0.3487 ± 0.0040	**62.77**
120 min	0.5472 ± 0.0007	**98.50**	120 min	0.2126 ± 0.0036	**38.27**
240 min	0.5374 ± 0.0063	**96.74**	240 min	0.0291 ± 0.0023	**5.24**

Table S5. The effects of 30 mg/kg SH-053-2′F-R-CH3 on the rat's behavior in the MWM. Two-way repeated measures ANOVA and overall *post hoc* results for latency to platform (s), total distance (m), distance swam in the peripheral annulus (%) and path efficiency. SOL = solvent; SH = SH-053-2′F-R-CH3; ns = not significant.

Factor	**Latency (s)**	**Total distance (m)**	**Distance in the peripheral ring (%)**	**Path efficiency**
Treatment: F(1,14)	1.478	1.717	5.804	1.819
p	0.244	0.211	0.030	0.199
Days: F(4,56)	16.205	12.385	7.634	10.177
p	< 0.001	< 0.001	< 0.001	< 0.001
Interaction: F(4,56)	0.233	0.150	2.066	0.519
p	0.919	0.962	0.097	0.722
SNK *post hoc* for Treatment				
SOL vs. 30 mg/kg SH	-	-	0.030	-

Table S6. The raw data obtained in the three-chamber test

YELLOW = excluded from T2 (sociability test)

RED = excluded from T3 (social cognition test)

MP-III-022 = 10 mg/kg MP-III-022, KET 15 = 15 mg/kg ketamine, SOL = solvent

Sociability data

Treatment	Distance (m)	Time RAT (s)	Time OBJECT (s)	Chamber RAT (s)	Chamber OBJECT (s)	Central chamber (s)
KET 15 + MP-III-022	4.218	513.7	0	536.9	0	63.1
KET 15 + MP-III-022	16.107	95.8	427.9	119.9	457.3	22.8
KET 15 + MP-III-022	10.686	0	262.7	0	304.3	295.7
KET 15 + MP-III-022	21.58	131.9	57.4	254.4	107.2	238.5
KET 15 + MP-III-022	10.966	135.7	308.7	152.4	343.5	104.1
KET 15 + MP-III-022	14.541	509.7	15.8	533	21.9	45.1
KET 15 + MP-III-022	21.416	121.1	246.7	199.8	326	74.2
KET 15 + MP-III-022	42.499	230.3	197.7	263.2	250.7	86.1
KET 15 + MP-III-022	16.968	476.4	0	579.8	0	20.2
KET 15 + MP-III-022	4.072	0	0	0	0	600
KET 15 + MP-III-022	7.713	514	0	560.5	0	39.5
KET 15 + MP-III-022	36.61	166.3	92.8	231.2	166.4	202.5
KET 15 + MP-III-022	17.984	144	125.6	202.5	190.5	207.1
KET 15 + MP-III-022	8.578	83.2	0	319.1	0	280.9
KET 15 + MP-III-022	15.291	32.6	230.8	41	264.6	294.4
KET 15 + MP-III-022	37.911	113.7	157.9	142.4	198.2	259.4
KET 15 + MP-III-022	32.702	175.3	114.7	227.1	153.6	219.3
KET 15 + SOL	6.338	11.1	35.3	13.6	48.9	537.5
KET 15 + SOL	9.036	229.6	24.1	295.1	27.5	277.3
KET 15 + SOL	10.092	262.7	233.1	313	258.8	28.3
KET 15 + SOL	7.377	0	0	1.7	0	598.3
KET 15 + SOL	11.279	260.1	0	296.9	0	303.1
KET 15 + SOL	28.288	159.2	56.3	196.2	111.5	292.3
KET 15 + SOL	17.606	147.6	135.6	183.5	207.2	209.3
KET 15 + SOL	9.096	0	0	6.5	0	593.5
KET 15 + SOL	16.866	154.8	174.9	210.9	273.2	115.9
KET 15 + SOL	26.22	150.7	121.8	215	202.1	182.8
KET 15 + SOL	15.671	416	0	547.9	0	52.1
KET 15 + SOL	6.89	42.6	41.7	67.7	63.4	468.9
KET 15 + SOL	3.992	0	0	0	0	600
KET 15 + SOL	23.77	134.5	77.1	245.9	191.2	162.8
SAL + MP-III-022	12.05	81.1	51.5	119.9	76.8	403.3
SAL + MP-III-022	0.105	0	0	0	0	600
SAL + MP-III-022	1.41	0	0	0	0	600
SAL + MP-III-022	12.009	0	362.6	0	420.5	179.5
SAL + MP-III-022	9.395	82.2	60.7	146.4	92.8	360.8
SAL + MP-III-022	29.375	164.1	119	213.2	162.2	224.6

SAL + MP-III-022	19.902	158.2	88.4	270.6	163.5	165.9
SAL + MP-III-022	11.167	99.7	38.1	148.4	49.5	402.2
SAL + MP-III-022	19.627	28.4	314.4	55.2	390.4	154.4
SAL + MP-III-022	5.805	47.3	39.2	51.4	72.5	476.1
SAL + MP-III-022	22.779	123.9	98.4	181.4	146.3	272.3
SAL + MP-III-022	12.731	86	55.3	103.6	88	408.3
SAL + MP-III-022	19.011	0	278.1	0	411.3	188.7
SAL + MP-III-022	25.034	169.7	31.9	333.7	77.4	188.9
SAL + MP-III-022	14.893	88.4	41.6	105.3	75	419.7
SAL + SOL	27.178	273.8	55	384.6	100.5	115
SAL + SOL	22.189	175.3	51.2	234.3	92.6	273.1
SAL + SOL	18.982	176.5	139.8	233	240.8	126.3
SAL + SOL	28.474	172.7	100.8	272.7	184.2	143.1
SAL + SOL	34.285	163.4	111.6	249.3	180.4	170.3
SAL + SOL	30.795	140.5	106.5	230.4	177.1	192.5
SAL + SOL	35.095	175.5	37.3	280.2	74.3	245.4
SAL + SOL	25.778	224.1	105.9	314.5	165.4	120.1
SAL + SOL	15.227	0	270.4	0	423.2	176.8
SAL + SOL	24.576	172.3	126.6	281.3	197.9	120.7

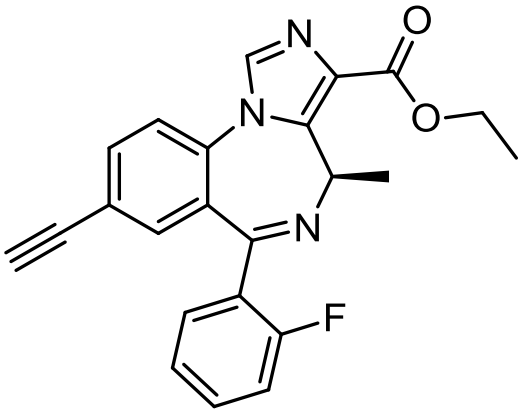
Social cognition data

Treatment	Distance (m)	Time NEW RAT (s)	Time OLD RAT (s)	Chamber NEW RAT (s)	Chamber OLD RAT (s)	Central chamber (s)
KET 15 + MP-III-022	32.709	84.9	182	118	250.2	231.8
KET 15 + MP-III-022	12.05	537.2	0	575.8	0.5	23.8
KET 15 + MP-III-022	3.916	438.3	0	472.6	2.1	125.3
KET 15 + MP-III-022	21.205	75.6	84.2	175.8	161.8	262.4
KET 15 + MP-III-022	15.075	0	403.1	0	442.6	157.4
KET 15 + MP-III-022	9.246	0	545.4	0	588.3	11.7
KET 15 + MP-III-022	11.018	83.9	334	119.4	410.1	70.5
KET 15 + MP-III-022	17.87	256.2	157.2	306.1	186.4	107.5
KET 15 + MP-III-022	16.841	0	564.5	0	593.9	6.1
KET 15 + MP-III-022	9.375	35.3	0	35.9	0	564.1
KET 15 + MP-III-022	4.265	0	526.7	0	531.4	68.6
KET 15 + MP-III-022	20.894	215.5	124.4	276.5	153.6	169.9
KET 15 + MP-III-022	14.718	16.8	185	60.4	370	169.6
KET 15 + MP-III-022	20.938	21.4	1.4	87.4	41.1	471.4
KET 15 + MP-III-022	9.553	294.8	76.3	344.7	79.6	175.7
KET 15 + MP-III-022	45.659	73	68.3	88.7	92.5	418.8
KET 15 + MP-III-022	24.058	85.3	178.4	162.8	251.7	185.4
KET 15 + SOL	23.125	122.3	178.6	210.4	271.9	117.7
KET 15 + SOL	26.755	66.1	90.2	158.6	232.4	209
KET 15 + SOL	4.058	99.5	456.5	124.8	458.4	16.8
KET 15 + SOL	5.463	18	0	21.9	0	578.1
KET 15 + SOL	3.895	0	586.7	0	598.5	1.5
KET 15 + SOL	15.287	65.2	177.9	88.8	235.6	275.6
KET 15 + SOL	19.23	298.7	88.2	320.1	120.5	159.4
KET 15 + SOL	14.618	198	21.6	232.4	26.6	341
KET 15 + SOL	9.795	207.1	54	344.5	84.3	171.2
KET 15 + SOL	14.656	65.8	108	196.7	146.9	256.4
KET 15 + SOL	12.412	134.1	52.2	293.1	131.4	175.5
KET 15 + SOL	6.503	58.6	0	96.5	0	503.5
KET 15 + SOL	0.02	0	0	0	0	1.9
KET 15 + SOL	16.954	40.6	149.3	157.1	288.9	154
SAL + MP-III-022	8.296	40.3	52.3	105.1	218.7	276.3
SAL + MP-III-022	4.093	0	20.6	0	86.7	513.3
SAL + MP-III-022	8.131	0.8	0.6	8.7	13.6	577.7
SAL + MP-III-022	2.018	0	0	0	0	600
SAL + MP-III-022	11.703	137.7	221.1	211.7	308.8	79.4
SAL + MP-III-022	18.238	134.5	109.9	201.9	186.9	211.3
SAL + MP-III-022	5.09	282.1	25.3	306.8	35.3	258
SAL + MP-III-022	2.12	495.6	0	496.7	0	103.3
SAL + MP-III-022	9.631	449.1	16.6	480.6	27.4	92
SAL + MP-III-022	8.486	432.5	0	445.7	5.4	148.9

SAL + MP-III-022	119.499	0	0	202.3	101.7	296.1
SAL + MP-III-022	22.394	63.8	58.5	165.8	141.6	292.7
SAL + MP-III-022	11.452	32.9	88.8	67.6	151	381.4
SAL + MP-III-022	20.354	108.6	21.6	224.9	108.7	266.4
SAL + MP-III-022	13.514	24	62.9	94.7	271.2	234.2
SAL + SOL	21.809	121.5	122.9	263.5	177.9	158.6
SAL + SOL	10.42	67.3	52.3	139.3	178.7	282
SAL + SOL	9.415	398.3	0	593.2	0	6.8
SAL + SOL	16.768	164.3	144.9	211.6	216	172.4
SAL + SOL	21.308	152.4	135.5	256.3	214.5	129.2
SAL + SOL	29.802	63.6	133.4	152.4	234.5	213.1
SAL + SOL	22.769	115.5	109.7	182.6	202.9	214.5
SAL + SOL	21.576	144.2	170.1	228.4	249.9	121.7
SAL + SOL	12.958	4.6	2.9	9.2	6.3	584.5
SAL + SOL	17.74	78.6	18.4	209.5	116.7	273.8

APPENDIX G. Manuscript Prepared by Etienne Sibille, *et al.* on the Anti-Depressant Effects of SH-053-2'F-R-CH_3.

Structure:



SH-053-2'F-R-CH_3

Sex-dependent, rapid anxiolytic- and antidepressant-like activity of an α5 subunit containing $GABA_A$ receptor positive allosteric modulator in the mouse unpredictable chronic mild stress model

Sean C Piantadosi[1,2], Beverly French[2], Michael M Poe[3], Tamara Timić[4], Bojan Marković[5], Mohan Pabba[6], Marianne L Seney[2], Miroslav M Savić[4], James M Cook[3], Etienne Sibille[1,2,6,*]

[1]Center for Neuroscience, University of Pittsburgh, Pittsburgh PA, USA; [2]Department of Psychiatry, University of Pittsburgh, Pittsburgh PA, USA; [3]Department of Chemistry and Biochemistry, UW-Milwaukee, Milwaukee WI, USA; [4]Department of Pharmacology, University of Belgrade, Belgrade, Serbia; [5]Department of Pharmaceutical Chemistry, University of Belgrade, Belgrade, Serbia; [6]Campbell Family Mental Health Research Institute of CAMH; Departments of Psychiatry, Pharmacology and Toxicology, University of Toronto, Toronto, ON, Canada;

*Correspondence: E Sibille, CAMH, 250 College street, Room 134, Toronto, ON M5T 1R8, Canada. E-mail address: Etienne.sibille@camh.ca; Phone: 416-535-8501 xt36751

Highlights

- Acute and chronic α5-PAM reduces anxiety- and depressive-like behavior induced by chronic mild stress in female mice
- Neither acute nor chronic α5-PAM treatment affected anxiety- and depressive-like behavior induced by chronic mild stress in male mice.
- Sex differences were not explained by differential pharmacokinetic or dose effects.
- α5-PAM treatment increased *Gabra5* expression in the hippocampus and prelimbic cortex of female, but not male mice.

Abstract

Current treatments for Major Depressive Disorder (MDD) acting on monoaminergic systems take weeks to achieve a therapeutic effect and have poor response and low remission rates. Recent research has implicated the GABAergic system in the pathophysiology of depression, including deficits in interneurons targeting the dendritic compartment of pyramidal cells. The present study evaluates whether SH-053-2'F-R-CH3 (denoted "α5-PAM"), a positive allosteric modulator selective for α5-subunit containing $GABA_A$ receptors found predominantly on pyramidal cell dendrites, has anxiolytic- and/or antidepressant-like-like effects. Female and male C57BL6/J mice were exposed to unpredictable chronic mild stress (UCMS) for 10 weeks and treated with α5-PAM acutely (30 minutes prior to assessing behavior) or chronically (weeks 3-10) before being assessed behaviorally (weeks 7-10). Acute and chronic α5-PAM treatments produce a pattern of decreased anxiety- and depressive-like behaviors (together denoted as “behavioral emotionality”) across various tests (elevated plus maze, open field, novelty suppressed feeding, and cookie test) only in females. Behavioral Z-scores across tests confirmed that both acute and chronic α5-PAM treatments produce significant decreases in behavioral emotionality in female but not male mice. Findings were replicated in independent cohorts. The characteristic behavioral responses to α5-PAM could not be accounted for by the observed differences in brain disposition between female and male mice. In mice exposed to UCMS, expression of the *Gabra5* gene was increased in the frontal cortex after acute treatment and in hippocampus after chronic treatment with α5-PAM in females only. Together, we showed that both, acute and chronic positive modulation of α5 subunit-containing $GABA_A$ receptors may elicit anxiolytic- and antidepressant-like effects in a sex-dependent manner, suggesting novel therapeutic modalities.

Keywords: Gabra5, alpha5, depression, interneurons, PAM, GABA

1. Introduction

Major depressive disorder (MDD) is a debilitating disorder characterized by low mood, anhedonia, physiological disturbance, and increased self-focus and rumination (Ferrari *et al*, 2013; Northoff and Sibille, 2014). Lifetime prevalence of MDD is higher in females than in males. Factors mediating this increase are still being investigated (Seney *et al*, 2013). Adding to the disease burden of MDD is the relative ineffectiveness of conventional antidepressant medications (roughly 30% remission rates), most of which act via the monoaminergic system (e.g. selective serotonin reuptake inhibitors – SSRIs) (Cipriani *et al*, 2009; Rush, 2010). Although drugs with rapid acting antidepressant effects have shown promise in preclinical studies and effectiveness in treating severely depressed individuals (Li *et al*, 2010; Zarate *et al*, 2012a; Zarate *et al*, 2012b) no existing antidepressant drug directly addresses the pathology observed in the depressed brain, providing a potential explanation for the limited efficacy of current antidepressants.

Converging evidence has long suggested a role for the inhibitory neurotransmitter gamma-amino butyric acid (GABA) in the pathophysiology of depression (Krystal *et al*, 2002; Luscher *et al*, 2011). Studies using magnetic resonance spectroscopy show decreases in GABA levels in depression in brain regions critical for emotion regulation (dorsolateral prefrontal cortex (dlPFC), subgenual anterior cingulate cortex (sgACC)) (Bajbouj *et al*, 2006; Sanacora *et al*, 2004; Sanacora *et al*, 1999). At the cellular level, reduced density of calbindin-positive interneurons were reported in frontal cortex (Rajkowska *et al*, 2007). At the molecular level, we previously reported alterations in GABA-related gene expression in dlPFC, sgACC, and amygdala (Guilloux *et al*, 2012; Seney *et al*, 2014; Sibille *et al*, 2010; Tripp *et al*, 2011). Preclinical evidence has also implicated the GABA system in the development of anxiety- and depressive-like behaviors. Mice with reduced GABA signaling exhibit increased depressive-like behavior (Earnheart *et al*, 2007; Shen *et al*, 2010). Further, chronic stress paradigms that produce anxiety- and depressive-like behavior in rodents, cause GABAergic deficits in the frontal cortex, including decreases in major GABA synthesizing enzymes (Gilabert-Juan *et al*, 2013; Herman and Larson, 2001).

Interestingly, this alteration in GABAergic signaling in MDD subjects appears to be restricted to interneuron subtypes that project to the dendritic compartment of pyramidal cells, and that are characterized by the expression of somatostatin (SST), neuropeptide Y (NPY) and cortistatin (CORT) neuropeptides (and that co-express calbindin). Cells targeting the perisomatic compartment, such as parvalbumin (PV)-or cholecystokinin (CCK)- expressing GABA neurons appear only sparingly affected (Guilloux *et al*, 2012; Sibille *et al*, 2010; Tripp *et al*, 2011). Recent work in mice has demonstrated that cortical SST cells are also affected in the unpredictable chronic mild stress (UCMS) model which induces elevated behavioral emotionality, and that UCMS-induced anxiety- and depressive-like behavior can re recapitulated in mice lacking SST (Lin and Sibille, 2015). Together these findings suggest a causal link between low SST expression and elevated behavioral emotionality. The UCMS model has been used to assess potential drug targets for treating human depression, as it has good construct (stress precipitates the UCMS phenotype as well as MDD episodes and disrupts similar biological pathways), predictive (chronic treatment with SSRIs reverses the UCMS phenotype), and face validity (behavioral features replicated) (Edgar *et al*, 2011; Isingrini *et al*, 2012; Lin *et al*, 2015).

Importantly, the structured anatomical distribution of $GABA_A$ receptors in the cortex provides a potential means of directly addressing GABAergic dysfunction within a specific compartment. Specifically, α5-containing $GABA_A$ receptors are predominantly expressed on dendritic branches of pyramidal cells where they mediate dendritic inhibition *in vitro* (Ali and Thomson, 2008; Wainwright *et al*, 2000), whereas α1 and α2 containing $GABA_A$ receptors are found near the soma (Packer *et al*, 2013). This anatomical proximity suggests a functional link between dendrite-preferring SST cells and the extra-synaptic α5 containing $GABA_A$ receptors that mediate tonic inhibition in the cortex (Bonin *et al*, 2007; Brickley and Mody, 2012). Knowing that GABA signaling is decreased in MDD and similarly in the rodent UCMS model, we set out to test whether increasing GABAergic tone specifically at the dendritic compartment may reverse UCMS-induced anxiety- and depressive-like behaviors. To directly test this hypothesis, we utilized the

$GABA_A$ receptor positive allosteric modulator (PAM), SH-053-2'F-R-CH3 (denoted further as α5-PAM), which has high affinity for $GABA_A$ receptors containing the α5 subunit (K_i=95.2nM) and lower affinity for $GABA_A$ receptors containing the α1- (K_i=759.1nM), α2- (K_i=948.2nM), and α3-subunits (K_i=768.8nM) (Savic *et al*, 2010). Based on the hypothesis that low GABA activity at the dendritic compartment following UCMS is involved in the expression of anxiety- and depressive-like behaviors, we predicted that enhancing GABA tone with α5-PAM would reduce UCMS-induced anxiety- and depressive-like behavior in female and male mice.

2. Methods

2.1. Animals. C57BL/6J mice (Jackson Laboratories, Bar Harbor, Maine USA) were housed under standard conditions with a 12/12 light/dark cycle and *ad libitum* access to food and water in accordance with the University of Pittsburgh Institutional Animal Care and Use Committee.

UCMS. Mice underwent 6 weeks of UCMS. Briefly, animals were exposed to 2-3 mild stressors each day throughout the light/dark cycle, including wet bedding, brief restraint, forced bath, no bedding, reduced space, and predator odor over a period of several weeks (see Lin et al. 2015 and Edgar et al., 2011). In one experiment, UCMS was augmented with single-cage isolation starting at the fourth week until sacrifice.

2.2. Drug treatment. Beginning on the third week of UCMS and continuing for ~50 days (including time for behavioral tests) until sacrifice, mice received daily i.p injections of vehicle (85% ddH_2O, 14% propylene glycol, 1% Tween 80) or 30mg/kg SH-053-2'F-R-CH3 (α5-PAM; synthesized in the laboratory of Dr. James M Cook) in a volume of 10mg/mL at least two hours prior to behavioral testing. Thirty minutes prior to behavioral testing, all animals received a second injection of either vehicle (for chronic α5-PAM treated animals and UCMS-vehicle treated animals) or α5-PAM acutely.

2.3. Pharmacokinetic study of α5-PAM. Male and female C57BL/6J (Military Farm, Belgrade, Serbia) were divided into six groups corresponding to predetermined time intervals following a

single 30mg/kg α5-PAM injection (5, 10, 20, 40, 60 and 180 min). Blood samples were collected in heparinized syringes via cardiac puncture of mice anesthetized with ketamine (100mg/kg i.p.; 10% Ketamidor, Richter Pharma Ag, Wels, Austria), and centrifuged at 2500rpm for 10min to obtain plasma. Thereafter, mice were decapitated and brains were weighed, homogenized in 2mL of methanol and centrifuged at 6000rpm for 20min. To determine the concentration of α5-PAM in plasma and supernatants of brain tissue homogenates, α5-PAM was extracted by solid phase extraction, using Oasis HLB cartridges (Waters Corporation, Milford, Massachusetts). The procedure of sample preparation and determination of α5-PAM by ultraperformance liquid chromatography–tandem mass spectrometry (UPLC–MS/MS) with Thermo Scientific Accela 600 UPLC system connected to a Thermo Scientific TSQ Quantum Access MAX triple quadrupole mass spectrometer (Thermo Fisher Scientific, San Jose, California) equipped with electrospray ionization (ESI) source, is described in (Obradovic *et al*, 2014).

2.4. Plasma protein and brain tissue binding studies. The rapid equilibrium dialysis assay used to determine free fraction of α5-PAM in mouse plasma and brain tissue was the same as in (Obradovic *et al*, 2014).

2.5. Behavioral testing. After five weeks of UCMS, animals were assessed in a battery of behavioral tests including (each test separated by 24 hours, UCMS continued throughout behavioral testing): *Elevated plus maze*: under red light, animals were placed on a plus maze with two open and two closed arms (30x5cm). Number of entries into all arms as well as the time spent in the open arms was recorded for 10min. *Open field test*: The open field test was conducted in a 43x43cm arena under bright (800lux) light. Using AnyMaze software (Stoelting, Wood Dale, IL USA), the center 50% of the arena was identified and animals were tracked for 10min. *Novelty suppressed feeding test*: Mice were food deprived for 24hours the day before testing. Testing occurred in brightly lit (~1000lux) open field arenas covered in bedding. A normal food pellet was placed into the brightly lit center and the latency for an animal to approach and bite the pellet was recorded over a 12min session. Immediately following the session, animals were placed into their

home cage and allowed to eat a weighed food pellet to assess hunger drive. *Cookie test*: The cookie test apparatus contains three identically sized chambers (40x20x20cm) separated by two offset dividers. The outer walls of each chamber were clear and the only difference between each was the color of the divider, with one divider shaded white and the other black. One week prior to experimentation, mice were habituated in their home cage to a piece (2±1g) of Keebler Fudge Stripe Cookie (Kellogg's Company, Battle Creek, MI USA). On the first and second day of testing, a piece of cookie (2±1g) was placed into the chamber separated by the black divider. Mice were then placed into the opposing chamber separated by the white divider and monitored for 10min. The latency for each mouse to bite the cookie was recorded. Data from day two of the cookie test are presented, after mice acclimated to the anxiogenic environment and their behavior is driven more prominently by reward-seeking, resulting in a decrease in latency to bite (Isingrini *et al*, 2011; Soumier and Sibille, 2014).

2.6. Tissue samples and micropunch procedure. 24hours after the final behavioral test, mice were injected with either an acute dose of α5-PAM or vehicle 30min prior to rapid perfusion (2ml 4%PFA). Brains were rapidly dissected and flash frozen on dry ice and 160μm thick coronal sections were obtained using a cryostat. The prelimbic cortex and dorsal hippocampus was dissected with a 1mm diameter micropunch and tissue samples were then frozen at -80℃. Total RNA was extracted with an RNAeasy FFPE kit (Qiagen, Germantown, MD USA). RNA concentration and quality (RIN) were then assessed using the Agilent RNA6000 Pico-Kit and Agilent 2100 Bioanalyzer (Agilent Technologies, Santa Clara, CA USA).

2.7. Real-time quantitative PCR. ~90ng of total RNA was used to generate cDNA via the qScript™ cDNA Supermix synthesis kit (Quanta Biosciences, Gaithersburg, MD USA). Real-time quantitative polymerase chain (qPCR) reactions were carried out using SYBR green fluorescence signal (Invitrogen, Carlsbad, CA USA) and an Opticon Monitor DNA Engine (Bio-Rad, Berkeley, CA USA). Gene of interest was *Gabra5,* coding for the α5-subunit of the $GABA_A$ receptor. Samples were run in triplicate and ΔC_t values were calculated by comparing the C_t values of

Gabra5 to the geometric mean of two reference genes, *β-Actin* and *glyceraldehyde 3-phosphate dehydrogenase* (*Gapdh*). Arbitrary signal intensity was calculated as $2^{-\Delta Ct}$*10000.

2.8. Antibodies. The following antibodies and their dilutions were used in this study: rabbit polyclonal anti-α5 (1:750; ThermoFisher Scientific, MA, USA), rabbit monoclonal anti-β_1-N^+/K^+-ATPase (NK-ATPase) (1:1000; Abcam, MA, USA), and mouse monoclonal anti-β-actin (1:100; Abcam, MA, USA).

2.9. Surface biotinylation. Dissected hippocampi were processed as described in (Pabba *et al*, 2014) with minor modifications.

2.10. Western blotting. Western blotting was performed using 5µg of protein resolved on 8% SDS-PAGE and transferred onto PVDF membranes and developed using IR-Dye conjugated secondary antibody and detection using LI-COR (NE, USA). Quantification of bands was performed using Image Studio™ Software (LI-COR, NE, USA). We analyzed α5 surface biotinylation in vehicle versus drug treated mice (N=6 females and 4 males per group). Total α5 band intensities were normalized to β-actin, whereas surface α5 band intensities were normalized to NK-ATPase.

2.11. Z-score generation & statistical analysis. To assess the consistency of effects of stress and drug treatment on overall anxiety- and depressive-like behavior, we calculated test-specific z-scores. These normalized scores integrate measures of behavioral emotionality over time and tests, yielding a combined measure of the UCMS-induced behavioral syndrome. For details, see (Guilloux *et al*, 2011). Behavioral and gene expression data were analyzed with a two-way (sex x treatment) or one-way analysis of variance (ANOVA), unless otherwise noted. Fisher's LSD *post-hoc* test was used to determine group differences only following a significant main effect or interaction in the ANOVA model. In certain tests, *a priori* predictions for UCMS versus non-stressed (NS) conditions lead to unpaired two-tailed *t*-tests being conducted. For western blot, statistical significance was determined using a two-tailed Student's *t*-test.

3. Results

3.1. Systemic administration of α5-PAM leads to rapid increase in brain levels in female and male mice.

Free concentrations of α5-PAM were calculated by multiplying the total plasma and brain concentrations with the appropriate free fractions (7.44% for plasma and 2.73% for brain tissue) determined by rapid equilibrium dialysis. Two-way repeated measure ANOVA for total brain concentration revealed a statistically significant difference between female and male mice [$F(1,4)=7.83$, $p<0.05$], and between time points [$F(5,20)=6.89$, $p<0.001$] with no significant interaction [$F(5,20)=1.05$, $p>0.05$]. α5-PAM plasma concentration were higher in female than male mice [$F(1,4)=16.54$; $p<0.05$] with a significant effect of time [$F(5,20)=12.27$, $p<0.001$] and no interaction [$F(5,20)=1.02$, $p>0.05$]. *Post-hoc* comparisons revealed significant differences between female and male mice in plasma C_{max} [$t(4)=-3.04$, $p<0.05$, Fig.1], confirming that higher concentrations were obtained in female mice. Furthermore, the AUC_{0-3} in brain is approximately 1.25X higher for females (4910.13±1032.02) than males (3944.49±560.30), suggesting that a cumulative 25% more ligand available in brain of female mice, after the same dose. However, at 30min, the amount of ligand in the brain of male and female mice was not statistically different (Fig.1). For this reason, we initially chose the 30mg/kg dose and 30min time point for evaluating the acute behavioral effects of α5-PAM in male and female mice.

3.2. α5-PAM reduces the stress-induced elevated anxiety- and anhedonia-like behaviors in female, but not male mice

We first sought to examine whether acute or chronic α5-PAM treatment would reduce anxiety- and depressive- like behaviors induced by UCMS in female and male mice. Individual OFT and EPM tests revealed no significant group differences, although trends were observed for acute and chronic α5-PAM treatment to reduce anxiety-like behavior in the EPM in female mice, whereas chronic treatment in male mice produced a potential anxiogenic response (Fig.S1).

There was a positive correlation between individual EPM and OFT anxiety measures separately in males (blue linear fit; R=0.411, F(28)=5.721, p<0.05) and females (red linear fit; R=0.421, F(21)=4.527, p<0.05), suggesting consistent behavior across tests. Therefore we calculated Z-anxiety scores encompassing both tests for each mouse (Fig.2A) and used those measures to assess group differences. ANOVA revealed a significant main effect of sex [F(1,48)=14.10, p<0.001] and an interaction between sex and treatment [F(2,48)=3.73, p<0.05]. Pairwise comparisons indicate that in female mice, both acute (p<0.05) and chronic (p<0.05) α5-PAM administration consistently decreased anxiety-like behaviors. By contrast, no difference in anxiety Z-scores were detected following α5-PAM in male mice (Fig.2B; p>0.05).

The NSF and cookie tests were used to measure depressive-like behaviors. The cookie test also includes an anhedonia-like component. In the NSF, we again observed a significant interaction between sex and treatment [F(2,48)=3.930, p<0.05] and a similar pattern of behavior in female mice, with acute (p<0.01) and chronic (p<0.01) α5-PAM treatment reducing latency to bite the food pellet compared to UCMS-vehicle treated animals. Again, no effect of either acute or chronic α5-PAM was observed in male mice (Fig.2C; p>0.05). In the cookie test, two-way ANOVA indicated a significant main effect of treatment [F(2,48)=3.504, p<0.05]. Follow-up comparisons uncovered a significant decrease in latency to bite the cookie in female mice following chronic α5-PAM administration (p<0.01) and a trend for acute treatment to reduce latency to bite (p=0.086). No significant difference in latency to bite was observed in male mice after acute or chronic α5-PAM treatment (Fig.3D).

Neither sex [F(1,48)=1.344, p>0.05] nor α5-PAM treatment [F(2,48)=1.721,p>0.05] altered the percentage of weight lost after 24 hours of food deprivation prior to the NSF test with no interaction between the two factors (Fig.3E; F(2,48)=1.775, p>0.05). Likewise, there was no effect of treatment on the amount of normal chow consumed in the home cage eight minutes after the NSF [Fig.3F; F(2,48)=1.441, p>0.05], though males did consume more relative to females

[F(1,48)=4.061, p<0.05]. Together, this suggests that differences in latency to bite are not due to a non-specific effect of treatment on hunger.

Although not statistically significant at 30min, pharmacokinetic data indicate greater accumulation of α5-PAM in the brain of female compared to male mice during the first 30min post injection (Fig.1). Therefore we tested a 25% higher dose (37.5mg/kg) in males. We found it also failed to reduce UCMS-induced anxiety- and anhedonia-/depressive-like behavior (Fig.S2). Finally, for locomotor activity, a two-way ANOVA revealed no significant effect of sex [Fig.S1E; F(1,48)=1.747, p>0.05] or treatment [F(2,47)=2.94, p<0.05], and no interaction [F(2,48)=1.36, p>0.05] between the two factors.

Together, these data indicate that acute and chronic treatments with α5-PAM result in a rapid reduction in stress-induced anxiety-like and anhedonia-like behaviors in female but not in male mice, without locomotion side–effects.

3.3. α5-PAM reduces UCMS-induced emotionality-like behavior in female mice to control non-stressed levels

The first studies tested whether treatment with α5-PAM has anxiolytic- or antidepressant-like activity in UCMS-exposed mice. We next sought to confirm these findings in an independent cohort of female mice, and further test whether acute or chronic treatment with α5-PAM could reverse UCMS-induced emotionality behaviors to levels measured in non-stressed control mice. In the EPM, no significant effect of either stress or treatment was found for time spent in the open arms [Fig.3A; F(3,66)=2.416, p>0.05]. A significant effect of treatment was observed in the percentage of crosses an animal made into the open arms [F(3,66)=5.069, p<0.01]. Pairwise comparisons indicate that UCMS-vehicle treated animals spent a smaller percentage of time in the open arms compared to non-stressed vehicle animals (Fig.3B; p<0.001). In the OFT, mice treated chronically with α5-PAM spent more time (Fig.3C; p<0.001) and had a higher percentage of their total distance traveled (Fig.3D; p<0.01) in the center of the arena compared to vehicle-

treated UCMS-exposed animals. A trend toward an increase in time spent in the center was also observed following acute α5-PAM treatment (Fig.3C; p=0.085).

In the NSF test, a significant effect of treatment was observed in the latency to bite the food pellet [F(3,66)=7.261, p<0.001]. Pairwise comparisons indicate that UCMS-vehicle treated animals took longer to bite the food pellet than non-stressed vehicle animals (p=0.010), and that both acute (p<0.001) and chronic (p<0.01) α5-PAM treatments reduced the latency to bite compared to UCMS-vehicle mice (Fig.3E). In the cookie test, there was a significant effect of treatment [F(3,66)=3.065, p<0.05] with *post hoc* comparisons revealing both acute (p<0.05) and chronic (p<0.05) α5-PAM treatment significantly reduced the latency to bite the cookie (Fig.3F). An overall Z-score was then calculated to assess the consistency of behaviors across tests. An effect of treatment on Z-emotionality score [F(3,66)=7.125, p<0.001] was observed, with pairwise comparisons highlighting an increase in emotionality behavior of UCMS-vehicle treated animals compared to non-stressed vehicle animals (p<0.001). Acute (p<0.001) and chronic (p<0.001) α5-PAM treatment significantly reduced Z-emotionality scores compared to the UCMS-vehicle group, hence confirming the prior results in female mice (Fig.2). Neither group were statistically different from the non-stressed vehicle group (Fig.3G; p>0.05).

3.4. α5-PAM fails to reduce anxiety- and depressive-like behaviors induced by combined isolation housing and UCMS in male mice

Given the inherent variability of the UCMS paradigm and the fact that the UCMS-induced phenotype can be more robust in female compared to male mice (Guilloux *et al*, 2011), we conducted an experiment in which male mice were single-housed during the final two weeks of UCMS, in order to potentiate the anxiety- and depressive-like UCMS-induced phenotypes (Ma *et al*, 2011). We detected a moderate positive correlation between Z-anxiety scores in these two tests (Fig.4A; R=0.273, F(34)=2.747, p=0.11), which combined show that UCMS-exposed and single–housed male mice exhibited a nearly-significant trend toward elevated anxiety-like

behavior (Fig.4B; $t(22)=1.619$, $p=0.06$). The combination of UCMS and social isolation also increased latency to bite a food pellet in the NSF (Fig.4C; $t(22)=2.088$, $p<0.05$), and latency to bite in the cookie test (Fig.4D; $t(22)=2.075$, $p<0.05$) relative to non-stressed vehicle-treated animals. Consistent with our prior observations, chronic treatment with α5-PAM did not alter the UCMS-induced behavioral phenotype of male mice in either the EPM, OFT, NSF or cookie test (Fig.4A-D; $p>0.05$). Emotionality z-scores indicated that combined UCMS and isolation housing robustly increases emotionality behavior in male mice compared to non-stressed controls (Fig.4E; $t(22)=3.101$, $p<0.01$), and confirmed the lack of effect of chronic α5-PAM treatment in male mice ($p>0.05$).

3.5. α5-PAM administration upregulates expression of the Gabra5 transcript in frontal cortex and hippocampus of female mice, but does not alter total or surface hippocampal Gabra5 protein levels

To evaluate the possibility that differing α5-subunit expression at baseline might explain the sex-specific behavioral effects of treatment, we assessed levels of *Gabra5* gene and protein expression within the frontal cortex and hippocampus of treated and untreated UCMS-exposed mice. Results show no difference in expression in either the prelimbic cortex or hippocampus as a factor of sex following UCMS exposure (Fig.5A-B, black bars; $p>0.05$). In frontal cortex, we observed a significant interaction between sex and treatment [$F(2,32)=3.508$, $p<0.05$], with *post hoc* comparisons indicating that acute α5-PAM treatment significantly increased *Gabra5* transcript expression in female mice (Fig.5A; $p<0.01$). No effect of chronic treatment was observed in male or female mice, though a non-significant increase was observed in female mice relative to vehicle treatment ($p=0.11$). In hippocampus, we again observed an interaction between sex and treatment [$F(2,26)=4.45$, $p<0.05$], with pairwise comparisons highlighting an increase in *Gabra5* expression in females after chronic α5-PAM treatment (Fig.5B; $p<0.01$). No changes in *Gabra5* expression were observed in males after either acute or chronic α5-PAM treatment ($p>0.05$). We

next sought to determine whether changes in RNA expression corresponded to *Gabra5* protein levels. We focused on the hippocampus due to high α5 levels in that region. We detected no difference in either total or surface *Gabra5* protein expression following either acute or chronic α5-PAM treatment in female (Fig.6A-B; $p>0.05$) or male mice (Fig.6C-D; $p>0.05$).

4. Discussion

4.1. Treatment with α5-PAM reduces anxiety- and anhedonia-/depressive-like behavior in female, but not male mice

We demonstrate that treatment with a $GABA_A$ receptor positive allosteric modulator with high affinity for α5 subunit-containing subtype (α5-PAM) (Savic *et al*, 2010) results in a rapid reduction in anxiety- and depressive-like behaviors in female mice exposed to UCMS (Fig.2&3). Moreover Z-normalization across tests suggests that both acute or chronic α5-PAM treatment was sufficient to reverse UCMS-induced anxiety- and depressive-like behaviors to WT levels, suggesting a rapid and sustained pharmacological effect (Fig.2&3). In contrast, treatment with α5-PAM did not alter either anxiety- or depressive-like behaviors in male mice (Fig.2&4). Results in both female and male mice were observed in two consecutive and separate cohorts. Importantly, the fact that acute and chronic α5-PAM treatment were effective in blocking UCMS-induced behavioral emotionality in female mice (Fig.2&3) raises the possibility that targeting the α5-containing $GABA_A$ receptors could have rapid anxiolytic and antidepressant effects.

Pharmacokinetic studies (Fig.1) show that the sex-specific behavioral differences were not explained by sex-dependent drug availability. Females displayed time-dependent elevated α5-PAM plasma levels compared to males (Fig.1). However, no effect of α5-PAM was observed in males at times when plasma levels were similar to females (30min; Fig.1) or when a 25% higher dose of α5-PAM was used (Fig. S2). Note that, even at Tmax, the estimated free brain concentrations in males (273nM) and females (313nM) were several times lower than the reported Ki values of α5-PAM at non-α5-$GABA_A$ receptors (Savic *et al*, 2010), thus demonstrating

selectivity of modulatory action of the ligand on mouse behavior in the used settings. Despite slight differences in the effect of acute versus chronic treatment (Fig.3A-D, S1), the data were qualitatively consistent across cohorts of mice in both sexes (Fig.2,3).

4.2. Sex-dependent effects of α5-PAM treatment parallel human sex-dependent molecular deficits and highlight modulation of extrasynaptic $GABA_A$ as a potential novel therapeutic modality

The observed sex difference in preclinical testing is potentially clinically interesting since women are twice as likely than men to experience a single episode of depression (Kessler, 2003) and display higher morbidity risk (Piccinelli and Wilkinson, 2000). These differences are not explained by diagnostic criteria, suggesting a biological predisposition in women (Angst and Dobler-Mikola, 1984). Interestingly, evidence suggest that dysfunction in SST interneurons may be more robust in females. In two frontocortical regions critical for emotion regulation, the sgACC and dlPFC, decreases in markers of dendritic targeting interneurons were more pronounced in female MDD compared to male MDD subjects and their matched controls (Seney *et al*, 2013; Sibille *et al*, 2010; Tripp *et al*, 2011; Tripp *et al*, 2012). This decrease in SST expression spanned all cortical layers of the sgACC in MDD subjects with greater effect sizes and significance in female subjects, suggesting a cellular vulnerability affecting all cortical SST neurons in MDD and more robustly in females (Seney *et al*, 2014).

In Lin & Sibille (2015), we showed that UCMS specifically affects expression of SST and GABA synthesizing molecules in SST neurons. The current pharmacological and behavioral results indicate that compounds that enhance α5-$GABA_AR$ mediated inhibition postsynaptic to SST cells may overcome or bypass the impact of the intrinsic vulnerability of SST cells to stress. That the potential therapeutic action of α5-PAM involves these cortical deficits is causally supported by our finding that acute treatment with α5-PAM upregulates expression of the *Gabra5* gene exclusively in female mice within the prelimbic cortex (homologous to the human sgACC). The lack of observed differences in α5 protein level may reflect the limitations and sensitivity of

the assays. In frontal cortex, low expression of total α5 protein precluded our ability to compare transcript and protein levels. In the hippocampus, where α5 mRNA and protein are highly expressed, we observed an increase in transcript expression following chronic α5-PAM treatment with no change in total or surface protein (Fig.5B & 6B), although a nominal non-significant increase was observed in males. Contributing to this discrepancy may be the 5-6 fold increase in protein half-life relative to mRNA, which results in much more dynamic mRNA regulation (Schwanhausser *et al*, 2011), or simply that at the time of sacrifice, translation of the α5 transcript was not elevated. It is worth noting that chronic α5-PAM treatment in female mice produced anhedonic- and anxiolytic-like effects with no down-regulation of the *Gabra5* transcript, commonly observed following chronic benzodiazepine administration (Uusi-Oukari and Korpi, 2010), which potentially explains the development of drug tolerance to benzodiazepine-like pan-$GABA_A$ receptor modulators (Vinkers and Olivier, 2012). In fact, sustained upregulation of α5 protein has been reported after exposure to anesthetics that act primarily as $GABA_A$ receptor modulators (Zurek *et al*, 2014). These findings highlight the specificity of α5-PAM for α5-subunit containing $GABA_A$ receptors and may alleviate concerns regarding a decrease in efficacy following chronic treatment.

Converging evidence from clinical data suggests an involvement of extrasynaptic $GABA_A$ receptors in psychiatric illness. Linkage studies have identified a susceptibility locus within the *GABRA5* gene (15q11-q13) for bipolar depression (Kato, 2007; Otani *et al*, 2005). Post-mortem studies have further examined the link between *GABRA5* gene expression and depression, with mixed findings. In the ACC and dlPFC, data suggest that expression of the *GABRA5* gene is increased in cortical layers 2-6 of subjects with bipolar depression and those with MDD (Choudary *et al*, 2005). In post-mortem dlPFC tissue from depressed suicides, no difference in *GABRA5* expression was observed (Merali *et al*, 2004). Similarly, in the amygdala of female post-mortem subjects, where decreases in SST and other GABA interneuron markers are present, no change in *GABRA5* gene expression was observed between MDD and matched controls (Guilloux *et al*,

2012). While this is the first study to demonstrate anxiolytic- and antidepressant-like effects of a selective α5-PAM compound, other studies have found that compounds with mixed α5 and α2 specificity do have anxiolytic effects in rodents (Savic *et al*, 2008; Savic *et al*, 2010). Moreover a recent study in the amygdala suggests that generalization of fear and anxiety is mediated by α5-subunit containing neurons in the central nucleus of the amygdala (Botta *et al*, 2015). Taken together, the data support a potential role for the α5-$GABA_A$ receptor in mood disorders, including anxiety and depression, though it is an area to study further, especially as it pertains to potential sex differences.

Data characterizing the expression of α5-$GABA_A$ receptors in a rodent model of depression are sparse, and our report is the first to examine potential sex-specific effects. Previous reports suggest that expression of the α5-subunit is increased in the frontal cortex following prolonged social isolation in male mice (Matsumoto *et al*, 2007). Expression of another extrasynaptic $GABA_A$ receptor subunit, the δ-subunit, is also increased after social isolation, a finding that correlates with increased tonic inhibition (Serra *et al*, 2006). A notable difference however is that the δ-subunit is not restricted to the dendritic compartment, as is the case for the α5-containing $GABA_A$ receptors (see **Introduction**). Interestingly, expression of extrasynaptic δ-$GABA_A$ receptor is modulated across the estrous cycle and sensitive to the neurosteroid progesterone (Maguire *et al*, 2005). Expression of extrasynaptic $GABA_A$ receptors is decreased at parturition and increased postpartum, providing support for hormonal modulation of these extrasynaptic receptors. Together, these preclinical data support the involvement of extrasynaptic $GABA_A$ receptors in the stress response and indicate sex-specific regulation of receptor expression.

4.3. Conclusions and therapeutic potential of targeting α5-containing $GABA_A$ receptors

Here we demonstrate that a $GABA_A$ α5-selective PAM can reverse anxiety- and depressive-like behavior induced by UCMS to non-stressed levels when administered acutely and

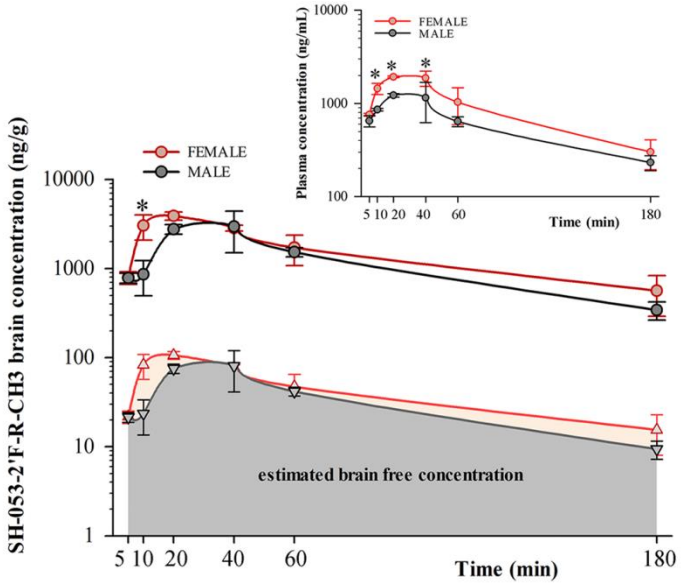
chronically to female mice (Fig.2 & 3). The effect on anxiety-like behaviors in females was mild and required behavioral z-score normalization across tests to identify consistent behavioral responses, but it was confirmed across two independent cohorts (Fig.2-3). By contrast, we observed a consistent lack of effect in male mice across separate cohorts and regardless of treatment regimen or dose (Fig.4 & S2). This lack of effect in males was not explained by pharmacokinetic differences (Fig.1). These data confirm previous reports that indicate a lack of anxiogenic/anxiolytic properties of α5-subunit modulation in male rodents either pharmacologically (Savic *et al*, 2008; Savic *et al*, 2010) or genetically (Collinson *et al*, 2002). Interestingly, a recent study in male rats found that two negative allosteric modulators (NAM) selective for the α5-subunit could reverse stress-induced anhedonia and deficits in AMPAR-mediated synaptic transmission within the hippocampus (Fischell *et al*, 2015). While these findings appear at odds with the data presented here, preclinical studies suggesting anxiogenic effects of α5-NAMs (Botta *et al*, 2015; Navarro *et al*, 2002), and of clinical and human post-mortem literature, they are in accordance with the actions of the rapid-acting antidepressant ketamine (Autry *et al*, 2011; Berman *et al*, 2000; Li *et al*, 2010). Together, these studies suggest that basal GABA tone or baseline cellular activity, for which sex may be a mediating factor, may influence which type of α5-modulator (positive or negative) may produce a therapeutic benefit. Support for this contention comes from the finding that while α5 $GABA_A$ receptor NAMs enhance memory in young rats, positive modulation is necessary to improve memory in older rats with excessive hippocampal activity and decreases in α5 transcript expression (Haberman *et al*, 2011; Koh *et al*, 2013). We believe that the same principle may exist in the UCMS condition, where animals are in a low GABA state due to dysfunction of SST cells, and potentially in MDD where low GABA content and dendritic targeting interneuron dysfunction is observed in analogous brain regions.

In summary, the present study supports the hypothesis that enhancing signaling specifically at α5-$GABA_A$ receptors may represent a novel therapeutic approach for mood disorders, including anxiety and depression, with the notable feature of rapid onset. Interestingly,

this treatment approach may be more beneficial to women, who are more severely affected by MDD. Future experiments should further explore the sex-dependent effects of treatment and propose the exact mechanism by which modulation of α5-$GABA_A$ receptors is exerting its effects in the UCMS condition.

Funding and Disclosure: The authors declare no conflict of interest. This work was supported by grants from the National Institute of Health (NIH) MH093723 (ES), MH096463 and HL118561 (JMC), and with the support of the Milwaukee Institute of Drug Discovery, and Bradley-Herzfeld Foundation (MMP and JC).

Acknowledgements: The authors would like to thank Jenna E Parrish for assistance in behavioral studies and Dr. Beverly Orser for careful comments on the manuscript.



	Male (Mean ± SEM)	Female (Mean ± SEM)
Plasma		
C_{max} (ng/mL)	1342.35 ± 171.13	2145.90 ± 201.16*
T_{max} (min)	26.66 ± 6.68	26.66 ± 6.68
$AUC_{0\text{-}3}$ (ng*h/mL)	1806.25 ± 210.79	2825.67 ± 563.59
$AUC_{0\text{-}\infty}$ (ng*h/mL)	2217.71 ± 238.16	3289.87 ± 786.27
β	0.61 ± 0.11	0.73 ± 0.09
$t_{1/2}$ (min)	71.90 ± 11.30	58.69 ± 7.96

	Male (Mean ± SEM)	Female (Mean ± SEM)
Brain		
C_{max} (ng/g)	3868.38 ± 942.19	4441.08 ± 308.71
T_{max} (min)	26.66 ± 6.68	16.66 ± 3.32
$AUC_{0\text{-}3}$ (ng*h/g)	3944.49 ± 560.30	4910.13 ± 1032.02
$AUC_{0\text{-}\infty}$ (ng*h/g)	4434.91 ± 490.89	5992.46 ± 1756.47
β	0.80 ± 0.18	0.72 ± 0.15
$t_{1/2}$ (min)	59.01 ± 15.84	64.36 ± 15.95
Estimated free concentration in T_{max} (nM)	272.60 ± 66.39	312.95 ± 21.75

Estimated brain free concentration in female
Estimated brain free concentration in male

Figure 1. Pharmacokinetic analysis of α5-PAM brain and plasma levels in female and male mice.

Measured plasma (inset) and estimated brain (main figure) concentration–time profiles of α5-PAM (30mg/kg) after intraperitoneal administration (n=3 per time point) in female and male mice. *p<0.05 between female and male mice in different time-points, according to Tukey post hoc test after two-way repeated ANOVA. The calculated plasma and brain pharmacokinetic parameters of α5-PAM are tabularly presented on the right. *p<0.05 between female and male mice according to t-test.

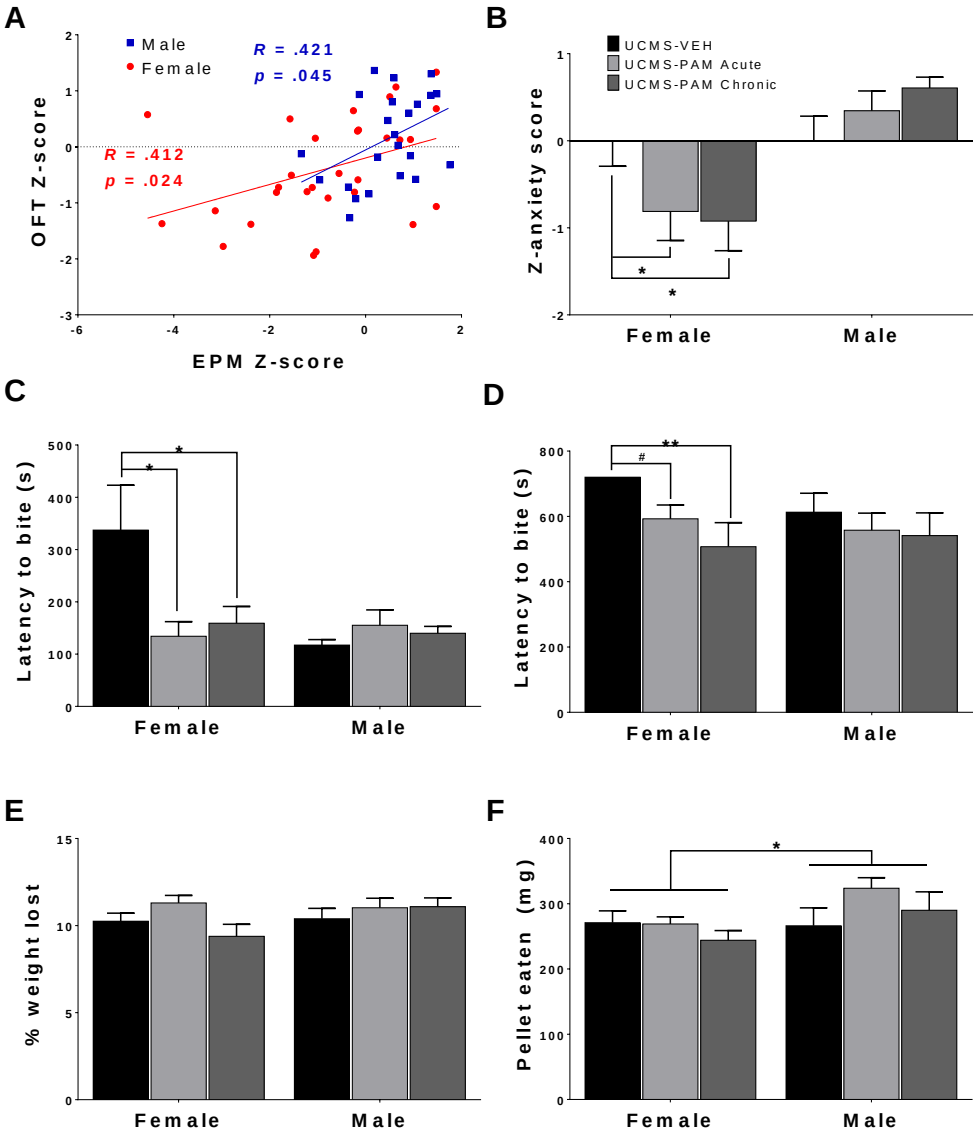


Figure 2. Effect of α5-PAM on anxiety- and depressive-like behavior induced by UCMS in female and male mice

A. Shown are significant positive correlations of Z-anxiety scores from the EPM and OFT. **B**. Female mice treated acutely and chronically with α5-PAM had reduced anxiety-like behavior across both tests while no effect of treatment was observed in male mice. **C**. Treatment with acute and chronic α5-PAM reduced latency to bite a food pellet in the NSF in female but not male mice. **D**. Chronic α5-PAM treatment reduced the latency to bite a piece of cookie in the cookie test in female mice, while a trend in the same direction was observed following acute treatment. No significant effect of α5-PAM was detected in males. **E.** No change in percentage of weight lost after 24 hour food deprivation after α5-PAM treatment. **F.** No change in amount of pellet consumed 5 minutes after the NSF test. *p<0.05, **p<0.01, ***p<0.001.

Figure 3

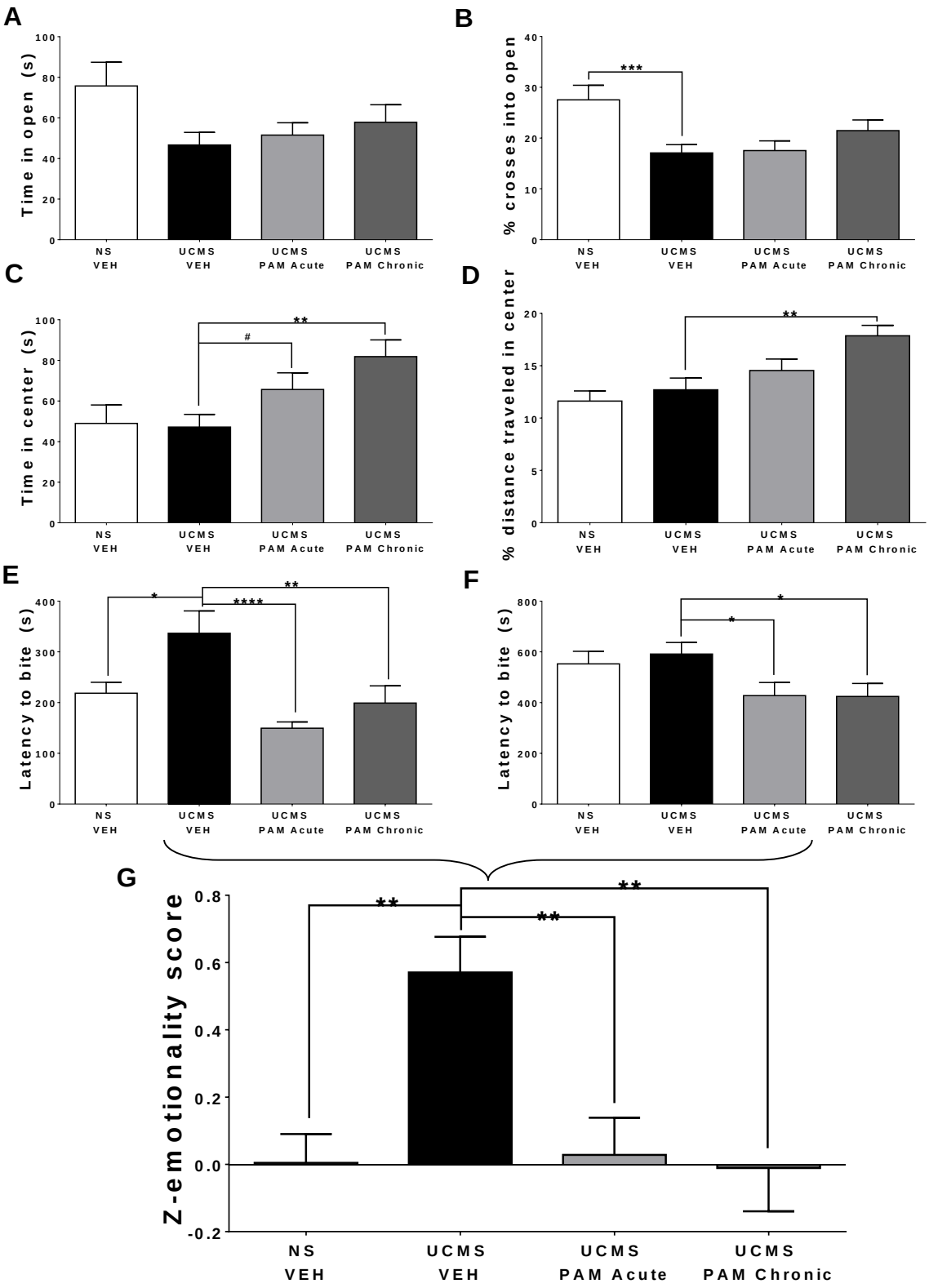

A
Time in open (s)
B
% crosses into open
C
Time in center (s)
D
% distance traveled in center
E
Latency to bite (s)
F
Latency to bite (s)
G
Z-emotionality score
NS VEH
UCMS VEH
UCMS PAM Acute
UCMS PAM Chronic

Figure 3. Treatment with α5-PAM normalizes anxiety- and depressive-like behavior induced by UCMS to non-stressed levels in female mice

A-B. UCMS reduced time spent in the open arms of the EPM. **C-D.** Chronic treatment with α5-PAM increased the amount of time spent and percentage of total distance traveled in the center of the open field, while a trend was observed for acute treatment to increase time in center. **E.** UCMS increased latency to bite in the NSF compared to NS-VEH treated animals, while both acute and chronic α5-PAM treatment reduced the increased latency following UCMS. **F.** Acute and chronic α5-PAM treatment reduced the latency to bite a piece of cookie in the cookie test compared to UCMS-VEH treated mice. **G.** Overall emotionality Z-score indicated an increase in emotionality in the UCMS-VEH treated mice that is normalized following acute and chronic α5-PAM administration. #p<0.1, *p<0.05, **p<0.01, ***p<0.001.

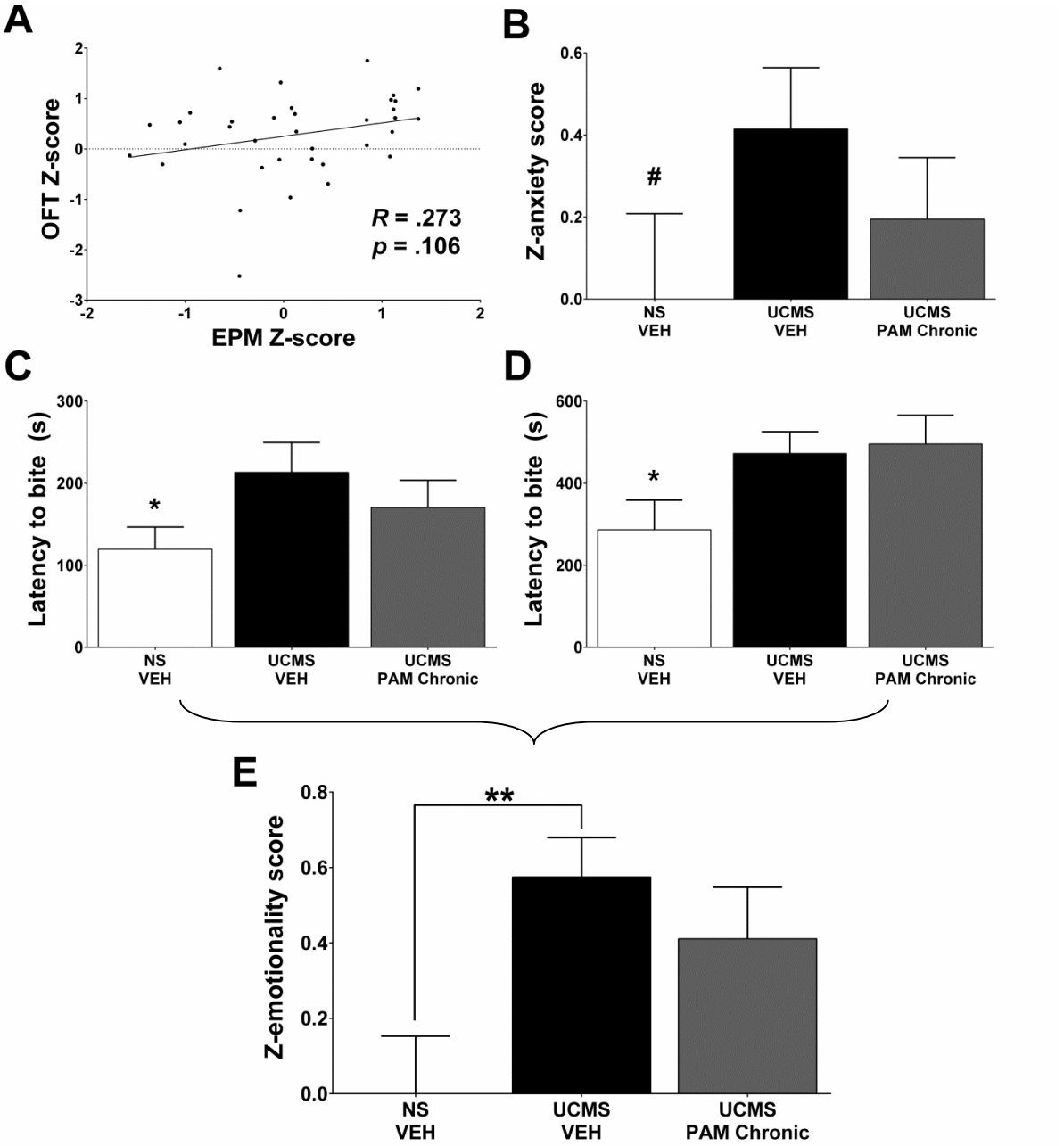


Figure 4. Chronic treatment with α5-PAM is ineffective at reducing anxiety- and depressive-like phenotypes induced by UCMS after the addition of isolation housing in male mice

A. Positive correlation in Z-anxiety scores observed in the EPM and OFT. **B.** UCMS increased Z-anxiety scores compared to NS-VEH animals, chronic α5-PAM treatment did not affect Z-anxiety scores. **C.** UCMS increases latency to bite in the cookie test relative to NS-VEH animals, no significant effect of α5-PAM administration. **D.** UCMS increases latency to bite a cookie while α5-PAM does not reduce this increased latency. **E.** Overall emotionality Z-scores are increased following UCMS-VEH treatment compared to NS-VEH mice. α5-PAM treatment does not mediate the increased emotionality induced by UCMS in male mice. #p<0.1, *p<0.05, **p<0.01, ***p<0.001.

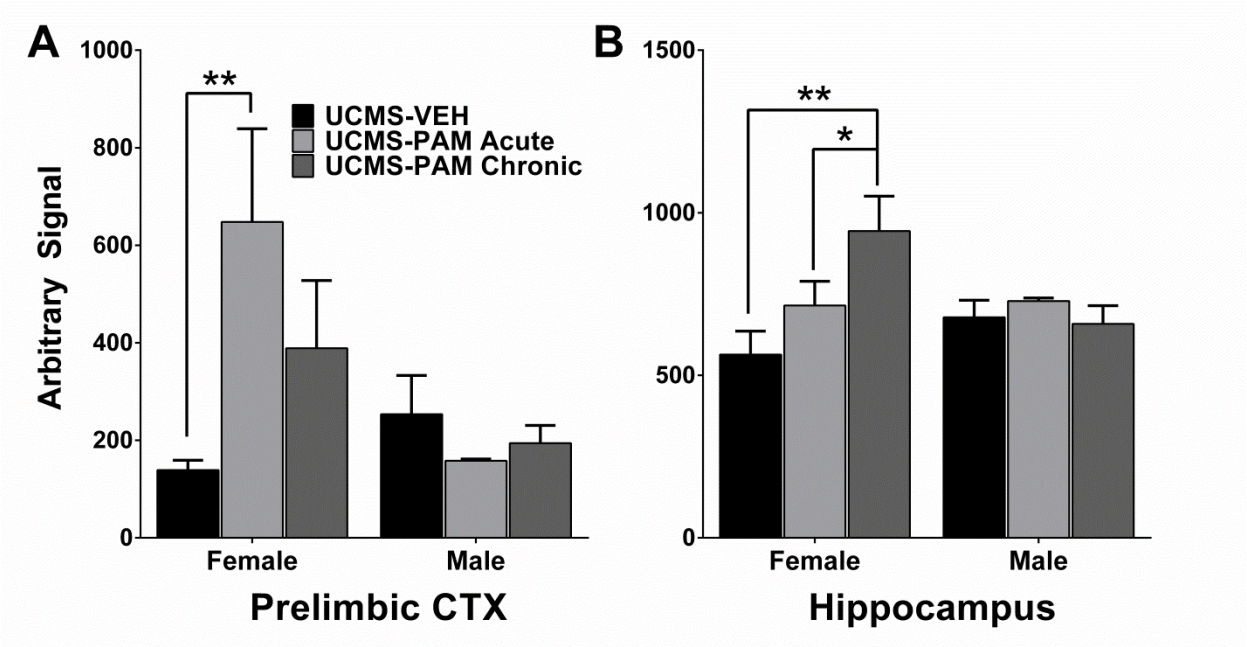


Figure 5. Treatment with α5-PAM increases Gabra5 transcript expression in the frontal cortex and hippocampus of female, but not male mice

A. Acute treatment with α5-PAM increases *Gabra5* expression in the frontal cortex of female mice exposed to UCMS. No change in *Gabra5* expression was observed following treatment in male mice. **B.** Chronic treatment with α5-PAM increases *Gabra5* expression in the hippocampus of female mice exposed to UCMS and compared to animals treated with α5-PAM acutely. No change in *Gabra5* expression was observed following either acute or chronic treatment in male mice. *p<0.05, **p<0.01.

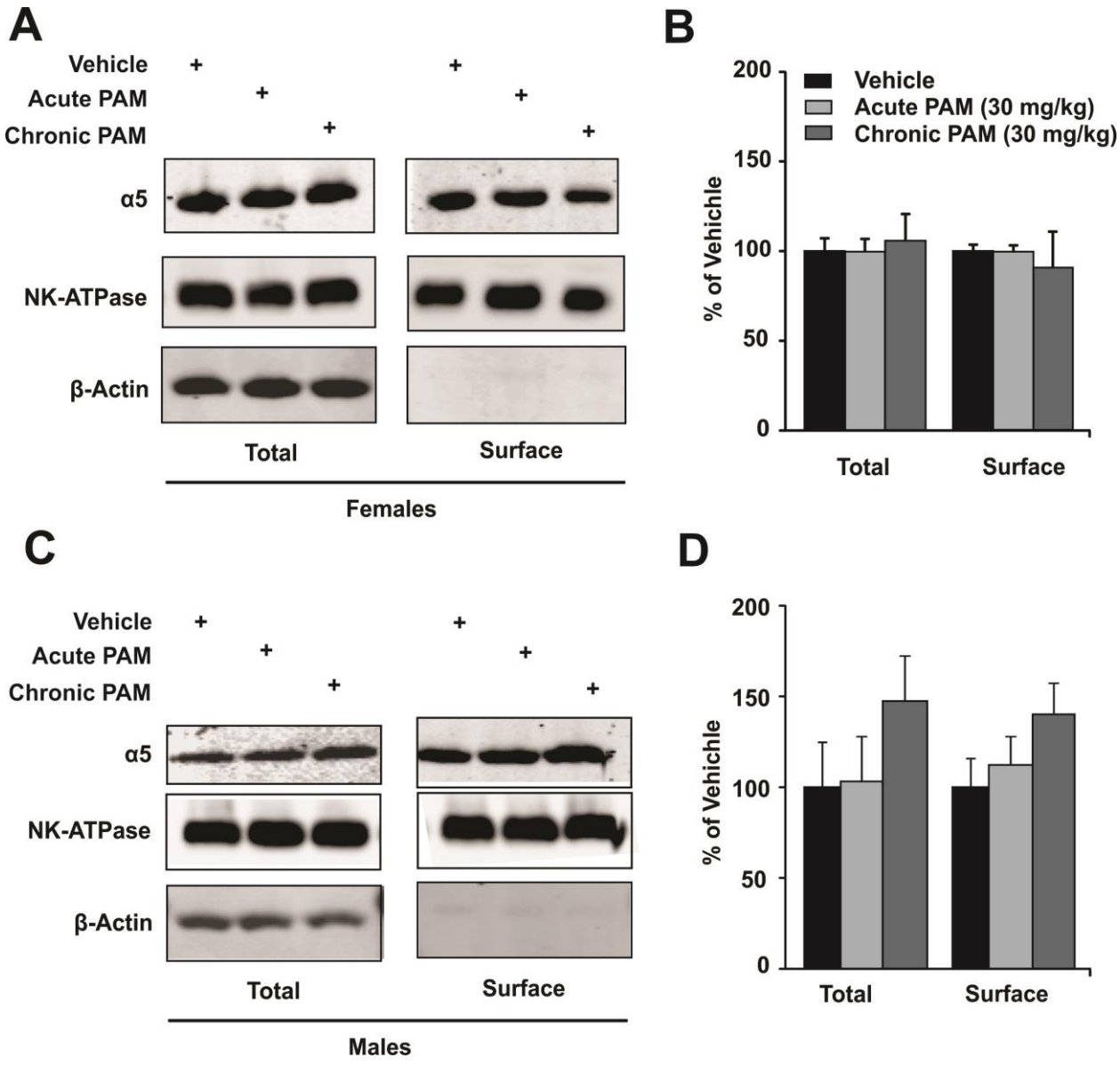


Figure 6. No change in either α5 subunit total or surface protein level in the hippocampus of male and female mice

A,**C.** Representative blots of two housekeeping proteins (NK-ATPase, β-Actin) as well as α5 at the surface and total protein levels following UCMS and either vehicle, acute, or chronic α5-PAM treatment in female (**A**) or male (**C**) mice. The absence of Actin signal in the "surface" lane indicates the selective enrichment in membrane proteins. **B**,**D**. No significant effect of treatment observed on either total or surface α5 protein in female (**B**) or male (**D**) mice.

References

Ali AB, Thomson AM (2008). Synaptic alpha 5 subunit-containing GABAA receptors mediate IPSPs elicited by dendrite-preferring cells in rat neocortex. *Cereb Cortex* **18**(6): 1260-1271.

Angst J, Dobler-Mikola A (1984). Do the diagnostic criteria determine the sex ratio in depression? *Journal of affective disorders* **7**(3-4): 189-198.

Autry AE, Adachi M, Nosyreva E, Na ES, Los MF, Cheng PF*, et al* (2011). NMDA receptor blockade at rest triggers rapid behavioural antidepressant responses. *Nature* **475**(7354): 91-95.

Bajbouj M, Lisanby SH, Lang UE, Danker-Hopfe H, Heuser I, Neu P (2006). Evidence for impaired cortical inhibition in patients with unipolar major depression. *Biol Psychiatry* **59**(5): 395-400.

Berman RM, Cappiello A, Anand A, Oren DA, Heninger GR, Charney DS*, et al* (2000). Antidepressant effects of ketamine in depressed patients. *Biol Psychiatry* **47**(4): 351-354.

Bonin RP, Martin LJ, MacDonald JF, Orser BA (2007). Alpha5GABAA receptors regulate the intrinsic excitability of mouse hippocampal pyramidal neurons. *J Neurophysiol* **98**(4): 2244-2254.

Botta P, Demmou L, Kasugai Y, Markovic M, Xu C, Fadok JP*, et al* (2015). Regulating anxiety with extrasynaptic inhibition. *Nat Neurosci* **18**(10): 1493-1500.

Brickley SG, Mody I (2012). Extrasynaptic GABA(A) receptors: their function in the CNS and implications for disease. *Neuron* **73**(1): 23-34.

Choudary PV, Molnar M, Evans SJ, Tomita H, Li JZ, Vawter MP*, et al* (2005). Altered cortical glutamatergic and GABAergic signal transmission with glial involvement in depression. *Proceedings of the National Academy of Sciences of the United States of America* **102**(43): 15653-15658.

Cipriani A, Furukawa TA, Salanti G, Geddes JR, Higgins JP, Churchill R*, et al* (2009). Comparative efficacy and acceptability of 12 new-generation antidepressants: a multiple-treatments meta-analysis. *Lancet* **373**(9665): 746-758.

Collinson N, Kuenzi FM, Jarolimek W, Maubach KA, Cothliff R, Sur C*, et al* (2002). Enhanced learning and memory and altered GABAergic synaptic transmission in mice lacking the alpha 5 subunit of the GABAA receptor. *J Neurosci* **22**(13): 5572-5580.

Earnheart JC, Schweizer C, Crestani F, Iwasato T, Itohara S, Mohler H*, et al* (2007). GABAergic control of adult hippocampal neurogenesis in relation to behavior indicative of trait anxiety and depression states. *J Neurosci* **27**(14): 3845-3854.

Edgar NM, Touma C, Palme R, Sibille E (2011). Resilient emotionality and molecular compensation in mice lacking the oligodendrocyte-specific gene Cnp1. *Transl Psychiatry* **1**: e42.

Ferrari AJ, Charlson FJ, Norman RE, Patten SB, Freedman G, Murray CJ*, et al* (2013). Burden of depressive disorders by country, sex, age, and year: findings from the global burden of disease study 2010. *PLoS medicine* **10**(11): e1001547.

Fischell J, Van Dyke AM, Kvarta MD, LeGates TA, Thompson SM (2015). Rapid Antidepressant Action and Restoration of Excitatory Synaptic Strength After Chronic Stress by Negative Modulators of Alpha5-Containing GABA Receptors. *Neuropsychopharmacology : official publication of the American College of Neuropsychopharmacology*.

Gilabert-Juan J, Castillo-Gomez E, Guirado R, Molto MD, Nacher J (2013). Chronic stress alters inhibitory networks in the medial prefrontal cortex of adult mice. *Brain Struct Funct* **218**(6): 1591-1605.

Guilloux JP, Douillard-Guilloux G, Kota R, Wang X, Gardier AM, Martinowich K*, et al* (2012). Molecular evidence for BDNF- and GABA-related dysfunctions in the amygdala of female subjects with major depression. *Mol Psychiatry* **17**(11): 1130-1142.

Guilloux JP, Seney M, Edgar N, Sibille E (2011). Integrated behavioral z-scoring increases the sensitivity and reliability of behavioral phenotyping in mice: Relevance to emotionality and sex. *J Neurosci Methods* **197**(1): 21-31.

Haberman RP, Colantuoni C, Stocker AM, Schmidt AC, Pedersen JT, Gallagher M (2011). Prominent hippocampal CA3 gene expression profile in neurocognitive aging. *Neurobiology of aging* **32**(9): 1678-1692.

Herman JP, Larson BR (2001). Differential regulation of forebrain glutamic acid decarboxylase mRNA expression by aging and stress. *Brain research* **912**(1): 60-66.

Isingrini E, Belzung C, Freslon JL, Machet MC, Camus V (2012). Fluoxetine effect on aortic nitric oxide-dependent vasorelaxation in the unpredictable chronic mild stress model of depression in mice. *Psychosomatic medicine* **74**(1): 63-72.

Isingrini E, Surget A, Belzung C, Freslon JL, Frisbee J, O'Donnell J*, et al* (2011). Altered aortic vascular reactivity in the unpredictable chronic mild stress model of depression in mice: UCMS causes relaxation impairment to ACh. *Physiol Behav* **103**(5): 540-546.

Kato T (2007). Molecular genetics of bipolar disorder and depression. *Psychiatry and clinical neurosciences* **61**(1): 3-19.

Kessler RC (2003). Epidemiology of women and depression. *Journal of affective disorders* **74**(1): 5-13.

Koh MT, Rosenzweig-Lipson S, Gallagher M (2013). Selective GABA(A) alpha5 positive allosteric modulators improve cognitive function in aged rats with memory impairment. *Neuropharmacology* **64**: 145-152.

Krystal JH, Sanacora G, Blumberg H, Anand A, Charney DS, Marek G*, et al* (2002). Glutamate and GABA systems as targets for novel antidepressant and mood-stabilizing treatments. *Molecular psychiatry* **7 Suppl 1**: S71-80.

Li N, Lee B, Liu RJ, Banasr M, Dwyer JM, Iwata M*, et al* (2010). mTOR-dependent synapse formation underlies the rapid antidepressant effects of NMDA antagonists. *Science* **329**(5994): 959-964.

Lin LC, Sibille E (2015). Somatostatin, neuronal vulnerability and behavioral emotionality. *Mol Psychiatry*.

Luscher B, Shen Q, Sahir N (2011). The GABAergic deficit hypothesis of major depressive disorder. *Mol Psychiatry* **16**(4): 383-406.

Ma XC, Jiang D, Jiang WH, Wang F, Jia M, Wu J*, et al* (2011). Social isolation-induced aggression potentiates anxiety and depressive-like behavior in male mice subjected to unpredictable chronic mild stress. *PloS one* **6**(6): e20955.

Maguire JL, Stell BM, Rafizadeh M, Mody I (2005). Ovarian cycle-linked changes in GABA(A) receptors mediating tonic inhibition alter seizure susceptibility and anxiety. *Nature neuroscience* **8**(6): 797-804.

Matsumoto K, Puia G, Dong E, Pinna G (2007). GABA(A) receptor neurotransmission dysfunction in a mouse model of social isolation-induced stress: possible insights into a non-serotonergic mechanism of action of SSRIs in mood and anxiety disorders. *Stress* **10**(1): 3-12.

Merali Z, Du L, Hrdina P, Palkovits M, Faludi G, Poulter MO*, et al* (2004). Dysregulation in the suicide brain: mRNA expression of corticotropin-releasing hormone receptors and GABA(A) receptor subunits in frontal cortical brain region. *J Neurosci* **24**(6): 1478-1485.

Navarro JF, Buron E, Martin-Lopez M (2002). Anxiogenic-like activity of L-655,708, a selective ligand for the benzodiazepine site of GABA(A) receptors which contain the alpha-5 subunit, in the elevated plus-maze test. *Prog Neuropsychopharmacol Biol Psychiatry* **26**(7-8): 1389-1392.

Northoff G, Sibille E (2014). Why are cortical GABA neurons relevant to internal focus in depression? A cross-level model linking cellular, biochemical and neural network findings. *Mol Psychiatry* **19**(9): 966-977.

Obradovic A, Joksimovic S, Poe MM, Ramerstorfer J, Varagic Z, Namjoshi O*, et al* (2014). Sh-I-048A, an in vitro non-selective super-agonist at the benzodiazepine site of GABAA receptors: the approximated activation of receptor subtypes may explain behavioral effects. *Brain research* **1554**: 36-48.

Otani K, Ujike H, Tanaka Y, Morita Y, Katsu T, Nomura A*, et al* (2005). The GABA type A receptor alpha5 subunit gene is associated with bipolar I disorder. *Neuroscience letters* **381**(1-2): 108-113.

Pabba M, Wong AY, Ahlskog N, Hristova E, Biscaro D, Nassrallah W*, et al* (2014). NMDA receptors are upregulated and trafficked to the plasma membrane after sigma-1 receptor activation in the rat hippocampus. *The Journal of neuroscience : the official journal of the Society for Neuroscience* **34**(34): 11325-11338.

Packer AM, McConnell DJ, Fino E, Yuste R (2013). Axo-dendritic overlap and laminar projection can explain interneuron connectivity to pyramidal cells. *Cerebral cortex* **23**(12): 2790-2802.

Piccinelli M, Wilkinson G (2000). Gender differences in depression. Critical review. *The British journal of psychiatry : the journal of mental science* **177**: 486-492.

Rajkowska G, O'Dwyer G, Teleki Z, Stockmeier CA, Miguel-Hidalgo JJ (2007). GABAergic neurons immunoreactive for calcium binding proteins are reduced in the prefrontal cortex in major depression. *Neuropsychopharmacology* **32**(2): 471-482.

Rush AJ (2010). Combining antidepressant medications: a good idea? *The American journal of psychiatry* **167**(3): 241-243.

Sanacora G, Gueorguieva R, Epperson CN, Wu YT, Appel M, Rothman DL*, et al* (2004). Subtype-specific alterations of gamma-aminobutyric acid and glutamate in patients with major depression. *Arch GenPsychiatry* **61**(7): 705-713.

Sanacora G, Mason GF, Rothman DL, Behar KL, Hyder F, Petroff OA*, et al* (1999). Reduced cortical gamma-aminobutyric acid levels in depressed patients determined by proton magnetic resonance spectroscopy. *Archives of general psychiatry* **56**(11): 1043-1047.

Savic MM, Huang S, Furtmuller R, Clayton T, Huck S, Obradovic DI*, et al* (2008). Are GABAA receptors containing alpha5 subunits contributing to the sedative properties of benzodiazepine site agonists? *Neuropsychopharmacology : official publication of the American College of Neuropsychopharmacology* **33**(2): 332-339.

Savic MM, Majumder S, Huang S, Edwankar RV, Furtmuller R, Joksimovic S*, et al* (2010). Novel positive allosteric modulators of GABAA receptors: do subtle differences in activity at alpha1 plus alpha5 versus alpha2 plus alpha3 subunits account for dissimilarities in behavioral effects in rats? *Progress in neuro-psychopharmacology & biological psychiatry* **34**(2): 376-386.

Schwanhausser B, Busse D, Li N, Dittmar G, Schuchhardt J, Wolf J*, et al* (2011). Global quantification of mammalian gene expression control. *Nature* **473**(7347): 337-342.

Seney ML, Chang LC, Oh H, Wang X, Tseng GC, Lewis DA*, et al* (2013). The Role of Genetic Sex in Affect Regulation and Expression of GABA-Related Genes Across Species. *Front Psychiatry* **4**: 104.

Seney ML, Tripp A, McCune S, Lewis D, Sibille E (2014). Laminar and cellular analyses of reduced somatostatin gene expression in the subgenual anterior cingulate cortex in major depression. *Neurobiol Dis* **73C**: 213-219.

Serra M, Mostallino MC, Talani G, Pisu MG, Carta M, Mura ML*, et al* (2006). Social isolation-induced increase in alpha and delta subunit gene expression is associated with a greater efficacy of ethanol on steroidogenesis and GABA receptor function. *Journal of neurochemistry* **98**(1): 122-133.

Shen Q, Lal R, Luellen BA, Earnheart JC, Andrews AM, Luscher B (2010). gamma-Aminobutyric acid-type A receptor deficits cause hypothalamic-pituitary-adrenal axis hyperactivity and antidepressant drug sensitivity reminiscent of melancholic forms of depression. *Biol Psychiatry* **68**(6): 512-520.

Sibille E, Morris HM, lewis DA (2010). GABA-related Transcripts in the Dorsolateral Prefrontal Cortex in Mood Disorders. *submitted*.

Soumier A, Sibille E (2014). Opposing Effects of Acute Versus Chronic Blockade of Frontal Cortex Somatostatin-Positive Inhibitory Neurons on Behavioral Emotionality in Mice. *Neuropsychopharmacology : official publication of the American College of Neuropsychopharmacology*.

Tripp A, Kota RS, Lewis DA, Sibille E (2011). Reduced somatostatin in subgenual anterior cingulate cortex in major depression. *Neurobiol Dis* **42**(1): 116-124.

Tripp A, Oh H, Guilloux JP, Martinowich K, Lewis DA, Sibille E (2012). Brain-derived neurotrophic factor signaling and subgenual anterior cingulate cortex dysfunction in major depressive disorder. *Am J Psychiatry* **169**(11): 1194-1202.

Uusi-Oukari M, Korpi ER (2010). Regulation of GABA(A) receptor subunit expression by pharmacological agents. *Pharmacological reviews* **62**(1): 97-135.

Vinkers CH, Olivier B (2012). Mechanisms Underlying Tolerance after Long-Term Benzodiazepine Use: A Future for Subtype-Selective GABA(A) Receptor Modulators? *Advances in pharmacological sciences* **2012**: 416864.

Wainwright A, Sirinathsinghji DJ, Oliver KR (2000). Expression of GABA(A) receptor alpha5 subunit-like immunoreactivity in human hippocampus. *Brain research Molecular brain research* **80**(2): 228-232.

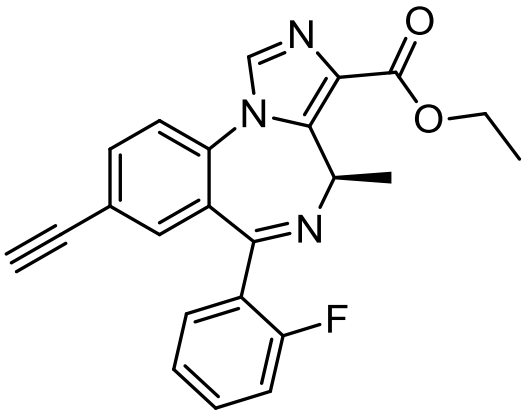
Zarate CA, Jr., Brutsche N, Laje G, Luckenbaugh DA, Venkata SL, Ramamoorthy A*, et al* (2012a). Relationship of ketamine's plasma metabolites with response, diagnosis, and side effects in major depression. *Biological psychiatry* **72**(4): 331-338.

Zarate CA, Jr., Brutsche NE, Ibrahim L, Franco-Chaves J, Diazgranados N, Cravchik A*, et al* (2012b). Replication of ketamine's antidepressant efficacy in bipolar depression: a randomized controlled add-on trial. *Biological psychiatry* **71**(11): 939-946.

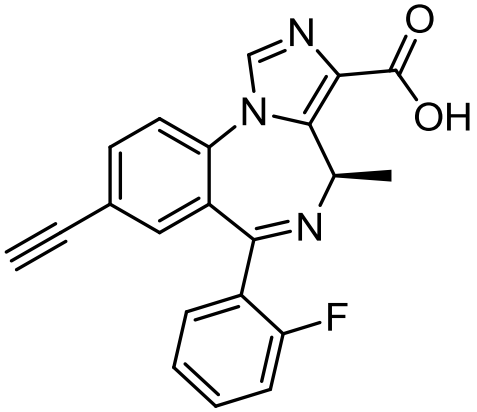
Zurek AA, Yu J, Wang DS, Haffey SC, Bridgwater EM, Penna A*, et al* (2014). Sustained increase in alpha5GABAA receptor function impairs memory after anesthesia. *J Clin Invest* **124**(12): 5437-5441.

APPENDIX H. Manuscript Prepared by Margot Ernst, *et al.* on the Effects of α5-GABA$_A$R Positive Allosteric Modulators in Bronchodilation.

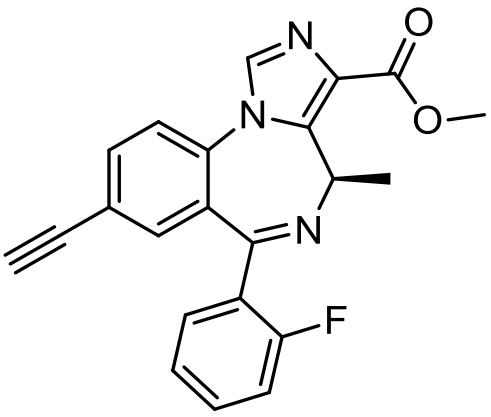
Structures:



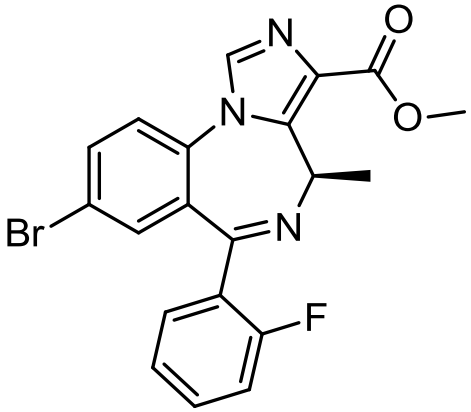
SH-053-2'F-R-CH$_3$



SH-053-2'F-R-CH$_3$-Acid



MP-III-004



MP-III-058

Imidazobenzodiazepines with improved $GABA_A$ $\alpha 5$ subunit selectivity, and their effect on airway smooth muscle relaxation

Roshan Puthenkalam, Marco Treven, Joachim Ramerstorfer, Friederike Steudle, Petra Scholze, George Gallos, Michael M. Poe, Kashi Reddy Methuku, Guanguan Li, Werner Sieghart, Anja Santrac, Miroslav Savic, Charles W. Emala, James M. Cook, and Margot Ernst

Center for Brain Research, Medical University of Vienna, Vienna, Austria (R.P., M.T., J.R., F.S., P.S., W.S., M.E.); Department of Chemistry and Biochemistry, University of Wisconsin-Milwaukee, Milwaukee, Wisconsin, United States (M.M.P., K.R.M., G.L., J.M.C.); Department of Anesthesiology, College of Physicians and Surgeons, Columbia University, New York, New York, United States (C.W.E.); Department of Pharmacology, Faculty of Pharmacy, University of Belgrade, Belgrade, Serbia (A.S., M.S.)

Running title

ABBREVIATIONS:

2-AG, 2-arachidonoyl glycerol; ASM, airway smooth muscle; BBB, blood brain barrier; CNS, central nervous system; NAM, negative allosteric modulator; PAM, positive allosteric modulator; SAM, silent allosteric modulator.

Numbers

Number of Pages

Number of Figures

Number of Tables

Number of References

Number of words in Abstract

Number of words in Introduction

Number of words in Discussion

Address correspondence to

Abstract

Visual Abstract

Introduction

$GABA_A$ receptors are GABA-gated chloride channels which are expressed in neurons, glial cells and several non-neuronal cell types (Gladkevich *et al.*, 2006; Olsen and Sieghart, 2008; Barragan *et al.*, 2015; Mizuta et al. 2008; Wan *et al.*, 2015) where they influence a variety of cellular processes through ligand-gated chloride flux. These receptors are pentamers of subunits that can belong to different subunit classes. The existence of six α, three β, three γ, the δ, ε, θ, π, and three ρ subunits in mammalian systems gives rise to an enormous diversity of $GABA_A$ receptor subtypes with distinct subunit composition and different pharmacological properties (Olsen and Sieghart, 2008).

$GABA_A$ receptors of the central nervous system (CNS) are the site of action of a variety of pharmacologically and clinically important drugs such as benzodiazepines, barbiturates, anesthetics and convulsants that allosterically modulate GABA-induced currents (Sieghart *et al.*, 2012; Sieghart, 2015). In addition to these synthetic drugs, a wide range of natural products (Khom *et al.*, 2010, Lorenz *et al.*, 2010; Hanrahan *et al.*, 2011) as well as some endogenous agents, such as neuroactive steroids (Belelli and Lambert, 2005), the endocannabinoid 2-AG ~~(Baur, Kielar, Richter, Ernst, Gerhard F Ecker, *et al.*, 2013~~), histamine (Saras *et al.*, 2008; Fleck *et al.*, 2012) and dopamine (Hoerbelt *et al.*, 2015) modulate $GABA_A$ receptors.

The best characterized site of drug action on $GABA_A$ receptors is the benzodiazepine binding site located at the extracellular α+/γ– interface of the receptors (Sigel and Lüscher, 2011; Richter *et al.*, 2012). Thus, their potency and efficacy is dependent on the subtype of both these subunits. In the CNS, benzodiazepine ligands exert mostly sedative-hypnotic, anxiolytic, ataxic, anticonvulsive and myo-relaxant properties (Sieghart, 2015). Studies on genetically modified mice carrying a point mutation at single types of α subunits, which renders the respective receptors insensitive to diazepam, revealed that benzodiazepine-induced behavioral responses seem to be predominantly mediated by $GABA_A$ receptors containing specific α subunits in distinct neuronal circuits (Rudolph *et al.*, 1999). Drugs

specifically interacting with certain $GABA_A$ receptor subtypes were thus expected to exhibit quite selective behavioral and pharmacological effects (Möhler, 2011). .

Due to the high similarity between the $\alpha 1,2,3$ and $\alpha 5$ subunits, the selective binding of compounds might not be attainable for all subtypes. However, the concept of efficacy-selectivity (also sometimes referred to as functional selectivity) has gained attention in recent years (Rudolph and Knoflach, 2011). This in turn has led to the development of ligands which bind to several subtypes with comparable affinity, but are "silent" allosteric modulators (SAM), or very weak allosteric modulators (near-SAM) at some subtypes, while acting as positive or negative allosteric modulators (PAM, NAM) at other subtypes (Rudolph and Knoflach, 2011). A pharmacophore based approach (He *et al.*, 1999; Huang *et al.*, 2000; Clayton *et al.*, 2007, 2015; Harris *et al.*, 2008) has led to an $\alpha 5-$ preferring chiral imidazobenzodiazepine SH-053-R-CH3 ((*R*)-ethyl-8-ethynyl-4-methyl-6-phenyl-4*H*-benzo[*f*]imidazo[1,5-*a*][1,4]diazepine-3-carboxylate) with pronounced binding and functional preference for the $\alpha 5$ subtype (Clayton *et al.*, 2007), and later a F-substituted analogue, SH-053-2'F-R-CH3 , was reported to display higher affinity (Savic et al. 2010).

Clinically applied $GABA_A$ receptor targeting drugs are currently mainly used for their various effects on the human CNS (Sieghart, 2015); however, considerable interest in these receptors expressed in peripheral tissues as potential therapeutic targets has emerged ((Gladkevich *et al.*, 2006; Barragan *et al.*, 2015; Wan *et al.*, 2015; Mizuta et al. 2008 ~~Yocum *et al.*, 2015~~) Sengupta *et al.*, 2014; Gallos *et al.*, 2015). Here we focus on $GABA_A$ receptors expressed in airway smooth muscle and their ability to induce relaxation of an established contraction which could have enormous clinical implications in bronchoconstrictive diseases such as asthma. In these cells, a restricted panel of subunits has been found and includes $\alpha 4$, $\alpha 5$, $\beta 3$, $\gamma 1-3$, δ, π, and θ (Mizuta *et al.*, 2008) subunits. So far, the composition, stoichiometry and arrangement of $GABA_A$ receptors that are expressed in these cells have not been identified. It was shown recently, however, that the $\alpha 5-$ preferring chiral imidazobenzodiazepine SH-053-2'F-R-CH3 relaxes airway smooth muscle (ASM) and

enhances chloride currents in cultured ASM cells (Gallos *et al.*, 2015), thus suggesting that benzodiazepine sensitive, $\alpha 5-$ containing receptors are present.

Here we developed and characterized compounds with improved $\alpha 5-$ preference compared to SH-053-2'F-R-CH3; gained first insights on issues of their blood brain barrier (BBB) penetration; and tested their ability to relax airway smooth muscle in *ex vivo* preparations.

Materials and Methods

Compounds

(list of all IUPAC names, and other compounds used in all experiments)

SH-053-2'F-R-CH3 ((R) stereoisomer of 8-ethynyl-6-(2-fluorophenyl)-4-methyl-4H-2,5,10b-triaza-benzo[e] azulene-3-carboxylic acid ethyl ester);

MP-III-004;

MP-III-58;

SH-053-2'F-R-CH3-acid;

SH-I-048a ((S)-7-bromo-5-(2- fluorophenyl)-3-methyl-1H-benzo[e][1,4]diazepin-2(3H)-one); Hz-166 (8-ethynyl-6-(20-pyridine)-4H-2,5,10b- triaza-benzo[e]azulene-3-carboxylic acid ethyl ester) were designed and synthesized at the Department of Chemistry and Biochemistry, University of Wisconsin—Milwaukee.

[3H]flunitrazepam (specific activity 83 Ci/mmmol) was purchased from Perkin Elmer NEN (New England Nuclear)(Waltham, Massachusetts, USA). Diazepam (7-chloro-1,3-dihydro-1-methyl-5-phenyl-2H-1,4, benzodiazepine-2-one) from Nycomed (Opfikon, Switzerland). Standard chemicals came from Sigma-Aldrich (St. Louis, Missouri, USA)

Culturing of human embryonic kidney 293 cells

Human embryonic kidney (HEK) 293 cells (American Type Culture Collection ATCC® CRL-1574™) were maintained in Dulbecco's modified Eagle medium (DMEM, high glucose, GlutaMAX™ supplement, Gibco 61965-059, ThermoFisher, Waltham, Massachusetts, USA) supplemented with 10% fetal calf serum (Sigma-Aldrich F7524, St. Louis, Missouria, USA), 100 U/ml Penicillin-Streptomycin (Gibco 15140-122, ThermoFisher, Waltham, Massachusetts, USA) and MEM (Non-Essential Amino Acids Gibco 11140-035, ThermoFisher, Waltham, Massachusetts, USA) on 10 cm cell culture dishes (Cell^{+}, Sarstedt, Nürnbrecht, Germany) at 37°C and 5% CO_2.

HEK 293 cells were transfected with cDNAs encoding rat $GABA_A$ receptor subunits subcloned into pCI expression vectors. The ratio of plasmids used for transfection with the calcium phosphate precipitation method (Chen and Okayama, 1987) were 3 µg α(1,2,3 or 5): 3 µg β3 and 15 µg γ2 per 10 cm dish. Medium was changed 4-6 hours after transfection.

Cells were harvested 72 days after transfection by scraping into phosphate buffered saline. After centrifugation (10 min, 12000 g, 4°C) cells were resuspended in TC50 (50 mM Tris-Citrate pH=7.1), homogenized with an ULTRA-TURRAX® (IKA, Staufen, Germany) and centrifuged (20 min, 50 000 g). Membranes were washed three times in TC50 as described above and frozen at -20°C until use.

Radioligand binding assay

Frozen membranes were thawed, resuspended in TC50 and incubated for 90 min at 4°C in a total of 500 µl of a solution containing 50 mM Tris/citrate buffer, pH=7.1, 150 mM NaCl and 2 nM [3H]flunitrazepam in the absence of presence of either 5 µM diazepam (to determine non-specific binding) (dissolved in DMSO, final DMSO concentration 0.5%). Membranes were filtered through Whatman GF/B filters and the filters were rinsed twice with 4 ml of ice-cold 50 mM Tris/citrate buffer. Filters were transferred to scintillation vials and subjected to scintillation counting after the addition of 3 ml Rotiszint Eco plus liquid scintillation cocktail. Non-specific binding determined in the presence of 5 µM diazepam was subtracted from total [3H]flunitrazepam binding to determine specific binding.

In order to determine the equilibrium binding constant KD of [3H]flunitrazepam for the various receptor subtypes, membranes were incubated with various concentrations of [3H]flunitrazepam in the absence or presence of 5 µM diazepam. These results are shown in the Supplementary Table 1 (Stamenic, 2015, submitted).

Data calculation

Saturation binding experiments were analyzed using the equation Y=Bmax*X/(KD+X).

Nonlinear regression analysis of the displacement curves used the equation: log(inhibitor) vs. response - variable slope with Top=100% and Bottom=0% Y=100/(1+10^((logIC50-x)*Hillslope)). Both analyses were performed using GraphPad Prism version 5.0a for Mac OS X, GraphPad Software, La Jolla California USA, www. graphpad.com.

Drug concentrations resulting in half maximal inhibition of specific [3H]flunitrazepam binding (IC50) were converted to Ki values by using the Cheng-Prusoff relationship (Cheng and Prusoff, 1973) Ki= IC50/(1+(S/KD)) with S being the concentration of the radioligand (2 nM) and the measured KD values (Stamenic, 2015, submitted and Supplementary Table 1).

Two-electrode voltage clamp electrophysiology

The modulation of $GABA_A$ receptor subtypes by the imidazobenzodiazepines was analyzed with electrophysiology as described previously (Varagic *et al.*, 2013). The cDNAs from the rat $\alpha 1$, $\alpha 2$, $\alpha 3$, $\alpha 5$, $\beta 3$ and $\gamma 2$ subunits were linearized with restriction endonucleases. mRNA was prepared with *in vitro* transcription using the mMachine® T7 transcription kit (Ambion, TX, USA). The RNA was capped on the 5' end and polyadenylated with yeast poly(A) polymerase.

Stage 5-6 oocytes from decapitated *Xenopus laevis* frogs (Nasco, WI, USA) were isolated and singled with a platinum wire. αx, $\beta 3$ and $\gamma 2$ mRNA were mixed in the ratio 1:1:5. An amount of 2.5 ng of the RNA mixture was injected into each cell. The cells were cultivated at 18°C in a modified Barths' medium (88 mM NaCl, 10 mM HEPES-NaOH (pH 7.4), 2.4 mM $NaHCO_3$, 1 mM KCl, 0.82 mM $MgSO_4$, 0.41 mM $CaCl_2$, 0.34 mM $Ca(NO_3)_2$) with 100 U/ml penicillin and 100 µg/ml streptomycin. The cells were then defolliculated 2 to 4 days after injection and examined using the two-electrode voltage clamp method on expression days 3 to 5. For current measurements the oocytes were impaled with two microelectrodes (1–3 MΩ) which were filled with 2 M KCl. The electrophysiological measurements were performed with a Warner OC-725C two-electrode voltage clamp (Warner Instrument, Hamden, CT, USA), a Dagan CA-1B Oocyte Clamp or a Dagan TEV-200A two-electrode voltage clamp

(Dagan Corporation, Mineapolis, MN, USA). Data were digitized, recorded and measured using a Digidata 1322A data acquisition system (Axon Instruments, Union City, CA, USA). Data were analyzed using GraphPad Prism. The cells were clamped at a holding potential of -60 mV. The perfusion medium was Xenopus Ringer (XR) solution (90 mM NaCl, 5 mM HEPES–NaOH (pH 7.4), 1 mM $MgCl_2$, 1 mM KCl and 1 mM $CaCl_2$). The application of buffer and compounds, respectively was done with gravity flow at 6 ml/min via a glass capillary placed directly above the cell. The compounds were applied with a GABA concentration which can elicit 3-5 % of maximal GABA current (GABA EC3-5 current) until the current trace reached the peak. Between each measurement the cells were washed for 3 min with buffer. Modulation of GABA EC3-5 currents was presented as % of the control current induced by the EC3-5 of GABA alone.

Quantification in rat plasma and brain tissue

Male outbred Wistar rats were supplied by Military Farm, Belgrade, Serbia. For each of four compounds tested, rats were divided into three dose groups, with three animals per group. All ligands were administered by intraperitoneal (i.p.) injection in a volume of 2 mL/kg. Compounds 1, 2 and 3 were dosed at 0.5, 2 and 10 mg/kg, while compound 4 was dosed at 1, 2.5 and 10 mg/kg. Twenty minutes after treatment administration, the blood samples were collected in heparinized syringes via cardiac puncture of rats anesthetized with ketamine solution (10% Ketamidor, Richter Pharma Ag, Wels, Austria, dosed i.p. at 100 mg/kg), and centrifuged at 2500 rpm for 10 min to obtain plasma. Thereafter, rats were decapitated and brains were weighed, homogenized in 5 mL of methanol and centrifuged at 6000 rpm for 20 min. To determine concentrations of the compounds 1, 2 and 3 in plasma and supernatants of brain tissue homogenates, compounds were extracted from these samples by solid phase extraction (SPE), using Oasis HLB cartridges (Waters Corporation, Milford, Massachusetts). The procedure of sample preparation and determination of the compounds by ultraperformance liquid chromatography–tandem mass spectrometry (UPLC–MS/MS) with Thermo Scientific Accela 600 UPLC system connected to a Thermo Scientific TSQ Quantum

Access MAX triple quadrupole mass spectrometer (Thermo Fisher Scientific, San Jose, California), equipped with electrospray ionization (ESI) source, has been already described in detail (Obradović *et al.*, 2014).

Even the modified protocols of SPE as a pretreatment procedure for UPLC–MS/MS could not yield satisfying results for compound 4. This could be due to the polarity and amphoteric qualities of this ligand. Instead, acetonitrile protein precipitation was used as preparation for UPLC–MS/MS. Plasma, brain supernatant, standard and internal standard solutions were prepared by the same way as before, for the standard SPE procedure. We then transferred 250 µL of plasma or brain supernatant to microcentrifuge tubes and added 50 µL of standard solution for calibration or pure methanol for samples and 50 µL of internal standard solution. After vortexing the mixture for 1 min at 1,000 rpm, 1500 µL of acetonitrile was added, vortexed again for 1 min at 1000 rpm and centrifuged for 10 min at 13,000 rcf. Supernatants were transferred to vials for UPLC–MS/MS analysis.

Plasma protein and brain tissue binding studies

A 48-well rapid equilibrium dialysis (RED) device (Thermo Scientific) was used to determine the free fraction of compound 1, 2 and 3 in fresh rat plasma and brain tissue. The free fraction of compound 4 was determined only in plasma, as it was shown in the above mentioned experiment that this compound is not able to pass the BBB. The protocol used was the same as in Obradović et al., 2014. Free concentrations were calculated by multiplying the measured total plasma and brain concentrations with the appropriate estimated free fractions.

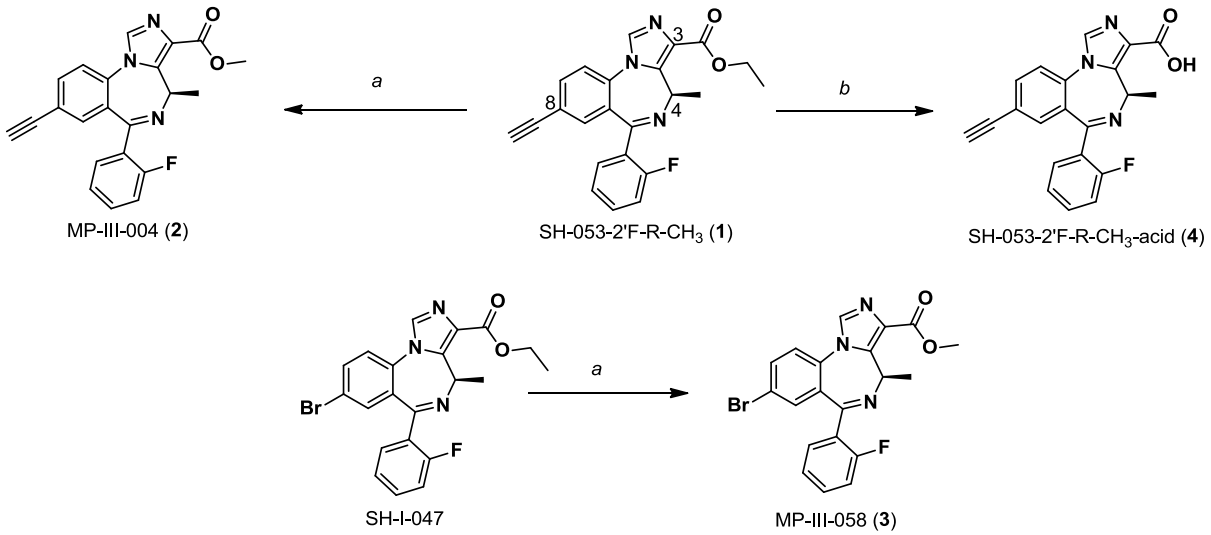
Force Measurements in Guinea Pig Tracheal Rings

All guinea pig protocols were approved by the Columbia University Animal Care and Use Committee. Studies were conducted as previously described (Gallos et al. 2015). Briefly, male Hartley guinea pigs (~400 g) were anesthetized with intraperitoneal pentobarbital (100 mg/kg) and their tracheas dissected free of epithelium and suspended in physiological buffer

with 10uM indomethacin in organ baths at 37°C and continuously bubbled with 95% O_2/5% CO_2. Tracheal rings were placed under a resting tension of 1.0g and allowed to equilibrate for 1h with buffer exchanges every 15min. Tracheal rings were pretreated with *N*-vanillylnonanamide (10 μM) to activate and then deplete nonadrenergic, noncholinergic nerves contained within the tissue. After buffer exchanges the tracheal rings were subjected to two cycles of increasing cumulative concentrations of acetylcholine (0.1 μM to 0.1 mM). Following extensive buffer exchanges, pyrilamine (10 μM), and tetrodotoxin (1 μM) were added to the buffers to block confounding effects of released histamine or nerve depolarization on endogenous airway smooth muscle contractile force. Tracheal rings were then contracted with 1uM substance P. After contractions achieved a steady-state plateau of increased force (typically 30 min), 50 μM of the indicated $GABA_A$ ligand or the vehicle control (0.1% ethanol) was added to the buffers. The maintenance of force was measured after 15 min and was expressed as a percent of the initial contractile substance P-induced force for each ring and the resultant relaxation was compared to the vehicle control.

Results

Scheme 1: Substitution pattern and numbering of chiral, α5- preferring imidazobenzodiazepines



Reagents and Conditions: *a*) NaOMe, MeOH, reflux, 0.5h, 87-95%; *b*) 3M NaOH, EtOH, 60°C, 1h; 1M HCl, 84%

Investigated compounds

α5- selective Compound	R8	R3	Lab code
1	ethynyl	ethyl ester	SH-053-2'F-R-CH3
2	ethynyl	methyl ester	MP-III-004
3	Br	methyl ester	MP-III-058
4	ethynyl	-COOH	SH-053-2'F-R-CH3-acid
Control compound			
5	Different chemotypes		Hz-166
6			SH-I-048a

Ligand **1** is published (Cook *et al.*, 2006) and is included here as a reference compound for α5– receptor preference. The R3 position on the imidazole ring was varied to include the methyl ester and the charged acid in compound **4**. The chemical synthesis and spectroscopic information on the newly synthesized ligands **2, 3** and **4** is provided as

supplementary information. Compounds **5** (ref) and **6** (ref) which are achiral and represent different chemotypes of benzodiazepine-site ligands were used as control compounds.

Modulatory effects of compounds on GABA-induced chloride currents

Ligand **1** is a published $\alpha5$- preferring chiral imidazobenzodiazepine (Fischer *et al.*, 2010) which already has been shown to relax airway smooth muscle (Gallos *et al.*, 2015). This compound possesses higher efficacy and affinity for the $\alpha5\beta3\gamma2$ receptor over $\alpha1,2,3\beta3\gamma2$ (see Fig 1. and TABLE 1), but still significant residual activity in other subtypes and a rather narrow window of separation between allosteric modulation of the $\alpha5$- and non-$\alpha5$- subtypes. Here we investigate how different substituents on the imidazobenzodiazepine scaffold lead to alterations and improvements of the efficacy preference for the $\alpha5$- subtype.

The imidazobenzodiazepine MP-III-004 (compound **2**) is the methyl ester analogue of compound **1**. It exhibits a marked drop in efficacy in the non-$\alpha5-$ subtypes compared to SH-053-2'F-R-CH3, see Fig. 1. While 1 μM SH-053-2'F-R-CH3 enhances EC3 (3% effective concentration) GABA currents to ~ 150 ($\alpha1,2$) and 200 ($\alpha3$)%, the modulation by the same concentration of compound **2** in the non-$\alpha5-$ subtypes is less than 150%. The compound with R8= Br, compound **3**, has a fairly similar receptor preference profile as its R8= ethynyl analogue (compound **2**), but a slightly higher apparent potency for the $\alpha5-$ subtype as it modulates the $\alpha5\beta3\gamma2$ receptors already at 100nM. Compound **4** is a charged compound with R3= COOH and displays very high efficacy, modulating the EC3 GABA current in the $\alpha5\beta3\gamma2$ subtype already by ~600% at only 100 nM compound concentration, see Fig. 1. At this low concentration, there is nearly no modulatory effect on the non-$\alpha5-$ subtypes, see Fig. 1. At higher concentrations it modulates the other subtypes too, but due to the very good window of separation in the lower concentration range activation of these subtypes can be avoided by appropriate dosing. Thus, the three analogues of SH-053-2'F-R-CH3 all display a wider concentration range in which they act on $\alpha5$-containing receptors exclusively compared to the parent compound.

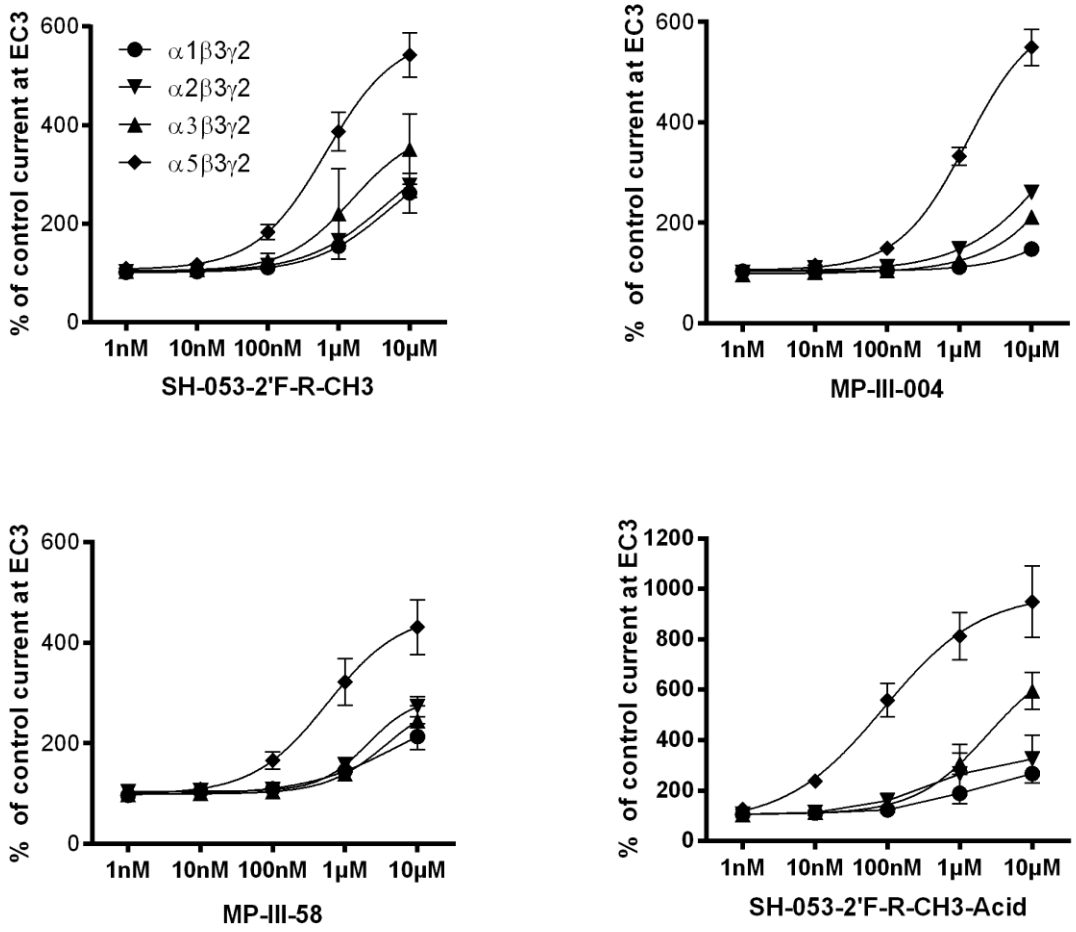


Fig. 1. Mean relative potentiation above the EC3 GABA current at the indicated compound concentrations is displayed with SEM, n= 3 or higher from at least two batches of oocytes. Note the different Y-axis scale for the strong modulator compound 4.

Binding selectivity

To evaluate binding selectivity, $\alpha 1,2,3,5\beta 3\gamma 2$ receptors were expressed individually in HEK 293 cells, and [3H]flunitrazepam displacement studies were performed with compounds 1-4 to compare binding selectivity for $\alpha 5-$ over non-$\alpha 5-$ containing receptors, see TABLE 1. The binding selectivity for $\alpha 5\beta 3\gamma 2$ of the reference compound **1** is about ten-fold over the $\alpha 1$-receptor (give first ref). The best binding selectivity was found for the acidic/ charged analogue SH-053-2'F-R-CH3-acid, which is approximately 60-fold selective for $\alpha 5-$ over $\alpha 1-$ containing receptors. All other tested compounds are equivalent or worse in $\alpha 5$- preference

compared to the parent compound **1**, see TABLE 1. The binding data suggests together with the efficacy data (Fig. 1) that compound **4** possesses both binding- and efficacy- preference for the α5- containing receptor subtype, while compounds **2** and **3** feature mostly efficacy selective action.

TABLE 1. Potency of [3H]flunitrazepam displacement in αxβ3γ2 receptors recombinantly expressed in HEK 293 cells. Data is reported as mean ± SEM from three displacement curves done in duplicates.

Cpd #	**Code Name**	**Ki ± SEM in μM**				
		α1	α2	α3	α5	α1/ α5
1	SH-053-2'F-R-CH3	1.8 ± 0.2	3.7 ± 0.3	1.7 ± 0.2	0.22 ± 0.02	8
2	MP-III-004	2.5 ± 0.2	3.2 ± 0.1	2.5 ± 0.3	0.4 ± 0.1	6
3	MP-III-058	0.35 ± 0.06	0.69 ± 0.05	0.58 ± 0.05	0.10 ± 0.01	3.5
4	SH-053-2'F-R-CH3-acid	1.9 ± 0.4	0.6 ± 0.1	1.1 ± 0.5	0.031 ± 0.005	**61**

Legend to TABLE 1: Membranes from HEK 293 cells expressing the indicated subunit combinations αxβ3γ2 were incubated with 2 nM [3H]flunitrazepam in the presence of various concentrations of the test compound. The concentrations resulting in half maximal inhibition of specific binding (as determined in the absence or presence of 5 μM diazepam) were converted to Ki values using the Cheng-Prusoff relationship (see Methods).

Free fraction and blood brain barrier penetration studies of the novel α5- preferring ligands

Among the possible future applications of these compounds is the exploitation of an airway smooth muscle relaxing effect (reported for SH-053-2'F-R-CH3 in Gallos et al. 2015) for the treatment of asthma bronchialis. If a compound should be applied as an aerosol, a low blood brain barrier (BBB) penetration is desirable to avoid central nervous system side effects. Since the brain α5β3γ2 receptor subtype is implicated in learning and memory (Soh and Lynch, 2015) and thought to be involved in tolerance development (van Rijnsoever *et al.*,

2004) and the amnestic effects of positive modulators such as diazepam (Antkowiak, 2015), a compound that cannot pass the BBB would be the most appropriate for peripheral administration. The plasma and brain concentrations, total and (estimated) free, of compounds **1**, **2** and **3** measured 20 min after intraperitoneal administration of 0.5, 2 and 10 mg/kg doses are presented in TABLE 2. It is notable that among these three brain-penetrant compounds, the measured free brain fractions and estimated free brain concentrations of compound **3** were lowest (TABLE 2), which may translate into a very favorable low side effect profile. For the charged compound **4** the protocol of the kinetic study had to be adapted (see Methods section). The quantification of brain samples demonstrated that compound **4** is essentially unable to pass the BBB, while free plasma fraction was as high as 18%, which may result in both, favorable central nervous system safety and good availability for eliciting pharmacological effects in peripheral tissues.

TABLE 2. Total and estimated free concentrations of SH-053-2''F-R-CH3, MP-III-004 and MP-III-058 (dosed at 0.5, 2 and 10 mg/kg) as well as SH-053-2''F-R-CH3- acid (dosed at 1, 2.5 and 10 mg/kg) in rat plasma and brain samples 20 min after i.p. administration.

Dose (mg/kg)		**0.5**	**2**	**10**
SH-053-2'F-R-CH3				
Plasma (nmol/L)	*Total*	38.83 ± 17.55	31.23 ± 14.89	337.57 ± 145.03
	Free	26.62 ± 12.03	21.41 ± 10.21	231.41 ± 99.41
Brain (nmol/kg)	*Total*	43.88 ± 18.47	66.59 ± 34.13	552.72 ± 241.70
	Free	1.70 ± 0.71	2.58 ± 1.32	21.39 ± 9.35
MP-III-004				
Plasma (nmol/L)	*Total*	64.47 ± 23.02	415.89 ± 58.91	1182.49 ± 546.09
	Free	22.78 ± 8.13	146.93 ± 20.81	417.77 ± 192.93
Brain (nmol/kg)	*Total*	125.88 ± 30.01	329.59 ± 26.55	1696.44 ± 269.70
	Free	7.89 ± 1.88	20.66 ± 1.66	106.37 ± 16.91
MP-III-058				
Plasma (nmol/L)	*Total*	13.43 ± 1.15	72.28 ± 38.07	94.59 ± 64.14
	Free	8.65 ± 0.74	46.55 ± 24.52	60.91 ± 41.30
Brain (nmol/kg)	*Total*	55.17 ± 4.98	268.15 ± 11.03	902.94 ± 395.01
	Free	0.66 ± 0.06	3.20 ± 0.13	10.79 ± 4.72
SH-053-2'F-R-CH3-acid				
Dose (mg/kg)		**1**	**2.5**	**10**

Plasma (nmol/L)	*Total*	510.24 ± 58.37	802.07 ± 426.95	1511.03 ± 814.51
	Free	91.75 ± 10.50	144.22 ± 76.77	271.71 ± 146.46

Effect of α5- containing $GABA_A$ receptor subtype selective compounds 2, 3 and 4 and control compounds in organ bath experiments on pre-contracted airway smooth muscle

In experiments as described previously (Gallos *et al.*, 2015), guinea pig airway smooth muscle was pre-contracted *ex vivo* by application of 1 μM substance P and subsequently treated with the test compounds, see Fig. 2.

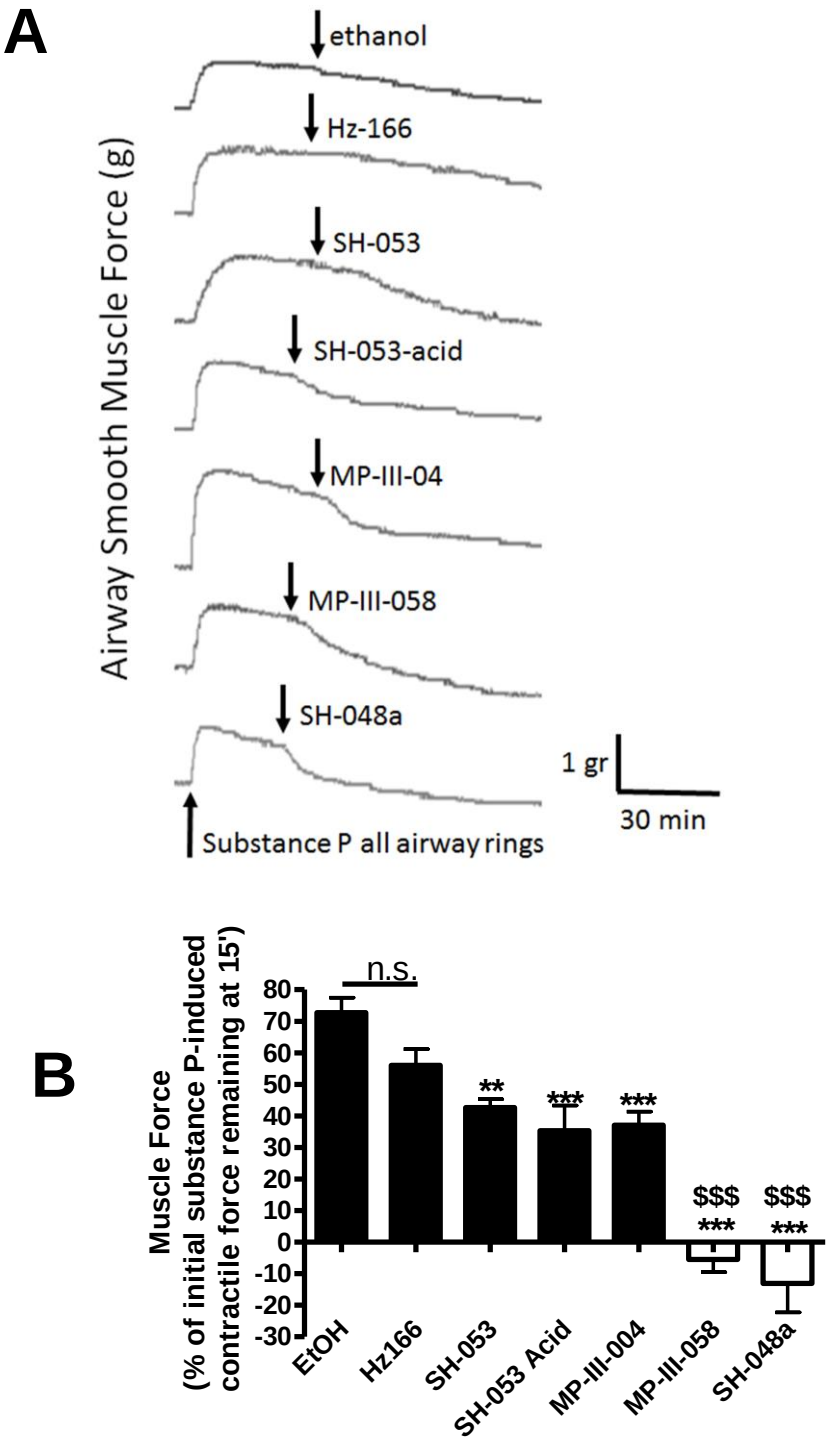


Fig. 2. Airway smooth muscle force relaxation in response to ligands with selectivity for α5 subunit containing $GABA_A$ receptors and the α2,3 selective ligand Hz-166 which is inactive in α5 subunit containing $GABA_A$

receptors. (**A**) Representative airway smooth muscle force tracings of guinea pig tracheal rings suspended *ex vivo* in organ baths and contracted with 1 µM substance P. At a plateau in contractile force, rings were treated with 50 µM of the indicated compound or the vehicle (0.1% ethanol) at times indicated by the arrows to assay for induced relaxation. There is a slow spontaneous decay in the substance P induced contraction but $GABA_A$ $\alpha5$ subunit-selective compounds induce active relaxation that is not seen with the ethanol vehicle or the $GABA_A$ $\alpha2,3$ subunit selective ligand Hz-166. (**B**) The amount of relaxation was measured 30 min after the addition of the test drug by comparing the remaining amount of contractile force at 30 min to the contractile force present just before test drug addition. ** and *** p< 0.01 and 0.001 compared to vehicle control, respectively; $$$ p< 0.001 compared to SH-053, n = 6-17.

All novel compounds with functional selectivity for the $\alpha5$- containing receptors performed as well as, or better than the parent **1** in the tissue bath experiments. Compound **3** exerted the strongest relaxing effect among the $\alpha5$- preferring test compounds and thus represents a considerably improved candidate for a future development towards a lead for an asthma medication compared to compound **1**. Compound **4** displays comparable effects as than the parent **1**, but offers the advantage of no blood brain barrier penetration, and thus also possibly represents an interesting follow up candidate.

Two additional compounds were included to investigate the specificity of the test compounds. Although the identity of individual $GABA_A$ subunits expressed in airway smooth muscle is known (Mizuta et al. 2008), the specific composition and stoichiometry of $GABA_A$ receptors expressed by the ASM cells is unknown. It was tacitly assumed that α, $\beta3$ and $\gamma2$ subunits would co-assemble to produce receptors like those seen in the CNS (Olsen and Sieghart, 2008). This assumption is plausible, and consistent with the previously published effects of the benzodiazepine- type ligands SH-053-2'F-R-CH3 (Gallos *et al.*, 2015) and the bretazenil analogues XHe-III-74 and CMD-54 (Yocum *et al.*, 2015) on intact ASM and isolated ASM cells. If the ASM relaxing effects are elicited by benzodiazepine- type positive modulation of GABA-elicited chloride flux via the $\alpha5/\gamma2$ (Gallos *et al.*, 2015) and $\alpha4/\gamma2$ (Yocum *et al.*, 2015) interfaces respectively, the compound Hz-166 which is an $\alpha2,3$

selective benzodiazepine- site ligand (Rivas *et al.*, 2009) should be inactive in the tissue bath experiments. Indeed, we found it to be inactive as hypothesized, see Fig. 2.

Hz-166 is also an imidazobenzodiazepine. To seek further evidence for a benzodiazepine-type mechanism by which the $\alpha 5$-selective ligands act in the ASM cells we included a compound which has a more distinct chemotype as additional control. SH-I-048a, an unselective modulator in all tested subtypes, is a 1,4- benzodiazepine ligand (ref to appropriate item – structure in scheme 1 or in SI?) with very high potency for diazepam sensitive benzodiazepine sites, high efficacy in $\alpha 1,2,3,5\beta 3\gamma 2$ receptors, but inactive in $\alpha 4\beta 3\gamma 2$ receptors (Obradović *et al.*, 2014). In the tissue bath experiment at 50 μM compound concentration it was as effective as the best $\alpha 5$- preferring test compound, see Fig. To nvestigate dose dependence of MP-III-058 and SH-I-048a, the tissue bath experiments were conducted at two additional lower concentrations. These experiments indicated that both compounds need to be present in the bath at concentrations higher than 10 μM for the relaxant effect to occur at high significance, see Fig. 3 (or supplementary Figure?). However, the effect observed at 25 μM was already approaching near saturation, see (see Fig 3. (or supplementary Figure?)). Interestingly, even though the binding potency in recombinantly expressed receptors is different by three orders of magnitude (Ki of 100 nM for MP-III-058 (TABLE 1) and 0.11 nM for Sh-I-048a (Obradović *et al.*, 2014) respectively), in the tissue bath experiments no difference in apparent potency was detected (see Fig 3. (or supplementary Figure?)). The reason for this lack of difference in apparent potency likely must be ascribed to different tissue penetration properties of these compounds.

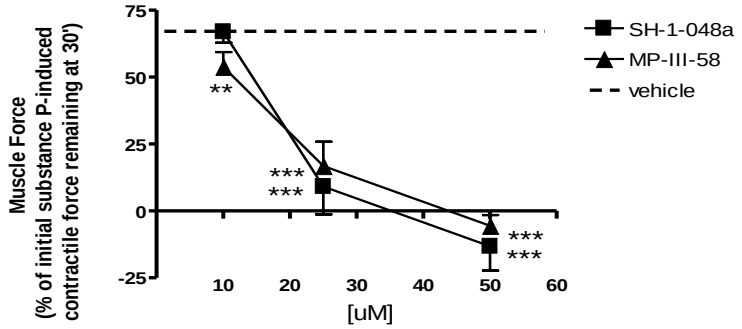


Figure X. Airway smooth muscle relaxation in response to ligands selective (MP-III-58) or non-selective (SH-1-048a) for $\alpha 5$ subunit containing $GABA_A$ channels. Guinea pig airway smooth muslce was contracted ex vivo to 1uM substance P and at a plateau in contractile force treated with the indicated ligand in 0.1% ethanol vehicle. The remaining amount of contractile force at 30 min was expressed as a percent of the initial substance P-induced force. ** $p<0.01$ and *** $p < 0.001$ compared to vehicle control (0.1% ethanol). n = 6-8.

Discussion

Subtype selective ligands of the benzodiazepine binding site subtypes would be highly desirable both as research tool compounds to study the role of individual receptor subtypes in CNS function (Drexler *et al.*, 2013), and to selectively modulate these receptors in all tissues in which they are expressed. Due to the high homology of the six α subunits, and particularly the four diazepam sensitive $\alpha 1,2,3,5$ subunits, truly selective compounds are still very sparse (Rudolph and Möhler, 2014). Here we present three derivatives of the $\alpha 5$-preferring compound SH-053-2'F-R-CH3 with improved properties. Two compounds display enhanced functional selectivity (i.e. lower efficacy in non-$\alpha 5$ receptors) (compounds **2** and **3)**, while one displays enhanced binding selectivity (i.e. an approximately 60-fold higher affinity for the $\alpha 5$- subtype, the carboxylic acid compound **4)**. Free fraction and blood brain barrier penetrations studies after intraperitoneal application of these compounds suggest that compound **2** would be suitable for CNS applications, as it displays a better brain-availability, and a better selectivity profile on central receptors compared to its parent compound **1**. In contrast, the brain free fraction of compound **3** is rather low, and compound **4** does not cross the BBB at all – making both these compounds very good candidates for peripheral applications.

A putative application of interest is as an aerosol to relax excessive contracted airway smooth muscle as it occurs in asthma bronchialis (Gallos et al. 2015). Airway smooth muscle cells express several $GABA_A$ receptor subunits. Among α subtypes, only the $\alpha4$ and $\alpha5$ are expressed (Mizuta *et al.*, 2008; Gallos *et al.*, 2015; Yocum *et al.*, 2015). It has been demonstrated previously, that targeting either of these subunits leads to relaxation of pre-contracted *ex vivo* airway smooth muscle from guinea pig, mouse and human (Gallos *et al.*, 2015; Yocum *et al.*, 2015), and that aerosol delivery of the $\alpha4$- preferring benzodiazepine-type compound XHe-III-74 can prevent ASM contraction by methacholine *in vivo* (Yocum *et al.*, 2015). While it was tacitly assumed so far that the ASM cells express $GABA_A$ receptors whose arrangement and stoichiometries correspond to those found in the CNS, this has so far not been investigated explicitly. However, the sensitivity of $\alpha4$ and $\alpha5$ positive ASM cells for benzodiazepine ligands (Gallos *et al.*, 2015; Yocum *et al.*, 2015) suggests that the receptors expressed by these cells contain "classical" benzodiazepine binding sites. More evidence for this hypothesis could be provided if the ASM relaxing effects of benzodiazepine- type compounds could be blocked by benzodiazepine- site antagonist compounds such as flumazenil. Unfortunately, these experiments are not feasible on cells that contain both $\alpha4-$ and $\alpha5-$ containing receptors, as flumazenil is a positive allosteric modulator of $\alpha4,6\beta3\gamma2$ receptors (Ramerstorfer *et al.*, 2010). While an $\alpha5$- preferring antagonist, XLi-093, has been published (Li *et al.*, 2003), this compound also modulates $\alpha4\beta3\gamma2$ receptors in the concentration range that would be needed for the tissue bath experiments (unpublished observations). Thus, no known "benzodiazepine antagonist" is a true antagonist on both these receptor subtypes that are putatively expressed by ASM cells. To circumvent this practical limitation, we performed control experiments with a benzodiazepine- type compound that has nearly no efficacy in $\alpha5$- containing receptors, namely the $\alpha2,3$- preferring compound Hz-166 (Rivas *et al.*, 2009). While it is structurally related to compounds **1**, **2** and **3**, and displays some overlapping CNS pharmacology (Fischer *et al.*, 2010), we show it to be inactive in guinea pig trachea preparations. While the

chemically similar Hz-166 is inactive, suggesting a subtype specific effect that parallels the effects seen in recombinant receptors, a chemically more distinct compound, SH-048a, that unselectively modulates all four diazepam sensitive receptor subtypes (Obradovic et al. 2014) was demonstrated here to also exert a pronounced relaxing effect in the tissue bath experiments with trachea ring preparations (see Figs 3 and 4).These observations together further support the working hypothesis that the receptors in the ASM cells that respond to our test compounds correspond to the CNS receptors, and that the compounds exert their effects by the classical benzodiazepine- mechanism and act on the $\alpha5+\gamma2-$ benzodiazepine site.

It turned out not to be possible to correlate properties such as affinity data from recombinant receptors with dose dependence in ASM relaxation, or efficacy of modulation at GABA EC3 with the degree of ASM relaxation. We tacitly attribute this to several possible causes that need further investigation in future experiments. Tissue penetration of the compounds is expected to steeply depend on physico-chemical properties such as electrostatics and lipophilicity of the compounds – the carboxylic acid compound **4** probably will not penetrate smooth muscle tissue very efficiently. Additionally, rapid degradation by tissue resident enzymes could be more limiting to the effects on ASM than apparent affinity or efficacy as seen in an isolated *in vitro* cell environment. Thus, for the more promising compounds **3** and **4** effective concentrations at several depths in the tissue samples should be investigated in future work. Furthermore, while the efficacy data obtained in recombinant receptors is obtained by applying a defined compound concentration, together with a known GABA concentration, directly to the receptors on the surface of the oocyte, the situation in the tissue bath experiment is profoundly different. Effective concentration of the compound is unknown, the level of tissue resident GABA is unknown, and furthermore, additional small molecules such as histamine or 2-AG that act on $GABA_A$ receptors also as allosteric modulators (Saras et al. 2008, Sigel et al. 2011) may be present at unknown concentrations and change the interactions between benzodiazepine-type compounds and the receptors.

In order to move forward with this putatively promising novel application of benzodiazepine type compounds, we conclude that all candidates that display the desired profile in recombinant experiments should be given consideration in *ex vivo* and downstream experiments, and that a pre-selection based on data from recombinant receptors should be done only with respect to the subtype selective action.

In conclusion, we present three novel chiral imidazobenzodiazepines derived from SH-053-2'F-R-CH3 with a superior $\alpha 5$- selective profile. Two of these compounds, **3** and **4**, show very favorable properties for peripheral application as ASM relaxants, while ligand **2** will possibly be suitable as a CNS-active selective agent featuring somewhat improved subtype selectivity compared to compound **1**. *Ex vivo* experiments identified compound **3** as best performing in airway smooth muscle relaxant properties, and thus this compound should be selected with high priority for follow up experiments as a prospect for the treatment of bronchoconstriction in diseases such as asthma in subsequent experiments (Yocum *et al.*, 2015). The $\alpha 5$-subunit is also found in T cells and dendritic cells of the immune system (Barragan et al. 2015), in reproductive organs (Akinci and Schofield 1999) and in airway epithelium (Xiang et al. 2007). ~~($\alpha 5$~~ The novel ligands presented here can be used also as tool compounds to study the function of $\alpha 5\gamma 2$- containing receptors in these cells, if they also form CNS-like benzodiazepine sensitive receptors there.

Acknowledgements

We thank Sabah Rehman for the support with the electrophysiological measurements and the data analysis.

Author contributions

Participated in research design: Sieghart, Savic, Emala, Cook, and Ernst.

Conducted experiments: Puthenkalam, Ramerstorfer, Steudle, Scholze, Poe, Reddy Methuku, Li, and Santrac.

Performed data analysis: Puthenkalam, Treven, Scholze, Poe, Emala, Ernst, and….

Wrote or contributed to the writing of the manuscript: Puthenkalam, Sieghart, Ernst, and….

Supplemental material

Supplementary Table 1. Equilibrium binding constant (KD) for the different receptor subtypes

α1β3γ2	α2β3γ2	α3β3γ2	α5β3γ2
7.2 ± 0.2 nM	2.9 ± 0.6 nM	4.1 ± 0.2 nM	2.2 ± 0.3 nM

Legend to Supplementary Table 1: Membranes from HEK 293 cells transfected with the subunit combinations as indicated were incubated with various concentrations of [3H]flunitrazepam in the absence or presence of either 5 µM diazepam (to determine unspecific binding). Results were analyzed using the equation Y=Bmax*X/(KD+X). KD values are presented as mean values ± SEM from 3-4 independent experiments performed in duplicates.

References

Antkowiak B (2015) Closing the gap between the molecular and systemic actions of anesthetic agents. *Adv Pharmacol* **72**:229–62.

Atack JR (2011) GABAA receptor subtype-selective modulators. I. α2/α3-selective agonists as non-sedating anxiolytics. *Curr Top Med Chem* **11**:1176–202.

Atack JR, Hallett DJ, Tye S, Wafford K a, Ryan C, Sanabria-Bohórquez SM, Eng W-S, Gibson RE, Burns HD, Dawson GR, Carling RW, Street LJ, Pike A, De Lepeleire I, Van Laere K, Bormans G, de Hoon JN, Van Hecken A, McKernan RM, Murphy MG, and Hargreaves RJ (2011) Preclinical and clinical pharmacology of TPA023B, a GABAA receptor α2/α3 subtype-selective partial agonist. *J Psychopharmacol* **25**:329–44.

Barragan A, Weidner JM, Jin Z, Korpi ER, and Birnir B (2015) GABAergic signalling in the immune system. *Acta Physiol (Oxf)* **213**:819–27.

Baur R, Kielar M, Richter L, Ernst M, Ecker GF, and Sigel E (2013) Molecular analysis of the site for 2-arachidonylglycerol (2-AG) on the ??2 subunit of GABAA receptors. *J Neurochem*, doi: 10.1111/jnc.12270.

Baur R, Kielar M, Richter L, Ernst M, Ecker GF, and Sigel E (2013) Molecular analysis of the site for 2-arachidonylglycerol (2-AG) on the β_2 subunit of GABA(A) receptors. *J Neurochem* **126**:29–36.

Belelli D, and Lambert JJ (2005) Neurosteroids: endogenous regulators of the GABA(A) receptor. *Nat Rev Neurosci* **6**:565–75.

Chen C, and Okayama H (1987) High-efficiency transformation of mammalian cells by plasmid DNA. *Mol Cell Biol* **7**:2745–52.

Cheng Y, and Prusoff WH (1973) Relationship between the inhibition constant (K1) and the concentration of inhibitor which causes 50 per cent inhibition (I50) of an enzymatic reaction. *Biochem Pharmacol* **22**:3099–108.

Chiara DC, Jayakar SS, Zhou X, Zhang X, Savechenkov PY, Bruzik KS, Miller KW, and Cohen JB (2013) Specificity of intersubunit general anesthetic-binding sites in the transmembrane domain of the human α1β3γ2 γ-aminobutyric acid type A (GABAA) receptor. *J Biol Chem* **288**:19343–57.

Clayton T, Chen JL, Ernst M, Richter L, Cromer BA, Morton CJ, Ng H, Kaczorowski CC, Helmstetter FJ, Furtmüller R, Ecker G, Parker MW, Sieghart W, and Cook JM (2007) An updated unified pharmacophore model of the benzodiazepine binding site on gamma-aminobutyric acid(a) receptors: correlation with comparative models. *Curr Med Chem* **14**:2755–75.

Clayton T, Poe MM, Rallapalli S, Biawat P, Savić MM, Rowlett JK, Gallos G, Emala CW, Kaczorowski CC, Stafford DC, Arnold LA, and Cook JM (2015) A Review of the Updated Pharmacophore for the Alpha 5 GABA(A) Benzodiazepine Receptor Model. *Int J Med Chem* **2015**:1–54.

Cook JM, Zhou H, Huang S, Sarma PVV., and Zhang C (2006) Stereospecific anxiolytic and anticonvulsant agents with reduced muscle-relaxant, sedative-hypnotic and ataxic effects.

Drexler B, Zinser S, Huang S, Poe MM, Rudolph U, Cook JM, and Antkowiak B (2013) Enhancing the function of alpha5-subunit-containing GABAA receptors promotes action potential firing of neocortical neurons during up-states. *Eur J Pharmacol* **703**:18–24.

Fischer BD, Licata SC, Edwankar R V, Wang Z-J, Huang S, He X, Yu J, Zhou H, Johnson EM, Cook JM, Furtmüller R, Ramerstorfer J, Sieghart W, Roth BL, Majumder S, and Rowlett JK (2010) Anxiolytic-like effects of 8-acetylene imidazobenzodiazepines in a rhesus monkey conflict

procedure. *Neuropharmacology* **59**:612–8, Elsevier Ltd.

Fleck MW, Thomson JL, and Hough LB (2012) Histamine-gated ion channels in mammals? *Biochem Pharmacol* **83**:1127–35.

Gallos G, Yocum GT, Siviski ME, Yim PD, Fu XW, Poe MM, Cook JM, Harrison N, Perez-Zoghbi J, and Emala CW (2015) Selective targeting of the α5-subunit of GABAA receptors relaxes airway smooth muscle and inhibits cellular calcium handling. *Am J Physiol Lung Cell Mol Physiol* **308**:L931–42.

Gladkevich A, Korf J, Hakobyan VP, and Melkonyan K V (2006) The peripheral GABAergic system as a target in endocrine disorders. *Auton Neurosci* **124**:1–8.

Hanrahan JR, Chebib M, and Johnston GAR (2011) Flavonoid modulation of GABA(A) receptors. *Br J Pharmacol* **163**:234–45.

Harris D, Clayton T, Cook J, Sahbaie P, Halliwell RF, Furtmüller R, Huck S, Sieghart W, and DeLorey TM (2008) Selective influence on contextual memory: physiochemical properties associated with selectivity of benzodiazepine ligands at GABAA receptors containing the alpha5 subunit. *J Med Chem* **51**:3788–803.

He X, Huang Q, Yu S, Ma C, McKernan R, and Cook JM (1999) Studies of molecular pharmacophore/receptor models for GABAA/BzR subtypes: binding affinities of symmetrically substituted pyrazolo[4,3-c]quinolin-3-ones at recombinant alpha x beta 3 gamma 2 subtypes and quantitative structure-activity relationship studi. *Drug Des Discov* **16**:77–91.

Hoerbelt P, Lindsley TA, and Fleck MW (2015) Dopamine directly modulates GABAA receptors. *J Neurosci* **35**:3525–36.

Huang Q, He X, Ma C, Liu R, Yu S, Dayer CA, Wenger GR, McKernan R, and Cook JM (2000) Pharmacophore/receptor models for GABA(A)/BzR subtypes (alpha1beta3gamma2, alpha5beta3gamma2, and alpha6beta3gamma2) via a comprehensive ligand-mapping approach. *J Med Chem* **43**:71–95.

Joksimović S, Divljaković J, Van Linn ML, Varagic Z, Brajković G, Milinković MM, Yin W, Timić T, Sieghart W, Cook JM, and Savić MM (2013) Benzodiazepine-induced spatial learning deficits in rats are regulated by the degree of modulation of α1 GABA(A) receptors. *Eur Neuropsychopharmacol* **23**:390–9.

Joksimović S, Varagic Z, Kovačević J, Van Linn M, Milić M, Rallapalli S, Timić T, Sieghart W, Cook JM, and Savić MM (2013) Insights into functional pharmacology of α_1 GABA(A) receptors: how much does partial activation at the benzodiazepine site matter? *Psychopharmacology (Berl)* **230**:113–23.

Khom S, Strommer B, Ramharter J, Schwarz T, Schwarzer C, Erker T, Ecker GF, Mulzer J, and Hering S (2010) Valerenic acid derivatives as novel subunit-selective GABAA receptor ligands - in vitro and in vivo characterization. *Br J Pharmacol* **161**:65–78.

Li X, Cao H, Zhang C, Furtmueller R, Fuchs K, Huck S, Sieghart W, Deschamps J, and Cook JM (2003) Synthesis, in Vitro Affinity, and Efficacy of a Bis 8-Ethynyl-4 H -imidazo[1,5 a]-[1,4]benzodiazepine Analogue, the First Bivalent α5 Subtype Selective BzR/GABA A Antagonist. *J Med Chem* **46**:5567–5570.

Lorenz M, Kabir MS, and Cook JM (2010) A two step synthesis of BzR/GABAergic active flavones via a Wacker-related oxidation. *Tetrahedron Lett* **51**:1095.

Magnaghi V, Ballabio M, Consoli A, Lambert JJ, Roglio I, and Melcangi RC (2006) GABA receptor-

mediated effects in the peripheral nervous system: A cross-interaction with neuroactive steroids. *J Mol Neurosci* **28**:89–102.

Miller PS, and Aricescu AR (2014) Crystal structure of a human GABAA receptor. *Nature*, doi: 10.1038/nature13293.

Mizuta K, Xu D, Pan Y, Comas G, Sonett JR, Zhang Y, Panettieri RA, Yang J, and Emala CW (2008) GABAA receptors are expressed and facilitate relaxation in airway smooth muscle. *Am J Physiol Lung Cell Mol Physiol* **294**:L1206–16.

Möhler H (2011) The rise of a new GABA pharmacology. *Neuropharmacology* **60**:1042–9.

Mortensen M, Ebert B, Wafford K, and Smart TG (2010) Distinct activities of GABA agonists at synaptic- and extrasynaptic-type GABAA receptors. *J Physiol* **588**:1251–68.

Mortensen M, and Smart TG (2006) Extrasynaptic alphabeta subunit GABAA receptors on rat hippocampal pyramidal neurons. *J Physiol* **577**:841–856.

Obradović AL, Joksimović S, Poe MM, Ramerstorfer J, Varagic Z, Namjoshi O, Batinić B, Radulović T, Marković B, Roth BL, Sieghart W, Cook JM, and Savić MM (2014) Sh-I-048A, an in vitro non-selective super-agonist at the benzodiazepine site of GABAA receptors: The approximated activation of receptor subtypes may explain behavioral effects. *Brain Res* **1554**:36–48.

Olsen RW, and Sieghart W (2008) International Union of Pharmacology. LXX. Subtypes of gamma-aminobutyric acid(A) receptors: classification on the basis of subunit composition, pharmacology, and function. Update. *Pharmacol Rev* **60**:243–60.

Ramerstorfer J, Furtmüller R, Vogel E, Huck S, and Sieghart W (2010) The point mutation gamma 2F77I changes the potency and efficacy of benzodiazepine site ligands in different GABAA receptor subtypes. *Eur J Pharmacol* **636**:18–27.

Richter L, de Graaf C, Sieghart W, Varagic Z, Mörzinger M, de Esch IJP, Ecker GF, and Ernst M (2012) Diazepam-bound GABAA receptor models identify new benzodiazepine binding-site ligands. *Nat Chem Biol* **8**:455–64.

Rivas FM, Stables JP, Murphree L, Edwankar R V, Edwankar CR, Huang S, Jain HD, Zhou H, Majumder S, Sankar S, Roth BL, Ramerstorfer J, Furtmüller R, Sieghart W, and Cook JM (2009) Antiseizure activity of novel gamma-aminobutyric acid (A) receptor subtype-selective benzodiazepine analogues in mice and rat models. *J Med Chem* **52**:1795–8.

Rudolph U, Crestani F, Benke D, Brünig I, Benson JA, Fritschy JM, Martin JR, Bluethmann H, and Möhler H (1999) Benzodiazepine actions mediated by specific gamma-aminobutyric acid(A) receptor subtypes. *Nature* **401**:796–800.

Rudolph U, and Knoflach F (2011) Beyond classical benzodiazepines: novel therapeutic potential of GABAA receptor subtypes. *Nat Rev Drug Discov* **10**:685–97, Nature Publishing Group.

Rudolph U, and Möhler H (2014) GABAA receptor subtypes: Therapeutic potential in Down syndrome, affective disorders, schizophrenia, and autism. *Annu Rev Pharmacol Toxicol* **54**:483–507.

Saras A, Gisselmann G, Vogt-Eisele AK, Erlkamp KS, Kletke O, Pusch H, and Hatt H (2008) Histamine action on vertebrate GABAA receptors: direct channel gating and potentiation of GABA responses. *J Biol Chem* **283**:10470–5.

Sauguet L, Shahsavar A, and Delarue M (2014) Crystallographic studies of pharmacological sites in pentameric ligand-gated ion channels ☆. , doi: 10.1016/j.bbagen.2014.05.007.

Savić MM, Majumder S, Huang S, Edwankar R V, Furtmüller R, Joksimović S, Clayton T, Ramerstorfer J, Milinković MM, Roth BL, Sieghart W, and Cook JM (2010) Novel positive allosteric modulators of GABAA receptors: do subtle differences in activity at alpha1 plus alpha5 versus alpha2 plus alpha3 subunits account for dissimilarities in behavioral effects in rats? *Prog Neuropsychopharmacol Biol Psychiatry* **34**:376–86, Elsevier Inc.

Seifi M, Brown JF, Mills J, Bhandari P, Belelli D, Lambert JJ, Rudolph U, and Swinny JD (2014) Molecular and functional diversity of GABA-A receptors in the enteric nervous system of the mouse colon. *J Neurosci* **34**:10361–78.

Sengupta S, Weeraratne SD, Sun H, Phallen J, Rallapalli SK, Teider N, Kosaras B, Amani V, Pierre-Francois J, Tang Y, Nguyen B, Yu F, Schubert S, Balansay B, Mathios D, Lechpammer M, Archer TC, Tran P, Reimer RJ, Cook JM, Lim M, Jensen FE, Pomeroy SL, and Cho Y-J (2014) α5-GABAA receptors negatively regulate MYC-amplified medulloblastoma growth. *Acta Neuropathol* **127**:593–603.

Sieghart W (2015) *Allosteric Modulation of GABAA Receptors via Multiple Drug-Binding Sites.*, 1st ed., Elsevier Inc.

Sieghart W, Ramerstorfer J, Sarto-Jackson I, Varagic Z, and Ernst M (2012) A novel GABA(A) receptor pharmacology: drugs interacting with the α(+) β(-) interface. *Br J Pharmacol* **166**:476–85.

Sigel E, and Lüscher BP (2011) A closer look at the high affinity benzodiazepine binding site on GABAA receptors. *Curr Top Med Chem* **11**:241–6.

Skolnick P (2012) Anxioselective anxiolytics: on a quest for the Holy Grail. *Trends Pharmacol Sci* **33**:611–20.

Smith KS, Engin E, Meloni EG, and Rudolph U (2012) Benzodiazepine-induced anxiolysis and reduction of conditioned fear are mediated by distinct GABAA receptor subtypes in mice. *Neuropharmacology* **63**:250–8.

Soh MS, and Lynch JW (2015) Selective Modulators of α5-Containing GABAA Receptors and their Therapeutic Significance. *Curr Drug Targets* **16**:735–46.

Stamenic TT (2015) A novel benzodiazepine MP-III-022 impairs spatial cognition and improves social recognition by stron selective positive modulation of GABAA receptors containing the □5 subunit. submitted.

van Rijnsoever C, Täuber M, Choulli MK, Keist R, Rudolph U, Mohler H, Fritschy JM, and Crestani F (2004) Requirement of alpha5-GABAA receptors for the development of tolerance to the sedative action of diazepam in mice. *J Neurosci* **24**:6785–90.

Varagic Z, Wimmer L, Schnürch M, Mihovilovic MD, Huang S, Rallapalli S, Cook JM, Mirheydari P, Ecker GF, Sieghart W, and Ernst M (2013) Identification of novel positive allosteric modulators and null modulators at the GABAA receptor α+β- interface. *Br J Pharmacol* **169**:371–83.

Wan Y, Wang Q, and Prud'homme GJ (2015) GABAergic system in the endocrine pancreas: a new target for diabetes treatment. *Diabetes Metab Syndr Obes* **8**:79–87.

Yocum GT, Gallos G, Zhang Y, Jahan R, Stephen MR, Varagic Z, Puthenkalam R, Ernst M, Cook JM, and Emala CW (2015) Targeting the GABA A Receptor α4 Subunit in Airway Smooth Muscle to Alleviate Bronchoconstriction. *Am J Respir Cell Mol Biol* rcmb.2015–0176OC.

Footnotes

This work was supported by the graduate school program Molecular Drug Targets MolTag [Grant W1232, FWF] (to R.P.), [Grant MH-096463 and HL-118561] (to ..), the Bradley-Herzfeld Foundation (UWMFDN) for a Catalyst Grant and acknowledge Shimadzu analytical Laboratory of Southeastern Wisconsin as well as the Milwaukee Institute of Drug Discovery (to …).

APPENDIX I. Provisional Patent on α5 $GABA_A$ Selective Agonists for the Treatment of Depression and Related Disorders

Submitted: March 18, 2016.

TREATMENTS OF COGNITIVE AND MOOD SYMPTOMS IN NEURODEGENERATIVE AND NEUROPSYCHIATRIC DISORDERS WITH ALPHA5-CONTAINING GABAA SELECTIVE AGONISTS

1. Summary

Provided herein are novel compounds. The compounds may include modulators of the $GABA_A$ receptor Alpha5 subunit. The compounds may include positive allosteric modulators of $GABA_A$ receptor Alpha5 subunit. Further provided are methods of making the compounds. Further provided herein are compositions and formulations including one or more of the compounds.

Further provided herein are methods of treating a disorder or condition. Further provided are methods of cognitive and mood remediation in neurological disorders. Further provided are methods of reversing stress-induced deficits in aspects of cognitive flexibility. The disorder may be selected from Alzheimer's Disease (AD), Major Depressive Disorder (MDD), cognitive deficits associated with Major Depressive Disorder (MDD), depression such as major depression and persistent depressive disorder and bipolar depression, schizophrenia, alcoholism, addiction, anxiety disorder, epilepsy, neuropathic pain, autism spectrum disorder, or a combination thereof. Anxiety disorder is divided into generalized anxiety disorder, phobic disorder, and panic disorder; each has its own characteristics and symptoms and they require different treatment. Particular examples of anxiety disorders include generalized anxiety disorder, panic disorder, phobias such as agoraphobia, social anxiety disorder, obsessive-compulsive disorder, post-traumatic stress disorder, separation anxiety and childhood anxiety disorders. There are many different epilepsy syndromes, each presenting with its own unique combination of seizure type, typical age of onset, EEG findings, treatment, and prognosis. Exemplary epilepsy syndromes include, e.g., Benign centrotemporal lobe epilepsy of childhood, Benign occipital epilepsy of childhood (BOEC), Autosomal dominant nocturnal frontal lobe epilepsy (ADNFLE), Primary reading epilepsy, Childhood absence epilepsy (CEA), Juvenile absence epilepsy, Juvenile myoclonic epilepsy (JME), Symptomatic localization-related epilepsies, Temporal lobe epilepsy (TLE), Frontal lobe epilepsy, Rasmussen's encephalitis, West syndrome, Dravet's syndrome, Progressive myoclonic epilepsies, and Lennox-Gastaut syndrome (LGS). Genetic, congenital, and developmental conditions are often associated with epilepsy among younger patients. Tumors might be a cause for patients over age 40. Head trauma and central nervous system infections may cause epilepsy at any age. Schizophrenia is a mental disorder characterized by a breakdown of thought processes and by poor emotional responsiveness. Particular types of schizophrenia include paranoid type, disorganized

type, catatonic type, undifferentiated type, residual type, post-schizophrenic depression and simple schizophrenia. Neuropathic pain encompasses a range of painful conditions of diverse origins including diabetic neuropathy, post-herpetic neuralgia and nerve injuries after surgery. It includes pain following paraplegia, hypersensitivity to non-painful stimuli (allodynia), for example after surgery or during migraine attacks, spontaneous pain, hyperalgesia and diffuse muscle tenderness of myofacial syndromes. Autism spectrum disorder encompasses a range of phenotypes expressed during neurodevelopment, characterized by persistent deficits in social communication and interaction across various contexts. The methods may include administering to a subject in need thereof a compound or composition as described herein.

2. Introduction

Neurological disorders as a whole, including neurodegenerative and neuropsychiatric disorders, represent the leading cause of disability and of years lost due to disability in the world. Currently there are no treatments for Alzheimer's Disease (AD). Anticholinergic drugs are used for the cognitive deficits in AD but with very limited success. Current treatments for Major Depressive Disorder (MDD) acting on monoaminergic systems are all derived from mechanisms of actions of drugs that were discovered by chance over 60 years ago. Current antidepressants take weeks to achieve a therapeutic effect and have poor response and low remission rates. Indeed, despite their wide use, current antidepressant drugs only work at best in 50% of patients with depression. Moreover there are no treatments for cognitive deficits associated with MDD. In addition, there are currently no drugs for the robust and early symptoms of depression in AD. MDD is often co-morbid with alcohol and addiction disorders, for which there are very limited treatment options as well.

We and others have described evidence for reduced expression and function of somatostatin (SST)-positive inhibitory γ-aminobutyric acid (GABA) neurons in neurological disorders, including AD, schizophrenia, bipolar depression, and major depression. SST-positive GABA neurons are a subtype of inhibitory neurons which are characterized by inhibiting the dendritic compartment of glutamatergic pyramidal neurons, the main excitatory cells in the brain. Signaling through SST neurons regulate information and neural processes and has been specifically implicated in regulating cognition and mood. The main function of SST-positive neurons is mediated by the neurotransmitter GABA and by a specific subtype of $GABA_A$ receptors which contain the alpha5 subunit. Alpha5-containing $GABA_A$ receptors are localized on the dendrites of pyramidal cells, the cellular compartment targeted by SST-positive neurons. Hence, the deficits in SST positive cells that is observed across neurological

disorders is postulated to result in reduced signaling though Alpha5-containing $GABA_A$ receptors. Targeting Alpha5-containing $GABA_A$ receptors may therefore have therapeutic value for cognitive and mood symptoms across brain disorders, and specifically in AD and MDD.

3. Description

The target for therapeutic intervention may include the inhibitory $GABA_A$ receptor Alpha5 subunit, the pharmacological effect may include positive allosteric modulation (Alpha5-PAM), and the therapeutic indication may include cognitive and mood remediation in neurological disorders (Alzheimer's disease, major depression, bipolar depression, schizophrenia, etc). Moreover, deficits in Alpha5-containing GABAA receptors have been reported in alcoholism and addiction, suggesting a therapeutic potential for alpha5-PAM in these disorders as well.

Alpha5-PAM may reverse stress-induced deficits in aspects of cognitive flexibility. Alpha5-PAM represents a novel mechanism of cognitive remediation and antidepressant action that is informed by the pathology of the illness (i.e. decreased SST-positive GABA cell markers).

We show in preclinical rodent models that drugs that augment signaling at Alpha5-containing GABAA receptors with an alpha5-PAM, can have antidepressant activity in rodent models of depression, and can reverse stress-induced deficits in aspects of cognitive flexibility, the ability of learning new rules, an important symptom dimension associated with neurological disorders. In control animals (i.e. non-stressed baseline) we show that strong alpha5-PAM modulation (i.e. high dose) causes mild muscle relaxation, devoid of ataxia or sedation characteristic for non-selective benzodiazepines, and some spatial learning and memory deficits. Finally, we show that mild alpha5-PAM modulation in control animals improved social recognition and acquisition of spatial learning in control animals (i.e. baseline).

Together this suggests that alpha5-PAM can remediate mood and cognitive symptoms in preclinical models of mood and cognitive disturbances (i.e., in disease states) with a mildly negative or positive behavioral profile in control animals (i.e., in non-disease states).

The market of the use of Alpha5-PAM compounds is extremely broad. It includes Alzheimer's disease (early stage; 10-30% of population between 65 and 85 years of age), late-life depression, adult depression (10% of population), treatment-resistant depression (5% of population) and other

categories of disorders characterized by reduced SST-positive GABA neurons and GABA inhibition (schizophrenia, bipolar disorders; 3% of the population).

a. Behavioral Findings

(1) Alpha5-PAM has antidepressant activity in rodent models of depression
These results are described in the Piantadosi et al manuscript.
This study was performed in mice and used the prototypical SH-053-2'F-R-CH3 alpha5-PAM, the parent compound of MP-III-022. Studies of antidepressant activity of MP-III-022 are on-going.

(2) Alpha5-PAM can reverse stress-induced deficits in aspects of cognitive flexibility.
These studies are described in Belzung and Sibille (See attached document). This study used MP-III-022 in mice.

3) Alpha5-PAM has mild myorelaxation and cognitive effects at high dose in control animals.
These studies are described in Savic paper (Stamenic et al). This study used MP-III-022 in rats.

(4) Alpha5-PAM has precognitive effects at mild doses in control animals.
These studies are described in Savic paper (Stamenic et al). They show improved social recognition and acquisition of spatial learning in control animals. This study used MP-III-022 in rats.

Together these results suggest that Alpha5-PAM represents a novel mechanism of cognitive remediation and antidepressant action. Patients with a range of brain diseases may benefit from Alpha5-PAM, including patients with AD, MDD, schizophrenia and bipolar disorders.

On-going on future studies include pharmacokinetic and pharmacodynamics evaluation of compounds herein, including their effects on mood-related and cognitive behaviors in rodents (such as mice and rats).

b. Compounds

Definitions

Definitions of specific functional groups and chemical terms are described in more detail below. For purposes of this invention, the chemical elements are identified in accordance with the

Periodic Table of the Elements, CAS version, Handbook of Chemistry and Physics, 75th Ed., inside cover, and specific functional groups are generally defined as described therein. Additionally, general principles of organic chemistry, as well as specific functional moieties and reactivity, are described in *Organic Chemistry*, Thomas Sorrell, University Science Books, Sausalito, 1999; Smith and March *March's Advanced Organic Chemistry*, 5th Edition, John Wiley & Sons, Inc., New York, 2001; Larock, *Comprehensive Organic Transformations*, VCH Publishers, Inc., New York, 1989; Carruthers, *Some Modern Methods of Organic Synthesis*, 3rd Edition, Cambridge University Press, Cambridge, 1987; the entire contents of each of which are incorporated herein by reference.

The term "acyl" refers to an alkylcarbonyl, cycloalkylcarbonyl, heterocyclylcarbonyl, arylcarbonyl or heteroarylcarbonyl substituent, any of which may be further substituted (e.g., with one or more substituents).

The term "alkyl" refers to a straight or branched hydrocarbon chain, containing the indicated number of carbon atoms. For example, C_1-C_{12} alkyl indicates that the alkyl group may have from 1 to 12 (inclusive) carbon atoms, and C_1-C_4 alkyl indicates that the alkyl group may have from 1 to 4 (inclusive) carbon atoms. An alkyl group may be optionally substituted. Examples of C_1-C_4 alkyl groups include methyl, ethyl, *n*-propyl, isopropyl, *n*-butyl, *sec*-butyl and *tert*-butyl.

The term "alkenyl" refers to a straight or branched hydrocarbon chain having one or more double bonds. Examples of alkenyl groups include, but are not limited to, allyl, propenyl, 2-butenyl, 3-hexenyl and 3-octenyl groups. One of the double bond carbons may optionally be the point of attachment of the alkenyl substituent. An alkenyl group may be optionally substituted.

The term "alkynyl" refers to a straight or branched hydrocarbon chain having one or more triple bonds. Examples of alkynyl groups include, but are not limited to, ethynyl, propargyl, and 3-hexynyl. One of the triple bond carbons may optionally be the point of attachment of the alkynyl substituent. An alkynyl group may be optionally substituted.

The term "aryl" refers to an aromatic monocyclic, bicyclic, or tricyclic hydrocarbon ring system, wherein any ring atom capable of substitution can be substituted (e.g., with one or more substituents). Examples of aryl moieties include, but are not limited to, phenyl, naphthyl, and anthracenyl.

The term "arylalkyl" refers to an alkyl moiety in which an alkyl hydrogen atom is replaced with an aryl group. Arylalkyl includes groups in which more than one hydrogen atom has been replaced with an aryl group. Examples of arylalkyl groups include benzyl, 2-phenylethyl, 3-phenylpropyl, 9-fluorenyl, benzhydryl, and trityl groups.

The term "cycloalkyl" as used herein refers to nonaromatic, saturated or partially unsaturated cyclic, bicyclic, tricyclic or polycyclic hydrocarbon groups having 3 to 12 carbons (e.g., 3, 4, 5, 6 or 7 carbon atoms). Any ring atom can be substituted (e.g., with one or more substituents). Cycloalkyl

groups can contain fused rings. Fused rings are rings that share one or more common carbon atoms. Examples of cycloalkyl groups include, but are not limited to, cyclopropyl, cyclobutyl, cyclopentyl, cyclohexyl, cyclohexenyl, cyclohexadienyl, methylcyclohexyl, adamantyl, norbornyl and norbornenyl.

The term "halo" or "halogen" as used herein refers to any radical of fluorine, chlorine, bromine or iodine.

The term "haloalkyl" as used herein refers to an alkyl in which one or more hydrogen atoms are replaced with a halogen, and includes alkyl moieties in which all hydrogens have been replaced with halogens (e.g., perfluoroalkyl such as CF_3).

The term "heteroaryl" as used herein refers to an aromatic 5-8 membered monocyclic, 8-12 membered bicyclic, or 11-14 membered tricyclic ring system having 1-3 heteroatoms if monocyclic, 1-6 heteroatoms if bicyclic, or 1-9 heteroatoms if tricyclic, said heteroatoms independently selected from O, N, S, P and Si (e.g., carbon atoms and 1-3, 1-6, or 1-9 heteroatoms independently selected from O, N, S, P and Si if monocyclic, bicyclic, or tricyclic, respectively). Any ring atom can be substituted (e.g., with one or more substituents). Heteroaryl groups can contain fused rings, which are rings that share one or more common atoms. Examples of heteroaryl groups include, but are not limited to, radicals of pyridine, pyrimidine, pyrazine, pyridazine, pyrrole, imidazole, pyrazole, oxazole, isoxazole, furan, thiazole, isothiazole, thiophene, quinoline, isoquinoline, quinoxaline, quinazoline, cinnoline, indole, isoindole, indolizine, indazole, benzimidazole, phthalazine, pteridine, carbazole, carboline, phenanthridine, acridine, phenanthroline, phenazine, naphthyridines and purines.

The term "heterocyclyl" as used herein refers to a nonaromatic, saturated or partially unsaturated 3-10 membered monocyclic, 8-12 membered bicyclic, or 11-14 membered tricyclic ring system having 1-3 heteroatoms if monocyclic, 1-6 heteroatoms if bicyclic, or 1-9 heteroatoms if tricyclic, said heteroatoms selected from O, N, S, Si and P (e.g., carbon atoms and 1-3, 1-6, or 1-9 heteroatoms of O, N, S, Si and P if monocyclic, bicyclic, or tricyclic, respectively). Any ring atom can be substituted (e.g., with one or more substituents). Heterocyclyl groups can contain fused rings, which are rings that share one or more common atoms. Examples of heterocyclyl groups include, but are not limited to, radicals of tetrahydrofuran, tetrahydrothiophene, tetrahydropyran, piperidine, piperazine, morpholine, pyrroline, pyrimidine, pyrrolidine, indoline, tetrahydropyridine, dihydropyran, thianthrene, pyran, benzopyran, xanthene, phenoxathiin, phenothiazine, furazan, lactones, lactams such as azetidinones and pyrrolidinones, sultams, sultones, and the like.

The term “hydroxy” refers to an –OH radical. The term "alkoxy" refers to an –O-alkyl radical. The term “aryloxy” refers to an –O-aryl radical. The term “haloalkoxy” refers to an –O-haloalkyl radical.

The term "substituent" refers to a group "substituted" on an alkyl, alkenyl, alkynyl, cycloalkyl, heterocyclyl, aryl, arylalkyl or heteroaryl group at any atom of that group. Suitable substituents include, without limitation: acyl, acylamido, acyloxy, alkoxy, alkyl, alkenyl, alkynyl, amido, amino, carboxy, cyano, ester, halo, hydroxy, imino, nitro, oxo (e.g., C=O), phosphonate, sulfinyl, sulfonyl, sulfonate, sulfonamino, sulfonamido, thioamido, thiol, thioxo (e.g., C=S), and ureido. In embodiments, substituents on a group are independently any one single, or any combination of the aforementioned substituents. In embodiments, a substituent may itself be substituted with any one of the above substituents.

The above substituents may be abbreviated herein, for example, the abbreviations Me, Et and Ph represent methyl, ethyl and phenyl, respectively. A more comprehensive list of the abbreviations used by organic chemists appears in the first issue of each volume of the Journal of Organic Chemistry; this list is typically presented in a table entitled Standard List of Abbreviations. The abbreviations contained in said list, and all abbreviations used by organic chemists of ordinary skill in the art, are hereby incorporated by reference.

For compounds, groups and substituents thereof may be selected in accordance with permitted valence of the atoms and the substituents, such that the selections and substitutions result in a stable compound, e.g., which does not spontaneously undergo transformation such as by rearrangement, cyclization, elimination, etc.

Where substituent groups are specified by their conventional chemical formulae, written from left to right, they optionally encompass substituents resulting from writing the structure from right to left, e.g., $-CH_2O-$ optionally also recites $-OCH_2-$.

In accordance with a convention used in the art, the group:

is used in structural formulas herein to depict the bond that is the point of attachment of the moiety or substituent to the core or backbone structure.

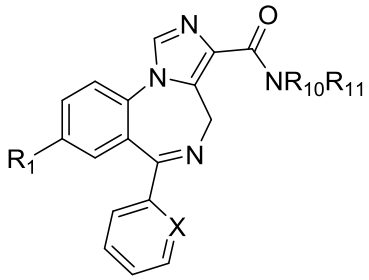
In the context of treating a disorder, the term “effective amount” as used herein refers to an amount of the compound or a composition comprising the compound which is effective, upon single or multiple dose administrations to a subject, in treating a cell, or curing, alleviating, relieving or improving a symptom of the disorder in a subject. An effective amount of the compound or composition may vary according to the application. In the context of treating a disorder, an effective amount may depend on factors such as the disease state, age, sex, and weight of the individual, and the ability of the compound to elicit a desired response in the individual. In an example, an effective

amount of a compound is an amount that produces a statistically significant change in a given parameter as compared to a control, such as in cells (e.g., a culture of cells) or a subject not treated with the compound.

It is specifically understood that any numerical value recited herein (e.g., ranges) includes all values from the lower value to the upper value, i.e., all possible combinations of numerical values between the lowest value and the highest value enumerated are to be considered to be expressly stated in this application. For example, if a concentration range is stated as 1% to 50%, it is intended that values such as 2% to 40%, 10% to 30%, or 1% to 3%, etc., are expressly enumerated in this specification. These are only examples of what is specifically intended.

MP-III-022 has PAM activity at the alpha5-containing GABAA receptor and presents the best efficacy, potency, ADME and toxicity data compared to related compounds.

Compounds may be of the following formula (I):



(I)

or a salt thereof, wherein:

X is selected from the group consisting of N, C-H, C-F, C-Cl, C-Br, C-I, and C-NO_2;

R_1 is selected from the group consisting of –Br, C≡CH, -C≡C-$Si(CH_3)_3$, -cyclopropyl, and bicycle[1.1.1]pentane (

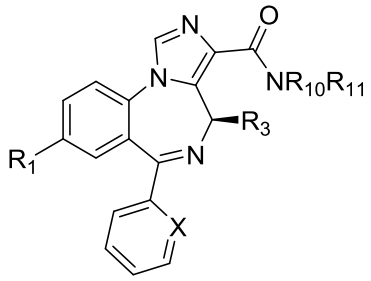
); and

R_{10} and R_{11} are independently selected from H, C1-6 alkyl, cycloalkyl, or together may form a cycloalkyl ring.

In some embodiments, X is N. In some embodiments, X is CH. In some embodiments, X is CF. In some embodiments, X is CCl. In some embodiments, X is CBr. In some embodiments, X is CI. In some embodiments, R_1 is –Br. In some embodiments, R_1 is -C≡CH. In some embodiments, R_1 is –

C≡C-Si(CH_3)$_3$. In some embodiments, R_1 is –cyclopropyl. In some embodiments, R_1 is bicycle[1.1.1]pentane.

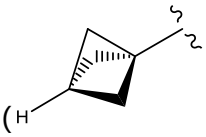
Compounds may be of the following formula (II):



(II)

or a salt thereof, wherein:

X is selected from the group consisting of N, C-H, C-F, C-Cl, C-Br, C-I, and C-NO_2;

R_1 is selected from the group consisting of –Br, -C≡CH, -C≡C-Si(CH_3)$_3$, -cyclopropyl, and bicycle[1.1.1]pentane (

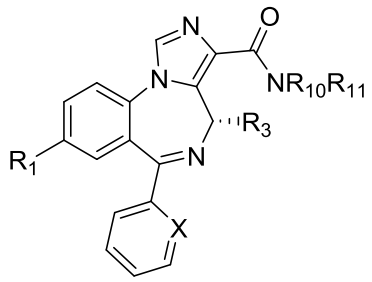
);

R_3 is selected from the group consisting of -H, -CH_3, -CH_2CH_3, -$CH(CH_3)_2$, -F, -Cl, -CF_3, and -CCl_3; and

R_{10} and R_{11} are independently selected from H, C1-6 alkyl, cycloalkyl, or together may form a cycloalkyl ring.

In some embodiments, X is N. In some embodiments, X is CH. In some embodiments, X is CF. In some embodiments, X is CCl. In some embodiments, X is CBr. In some embodiments, X is CI. In some embodiments, R_1 is –Br. In some embodiments, R_1 is -C≡CH. In some embodiments, R_1 is –C≡C-Si(CH_3)$_3$. In some embodiments, R_1 is –cyclopropyl. In some embodiments, R_1 is bicycle[1.1.1]pentane. In some embodiments, R_3 is -H. In some embodiments, R_3 is –CH_3. In some embodiments, R_3 is –CH_2CH_3. In some embodiments, R_3 is –$CH(CH_3)_2$. In some embodiments, R_3 is F. In some embodiments, R_3 is Cl. In some embodiments, R_3 is –CF_3. In some embodiments, R_3 is –CCl_3.

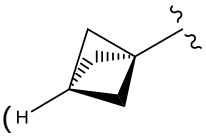
Compounds may be of the following formula (III):



(III)

or a salt thereof, wherein:

X is selected from the group consisting of N, C-H, C-F, C-Cl, C-Br, C-I, and C-NO_2;

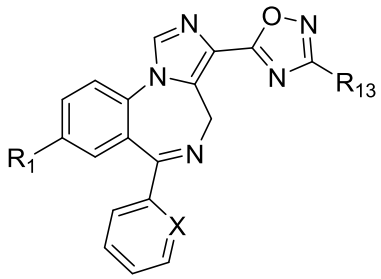
R_1 is selected from the group consisting of –Br, -C≡CH, -C≡C-$Si(CH_3)_3$, -cyclopropyl, and bicycle[1.1.1]pentane ();

R_3 is selected from the group consisting of -H, -CH_3, -CH_2CH_3, -$CH(CH_3)_2$, -F, -Cl, -CF_3, and -CCl_3; and

R_{10} and R_{11} are independently selected from H, C1-6 alkyl, cycloalkyl, or together may form a cycloalkyl ring.

In some embodiments, X is N. In some embodiments, X is CH. In some embodiments, X is CF. In some embodiments, X is CCl. In some embodiments, X is CBr. In some embodiments, X is CI. In some embodiments, R_1 is –Br. In some embodiments, R_1 is -C≡CH. In some embodiments, R_1 is –C≡C-$Si(CH_3)_3$. In some embodiments, R_1 is –cyclopropyl. In some embodiments, R_1 is bicycle[1.1.1]pentane. In some embodiments, R_3 is -H. In some embodiments, R_3 is –CH_3. In some embodiments, R_3 is –CH_2CH_3. In some embodiments, R_3 is –$CH(CH_3)_2$. In some embodiments, R_3 is F. In some embodiments, R_3 is Cl. In some embodiments, R_3 is –CF_3. In some embodiments, R_3 is –CCl_3.

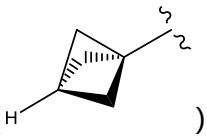
Compounds may be of the following formula (IV):



(IV)

or a salt thereof, wherein:

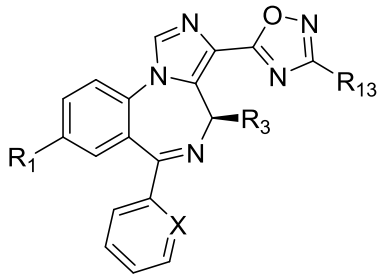
X is selected from the group consisting of N, C-H, C-F, C-Cl, C-Br, C-I, and C-NO_2;

R_1 is selected from the group consisting of –Br, -C≡CH, -C≡C-Si$(CH_3)_3$, -cyclopropyl, and bicycle[1.1.1]pentane (); and

R_{13} is selected from the group consisting of H, C_{1-6} alkyl, and cycloalkyl.

In some embodiments, X is N. In some embodiments, X is CH. In some embodiments, X is CF. In some embodiments, X is CCl. In some embodiments, X is CBr. In some embodiments, X is CI. In some embodiments, R_1 is –Br. In some embodiments, R_1 is -C≡CH. In some embodiments, R_1 is –C≡C-Si$(CH_3)_3$. In some embodiments, R_1 is –cyclopropyl. In some embodiments, R_1 is bicycle[1.1.1]pentane.

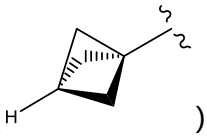
Compounds may be of the following formula (V):



(V)

or a salt thereof, wherein:

X is selected from the group consisting of N, C-H, C-F, C-Cl, C-Br, C-I, and C-NO_2;

R_1 is selected from the group consisting of –Br, -C≡CH, -C≡C-Si$(CH_3)_3$, -cyclopropyl, and bicycle[1.1.1]pentane ();

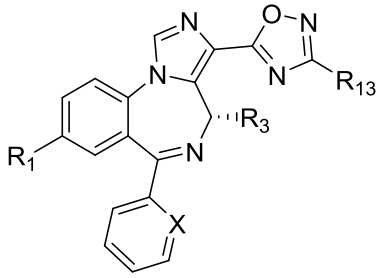
R_3 is selected from the group consisting of -H, -CH_3, -CH_2CH_3, -$CH(CH_3)_2$, -F, -Cl, -CF_3, and -CCl_3; and

R_{13} is selected from the group consisting of H, C_{1-6} alkyl, and cycloalkyl.

In some embodiments, X is N. In some embodiments, X is CH. In some embodiments, X is CF. In some embodiments, X is CCl. In some embodiments, X is CBr. In some embodiments, X is CI. In some embodiments, R_1 is –Br. In some embodiments, R_1 is -C≡CH. In some embodiments, R_1 is –

C≡C-Si(CH_3)$_3$. In some embodiments, R_1 is –cyclopropyl. In some embodiments, R_1 is bicycle[1.1.1]pentane. In some embodiments, R_3 is -H. In some embodiments, R_3 is –CH_3. In some embodiments, R_3 is –CH_2CH_3. In some embodiments, R_3 is –$CH(CH_3)_2$. In some embodiments, R_3 is F. In some embodiments, R_3 is Cl. In some embodiments, R_3 is –CF_3. In some embodiments, R_3 is –CCl_3.

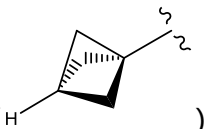
Compounds may be of the following formula (VI):



(VI)

or a salt thereof, wherein:

X is selected from the group consisting of N, C-H, C-F, C-Cl, C-Br, C-I, and C-NO_2;

R_1 is selected from the group consisting of –Br. -C≡CH, -C≡C-Si(CH_3)$_3$, -cyclopropyl, and bicycle[1.1.1]pentane (

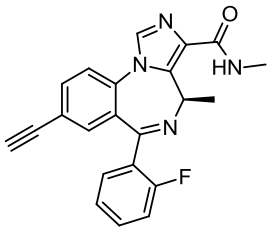
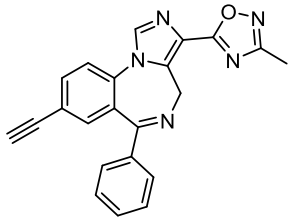
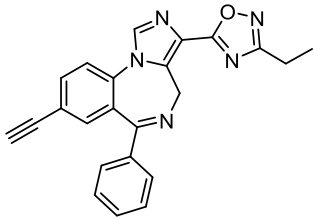
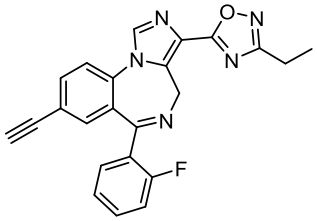
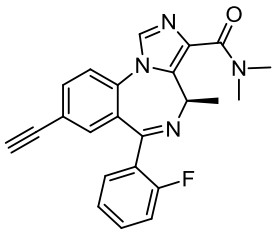
);

R_3 is selected from the group consisting of -H, -CH_3, -CH_2CH_3, -$CH(CH_3)_2$, -F, -Cl, -CF_3, and -CCl_3; and

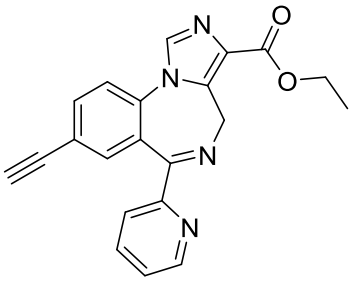
R_{13} is selected from the group consisting of H, C_{1-6} alkyl, and cycloalkyl.

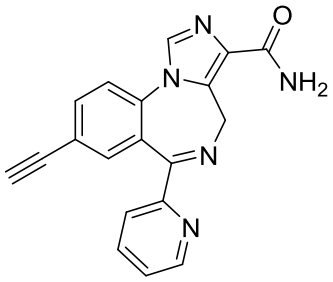
In some embodiments, X is N. In some embodiments, X is CH. In some embodiments, X is CF. In some embodiments, X is CCl. In some embodiments, X is CBr. In some embodiments, X is CI. In some embodiments, R_1 is –Br. In some embodiments, R_1 is -C≡CH. In some embodiments, R_1 is –C≡C-Si(CH_3)$_3$. In some embodiments, R_1 is –cyclopropyl. In some embodiments, R_1 is bicycle[1.1.1]pentane. In some embodiments, R_3 is -H. In some embodiments, R_3 is –CH_3. In some embodiments, R_3 is –CH_2CH_3. In some embodiments, R_3 is –$CH(CH_3)_2$. In some embodiments, R_3 is F. In some embodiments, R_3 is Cl. In some embodiments, R_3 is –CF_3. In some embodiments, R_3 is –CCl_3.

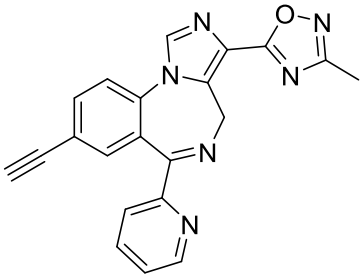
In some embodiments, for formulas (IV)-(VI), R_{13} is not C_{1-6} alkyl, particularly ethyl. In some embodiments, for formulas (I)-(VI), the compound is not one or more of:

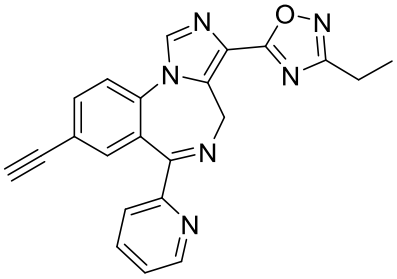

,

,

,

, or

,.

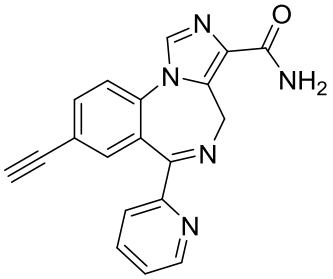
Compounds may be selected from the following:

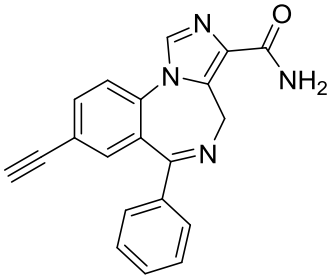

HZ-166

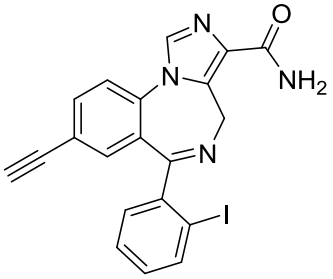

MP-II-065

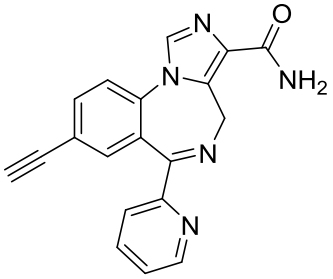

MP-III-085

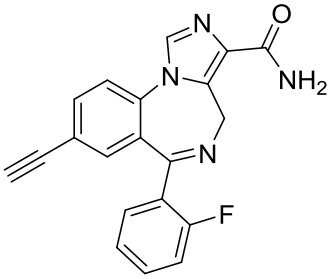

MP-III-080

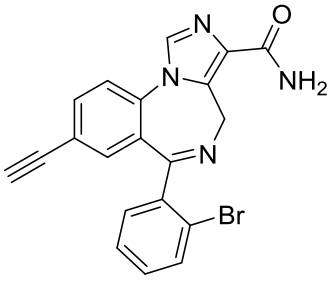


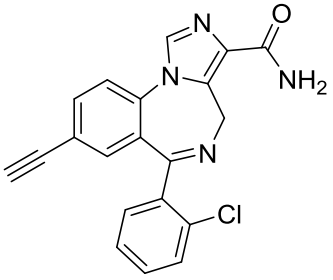


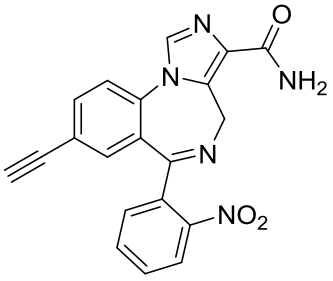


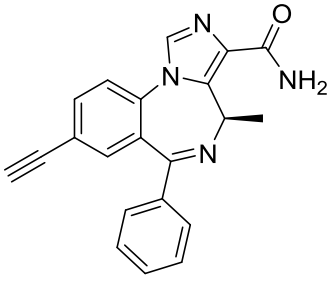


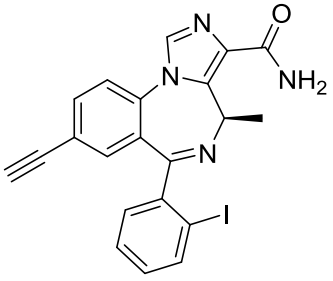


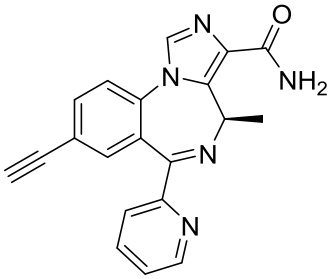


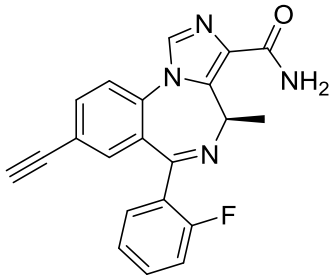


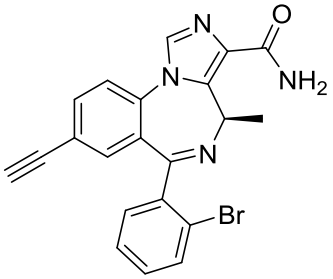


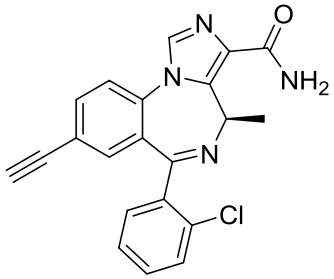


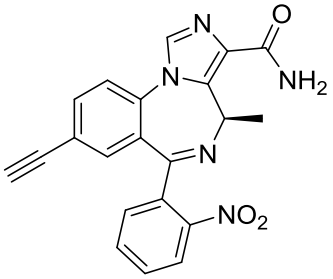


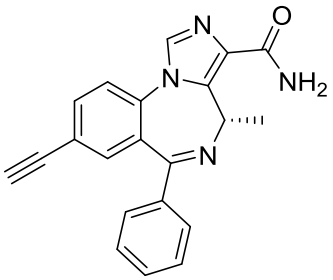


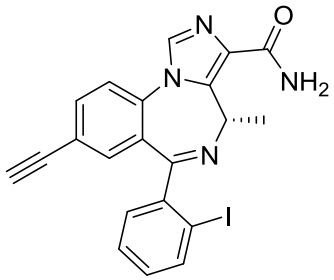


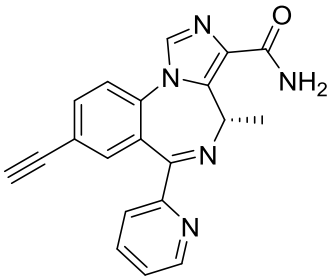


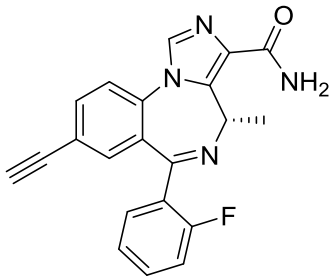


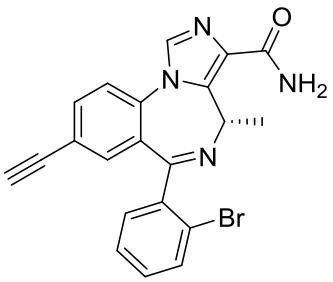


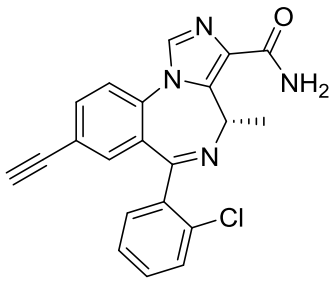


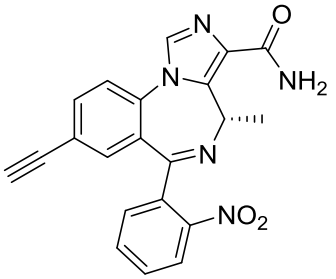


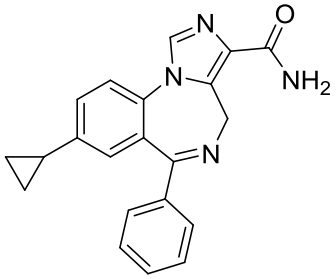


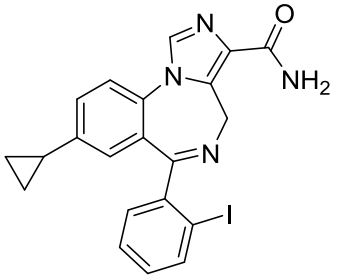


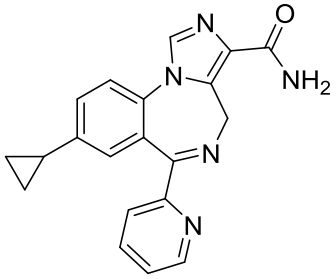


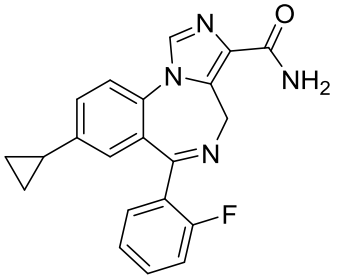


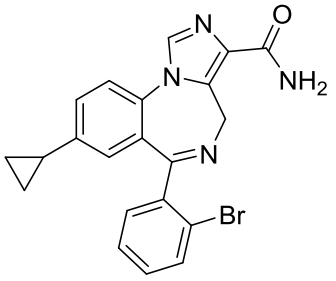


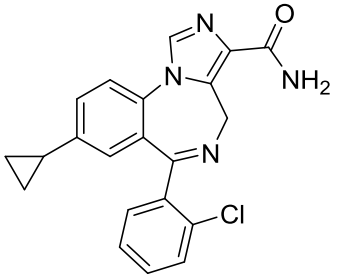


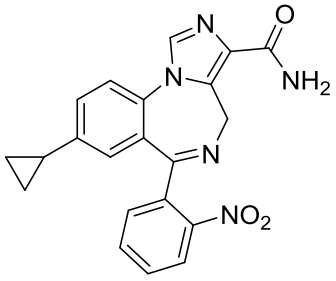


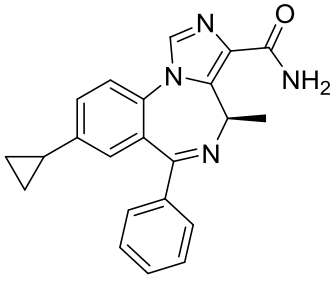


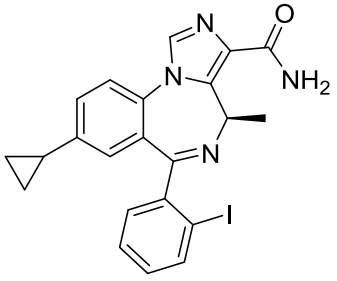


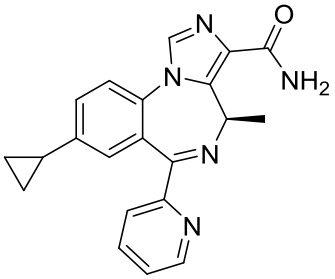


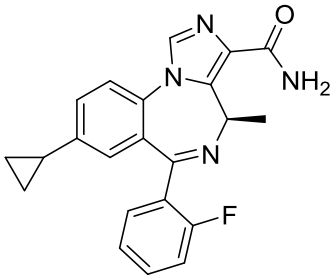


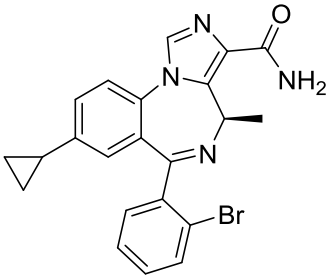


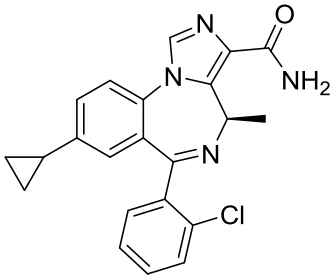


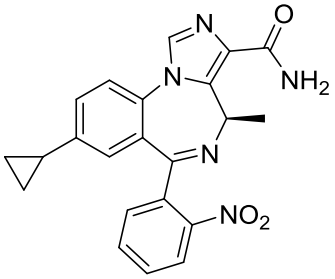


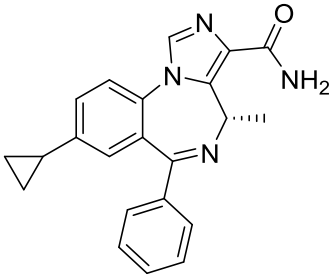


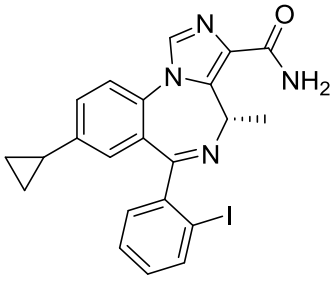


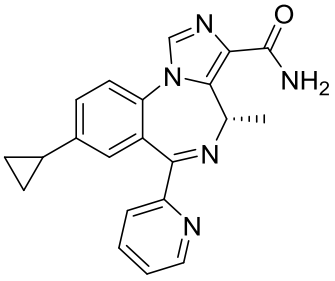


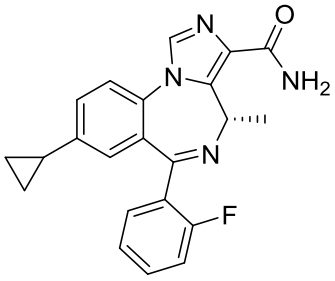


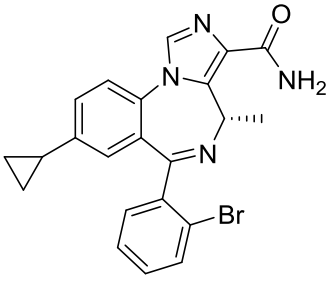


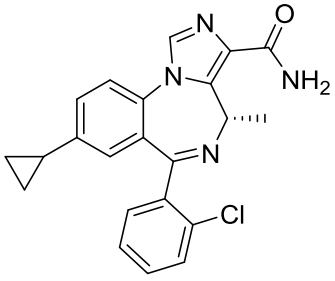


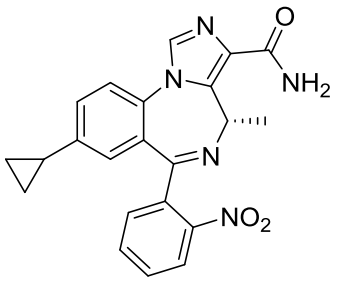


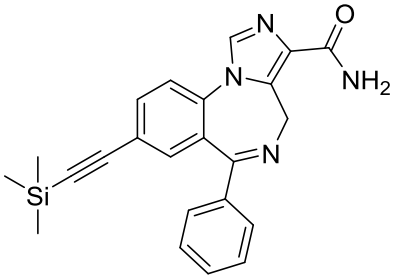


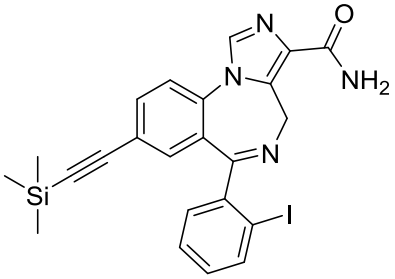


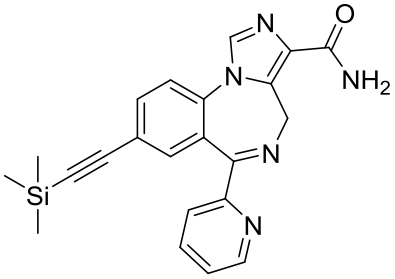


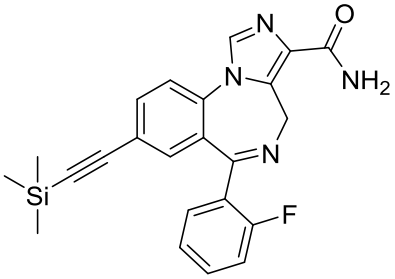


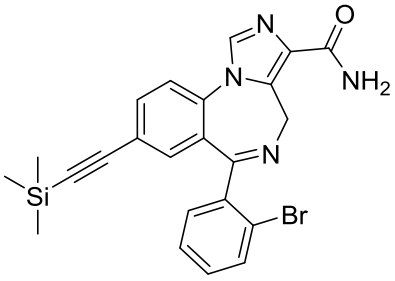


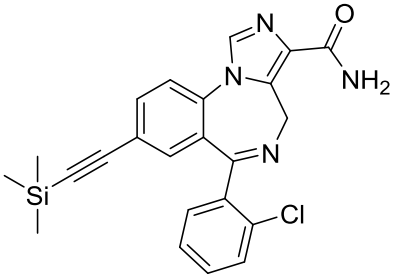


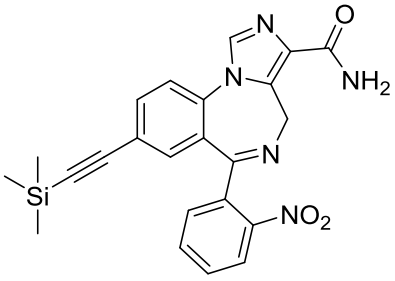


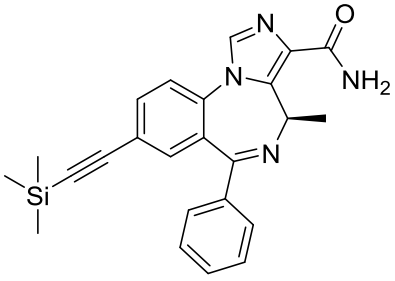


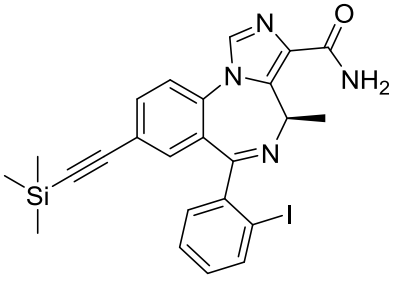


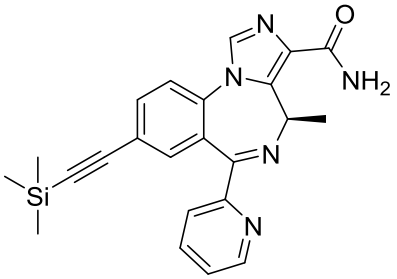


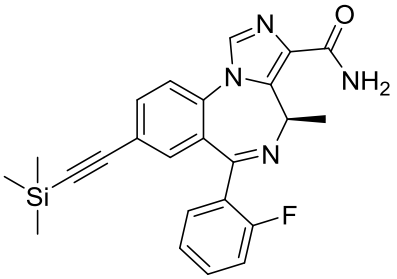


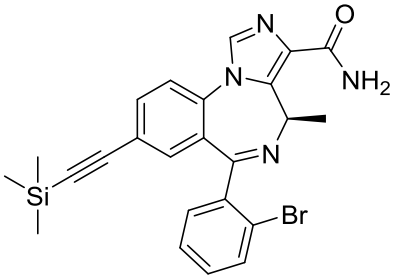


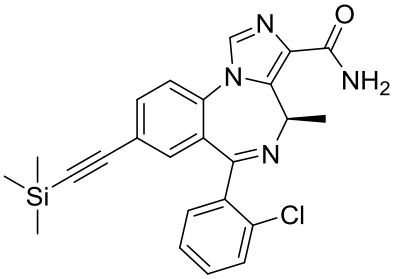


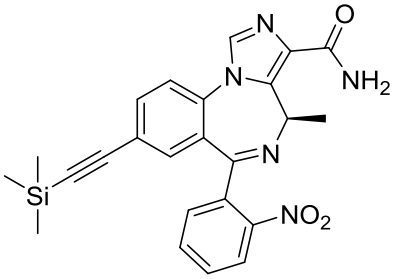


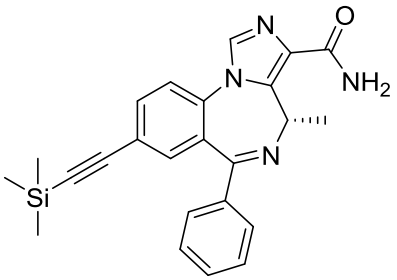


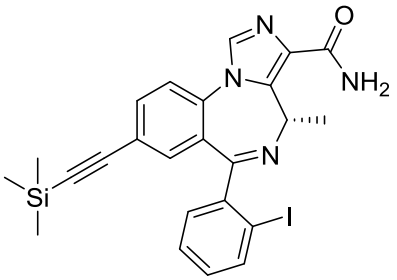


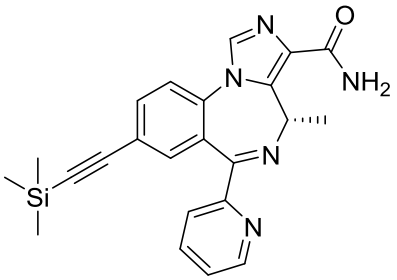


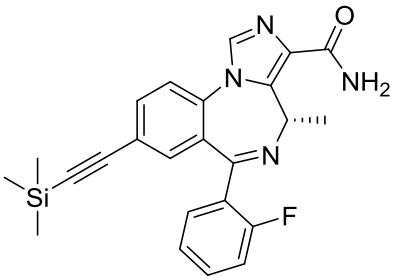


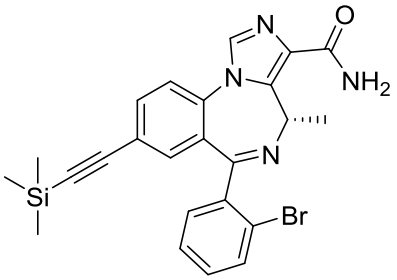


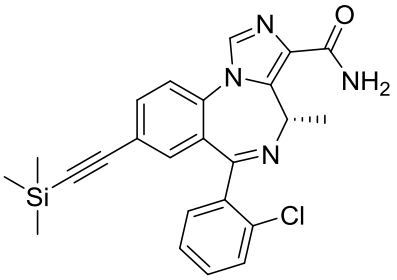


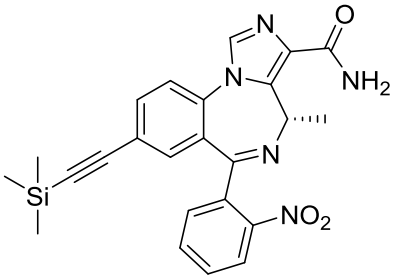


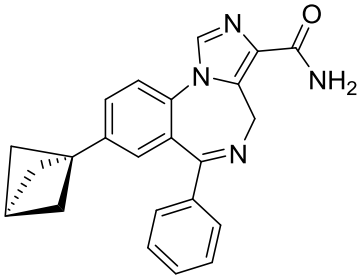


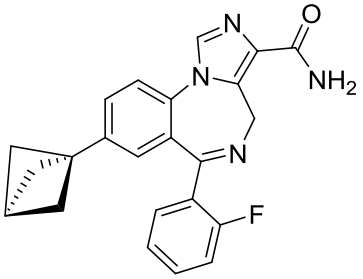


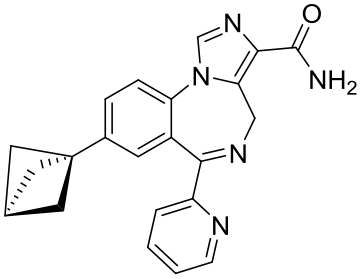


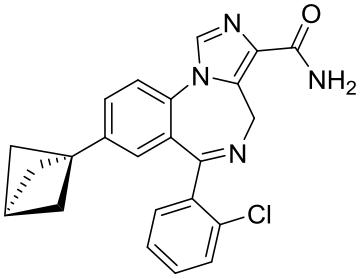


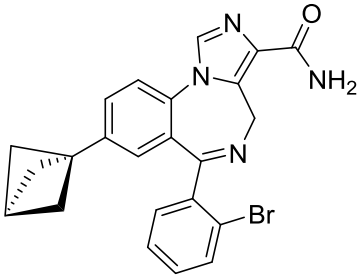


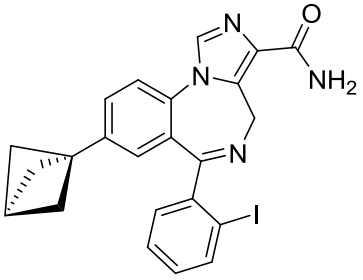


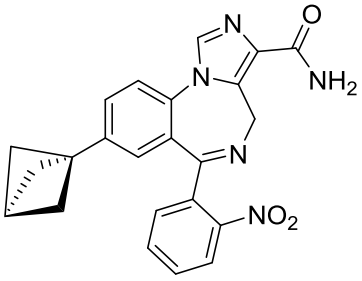


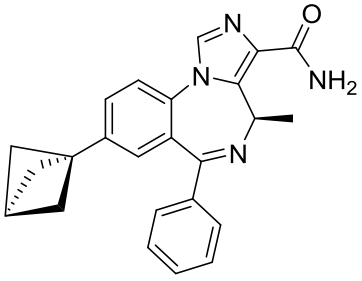


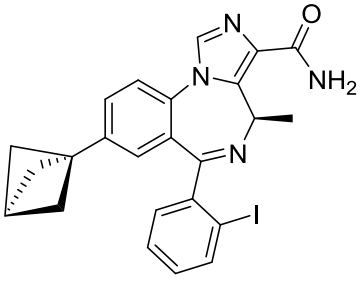


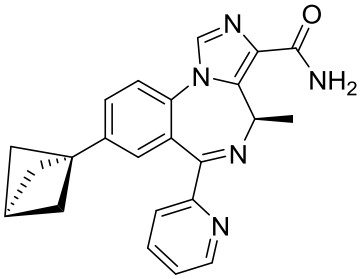


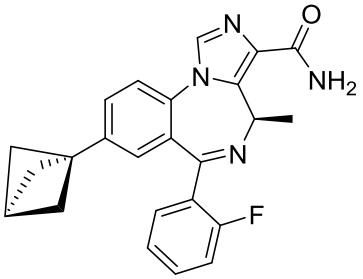


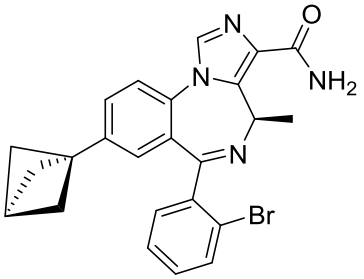


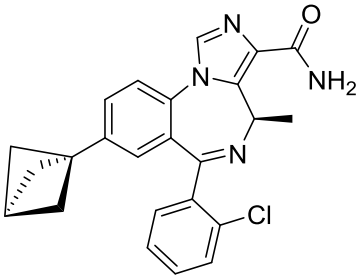


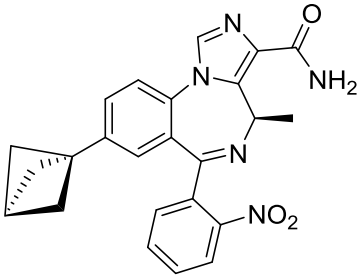


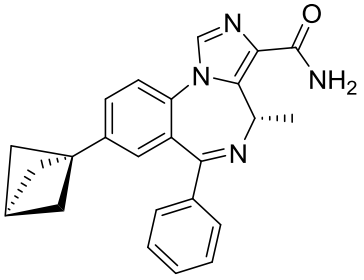


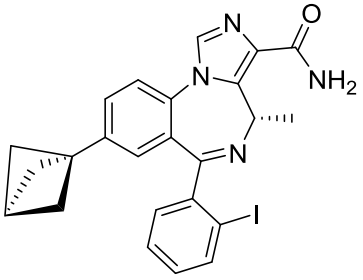


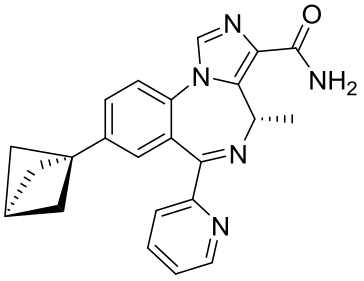


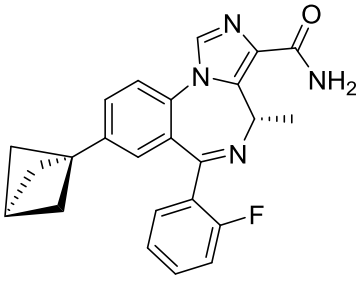


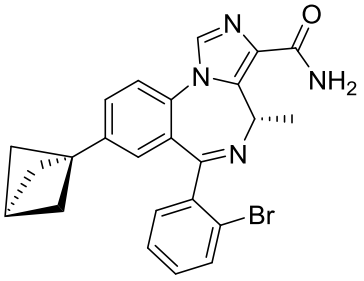


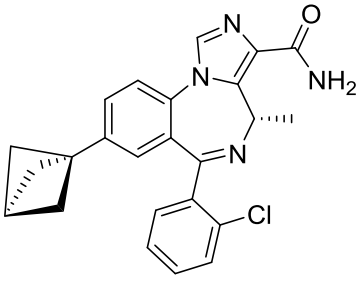


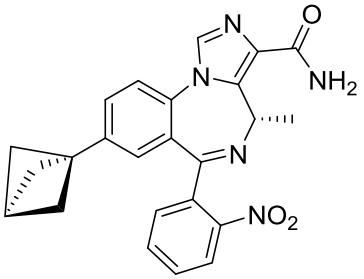




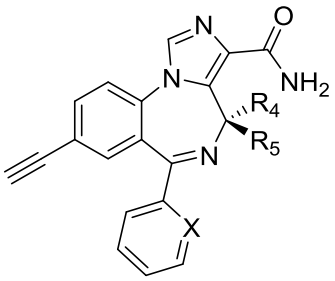


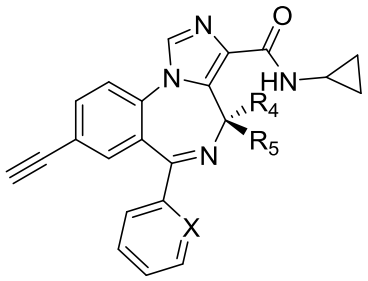


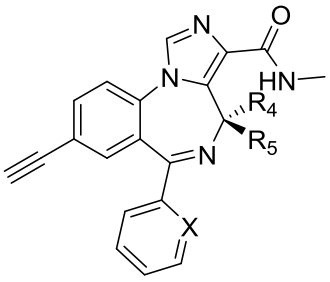


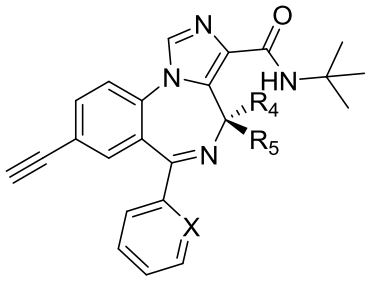


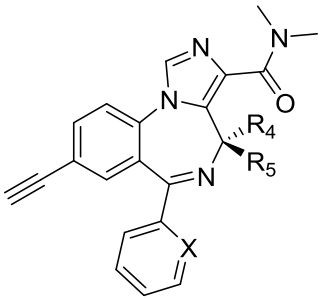
Compounds may further include the following, wherein X = CH, CF, CCl, N; R4 = H, CH_3; and R5 = H, CH_3:

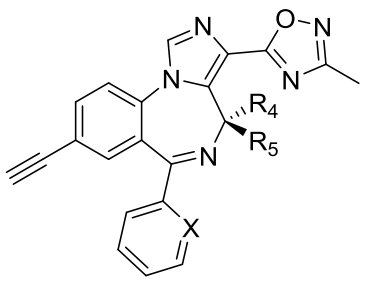


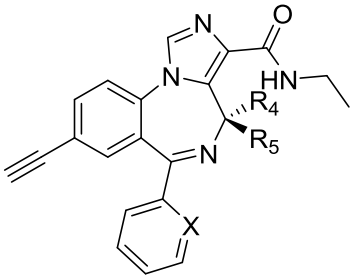


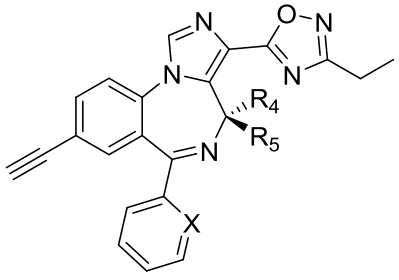


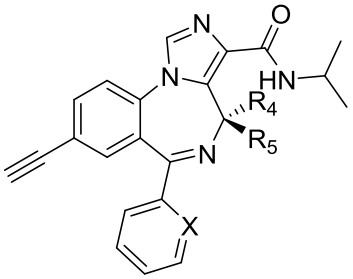


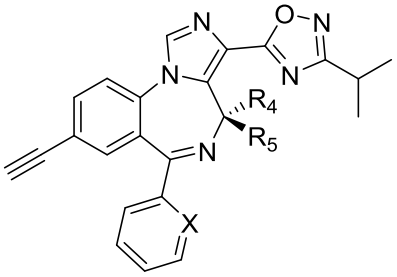


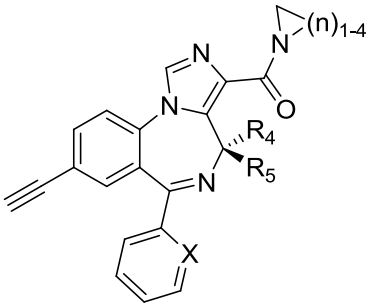




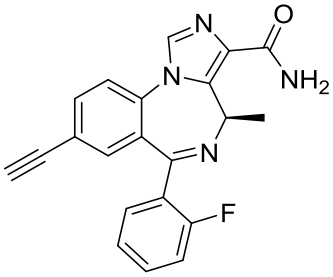




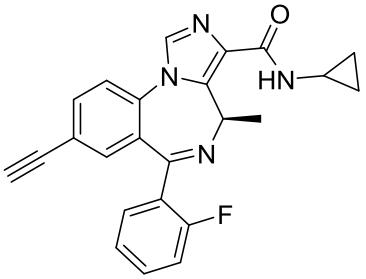


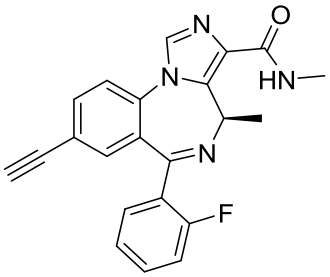


Compounds may further include the following:

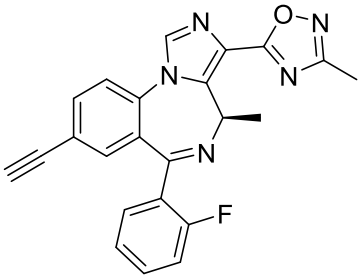


MP-III-019.B

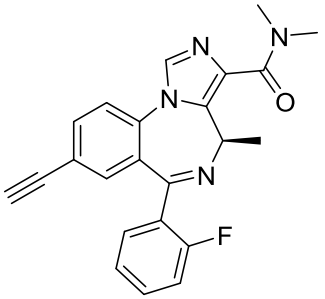


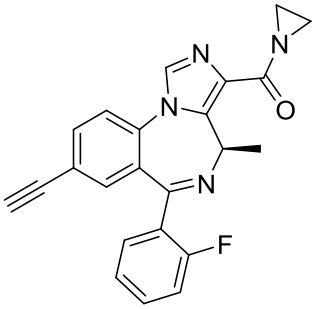


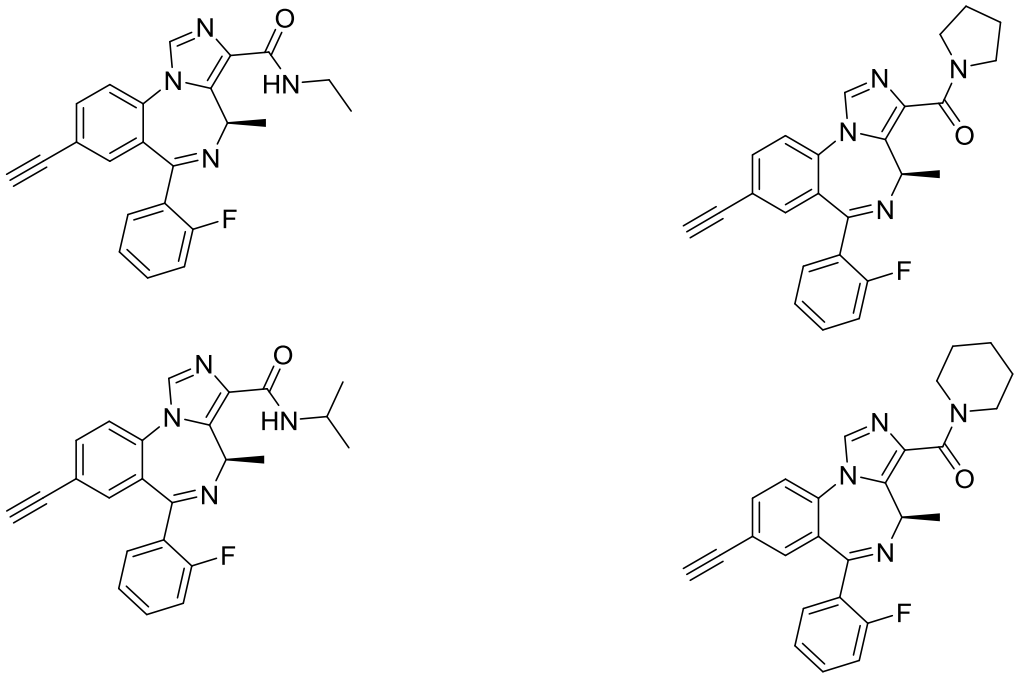
MP-III-022



MP-IV-004

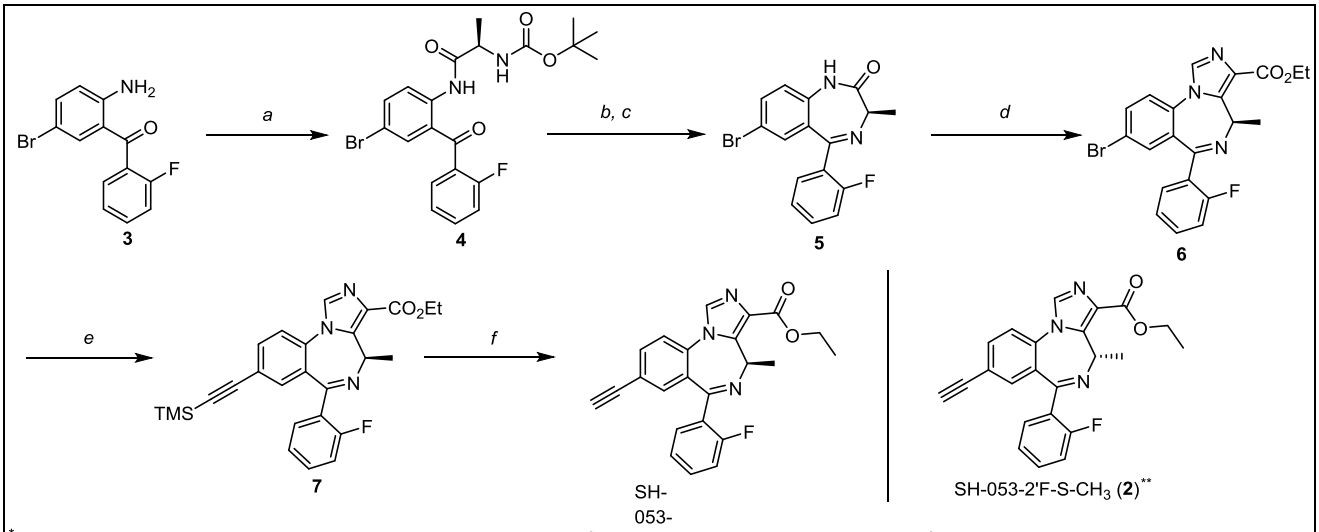






c. Synthesis

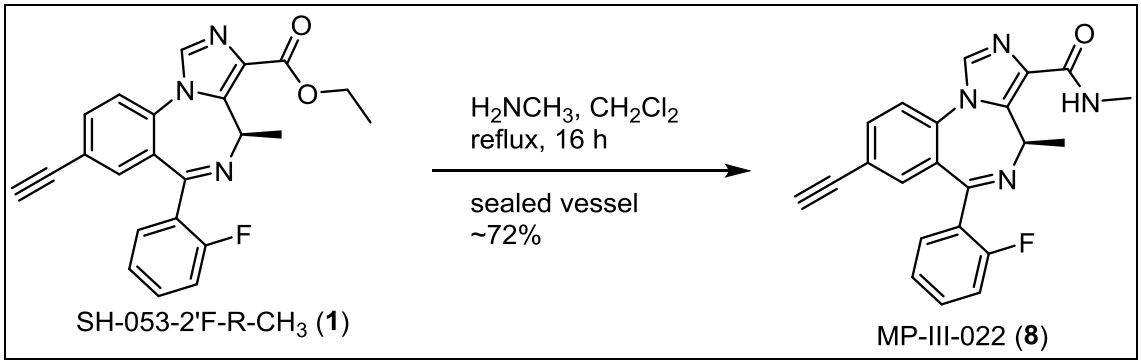
Scheme 1. Synthesis of SH-053-2'F-(*R/S*)-CH3.



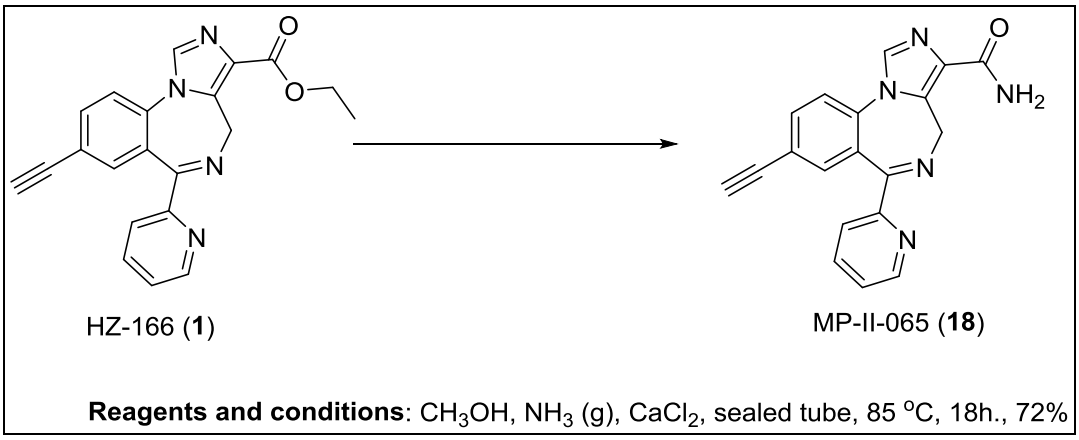
* *Reagents and Conditions*: a) D-Boc-alanine, DCC, CH_2Cl_2, 0 °C to r.t., 87%; b) CH_2Cl_2, HCl (g), 0 °C to r.t.; c) methanol/water, pH 8.5 (1 M NaOH), r.t., 75% over two steps; d) THF, K-*t*-BuO, $ClPO(OEt)_2$, $CNCH_2CO_2Et$, -78 °C to r.t., 78%; e) $Pd(PPh_3)_2(OAc)_2$, TMS-acetylene, Et_3N, CH_3CN, reflux, 12h., 91%; f) TBAF, THF, water, -78 °C, 95%

** Compound **2** synthesized with comparable yields using L-Boc-alanine in step *a.*

Scheme 2. Synthesis of MP-III-022.



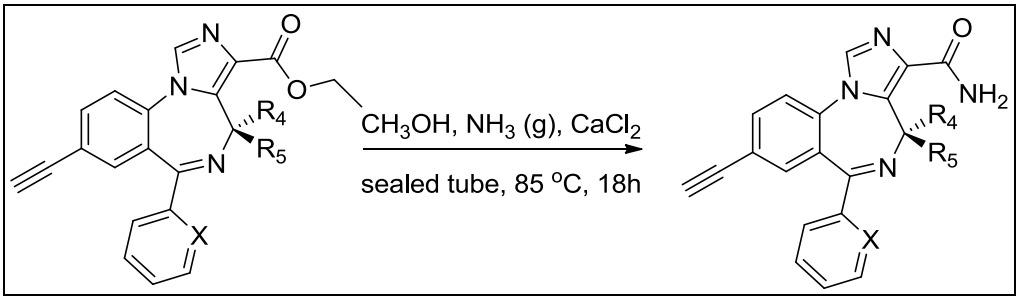
Scheme 3. Synthesis of MP-II-065.



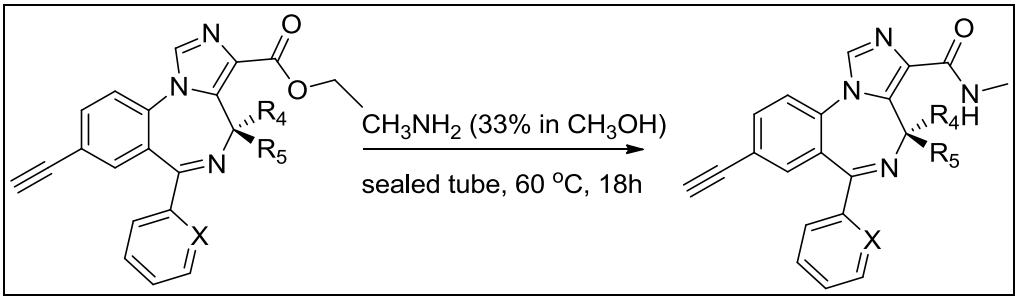
8-ethynyl-6-(pyridin-2-yl)-4*H*-benzo[*f*]imidazo[1,5-a][1,4]diazepine-3-carboxamide MP-II-065 (**18**) Ethyl ester **1** (1 g, 2.81 mmol) and calcium chloride (311 mg, 2.81 mmol) were placed inside a sealable vessel with a stir bar. Methanol (dry, 20 mL) was added and a septum was placed to seal the vessel. In a separate flask, ammonia (g) was bubbled into methanol (dry, 20 mL) until saturated, about 10 minutes. The ammonia-methanol solution was added to the vessel containing **1** and the vessel was sealed with a screw cap. The reaction mixed was heated and stirred at 85 ^oC for 18 hours. The reaction was allowed to cool and the methanol was removed under reduced pressure. The solid which remained was dissolved in ethyl acetate and filtered to remove the calcium chloride. The filtrate was washed with brine, dried (Na_2SO_4) and solvent removed under reduced pressure. The residue that remained was purified using a flash column chromatography (EtOAc with 1% methanol and 1% trimethylamine) to afford pure **18** as a white solid (661 mg, 72%); ^1H NMR (300 MHz, $CDCl_3$) δ 8.57 (d, *J* = 4.6 Hz, 1H), 8.14 (d, *J* = 8.0 Hz, 1H), 7.84 (s, 2H), 7.81 – 7.73 (m, 1H), 7.61 – 7.51 (m, 2H), 7.42 – 7.32 (m, 1H), 7.01 (s, 1H), 6.26 (s, 1H), 5.38 (s, 1H), 4.13 (s, 1H), 3.17 (s, 1H); ^{13}C NMR (300 MHz, $CDCl_3$) δ 167.38, 164.71, 156.59, 148.59, 136.87, 136.52, 136.32, 135.53, 135.14, 133.29,

131.01, 127.14, 124.72, 124.04, 122.76, 121.07, 81.77, 79.35, 44.80; HPLC-MS (ESI) *m/z* (M+H) 328.12.

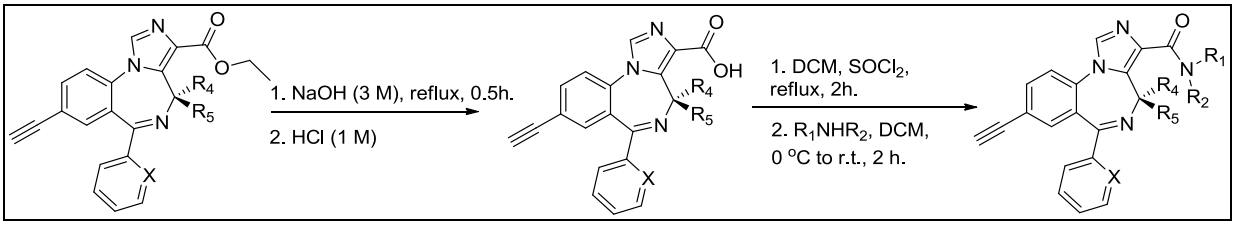
SCHEME 4. General synthetic route to carboxamides.



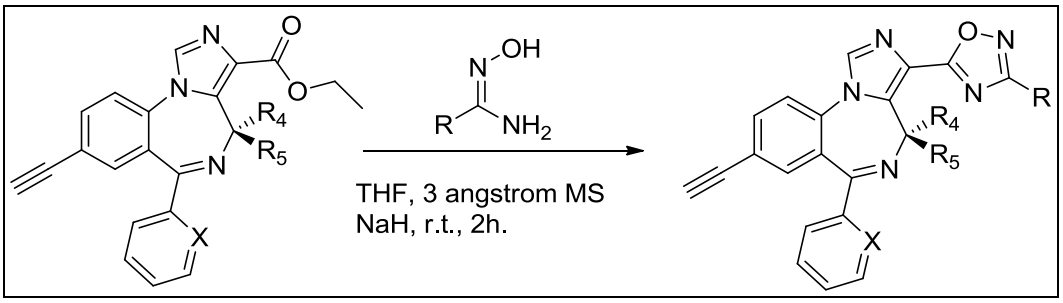
SCHEME 5. General synthetic route to methylamides.



SCHEME 6. General synthetic route to amides.



SCHEME 7. General synthetic route to oxadiazoles.



4. Examples

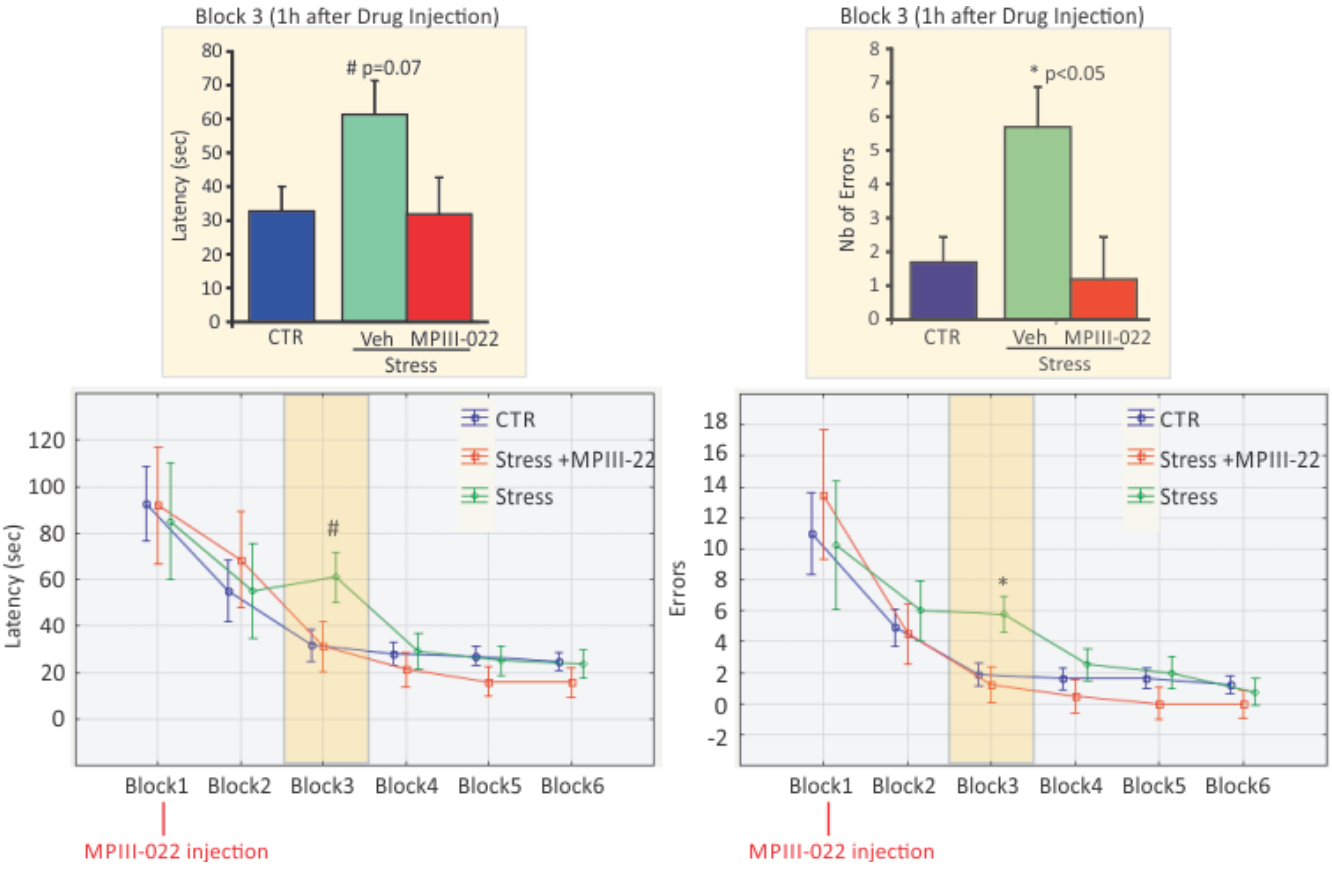
EXAMPLE 1

Results - Effects of MP-III-022 on cognition in mice

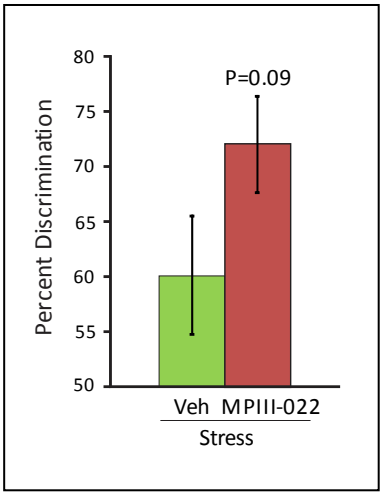
Mice (C57B6; n=10/group) were subjected to unpredictable chronic mild stress (UCMS), a validated paradigm to induce depressive-like behaviors in rodents. We previously showed that UCMS also induced molecular deficits in SST neurons (Lin and Sibille, 2015). The progression of the UCMS effects is monitored weekly by the progressive degradation of the fur coat quality. At the beginning of the 6^{th} week of UCMS, mice are tested for cognitive functions including flexibility and inhibition of learned behavior using the cross water maze protocol. Groups included UCMS-exposed and control animals. Mice were treated during (following block1; see methods) to behavioral testing with MP-III-022 (5 mg/kg) or vehicle. A control (non-stressed) group treated with MP-III-022 was not included as we separately showed no effect of the drug in that control group.

Results indicated that UCMS induced a significant deficit in the ability to inhibit over-training, an aspect of cognitive flexibility following over-training in one task. This manifested as increased latency to perform the new rule and increased number of errors.

MP-III-022 reversed those deficits in UCMS-exposed mice, as demonstrated by latency to switch strategy and number of errors being at control non-stress levels. See Yellow section of tests in figure below.



In a separate cohort, we assessed the effects of MPIII-022 on the cognitive performance of UCMS-exposed animals using the object recognition test. Acute administration of MPIII-022 (30 min before the test) increased the time that mice spent in the vicinity of the novel object compared to saline-treated UCMS-exposed mice. This translates as an increased percent discrimination novel versus familiar object ($p<0.09$), indicating that MP-III-022 increased the ability of mice to discriminate between a familiar or a novel object.



Methods

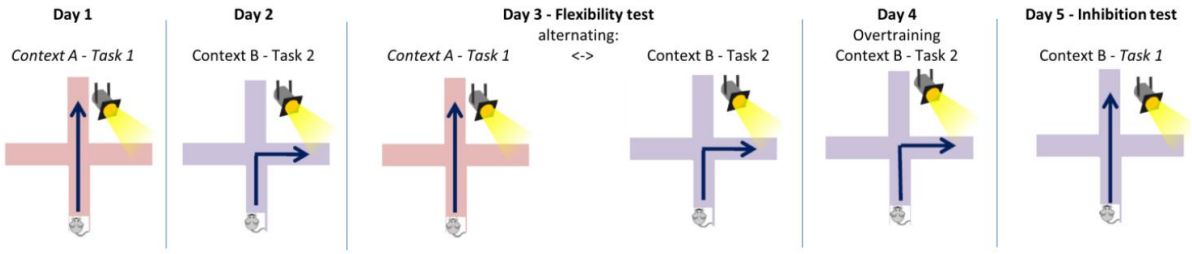
Unpredictable Chronic Mild Stress (UCMS)

Mice were subjected to various stressors according to a “random” schedule for seven weeks. UCMS-exposed mice were maintained under standard laboratory conditions but were isolated in small individual cages (24x11x12cm) while non-stressed controls were group-housed in standard laboratory cages (42x28x18cm). The stressors were: altered bedding (sawdust change, removal or damp; substitution of sawdust with 21°C water, rat or cat feces); cage tilting (45°); cage exchange (mice positioned in the empty cage of another male); and altered length and time of light/dark cycle. Body weight and coat state were assessed weekly, as markers of the progression of the UCMS-evoked syndrome. The total score resulted from the sum of scores obtained from the head, neck, dorsal coat, ventral coat, tail, forepaws and hindpaws (0= well-groomed, 1= unkempt).

Drug administration

Half of the mice subject to the UCMS paradigm were injected with MP-III-022 at a dose of 5 mg/kg i.p. or vehicle on the inhibition test day (see description below), right after the Block 1 trials. This time point also corresponds to 30min before the start of Block 2 trials since there is a 30min interval between blocks.

Cross Water Maze Protocol



Materials:

- Water maze labyrinth composed of four arms perpendicular to each other, each 10 cm wide and 50 cm long. North arm is thus distinguishable from South, East and West arms. Labyrinth is filled with about 15 cm of water (so mice cannot walk) to a temperature 21 ± 1°C (cold enough to motivate mice to move).
- A movable platform submerged just below the water surface that can be positioned at the end of either arm in a variable manner

- To increase swimming difficulties, small lens (PVC capsules of 3mm) can be placed on the water surface. Some conditions need entire surface of the water maze covered by lens.

Method:

Learning 1 (Day 1)

- Learning takes place through sessions that can also call blocks, within each block there is 5 trials. A mouse will do 5 trials to complete a Block. Then, when all mice did the Block 1, starts Block 2 and so on until Block 6.
- In each block, the number of correct answers (arrive platform before 60 sec) is assessed, which can vary from 0 to 5.
- Retrieve mouse on platform by 1 min between each trial.

The time between 2 blocks is the time it takes to test all other mice in this block.

Group 1: Clear water / go straight

Group 2: Clear water / go to clue

Group 3: Lens water / go straight

Group 4: Lens water / go to clue

Learning 2 (Day 2)

- Procedure is similar to Learning 1, just change conditions of learning.

Group 1: Lens water / go to clue

Group 2: Lens water / go straight

Group 3: Clear water / go to clue

Group 4: Clear water / go straight

Flexibility (Day 3)

- After two days of learning, mice are participating in flexibility test. This test consists in alternate the two conditions learned. Similar to precedent days, this test consists of six blocks of five trials. Mice carry five trials with Learning 1 (Block 1). Then when all mice do Block 1, starts Block 2 (Learning 2), later Block 3 (Learning 1), Block 4 (Learning 2), Block 5 (Learning 1) and finally Block 6 (Learning 2).
- On Flexibility test we measure:

Swimming time is the time required to find platform on each trial.-

Failures are defined by the mouse not directly reach to the platform.

Perseverance failures consist in the mouse fails to find the platform by using the precedent strategy. For example, if precedent block was "clear water go straight," and during current block (lens water go to clue), mouse goes straight, then we consider it a perseverance failure.
Hesitations are defined when mouse is seeking its way in the central intersection of the maze, or when the mouse turned back at the entrance of an arm without fully enter.
Group 1: Blocks 1, 3 and 5: Clear water / go straight.
Blocks 2, 4 and 6: Lenses water / go to clue.
Group 2: Blocks 1, 3 and 5: Clear water / go to clue.
Blocks 2, 4 and 6: Lenses water / go straight.
Group 3: Blocks 1, 3 and 5: Lenses water / go straight.
Blocks 2, 4 and 6: Clear water / go to clue.
Group 4: Blocks 1, 3 and 5: Lenses water / go to clue.
Blocks 2, 4 and 6: Clear water / go straight.

Overtraining (Day 4)
- Procedure is similar to Learning 2.
Group 1: Lens water / go to clue
Group 2: Lens water / go straight
Group 3: Clear water / go to clue
Group 4: Clear water / go straight

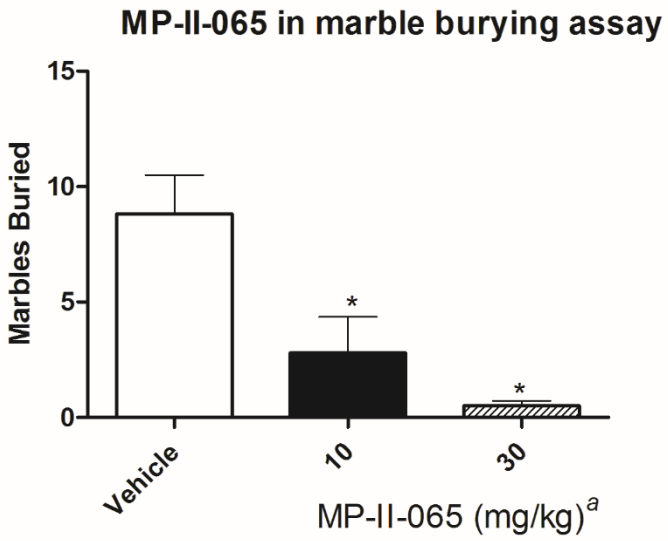
Inhibition (Day 5)
- Mice start first Block with precedent learning (same condition of overtraining), and Blocks 2 to 6 will change condition for a new condition. Therefore, mice will have a spontaneous tendency to respond to learning in which they have been over-trained. During the test phase, we measure their ability to inhibit this response.
- On Inhibition test we measure swim time, failures and perseverance as described above. We measure time spend in the wrong arms as an additional measure of cognitive deficit
Group 1: Lens water / go straight
Group 2: Clear water / go straight
Group 3: Lens water / go to clue
Group 4: Clear water / go to clue

Novel object recognition test

Mice are habituated for 10 min to ~70x70 cm width and 33 cm height chamber and the presence of 2 identical objects (30 cm appart, 17 cm from the walls of the arena) once a day for 3 sessions. The last session is recorded from above for 10 min. Two and a half hours after the last session, mice are injected with vehicle or MPIII-022. Thirty minutes later, the mouse is placed back in the arena where one of the familiar object is replaced by a new one. This session also lasts for 10 min and is recorded. Since mice have a natural exploratory tendency and should remember the first object, animals should spend more time exploring the novel object. Time spent in proximity of the each object for each recorded session is measured using ANY-Maze tracking system. Object discrimination is determined as the percent time spent with the novel objet over the percent time spent with the both objects.

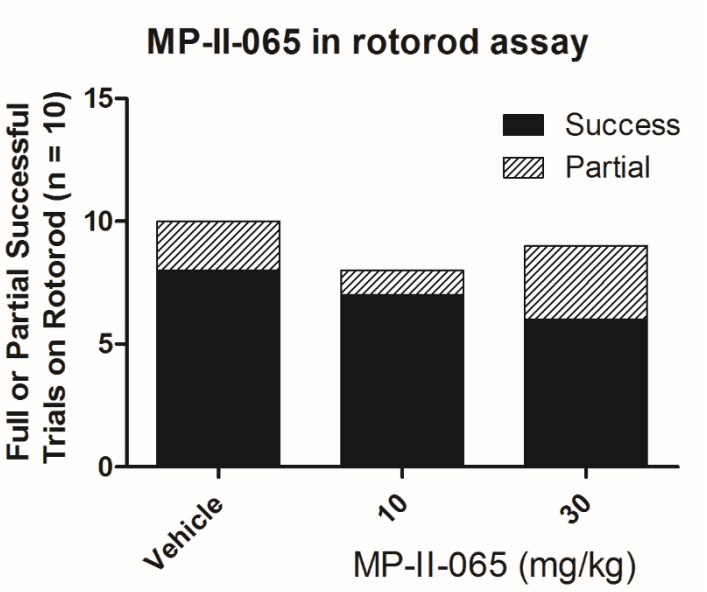
EXAMPLE 2

Assessment of MP-II-065 was assessed in the marble burying assay. Male NIH Swiss mice (n = 10) were dosed i.p. with vehicle (1% carboxymethyl cellulose) or MP-II-065 (10 or 30 mg/kg) 30 minutes prior to being tested in the marble burying assay. Results were analyzed using ANOVA (Dunnett's test: * P < 0.05). [a] Sedation-like effects were observed at 10 and 30 mg/kg. Results are shown in the Figure below.



MP-II-065 was assessed in the rotorod assay. Male NIH Swiss mice (n = 10) were dosed i.p. with vehicle (1% carboxymethyl cellulose) or MP-II-065 (10 or 30 mg/kg) 30 minutes prior to being tested on the rotorod. Mice were placed on a rod for two minutes at 4 revolutions per minute. Mice

that did not fall were designated a “Success”, while mice that fell once during the timing were given a “Partial” designation. Mice that fell twice failed the testing. Results are shown in the Figure below.



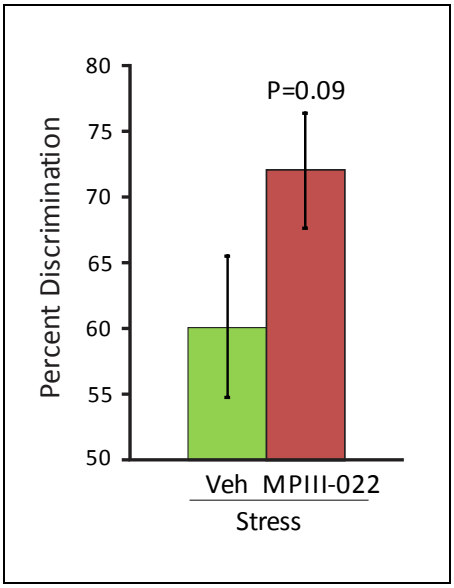
EXAMPLE 3

The effects of MPIII-022 were examined in another cognitive task: the object recognition test. In a separate cohort, we assessed the effects of MPIII-022 on the cognitive performances of animals subjected to chronic stress using the object recognition test.

Acute administration of MPIII-022 (30 min before the test) increased the ability of mice to discriminate between a familiar or a novel object. MPIII-022-treated mice spent more time in the vicinity of the novel object while mice only subjected to chronic unpredictable mild stress favored the familiar object. This translates as an increased percent discrimination novel versus familiar object ($p<0.09$)

Methods: Mice are habituated for 10 min to ~70x70 cm width and 33 cm height chamber and the presence of 2 identical objects (30 cm appart, 17 cm from the walls of the arena) once a day for 3 sessions. The last session is recorded from above for 10 min. Two and a half hours after the last session, mice are injected with vehicle or MPIII-022. Thirty minutes later, the mouse is placed back in the arena where one of the familiar object is replaced by a new one. This session also lasts for 10 min and is recorded. Since mice have a natural exploratory tendency and should remember the first

object, animals should spend more time exploring the novel object. Time spent in proximity of the each object for each recorded session is measured using ANY-Maze tracking system. Object discrimination is determined as the percent time spent with the novel objet over the percent time spent with the both objects.



APPENDIX J. PCT Patent on α2/α3 $GABA_A$ Selective Ligands for the Treatment of Anxiety, Epilepsy, Neuropathic Pain and Depression

Patent No.: PCT/US2016/035761

Submitted: March 18, 2016.

GABAERGIC LIGANDS AND THEIR USES

CROSS-REFERENCE TO RELATED APPLICATIONS

[0001] This application claims the benefit of U.S. Provisional Application Serial No. 62/135,854, filed March 20, 2015, which is incorporated by reference herein.

STATEMENT REGARDING FEDERALLY SPONSORED RESEARCH OR DEVELOPMENT

[0002] This invention was made with United States government support under NIH grant number RO1 NS076517, and NIH grant number RO1 MH09463. The United States government has certain rights to this invention.

BACKGROUND

[0003] Gamma-aminobutyric acid (GABA) is the major inhibitory neurotransmitter in the central nervous system. GABA receptors are heteromeric, and are divided into three main classes: (1) $GABA_A$ receptors, which are members of the ligand-gated ion channel superfamily; (2) $GABA_B$ receptors, which may be members of the G-protein linked receptor superfamily; and (3) $GABA_C$ receptors, also members of the ligand-gated ion channel superfamily, but their distribution is confined to the retina. Benzodiazepine receptor ligands do not bind to $GABA_B$ and $GABA_C$ receptors. Since the first cDNAs encoding individual $GABA_A$ receptor subunits were cloned the number of known members of the mammalian family has grown to 21 including α, β, and γ subunits (6α, 4β, 4γ, 1δ, 1ε, 1π, 1θ, and 3ρ).

[0004] A characteristic property of $GABA_A$ receptors is the presence of a number of modulatory sites, one of which is the benzodiazepine (BZ) site. The benzodiazepine binding site is the most explored of the $GABA_A$ receptor modulatory sites, and is the site through which benzodiazepine-based anxiolytic drugs exert their effect. Before the cloning of the $GABA_A$ receptor gene family, the benzodiazepine binding site was historically subdivided into two subtypes, BENZODIAZEPINE1 and BENZODIAZEPINE2, on the basis of radioligand binding studies on synaptosomal rat membranes. The BENZODIAZEPINE1 subtype has been shown to be pharmacologically equivalent to a $GABA_A$ receptor comprising the α1 subunit in combination with a β subunit and γ2. It has been indicated that an α subunit, a β subunit and a γ subunit constitute the minimum requirement for forming a fully functional Benzodiazepine/$GABA_A$ receptor.

[0005] Receptor subtype assemblies for BZ-sensitive $GABA_A$ receptors include amongst others the subunit combinations α1β2/3γ2, α2β2/3γ2, α3 β2/3γ2, α4 β2/3γ2, and α5 β2/3γ2. Subtype assemblies containing an α1 subunit (α1β2γ2) are present in most areas of the brain and are thought to account for 40-50% of $GABA_A$ receptors in the rat. Subtype assemblies containing α2 and α3 subunits respectively are thought to account for about 25% and 17% of $GABA_A$ receptors in the rat. Subtype assemblies containing an α5 subunit (α5β3γ2) are expressed predominately in the hippocampus and cortex and are thought to represent about 5% of $GABA_A$ receptors in the rat. Two other major populations are the α2β2/3γ2 and α3β2/3γ2 subtypes as stated above. Together these constitute approximately a further 35% of the total $GABA_A$ receptor population. Pharmacologically this combination appears to be equivalent to the BENZODIAZEPINE2 subtype as defined previously by radioligand binding, although the BENZODIAZEPINE2 subtype may also include certain α5-containing subtype assemblies.

[0006] The present pharmacology of agonists acting at the BZ site of $GABA_A$ receptors suggests that α1 containing receptors mediate sedation, anticonvulsant activity, ataxia, and anterograde amnesia, while α2 and/or α3 $GABA_A$ receptors mediate anxiolytic activity. α5 containing $GABA_A$ receptors are involved in memory functions (U. Rudolph et al., *Nature* 1999, 401, 796; K. Löw et al., *Science* 2000, 290, 131; McKernan *Nature Neurosci*. 2000, 3, 587; F. Crestani et al., *Proc. Nat. Acad. Sci. USA* 2002, 99, 8980; M.S. Chambers et al., *J. Med. Chem.* 2003, 46, 2227).

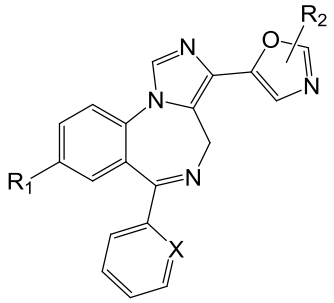
[0007] It is believed that agents acting selectively as benzodiazepine agonists at $GABA_A$/α2, $GABA_A$/α3, and/or $GABA_A$/α5 receptors possess desirable properties. Compounds which are modulators of the benzodiazepine binding site of the $GABA_A$ receptor by acting as benzodiazepine agonists are referred to hereinafter as "$GABA_A$ receptor agonists." The $GABA_A$/α1-selective (α1β2γ2) agonists alpidem and zolpidem are clinically prescribed as hypnotic agents, suggesting that at least some of the sedation associated with known anxiolytic drugs which act at the Benzodiazepine 1 binding site is mediated through $GABA_A$ receptors containing the α1 subunit. Recently, two studies have shown that the majority of additive properties of diazepam are mediated by α1 subtypes (N. A. Ator et. al., *J. Pharm. Exp. Thera.* 2010, 332, 4-16; K. R. Tan et. al., *Nature*, 463, 769-774).

[0008] It is also known that some benzodiazepine derivatives, such as QH-ii-066, bind with high affinity to $GABA_A$/α5 receptors (K_i<10 nM), intermediate affinity to $GABA_A$/α2 and

$GABA_A/\alpha 3$ (Ki<50 nM), and poorer affinity to $GABA_A/\alpha 1$ receptors (Ki>70 nM), unlike diazepam which binds with high affinity to all four diazepam-sensitive $GABA_A$ receptors (Ki<25 nM), as disclosed in Huang, *et al., J. Med. Chem.* 2000, 43, 71-95. However, such benzodiazepine derivatives may contain ester linkages, and are thus sensitive to hydrolysis *in vivo* (e.g., by esterases). What is needed are GABAergic receptor subtype selective ligands that lack ester linkages, and are less sensitive to hydrolysis *in vivo* by esterases.

SUMMARY

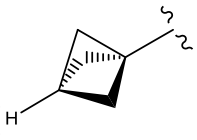
[0009] In one aspect, the invention provides a compound of formula (I):



(I)

or a salt thereof, wherein:

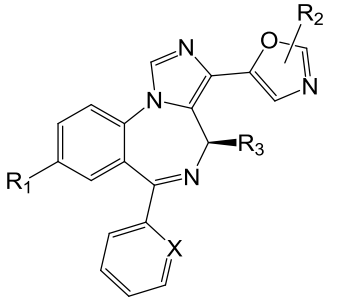
X is selected from the group consisting of N, C-H, C-F, C-Cl, C-Br, C-I, and C-NO_2;

R_1 is selected from the group consisting of -C≡CH, -C≡C-Si(CH_3)$_3$, -cyclopropyl, and bicycle[1.1.1]pentane (); and

R_2 is selected from the group consisting of -H, -CH_3, -CH_2CH_3 and -$CH(CH_3)_2$.

[0010] In some embodiments of the compound of formula (I), R_2 is -H.

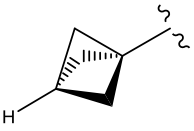
[0011] In another aspect, the invention provides a compound of formula (II):



(II)

or a salt thereof, wherein:

X is selected from the group consisting of N, C-H, C-F, C-Cl, C-Br, C-I, and C-NO_2;

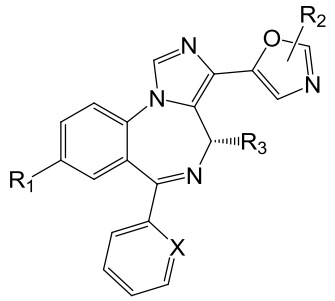
R_1 is selected from the group consisting of -C≡CH, -C≡C-Si$(CH_3)_3$, -cyclopropyl, and bicycle[1.1.1]pentane ();

R_2 is selected from the group consisting of -H, -CH_3, -CH_2CH_3, and -$CH(CH_3)_2$; and

R_3 is selected from the group consisting of -H, -CH_3, -CH_2CH_3, -$CH(CH_3)_2$, -F, -Cl, -CF_3, and -CCl_3.

[0012] In some embodiments of the compound of formula (II), R_2 is -H.

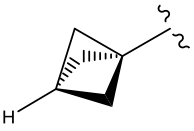
[0013] In another aspect, the invention provides a compound of formula (III):



(III)

or a salt thereof, wherein:

X is selected from the group consisting of N, C-H, C-F, C-Cl, C-Br, C-I, and C-NO_2;

R_1 is selected from the group consisting of -C≡CH, -C≡C-Si$(CH_3)_3$, -cyclopropyl, and bicycle[1.1.1]pentane ();

R_2 is selected from the group consisting of -H, -CH_3, -CH_2CH_3, and -$CH(CH_3)_2$; and

R_3 is selected from the group consisting of -H, -CH_3, -CH_2CH_3, -$CH(CH_3)_2$, -F, -Cl, -CF_3, and -CCl_3.

[0014] In some embodiments of the compound of formula (III), R_2 is –H.

[0015] In another aspect, the invention provides a method of treating a disorder selected from an anxiety disorder, depression, epilepsy, schizophrenia and neuropathic pain in a subject in need of treatment, comprising administering to the subject an effective amount of a compound of formula (I), (II), or (III).

[0016] Other aspects and embodiments are encompassed by the disclosure and will become apparent in light of the following description.

BRIEF DESCRIPTION OF THE DRAWINGS

[0017] **FIG. 1** is a synthetic scheme for the synthesis of the bioisosteres.

[0018] **FIG. 2** are ORTEP views of the crystal structure of **7c** (SH-I-85), **9a** (KRM-II-81), **9c** (KRM-II-18B), **10a**, and **11a** (displacement ellipsoids are at the 50% level).

[0019] **FIG. 3** are structures of compounds. Shown in A) are the imidazobenzodiazepine-bioisosteres, and shown in B) are structurally related compounds.

[0020] **FIG. 4** is a graph of dose versus inverted screen failures for KRM-II-81, HZ-166, and diazepam in the inverted screen assay. Male Sprague-Dawley rats (n = 5) were dosed i.p. (vehicle = 1% carboxymethyl cellulose) with diazepam (3, 10, or 30 mg/kg), KRM-II-81 (10, 30, or 60 mg/kg), or HZ-166 (30 mg/kg) 30 minutes prior to testing. Results were analyzed using ANOVA (Dunnett's test: * $P < 0.05$).

[0021] **FIG. 5** are graphs showing results from the rotorod assay for A) HZ-166 and KRM-II-81; B) MP-III-085, KRM-II-82 and KRM-II-18B; C) MP-III-080 and KRM-III-78; D) KRM-III-59; E) KRM-III-66 and KRM-III-65; F) KRM-III-79 and KRM-III-67. Male NIH Swiss mice (n = 10) were dosed i.p. with vehicle (1% carboxymethyl cellulose) or one of the test compounds (10 or 30 mg/kg) 30 minutes prior to being tested on the rotorod. Mice were placed on a rod for two minutes at 4 revolutions per minute. Mice that did not fall were designated a "Success", while mice that fell once during the timing were given a "Partial" designation. Mice that fell twice failed the testing.

[0022] **FIG. 6** is a graph of dose versus percent seizures, showing protection from MET-induced seizures by KRM-II-81, HZ-166, and diazepam. Male CD-1 mice (n = 10) were dosed i.p. 30 minutes prior to being tested. Results were analyzed using ANOVA (Dunnett's test versus vehicle: * $P < 0.05$).

[0023] **FIG. 7** is a graph of dose versus percent seizures, showing protection against scMET by KRM-II-81, HZ-166, and diazepam. Male Sprague-Dawley rats (n = 5) were dosed i.p. with KRM-II-81, HZ-166, or diazepam 30 minutes prior to testing. A 35 mg/kg subcutaneous dose of pentylenetetrazole was given and the percent outcome of seizure was recorded. Results were analyzed using ANOVA (Dunnett's test: * $P < 0.05$).

[0024] **FIG. 8** is a graph of dose versus pentylenetetrazole (scMet), showing the threshold against scMET seizures by KRM-II-81, HZ-166, and diazepam. Male Sprague-Dawley rats (n = 8) were dosed i.p. with KRM-II-81 or HZ-166 (3, 10, 30, or 60 mg/kg) or diazepam (0.1, 0.3, or

1 mg/kg) 30 minutes prior to infusion of PTZ until a convulsion is achieved. Results were analyzed using ANOVA (Dunnett's test: * $P < 0.05$).

[0025] **FIG. 9** are graphs showing the number of marbles buried for each dose of compound in the marble burying assay for A) HZ-166 and KRM-II-81; B) MP-III-085, KRM-II-82 and KRM-II-18B; C) MP-III-080 and KRM-III-78; D) KRM-III-59; E) KRM-III-66 and KRM-III-65; F) KRM-III-79 and KRM-III-67. Male NIH Swiss mice (n = 10) were dosed i.p. with vehicle (1% carboxymethyl cellulose) or one of the test compounds (10 or 30 mg/kg) 30 minutes prior to being tested in the marble burying assay. Results were analyzed using ANOVA (Dunnett's test: * $P < 0.05$). [a] Sedation-like effects were observed at 30 mg/kg. [b] Sedation-like effects were observed at 10 and 30 mg/kg. [c] Modest sedation-like effects were observed at 30 mg/kg.

[0026] **FIG. 10** is a graph of the concentration of KRM-II-81 versus percent of control for KRM-II-81 analyzed in the Vogel conflict procedure. After a baseline was established using a vehicle (1% 2-hydroxyethyl cellulose), male Sprague-Dawley rats (n = 6-8) were dosed i.p. with either KRM-II-81 (3, 10, 30, or 60 mg/kg) or chlordiazepoxide (20 mg/kg) 30 minutes prior to testing. Results were analyzed using ANOVA (Dunnett's test: * $P < 0.05$; Student t-test: ** $P < 0.05$).

[0027] **FIG. 11** is a graph of time versus withdrawal threshold for KRM-II-81, Gabapentin, and vehicle, showing the effect of KRM-II-81 on antihyperalgesia in the von Frey filament assay. Male Sprague-Dawley rats (n = 5) were dosed i.p. either vehicle, KRM-II-81 (30 mg/kg), or gabapentin (50 mg/kg) and tested in the von Frey filament assay after undergoing SNL 90 days prior. Results were analyzed using ANOVA (Dunnett's test: * $P < 0.05$).

[0028] **FIG. 12** are graphs of compound concentration versus % MPE, showing that $GABA_A$ receptor PAMs, Midazolam (nonselective PAM), HZ166, KRM-II-18B, and KRM-II-81 dose-dependently attenuated mechanical hyperalgesia in a CFA-induced inflammatory pain rat model. Raw data (paw withdrawal threshold, expressed in g of von Frey filament) was converted to a maximal possible effect value according the following equation:

% MPE = [(test threshold (g)- control threshold (g) / (pre-CFA threshold – control threshold)] x 100.

[0029] **FIG. 13** are graphs of compound concentration versus paw withdrawal threshold, showing that the benzodiazepine site antagonist flumazenil shifted the dose-effect curves of PAMs rightward, indicating the effect is modulated by the benzodiazepine receptor.

[0030] **FIG. 14** are graphs of compound concentration or does versus % MPE in a three-assay comparison, showing that midazolam produced antihyperalgesic, rate-suppressing, and muscle-relaxant activity at similar doses. The subunit-selective $GABA_A$ receptor PAMs HZ166, KRM-II-81, and KRM-II-18B seemed to selectively produce antihyperalgesic effect and produce rate-suppressing and muscle-relaxant activity at much larger doses.

[0031] **FIG. 15** is a graph of time versus concentration for male Sprague-Dawley rats (n = 3 per time point) when given either a 1 mg/kg i.v. or 10 mg/kg i.p. dose. The total plasma concentrations were taken at various time points.

[0032] **FIG. 16** is a graph of immobility illustrating the antidepressant effects of KRM-II-81 assessed in the forced swim test. Male NIH Swiss mice (n = 7 – 8) were dosed i.p. with vehicle (1% HEC, 0.25% Tween 80, 0.05% antifoam), KRM-II-81 (3, 10, or 30 mg/kg), or imipramine (15 mg/kg) and assessed in the forced swim test. Results were analyzed using ANOVA (Dunnett's test * $P < 0.05$).

DETAILED DESCRIPTION

[0033] The present invention provides compounds that may be alpha 2, alpha 3, or alpha2/alpha3 GABAergic receptor subtype selective ligands, pharmaceutical compositions, and methods of use of such ligands and compositions in treatment of anxiety disorders, depression, epilepsy, schizophrenia and neuropathic pain. In embodiments, such alpha 2, alpha 3 or alpha2/alpha3 GABAergic receptor subtype selective ligands lack ester linkages and are thus relatively insensitive to hydrolysis by esterases.

Definitions

[0034] Definitions of specific functional groups and chemical terms are described in more detail below. For purposes of this invention, the chemical elements are identified in accordance with the Periodic Table of the Elements, CAS version, Handbook of Chemistry and Physics, 75th Ed., inside cover, and specific functional groups are generally defined as described therein. Additionally, general principles of organic chemistry, as well as specific functional moieties and reactivity, are described in *Organic Chemistry*, Thomas Sorrell, University Science Books, Sausalito, 1999; Smith and March *March's Advanced Organic Chemistry*, 5th Edition, John Wiley & Sons, Inc., New York, 2001; Larock, *Comprehensive Organic Transformations*, VCH Publishers, Inc., New York, 1989; Carruthers, *Some Modern Methods of Organic Synthesis*, 3rd

Edition, Cambridge University Press, Cambridge, 1987; the entire contents of each of which are incorporated herein by reference.

[0035] The term "acyl" refers to an alkylcarbonyl, cycloalkylcarbonyl, heterocyclylcarbonyl, arylcarbonyl or heteroarylcarbonyl substituent, any of which may be further substituted (e.g., with one or more substituents).

[0036] The term "alkyl" refers to a straight or branched hydrocarbon chain, containing the indicated number of carbon atoms. For example, C_1-C_{12} alkyl indicates that the alkyl group may have from 1 to 12 (inclusive) carbon atoms, and C_1-C_4 alkyl indicates that the alkyl group may have from 1 to 4 (inclusive) carbon atoms. An alkyl group may be optionally substituted. Examples of C_1-C_4 alkyl groups include methyl, ethyl, *n*-propyl, isopropyl, *n*-butyl, *sec*-butyl and *tert*-butyl.

[0037] The term "alkenyl" refers to a straight or branched hydrocarbon chain having one or more double bonds. Examples of alkenyl groups include, but are not limited to, allyl, propenyl, 2-butenyl, 3-hexenyl and 3-octenyl groups. One of the double bond carbons may optionally be the point of attachment of the alkenyl substituent. An alkenyl group may be optionally substituted.

[0038] The term "alkynyl" refers to a straight or branched hydrocarbon chain having one or more triple bonds. Examples of alkynyl groups include, but are not limited to, ethynyl, propargyl, and 3-hexynyl. One of the triple bond carbons may optionally be the point of attachment of the alkynyl substituent. An alkynyl group may be optionally substituted.

[0039] The term "aryl" refers to an aromatic monocyclic, bicyclic, or tricyclic hydrocarbon ring system, wherein any ring atom capable of substitution can be substituted (e.g., with one or more substituents). Examples of aryl moieties include, but are not limited to, phenyl, naphthyl, and anthracenyl.

[0040] The term "arylalkyl" refers to an alkyl moiety in which an alkyl hydrogen atom is replaced with an aryl group. Arylalkyl includes groups in which more than one hydrogen atom has been replaced with an aryl group. Examples of arylalkyl groups include benzyl, 2-phenylethyl, 3-phenylpropyl, 9-fluorenyl, benzhydryl, and trityl groups.

[0041] The term "cycloalkyl" as used herein refers to nonaromatic, saturated or partially unsaturated cyclic, bicyclic, tricyclic or polycyclic hydrocarbon groups having 3 to 12 carbons (e.g., 3, 4, 5, 6 or 7 carbon atoms). Any ring atom can be substituted (e.g., with one or more

substituents). Cycloalkyl groups can contain fused rings. Fused rings are rings that share one or more common carbon atoms. Examples of cycloalkyl groups include, but are not limited to, cyclopropyl, cyclobutyl, cyclopentyl, cyclohexyl, cyclohexenyl, cyclohexadienyl, methylcyclohexyl, adamantyl, norbornyl and norbornenyl.

[0042] The term "halo" or "halogen" as used herein refers to any radical of fluorine, chlorine, bromine or iodine.

[0043] The term "haloalkyl" as used herein refers to an alkyl in which one or more hydrogen atoms are replaced with a halogen, and includes alkyl moieties in which all hydrogens have been replaced with halogens (e.g., perfluoroalkyl such as CF_3).

[0044] The term "heteroaryl" as used herein refers to an aromatic 5-8 membered monocyclic, 8-12 membered bicyclic, or 11-14 membered tricyclic ring system having 1-3 heteroatoms if monocyclic, 1-6 heteroatoms if bicyclic, or 1-9 heteroatoms if tricyclic, said heteroatoms independently selected from O, N, S, P and Si (e.g., carbon atoms and 1-3, 1-6, or 1-9 heteroatoms independently selected from O, N, S, P and Si if monocyclic, bicyclic, or tricyclic, respectively). Any ring atom can be substituted (e.g., with one or more substituents). Heteroaryl groups can contain fused rings, which are rings that share one or more common atoms. Examples of heteroaryl groups include, but are not limited to, radicals of pyridine, pyrimidine, pyrazine, pyridazine, pyrrole, imidazole, pyrazole, oxazole, isoxazole, furan, thiazole, isothiazole, thiophene, quinoline, isoquinoline, quinoxaline, quinazoline, cinnoline, indole, isoindole, indolizine, indazole, benzimidazole, phthalazine, pteridine, carbazole, carboline, phenanthridine, acridine, phenanthroline, phenazine, naphthyridines and purines.

[0045] The term "heterocyclyl" as used herein refers to a nonaromatic, saturated or partially unsaturated 3-10 membered monocyclic, 8-12 membered bicyclic, or 11-14 membered tricyclic ring system having 1-3 heteroatoms if monocyclic, 1-6 heteroatoms if bicyclic, or 1-9 heteroatoms if tricyclic, said heteroatoms selected from O, N, S, Si and P (e.g., carbon atoms and 1-3, 1-6, or 1-9 heteroatoms of O, N, S, Si and P if monocyclic, bicyclic, or tricyclic, respectively). Any ring atom can be substituted (e.g., with one or more substituents). Heterocyclyl groups can contain fused rings, which are rings that share one or more common atoms. Examples of heterocyclyl groups include, but are not limited to, radicals of tetrahydrofuran, tetrahydrothiophene, tetrahydropyran, piperidine, piperazine, morpholine, pyrroline, pyrimidine, pyrrolidine, indoline, tetrahydropyridine, dihydropyran, thianthrene, pyran,

benzopyran, xanthene, phenoxathiin, phenothiazine, furazan, lactones, lactams such as azetidinones and pyrrolidinones, sultams, sultones, and the like.

[0046] The term “hydroxy” refers to an –OH radical. The term "alkoxy" refers to an –O-alkyl radical. The term “aryloxy” refers to an –O-aryl radical. The term “haloalkoxy” refers to an –O-haloalkyl radical.

[0047] The term "substituent" refers to a group "substituted" on an alkyl, alkenyl, alkynyl, cycloalkyl, heterocyclyl, aryl, arylalkyl or heteroaryl group at any atom of that group. Suitable substituents include, without limitation: acyl, acylamido, acyloxy, alkoxy, alkyl, alkenyl, alkynyl, amido, amino, carboxy, cyano, ester, halo, hydroxy, imino, nitro, oxo (e.g., C=O), phosphonate, sulfinyl, sulfonyl, sulfonate, sulfonamino, sulfonamido, thioamido, thiol, thioxo (e.g., C=S), and ureido. In embodiments, substituents on a group are independently any one single, or any combination of the aforementioned substituents. In embodiments, a substituent may itself be substituted with any one of the above substituents.

[0048] The above substituents may be abbreviated herein, for example, the abbreviations Me, Et and Ph represent methyl, ethyl and phenyl, respectively. A more comprehensive list of the abbreviations used by organic chemists appears in the first issue of each volume of the Journal of Organic Chemistry; this list is typically presented in a table entitled Standard List of Abbreviations. The abbreviations contained in said list, and all abbreviations used by organic chemists of ordinary skill in the art, are hereby incorporated by reference.

[0049] For compounds, groups and substituents thereof may be selected in accordance with permitted valence of the atoms and the substituents, such that the selections and substitutions result in a stable compound, e.g., which does not spontaneously undergo transformation such as by rearrangement, cyclization, elimination, etc.

[0050] Where substituent groups are specified by their conventional chemical formulae, written from left to right, they optionally encompass substituents resulting from writing the structure from right to left, e.g., $-CH_2O-$ optionally also recites $-OCH_2-$.

[0051] In accordance with a convention used in the art, the group:



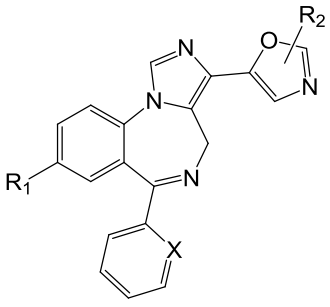
is used in structural formulas herein to depict the bond that is the point of attachment of the moiety or substituent to the core or backbone structure.

[0052] In the context of treating a disorder, the term "effective amount" as used herein refers to an amount of the compound or a composition comprising the compound which is effective, upon single or multiple dose administrations to a subject, in treating a cell, or curing, alleviating, relieving or improving a symptom of the disorder in a subject. An effective amount of the compound or composition may vary according to the application. In the context of treating a disorder, an effective amount may depend on factors such as the disease state, age, sex, and weight of the individual, and the ability of the compound to elicit a desired response in the individual. In an example, an effective amount of a compound is an amount that produces a statistically significant change in a given parameter as compared to a control, such as in cells (e.g., a culture of cells) or a subject not treated with the compound.

[0053] It is specifically understood that any numerical value recited herein (e.g., ranges) includes all values from the lower value to the upper value, i.e., all possible combinations of numerical values between the lowest value and the highest value enumerated are to be considered to be expressly stated in this application. For example, if a concentration range is stated as 1% to 50%, it is intended that values such as 2% to 40%, 10% to 30%, or 1% to 3%, etc., are expressly enumerated in this specification. These are only examples of what is specifically intended.

Compounds

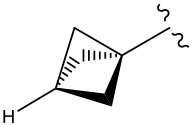
[0054] Compounds may be of the following formula (I):



(I)

or a salt thereof, wherein:

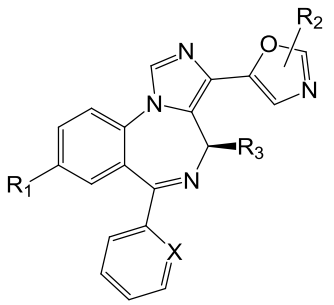
X is selected from the group consisting of N, C-H, C-F, C-Cl, C-Br, C-I, and C-NO_2;

R_1 is selected from the group consisting of -C≡CH, -C≡C-Si(CH_3)$_3$, -cyclopropyl, and bicycle[1.1.1]pentane (); and

R_2 is selected from the group consisting of -H, -CH_3, -CH_2CH_3 and -$CH(CH_3)_2$.

[0055] In some embodiments, X is N. In some embodiments, X is CH. In some embodiments, X is CF. In some embodiments, X is CCl. In some embodiments, X is CBr. In some embodiments, X is CI. In some embodiments, R_1 is -C≡CH. In some embodiments, R_1 is –C≡C-$Si(CH_3)_3$. In some embodiments, R_1 is –cyclopropyl. In some embodiments, R_1 is bicycle[1.1.1]pentane. In some embodiments, R_2 is -H. In some embodiments, R_2 is –CH_3. In some embodiments, R_2 is –CH_2CH_3. In some embodiments, R_2 is –$CH(CH_3)_2$. In particular embodiments, in compounds of formula (I), R_2 is H.

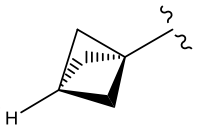
[0056] Compounds may be of the following formula (II):



(II)

or a salt thereof, wherein:

X is selected from the group consisting of N, C-H, C-F, C-Cl, C-Br, C-I, and C-NO_2;

R_1 is selected from the group consisting of -C≡CH, -C≡C-$Si(CH_3)_3$, -cyclopropyl, and bicycle[1.1.1]pentane ();

R_2 is selected from the group consisting of -H, -CH_3, -CH_2CH_3, and -$CH(CH_3)_2$; and

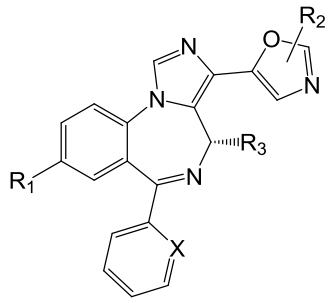
R_3 is selected from the group consisting of -H, -CH_3, -CH_2CH_3, -$CH(CH_3)_2$, -F, -Cl, -CF_3, and -CCl_3.

[0057] In some embodiments, X is N. In some embodiments, X is CH. In some embodiments, X is CF. In some embodiments, X is CCl. In some embodiments, X is CBr. In some embodiments, X is CI. In some embodiments, R_1 is -C≡CH. In some embodiments, R_1 is –C≡C-$Si(CH_3)_3$. In some embodiments, R_1 is –cyclopropyl. In some embodiments, R_1 is bicycle[1.1.1]pentane. In some embodiments, R_2 is -H. In some embodiments, R_2 is –CH_3. In some embodiments, R_2 is –CH_2CH_3. In some embodiments, R_2 is –$CH(CH_3)_2$. In some embodiments, R_3 is -H. In some embodiments, R_3 is –CH_3. In some embodiments, R_3 is –

CH_2CH_3. In some embodiments, R_3 is $–CH(CH_3)_2$. In some embodiments, R_3 is F. In some embodiments, R_3 is Cl. In some embodiments, R_3 is $–CF_3$. In some embodiments, R_3 is $–CCl_3$.

[0058] In particular embodiments, in compounds of formula (II), R_2 is H.

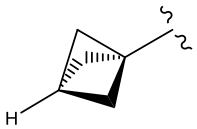
[0059] Compounds may be of the following formula (III):



(III)

or a salt thereof, wherein:

X is selected from the group consisting of N, C-H, C-F, C-Cl, C-Br, C-I, and C-NO_2;

R_1 is selected from the group consisting of -C≡CH, -C≡C-$Si(CH_3)_3$, -cyclopropyl, and bicycle[1.1.1]pentane ();

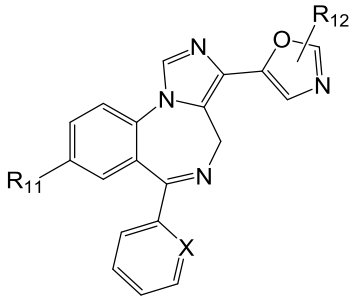
R_2 is selected from the group consisting of -H, $-CH_3$, $-CH_2CH_3$, and $-CH(CH_3)_2$; and

R_3 is selected from the group consisting of -H, $-CH_3$, $-CH_2CH_3$, $-CH(CH_3)_2$, -F, -Cl, $-CF_3$, and $-CCl_3$.

[0060] In some embodiments, X is N. In some embodiments, X is CH. In some embodiments, X is CF. In some embodiments, X is CCl. In some embodiments, X is CBr. In some embodiments, X is CI. In some embodiments, R_1 is -C≡CH. In some embodiments, R_1 is –C≡C-$Si(CH_3)_3$. In some embodiments, R_1 is –cyclopropyl. In some embodiments, R_1 is bicycle[1.1.1]pentane. In some embodiments, R_2 is -H. In some embodiments, R_2 is $–CH_3$. In some embodiments, R_2 is $–CH_2CH_3$. In some embodiments, R_2 is $–CH(CH_3)_2$. In some embodiments, R_3 is -H. In some embodiments, R_3 is $–CH_3$. In some embodiments, R_3 is $–CH_2CH_3$. In some embodiments, R_3 is $–CH(CH_3)_2$. In some embodiments, R_3 is F. In some embodiments, R_3 is Cl. In some embodiments, R_3 is $–CF_3$. In some embodiments, R_3 is $–CCl_3$.

[0061] In particular embodiments, in compounds of formula (III), R_2 is H.

[0062] Compounds may be of the following formula (IV):



(IV)

or a salt thereof, wherein:

X is selected from the group consisting of N, C-H, C-F, C-Cl, C-Br, C-I, and C-NO_2;

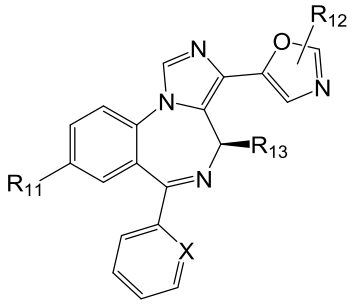
R_{11} is Br; and

R_{12} is selected from the group consisting of -H, -CH_3, -CH_2CH_3 and -$CH(CH_3)_2$.

[0063] In some embodiments, X is N. In some embodiments, X is CH. In some embodiments, X is CF. In some embodiments, X is CCl. In some embodiments, X is CBr. In some embodiments, X is CI. In some embodiments, R_2 is -H. In some embodiments, R_2 is –CH_3. In some embodiments, R_{12} is –CH_2CH_3. In some embodiments, R_{12} is –$CH(CH_3)_2$.

[0064] In particular embodiments, in compounds of formula (IV), R_{12} is H.

[0065] Compounds may be of the following formula (V):



(V)

or a salt thereof, wherein:

X is selected from the group consisting of N, C-H, C-F, C-Cl, C-Br, C-I, and C-NO_2;

R_{11} is Br;

R_{12} is selected from the group consisting of -H, -CH_3, -CH_2CH_3, and -$CH(CH_3)_2$; and

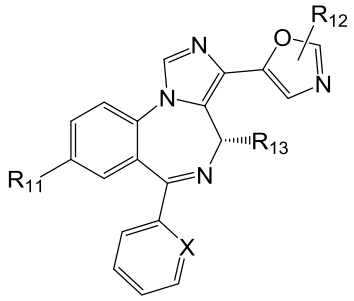
R_{13} is selected from the group consisting of -H, -CH_3, -CH_2CH_3, -$CH(CH_3)_2$, -F, -Cl, -CF_3, and -CCl_3.

[0066] In some embodiments, X is N. In some embodiments, X is CH. In some embodiments, X is CF. In some embodiments, X is CCl. In some embodiments, X is CBr. In some embodiments, X is CI. In some embodiments, R_{12} is -H. In some embodiments, R_{12} is –

CH_3. In some embodiments, R_{12} is $–CH_2CH_3$. In some embodiments, R_{12} is $–CH(CH_3)_2$. In some embodiments, R_{13} is -H. In some embodiments, R_{13} is $–CH_3$. In some embodiments, R_{13} is $–CH_2CH_3$. In some embodiments, R_{13} is $–CH(CH_3)_2$. In some embodiments, R_{13} is F. In some embodiments, R_{13} is Cl. In some embodiments, R_{13} is $–CF_3$. In some embodiments, R_{13} is $–CCl_3$.

[0067] In particular embodiments, in compounds of formula (V), R_{12} is H.

[0068] Compounds may be of the following formula (VI):



(VI)

or a salt thereof, wherein:

X is selected from the group consisting of N, C-H, C-F, C-Cl, C-Br, C-I, and $C-NO_2$;

R_{11} is Br;

R_{12} is selected from the group consisting of -H, $-CH_3$, $-CH_2CH_3$, and $-CH(CH_3)_2$; and

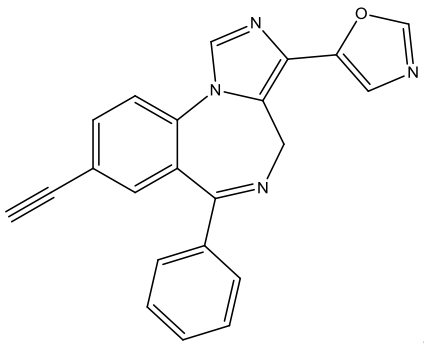
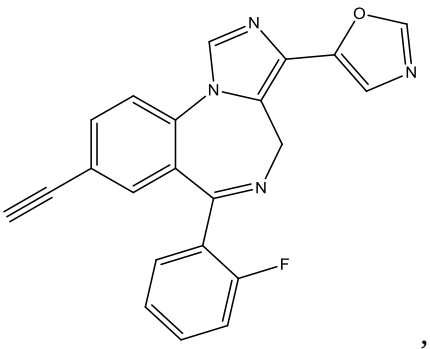
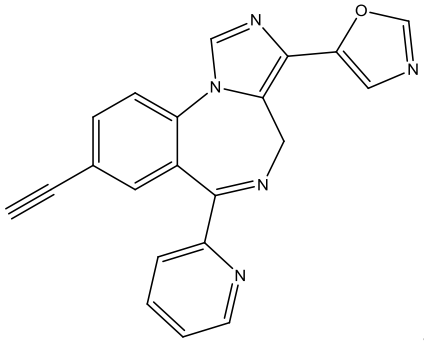
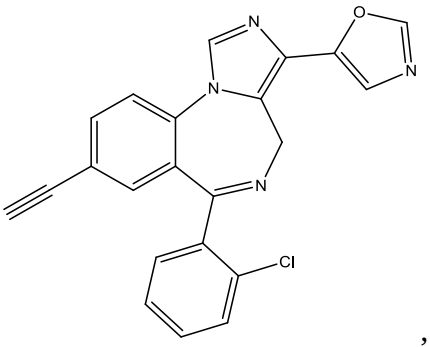
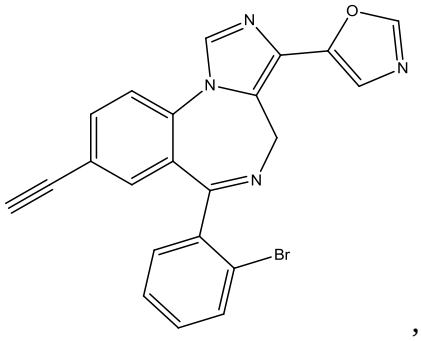
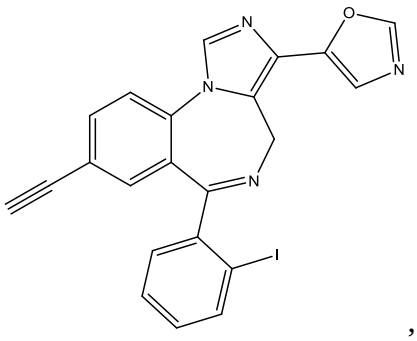
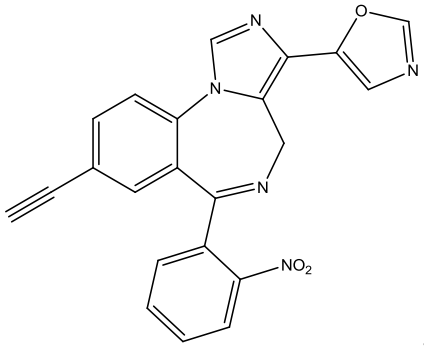
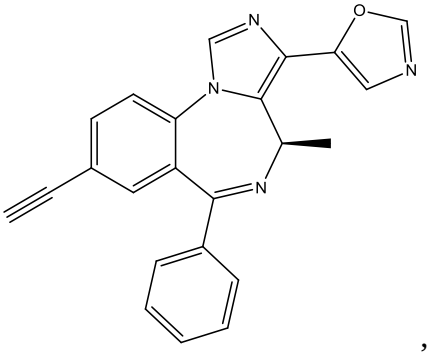
R_{13} is selected from the group consisting of -H, $-CH_3$, $-CH_2CH_3$, $-CH(CH_3)_2$, -F, -Cl, $-CF_3$, and $-CCl_3$.

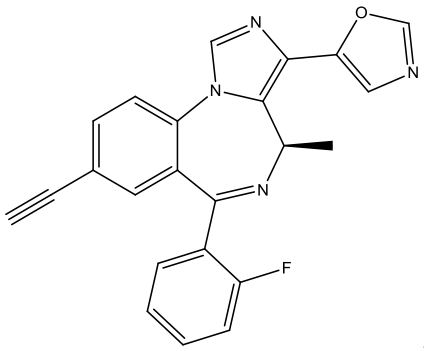
[0069] In some embodiments, X is N. In some embodiments, X is CH. In some embodiments, X is CF. In some embodiments, X is CCl. In some embodiments, X is CBr. In some embodiments, X is CI. In some embodiments, R_{12} is -H. In some embodiments, R_{12} is $–CH_3$. In some embodiments, R_{12} is $–CH_2CH_3$. In some embodiments, R_{12} is $–CH(CH_3)_2$. In some embodiments, R_{13} is -H. In some embodiments, R_{13} is $–CH_3$. In some embodiments, R_{13} is $–CH_2CH_3$. In some embodiments, R_{13} is $–CH(CH_3)_2$. In some embodiments, R_{13} is F. In some embodiments, R_{13} is Cl. In some embodiments, R_{13} is $–CF_3$. In some embodiments, R_{13} is $–CCl_3$.

[0070] In particular embodiments, in compounds of formula (VI), R_2 is H.

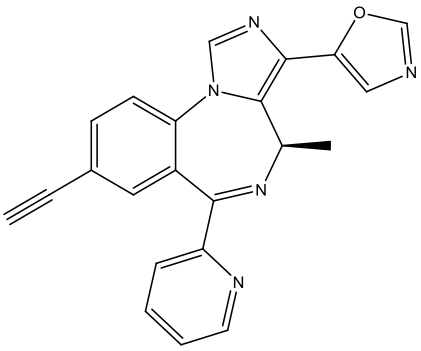
[0071] Suitable compounds include the following:

OTT1436

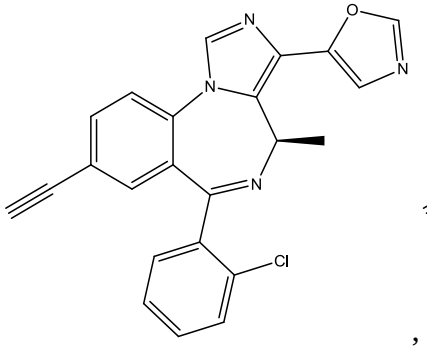

,

,

,

,

,

,

,

,


N
O
N
N
N
F

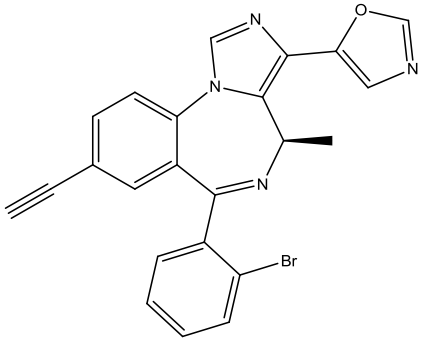
,


N
O
N
N
N
N

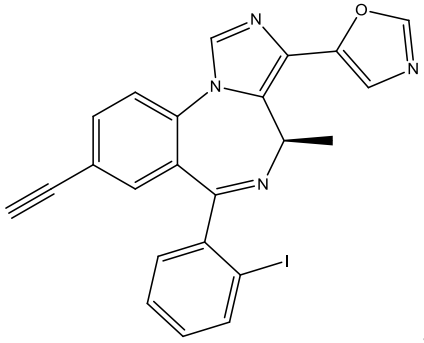
,


N
O
N
N
N
Cl

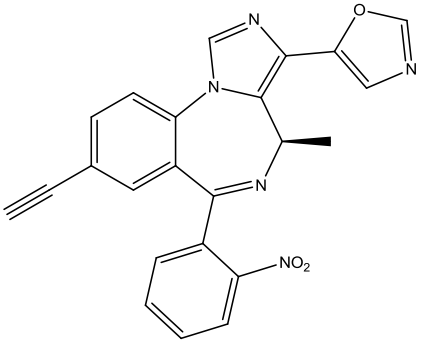
,


N
O
N
N
N
Br

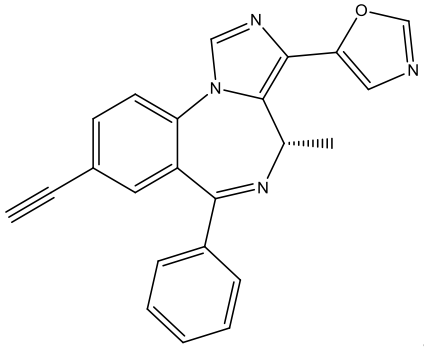
,


N
O
N
N
N
I

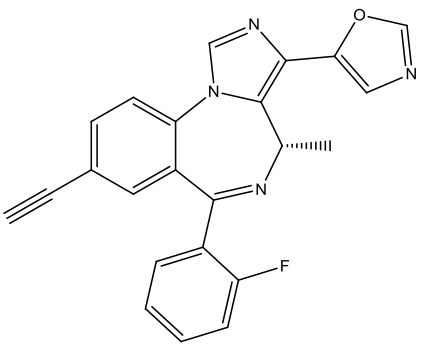
,


N
O
N
N
N
NO2

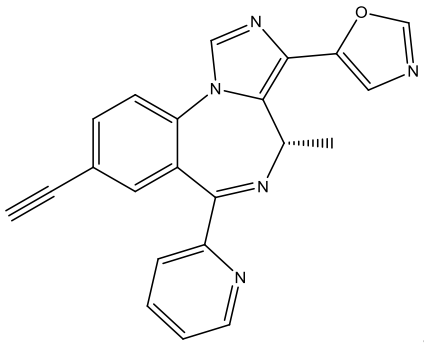
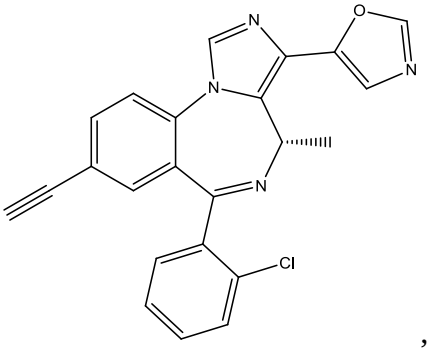
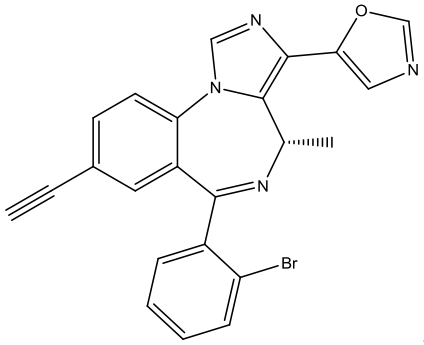
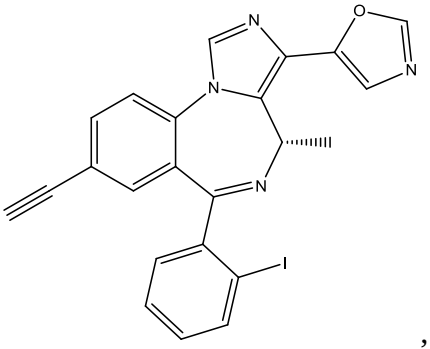
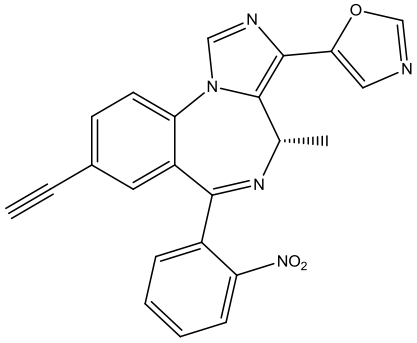
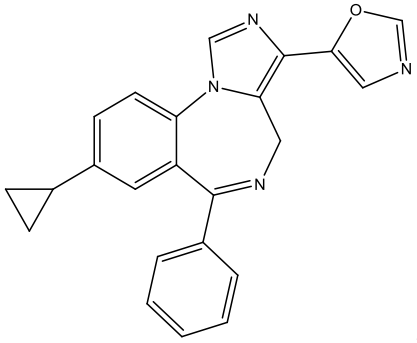
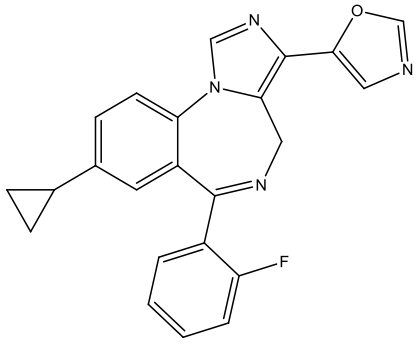
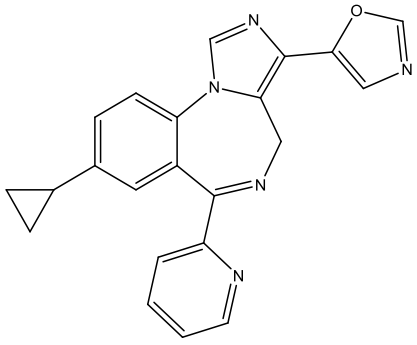
,

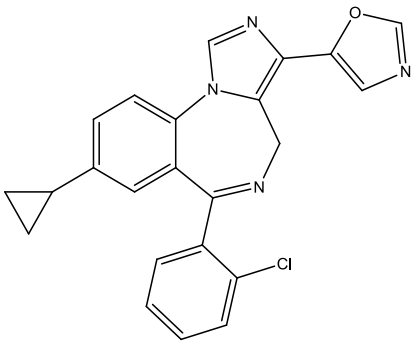

N
O
N
N
N

,

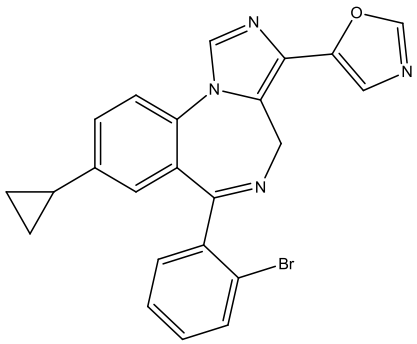

N
O
N
N
N
F

,

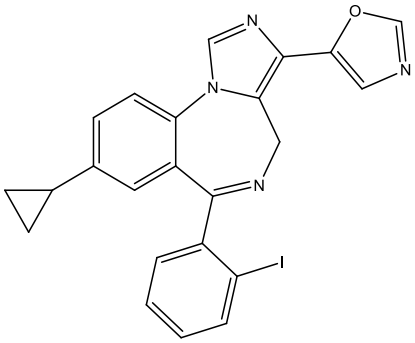



Br

I

NO2


F



N
O
N
N
N
Cl

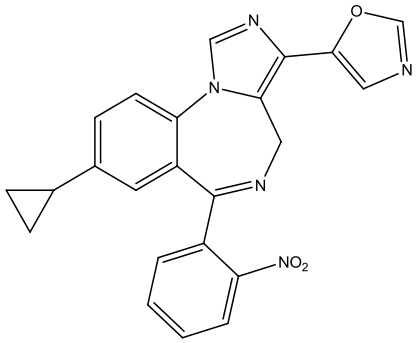
,


N
O
N
N
N
Br

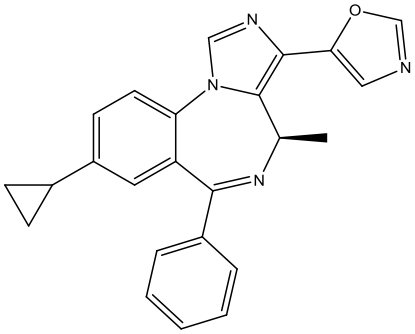
,


N
O
N
N
N
I

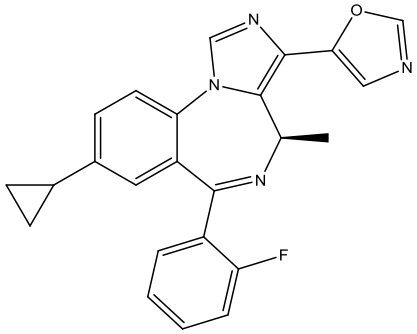
,


N
O
N
N
N
NO2

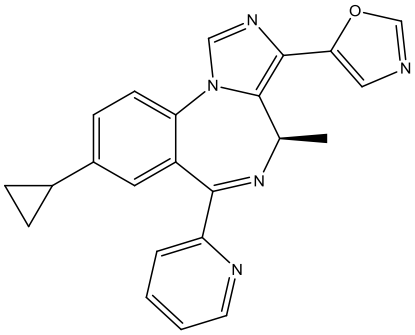
,


N
O
N
N
N

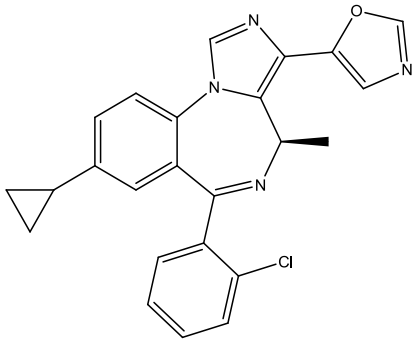
,


N
O
N
N
N
F

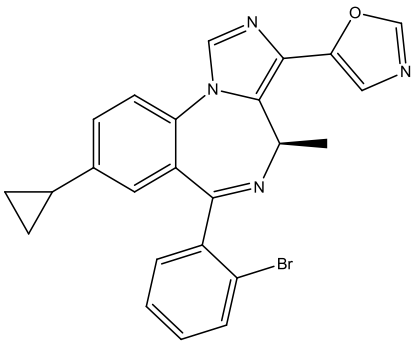
,


N
O
N
N
N
N

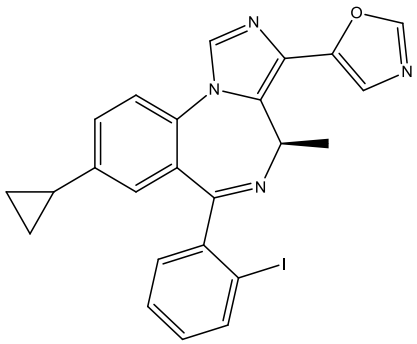
,


N
O
N
N
N
Cl

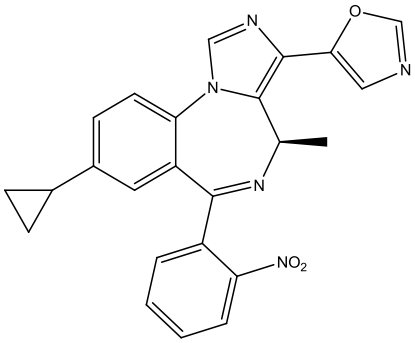
,


N
O
N
N
N
Br

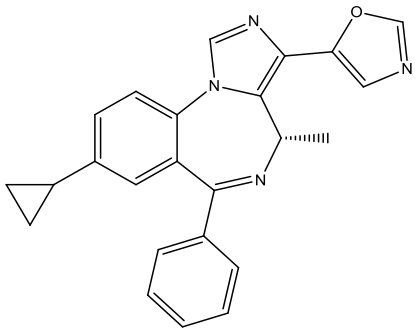
,


N
O
N
N
N
I

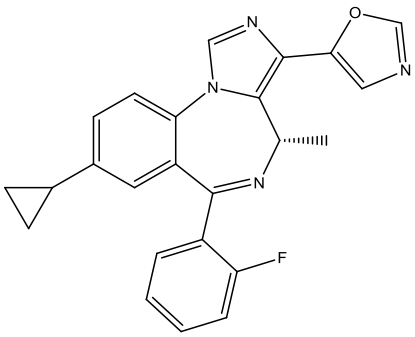
,


N
O
N
N
N
NO2

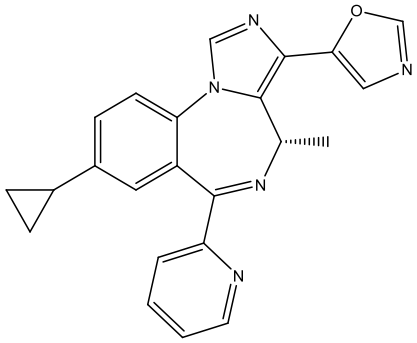
,


N
O
N
N
N

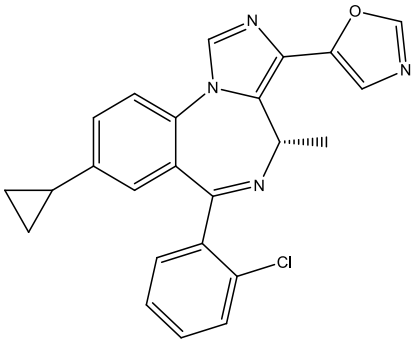
,


N
O
N
N
N
F

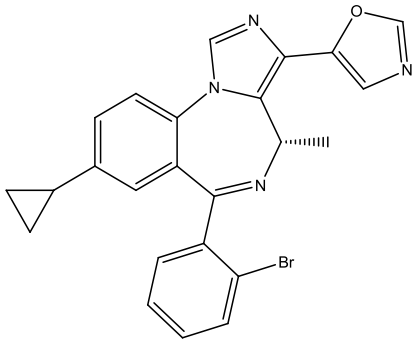
,


N
O
N
N
N
N

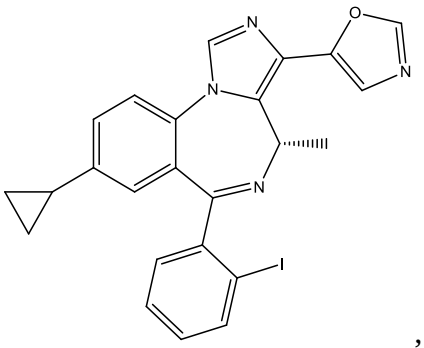
,


N
O
N
N
N
Cl

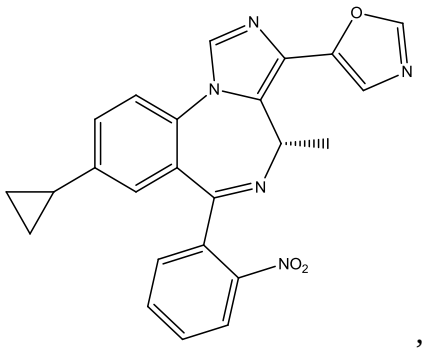
,


N
O
N
N
N
Br

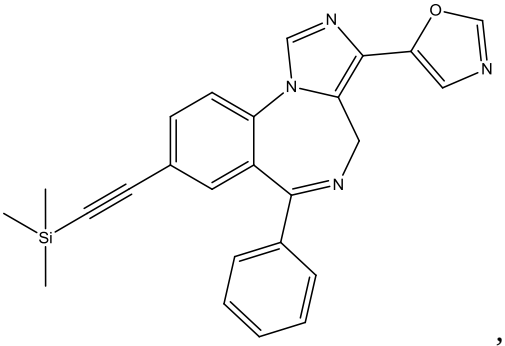
,


N
O
N
N
N
I

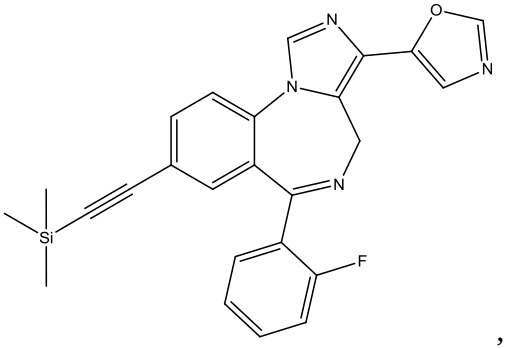
,


N
O
N
N
N
NO2

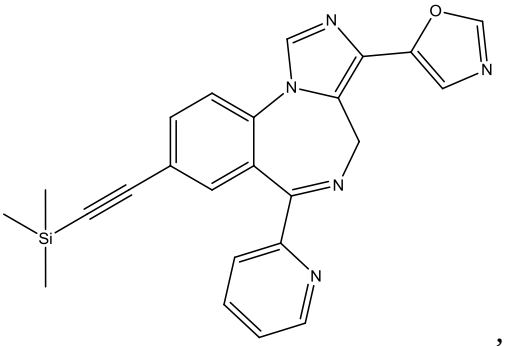
,


N
O
N
N
N
Si

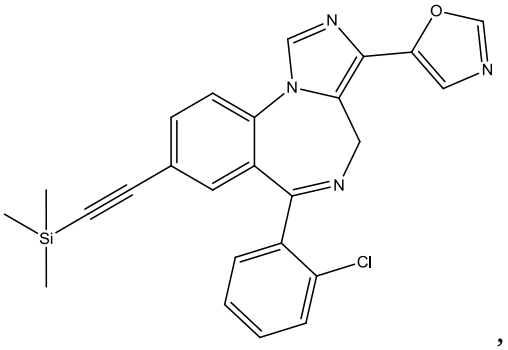
,


N
O
N
N
N
Si
F

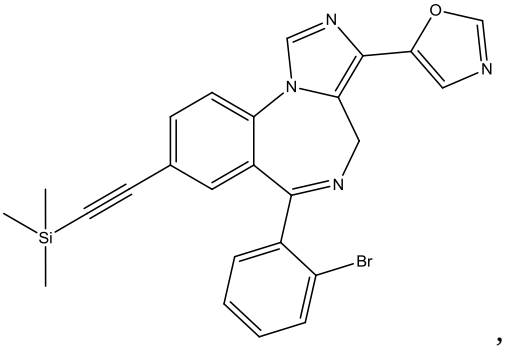
,


N
O
N
N
N
Si
N

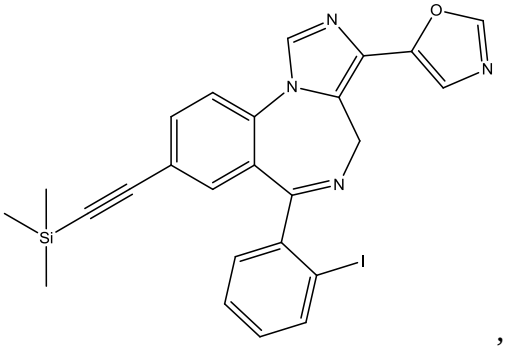
,


N
O
N
N
N
Si
Cl

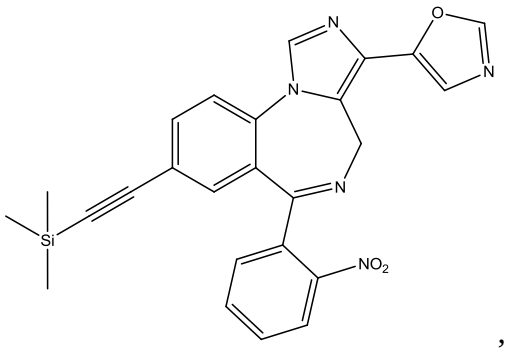
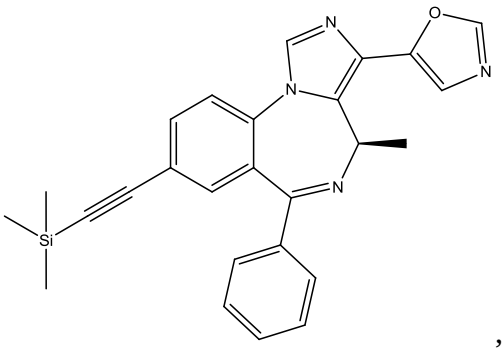
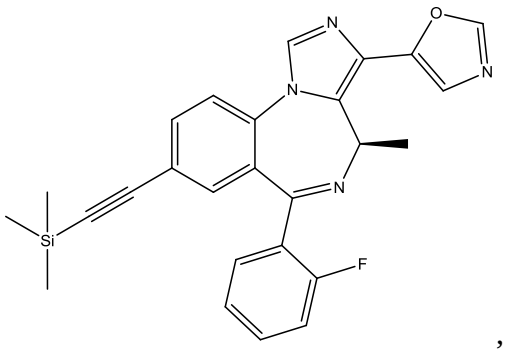
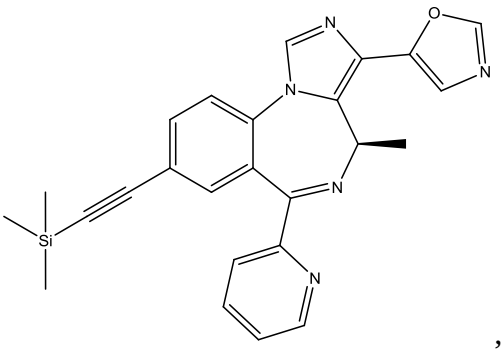
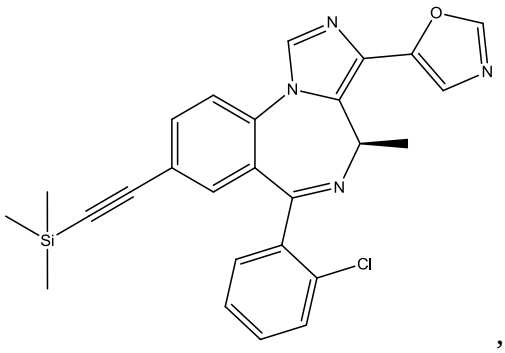
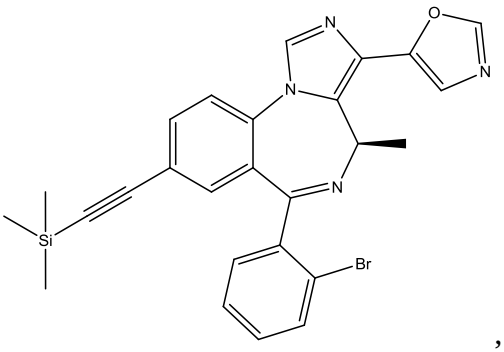
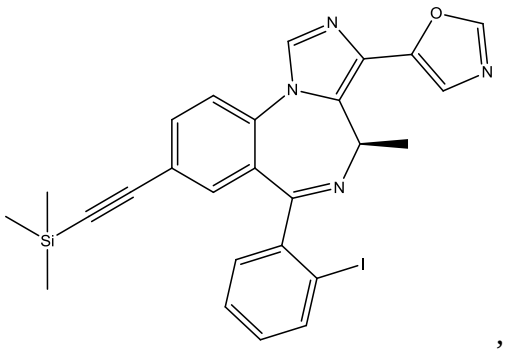
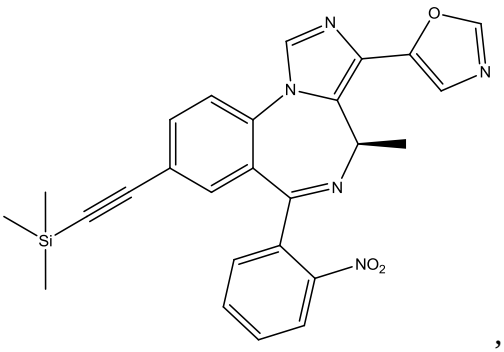
,

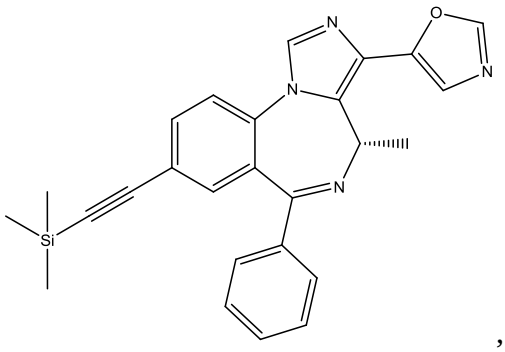
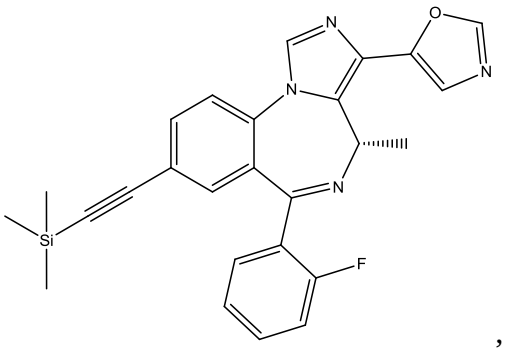
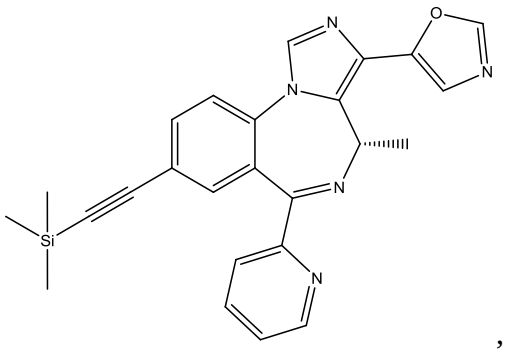
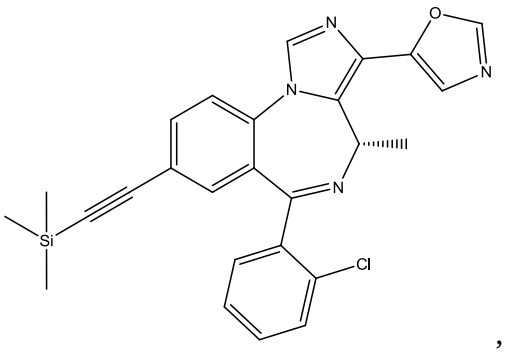
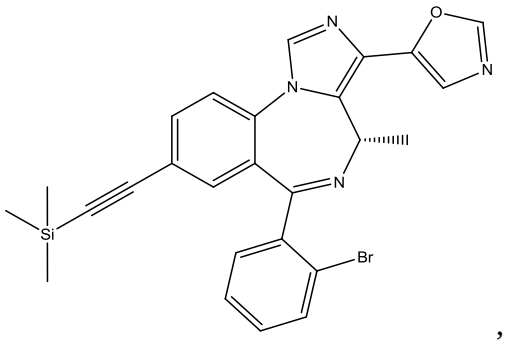
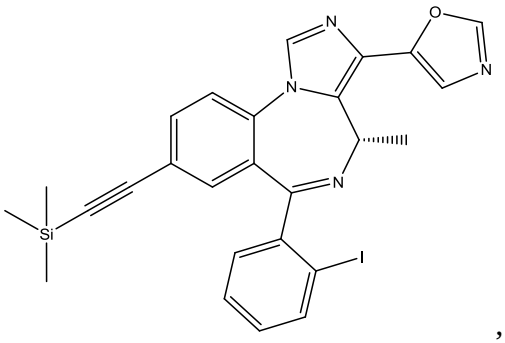
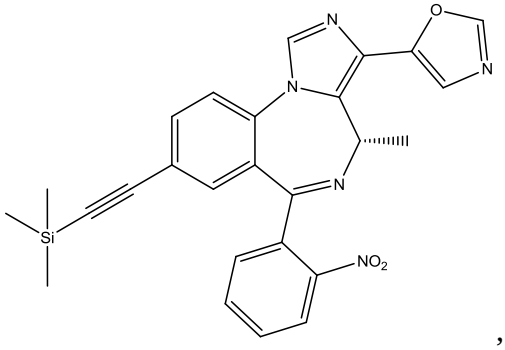
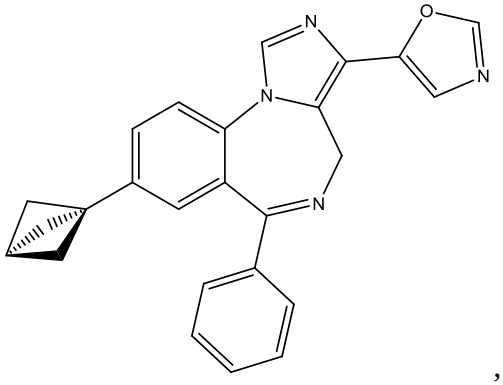

N
O
N
N
N
Si
Br

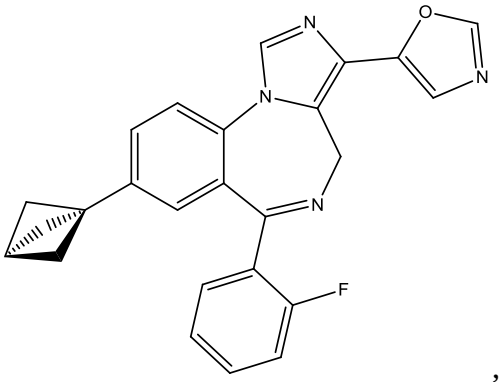
,


N
O
N
N
N
Si
I

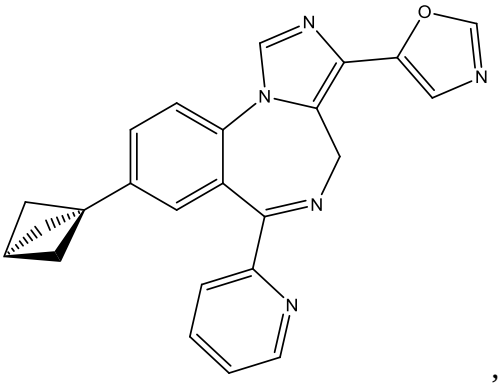
,

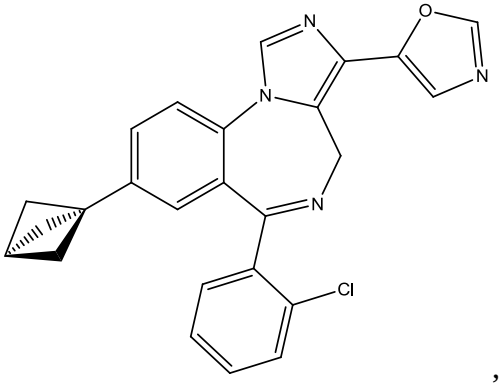

,

,

,

,

,

,

,

,


N
O
N
N
N
N
F

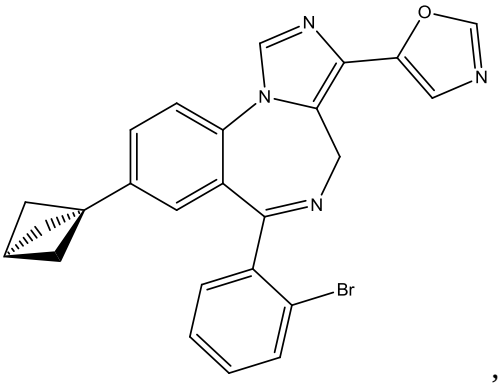
,


N
O
N
N
N
N

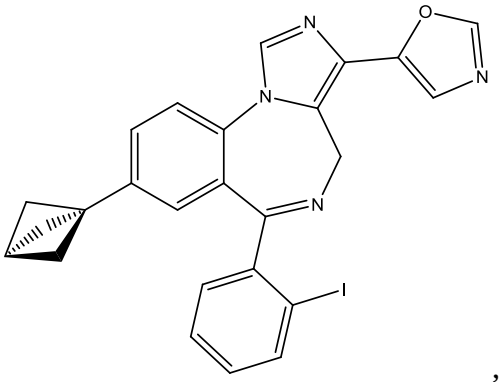
,


N
O
N
N
N
N
Cl

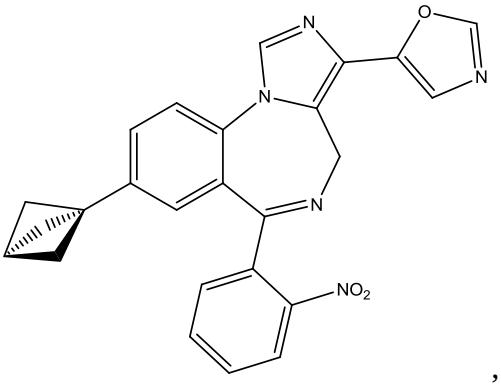
,


N
O
N
N
N
N
Br

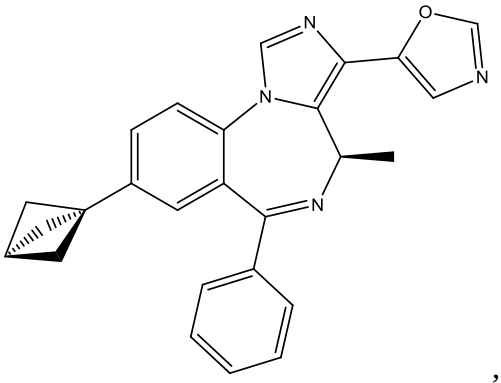
,


N
O
N
N
N
N
I

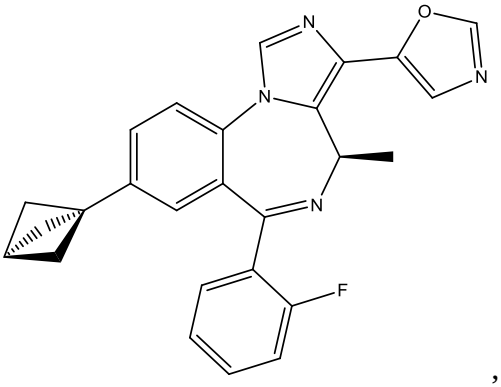
,


N
O
N
N
N
N
NO2

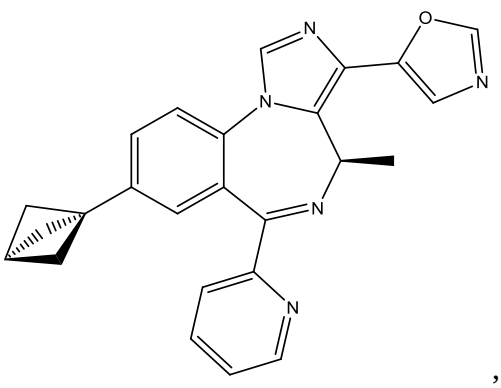
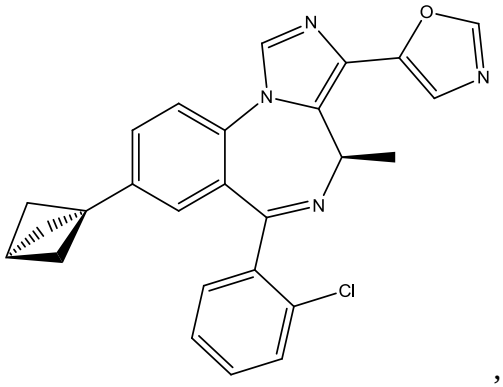
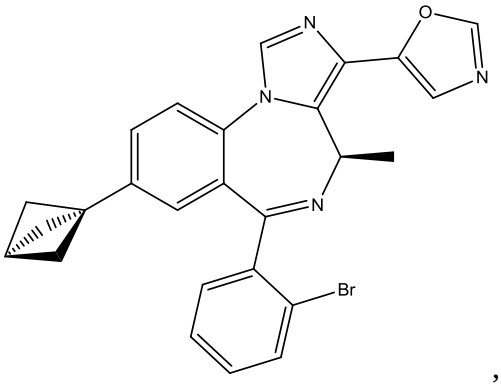
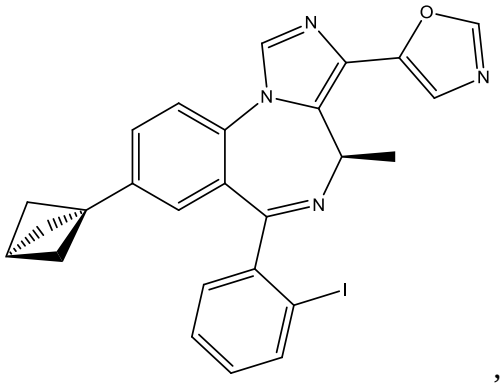
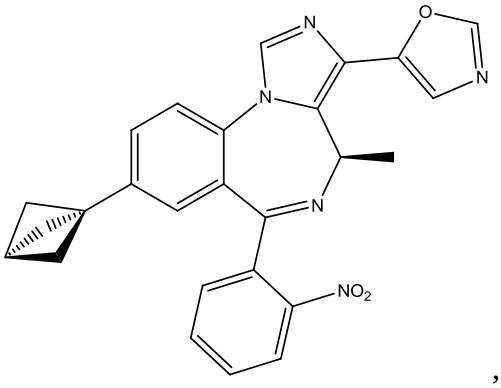
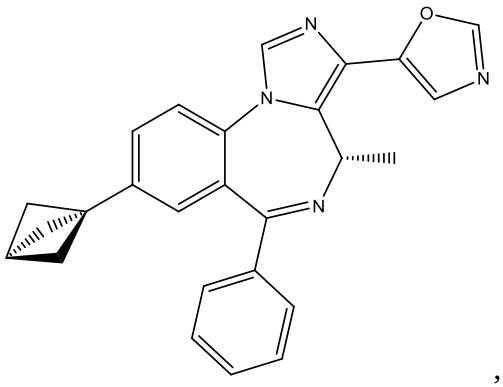
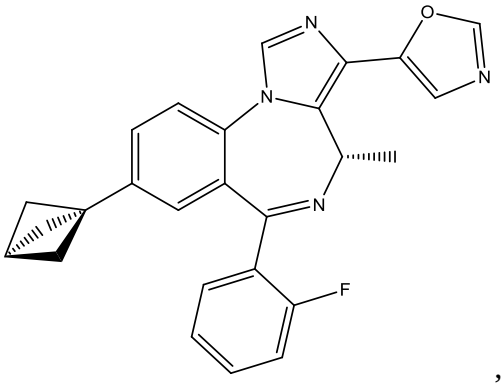
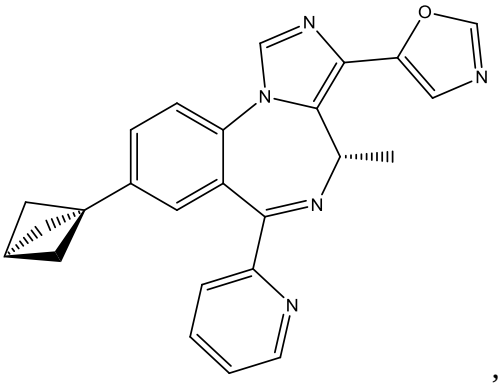
,

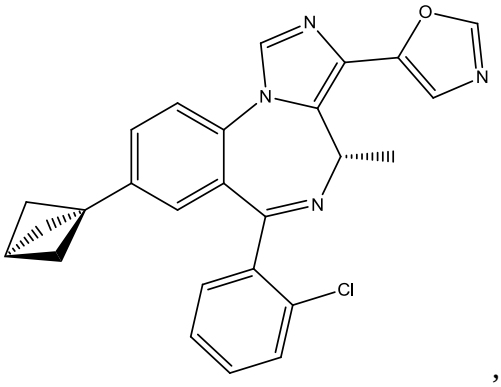

N
O
N
N
N
N

,

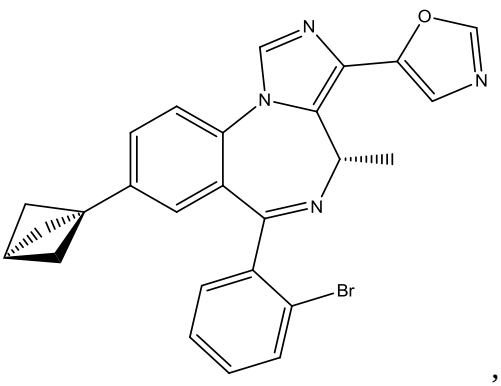

N
O
N
N
N
N
F

,

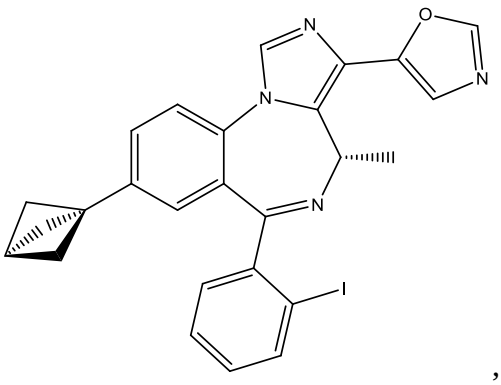










N
O
N
N
N
Cl

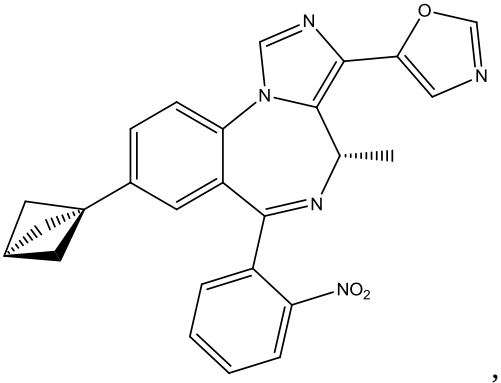
,


N
O
N
N
N
Br

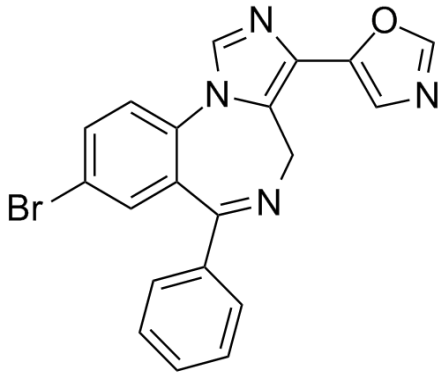
,


N
O
N
N
N
I

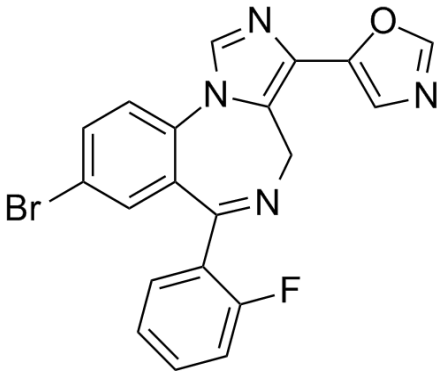
,


N
O
N
N
N
NO2

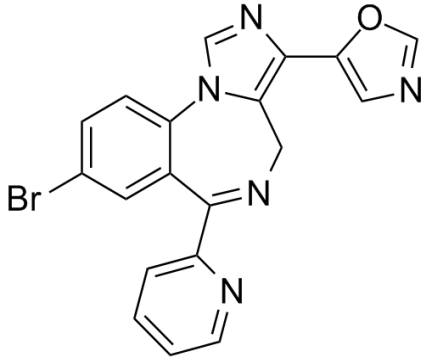
,


N
O
N
N
N
Br

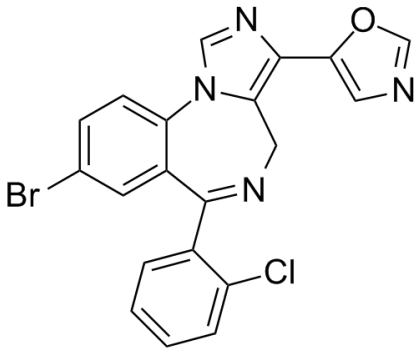
,


N
O
N
N
N
Br
F

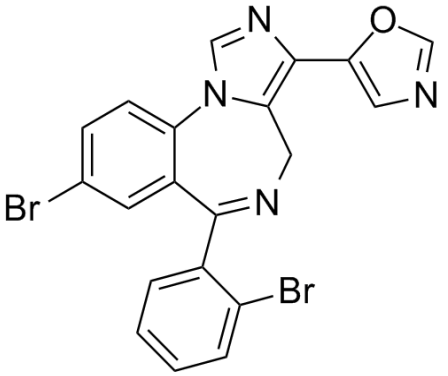
,


N
O
N
N
N
Br
N

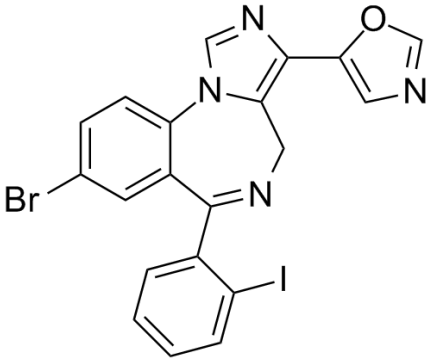
,


N
O
N
N
N
Br
Cl

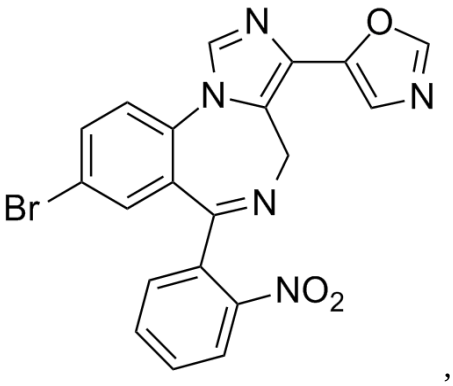
,


N
O
N
N
Br
N
Br

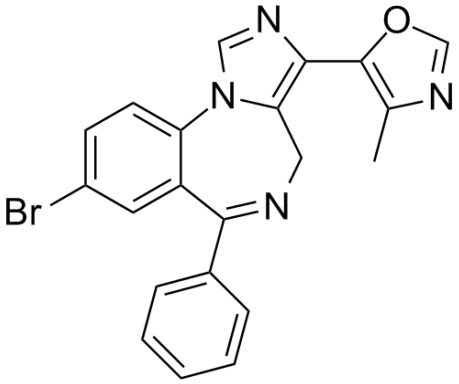
,


N
O
N
N
Br
N
I

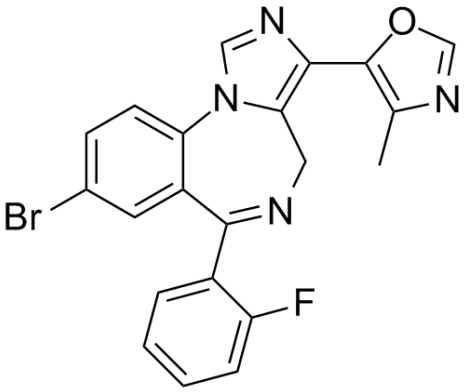
,


N
O
N
N
Br
N
NO2

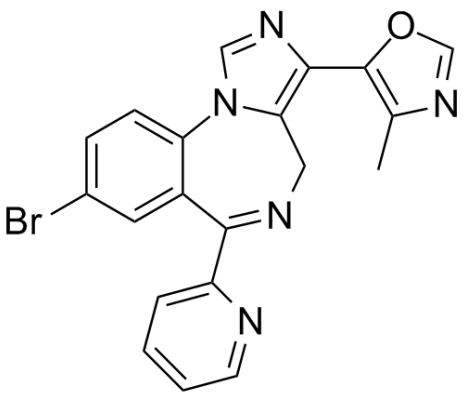
,


N
O
N
N
Br
N

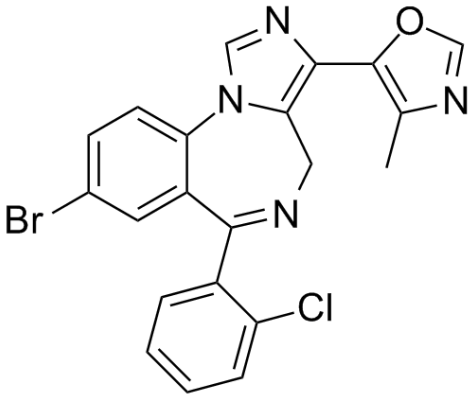
,


N
O
N
N
Br
N
F

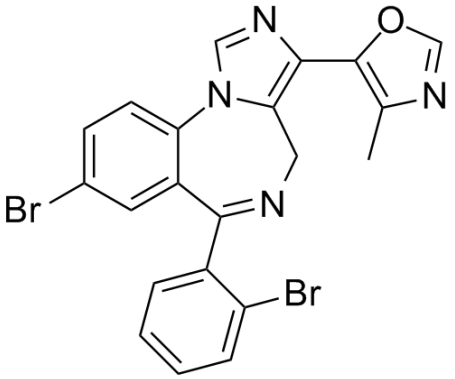
,


N
O
N
N
N
Br
N

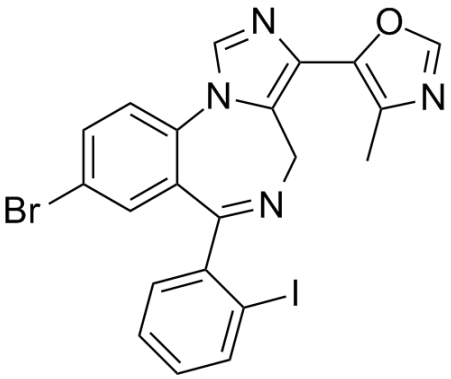
,


N
O
N
N
N
Br
Cl

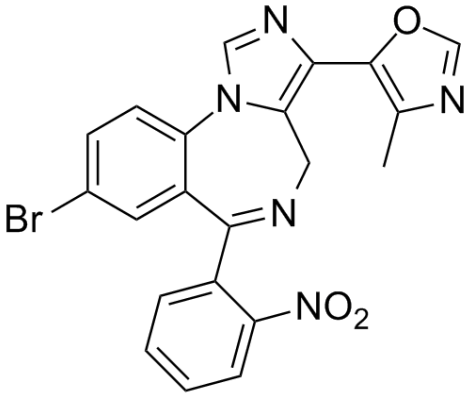
,


N
O
N
N
N
Br
Br

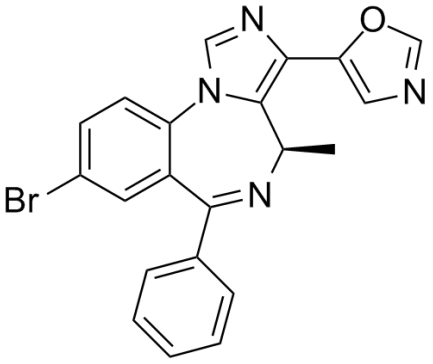
,


N
O
N
N
N
Br
I

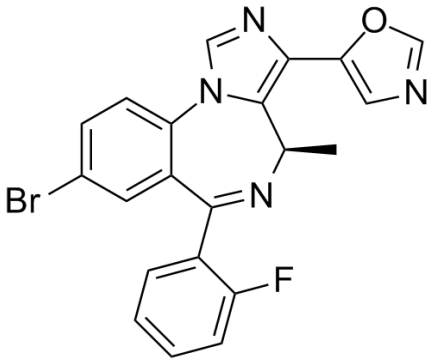
,


N
O
N
N
N
Br
NO2

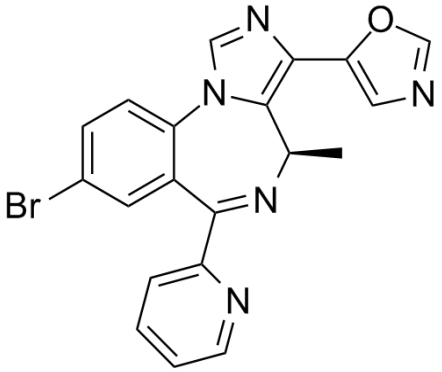
,


N
O
N
N
N
Br

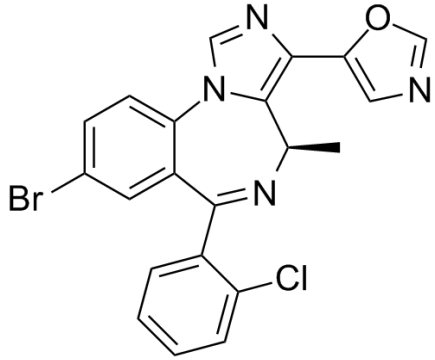
,


N
O
N
N
N
Br
F

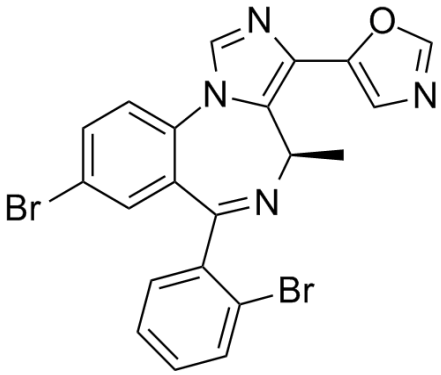
,


N
O
N
N
Br
N
N

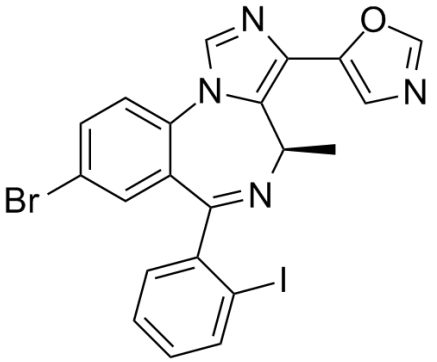
,


N
O
N
N
Br
N
Cl

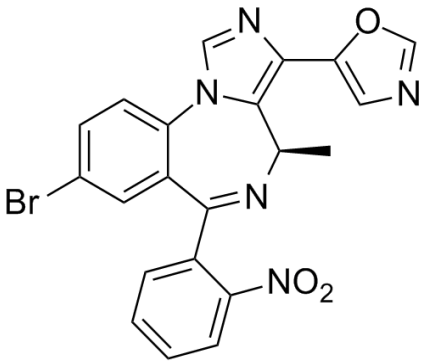
,


N
O
N
N
Br
N
Br

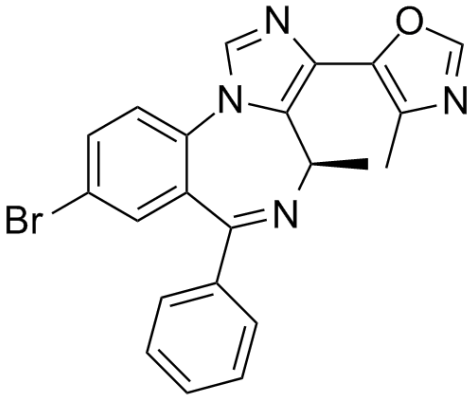
,


N
O
N
N
Br
N
I

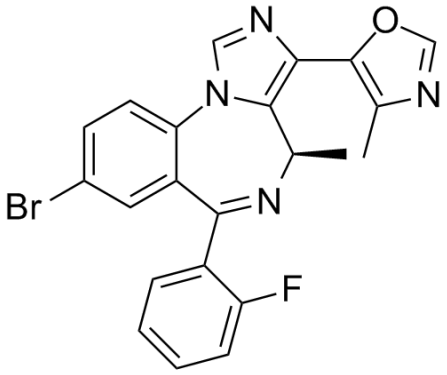
,


N
O
N
N
Br
N
NO2

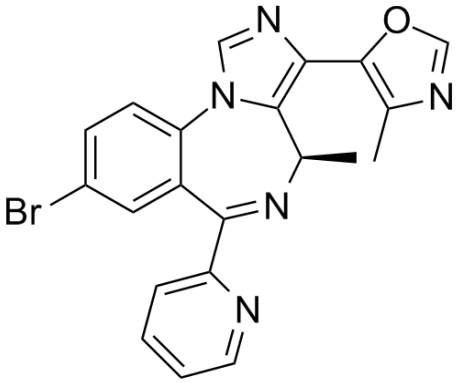
,


N
O
N
N
N
Br

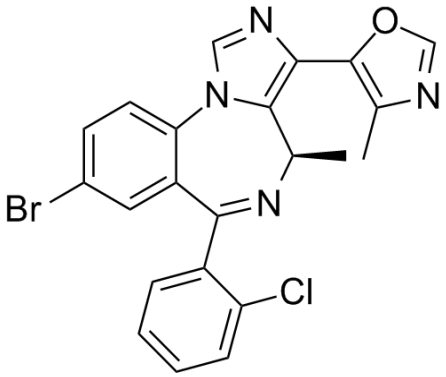
,


N
O
N
N
N
Br
F

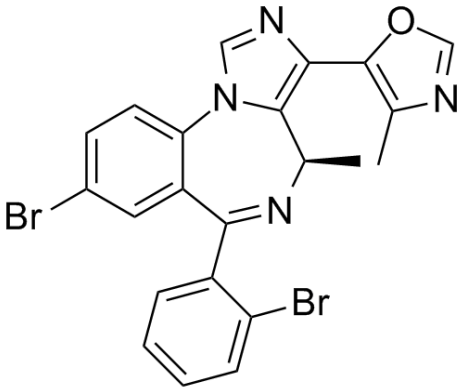
,


N
O
N
N
N
Br
N

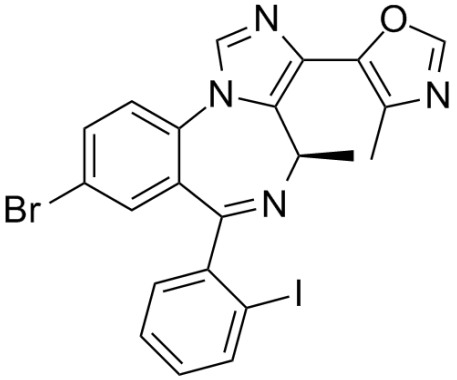
,


N
O
N
N
N
Br
Cl

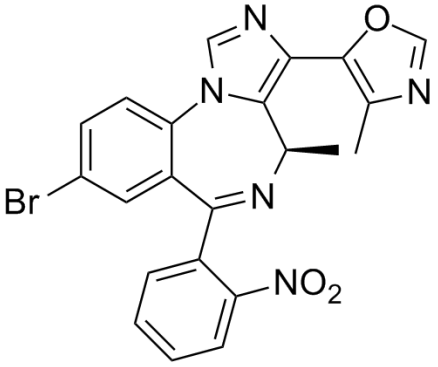
,


N
O
N
N
N
Br
Br

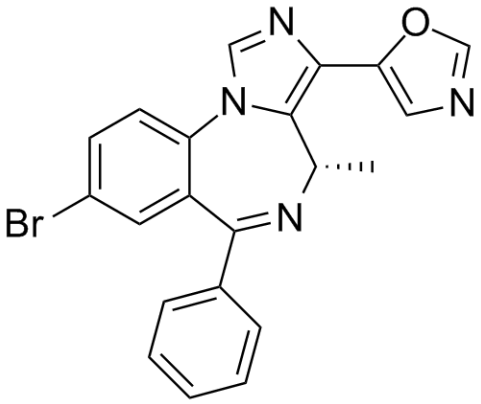
,

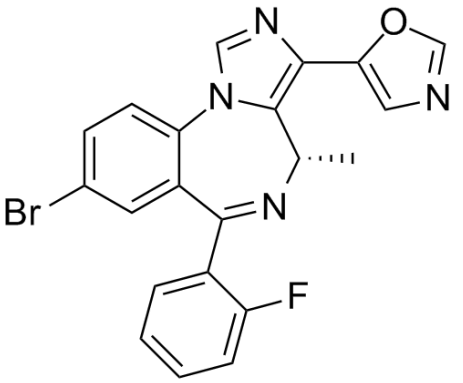

N
O
N
N
N
Br
I

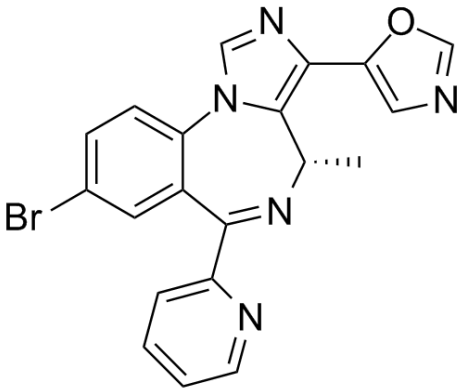
,


N
O
N
N
N
Br
NO2

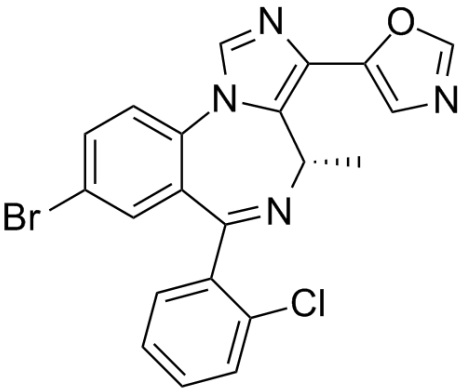
,


N
O
N
N
Br
N

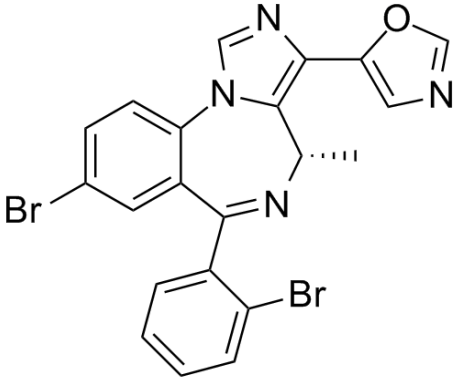

N
O
N
N
Br
N
F


N
O
N
N
Br
N
N

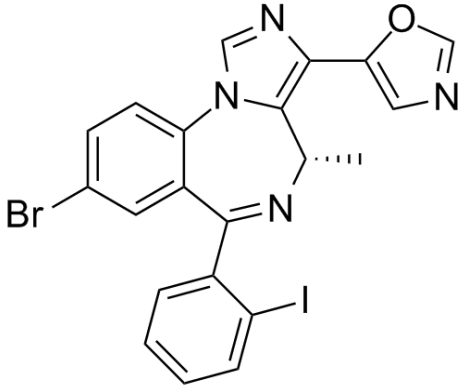
,


N
O
N
N
Br
N
Cl

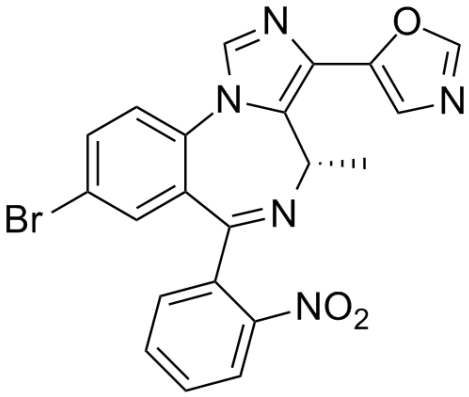
,


N
O
N
N
Br
N
Br

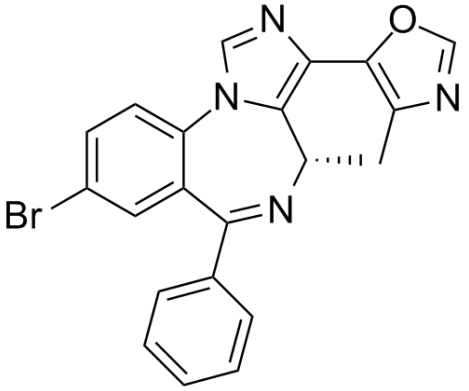
,


N
O
N
N
Br
N
I

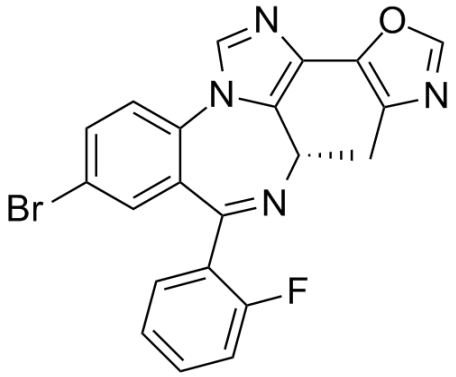
,


N
O
N
N
Br
N
NO2

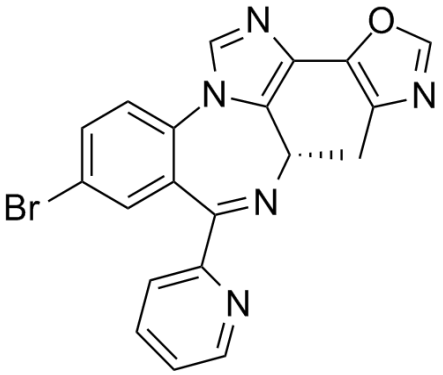
,


N
O
N
N
Br
N

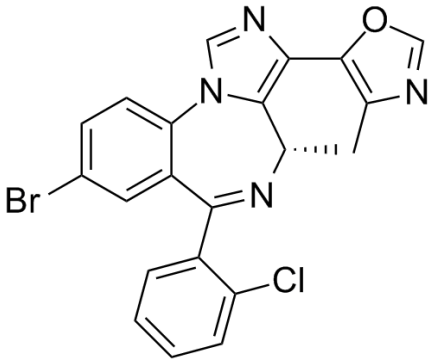
,


N
O
N
N
Br
N
F

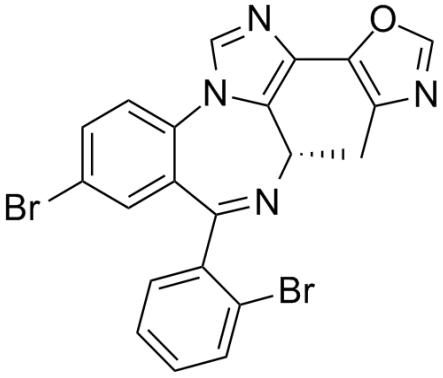
,


N
O
N
N
Br
N
N

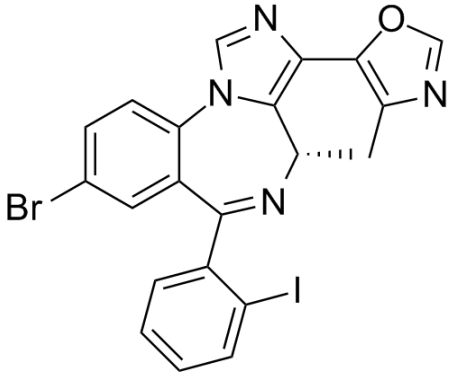
,


N
O
N
N
Br
N
Cl

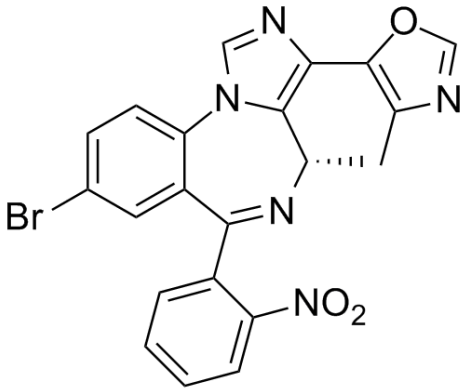
,


N
O
N
N
Br
N
Br

,

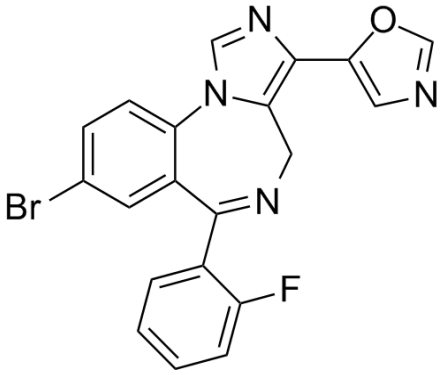

N
O
N
N
Br
N
I

, and



.

[0072] In some embodiments, the compound is not



.

[0073] For compounds of formula (I), (II), (III), (IV), (V), and (VI), groups and substituents thereof may be selected in accordance with permitted valence of the atoms and the substituents, such that the selections and substitutions result in a stable compound, e.g., which does not spontaneously undergo transformation such as by rearrangement, cyclization, elimination, etc.

[0074] Compounds of formula (I), (II), (III), (IV), (V), and (VI) include compounds that differ only in the presence of one or more isotopically enriched atoms. For example, compounds may have the present structures except for the replacement of hydrogen by deuterium or tritium, or the replacement of a carbon by a ^{13}C- or ^{14}C-enriched carbon.

[0075] A compound of formula (I), (II), (III), (IV), (V), or (VI) can be in the form of a salt, e.g., a pharmaceutically acceptable salt. The term "pharmaceutically acceptable salt" includes salts of the active compounds that are prepared with relatively nontoxic acids or bases, depending on the particular substituents found on the compounds. Suitable pharmaceutically acceptable salts of the compounds of this invention include acid addition salts which may, for example, be formed by mixing a solution of the compound according to the invention with a

solution of a pharmaceutically acceptable acid such as hydrochloric acid, sulfuric acid, methanesulfonic acid, fumaric acid, maleic acid, succinic acid, acetic acid, benzoic acid, oxalic acid, citric acid, tartaric acid, carbonic acid or phosphoric acid. Furthermore, where the compounds of the invention carry an acidic moiety, suitable pharmaceutically acceptable salts thereof may include alkali metal salts, e.g. sodium or potassium salts, alkaline earth metal salts, e.g. calcium or magnesium salts; and salts formed with suitable organic ligands, e.g. quaternary ammonium salts.

[0076] Neutral forms of the compounds may be regenerated by contacting the salt with a base or acid and isolating the parent compound in a conventional manner. The parent form of the compound differs from the various salt forms in certain physical properties, such as solubility in polar solvents, but otherwise the salts are equivalent to the parent form of the compound for the purposes of this disclosure.

[0077] In addition to salt forms, the present invention may also provide compounds of formula (I), (II) (III), (IV), (V), or (VI) that are in a prodrug form. Prodrugs of the compounds are those compounds that readily undergo chemical changes under physiological conditions to provide the compounds. Prodrugs can be converted to the compounds of the present invention by chemical or biochemical methods in an *ex vivo* environment. For example, prodrugs can be slowly converted to the compounds of the present invention when placed in a transdermal patch reservoir with a suitable enzyme or chemical reagent.

[0078] Compounds of formula (I), (II) (III), (IV), (V), and (VI) can be, for example, an enantiomerically enriched isomer of a stereoisomer described herein. Enantiomer, as used herein, refers to either of a pair of chemical compounds whose molecular structures have a mirror-image relationship to each other. For example, a compound may have an enantiomeric excess of at least about 10%, 15%, 20%, 25%, 30%, 35%, 40%, 45%, 50%, 55%, 60%, 65%, 70%, 75%, 80%, 85%, 90%, 95%, 96%, 97%, 98%, or 99%.

[0079] A preparation of a compound of formula (I), (II) (III), (IV), (V), or (VI) may be enriched for an isomer of the compound having a selected stereochemistry, e.g., R or S, corresponding to a selected stereocenter. For example, the compound may have a purity corresponding to a compound having a selected stereochemistry of a selected stereocenter of at least about 60%, 65%, 70%, 75%, 80%, 85%, 90%, 95%, 96%, 97%, 98%, or 99%. A compound can, for example, include a preparation of a compound disclosed herein that is

enriched for a structure or structures having a selected stereochemistry, e.g., R or S, at a selected stereocenter.

[0080] In some embodiments, a preparation of a compound of formula (I), (II) (III), (IV), (V), or (VI) may be enriched for isomers (subject isomers) which are diastereomers of the compound. Diastereomer, as used herein, refers to a stereoisomer of a compound having two or more chiral centers that is not a mirror image of another stereoisomer of the same compound. For example, the compound may have a purity corresponding to a compound having a selected diastereomer of at least about 60%, 65%, 70%, 75%, 80%, 85%, 90%, 95%, 96%, 97%, 98%, or 99%.

[0081] When no specific indication is made of the configuration at a given stereocenter in a compound, any one of the configurations or a mixture of configurations is intended.

[0082] Compounds may be prepared in racemic form or as individual enantiomers or diastereomers by either stereospecific synthesis or by resolution. The compounds may, for example, be resolved into their component enantiomers or diastereomers by standard techniques, such as the formation of stereoisomeric pairs by salt formation with an optically active base, followed by fractional crystallization and regeneration of the free acid. The compounds may also be resolved by formation of stereoisomeric esters or amides, followed by chromatographic separation and removal of the chiral auxiliary. Alternatively, the compounds may be resolved using a chiral HPLC column. The enantiomers also may be obtained from kinetic resolution of the racemate of corresponding esters using lipase enzymes.

[0083] A compound of formula (I), (II) (III), (IV), (V), or (VI) can also be modified by appending appropriate functionalities to enhance selective biological properties. Such modifications are known in the art and include those that increase biological penetration into a given biological system (e.g., blood, lymphatic system, central nervous system), increase oral availability, increase solubility to allow administration by injection, alter metabolism, and/or alter rate of excretion. Examples of these modifications include, but are not limited to, esterification with polyethylene glycols, derivatization with pivolates or fatty acid substituents, conversion to carbamates, hydroxylation of aromatic rings, and heteroatom substitution in aromatic rings.

Synthesis of Compounds

[0084] Compounds of formula (I), (II) (III), (IV), (V), and (VI) may be synthesized from commercially available starting materials. Exemplary syntheses are illustrated below in the

Examples. The starting materials (**1**, **4**, **9**, and **14**) in Schemes I, II, III, and IV have been previously synthesized ("Stereospecific anxiolytic and anticonvulsant agents with reduced muscle-relaxant, sedative-hypnotic and ataxic effects," Cook, J.M.; Zhou, H.; Huang, S.; Sarma, P.V.V.S.; Zhang, C., U.S. Patent Publication No. 2006/0003995 A1, Published January 5, 2006).

[0085] Relevant references include the following:

van Leusen, A.M.; Hoogenboom, B.E.; Sideruis, H., "A novel and efficient synthesis of oxazoles from tosylmethylisocyanide and carbonyl compounds", *Tetrahedron Letters*, **13**, 2369-2372, 1972;

Webb, M.R.; Donald, C.; Taylor, R.J.K., "A general route to the *Streptomyces*-derived inthomycin family: the first synthesis of (+)-inthomycin B", *Tetrahedron Letters*, **47**, 549-552, 2006; and

Bull, J.A.; Balskus, E.P.; Horan, R.A.J.; Langner, M.; Ley, S.V., "Total synthesis of potent antifungal marine bisoxazole natural products bengazoles A and B", *Chem. Eur. J.*, **13**, 5515-5538, 2007

[0086] Other methods of synthesizing the compounds of the formulae herein will be evident to those of ordinary skill in the art. Synthetic chemistry transformations and protecting group methodologies (protection and deprotection) useful in synthesizing the compounds are known in the art and include, for example, those such as described in R. Larock, *Comprehensive Organic Transformations*, VCH Publishers (1989); T.W. Greene and P.G.M. Wuts, *Protective Groups in Organic Synthesis*, 2d. Ed., John Wiley and Sons (1991); L. Fieser and M. Fieser, *Fieser and Fieser's Reagents for Organic Synthesis*, John Wiley and Sons (1994); and L. Paquette, ed., *Encyclopedia of Reagents for Organic Synthesis*, John Wiley and Sons (1995), and subsequent editions thereof.

Evaluation of compounds

[0087] Compounds may be analyzed using a number of methods, including receptor binding studies and in vivo methods.

[0088] For example, the $GABA_A$ subunit selectivity of compounds can be evaluated, for example, using competitive binding assays. Such assays have been described (Choudhary et al. *Mol Pharmacol.* 1992, *42*, 627-33; Savić et al. *Progress in Neuro-Psychopharmacology & Biological Psychiatry*, 2010, 34, 376–386). The assays involve the use of a radiolabeled compound known to bind to $GABA_A$ receptors, such as [^{3}H]flunitrazepam. Membrane proteins

can be harvested and incubated with the radiolabeled compound, and non-specific binding can be evaluated by comparing binding of the radiolabeled compound to another, non-labeled compound (e.g., diazepam). Bound radioactivity can be quantified by liquid scintillation counting. Membrane protein concentrations can be determined using commercially available assay kits (e.g., from Bio-Rad, Hercules, CA).

[0089] Compounds can also be evaluated in electrophysiological assays in *Xenopus* oocytes. Compounds can be preapplied to the oocytes before the addition of GABA, which can then be coapplied with the compounds until a peak response is observed. Between applications, oocytes can be washed to ensure full recovery from desensitization. For current measurements, the oocytes can be impaled with microelectrodes, and recordings performed using voltage clamps.

[0090] Compounds described herein may be $GABA_A$ receptor ligands which exhibit anxiolytic activity due to increased agonist efficacy at $GABA_A/\alpha 2$, $GABA_A/\alpha 3$, $GABA_A/\alpha_{2/3}$ and/or $GABA_A/\alpha 5$ receptors. The compounds may possess at least 2-fold, suitably at least 5-fold, and advantageously at least a 10-fold, selective efficacy for the $GABA_A/\alpha 2$, $GABA_A/\alpha 3$, and/or $GABA_A/\alpha 5$ receptors relative to the $GABA_A/\alpha 1$ receptors. However, compounds which are not selective in terms of their agonist efficacy for the $GABA_A/\alpha 2$, $GABA_A/\alpha 3$, and/or $GABA_A/\alpha 5$ receptors are also encompassed within the scope of the present invention. Such compounds will desirably exhibit functional selectivity by demonstrating anxiolytic activity with decreased sedative-hypnotic/muscle relaxant/ataxic activity due to decreased efficacy at $GABA_A/\alpha 1$ receptors.

[0091] GABAergic receptor subtype selective compounds which are ligands of the $GABA_A$ receptors acting as agonists or partial agonists are referred to hereinafter as "$GABA_A$ receptor agonists" or "$GABA_A$ receptor partial agonists" or "agonists" or "partial agonists". In particular these are compounds that are ligands of the benzodiazepine (BZ) binding site of the $GABA_A$ receptors, and hence acting as BZ site agonists or partial agonists. Such ligands also include compounds acting at the GABA site or at modulatory sites other than the benzodiazepine site of $GABA_A$ receptors.

[0092] GABAergic receptor subtype selective compounds act preferably by selectively or preferentially activating as agonists or partial agonists the $GABA_A/\alpha_2$ receptors, $GABA_A/\alpha_3$ receptors, or $GABA_A/\alpha_{2/3}$ as compared to the $GABA_A/\alpha_1$ receptors. A selective or preferential

therapeutic agent has less binding affinity or efficacy to the $GABA_A/\alpha_1$ receptors compared to the $GABA_A/\alpha_2$, $GABA_A/\alpha_3$, or $GABA_A/\alpha_{2/3}$ receptors. Alternatively, the agent binds to $GABA_A/\alpha_1$, $GABA_A/\alpha_2$ and $GABA_A/\alpha_3$ receptors with a comparable affinity but exerts preferential efficacy of receptor activation at $GABA_A/\alpha_2$, $GABA_A/\alpha_3$, $GABA_A/\alpha_{2/3}$, or $GABA_A/\alpha_5$ receptors compared to the $GABA_A/\alpha_1$ receptors. A selective agent of the present invention can also have a greater or lesser ability to bind or to activate $GABA_A/\alpha_5$ receptors relative to $GABA_A/\alpha_2$ and $GABA_A/\alpha_3$ receptors. The Bz/GABA agonists act at the benzodiazepine site of the respective $GABA_A$ receptors but are not restricted to this drug binding domain in its receptor interactions.

[0093] Other methods for evaluating compounds are known to those skilled in the art. For example, an assessment of anxiolytic effects of compounds can be accomplished objectively and quantitatively with operant-based conflict procedures, as described in Fischer et al. *Neuropharmacology* 59 (2010) 612-618. Briefly, behavior which is positively reinforced can be suppressed in these procedures by response-contingent administration of a noxious stimulus such as mild electric shock. If a compound has an anxiolytic effect it increases the rates of responding that are normally suppressed by response-contingent delivery of shock. The strength of conflict procedures is their predictive validity with respect to expected therapeutic effects in humans. Results from the Fischer et al. indicate that benzodiazepine-like drugs that have pharmacological activity for $\alpha 2GABA_A$ and/or $\alpha 3GABA_A$ receptors and low receptor activity at α $1GABA_A$ and $\alpha 5GABA_A$ receptors may be useful, particularly as non-sedating anxiolytics and agents to treat neuropathic pain.

[0094] Anxiolytic activity and locomotor activity can evaluated in the light/dark box by a method developed by Crawley (*Neurosci Biobehav Rev* 1985, 9, 37-44). The light/dark box is an extremely simple noninvasive test for anxiolytic activity. Mice or rats are administered new agents 15-30 minutes prior to testing and placed in the dark portion of the light/dark box. The amount of time it takes the animals to enter the light side and how long they stay versus controls (e.g., diazepam) are a measure of anxiolytic activity. The amount of exploration (or lack thereof) can be used as a preliminary measure of sedation.

[0095] The marble burying assay (Deacon, *Nat Protocols*, 2006, *1*, 122; Kinsey et al., *Pharmacol Biochem Behav* 2011, *98*, 21) is another anxiolytic test. Mice or rats are pretreated the test compound 1 h before being placed in a cage filled with wood chip bedding. The rodents

are then timed and the number of mables buried are counted. A reduction in marble burying compared to control is considered an anxiolytic effect.

[0096] In the elevated plus maze (Savic et al. *Pharmacol Biochem Behav* 2004, *79*, 279-290), test compounds can be administrated ip 15 minutes prior to testing at which time mice can be placed in the center of the maze under a bright light condition. The number of crosses as well as the time spent in the open and closed arms of the maze for the following 15 minutes can be recorded. Control values for the percentage of entries into the open arms, percentage of time spent in the open arms, and total entries can be correlated to values obtained with controls (e.g., diazepam). Promising compounds may not suppress locomotor activity at up to 100 mg/kg and may be anxiolytic.

[0097] For evaluation of potential to treat schizophrenia, compounds may be tested using a mouse model as described in Gill et al. *Neuropsychopharmacology* 2011, 36: 1903-1911. This mouse model of schizophrenia arises from a development disturbance induced by the administration of a DNA-methylating agent, methylazoxymethanol acetate (MAM), to pregnant dams on gestational day 17. The MAM-treated offspring display structural and behavioral abnormalities, consistent with those observed in human patients with schizophrenia. Antagonism or genetic deletion of the α5GABA$_A$ receptor (α5GABA$_A$ R) leads to behaviors that resemble some of the behavioral abnormalities seen in schizophrenia, including prepulse inhibition to startle and impaired latent inhibition. The MAM model can be used to show the effectiveness of a benzodiazepine-positive allosteric modulator (PAM) compound selective for the α5 subunit of the GABA$_A$R. In Gill et al., the pathological increase in tonic dopamine transmission in the brain was reversed, and behavioral sensitivity to psychostimulants observed in MAM rats was reduced. The data suggests that such compounds would be effective in alleviating dopamine-mediated psychosis.

[0098] Compounds selective for GABA$_A$ receptor subunits can be tested for the ability to suppress seizures in several standard rat and mouse models of epilepsy, as described in U.S. Patent Application Publication No. US 2011/0261711. Anticonvulsant activity of compounds can be compared to diazepam. The standard models incorporated into anticonvulsant screening include the maximal electroshock test (MES), the subcutaneous Metrazol test (scMet), and evaluations of toxicity (TOX). The data for each condition can be presented as a ratio of either

the number of animals protected or toxic (loss of locomotor activity) over the number of animals tested at a given time point and dose.

[0099] The MES is a model for generalized tonic-clonic seizures and provides an indication of a compound's ability to prevent seizure spread when all neuronal circuits in the brain are maximally active. These seizures are highly reproducible and are electrophysiologically consistent with human seizures. For all tests based on MES convulsions, 60 Hz of alternating current (50 mA in mice, 150 in rats) is delivered for by corneal electrodes which have been primed with an electrolyte solution containing an anesthetic agent (0.5% tetracaine HCL). For Test 1, mice are tested at various intervals following doses of 30, 100 and 300 mg/kg of test compound given by ip injection of a volume of 0.01 mL/g. In Test 2, rats are tested after a dose of 30 mg/kg (po) in a volume of 0.04 mL/g. Test 8 uses varying doses administered via i.p. injection, again in a volume of 0.04 ml/g. An animal is considered "protected" from MES-induced seizures upon abolition of the hindlimb tonic extensor component of the seizure (Swinyard, E. A., et al. in Antiepileptic Drugs, Levy, R. H. M., et al., Eds.; Raven Press: New York, 1989; pp 85-102; White, H. S., et al., Ital J Neurol Sci. 1995a, 16, 73-7; White, H. S., et al., in Antiepileptic Drugs, Levy, R. H. M., Meldrum, B. S., Eds.; Raven Press: New York, pp 99-110, 1995b).

[00100] Subcutaneous injection of the convulsant Metrazol produces clonic seizures in laboratory animals. The scMet test detects the ability of a test compound to raise the seizure threshold of an animal and thus protect it from exhibiting a clonic seizure. Animals can pretreated with various doses of the test compound (in a similar manner to the MES test, although a dose of 50 mg/kg (po) is the standard for Test 2 scMet). At the previously determined TPE of the test compound, the dose of Metrazol which will induce convulsions in 97% of animals (CD.sub.97: 85 mg/kg mice) is injected into a loose fold of skin in the midline of the neck. The animals can be placed in isolation cages to minimize stress (Swinyard et al. J. Physiol. 1961, 132, 97-0.102) and observed for the next 30 minutes for the presence or absence of a seizure. An episode of clonic spasms, approximately 3-5 seconds, of the fore and/or hindlimbs, jaws, or vibrissae is taken as the endpoint. Animals which do not meet this criterion are considered protected.

[00101] To assess a compound's undesirable side effects (toxicity), animals may monitored for overt signs of impaired neurological or muscular function. In mice, the rotorod procedure

(Dunham, M. S. et al. J. Amer. Pharm. Ass. Sci. Ed. 1957, 46, 208-209) is used to disclose minimal muscular or neurological impairment. When a mouse is placed on a rod that rotates at a speed of 6 rpm, the animal can maintain its equilibrium for long periods of time. The animal is considered toxic if it falls off this rotating rod three times during a 1-min period. In rats, minimal motor deficit is indicated by ataxia, which is manifested by an abnormal, uncoordinated gait. Rats used for evaluating toxicity are examined before the test drug is administered, since individual animals may have peculiarities in gait, equilibrium, placing response, etc., which might be attributed erroneously to the test substance. In addition to MMI, animals may exhibit a circular or zigzag gait, abnormal body posture and spread of the legs, tremors, hyperactivity, lack of exploratory behavior, somnolence, stupor, catalepsy, loss of placing response and changes in muscle tone.

[00102] To further characterize the anticonvulsant activity of compounds, a hippocampus kindling screen can be performed. This screen is a useful adjunct to the traditional MES and scMet tests for identification of a substance potential utility for treating complex partial seizures.

[00103] Benzodiazepines can be highly effective drugs in certain treatment paradigms. They are routinely employed for emergency situations such as status epilepticus and other acute conditions. But their use in chronic convulsant diseases has been limited due to side effects such as sedation and with high doses respiratory depression, hypotension and other effects. Further it has long been purported that chronic administration of this class of drugs can lead to tolerance to the anticonvulsant effects. This has limited their utility as first line treatment for chronic anticonvulsant conditions. Discovery of a potent BDZ with a decreased side effect profile and efficacy over extended treatment periods would be highly desirable.

[00104] In order to assess the effects of tolerance of compounds, whether tolerance could be detected using a chronic (5 day) dose of the candidate drug can be studied. With typical benzodiazepines (for example diazepam), tolerance to the anticonvulsant effects of the drug are evident before 5 days have passed, consequently studies can be done for only 5 days. The dose to be used may be the predetermined ED50 against the scMet seizure model.

Compositions and Routes of Administration

[00105] In another aspect, the invention provides pharmaceutical compositions comprising one or more compounds of this invention in association with a pharmaceutically acceptable carrier. Such compositions may be in unit dosage forms such as tablets, pills, capsules, powders,

granules, sterile parenteral solutions or suspensions, metered aerosol or liquid sprays, drops, ampoules, auto-injector devices or suppositories; for oral, parenteral, intranasal, sublingual or rectal administration, or for administration by inhalation or insufflation. It is also envisioned that compounds may be incorporated into transdermal patches designed to deliver the appropriate amount of the drug in a continuous fashion. For preparing solid compositions such as tablets, the principal active ingredient is mixed with a pharmaceutical carrier, e.g. conventional tableting ingredients such as corn starch, lactose, sucrose, sorbitol, talc, stearic acid, magnesium stearate, dicalcium phosphate or gums, and other pharmaceutical diluents, e.g. water, to form a solid preformulation composition containing a homogeneous mixture for a compound of the present invention, or a pharmaceutically acceptable salt thereof. When referring to these preformulation compositions as homogeneous, it is meant that the active ingredient is dispersed evenly throughout the composition so that the composition may be easily subdivided into equally effective unit dosage forms such as tablets, pills and capsules. This solid preformulation composition is then subdivided into unit dosage forms of the type described above containing from 0.1 to about 500 mg of the active ingredient of the present invention. Typical unit dosage forms contain from 1 to 100 mg, for example, 1, 2, 5, 10, 25, 50, or 100 mg, of the active ingredient. The tablets or pills of the novel composition can be coated or otherwise compounded to provide a dosage form affording the advantage of prolonged action. For example, the tablet or pill can comprise an inner dosage and an outer dosage component, the latter being in the form of an envelope over the former. The two components can be separated by an enteric layer, which serves to resist disintegration in the stomach and permits the inner component to pass intact into the duodenum or to be delayed in release. A variety of materials can be used for such enteric layers or coatings, such materials including a number of polymeric acids and mixtures of polymeric acids with such materials as shellac, cetyl alcohol and cellulose acetate.

[00106] The liquid forms in which the compositions of the present invention may be incorporated for administration orally or by injection include aqueous solutions, suitably flavored syrups, aqueous or oil suspensions, and flavored emulsions with edible oils such as cottonseed oil, sesame oil, coconut oil or peanut oil, as well as elixirs and similar pharmaceutical vehicles. Suitable dispersing or suspending agents for aqueous suspensions include synthetic and natural gums such as tragacanth, acacia, alginate, dextran, sodium carboxymethylcellulose, methylcellulose, polyvinylpyrrolidone or gelatin.

[00107] Suitable dosage level is about 0.01 to 250 mg/kg per day, about 0.05 to 100 mg/kg per day, or about 0.05 to 5 mg/kg per day. The compounds may be administered on a regimen of 1 to 4 times per day, or on a continuous basis via, for example, the use of a transdermal patch.

[00108] Pharmaceutical compositions for enteral administration, such as nasal, buccal, rectal or, especially, oral administration, and for parenteral administration, such as intravenous, intramuscular, subcutaneous, peridural, epidural or intrathecal administration, are suitable. The pharmaceutical compositions comprise from approximately 1% to approximately 95% active ingredient, or from approximately 20% to approximately 90% active ingredient.

[00109] For parenteral administration including intracoronary, intracerebrovascular, or peripheral vascular injection/infusion preference is given to the use of solutions of the subunit selective GABAA receptor agonist, and also suspensions or dispersions, especially isotonic aqueous solutions, dispersions or suspensions which, for example, can be made up shortly before use. The pharmaceutical compositions may be sterilized and/or may comprise excipients, for example preservatives, stabilizers, wetting agents and/or emulsifiers, solubilizers, viscosity-increasing agents, salts for regulating osmotic pressure and/or buffers and are prepared in a manner known per se, for example by means of conventional dissolving and lyophilizing processes.

[00110] For oral pharmaceutical preparations suitable carriers are especially fillers, such as sugars, for example lactose, saccharose, mannitol or sorbitol, cellulose preparations and/or calcium phosphates, and also binders, such as starches, cellulose derivatives and/or polyvinylpyrrolidone, and/or, if desired, disintegrators, flow conditioners and lubricants, for example stearic acid or salts thereof and/or polyethylene glycol. Tablet cores can be provided with suitable, optionally enteric, coatings. Dyes or pigments may be added to the tablets or tablet coatings, for example for identification purposes or to indicate different doses of active ingredient. Pharmaceutical compositions for oral administration also include hard capsules consisting of gelatin, and also soft, sealed capsules consisting of gelatin and a plasticizer, such as glycerol or sorbitol. The capsules may contain the active ingredient in the form of granules, or dissolved or suspended in suitable liquid excipients, such as in oils.

[00111] Transdermal application is also considered, for example using a transdermal patch, which allows administration over an extended period of time, e.g. from one to twenty days.

Methods of Treatment

[00112] Compounds may be used in methods of treatment or prevention of anxiety disorders, depression, epilepsy, schizophrenia, and/or neuropathic pain.

[00113] Anxiety disorder is a term covering several different forms of a type of mental illness of abnormal and pathological fear and anxiety. Current psychiatric diagnostic criteria recognize a wide variety of anxiety disorders. Recent surveys have found that as many as 18% of Americans may be affected by one or more of them. The term anxiety covers four aspects of experiences an individual may have: mental apprehension, physical tension, physical symptoms and dissociative anxiety. Anxiety disorder is divided into generalized anxiety disorder, phobic disorder, and panic disorder; each has its own characteristics and symptoms and they require different treatment. The emotions present in anxiety disorders range from simple nervousness to bouts of terror. Standardized screening clinical questionnaires such as the Taylor Manifest Anxiety Scale or the Zung Self-Rating Anxiety Scale can be used to detect anxiety symptoms, and suggest the need for a formal diagnostic assessment of anxiety disorder.

[00114] Particular examples of anxiety disorders include generalized anxiety disorder, panic disorder, phobias such as agoraphobia, social anxiety disorder, obsessive-compulsive disorder, post-traumatic stress disorder, separation anxiety and childhood anxiety disorders.

[00115] Depression is a state of low mood and is generally caused by genetic, psychological and social factors. Depression can leave those affected feeling down and unable to enjoy activities. Approximately 4.3% of the world population suffers from depression, while lifetime prevalence ranges from 8-12%. Particular examples of depression are major depressive disorder, persistent depressive disorder and bipolar disorder, which itself has extreme lows as a characteristic.

[00116] Epilepsy is a common chronic neurological disorder that is characterized by recurrent unprovoked seizures. These seizures are transient signs and/or symptoms due to abnormal, excessive or synchronous neuronal activity in the brain. There are many different epilepsy syndromes, each presenting with its own unique combination of seizure type, typical age of onset, EEG findings, treatment, and prognosis. Exemplary epilepsy syndromes include, e.g., Benign centrotemporal lobe epilepsy of childhood, Benign occipital epilepsy of childhood (BOEC), Autosomal dominant nocturnal frontal lobe epilepsy (ADNFLE), Primary reading epilepsy, Childhood absence epilepsy (CEA), Juvenile absence epilepsy, Juvenile myoclonic epilepsy

(JME), Symptomatic localization-related epilepsies, Temporal lobe epilepsy (TLE), Frontal lobe epilepsy, Rasmussen's encephalitis, West syndrome, Dravet's syndrome, Progressive myoclonic epilepsies, and Lennox-Gastaut syndrome (LGS). Genetic, congenital, and developmental conditions are often associated with epilepsy among younger patients. Tumors might be a cause for patients over age 40. Head trauma and central nervous system infections may cause epilepsy at any age.

[00117] Schizophrenia is a mental disorder characterized by a breakdown of thought processes and by poor emotional responsiveness. It most commonly manifests itself as auditory hallucinations, paranoid or bizarre delusions, or disorganized speech and thinking, and it is accompanied by significant social or occupational dysfunction. The onset of symptoms typically occurs in young adulthood, with a global lifetime prevalence of about 0.3–0.7%. Diagnosis is based on observed behavior and the patient's reported experiences. Genetics, early environment, neurobiology, and psychological and social processes appear to be important contributory factors. Current research is focused on the role of neurobiology, although no single isolated organic cause has been found. Particular types of schizophrenia include paranoid type, disorganized type, catatonic type, undifferentiated type, residual type, post-schizophrenic depression and simple schizophrenia.

[00118] Neuropathic pain encompasses a range of painful conditions of diverse origins including diabetic neuropathy, post-herpetic neuralgia and nerve injuries after surgery. It includes pain following paraplegia, hypersensitivity to non-painful stimuli (allodynia), for example after surgery or during migraine attacks, spontaneous pain, hyperalgesia and diffuse muscle tenderness of myofacial syndromes. Back pain, cancer pain and AIDS associated pain also qualify as neuropathic pain. Currently prescribed drugs for neuropathic pain are often addictive, are not effective for all patients and have various side effects including tolerance, addiction, sedation, liver toxicity. The financial burden from the loss of productivity in the US alone numbers in the billions of dollars notwithstanding the misery these patients suffer.

[00119] In another aspect, the invention provides a method of treating a disorder selected from an anxiety disorder, depression, epilepsy, schizophrenia and neuropathic pain, in a subject in need of treatment, comprising administering to the subject an effective amount of a compound of

[00120] In an aspect, the invention provides a method of treating an anxiety disorder in a subject in need of treatment, comprising administering to the subject an effective amount of a

compound of formula (I), (II) (III), (IV), (V), or (VI). In embodiments, the anxiety disorder is selected from the group consisting of generalized anxiety disorder, panic disorder, phobias such as agoraphobia, social anxiety disorder, obsessive–compulsive disorder, post-traumatic stress disorder, separation anxiety and childhood anxiety disorders.

[00121] In an aspect, the invention provides a method of treating depression in a subject in need of treatment, comprising administering to the subject an effective amount of a compound of formula (I), (II) (III), (IV), (V), or (VI).

[00122] In an aspect, the invention provides a method of treating schizophrenia in a subject in need of treatment, comprising administering to the subject an effective amount of a compound of formula (I), (II) (III), (IV), (V), or (VI). In embodiments, the schizophrenia may be selected from the group consisting of paranoid type, disorganized type, catatonic type, undifferentiated type, residual type, post-schizophrenic depression and simple schizophrenia.

[00123] In an aspect, the invention provides a method of treating epilepsy in a subject in need of treatment, comprising administering to the subject an effective amount of a compound of formula (I), (II) (III), (IV), (V), or (VI). In another aspect, the invention provides a method of treating seizures in a subject in need of treatment, comprising administering to the subject an effective amount of a compound of formula (I), (II) (III), (IV), (V), or (VI).

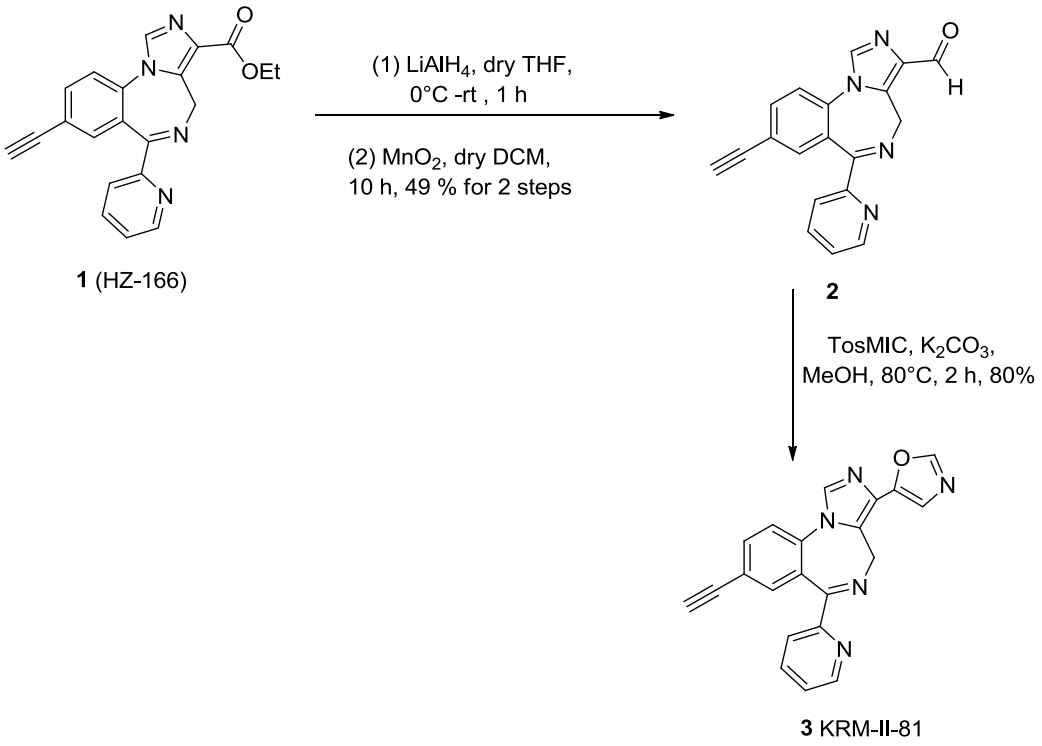
[00124] In an aspect, the invention provides a method of treating neuropathic pain in a subject in need of treatment, comprising administering to the subject an effective amount of a compound of formula (I), (II) (III), (IV), (V), or (VI).

[00125] The following non-limiting examples are intended to be purely illustrative of some aspects and embodiments, and show specific experiments that were carried out in accordance with the disclosure.

EXAMPLES

Example 1. Compound Syntheses

Scheme I. Synthesis of KRM-II-81 (**3**).



1 (HZ-166) **2** **3** KRM-II-81

8-Ethynyl-6-(pyridin-2-yl)-4H-benzo[f]imidazo[1,5-a][1,4]diazepine-3-carbaldehyde (**2**)

[00126] The ethyl ester of 2'-pyridylbenzimidazodiazepine **1** (1.5 g, 4.21 mmol) was placed in an oven dried two neck round bottom flask and was then dissolved in dry THF. The reaction mixture was stirred at 0^{o}C and $LiAlH_4$ (320 mg, 8.42 mmol) was added to the reaction mixture at 0 ^{o}C. After 10 min the reaction mixture was stirred at rt for up to 45 min under an argon atmosphere. After 45 min at rt analysis of the mixture by TLC (silica gel 1: 9 MeOH/EtOAc) indicated the absence of starting ester **1**. The reaction mixture was slowly quenched with an aq saturated sodium sulfate solution (20 mL) at 0^{o}C and then the reaction mixture was diluted with ethyl acetate (50 mL). After this the mixture was filtered through a small bed of Celite. Water was added to the filtrate and it was extracted with ethyl acetate (3x 30 mL). The combined organic layers were washed with water and brine successively and dried (Na_2SO_4). After this the solvent was removed under reduced pressure to furnish the mixture of alcohols (imine alcohol 40% and reduced imine alcohol 60%, via analysis by H^1NMR spectroscopy) as a yellow solid.

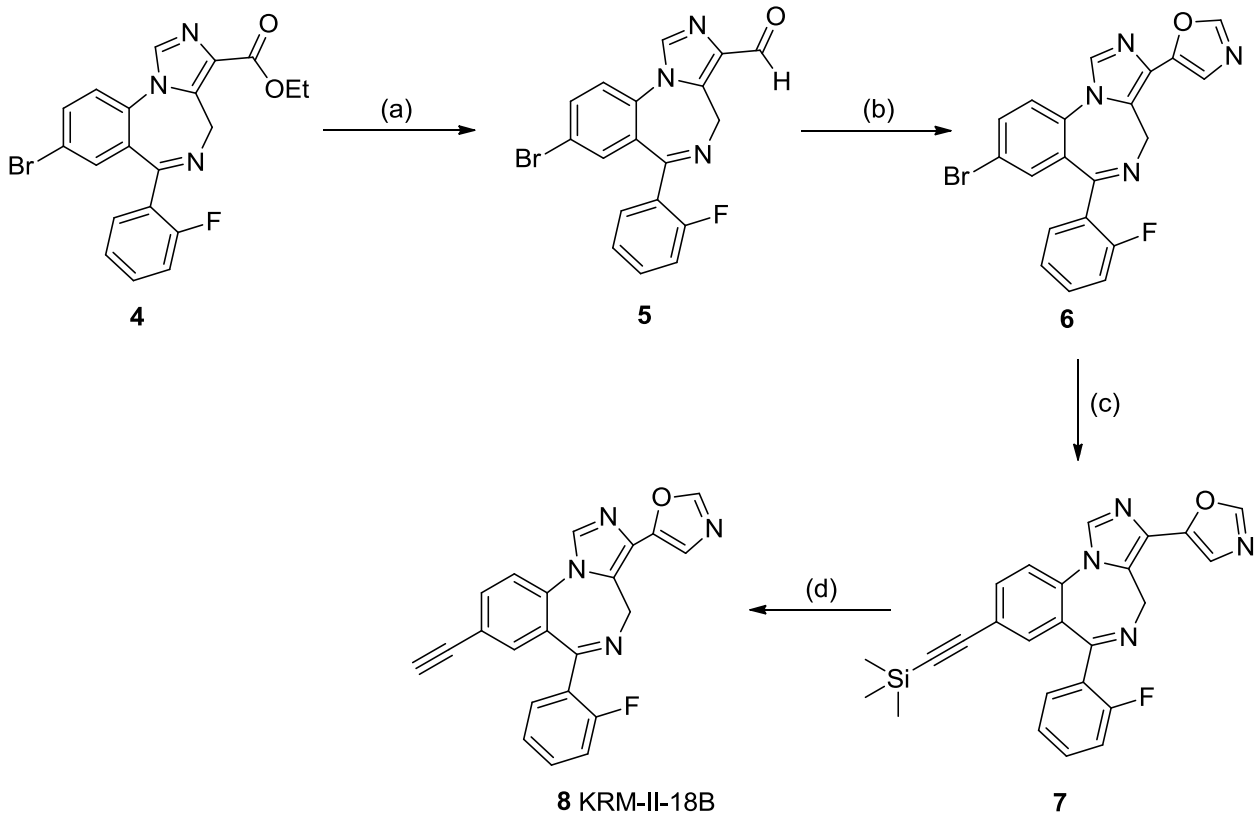
This mixture of alcohols was used directly in the next step. The mixture of 2'-pyridylalcohols (4.45 g, 4.61 mmol) were dissolved in dry DCM (60 mL) under an argon atmosphere, and activated MnO_2 (4.01 g, 46.10 mmol) and Na_2CO_3 were added to the reaction mixture at 0^oC. The mixture was stirred at room temperature for 12 hours. After completion of the reaction as indicated by TLC (complete conversion of alcohol to aldehyde), the reaction mixture was diluted with DCM (50 mL) and it was filtered through a small pad of Celite. The solvent was removed under reduced pressure to get the crude 2'-pyridyl aldehyde along with some other byproducts by TLC (1:9 MeOH/EtOAc). This material was purified by flash column chromatography using EtOAc/DCM (2:1 and 1 mL MeOH + 1 mL TEA for 100 mL) to afford the pure 2' pyridyl aldehyde **2** as a white solid (650 mg, 49.2% over two steps); mp: 238-240^oC; ^1H NMR (500 MHz, $CDCl_3$) δ 10.05 (s, 1H), 8.56 (d, *J* = 5.0 Hz, 1H), 8.08 (d, *J* = 7.5 Hz, 1H), 7.97 (s, 1H), 7.78 (ddd, *J* = 1.5, 6.0 Hz, 1H), 7.77 (dd, *J* = 1.5, 7.0 Hz, 1H), 7.55-7.57 (m, 2H), 7.38 (ddd, *J* = 1.5, 5.0 Hz, 1H), 6.00 (br s, 1H), 4.17 (br s, 1H), 3.16(s, 1H): ^{13}C NMR (75 MHz, $CDCl_3$) δ 186.9, 167.7, 156.2, 148.6, 137.7, 137.1, 136.7, 136.3, 135.4, 135.3, 135.0, 127.1, 124.9, 124.0, 122.8, 121.5, 81.5, 79.7, 44.4. (ESI) MS: *m/z* 313 $(M+H)^+$.

5-(8-Ethynyl-6-(pyridin-2-yl)-4H-benzo[f]imidazo[1,5-a][1,4]diazepin-3-yl)oxazole (3, KRM-II-81)

[00127] The toluenesulfonylmethyl isocyanide (TosMIC, 640 mg, 3.30 mmol) was placed in a dry two neck round bottom flask and dissolved in dry MeOH (50 mL) under an argon atmosphere. At room temperature, K_2CO_3 (1.30 g, 9.99 mmol) was added as well as 2' pyridyldiazepine carboxaldehyde **2** (650 mg, 2.08 mmol) to the reaction mixture and it was heated to reflux for 3 to 4 h. After completion of the reaction on analysis by TLC (silica gel, 1:10 MeOH and EtOAc) which indicated the absence of aldehyde starting material and complete conversion into an oxazole of lower R_f. The reaction mixture was then quenched with cold water. After this, 1/3 of the solvent was removed under reduced pressure and the work up followed with ethyl acetate (3x30 mL). The combined organic layers were washed with water and brine successively and dried (Na_2SO_4). The solvent was then removed under reduced pressure and the residue was purified by silica gel flash chromatography to give the pure 2' pyridyldiazepine oxazole as a white solid (510 mg, 72%); mp: 220-222 ^oC ^1H NMR (300 MHz, $CDCl_3$) δ 8.62 (d, *J* = 4.2 Hz, 1H), 8.12 (s, 1H), 8.06 (d, *J* = 7.8 Hz, 1H), 7.96 (s, 1H), 7.85 (ddd, *J* = 1.8, 6.0 Hz, 1H), 7.79 (dd, *J* = 1.8, 6.6 Hz, 1H), 7.62 (d, *J* = 8.4 Hz, 1H), 7.55 (d, *J* = 1.5 Hz, 1H), 7.53 (s,

1H), 7.41 (ddd, *J* = 1.5, 4.8 Hz, 1H), 5.78 (d, *J* = 12.9 Hz, 1H), 4.31 (d, *J* = 12.9 Hz, 1H). ^{13}C NMR (75 MHz, $CDCl_3$) δ 167.9, 156.7, 149.9, 149.0, 146.6, 137.0, 136.4, 135.8, 135.5, 135.3, 129.8, 127.5, 127.0, 124.9, 124.0, 122.8, 122.7, 121.0, 81.8.7, 79.5, 45.3; HRMS (ESI *m/z*) for $C_{21}H_{13}N_5O$ calcd 352.1188, found 352.1193 $(M+H)^+$.

Scheme II. Synthesis of KRM-II-18B (**8**).



Reagents and conditions: (a) DIBAL-H, -78 °C 2 h, 75%, (b) TosMIC, K_2CO_3, MeOH, 80 °C, 2 h, 77%, (c)TMS acetylene, $Pd(OAc)_2$ ($PPh_{3)2}$, TEA/CH_3CN, rf, 10 h, 92%, (d) TBAF xH_2O, THF, 0°C- rt, 1 h, 88%,

8-Bromo-6-(2-fluorophenyl)-4H-benzo[f]imidazo[1,5-a][1,4]diazepine-3-carbaldehyde (5)

[00128] A solution of diisobutylaluminumhydride (6.25 mL of 1.2 M solution in toluene, 20% w/v) was added dropwise to a vigorously stirred solution of the ester **4** (1.5 g, 3.51 mmol) in anhydrous dichloromethane (40 mL) under an argon atmasphere at –78°C (dry ice-ethyl acetate). After this, the reaction mixture was stirred for an additional 2-3 h at –78°C, and was monitored by TLC every 30 min after 1 h. The temperature must not get above –78°C. If the temperature gets above –78°C or if the reaction continues more than 3 h at –78°C other byproducts are formed (imine reduced aldehyde and ester to alcohol). After completion of the reaction, excess

DIBAL-H was quenched by careful addition of dry methanol (5 mL), followed by 5% aq HCl (10 mL). After this the resulting mixture was allowed to warm to room temperature. If the reaction mixture formed an aluminum-related emulsion, a saturated aq solution of Rochelle's salt and DCM (50 mL) were added to the reaction mixture. It was then filtered through a small pad of Celite and then the organic layer was separated. The aq layer which remained was extracted with DCM (2x30 mL). The combined organic layers were washed with brine and dried (Na_2SO_4). The solvent was removed under reduced pressure to afford the crude aldehyde. This residue was purified by flash chromatography (2:1 ethyl acetate/hexane) to afford the pure diazepine aldehyde **5** as a white solid (1.0 g, 74.6%); mp 120-122^oC; ^1H NMR (300 MHz, $CDCl_3$) δ 10.07 (s, 1H), 8.01 (s, 1H), 7.80 (dd, *J* = 1.8, 6.6 Hz, 1H), 7.67 (ddd, *J* = 1.5, 6.0 Hz, 1H), 7.45-7.52 (m, 3H), 7.25-7.30 (m, 1H), 7.04 (t, *J* = 9.3 Hz, 1H), 6.02 (br s, 1H), 4.15 (br s, 1H). LCMS: *m/z* 385 (M+H).

General synthetic procedure for oxazole containing benzimidazodiazepines.

5-(8-Bromo-6-(2-fluorophenyl)-4H-benzo[f]imidazo[1,5-a][1,4]diazepin-3-yl)oxazole (6)

[00129] The toluenesulfonylmethyl isocyanide (TOSMIC, 300 mg, 1.56 mmol) was placed in a dry two neck round bottom flask and dissolved in dry MeOH (30 mL) under an argon atmosphere. At room temperature, K_2CO_3 (649 mg, 1.53 mmol) was added as well as the 2'fluoro diazepine carboxaldehyde **5** (647 mg, 1.62 mmol) to the reaction mixture and it was heated to reflux for 3 to 4 h. After completion of the reaction on analysis by TLC (silica gel, 2:1 EtOAc and hexane), which indicated the absence of aldehyde starting material and complete conversion to the oxazole of lower R_f, the reaction mixture was then quenched with cold water. After this, 1/3 of the solvent was removed under reduced pressure and the work up followed with ethyl acetate (3x40 mL). The combined organic layers were washed with water, brine successively and dried (Na_2SO_4). The solvent was then removed under reduced pressure and the residue was purified by silica gel flash chromatography to give the pure 2' 2'fluorodiazepine oxazole **6** as white solid (550 mg, 76.7 % yield); mp:190-192 ^oC; ^1H NMR (300 MHz, $CDCl_3$) δ 8.01 (s, 1H), 7.92 (s, 1H), 7.77 (dd, *J* = 2.1, 6.6 Hz, 1H), 7.77 (ddd, *J* = 1.5, 6.0 Hz, 1H), 7.52 (s, 1H), 7.46-7.52 (m, 3H), 7.23-7.28 (m, 1H), 7.04 (t, *J* = 8.4 Hz, 1H), 5.75 (br s, 1H), 4.26 (br s, 1H). ^{13}C NMR (300 MHz, $CDCl_3$) δ 165.0, 161.8, 158.5, 149.8, 146.5, 135.1, 134.9, 133.6, 133.3, 132.5,

131.1, 130.4, 129.7, 127.6, 124.6, 124.0, 122.6, 120.9, 116.4, 116.1, 45.3; HRMS (ESI-TOF *m/z*) for $C_{20}H_{12}N_4OFBr$ calcd 423.0263, found 423.0251 $(M+H)^+$.

5-(6-(2-Fluorophenyl)-8-((trimethylsilyl)ethynyl)-4H-benzo[f]imidazo[1,5-a][1,4] diazepin-3-yl)oxazole (**7**)

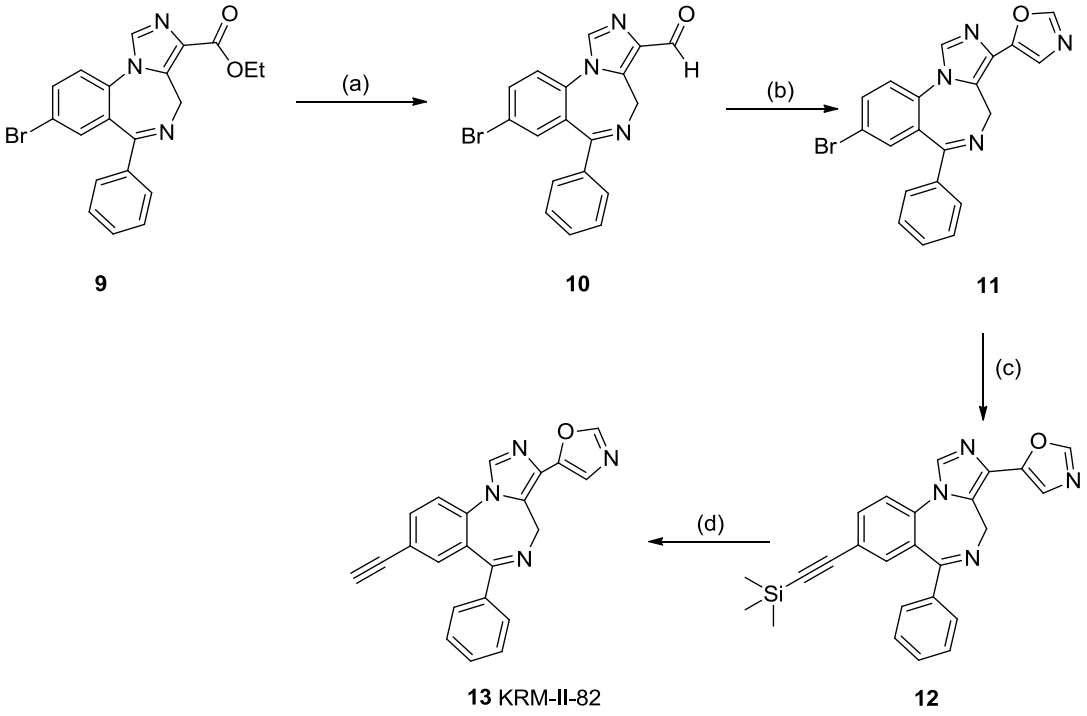
[00130] The 2'fluorodiazepine diazepine bromide **6** (100 mg, 0.23 mmol) and bis(triphenylphosphine)-palladium (II) acetate (10 mg, 0.011 mmol) were added to an oven dried two neck round bottom flask, after which the round bottom flask was fitted with a rubber septum. It was then evacuated under vaccum and back filled with argon. After this, a mixed dry solvent system of CH_3CN:TEA (1:2 ratio) and trimethylsilylacetylene (0.04 mL, 0.26 mmol) were added to the round bottom flask with a syringe under a positive pressure of argon. The round bottom flask was fitted with a reflex condenser and the reaction mixture was degased under vaccum and argon, the process was repeated three times, after which the reaction mixture was slowly heated to 90^{o}C. After stirring for 10 h, the reaction mixture was diluted with ethyl acetate and filtered through a bed of Celite. The organic layer was washed with brine and dried (Na_2SO_4). The solvent was then removed under reduced pressure to furnish a crude solid. This material was purified by flash chromatography (3:1 ethyl acetate/hexane) to afford the pure trimethylsilylacetylene 2'fluorodiazepine intermediate as a light brown solid **7** (90 mg, 92.6% yield). ^{1}H NMR (300 MHz, $CDCl_3$) δ 8.02 (s, 1H), 7.92 (s, 1H), 7.60-7.74 (m, 3H), 7.40-7.57 (m, 3H), 7.23-7.28 (m, 1H), 7.04 (t, *J* = 9.0 Hz, 1H), 5.73 (br s, 1H), 4.24 (br s, 1H), 0.24 (s, 9H); HRMS (ESI-TOF *m/z*) for $C_{25}H_{21}N_4OFSi$ calcd 441.1543, found 441.1541 $(M+H)^+$.

5-(8-Ethynyl-6-(2-fluorophenyl)-4H-benzo[f]imidazo[1,5-a][1,4]diazepin-3-yl)oxazole KRM-II-18B (**8**)

[00131] A solution of 2'-fluorodiazepine trimethylsilylacetylene **7** (90 mg, 0.20 mmol) was dissolved in dry THF and kept at 0°C after which tetrabutylammonium iodide (0.05 mL, 024 mmol) was added slowly to the reaction mixture at 0°C. After 10 min the reaction mixture was stirred at room temperature for 2 h under an argon atmosphere. After TLC (silica gel) indicated the absence of starting material, this reaction mixture was quenched by slow addition of ice cold water and the combined layers were extracted with ethyl acetate (3×20 mL). The combined organic layers were washed with water and brine. This solution was dried (Na_2SO_4) and the solvent was removed under reduced pressure to furnish a solid. This material was then purified

by flash chromatography (4:1 ethyl acetate/hexane) to afford the pure 8-acetyleno-2'-fluorodiazepine oxazole **8** as a white solid (80 mg, 88% yield); mp 212-214; ^{1}H NMR (300 MHz, $CDCl_3$) δ 8.03 (s, 1H), 7.93 (s, 1H), 7.75 (d, *J* = 7.8 Hz, 1H), 7.57-7.63 (m, 2H), 7.44-7.53 (m, 3H), 7.23-7.28 (m, 1H), 7.04 (t, *J* = 9.0 Hz, 1H), 5.74 (br s, 1H), 4.26 (br s, 1H), 3.16 (s, 1H). ^{13}C NMR (300 MHz, $CDCl_3$) δ 165.5, 161.9, 158.5, 149.8, 146.5, 135.4, 135.0, 134.3, 132.3, 131.1, 129.8, 128.9, 127.8, 127.5, 124.5, 122.6, 121.6, 116.4, 116.1, 81.4, 79.6, 45.0; HRMS (ESI-TOF *m/z*) for $C_{22}H_{13}N_4OF$ calcd 369.1144, found 369.1146 $(M+H)^+$.

Scheme III. Synthesis of KRM-II-82



Reagents and conditions: (a) DIBAL-H, -78 °C 2 h, 76%, (b) TosMIC, K_2CO_3, MeOH, 80 °C, 2 h, 78%, (c)TMS acetylene, $Pd(OAc)_2$ (PPh_3)2, TEA/CH_3CN, rf, 10 h, 84%, (d) TBAF xH_2O, THF, 0°C- rt, 1 h, 90%,

8-Bromo-6-phenyl-4H-benzo[f]imidazo[1,5-a][1,4]diazepine-3-carbaldehyde (10)

[00132] A solution of diisobutylaluminumhydride (8.5 mL of 1.2 M solution in toluene, 20% w/v) was added dropwise to a vigorously stirred solution of the ester **9** (2.7 g, 6.58 mmol) in anhydrous dichloromethane (50 mL) under an argon atmasphere at –78^{o}C (dry ice-ethyl acetate). After this the reaction mixture was stirred for an additional 2-3 h at –78^{o}C, and was monitored by TLC every 30 min after 1 h. The temperature must not get above –78^{o}C. If the temperature gets above –78^{o}C or if the reaction continues more than 3 h at –78^{o}C other byproducts are formed

(imine reduced aldehyde and ester to alcohol). After completion of the reaction, excess DIBAL-H was quenched by careful addition of dry methanol (5 mL), followed by 5% aq HCl (10 mL). After this the resulting mixture was allowed to warm rt. If the reaction mixture forms an aluminum-related emulsion, a saturated aq solution of Rochelle's salt and DCM (50 mL) were added to the reaction mixture. It was then filtered through a small pad of Celite and then the organic layer was separated. The aq layer which remained was extracted with DCM (2x30 mL). The combined organic layers were washed with brine and dried (Na_2SO_4). The solvent was removed under reduced pressure to afford the crude aldehyde. This residue was purified by flash chromatography (2:1 ethyl acetate/hexane) to afford the pure diazepine aldehyde **10** as a white solid (2.0 g, 76%); mp 192-194^oC; ^1H NMR (300 MHz, $CDCl_3$) δ 10.06 (s, 1H), 8.01 (s, 1H), 7.84 (d, *J* = 8.4 Hz, 1H), 7.62 (s, 1H), 7.47-7.54 (m, 4H), 7.39-7.44 (m, 2H), 5.98 (d, *J* = 12.6 Hz, 1H), 4.02 (d, *J* = 12.3 Hz, 1H). LCMS: *m/z* 367 (M+2).

5-(8-Bromo-6-phenyl-4H-benzo[f]imidazo[1,5-a][1,4]diazepin-3-yl)oxazole (11)

[00133] The reaction was performed following the same procedure for **6** employing TosMIC (350 mg, 1.79 mmol), K_2CO_3 (7.4 g, 6.90 mmol) and diazepine aldehyde **10** (720 mg, 2.30 mmol). This afforded the crude compound which was purified by flash silica gel chromatography (4:1 ethyl acetate/hexane) to give a white solid **11** (601 mg, 78.0 % yield): mp 225-227 ^oC; ^1H NMR (300 MHz, $CDCl_3$) δ 8.05 (s, 1H), 7.92 (s, 1H), 7.81 (dd, *J* = 1.8, 6.6 Hz, 1H), 7.82 (d, *J* = 8.4 Hz, 1H), 7.53-7.57 (m, 3H), 7.43-7.49 (m, 2H), 7.39-7.43 (m, 2H), 5.75 (d, *J* = 12.6 Hz, 1H), 4.24 (d, *J* = 12.6 Hz, 1H). ^{13}C NMR (300 MHz, $CDCl_3$) δ 167.9, 156.7, 149.9, 148.9, 146.6, 137.0, 136.4, 135.8, 135.4, 135.3, 129.8, 127.5, 127.0, 124.9, 124.0, 122.8, 122.6, 121.0, 45.3; HRMS (ESI-TOF *m/z*) for $C_{20}H_{13}N_4OBr$ calcd 405.0349, found 405.0345 $(M+H)^+$.

5-(6-Phenyl-8-((trimethylsilyl)ethynyl)-4H-benzo[f]imidazo[1,5-a][1,4]diazepin-3-yl)oxazole (12)

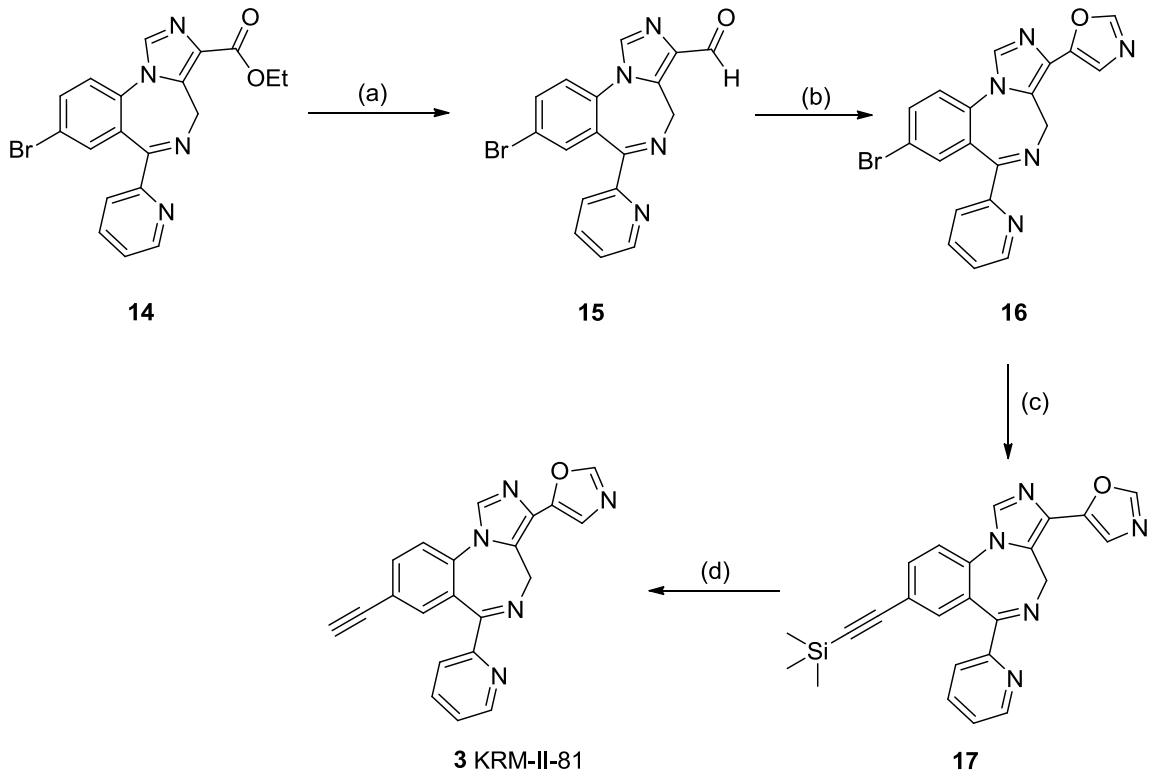
[00134] The trimethylsilylacetylenodiazepine **12** was prepared according to the method described for **7**, employing the bromodiazepine oxazole **11** (700 mg, 1.72 mmol), bis(triphenylphosphine)palladium(II)acetate (64 mg, 0.0864 mmol) and trimethylsilyl acetylene (0.3 mL, 2.07 mmol). The residue which resulted was purified by silica gel flash column chromatography (3:1 ethyl acetate/hexane) to give a light yellow solid **12** (650 mg, 89.6% yield); mp 107-109 ^oC; ^1H NMR (300 MHz, $CDCl_3$) δ 8.05 (s, 1H), 7.92 (s, 1H), 7.81 (dd, *J* = 1.8, 6.6

Hz, 1H), 7.82 (d, *J* = 8.4 Hz, 1H), 7.53-7.57 (m, 3H), 7.43-7.49 (m, 2H), 7.39-7.43 (m, 2H), 5.75 (d, *J* = 12.6 Hz, 1H), 4.24 (d, *J* = 12.6 Hz, 1H), 0.25 (s, 9H); HRMS (ESI-TOF *m/z*) for $C_{25}H_{22}N_4OSi$ calcd 423.1638, found 423.1636 $(M+H)^+$.

5-(8-Ethynyl-6-phenyl-4H-benzo[f]imidazo[1,5-a][1,4]diazepin-3-yl)oxazole KRM-II-82 (**13**)

[00135] The acetylenodiazepine oxazole **13** was prepared, according to the method described for **8**, which employed the TMS-acetylenodiazepine oxazole **12** (500 mg, 1.18) and TBAF (0.5 mL, 1.76 mmol). After workup, the residue was purified by silica gel flash column chromatography (4:1 ethyl acetate/hexane) to afford acetylenodiazepine oxazole **13** as a white solid (370 mg, 90% yield); mp 120-122 ºC. ^{1}H NMR (300 MHz, $CDCl_3$) δ 8.08 (s, 1H), 7.93 (s, 1H), 7.81 (dd, *J* = 1.8, 6.6 Hz, 1H), 7.81 (d, *J* = 8.4 Hz, 1H), 7.53-7.57 (m, 3H), 7.43-7.49 (m, 2H), 7.39-7.43 (m, 2H), 5.75 (d, *J* = 12.9 Hz, 1H), 4.24 (d, *J* = 12.9 Hz, 1H), 3.18 (s, 1H).^{13}C NMR (300 MHz, $CDCl_3$) δ 167.9, 156.7, 149.9, 148.9, 146.6, 137.0, 136.4, 135.8, 135.4, 135.3, 129.8, 127.5, 127.0, 124.9, 124.0, 122.8, 122.6, 121.0, 81.8, 79.5, 45.2; HRMS (ESI-TOF *m/z*) for $C_{22}H_{14}N_4O$ calcd 351.1246, found 351.1240 $(M+H)^+$.

Scheme IV. Alternate Synthetic Route to KRM-II-81 (**3**).



Reagents and conditions: (a) (i) $LiAlH_4$, dry THF, 0°C -rt, 1 h, (ii) MnO_2, dry CH_2Cl_2, 57% over 2 steps) (b) TosMIC, K_2CO_3, MeOH, 80 °C, 2 h, 73%, (c) TMS acetylene, $Pd(OAc)_2$ ($PPh_{3)2}$, TEA/CH_3CN, rf, 10 h, 80%, (d) TBAF xH_2O, THF, 0°C- rt, 1 h, 82%,

8-Bromo-6-(pyridin-2-yl)-4H-benzo[f]imidazo[1,5-a][1,4]diazepine-3-carboxaldehyde(15)

[00136] The ethyl ester of 2'-pyridylbenzimidazodiazepine **14** (500 mg, 1.22 mmol) was placed in an oven dried two neck round bottom flask and was then dissolved in dry THF. The reaction mixture was stirred at 0°C and $LiAlH_4$ (93 mg, 2.43 mmol) was added to the reaction mixture at 0 °C. After 10 min the reaction mixture was stirred at rt up to 45 min under an argon atmosphere. After 45 min at rt analysis of the mixture by TLC (silica gel 1: 9 MeOH/EtOAc) indicated the absence of starting ester **14**. The reaction mixture was slowly quenched with a saturated aq solution of sodium sulfate (10 mL) at 0°C and then the reaction mixture was diluted with ethyl acetate (30 mL). After this the mixture was filtered through a small pad of Celite and then the filtrate was extracted with ethyl acetate (3x 30 mL). The combined organic layers were washed with water and brine successively. After this, the solvent was removed under reduced pressure to furnish the mixture of alcohols (imine alcohol 60% and reduced imine alcohol 40%, via analysis by H^1NMR spectroscopy) as a yellow solid. This mixture of alcohols was used

directly in the next step. The mixture of 2'-pyridylalcohols (455 mg, 1.22 mmol) were dissolved in dry DCM (30 mL) under an argon atmosphere, and activated MnO_2 (278 mg, 14.4 mmol) was added to the reaction mixture at 0°C. The mixture was stirred at rt overnight. After completion of the reaction as indicated by TLC (complete conversion of alcohol to aldehyde), the reaction mixture was diluted with DCM/EtOAc (30 mL) and was filtered through a small pad of Celite. The solvent was removed under reduced pressure to get the crude 2'-pyridyl aldehyde along with some other byproducts by TLC (1:9 MeOH/EtOAc). This material was purified by flash column chromatography using EtOAc/DCM (2:1 and 1 mL MeOH + 1 mLTEA for 100 mL) to afford the pure 2' pyridyl aldehyde **15** as a white solid (289 mg, 56.7% over two steps); mp: 220-222 °C. ^{1}H NMR (300 MHz, $CDCl_3$) δ 10.07 (s, 1H), 8.56 (d, *J* = 2.4 Hz, 1H), 8.13 (d, *J* = 7.8 Hz, 1H), 7.96 (s, 1H), 7.80-7.86 (m, 2H), 7.62 (s, 1H), 7.49 (d, *J* = 8.4 Hz, 1H), 7.40 (t, *J* = 7.2 Hz, 1H), 6.10 (br s, 1H), 4.15 (br s, 1H). LCMS: *m/z* 368 $(M+2)^+$.

5-(8-Bromo-6-(pyridin-2-yl)-4H-benzo[f]imidazo[1,5-a][1,4]diazepin-3-yl)oxazole (16)

[00137] The 2' pyridyldiazepine oxazole **16** was prepared according to the method described for **6** employing TosMIC (160 mg, 0.81 mmol), K_2CO_3 (223 mg, 18.46 mmol) and 2' pyridyldiazepine carboxaldehyde **15** (200 mg, 1.62 mmol). This afforded the crude oxazole which was purified by flash silica gel chromatography (silica gel, 1:10 MeOH and EtOAc) to give pure 2' pyridyldiazepine oxazole **16** as a white solid (160 mg, 73%); mp:226-228 °C; ^{1}H NMR (500 MHz, $CDCl_3$) δ 8.62 (d, *J* = 4.5 Hz, 1H), 8.24 (s, 1H), 8.08 (d, *J* = 8.0 Hz, 1H), 7.96 (s, 1H), 7.82-7.87 (m, 2H), 7.57-7.59 (m, 2H), 7.40-7.43 (m, 1H), 5.78 (d, *J* = 12.5 Hz, 1H), 4.32 (d, *J* = 12.5 Hz, 1H), (ESI) MS: *m/z* 368 $(M+H)^+$.)$^+$. ^{13}C NMR (300 MHz, $CDCl_3$) δ 167.2, 155.9, 150.1, 148.7, 145.4, 137.2, 135.3, 135.2, 134.4, 133.3, 129.6, 128.3, 126.9, 125.1, 124.5, 124.1, 123.4, 120.8, 44.9; HRMS (ESI-TOF *m/z*) for $C_{19}H_{12}N_5OBr$ calcd 406.0299, found 406.0298 $(M+H)^+$.

5-(6-(Pyridin-2-yl)-8-((trimethylsilyl)ethynyl)-4H-benzo[f]imidazo[1,5-a][1,4]diazepin-3-yl)oxazole (**17**)

[00138] The 2'pyridyltrimethylsilylacetylenodiazepine **17** was prepared, according to the method described for **7**, which employed the 2' pyridyldiazepine bromide **16** (160 mg, 0.394 mmol) bis(triphenylphosphine)palladium(II)acetate (15.0 mg, 0.02 mmol) and trimethylsilyl acetylene (0.3 mL, 2.07 mmol). After work up, the residue which resulted was purified by silica

gel flash column chromatography (4:1 ethyl acetate/DCM and 1 mL MeOH and 1 mL TEA for 100 mL) to give a light brown solid **17** (133 mg, 80%). ^{1}H NMR (300 MHz, $CDCl_3$) δ 8.63 (d, *J* = 4.1 Hz, 1H), 8.26 (s, 1H), 8.06 (d, *J* = 8.0 Hz, 1H), 7.97 (s, 1H), 7.82-7.88 (m, 2H), 7.57-7.59 (m, 2H), 7.40-7.43 (m, 1H), 5.78 (d, *J* = 12.1 Hz, 1H), 4.32 (d, *J* = 12.1 Hz, 1H), 0.24 (s, 9H).

5-(8-Ethynyl-6-(pyridin-2-yl)-4*H*-benzo[*f*]imidazo[1,5-a][1,4]diazepin-3-yl)oxazole KRM-II-81 (**3**)

[00139] The 2'-pyridyl-8-acetylenediazepines oxazole **3** was prepared, according to the method described for **8**, employing the 2'-pyridyltrimethylsilylacetylene diazepine **17** (600 mg, 1.4 mmol), and TBAF (0.48 mL, 1.7 mmol). After workup the residue was purified by flash chromatography (4:1 ethyl acetate/DCM, 1 mL MeOH and 1 mL TEA for 100 mL) to afford the pure 2'-pyridyl-8-acetylenediazepines oxazole **3** as a white solid (410 mg, 82%); mp: 230-232 ^{o}C; ^{1}H NMR (300 MHz, $CDCl_3$) δ 8.62 (d, *J* = 4.2 Hz, 1H), 8.12 (s, 1H), 8.06 (d, *J* = 7.8 Hz, 1H), 7.96 (s, 1H), 7.85 (ddd, *J* = 1.8, 6.0 Hz, 1H), 7.79 (dd, *J* = 1.8, 6.6 Hz, 1H), 7.62 (d, *J* = 8.4 Hz, 1H), 7.55 (d, *J* = 1.5 Hz, 1H), 7.53 (s, 1H), 7.41 (ddd, *J* = 1.5, 4.8 Hz, 1H), 5.78 (d, *J* = 12.9 Hz, 1H), 4.31 (d, *J* = 12.9 Hz, 1H). ^{13}C NMR (300 MHz, $CDCl_3$) δ 167.9, 156.7, 149.9, 149.0, 146.6, 137.0, 136.4, 135.8, 135.5, 135.3, 129.8, 127.5, 127.0, 124.9, 124.0, 122.8, 122.7, 121.0, 81.8.7, 79.5, 45.3; HRMS (ESI-TOF *m/z*) for $C_{21}H_{13}N_5O$ calcd 352.1188, found 352.1193 $(M+H)^+$.

Example 2. Compound Assays

Explanation of Terms

[00140] **EC3**: A concentration of GABA eliciting 3% of the maximal GABA-elicited current amplitude of the individual oocyte.

[00141] **log[M]**: Represents the logarithm of molar concentration

Assays Of Competitive Binding To αxβ3γ2 GABAA Receptors

[00142] The $GABA_A$ subunit selectivity of several compounds prepared as described above were determined using competitive binding assays. Competition binding assays were performed in a total volume of 0.5 mL at 4°C for 1 h using [^{3}H]flunitrazepam as the radioligand (Savić, M. M.; Cook, J. M. et al. *Progr. Neuro. Psychopharm. Biol. Psy.* **2010**, *34*, 376-386). A total of 6 μg of cloned human $GABA_A$ receptor DNA containing desired α subtype along with β2 and γ2 subunits were used for transfecting HEK 293T cell line using Fugene 6 (Roche Diagnostic) transfecting reagent. Cells were harvested 48 h

after transfection, washed with Tris–HCl buffer (pH 7.0) and Tris Acetate buffer (pH 7.4) and resulting pellets were stored at -80°C until assayed. On the day of the assay, pellets containing 20-50 μg of $GABA_A$ receptor harvested with hypotonic buffer (50 mM Tris–acetate, pH 7.4, at 4°C) was incubated with the radiolabel as previously described. Non-specific binding was defined as radioactivity bound in the presence of 100 μM diazepam and represented less than 20% of total binding. Membranes were harvested with a Brandel cell harvester followed by three ice-cold washes onto polyethyleneimine-pretreated (0.3%) Whatman GF/C filters. Filters were dried overnight and then soaked in Ecoscint A liquid scintillation cocktail (National Diagnostics; Atlanta, GA). Bound radioactivity was quantified by liquid scintillation counting. Membrane protein concentrations were determined using an assay kit from Bio-Rad (Hercules, CA) with bovine serum albumin as the standard.

Electrophysiological experiments

[00143] Oocytes will be injected according to a standard method (Savic *et al. Prog. Neuropsychopharmacol. Biol. Psychiatry* 2010, 34(2):376-386) with different combinations of cDNA's comprised of different α-GABAergic cDNA's in combination with β3 and γ2 GABAergic cDNAs to express the different $GABA_A$ ion channels (Savic *et al. Prog. Neuropsychopharmacol. Biol. Psychiatry* 2010, 34(2):376-386). These will be used for the oocyte studies, applying an EC3 of GABA and then the drug being tested. For electrophysiological recordings, oocytes will be placed on a nylon-grid in a bath of Xenopus Ringer solution (XR, containing 90 mM NaCl, 5 mM HEPES-NaOH (pH 7.4), 1 mM $MgCl_2$, 1 mM KCl and 1 mM $CaCl_2$). The oocytes will be constantly washed by a flow of 6 ml/min XR which could be switched to XR containing GABA and/or drugs. Drugs were diluted into XR from DMSO-solutions resulting in a final concentration of 0.1 % DMSO perfusing the oocytes. Drugs will be preapplied for 30 sec before the addition of GABA, which will be coapplied with the drugs until a peak response was observed. Between two applications, oocytes will be washed in XR for up to 15 min to ensure full recovery from desensitization. For current measurements the oocytes will be impaled with two microelectrodes (2–3 mΩ) which were filled with 2 mM KCl. All recordings will be performed at room temperature at a holding potential of –60 mV using a Warner OC-725C two-electrode voltage clamp (Warner Instruments, Hamden, CT). Data will be digitized, recorded and measured using a Digidata 1322A data acquisition system (Axon

Instruments, Union City, CA). Results of concentration response experiments will be fitted using GraphPad Prism 3.00 (GraphPad Software, San Diego, CA).

[00144] The equation to be used for fitting concentration response curves will be Y=Bottom + (Top-Bottom)/(1+10^((LogEC50-X)*HillSlope)); X represents the logarithm of concentration, Y represents the response; Y starts at Bottom and goes to Top with a sigmoid shape. This is identical to the "four parameter logistic equation."

[00145] Concentration–effect curves can be prepared for various compounds tested on α1β3γ2, α2β3γ2, α3β3γ2, andα5β3γ2 $GABA_A$ receptors, using an EC3 GABA concentration.

Metabolic Stability for $GABA_A$ Receptor Ligands Using Human Liver Microsomes

[00146] The metabolic stability of $GABA_A$ receptor ligands using human liver microsomes will be studied. The test articles will be incubated at two concentrations (1 and 10 μM) and aliquots (100 μL) were removed at various time points (0, 15, 30, and 60 minutes), and analyzed by LC-MS/MS.

Example 3. Binding and Brain Fractions

[00147] KRM-II-81 was shown to have a great affinity in the nanomolar range for the α3-subtype (0.97 μM), complemented by a low affinity for the α1-subtype (testing was halted at greater than 20 μM). This α3 binding is comparable to the nonsedating anxiolytic, HZ-166 (0.84 μM). In a 10 mg/kg oral dose in rats, a concentration of 644 ng/g of KRM-II-81 was found unbound in the brain, indicating a great pharmacokinetic-profile. In addition, KRM-II-81 was not found to be a substrate of CYP3A4, CYP2D6, or CYP2C9; all of which are responsible for the metabolism of many other clinically used drugs.

Example 4. Marble Burying Assay

[00148] The marble burying assay is designed to measure the anxiolytic-effect of a compound. When mice are nervous, they will bury marbles. As there becomes a decrease in amount of marbles buried, the better anxiolytic effect of a compound. Herein, KRM-II-81 is shown to be a better anxiolytic than HZ-166, which is a published anxiolytic (Fischer *et al. Neuropharmacology*, 2010, **59**, 612). KRM-II-81 also displayed less sedative effects than HZ-166 based on the rotarod assay, which implies that it have little to no amnesic or addictive properties.

Example 5. Pharmacokinetics

[00149] A 10 mg/kg P.O. dose was given for each of the compounds; however, HZ-166 used mice while KRM-II-81 used rats. Although these are different species, the numbers can still be compared. Data are summarized in **TABLE 1**.

TABLE 1: Highest concentration of compound, C_{max}, found in blood at time T_{max}.

	HZ-166	KRM-II-81
C_{max}	4.11 ng/mL	1746 ng/mL
T_{max}	5.58 hours	1.3 hours

[00150] This data shows that the concentration of KRM-II-81 is nearly 500-times more concentrated in the blood than HZ-166. This leads to a higher concentration of the compound getting into the brain, which leads to a more effective compound. This data coupled with the brain unbound concentration ($[brain]_u$) of 644 ng/g and an 18% free fraction gives KRM-II-81 an exceptional profile. This is also superior to MP-III-080, which was also evaluated for the brain concentrations one hour after a 10 mg/kg oral dose. MP-III-080 produced a $[brain]_u$ of 340 ng/g and an 11% free fraction.

[00151] *In vitro* metabolism studies were done in mouse, rat, human, and dogs cells (**TABLE 2**).

TABLE 2: Percent of compound metabolized by in individual species.

Mouse % Metabolized	Rat % Metabolized	Human % Metabolized	Dog % Metabolized
10.1	9.6	8.6	5.9

[00152] In summary, the max concentration of the nonsedating anxiolytic/anticonvulsant/ antinociceptive agent HZ-166 in rodents was 4.11 ng/mL; while KRM-II-81 came in at 1746 ng/mL. KRM-II-81 was found in the blood at nearly a 500-times higher concentration.

Example 6. Synthesis of Compounds

[00153] Compounds shown in **FIG. 3** were synthesized according to the scheme shown in **FIG. 1**, with intermediates further shown in **FIG. 2**.

8-Bromo-6-(pyridin-2-yl)-4H-benzo[f]imidazo[1,5-a][1,4]diazepine-3-carbaldehyde (**6a**), **Method 1**

[00154] The ethyl ester of 2'-pyridyl benzimidazodiazepine **5a** (500 mg, 1.21 mmol) was placed in an oven dried two neck round bottom flask and was then dissolved in dry THF. The reaction mixture was stirred at 0^{o}C and $LiAlH_4$ (50 mg, 1.34 mmol) was added to the reaction mixture at 0^{o}C. After 10 min the reaction mixture was stirred at room temperature up to 45 min to 1 h under an argon atmosphere. After 45-60 min at room temperature analysis of the mixture by TLC (silica gel 1: 9 MeOH/EtOAc) indicated the absence of starting ester **5a**. The reaction mixture was slowly quenched with a saturated aqueous solvent of sodium sulfate (10 mL) at 0°C and then the reaction mixture was diluted with ethyl acetate (30 mL). After this, the mixture was filtered through a small pad of Celite and then the filtrate was extracted with ethyl acetate (3 x 30 mL). The combined organic layers were washed with brine and dried over Na_2SO_4. The solvent was then removed under reduced presser to furnish the mixture of alcohols (imine alcohol 60% and reduced imine alcohol 40%, via analysis by H^1NMR spectroscopy) as a yellow solid. This mixture of alcohols was used directly in the next step. The mixture of 2'-pyridylalcohols (455 mg, 1.22 mmol) was dissolved in dry DCM (30 mL) under an argon atmosphere, after which Na_2CO_3 (384 mg, 3.66 mmol) and activated MnO_2 (278 mg, 14.4 mmol) were added to the reaction mixture at 0°C. The mixture was stirred at room temperature overnight. After completion of the reaction as indicated by TLC, the reaction mixture was diluted with DCM (30 mL) and was filtered through a small pad of Celite. The solvent was removed under reduced pressure to give the crude 2'-pyridyl aldehyde along with some other byproducts by TLC (1:9 MeOH/EtOAc). This material was purified by flash column chromatography using EtOAc/DCM/Hexane (2:1:1 and 1 mL MeOH + 1 mLTEA for 100 mL) to afford the pure 2' pyridyl aldehyde **6a** as a white solid (180 mg, 39.8% over two steps); mp: 220-222 ^{o}C. ^{1}H NMR (300 MHz, $CDCl_3$) δ 10.07 (s, 1H), 8.56 (d, *J* = 2.4 Hz, 1H), 8.13 (d, *J* = 7.8 Hz, 1H), 7.96 (s, 1H), 7.80-7.86 (m, 2H), 7.62 (s, 1H), 7.49 (d, *J* = 8.4 Hz, 1H), 7.40 (t, *J* = 7.2 Hz, 1H), 6.10 (br s, 1H), 4.15 (br s, 1H). (ESI) MS: *m/z* 368 $(M+H)^+$. ^{13}C NMR (75 MHz, $CDCl_3$) δ 186.7, 167.6, 156.3, 148.5, 137.7, 137.1, 136.8, 136.4, 135.5, 135.4, 135.0, 127.1, 124.9, 124.1, 122.9, 121.6, 81.5, 79.8, 44.3; HRMS (ESI-TOF *m/z*) for $C_{17}H_{11}BrN_4O$ calcd 367.0176 found 367.0189 (M+H)+.

8-Bromo-6-phenyl-4H-benzo[f]imidazo[1,5-a][1,4]diazepine-3-carbaldehyde (6b), Method 2

[00155] A solution of diisobutylaluminum hydride (8.5 mL of 1.0 M solution in hexane) was added dropwise to a vigorously stirred solution of the ester **5b** (2.7 g, 6.58 mmol) in anhydrous dichloromethane (50 mL) under an argon atmasphere at –78°C (dry ice-ethyl acetate). The reaction mixture was stirred for an additional 2-3 h at –78°C, and was monitored by TLC every 30 min. The temperature cannot be allowed to above –78°C. If the temperature gets above –78°C other byproducts are formed (imine reduced aldehyde and alcohols). After completion of the reaction excess DIBAL-H was quenched by careful addition of dry methanol (5 mL), followed by 5% aq HCl (10 mL). After this the resulting mixture was allowed to warm to room temperature. If the reaction mixture forms an aluminum emulsion, a saturated solution aqueous solution of Rochelle's salt and DCM (50 mL) were added to the reaction mixture. It was then filtered through a pad of Celite and then the organic layer was separated. The aqueous layer which remained was extracted with DCM (2x30 mL). The combined organic layers were washed with brine and dried (Na_2SO_4). The solvent was removed under reduced pressure to afford the crude aldehyde. This residue was purified by flash chromatography (2:1 ethyl acetate/hexane) to afford the pure diazepine aldehyde **6b** as a white solid, (2.0 g, 78%); mp 192-194^{o}C. ^{1}H NMR (300 MHz, $CDCl_3$) δ 10.06 (s, 1H), 8.01 (s, 1H), 7.84 (d, *J* = 8.4 Hz, 1H), 7.62 (s, 1H), 7.47-7.54 (m, 4H), 7.39-7.44 (m, 2H), 5.98 (d, *J* = 12.6 Hz, 1H), 4.02 (d, *J* = 12.3 Hz, 1H). ^{13}C NMR (75 MHz, $CDCl_3$) δ 186.6, 168.2, 138.9, 138.3, 136.7, 135.2, 135.0, 134.8, 134.1, 130.9, 129.8, 129.3, 128.4, 124.2, 121.1, 44.2; HRMS (ESI-TOF *m/z*) for $C_{18}H_{12}BrN_3O$ calcd 366.0230 found 366.0236 (M+H)+.

8-Bromo-6-(2-fluorophenyl)-4H-benzo[f]imidazo[1,5-a][1,4]diazepine-3-carbaldehyde (6c)

[00156] The aldehyde **6c** was prepared according to the method described for pyridine **6b,** employing the 2'-F ethyl ester **5c (**1.5 g, 3.51 mmol) and DIBAL-H (6.25 mL of 1.2 M solution in toluene, 20% w/v), to afford the pure aldehyde **6c** as a white solid (1.0 g, 74.6%); mp 120-122^{o}C. ^{1}H NMR (300 MHz, $CDCl_3$): δ 10.07 (s, 1H), 8.01 (s, 1H), 7.80 (dd, *J* = 1.8, 6.6 Hz, 1H), 7.67 (ddd, *J* = 1.5, 6.0 Hz, 1H), 7.45-7.52 (m, 3H), 7.25-7.30 (m, 1H), 7.04 (t, *J* = 9.3 Hz, 1H), 6.02 (br s, 1H), 4.15 (br s, 1H). ^{13}C NMR (75 MHz, $CDCl_3$) δ 186.6, 165.6, 161.8, 158.5, 137.8, 136.8, 135.4, 135.2, 134.1, 133.5, 132.6, 132.4, 131.3, 129.2, 127.6, 127.5, 122.5, 122.1, 116.4, 116.1, 44.2. HRMS (ESI-TOF *m/z*) for $C_{18}H_{11}BrFN_3O$ calcd 384.0145 found 384.0142 (M+H)+.

General synthetic procedure for oxazole containing benzimidazodiazepines through Van Leusen reaction via Baldwin's rules

5-(8-Bromo-6-(pyridin-2-yl)-4H-benzo[f]imidazo[1,5-a][1,4]diazepin-3-yl)oxazole (**7a**)

[00157] The 2' pyridyldiazepine carboxaldehyde **6a** (200 mg, 0.54 mmol) was placed in a dry two neck round bottom flask and dissolved in dry MeOH (30 mL) under an argon atmosphere. At rt, toluenesulfonylmethyl isocyanide (TosMIC, 130 mg, 0.65 mmol) was added as well as K_2CO_3 (225 mg, 1.6 mmol), The reaction mixture was heated to reflux for 3 to 4 h. After completion of the reaction on analysis by TLC (silica gel, 1:10 MeOH and EtOAc) this indicated the absence of aldehyde starting material and complete conversion to an oxazole of lower R_f. The reaction mixture was then quenched with cold water. After this 33% of the solvent was removed under reduced pressure and the solution was extracted with ethyl acetate (3x40 mL). The combined organic layers were washed with water and brine successively and dried (Na_2SO_4). The solvent was then removed under reduced pressure and the residue was purified by silica gel flash chromatography using EtOAc/DCM/Hexane (2:1:1 and 1 mL MeOH + 1 mLTEA for 100 mL) to give the pure 2' pyridyldiazepine oxazole as white solid (170 mg, 77%); mp: 226-228 ^oC. ^1H NMR (500 MHz, $CDCl_3$) δ 8.62 (d, *J* = 4.5 Hz, 1H), 8.24 (s, 1H), 8.08 (d, *J* = 8.0 Hz, 1H), 7.96 (s, 1H), 7.82-7.87 (m, 2H), 7.57-7.59 (m, 2H), 7.40-7.43 (m, 1H), 5.78 (d, *J* = 12.5 Hz, 1H), 4.32 (d, *J* = 12.5 Hz, 1H), (ESI) MS: *m/z* 368 $(M+H)^+$. $)^+$. ^{13}C NMR (300 MHz, $CDCl_3$) δ 167.2, 155.9, 150.1, 148.7, 145.4, 137.2, 135.3, 135.2, 134.4, 133.3, 129.6, 128.3, 126.9, 125.1, 124.5, 124.1, 123.4, 120.8, 44.9; HRMS (ESI *m/z*) for $C_{19}H_{12}BrN_5O$ calcd 406.0299, found 406.0298 $(M+H)^+$.

5-(8-Bromo-6-phenyl-4*H*-benzo[*f*]imidazo[1,5-*a*][1,4]diazepin-3-yl)oxazole (**7b**)

[00158] The reaction was performed following the same procedure for **7a,** employing diazepine aldehyde **6b** (720 mg, 1.9 mmol), TosMIC (460 mg, 2.36 mmol) and K_2CO_3 (977 mg, 7.08 mmol). This afforded the crude oxazole which was purified by flash silica gel chromatography (4:1 ethyl acetate/hexane) to give a white solid **7b** (601 mg, 78 % yield); mp 225-227 ^oC. ^1H NMR (300 MHz, $CDCl_3$) δ 8.05 (s, 1H), 7.92 (s, 1H), 7.81 (dd, *J* = 1.8, 6.6 Hz, 1H), 7.82 (d, *J* = 8.4 Hz, 1H), 7.53-7.57 (m, 3H), 7.43-7.49 (m, 2H), 7.39-7.43 (m, 2H), 5.75 (d, *J* = 12.6 Hz, 1H), 4.24 (d, *J* = 12.6 Hz, 1H). ^{13}C NMR (300 MHz, $CDCl_3$) δ 167.9, 156.7, 149.9, 148.9, 146.6, 137.0, 136.4, 135.8, 135.4, 135.3, 129.8, 127.5, 127.0, 124.9, 124.0, 122.8, 122.6, 121.0, 45.3; HRMS (ESI *m/z*) for $C_{20}H_{13}N_4OBr$ calcd 405.0349, found 405.0345 $(M+H)^+$.

5-(8-Bromo-6-(2-fluorophenyl)-4H-benzo[f]imidazo[1,5-a][1,4]diazepin-3-yl)oxazole (**7c**)

[00159] The 2'-F oxazole **7c** was prepared according to the method described for **7a** employing 2'-F diazepine aldehyde **6c** (649 mg, 1.53 mmol), TosMIC (330 mg, 1.68 mmol) and K_2CO_3 (640 mg, 4.60 mmol). This afforded the crude oxazole which was purified by flash silica gel chromatography (3:1 ethyl acetate/hexane) to give 2'-F oxazole **7c** as a white solid (550 mg, 76.7 % yield); mp:190-192 ºC.^{1}H NMR (300 MHz, $CDCl_3$) δ 8.01 (s, 1H), 7.92 (s, 1H), 7.77 (dd, *J* = 2.1, 6.6 Hz, 1H), 7.77 (ddd, *J* = 1.5, 6.0 Hz, 1H), 7.52 (s, 1H), 7.46-7.52 (m, 3H), 7.23-7.28 (m, 1H), 7.04 (t, *J* = 8.4 Hz, 1H), 5.75 (br s, 1H), 4.26 (br s, 1H). ^{13}C NMR (300 MHz, $CDCl_3$) δ 165.0, 161.8, 158.5, 149.8, 146.5, 135.1, 134.9, 133.6, 133.3, 132.5, 131.1, 130.4, 129.7, 127.6, 124.6, 124.0, 122.6, 120.9, 116.4, 116.1, 45.3; HRMS (ESI-TOF *m/z*) for $C_{20}H_{12}N_4OFBr$ calcd 423.0263, found 423.0251 $(M+H)^+$.

5-(8-Bromo-6-(pyridin-2-yl)-4H-benzo[f]imidazo[1,5-a][1,4]diazepin-3-yl)-4-methyloxazole (7d)

[00160] The 2'-N methyl oxazole **7d** was prepared according to the method described for **7a,** employing 2'-N aldehyde **6a** (300 mg, .815 mmol), 1-((1-isocyanoethyl)sulfonyl)-4-methylbenzene (α-methyl TosMIC, 196 mg, 0.978 mmol) and K_2CO_3 (340 mg, 2.44 mmol). This afforded the crude oxazole which was purified by flash silica gel chromatography EtOAc/DCM (1:1 and 1 mL MeOH + 1 mLTEA for 100 mL) to give 2'-N methyl oxazole **7d** as a half white solid (250 mg, 73 % yield); mp 228-230 ºC. ^{1}H NMR (500 MHz, $CDCl_3$) δ 8.60 (d, *J* = 3.6 Hz, 1H), 8.07 (d, *J* = 7.5 Hz, 1H), 7.96 (s, 1H), 7.77-7.86 (m, 3H), 7.57 (s, 1H), 7.47 (d, *J* = 8.7 Hz, 1H), 7.38 (t, *J* = 5.4 Hz, 1H),), 5.71 (d, *J* = 11.7 Hz, 1H), 4.28 (d, *J* = 12.3 Hz, 1H), 2.52 (s, 3H); ^{13}C NMR (300 MHz, $CDCl_3$) δ 167.0, 156.4, 148.7, 140.6, 136.9, 135.2, 134.9, 134.8, 132.7, 129.8, 128.4, 128.1, 124.8, 124.1, 123.8, 120.1, 45.2, 12.37; HRMS (ESI-TOF *m/z*) for $C_{20}H_{14}N_5OBr$ calcd 420.0450, found 420.0456 $(M+H)^+$.

5-(8-Bromo-6-phenyl-4H-benzo[f]imidazo[1,5-a][1,4]diazepin-3-yl)-4-methyloxazole (7e)

[00161] The methyl 2'-H methyl oxazole compound **7e** was prepared according to the method described for **7a**, employing the 2'-H aldehyde **6b** (500 mg, 1.366 mmol), 1-((1-isocyanoethyl)sulfonyl)-4-methylbenzene (α-methyl TosMIC, 342 mg, 1.6 mmol) and K_2CO_3 (565 mg, 4.0mmol). This afforded the crude solid which was purified by flash chromatography (4:1 ethyl acetate/hexane) to give a half white 2'-H methyl oxazole as a solid **7e** (450 mg, 78 % yield); mp 236-238 ºC. ^{1}H NMR (300 MHz, $CDCl_3$) δ 7.99 (s, 1H), 7.85 (s, 1H), 7.80 (dd, *J* =

3.0, 8.4 Hz, 1H), 7.58 (d, *J* = 2.1 Hz, 1H), 7.47-7.53 (m, 3H), 7.37-7.42 (m, 3H), 5.67 (d, *J* = 13.2 Hz, 1H), 4.20 (d, *J* = 12.6 Hz, 1H), 2.52 (s, 3H). ^{13}C NMR (75 MHz, $CDCl_3$) δ 168.0, 148.6, 140.6, 139.3, 135.0, 134.9, 134.8, 134.4, 132.7, 130.6, 130.3, 129.6, 129.3, 128.4, 128.2, 124.1, 120.2, 45.1, 12.3; HRMS (ESI-TOF *m/z*) for $C_{21}H_{15}N_4OBr$ calcd 419.0500, found 419.0502 $(M+H)^+$.

5-(8-Bromo-6-(2-fluorophenyl)-4H-benzo[f]imidazo[1,5-a][1,4]diazepin-3-yl)-4-methyloxazole (7f)

[00162] The 2'-F methyl oxazole **7f** was prepared according to the method described for **7a**, employing the 2'-F aldehyde **6c** (300 mg, 0.782 mmol), 1-((1-isocyanoethyl)sulfonyl)-4-methylbenzene (α-methyl TosMIC, 196 mg, 0.938 mmol) and K_2CO_3 325 mg, 2.34 mmol). This afforded the crude solid which was purified by flash chromatography (4:1 ethyl acetate/hexane) to give a half white 2'-F methyl oxazole as a solid **7f** (260 mg, 76 % yield); mp 138-140 ^oC. ^{1}H NMR (500 MHz, $CDCl_3$) δ 8.04 (s, 1H), 7.84 (s, 1H), 7.78 (d, *J* = 8.0 Hz, 1H), 7.77 (t, *J* = 7.0 Hz, 1H), 7.46-7.52 (m, 3H), 7.23-7.28 (m, 1H), 7.05 (t, *J* = 8.5 Hz, 1H), 5.72 (br s, 1H), 4.24 (br s, 1H), 2.53 (s, 3H); ^{13}C NMR (75 MHz, $CDCl_3$) δ 164.8, 161.8, 158.5, 148.75, 140.65, 135.1, 134.7, 133.7, 133.2, 132.8, 132.4, 132.3, 131.2, 131.1, 130.4, 129.9, 128.2, 127.6, 127.5, 124.5, 124.1, 120.7, 116.4, 116.1, 45.3, 12.3. HRMS (ESI-TOF *m/z*) for $C_{21}H_{14}N_4OFBr$ calcd 437.0403 found 437.0408 $(M+H)^+$.

General synthetic procedures for Sonogashira coupling

5-(6-(Pyridin-2-yl)-8-((trimethylsilyl)ethynyl)-4H-benzo[f]imidazo[1,5-a][1,4]diazepin-3-yl)oxazole (**8a**)

[00163] The 2'-N bromide **7a** (200 mg, 0.50 mmol) and bis(triphenylphosphine)-palladium (II) acetate (18 mg, 0.024 mmol) were added to an oven dried two neck round bottom flask, after which the round bottom flask was fitted with a rubber septum. It was then evacuated under vaccum and back filled with argon three times. After this, a mixed dry solvent system of CH_3CN:TEA (1:2 ratio) and trimethylsilylacetylene (0.3 mL, 2.07 mmol) were added to the round bottom flask with a syringe under a positive pressure of argon. The round bottom flask was fitted with a reflex condenser and the reaction mixture was degased under vaccum and argon, the process was repeated two to three times, after which the reaction mixture was slowly heated to 90°C. After stirring for 10 h, the reaction mixture was filtered through a bed of Celite. The organic layer was washed with brine and dried (Na_2SO_4). The solvent was then removed under

reduced pressure to furnish a crude solid. This material was purified by flash chromatography using EtOAc/DCM/Hexane (2:1:1 and 1 mL MeOH + 1 mLTEA for 100 mL) to afford the pure 2'-N trimethylsilylacetylene intermediate as a light brown solid (170 mg, 80.6% yield); mp 208-210 ^{o}C. ^{1}H NMR (300 MHz, $CDCl_3$) δ 8.63 (d, *J* = 4.1 Hz, 1H), 8.26 (s, 1H), 8.06 (d, *J* = 8.0 Hz, 1H), 7.97 (s, 1H), 7.82-7.88 (m, 2H), 7.57-7.59 (m, 2H), 7.40-7.43 (m, 1H), 5.78 (d, *J* = 12.3 Hz, 1H), 4.32 (d, *J* = 12.3 Hz, 1H), 0.22 (s, 9H); ^{13}C NMR (75 MHz, $CDCl_3$) δ 167.6, 149.8, 146.5, 139.5, 135.3, 134.8, 132.1, 131.9, 131.6, 130.5, 130.2, 129.3, 128.6, 128.3, 127.8, 127.1, 122.5, 122.4, 122.2, 102.5, 97.4, 44.9, -.0.22; HRMS (ESI-TOF *m/z*) for $C_{24}H_{21}N_5OSi$ calcd 424.1816, found 424.1810 $(M+H)^+$.

5-(6-Phenyl-8-((trimethylsilyl)ethynyl)-4H-benzo[f]imidazo[1,5-a][1,4]diazepin-3-yl)oxazole (**8b**)

[00164] The 2'-H trimethylsilylacetylenediazepine oxazole **8b** was prepared according to the method described for **8a**, employing the 2'-H bromodiazepine oxazole **7b** (700 mg, 1.72 mmol), bis(triphenylphosphine)palladium(II)acetate (64 mg, 0.0864 mmol) and trimethylsilylacetylene (0.3 mL, 2.07 mmol). The residue which resulted was purified by silica gel flash column chromatography (4:1 ethyl acetate/hexane) to give a white solid **8b** (650 mg, 89.6% yield); mp 126-128 ^{o}C. ^{1}H NMR (300 MHz, $CDCl_3$) δ 8.00 (s, 1H), 7.93 (s, 1H), 7.81 (dd, *J* = 1.5, 8.4 Hz, 1H), 7.65-7.72 (m, 1H), 7.51-7.57 (m, 4H), 7.38-7.47 (m, 4H), 5.70 (d, *J* = 12.6 Hz, 1H), 4.19 (d, *J* = 12.6 Hz, 1H), 0.25 (s, 9H); ^{13}C NMR (300 MHz, $CDCl_3$) δ 168.8, 149.8, 146.5, 139.5, 135.3, 134.8, 132.1, 131.9, 131.6, 130.5, 130.2, 129.3, 128.6, 128.3, 127.8, 127.1, 122.5, 122.4, 122.2, 102.5, 97.4, 44.9, -0.23; HRMS (ESI-TOF *m/z*) for $C_{25}H_{22}N_4OSi$ calcd 423.1630, found 423.1636 $(M+H)^+$.

5-(6-(2-Fluorophenyl)-8-((trimethylsilyl)ethynyl)-4H-benzo[f]imidazo[1,5-a][1,4] diazepin-3-yl)oxazole (**8c**)

[00165] The 2'-F trimethylsilylacetylenediazepine oxazole **8c** was prepared according to the method described for **8a**, employing the 2'-F bromodiazepine oxazole **7c** (100 mg, 0.23 mmol) bis(triphenylphosphine)palladium(II)acetate (10 mg, 0.011 mmol) and trimethylsilylacetylene (0.04 mL, 0.26 mmol). After work up the residue which resulted was purified by silica gel flash column chromatography (4:1 ethyl acetate/hexane) to give a light brown solid **8c** (90 mg, 92.6% yield). ^{1}H NMR (300 MHz, $CDCl_3$) δ 8.02 (s, 1H), 7.92 (s, 1H), 7.60-7.74 (m, 3H), 7.40-7.57 (m, 3H), 7.23-7.28 (m, 1H), 7.04 (t, *J* = 9.0 Hz, 1H), 5.73 (br s, 1H), 4.24 (br s, 1H), 0.24 (s, 9H). ^{13}C

NMR (75 MHz, $CDCl_3$) δ 165.6, 161.9, 158.4, 148.7, 140.7, 135.4, 134.7, 134.3, 133.7, 132.7, 132.1, 131.1, 131.3, 129.9, 128.8, 128.3, 128.1, 124.4, 122.4, 116.5, 116.2, 102.5, 97.2, 45.1, -0.23; HRMS (ESI-TOF *m/z*) for $C_{25}H_{21}N_4OFSi$ calcd 441.1543, found 441.1541 $(M+H)^+$.

4-Methyl-5-(6-phenyl-8-((trimethylsilyl)ethynyl)-4H-benzo[f]imidazo[1,5-a][1,4] diazepin-3-yl)oxazole (8e)

[00166] The 2'-H trimethylsilylacetylenediazepine methyl oxazole **8e** was prepared according to the method described for **8a**, employing the bromo 2'-H trimethylsilylacetylenediazepine methyl oxazole **7e** (250 mg, 1.72 mmol), bis(triphenylphosphine)palladium(II)acetate (17 mg, 0.0238 mmol) and trimethylsilyl acetylene (0.074 mL, 0.52 mmol). The residue which resulted was purified by silica gel flash column chromatography (4:1 ethyl acetate/hexane) to give a light brown solid **8b** (188 mg, 90 % yield); mp130-132°C. ^1H NMR (300 MHz, $CDCl_3$) δ 8.00 (s, 1H), 7.93 (s, 1H), 7.81 (dd, *J* = 1.5, 8.4 Hz, 1H), 7.65-7.72 (m, 1H), 7.51-7.57 (m, 4H), 7.38-7.47 (m, 4H), 5.70 (d, *J* = 12.6 Hz, 1H), 4.19 (d, *J* = 12.6 Hz, 1H), 0.25 (s, 9H); ^{13}C NMR (300 MHz, $CDCl_3$) δ 168.8, 149.8, 146.5, 139.5, 135.3, 134.8, 132.1, 131.9, 131.6, 130.5, 130.2, 129.3, 128.6, 128.3, 127.8, 127.1, 122.5, 122.4, 122.2, 102.5, 97.4, 44.9, -0.23; HRMS (ESI-TOF *m/z*) for $C_{26}H_{24}N_4OSi$ calcd 437.1638, found 437.1636 $(M+H)^+$.

5-(6-(2-Fluorophenyl)-8-((trimethylsilyl)ethynyl)-4H-benzo[f]imidazo[1,5-a][1,4] diazepin-3-yl)-4-methyloxazole (8f)

[00167] The 2'-F trimethylsilylacetylenediazepine methyl oxazole **8f** was prepared according to the method described for **8a**, employing the bromo 2'-F trimethylsilylacetylenediazepine methyl oxazole **7f** (900 mg, 2.059 mmol), bis(triphenylphosphine)palladium(II)acetate (77 mg, 0.103 mmol) and trimethyl silylacetylene (0.321 mL, 2.65 mmol). The residue which resulted was purified by silica gel flash column chromatography (4:1 ethyl acetate/hexane) to give a brown solid **8f** (800 mg, 87 % yield); mp 209-211 ^oC. ^1H NMR (300 MHz, $CDCl_3$) δ 8.03 (s, 1H), 7.83 (s, 1H), 7.71 (dd, *J* = 1.8, 8.1 Hz, 1H), 7.63 (td, *J* = 1.8, 7.5 Hz, 1H), 7.40-7.53 (m, 3H), 7.23-7.28 (m, 1H), 7.04 (t, *J* = 10.2 Hz, 1H), 5.69 (br s, 1H), 4.21 (br s, 1H), 2.53 (s, 3H), 0.25 (s, 9H); ^{13}C NMR (75 MHz, $CDCl_3$) δ 165.4, 161.9, 158.5, 148.6, 140.7, 135.3, 134.6, 134.2, 133.7, 132.7, 132.1, 131.0, 131.2, 129.9, 128.8, 128.2, 128.0, 124.4, 122.4, 116.4, 116.1, 102.6, 97.1, 45.1, 12.3, -0.23; HRMS (ESI-TOF *m/z*) for $C_{26}H_{23}N_4OFSi$ calcd 455.1690, found 455.1698 $(M+H)^+$.

5-(8-Ethynyl-6-(pyridin-2-yl)-4*H*-benzo[*f*]imidazo[1,5-a][1,4]diazepin-3-yl)oxazole (**9a**)

[00168] A solution of 2'-N trimethylsilylacetylene oxazole intermediate **8a** (150 mg, 0.35 mmol) was dissolved in dry THF and kept at 0°C after which tetrabutylammonium iodide (0.12 mL, 0.39 mmol) was added slowly to the reaction mixture at 0°C. After 10 min the reaction mixture was stirred at room temperature for 2 h under an argon atmosphere. After TLC on silica gel indicated the absence of starting material, this reaction mixture was quenched by slow addition of ice cold water and the combined layers were extracted with ethyl acetate (3×30 mL). The combined organic layers were washed with water and brine. This solution was dried over Na_2SO_4 and the solvent was removed under reduced pressure to furnish a solid. This material was then purified by flash chromatography using EtOAc/DCM/Hexane (2:1:1 and 1 mL MeOH + 1 mLTEA for 100 mL) to afford the pure 2'-N acetyleno oxazole **9a** as a white solid (101 mg, 82% yield); mp 220-222 °C. ^{1}H NMR (300 MHz, $CDCl_3$) δ 8.62 (d, *J* = 4.2 Hz, 1H), 8.12 (s, 1H), 8.06 (d, *J* = 7.8 Hz, 1H), 7.96 (s, 1H), 7.85 (ddd, *J* = 1.8, 6.0 Hz, 1H), 7.79 (dd, *J* = 1.8, 6.6 Hz, 1H), 7.62 (d, *J* = 8.4 Hz, 1H), 7.55 (d, *J* = 1.5 Hz, 1H), 7.53 (s, 1H), 7.41 (ddd, *J* = 1.5, 4.8 Hz, 1H), 5.78 (d, *J* = 12.9 Hz, 1H), 4.31 (d, *J* = 12.9 Hz, 1H). ^{13}C NMR (75 MHz, $CDCl_3$) δ 167.9, 156.7, 149.9, 149.0, 146.6, 137.0, 136.4, 135.8, 135.5, 135.3, 129.8, 127.5, 127.0, 124.9, 124.0, 122.8, 122.7, 121.0, 81.8.7, 79.5, 45.3; HRMS (ESI-TOF *m/z*) for $C_{21}H_{13}N_5O$ calcd 352.1188, found 352.1193 $(M+H)^+$.

5-(8-Ethynyl-6-phenyl-4H-benzo[f]imidazo[1,5-a][1,4]diazepin-3-yl)oxazole (**9b**)

[00169] The 2'-H acetyleno oxazole **9b** was prepared according to the method described for **7a**, employing the 2'-H trimethylsilylacetylenodiazepine oxazole **8b** (500 mg, 1.18) and TBAF (0.5 mL, 1.76 mmol). After workup, the residue was purified by silica gel flash column chromatography (4:1 ethyl acetate/hexane) to afford 2'-H acetyleno oxazole **9b** as a white solid (370 mg, 90% yield); mp 120-122°C. ^{1}H NMR (300 MHz, $CDCl_3$) δ 8.08 (s, 1H), 7.93 (s, 1H), 7.81 (dd, *J* = 1.8, 6.6 Hz, 1H), 7.81 (d, *J* = 8.4 Hz, 1H), 7.53-7.57 (m, 3H), 7.43-7.49 (m, 2H), 7.39-7.43 (m, 2H), 5.75 (d, *J* = 12.9 Hz, 1H), 4.24 (d, *J* = 12.9 Hz, 1H), 3.18 (s, 1H).^{13}C NMR (300 MHz, $CDCl_3$) δ 167.9, 156.7, 149.9, 148.9, 146.6, 137.0, 136.4, 135.8, 135.4, 135.3, 129.8, 127.5, 127.0, 124.9, 124.0, 122.8, 122.6, 121.0, 81.8, 79.5, 45.2; HRMS (ESI-TOF *m/z*) for $C_{22}H_{14}N_4O$ calcd 351.1246, found 351.1240 $(M+H)^+$.

5-(8-Ethynyl-6-(2-fluorophenyl)-4H-benzo[f]imidazo[1,5-a][1,4]diazepin-3-yl)oxazole (**9c**)

[00170] The 2'-F acetyleno oxazole **9c** was prepared according to the method described for **9a**, employing the 2'-F TMS-acetyleno-2'-fluorodiazepine oxazole **8c** (90 mg, 0.20 mmol), and TBAF (0.05 mL, 024 mmol). After workup the residue was purified by silica gel flash column chromatography (4:1 ethyl acetate/hexane) to give the 2'-F acetyleno oxazole **9c** as a white solid (80 mg, 88% yield); mp 212-214°C. ^{1}H NMR (300 MHz, $CDCl_3$) δ 8.03 (s, 1H), 7.93 (s, 1H), 7.75 (d, *J* = 7.8 Hz, 1H), 7.57-7.63 (m, 2H), 7.44-7.53 (m, 3H), 7.23-7.28 (m, 1H), 7.04 (t, *J* = 9.0 Hz, 1H), 5.74 (br s, 1H), 4.26 (br s, 1H), 3.16 (s, 1H). ^{13}C NMR (300 MHz, $CDCl_3$) δ 165.5, 161.9, 158.5, 149.8, 146.5, 135.4, 135.0, 134.3, 132.3, 131.1, 129.8, 128.9, 127.8, 127.5, 124.5, 122.6, 121.6, 116.4, 116.1, 81.4, 79.6, 45.0; HRMS (ESI-TOF *m/z*) for $C_{22}H_{13}N_4OF$ calcd 369.1144, found 369.1146 $(M+H)^+$.

5-(8-Ethynyl-6-phenyl-4H-benzo[f]imidazo[1,5-a][1,4]diazepin-3-yl)-4-methyloxazole (9e)

[00171] The 2'-H acetyleno methyl oxazole **9e** was prepared according to the method described for **9a**, employing the TMS-acetyleno-2'-H methyl oxazole **8c** (250 mg, 0.573 mmol), and TBAF (0.19 mL, 0.68 mmol). After workup the residue was purified by silica gel flash column chromatography (4:1 ethyl acetate/hexane) to give the 2'-H acetyleno methyl oxazole **9e** as a white solid (190 mg, 91% yield); mp 228-230°C. ^{1}H NMR (300 MHz, $CDCl_3$) δ 8.01 (s, 1H), 7.85 (s, 1H), 7.77 (dd, *J* = 1.8, 8.4 Hz, 1H), 7.56-7.60 (m, 2H), 7.49-7.53 (m, 2H), 7.37-7.46 (m, 3H), 5.67 (d, *J* = 12.9 Hz, 1H), 4.20 (d, *J* = 12.9 Hz, 1H), 3.17 (s, 1H), 2053 (s, 3H); ^{13}C NMR (300 MHz, $CDCl_3$) δ 168.5, 148.7, 140.6, 139.5, 135.9, 135.8, 135.3, 134.5, 132.8, 130.5, 130.3, 129.3, 128.3, 128.2, 128.0, 122.6, 121.0, 81.5, 79.6, 45.3, 12.3; HRMS (ESI-TOF *m/z*) for $C_{23}H_{16}N_4O$ calcd 365.1400 found 365.1397 $(M+H)^+$.

5-(8-Ethynyl-6-(2-fluorophenyl)-4H-benzo[f]imidazo[1,5-a][1,4]diazepin-3-yl)-4-methyloxazole (9f)

[00172] The 2'-F acetyleno methyl oxazole **9e** was prepared according to the method described for **9a**, employing the TMS-acetyleno-2'-H methyl oxazole **8c** (500 mg, 1.147 mmol), and TBAF (0.390 mL, 1.37 mmol). After workup the residue was purified by silica gel flash column chromatography (4:1 ethyl acetate/hexane) to give the 2'-F acetyleno methyl oxazole **9f** as a white solid (395 mg, 90 % yield); mp 145-147°C. ^{1}H NMR (300 MHz, $CDCl_3$) δ 8.03 (s, 1H), 7.84 (s, 1H), 7.74 (d, *J* = 7.8 Hz, 1H), 7.55-7.65 (m, 2H), 7.46 (s, 2H), 7.22-7.28 (m, 1H), 7.03 (t, *J* = 8.1 Hz, 1H), 5.70 (br s, 1H), 4.25 (br s, 1H), 3.16 (s, 1H), 2.53 (s, 3H). ^{13}C NMR (75

MHz, $CDCl_3$) δ 165.4, 161.9, 158.5, 148.7, 140.6, 135.4, 134.6, 134.2, 132.8, 132.2, 132.1, 131.2, 131.1, 129.9, 128.9, 128.3, 127.9, 127.8, 124.5, 124.4, 122.5, 121.4, 116.4, 116.1, 81.5, 79.9, 45.1, 12.3; HRMS (ESI-TOF *m/z*) for $C_{23}H_{15}N_4OF$ calcd 383.1300 found 383.1303 $(M+H)^+$.

General synthetic procedures for Sonogashira coupling and desilylation

Ethyl-8-ethynyl-6-(pyridin-2-yl)-4H-benzo[f]imidazo[1,5-a][1,4]diazepine-3-carboxylate (**10a**)

[00173] The 2'-N bromide ethyl ester **5a** (17.0 g, 41.2 mmol) and bis(triphenylphosphine)-palladium (II) acetate (1.50 g, 2.06 mmol) were added to an oven dried two neck round bottom flask, after which the round bottom flask was fitted with a rubber septum. It was then evacuated under vaccum and back filled with argon three times. After this, a mixed dry solvent system of CH_3CN:TEA (1:2 ratio) and trimethylsilylacetylene (6.4 mL, 45.40 mmol) were added to the round bottom flask with a syringe under a positive pressure of argon. The round bottom flask was fitted with a reflex condenser and the reaction mixture was degased under vaccum and argon, the process was repeated two to three times, after which the reaction mixture was slowly heated to 90°C. After stirring for 10 h, the reaction mixture was filtered through a bed of Celite. The organic layer was washed with brine and dried (Na_2SO_4). The solvent was then removed under reduced pressure to furnish a crude solid. This material was purified by flash chromatography using EtOAc/DCM/Hexane (2:1:1 and 1 mLTEA for 100 mL) to afford the pure 2'-N trimethylsilyl acetyleno intermediate (14.12 g, 80 % yield) as a light brown solid. And this intermediate (14.12 mg, 3.30 mmol) was dissolved in dry THF and kept at 0°C after which tetrabutylammonium iodide (10.30 mL, 3.62 mmol) was added slowly to the reaction mixture at 0°C. After 10 min the reaction mixture was stirred at room temperature for 2 h under an argon atmosphere. After TLC on silica gel indicated the absence of starting material, this reaction mixture was quenched by slow addition of ice cold water and the combined layers were extracted with ethyl acetate (2×150 mL). The combined organic layers were washed with water and brine. This solution was dried over Na_2SO_4 and the solvent was removed under reduced pressure to furnish a solid. This material was then purified by flash chromatography using EtOAc/DCM/Hexane (2:1:1 and 1 mLTEA for 100 mL) to afford the pure 2'-N acetyleno ethyl ester **10a** as a white solid (9.63 g, 82 % yield); mp 248-250°C. ^1H NMR (300 MHz, $CDCl_3$) δ 8.58 (d, *J* = 4.8 Hz, 1H), 8.07 (d, *J* = 7.8 Hz, 1H), 7.92 (s, 1H), 7.82 (td, *J* = 1.8, 7.8 Hz, 1H),

7.57-7.59 (dd, *J* = 1.5, 8.4 Hz, 1H), 7.54-7.57 (m, 2H), 7.37 (td, *J* = 0.9, 4.8 Hz, 1H), 6.14 (d, *J* = 9.9 Hz, 1H), 4.42 (q, *J* = 3.9, 7.2 Hz, 2H), 4.16 (d, *J* = 10.2 Hz, 1H), 3.17 (s, 1H), 1.44 (t, *J* = 7.2 Hz, 1H); ^{13}C NMR (75 MHz, $CDCl_3$) δ 167.5, 162.9, 156.2, 148.6, 138.3, 137.1, 136.1, 135.4, 135.3, 134.5, 129.2, 127.0, 124.9, 124.1, 122.9, 121.3, 81.6, 79.5, 60.8, 45.0, 14.4; HRMS (ESI-TOF *m/z*) for $C_{21}H_{16}N_4O$ calcd 357.1340, found 357.1346 $(M+H)^+$.

Ethyl 8-ethynyl-6-phenyl-4H-benzo[f]imidazo[1,5-a][1,4]diazepine-3-carboxylate (**10b**)

[00174] The 2'-H acetyleno ethyl ester **10b** was prepared according to the method described for **10a**, employing the 2'-H bromodiazepine ethyl ester **5b** (10.0 g, 24.40 mmol), bis(triphenylphosphine)palladium(II)acetate (913 mg, 1.22 mmol) and trimethylsilylacetylene (3.82 mL, 26.84 mmol). The residue was purified by flash chromatography (3:1 ethyl acetate/hexane) to afford the 2'-H trimethylsilyl acetyleno intermediate (9.48 mg, 91.0% yield). And this intermediate (9.48 mg, 22.20 mmol). was treated with tetrabutylammonium iodide (7.0 mL, 24.42 mmol), this resulting material was purified by flash column chromatography using EtOAc/Hexane (4:1) to afford the pure 2'-H acetyleno ethyl ester **10b** as a white solid (7.33 mg, 93.0% yield); mp 237-239 ºC. ^{1}H NMR (300 MHz, $CDCl_3$) δ 8.00 (s, 1H), 7.81 (dd, *J* = 1.8, 8.3 Hz, 1H), 7.65-7.72 (m, 2H), 7.51-7.57 (m, 3H), 7.38-7.47 (m, 2H), 6.11 (d, *J* = 12.6 Hz, 1H), 4.41-4.48 (m, 2H), 4.19 (d, *J* = 12.6 Hz, 1H), 3.20 (s, 1H), 1.44 (t, *J* = 7.3 Hz, 3H); ^{13}C NMR (75 MHz, $CDCl_3$) δ 168.3, 138.8, 138.4, 136.7, 135.3, 135.0, 134.8, 134.1, 130.9, 129.8, 129.2, 128.3, 124.2, 121.1, 81.3, 80.0, 60.6, 44.2, 14.7; HRMS (ESI-TOF *m/z*) for $C_{22}H_{17}N_3O_2$ calcd 356.1390 found 356.1394 (M+H)+.

Ethyl-8-ethynyl-6-(2-fluorophenyl)-4H-benzo[f]imidazo[1,5-a][1,4]diazepine-3-carboxylate (**10c**)

[00175] The 2'-F acetyleno ethyl ester **10c** was prepared according to the method described for **10a**, employing the 2'-F bromodiazepine ethyl ester **5c** (7 g, 16.35 mmol), bis(triphenylphosphine)palladium(II)acetate (612 mg, 0.817 mmol) and trimethylsilylacetylene (2.56 mL, 18.0 mmol). The residue was purified by flash chromatography (3:1 ethyl acetate/hexane) to afford the 2'-F trimethylsilyl acetyleno intermediate (6.47 g, 89.0% yield). And this intermediate (6.47 g, 14.55 mmol) was treated with tetrabutylammonium iodide (4.54 mL, 16.0 mmol), this resulting material was purified by flash column chromatography using EtOAc/Hexane (4:1) to afford the pure 2'-F acetyleno ethyl ester **10c** as a white solid (4.89 g, 90.0% yield); mp 232-234 ºC. ^{1}H NMR (300 MHz, $CDCl_3$) δ 7.97 (s, 1H), 7.64 (dd, *J* = 1.5, 8.1

Hz, 1H), 7.65 (td, *J* = 1.8, 7.5 Hz, 1H), 7.57 (d, *J* = 8.4 Hz, 1H), 7.42-7.48 (m, 2H), 7.23-7.28 (m, 1H), 7.02 (t, *J* = 9.9 Hz, 1H), 6.11 (br s, 1H), 4.43 (q, *J* = 3.6, 6.9 Hz, 2H), 4.14 (br s, 1H), 3.16 (s, 1H), 1.43 (t, *J* = 6.9 Hz, 3H); ^{13}C NMR (300 MHz, $CDCl_3$) δ 165.5, 162.8, 161.8, 158.5, 138.3, 135.5, 135.3, 134.5, 134.3, 134.1, 134.0, 132.3, 132.2, 131.2, 129.4, 129.0, 127.7, 127.5, 124.4, 122.7, 121.9, 116.3, 116.0, 81.3, 79.8, 60.7, 44.8, 14.8; HRMS (ESI-TOF *m/z*) for $C_{22}H_{16}N_3O_2F$ calcd 374.1290, found 374.1299 $(M+H)^+$.

8-Ethynyl-6-(pyridin-2-yl)-4H-benzo[f]imidazo[1,5-a][1,4]diazepine-3-carbaldehyde (11a), Method 1

[00176] The reaction was performed following the same procedure for **6a,** employing the 2'-pyridyl ethyl ester (HZ-166) **10a** (3.0 g, 8.42 mmol) and $LiAlH_4$ (360 mg, 9.27 mmol). This afforded the crude mixture of alcohols (1:0.4 ratio); this mixture of alcohols was used directly in the next step. The mixture of 2'-pyridylalcohols (2.5 g, 8.00 mmol) was dissolved in dry DCM (200 mL) under an argon atmosphere, after which Na_2CO_3 (2.8 g, 24 mmol) and activated MnO_2 (10.5 g, 120 mmol) were added to the reaction mixture at 0°C. The mixture was stirred at room temperature overnight. After 12-14 h, the reaction mixture was diluted with DCM (50 mL) and was filtered through a pad of Celite. The desired aldehyde **11a** was purified by flash silica gel chromatography (2:1:1 ethyl acetate/DCM/hexane and 1 mL MeOH + 1 mLTEA for 100 mL) to give a white solid **11a** (1.02 g, 40 % yield for 2 steps); mp 238-240°C. ^{1}H NMR (500 MHz, $CDCl_3$) δ 10.05 (s, 1H), 8.56 (d, *J* = 5.0 Hz, 1H), 8.08 (d, *J* = 7.5 Hz, 1H), 7.97 (s, 1H), 7.78 (ddd, *J* = 1.5, 6.0 Hz, 1H), 7.77 (dd, *J* = 1.5, 7.0 Hz, 1H), 7.55-7.57 (m, 2H), 7.38 (ddd, *J* = 1.5, 5.0 Hz, 1H), 6.00 (br s, 1H), 4.17 (br s, 1H), 3.16 (s, 1H): ^{13}C NMR (75 MHz, $CDCl_3$) δ 186.9, 167.7, 156.2, 148.6, 137.7, 137.1, 136.7, 136.3, 135.4, 135.3, 135.0, 127.1, 124.9, 124.0, 122.8, 121.5, 81.5, 79.7, 44.4 HRMS (ESI-TOF *m/z*) for $C_{19}H_{12}N_4O$ calcd 113.1080 found 313.1084 (M+H)+.

8-Ethynyl-6-phenyl-4H-benzo[f]imidazo[1,5-a][1,4]diazepine-3-carbaldehyde (11b) Method 2

[00177] The aldehyde **11b** was prepared according to the method described for pyridine **6b,** employing the 2'H 8-ethynyl ethyl ester **10b (**4.5 g, 12.6 mmol) and DIBAL-H (22.5 mL of 1.2 M solution in toluene, 20% w/v), to afford the pure compound **11b** as a white solid (3.15 g, 80.0%); mp 117-119 °C. ^{1}H NMR (300 MHz, $CDCl_3$) δ 10.07 (s, 1H), 8.01 (s, 1H), 7.80 (dd, *J* = 1.8, 8.1 Hz, 1H), 7.58-7.62 (m, 2H), 7.46-7.53 (m, 3H), 7.36-7.43 (m, 2H), 5.98 (d, *J* = 12 Hz,

H), 4.13 (d, *J* = 12 Hz, 1H). 3.20 (s, 1H).^{13}C NMR (75 MHz, $CDCl_3$) δ 186.7, 168.3, 138.8, 138.4, 136.7, 135.3, 135.0, 134.8, 134.1, 130.9, 129.8, 129.2, 128.3, 124.2, 121.1, 81.3, 80.0, 44.2; HRMS (ESI-TOF *m/z*) for $C_{20}H_{13}N_3O$ calcd 312.0231 found 312.0236 (M+H)+.

8-Ethynyl-6-(2-fluorophenyl)-4H-benzo[f]imidazo[1,5-a][1,4]diazepine-3-carbaldehyde (11c)

[00178] The aldehyde **11c** was prepared according to the method described for pyridine **6b,** employing the 2'F 8-ethynyl ethyl ester **10c (**770 mg, 2.06 mmol) and DIBAL-H (4 mL of 1.2 M solution in toluene, 20% w/v), to afford the pure aldehyde **11c** as a white solid (530 mg, 78.0%); mp 190-192 ^{o}C. ^{1}H NMR (300 MHz, $CDCl_3$) δ 10.08 (s, 1H), 8.04 (s, 1H), 7.77 (d, *J* = 8.4 Hz, 1H), 7.67 (t, *J* = 7.5 Hz, 1H), 7.60 (d, *J* = 8.4 Hz, 1H), 7.44-7.50 (m, 2H), 7.25-7.30 (m, 1H), 7.04 (t, *J* = 9.0 Hz, 1H), 6.00 (br s, 1H), 4.13 (br s, 1H), 3.18 (s, 1H). ^{13}C NMR (75 MHz, $CDCl_3$) δ 186.7, 165.7, 161.8, 158.5, 137.8, 136.8, 135.4, 135.2, 134.1, 133.7, 132.5, 132.4, 131.2, 129.2, 127.5, 127.4, 122.6, 122.2, 116.4, 116.1, 81.3, 80.0, 44.2; HRMS (ESI-TOF *m/z*) for $C_{20}H_{12}FN_3O$ calcd 330.1030 found 330.1037 (M+H)+.

General synthetic procedure for oxazole containing benzimidazodiazepines through Van Leusen reaction via Baldwin's rules.

5-(8-Ethynyl-6-(pyridin-2-yl)-4*H*-benzo[*f*]imidazo[1,5-a][1,4]diazepin-3-yl)oxazole (9a)

[00179] The 2'-N aldehyde **11a** (1.1 g, 3.52 mmol) was placed in a dry two neck round bottom flask and dissolved in dry MeOH (100 mL) under an argon atmosphere. At rt, TosMIC (825 mg, 4.23 mmol) was added as well as K_2CO_3 (1.30 g, 9.75 mmol) to the reaction mixture and it was allowed to heat reflux for 2 to 3 h. After completion of the reaction on analysis by TLC (silica gel, 1:10 MeOH and EtOAc) which indicated the absence of aldehyde starting material and complete conversion of oxazole of lower R_f. The reaction mixture was then quenched with cold water. After this 33% of the solvent was removed under reduced pressure and the work up followed with ethyl acetate (3x30 mL). The combined organic layers were washed with water and brine successively and dried (Na_2SO_4). The solvent was then removed under reduced pressure and the residue was purified by silica gel flash chromatography to give the pure 2'-N oxazole **9a** as a white solid (910 mg, 73.4%); mp: 220-222^{o}C. ^{1}H NMR (300 MHz, $CDCl_3$) δ 8.62 (d, *J* = 4.2 Hz, 1H), 8.12 (s, 1H), 8.06 (d, *J* = 7.8 Hz, 1H), 7.96 (s, 1H), 7.85 (ddd, *J* = 1.8, 6.0 Hz, 1H), 7.79 (dd, *J* = 1.8, 6.6 Hz, 1H), 7.62 (d, *J* = 8.4 Hz, 1H), 7.55 (d, *J* = 1.5 Hz, 1H), 7.53 (s, 1H), 7.41 (ddd, *J* = 1.5, 4.8 Hz, 1H), 5.78 (d, *J* = 12.9 Hz, 1H), 4.31 (d, *J* = 12.9 Hz, 1H).

^{13}C NMR (75 MHz, $CDCl_3$) δ 167.9, 156.7, 149.9, 149.0, 146.6, 137.0, 136.4, 135.8, 135.5, 135.3, 129.8, 127.5, 127.0, 124.9, 124.0, 122.8, 122.7, 121.0, 81.8.7, 79.5, 45.3; HRMS (ESI-TOF *m/z*) for $C_{21}H_{13}N_5O$ calcd 352.1188, found 352.1193 $(M+H)^+$.

5-(8-Ethynyl-6-phenyl-4H-benzo[f]imidazo[1,5-a][1,4]diazepin-3-yl)oxazole (**9b**)

[00180] The 2'-H oxazole compound **9b** was prepared according to the method described for **9a**, employing the 2'-H aldehyde **11b** (3.30 g, 10.61 mmol), TosMIC, 2.50 g, 12.7 mmol) and K_2CO_3 (4.3 g, 31.80 mmol). This afforded the crude solid which was purified by flash chromatography (4:1 ethyl acetate/hexane) to give a white solid **9b** (2.90 g, 78% yield); mp 120-122 ^oC. ^{1}H NMR (300 MHz, $CDCl_3$) δ 8.08 (s, 1H), 7.93 (s, 1H), 7.81 (dd, *J* = 1.8, 6.6 Hz, 1H), 7.81 (d, *J* = 8.4 Hz, 1H), 7.53-7.57 (m, 3H), 7.43-7.49 (m, 2H), 7.39-7.43 (m, 2H), 5.75 (d, *J* = 12.9 Hz, 1H), 4.24 (d, *J* = 12.9 Hz, 1H), 3.18 (s, 1H).^{13}C NMR (300 MHz, $CDCl_3$) δ 167.9, 156.7, 149.9, 148.9, 146.6, 137.0, 136.4, 135.8, 135.4, 135.3, 129.8, 127.5, 127.0, 124.9, 124.0, 122.8, 122.6, 121.0, 81.8, 79.5, 45.2; HRMS (ESI-TOF *m/z*) for $C_{22}H_{14}N_4O$ calcd 351.1246, found 351.1240 $(M+H)^+$.

5-(8-Ethynyl-6-(2-fluorophenyl)-4H-benzo[f]imidazo[1,5-a][1,4]diazepin-3-yl)oxazole (**9c**)

[00181] The 2'-F oxazole **9c** was prepared according to the method described for **9a**, employing the 2'-N aldehyde **11c** (500 mg, 1.51 mmol), TosMIC, 366 mg, 1.82 mmol) and K_2CO_3 (629 mg, 4.56 mmol). This afforded the crude solid which was purified by flash chromatography (4:1 ethyl acetate/hexane) to give 2'-F oxazole as a white solid **9b** (446 mg, 80% yield); mp 212-214°C. ^{1}H NMR (300 MHz, $CDCl_3$) δ 8.03 (s, 1H), 7.93 (s, 1H), 7.75 (d, *J* = 7.8 Hz, 1H), 7.57-7.63 (m, 2H), 7.44-7.53 (m, 3H), 7.23-7.28 (m, 1H), 7.04 (t, *J* = 9.0 Hz, 1H), 5.74 (br s, 1H), 4.26 (br s, 1H), 3.16 (s, 1H). ^{13}C NMR (300 MHz, $CDCl_3$) δ 165.5, 161.9, 158.5, 149.8, 146.5, 135.4, 135.0, 134.3, 132.3, 131.1, 129.8, 128.9, 127.8, 127.5, 124.5, 122.6, 121.6, 116.4, 116.1, 81.4, 79.6, 45.0; HRMS (ESI-TOF *m/z*) for $C_{22}H_{13}N_4OF$ calcd 369.1144, found 369.1146 $(M+H)^+$.

5-(8-Ethynyl-6-(pyridin-2-yl)-4H-benzo[f]imidazo[1,5-a][1,4]diazepin-3-yl)-4-methyloxazole (9d)

[00182] The 8-ethynyl 2'-N methyl oxazole **9d** was prepared according to the method described for **9a,** employing 2'-N aldehyde **11a** (700 mg, 2.23 mmol), α-methyl TosMIC (560 mg, 2.683 mmol) and K_2CO_3 (925 mg, 6.709 mmol). This afforded the crude oxazole which was purified by flash silica gel chromatography EtOAc/DCM (1:1 and 1 mL MeOH + 1 mLTEA for

100 mL) to give 8-ethynyl 2'-N methyl oxazole **9d** as a half white solid (600 mg, 74% yield); mp 209-211°C. ^{1}H NMR (500 MHz, $CDCl_3$) δ 8.60 (d, *J* = 4.5 Hz, 1H), 8.04 (d, *J* = 7.5 Hz, 1H), 7.98 (s, 1H), 7.86 (s, 1H), 7.81 (t, *J* = 7.5 Hz, 1H), 7.76 (dd, *J* = 1.5, 8.5 Hz, 1H), 7.57 (d, *J* = 8.5 Hz, 1H), 7.54 (d, *J* = 1.0 Hz, 1H), 7.37 (t, *J* = 7.5 Hz, 1H),), 5.70 (d, *J* = 12.0 Hz, 1H), 4.28 (d, *J* = 12.5 Hz, 1H), 3.16 (s, 1 H), 2.53 (s, 3H); ^{13}C NMR (75 MHz, $CDCl_3$) δ 167.6, 156.7, 148.8, 148.7, 140.7, 136.8, 136.2, 135.9, 135.3, 134.8, 132.8, 129.8, 128.2, 126.9, 124.7, 123.9, 122.7, 120.7, 81.8, 79.2, 45.3, 12.3; HRMS (ESI-TOF *m/z*) for $C_{22}H_{15}N_5O$ calcd 366.1340 found 366.1349 $(M+H)^+$.

5-(8-Ethynyl-6-phenyl-4H-benzo[f]imidazo[1,5-a][1,4]diazepin-3-yl)-4-methyloxazole (9e)

[00183] The 8-ethynyl 2'-H methyl oxazole **9e** was prepared according to the method described for **9a**, employing the 2'-H aldehyde **11b** (250 mg, 0.803 mmol), α-methyl TosMIC **(**201 mg, 0.967 mmol) and K_2CO_3 (332 mg, 2.4 mmol). This afforded the crude solid which was purified by flash chromatography (4:1 ethyl acetate/hexane) to give half white 8-ethynyl 2'-H methyl oxazole as a solid **9e** (242 mg, 82% yield); mp 228-230°C. (300 MHz, $CDCl_3$) δ 8.01 (s, 1H), 7.85 (s, 1H), 7.77 (dd, *J* = 1.8, 8.4 Hz, 1H), 7.56-7.60 (m, 2H), 7.49-7.53 (m, 2H), 7.37-7.46 (m, 3H), 5.67 (d, *J* = 12.9 Hz, 1H), 4.20 (d, *J* = 12.9 Hz, 1H), 3.17 (s, 1H), 2053 (s, 3H); ^{13}C NMR (300 MHz, $CDCl_3$) δ 168.5, 148.7, 140.6, 139.5, 135.9, 135.8, 135.3, 134.5, 132.8, 130.5, 130.3, 129.3, 128.3, 128.2, 128.0, 122.6, 121.0, 81.5, 79.6, 45.3, 12.3; HRMS (ESI-TOF *m/z*) for $C_{23}H_{16}N_4O$ calcd 365.1400 found 365.1397 $(M+H)^+$.

5-(8-Ethynyl-6-(2-fluorophenyl)-4H-benzo[f]imidazo[1,5-a][1,4]diazepin-3-yl)-4-methyloxazole (9f)

[00184] The 8-ethynyl 2'-F methyl oxazole **9f** was prepared according to the method described for **9a**, employing the 8-ethynyl 2'-F aldehyde **11c** (500 mg, 1.52 mmol), α-methyl TosMIC (381 mg, 1.82 mmol) and K_2CO_3 (630 mg, 4.55 mmol). This afforded the crude solid which was purified by flash chromatography (4:1 ethyl acetate/hexane) to give a half white 8-ethynyl 2'-F methyl oxazole as a solid **9f** (450 mg, 78 % yield); mp 145-147°C; ^{1}H NMR (300 MHz, $CDCl_3$) δ 8.03 (s, 1H), 7.84 (s, 1H), 7.74 (d, *J* = 7.8 Hz, 1H), 7.55-7.65 (m, 2H), 7.46 (s, 2H), 7.22-7.28 (m, 1H), 7.03 (t, *J* = 8.1 Hz, 1H), 5.70 (br s, 1H), 4.25 (br s, 1H), 3.16 (s, 1H), 2.53 (s, 3H). ^{13}C NMR (75 MHz, $CDCl_3$) δ 165.4, 161.9, 158.5, 148.7, 140.6, 135.4, 134.6, 134.2, 132.8, 132.2, 132.1, 131.2, 131.1, 129.9, 128.9, 128.3, 127.9, 127.8, 124.5, 124.4, 122.5,

121.4, 116.4, 116.1, 81.5, 79.9, 45.1, 12.3; HRMS (ESI-TOF *m/z*) for $C_{23}H_{15}N_4OF$ calcd 383.1300 found 383.1303 $(M+H)^+$.

Example 7. In Vitro Analysis

FLIPR Binding

[00185] The FLIPR functional assay is used to determine the EC_{50} at the α1 and α3 $GABA_A$ receptor subtypes. A high EC_{50} for the α1 subtype would indicate a low chance of adverse effects, including sedation, ataxia, and muscle relaxation. A low α3 EC_{50} would indicate potential effectiveness as an anxiolytic, antihyperalgesic, and likely an anticonvulsant. See, for example, Liu et al. (*Assay. Drug. Dev. Technol.* 2008, 6, 781-6) and Joesch et al. (*J. Biomol. Screen.* 2008, 13, 218-28).

[00186] Compounds tested were synthesized internally and solubilized in DMSO at a 10 mM concentration. GABA was purchase from Sigma (#A2129) and prepared at 100 mM in water.

[00187] HEK-293 cells were stably transfected with the α1, β3, γ2 GABA A receptor subunits (GenBank accession numbers NM_000806.3, NM_000814.5, and NM_198904.1, respectively) or α3, β3, γ2 (NM_000808 for α3) where obtained from ChanTest Co. (Catalog # CT6216 and CT6218, respectively).

[00188] Cells were cultivated in Dulbeco's Modified Eagle's Medium (DMEM, Sigma D5796) supplemented with 10 % Fetal Bovine Serum (FBS, Gibco 16000), 0.5 mg/mL Geneticin (Gibco), 0.04 mg/mL Hygromycin B (Gibco), 0.1 mg/mL Zeocin (Gibco) and 20 mM HEPES (Sigma). Cells were grown at 37ºC in a humidified atmosphere of 5% CO_2. In the experiments described here frozen cells were used. For this purpose, cells were gown and maintained under confluency during 2-3 weeks and then frozen down at different cell densities using Recovery™ Cell Culture Freezing Medium (Gibco).

[00189] 18 hours prior to the experiment, cells were quickly thawed at 37ºC and seeded on Poly-D-Lys 384 plates (Corning 356663) at a density of 25,000 cells/well and in 25 µL of complete cell medium as described above.

[00190] Membrane potential changes induced by the flux of ions through the receptor were measured as relative fluorescence units (RFU) using the Fluorometric Imaging Plate Reader (FLIPR Tetra®, Molecular Devices) and the FLIPR Membrane Potential Blue Assay kit (Molecular Devices). Prior to the addition of the compounds the medium was removed and cells

were loaded with 20 µL of dye prepared in assay buffer composed of Hank's Balanced Salt Solution (HBSS with Ca^{+2} and Mg^{+2}; Gibco 14025) with 20 mM Hepes. After 1 hour of incubation at room temperature (RT), the plate was placed into the FLIPR instrument and experiments were run adding first 10 µL from the 1st addition plate (compound plate) and after a 3 minutes incubation adding 20 µL of the 2nd addition or agonist plate. The response to this last GABA addition was monitored for another 3 minutes.

[00191] *1st addition plates or compound plates.* First addition plates containing the compounds to be tested were prepared as follows: compounds in 10 mM dimethyl sulfoxide (DMSO) stock were serially diluted from column 3 to 12 and 13 to 22 in 100 % DMSO using Corning 3657 plates and a Tecan Freedom Evo ® platform. Then, compounds were further diluted 1:100 in assay buffer. A GABA EC_0 (assay buffer alone) and EC_{100} (150 or 100 µM final GABA concentration after 1st addition for α1 or α3-containing receptor cell lines, respectively) were also included in these plates and used as minimum and maximum response controls, respectively, to analyse any possible compound agonist response.

[00192] *2nd addition plate or agonist plate.* Second addition plates were generated using a GABA EC_{20} to test potentiation profile of the compounds. EC_{20} and EC_{100} GABA (final assay concentrations) were used as minimum and maximum response controls, respectively. EC_{20} was 2 or 1.2 µM final GABA concentration for α1 or α3-containing receptor cell lines, respectively.

[00193] *Data analysis.* The difference between the maximum and the minimum (Max-Min) fluorescence reached during the first addition or read interval and the second read interval were used for data analysis (agonist and potentiation, respectively). Data was normalized according to the following formula:

$$\%\text{activation} = 100 \times \left(\frac{\text{Test well} - \text{Median EC0 or 20 Control}}{\text{Median EC100 Control} - \text{Median EC0 or EC20 Control}}\right)$$

wherein "Test well" refers to those that contain test compounds.

[00194] EC_{50} and maximum stimulation values were determined from concentration-response curves at 10 distinct concentrations. The four-parameter logistic model was used to fit each data set.

[00195] All compounds (HZ-166, MP-III-085, MP-III-080, KRM-II-81, KRM-II-82, KRM-II-18B, KRM-II-97, KRM-II-73, and SH-I-085) displayed a α1 EC_{50} above 20 µM (the highest

concentration tested) while also exhibiting α3 activity, with EC_{50} in, or near, the nanomolar range (**TABLE 3**).

Liver Microsomal Stability Studies

[00196] *In vitro* liver microsomal studies were completed to measure the stability of the compounds against degradation in various species' liver microsomes.

[00197] Compound was incubated in hepatic microsomes over a 30-minute incubation period at 37ºC. Incubations both with and without NADPH (2 mM) were performed in a 96-well plate format. The reaction was initiated with the addition of substrate and was terminated by protein precipitation. All incubations were performed using a final substrate concentration of 4 μM in 50 mM sodium phosphate buffer, pH 7.4. The final organic solvent content was 0.5 % acetonitrile and 0.02% DMSO. The amount of enzyme present was fixed at 1.11 mg/mL protein irrespective of the species of microsomes used. Samples were analyzed by LC/MS-MS to determine the percent loss in the NAPDH incubations relative to the NADPH free incubations.

[00198] Although HZ-166 and other BZDs had been shown to be stable against human liver microsomes, short half lives in *in vivo* studies indicated poor stability in rodents, which can be a hindrance in fully evaluating compounds in preclinical studies in rodents. Results are shown in **TABLE 3**.

TABLE 3. Compound binding affinities (α1 and α3) and liver microsomal stability.

Compound	α1 Binding	α3 Binding	Human	Dog	Mouse	Rat
	EC_{50} (μM)		Liver microsome stability (reported in % remaining) Conditions: 37ºC, 4 μM compound, 30 minutes			
HZ-166	> 20	0.844	80	97	54	50
MP-III-085	> 20	5.15	81	93	85	93
MP-III-080	> 20	3.02	91	97	92	94
KRM-II-81	> 20	0.937	91	94	90	90
KRM-II-82	> 20	0.0321	74	86	73	72
KRM-II-18B	> 20	0.0112	78	87	79	68
KRM-II-97	> 20	0.629	94	85	86	75
KRM-II-73	> 20	0.115	78	89	70	77

SH-I-085	> 20	0.0249	62	77	67	61

Example 8. Motor Impairment

Inverted Screen

[00199] The inverted screen test is used to measure whether or not a test compound induces muscle relaxation. When a test subject is placed on a wire screen which is then inverted, the reaction is to climb to the opposite side so they are no longer hanging upside down. If a compound promotes muscle relaxation, the test subjects will either fall off, or hang onto the screen without being able to climb to the opposite side.

[00200] Male Sprague-Dawley rats (n = 5) were dosed i.p. (vehicle = 1% carboxymethyl cellulose) with diazepam (3, 10, or 30 mg/kg), KRM-II-81 (10, 30, or 60 mg/kg) or HZ-166 (30 mg/kg) 30 minutes prior to testing. Rats were placed onto the top of a wire screen, which was then inverted so that the rats were hanging upside down. Rats were observed for 60 seconds, at which point they were score (0 = climbed over; 1 = hanging onto screen; 2 = fell off). Results were analyzed using ANOVA (Dunnett's test: $^{*}P < 0.05$).

[00201] Neither HZ-166 nor KRM-II-81 induced significant muscle relaxation (**FIG. 4**); however, signs of muscle relaxation began to appear at 30 mg/kg for HZ-166, while the same slight signs occurred at 60 mg/kg for KRM-II-81. Non-dosed rats were able to climb to the top of the screen when inverted (score of 0.4 ± 0.4). Diazepam but not KRM-II-81 or HZ-166 produced full motor impairment.

Rotorod

[00202] The rotorod assay (**FIG. 5**) is used to determine the ataxic effects, generally stemming from the α1 subtype, that compounds have in test subjects. Mice are trained to run on a slow, rotating cylinder for two minutes, and failure to stay on the rod may be due to ataxia. HZ-166 has previously been shown to have no ataxic complications in doses over 100 mg/kg. Each set of compounds were tested against a vehicle.

[00203] Male NIH Swiss mice (n = 10/group) were trained on a rotorod (Ugo Basile 7650) at 4 r.p.m. for two minutes per training session prior to testing. On test day, mice were dosed i.p. with either vehicle (1% carboxymethyl cellulose) or one of the test compounds (10 or 30 mg/kg) 30 minutes prior to testing. Once placed on the rotorod, mice were observed for falling. Mice

that did not fall off during testing were given a "success" designation, while mice that fell off once during the 2 minutes of testing were scored as "partial." Mice that fell twice failed the trial.

[00204] The majority of compounds tested well at 10 mg/kg, while KRM-II-82, KRM-II-18B, and KRM-III-69 failed multiple times at 30 mg/kg.

[00205] KRM-II-81 still appeared to be the best compound in rotarod assays as it exhibited no significant ataxic concerns (rotarod) without observed signs of sedation.

Example 9. Anticonvulsant Activity

Maximal Electroshock (MES)-induced convulsion protection

[00206] The maximal electroshock (MES) assay is designed to determine how well a test compound can prevent seizures induced by applying a voltage stimuli to a mouse. HZ-166 has previously been shown to be effective in this assay, as well as giving protection against scMET-induced seizures.

[00207] Male CD (n = 10) were pretreated i.p. with vehicle (1% carboxymethyl cellulose), KRM-II-81 (3, 10, 30 mg/kg), or HZ-166 (3, 10, 30 mg/kg). Mice were subjected to electrical induced tonic seizures and examined for anticonvulsant effects 30 minutes after treatment. Mice were then given a 7mA electroshock using a Wahlquist Model H for 0.2 seconds and observed for the presence or absence of seizure activity. Each mouse is tested only once and euthanized immediately following the test.

[00208] KRM-II-81 is shown to display greater effectiveness than HZ-166 (**FIG. 6**). Both diazepam and KRM-II-81 fully protected against seizure induction, whereas HZ-166 (up to 60 mg/kg) did not.

scMET-induced seizure protection

[00209] A subcutaneous (sc) injection of pentylenetetrazol (PTZ), also known as metrazole (MET), is known to induce clonic and tonic seizures, demonstrated by loss of righting (inability to orient itself in an upright position). Test subjects were given a test compound, followed by a 35 mg/kg dose of MET and observed for convulsions (**FIG. 7**).

[00210] Male Sprague-Dawley rats (n = 5) were dosed i.p. (vehicle = 1% carboxymethyl cellulose) with either diazepam (3 or 10 mg/kg), KRM-II-81 (10, 30 or 60 mg/kg), or HZ-166 (30 mg/kg) 30 minutes prior to testing. Pentylenetetrazole (in saline) was dosed at 35 mg/kg i.p.,

and rats were observed for 30 minutes for signs of seizures. Results were analyzed using ANOVA (Dunnett's test: * $P < 0.05$).

[00211] Mice were then dosed i.p. with 5, 10, 25, or 50 mg/kg of KRM-II-81. 30 minutes later, a subcutaneous dose of pentylenetetrazole was administered, and the mice were observed for seizures. KRM-II-81 performed very well (**TABLE 4**), protecting most mice, with an ED_{50} of 10.94 mg/kg at the half hour time point.

[00212] Diazepam achieved significant protection at 10 mg/kg, KRM-II-81 at 30 mg/kg, while previously shown anticonvulsant HZ-166 had little effect at 30 mg/kg. This indicates that KRM-II-81 has greater therapeutic potential against convulsions than HZ-166.

TABLE 4. Assessment of KRM-II-81 in the scMET test for anticonvulsant activity.[*]

Dose (mg/kg)	5	10	25	50
Protected	0/8	5/8	7/8	8/8

[*] ED_{50} = 10.94 mg/kg

PTZ-induced seizure threshold

[00213] Following the evaluation of protection against scMET (35 mg/kg), KRM-II-81, HZ-166, and diazepam were tested to determine at what threshold of scMET each compound can protect against seizures at various concentrations. After a pretreatment of test compound, MET was intravenously administered to a test subject until a convulsions were observed.

[00214] Male Sprague-Dawley rats (n = 8; from Harlan Sprague Dawley, Indianapolis, IN) were dosed i.p. (vehicle = 1% carboxymethyl cellulose) with diazepam (0.1, 0.3, or 1 mg/kg) or a test compound (3, 10, 30, or 60 mg/kg) 30 minutes prior to testing. Pentylenetetrazole was administered i.v. to each group (10 mg/mL at 0.5 mL/minute) until each animal exhibited a clonic convulsion, or for four minutes. Each animal was used only once and was euthanized post testing. Results were analyzed using ANOVA (Dunnett's test: * $P < 0.05$).

[00215] HZ-166 displayed little protection against MET (35 mg/kg) at concentrations varying from 3 mg/kg to 60 mg/kg, while KRM-II-81 began to exhibit a significant protection against seizures, requiring a 71 mg/kg dose of MET when pretreated with 10 mg/kg of KRM-II-81 (**FIG. 8**). Both diazepam and KRM-II-81 significantly increased the seizure threshold to PTZ with KRM-II-81 producing larger maximal effect.

Example 10. Anxiolytic Activity

Anxiolytic Marble Burying Assay

[00216] The marble burying assay is used to determine the anxiolytic activity of a given compound. Mice are placed in a tub containing 20 marbles placed over a bed of sawdust. Defensive burying (Broekkamp 1986) is the natural reaction for the mice. When given an anxiolytic, such as diazepam, the mice are less likely to defensively bury the marbles.

[00217] Experiments were carried out by the methods described in Li et al. (*Life Sciences* 2006, **78**, 1933-1939). Separate groups of mice were used in these experiments and were conducted in a dimly lit testing room. After 60 min acclimation to the experimental room, mice were placed in a 17 x 28 x 12 cm high plastic tub with 5 mm sawdust shavings (Harlan Sani-Chips, Harlan-Teklad, Indianapolis, IN, USA) on the floor, which was covered with 20 blue marbles (1.5 cm diameter) placed in the center. Mice were left in the tub for 30 min. The number of marbles buried (2/3 covered with sawdust) was counted and submitted to inter-observer reliability assessment.

[00218] All compounds are shown to display a significant reduction in marbles buried at 30 mg/kg (**FIG. 9**), while MP-III-080 and KRM-III-69 show a reduction at 10 mg/kg. However, sedation was also observed in these three compounds, which likely led to the reduction in marble burying (both at 10 and 30 mg/kg) for MP-III-080, and KRM-III-69.

[00219] KRM-II-81 still appeared to be the best compound in the marble burying assay as it had good activity in the marble burying without observed signs of sedation.

Vogel conflict model for anxiety

[00220] The Vogel conflict procedure is used to determine the anxiolytic effects a compound exerts on a test subject, and HZ-166 has previously been shown to be effective in rhesus monkeys. Subjects are withheld from water prior to testing. Once given water during testing, they will either be unpunished, where they are free to drink without consequence, or punished, where a small electrical shock is applied after every 20^{th} lick. In vehicle punished, is it is expected that the rats hesitate from drinking due to the anxiousness of being shocked. When given an anxiolytic, the mice will continue to drink water despite the electrical shock.

[00221] Experiments were conducted as described in the protocol of Alt et al. (*Neuropharmacology* 2007, **52**, 1482-1487). Experimentally-naive adult male Sprague-Dawley

rats (Harlan Industries, Indianapolis, IN), weighing between 200 and 300 g, were used as subjects. The rats were housed in Plexiglas cages (4 per cage) and given free access to Lab Diet #5001 for rodents (PMI Nutrition International Inc., St. Louis, MO). Water was withheld for 20-24 hours prior to the first training session. A 12-hr light/dark cycle was maintained, and all experimental sessions were conducted during the light phase of the cycle at about the same time each day. All experiments were conducted in accordance with the NIH regulations of animal care covered in "Principles of Laboratory Animal Care", NIH publication 85-23, and were approved by the Institutional Animal Care and Use Committee.

[00222] *Apparatus.* The experiments were conducted using operant behavior test chambers ENV-007 (Med Associates Inc., Georgia, Vermont, USA), 30.5 x 24.1 x 29.2 cm. The test chambers were contained within light and sound attenuating shells. On the front wall of the chamber, a food trough was mounted 2 cm off the grid floor on the centerline. Two response levers were centered 8 cm off the centerline and 7 cm off the grid floor. Three lights were located above each response lever at 15 cm off the grid floor. Responding on the levers was without consequences for all sessions. On the rear of the chamber, a sipping tube was mounted 3 cm off the grid floor and 3 cm from the door. The sipping tube was wrapped with electrical tape to prevent the circuit from being completed if the animals were holding/touching the tube. All events were controlled and licking data was recorded by a Compaq computer running MED-PC Version IV (Med Associates Inc., Georgia, Vermont, USA).

[00223] *Sipper tube training.* Rats were put into the chamber on day 1 and 2 with white noise and the houselight illuminated, and allowed to drink for a total of six minutes after the first lick was made. The six minutes was broken into two components, the first three minutes was recorded as the unpunished component and the second three minutes were recorded as the punished component. During the two training days no shock was delivered in the punished component. After training, animals were returned to the home cage and given access to water for 30 minutes. For the second and third tests for each group, water was withheld for 24 hours before the training session. Animals were re-trained for one day. After training, animals were returned to the home cage and given access to water for 30 minutes.

[00224] *Sipper tube testing.* On day 3, animals were weighed and injected with either vehicle or compound and returned to the home cage. Thirty minutes after injection, animals were placed into the test chamber. The session was identical to the training session except that during the

punishment component the sipper tube delivered a brief electrical shock (100 milliseconds, 0.5 mA) after every 20th lick (FR20).

[00225] *Data Analysis.* The mean number of licks for both the unpunished and punished components were analyzed. In addition, data were also expressed as a percent of control values. The calculation was done using the mean number of licks for the control group in both components. Individual animal means (percent control) were calculated for animals receiving drug utilizing the formula: number of licks divided by mean number of licks by control group times 100 for each respective component. Dose-effect functions were analyzed by ANOVA followed by post-hoc Dunnett's test with vehicle treatment as the control standard. The proportion of animals exhibiting specified numbers of responses was analyzed by Fisher's exact probability test comparing vehicle control to drug values. Statistical probabilities ≤ 0.05 were considered significant.

[00226] As shown in **FIG. 10**, KRM-II-81 exhibited a significant increase in punished licking as compared to control at 10 mg/kg, indicating a powerful anxiolytic effect. Chordiazepoxide was run as a positive control. Both the anxioltyic, chlordiazepoxide, and KRM-II-81 increased punished licking.

Example 11. Antihyperalgesic Activity

Tactile hypersensitivity in spinal nerve ligated (SNL) rats

[00227] The von Frey filament test is used to test for antihyperalgesia, or an increased sensitivity to pain. HZ-166 has been shown to perform well in this assay. The von Frey filaments are used to apply pressure to the forelimbs of test subjects at set amounts. When pressure becomes too great, the forelimb is withdrawn and the amount of force applied recorded. The spinal nerve ligation induced hyperalgesia, reducing the amount of force a limb can take before being withdrawn.

[00228] Test compounds were given to test the effectiveness of combating the hyperalgesic effect of SNL. Male Sprague-Dawley rats went through SNL at least 90 days prior to the von Frey testing. Rats were first tested without given an injection to determine a baseline. Following baseline establishment, rats (n = 5 for all groups) were dosed i.p. with vehicle (1% carboxymethyl cellulose), KRM-II-81 (30 mg/kg), or gabapentin (50 mg/kg). Subjects were then tested every hour for four hours to determine the antihyperalgesic effect of the test compounds.

For testing, pressure using von Frey filaments was applied to the forelimb of the rat. Pressure was increased until the limb was withdrawn, and the amount of pressure was recorded.

[00229] In **FIG. 11**, rats given vehicle were only able to withstand an average of 5-6 grams of force before the forelimb is withdrawn. Both gabapentin (50 mg/kg) and KRM-II-81 (30 mg/kg) were active as antihyperalgesics, increasing the amount of force that can be handled before forelimb withdrawal. However, KRM-II-81 (at one hour) was able to reach significance, while gabapentin was not. This indicates that KRM-II-81 is a potential therapeutic for the treatment for neuropathic pain. With vehicle, rats were able to withstand ~5 g. of force before removing paw. KRM and gabapentin increase this pain threshold to ~12 g. of force from 1-2 hours, with KRM slightly more effective (doses unknown). The results indicate that KRM-II-81 was able to reverse the effects of hyperalgesia, allowing rats to withstand more force in the von Frey filament test after SNL surgery.

Example 12. GABA-A Receptor PAM

Model of Pain

[00230] Complete Freund's adjuvant (CFA) contains *Mycobacterium butyricum,* inducing inflammation and an increase in paw thickness. 0.1 mL of CFA was injected in the right hind paw of Sprague Dawley male rats under isoflurane anaesthesia.

[00231] *Food-maintained operant responding (rate response).* Rats (n=7) were placed in a chamber consisting of two (one active) levers. Rats were trained to press a lever (left) for a food pellet under a multiple-cycle procedure. Each cycle started with a 15 min inactive period (dark chamber and no programmed consequence), followed by a 5 min active period (cue light above the active lever lit up). The active period was set on a FR10 schedule and rats could receive a maximum of 5 food pellets. The cue light was terminated either after 5 minutes or once 5 food pellets were delivered. After each active period (every 20 minutes), rats received the next dose of drug for a duration of 2 hours. Data (rate per minute) was collected using Graphic State 3.03 software and interface (Coulbourn Instruments Inc.)

[00232] *Mechanical hyperalgesia.* Mechanical hyperalgesia was measured 3 days after CFA treatment. Rats (n=6) were placed in elevated boxes with a mesh floor. Von Frey filaments (expressed in g) were applied perpendicularly to the hindpaws, starting with the lowest filament (1.4 g) then increased until hindpaw withdrawal was observed. After each measurement, rats

received the next dose of drug (every 20 min) until the maximum threshold (26 g) was observed. For the antagonist study, rats were pretreated with the benzodiazepine site antagonist flumazenil (10 min) and then received the next dose of drug (every 20 min) until the pre-CFA threshold was observed.

[00233] *Horizontal wire test.* Rats (n=10) were lifted by the tail and allowed to grasp a horizontally strung wire with their forepaws and released. The inability to complete this task (within 3 seconds) was recorded 20 minutes after each injection of drug.

[00234] *Drugs.* The following drugs were used: HZ166, KRM-II-18B, and KRM-II-81, and were dissolved in a mixture containing 20% Dimethyl sulfoxide (DMSO), 10% Emulphor-620 (Rhodia Inc.), and 70% of 0.9% saline. Flumazenil (purchased from Cayman Chemical Company, MI) was dissolved in a mixture containing 10% ethanol, 40% propylene glycol, and 50% sterile water. Midazolam (Akorn, Inc.) was dissolved in 0.9% saline. Doses were expressed as the weight of the drug in milligrams per kilogram of body weight and drugs were administered intraperitoneally.

[00235] *Results.* Results are shown in **FIG. 12**, **FIG. 13**, and **FIG. 14**. This data demonstrated that KRM-II-81 and KRM-II-18B are much more active against hyperalgesia in the von Frey filament assay and on par with the performance of midazolam.

Example 13. Pharmacokinetics and concentrations in brain of KRM-II-81 administered to rats by IV and IP

[00236] The single-dose pharmacokinetics were determined in femoral artery/vein cannulated Sprague-Dawley rats. The rats received a 1 mg/kg intravenous and 10 mg/kg oral gavage dose of compound. Blood samples were collected at 0.08 (IV only), 0.25, 0.5, 1, 2, 4, 8, 12, and 24 hours after initiation of compound administration. Plasma was obtained via centrifugation. Plasma samples were then analyzed by LC-MS, and pharmacokinetic parameters calculated using Watson (version 7.4; Thermo Fisher Scientific). Calculated parameters include clearance (Cl), volume of distribution (Vdss), area-under-the-curve (AUC), half-life (T1/2), maximum plasma concentration (Cmax), time of maximum concentration (Tmax), and bioavailability (%F).

[00237] Male Sprague-Dawley rats were given either a 1 mg/kg oral dose or 10 mg/kg i.p. dose. Plasma concentrations were taken at 0.08, 0.25, 0.5, 1.0, 2, 4, 8, 12, and 24 hours (three rats per time point for each dose). The time-plasma concentration profiles are shown in **FIG. 15**.

[00238] Following a 1 mg/kg IV dose in rat, KRM-II-81 had a mean clearance of 21.7 mL/min/kg with a mean Vdss of 1.4 L/kg and a mean T ½ of 1.4 hours. Following a 10 mg/kg IP dose in rat, the mean AUC was 16500 nM*hrs with a Cmax of 3090 nM occurring at 2.0 hours. The mean IP T ½ was 3.1 hours and the mean bioavailability was 69%. The 1 hour brain concentration following a 10 mg/kg IP dose was 6630 nM with a Kp,uu of 0.53. The 4 hour brain concentration was 2050 nM with a Kp,uu of 0.67.

Example 14. Forced Swim Test

[00239] The forced swim test is used as a primary screen for the antidepressant nature of a test compound. Mice are placed in a cylinder filled with a small amount of water. Mice that are more mobile after a dosing of a compound are determined to be less depressed.

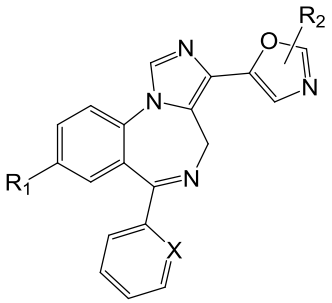
[00240] The experiment was carried out as described by Porsolt et al. (*Arch. Int. Pharmacodyn. Ther.* **1977**, *229*, 327-366). Male NIH Swiss mice (n = 7 – 8) were dosed i.p. with vehicle (1% HEC, 0.25% Tween 80, 0.05% antifoam), KRM-II-81 (3, 10, or 30 mg/kg), or imipramine (15 mg/kg) and assessed in the forced swim test. Mice were placed individually in clear plastic cylinders (10 cm in diameter x 25 cm in height) filled to 6 cm with 22 – 25^{o}C water for 6 minutes. The duration of immobility was recorded during the last 4 minutes of a 6-minute trial. A mouse was regarded as immobile when floating motionless or making only those movements necessary to keep its head above the water.

[00241] Results are shown in **FIG. 16**. Results were analyzed using ANOVA (Dunnett's test * $P < 0.05$). KRM-II-81 demonstrated antidepressant effects at 10 and 30 mg/kg. Imipramine was used as a positive control.

[00242] All patents, publications and references cited herein are hereby fully incorporated by reference. In case of conflict between the present disclosure and incorporated patents, publications, and references, the present disclosure should control.

CLAIMS

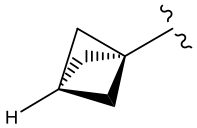
1. A compound of formula (I):



(I)

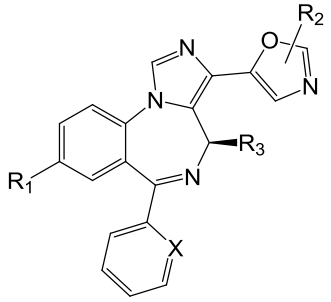
or a salt thereof, wherein:

X is selected from the group consisting of N, C-H, C-F, C-Cl, C-Br, C-I, and C-NO_2;

R_1 is selected from the group consisting of -C≡CH, -C≡C-Si$(CH_3)_3$, -cyclopropyl, and bicycle[1.1.1]pentane (); and

R_2 is selected from the group consisting of -H, -CH_3, -CH_2CH_3 and -CH$(CH_3)_2$.

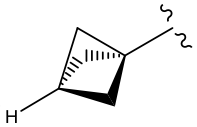
2. A compound of formula (II):



(II)

or a salt thereof, wherein:

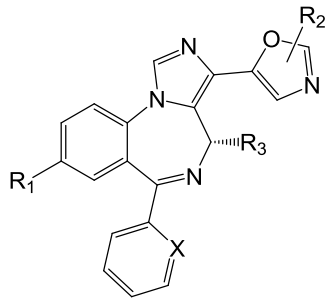
X is selected from the group consisting of N, C-H, C-F, C-Cl, C-Br, C-I, and C-NO_2;

R_1 is selected from the group consisting of -C≡CH, -C≡C-Si$(CH_3)_3$, -cyclopropyl, and bicycle[1.1.1]pentane ();

R_2 is selected from the group consisting of -H, -CH_3, -CH_2CH_3, and -CH$(CH_3)_2$; and

R_3 is selected from the group consisting of -H, -CH_3, -CH_2CH_3, -$CH(CH_3)_2$, -F, -Cl, -CF_3, and -CCl_3.

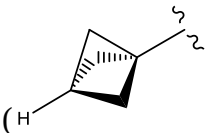
3. A compound of formula (III):



(III)

or a salt thereof, wherein:

X is selected from the group consisting of N, C-H, C-F, C-Cl, C-Br, C-I, and C-NO_2;

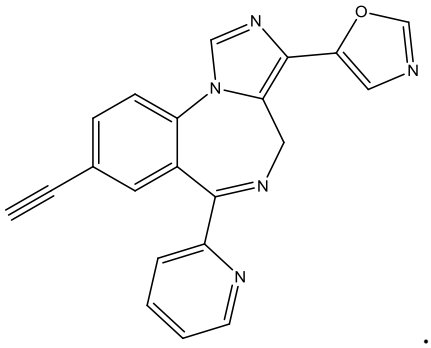
R_1 is selected from the group consisting of -C≡CH, -C≡C-$Si(CH_3)_3$, -cyclopropyl, and bicycle[1.1.1]pentane ();

R_2 is selected from the group consisting of -H, -CH_3, -CH_2CH_3, and -$CH(CH_3)_2$; and

R_3 is selected from the group consisting of -H, -CH_3, -CH_2CH_3, -$CH(CH_3)_2$, -F, -Cl, -CF_3, and -CCl_3.

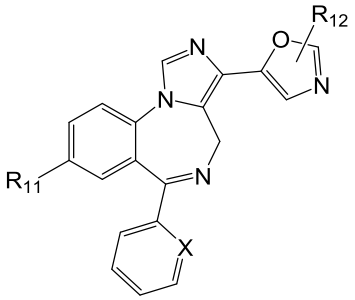
4. The compound of any of claims 1-3, wherein R_1 is -C≡CH.

5. The compound of any of claims 1-4, wherein the compound has the following formula:



.

6. A compound of formula (IV):



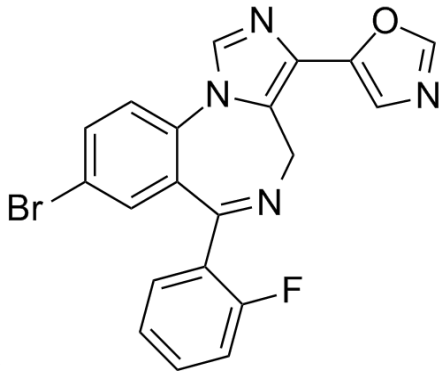
(IV)

or a salt thereof, wherein:

X is selected from the group consisting of N, C-H, C-F, C-Cl, C-Br, C-I, and C-NO_2;

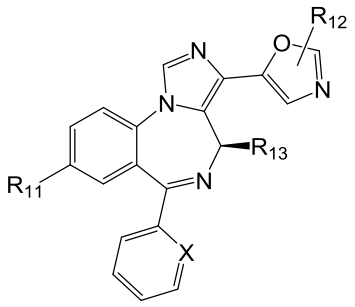
R_{11} is Br; and

R_{12} is selected from the group consisting of -H, -CH_3, -CH_2CH_3 and -$CH(CH_3)_2$,



with the proviso that the compound is not .

7. A compound of formula (V):



(V)

or a salt thereof, wherein:

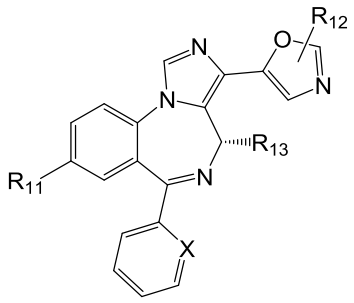
X is selected from the group consisting of N, C-H, C-F, C-Cl, C-Br, C-I, and C-NO_2;

R_{11} is Br;

R_{12} is selected from the group consisting of -H, -CH_3, -CH_2CH_3, and -$CH(CH_3)_2$; and

R_{13} is selected from the group consisting of -H, $-CH_3$, $-CH_2CH_3$, $-CH(CH_3)_2$, -F, -Cl, $-CF_3$, and $-CCl_3$.

8. A compound of formula (VI):



(VI)

or a salt thereof, wherein:

X is selected from the group consisting of N, C-H, C-F, C-Cl, C-Br, C-I, and $C-NO_2$;

R_{11} is Br;

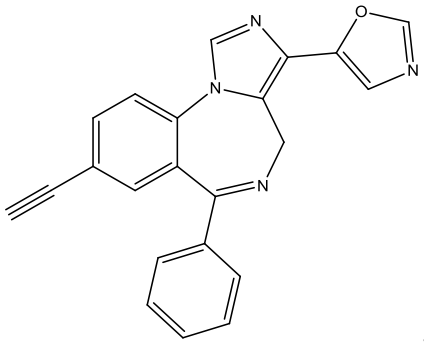
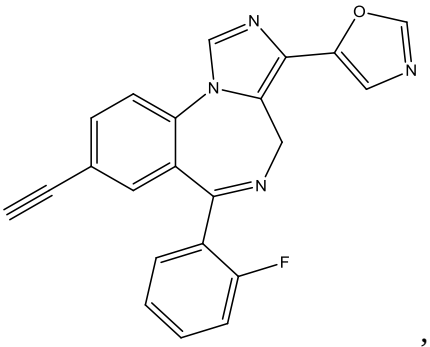
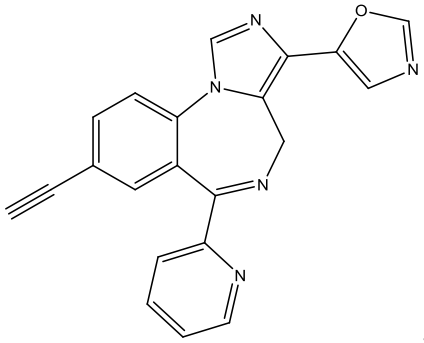
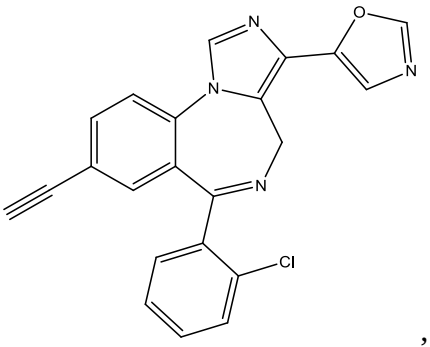
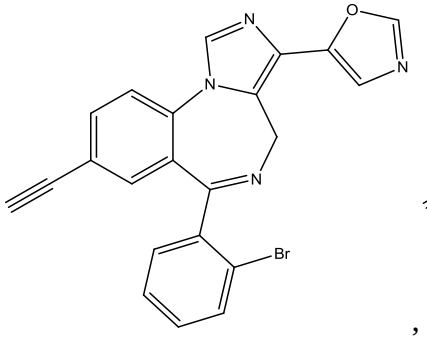
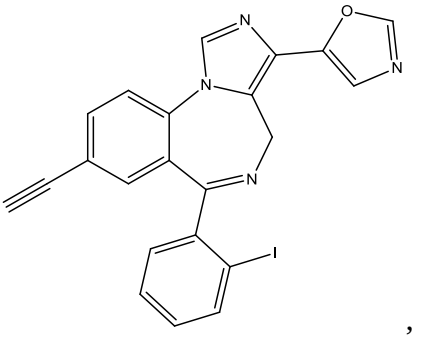
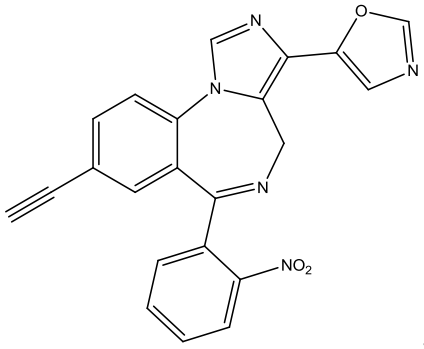
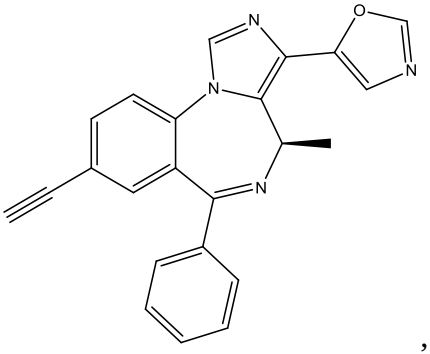
R_{12} is selected from the group consisting of -H, $-CH_3$, $-CH_2CH_3$, and $-CH(CH_3)_2$; and

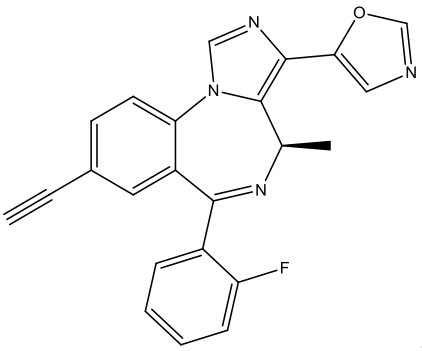
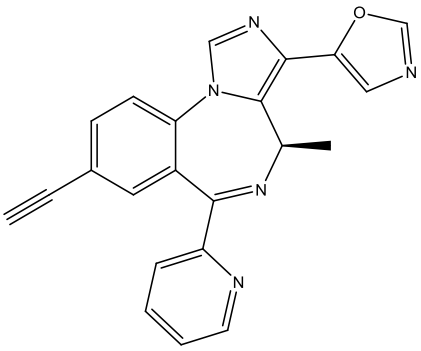
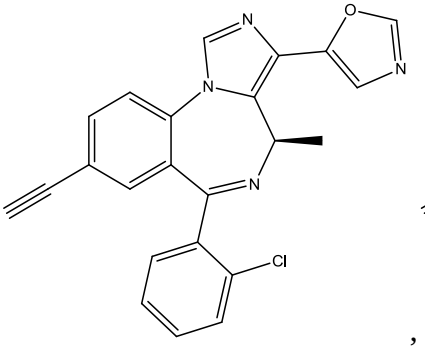
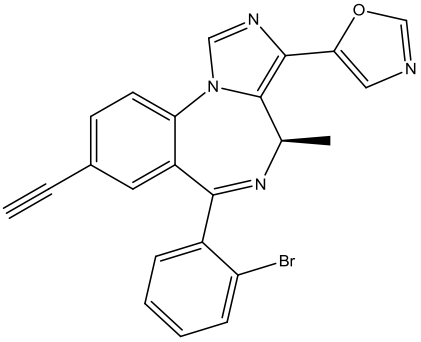
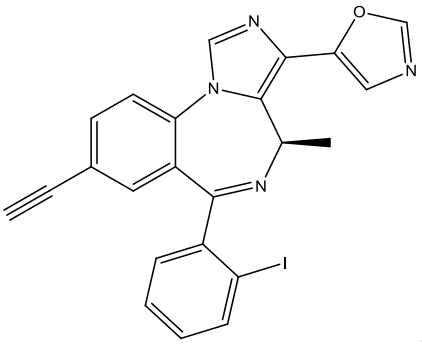
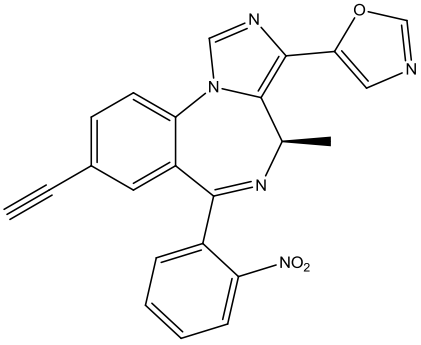
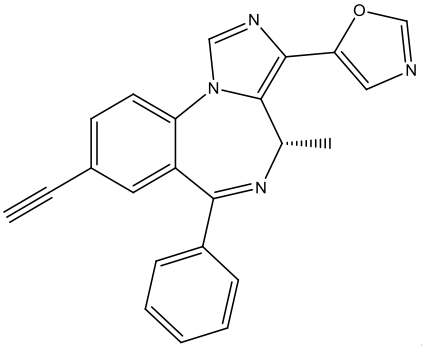
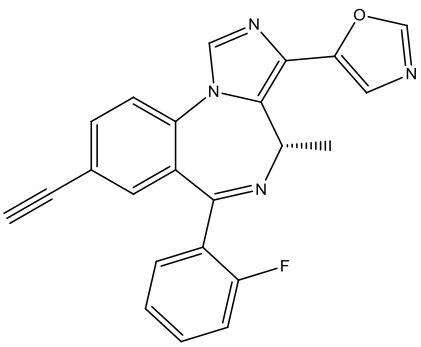
R_{13} is selected from the group consisting of -H, $-CH_3$, $-CH_2CH_3$, $-CH(CH_3)_2$, -F, -Cl, $-CF_3$, and $-CCl_3$.

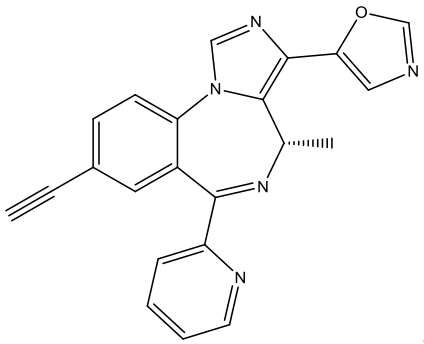
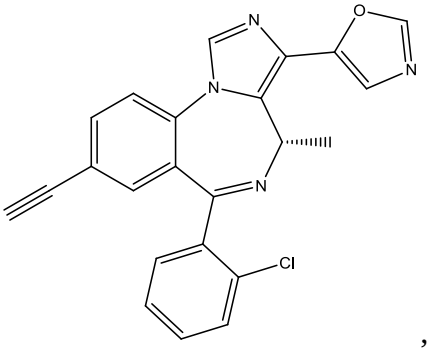
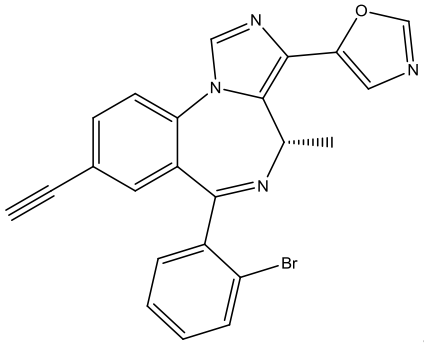
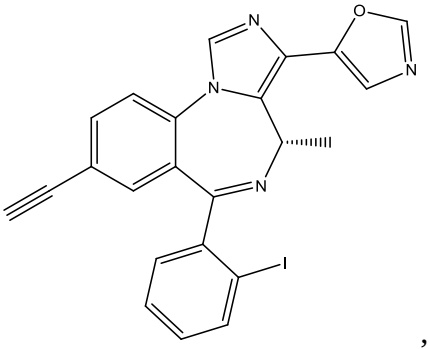
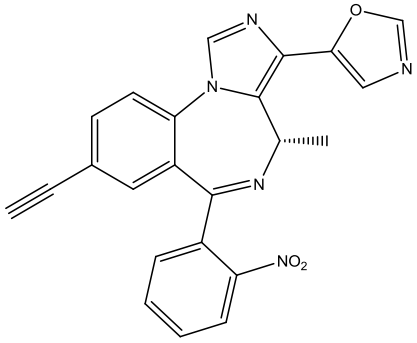
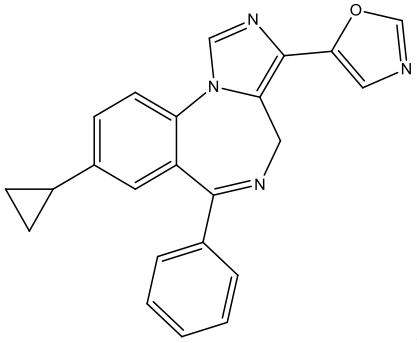
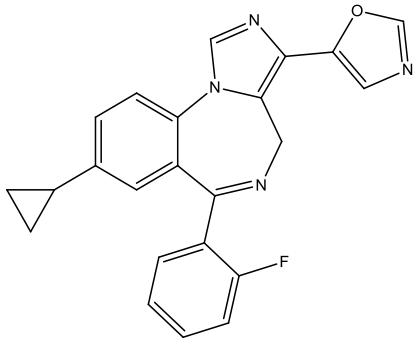
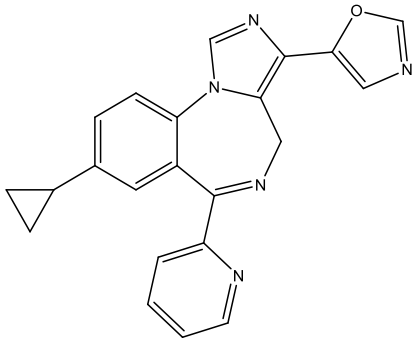
9. The compound of any of claims 1-8, wherein R_2 is -H.

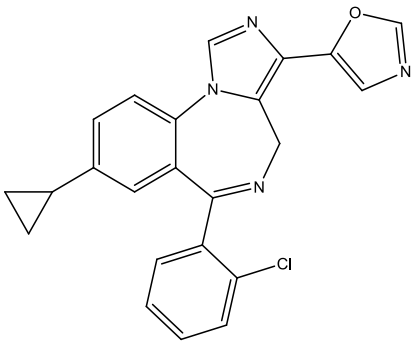
10. The compound of any of claims 1-9, wherein X is N.

11. A compound selected from the group consisting of:

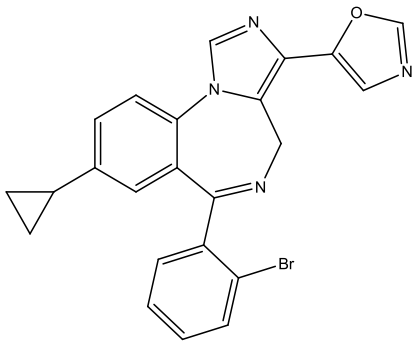

,

,

,

,

,

,

,

,


N
O
N
N
N
F
,

N
O
N
N
N
N
,

N
O
N
N
N
Cl
,

N
O
N
N
N
Br
,

N
O
N
N
N
I
,

N
O
N
N
N
NO2
,

N
O
N
N
N
,

N
O
N
N
N
F
,

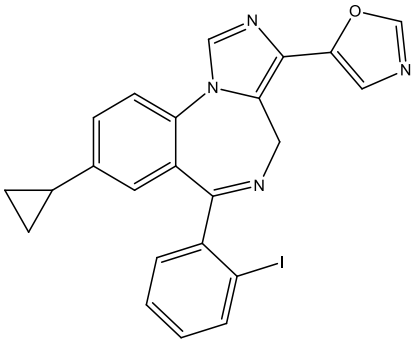

,

,

,

,

,

,

,

,


N
O
N
N
N
Cl

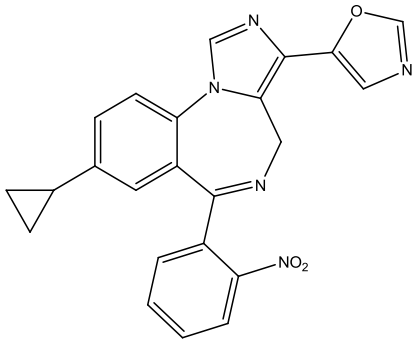
,


N
O
N
N
N
Br

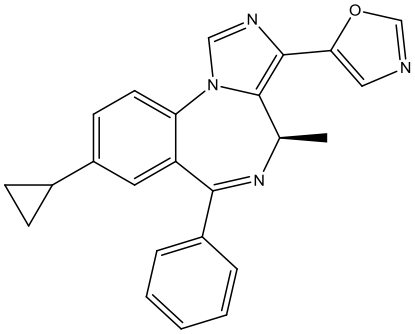
,


N
O
N
N
N
I

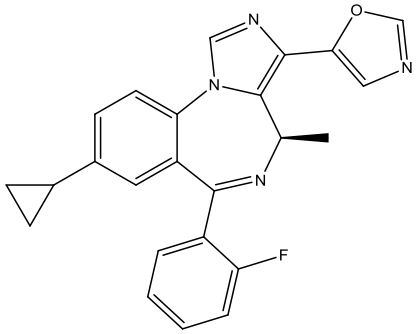
,


N
O
N
N
N
NO2

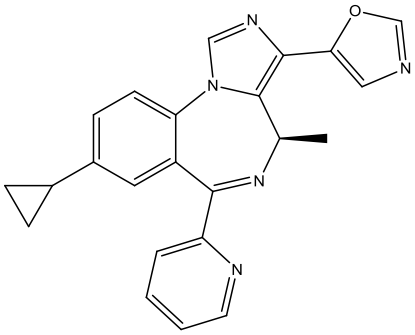
,


N
O
N
N
N

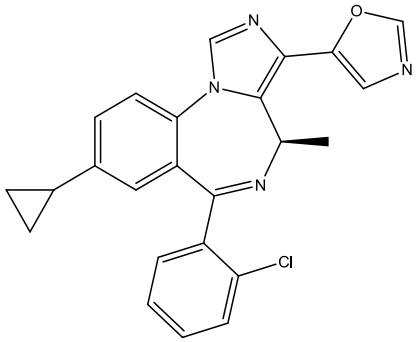
,


N
O
N
N
N
F

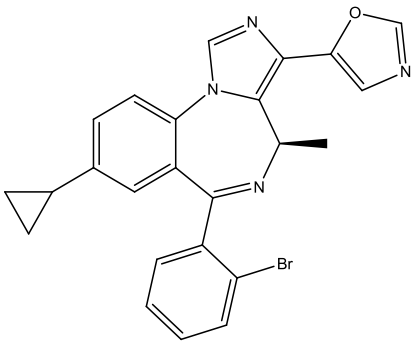
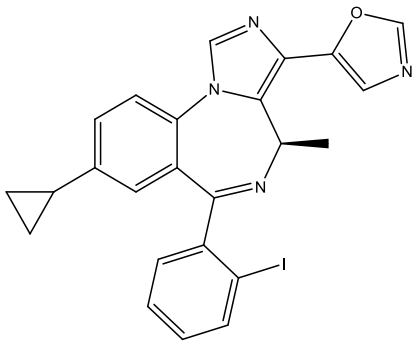
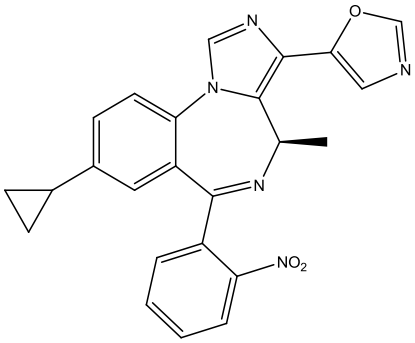
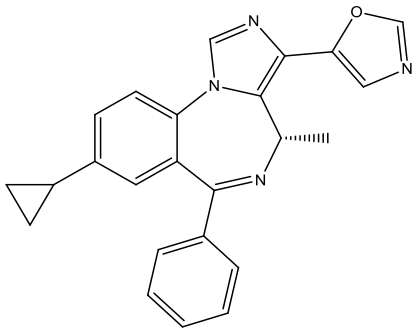
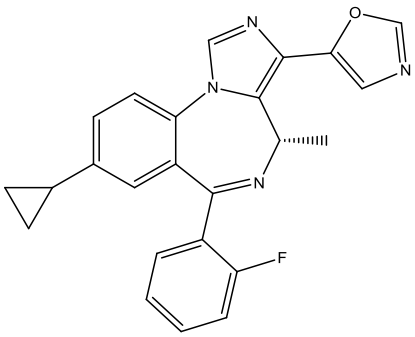
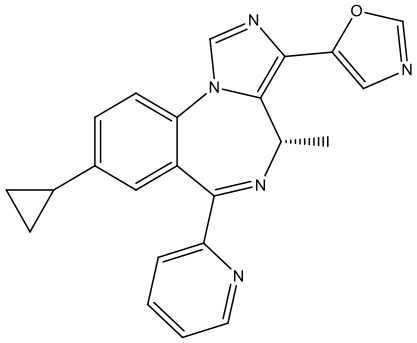
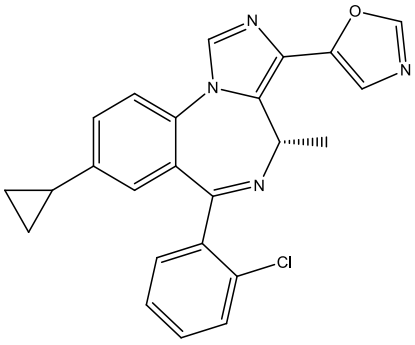
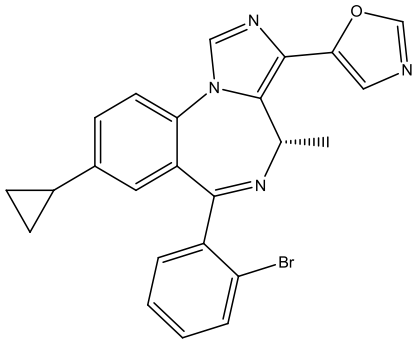
,

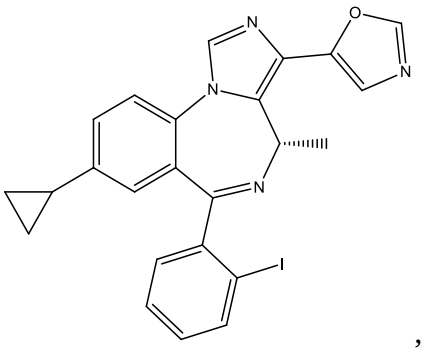

N
O
N
N
N
N

,

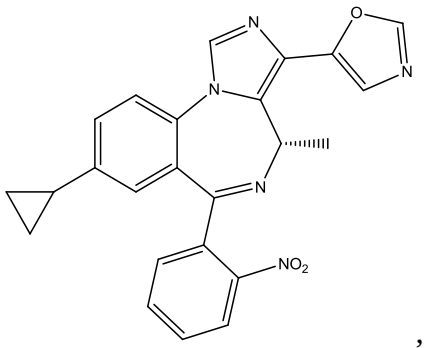

N
O
N
N
N
Cl

,

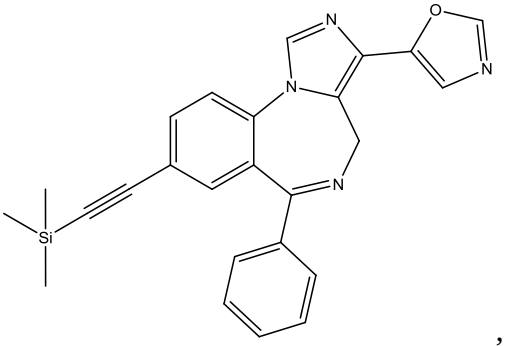

N
O
N
N
N
Br
,

N
O
N
N
N
I
,

N
O
N
N
N
NO2
,

N
O
N
N
N
,

N
O
N
N
N
F
,

N
O
N
N
N
N
,

N
O
N
N
N
Cl
,

N
O
N
N
N
Br
,


N
O
N
N
N
I

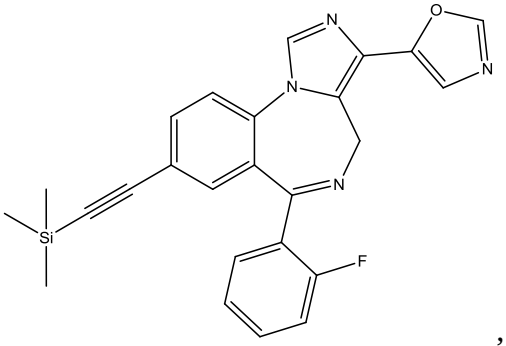
,


N
O
N
N
N
NO2

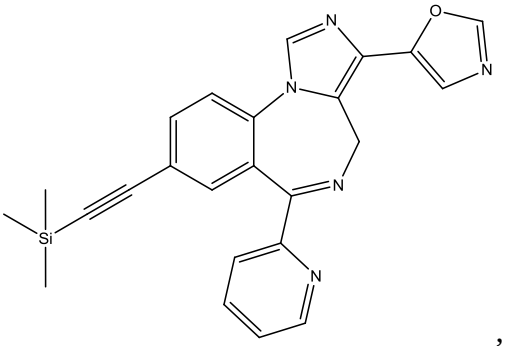
,


N
O
N
N
N
Si

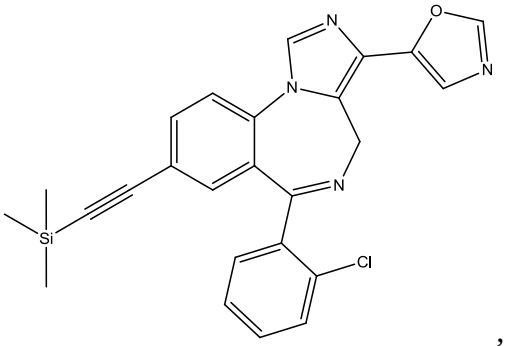
,


N
O
N
N
N
Si
F

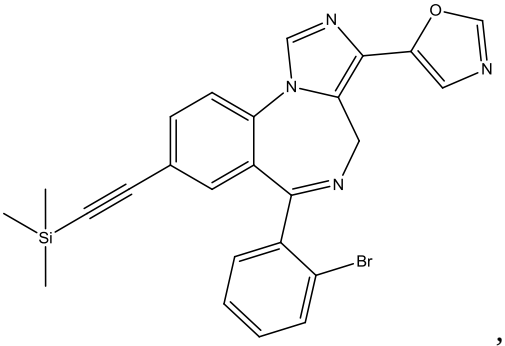
,


N
O
N
N
N
Si
N

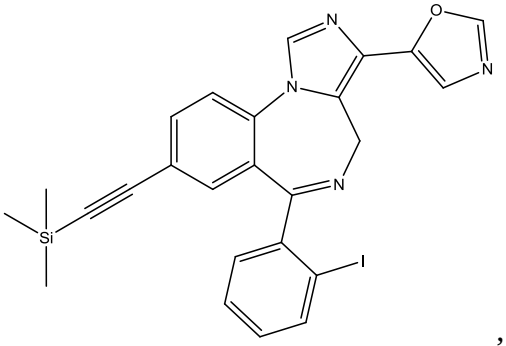
,


N
O
N
N
N
Si
Cl

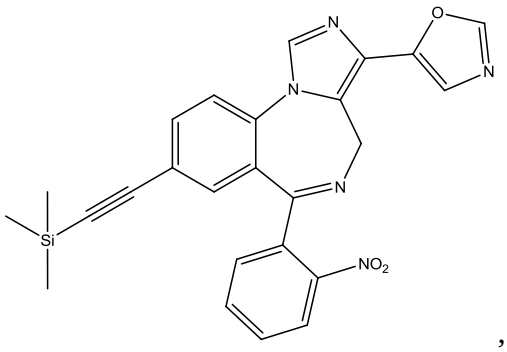
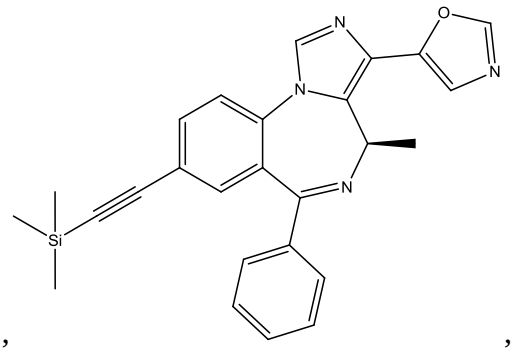
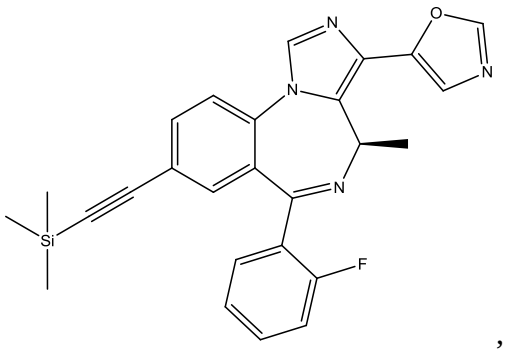
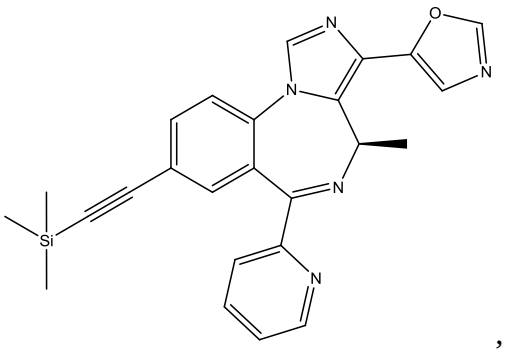
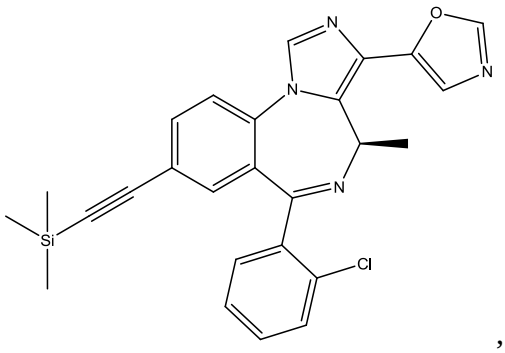
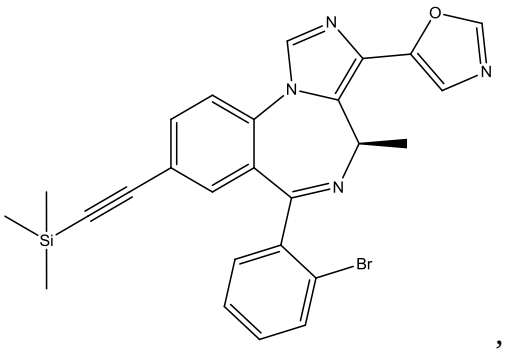
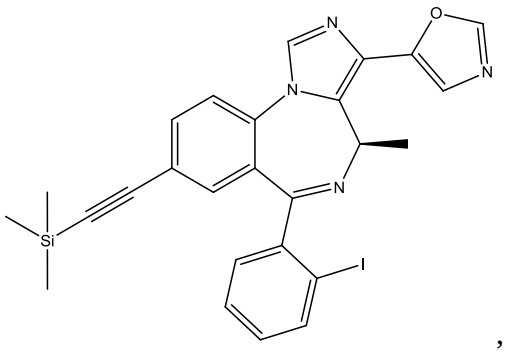
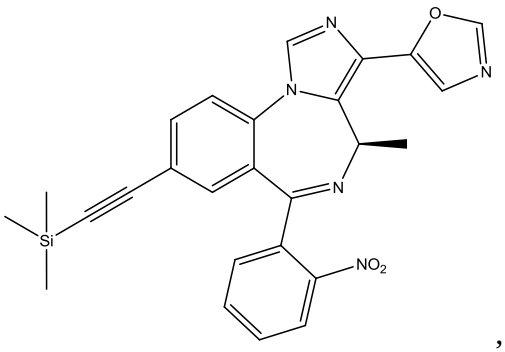
,

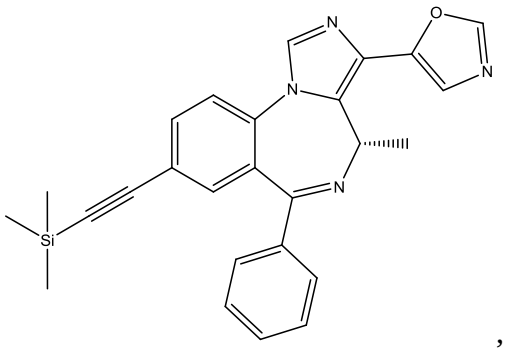
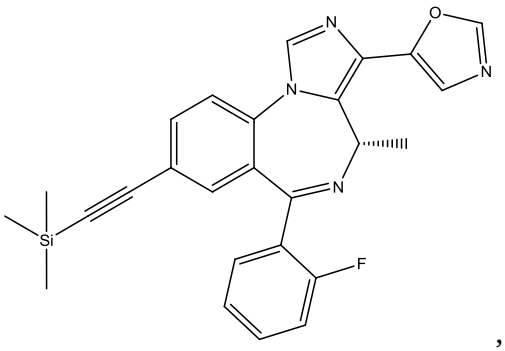
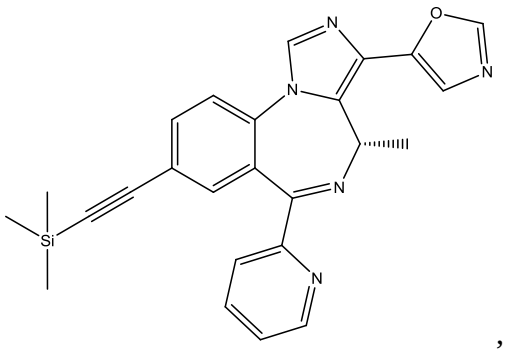
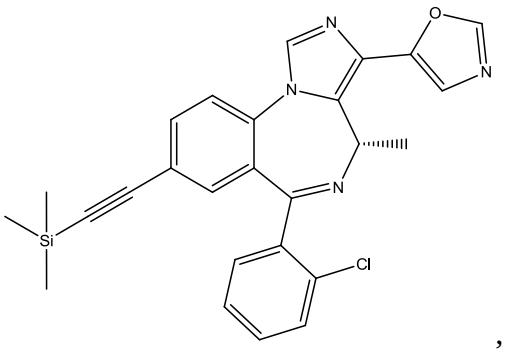
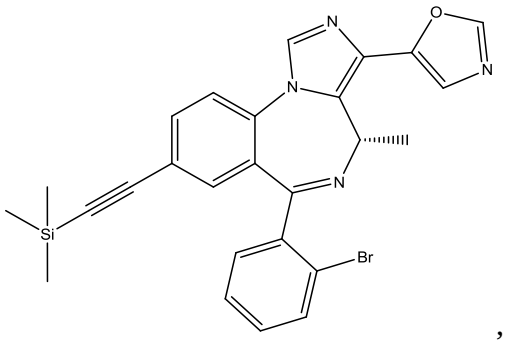
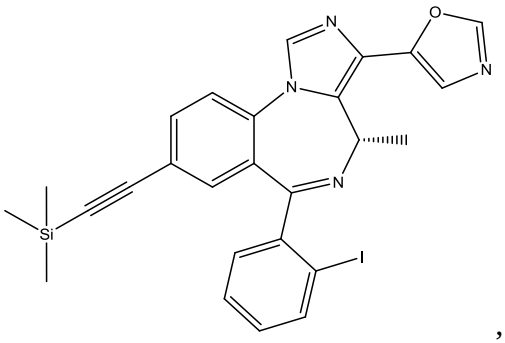
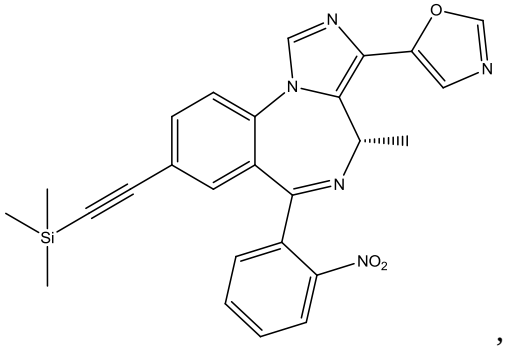
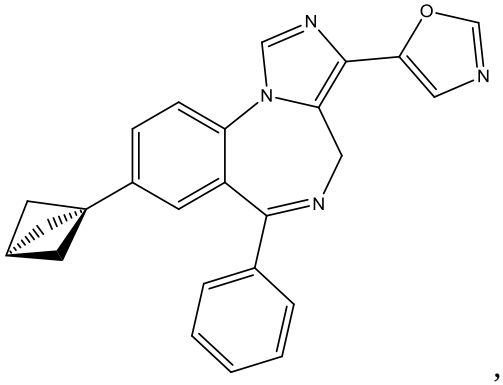

N
O
N
N
N
Si
Br

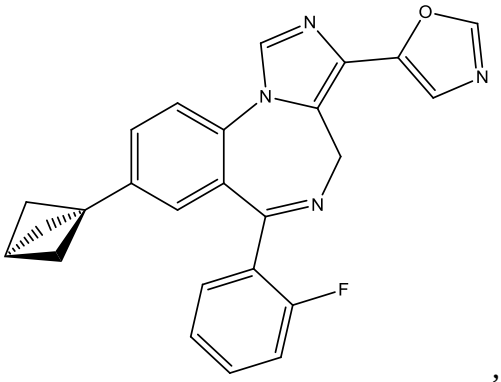
,


N
O
N
N
N
Si
I

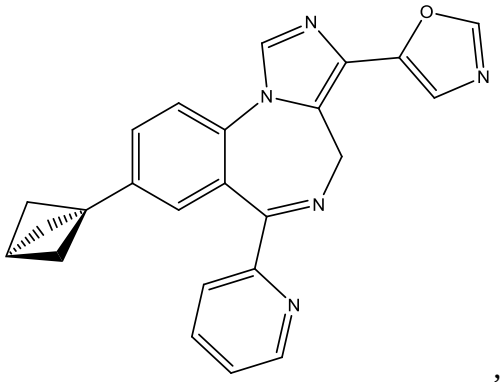
,

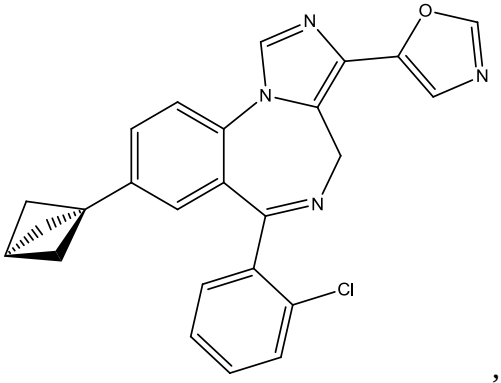

,

,

,

,

,

,

,

,


N
O
N
N
N
N
F

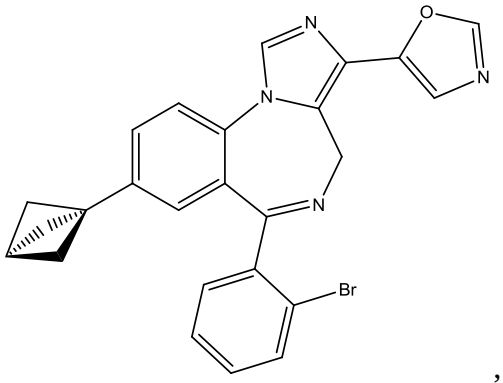
,


N
O
N
N
N
N

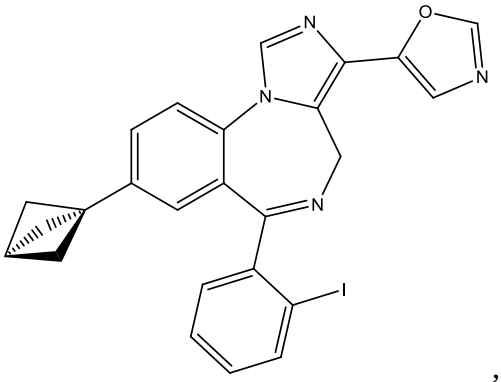
,


N
O
N
N
N
N
Cl

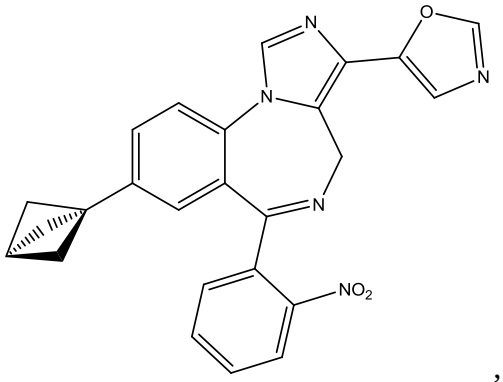
,


N
O
N
N
N
N
Br

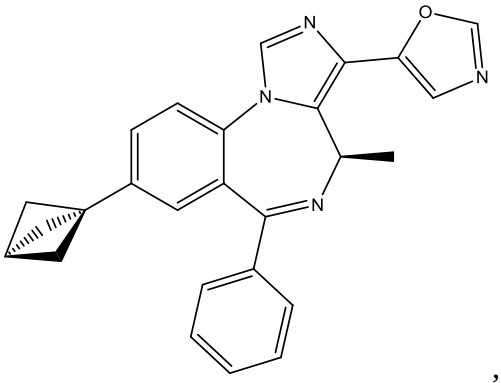
,


N
O
N
N
N
N
I

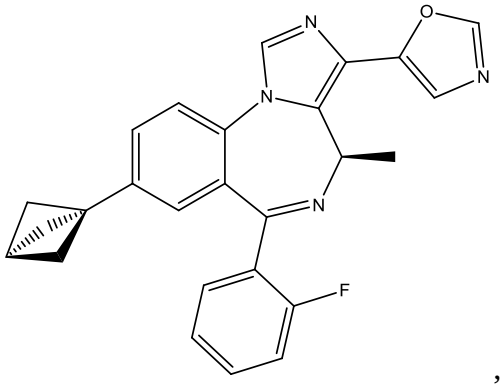
,


N
O
N
N
N
N
NO2

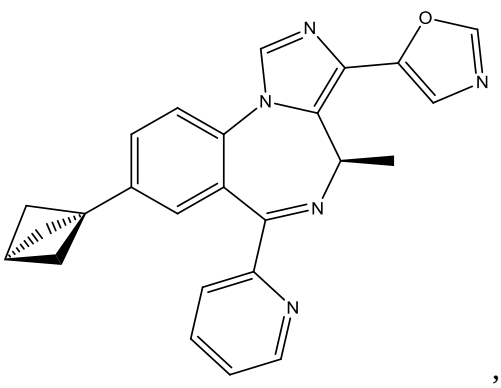
,


N
O
N
N
N
N

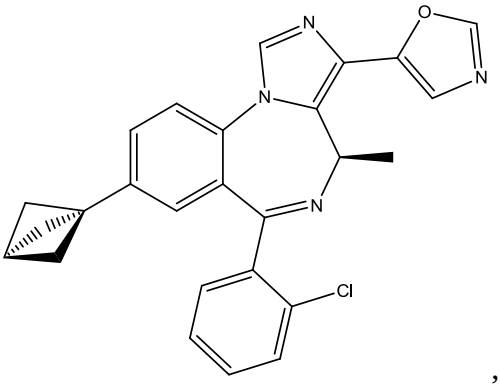
,


N
O
N
N
N
N
F

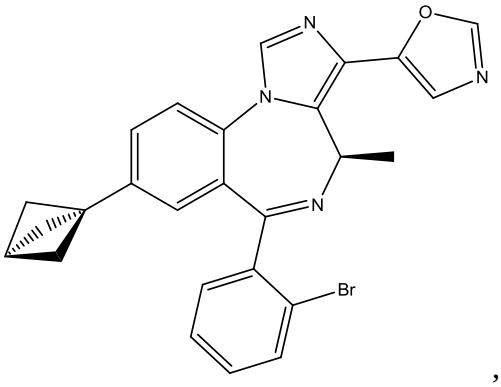
,


N
O
N
N
N
N

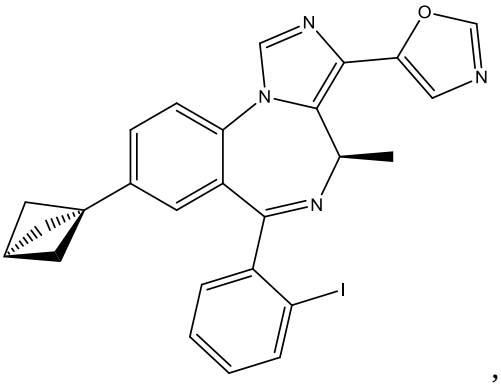
,


N
O
N
N
N
Cl

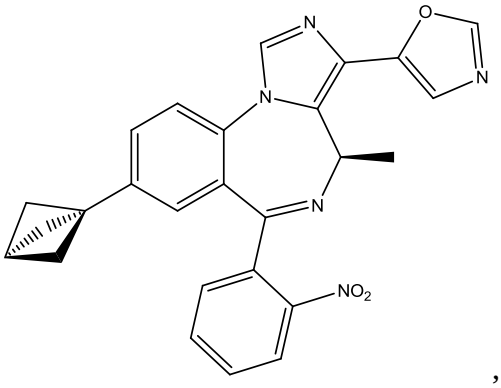
,


N
O
N
N
N
Br

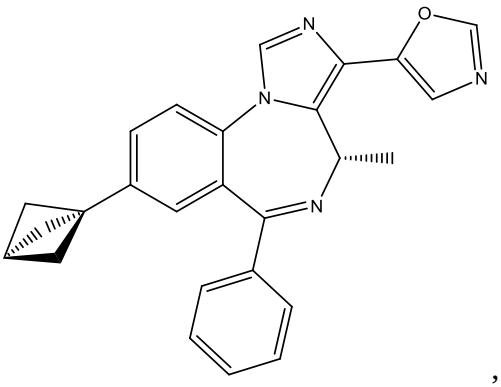
,


N
O
N
N
N
I

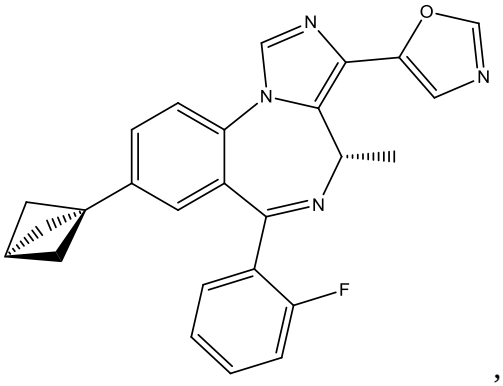
,


N
O
N
N
N
NO2

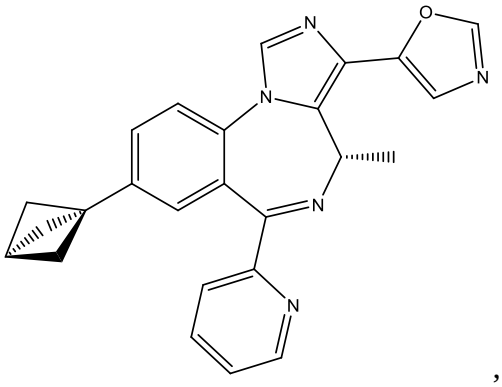
,


N
O
N
N
N

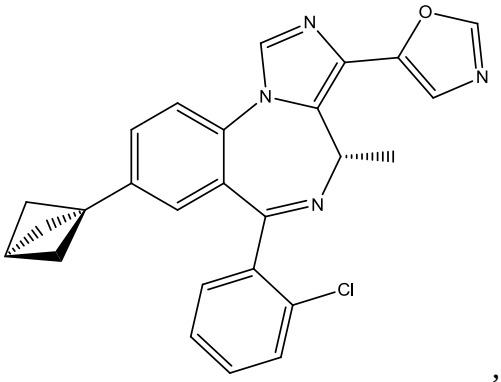
,


N
O
N
N
N
F

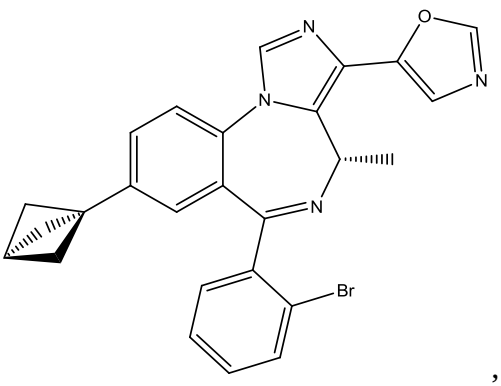
,


N
O
N
N
N
N

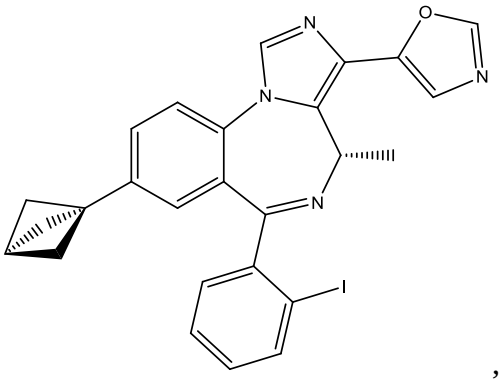
,



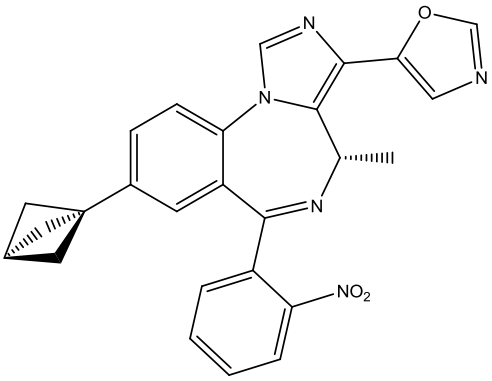
,



,

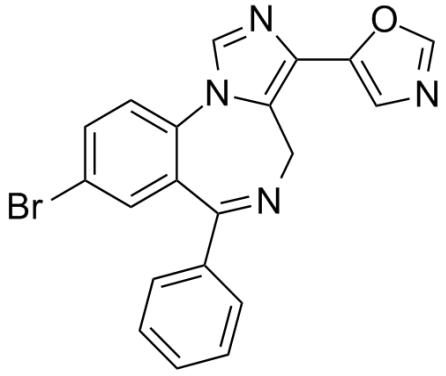


, and

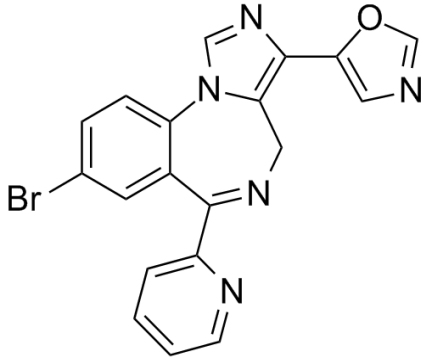


.

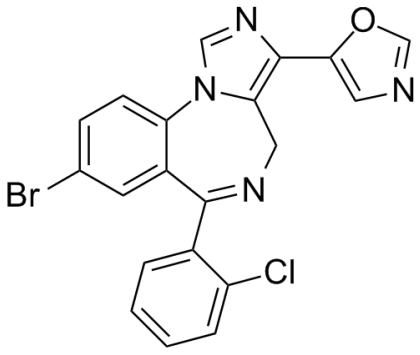
12. A compound selected from the group consisting of:



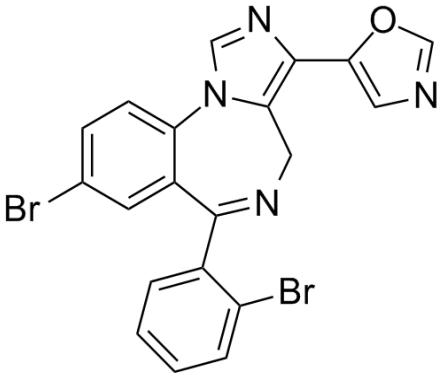
,



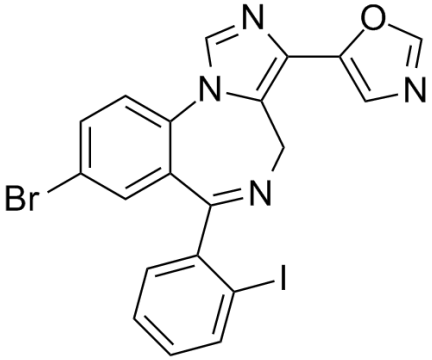
,



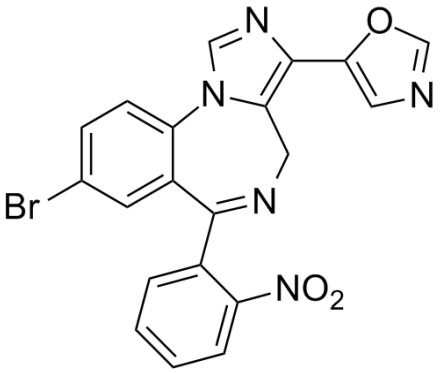
,


N
O
N
N
Br
N
Br

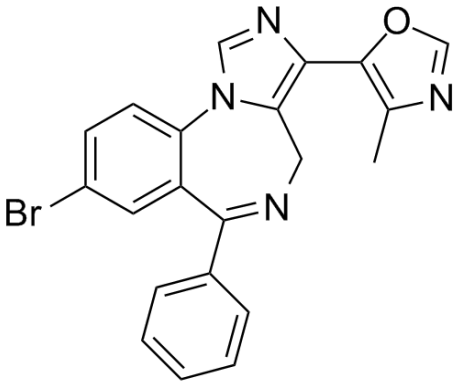
,


N
O
N
N
Br
N
I

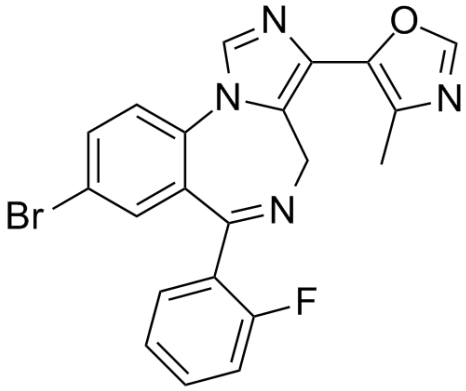
,


N
O
N
N
Br
N
NO2

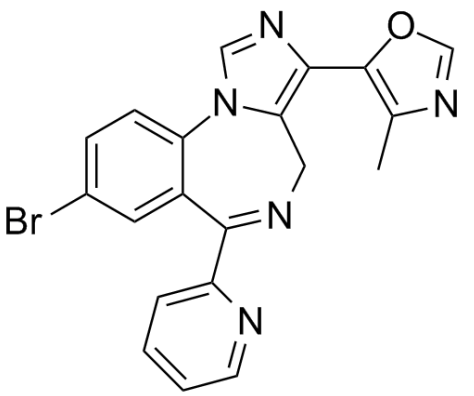
,


N
O
N
N
Br
N

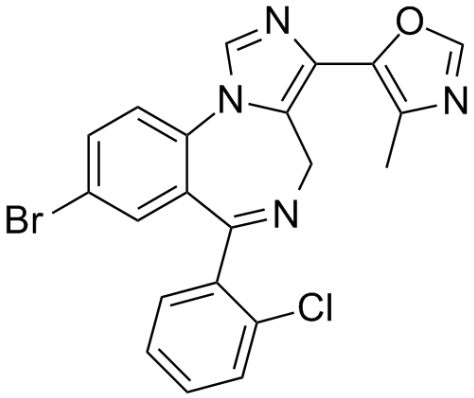
,


N
O
N
N
Br
N
F

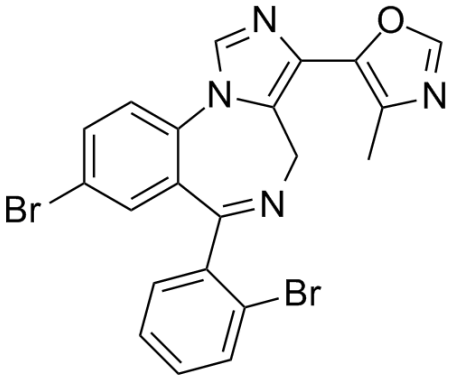
,


N
O
N
N
N
Br
N

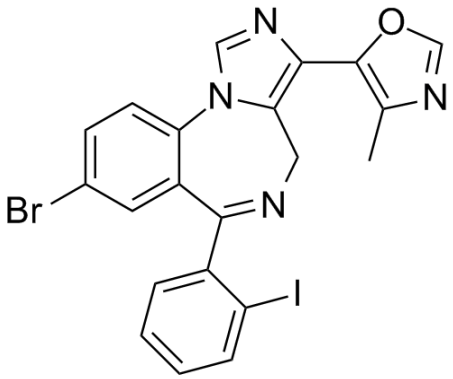
,


N
O
N
N
N
Br
Cl

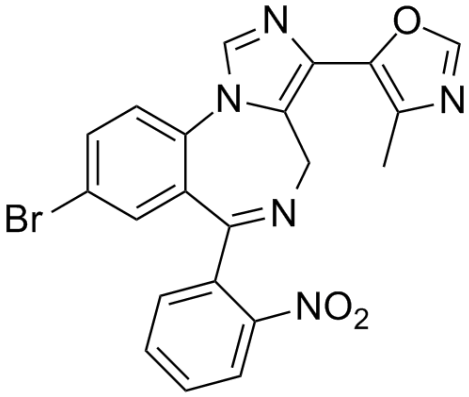
,


N
O
N
N
N
Br
Br

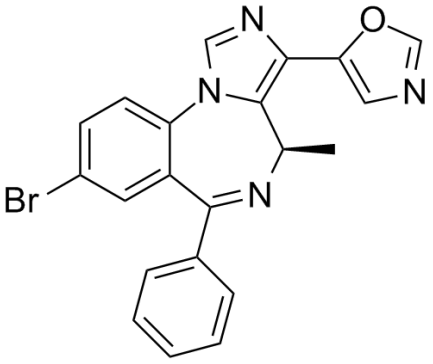
,


N
O
N
N
N
Br
I

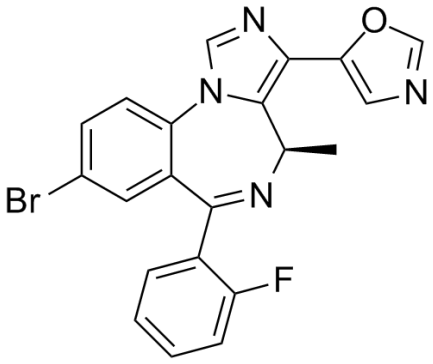
,


N
O
N
N
N
Br
NO2

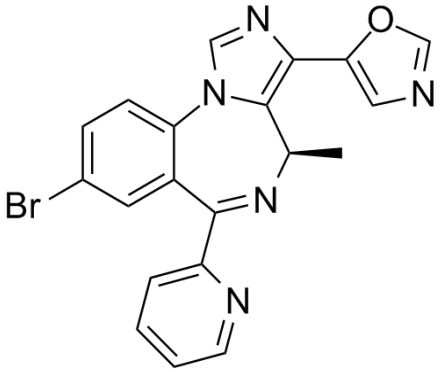
,


N
O
N
N
N
Br

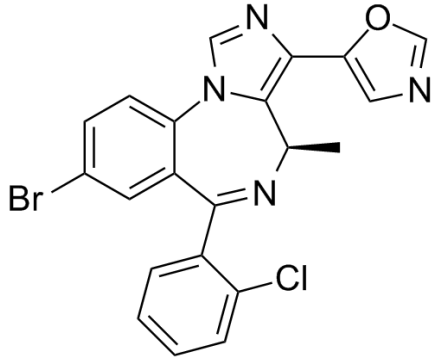
,


N
O
N
N
N
Br
F

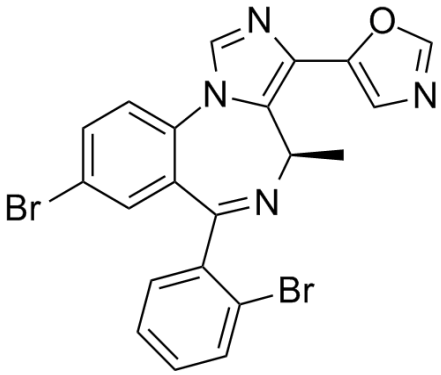
,


N
O
N
N
Br
N
N

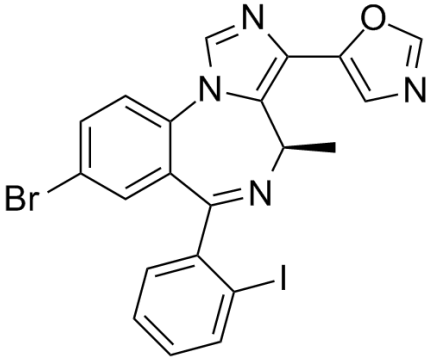
,


N
O
N
N
Br
N
Cl

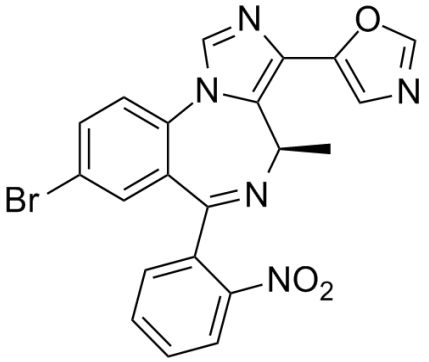
,


N
O
N
N
Br
N
Br

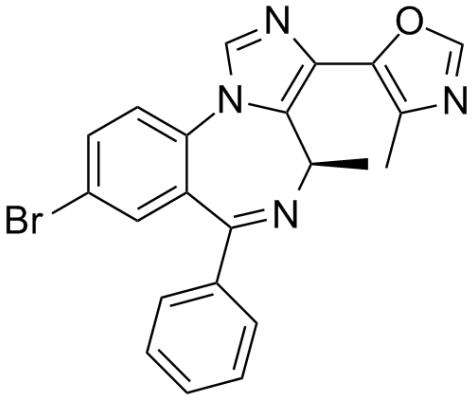
,


N
O
N
N
Br
N
I

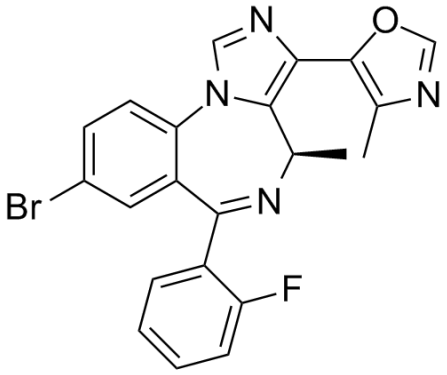
,


N
O
N
N
Br
N
NO2

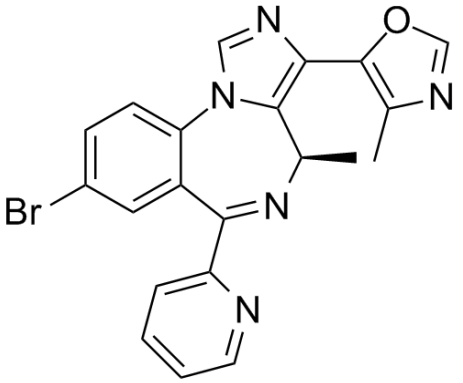
,


N
O
N
N
N
Br

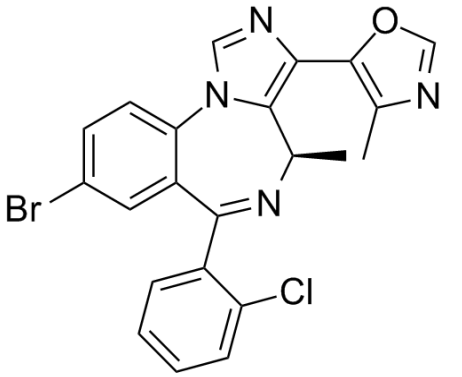
,


N
O
N
N
N
Br
F

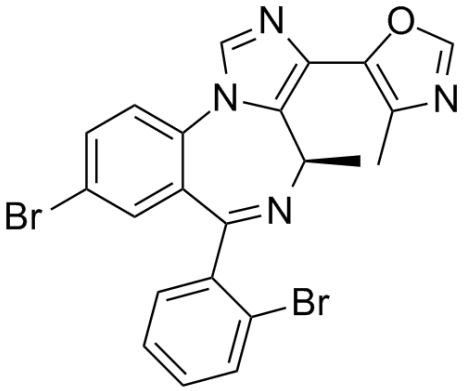
,


N
O
N
N
N
Br
N

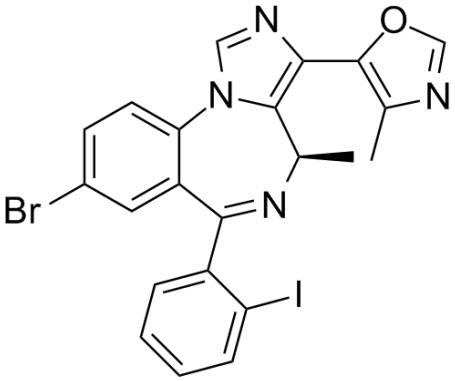
,


N
O
N
N
N
Br
Cl

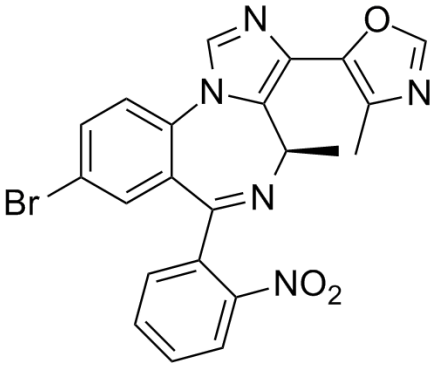
,


N
O
N
N
N
Br
Br

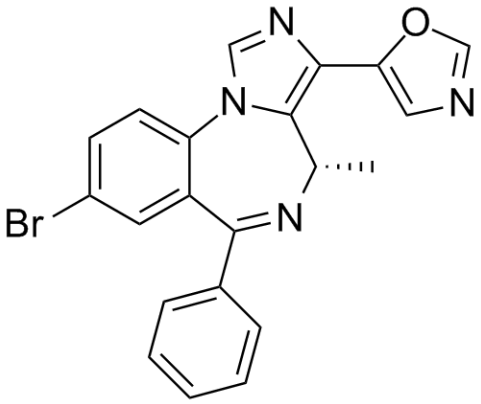
,

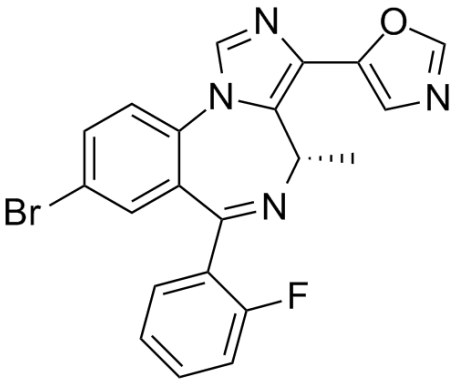

N
O
N
N
N
Br
I

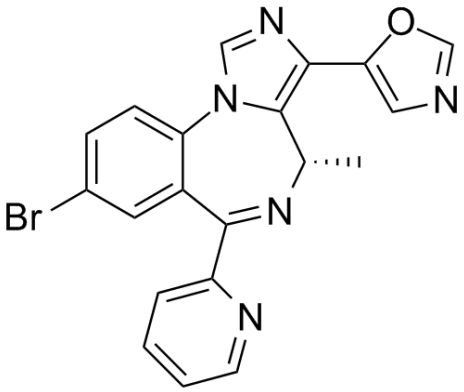
,


N
O
N
N
N
Br
NO2

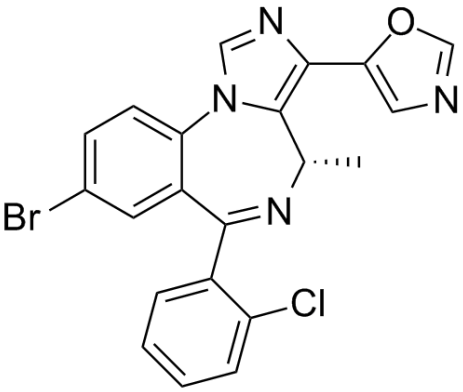
,


N
O
N
N
Br
N

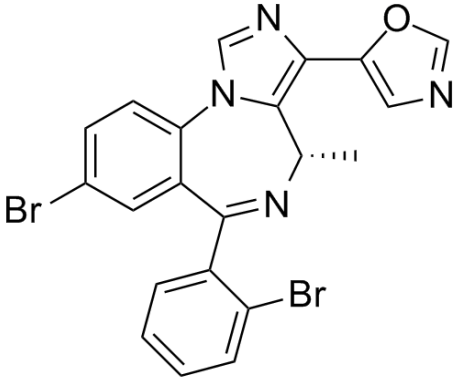

N
O
N
N
Br
N
F


N
O
N
N
Br
N
N

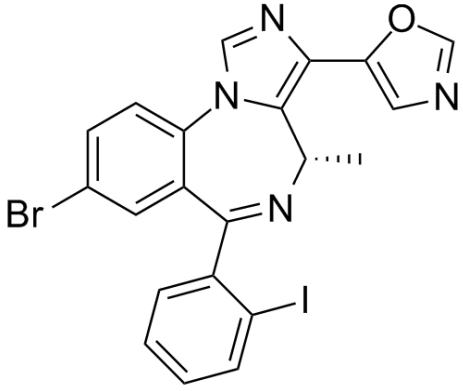
,


N
O
N
N
Br
N
Cl

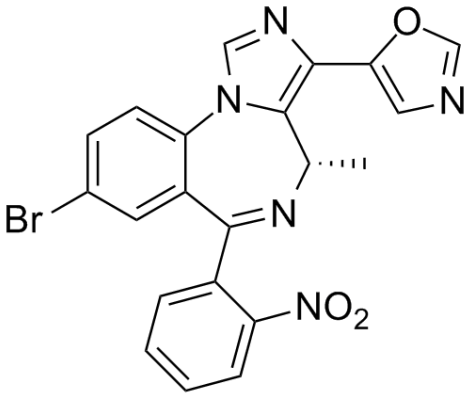
,


N
O
N
N
Br
N
Br

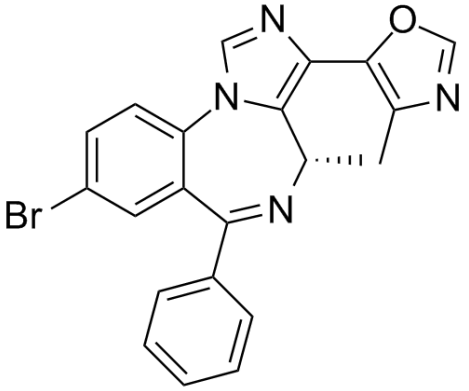
,


N
O
N
N
Br
N
I

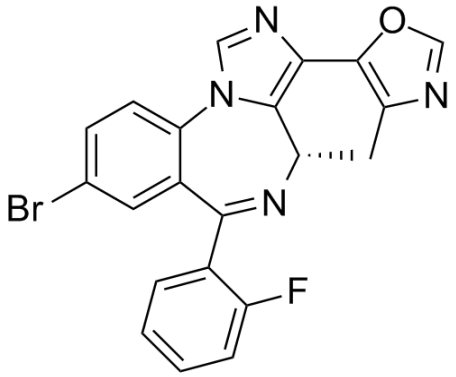
,


N
O
N
N
Br
N
NO2

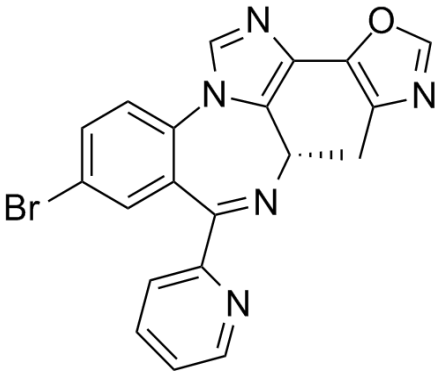
,


N
O
N
N
Br
N

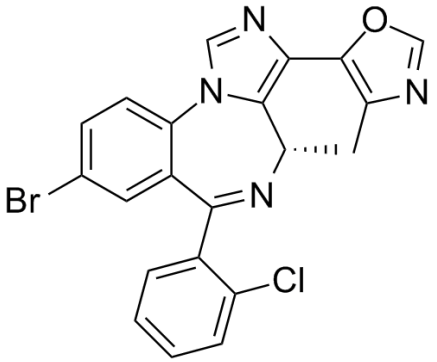
,


N
O
N
N
Br
N
F

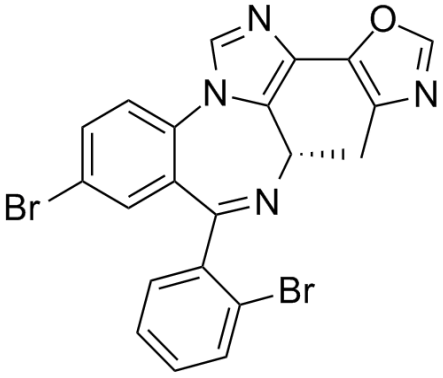
,


N
O
N
N
Br
N
N

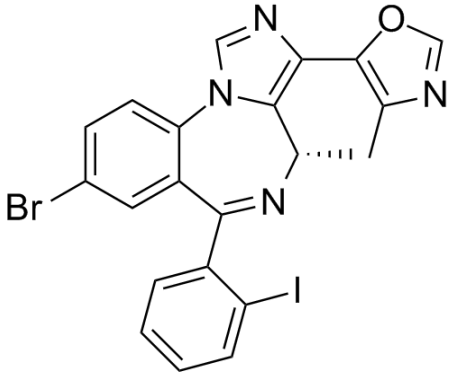
,


N
O
N
N
Br
N
Cl

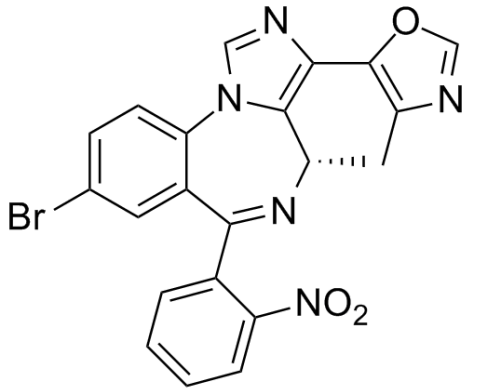
,


N
O
N
N
Br
N
Br

,


N
O
N
N
Br
N
I

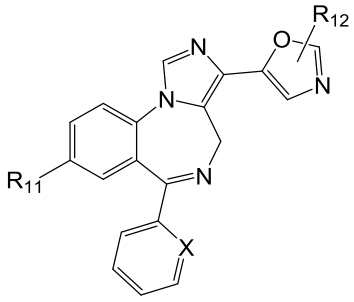
, and



.

13. A pharmaceutical composition comprising a compound according to any of claims 1-12; and a carrier.

14. A pharmaceutical composition comprising a compound according to Formula IV and a carrier, wherein the compound of Formula IV is



(IV)

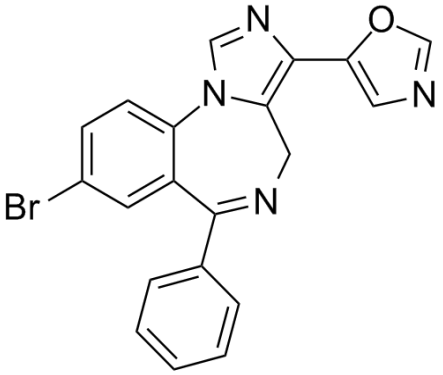
or a salt thereof, wherein:

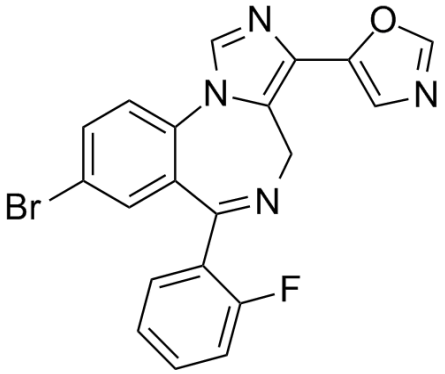
X is selected from the group consisting of N, C-H, C-F, C-Cl, C-Br, C-I, and C-NO_2;

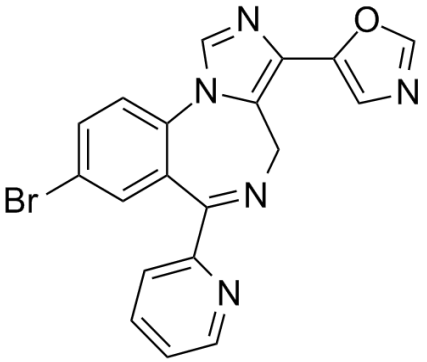
R_{11} is Br; and

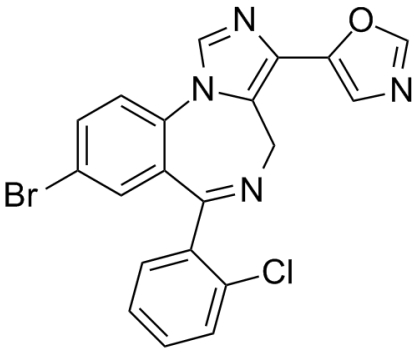
R_{12} is selected from the group consisting of -H, -CH_3, -CH_2CH_3 and -$CH(CH_3)_2$..

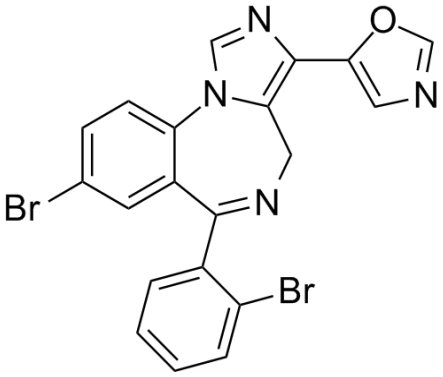
15. The pharmaceutical composition of claim 14, wherein the compound is selected from the group consisting of:

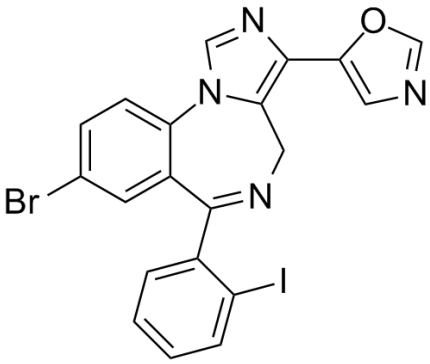


,


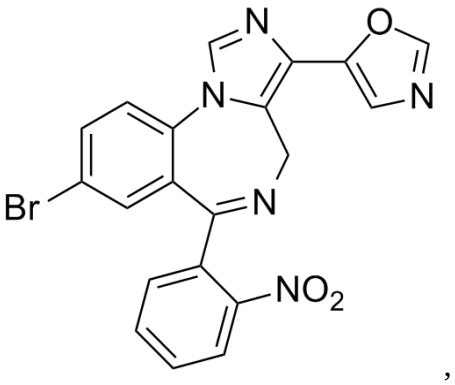
,


,


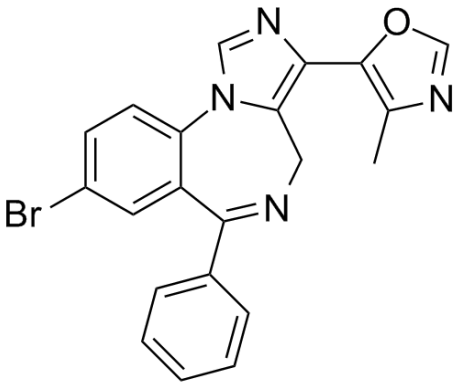
,


,


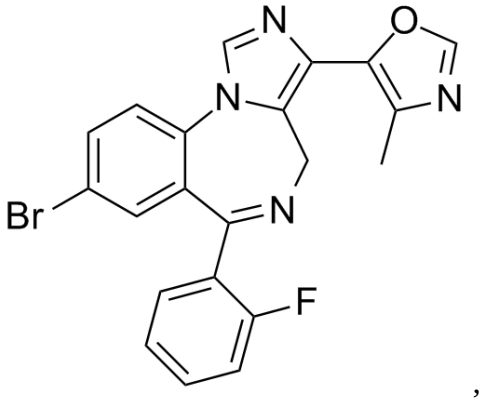
,


N
O
N
N
Br
N
NO2

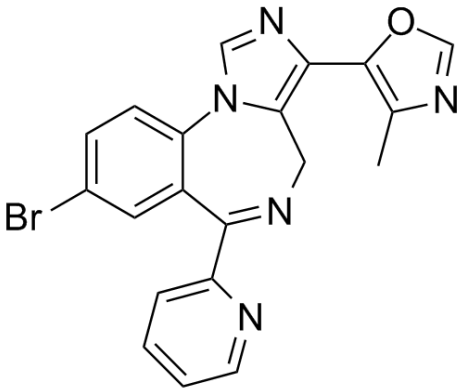
,


N
O
N
N
Br
N

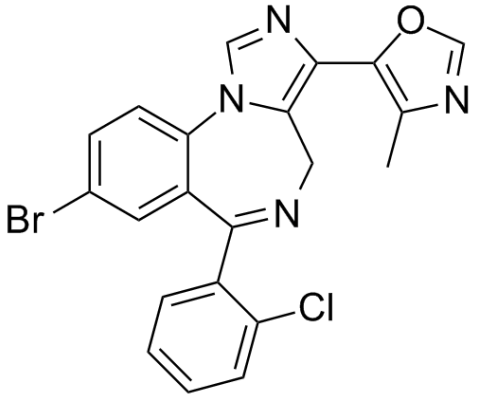
,


N
O
N
N
Br
N
F

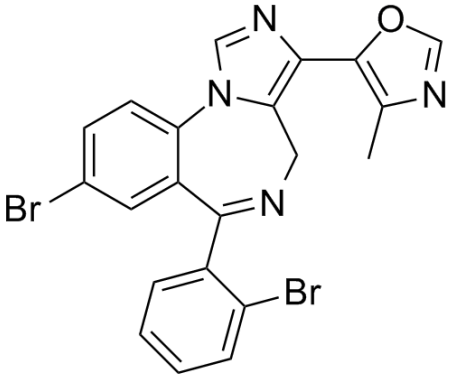
,


N
O
N
N
Br
N
N

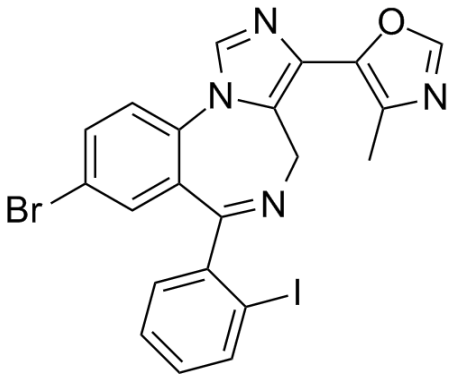
,


N
O
N
N
Br
N
Cl

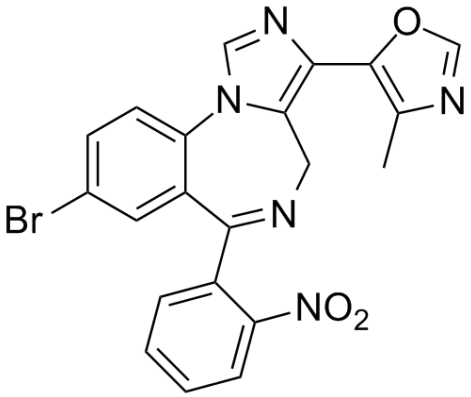
,


N
O
N
N
Br
N
Br

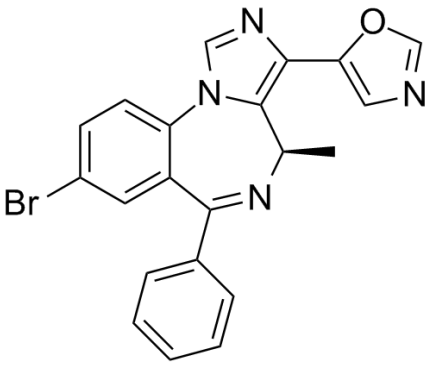
,


N
O
N
N
Br
N
I

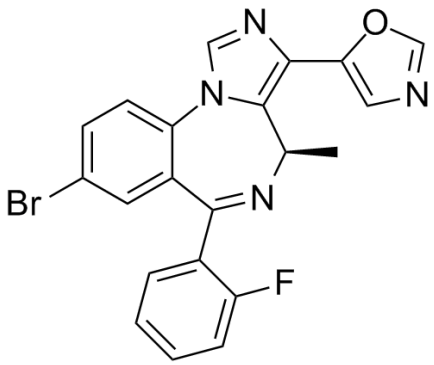
,


N
O
N
N
Br
N
NO2

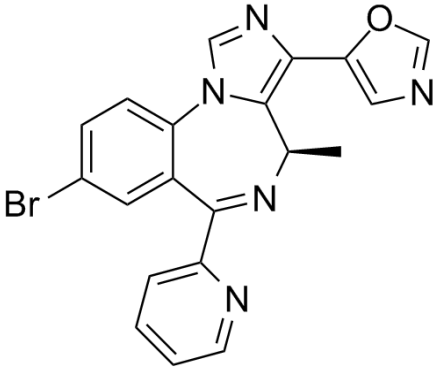
,


N
O
N
N
Br
N

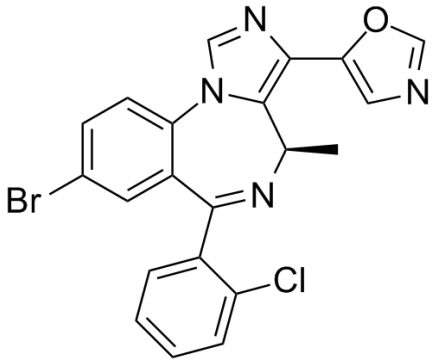
,


N
O
N
N
Br
N
F

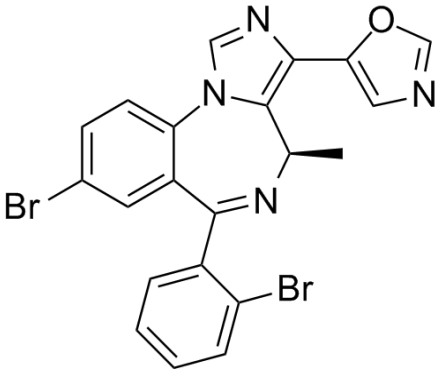
,


N
O
N
N
Br
N
N

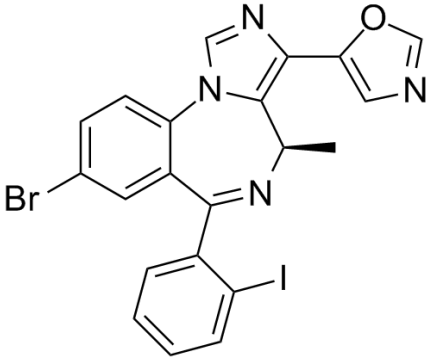
,


N
O
N
N
Br
N
Cl

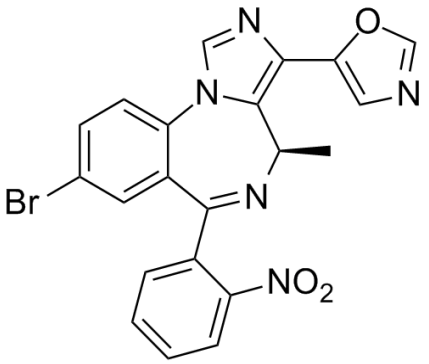
,


N
O
N
N
Br
N
Br

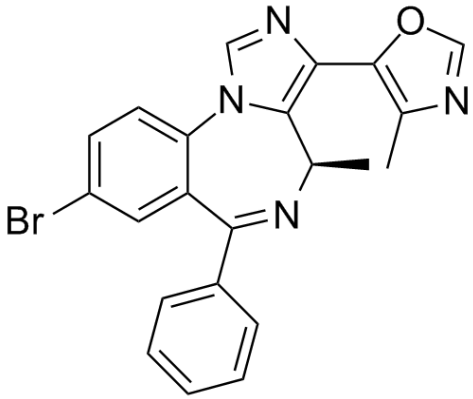
,


N
O
N
N
Br
N
I

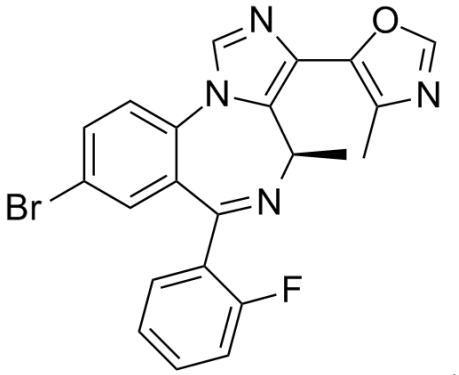
,


N
O
N
N
Br
N
NO2

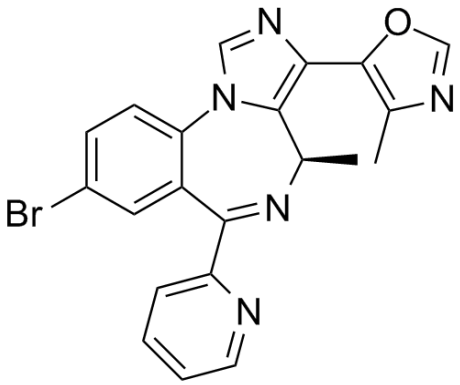
,


N
O
N
N
Br
N

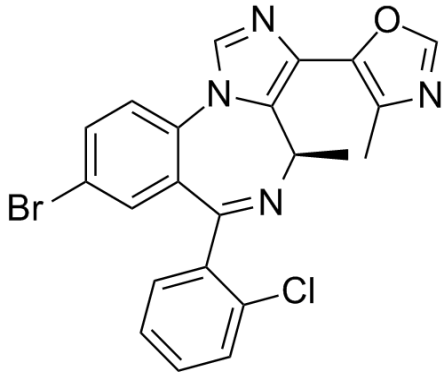
,


N
O
N
N
Br
N
F

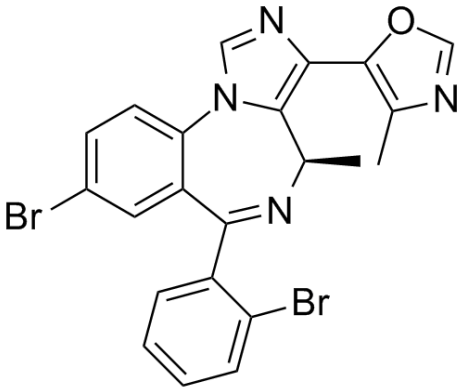
,


N
O
N
N
Br
N
N

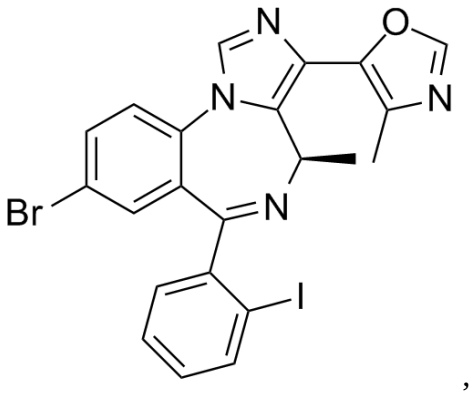
,


N
O
N
N
Br
N
Cl

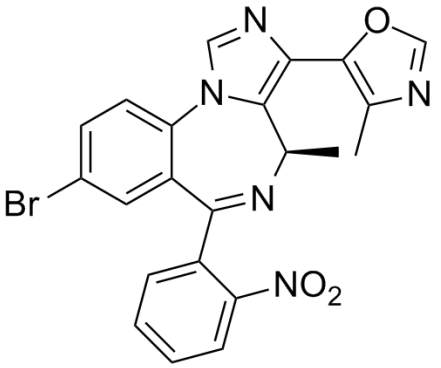
,


N
O
N
N
N
Br
Br

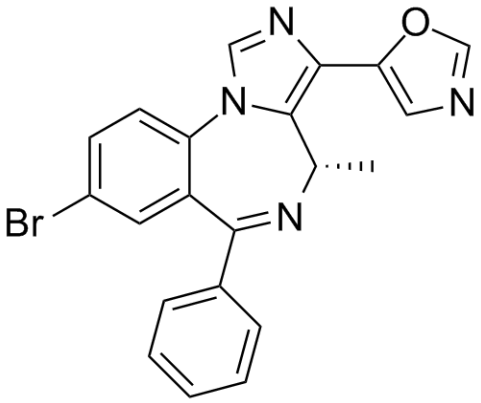
,

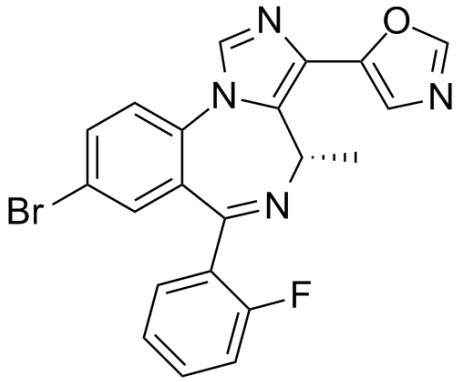

N
O
N
N
N
Br
I

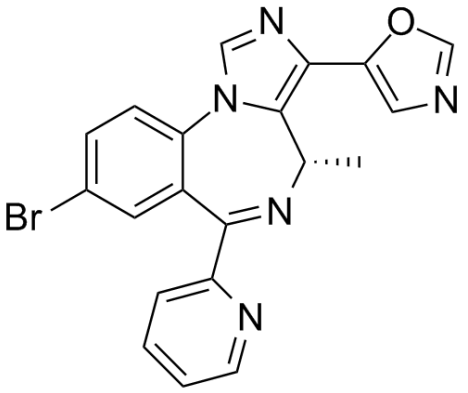
,


N
O
N
N
N
Br
NO2

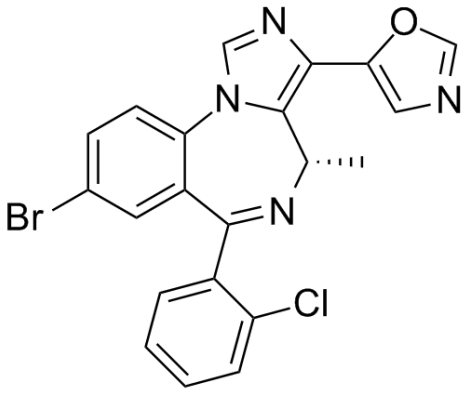
,


N
O
N
N
N
Br

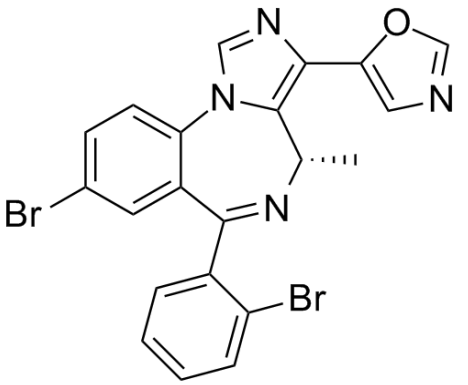

N
O
N
N
N
Br
F


N
O
N
N
N
Br
N

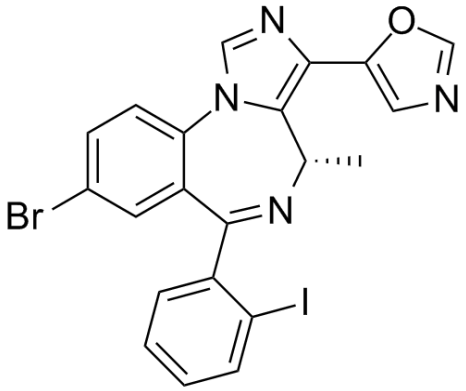
,


N
O
N
N
N
Br
Cl

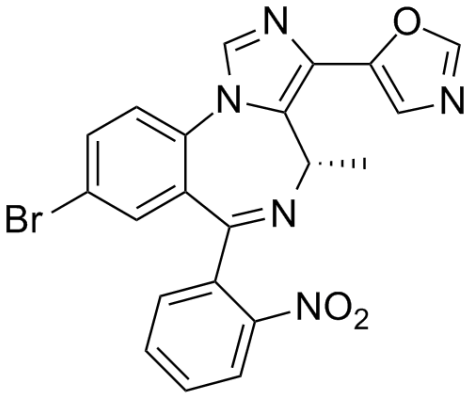
,


N
O
N
N
Br
N
Br

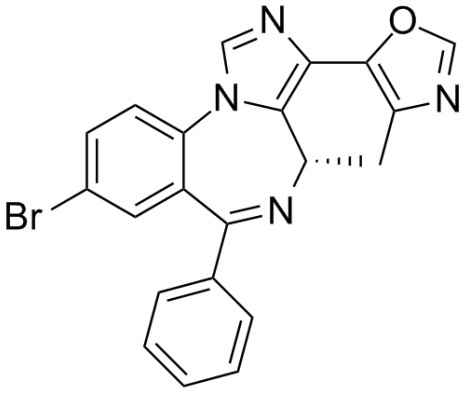
,


N
O
N
N
Br
N
I

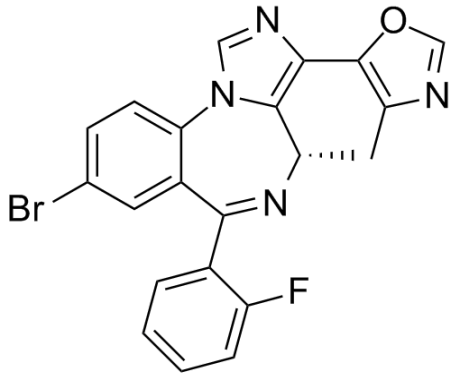
,


N
O
N
N
Br
N
NO2

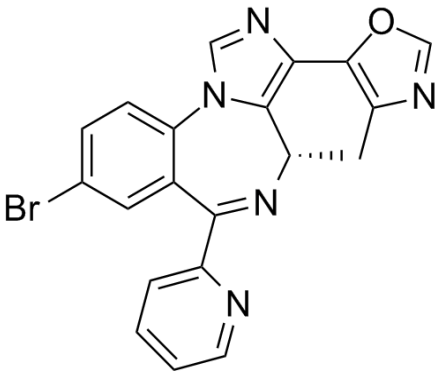
,


N
O
N
N
Br
N

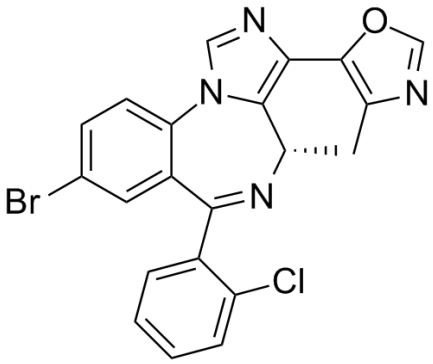
,


N
O
N
N
Br
N
F

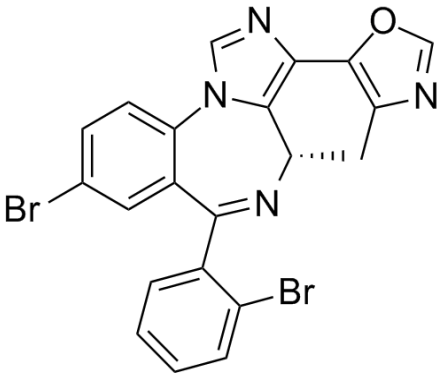
,



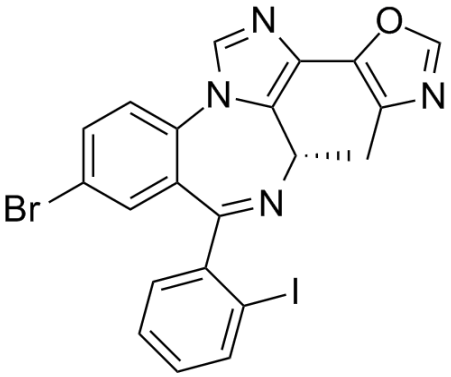
,



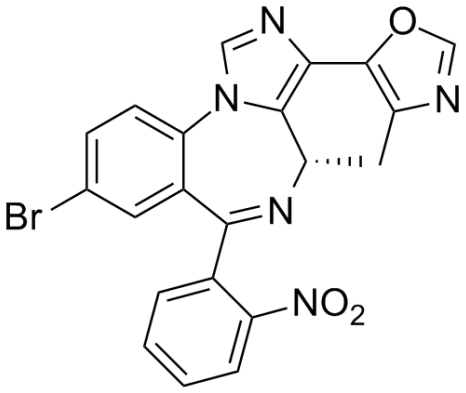
,



,



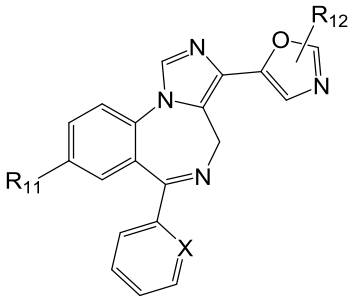
, and



.

16. A method of treating a disorder selected from an anxiety disorder, depression, epilepsy, schizophrenia and neuropathic pain in a subject in need of treatment, comprising administering to the subject an effective amount of a compound of any of claims 1-12 or a composition of claims 13-15.

17. A method of treating a disorder selected from an anxiety disorder, depression, epilepsy, schizophrenia and neuropathic pain in a subject in need of treatment, comprising administering to the subject an effective amount of a compound according to Formula IV:



(IV)

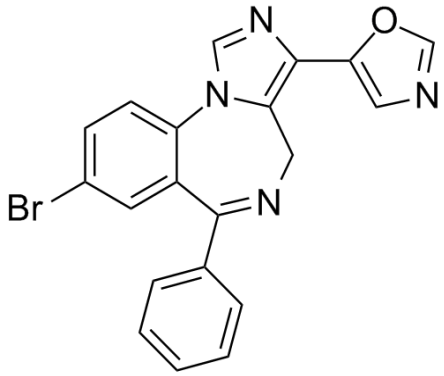
or a salt thereof, wherein:

X is selected from the group consisting of N, C-H, C-F, C-Cl, C-Br, C-I, and C-NO_2;

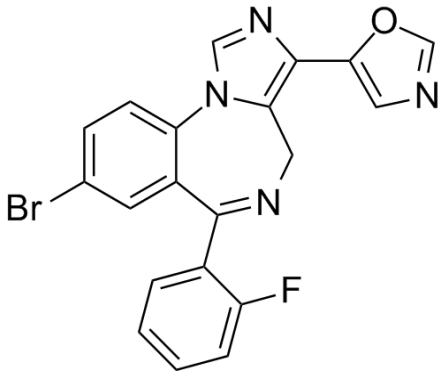
R_{11} is Br; and

R_{12} is selected from the group consisting of -H, -CH_3, -CH_2CH_3 and -$CH(CH_3)_2$..

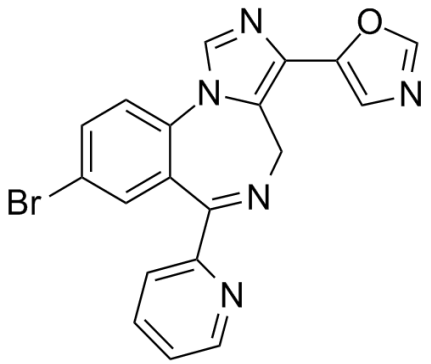
18. The method according to claim 17, wherein the compound is selected from the group consisting of:



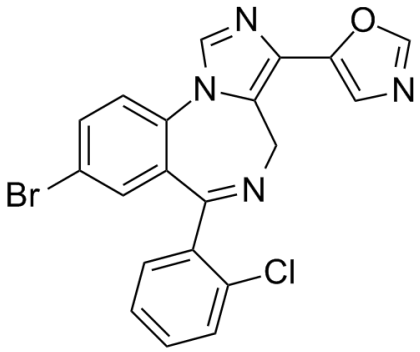
,



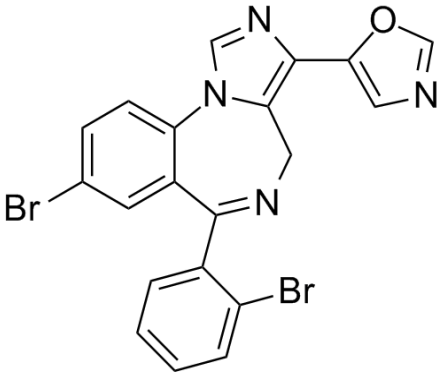
,



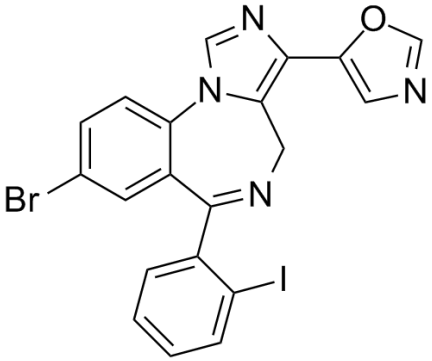
,



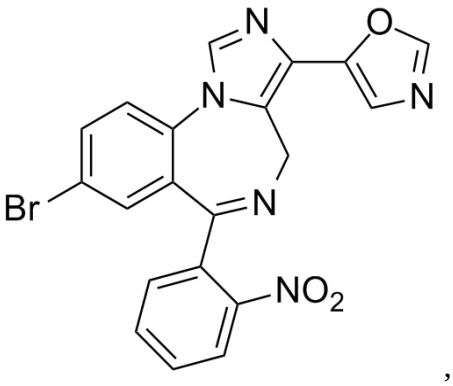
,


N
O
N
N
Br
N
Br

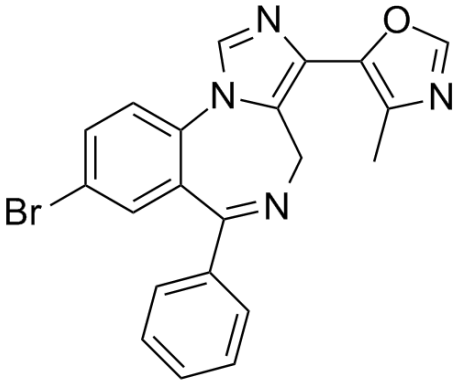
,


N
O
N
N
Br
N
I

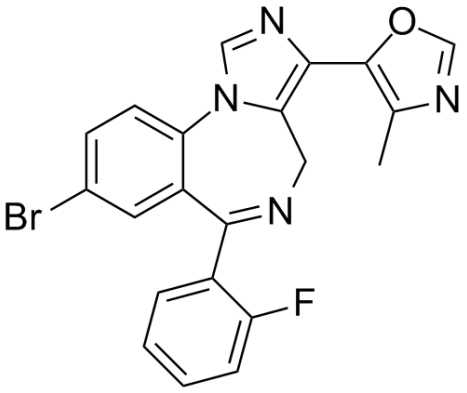
,


N
O
N
N
Br
N
NO2

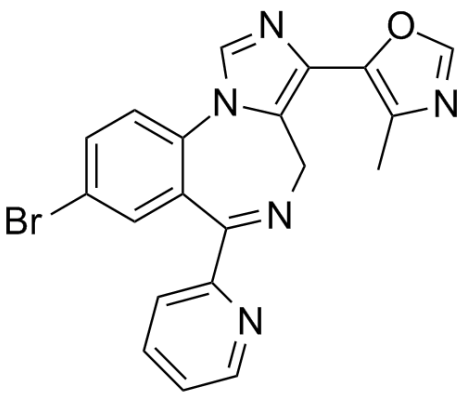
,


N
O
N
N
Br
N

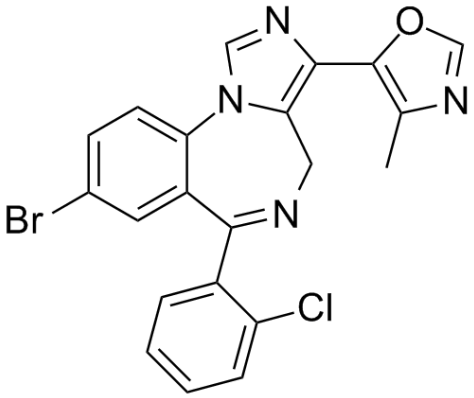
,


N
O
N
N
Br
N
F

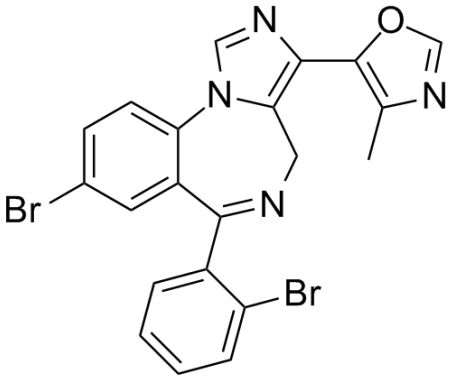
,


N
O
N
N
N
Br
N

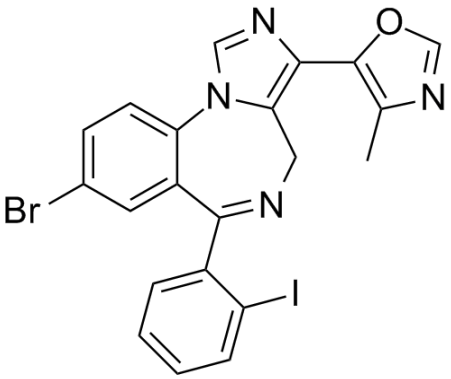
,


N
O
N
N
N
Br
Cl

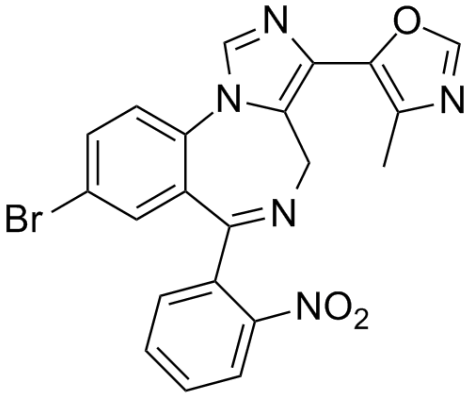
,


N
O
N
N
N
Br
Br

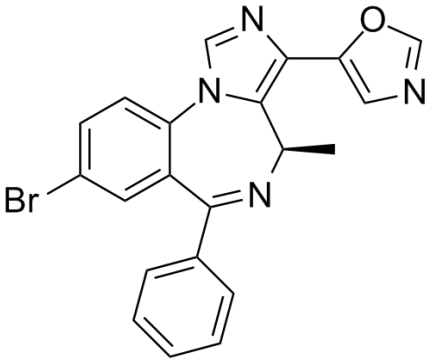
,


N
O
N
N
N
Br
I

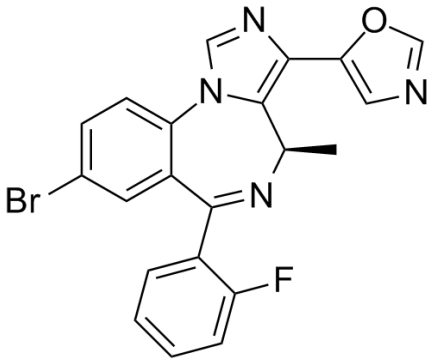
,


N
O
N
N
N
Br
NO2

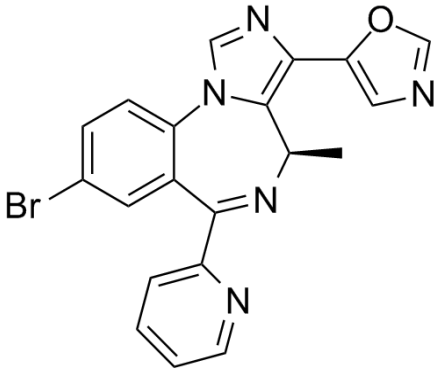
,


N
O
N
N
N
Br

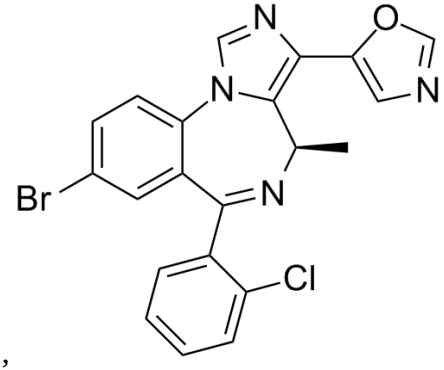
,


N
O
N
N
N
Br
F

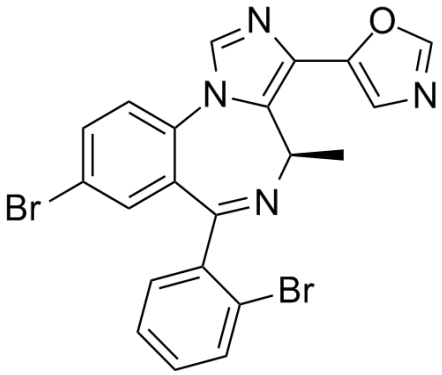
,


N
O
N
N
Br
N
N

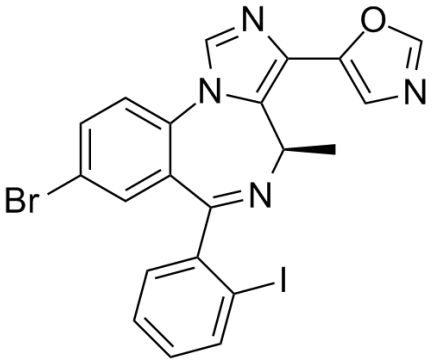
,


N
O
N
N
Br
N
Cl

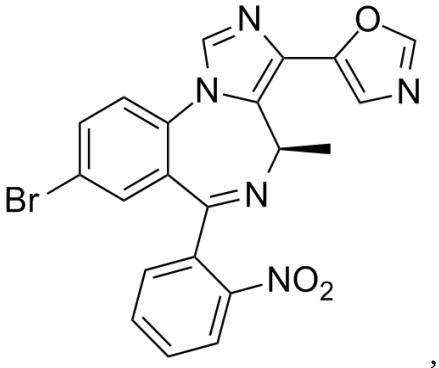
,


N
O
N
N
Br
N
Br

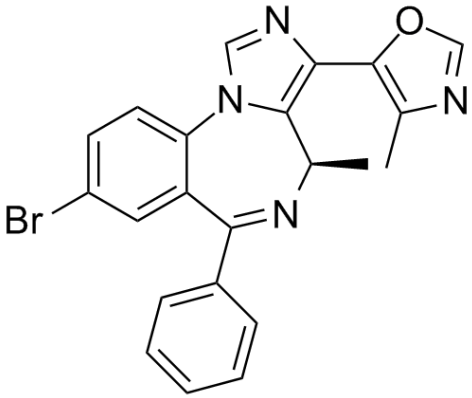
,


N
O
N
N
Br
N
I

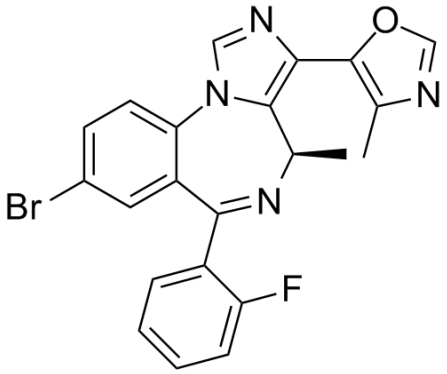
,


N
O
N
N
Br
N
NO2

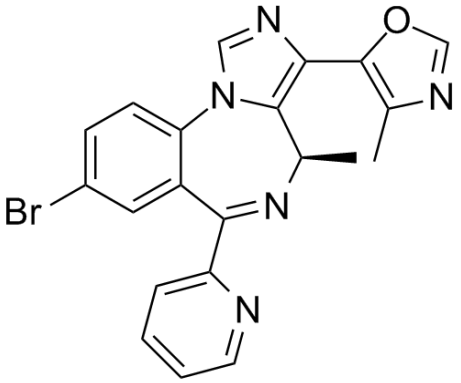
,


N
O
N
N
N
Br

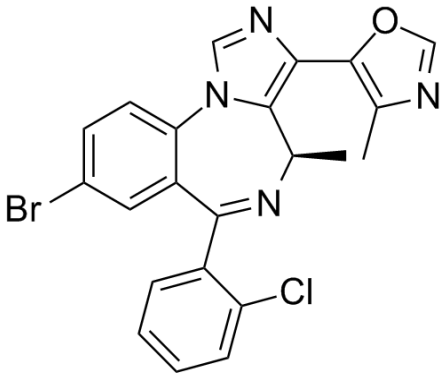
,


N
O
N
N
N
Br
F

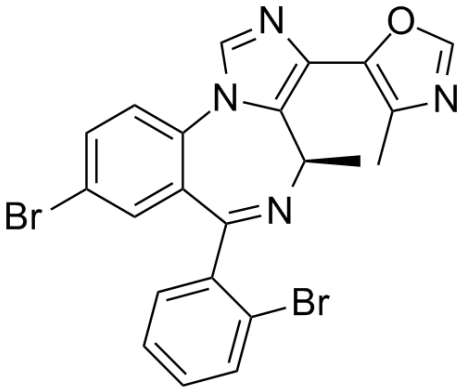
,


N
O
N
N
N
Br
N

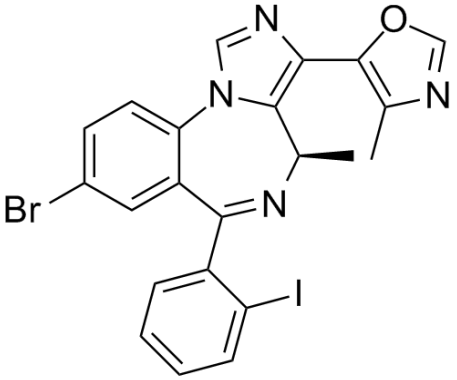
,


N
O
N
N
N
Br
Cl

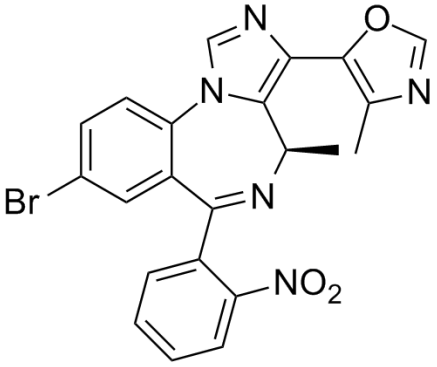
,


N
O
N
N
N
Br
Br

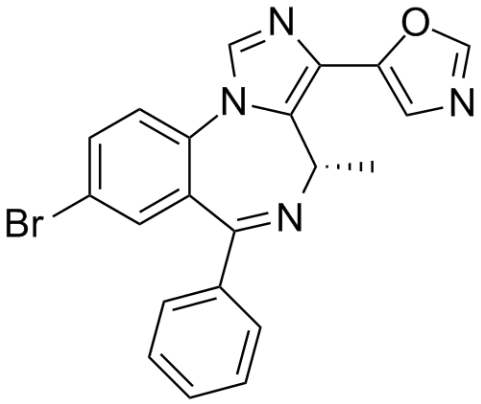
,

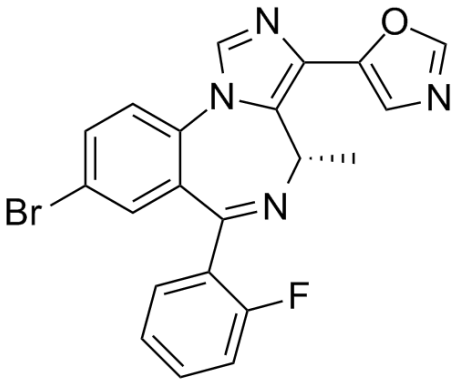

N
O
N
N
N
Br
I

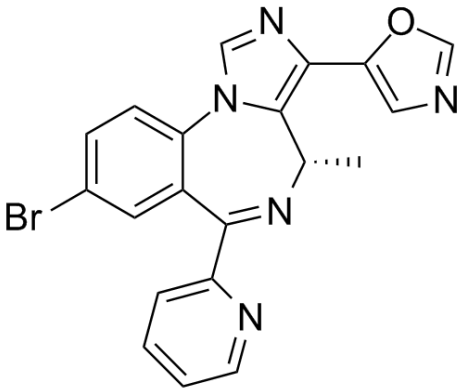
,


N
O
N
N
N
Br
NO2

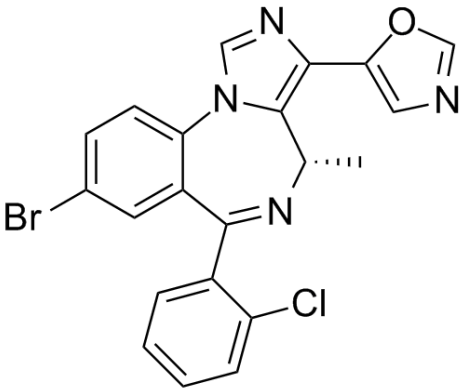
,


N
O
N
N
Br
N

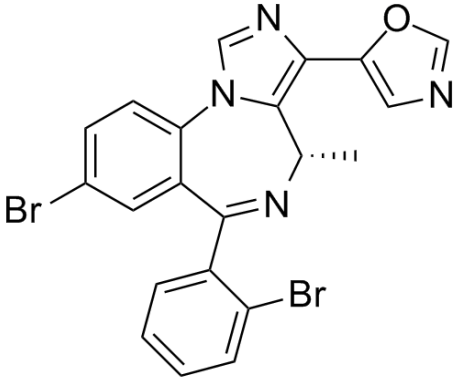

N
O
N
N
Br
N
F


N
O
N
N
Br
N
N

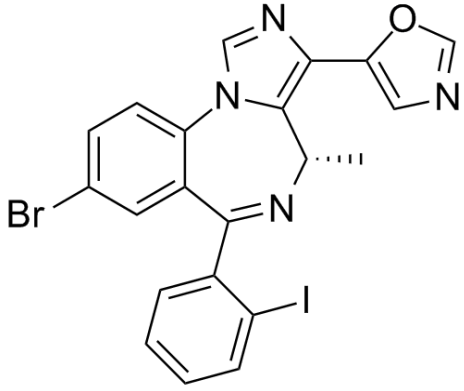
,


N
O
N
N
Br
N
Cl

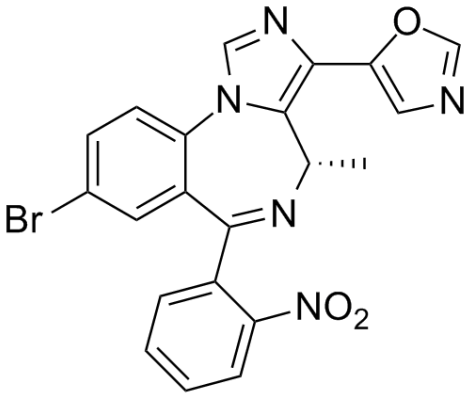
,


N
O
N
N
Br
N
Br

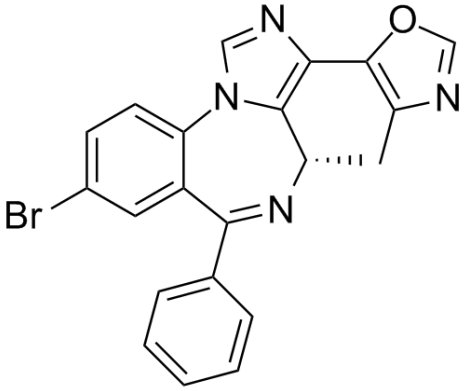
,


N
O
N
N
Br
N
I

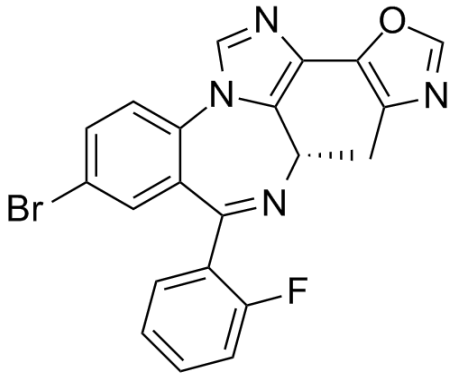
,


N
O
N
N
Br
N
NO2

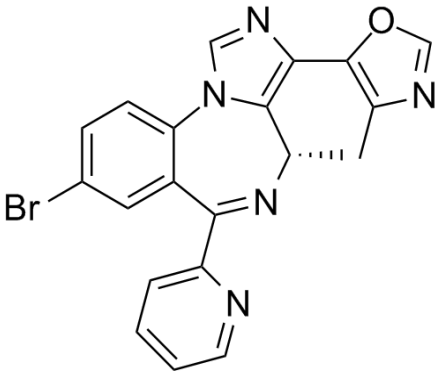
,


N
O
N
N
Br
N

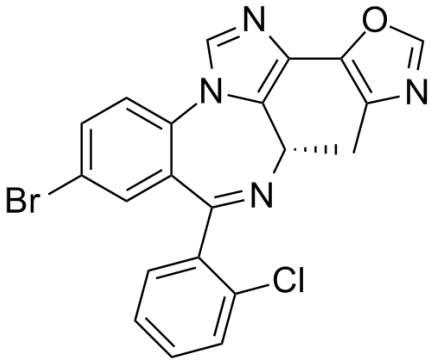
,


N
O
N
N
Br
N
F

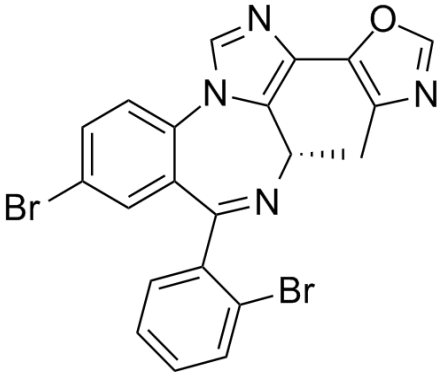
,


N
O
N
N
Br
N
N

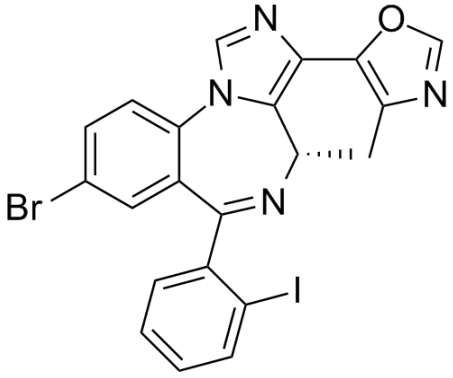
,


N
O
N
N
Br
N
Cl

,

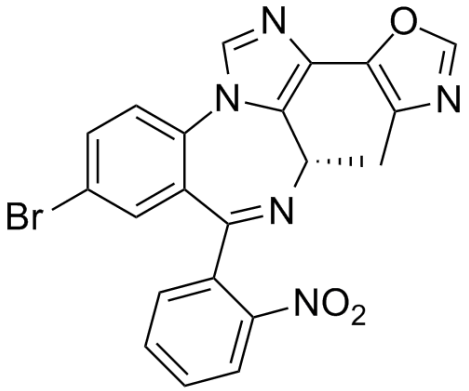

N
O
N
N
Br
N
Br

,


N
O
N
N
Br
N
I

, and

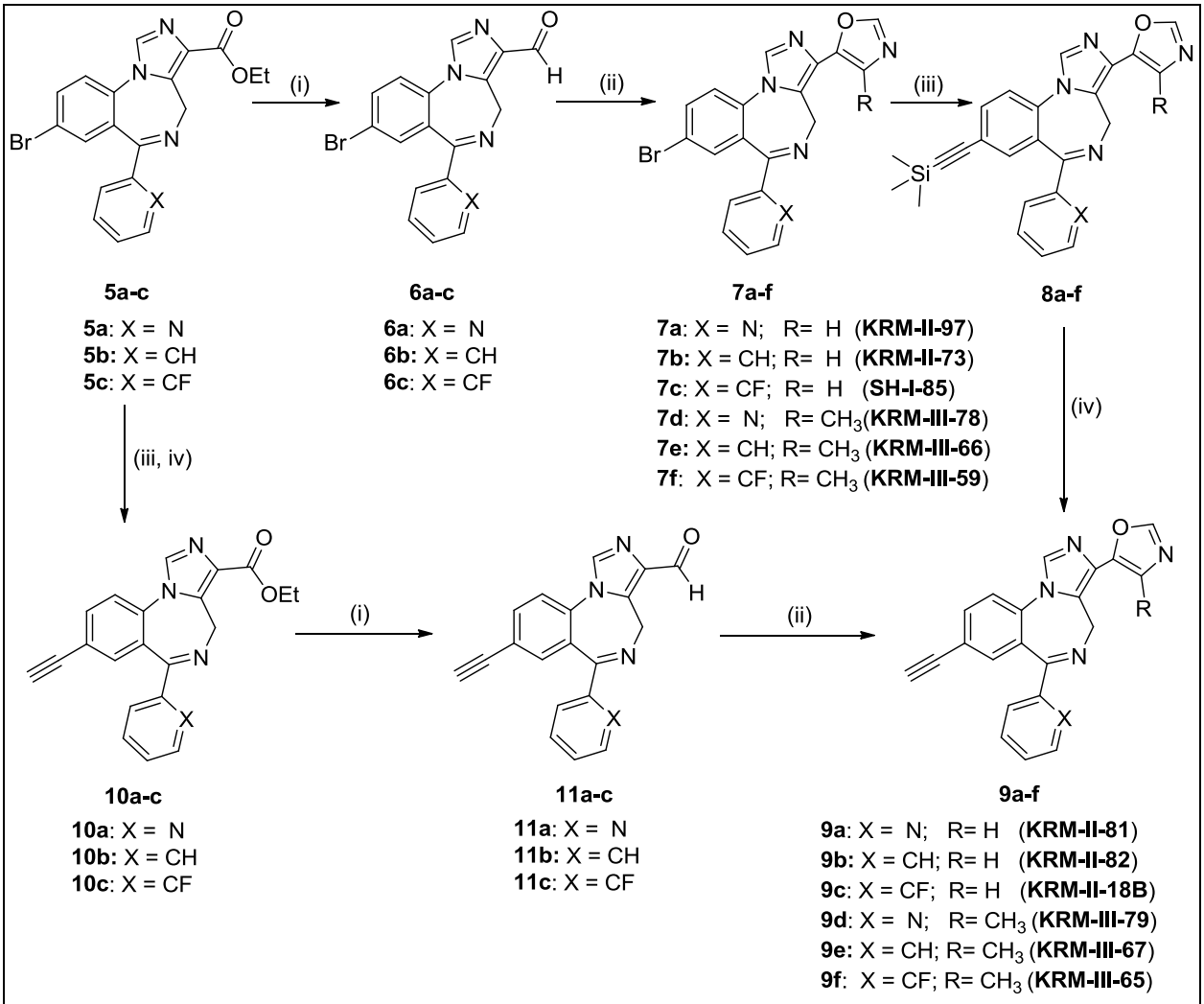
OTT1436



.

ABSTRACT

Described herein are α3 or α2 or α2/α3 GABAergic receptor subtype selective ligands, pharmaceutical compositions, and methods of use of such ligands and compositions in treatment of anxiety disorders, epilepsy and schizophrenia with reduced sedative and ataxic side effects. In embodiments, such as α3 or α2 or α2/α3 GABAergic receptor subtype selective ligands lack ester linkages and may be thus relatively insensitive to hydrolysis by esterases.



Reagents and conditions: (i) **Method 1** (a) $LiAlH_4$, dry THF, 0°C -rt ,1h, (b) MnO_2, Na_2CO_3, dry CH_2Cl_2 (for **6a** and **11a**,40 % over 2 steps), **Method 2.** DIBAL-H, -78 °C 2-3 h, (74-80% **6b**, **6c, 11b** and **11c**), (ii) TOSMIC **(**for R= H) or α–Methyl TOSMIC (for R= CH_3), K_2CO_3, MeOH, 80-90 °C, 2-3 h, 73-82%, (iii) TMS acetylene, $Pd(OAc)_2$ ($PPh_{3)2}$, TEA/CH_3CN (1:1), rf, 10 h, 80-93 %, (iv) TBAF, THF, 0°C- rt, 1-2 h, 82-93%.

FIG. 1

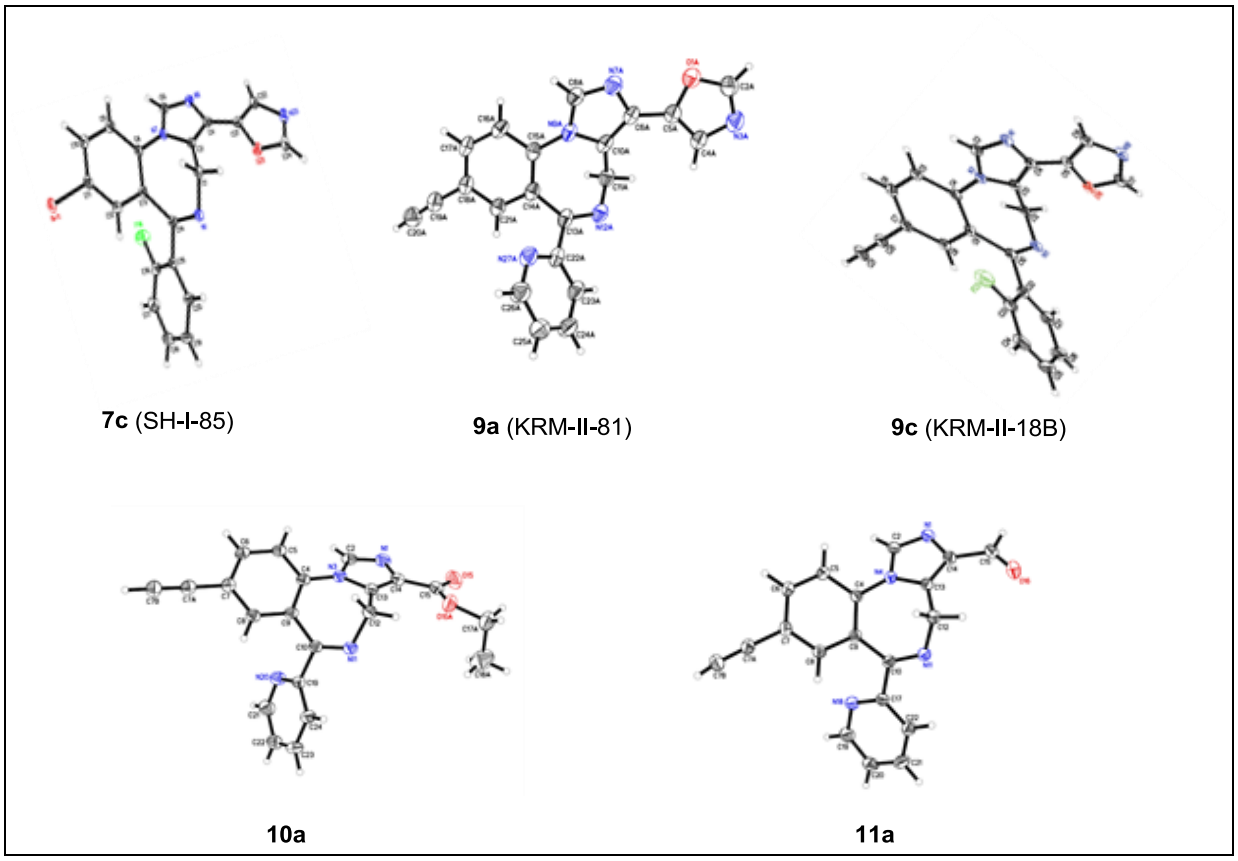


FIG. 2

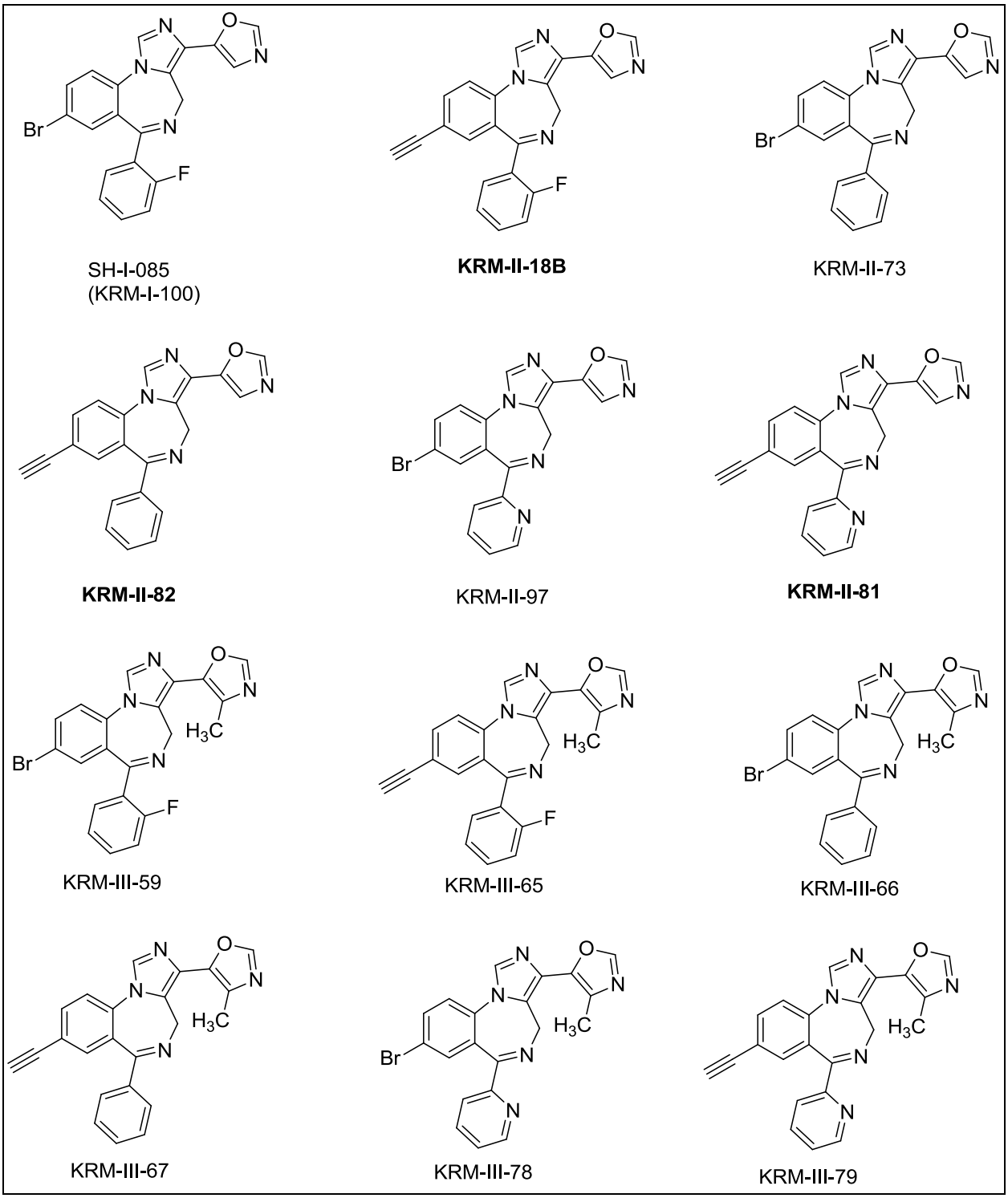

SH-I-085
(KRM-I-100)
KRM-II-18B
KRM-II-73
KRM-II-82
KRM-II-97
KRM-II-81
KRM-III-59
KRM-III-65
KRM-III-66
KRM-III-67
KRM-III-78
KRM-III-79

FIG. 3A

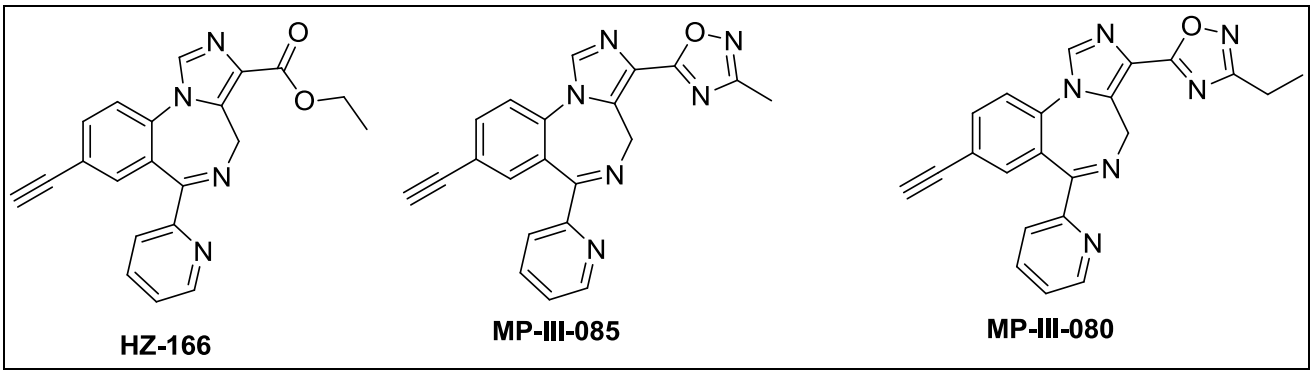


FIG. 3B

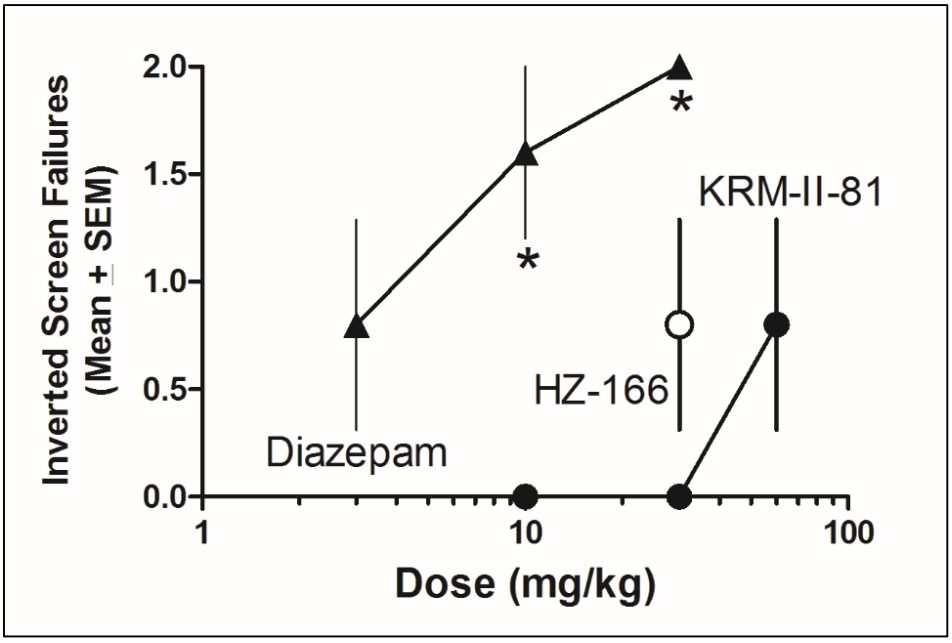

Inverted Screen Failures
(Mean ± SEM)
2.0
1.5
1.0
0.5
0.0
1
10
100
Dose (mg/kg)
*
*
KRM-II-81
HZ-166
Diazepam

FIG. 4

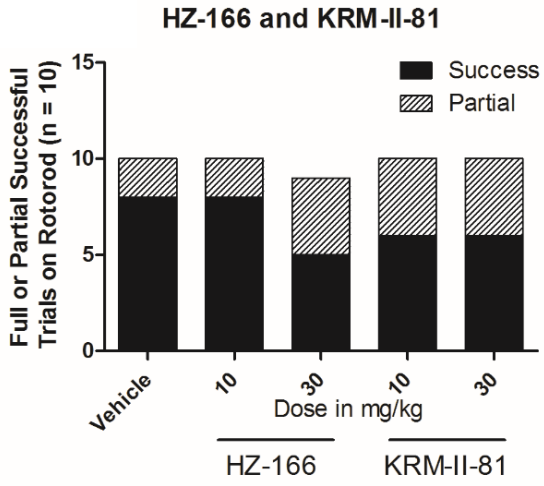


FIG. 5A

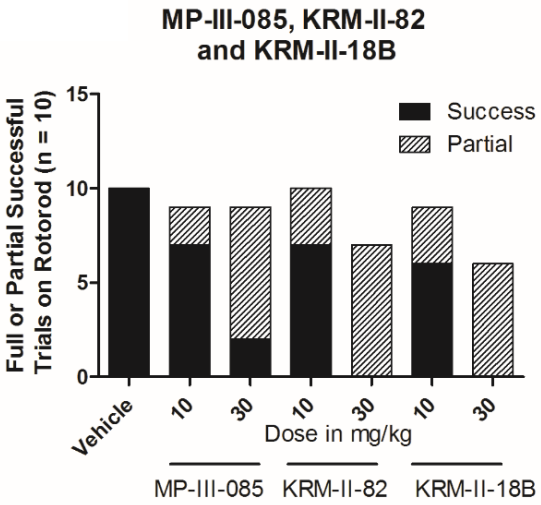


FIG. 5B

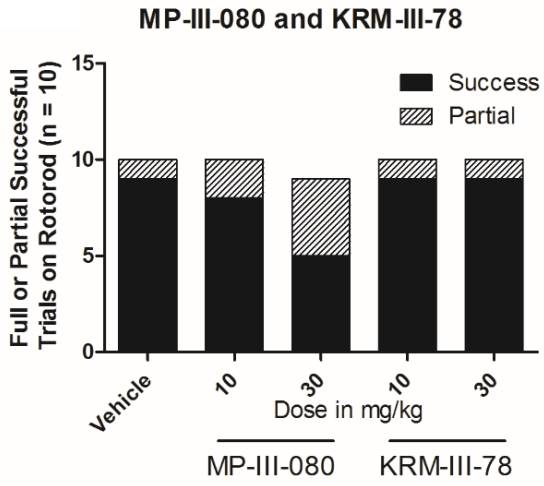


FIG. 5C

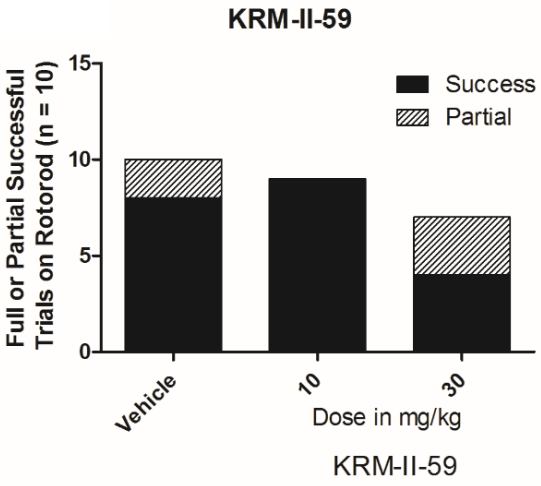


FIG. 5D

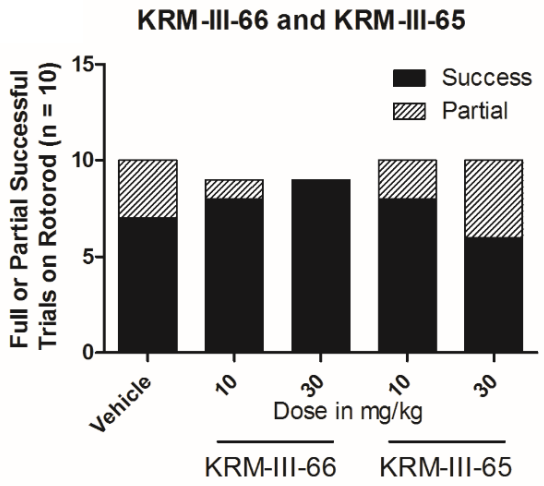


FIG. 5E

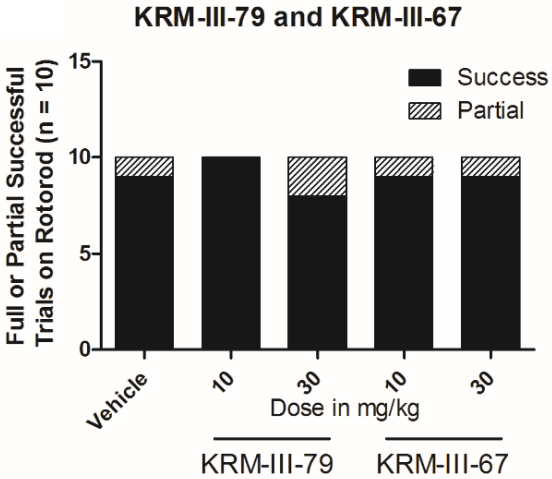


FIG. 5F

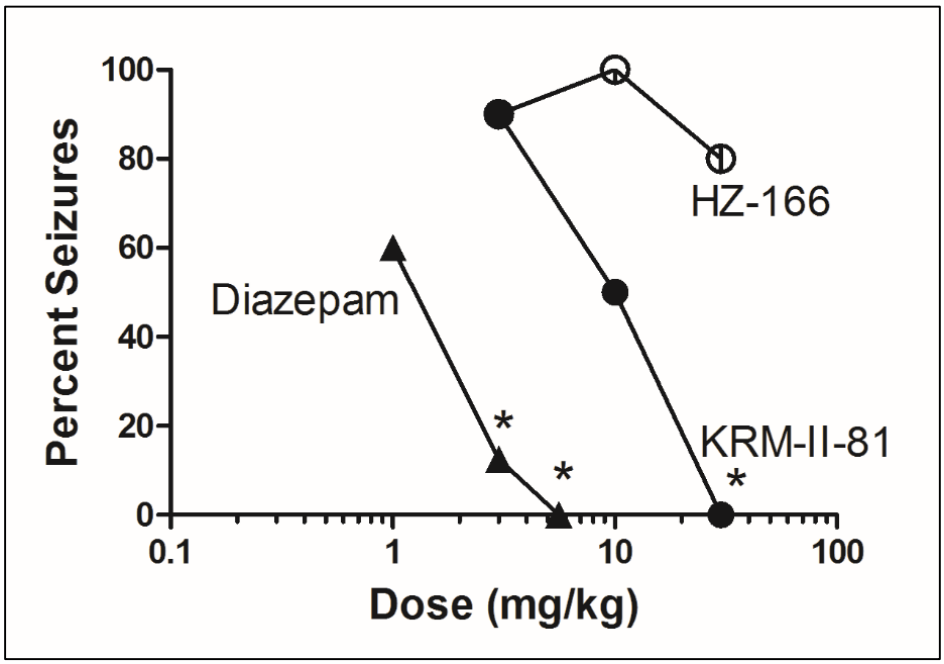

Percent Seizures
100
80
60
40
20
0
0.1
1
10
100
Dose (mg/kg)
Diazepam
HZ-166
KRM-II-81
*
*
*

FIG. 6

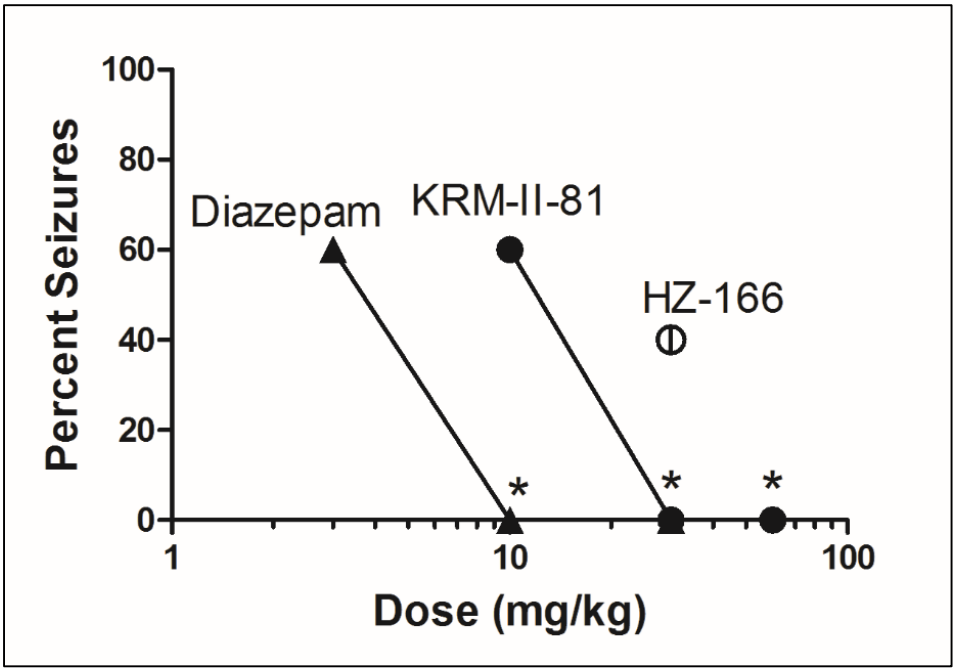

Percent Seizures
100
80
60
40
20
0
Diazepam
KRM-II-81
HZ-166
*
*
*
1
10
100
Dose (mg/kg)

FIG. 7

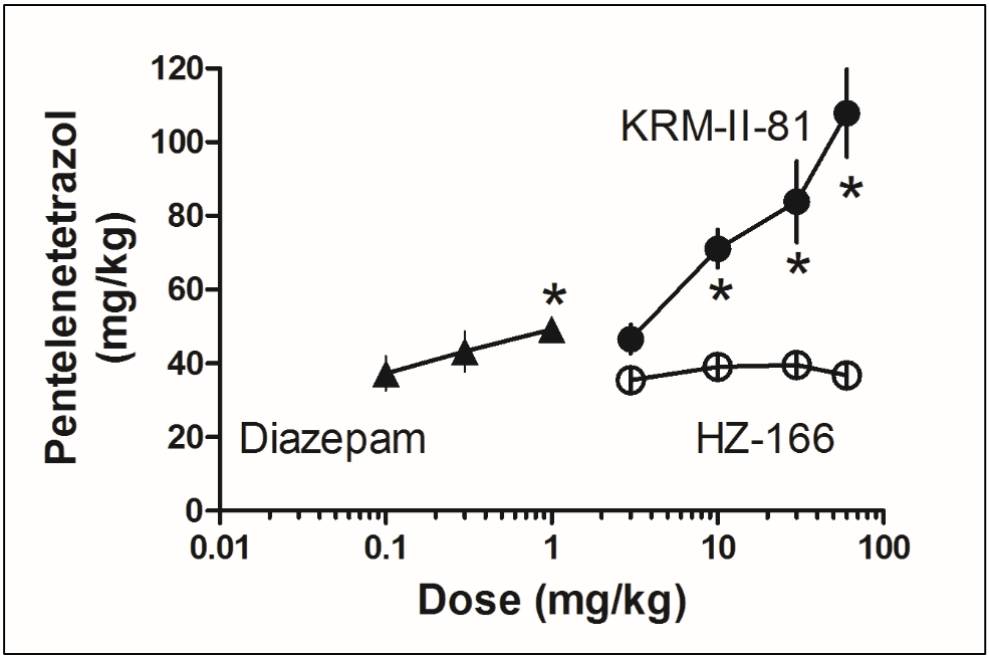

Pentelenetetrazol (mg/kg)
120
100
80
60
40
20
0
KRM-II-81
*
*
*
*
Diazepam
HZ-166
0.01
0.1
1
10
100
Dose (mg/kg)

FIG. 8

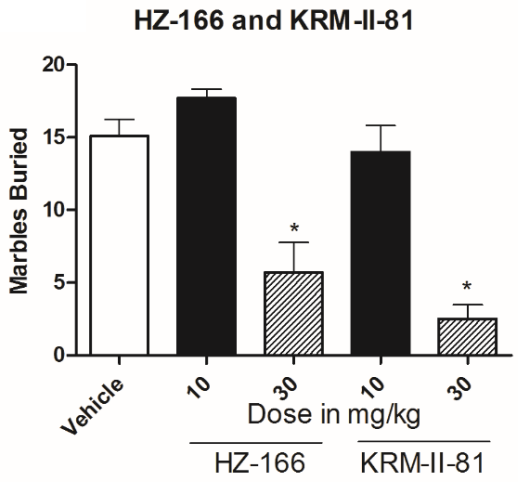


FIG. 9A

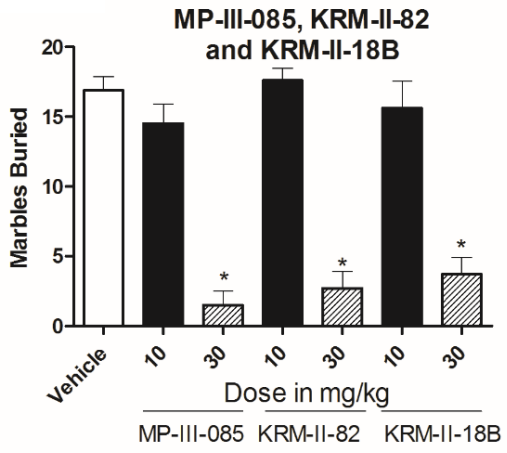


FIG. 9B

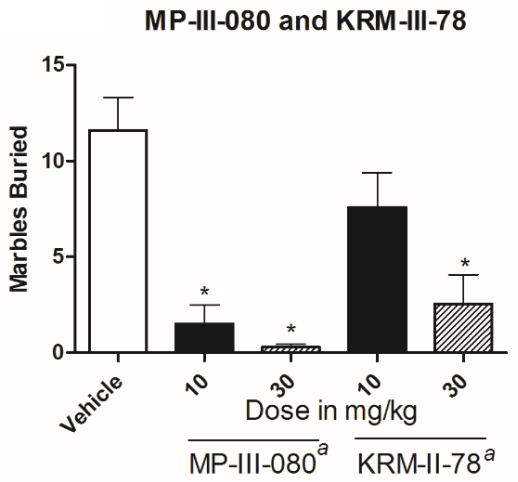


FIG. 9C

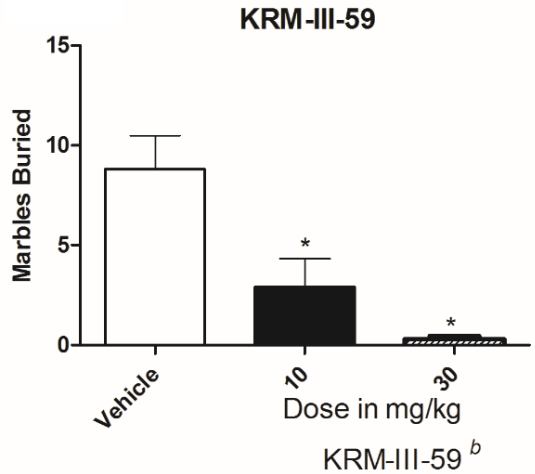


FIG. 9D

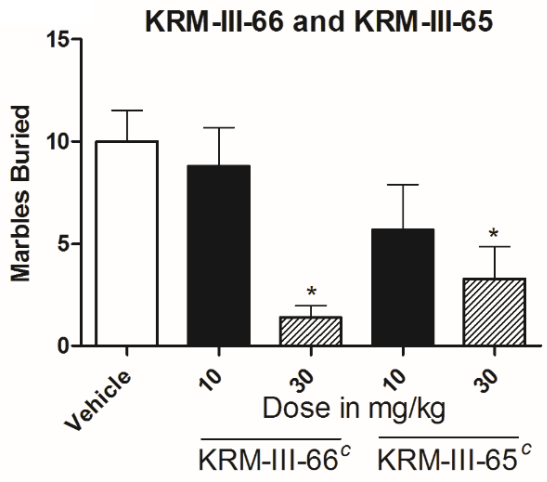


FIG. 9E

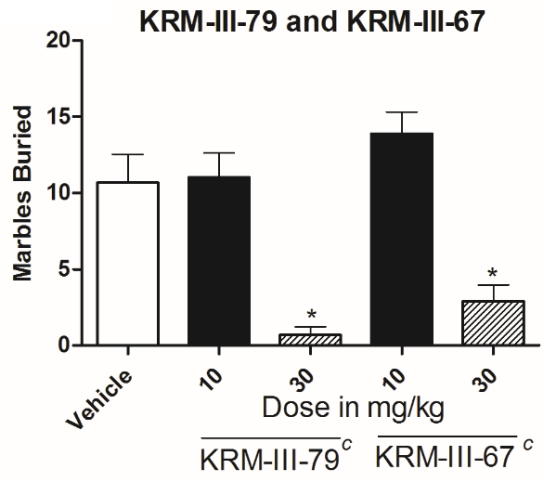


FIG. 9F

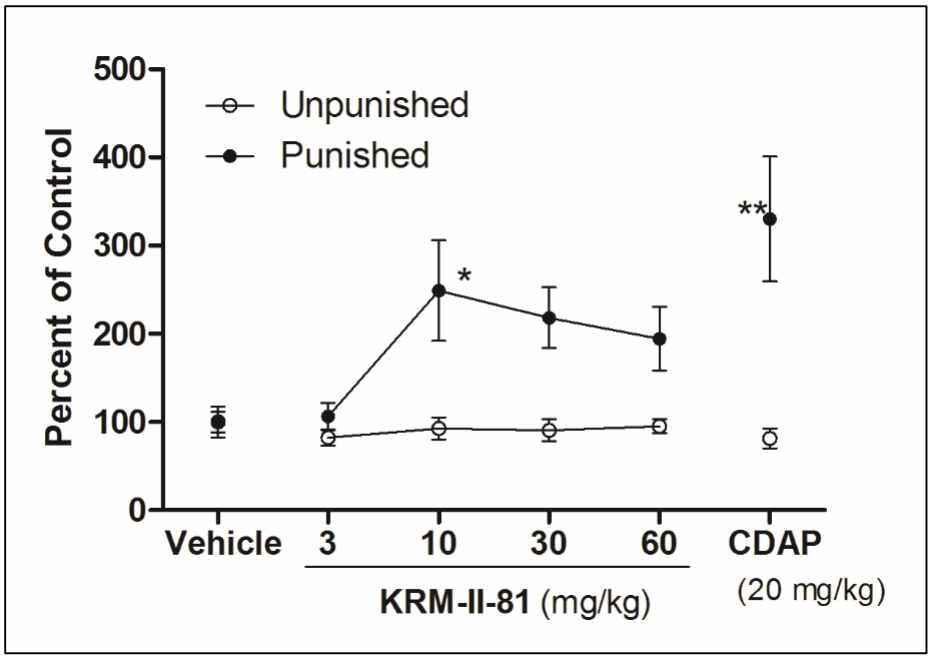

500
400
300
200
100
0
Percent of Control
Unpunished
Punished
*
**
Vehicle
3
10
30
60
CDAP
(20 mg/kg)
KRM-II-81 (mg/kg)

FIG. 10

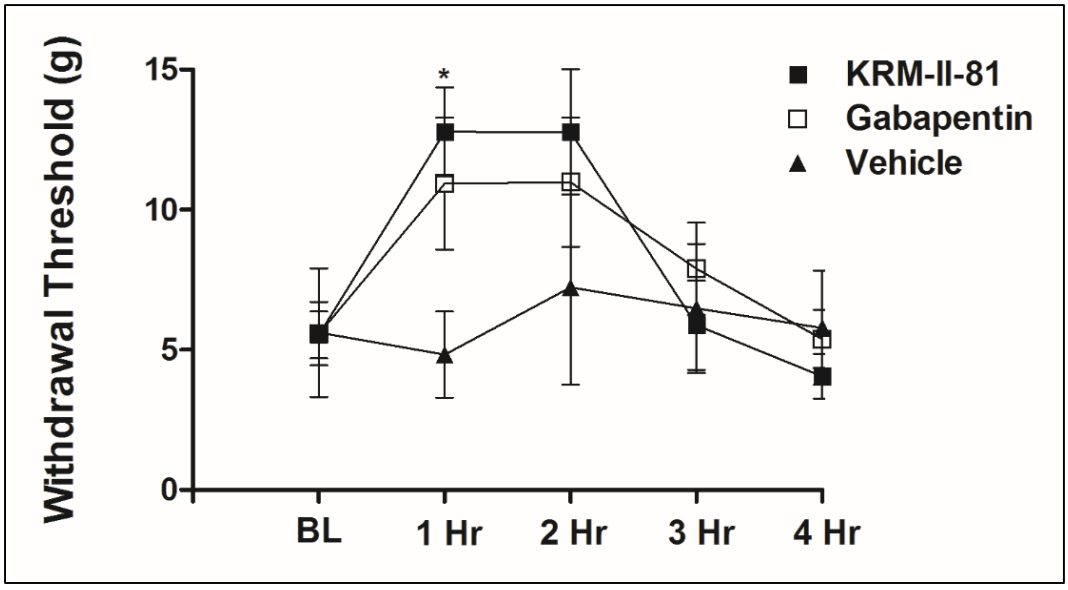

15
10
5
0
Withdrawal Threshold (g)
*
KRM-II-81
Gabapentin
Vehicle
BL
1 Hr
2 Hr
3 Hr
4 Hr

FIG. 11

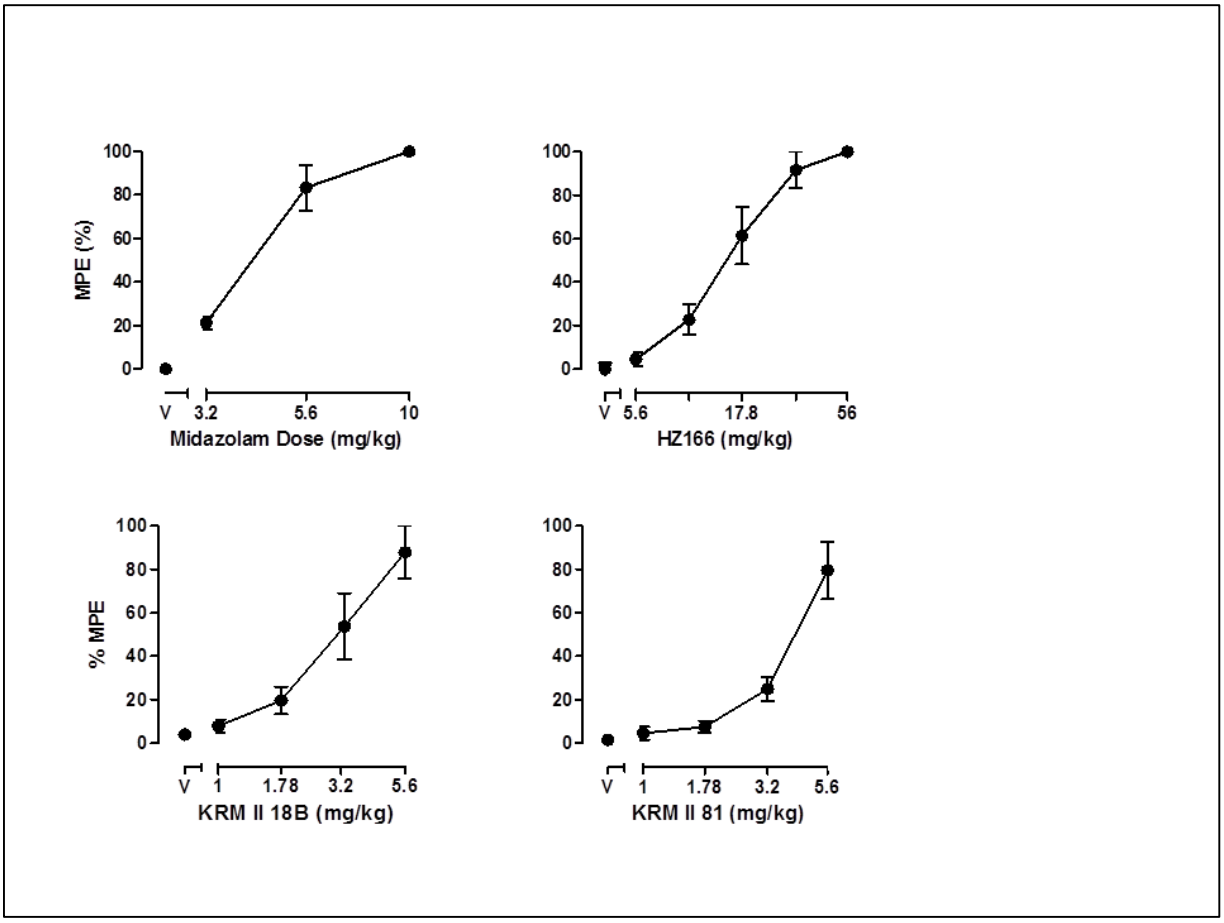

MPE (%)
100
80
60
40
20
0
V
3.2
5.6
10
Midazolam Dose (mg/kg)
V
5.6
17.8
56
HZ166 (mg/kg)
% MPE
V
1
1.78
3.2
5.6
KRM II 18B (mg/kg)
KRM II 81 (mg/kg)

FIG. 12

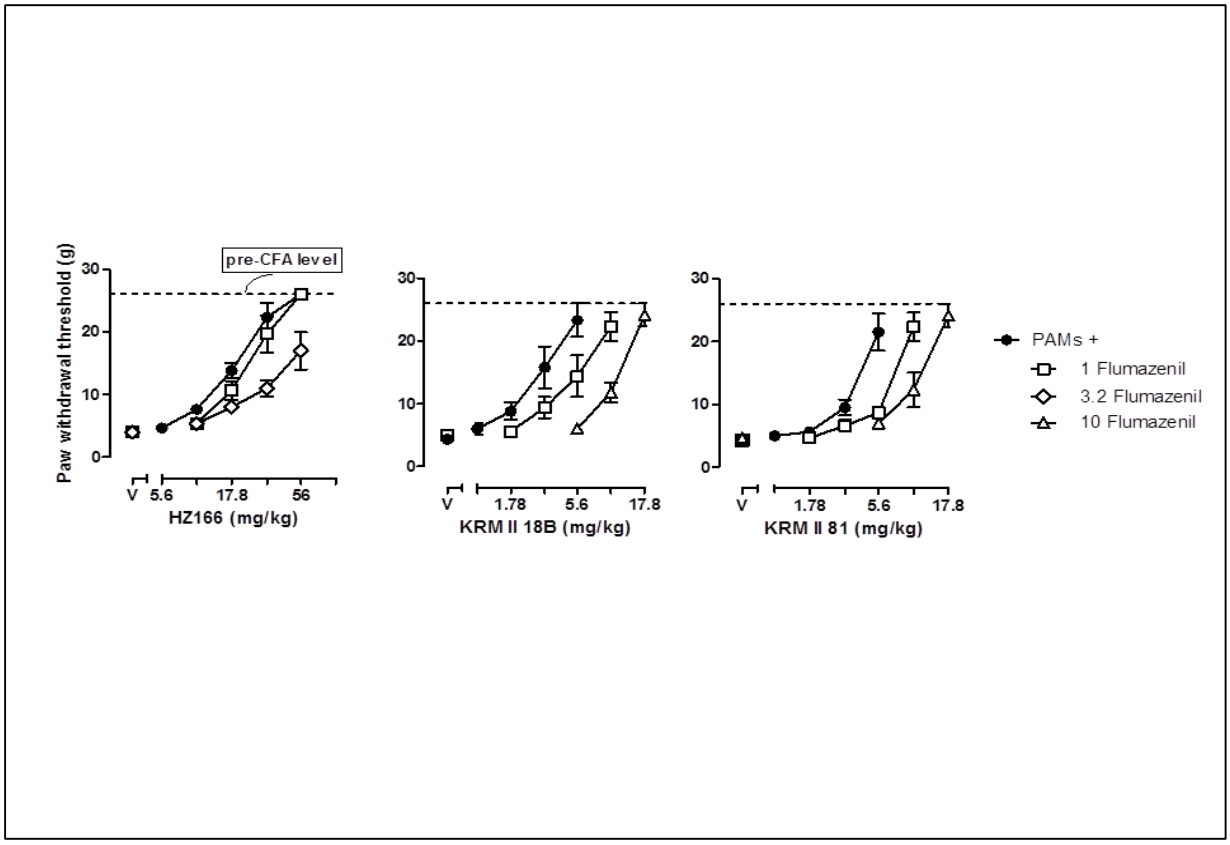

pre-CFA level
Paw withdrawal threshold (g)
30
20
10
0
V
5.6
17.8
56
HZ166 (mg/kg)
V
1.78
5.6
17.8
KRM II 18B (mg/kg)
V
1.78
5.6
17.8
KRM II 81 (mg/kg)
PAMs +
1 Flumazenil
3.2 Flumazenil
10 Flumazenil

FIG. 13

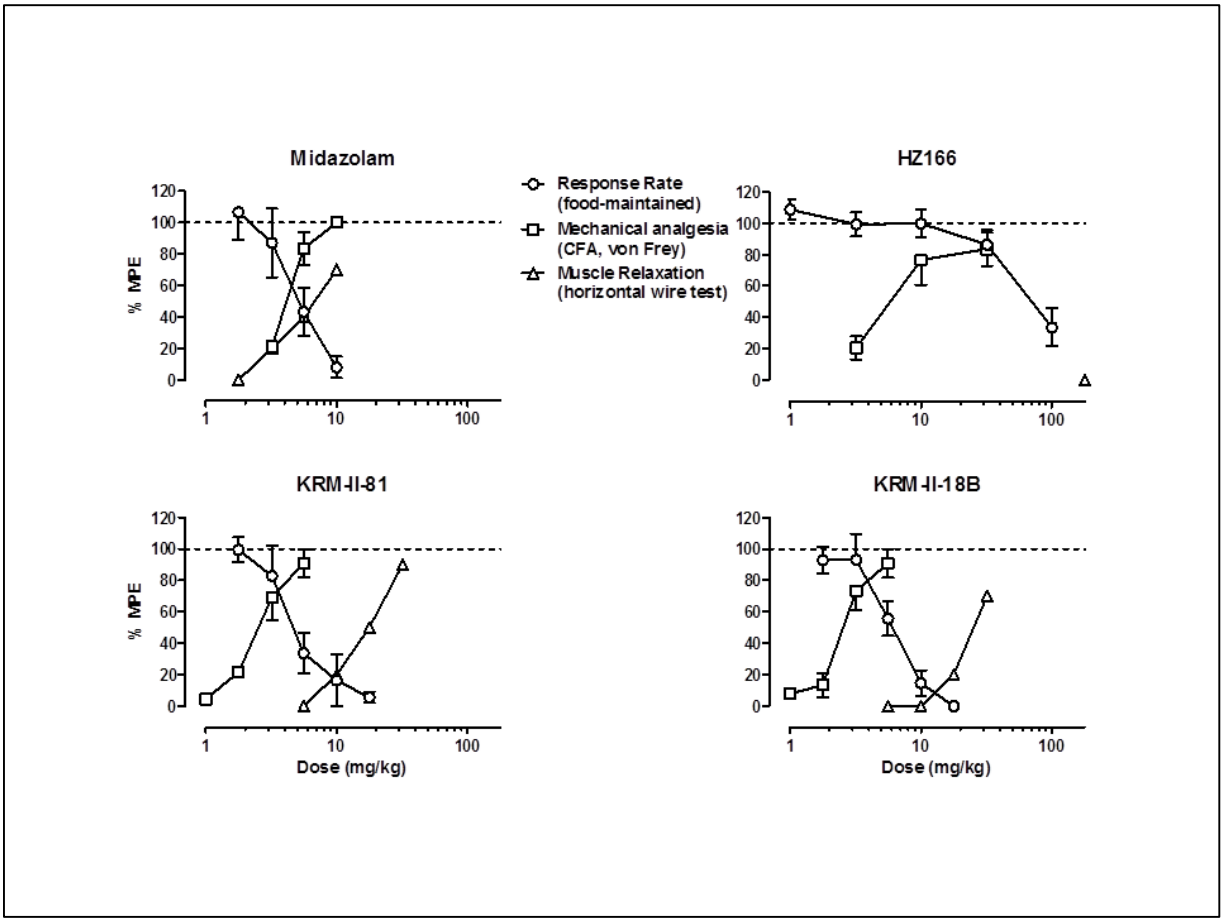

Midazolam
HZ166
KRM-II-81
KRM-II-18B
Response Rate (food-maintained)
Mechanical analgesia (CFA, von Frey)
Muscle Relaxation (horizontal wire test)
% MPE
Dose (mg/kg)

FIG. 14

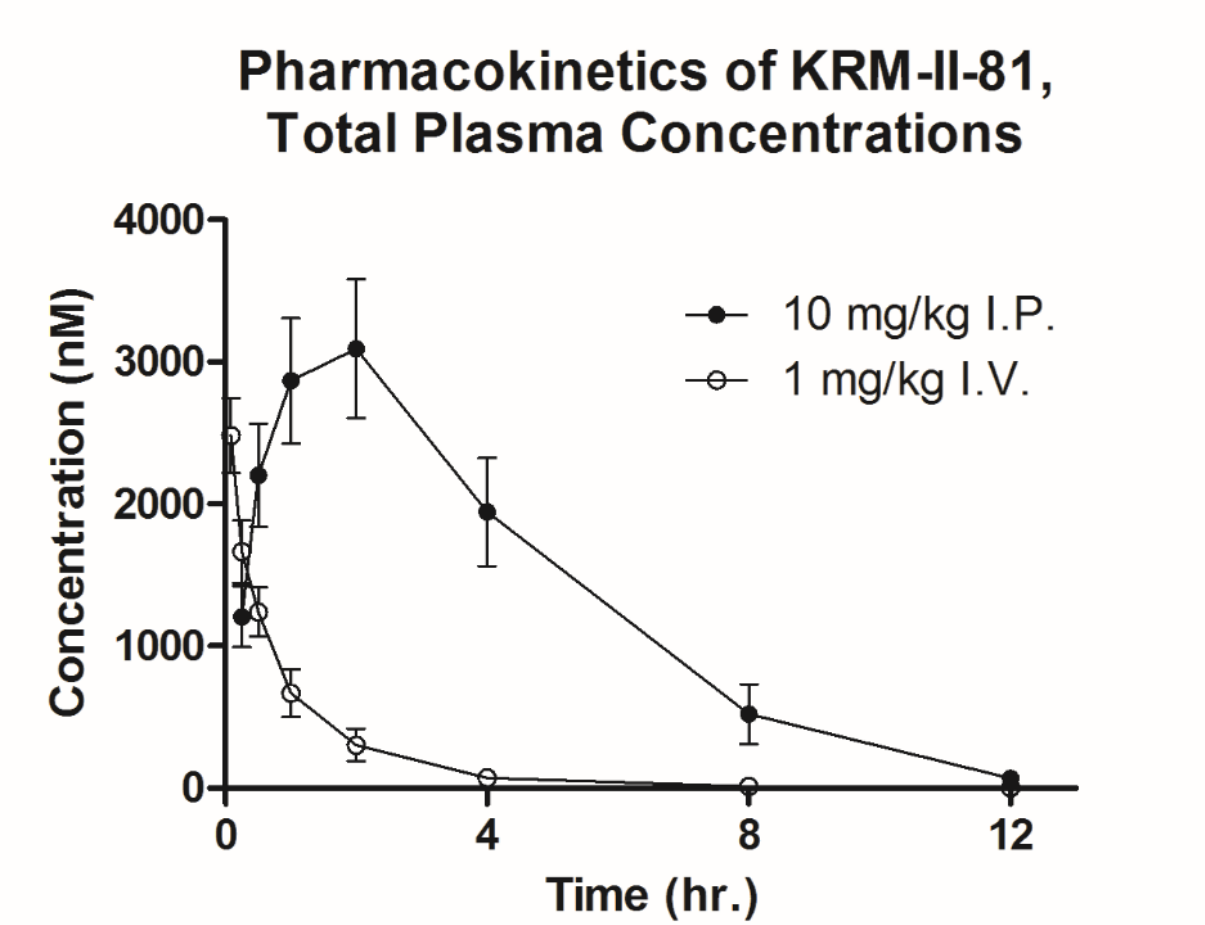

Pharmacokinetics of KRM-II-81,
Total Plasma Concentrations
Concentration (nM)
4000
3000
2000
1000
0
0
4
8
12
Time (hr.)
10 mg/kg I.P.
1 mg/kg I.V.

FIG. 15

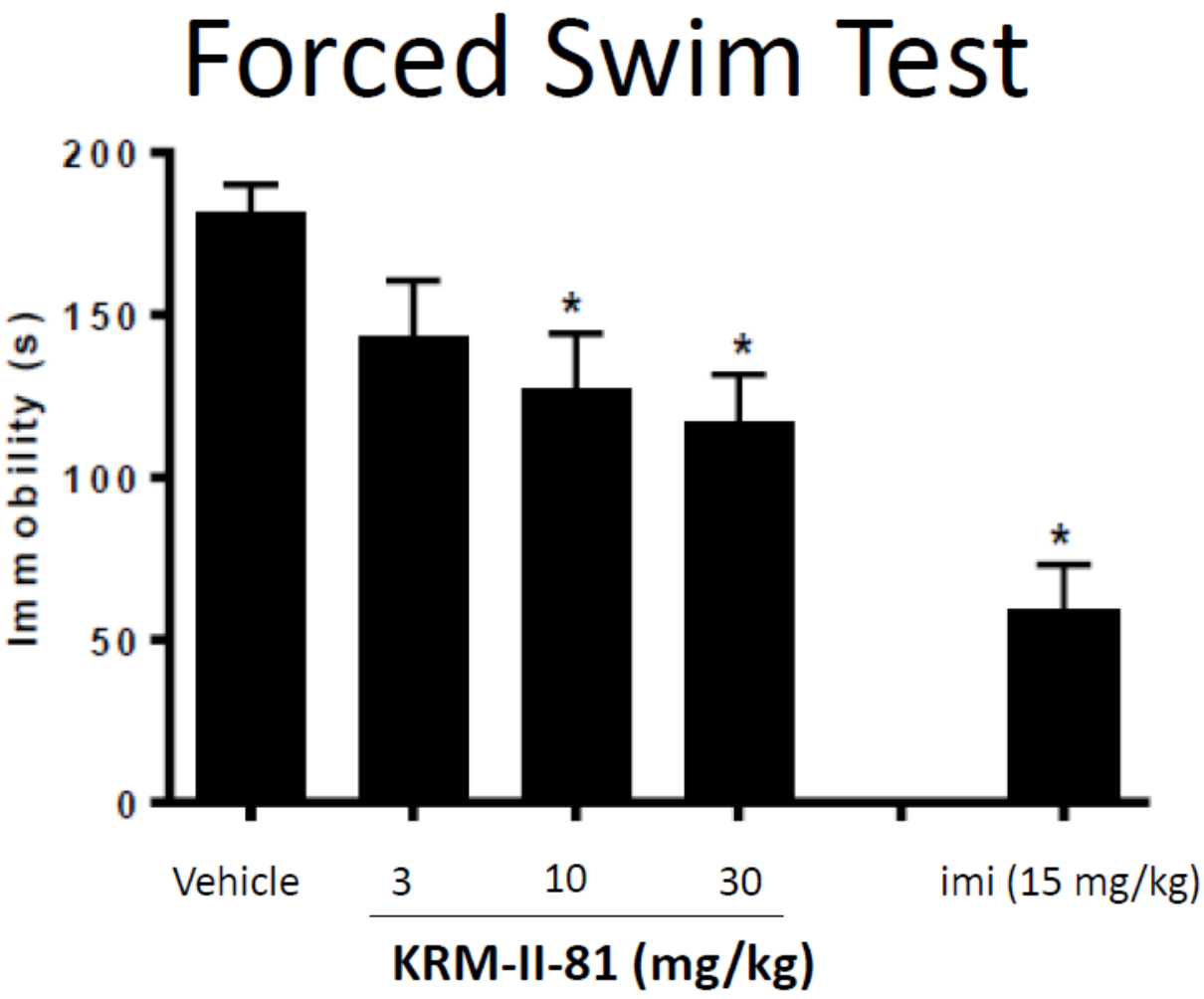

Forced Swim Test
200
150
100
50
0
Immobility (s)
*
*
*
Vehicle
3
10
30
imi (15 mg/kg)
KRM-II-81 (mg/kg)

FIG. 16

APPENDIX K. Crystal Structures (from Jeff Deschampes)

List of Figures:

1. HZ-166 (cook152)
2. MP-II-050 (cook153)
3. KRM-II-81 (1)*
4. KRM-II-81 (2)
5. KRM-II-81 (3)
6. KRM-II-81 (4)
7. KRM-II-81 (5)
8. SH-I-085 (KRM-I-100; cook128)
9. KRM-II-18B

* The code number for KRM-II-81 is cook149

List of Tables (data for KRM-II-81):

1. Crystal data and structure refinement for KRM-II-81 (cook149).
2. Atomic coordinates (x 10^4) and equivalent isotropic displacement parameters ($Å^2$x 10^3) for KRM-II-81 (cook149). U(eq) is defined as one third of the trace of the orthogonalized U^{ij} tensor.
3. Bond lengths [Å] and angles [°] for KRM-II-81 (cook149).
4. Anisotropic displacement parameters ($Å^2$x 10^3) for KRM-II-81 (cook149). The anisotropic displacement factor exponent takes the form: $-2\pi^2[h^2a^{*2}U^{11} + ... + 2 h k a^* b^* U^{12}]$
5. Hydrogen coordinates (x 10^4) and isotropic displacement parameters ($Å^2$x 10^3) for KRM-II-81 (cook149).
6. Torsion angles [°] for KRM-II-81 (cook149).
7. Hydrogen bonds for KRM-II-81 (cook149) [Å and °].

Fig.1

HZ-166
Code - cook152

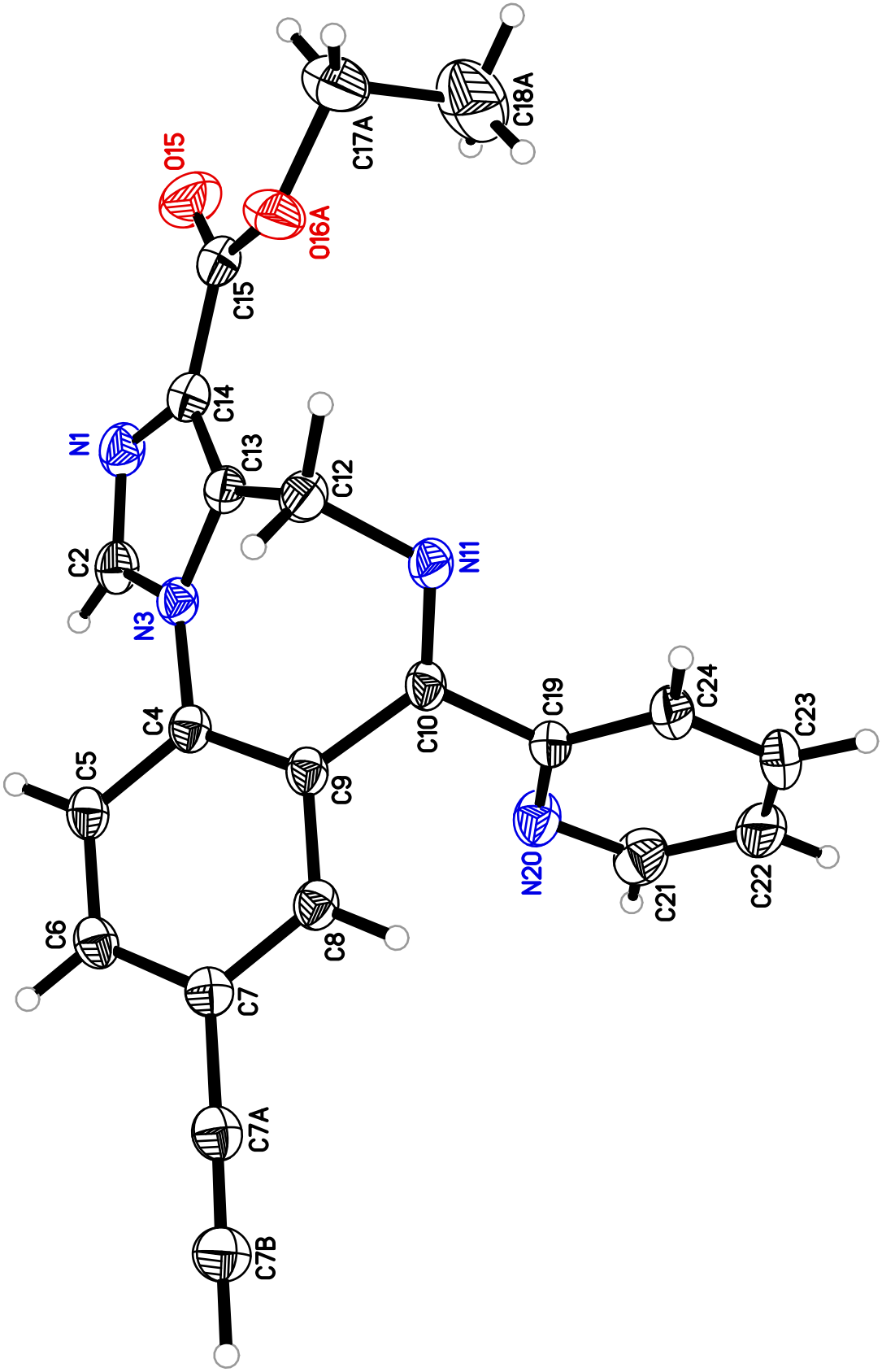


Fig.2

MP-II-050
Code - cook153

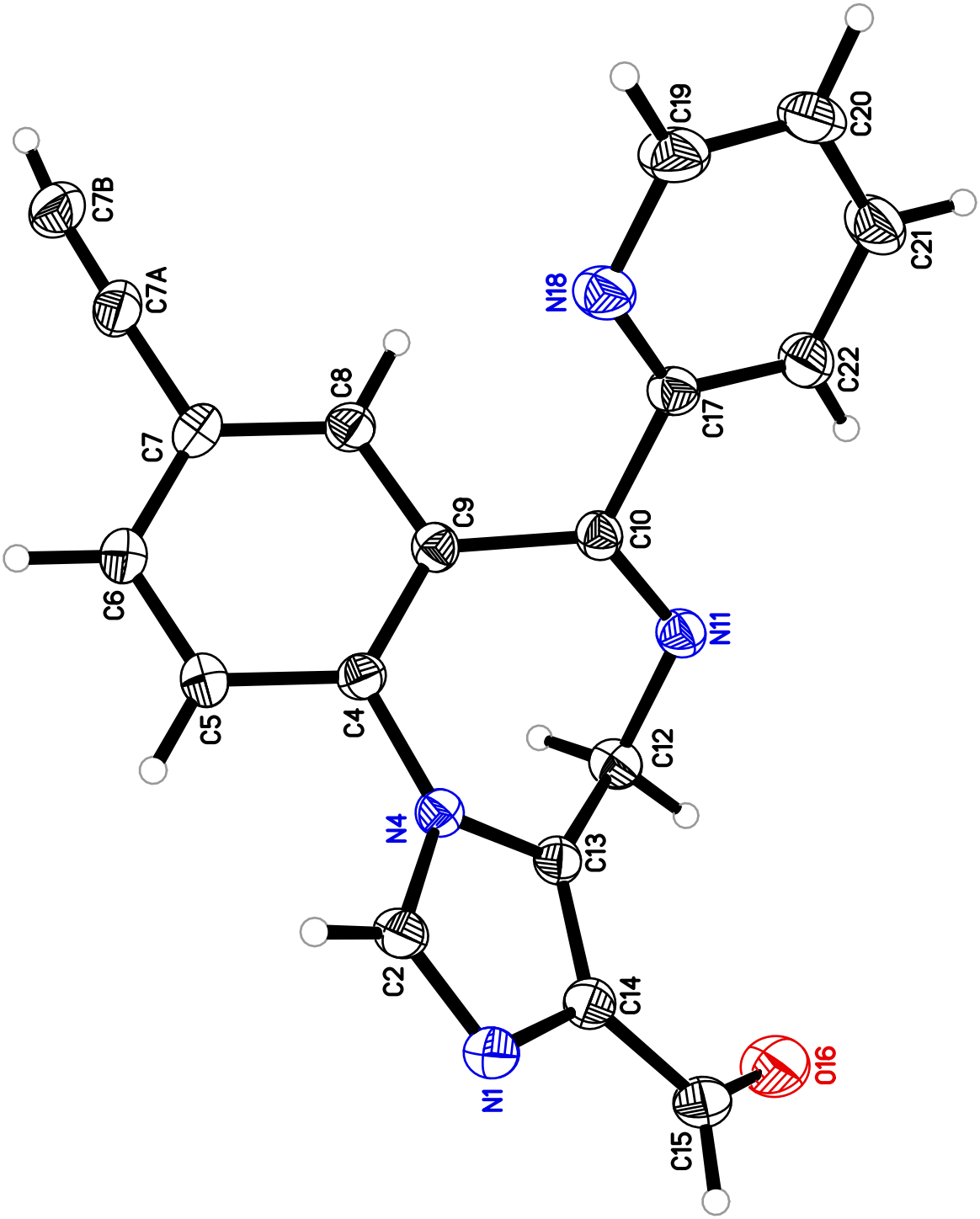


Fig.3

KRM-II-81
Code - cook149 (1)

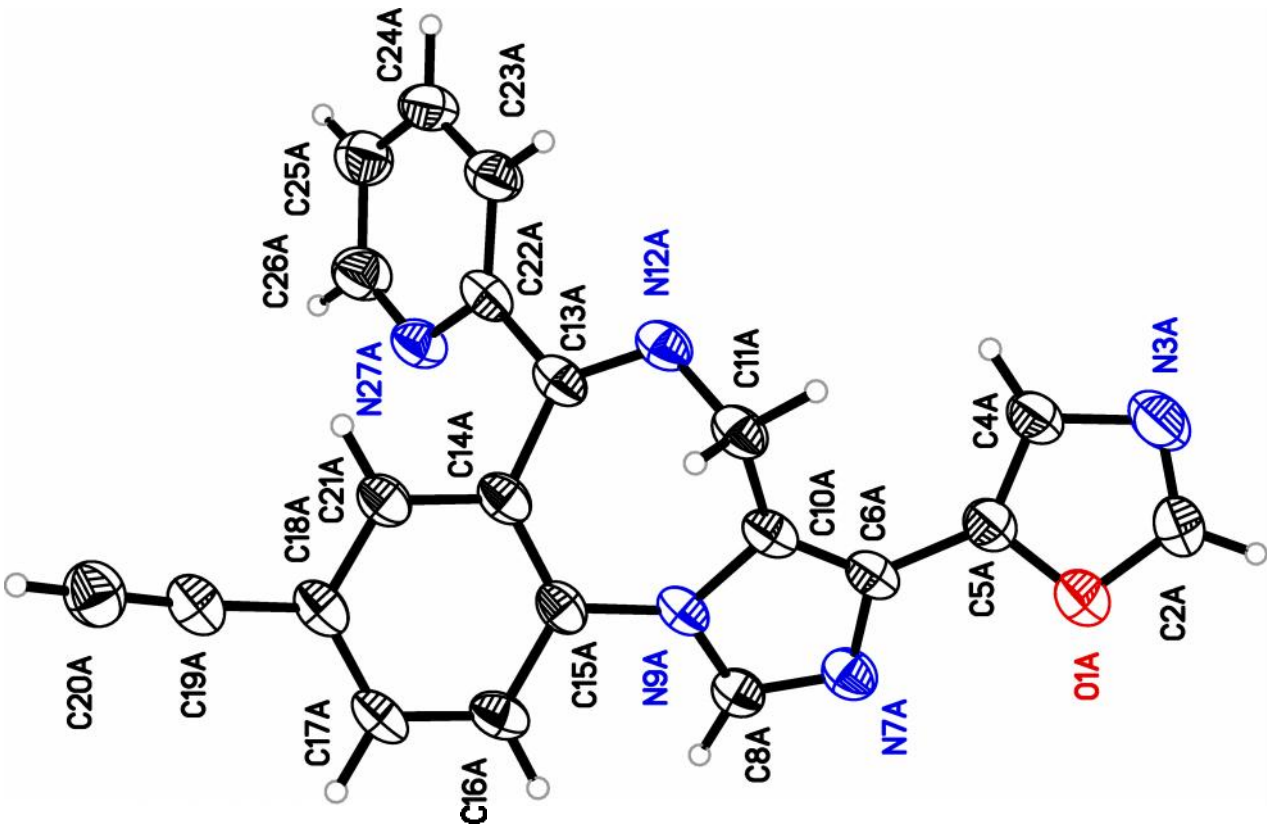


Fig.4

KRM-II-81
Code - cook149 (2)

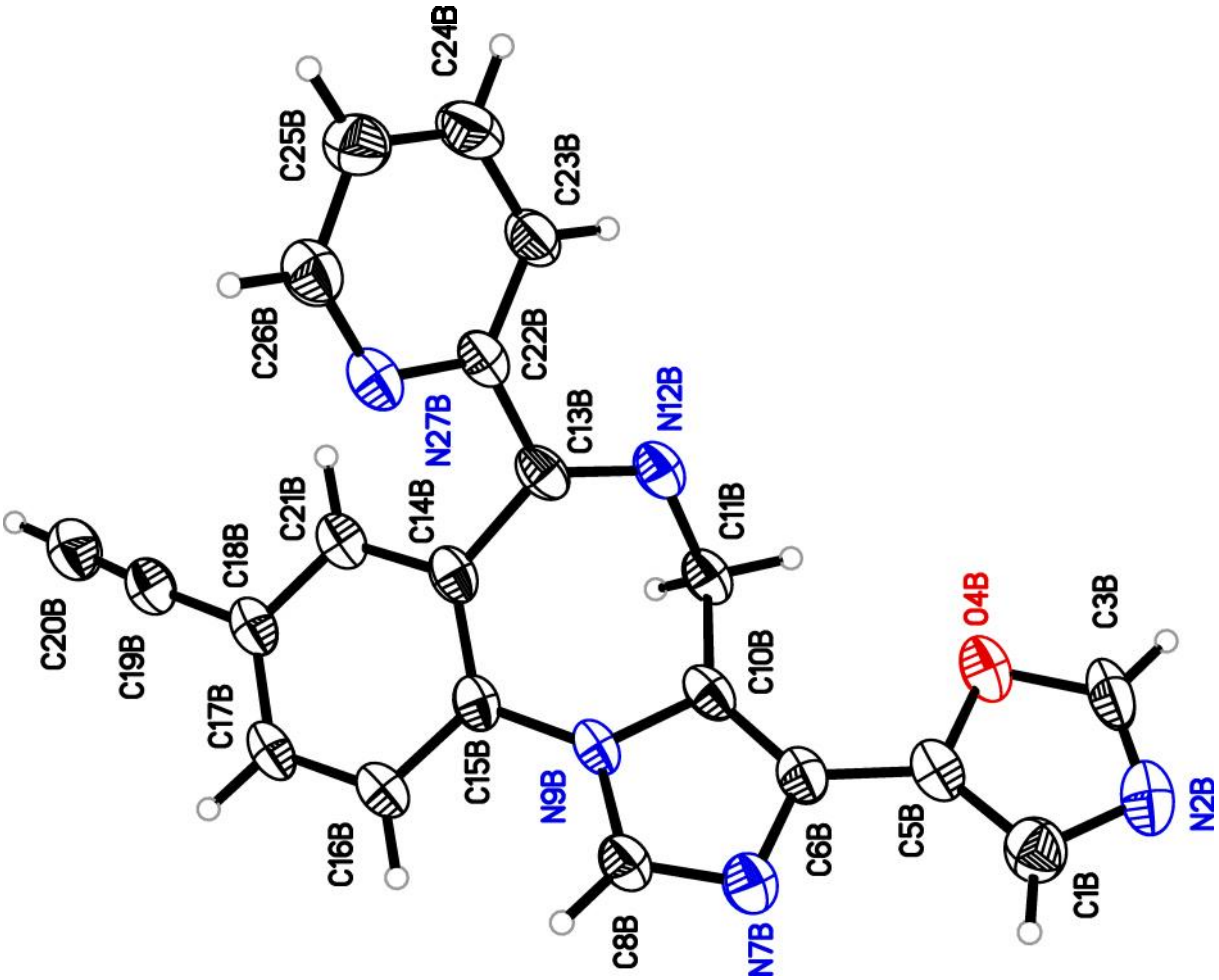


Fig.5

KRM-II-81
Code - cook149 (3)

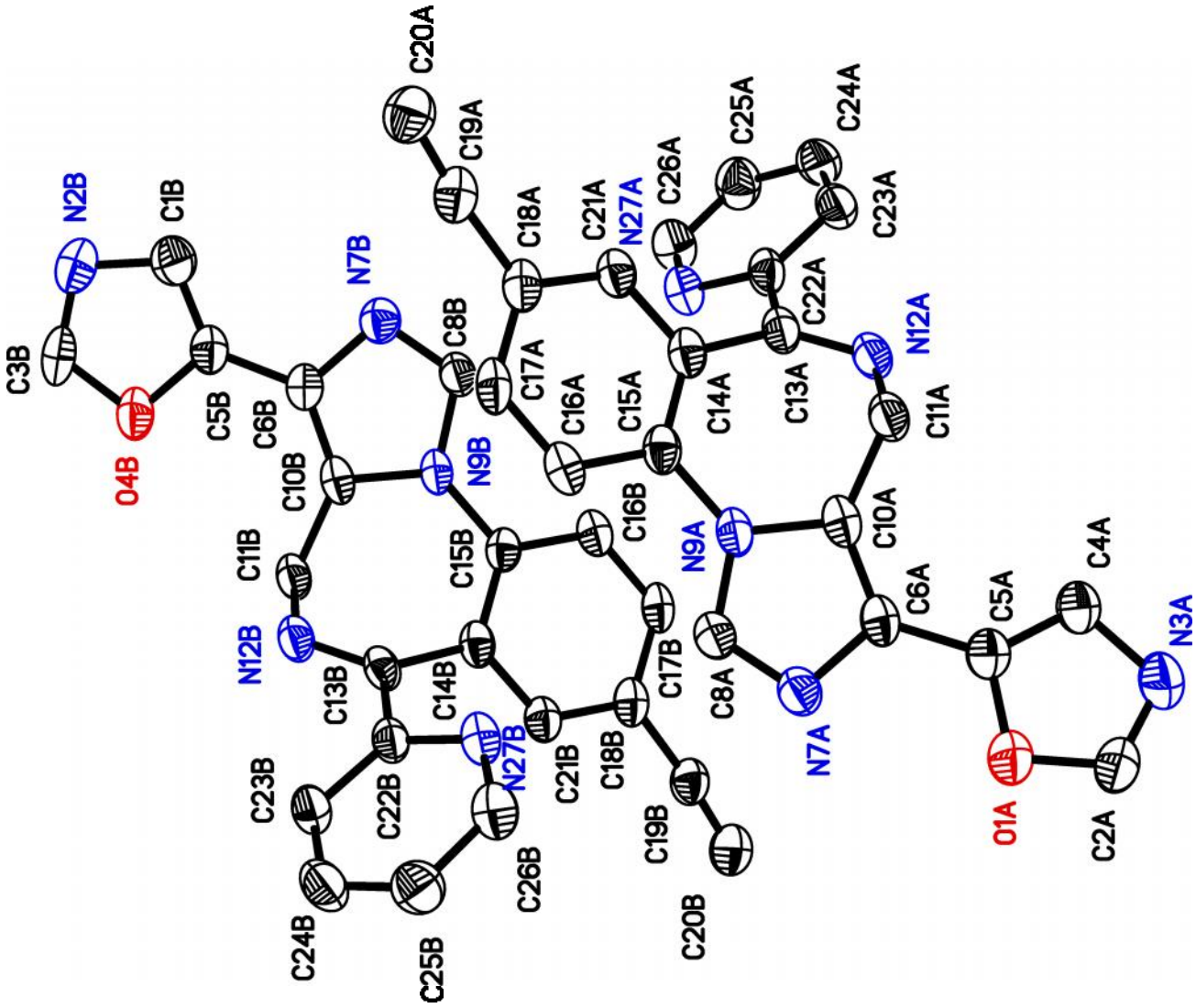


Fig.6

KRM-II-81
Code - cook149 (4)

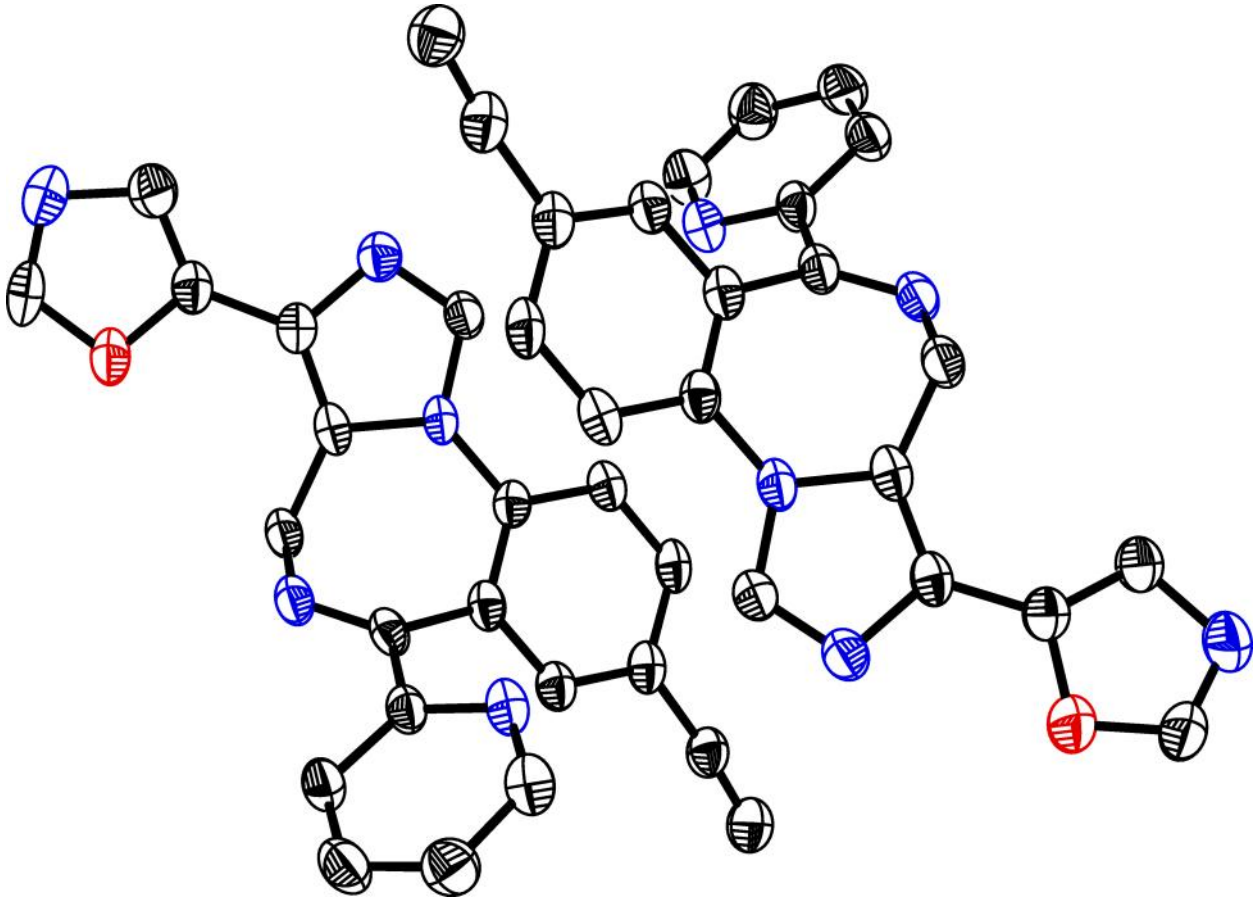


Fig.7

KRM-II-81
Code - cook149 (5)

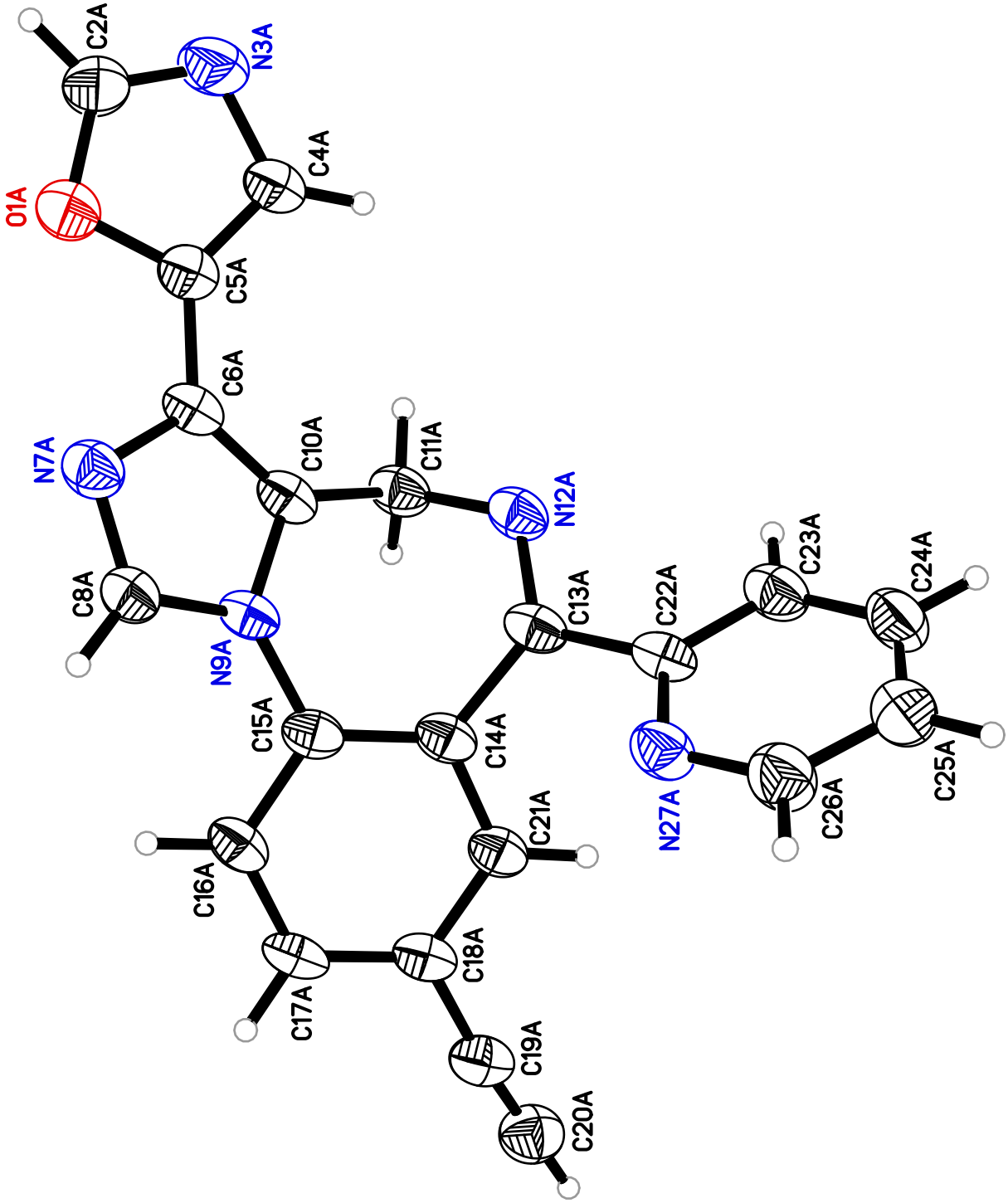


Fig.8

SH-I-085 (KRM-I-100)
Code - cook128

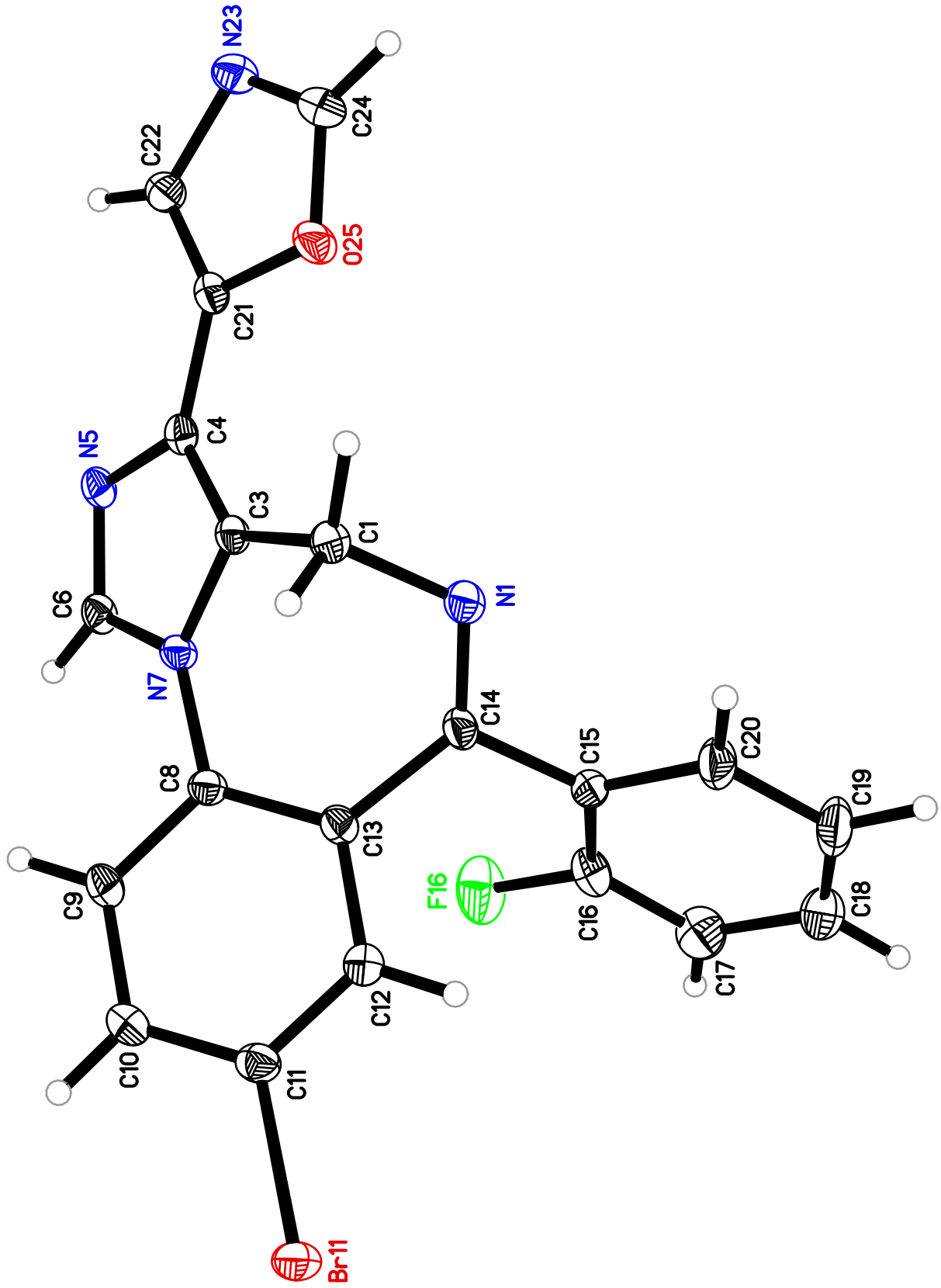


Fig.9

KRM-II-18B
Code - cook134

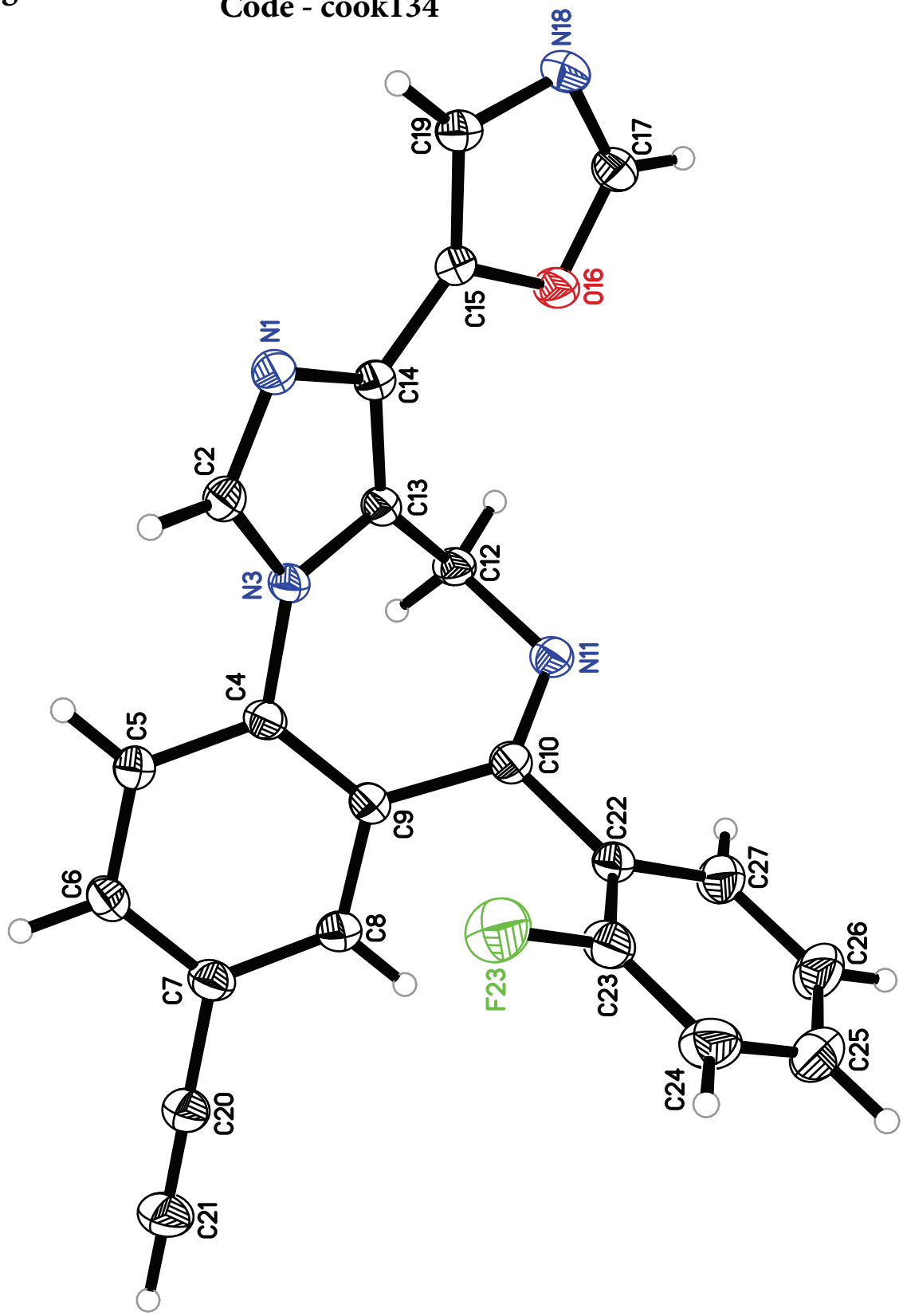


Table 1. Crystal data and structure refinement for KRM-II-81 (cook149).

Empirical formula	$C_{21}H_{13}N_5O$	
Formula weight	351.36	
Temperature	150(2) K	
Wavelength	1.54178 Å	
Crystal system	Monoclinic	
Space group	$P2_1/n$	
Unit cell dimensions	a = 17.6247(13) Å	α= 90°.
	b = 8.2158(7) Å	β= 102.499(5)°.
	c = 23.1472(17) Å	γ = 90°.
Volume	3272.3(4) $Å^3$	
Z	8	
Density (calculated)	1.426 Mg/m^3	
Absorption coefficient	0.749 mm^{-1}	
F(000)	1456	
Crystal size	0.115 x 0.100 x 0.010 mm^3	
θ range for data collection	2.871 to 68.957°.	
Index ranges	-21<=h<=20, -9<=k<=6, -27<=l<=27	
Reflections collected	17063	
Independent reflections	5806 [$R_{(int)}$ = 0.0579]	
Completeness to θ = 67.679°	96.8 %	
Absorption correction	Semi-empirical from equivalents	
Max. and min. transmission	0.7456 and 0.5364	
Refinement method	Full-matrix least-squares on F^2	
Data / restraints / parameters	5806 / 0 / 495	
Goodness-of-fit on F^2	1.023	
Final R indices [I>2σ(I)]	R_1 = 0.0628, wR_2 = 0.1596	
R indices (all data)	R_1 = 0.1158, wR_2 = 0.1894	
Largest diff. peak and hole	0.302 and -0.275 $e.Å^{-3}$	

Table 2. Atomic coordinates (x 10^4) and equivalent isotropic displacement parameters ($Å^2$x 10^3) for KRM-II-81 (cook149). U(eq) is defined as one third of the trace of the orthogonalized U^{ij} tensor.

	x	y	z	U(eq)
O(1A)	8188(1)	6079(4)	4697(1)	55(1)
C(2A)	8979(2)	6002(6)	4859(2)	57(1)
N(3A)	9337(2)	6371(4)	4461(2)	56(1)
C(4A)	8737(2)	6737(5)	3969(2)	44(1)
C(5A)	8049(2)	6547(4)	4113(2)	39(1)
C(6A)	7246(2)	6713(4)	3803(2)	35(1)
N(7A)	6651(2)	5935(3)	4000(1)	38(1)
C(8A)	6016(2)	6323(4)	3616(1)	35(1)
N(9A)	6161(1)	7288(3)	3172(1)	34(1)
C(10A)	6957(2)	7575(4)	3294(2)	34(1)
C(11A)	7298(2)	8680(4)	2913(2)	37(1)
N(12A)	7233(2)	7964(3)	2322(1)	36(1)
C(13A)	6548(2)	7842(4)	2002(2)	34(1)
C(14A)	5812(2)	8368(4)	2165(2)	34(1)
C(15A)	5616(2)	8035(4)	2705(1)	32(1)
C(16A)	4886(2)	8448(4)	2802(2)	37(1)
C(17A)	4366(2)	9294(4)	2373(2)	38(1)
C(18A)	4571(2)	9755(4)	1848(2)	36(1)
C(19A)	4084(2)	10791(5)	1420(2)	41(1)
C(20A)	3750(2)	11719(5)	1069(2)	47(1)
C(21A)	5275(2)	9212(4)	1742(2)	35(1)
C(22A)	6474(2)	7118(4)	1395(2)	35(1)
C(23A)	7042(2)	7366(4)	1073(2)	41(1)
C(24A)	6949(2)	6617(5)	526(2)	49(1)
C(25A)	6311(2)	5666(5)	324(2)	50(1)
C(26A)	5772(2)	5512(5)	671(2)	48(1)
N(27A)	5835(2)	6217(4)	1195(1)	39(1)
C(1B)	1719(2)	6428(5)	352(2)	45(1)
N(2B)	920(2)	6201(4)	202(1)	50(1)
C(3B)	772(2)	5342(5)	622(2)	48(1)
O(4B)	1402(1)	4961(3)	1054(1)	45(1)
C(5B)	2011(2)	5689(4)	867(2)	36(1)
C(6B)	2787(2)	5522(4)	1222(1)	34(1)
N(7B)	3399(2)	6258(3)	1024(1)	36(1)
C(8B)	4021(2)	5888(4)	1422(1)	34(1)
N(9B)	3850(1)	4974(3)	1874(1)	30(1)
C(10B)	3052(2)	4722(4)	1744(1)	32(1)
C(11B)	2692(2)	3691(4)	2136(1)	35(1)
N(12B)	2774(1)	4440(3)	2724(1)	35(1)
C(13B)	3458(2)	4484(4)	3044(1)	31(1)

Table 2. (continued)

	x	y	z	U(eq)
C(14B)	4183(2)	3862(4)	2879(1)	32(1)
C(15B)	4383(2)	4209(4)	2337(1)	30(1)
C(16B)	5115(2)	3768(4)	2247(2)	35(1)
C(17B)	5630(2)	2915(4)	2676(2)	35(1)
C(18B)	5409(2)	2431(4)	3194(2)	34(1)
C(19B)	5887(2)	1406(4)	3621(2)	37(1)
C(20B)	6230(2)	473(5)	3971(2)	46(1)
C(21B)	4701(2)	2964(4)	3295(2)	33(1)
C(22B)	3565(2)	5164(4)	3657(1)	32(1)
C(23B)	2986(2)	5037(4)	3974(2)	39(1)
C(24B)	3128(2)	5581(5)	4550(2)	46(1)
C(25B)	3833(2)	6261(5)	4793(2)	46(1)
C(26B)	4381(2)	6361(4)	4446(2)	43(1)
N(27B)	4259(1)	5836(3)	3887(1)	37(1)

Table 3. Bond lengths [Å] and angles [°] for KRM-II-81 (cook149).

O(1A)-C(2A)	1.364(4)	O(1A)-C(5A)	1.374(4)
C(2A)-N(3A)	1.261(5)	C(2A)-H(2A)	0.9500
N(3A)-C(4A)	1.408(5)	C(4A)-C(5A)	1.336(4)
C(4A)-H(4A)	0.9500	C(5A)-C(6A)	1.447(4)
C(6A)-C(10A)	1.373(5)	C(6A)-N(7A)	1.389(4)
N(7A)-C(8A)	1.310(4)	C(8A)-N(9A)	1.366(4)
C(8A)-H(8A)	0.9500	N(9A)-C(10A)	1.390(4)
N(9A)-C(15A)	1.420(4)	C(10A)-C(11A)	1.481(4)
C(11A)-N(12A)	1.471(4)	C(11A)-H(11C)	0.9900
C(11A)-H(11D)	0.9900	N(12A)-C(13A)	1.277(4)
C(13A)-C(14A)	1.490(4)	C(13A)-C(22A)	1.505(5)
C(14A)-C(21A)	1.391(5)	C(14A)-C(15A)	1.395(4)
C(15A)-C(16A)	1.394(4)	C(16A)-C(17A)	1.384(5)
C(16A)-H(16A)	0.9500	C(17A)-C(18A)	1.392(5)
C(17A)-H(17A)	0.9500	C(18A)-C(21A)	1.390(4)
C(18A)-C(19A)	1.441(5)	C(19A)-C(20A)	1.175(5)
C(20A)-H(20A)	0.88(5)	C(21A)-H(21A)	0.9500
C(22A)-N(27A)	1.344(4)	C(22A)-C(23A)	1.386(4)
C(23A)-C(24A)	1.387(5)	C(23A)-H(23A)	0.9500
C(24A)-C(25A)	1.366(5)	C(24A)-H(24A)	0.9500
C(25A)-C(26A)	1.375(5)	C(25A)-H(25A)	0.9500
C(26A)-N(27A)	1.326(4)	C(26A)-H(26A)	0.9500
C(1B)-C(5B)	1.337(5)	C(1B)-N(2B)	1.387(4)
C(1B)-H(1B)	0.9500	N(2B)-C(3B)	1.274(5)
C(3B)-O(4B)	1.360(4)	C(3B)-H(3B)	0.9500
O(4B)-C(5B)	1.378(4)	C(5B)-C(6B)	1.441(4)
C(6B)-C(10B)	1.366(5)	C(6B)-N(7B)	1.397(4)
N(7B)-C(8B)	1.307(4)	C(8B)-N(9B)	1.373(4)
C(8B)-H(8B)	0.9500	N(9B)-C(10B)	1.388(4)
N(9B)-C(15B)	1.411(4)	C(10B)-C(11B)	1.482(4)
C(11B)-N(12B)	1.471(4)	C(11B)-H(11A)	0.9900
C(11B)-H(11B)	0.9900	N(12B)-C(13B)	1.271(4)
C(13B)-C(22B)	1.498(4)	C(13B)-C(14B)	1.500(4)
C(14B)-C(21B)	1.387(4)	C(14B)-C(15B)	1.404(4)
C(15B)-C(16B)	1.399(4)	C(16B)-C(17B)	1.382(5)
C(16B)-H(16B)	0.9500	C(17B)-C(18B)	1.397(4)
C(17B)-H(17B)	0.9500	C(18B)-C(21B)	1.388(4)
C(18B)-C(19B)	1.427(5)	C(19B)-C(20B)	1.183(5)
C(20B)-H(20B)	0.93(4)	C(21B)-H(21B)	0.9500
C(22B)-N(27B)	1.342(4)	C(22B)-C(23B)	1.385(4)
C(23B)-C(24B)	1.378(5)	C(23B)-H(23B)	0.9500
C(24B)-C(25B)	1.368(5)	C(24B)-H(24B)	0.9500
C(25B)-C(26B)	1.385(5)	C(25B)-H(25B)	0.9500

Table 3. (continued)

C(26B)-N(27B)	1.337(4)	C(26B)-H(26B)	0.9500
C(2A)-O(1A)-C(5A)	103.8(3)	N(3A)-C(2A)-O(1A)	115.5(3)
N(3A)-C(2A)-H(2A)	122.3	O(1A)-C(2A)-H(2A)	122.3
C(2A)-N(3A)-C(4A)	103.6(3)	C(5A)-C(4A)-N(3A)	109.6(3)
C(5A)-C(4A)-H(4A)	125.2	N(3A)-C(4A)-H(4A)	125.2
C(4A)-C(5A)-O(1A)	107.4(3)	C(4A)-C(5A)-C(6A)	135.0(3)
O(1A)-C(5A)-C(6A)	117.6(3)	C(10A)-C(6A)-N(7A)	110.6(3)
C(10A)-C(6A)-C(5A)	128.1(3)	N(7A)-C(6A)-C(5A)	121.3(3)
C(8A)-N(7A)-C(6A)	105.1(3)	N(7A)-C(8A)-N(9A)	112.4(3)
N(7A)-C(8A)-H(8A)	123.8	N(9A)-C(8A)-H(8A)	123.8
C(8A)-N(9A)-C(10A)	106.9(3)	C(8A)-N(9A)-C(15A)	128.1(3)
C(10A)-N(9A)-C(15A)	124.7(3)	C(6A)-C(10A)-N(9A)	105.0(3)
C(6A)-C(10A)-C(11A)	134.7(3)	N(9A)-C(10A)-C(11A)	120.3(3)
N(12A)-C(11A)-C(10A)	110.4(3)	N(12A)-C(11A)-H(11C)	109.6
C(10A)-C(11A)-H(11C)	109.6	N(12A)-C(11A)-H(11D)	109.6
C(10A)-C(11A)-H(11D)	109.6	H(11C)-C(11A)-H(11D)	108.1
C(13A)-N(12A)-C(11A)	116.4(3)	N(12A)-C(13A)-C(14A)	126.5(3)
N(12A)-C(13A)-C(22A)	116.9(3)	C(14A)-C(13A)-C(22A)	116.6(3)
C(21A)-C(14A)-C(15A)	117.7(3)	C(21A)-C(14A)-C(13A)	117.6(3)
C(15A)-C(14A)-C(13A)	124.6(3)	C(16A)-C(15A)-C(14A)	120.8(3)
C(16A)-C(15A)-N(9A)	118.6(3)	C(14A)-C(15A)-N(9A)	120.6(3)
C(17A)-C(16A)-C(15A)	119.9(3)	C(17A)-C(16A)-H(16A)	120.0
C(15A)-C(16A)-H(16A)	120.0	C(16A)-C(17A)-C(18A)	120.4(3)
C(16A)-C(17A)-H(17A)	119.8	C(18A)-C(17A)-H(17A)	119.8
C(21A)-C(18A)-C(17A)	118.5(3)	C(21A)-C(18A)-C(19A)	119.3(3)
C(17A)-C(18A)-C(19A)	122.3(3)	C(20A)-C(19A)-C(18A)	173.7(4)
C(19A)-C(20A)-H(20A)	179(4)	C(18A)-C(21A)-C(14A)	122.3(3)
C(18A)-C(21A)-H(21A)	118.9	C(14A)-C(21A)-H(21A)	118.9
N(27A)-C(22A)-C(23A)	123.0(3)	N(27A)-C(22A)-C(13A)	115.8(3)
C(23A)-C(22A)-C(13A)	121.1(3)	C(22A)-C(23A)-C(24A)	118.0(3)
C(22A)-C(23A)-H(23A)	121.0	C(24A)-C(23A)-H(23A)	121.0
C(25A)-C(24A)-C(23A)	119.5(3)	C(25A)-C(24A)-H(24A)	120.3
C(23A)-C(24A)-H(24A)	120.3	C(24A)-C(25A)-C(26A)	118.3(4)
C(24A)-C(25A)-H(25A)	120.8	C(26A)-C(25A)-H(25A)	120.8
N(27A)-C(26A)-C(25A)	124.2(4)	N(27A)-C(26A)-H(26A)	117.9
C(25A)-C(26A)-H(26A)	117.9	C(26A)-N(27A)-C(22A)	117.0(3)
C(5B)-C(1B)-N(2B)	109.7(3)	C(5B)-C(1B)-H(1B)	125.2
N(2B)-C(1B)-H(1B)	125.2	C(3B)-N(2B)-C(1B)	104.3(3)
N(2B)-C(3B)-O(4B)	114.7(3)	N(2B)-C(3B)-H(3B)	122.6
O(4B)-C(3B)-H(3B)	122.6	C(3B)-O(4B)-C(5B)	103.7(3)
C(1B)-C(5B)-O(4B)	107.5(3)	C(1B)-C(5B)-C(6B)	133.4(3)
O(4B)-C(5B)-C(6B)	119.1(3)	C(10B)-C(6B)-N(7B)	110.9(3)

Table 3. (continued)

C(10B)-C(6B)-C(5B)	130.7(3)	N(7B)-C(6B)-C(5B)	118.4(3)
C(8B)-N(7B)-C(6B)	105.0(3)	N(7B)-C(8B)-N(9B)	112.0(3)
N(7B)-C(8B)-H(8B)	124.0	N(9B)-C(8B)-H(8B)	124.0
C(8B)-N(9B)-C(10B)	107.2(3)	C(8B)-N(9B)-C(15B)	127.1(2)
C(10B)-N(9B)-C(15B)	125.1(3)	C(6B)-C(10B)-N(9B)	104.9(3)
C(6B)-C(10B)-C(11B)	135.0(3)	N(9B)-C(10B)-C(11B)	120.1(3)
N(12B)-C(11B)-C(10B)	111.0(3)	N(12B)-C(11B)-H(11A)	109.4
C(10B)-C(11B)-H(11A)	109.4	N(12B)-C(11B)-H(11B)	109.4
C(10B)-C(11B)-H(11B)	109.4	H(11A)-C(11B)-H(11B)	108.0
C(13B)-N(12B)-C(11B)	116.2(3)	N(12B)-C(13B)-C(22B)	118.1(3)
N(12B)-C(13B)-C(14B)	126.5(3)	C(22B)-C(13B)-C(14B)	115.3(3)
C(21B)-C(14B)-C(15B)	118.2(3)	C(21B)-C(14B)-C(13B)	118.3(3)
C(15B)-C(14B)-C(13B)	123.4(3)	C(16B)-C(15B)-C(14B)	120.0(3)
C(16B)-C(15B)-N(9B)	119.0(3)	C(14B)-C(15B)-N(9B)	121.0(3)
C(17B)-C(16B)-C(15B)	120.5(3)	C(17B)-C(16B)-H(16B)	119.8
C(15B)-C(16B)-H(16B)	119.8	C(16B)-C(17B)-C(18B)	120.0(3)
C(16B)-C(17B)-H(17B)	120.0	C(18B)-C(17B)-H(17B)	120.0
C(21B)-C(18B)-C(17B)	118.8(3)	C(21B)-C(18B)-C(19B)	119.2(3)
C(17B)-C(18B)-C(19B)	122.0(3)	C(20B)-C(19B)-C(18B)	174.5(4)
C(19B)-C(20B)-H(20B)	178(3)	C(14B)-C(21B)-C(18B)	122.2(3)
C(14B)-C(21B)-H(21B)	118.9	C(18B)-C(21B)-H(21B)	118.9
N(27B)-C(22B)-C(23B)	122.3(3)	N(27B)-C(22B)-C(13B)	116.5(3)
C(23B)-C(22B)-C(13B)	121.2(3)	C(24B)-C(23B)-C(22B)	119.2(3)
C(24B)-C(23B)-H(23B)	120.4	C(22B)-C(23B)-H(23B)	120.4
C(25B)-C(24B)-C(23B)	119.3(3)	C(25B)-C(24B)-H(24B)	120.4
C(23B)-C(24B)-H(24B)	120.4	C(24B)-C(25B)-C(26B)	118.2(3)
C(24B)-C(25B)-H(25B)	120.9	C(26B)-C(25B)-H(25B)	120.9
N(27B)-C(26B)-C(25B)	123.7(3)	N(27B)-C(26B)-H(26B)	118.2
C(25B)-C(26B)-H(26B)	118.2	C(26B)-N(27B)-C(22B)	117.4(3)

Table 4. Anisotropic displacement parameters ($Å^2 x\ 10^3$) for KRM-II-81 (cook149). The anisotropic displacement factor exponent takes the form: $-2\pi^2[\ h^2 a^{*2} U^{11} + ... + 2\ h\ k\ a^*\ b^*\ U^{12}\ ]$

	U^{11}	U^{22}	U^{33}	U^{23}	U^{13}	U^{12}
O(1A)	33(1)	83(2)	49(2)	8(2)	9(1)	-1(1)
C(2A)	34(2)	86(3)	47(2)	7(2)	2(2)	-1(2)
N(3A)	32(2)	70(2)	67(2)	14(2)	12(2)	1(2)
C(4A)	31(2)	54(3)	50(2)	4(2)	12(2)	6(2)
C(5A)	33(2)	41(2)	43(2)	-1(2)	8(2)	2(2)
C(6A)	25(2)	36(2)	45(2)	-4(2)	10(1)	1(1)
N(7A)	33(2)	36(2)	47(2)	3(1)	11(1)	-2(1)
C(8A)	30(2)	36(2)	41(2)	0(2)	10(2)	-2(2)
N(9A)	22(1)	35(2)	44(2)	0(1)	8(1)	-2(1)
C(10A)	26(2)	33(2)	46(2)	-6(2)	12(1)	-2(1)
C(11A)	27(2)	36(2)	49(2)	3(2)	10(1)	-4(2)
N(12A)	28(1)	34(2)	48(2)	3(1)	12(1)	-3(1)
C(13A)	25(2)	30(2)	49(2)	3(2)	10(2)	0(1)
C(14A)	25(2)	31(2)	45(2)	-5(2)	7(1)	-3(1)
C(15A)	25(2)	27(2)	42(2)	-4(2)	5(1)	-3(1)
C(16A)	27(2)	39(2)	48(2)	-5(2)	14(2)	-5(2)
C(17A)	20(2)	38(2)	55(2)	-5(2)	8(2)	2(2)
C(18A)	25(2)	33(2)	49(2)	-3(2)	6(2)	0(1)
C(19A)	31(2)	38(2)	51(2)	-6(2)	5(2)	2(2)
C(20A)	45(2)	44(3)	52(2)	-3(2)	7(2)	3(2)
C(21A)	26(2)	34(2)	43(2)	-2(2)	7(1)	-4(1)
C(22A)	24(2)	32(2)	49(2)	1(2)	9(1)	3(1)
C(23A)	32(2)	41(2)	52(2)	7(2)	14(2)	1(2)
C(24A)	39(2)	60(3)	51(2)	9(2)	22(2)	8(2)
C(25A)	43(2)	61(3)	47(2)	-7(2)	11(2)	0(2)
C(26A)	40(2)	54(3)	51(2)	-7(2)	13(2)	-5(2)
N(27A)	30(1)	43(2)	47(2)	-5(2)	11(1)	-5(1)
C(1B)	40(2)	47(2)	49(2)	-1(2)	7(2)	-6(2)
N(2B)	35(2)	54(2)	57(2)	-1(2)	-1(2)	6(2)
C(3B)	24(2)	57(3)	59(2)	-9(2)	1(2)	8(2)
O(4B)	26(1)	53(2)	54(2)	-1(1)	5(1)	-1(1)
C(5B)	28(2)	33(2)	48(2)	-4(2)	8(2)	1(2)
C(6B)	26(2)	36(2)	39(2)	-4(2)	6(1)	0(1)
N(7B)	32(1)	34(2)	42(2)	-1(1)	7(1)	-1(1)
C(8B)	25(2)	34(2)	43(2)	2(2)	9(1)	-1(1)
N(9B)	19(1)	31(2)	40(2)	-2(1)	7(1)	-1(1)
C(10B)	22(2)	32(2)	44(2)	-7(2)	10(1)	-4(1)
C(11B)	23(2)	37(2)	45(2)	0(2)	9(1)	-3(1)
N(12B)	24(1)	35(2)	45(2)	1(1)	9(1)	-3(1)
C(13B)	25(2)	25(2)	45(2)	2(2)	13(1)	-3(1)

Table 4. (continued)

	U^{11}	U^{22}	U^{33}	U^{23}	U^{13}	U^{12}
C(14B)	23(2)	29(2)	43(2)	-4(2)	6(1)	-3(1)
C(15B)	23(2)	27(2)	37(2)	-3(2)	4(1)	-1(1)
C(16B)	26(2)	36(2)	45(2)	-2(2)	11(1)	-2(1)
C(17B)	20(2)	36(2)	49(2)	-5(2)	8(1)	2(1)
C(18B)	24(2)	32(2)	45(2)	-6(2)	7(1)	1(1)
C(19B)	29(2)	38(2)	45(2)	0(2)	9(2)	5(2)
C(20B)	37(2)	48(3)	53(2)	-1(2)	9(2)	5(2)
C(21B)	26(2)	30(2)	43(2)	-1(2)	9(1)	1(1)
C(22B)	24(2)	30(2)	43(2)	4(2)	10(1)	2(1)
C(23B)	27(2)	45(2)	46(2)	2(2)	12(1)	1(2)
C(24B)	39(2)	53(3)	53(2)	4(2)	22(2)	0(2)
C(25B)	48(2)	49(2)	44(2)	-2(2)	14(2)	4(2)
C(26B)	35(2)	42(2)	51(2)	-5(2)	10(2)	-3(2)
N(27B)	27(1)	37(2)	50(2)	-3(1)	10(1)	-2(1)

Table 5. Hydrogen coordinates (x 10^4) and isotropic displacement parameters (Å^{2}x 10^3) for KRM-II-81 (cook149).

	x	y	z	U(eq)
H(2A)	9243	5692	5246	68
H(4A)	8811	7070	3592	53
H(8A)	5511	5974	3643	42
H(11C)	7023	9739	2877	44
H(11D)	7852	8878	3096	44
H(16A)	4747	8149	3161	45
H(17A)	3866	9562	2437	45
H(21A)	5393	9425	1368	41
H(23A)	7483	8029	1224	49
H(24A)	7326	6764	292	58
H(25A)	6241	5125	-46	60
H(26A)	5327	4858	526	58
H(1B)	2014	7018	124	54
H(3B)	261	4994	633	58
H(8B)	4532	6213	1402	40
H(11A)	2134	3538	1956	42
H(11B)	2943	2607	2179	42
H(16B)	5260	4058	1888	42
H(17B)	6134	2658	2618	42
H(21B)	4568	2705	3660	39
H(23B)	2495	4579	3796	47
H(24B)	2741	5484	4777	56
H(25B)	3945	6654	5188	55
H(26B)	4872	6829	4615	51
H(20B)	6510(20)	-240(60)	4250(20)	79(15)
H(20A)	3500(30)	12390(60)	800(20)	97(19)

Table 6. Torsion angles [°] for KRM-II-81 (cook149).

C(5A)-O(1A)-C(2A)-N(3A)	0.7(5)	O(1A)-C(2A)-N(3A)-C(4A)	-0.2(5)
C(2A)-N(3A)-C(4A)-C(5A)	-0.4(5)	N(3A)-C(4A)-C(5A)-O(1A)	0.8(4)
N(3A)-C(4A)-C(5A)-C(6A)	-178.9(4)	C(2A)-O(1A)-C(5A)-C(4A)	-0.9(4)
C(2A)-O(1A)-C(5A)-C(6A)	178.9(3)	C(4A)-C(5A)-C(6A)-C(10A)	-20.5(7)
O(1A)-C(5A)-C(6A)-C(10A)	159.8(3)	C(4A)-C(5A)-C(6A)-N(7A)	158.4(4)
O(1A)-C(5A)-C(6A)-N(7A)	-21.3(5)	C(10A)-C(6A)-N(7A)-C(8A)	0.1(4)
C(5A)-C(6A)-N(7A)-C(8A)	-179.0(3)	C(6A)-N(7A)-C(8A)-N(9A)	1.1(4)
N(7A)-C(8A)-N(9A)-C(10A)	-1.8(4)	N(7A)-C(8A)-N(9A)-C(15A)	-175.1(3)
N(7A)-C(6A)-C(10A)-N(9A)	-1.2(4)	C(5A)-C(6A)-C(10A)-N(9A)	177.8(3)
N(7A)-C(6A)-C(10A)-C(11A)	176.0(3)	C(5A)-C(6A)-C(10A)-C(11A)	-5.0(6)
C(8A)-N(9A)-C(10A)-C(6A)	1.8(4)	C(15A)-N(9A)-C(10A)-C(6A)	175.3(3)
C(8A)-N(9A)-C(10A)-C(11A)	-176.0(3)	C(15A)-N(9A)-C(10A)-C(11A)	-2.4(5)
C(6A)-C(10A)-C(11A)-N(12A)	115.3(4)	N(9A)-C(10A)-C(11A)-N(12A)	-67.8(4)
C(10A)-C(11A)-N(12A)-C(13A)	68.2(4)	C(11A)-N(12A)-C(13A)-C(14A)	0.7(5)
C(11A)-N(12A)-C(13A)-C(22A)	179.7(3)	N(12A)-C(13A)-C(14A)-C(21A)	135.5(4)
C(22A)-C(13A)-C(14A)-C(21A)	-43.5(4)	N(12A)-C(13A)-C(14A)-C(15A)	-46.3(5)
C(22A)-C(13A)-C(14A)-C(15A)	134.6(3)	C(21A)-C(14A)-C(15A)-C(16A)	3.9(5)
C(13A)-C(14A)-C(15A)-C(16A)	-174.3(3)	C(21A)-C(14A)-C(15A)-N(9A)	-175.2(3)
C(13A)-C(14A)-C(15A)-N(9A)	6.7(5)	C(8A)-N(9A)-C(15A)-C(16A)	28.9(5)
C(10A)-N(9A)-C(15A)-C(16A)	-143.3(3)	C(8A)-N(9A)-C(15A)-C(14A)	-152.1(3)
C(10A)-N(9A)-C(15A)-C(14A)	35.8(5)	C(14A)-C(15A)-C(16A)-C(17A)	-4.3(5)
N(9A)-C(15A)-C(16A)-C(17A)	174.8(3)	C(15A)-C(16A)-C(17A)-C(18A)	-0.9(5)
C(16A)-C(17A)-C(18A)-C(21A)	6.1(5)	C(16A)-C(17A)-C(18A)-C(19A)	-172.9(3)
C(17A)-C(18A)-C(21A)-C(14A)	-6.6(5)	C(19A)-C(18A)-C(21A)-C(14A)	172.5(3)
C(15A)-C(14A)-C(21A)-C(18A)	1.6(5)	C(13A)-C(14A)-C(21A)-C(18A)	179.9(3)
N(12A)-C(13A)-C(22A)-N(27A)	145.7(3)	C(14A)-C(13A)-C(22A)-N(27A)	-35.2(4)
N(12A)-C(13A)-C(22A)-C(23A)	-33.6(5)	C(14A)-C(13A)-C(22A)-C(23A)	145.5(3)
N(27A)-C(22A)-C(23A)-C(24A)	-1.4(5)	C(13A)-C(22A)-C(23A)-C(24A)	177.9(3)
C(22A)-C(23A)-C(24A)-C(25A)	-0.3(6)	C(23A)-C(24A)-C(25A)-C(26A)	1.2(6)
C(24A)-C(25A)-C(26A)-N(27A)	-0.7(6)	C(25A)-C(26A)-N(27A)-C(22A)	-0.9(6)
C(23A)-C(22A)-N(27A)-C(26A)	1.9(5)	C(13A)-C(22A)-N(27A)-C(26A)	-177.4(3)
C(5B)-C(1B)-N(2B)-C(3B)	-0.5(4)	C(1B)-N(2B)-C(3B)-O(4B)	0.4(4)
N(2B)-C(3B)-O(4B)-C(5B)	-0.1(4)	N(2B)-C(1B)-C(5B)-O(4B)	0.5(4)
N(2B)-C(1B)-C(5B)-C(6B)	179.5(4)	C(3B)-O(4B)-C(5B)-C(1B)	-0.2(4)
C(3B)-O(4B)-C(5B)-C(6B)	-179.4(3)	C(1B)-C(5B)-C(6B)-C(10B)	-178.8(4)
O(4B)-C(5B)-C(6B)-C(10B)	0.2(5)	C(1B)-C(5B)-C(6B)-N(7B)	0.6(6)
O(4B)-C(5B)-C(6B)-N(7B)	179.6(3)	C(10B)-C(6B)-N(7B)-C(8B)	0.5(4)
C(5B)-C(6B)-N(7B)-C(8B)	-179.0(3)	C(6B)-N(7B)-C(8B)-N(9B)	-1.0(4)
N(7B)-C(8B)-N(9B)-C(10B)	1.1(4)	N(7B)-C(8B)-N(9B)-C(15B)	172.0(3)
N(7B)-C(6B)-C(10B)-N(9B)	0.2(4)	C(5B)-C(6B)-C(10B)-N(9B)	179.6(3)
N(7B)-C(6B)-C(10B)-C(11B)	-176.6(3)	C(5B)-C(6B)-C(10B)-C(11B)	2.8(7)
C(8B)-N(9B)-C(10B)-C(6B)	-0.8(3)	C(15B)-N(9B)-C(10B)-C(6B)	-171.9(3)
C(8B)-N(9B)-C(10B)-C(11B)	176.7(3)	C(15B)-N(9B)-C(10B)-C(11B)	5.5(5)

Table 6. (continued)

C(6B)-C(10B)-C(11B)-N(12B)	-118.0(4)	N(9B)-C(10B)-C(11B)-N(12B)	65.6(4)
C(10B)-C(11B)-N(12B)-C(13B)	-69.3(4)	C(11B)-N(12B)-C(13B)-C(22B)	-177.2(3)
C(11B)-N(12B)-C(13B)-C(14B)	0.5(5)	N(12B)-C(13B)-C(14B)-C(21B)	-135.6(3)
C(22B)-C(13B)-C(14B)-C(21B)	42.1(4)	N(12B)-C(13B)-C(14B)-C(15B)	47.6(5)
C(22B)-C(13B)-C(14B)-C(15B)	-134.6(3)	C(21B)-C(14B)-C(15B)-C(16B)	-5.2(5)
C(13B)-C(14B)-C(15B)-C(16B)	171.5(3)	C(21B)-C(14B)-C(15B)-N(9B)	173.6(3)
C(13B)-C(14B)-C(15B)-N(9B)	-9.6(5)	C(8B)-N(9B)-C(15B)-C(16B)	-26.0(5)
C(10B)-N(9B)-C(15B)-C(16B)	143.3(3)	C(8B)-N(9B)-C(15B)-C(14B)	155.1(3)
C(10B)-N(9B)-C(15B)-C(14B)	-35.5(5)	C(14B)-C(15B)-C(16B)-C(17B)	3.5(5)
N(9B)-C(15B)-C(16B)-C(17B)	-175.4(3)	C(15B)-C(16B)-C(17B)-C(18B)	2.5(5)
C(16B)-C(17B)-C(18B)-C(21B)	-6.5(5)	C(16B)-C(17B)-C(18B)-C(19B)	173.4(3)
C(15B)-C(14B)-C(21B)-C(18B)	1.1(5)	C(13B)-C(14B)-C(21B)-C(18B)	-175.8(3)
C(17B)-C(18B)-C(21B)-C(14B)	4.7(5)	C(19B)-C(18B)-C(21B)-C(14B)	-175.1(3)
N(12B)-C(13B)-C(22B)-N(27B)	-152.5(3)	C(14B)-C(13B)-C(22B)-N(27B)	29.6(4)
N(12B)-C(13B)-C(22B)-C(23B)	30.2(5)	C(14B)-C(13B)-C(22B)-C(23B)	-147.8(3)
N(27B)-C(22B)-C(23B)-C(24B)	-1.6(5)	C(13B)-C(22B)-C(23B)-C(24B)	175.6(3)
C(22B)-C(23B)-C(24B)-C(25B)	1.2(6)	C(23B)-C(24B)-C(25B)-C(26B)	-0.6(6)
C(24B)-C(25B)-C(26B)-N(27B)	0.3(6)	C(25B)-C(26B)-N(27B)-C(22B)	-0.6(5)
C(23B)-C(22B)-N(27B)-C(26B)	1.3(5)	C(13B)-C(22B)-N(27B)-C(26B)	-176.1(3)

Table 7. Hydrogen bonds for KRM-II-81 (cook149) [Å and °].

D-H...A	d(D-H)	d(H...A)	d(D...A)	<(DHA)
C(8A)-H(8A)...N(27B)	0.95	2.40	3.314(4)	162.5
C(8B)-H(8B)...N(27A)	0.95	2.45	3.361(4)	161.9
C(11B)-H(11A)...O(4B)	0.99	2.50	3.173(4)	125.4
C(26B)-H(26B)...N(2B)#1	0.95	2.61	3.518(5)	161.0

Symmetry transformations used to generate equivalent atoms:
#1 x+1/2,-y+3/2,z+1/2

APPENDIX L. Results from the Psychoactive Drug Screening Program

Table 1. *Primary Results*

Note: The PDSP has a low threshold for "hits" at primary assays. They perform a large number of secondary assays using a relatively low threshold in order not to miss potential high-affinity compounds. The likelihood of an actual, high-affinity, "hit" is still very low. Thus, one should not over-interpret results from primary assays.

Data represent mean % inhibition (n = 4 determinations) for compound tested at receptor subtypes. Significant inhibition is considered > 50%. In cases where negative inhibition (-) is seen, this represents a stimulation of binding. Occasionally, compounds at high concentrations will non-specifically increase binding.

The default concentration for primary binding experiments is 10 µM.

Legend:

1° Assay Scheduled	Complete	2° Assay Scheduled	2° Assay or Functional Completed
Redo	In Progress	Pending Approval	

CMPD	Code Name	5-HT1A	5-HT1B	5-HT1D	5-ht1e	5-HT2A
473	JY-XHe-053	42	53	45	-15	1
962	HZ-166					
1031	XHe-II-053					
30605	MP-III-024	12.2	20.1	5.7	13.1	-3
30606	MP-II-064	0.5	11.6	22.6	8	-5.6
30607	MP-II-068	-2.9	2.2	14.3	7.5	14
30608	MP-III-002	5.4	17	12.5	4.8	-1.5
30609	MP-II-075	55	19	18.5	-1.6	-12.1
30611	SH-053-2'F-R-CH3	18	9.3	16.4	-8.8	-10.7
30612	SH-053-2'F-S-CH3	8.5	4.8	12.8	-4.6	19.4
30613	MP-III-004	37.5	0.6	32.5	-3.3	9.4
30614	MP-III-021	18.8	3.3	34.4	-12.5	-0.9
30615	MP-III-019.A	-1.4	2.1	37	-9.5	-9.6
30616	MP-III-018.A	8.3	2.4	23.1	-5.8	38.5
30617	MP-III-022	1.7	0.9	9.6	-2	8.8
30618	MP-III-023	6.9	2.3	20.1	-0.3	12.4
30619	SH-I-085	22.9	9.4	14	-12	7
30620	KRM-I-56	2.8	4.3	17.5	-9.1	8.8
30621	KRM-I-55	0.3	-2.3	2.6	-8	6.8
37713	MP-III-068	2.4	5.6	-0.7	3.1	-20
37714	MP-III-080	18.8	11	-3.5	2.2	-11.7
37715	MP-III-085	7.3	2.8	2.4	3.5	-16
37717	SH-053-2'F-R-CH3-Acid	0.8	5.4	-2.3	1.6	-7.2
37718	SH-053-2'F-S-CH3-Acid	7.1	14.2	-2.9	-1	4.8
37719	MP-III-018.B	12	3.1	-2.5	1.6	-0.2
37720	MP-III-019.B	1.5	14.2	-9.2	2.7	17.3
37721	MP-IV-004	8.7	8.2	-7	0.7	32.8
37723	MP-IV-005	19.6	17.3	2.2	-1.1	18.9
37725	MP-IV-010	19.4	28.7	6	-6.7	-0.6
37728	SH-I-085	43.4	28.8	13.9	-9.6	-3.1
37729	KRM-II-18B	51.2	27.6	16	-2.9	3.5
37730	KRM-II-73	43.4	29.3	15.7	-6.8	-3.7
37731	KRM-II-82	56.6	38.8	20.1	-2.7	7.7
37732	KRM-II-97	22.9	5.9	-0.4	-3.3	16.8
37733	KRM-II-81	29.5	-1.6	-0.3	4.9	16
37734	KRM-II-68	15.5	-5.2	3.6	10	20.1
37735	KRM-II-08	9.6	3.6	9.2	1.1	-2.3
37736	KRM-II-3B	17.8	1.2	6.9	-2.7	11

Code Name	5-HT2B	5-HT2C	5-HT3	5-ht5a	5-HT6	5-HT7	Alpha1A	Alpha1B
JY-XHe-053		1	-2	23	14	9	13	12.3
HZ-166								
XHe-II-053								
MP-III-024	14.5	1.1	-1.3	2.3(AVE)	9.7	1.3	2.8	34.9
MP-II-064	-5.2	2.9	-0.2	7.8(AVE)	43.9	-9.8	0.3	-22.1
MP-II-068	-5.6	29.5	-4.4	13.4(AVE)	36.4	14.4	0.9	6.6
MP-III-002	16.3	27.3	-4.7	-1.3(AVE)	9.5	-4.8	3.1	-8.6
MP-II-075	17.8	11.6	-6	-2.6(AVE)	10.0	5.7	2	-4.1
SH-053-2'F-R-CH3	17.3	17.4	-3.8	11.5(AVE)	16.8	8.2	4.8	-3.7
SH-053-2'F-S-CH3	20.4	23.4	-10.7	4.9(AVE)	8.6	7.9	3.9	-7.1
MP-III-004	44.2	24.5	36.6	-3.9(AVE)	11.1	24.4	7.7	2.4
MP-III-021	36.6	14.6	1.1	1.4(AVE)	4.1	47.8	1.7	-7
MP-III-019.A	50	19.6	-6.5	7.7(AVE)	18.5	32.9	1.3	-4.7
MP-III-018.A	47.3	17.2	-2.9	11.6(AVE)	4.8	38.2	2	-3.6
MP-III-022	10.4	15.8	-1.7	3.5(AVE)	14.1	-1.8	-5.3	39.6
MP-III-023	44.5	35	6.1	9.5(AVE)	20.3	3.2	-11.4	23.4
SH-I-085	54.7	14.8	-5.3	12.2(AVE)	18.8	18.6	-11	22
KRM-I-56	23	5.2	-8.5	10.7(AVE)	13	18.7	-8.8	4
KRM-I-55	66.1	28.1	5.3	10.0(AVE)	-4.7	4.8	2	23.4
MP-III-068	-16.8	-4.7	-15.3	-9.2	-15.2	2.6	15.3	15.8
MP-III-080	1.3	92.6	-11.4	11.9	-17.6	18.9	11	3.5
MP-III-085	-6.4	-3.7	-6.6	-0.9	2.8	14.7	5.1	-5.6
SH-053-2'F-R-CH3-Acid	-9.7	8.6	-14.4	-1.1	-9.6	0	11.1	-17.4
SH-053-2'F-S-CH3-Acid	-8.9	-0.6	-1.2	-6.8	-5	-7.1	2.2	-15.2
MP-III-018.B	-8.4	10.2	6.3	3.7	11.2	-1.9	9.3	12.3
MP-III-019.B	0.8	14	0.9	9.4	2.2	4.5	16.7	-3.9
MP-IV-004	-8.2	10.4	0.8	12.2	21.1	3.1	12.9	1.5
MP-IV-005	1.4	11.2	-0.3	11.8	21.6	7	13.2	8.3
MP-IV-010	0.2	-1.9	12.8	11.3	21.2	-5.4	2.1	14.6
SH-I-085	5.9	24.1	3.9	14.6	-0.3	10.2	4.2	27
KRM-II-18B	-8.5	21.8	4.9	18.4	8.2	-4.5	4.3	26.1
KRM-II-73	-8.9	24.2	17.3	18.9	-1.7	8.1	-0.2	18.7
KRM-II-82	-11.3	16.4	11.5	14	-5.4	1.8	2.2	27.4
KRM-II-97	-5.5	21.9	13.3	8.1	-1.5	5.4	5.2	17.8
KRM-II-81	-1.5	17.3	6.7	9.4	-1.3	4.3	-9.6	22.3
KRM-II-68	-3.1	10.7	12.5	3.9	7.3	1.7	7.4	9.7
KRM-II-08	8	15.3	18	17.6	11.6	10.9	10.2	27.9
KRM-II-3B	88.9	65.9	-6.7	26.3	20.8	13	2.5	8.1

Code Name	Alpha1D	Alpha2A	Alpha2B	Alpha2C	Beta1	Beta2
JY-XHe-053		67	59.3	74.7	9.4	4.3
HZ-166						
XHe-II-053						
MP-III-024	15.6(AVE)	-3	24.3(AVE)	-7.4(AVE)	26.8(AVE)	11.4
MP-II-064	5.3(AVE)	12.2	7.0(AVE)	1.2(AVE)	26.3(AVE)	26.5
MP-II-068	-0.8(AVE)	10.3	16.9(AVE)	-1.2(AVE)	19.9(AVE)	17.7
MP-III-002	-9.9(AVE)	11.7	9.9(AVE)	1.7(AVE)	1.9(AVE)	0.6
MP-II-075	-6.3(AVE)	14.2	55.0(AVE)	23.5(AVE)	14.9(AVE)	4.3
SH-053-2'F-R-CH3	13.6(AVE)	9.4	9.6(AVE)	18.2(AVE)	30.6(AVE)	-1.2
SH-053-2'F-S-CH3	10.7(AVE)	16.6	18.9(AVE)	18.9(AVE)	19.4(AVE)	-1.8
MP-III-004	7.5(AVE)	14.4	13.6(AVE)	19.3(AVE)	14.5(AVE)	16.8
MP-III-021	5.4(AVE)	8	10.5(AVE)	1.7(AVE)	21.4(AVE)	22.9
MP-III-019.A	8.5(AVE)	-4.8	3.3(AVE)	-4.3(AVE)	21.4(AVE)	31.1
MP-III-018.A	12.8(AVE)	11.6	17.1(AVE)	2.9(AVE)	42.9(AVE)	19
MP-III-022	6.7(AVE)	1.9	0.7(AVE)	1.8(AVE)	32.2(AVE)	18
MP-III-023	-1.2(AVE)	-1.0	4.3(AVE)	27.5(AVE)	26.5(AVE)	5.6
SH-I-085	26.8(AVE)	8.5	28.3(AVE)	12.8(AVE)	19.2(AVE)	5.2
KRM-I-56	6.1(AVE)	10.5	15.7(AVE)	23.9(AVE)	36.5(AVE)	9.4
KRM-I-55	5.3(AVE)	14.4	9.6(AVE)	10.9(AVE)	25.1(AVE)	16.5
MP-III-068	2.5	5	23.8	-5.2	-19.4	29.4
MP-III-080	-10.5	23	35	1.2	-19.9	8.2
MP-III-085	-18.4	11.7	23.8	-7.3	-16.7	-8.2
SH-053-2'F-R-CH3-Acid	-17.9	13.4	-1.7	-10.4	13.2	93.6
SH-053-2'F-S-CH3-Acid	-9.1	21.2	16.2	0.9	-5.9	19.7
MP-III-018.B	-8.9	5	21.1	-5.3	-14.1	19.2
MP-III-019.B	-4.6	29.4	18.3	19.3	-2.1	3.1
MP-IV-004	4.5	22	9.7	3.8	-3.7	7.8
MP-IV-005	5.9	30.5	20.5	20.9	5.6	22.2
MP-IV-010	9	14.1	28.8	30.9	6.4	20.5
SH-I-085	3.6	14.9	37.8	11	-17.1	26.7
KRM-II-18B	12	13.4	23.7	2.6	11.6	-8.2
KRM-II-73	8.6	17	50	20	6.9	-18
KRM-II-82	6.8	16.3	36.3	13.1	-6.6	-10.5
KRM-II-97	13.5	15	79.5	17.6	-4.6	-18.7
KRM-II-81	0.1	20.9	55	0.1	-12.2	-28.4
KRM-II-68	-6.1	14.7	12.2	4.2	-9.6	-12.2
KRM-II-08	-11.6	27.7	2.6	-6.7	-13.3	-7.2
KRM-II-3B	-4.7	37.1	26.2	23.7	-6.1	-5.2

Code Name	Beta3	BZP Rat Brain Site	Calcium Channel	CB1	D1
JY-XHe-053			30.3	59	22
HZ-166					
XHe-II-053					
MP-III-024	6.0(AVE)	80.2(AVE)			9.4
MP-II-064	-21.1(AVE)	68.9(AVE)			13.6
MP-II-068	19.7(AVE)	95.5(AVE)			28.7
MP-III-002	-5.5(AVE)	90.9(AVE)			6.8
MP-II-075	-3.9(AVE)	97.9(AVE)			35.1
SH-053-2'F-R-CH3	-7.2(AVE)	83.7(AVE)			12.3
SH-053-2'F-S-CH3	0.3(AVE)	91.5(AVE)			11.2
MP-III-004	-12.4(AVE)	76.3(AVE)			16
MP-III-021	-11.0(AVE)	87.3(AVE)			33.2
MP-III-019.A	1.0(AVE)	49.0(AVE)			15.2
MP-III-018.A	7.9(AVE)	93.1(AVE)			14.2
MP-III-022	0.2(AVE)	93.5(AVE)			9.7
MP-III-023	18.5(AVE)	97.0(AVE)			2.4
SH-I-085	15.7(AVE)	98.2(AVE)			26.7
KRM-I-56	15.1(AVE)	97.5(AVE)			-5.4
KRM-I-55	0.1(AVE)	96.0(AVE)			-6.1
MP-III-068	-2.5	87.6			-4.6
MP-III-080	15.4	88.2			11.1
MP-III-085	-1.3	81.7			4
SH-053-2'F-R-CH3-Acid	-6.5	93.4			-10.4
SH-053-2'F-S-CH3-Acid	-16.2	92.9			-4.3
MP-III-018.B	6.5	96.6			4.9
MP-III-019.B	16.6	94.1			10
MP-IV-004	14.8	63.4			9.3
MP-IV-005	29.6	67.7			20.5
MP-IV-010	38.2	64.1			27.8
SH-I-085	-0.5	97			19.5
KRM-II-18B	-1.4	96.8			12.9
KRM-II-73	-8.5	96.9			26.4
KRM-II-82	-2.9	94.6			18
KRM-II-97	-5.8	93.4			8.1
KRM-II-81	-14	85.6			14.3
KRM-II-68	-7.4	74.8			0.6
KRM-II-08	-12.4	94.8			5.5
KRM-II-3B	5.9	69.4			25.3

Code Name	D2	D3	D4	D5	DAT	DOR
JY-XHe-053	9	-36	-5	-1	-8	43.8
HZ-166						
XHe-II-053						
MP-III-024	3.2(AVE)	3.9(AVE)	14	9.7(AVE)	4.4(AVE)	15.4(AVE)
MP-II-064	4.5(AVE)	-8.0(AVE)	34.8	20.1(AVE)	39.9(AVE)	16.8(AVE)
MP-II-068	1.8(AVE)	-4.7(AVE)	2.9	19.2(AVE)	31.4(AVE)	22.2(AVE)
MP-III-002	6.6(AVE)	2.4(AVE)	7.6	5.8(AVE)	27.0(AVE)	7.5(AVE)
MP-II-075	17.0(AVE)	16.9(AVE)	14.1	23.6(AVE)	27.6(AVE)	19.1(AVE)
SH-053-2'F-R-CH3	9.6(AVE)	2.4(AVE)	23.1	5.9(AVE)	35.3(AVE)	22.4(AVE)
SH-053-2'F-S-CH3	7.9(AVE)	6.8(AVE)	3.1	25.1(AVE)	38.1(AVE)	25.2(AVE)
MP-III-004	22.7(AVE)	9.6(AVE)	-5.5	19.6(AVE)	32.3(AVE)	21.0(AVE)
MP-III-021	20.1(AVE)	7.5(AVE)	4.9	21.7(AVE)	36.9(AVE)	20.2(AVE)
MP-III-019.A	14.3(AVE)	-9.8(AVE)	42.5	20.6(AVE)	65.4(AVE)	13.6(AVE)
MP-III-018.A	3.7(AVE)	12.9(AVE)	-7.4	8.1(AVE)	34.0(AVE)	27.1(AVE)
MP-III-022	12.6(AVE)	11.1(AVE)	-7.1	1.0(AVE)	48.6(AVE)	16.9(AVE)
MP-III-023	14.8(AVE)	6.2(AVE)	-15.7	14.1(AVE)	41.6(AVE)	15.0(AVE)
SH-I-085	13.6(AVE)	4.2(AVE)	2	13.9(AVE)	33.6(AVE)	35.2(AVE)
KRM-I-56	0.1(AVE)	6.1(AVE)	-15.6	16.1(AVE)	43.4(AVE)	21.7(AVE)
KRM-I-55	4.8(AVE)	9.0(AVE)	-21.7	10.8(AVE)	27.5(AVE)	17.9(AVE)
MP-III-068	-10.3	-5	-4.7	-17.2	7.8	18.7
MP-III-080	-5.8	12.1	-0.3	11.7	-6.4	0
MP-III-085	5.7	-0.3	-3.1	-17.2	-2.9	-3.9
SH-053-2'F-R-CH3-Acid	-14.8	-4.3	-4.6	-16.2	-1.5	-3.9
SH-053-2'F-S-CH3-Acid	-8.4	-2.8	-3.7	-13.3	3.6	17.6
MP-III-018.B	1.3	2.3	-6.5	-9.1	11	9.7
MP-III-019.B	-4.8	20.4	-6.2	-0.4	21.8	-9.9
MP-IV-004	-1.1	6.9	-2.9	11.6	32.2	9.8
MP-IV-005	-0.8	10	4.7	30.7	26.6	23.4
MP-IV-010	25.1	15	4.8	28.7	13.5	5.1
SH-I-085	29.4	1.5	-4.5	13.3	17.8	11
KRM-II-18B	13.9	4.6	-1.8	5.9	18.9	20.1
KRM-II-73	21.6	3.3	5	9	19.3	31.7
KRM-II-82	15.4	9.4	7.6	1	20.3	19.6
KRM-II-97	23.6	9.9	3.2	14	21.3	8.3
KRM-II-81	13.6	6.6	-2.8	-7	26.9	15.2
KRM-II-68	16.4	11.2	-1	-8.7	39.5	-6
KRM-II-08	19.1	17	4.3	5.1	-15.2	-7.2
KRM-II-3B	-1.7	35.8	-12	-2.9	-17.7	11.9

Code Name	GABA a1	GABAA	H1	H2	H3	H4	HERG
JY-XHe-053	99	-12.4		26.2	7.4	-13.8	
HZ-166	92.6						
XHe-II-053	99						
MP-III-024		-14.0(AVE)	36.3	-1.1	4.2	-9.0(AVE)	
MP-II-064		-6.5(AVE)	32.4	-14.3	-15.2	-6.4(AVE)	
MP-II-068		-12.6(AVE)	48.0	-12	-7.9	16.0(AVE)	
MP-III-002		-13.0(AVE)	50.4	-36.6	2.2	25.2(AVE)	
MP-II-075		-25.1(AVE)	56.5	3.2	16.2	25.6(AVE)	
SH-053-2'F-R-CH3		-12.2(AVE)	35.6	1	-2.6	9.7(AVE)	
SH-053-2'F-S-CH3		-12.6(AVE)	50.0	-7	0.4	13.9(AVE)	
MP-III-004		-6.0(AVE)	44.5	-9	-6.6	12.9(AVE)	
MP-III-021		-13.4(AVE)	44.8	-5.8	-1.8	12.1(AVE)	
MP-III-019.A		-11.1(AVE)	59.5	8.6	-19.1	20.5(AVE)	
MP-III-018.A		-10.4(AVE)	53.7	-2.7	-1.2	16.5(AVE)	
MP-III-022		-19.5(AVE)	25.5	5.5	12.5	10.4(AVE)	
MP-III-023		-24.4(AVE)	17.3	-3.2	12	14.1(AVE)	
SH-I-085		-17.7(AVE)	3.2	-5.5	4.8	-6.3(AVE)	
KRM-I-56		-5.8(AVE)	-9.3	-4.7	9.4	3.1(AVE)	
KRM-I-55		-2.9(AVE)	-9.3	-10.2	15.5	-4.5(AVE)	
MP-III-068		9.4	24.9	12.4	2.3	-3.2	
MP-III-080		-0.6	89.3	2.6	7.9	7.1	
MP-III-085		-18.2	90.2	-1.9	-5.9	-3.1	
SH-053-2'F-R-CH3-Acid		-15.2	86.7	-5.4	-1.3	14	
SH-053-2'F-S-CH3-Acid		-3.8	78	7.7	8	-7.6	
MP-III-018.B		-14.4	71.3	1.2	3	-1.1	
MP-III-019.B		-19.4	58.3	-0.8	-0.2	-0.1	
MP-IV-004		-8.5	44.1	-6.9	-5.5	8.4	
MP-IV-005		-5.6	20.8	0.7	-1.2	5.6	
MP-IV-010		-7.6	19	28.2	-17.9	5.7	
SH-I-085		-1.2	19.3	11.6	16.2	15.5	
KRM-II-18B		-11.2	5.1	9.6	22.2	19	
KRM-II-73		-17.5	-8.1	0.7	16.6	14.8	
KRM-II-82		-15.3	-11.3	19.6	13.1	32.8	
KRM-II-97		-14.8	-32.6	-4.7	2.4	15.2	
KRM-II-81		-7.9	-13.5	-11.7	8.6	11.7	
KRM-II-68		-0.6	4.2	79.1	-1	4.9	
KRM-II-08		-19.8	89	1.7	-11.4	20.5	
KRM-II-3B		-16.1	42.9	-0.7	-6.8		

Code Name	HERG binding	KOR	M1	M2	M3	M4	M5
JY-XHe-053		26	-4.2	12.3	21.8	30.6	6.4
HZ-166							
XHe-II-053							
MP-III-024	-0.0	40.0(AVE)	-10.6	-5.7	12.0(AVE)	3.3(AVE)	-1.4
MP-II-064	8.1	35.5(AVE)	5.7	-1.5	-5.7(AVE)	-3.5(AVE)	21.7
MP-II-068	-6.9	82.8(AVE)	-10.7	16.5	-14.6(AVE)	21.9(AVE)	4.9
MP-III-002	1.1	12.6(AVE)	-7.2	11.2	6.8(AVE)	-1.6(AVE)	-2.6
MP-II-075	14.7	84.1(AVE)	-8.4	23.8	16.2(AVE)	4.4(AVE)	2.1
SH-053-2'F-R-CH3	10.6	90.9(AVE)	-4.9	17.9	26.1(AVE)	7.7(AVE)	0
SH-053-2'F-S-CH3	15.3	95.7(AVE)	-8.5	11.7	12.8(AVE)	12.6(AVE)	-1.9
MP-III-004	21.7	80.3(AVE)	-7.8	-0.7	7.9(AVE)	1.0(AVE)	3.6
MP-III-021	16.1	97.5(AVE)	-6.2	2.9	9.3(AVE)	5.8(AVE)	0.8
MP-III-019.A	15	45.5(AVE)	-4.5	2.1	1.7(AVE)	9.2(AVE)	6
MP-III-018.A	27.6	71.1(AVE)	-7.2	-3.2	2.3(AVE)	43.3(AVE)	8.3
MP-III-022	25.3	87.0(AVE)	-11.4	4.7	-0.9(AVE)	-3.9(AVE)	5.7
MP-III-023	9.4	96.1(AVE)	-2.2	10	9.1(AVE)	-2.3(AVE)	2.6
SH-I-085	4.1	95.6(AVE)	-10.2	0.6	10.8(AVE)	1.4(AVE)	2.4
KRM-I-56	37.6	7.6(AVE)	-2	-2.6	14.5(AVE)	0.3(AVE)	6.3
KRM-I-55	-10.8	2.7(AVE)	-5.2	0.3	19.7(AVE)	1.6(AVE)	6
MP-III-068	-10.5	28.5	7.2	19.5	15.4	18.2	-2.7
MP-III-080	5.3	46.6	4	25.9	7.8	26.6	11.5
MP-III-085	-6.4	40.2	6.2	16.3	3.3	29.4	-5.9
SH-053-2'F-R-CH3-Acid	0.7	16.4	11.9	21.1	8.6	29	-3.9
SH-053-2'F-S-CH3-Acid	-4.4	20.1	5.8	20.7	12.3	20.7	-0.1
MP-III-018.B	0.4	50.9	10.6	50	16.7	29.7	6.6
MP-III-019.B	2	62.1	4.2	50	8.1	28.6	14.1
MP-IV-004	18.6	86	-9.8	26.5	-5.5	27.7	12.4
MP-IV-005	18.5	89.3	-11.3	22.3	7.3	22.2	12
MP-IV-010	28.8	93.6	-11.2	10.5	-0.4	8.4	26.2
SH-I-085	17.8	91.3	-3.4	17.1	-3.9	14.2	28.2
KRM-II-18B	17.6	88.9	-1.4	4.9	7.7	9	30.5
KRM-II-73	17.9	83.1	-4.5	6.6	4.9	15.4	50
KRM-II-82	16.3	77.9	-4.3	0	3.8	13.5	33.5
KRM-II-97	20	61.6	10.1	3.5	6.7	12	38.3
KRM-II-81	-16.4	45.9	3.2	2.4	-8.9	11.2	37.5
KRM-II-68	6.1	20.3	6.9	0.1	-8.3	12.8	26.2
KRM-II-08	3	80.2	11.8	3.5	-0.1	18	25.4
KRM-II-3B	-9.2	54.7	-5	-1.3	15.2	-7.5	10.3

Code Name	mGlur5	MOR	NET	NMDA	Oxytocin	PBR	SERT
JY-XHe-053		5	46	-7.2(AVE)			103.0
HZ-166							
XHe-II-053							
MP-III-024	-1.8	-5.4(AVE)	-1.6		20.4	20.8(AVE)	-1.3
MP-II-064	-19.8	-1.4(AVE)	2.5		14.3	38.4(AVE)	8.9
MP-II-068	36.5	10.0(AVE)	-3.6		4.5	59.5(AVE)	-13.2
MP-III-002	10.1	7.4(AVE)	-11		8.1	24.0(AVE)	-7.4
MP-II-075	-18.5	8.4(AVE)	-0.1		24.1	81.8(AVE)	-11.5
SH-053-2'F-R-CH3	31.7	15.7(AVE)	-11.3		13.9	12.3(AVE)	-14.3
SH-053-2'F-S-CH3	24.8	15.6(AVE)	-5.5		18.1	18.2(AVE)	-9.5
MP-III-004	4.8	-2.2(AVE)	-14.2		42.1	30.1(AVE)	-12.5
MP-III-021	-5.1	2.1(AVE)	-11.8		16.8	25.5(AVE)	-9
MP-III-019.A	-7.3	2.7(AVE)	-22		15.9	22.5(AVE)	-4.2
MP-III-018.A	54.4	8.8(AVE)	-6.4		7.6	1.9(AVE)	5.4
MP-III-022	29.1	4.1(AVE)	-11.4		12.5	16.6(AVE)	-6.1
MP-III-023	-0.6	-5.7(AVE)	7.9		21.8	15.1(AVE)	-10
SH-I-085	28.6	10.8(AVE)	-26.8		30.2	60.4(AVE)	1.1
KRM-I-56	39	9.0(AVE)	60.4		37	11.1(AVE)	-11.8
KRM-I-55	-16.9	2.7(AVE)	39.8		55.3	-2.6(AVE)	-9.9
MP-III-068		24.8	-11.3			61.8	-12.7
MP-III-080		-1.1	-3.4			84.8	-13.4
MP-III-085		-4.3	-17.8			75.2	40.7
SH-053-2'F-R-CH3-Acid		-9.2	11.4			12.8	-26.8
SH-053-2'F-S-CH3-Acid		-2.5	38.9			17.7	2.1
MP-III-018.B		2	38.5			22.3	-5.4
MP-III-019.B		2	32.8			34.4	-2
MP-IV-004		7	19			47.6	10.9
MP-IV-005		20.6	27.2			38.2	13.3
MP-IV-010		32.7	-2.2			27.7	21.7
SH-I-085		10.9	-12.1			80.3	6.4
KRM-II-18B		10.9	-2.2			38.4	11.5
KRM-II-73		10.5	16.6			67.9	3.5
KRM-II-82		5.4	9.8			42.7	21.1
KRM-II-97		18.1	26.6			93.4	0.7
KRM-II-81		6.5	41.1			93.1	-9.1
KRM-II-68		6.1	37.3			37.8	-3.7
KRM-II-08		5	38.3			81.6	7.7
KRM-II-3B		-12.3	39.4			66.5	33.4

Code Name	Sigma 1	Sigma 2	V1A	V1B	V2
JY-XHe-053			-6	-18	-13
HZ-166					
XHe-II-053					
MP-III-024	16.5(AVE)	-22.7(AVE)	7.2	10.5	4.6
MP-II-064	9.1(AVE)	0.1	10.6	18.1	3.7
MP-II-068	-2.0(AVE)	2.3	13.8	-7.4	6
MP-III-002	6.4(AVE)	-15.9(AVE)	6.7	18.6	8.3
MP-II-075	4.3(AVE)	-18.4	11.7	24.1	17.9
SH-053-2'F-R-CH3	-5.3(AVE)	-2.8	9.2	31.3	2
SH-053-2'F-S-CH3	-3.0(AVE)	-5.0	10.7	32.3	7.5
MP-III-004	7.5(AVE)	-7.1	4.7	18.1	5.6
MP-III-021	8.9(AVE)	5.5	9.7	13.2	9.1
MP-III-019.A	3.2(AVE)	-22.5(AVE)	7.1	10	6.6
MP-III-018.A	-0.7(AVE)	-8.4	17.4	-2.5	8.6
MP-III-022	-8.1(AVE)	-7.6	5.4	17.9	15.7
MP-III-023	-15.3(AVE)	-9.9	10	23.1	14.1
SH-I-085	-12.7(AVE)	30.3	14.6	44.7	4.2
KRM-I-56	9.8(AVE)	-1	18.4	48	8
KRM-I-55	-5.6(AVE)	-5.1	8.8	26.8	9.3
MP-III-068	25.5	-16.6			
MP-III-080	36.3	24.1			
MP-III-085	25	59.1			
SH-053-2'F-R-CH3-Acid	0.5	-3.3			
SH-053-2'F-S-CH3-Acid	12.6	-3.8			
MP-III-018.B	18.5	11.6			
MP-III-019.B	28	26.2			
MP-IV-004	22.2	62.4			
MP-IV-005	25.3	63.2			
MP-IV-010	34.9	64.2			
SH-I-085	11.6	44.8			
KRM-II-18B	-1.5	45.8			
KRM-II-73	6.3	58.1			
KRM-II-82	-5.5	47.5			
KRM-II-97	-13.1	30.7			
KRM-II-81	-14.9	34.5			
KRM-II-68	-8.2	14.9			
KRM-II-08	-6.3	41.5			
KRM-II-3B	17.5	54.6			

Table 2. *Secondary Results*

Unless otherwise indicated (see Note), data represent K_i (nM) values obtained from non-linear regression of radioligand competition binding isotherms. K_i values are calculated from best fit IC_{50} values using the Cheng-Prusoff equation.

Note: When the Hill coefficient (nH) is significantly different from -1 (assessed by F test), the IC_{50} and nH are reported instead of the K_i.

A * next to a value denotes IC_{50}.

Legend:

Complete	2° Assay Scheduled	1° Assay <50%	Redo
In Progress	Pending Approval	Under Review	

CMPD	Code Name	5-HT1A	5-HT1B	5-HT2B	5-HT2C
473	JY-XHe-053		>10000		
962	HZ-166				
1031	XHe-II-053				
30605	MP-III-024				
30606	MP-II-064				
30607	MP-II-068				
30608	MP-III-002				
30609	MP-II-075	2,062.00			
30611	SH-053-2'F-R-CH3				
30612	SH-053-2'F-S-CH3				
30613	MP-III-004				
30614	MP-III-021				
30615	MP-III-019.A			>10,000	
30616	MP-III-018.A				
30617	MP-III-022				
30618	MP-III-023				
30619	SH-I-085			>10,000	
30620	KRM-I-56				
30621	KRM-I-55			3,665.00	
37713	MP-III-068				
37714	MP-III-080				1,319.0(AVE)
37715	MP-III-085				
37717	SH-053-2'F-R-CH3-Acid				
37718	SH-053-2'F-S-CH3-Acid				
37719	MP-III-018.B				
37720	MP-III-019.B				
37721	MP-IV-004				
37723	MP-IV-005				
37725	MP-IV-010				
37728	SH-I-085				
37729	KRM-II-18B	3,372.0(AVE)			
37730	KRM-II-73				
37731	KRM-II-82	2,383.7(AVE)			
37732	KRM-II-97				
37733	KRM-II-81				
37734	KRM-II-68				
37735	KRM-II-08				
37736	KRM-II-3B			852.5(AVE)	1,066.5(AVE)

Code Name	Alpha2A	Alpha2B	Alpha2C	Beta1	Beta2
JY-XHe-053	3,484.00	3,975.00	2,105.00		
HZ-166					
XHe-II-053					
MP-III-024					
MP-II-064					
MP-II-068					
MP-III-002					
MP-II-075		1,760.00			
SH-053-2'F-R-CH3					
SH-053-2'F-S-CH3				7,214.00	
MP-III-004					
MP-III-021				>10,000	
MP-III-019.A				>10,000	
MP-III-018.A				>10,000	
MP-III-022					
MP-III-023			>10,000		
SH-I-085					
KRM-I-56				>10,000	
KRM-I-55					
MP-III-068					
MP-III-080					
MP-III-085					
SH-053-2'F-R-CH3-Acid					>10,000
SH-053-2'F-S-CH3-Acid					
MP-III-018.B					
MP-III-019.B					
MP-IV-004					
MP-IV-005					
MP-IV-010					
SH-I-085					
KRM-II-18B					
KRM-II-73		4,565.7(AVE)			
KRM-II-82					
KRM-II-97		834.3(AVE)			
KRM-II-81		2,876.7(AVE)			
KRM-II-68					
KRM-II-08					
KRM-II-3B					

Code Name	BZP Rat Brain Site	CB1	DAT	GABA a1	H1	H2
JY-XHe-053		4,771.00		47.4		
HZ-166						
XHe-II-053						
MP-III-024	277					
MP-II-064	590		>10,000			
MP-II-068	42		>10,000			
MP-III-002	109		7,603.00		>10,000	
MP-II-075	21				>10,000	
SH-053-2'F-R-CH3	379		>10,000			
SH-053-2'F-S-CH3	111		>10,000		>10,000	
MP-III-004	445					
MP-III-021	219					
MP-III-019.A	3,246.00		6,482.00		>10,000	
MP-III-018.A	139		5,857.00		>10,000	
MP-III-022	83		>10,000			
MP-III-023	37		>10,000			
SH-I-085	11		>10,000			
KRM-I-56	2.8		>10,000			
KRM-I-55	29					
MP-III-068	244.7(AVE)					
MP-III-080	263.3(AVE)				9,436.7(AVE)	
MP-III-085	339.0(AVE)				10,000.0(AVE)	
SH-053-2'F-R-CH3-Acid	32.3(AVE)				10,000.0(AVE)	
SH-053-2'F-S-CH3-Acid	52.7(AVE)				10,000.0(AVE)	
MP-III-018.B	27.7(AVE)				924.3(AVE)	
MP-III-019.B	88.3(AVE)				10,000.0(AVE)	
MP-IV-004	941.0(AVE)					
MP-IV-005	710.0(AVE)					
MP-IV-010	1,051.0(AVE)					
SH-I-085	10.8(AVE)					
KRM-II-18B	38					
KRM-II-73	56.0(AVE)					
KRM-II-82	134.7(AVE)					
KRM-II-97	150.3(AVE)					
KRM-II-81	382.0(AVE)					
KRM-II-68	475.7(AVE)					3,516.00
KRM-II-08	6.4(AVE)				9,333.3(AVE)	
KRM-II-3B	1,114.0(AVE)				1.2	

Code Name	KOR	M2	M4	M5	mGlur5
JY-XHe-053					
HZ-166					
XHe-II-053					
MP-III-024					
MP-II-064					
MP-II-068	550				
MP-III-002					
MP-II-075	547				
SH-053-2'F-R-CH3	240				
SH-053-2'F-S-CH3	90				
MP-III-004	599				
MP-III-021	122				
MP-III-019.A	3,367.00				
MP-III-018.A	1,182.00		>10,000		1,358.0(AVE)
MP-III-022	381				
MP-III-023	119				
SH-I-085	162				
KRM-I-56					
KRM-I-55					
MP-III-068					
MP-III-080					
MP-III-085					
SH-053-2'F-R-CH3-Acid					
SH-053-2'F-S-CH3-Acid					
MP-III-018.B	3,072.0(AVE)	10,000.0(AVE)			
MP-III-019.B	2,621.0(AVE)	10,000.0(AVE)			
MP-IV-004	637.0(AVE)				
MP-IV-005	379.5(AVE)				
MP-IV-010	149.0(AVE)				
SH-I-085	219.5(AVE)				
KRM-II-18B	375.5(AVE)				
KRM-II-73	900.5(AVE)			10,000.0(AVE)	
KRM-II-82	1,084.0(AVE)				
KRM-II-97	2,102.5(AVE)				
KRM-II-81					
KRM-II-68					
KRM-II-08	713.0(AVE)				
KRM-II-3B	3,627.0(AVE)				

Code Name	NET	Oxytocin	PBR	SERT	Sigma 2
JY-XHe-053				>10000	
HZ-166					
XHe-II-053					
MP-III-024					
MP-II-064					
MP-II-068			1,671.00		
MP-III-002					
MP-II-075			439		
SH-053-2'F-R-CH3					
SH-053-2'F-S-CH3					
MP-III-004					
MP-III-021					
MP-III-019.A					
MP-III-018.A					
MP-III-022					
MP-III-023					
SH-I-085			1,226.00		
KRM-I-56	644				
KRM-I-55		>10,000			
MP-III-068			2,501.3(AVE)		
MP-III-080			943.5(AVE)		
MP-III-085			2,241.5(AVE)		6,994.3(AVE)
SH-053-2'F-R-CH3-Acid					
SH-053-2'F-S-CH3-Acid					
MP-III-018.B					
MP-III-019.B					
MP-IV-004					1,730.0(AVE)
MP-IV-005					2,054.3(AVE)
MP-IV-010					2,070.5(AVE)
SH-I-085			1,338.0(AVE)		
KRM-II-18B					
KRM-II-73			3,318.0(AVE)		1,579.7(AVE)
KRM-II-82					
KRM-II-97			311.0(AVE)		
KRM-II-81			560.0(AVE)		
KRM-II-68					
KRM-II-08			1,055.0(AVE)		
KRM-II-3B			3,757.7(AVE)		3,061.3(AVE)

MICHAEL M. POE CIRRICULUM VITAE

EDUCATION

- **B.S.,** Chemistry, University of Minnesota-Duluth, Duluth, MN, 2004 – 2008.
    - Research: Synthesis of lactones and lactams under supervision of Dr. Robert Carlson

POSITIONS HELD

- Student Paraprofessional, Environmental Proection Agency (EPA), Duluth, MN, 2008 – 2009.
- Teaching (2009 – 2011) and Research (2011 – present) Assistant, Department of Chemistry and Biochemistry, UW-Milwaukee, Milwaukee, WI, 2009 – present.

RESEARCH EXPERIENCE

- **EPA**: Analysis of rainbow trout viability in arsenic contaminated waters using analytical techniques
    - Responsible for conducting experiments which included feeding fish arsenic-laced food (with chromium as a marker) and analyzing the collected fecal matter for lack of absorption of nutrients. Instrumentation included flame atomic absorption, LC-MS, and fluorescence, as well as extractions for lipid content. At the end of the study, fish were sacrificed and the extracted intestine was inverted and washed with [^{3}H]-glucose and measured for sugar absorption by a liquid scintillation counter.
- **UWM**: Synthesis of subtype-selective benzodiazepine receptor ligands for therapeutic use (P.I. James M. Cook)
    - Organic/medicinal chem. highlights (*Research Summary* available if not yet provided)
        - Multi-step synthesis starting at over 100 g. scale
        - Supply collaborators with mg- to gram- quantities
        - Over 100 novel ligands synthesized
        - Experience with wide-range of reagents and reactions
        - Also performed many simple transformations for complete SAR studies
        - Developed ligand undergoing extensive preclinical studies (PCT Patent)
    - Laboratory Techniques
        - 1D and 2D NMR
        - Flash column chromatography
        - Mass spectrometry (single quadrupole)
        - Mammalian cell culture (HEK293)
        - *In vitro* liver microsomal stability studies
        - Animal studies, including drug administration, rotorod studies, and organ harvesting
    - Additional experience outside of lab work included:
        - Wrote and received a UWM Catalyst Grant ($56,000); P.I. James M. Cook
        - Assisted in writing of two funded NIH R01 Grants; P.I. James M. Cook
        - Wrote Provisional and PCT Patent, "GABAergic Ligands to Treat CNS Disorders including Anxiety and Depression as well as Neuropathic Pain"; conversion to PCT, March 2016; P.I. James M. Cook
        - Group safety representative

PUBLICATIONS AND PRESENTATIONS

Scholarly Publications (*Published and Accepted*)

1. Drexler, Berthold; Zinser, Stefan, Huang, Shengming; **Poe, Michael M**.; Rudolph, Uwe; Cook, James M.; Antkowiak, Bernd, "Enhancing the function of alpha5-subunit-containing GABAA receptors promotes action potential firing of neocortical neurons during up-states," *European Journal of Pharmacology*, **703**, 18-24 (2013).

2. Gill, Kathryn M.; Cook, James M.; **Poe, Michael M**.; Grace, Anthony A., "Prior antipsychotic drug treatment prevents response to novel antipsychotic agent in the methylazoxymethanol acetate model of schizophrenia," *Schizophrenia Bulletin*, **40**(2), 341-350 (2014).

3. Obradovic, Aleksandar Lj; Joksimovic, Srdan; Batinic, Bojan; Radulovic, Tamara; **Poe, Michael M**.; Namjoshi, Ojas; Cook, James M.; Ramerstorfer, Joachim; Varagic, Zdravko; Sieghart, Werner; Karovic, Bojan; Roth, Brian; Savic, Miroslaw M., "SH-I-048A, an *in vitro* nonselective super-agonist at the benzodiazepine site of GABAA receptors: the approximated activation of receptor subtypes may explain behavioral effects," *Brain Research*, **1554**, 36-48 (2014).

4. Obradović, A.Lj; Joksimović, S.; **Poe, M.M**.; Timić, T.; Cook, J.M.; Savić, M.M., "Delayed behavioral effects of SH-I-048A, a novel nonselective positive modulator of $GABA_A$ receptors, after peripheral nerve injury in rats," *Acta Veterinaria*, **64**(2), 189-199 (2014).

5. Richetto, Juliet; Labouesse, Marie A.; **Poe, Michael M**.; Cook, James M.; Grace, Anthony A.; Riva, Marco A.; Meyer, Urs, "Behavioral effects of the benzodiazepine positive allosteric modulator SH-053-2'F-S-CH_3 in an immune-mediated neurodevelopmental disruption model," *Int. J. Neuropsychopharmacol.*, **18**, (2015).

6. Gallos, George; Yocum, Gene T.; Siviski, Matthew E.; Yim, Peter D.; Fu, Xiao Wen; **Poe, Michael M**.; Cook, James M.; Harrison, Neil; Perez-Zoghbi, Jose; Emala Sr., Charles W., "Selective targeting of the α5 subunit of $GABA_A$ receptors relaxes airway smooth muscle and inhibits cellular calcium handling," *American Journal of Physiology. Lung Cellular and Molecular Physiology*, **308**, L931-L942 (2015).

7. Clayton, Terry[†]; **Poe, Michael M.[†]**; Rallapalli, Sundari; Biawat, Poonam; Savić, Miroslav M.; Rowlett, James K.; Gallos, George; Emala, Charles W.; Kaczorowski, Catherine C.; Stafford, Douglas C.; Arnold, Leggy A.; Cook, James M., "A review of the updated pharmacophore for the alpha 5 GABA(A) benzodiazepine receptor model," *International Journal of Medicinal Chemistry*, doi:10.1155/2015/430248 (2015).

8. Botta, Paolo; Demmou, Lynda; Kasugai, Yu; Markovic, Milica; Xu, Chun; Fadok, Jonathan P.; Lu, Tingjai; **Poe, Michael M**.; Xu, Li; Cook, James M.; Rudolph, Uwe; Sah, Pankaj; Feeraguti; Francesco; Lüthi, Andreas, "Regulating anxiety with extrasynaptic inhibition," *Nature Neuroscience*, **18**, 1493-1500 (2015).

9. Heise, Christopher; Taha, Elham; Murru, Lucca; Ponzoni, Luisa; Cattaneo, Angela; Guarnieri, Fabrizia C.; Montani, Caterine; Mossa, Adele; Vezzoli, Elena; Ippolito, Guilio; Zapata, Jonathan; Berrera, Iliana; Ryazanov, Alexey G.; Cook, James; **Poe, Michael**; Stephen, Michael; Kopanitsa, Maksym; Benfante, Roberta; Rusconi, Francesco; Braida, Baniela; Francolini, Maura; Proud, Chris; Valtorta, Flavia; Passafaro, Maria; Sala, Mariaelvina; Bachi, Angela; Verpelli, Chiara; Rosenblum, Kobi; Sala, Carlo, "eEF2 pathway controls dentate

gyrus dependent behavior and excitation-inhibition balance," *Cerebral Cortex*, doi:10.1093/cercor/bhw075 (2016).

10. Jonas, Oliver; Calligaris, David; Methuku, Kashi Reddy; **Poe, Michael M**.; Pierre Francois, Jessica; Tranghese, Frank; Changelian, Armen; Sieghart, Werner; Ernst, Margot; Pomeranz Krummel, Daniel A.; Cook, James M.; Pomeroy, Scott L.; Cima, Michael; Agar, Nathalie Y.R.; Langer, Robert; Sengupta, Soma, "First *in vivo* testing of compounds targeting Group 3 medulloblastomas using an implantable microdevice as a new paradigm for drug development," *Journal of Biomedical Nanotechnology*, **12** (6), 1297 – 1302 (2016).

11. Forkuo, Gloria; Guthrie, Margaret; Yuan, Nina; Nieman, Amanda; Kodali, Revathi; Jahan, Rajwana; Yocum, G. Thomas; Stephen, Michael; **Poe, Michael**; Li, Guanguan; Yu, Olivia; Hartzler, Benjamin; Zahn, Nicholas; Emala, Charles; Stafford, Douglas; Cook, James; Arnold, Leggy, "Development of $GABA_A$ receptor subtype-selective imidazobenzodiazepines as novel asthma treatments," *Molecular Pharmaceutics*, **13**, 2026 – 2038 (2016).

Scholarly Publications (*Submitted and In Preparation*)

1. **Poe, Michael M**.; Methuku, Kashi R.; Li, Guanguan; Verma, Ashwini; Teske, Kelly A.; Stafford, Douglas C.; Arnold, Leggy A.; Cramer, Jeffrey W.; Jones, Timothy M.; Cerne, Rok; Krambis, Michael J.; Witkin, Jeffrey M.; Jambrina, Enrique; Rehman, Sabah; Ernst, Margot; Cook, James M.; Schkeryantz, Jeffrey M, "Synthesis and characterization of a novel $GABA_A$ receptor ligand that combines outstanding metabolic stability, pharmacokinetics and anxiolytic activity," *Journal of Medicinal Chemistry*, Submitted (2016).

2. Piantadosi, Sean C.; French, Beverly; Timic, Tamara; **Poe, Michael M**.; Markovic, Bojan; Pabba, Mohan; Savic, Miroslav M.; Cook, James M.; Sibille, Etienne, "Sex-dependent rapid mild antidepressant activity of an α5 subunit containing $GABA_A$ receptor positivie allosteric modulator in the mouse unpredictable chronic mild stress model," *Frontiers in Pharmacology*, Submitted (2016).

3. Stamenić, Tamara Timić; **Poe, Michael M**.; Rehman, Sabah; Santrač, Anja; Divović, Branka; Scholze, Petra; Ernst, Margot; Cook, James M.; Savić, Miroslav M., "A novel benzodiazepine MP-III-022 impairs spatial cognition and improves social recognition by strong selective positive modulation of $GABA_A$ receptors containing the α5 subunit," *ACS Chemical Neuroscience*, Submitted (2016).

4. Yuan, Nina Y.; **Poe, Michael M**.; Witzigmann, Christopher; Cook, James M.; Stafford, Douglas; Arnold, Leggy A., "Characterization of GABA(A) receptor ligands with automated patch-clamp using human neurons derived from pluripotent stem cells," *Journal of Pharmacological and Toxicological Methods*, Submitted (2016).

5. Kannampalli, Pradeep; Babygirija, Reji; Zhang, Jiang; **Poe, Michael M.**; Li, Guanguan; Cook, James M.; Shaker, Reza; Banerjee, Banani; Sengupta, Jyoti, "Neonatal bladder inflammation induces long-term visceral pain and altered responses of spinal neurons in adult rats," *Pain*, Submitted (2016).

6. **Poe, Michael M**.; *et al.*, "Chiral imidazobenzodiazepine enantiomers for the treatment of different progressions of schizophrenia," *Manuscript in Preparation* (Target: *ACS Chemical Neuroscience*)

Contributions Acknowledged

1. Paul et al., "Antihyperalgesia by α2-$GABA_A$ receptors occurs via a genuine spinal action and does not involve supraspinal site," *Neuropsychopharmacology*, **39**, 477-487 (2014).

2. Ralvenius et al., "Analgesia and unwanted benzodiazepine effects in point-mutated mice expressing only one benzodiazepine-sensitive $GABA_A$ receptor subtype," *Nature Communications*, **6**, 1-12 (2015).

Patents

1. "GABAergic receptor subtype selective ligands and their uses," Cook, James M.; Clayton, Terry S.; Jain, Hiteshkumar D.; Johnson, Yun T.; Rallipalli, Sundari K.; Wang, Zhi-jian; Namjoshi, Ojas A.; **Poe, Michael M**., Patent No. US 2015/0258128 A1; Pub. Date Nov. 22, 2012.

2. "GABAergic receptor subtype selective ligands and their uses," Cook, J.M., Clayton, T., Jain, H.D., Rallapalli, S. K., Johnson, Y. T.,Yang, J.,**Poe, M.M**., Namjoshi, O. A., Wang, Z. Patent No. US 9,006,233 B2; Date of Patent April 14, 2015.

3. "GABAergic ligands to treat CNS disorders including anxiety and depression as well as neuropathic pain," Cook, James M.; **Poe, Michael M**.; Methuku, Kashi R.; Li, Guanguan. Provisional Application Filed on March 20, 2015; PCT conversion, March 2016.

4. Cook, James M.; **Poe, Michael M.**; Li, Guanguan; Sibille, Etienne; Savic, Miroslav M.; Banasr, Mounira. Provisional Application Filed on March 18, 2016.

Papers Presented at Professional Meetings

"Synthesis of nonsedating anxiolytics active against neurophatic pain as well as seizures", Z.J. Wang, A. Di Lio, S.K. Rallapalli, R.V. Edwankar, M.M. Poe, J.M. Cook, H.U. Zeilhofer, 241st ACS National Meeting, Anaheim CA, March 27-31, (Abst. MEDI 129), 2011.

"Withdrawal from Repeated Haloperidol Reduces the Efficacy of Subsequent Novel Antipsychotic Treatment in MAM Model of Schizophrenia", T. Grace, et al., M. Poe, J.M. Cook, Society for Neuroscience Meeting, San Diego, Fall, 2013.

"Reversal of Ketamine-Induced Cognitive Impairment by an α2/α3 $GABA_A$ Receptor Modulator in Rhesus Monkeys", Z. Meng, M.M. Poe, Zhi-jian Wang, J.M. Cook, J.K. Rowlett, Society for Neuroscience Meeting, San Diego, Fall, 2013.

"Synthesis of Benzodiazepines Active Against Neuropathic Pain as well as Schizophrenia", **M. Poe**, Z. Wang, A. Di Lio, S. Rallapalli, R. Edwankar, J. Cook, H.U. Zeilhofer, 245th ACS National Meeting, New Orleans LA, April 7-11, (Abst. MEDI 371), 2013.

"MK-801-Induced Hyperlocomotion in Rats is Affected by Modulation of α5-Containing GABA Receptors", T. Timic, S. Joksimovic, M.M. Poe, J. Ramerstorfer, P. Biawat, T. Radulovic, B. Roth, W. Sieghart, J.M. Cook, M. Savic, 26th ECNP Congress, Barcelona, Spain, Oct. 2013.

"Role of Alpha 3 $GABA_A$ Receptor Modulation in the Anti-Conflict Effects of Benzodiazepine – Type Drugs in Monkeys," Sawyer, E.; Fischer, B.; Meng, Z.; Poe, M.; Namjoshi,O.; Cook, J.;

Rowlett, J., presented at The CPDD Meeting, San Diego, CA. Hilton Bayfront Hotel, June 17-21 (2013).

"Synthesis of Natural Products and related Heterocyclic Compounds. Search for Agents to Treat Neuropathic Pain, Epilepsy and Anxiety Disorders as well as Simple Molecules to Treat TB and MRSA Infections", J.M. Cook, C.R. Edwankar, M.M. Poe, V.V.N.P.B. Tiruveedhula, C.M. Witzigmann; Mona Symposium, Mona, Jamaica, January 6-9, 2014.

"Chiral Subtype Selective imidazobenzodiazepines Important as Potential Agents to Treat Schizophrenia," **M.M. Poe**, N. Raddatz, D. Baker, J.M. Cook; 247th ACS National Meeting, Dallas, TX, March 16-20, (Abst. MEDI 282), 2014.

"Effects of HZ-166, a Novel α2 and α3 Subunit-containing $GABA_A$ Receptor Agonist, on Inflammatory Pain and Operant Behavior," Fischer, B.D.; Kroll, C.; Poe, M.M.; Cook, J.M., CPDD National Meeting, San Juan, Puerto Rice, June 14-19, 2014.

"Positive Modulation at α5-$GABA_A$ Receptors is not Beneficial for Cognitive Deficits Induced by MK-801 in Water Maze in Rats", Timić Stamenić, T.; Joksimović, S.; Milić, M.; Batinić, B.; Poe, M.M.; Cook, J.M.; Savić, M.M., 27th Congress of the European College of Neuropsychopharmacology (ECNP), Berlin, Germany, October 18-21, (Eur Neuropsychopharmacol 2014; 24 Suppl 2: S325), 2014.

"A novel Trojan horse for in-vivo sensitivity testing of medulloblastoma therapies", Sengupta, S.; Jonas, O.; Calligaris, D.; Cook, J.M.; Poe, M.M.; Methuku, K.; Archer, T.; Francois, J.P.; Tranghese, F.; Pomeroy, S.; Agar, N.; Langer, R., Society for Neuro-Oncology 19th Annual Meeting, Miami, Florida, November 13-16, 2014.

"Benzodiazepine receptor ligands as analgesics", Fischer, B.D.; Hamade, B.Z.; Poe, M.M.; Cook, J.M., 2015 Behavioral Pharmacology Society Meeting, Boston, MA, March 27-28, 2015.

"Behavioral effects of the novel benzodiazepine analog methyl 8-ethynyl-6-(pyridine-2-yl)-4*H*-benzo[*f*]imidazo[1,5-*a*][1,4]diazepine-3-carboxylate (MP-III-024)", Hamade, B.Z.; Poe, M.M.; Cook, J.M., Annual Metting of the American Society for Pharmacology and Experimental Therapeutics, Boston, MA, March 28, 2015.

"Imidazobenzodiazepines for improving α5-$GABA_A$R subtype selectivity and their pharmacological relevance," **M.M. Poe**, G. Gallos, R. Puthenkalam, M.M. Savic, C.W. Emala Sr., M. Ernst, JmM. Cook; 250th ACS National Meeting, Boston, MA, August 16-20, (Abst. MEDI 70), 2015.

"Metabolic studies of drug candidates for neurological disorders and asthma based on $GABA_A$ receptor subtype selective ligands using mass spectrometry," R. Kodali, M. Guthrie, M. Poe, M.R. Stephen, R. Jahan, C.W. Emala, J.M. Cook, D. Stafford, A. Arnold; 250th ACS National Meeting, Boston, MA, August 16-20, (Abst. MEDI 432), 2015.

"Development of a Liquid Chromatography-Tandem Mass Spectrometry (LC-MS/MS) Method for Quantification of Subtype-Selective $GABA_A$ Receptor Ligands following Liquid-Liquid Extraction (LLE) and on-line Solid-Phase Extraction (SPE)," M.L. Guthrie, M.M. Poe, J.M. Cook, A. Arnold, 250th ACS National Meeting, Boston, MA, August 16-20, (Abst. ANYL 133), 2015.

"Novel α5 Selective Benzodiazepine Site Ligands," Rehman, S.; Puthenkalam, R.; Scholze, P.; Steudle, F.; Poe, M.; Li, G.; Cook, J.M.; Savic, M.; Timic, T.; Emala, C.; Gallos, G.; Ernst, M., 14th Austrian Neuroscience Association Meeting, Salzburg, Austria, September 23-25, 2015.

"A Novel, α2-, 3-selective $GABA_A$ Receptor Modulator with Improved Central Penetrability and Associated Antiepileptic and Anti-Pain Efficacy," J.M. Witkin, K.R. Methuku, J.M. Schkeryantz, S.D. Gleeson, A. Okun, F. Porecca, J.W. Cramer, T.M. Jones, J.T. Catlow, X. Li, M.M. Poe, G. Li, A. Arnold, J.M. Cook, APSET Meeting, San Diego, CA, April 2-6, 2016.

"Attaining *in vivo* selectivity of positive modulation of α3 $GABA_A$ receptors in rats: a hard task," B. Batinic, T. Stankovic, M.M. Poe, J.M. Cook, M.M. Savic, ECNP Workshop for Junior Scientists, Nice, France, March 17 – 20, 2016.

MEMBERSHIPS

- Member of the American Chemical Society (2011 – present)
- Member of the American Chemical Society – *Med. Chem. Division* (2012 – present)